OCS Study
MMS 2001-064

Deepwater Physical Oceanography Reanalysis and Synthesis of Historical Data

Synthesis Report

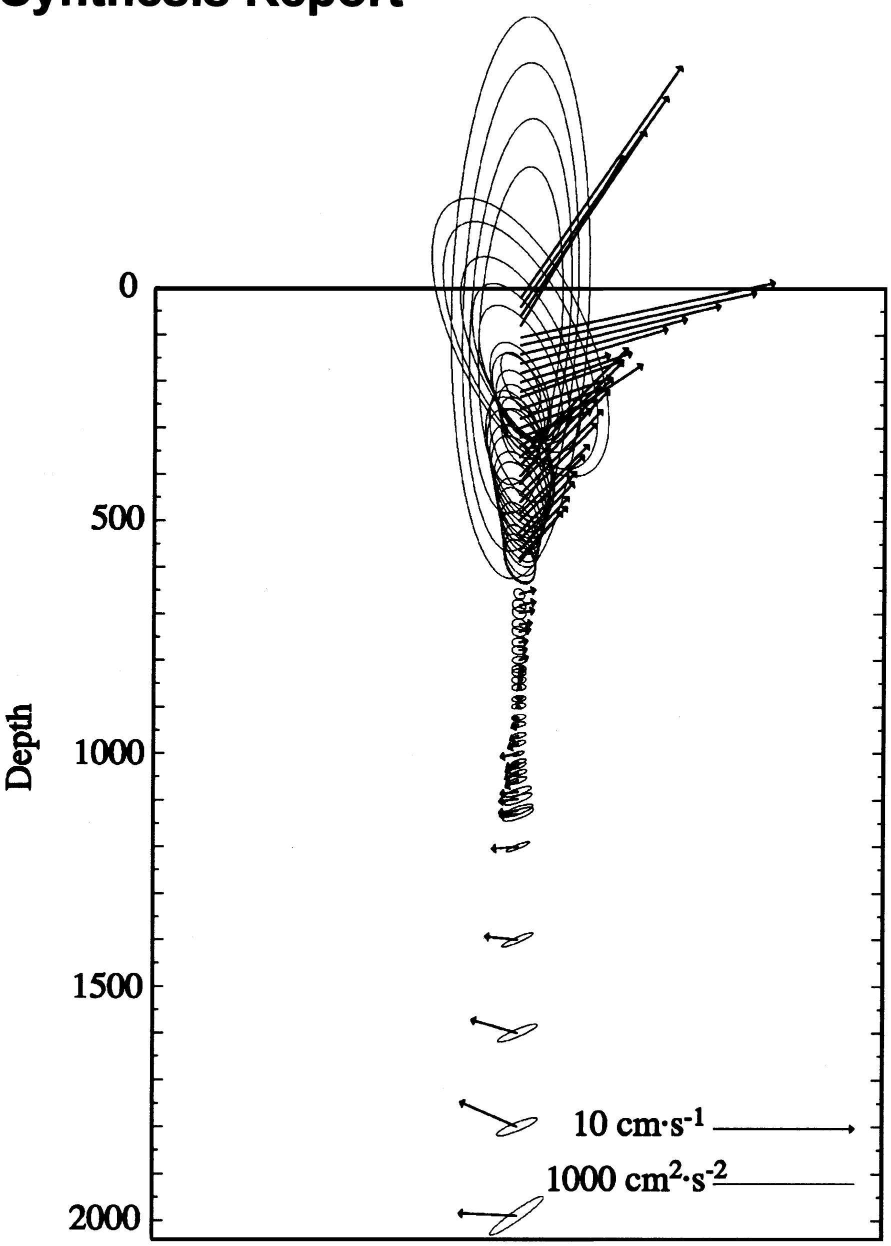

U.S. Department of the Interior
Minerals Management Service
Gulf of Mexico OCS Region

OCS Study
MMS 2001-064

Deepwater Physical Oceanography Reanalysis and Synthesis of Historical Data

Synthesis Report

Authors

Worth D. Nowlin, Jr.
Ann E. Jochens
Steven F. DiMarco
Robert O. Reid
Matthew K. Howard

Prepared under MMS Contract
1435-01-98-CT-30910
by
Texas A&M University
Department of Oceanography
College Station, Texas 77843-3146

Published by

U.S. Department of the Interior
Minerals Management Service
Gulf of Mexico OCS Region

New Orleans
August 2001

DISCLAIMER

REPORT AVAILABILITY

Extra copies of the report may be obtained from the Public Information Office (Mail Stop 5034) at the following address:

U.S. Department of the Interior
Minerals Management Service
Gulf of Mexico OCS Region
Public Information Office (MS 5034)
1201 Elmwood Park Boulevard
New Orleans, Louisiana 70123-2394

Telephone: (504) 736-2519 or
1-800-200-GULF

CITATION

Suggested citation:

Nowlin, W. D., Jr., A. E. Jochens, S. F. DiMarco, R. O. Reid, and M. K. Howard. 2001. Deepwater Physical Oceanography Reanalysis and Synthesis of Historical Data: Synthesis Report. OCS Study MMS 2001-064, U.S. Dept. of the Interior, Minerals Management Service, Gulf of Mexico OCS Region, New Orleans, LA. 528 pp.

ABOUT THE COVER

The cover art depicts record-length current vectors and variance ellipses for records of duration greater than 100 d from MMS mooring I1 at 89.784°W, 27.293°N. The record shows strong surface intensified currents and variability associated with the extended presence near the mooring of Loop Current Eddy Juggernaut, minimum currents and variance in the depth interval of 800-1000 m, and intensification of currents and variance with depth below that level.

ACKNOWLEDGMENTS

This report would not have been possible without the contributions of a large number of people at Texas A&M University (TAMU) and the University of Colorado (CU). Each Deepwater principal investigator (PI) contributed substantially to the success of this project. The principal investigators, their affiliations, and their tasks are:

Worth D. Nowlin, Jr.	TAMU	Program Manager, PI for Task 2, Co-PI for Task 4
Steven F. DiMarco	TAMU	Co-PI for Task 1
Matthew K. Howard	TAMU	PI for Task 1
Ann E. Jochens	TAMU	PI for Task 4
Lakshmi Kantha	CU	Co-PI for Task3
Robert O. Reid	TAMU	PI for Task 3, Co-PI for Task 2

Jei-Kook Choi, postdoc at CU, generated the model output. A number of students at TAMU participated in various aspects of the Deepwater project. Yue Fang and Ou Wang, graduate students in physical oceanography, and Tecky Surawijaya, graduate student in ocean engineering, worked tirelessly on data quality control efforts. Todd Ooten, undergraduate student in mathematics, prepared the drifter data sets for final QA/QC processing and analysis. Xia Xiang Dong, graduate student in physical oceanography, and Michael Flinn, graduate student in biological oceanography, also assisted in the data quality control processing effort. Thanks go to all these for their contributions to the success of this project. Thanks also to Dave Brooks for his assistance. We greatly appreciate the efforts of Susan Martin in helping us put together this document for printing, as well as the assistance of Maureen Reap.

We appreciate the help of the Science Review Board: Cortis Cooper of Chevron Petroleum Technology, Ken Schaudt of Marathon Oil Company, and Robert Smith of Oregon State University. Their suggestions early on in the project broadened the nature of the model output data set used for analysis and provided additional ideas to be considered in this deepwater Gulf circulation study.

A special thanks go to Ken Schaudt, Certified Consulting Meteorologist, for his substantial efforts to assist us in obtaining data from the petroleum industry and for providing data sets from Marathon. Cortis Cooper also helped greatly in this regard and gave us the data sets from Chevron. We thank the members of the petroleum industry who helped to identify data sets and provided us with many of their existing data, including Dave Peters of Conoco, Tom Mitchell of Texaco, Dave Driver of BP-Amoco, Michael Vogel and George Forristall of Shell, Markku Santala of Exxon, Walter Spring of Mobil, Mike Utt of Unocal, and David Tubbs of Burlington Resources. We appreciate the help of Peter Hamilton of Science Applications International Corporation, Bruce Magnell of Woods Hole Group, Dave Szabo of Fugro-GEOS, and Robert Hamilton of Evans-Hamilton, Inc., for their help in providing to us many of the industry data sets.

Van Waddell and Peter Hamilton assisted us in obtaining the newest data sets collected under MMS sponsorship by Science Applications International Corporation. The addition of their data sets provided several of the non-proprietary, long time series contining many interesting events.

Thanks to Wilford Gardner and Doug Biggs of the Department of Oceanography of TAMU and Norman Guinasso and Gary Wolff of the Geochemical and Environmental Research Group (GERG) of TAMU for providing data sets and providing permission to include many of them in the database; Bill Bryant and Dan Bean of TAMU-Oceanography for providing information on the geology of the furrows; Ian MacDonald of GERG for making possible collection of preliminary hydrographic data from a Gulf of Mexico furrow during an ALVIN dive; Wilton Sturges of Florida State University for providing the "lost" Yucatan sill data set; Robert L. Leben, Colorado Center for Astrodynamics Research, CU, for production of daily sea surface height anomaly fields from satellite altimeter data; William Wiseman of Louisiana State University and Robert Weisberg of the University of South Florida for data from their projects in the Gulf; Alberto Vazquez for providing a number of hydrographic data sets from Mexican waters, and Walter Johnson and Jim Price of MMS for providing us with their surface drifter data. Mary Hollinger and Francis Mitchell of NODC were particularly helpful in promptly meeting our requests for data from the NODC data base.

Finally, we thank Alexis Lugo-Fernández, our contracting officer's technical representative, for making available to us the databases and reports from the Eddy Joint Industry Project (EJIP) and Climatology and Simulation of Eddies study (CASE); these have substantially augmented the data sets available to us for analysis and have aided us in our interpretations. We greatly appreciate his enthusiasm and thoughtful oversight of our project; he has contributed much to the success of this project.

The Deepwater Principal Investigators

TABLE OF CONTENTS

TABLE OF CONTENTS (continued)

TABLE OF CONTENTS (continued)

LIST OF FIGURES

LIST OF FIGURES (continued)

LIST OF FIGURES (continued)

LIST OF FIGURES (continued)

LIST OF FIGURES (continued)

LIST OF FIGURES (continued)

LIST OF FIGURES (continued)

LIST OF FIGURES (continued)

LIST OF FIGURES (continued)

LIST OF FIGURES (continued)

LIST OF TABLES

LIST OF TABLES (continued)

ACRONYMS AND ABBREVIATIONS

ADCP	acoustic Doppler current profiler
AVHRR	advanced very high resolution radiometer satellite
AXBT	air-deployed XBT
AXCP	air-deployed XCP
CASE	Climatology and Simulation of Eddies study
CCAR	Colorado Center for Astrodynamics Research
C_L	Longitudinal Decorrelation Scale
CODAR	Coastal Ocean Dynamics Applications Radar
CSR	Center for Space Research at the University of Texas
C_T	Transverse Decorrelation Scale
CTD	conductivity-temperature-depth sensors
CU	University of Colorado
CUPOM	CU implementation of the Princeton Ocean Model
ECMWF	European Center for Mid-range Weather Forecasting
EOF	empirical orthogonal function
EIS	DeSoto Canyon Eddy Intrusion Study of SAIC
EJIP	Eddy Joint Industry Project
GEK	geomagnetic electrokinetograph
GERG	Geochemical and Environmental Research Group at TAMU
GOMOMS	Gulf of Mexico Ocean Monitoring System
GOOS	Global Ocean Observing System
HF	High-Frequency (radars)
IES	inverted echo sounder
LATEX	Louisiana-Texas Shelf Physical Oceanography Program
LATEX A	Texas-Louisiana Shelf Circulation and Transport Processes Study
LC	Loop Current
LCE	Loop Current Eddy
NEGOM	Northeastern Gulf of Mexico Physical Oceanography Program, Chemical Oceanography and Hydrography Study
MAMES	Mississippi-Alabama Continental Shelf Ecosystem Study
MBT	mechanical bathythermograph
MMS	Minerals Management Service, U.S. Department of the Interior
NASA	National Aeronautics and Space Administration
NOAA	National Oceanic and Atmospheric Administration
NODC	National Oceanographic Data Center
NOPP	National Ocean Partnership Program
OSU MSL	Ohio State University Mean Sea Level
PI	principal investigator
QA/QC	quality assurance/quality control
RAFOS	SOFAR spelled backwards (SOFAR = sound fixing and ranging float)
R/V	research vessel
S	salinity
SAIC	Science Applications International Corporation
SCULP	Surface Current Lagrangian Program
SIO	Scripps Institute of Oceanography
SRB	Scientific Review Board
SSH	sea surface height
SSHA	sea surface height anomaly

ACRONYMS AND ABBREVIATIONS (continued)

SST	sea surface temperature
STD	salinity-temperature-depth sensors
SVD	singular value decomposition
T	temperature
TAMU	Texas A&M University
TAMUG	Texas A&M University–Galveston
TRW	topographic Rossby wave
UCT or UTC	universal coordinated time
XBT	expendable bathythermograph probe
XCP	expendable current profiler

1 EXECUTIVE SUMMARY

1.1 Introduction

The Minerals Management Service (MMS) of the U. S. Department of the Interior funded the Deepwater Physical Oceanography Reanalysis and Synthesis of Historical Data Study in the Gulf of Mexico. MMS awarded the contract to the Texas A&M Research Foundation in July 1998. Under the contract, scientists at Texas A&M University (TAMU) and the University of Colorado (CU) conducted the study. The basic study area is bounded by the shelf edge (~200-m isobath) and the 25°N latitude, which is the southern boundary; it extends from sea surface to sea floor. MMS has four objectives for the study. First is to create an inventory of physical oceanographic data and compile it into a single database on a CD-ROM. Second is to conduct analyses and interpretations of the physical oceanographic data to identify physical processes and phenomena. Third is to produce a climatology of the processes from available data and analyses and to prioritize the processes in terms of importance to improved understanding, simulation, and prediction of deepwater circulation. Fourth is to provide criteria and constraints useful in design of future field observations and numerical modeling efforts. Study results will provide MMS with information needed to direct its resources more efficiently and effectively in the review and assessment of potential environmental impacts of offshore oil and gas operations in the deepwater Gulf of Mexico.

1.2 Data Assembly

An inventory of historical and concurrent physical oceanographic data sets was compiled. Data included were current measurements from moored single-point current meters, acoustic Doppler current profilers, and expendable current profilers; hydrographic observations from bottles, salinity-temperature-depth and conductivity-temperature-depth (CTD) sensors, mechanical bathythermographs, and expendable bathythermographs (XBT); drifting buoy trajectories; and inverted echo sounder data. As many of these data sets as possible were obtained from MMS, the National Oceanographic Data Center, other federal and state agencies, national laboratories, universities, Mexican institutions, and the private sector, particularly the oil and gas industry. Data were quality controlled. Data that were provided without restrictions on use were compiled into a database and put on a CD-ROM with an accompanying descriptive technical report.

Examination of the spatial location and temporal duration of the data reveal a number of data gaps. Except in the central Gulf, there are few current data sets in water depths of 1000 m or more, and few stations are available south of 25°N. Most current measurements are made in the upper 800 m, with deeper waters sparsely sampled. Very few current records have a duration as long as one year. High quality CTD measurements, with excellent vertical spatial resolution, are relatively sparse in deep water. There are fewer hydrographic data in winter months. All data are sparse in the southwestern Gulf.

Selected ancillary data sets were assembled to aid in the interpretations, including meteorology, river discharge, sea surface height (SSH) from satellite altimeter, and sea surface temperature (SST) from Advanced Very High Resolution Radiometer satellites. Additionally, output from a high-resolution, 3-dimensional, circulation model was obtained for 1993–1999. The model, called by the acronym CUPOM, is the CU version of the Princeton Ocean Model adapted for the Gulf of Mexico. The horizontal resolution is 1/12°, and the vertical resolution is 24 sigma levels. The model assimilates SSH and SST data. Ancillary and model data are not included in the CD-ROM database.

1.3 General Hydrography and Circulation of Deepwater Gulf

The circulation within the Gulf of Mexico is driven principally by two sources of energy. The main source consists of the Yucatan Current and other circulation features that enter the Gulf from the Caribbean Sea through the Yucatan Channel. Effects are seen as a Loop Current (the extension of the Yucatan Current through the eastern Gulf and into the Florida Straits), the warm-core rings that detach from the Loop Current and their subsequent distribution of energy throughout the Gulf, and the effects of the Loop Current and ring separation on the deep circulation within the basin. Transport estimates for the Loop Current system are approximately 30 Sverdrups with seasonal fluctuations of about 10%. The second major energy source is wind stress forcing. Effects are seen as low-frequency regional circulation patterns forced by low-frequency regional wind patterns and as episodic currents forced by high frequency atmospheric events including tropical cyclones, extratropical cyclones, cold air outbreaks, and other frontal passages. Thermohaline forcing is known to be important over the Gulf shelves, e.g., buoyancy forcing by river discharge affects the nearshore coastal currents over the shelves. However, no thermohaline forcing of consequence or significant water mass formation are known to occur in the deepwater Gulf.

1.4 Large Scale Circulation and Its Variability

Large scale circulation was examined using geostrophic shear fields from hydrography, statistics from the near-surface drifter velocity field, the CUPOM model circulation, and SSH fields. High-quality temperature and salinity data were used to compute the mean and standard deviation of dynamic topography of the sea surface relative to 800 m and of 1500 m relative to 800 m (current data, model output, and prior hydrographic studies indicate 800-1000 m is a reasonable depth separating surface-intensified upper ocean currents from nearly barotropic deep currents within the Gulf). Near-surface current velocities estimated from drifter data were grouped in 0.5° x 0.5° bins and averaged to determine mean currents and their variance ellipses. Model mean currents and their variance ellipses were calculated over the years 1993-1998 for the sea surface and 500-m, 1000-m, 2000-m, and 3000-m surfaces. Mean SSH, which provides our best estimate of the mean circulation from satellite altimeter data, was determined by averaging the SSH output of the 1993-1999 CUPOM model run; the standard deviation was determined from the SSH anomaly fields.

The dominant feature in the mean fields of the upper layer is the Loop Current. A closed anticyclonic feature is present within the Loop Current. In addition to the strong inflow on the west side of the Yucatan Channel, the drifter field shows an outflow just west of Cuba. The largest variability is in the region of the Loop Current and eddy separations in the northeastern Gulf. Variance ellipses generally are aligned parallel with the inflow and outflow limbs of the Loop Current. Both the SSH field and surface dynamic topography have a slight lowering of sea level around the margins relative to the center, suggesting slight anticyclonic circulation. The fields exhibit evidence of anticyclonic circulation in the west central Gulf, centered about 24°N 95°W, that is consistent with the forcing of the surface circulation by the annual cycle of wind stress curl. The fields also exhibit indications of cyclonic circulation in the Bay of Campeche. The dynamic topography of 1500 m relative to 800 m indicates there is a cyclone beneath the Loop Current and that the circulation in the western Gulf is cyclonic at depth. The model results also show a cyclone beneath the Loop Current, most predominantly on the 1000-m and 2000-m surfaces. They also indicate cyclonic flow around the basin near the 2000-m to 3000-m isobaths. The strong effect of the bathymetry on the directionality of the variability is seen in the orientation of the model variance ellipses along the margins of each isobath.

1.5 Identification of Energetic Current Events

The inventory of identified processes and phenomena was carried out in three steps: identification of energetic currents, identification of possible processes/phenomena, and categorization of currents by class. Each time series of currents was examined for the occurrence of energetic currents. Energetic current events were considered to have occurred when the magnitudes of currents over the period of an event were considerably greater than the background currents for the region and/or for situations where the currents had characteristics known to be associated with particular classes of events. The possible processes and phenomena were identified from the literature and from the character of the energetic currents observed. Five broad classes of energetic current events were identified: Loop Current and surface-intensified eddies; deep barotropic and bottom-trapped motions; atmospheric storm generated motions; internal waves generated by topographic influence; and mid-water current jets. Current records were compared and, where appropriate, matched in time and space to known occurrences of the Loop Current, Loop Current Eddies, other anticyclonic or cyclonic rings, tropical storms, hurricanes, extratropical (winter) cyclones, frontal passages, and other energetic wind events. The energetic portions of each record were then inventoried according to type of phenomena or process (Section 6.4).

1.6 Climatology of Processes and Phenomena

The climatology of processes and phenomena consisted of general current statistics, current roses and persistence tables, current speed versus depth by region, record-length velocities and variances, eddy kinetic energy distributions, energy spectra, vertical empirical orthogonal functions, and a detailed examination of the statistics for each event type. Ten major categories of physical processes and phenomena were identified for prioritization for futher consideration.

These then were prioritized as to the need for additional data for improved understanding, simulation, and prediction of slope and subsurface circulation. Three major criteria were selected for use in determining the priority. These were the need for improved level of understanding, the need for improved ability to simulate and predict, and the ability to make the desired measurements (see Section 7.3.2). The categories and their priority rankings are shown below, with 1 being the highest rated in terms of the need for additional measurements.

1. Deep barotropic & bottom-intensified motions
2. General circulation—deep currents
3. Currents associated with furrows
4. Eddy induced currents
5. Loop Current
6. General circulation—surface currents from local wind forcing
7. Subsurface, mid-water column motions
8. Hurricane/tropical storm-induced motions
9. Other energetic wind event induced motions
10. Topographically generated near-inertial motion

1.7 Measurement System Design Criteria

The primary region of interest for gathering more data to characterize energetic phenomena and processes in the Gulf is the north-central slope and rise and northwest corner of the deepwater Gulf. This is the deepwater region where the future oil discoveries are expected to occur. The highest priority phenomena/processes are considered to be the currents in deep water. These include: (1) deep barotropic and bottom-intensified motions, particularly deep anticyclonic-cyclonic eddy pairs and topographic Rossby waves; (2) the deep general circulation; and (3) currents associated with furrows. Current and hydrographic data and model output were examined for the presence of the top three processes. Characteristics of these processes, in terms of spatial and temporal scales, were estimated. Deep eddies and topographic Rossby waves have time scales of 10 to 100 days and spatial scales of hundreds of kilometers. The deep circulation has spatial scales ranging from eddy size (200-400 km) to basin scale (> 400 km), with time scales that are long (> 2 d) but uncertain. Furrow fields have cross-isobath scales of ~35 km and along-isobath scales of over 100 km; time scales of currents associated with these fields are unknown. Measurement arrays were developed for each priority process using, among other factors, the characteristic scales to determine optimal spatial locations and temporal duration.

1.8 Conclusions and Recommendations

Several general conclusions were made from this study. (1) The general surface circulation for the Gulf is rather well described and understood in terms of forcing and response. (2) There appear to be adequate data to characterize surface features such as the Loop Current and anticyclonic eddies, but not to understand the processes of eddy evolution and decay. Moreover, models and their inflow conditions are not yet adequate to hindcast or forecast them with the needed degree of skill. (3) The data are inadequate to fully characterize the deep subsurface processes, which include barotropic deep events in the form of topographic Rossby waves or deep eddies, or to determine the influence of surface processes, such as LCE separation events, on such deep processes. (4) The verification of mid-water jets remains problematical; a few (perhaps 8) events have been documented, but the data quality remains in doubt. (5) There is no convincing evidence of topographically generated near-inertial motion in the Gulf. (6) Knowledge of the general deep Gulf circulation is based principally on model output and speculation using sparse observations and their derived properties. However, the sparse, existing data sets tend to confirm the speculation and model results. (7) The processes responsible for the mega-furrows near the Sigsbee Escarpment in the north-central Gulf are not understood.

Three types of recommendations are made: specific measurement programs, systematic monitoring operations, and model improvements. The specific measurement programs are: (1) a moored array near the Sigsbee Escarpment in the north-central Gulf designed to measure barotropic deep motions propagated along this boundary; (2) a thin array of current moorings over the abyssal plain to detect and describe deep eddy pairs and surface-intensified eddies propagating across the Gulf; (3) a Lagrangian float experiment in the deep basin designed to obtain statistics regarding the deep circulation and its variability and to give indications of deep flow through the Yucatan Channel; and (4) an experiment to characterize currents and determine processes responsible for the mega-furrows in the north-central Gulf. The systematic monitoring operations are: (1) to enhance the environmental observations obtained on the drill vessels and production platforms of the petroleum industry; (2) to monitor surface currents with pairs of high frequency radars; (3) to use automated sea level and meteorological stations on both sides of the Yucatan Channel and between Cuba and Key West to monitor the transport of the inflow and outflow; and (4) to obtain regular surface estimates of velocity and temperature and subsurface measurements of temperature and salinity by comprehensive inclusion of the Gulf of Mexico in the operational deployment programs for surface drifters, ship-of-opportunity XBTs, and Argos profiling floats. To enhance the capabilities of numerical models for providing needed environmental information, periodic, careful comparisons should be made between results from the many available models, corroborated by available observations, and improvements should be made to Gulf of Mexico circulation models, including notably better boundary conditions for regional models and improved data assimilation capabilities.

2 INTRODUCTION

2.1 Background

The Minerals Management Service (MMS) of the U. S. Department of the Interior is charged with managing the federal offshore oil and gas resource. As a result of the Deep Water Royalty Relief Act and the evolution of new exploration and production technologies, oil and gas leasing activity accelerated substantially, beginning in 1995, in waters of the Gulf of Mexico deeper than 300 m (Carney 1997). In April 1997, MMS sponsored an environmental deepwater workshop in New Orleans, LA, to identify environmental and socioeconomic issues related to the expansion of oil and gas operations off the continental shelf into the deepwater Gulf of Mexico and to provide recommendations on studies needed to fill gaps in knowledge (Carney 1997). One recommendation was that a synthesis of historical physical oceanographic data be completed prior to implementation of any major observational study of the deepwater physical oceanography.

In July 1998, MMS awarded the contract for the Deepwater Physical Oceanography Reanalysis and Synthesis of Historical Data study (Deepwater Study) to the Texas A&M Research Foundation. Under the contract, scientists at Texas A&M University (TAMU) and the University of Colorado (CU) conduct the Deepwater Study. In addition to support from the MMS, financial backing for the Deepwater Study was provided by Texas A&M University and the Texas Institute of Oceanography.

The Deepwater Study is part of a comprehensive program designed to gather necessary physical oceanography data for waters over the slope of the northern Gulf of Mexico. Its main foci are data assembly and quality control, data synthesis, identification of physical processes operating in the deepwater Gulf, and development of recommendations for experimental designs for future field studies. Study results should provide MMS with the information needed to direct its resources more efficiently and effectively as they review and assess potential environmental impacts of offshore oil and gas operations in the deepwater Gulf of Mexico.

2.2 Program Overview and Objectives

The study area is bounded by the 200-m isobath, which is roughly the shelf edge, and the 25°N latitude (Figure 2.2-1) and extends from the sea surface to the sea floor. MMS had four objectives for the Deepwater Study. These are:

1. *Create an inventory of physical oceanographic data and compile it into a single database on a CD-ROM*. The inventory will consist of historical physical oceanographic data, together with data collected by concurrent programs and related numerical ocean circulation model outputs, in the study domain. Data collected will be acquired from the MMS, other state and federal agencies, national laboratories, universities, Mexican institutions, and the private sector, especially the oil and gas industry. As many of the data sets identified in the inventory as possible will be assembled, quality controlled as feasible (dependent on availability of metadata), and compiled into a database on a CD-ROM with accompanying descriptive technical report. The inventory, but not the CD-ROM, also will include ancillary data (e.g., river discharge rates, surface meteorological fields, sea level measurements, and satellite observations) needed to aid in the study of the in situ physical oceanographic data.

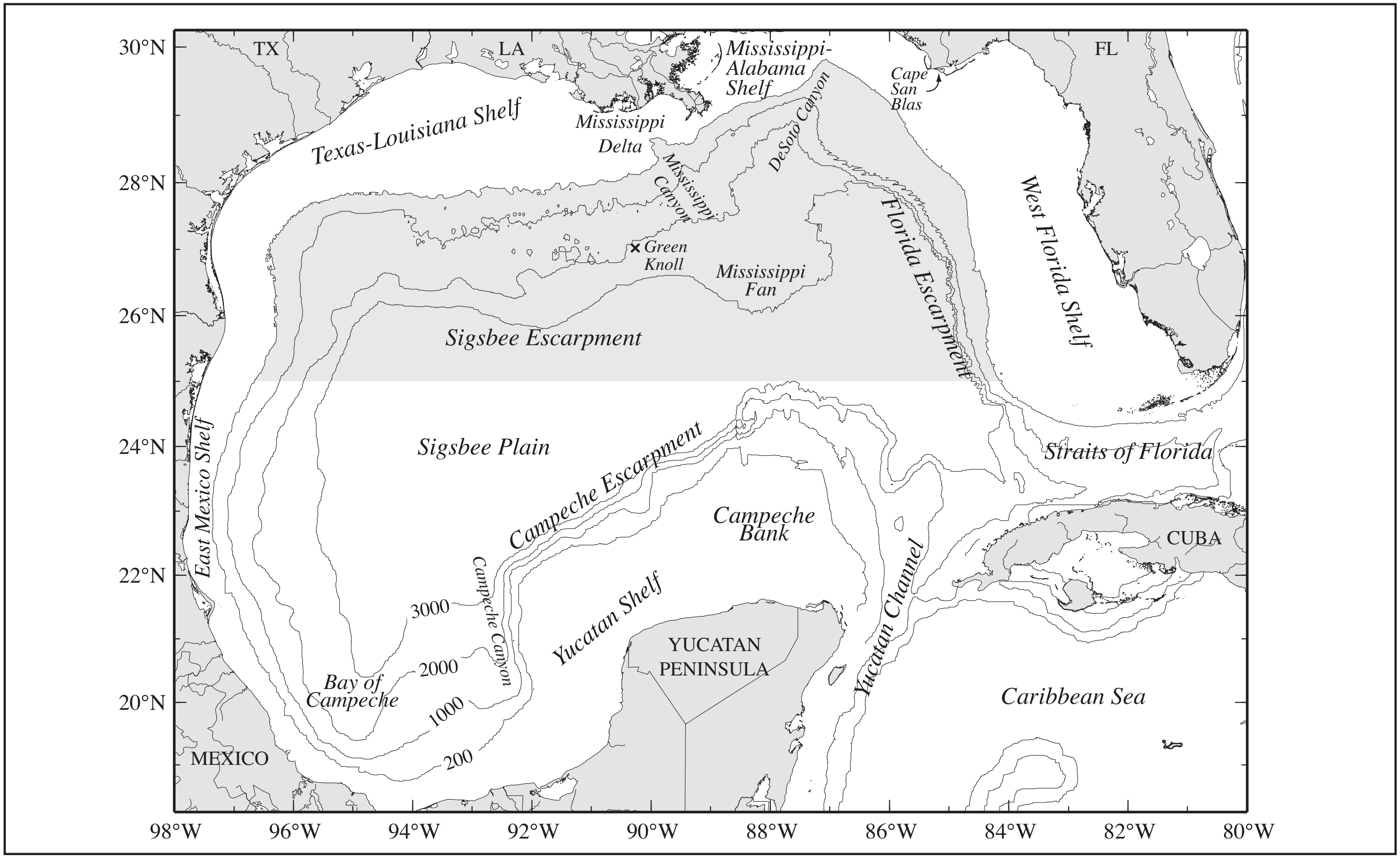

Figure 2.2-1. Study domain (shaded area) for the Deepwater Study with bathymetry and geographical locations in the Gulf of Mexico.

2. *Conduct analyses and interpretations of the physical oceanographic data based on analytical solutions to identify physical processes*. The assembled data sets will be examined using quantitative mathematical and statistical techniques to identify and resolve characteristics of phenomena and processes present in the study domain. This will focus on estimation of the temporal and spatial scales, amplitudes, phase relationships, dominant patterns, and causal factors of currents and property distributions associated with these phenomena and processes. Model output as well as data will be examined.

3. *Produce a climatology of these physical processes from available data and analyses*. The frequency of occurrence of the identified phenomena and physical processes and statistical estimates of their associated properties (produced as objective 2) will be compiled. This will constitute a climatology of these processes and phenomena. The identified physical phenomena and processes will be prioritized in terms of importance to improved understanding, simulation, and prediction of deepwater circulation. The synthesis will concentrate on identifying important processes and illustrating these with observational (and, if appropriate, model) data, and on formulating hypotheses regarding the underlying mechanisms that can be used for prediction (if understanding is adequate).

4. *Provide criteria and constraints useful in the design of future field observations and numerical modeling efforts*. Based on design criteria developed, optimal designs for moored arrays to study the prioritized physical phenomena and processes over the continental slope, rise, and plain of the northern Gulf of Mexico west of approximately 89°W will be recommended.

To accomplish these objectives, four tasks were set out for the Deepwater Study. Each task has two Principal Investigators (PI) who are responsible directly to the Program Manager for successful completion of that task. Program management is directed by Dr. Worth D. Nowlin, Jr., Program Manager. The four tasks are:

Task 1 (Data Inventory and Collection): Dr. Matthew K. Howard (PI) and Dr. Steven F. DiMarco (Co-PI) of TAMU are responsible for Task 1. The goal of this task is to produce a high-quality comprehensive database of physical oceanographic data for the Gulf of Mexico from existing data and model outputs. Major task activities are to create an inventory of existing data, ancillary data, and selected model outputs; to acquire such data and outputs; to perform Quality Assurance/Quality Control (QA/QC) processing on the data; to generate metadata, supporting documentation, and plots; and to make the non-proprietary physical oceanographic database available on CD-ROM with a technical report detailing QA/QC procedures and results.

Task 2 (Data Analysis and Synthesis): Dr. Worth D. Nowlin, Jr. (PI) and Professor Robert O. Reid (Co-PI) of TAMU are responsible for Task 2. The goal of this task is to fully analyze the database acquired by Task 1 and develop a synthesis of the physical phenomena and processes present in the data. The major activities are to examine the data sets using quantitative statistical and mathematical techniques to identify and resolve the characteristics of physical phenomena and processes in the data; use the ancillary data to identify possible causal mechanisms for the phenomena and processes; compile the frequency of occurrence of the identified phenomena and processes and statistical estimates of their associated properties (the climatology); and prioritize the phenomena and processes in terms of their importance to improving understanding, simulation, and prediction of slope and subsurface circulation.

Task 3 (Design Criteria of Field Study and Numerical Modeling): Professor Robert O. Reid of TAMU (PI) and Dr. Lakshmi Kantha of CU (Co-PI) are responsible for Task 3. The goal of this task is to develop optimal designs of mooring systems, to be located in the deepwater off Louisiana and in the northwest corner of the Gulf, for detection and quantification of the high priority phenomena and processes identified in Task 2.

Task 4 (Information/Data Synthesis and Technical Reports): Dr. Ann E. Jochens (PI) and Dr. Worth D. Nowlin, Jr. (Co-PI) of TAMU are responsible for Task 4. The goal of this task is to compile the results from Tasks 1, 2, and 3 into the final synthesis report.

2.3 Scientific Review Board

The Scientific Review Board (SRB) for the Deepwater Study is composed of three members from the oceanographic community. Table 2.3-1 shows the members and their affiliations. The purpose of the SRB is to review the progress and scientific value of the study and recommend improvements, provide advice on identification of data sources and plans for technical reports, and review and comment on the draft Synthesis Report. A meeting of the SRB was held 11-12 November 1998 in College Station, Texas, to review the plans for the study and obtain SRB advice. Throughout the study period, the SRB members provided significant assistance in assembly of data sets.

Table 2.3-1. Members of the Deepwater Study Scientific Review Board.

Member	Affiliation
Dr. Cortis K. Cooper	Chevron Petroleum Technology
Mr. Kenneth J. Schaudt	Marathon Oil Company
Dr. Robert L. Smith	College of Oceanic and Atmospheric Sciences Oregon State University

2.4 Report Organization

This is the final report of the Deepwater Study. The Executive Summary, Section 1, provides a brief review of the findings, results, and significance of this study. Descriptions of the data base assembled and the quality control processing methods used are given in Section 3. Sections 4 and 5 provide the overview of the general hydrography and large-scale circulation from both the literature and the results of this study. Classes of energetic current events are discussed in Section 6, and those identified in the data sets are inventoried. The climatology of processes and phenomena is given in Section 7. Section 8 presents the moored array design criteria. Section 9 gives the conclusions and recommendations. References are in Section 10.

3 DATA BASE AND METHODS

3.1 Data Types

The data assembled for the Deepwater Study fall into two categories: basic and ancillary. Basic data sets consist of the physical oceanographic data that are used in the analysis. Ancillary data are supplemental data used in the interpretations. Some of the basic data are proprietary, which means these data are used in this report only to the extent permitted by the data source; specific details from these records are not included. Except for proprietary data, basic data are included on the CD-ROM. Ancillary data are not.

Basic data are current measurements from moored or fixed single-point current meters, acoustic Doppler current profilers (ADCP), and expendable current profilers (XCP); hydrographic observations from bottles, salinity-temperature-depth (STD) and conductivity-temperature-depth (CTD) sensors, mechanical bathythermographs (MBT), and expendable bathythermographs (XBT); drifting buoy trajectories; and inverted echo sounder (IES) data. Current measurements include east-west and north-south velocity components, time series of temperature, salinity, and pressure when available, and percent good for ADCP data if available. Hydrographic observations include temperature, salinity or conductivity, and density or depth, with dissolved oxygen and nutrient data when available. Drifter data are latitude, longitude, date, and time. A limited number of the drifter data include sea surface temperature. IES data consist of time series of acoustic travel time and, when available, temperature and pressure. Data sets have metadata giving locations (latitude, longitude, depth), times, measurement units, and other information. Times are in Universal Coordinated Time (UTC), unless otherwise noted.

Ancillary data sets include meteorological, river discharge, coastal sea level, and satellite data. Two main types of satellite data were assembled: sea surface height (SSH) from satellite altimeter and sea surface temperature (SST) from Advanced Very High Resolution Radiometer (AVHRR) satellites. Additionally, output from a numerical circulation model run in hindcast mode for 1993 through 1999 were obtained for use in the analysis of the data and in development of design criteria for moored arrays.

3.2 Data Assembly

Data assembly commenced with the identification of possible sources of physical oceanographic data sets in the deepwater Gulf. Although the contract specified assembly of data north of 25°N in water depths of 300 m or more, on recommendation of the Deepwater Science Review Board and for database completeness, we sought Gulf-wide data in water depths of more than 200 m. Specific requests were made for known data sets. General requests for data were made to academic scientists, federal, state, and local agencies, consulting firms, petroleum industry representatives, and sources in Mexico. A substantial set of data was obtained through the National Oceanographic Data Center (NODC) of the National Oceanic and Atmospheric Administration (NOAA).

Locations of current and IES data sets are shown in Figure 3.2-1. Note that, except in the central Gulf, there are not many data sets in water depths of 1000 m or more and few stations are available south of 25°N. Names, sources, and general locations and dates of the current and IES data sets are given in Table 3.2-1; information on proprietary data are not included. Examination of the depths of the measurements indicates that most measurements were made in the upper 800 m. Efforts were made to obtain other known data sets, but they either were

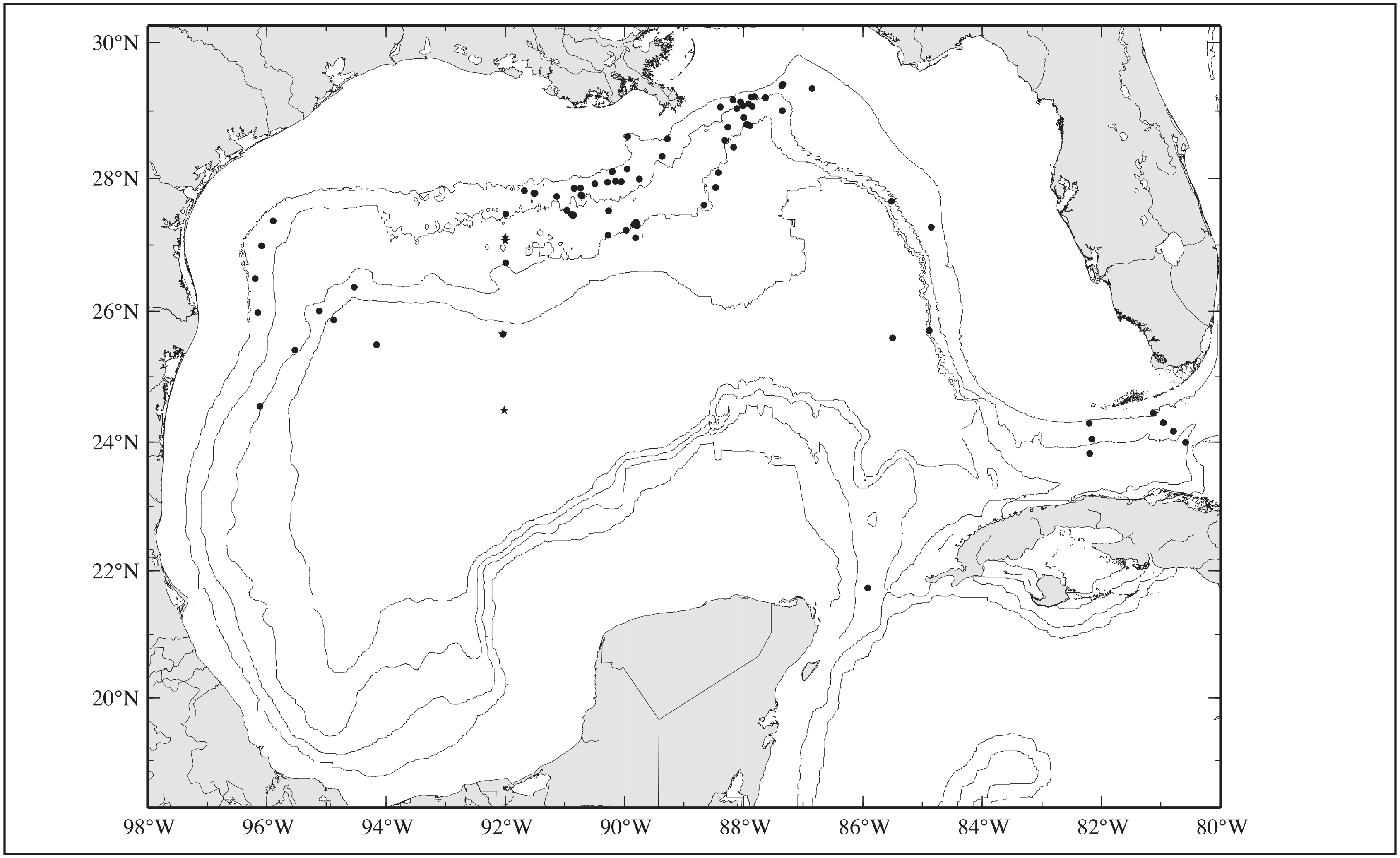

Figure 3.2-1. Locations of current (circles) and IES (stars) measurements in the deepwater Gulf of Mexico. Bathymetric contours shown are 200, 1000, 2000, and 3000 m.

Table 3.2-1. Current and IES measurements in the deepwater Gulf of Mexico. Start and end dates cover the period of any sampling at a site; not all instruments measured for the entire period. Instrument depths and locations are approximate because of multiple deployments in one location. Data are currents [C], temperature [T], salinity [S], and acoustic travel time [A]. Pressure was measured on few instruments (not shown). Instruments used were current meters (CM), acoustic Doppler current profilers (ADCP), and current profilers (CP). T on ADCP was usually limited to the top measurement. Selected major references using the data are indicated in the last column, which gives the key to the citations at the end of the table. Proprietary data sets are not included

Data Source	Name	Water Depth (m)	Nominal Instrument Depths (m) [ADCP bin size (m)]	Latitude (°N)	Longitude (°W)	Start Date	End Date	Data Types	Ref
NOAA-AOML	M1	1047	130, 215	29.0388	88.1130	07/17/1977	11/16/1977	CM: C	1
NOAA-AOML	M2	1050	94, 194, 994	29.1083	87.9187	07/17/1977	10/18/1977	CM: C	1
NOAA-AOML	M3	1047	90, 190, 985	29.1900	87.6367	10/18/1977	06/16/1978	CM: C	1
NOAA-AOML	M3	1033	70, 168, 970	29.1983	87.6383	06/17/1978	08/23/1978	CM: C	1
NOAA-AOML	T1	1050	150, 250, 550, 950	27.6633	85.5167	06/12/1978	06/26/1979	CM: C	1
TAMU-Brooks	N	730	200, 450, 700	26.9933	96.0933	07/17/1980	02/10/1981	CM: C	2, 3
TAMU-Brooks	C	730	200, 450, 575, 700	26.5000	96.1917	07/17/1980	02/11/1981	CM: C	2, 3
TAMU-Brooks	S	730	200, 450, 700	25.9900	96.1517	07/17/1980	02/09/1981	CM: C	2, 3
SAIC-5YR	A	1697	172, 400, 738, 1100, 1600	25.7150	84.8850	01/27/1983	02/01/1986	CM: C, T	4, 5, 6
SAIC-5YR	G	3200	177, 397, 703, 1565, 2364, 3174	25.6003	85.4995	02/03/1984	01/31/1986	CM: C	4, 5, 6
SAIC-5YR	P	2000	300, 1000, 1500	26.0117	95.1217	06/11/1985	05/04/1986	CM: C	4, 9
SAIC-5YR	Q	3000	100	25.8717	94.8800	06/15/1985	05/04/1986	CM: C	4, 9
SAIC-5YR	R	3500	100, 300, 750, 1000	25.4917	94.1600	06/15/1985	10/21/1985	CM: C	4, 9
SAIC-5YR	S	1503	100, 300, 750, 1000	25.4115	95.5300	06/12/1985	05/04/1986	CM: C	4, 9
SAIC-5YR	T	2200	100, 300, 1000	24.5532	96.1183	06/13/1985	05/02/1986	CM: C	4, 9
SAIC-5YR	EE	845	100, 300, 305, 725	27.4683	91.9932	04/05/1987	10/31/1988	CM: C	7, 8
SAIC-5YR	FF	1750	100, 300, 305, 725, 1650	26.7400	91.9950	04/06/1987	10/31/1988	CM: C	4, 7, 8
SAIC-5YR	GG	3000	100, 300, 305, 725, 1650, 2500	25.6532	92.0333	04/06/1987	10/30/1988	CM: C	4, 7, 8
SAIC-5YR	IES1	3000	2999	25.6567	92.0400	04/06/1987	10/30/1988	IES: A	8
TAMU-LATEX	M12	515	18, 105, 495	27.9240	90.4950	04/15/1992	12/07/1993	CM: C, T, S	10-14
TAMU-LATEX	M49	510	14, 102, 493	27.3690	95.8940	04/09/1992	12/06/1994	CM: C, T, S	10-14
TAMU-LATEX	M42	1540	1559	27.069	92.001	07/24/1992	07/23/1993	IES: T	17
TAMU-LATEX	M42	2220	2217	27.119	92.001	07/25/1993	07/25/1994	IES: A, T	17

Table 3.2-1. Current and IES measurements in the deepwater Gulf of Mexico (continued)

Data Source	Name	Water Depth (m)	Instrument Depths (m) [ADCP bin size (m)]	Latitude (°N)	Longitude (°W)	Start Date m/d/y	End Date m/d/y	Data Types	Ref
SAIC-EIS	A2	500	12-90 [4]	29.0592	88.3900	03/20/1997	07/09/1997	ADCP: C	18
SAIC-EIS	A2	500	200, 300, 490	29.0592	88.3900	03/21/1997	03/31/1999	CM: C	18
SAIC-EIS	A3	1300	8-80 [4]	28.7662	88.2650	03/20/1997	03/31/1999	ADCP: C	18
SAIC-EIS	A3	1300	500, 1310	28.7662	88.2650	03/20/1997	03/31/1999	CM: C	18
SAIC-EIS	B2	500	12-90 [4]	29.2120	87.8722	03/27/1997	04/01/1999	ADCP: C	18
SAIC-EIS	B2	500	200, 300, 490	29.2120	87.8722	03/28/1997	04/01/1999	CM: C	18
SAIC-EIS	B3	1300	12-80 [4]	29.0705	87.8568	03/22/1997	04/01/1999	ADCP: C	18
SAIC-EIS	B3	1300	500, 1290	29.0705	87.8568	03/22/1997	04/01/1999	CM: C	18
SAIC-EIS	C2	500	8-90, [4]	29.3712	87.3563	03/24/1997	04/02/1999	ADCP: C	18
SAIC-EIS	C2	500	200, 300, 490	29.3712	87.3563	03/24/1997	04/02/1999	CM: C	18
SAIC-EIS	C3	1300	8-80, [4]	29.0032	87.3532	03/24/1997	04/02/1999	ADCP: C	18
SAIC-EIS	C3	1300	500, 1290	29.0032	87.3532	03/24/1997	04/02/1999	CM: C	18
SAIC-EIS	D2	500	8-90, [4]	29.3348	86.8520	03/24/1997	04/03/1999	ADCP: C	18
SAIC-EIS	D2	500	200, 300, 490	29.3348	86.8520	03/24/1997	04/03/1999	CM: C	18
SAIC-MMS	I1	2001	12-1130 [4 or 8]	27.2933	89.7845	08/29/1999	08/26/2000	ADCP: C	
SAIC-MMS	I1	2001	800, 1000, 1200, 1400, 1600, 1800, 1989	27.2933	89.7845	08/29/1999	08/26/2000	CM: C	
SAIC-MMS	I2	1998	1600, 1800, 1989	27.2280	89.9710	08/29/1999	08/27/2000	CM: C	
SAIC-MMS	I3	2175	1775, 1975, 2164	27.1160	89.8138	08/29/1999	08/26/2000	CM: C	
TAMU-Burden	MC	300	250, 297	28.6190	89.9430	05/18/1998	11/12/1998	CM: C	15
TAMU-GERG	CHEMO	545	247, 537	27.7825	91.5047	08/08/1997	05/22/1998	CM: C, T	16
GERG-MAMES	C	430	20, 150, 426	29.3983	87.3450	12/30/1987	02/10/1990	CM: C, T, S	19
GERG-MAMES	E	430	20, 150, 426	29.1597	88.1753	02/15/1989	10/22/1989	CM: C, T, S	19
NOAA-Yucatan	YS	2040	1895	21.7333	85.9167	11/03/1977	10/19/1980	CM: C, T	20
SAIC-FL Straits	A1	245	75, 150	24.2948	82.2033	11/28/1990	08/17/1991	CM: C, T, S	21
SAIC-FL Straits	A2	820	145, 300, 600	24.0533	82.1617	02/17/1991	08/17/1991	CM: C, T	21
SAIC-FL Straits	A3	1500	145, 300, 600, 1000,1400	23.8283	82.1967	02/17/1991	08/17/1991	CM: C, T	21
SAIC-FL Straits	B1	200	75, 150	24.4517	81.1317	11/27/1990	08/16/1991	CM: C, T, S	21
SAIC-FL Straits	B2	320	75, 200	24.3017	80.9600	11/27/1990	08/19/1991	CM: C, T, S	21
SAIC-FL Straits	B3	850	30, 48, 66, 84, 102,120, 138, 156, 174, 192, 210, 228, 246, 273, 293, 300, 600, 805	24.1750	80.7933	11/26/1990	05/05/1991	CM: C, T	21

Table 3.2-1. Current and IES measurements in the deepwater Gulf of Mexico (continued)

Data Source	Name	Water Depth (m)	Instrument Depths (m) [ADCP bin size (m)]	Latitude (°N)	Longitude (°W)	Start Date	End Date	Data Types	Ref
SAIC-FL Straits	B4	1080	145, 300, 600, 1000	24.0000	80.5850	11/25/1990	05/06/1991	CM: C, T	21
Industry	GC137	350	38, 79, 107, 156, 306	27.8228	91.6808	12/16/1980	01/18/1981	CM: C, T	
Industry	GC184	435	35, 65, 100, 150, 400	27.7780	91.5213	01/19/1981	04/22/1981	CM: C, T	
Industry	GC110	489	10, 30, 50, 70, 90, 110, 130, 150, 170, 190, 213, 305	27.8533	90.8483	03/21/1984	07/04/1984	CP: C, T	
Industry	MC366	222	10, 30, 50, 70, 90, 110, 130, 150, 170	28.5883	89.2797	12/17/1984	12/26/1984	CP: C, T	
Industry	GC110	489	30, 61, 91, 121, 152, 182, 213, 243, 274, 304, 335, 365, 396	27.8566	90.8456	03/29/1989	03/29/1989	CP: C	
Industry	EW873A	236	20	28.1064	90.2020	06/30/1991	09/02/1991	CM: C	
Industry	EW873B	236	23-231, [8]	28.1064	90.2020	09/06/1991	09/13/1991	ADCP: C, T	
Industry	EW873C	236	23-231, [8]	28.1064	90.2020	09/20/1991	12/24/1991	ADCP: C, T	
Industry	EW1006	584	12-460, [8]	27.9576	90.1512	09/15/1993	12/08/1993	ADCP: C, T	
Industry	GC20094	895	23-463, [8]	27.7457	90.7310	02/12/1994	06/02/1994	ADCP: C, T	
Industry	EW873	236	23-223, [8]	28.1010	90.2021	05/21/1994	06/02/1994	ADCP: C, T	
Industry	GC20095	877	21-741, [8]	27.7569	90.7301	06/25/1995	07/16/1995	ADCP: C, T	
Industry	GC245	889	21-733, [8]	27.7369	90.7145	09/07/1995	11/13/1995	ADCP: C, T	
Industry	MC972	769	21-445, [8]	27.9953	89.7528	11/17/1995	12/18/1995	ADCP: C, T	
Industry	EW1008	1172	23-583, [8]	27.9567	90.0508	10/22/1997	12/15/1997	ADCP: C, T	
Industry	GC112A	536	23-535, [8]	27.8553	90.7348	12/28/1997	01/28/1998	ADCP: C, T	
Industry	GC112B	536	23-535, [8]	27.8553	90.7348	01/28/1998	02/26/1998	ADCP: C, T	
Industry	MC628	838	20-804, [16]	28.3323	89.3669	01/21/1997	07/03/1997	ADCP: C	
Industry	AT378	1843	20-772, [16]	27.6019	88.6663	07/11/1997	12/06/1997	ADCP: C	
Industry	GC236	674	20-628, [16]	27.7302	91.1419	04/09/1998	05/14/1998	ADCP: C	
Industry	AT118	2371	20-740, [16]	27.8655	88.4742	08/14/1998	12/03/1998	ADCP: C	

Table 3.2-1. Current and IES measurements in the deepwater Gulf of Mexico (continued)

References:

1 Molinari and Mayer 1982
2 Brooks 1983
3 Brooks 1984
4 Hamilton 1990
5 Science Applications International Corporation 1986
6 Science Applications International Corporation 1987
7 Hamilton 1992
8 Science Applications International Corporation 1989
9 Science Applications International Corporation 1988
10 Cho et al. 1998
11 Hamilton et al. 1999
12 DiMarco et al. 1997
13 Nowlin et al. 1998a and b
14 DiMarco and Reid 1998
15 Burden 1999
16 Guinasso 2000
17 Howard and DiMarco 1998
18 Hamilton et al. 2000
19 Brooks 1991
20 Maul et al. 1985
21 Lee et al. 1995

no longer available from the sources contacted (e.g., principal investigators and/or federal repositories) or the sources did not wish to release the data to the study, even on a proprietary basis. Time lines for current measurements are shown in Figure 3.2-2. These indicate that very few instruments sampled for periods of one year or more. Many proprietary data sets were of short duration (order of one month or less). Names, sources, and general locations and dates of shipboard ADCP data are given in Table 3.2-2.

Table 3.2-2. Shipboard ADCP measurements in the deep water Gulf of Mexico. Listed are those data sets that are included in the CD-ROM database.

Program	**Region**	**Dates**	**Data Source**
LATEX A – M02	NW Gulf shelf & slope	13–27 July 1992	TAMU
LATEX A – H03	NW Gulf shelf & slope	6–12 November 1992	TAMU
LATEX A – H04	NW Gulf shelf & slope	5–13 February 1993	TAMU
LATEX A – H05	NW Gulf shelf & slope	26 April – 11 May 1993	TAMU
LATEX A – H06	NW Gulf shelf & slope	26 July – 7 August 1993	TAMU
LATEX A – H07	NW Gulf shelf & slope	6–21 November 1993	TAMU
LATEX A – H08	NW Gulf shelf & slope	24 April – 7 May 1994	TAMU
LATEX A – H09	NW Gulf shelf & slope	27 July – 7 August 1994	TAMU
LATEX A – H10	NW Gulf shelf & slope	2–13 November 1994	TAMU
GULFCET II	west & central Gulf slope	11–27 October 1996	TAMUG/TAMU
GULFCET II	eastern Gulf slope	6–22 August 1997	TAMUG/TAMU
GOMOMS	central Gulf	19 April – 3 May 1998	TAMU/GERG
GOMOMS	eastern Gulf/Caribbean	7–29 October 1999	TAMU/GERG

Locations of all hydrographic stations are shown in Figures 3.2-3 (CTD data), 3.2-4 (bottle data, including temperature, salinity, dissolved oxygen, and nutrients; STD data), 3.2-5 (both air and ship deployed XBTs), and 3.2-6 (MBTs). Note: STD data were sub-sampled by NODC to simulate the discrete levels associated with bottle data. These figures show the relative sparseness of CTD data from the deepwater Gulf. Major sets of hydrographic observations are listed in Table 3.2-3 by vessel name, sampling dates, sources, and numbers of profiles taken. Data were grouped together according to ship name and dates in close sequential proximity to each other. The total number of profiles in water depths of more than 200 m by 1° squares is given in Figures 3.2-7 (CTD), 3.2-8 (bottles), 3.2-9 (XBTs), and 3.2-10 (MBTs). Examination of numbers of profiles by month reveals fewer data sets in the winter months. Although there are a large number of MBT profiles, they are of limited usefulness and must be used with caution because they are much less accurate and reliable than XBTs and most stop at 250 m or less, much shallower than the 500- to 1800-m depths of XBTs (Emery and Thomson 1997).

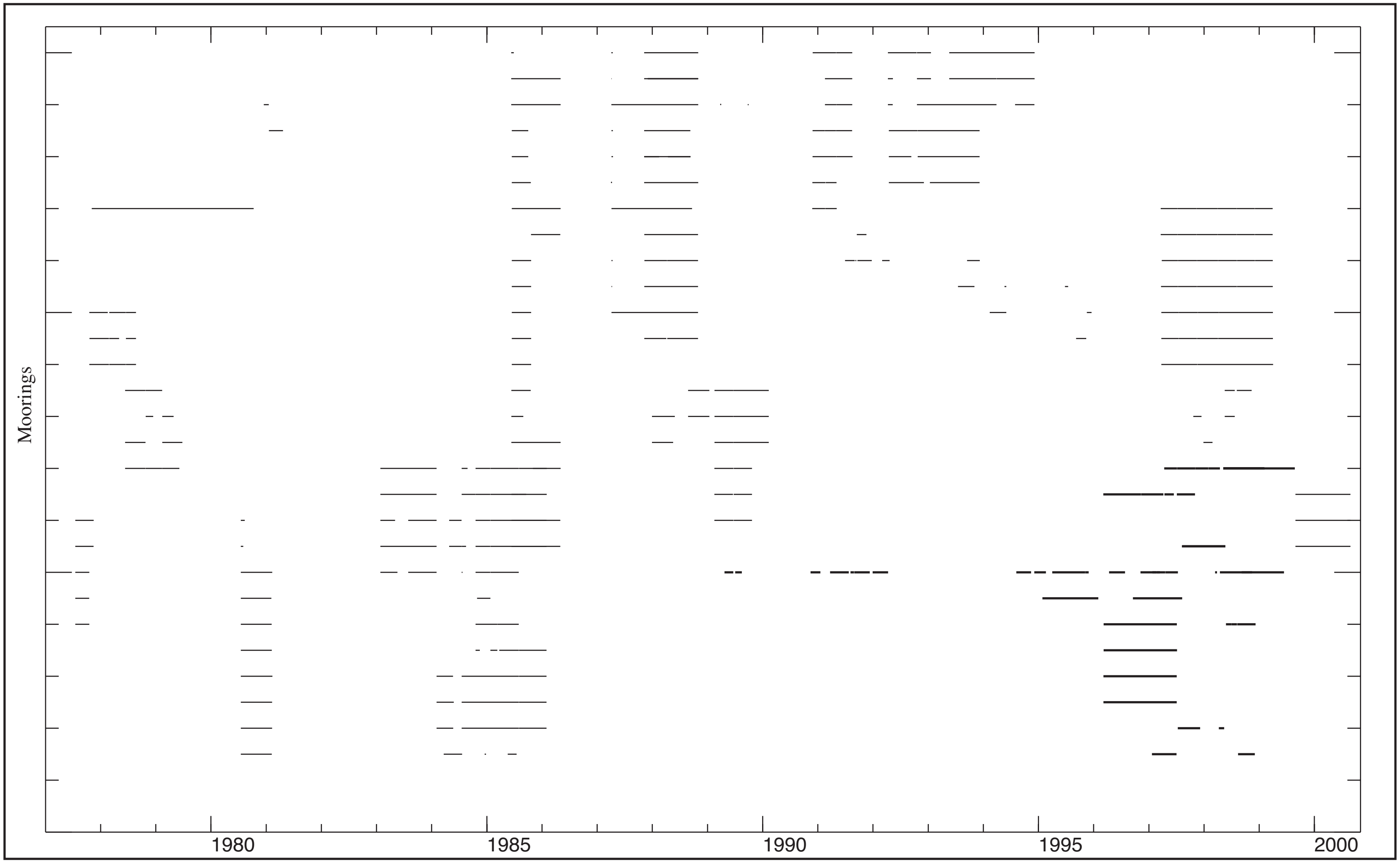

Figure 3.2-2. Composite of time lines for current measurements in the deepwater Gulf of Mexico. Time lines for current measurements at more than one location may be shown at the same level. See Section 6.3 for particular time lines of specific moorings. Heavy lines denote proprietary data sets.

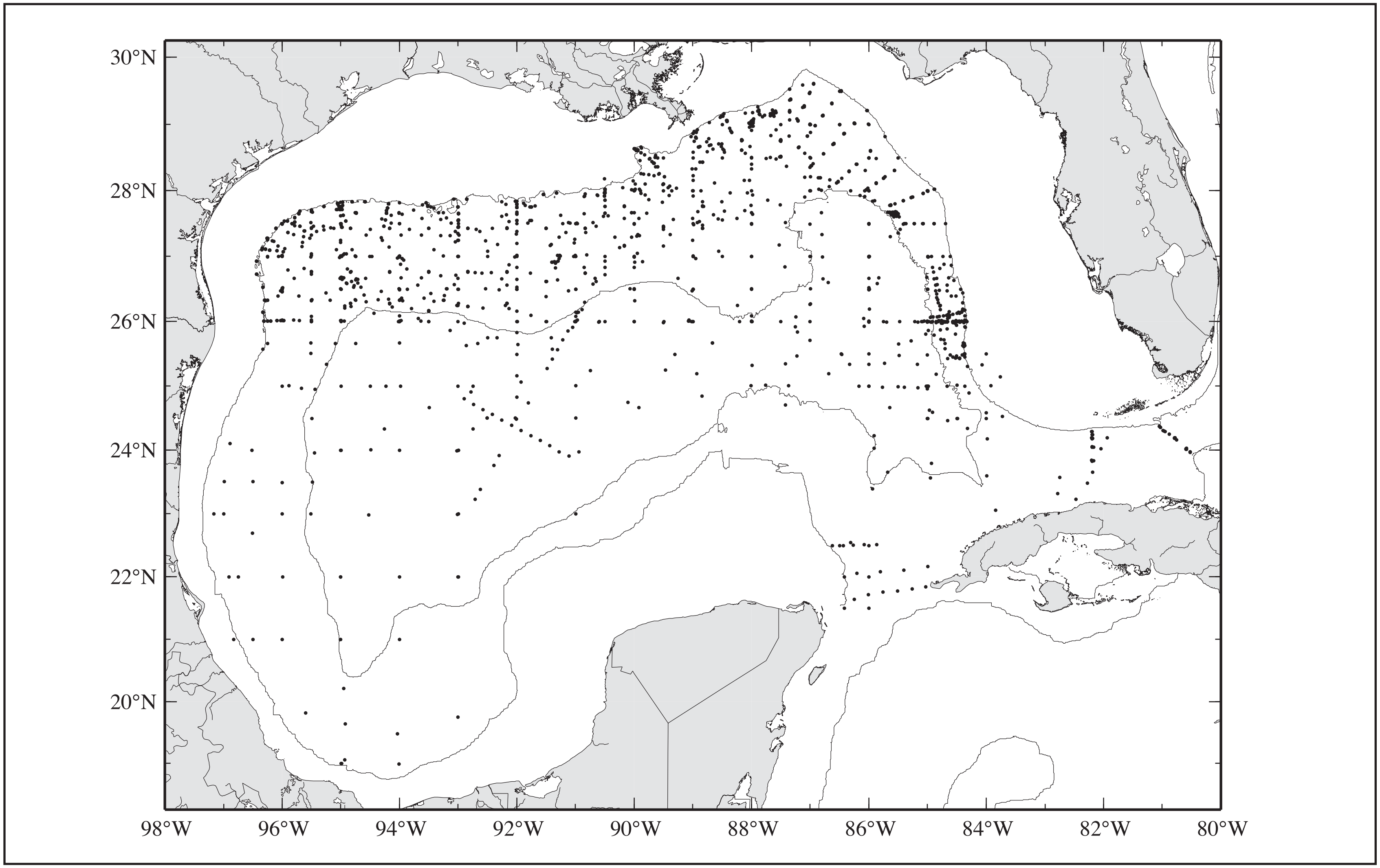

Figure 3.2-3. Locations of CTD stations in the deep water Gulf of Mexico. Bathymetric contours shown are 200 and 3000 m.

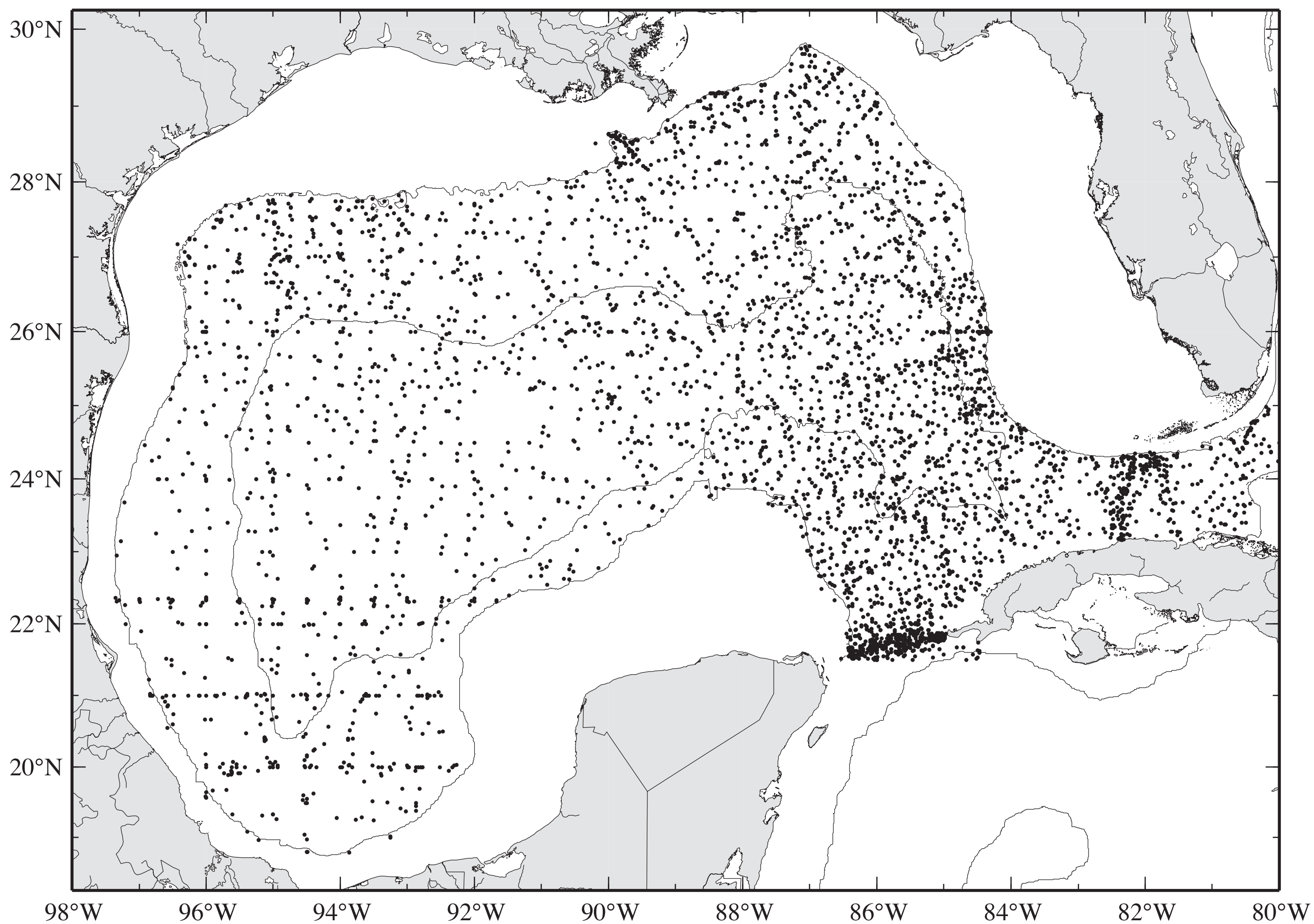

Figure 3.2-4. Locations of bottle and STD stations in the deepwater Gulf of Mexico. Bathymetric contours shown are 200 and 3000 m.

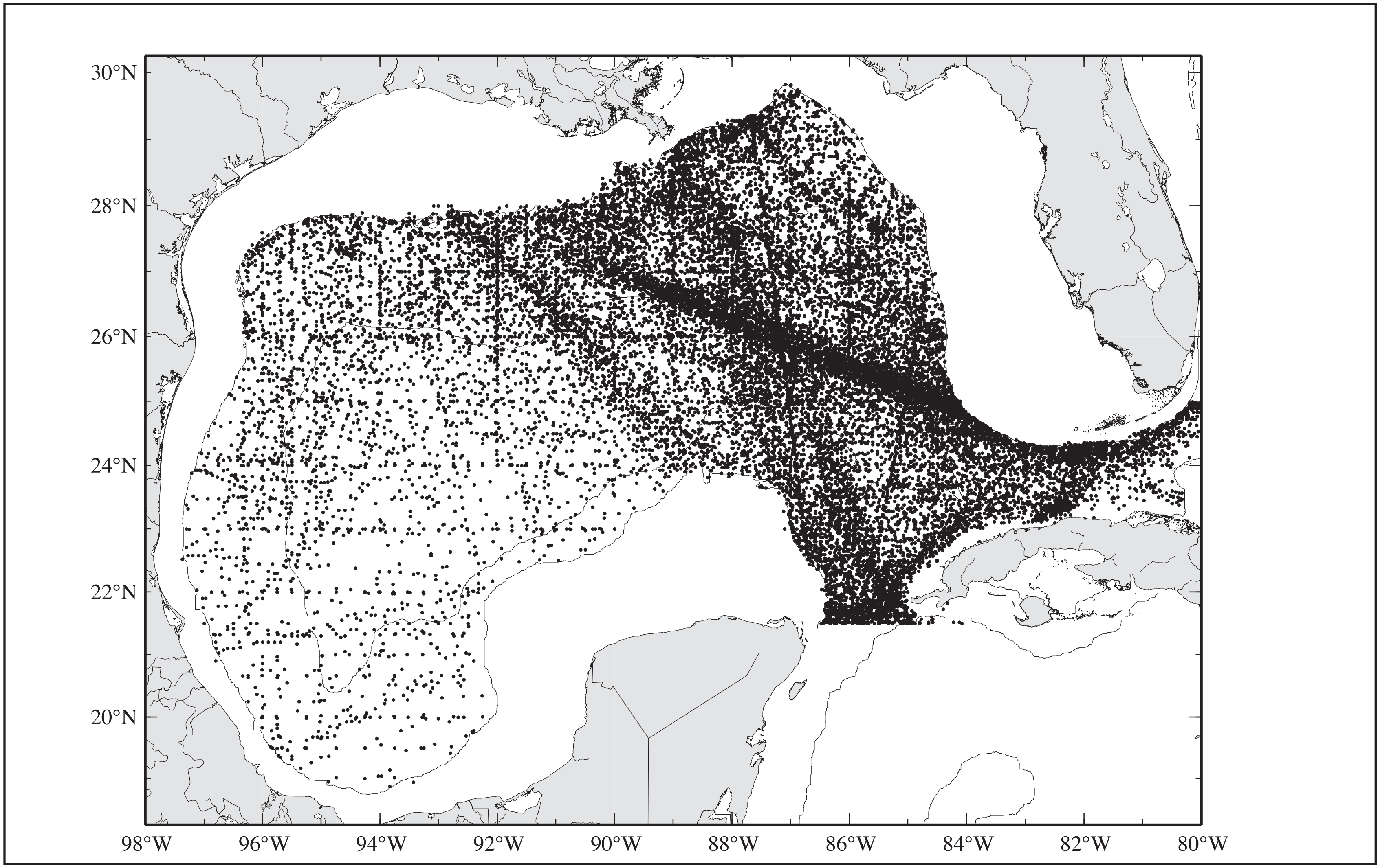

Figure 3.2-5. Locations of XBT stations in the deepwater Gulf of Mexico. Bathymetric contours shown are 200 and 3000 m.

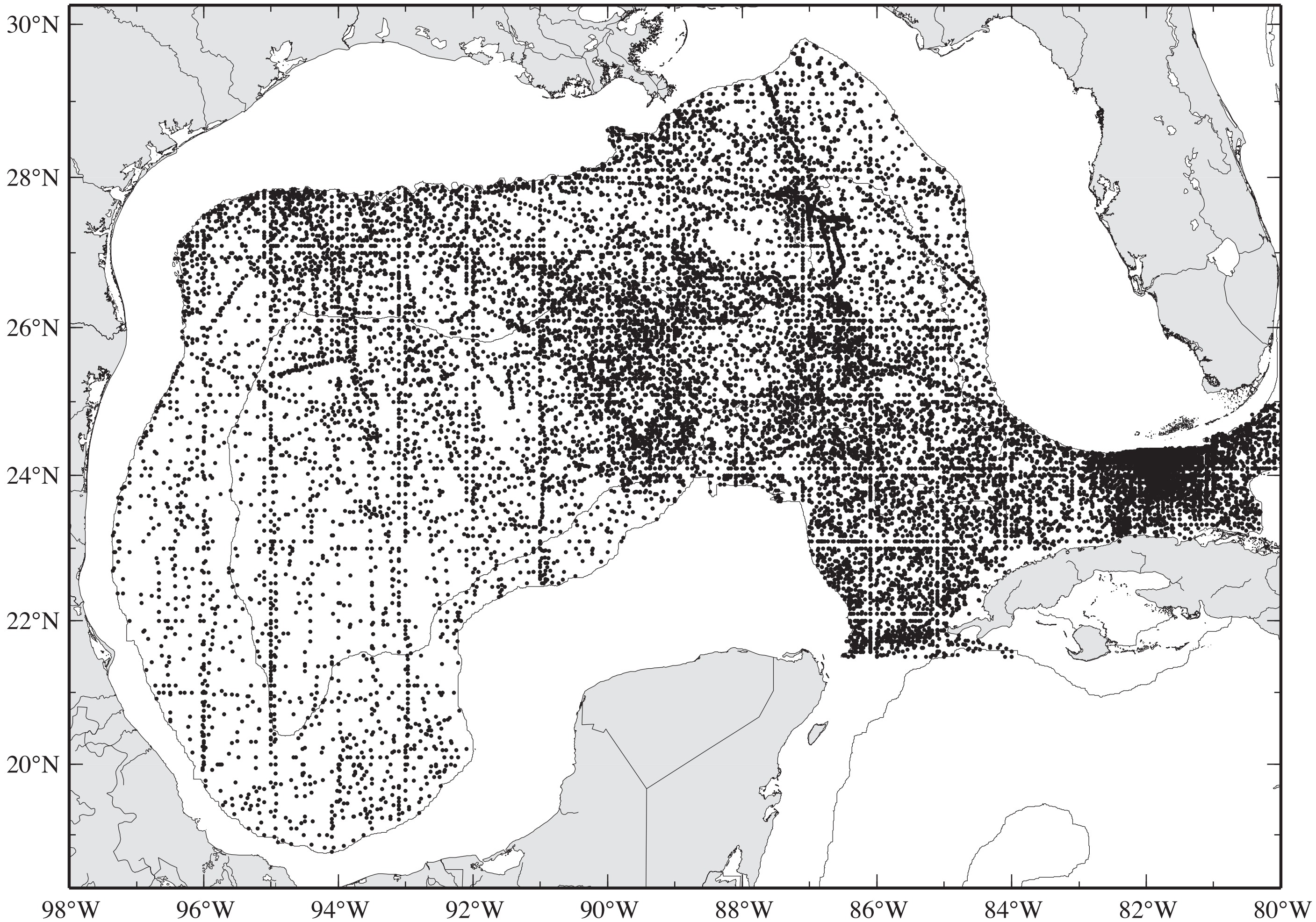

Figure 3.2-6. Locations of MBT stations in the deepwater Gulf of Mexico. Bathymetric contours shown are 200 and 3000 m.

Table 3.2-3. Major hydrographic data sets in the deepwater Gulf of Mexico. Shown are vessel name, cruise identifier, dates of the cruise, data types, number of stations, and data source. Data types are temperature (T), salinity/conductivity (S), oxygen (O), and nutrients (N); depth is available for all data types. Proprietary data sets are not included. Only stations in water depths of 200 m or more are included in the counts.

Vessel Name	Cruise ID	Start and end dates (mm/dd/yyyy)	Data types	No. of station	Data source
ACUSHNET	SAR-5-75	08/24/1975 – 09/20/1975	T, S	49	USCG
ACUSHNET	SAR-1-76	02/18/1976 – 03/18/1976	T, S	53	USCG
AKADEMIK, KOVALGVSKIY		11/03/1964 – 12/16/1964	T, S	04	ARI
AKADEMIK, KOVALGVSKIY		03/28/1965 – 05/31/1965	T, S, O	51	ARI
AKADEMIK, KNIPOVICH	CUBA V	07/13/1969 – 07/14/1969	T, S, O	04	FRC
AKADEMIK, KURCHATOV	14	04/03/1973 – 04/07/1973	T, S, O, N	04	IO
AKADEMIK, KOROLYOV	30	10/25/1981 – 10/26/1981	T, S	04	WDCB
ALAMINOS		12/07/1963 – 12/08/1963	T, S, O	04	NODC
ALAMINOS		01/17/1964 – 01/26/1964	T, S, O, N	19	NODC
ALAMINOS		02/27/1964 – 03/02/1964	T, S, O, N	08	NODC
ALAMINOS	64-1A-8	05/25/1964 – 05/27/1964	T, S	05	SUSIO
ALAMINOS	65-A-1	02/07/1965 – 02/07/1965	T, S, O	04	TAMU
ALAMINOS	65-A-2	02/27/1965 – 02/28/1965	T, S	04	SUSIO
ALAMINOS	65-A-7	05/18/1965 – 05/20/1965	T, S	05	SUSIO
ALAMINOS	65-A-11	08/11/1965 – 08/22/1965	T, S, O	30	TAMU
ALAMINOS	65-A-12	09/03/1965 – 09/06/1965	T, S	07	TAMU
ALAMINOS	65-A-13	09/12/1965 – 09/23/1965	T, S, O	58	TAMU
ALAMINOS		09/09/1967 – 09/13/1967	T, S, O, N	17	NODC
ALAMINOS	68-A-2	02/16/1968 – 03/06/1968	T, S, O	105	TAMU
ALAMINOS	68-A-5	04/22/1968 – 05/25/1968	T, S, O	72	SUSIO
ALAMINOS	68-A-8	08/18/1968 – 09/04/1968	T, S, O	78	TAMU
ALAMINOS	68-A-9	09/11/1968 – 09/15/1968	T, S, O	08	TAMU
ALAMINOS	69-A-7	05/01/1969 – 05/27/1969	T, S, O	120	SUSIO
ALAMINOS	69-A-8	06/08/1969 – 06/15/1969	T, S, O	10	TAMU
ALAMINOS	69-A-10	07/12/1969 – 07/29/1969	T, S, O, N	21	TAMU
ALAMINOS	69-A-12	09/09/1969 – 09/21/1969	T, S, O, N	52	SUSIO
ALAMINOS	70-A-3	02/05/1970 – 03/03/1970	T, S, O, N	04	SUSIO
ALAMINOS	70-A-6	04/03/1970 – 04/24/1970	T, S, O, N	62	TAMU
ALAMINOS	70-A-7	05/04/1970 – 05/11/1970	T, S, O, N	48	SUSIO
ALAMINOS	70-A-9	06/12/1970 – 06/22/1970	T, S	60	SUSIO
ALAMINOS	70-A-14	10/22/1970 – 11/02/1970	T, S, O, N	73	SUSIO
ALAMINOS	72-A-7	03/26/1972 – 03/29/1972	T, S, O	08	TAMU
ALAMINOS		04/29/1972 – 04/30/1972	T, S	08	NODC
ALAMINOS	72-A-9	05/02/1972 – 05/21/1972	T, S, O, N	53	TAMU
ALAMINOS	73-A-8	05/18/1973 – 06/03/1973	T, S, O, N	51	SUSIO
ALASKA	1-1A	04/22/1951 – 08/19/1951	T, S	67	TAMU
ALASKA	4-2A	01/09/1952 – 06/04/1952	T, S, N	66	TAMU
ALASKA	10-2B	02/24/1953 – 05/03/1953	T, S, N	27	TAMU
ALBATROSS		11/16/1919 – 11/24/1919	T, S	09	NODC
ALIOT	3232	01/28/1971 – 07/18/1971	T, S, O	35	CIO
ALTAIR	AL-8601	01/24/1986 – 02/03/1986	T, S, O, N	45	SAIC
ANTARES		01/15/1972 – 03/27/1972	T, S, O	21	NODC
ANTARES		05/11/1972 – 05/13/1972	T, S	09	NODC
ANTARES		10/04/1972 – 10/29/1972	T, S	17	NODC
ANTARES		01/16/1973 – 01/18/1973	T, S	08	NODC
ANTARES		02/25/1973 – 02/26/1973	T, S	05	NODC
ANTARES	95ANT	06/14/1995 – 06/17/1995	T, S	11	TAMU
ATLANTIS I		05/04/1933 – 05/05/1993	T, S, O	05	NODC
ATLANTIS I		03/01/1934 – 03/04/1934	T, S, O	11	NODC
ATLANTIS I		02/16/1935 – 04/13/1935	T, S, O	67	NODC
ATLANTIS I		03/21/1937 – 03/28/1937	T, S	17	NODC
ATLANTIS I		05/16/1939 – 04/19/1942	T, S	12	NODC
ATLANTIS I		01/26/1947 – 03/16/1947	T, S	22	NODC
BACHE		03/13/1914 – /0//1/1914	T, S	05	NODC
BELLOWS	B-7104A	08/24/1971 – 09/01/1971	T, S	12	SUSIO
BELLOWS	004	05/09/1972 – 05/18/1972	T, S	28	SUSIO
BELLOWS	007	08/21/1972 – 08/25/1972	T, S	15	SUSIO

Table 3.2-3. Major hydrographic data sets in the deepwater Gulf of Mexico. (continued)

Vessel name	Cruise ID	Start and end dates (mm/dd/yyyy)	Data types	No. of station	Data source
BELLOWS	011	09/29/1972 – 09/30/1972	T, S	06	SUSIO
BELLOWS	013	11/01/1972 – 11/05/1972	T, S	13	SUSIO
BELLOWS	015	12/07/1972 – 12/11/1972	T, S	13	SUSIO
BELLOWS	7306	05/03/1973 – 05/06/1973	T, S	04	SUSIO
BELLOWS	B-7312	06/04/1973 – 06/05/1973	T, S	04	SUSIO
BELLOWS	B-7313	07/06/1973 – 07/10/1973	T, S	13	SUSIO
BELLOWS	B-7315	08/11/1973 – 08/14/1973	T, S	25	SUSIO
BELLOWS	B-7320	10/23/1973 – 10/26/1973	T, S	04	SUSIO
BELLOWS	B-7321	11/16/1973 – 11/17/1973	T, S	08	SUSIO
BRAMAN, DAN	8C-7120	08/10/1971 – 08/11/1971	T, S	07	SUSIO
CAPE FLORIDA	CF8405	05/06/1984 – 05/17/1984	T, S, O, N	40	SAIC
CARYN		05/17/1956 – 05/18/1956	T, S, O	10	NODC
CHAIN		05/24/1962 – 05/27/1962	T, S, N	11	NODC
CORIOLIS		10/28/1973 – 11/01/1973	T, S	07	POI
DANA II		02/01/1922 – 02/06/1922	T, S, O	10	CCF
DROGUE	D-3-63	05/28/1963 – 05/30/1963	T, S	04	SUSIO
DROGUE	D-6-63	06/28/1963 – 07/01/1963	T, S	04	SUSIO
DROGUE	002	04/10/1964 – 04/11/1964	T, S	06	SUSIO
DROGUE	D-7-64	06/30/1964 – 07/02/1964	T, S	06	SUSIO
DROGUE	D-8-64	08/03/1964 – 08/06/1964	T, S	06	SUSIO
DROGUE	D-09-64	08/31/1964 – 09/03/1964	T, S	08	SUSIO
DROGUE	D-11-64	11/02/1964 – 11/03/1964	T, S	08	SUSIO
DROGUE	D-11C-64	12/15/1964 – 12/16/1964	T, S	05	SUSIO
DROGUE	65D2	03/03/1965 – 03/31/1965	T, S	11	SUSIO
DROGUE	004	04/05/1965 – 04/08/1965	T, S	12	SUSIO
DROGUE	5	05/10/1965 – 05/11/1965	T, S	05	SUSIO
DROGUE	6-65	05/19/1965 – 06/25/1965	T, S	26	SUSIO
DROGUE	D-11-65	07/21/1965 – 07/21/1965	T, S	11	SUSIO
DROGUE	D-12-65	08/16/1965 – 08/25/1965	T, S	31	SUSIO
DROGUE	D-13-65	09/14/1965 – 09/14/1965	T, S	07	SUSIO
DROGUE	D-14-65	09/17/1965 – 09/17/1965	T, S	07	SUSIO
DROGUE	D-15-65	10/12/1965 – 10/14/1965	T, S	20	SUSIO
DROGUE	D-16-65	10/26/1965 – 10/27/1965	T, S	17	SUSIO
DROGUE	D-17-65	11/15/1965 – 11/16/1965	T, S	18	SUSIO
DROGUE	D-18-65	11/19/1965 – 11/19/1965	T, S	12	SUSIO
DROGUE	D-19-65	12/13/1965 – 12/16/1965	T, S	17	SUSIO
EASTWARD	E-19	03/08/1971 – 03/10/1971	T, S	5	DUKE
EXPLORER		03/30/1960 – 04/08/1960	T, S	12	NODC
FOTON (SRT-M-8024)	3314	10/05/1971 – 10/05/1971	T, S, O, N	6	CIO
FOTON (SRT-M-8024)	3315	11/04/1971 – 11/05/1971	T, S, O	6	CIO
FOTON (SRT-M-8024)	3239	11/06/1971 – 11/06/1971	T, S	4	CIO
FOTON (SRT-M-8024)	3316	11/24/1971 – 11/24/1971	T, S	6	CIO
GERDA		10/20/1957 – 08/07/1960	T, S, O, N	44	NODC
GERDA	6110	03/01/1961 – 11/20/1961	T, S, O, N	20	MIAMI
GERDA		04/24/1962 – 06/14/1962	T, S, O, N	19	NODC
GERDA	6405	03/27/1964 – 12/21/1964	T, S	9	MIAMI
GERDA	6506	01/29/1965 – 12/16/1965	T, S	11	MIAMI
GERDA	G-7027	10/02/1970 – 10/03/1970	T, S	15	MIAMI
GERDA	008	05/05/1972 – 05/08/1972	T, S	4	SUSIO
GERONIMO	6	11/01/1965 – 11/02/1965	T, S, O, N	6	NMFS-M
GERONIMO	GO-12	02/22/1967 – 03/31/1967	T, S	87	NMFS-G
GERONIMO	GO-16	08/18/1967 – 10/07/1967	T, S	113	NODC
GILLISS		04/01/1964 – 10/08/1964	T, S	33	NODC
GILLISS	7303	02/25/1973 – 03/11/1973	T, S	52	MIAMI
GILLISS	MIA	06/05/1973 – 06/14/1973	T, S	55	MIAMI
GIRON II	CUBA I	08/01/1966 – 08/01/1966	T, S	4	FRC
GOSNOLD	152	11/24/1969 – 12/13/1969	T, S	20	WHOI
GYRE	I	04/02/1982 – 04/07/1982	T, S, O, N	34	WCC
GYRE	87G03	04/02/1987 – 04/04/1987	T, S	5	TAMU
GYRE	87G04	04/12/1987 – 04/16/1987	T, S, O, N	12	TAMU
GYRE	87G10	10/27/1987 – 10/28/1987	T, S, O, N	4	TAMU
GYRE	87G11	11/18/1987 – 11/23/1987	T, S, O, N	12	TAMU

Table 3.2-3. Major hydrographic data sets in the deepwater Gulf of Mexico. (continued)

Vessel name	Cruise ID	Start and end dates (mm/dd/yyyy)	Data types	No. of station	Data source
GYRE	87G12	11/29/1987 – 12/29/1987	T, S, O, N	11	TAMU
GYRE	88G05	10/15/1988 – 10/17/1988	T, S, O, N	51	TAMU
GYRE	89G06	05/17/1989 – 05/24/1989	T, S	22	TAMU
GYRE	89G15	11/13/1989 – 11/17/1989	T, S	21	TAMU
GYRE	90G04	02/19/1990 – 02/23/1990	T, S	15	TAMU
GYRE	90G05	02/27/1990 – 02/28/1990	T, S	9	TAMU
GYRE	91G02	03/04/1990 – 03/09/1990	T, S, O, N	11	TAMU
GYRE	90G10	07/11/1990 – 07/15/1990	T, S, O, N	27	TAMU
GYRE	90G14	10/01/1990 – 10/15/1990	T, S	35	TAMU
GYRE	90G15	10/13/1990 – 10/15/1990	T, S	9	TAMU
GYRE	91G02	03/02/1991 – 03/09/1991	T, S	36	TAMU
GYRE	91G04	06/15/1991 – 06/15/1991	T, S, O, N	25	TAMU
GYRE	92G01	01/08/1992 – 01/29/1992	T, S, O, N	26	TAMU
GYRE	92G03	03/16/1992 – 03/20/1992	T, S	37	TAMU
GYRE	92G04	04/01/1992 – 04/09/1992	T, S	23	TAMU
GYRE	92G05	05/01/1992 – 05/08/1992	T, S	17	TAMU
GYRE	92G07	06/21/1992 – 06/25/1992	T, S	29	TAMU
GYRE	92G08	08/01/1992 – 08/07/1992	T, S	21	TAMU
GYRE	92G09	09/26/1992 – 09/27/1992	T, S	8	TAMU
GYRE	92G10	10/02/1992 – 10/04/1992	T, S	11	TAMU
GYRE	92G13	10/04/1992 – 10/31/1992	T, S	46	TAMU
GYRE		01/08/1993 – 01/14/1993	T, S	54	TAMU
GYRE	93G02	02/06/1993 – 02/12/1993	T, S	22	TAMU
GYRE	93G10	09/10/1993 – 09/16/1993	T, S	5	TAMU
GYRE	93G11	09/25/1993 – 10/06/1993	T, S	7	TAMU
GYRE	93G12	10/28/1993 – 11/03/1993	T, S	17	TAMU
GYRE	94G01	04/24/1994 – 05/07/1994	T, S	55	TAMU
GYRE	94G05	07/18/1994 – 07/20/1994	T, S	17	TAMU
GYRE	94G07	08/10/1994 – 08/20/1994	T, S	34	TAMU
GYRE	94G08	10/19/1994 – 10/24/1994	T, S	126	TAMU
GYRE	94G09	11/02/1994 – 11/13/1994	T, S	54	TAMU
GYRE	95G03	06/13/1995 – 06/16/1995	T, S, O, N	11	TAMU
GYRE	96G06	10/12/1996 – 10/27/1996	T, S, O	8	TAMU
GYRE	97G08	08/07/1997 – 08/21/1997	T, S, O	10	TAMU
GYRE	97G14	11/16/1997 – 11/26/1997	T, S	48	TAMU
GYRE	98G05	05/05/1998 – 05/15/1998	T, S	48	TAMU
GYRE	98G10	07/26/1998 – 08/06/1998	T, S	43	TAMU
GYRE	98G15	11/13/1998 – 11/24/1998	T, S	46	TAMU
HAMILTON	HT1	02/18/1971 – 03/04/1971	T, S	6	USCG
HIDALGO		03/27/1958 – 02/26/1959	T, S, O	20	NODC
HIDALGO	59-H-12	10/24/1959 – 11/04/1959	T, S	19	TAMU
HIDALGO	60-H-3	02/17/1960 – 02/27/1960	T, S	4	TAMU
HIDALGO	60-H-6	05/19/1960 – 05/28/1960	T, S	16	TAMU
HIDALGO	61-H-6	03/23/1961 – 04/07/1961	T, S, O	7	TAMU
HIDALGO	61-H-9	05/23/1961 – 06/06/1961	T, S, O	16	TAMU
HIDALGO	61-H-16	10/15/1961 – 10/17/1961	T, S, O	5	TAMU
HIDALGO	61-H-18	10/20/1961 – 11/02/1961	T, S	16	SUSIO
HIDALGO	61-H-19	11/11/1961 – 11/13/1961	T, S, O	5	TAMU
HIDALGO	62-H-1	01/17/1962 – 01/19/1962	T, S, O	5	TAMU
HIDALGO	62-H-3	02/14/1962 – 03/31/1962	T, S, O	90	NODC
HIDALGO	62-H-4	05/12/1962 – 05/25/1962	T, S, O	10	TAMU
HIDALGO	62-H-15	10/31/1962 – 11/12/1962	T, S	6	SUSIO
HYDROGRAPHER		10/23/1953 – 06/26/1962	T, S	39	NODC
ISELIN COLUMBUS	7304	02/02/1973 – 02/13/1973	T, S	22	MIAMI
ISELIN COLUMBUS	7311	07/02/1973 – 07/04/1973	T, S	6	SUSIO
ISELIN COLUMBUS	7318	10/14/1973 – 10/18/1973	T, S	17	MIAMI
ISELIN COLUMBUS	7319	10/30/1973 – 11/04/1973	T, S	6	MIAMI
ISELIN COLUMBUS	7320	11/08/1973 – 11/11/1973	T, S	5	SUSIO
ISELIN COLUMBUS	7321	11/27/1973 – 12/08/1973	T, S	23	MIAMI
ISLAND WATERS	001	05/04/1970 – 05/13/1970	T, S	21	SUSIO
ISLAND WATERS	7004B	06/12/1970 – 06/24/1970	T, S	90	SUSIO
JUSTO SIERRA	JS085	03/05/1985 – 03/23/1985	T, S, O	28	SIO

Table 3.2-3. Major hydrographic data sets in the deepwater Gulf of Mexico. (continued)

Vessel name	Cruise ID	Start and end dates (mm/dd/yyyy)	Data types	No. of station	Data source
KANE	939014	06/10/1969 – 09/09/1969	T, S, O	148	NOO
KANE	003	09/28/1969 – 11/30/1969	T, S, N	13	NOO
LYNCH		06/22/1966 – 09/09/1967	T, S	12	NODC
MALCOLM BALDRIDGE	RP9RE-71	08/27/1971 – 09/01/1971	T, S	33	AOML
MALCOLM BALDRIDGE	1176	10/08/1976 – 11/14/1976	T, S	68	AOML
MALCOLM BALDRIDGE		07/13/1977 – 07/23/1977	T, S	19	AOML
MALCOLM BALDRIDGE	1777	10/19/1977 – 10/30/1977	T, S	22	AOML
MIKHAIL LONOMOSON	20	02/21/1967 – 03/04/1967	T, S, O, N	4	ARI
MT MITCHELL		05/05/1989 – 08/06/1991	T, S	43	NODC
OLENTY		02/24/1964 – 03/17/1964	T, S, O, N	11	NODC
OREGON II	0-7129	08/10/1971 – 08/27/1971	T, S	36	SUSIO
OREGON II	039	08/02/1972 – 08/07/1972	T, S	8	SUSIO
OREGON II	199	04/22/1992 – 05/23/1992	T, S, O	204	TAMU
OREGON II	203	01/06/1993 – 02/11/1993	T, S, O	174	TAMU
OREGON II	220L3	05/31/1996 – 06/08/1996	T, S	4	TAMU
PELICAN	8502	10/22/1985 – 10/25/1985	T, S	19	SAIC
PELICAN	87-13	04/07/1987 – 04/09/1987	T, S	17	SAIC
PELICAN	Cruise 2	08/11/1992 – 08/23/1992	T, S, O	75	TAMU
PELICAN	Cruise 3	11/10/1992 – 11/10/1992	T, S, O	76	TAMU
PELICAN	Cruise 4	02/12/1993 – 02/24/1993	T, S, O	73	TAMU
PELICAN	Cruise 5	05/25/1993 – 05/28/1993	T, S, O	75	TAMU
PELICAN	Cruise 6	08/28/1993 – 09/05/1993	T, S, O	63	TAMU
PELICAN	Cruise 7	12/05/1993 – 12/12/1993	T, S, O	55	TAMU
PETO	CUBA III	02/18/1967 – 02/18/1967	T, S, O	4	FRC
PILLSBURY, J.E.	P-6803	04/11/1968 – 04/27/1968	T, S, O, N	13	MIAMI
PILLSBURY, J.E.	004	04/12/1969 – 05/11/1970	T, S	33	MIAMI
POWELL, J.W.	91P03	06/10/1991 – 06/13/1994	T, S	6	TAMU
POWELL, J.W.	92P10	11/05/1992 – 11/12/1992	T, S	18	TAMU
POWELL, J.W.	93P06	04/28/1993 – 05/11/1993	T, S	45	TAMU
POWELL, J.W.	93P11	07/28/1993 – 08/06/1993	T, S	42	TAMU
POWELL, J.W.	93P14	11/10/1993 – 11/21/1993	T, S	45	TAMU
POWELL, J.W.	94P10	07/27/1994 – 08/07/1994	T, S	56	TAMU
REHOBOTH	7	12/03/1950 – 12/09/1950	T, S, O	13	NOO
SAN PABLO	7	12/02/1950 – 12/09/1950	T, S, O	14	NOO
SAN PABLO		02/22/1968 – 05/28/1968	T, S	8	NODC
SARDINA	CUBA IV	06/29/1968 – 06/29/1968	T, S, O	4	FRC
SEAWARD EXPLORER	9103	02/17/1991 – 02/22/1991	T, S	7	SAIC
SEAWARD EXPLORER	9112	05/03/1991 – 05/08/1991	T, S	9	SAIC
SEAWARD EXPLORER	9117	08/18/1991 – 08/21/1991	T, S	10	SAIC
SEAWARD EXPLORER	9120	11/12/1991 – 11/13/1991	T, S	5	SAIC
SRT-M8030	CUBA VI	03/13/1970 – 04/05/1970	T, S	5	FRC
SRT-R9029	CUBA I	08/12/1966 – 10/14/1969	T, S, O, N	59	FRC
STAGE TIDE	ST-1-65	08/21/1965 – 08/21/1965	T, S	6	SUSIO
SUN COASTER	II	09/14/1982 – 09/18/1982	T, S	6	WCC
SUN COASTER	GM01	03/09/1983 – 03/20/1983	T, S, O, N	35	SAIC
SUN COASTER	SC8310	11/12/1983 – 11/19/1983	T, S, O, N	44	SAIC
TAYLOR, MABEL		01/26/1932 – 04/27/1932	T, S	60	
TRIDENT	68	04/19/1969 – 04/24/1969	T, S, O	14	URI
TRIDENT	127	12/01/1972 – 12/11/1972	T, S	22	URI
TURSIOPS	T7015	05/02/1970 – 05/11/1970	T, S, O	17	FSU
TURSIOPS	7020	10/24/1970 – 11/01/1970	T, S	17	SUSIO
TURSIOPS	TI-7121	08/17/1971 – 08/24/1971	T, S	19	SUSIO
TURSIOPS	11	05/15/1972 – 05/18/1972	T, S, N	10	FSU
UNDAUNTED		06/02/1966 – 06/06/1966	T, S, O, N	16	NODC
VIRGILIO URIBE	C12	10/31/1970 – 11/13/1970	T, S, O	39	NODC
VIRGILIO URIBE	VU/71-02	01/18/1971 – 01/21/1971	T, S, O	7	NIO
VIRGILIO URIBE	VU/71/08	04/28/1971 – 05/09/1971	T, S, O	19	NIO
VIRGILIO URIBE	711	05/24/1971 – 06/09/1971	T, S, O	40	UN
VIRGILIO URIBE	VU/71-14	07/21/1971 – 07/28/1971	T, S, O	20	NIO
VIRGILIO URIBE	712	08/04/1971 – 09/03/1971	T, S, O	44	UN
VIRGILIO URIBE	VU/71-20	10/10/1971 – 10/17/1971	T, S, O	20	NIO
VIRGILIO URIBE	713	10/27/1971 – 11/10/1971	T, S, O	39	UN

Table 3.2-3. Major hydrographic data sets in the deepwater Gulf of Mexico. (continued)

Vessel name	Cruise ID	Start and end dates (mm/dd/yyyy)	Data types	No. of station	Data source
VIRGILIO URIBE	VU/72/02	01/11/1972 – 01/19/1972	T, S, O	21	NIO
VIRGILIO URIBE	721	04/25/1972 – 05/19/1972	T, S, O	40	UN
VIRGILIO URIBE	VU	05/23/1973 – 06/05/1973	T, S, O	27	UN
VIRGINIA KEY	009	04/27/1973 – 04/29/1973	T, S	14	SUSIO
VIRGINIA KEY		06/02/1973 – 06/04/1973	T, S	14	SUSIO
VIRGINIA KEY	016	07/07/1973 – 07/09/1973	T, S	14	SUSIO
VIRGINIA KEY	021	08/12/1973 – 08/15/1973	T, S	12	SUSIO
VIRGINIA KEY	027	09/18/1973 – 09/20/1973	T, S	12	SUSIO
VIRGINIA KEY	7806	06/12/1978 – 06/15/1978	T, S	5	AOML
VIRGINIA KEY	7808	08/19/1978 – 08/23/1978	T, S	15	AOML
VIRGINIA KEY	7810	10/26/1978 – 11/02/1978	T, S	13	AOML
VIRGINIA KEY	1278	12/18/1978 – 12/19/1978	T, S	12	AOML
VIRGINIA KEY		02/14/1979 – 05/20/1979	T, S	65	AOML
WHITING		06/20/1989 – 11/10/1989	T, S	15	NOS
WHITING	535	07/27/1990 – 11/20/1990	T, S	16	NOS

Key to Data Sources:
AOML: NOAA, Atlantic Oceanographic and Meteorological Laboratories
ARI: Atlantic Research Institute of Fishing Econ. and Ocean. (ATLATNIRO)
CCF: Collection, Carlsberg Foundation, Charlottenlund, Denmark
CIO: Cuban Institute of Technological Investigations, Havana
DUKE: Duke University
FRC: Fisheries Research Center, Havana
FSU: Florida State University
IO: Institute of Oceanology, AS USSR, Moscow
MIAMI: Rosenstiel School of Marine and Atmospheric Science, University of Miami
NIO: National Institute of Fisheries, Mexico
NMFS-M: NOAA, National Marine Fisheries Service, Miami, FL
NMFS-G: NOAA, National Marine Fisheries Service, Galveston, TX
NODC: NOAA, National Oceanographic Data Center
NOO: U.S. Naval Oceanographic Office, Bay St. Louis, MS
NOS: NOAA, National Ocean Service, Norfolk, VA
POI: Pacific Oceanological Institute (VLADIVOSTOK)
SAIC: Science Applications International Corporation
SIO: Scripps Institute of Oceanography
SUSIO: State University System of Florida, Institute of Oceanography, St. Petersburg, FL
TAMU: Texas A&M University
UN: University National of Mexico, Institute of Geophysics, Mexico City
URI: University of Rhode Island
USCG: U.S. Coast Guard
WCC: Woodward-Clyde Consultants
WDCB: World Data Center B
WHOI: Woods Hole Oceanographic Institution

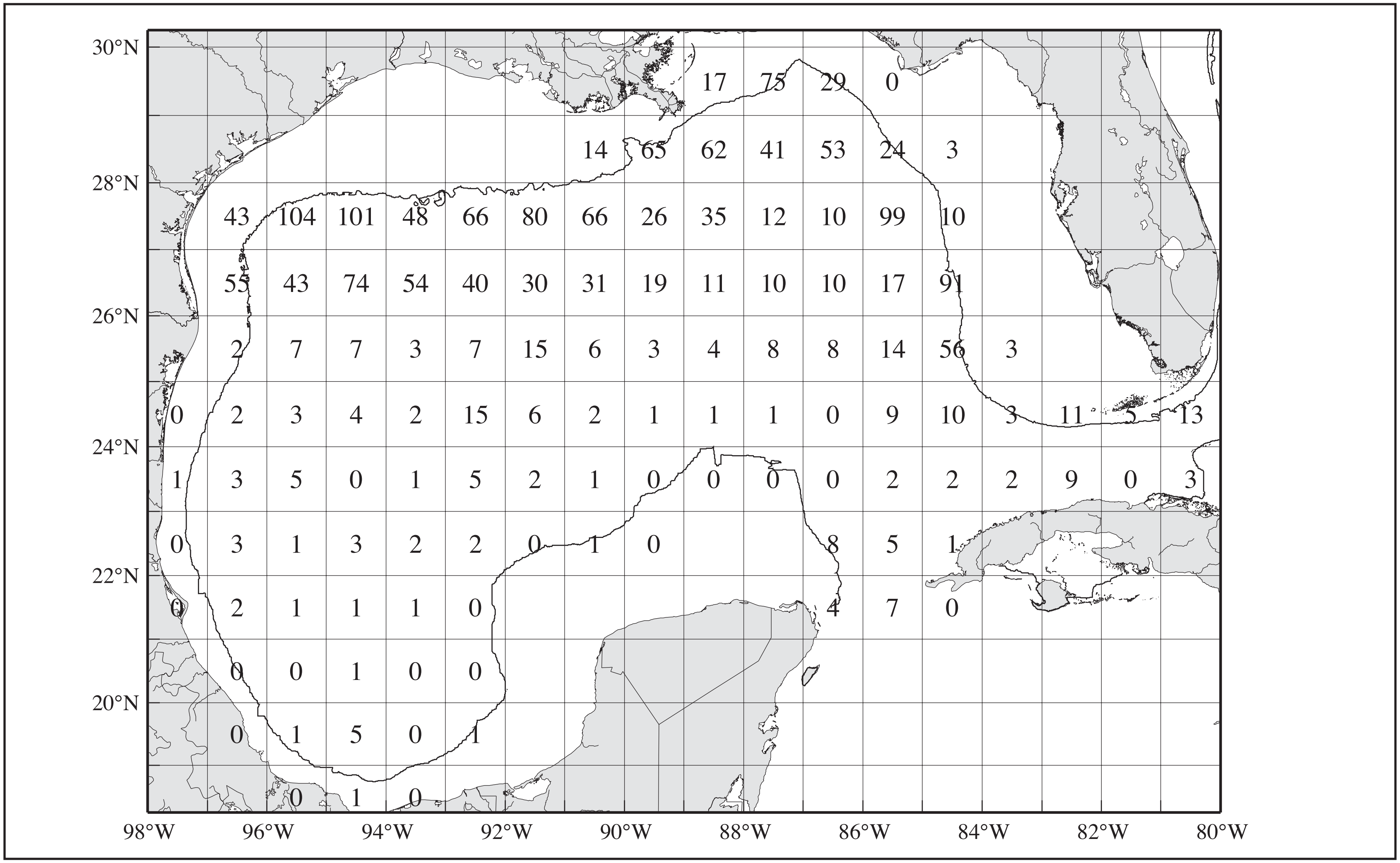

Figure 3.2-7. Number of CTD stations in water depths of 200 m or more by 1° squares in the Gulf of Mexico. The 200-m isobath is shown.

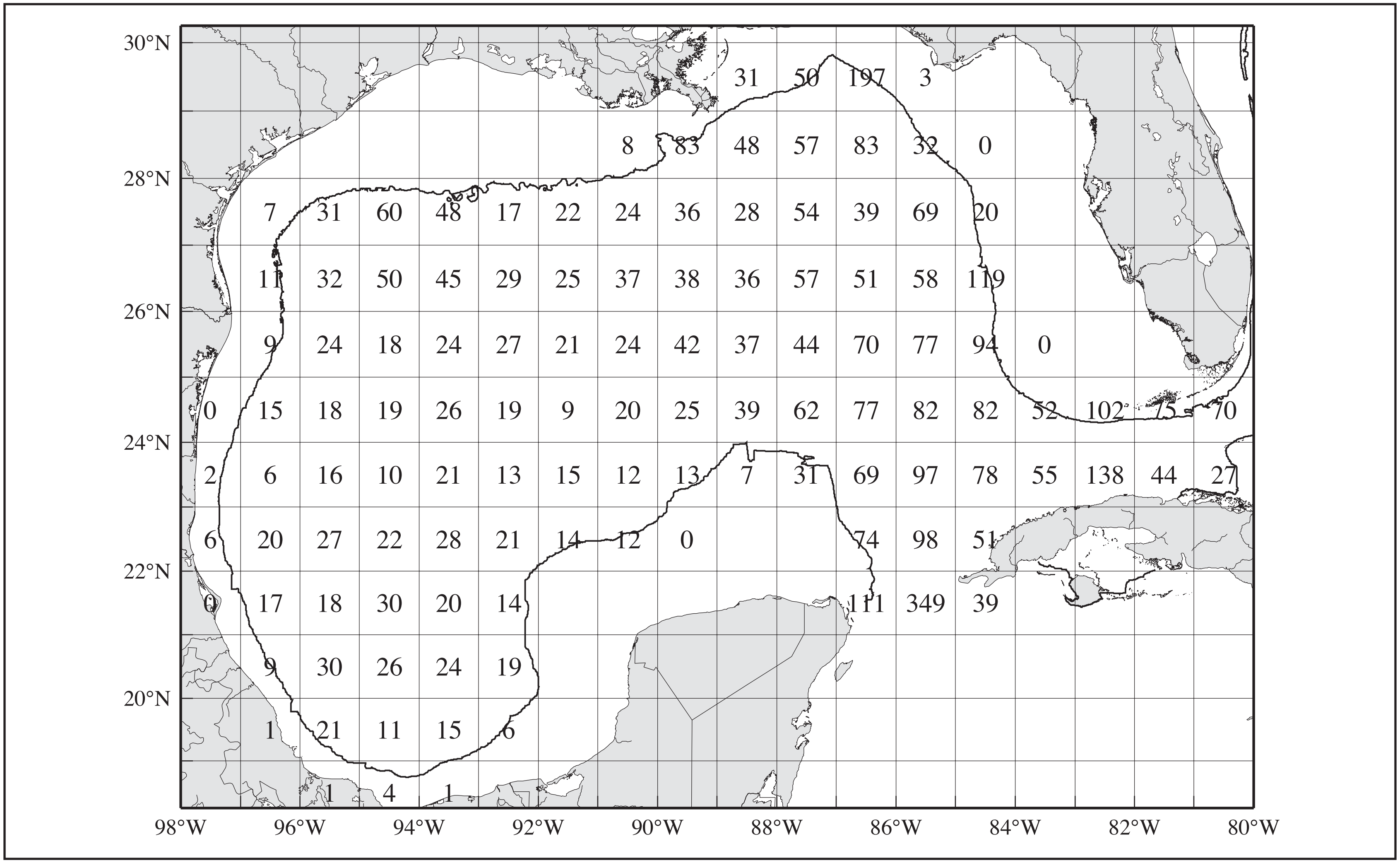

Figure 3.2-8. Number of bottle stations in water depths of 200 m or more by 1° squares in the Gulf of Mexico. The 200-m isobath is shown.

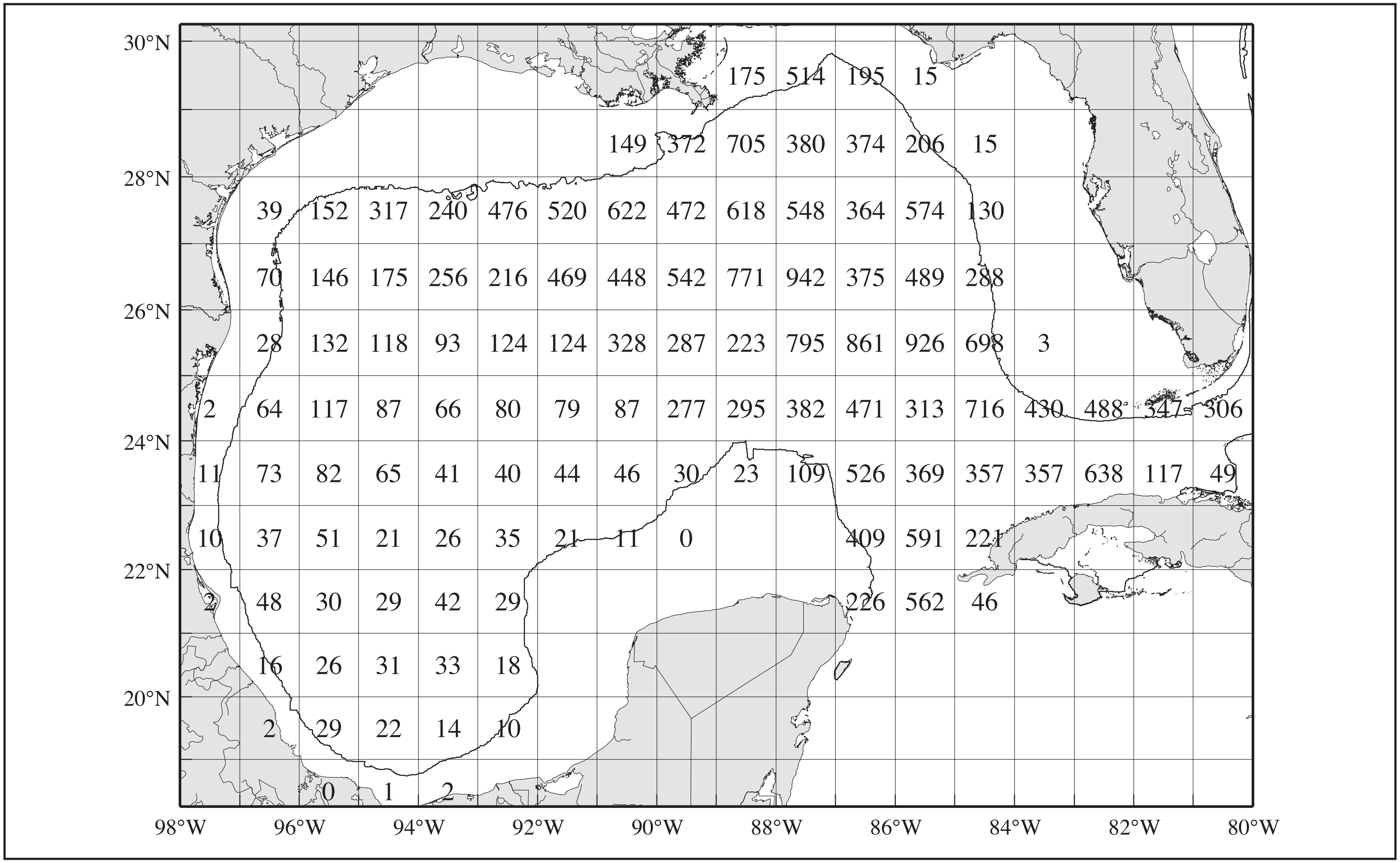

Figure 3.2-9. Number of XBT stations in water depths of 200 m or more by 1° squares in the Gulf of Mexico. The 200-m isobath is shown.

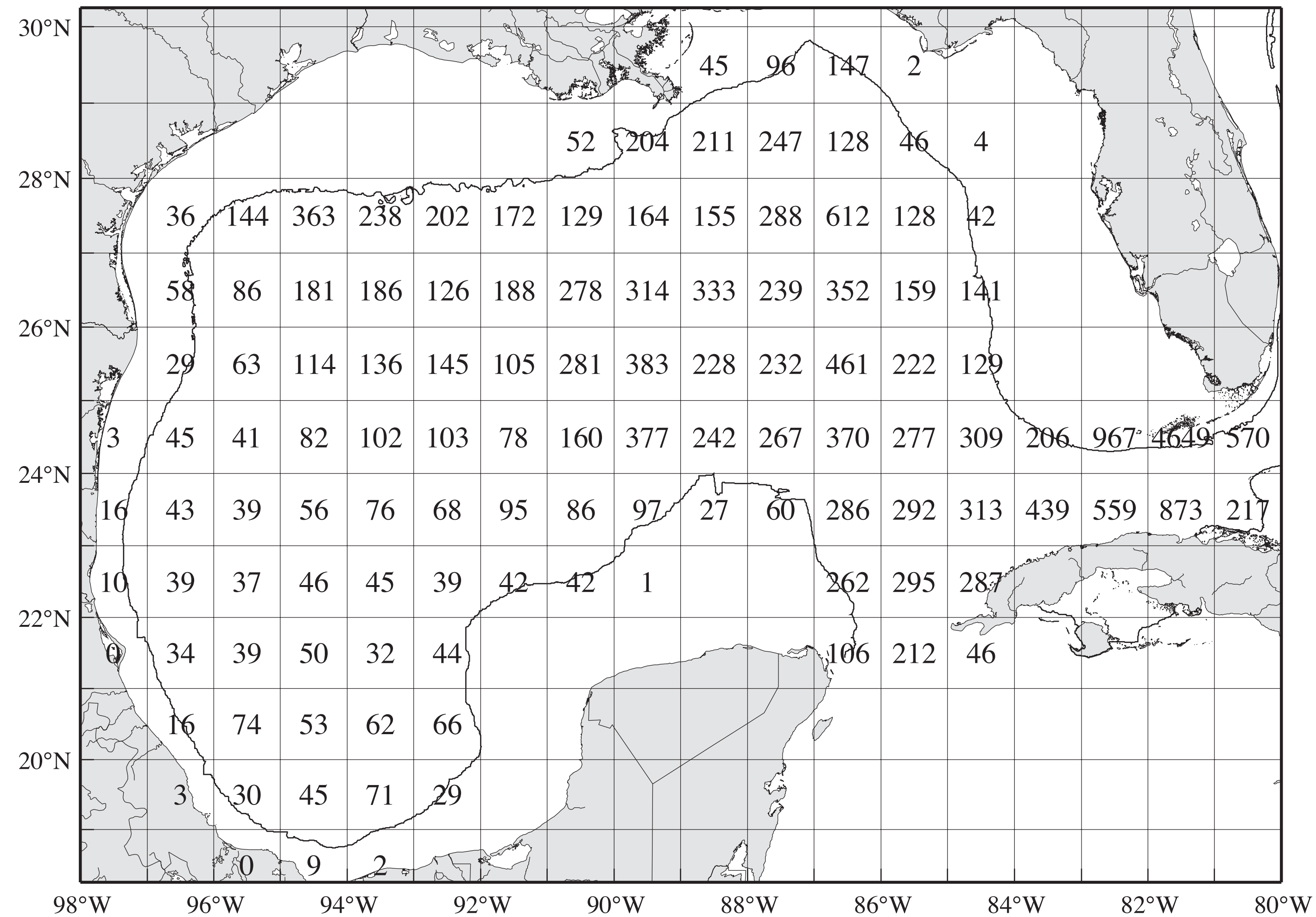

Figure 3.2-10. Number of MBT stations in water depths of 200 m or more by 1° squares in the Gulf of Mexico. The 200-m isobath is shown.

Drifters float at the sea surface, move with surface or near-surface currents, depending on whether they are drogued and at what depth, and telemeter their locations via satellite several times each day. Floats sink to a selected density surface, move with currents at that depth, and surface every 1-2 weeks to send their location by satellite before returning to the selected density surface. Drifter and float data for 1989 through 1999 in the Gulf of Mexico were obtained from the University of Texas Center for Space Research (CSR), which has a ground station that receives satellite transmissions from buoys, floats, and other platforms. Because the sources of the drifter data were not the originators, very limited metadata were available. Therefore, only selected drifter data sets, for which metadata are available from the data originator, are included on the CD-ROM. These are listed in Table 3.2-4. Deployment locations by 1° x 1° boxes and season are presented in Section 5.2.

Drifter fixes were extracted from the full CSR data set of drifter, float, and platform fixes. A major set of drifter data was from the MMS-sponsored Surface Current Lagrangian Program (SCULP) over the LATEX and NEGOM shelves. Many of these drifters moved off shelf into the deep water of the Gulf. The SCULP drifters followed the surface currents, rather than the deeper currents followed by other drifters. For data analysis, the SCULP data set was separated from the remainder of the drifter data.

Ancillary data sets that were assembled are listed in Table 3.2-5. Additional proprietary ancillary information was provided by the petroleum industry and MMS. This information included most EddyWatch charts produced from September 1984 through December 1998 by Horizon Marine, Inc., and various survey reports on Loop Current eddies. EddyWatch charts are analysis products, based on SST fields, drifter tracks, and XBT/CTD profiles, that tracked the Loop Current and Loop Current eddies (LCEs). They were issued on approximately a weekly basis over much of the period.

Model output from a seven-year run of a high-resolution, 3-dimensional numerical model of the Gulf of Mexico was obtained for use in the analysis and array design. The model was developed by Dr. Lakshmi Kantha and colleagues at the University of Colorado (CU) with partial support from an industry-sponsored study on Climatology and Simulation of Eddies (CASE). It is the CU version of the Princeton Ocean Model adapted for the Gulf of Mexico, referred to by the acronym CUPOM. The horizontal resolution is 1/12° and the vertical resolution is 24 sigma levels. The model run was for the years 1993 through 1999. The model assimilates altimeter data for the region in 1000-m water depth or more. It also assimilates satellite sea surface temperature data, but uses climatological sea surface salinity. The 6-hourly, 1.125° resolution ECMWF wind stresses are used for the wind forcing. The inflow boundary is at 21.333°N in the Yucatan Channel, with a geophysically balanced inflow prescribed using typical monthly temperature and salinity profiles. The outflow boundary is at the Florida Straits; the boundary condition is set to be balanced and in phase with the inflow boundary. The data assimilation module is the same as in Horton et al. (1997) and Clifford et al. (1997). Details of the specifics with respect to the Gulf of Mexico can be found in Kantha et al. (1999).

Model output saved for use in the Deepwater Study consisted of:

- Two-dimensional fields at daily intervals of sea surface height, sea surface temperature, sea surface east-west and north-south velocity components; bottom (where the bottom is the lowest sigma level) temperature, salinity, and velocity components; and surface wind stress components at each grid point in the model domain.

Table 3.2-4. Drifter data sets in the deepwater northern Gulf of Mexico that are included in the CD-ROM database.

Program Name	Sample Depth (m)	Deployment Region	Sampling Period	Number	Data Source
LATEX A	6	NW Gulf	April 1992 to December 1994	19	TAMU
LATEX C	50, 100, 200	NW Gulf	April 1992 to December 1994	25	SAIC
SCULP I	surface	NW Gulf	June 1993 to December 1994	374	MMS/SIO
SCULP II	surface	NE Gulf	February 1996 to May 1997	344	MMS/SIO
NEGOM deployed	surface	NE Gulf	November 1997 to January 1999	32	MMS

Table 3.2-5. Gulf of Mexico ancillary data assembled in support of the Deepwater Study.

Data Type	Dates	Sources
Sea surface height anomaly fields (blended TOPEX/Poseidon and ERS-1&2 satellite altimeter product)	mid-April 1992 - August 2000	Dr. Robert L. Leben, Colorado Center for Astrodynamics Research, University of Colorado
Sea surface temperature fields (satellite AVHRR)	April 1992 - August 2000	Johns-Hopkins University, Applied Physics Laboratory; U.S. Geological Survey; NOAA COASTWATCH; and NASA Physical Oceanography Distributed Active Archive Center
River discharge: Mississippi and rivers discharging into the northeast Gulf	Historical records through 1998.	U.S. Geological Survey; Army Corps of Engineers
Meteorological: wind speed and direction, barometric pressure, air and sea surface temperature, relative humidity, dew point	1972-present	National Data Buoy Center, various airports

- Two-dimensional fields of east-west and north-south velocity components, temperature, and salinity at daily intervals and interpolated to selected level surfaces corresponding to depths of 500, 1000, and 2000 m at each grid point in the model domain.

- Time series of hourly east-west and north-south velocity components, temperature, and salinity at 134 selected sites (Figure 3.2-11, solid circles). These sites were selected as the positions of known current measurements and potential measurement locations.

- Three-dimensional fields at 6-hourly intervals of east-west and north-south velocity components, temperature, and salinity at the full spatial resolution of 1/12° and 24 sigma levels for (1) the region bounded north of 26°N, west of 88°W and deeper than 200 m (this is the region of lease blocks for potential deep drilling by industry and is the region for which an optimal measurement array design is sought as Task 3 of the Deepwater Study), (2) the region east of 88°W and north of 26°N that is between 200-m and 3000-m water depths, and (3) the region in the western Gulf between 24°N and 26°N that is in water depths between 200-m and 3000-m (Figure 3.2-11, shaded area).

- Two-dimensional vertical sections of east-west and north-south velocity components, temperature, and salinity at each grid point along selected vertical transects (Figure 3.2-11, solid lines). Sections north of and including 26°N were saved at hourly intervals. Sections south of 26°N were saved at 6-hourly intervals.

Model outputs were used to supplement the historical data base in the analysis of physical processes and phenomena and to aid in development of the field array design criteria.

3.3 Data Quality Control

Data were subjected to quality assurance/quality control (QA/QC) procedures that were reviewed by the SRB and approved by MMS. These procedures follow those applied to data sets collected by TAMU during the Texas-Louisiana Shelf Circulation and Transport Processes Study of the Louisiana-Texas Shelf Physical Oceanography Program (LATEX) and the Chemical Oceanography and Hydrography Study of the Northeastern Gulf of Mexico Physical Oceanography Program (NEGOM), both sponsored by MMS. The rigor of the procedures applied to a particular data set depended in part on the level of QA/QC performed by the data source. Where acceptable QA/QC had been performed, the Deepwater QA/QC was more limited in extent than that applied to new data sets or to data where the QA/QC was unknown or suspect. All data included in the database were examined. The non-proprietary portion of the database is in ASCII format on a CD-ROM that is compatible with ISO Standard 9660. Results of QA/QC are included in the Technical Report that accompanies the database (DiMarco et al. 2001). QA/QC procedures are summarized below.

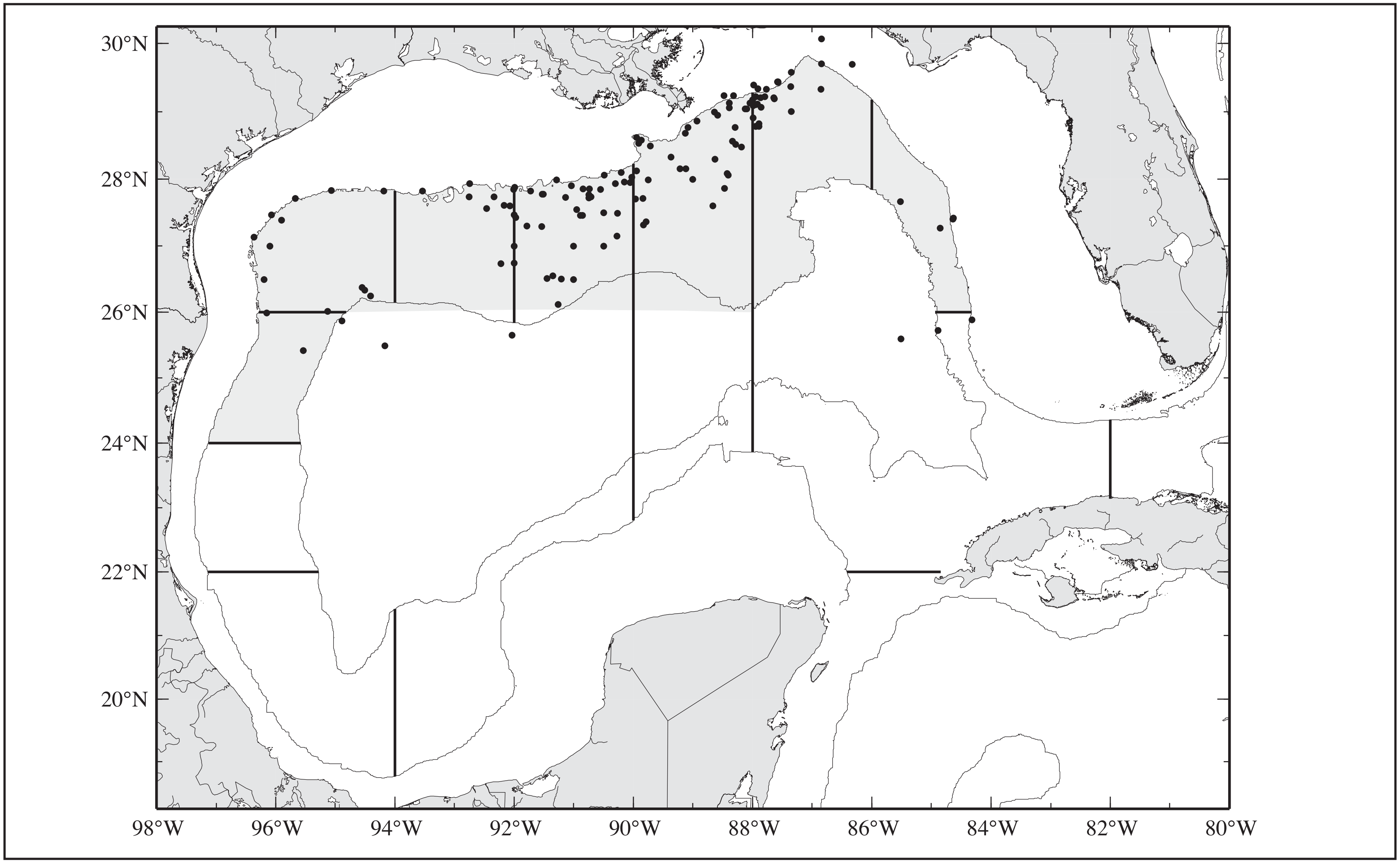

Figure 3.2-11. Model output for the Deepwater Study. Shown are time series stations (solid circles), selected vertical transects (solid lines), and region of 3-dimensional fields at full spatial resolution (shaded region). Bathymetric contours shown are 200 and 3000 m.

3.3.1 Metadata

Metadata were examined and corrected where possible. If the data set had fatally flawed metadata, it was rejected from the database. The three kinds of fatal flaws were no measurement location (geographical location or depth of sensor), unspecified type of data, and no sampling date or time information. Metadata included in database, as available, were:

1. Measurement location
2. Measurement depth
3. Date and time information
4. Data type
5. Sampling interval (spatial or temporal, as applicable to data type)
6. Measurement units
7. Source (data originator)
8. Program name
9. Contact
10. Total water depth
11. Quality code
12. Selected metadata from original data files
13. Identification of corrections or transformations of data from Deepwater QA/QC

3.3.2 Duplicate Data Sets

Duplicate or near-duplicate data sets were identified and eliminated from the database. The highest quality data set of the duplicates was retained by considering mainly the source of each data set, the level of data processing, how much the data were sub-sampled, and consistency with information in the published literature.

3.3.3 QA/QC Procedures

All data sets were screened to remove sets with fatal metadata flaws, duplications, or locations in less than 200 m of water depth. Data then were processed using the procedures described below. Details are provided in DiMarco et al. (2001).

Time series data: Time series data are included in the database. Data types include currents from moored single-point meters or moored or suspended ADCP, time series of salinity, temperature, pressure, and acoustic travel time (inverted echo sounder), shipboard ADCP, XCP/AXCP, and drifter trajectories. The primary QA/QC of time series data followed the procedures used in LATEX and NEGOM as follows

1. For current meter data: DiMarco et al. (1997)
2. For ADCP data: Jochens and Nowlin (2000); Bender and Kelly (1998)
3. For drifter data: Howard and DiMarco (1998)
4. For IES data: DiMarco et al. (1997)
5. For shipboard ADCP data: Jochens and Nowlin (2000); Bender and Kelly (1998)
6. For expendable sensor data: Howard and DiMarco (1998).

The procedure consisted of display and visual and/or statistical inspection of each basic data set. Data were plotted as vector stick plots and/or as plots of property versus time. Plots were inspected to identify outliers, spurious, or other bad data. Bad data were corrected using value replacement (linear interpolation) for short interval gaps or by replacement with a "bad or no data" flag (typically -999.0, -9.0, etc.). For shipboard ADCP and XCP/AXCP, the QA/QC of the data source was generally accepted as adequate. QA/QC of drifter data is described in Section 5.2. Secondary QA/QC consisted of corrections based on feedback from investigators using the database. Correction information was added to the metadata.

Each current meter and moored/suspended ADCP data set was given a quality code rating. The protocol for quality control codes consists of four categories: data quality, percent gaps/zeros, metadata completeness, and special. Data quality is determined to be good, suspect, or reject based on a number of factors including, but not limited to, visual analysis of time-series plots, statistical and spectral analysis, and comparison to historical, synoptic and ancillary data sets. A rejected data set is considered useless for analysis purposes. The number of gaps and zeros in the data set are determined, and the data set then is rated by the percent of the record that contains data gaps or zeros. The metadata are classified as complete or fatally flawed. "Complete" signifies essential metadata are available. "Fatally flawed" indicates one or more of the following is unknown: date and time, location, reasonable knowledge of position in water column. The final category considers three objective criteria that might indicate data interpretation could be compromised. If the only location (latitude, longitude, or total water depth) available is the lease block of the measurement, then the center of the lease block is used to determine the location and the quality code is downgraded. Two criteria apply to ADCP data: if there was no percent good data given or if the ADCP was freely suspended, then the quality code is downgraded. Table 3.3-1 shows the protocol. Each data file was given the code of the lowest class in which it qualified. Files coded "F" were not used in the analysis and were not included in the final CD-ROM.

Table 3.3-1. Quality codes for deepwater current data archive.

QC Code	Data Quality	Percent Gaps or Zeros	Metadata Completeness	Special
A	good	< 1	complete	
B	good	1–10	complete	no % good data available for the ADCP record; lease block center was used for latitude, longitude, and/or bottom depth
C	suspect	11–50	complete	freely suspended ADCP
D	suspect	51–90	complete	
F	reject	91–100	fatally flawed	

Hydrographic data: Hydrographic data were included in the database. Data types included conductivity/salinity-temperature-depth profiles, nutrients, dissolved oxygen, bottle salinity, XBT/AXBT, and MBT. The primary QA/QC of these data followed the procedures used in LATEX and NEGOM as follows

1. For hydrographic data: Jochens et al. (1998)
2. For expendable sensor data: Howard and DiMarco (1998).

The procedure consisted of two steps: rejection of suspect casts and QA/QC of the remaining casts. Suspect casts included those with uncorrectable locations given as being on land or with uncorrectable problems associated with the bottom depth.

The bottom depths for each cast were examined for reasonableness. Three major bottom depth categories were found: (1) no bottom depth was given; (2) the deepest datum was greater than the bottom depth given; and (3) the bottom depth given was greater than the depth of the deepest datum for the cast. For case (1) of no bottom depth given, the "best" depth for that location was assigned to the cast. The bathymetric data sets used to determine the "best" depths were the 50-m and 300-m horizontal resolution data sets from Bryant and Liu of TAMU, 1-km resolution data set from NOAA National Geophysical Data Center, and 3- to 10-km resolution data sets from Scripps Institute of Oceanography. For class (2) where the deepest datum was greater than the bottom depth, the given bottom depth was replaced with the best depth, if the best depth was greater than the deepest datum; otherwise, the given depth was replaced with the depth of the deepest datum plus one meter. For case (3) of bottom depth greater than deepest datum, the absolute value of the difference between the best and given bottom depths was calculated. If this value was greater than 10% of the best depth, then the depths were examined in detail and a selection for bottom depth was made (DiMarco et al. 2001). Otherwise the given depth was used as the bottom depth.

Data were screened for minima and maxima outside of the acceptable limits shown in Table 3.3-2, with extreme outliers noted in the metadata and removed from further consideration. The QA/QC then included preparation of various plots (including ensemble property-property plots, particularly T-S plots) that were inspected.

Table 3.3-2. Acceptable limits applied in QA/QC of hydrographic data sets.

Parameter	Minimum	Maximum
Temperature	3°C	33°C
Salinity	15	37
Oxygen	1 $mL \cdot L^{-1}$	6 $mL \cdot L^{-1}$
Nitrate	0 µM	35 µM
Phosphate	0 µM	4 µM
Silicate	0 µM	30 µM

A climatology of T-S in the waters below 100 m and with temperatures less than 15°C was developed. Twenty-two cruises known to be of high data quality and providing good areal coverage of the deep water were selected against which to assess the temperature and salinity quality of all Gulf stations (Table 3.3-3). Figure 3.3-1 shows the combined locations of all stations from these 22 cruises, with a total of 592 stations, which span the time period 1962-1993. For each cruise data were examined in T-S space and extreme outliers flagged in the metadata and removed from consideration. Then salinity and temperature were binned by density, and salinity was fit as a function of temperature using data from the 22 cruises. Climatological T-S curves were produced for the eastern (east of 89°W; 285 stations) and western (307 stations) Gulf as well as for the entire Gulf. In Figure 3.3-2 are shown the three

Table 3.3-3. Twenty-two cruises with known high quality data used to formulate the T-S curves for QA/QC of the temperature and salinity data. BDO denotes bottle or sub-sampled STD data.

Cruise Name	Cruise Dates	No. of Stations	Data Type
Hidlago 62-H-3	14 February-31 March 1962	90	BDO
Hidlago 62-H-4	12-25 May 1962	10	BDO
Alaminos 6312	7-8 December 1963	4	BDO
Alaminos 64-A-2	17-26 January 1964	19	BDO
Alaminos 64-A-3	27 February-2 March 1964	7	BDO
Alaminos 65-A-1	7 February 1965	4	BDO
Alaminos 65-A-2	27-28 February 1965	4	BDO
Alaminos 65 A-7	18-20 May 1965	5	BDO
Alaminos 65-A-12	3-6 September 1965	7	BDO
Alaminos 65-A-13	12-23 September 1965	58	BDO
Alaminos 66-A-15	6-12 November 1966	10	BDO
Geronimo G0-12	22 February-31 March 1967	86	BDO
San Pablo 6802	22 February-9 October 1968	10	BDO
Kane 6906	10 June-18 August 1969	117	BDO
Kane 6910	16 October-30 November 1969	11	BDO
SunCoaster SC8310	12-19 November 1983	41	BDO
		3	CTD
Justo Sierra JS085	5-23 March 1985	27	BDO
		1	CTD
Gyre 89G15	13-17 November 1989	10	BDO
		10	CTD
Gyre 90G15	13-15 October 1990	8	BDO
		3	CTD
Gyre 91G02	3-9 March 1991	16	CTD
Gyre 91G04	15-18 June 1991	5	BDO
		3	CTD
Pelican 9312	5-12 December 1993	23	CTD

curves. As expected, the T-S curve for the western Gulf shows higher salinities at the salinity minimum (core of the residual Antarctic Intermediate Waters) than does the curve for the eastern Gulf, the maximum difference being of order 0.04 (in agreement with the work of Carruthers, 1972). For the bottom waters and for waters near 15°C the two curves agree well. It was decided to use the T-S curve fit for the entire Gulf against which to quality control other cruise data.

All remaining stations with temperature and salinity observations were plotted by cruise showing the climatological T-S curve and indicating which samples were outside ± 2 and ± 3 standard deviations in salinity for given temperature. Extreme outliers were identified as "bad" in the metadata and removed from further consideration, though kept in the data set. Cruises with large numbers of points (in some cases all points) outside the limits of ± 2 standard deviations were flagged as "bad" in the metadata and removed to a separate data set.

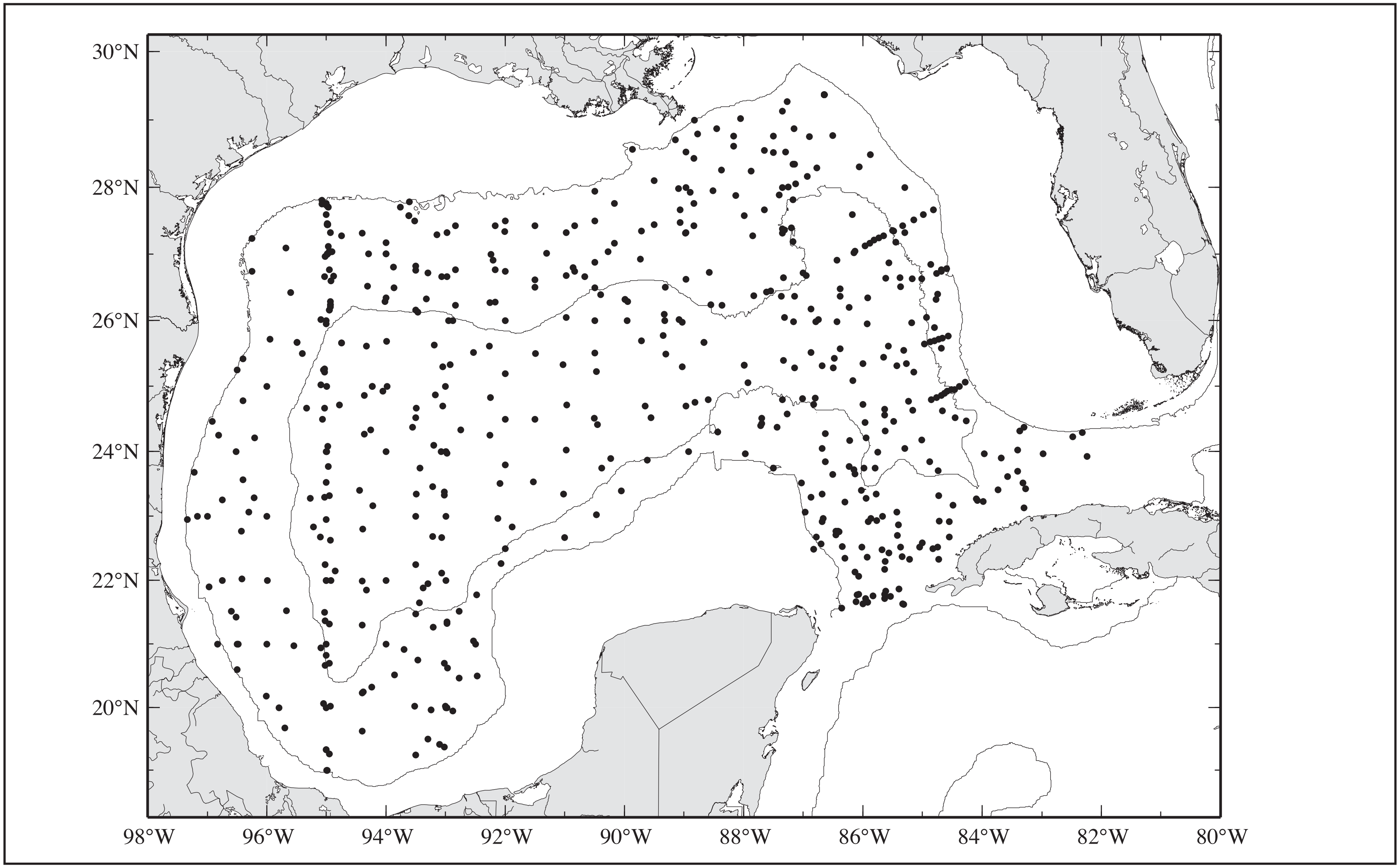

Figure 3.3-1. Basemap showing locations of 592 T-S profiles from 22 cruises (1962-1993) which have high-quality data and broad geographic coverage. Contours shown are 200 and 3000 m.

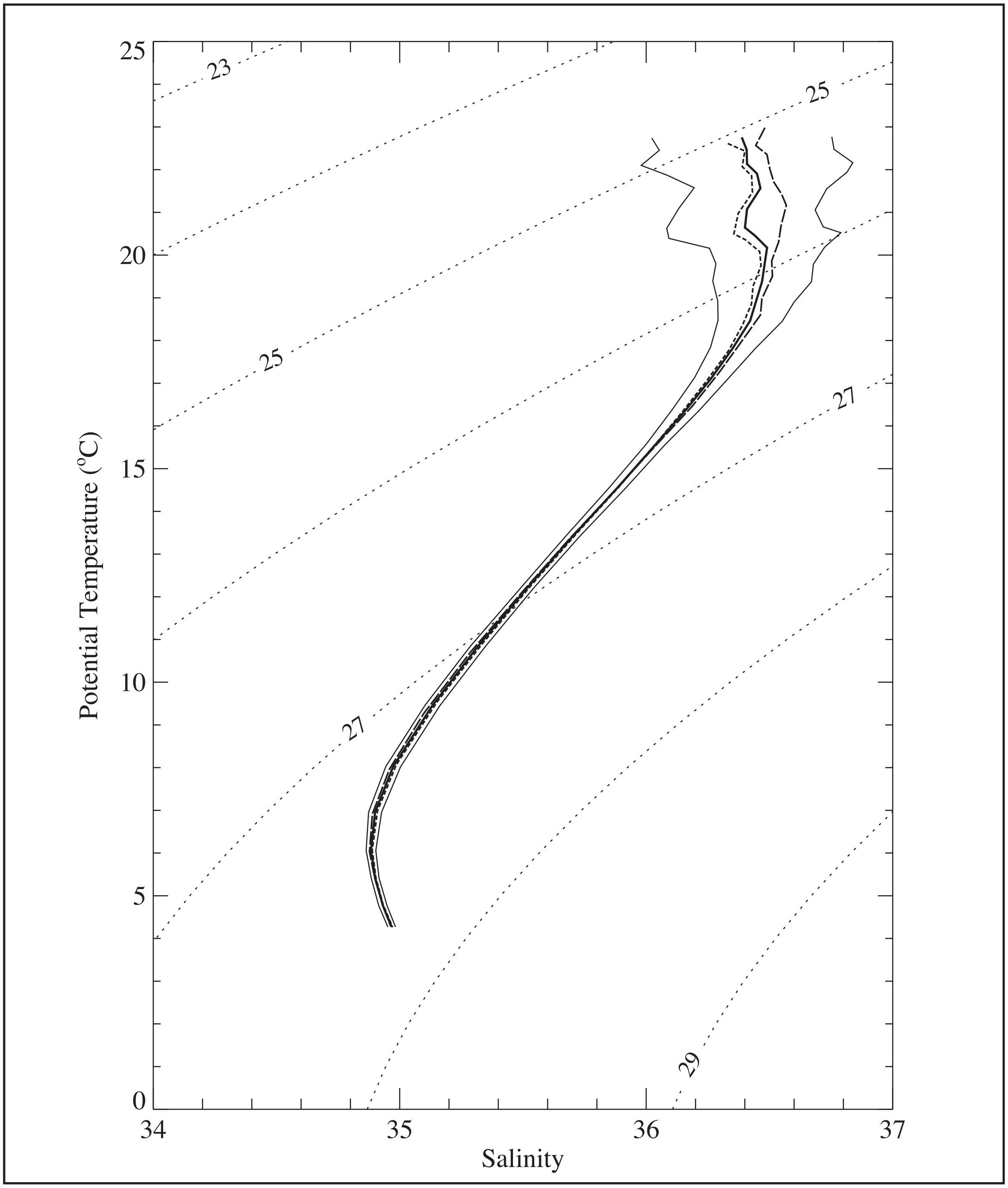

Figure 3.3-2 Mean T-S relationships between $\sigma_\theta = 25.0$ and 28.0 for 22 selected cruises having high-quality data. Curves for all stations (thick line), stations west of 89°W (307 stations; dashed), stations east of 89°W (285 stations; dash-dot), and ± 2.3 standard deviations about mean for all stations (thin lines).

Then all remaining data were screened for data to be flagged as "suspect" and not used in our calculations. We used two criteria. We wished to reject observations falling outside of the 98% probability limits from our standard T-S curve for $T \leq 17°C$; for a normal distribution of salinity about the curve, this limit corresponds to 2.3 standard deviation about the curve. We also wished to reject stations having large numbers of suspect observations for $T \leq 17°C$ on the grounds that such stations would not produce good estimates of geostrophic shear.

We calculated for each station the percentage of observations $T \leq 17°C$ with S outside 2.3 standard deviations about the standard curve. Stations with greater than 30% of such observations were classified as suspect. For the remaining stations, observations were classified as suspect if salinity fell outside 2.3 standard deviations from the standard T-S curve for $T \leq 17°C$.

Nutrient data collected before 1972 were flagged as "suspect" because of lack of reliable laboratory analysis techniques in the early years. Dissolved oxygen data derived from continuous profilers were likewise flagged as suspicious because of the wide variety of correction procedures applied. Secondary QA/QC of all data consisted of corrections based on feedback from investigators using the database. Correction information was added to the metadata.

Ancillary data: Ancillary data (river discharge, meteorological, and sea-level gauge data) and satellite remote sensing fields (SSH and SST) were used for analysis only and were not included in the database. Generally the QA/QC of the data source was accepted. When used in analysis, data were plotted and examined for possible outliers and fields were plotted and examined for possible erroneous or suspect features. Problem data points and fields were not used in the analysis.

Selected numerical model output: Selected numerical model output was used in the analysis, but not included in the database.

4 OVERVIEW OF GENERAL HYDROGRAPHY AND CIRCULATION OF DEEPWATER GULF

This section is a brief overview of the energetics, circulation and water masses of the Gulf of Mexico. It does not contain details or extensive references. For further details the reader is referred to the data search and literature synthesis report for the deepwater region of the Gulf prepared by Continental Shelf Associates, Inc., with support from the Minerals Management Service (Continental Shelf Associates, Inc. 2000). That report contains several hundred pertinent references to the physical oceanography discussed below.

The circulation within the Gulf of Mexico is driven principally by two sources of energy. The main source of energy consists of the Yucatan Current and other circulation features that enter the Gulf from the Caribbean Sea through the Yucatan Channel. Effects are seen as the Loop Current (the extension of the Yucatan Current through the eastern Gulf and into the Florida Straits), the current rings that detach from the Loop Current and their subsequent distribution of energy throughout the Gulf, and the effects of the Loop Current and ring separation on the deep circulation within the basin. The second major energy source is wind stress forcing within the Gulf. Effects are seen as low frequency regional circulation patterns forced by low frequency regional wind patterns and as episodic currents forced by high frequency atmospheric events, including tropical cyclones, extratropical cyclones, cold air outbreaks, and other frontal passages. Thermohaline forcing is known to be important over the shelves of the Gulf, e.g., buoyancy forcing by river discharge affects the nearshore coastal currents over the continental shelves. However, no thermohaline forcing of consequence or water mass formation are known to occur in the deepwater region of the Gulf.

The Yucatan Current enters the Gulf from the Cayman Basin of the Caribbean Sea as a westward-intensified boundary current. Surface speeds in its core may exceed 200 $cm \cdot s^{-1}$. A southward surface counterflow has long been documented to exist off Cape San Antonio at the western end of Cuba. There is evidence in some data for a southward counterflow in the westward reaches of the Yucatan Channel just off the Campeche Shelf of Mexico.

The density structure within the Yucatan Channel shows shear within and beneath the main inflow of the Yucatan Current extending essentially to the sill depth (approximately 2000 m) of the channel. The current is strongly surface intensified, as documented from numerous observations. However, the magnitude and direction of barotropic components are unknown, as is the optimal reference level. The inflow of the Yucatan Current, and its continuation as a Loop Current through the eastern Gulf and then into the open Atlantic through the Florida Straits, extends in depth at least down to the sill depth of the Florida Straits (somewhat less than 800 m). The direction of deep currents within the Yucatan Channel and beneath the Loop Current in the open Gulf still is open to conjecture. The first intensive direct measurements are underway, and results are not yet available.

Transport estimates for the Loop Current system are approximately 30 Sverdrups with seasonal signals of about 10%. However, one difficulty in interpreting estimates of transport made over short time periods results because tidal transports through the channels are of the same magnitude as the total transport.

It should be understood clearly that the Loop Current system is neither stationary nor regular (or even deterministic) in its behavior. In addition to the mentioned counterflows through the Yucatan Channel, bottom and lateral counterflows are known to occur in the Florida Straits near Florida and south of the Florida Keys at the entrance to the straits. The maximum speeds, point of departure from the Campeche Shelf, and velocity distribution of the core of the Yucatan

Current are known to vary considerably. These factors may influence the extent of encroachment of the Loop Current into the eastern Gulf, as well as its stability.

Closed current rings form and separate from the Loop Current. Those of principal importance are large anticyclonic rings, with current cores similar in properties to the waters of Caribbean type comprising most of the Loop Current and enclosed by that current within the Gulf. Secondary rings (usually cyclonic) and near-surface filaments or streamers also emanate from the Loop Current and at times may extend well over the slopes and onto the continental shelves.

Anticyclonic rings formed from the Loop Current are commonly referred to as Loop Current Eddies (LCEs). They have been observed to separate at intervals ranging from 3 to 17 months; the frequency of separation shows a peak near 12 mo with secondary peaks at 9 and 6 mo. After formation, LCEs display a wide variety of behavior. They may remain for considerable lengths of time (months) in the eastern Gulf or immediately begin to move generally westward, with average drift speeds of order 5 $km \cdot d^{-1}$. They have been observed to interact with one another, the slopes/shelves, with cyclonic rings, and even with the Loop Current itself (on occasion re-attaching to that current). Cyclonic rings are numerous and are formed, at least in part, by the interaction of LCEs with other rings or bathymetry. These surface-intensified ring currents extend into the water column to depths of about 700-800 m. The surface waters of the western Gulf are normally populated by an array of rings of different size, shape, and vorticity. The average life of a LCE is of order one year.

The waters entering the deepwater Gulf through the Yucatan Channel naturally are those found in the northwestern Caribbean Sea. From top to bottom the principal water masses are: Subtropical Underwater, 18°C Water, Tropical Atlantic Central Water, Antarctic Intermediate Water, and Upper North Atlantic Deep Water. Each of these water masses is distinguished by one or more extrema or inflection points in the distributions of property values versus depth, or density. Subtropical Underwater, derived from the subtropical surface waters north and south of the Equator, is characterized in the Caribbean by a pronounced salinity maximum (34.6-34.8), and the same characteristics are brought into the Gulf by the Loop Current. Therefore, those same high salinities are found within the newly formed LCEs. Convective mixing along the western edge of the Loop Current as it passes through Yucatan Channel decreases salinity at the Subtropical underwater core; similarly, as LCEs age and spin down, mixing decreases the salinity at this core within the rings. Thus the waters of the interior Gulf may be differentiated from those within the Loop Current and most anticyclonic LCEs by the difference in salinity at the core of the Subtropical Underwater. That core is found at depths of 150-250 m. The depth of the core, and of other surfaces marking specific property values, e.g., isotherms, are depressed within the anticyclonic rings and raised within the cyclonic rings. The magnitude of that vertical offset is a measure of the strength of the circulation in the feature, and horizontal distributions of isotherm depths as well as sea surface height give reasonable estimations of the presence and strength of surface-intensified eddies in the Gulf.

At least two low-frequency, surface-intensified circulation features within the deepwater Gulf are believed to be forced by local wind stress. (A number of others are recognized within the shelf circulation regimes of the Gulf.) A large circulation feature appears as an east-west elongated anticyclone with westward intensification along the Mexican-U.S. boundary. It is centered north-south at approximately 24°N. The volume transport and speeds in this feature have an annual cycle, with maximum values in July and minimum in October, in response to the wind stress curl over the western Gulf. The transport varies from about 2.5 to 7.5 Sverdrups; the maximum drift speeds in the western boundary current vary from about 5 to 25-30 $cm \cdot s^{-1}$. In the Bay of Campeche, centered near 20°N, 94.5°W, is a cyclonic circulation feature with apparent annual signal. It is a maximum, with transports of order 3 Sv, in the summer, consistent with the minimum positive wind torque that occurs in that season. Both of these features have been the subject of some debate, but evidence seems strong enough to consider them as highly likely.

Strong, episodic wind events that force the Gulf include tropical cyclones (especially hurricanes), extratropical cyclones, cold air outbreaks, and other frontal passages. Tropical conditions normally prevail over the Gulf from May or June until October or November; the nominal hurricane season is 1 June through 30 November. Hurricane forced currents in the mixed layer may exceed 150 $cm \cdot s^{-1}$, and when combined with wave orbital velocity, may exceed 300 $cm \cdot s^{-1}$. Hurricane induced currents at 200 m have been observed to be approximately 100 $cm \cdot s^{-1}$ in several instances, and even at 700 m may reach 10-20 $cm \cdot s^{-1}$.

From October or November until March or April the Gulf experiences intrusions of cold, dry continental air masses. These result in cold air outbreaks and the formation of extratropical cyclones. These cyclogenesis events, which occur some 10 times per season, are known to cause very energetic currents over the continental shelves, and even over the upper continental slopes; speeds of 50-75 $cm \cdot s^{-1}$ in the surface layer and exceeding 20 $cm \cdot s^{-1}$ down to depths of 200 m have been observed.

The strong atmospheric events decay as series of inertial oscillations lasting of order 5-10 days. They may propagate laterally and downward to considerable depths (~1000 m) as coherent wave trains with amplitudes of 25-50 $cm \cdot s^{-1}$.

At least two large upwelling regions exist in the Gulf. Upwelling in one region, located along the western shelf off Mexico and Texas, appears annually as the regional wind stress turns northward in summer, producing upwelling favorable conditions (Nowlin et al. 1998b). Another region is located over the broad Campeche Shelf and is driven principally by impingement of the Yucatan Current onto the shelf (Cochrane 1969). The flow runs nearly parallel to the local isobaths, producing a near-bottom Ekman layer with transports directed up slope over the shelf.

Below approximately 800 m, knowledge of both the general circulation and mesoscale features present in the Gulf of Mexico are much more speculative than for the upper layer circulation. However, based on analyses of a combination of numerical model output and observations, some pictures are emerging.

Based on model output and reasonable choice of reference levels applied to geostrophic calculations, the long-term mean circulation of the deep Gulf is cyclonic. Moreover it appears to be intensified offshore from steep topography in the slope and rise, e.g., the Sigsbee Escarpment on the north Central Gulf, the Campeche Shelf, or the West Florida Shelf.

Based on sparse arrays of current meters, it has been inferred that low-frequency fluctuations with periods greater than 10 d propagate from east to west in the deep Gulf with group speeds near 9 $km \cdot d^{-1}$, faster than typical observed westward travel speeds for LCEs. These deep motions were observed to be highly coherent in the vertical with bottom intensification and have been attributed to topographic Rossby waves. Speeds within these deep motions are observed to be as great as 30 $cm \cdot s^{-1}$ beneath the Loop Current, but less in the central and western Gulf. It is speculated that these deep perturbations are excited by the Loop Current, perhaps when LCEs separate (Hamilton 1990).

High resolution numerical circulation models of the Gulf evidence both cyclonic and anticyclonic eddies in the deep basin waters. They form in the eastern Gulf under the Loop Current regime and propagate into the western Gulf guided by topography. In at least two models deep eddies appear to form as LCEs are formed. It is suggested that an anticyclone and a stronger cyclone are formed in the lower layer in response to a westward moving newly formed anticyclonic LCE in the upper layer. Evidence from one model is that the deep eddy pair remains coupled with the upper ring, although the two deep rings rotate cyclonically as a pair, and that the deep anticyclone decays more rapidly than the deep cyclone.

On the continental slope and rise of the north-central Gulf of Mexico a previously unexplored bed form was found (Bryant et al. 2000a, 2000b, 2001; Scott et al. 2001). Just offshore of, and perhaps on, the Sigsbee Escarpment are mega-furrows with depths of 5 to 10 m and widths of 10s of m eroded into Holocene deposits blanketing this region. These furrows are spaced on the order of 100 m apart and extend unbroken for distances of order 100 km, generally oriented nearly along isobaths. Water depths range from 2000 to 3000 m. See further discussion in Section 6.1.3. Global observations demonstrate that such bed forms are widespread features.

These features are observed to change character with distance from the escarpment, and those changes are in good agreement with published laboratory studies of submarine erosion in unconsolidated sediments, showing that furrows of different separation, wavelengths, and fundamental character occur for different flow rates (Flood 1983; Dzulynski 1965; Allen 1969). The tentative conclusion is that bottom currents responsible for these features have along-isobath components and increase in strength toward the escarpment. Speculation based on laboratory experiments is that near-bottom speeds of currents responsible for the inshore furrows might be 50 $cm \cdot s^{-1}$ or even in excess of 100 $cm \cdot s^{-1}$. These currents might be sporadic or quasi-permanent. These furrows and the currents responsible for them may also exist over a considerable part of the yet unexplored base of the continental slope in the Gulf of Mexico. These mega-furrows may be related to the mean circulation within the deep basin. However, topographic waves or deep eddies can not be ruled out as potential causative factors. Nearly barotropic currents fluctuating essentially along-isobath with amplitudes reaching 100 $cm \cdot s^{-1}$ and periods of order 10 d have been observed above the bottom in the region just inshore from the mega-furrows.

Finally, mention must be given to the occasional observations of subsurface-intensified currents of short duration. High-speed current cores have been reported with maxima in the depth range of 100 to about 400 m and with maximum speeds of 100 $cm \cdot s^{-1}$ (or perhaps greater). Occurrences based on reliable data certainly are rare, but they are confirmed. Moreover, such events can also be seen in the output of numerical circulation models. Occurrences seem confined to regions over the upper continental slope. Their causal mechanism(s) are yet unknown.

5 LARGE-SCALE CIRCULATION AND ITS VARIABILITY FROM OUR STUDY

5.1 Geostrophic Shear Fields from Hydrography

The depth of 800 m was used as a reference level for our examination of geostrophic shear in the Gulf of Mexico because, based on direct current observations (Section 7.1), it seems a reasonable depth separating surface-intensified upper ocean currents from nearly barotropic deep currents within the Gulf. Near 800 m, both mean speeds and their standard deviations reach a minimum with depth, based on long current meter records. We note also that the inverse analysis of Hofmann and Worley (1986) showed that currents in the Gulf of Mexico at depths below 800-1000 m were often reversed relative to currents at shallower depths. Moreover, we have found from examination of model output (discussed in Section 5.3) that averaged currents above and below about 800 m behave quite independently.

For analysis of the large scale geostrophic circulation of the Gulf of Mexico, we used only temperature and salinity data that passed the quality control procedures described in Section 3.3.3. Shown in Figure 5.1-1 are the number of quality controlled stations with samples to at least 800 m within each 0.5°x 0.5° bin in the Gulf of Mexico. For stations with reported surface observations within 20 m of the sea surface, we used as surface values of temperature and salinity those values at the shallowest reported depths. Stations not having observations within 20 m of the sea surface (2.5%) were not used. In Figures 5.1-2 and 5.1-3 are shown, respectively, the bin-averaged values of dynamic topography of the sea surface relative to 800 db (area average removed) and the standard deviation of the values within each bin.

The hand-contoured field of dynamic topography of the sea surface relative to 800 db using the values in Figure 5.1-2 is shown in Figure 5.1-4. The dominant feature seen is the Loop Current, with a dynamic range in excess of 40 dyn cm for that part of the loop extending with continuity past 25°N. The dynamic ranges of closed anticyclonic features within the Loop Current exceed 60 dyn cm. It might be noted that for the Loop Current region the mean standard deviation is about 18 dyn cm and the mean sample size per bin is about 5; therefore the mean standard error of estimate for that region is about 8 dyn cm. This fact might be kept in mind when viewing the figure. Additionally, it should be noted that the asynoptic and unequal temporal and spatial distribution of data going into the mean dynamic topography fields makes uncertain the credibility of the derived mean flow field.

The eastern and western regions of the Gulf seem separated by a region of minimum sea surface height near 90°W. In the far west there appears an anticyclone off the Mexican coast centered near 24°N, 95°-96°W, in agreement with the findings of Sturges (1993). This circulation feature has a dynamic range of ~20 dyn cm. An alternative explanation is that the migration of the anticyclonic LCEs and their decay in the western Gulf may cause a mean anticyclone (Elliott, 1982). However, this explanation has largely been refuted by the work of Sturges (1993). Within Campeche Bay is seen a cyclonic circulation feature with dynamic range of ~10 dyn cm. This is in agreement with the findings of Vazquez (1993).

Figures 5.1-5 and 5.1-6 show, respectively, the number of quality controlled profiles reaching 1500 m and bin-averaged values of dynamic topography of the 1500-db surface relative to 800 db for each bin. The standard deviation for the 1500/800 field was not calculated because of the small sample size. The area mean of dynamic topography was subtracted from each value shown. The hand-contoured field of dynamic topography is shown in Figure 5.1-7. Note that in this representation larger negative values correspond to cyclonic and larger positive values to anticyclonic circulation features. Thus, beneath the Loop Current is seen a cyclone with

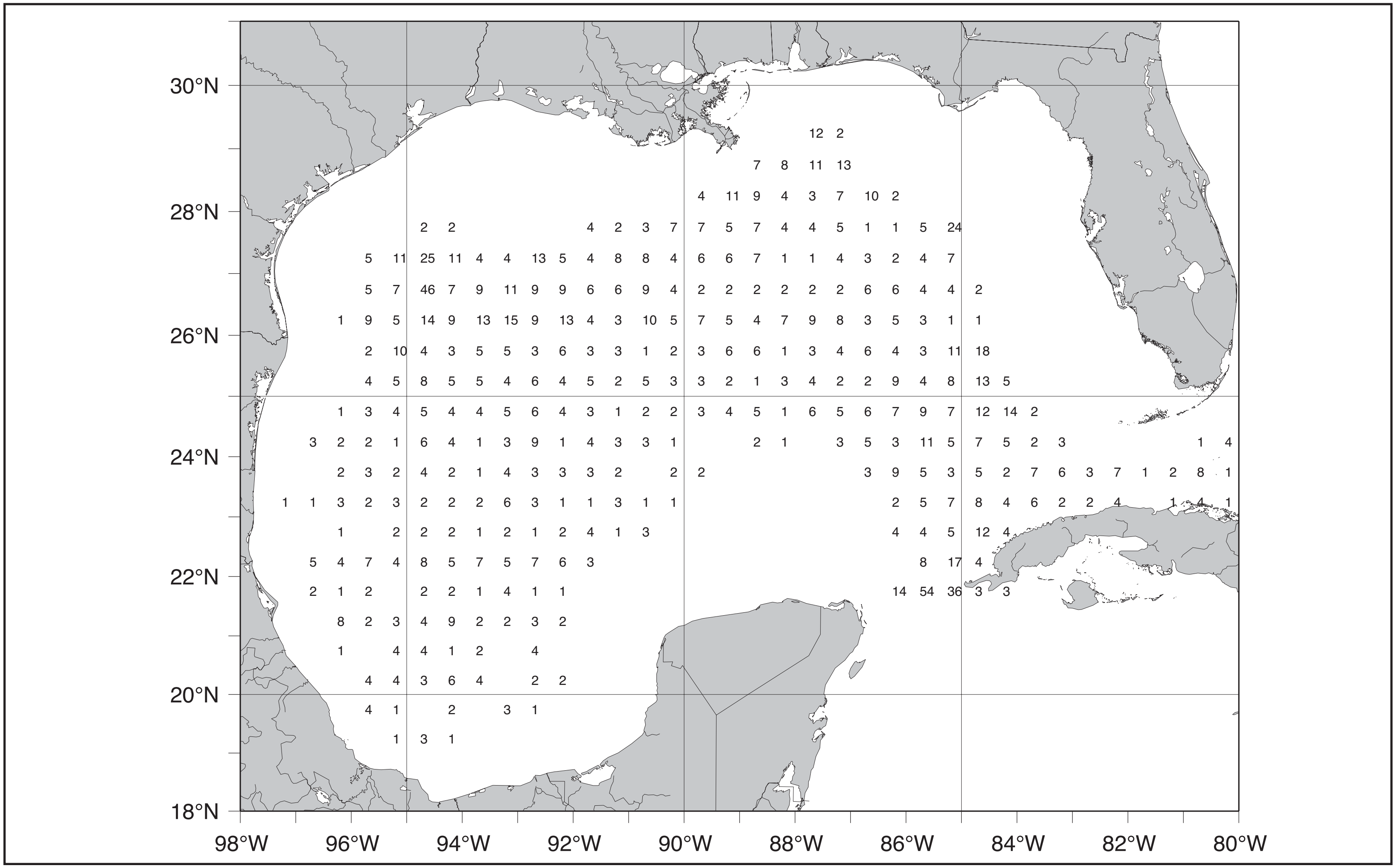

Figure 5.1-1. Number of stations with quality controlled temperature and salinity observations to at least 800 m for each 0.5° x 0.5° bin in the Gulf of Mexico. The total number is 1630.

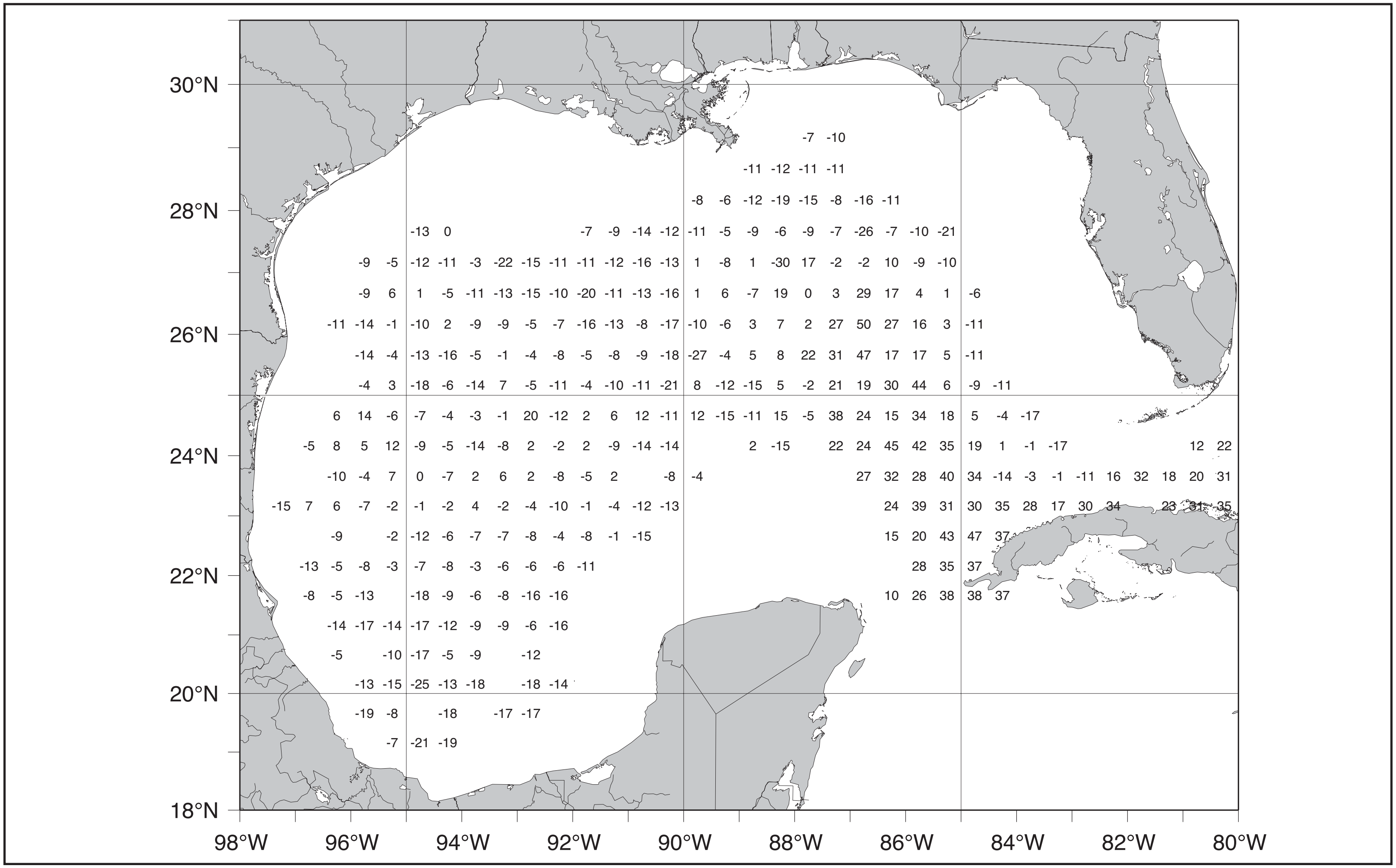

Figure 5.1-2. Bin-averaged dynamic height (dyn cm) at the sea surface relative to 800 db. An area average of 118 dyn cm was removed.

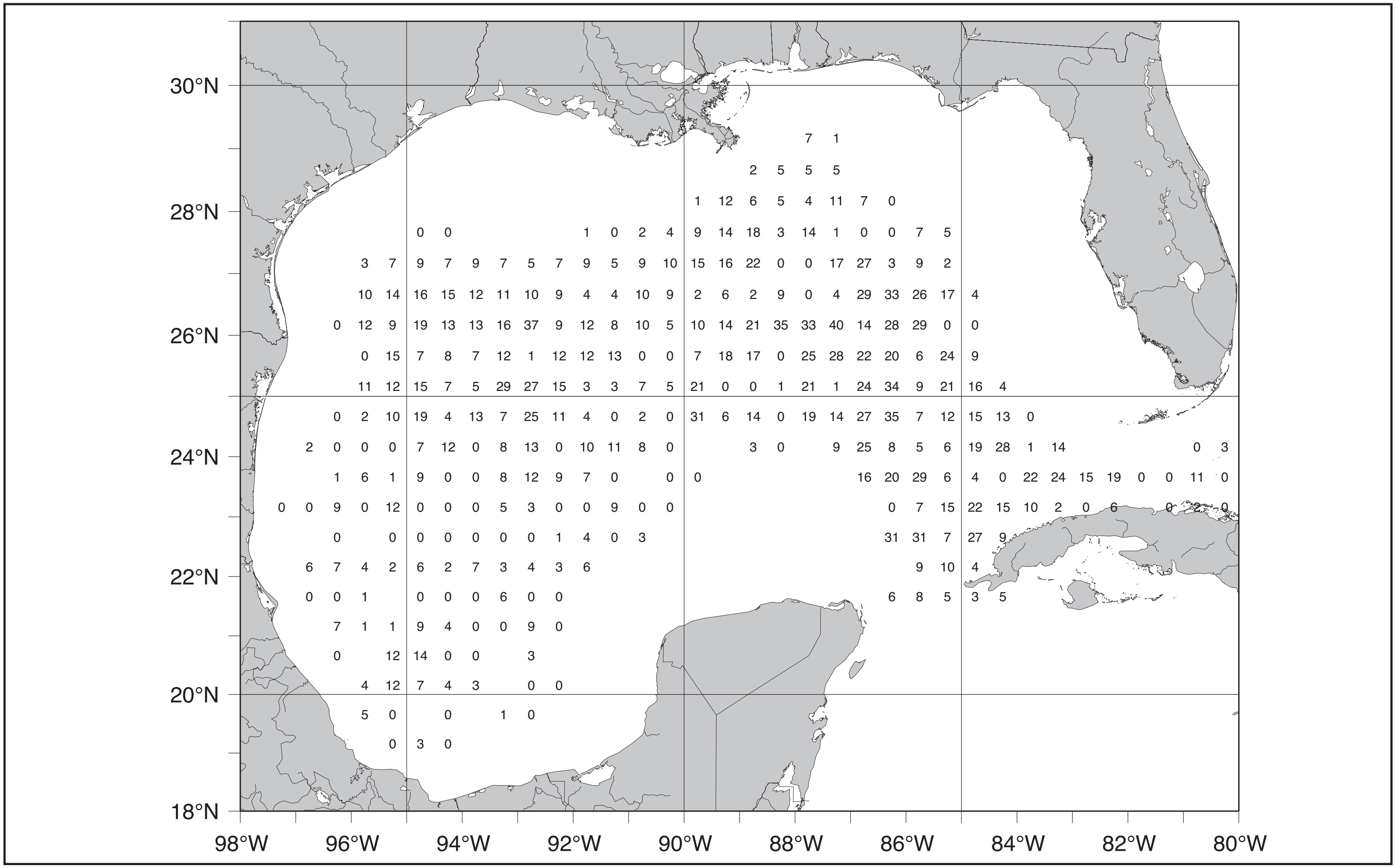

Figure 5.1-3. Standard deviation (dyn cm) of values of dynamic height of sea surface relative to 800 db within each 0.5°x 0.5° bin.

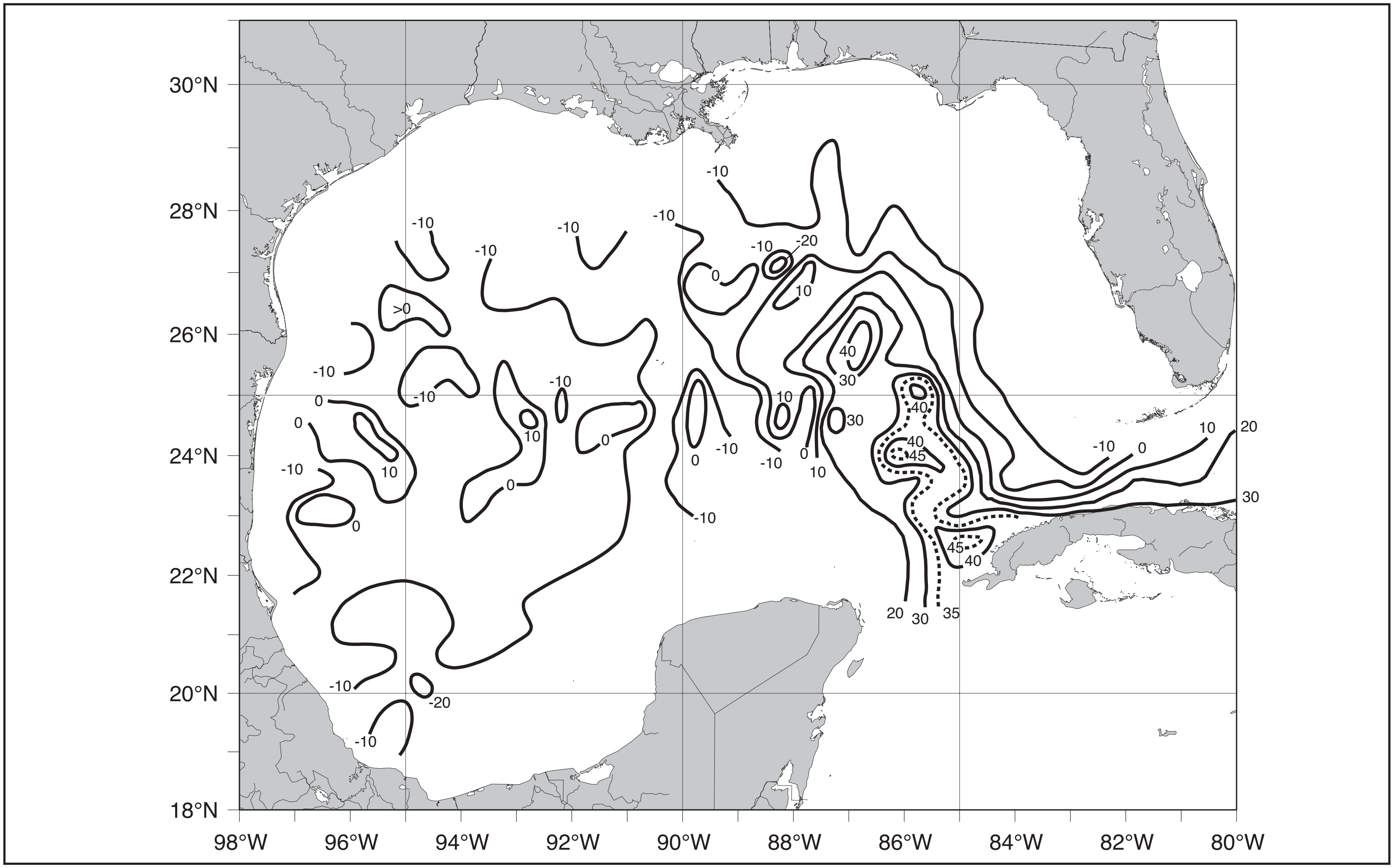

Figure 5.1-4. Hand-contoured dynamic topography of sea surface relative to 800 db using the values shown in Figure 5.1-2.

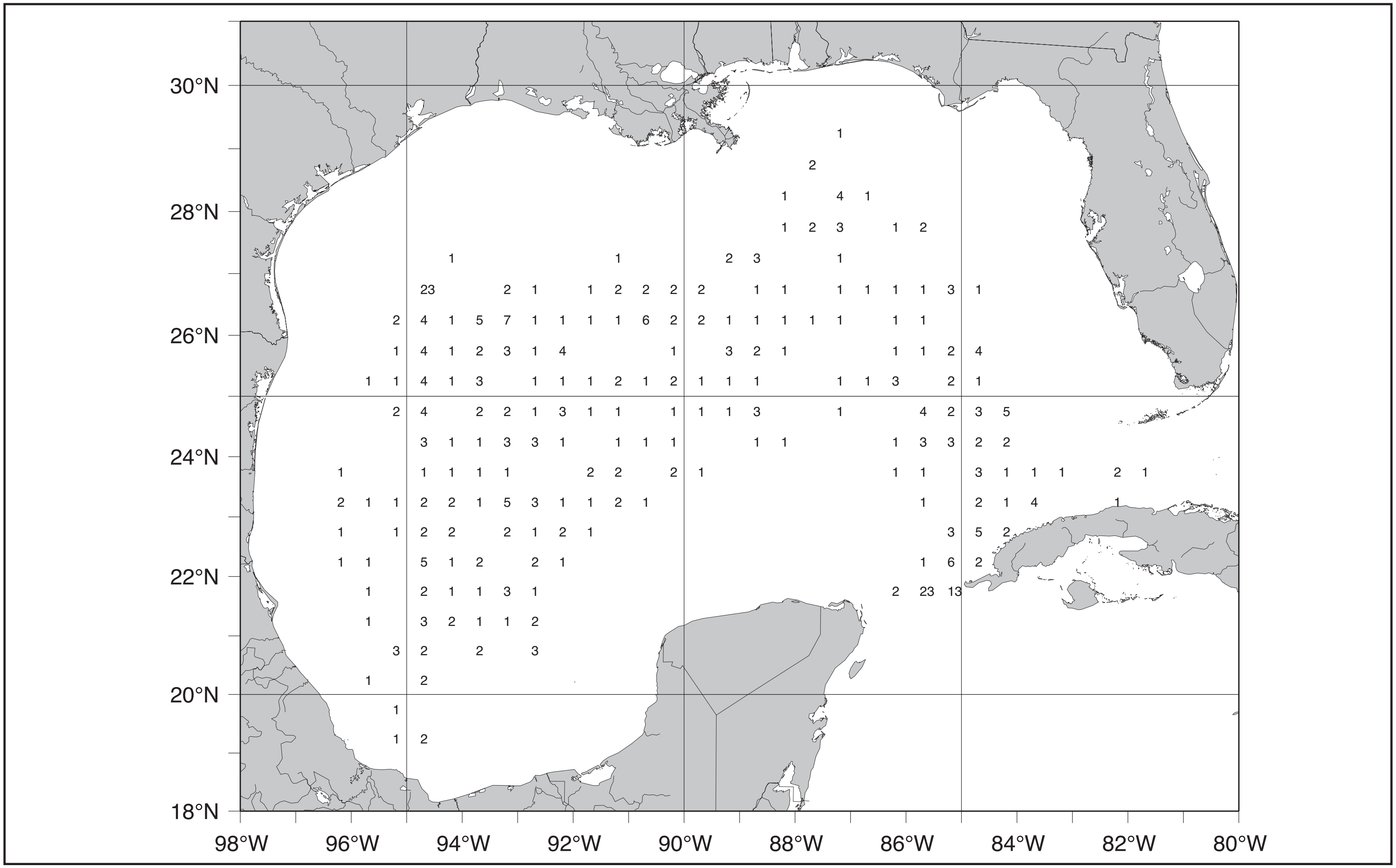

Figure 5.1-5. Number of stations with quality controlled temperature and salinity observations to at least 1500 m for each 0.5° x 0.5° bin in the Gulf of Mexico. The total number is 408.

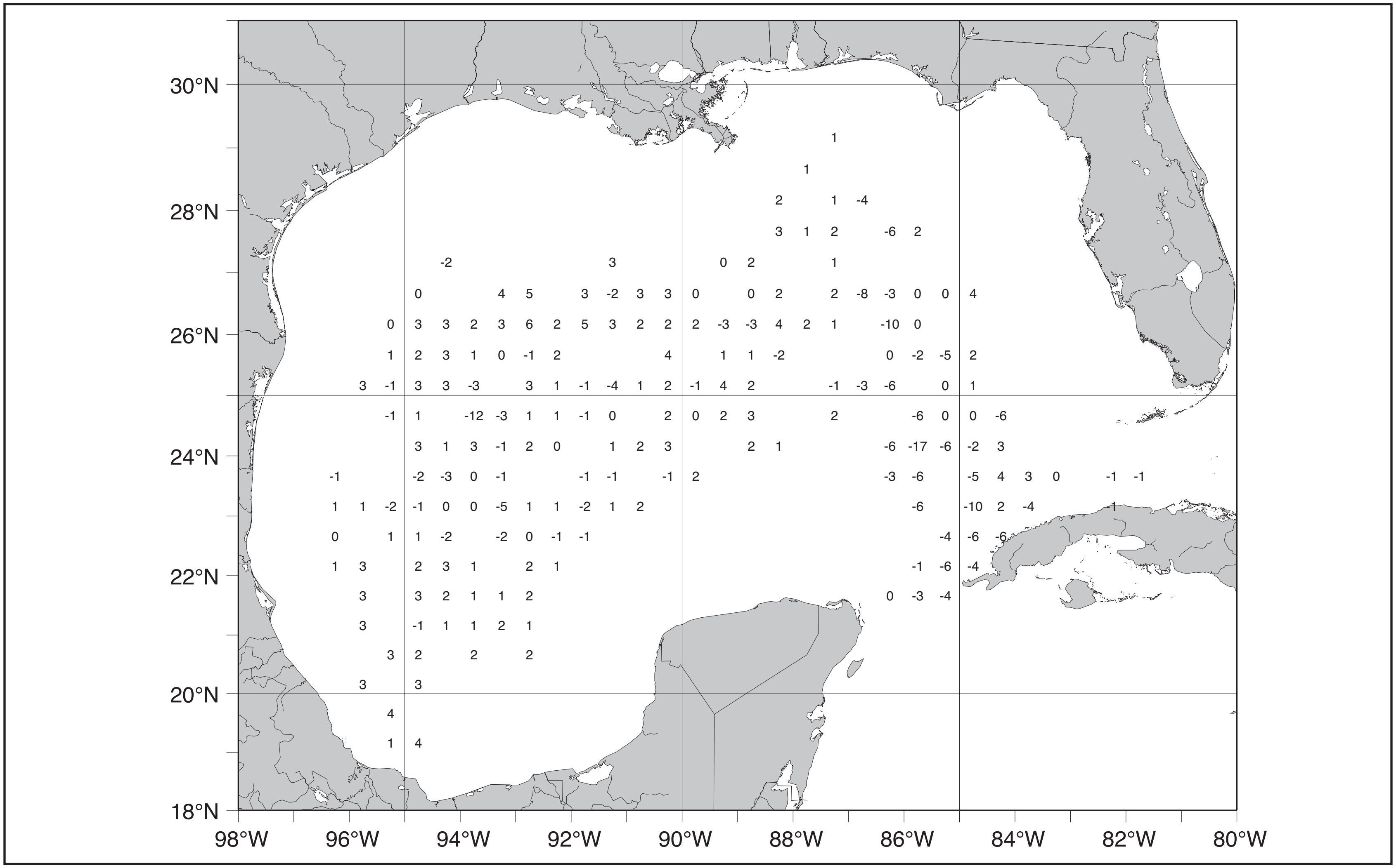

Figure 5.1-6. Bin-averaged dynamic height (dyn cm) of 1500-db surface relative to 800 db. An area average of 40.6 dyn cm was removed from all bin averages.

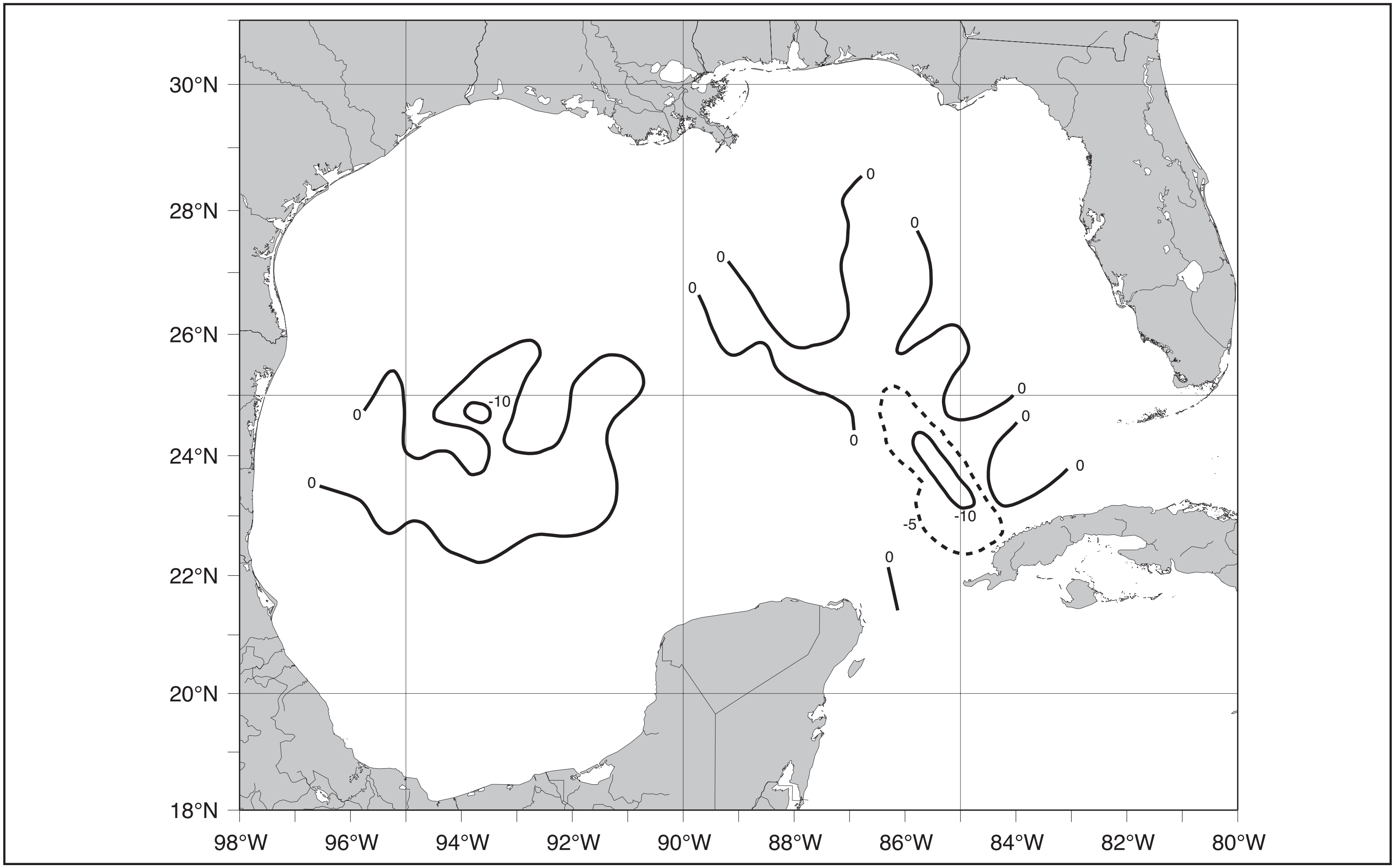

Figure 5.1-7. Hand-contoured dynamic topography of 1500 db relative to 800 db using the values shown in Figure 5.1-6.

dynamic range of ~10 dyn cm. This is separated from a weaker anticyclonic circulation feature just to its northwest. The circulation in the western Gulf is essentially cyclonic. These patterns are in agreement with the results of the CUPOM output discussed in Section 5.4.

Perhaps the most carefully executed hydrographic survey of the whole Gulf was carried out in February and March 1962 aboard the *R/V Hidalgo* (McLellan and Nowlin 1963; Nowlin and McLellan 1967). We have re-examined data from that quasi-synoptic survey of the Gulf, called cruise 62-H-3. Shown in Figures 5.1-8 and 5.1-9 are the values of dynamic topography (dyn cm) of the sea surface relative to 800 db (area average removed) and of 1500 db relative to 800 db. In Figures 5.1-10 and 5.1-11 are shown the hand-contoured fields of dynamic topography based on the values in Figures 5.1-8 and 5.1-9, respectively.

Of course, the contoured fields of dynamic topography for cruise 62-H-3 are quite smooth because there are relatively few observations on which to base the contouring. The large closed contour of SSH within the Loop Current is more than 60 dyn cm higher than the northeastern side of the outflow to the Straits of Florida and some 45-50 dyn cm higher than the western side of the inflow from the Yucatan Channel, where water depths are less than 800 m. The sea surface is depressed around the margins of the basin, as is the case for the mean hydrographic SSH field and for the field of model SSH output (Section 5.3). There is some hint of increasing dynamic topography to the west centered near 24°N (see also Figure 5.1-8) and a general lowering of sea level in the Bay of Campeche. Again this is consistent with the mean dynamic topography. Similar features were seen by Nowlin and McLellan (1967) in their map of dynamic topography of the sea surface relative to 1000 db. The dynamic topography of 1500 db relative to 800 db for cruise 62-H-3 shows a pattern remarkably similar to that shown by the mean field (Figure 5.1-7).

5.2 Statistical Description of Near-Surface Velocity Field from Drifters

The drifter data set acquired is described in Section 3.1. We used the drogued drifter data (excluding SCULP data) to produce a climatology of near-surface flow. The drifters used were drogued at depths from 6 to 200 m.

The drifter fixes were subjected to initial quality control procedures. Records with only one or two points were removed. Removed from further consideration were fixes that: gave locations over land, resulted in speeds between consecutive fixes of more than 350 $cm \cdot s^{-1}$, or that were within 1 km in space and 1 hr in time from a consecutive fix. Positions of all individual drifters were plotted and examined by eye for unusual behavior, including quasi-stationary behavior and positions clearly generated to test drifter functionality while aboard a platform. Drifter records with gaps longer than 2 days were treated as separate records. The resulting data set consists of 1397 records, from the period 1989-1999.

Drifter positions were fit with a moving cubic spline to produce drifter positions at 6-hr intervals. Velocities were obtained for each pair of fixes. Then consecutive velocities were averaged to obtain the velocity corresponding to each spline-fit drifter location except the first and last position in a drifter record. The resulting drifter velocity estimates were grouped in 0.5°x 0.5° bins and averaged for selected time periods. If there were fewer than 10 estimates in a bin for the time period, no average was reported.

In Figure 5.2-1 are shown the total number of drifter velocity estimates for each 0.5° bin in the Gulf of Mexico and northwestern Cayman Basin. Numbers over the deep water Gulf are in the hundreds except for southern Campeche Bay where numbers are smaller. Numbers and data are plotted at the center of the 0.5° bins; any datum or number that appears to be over land

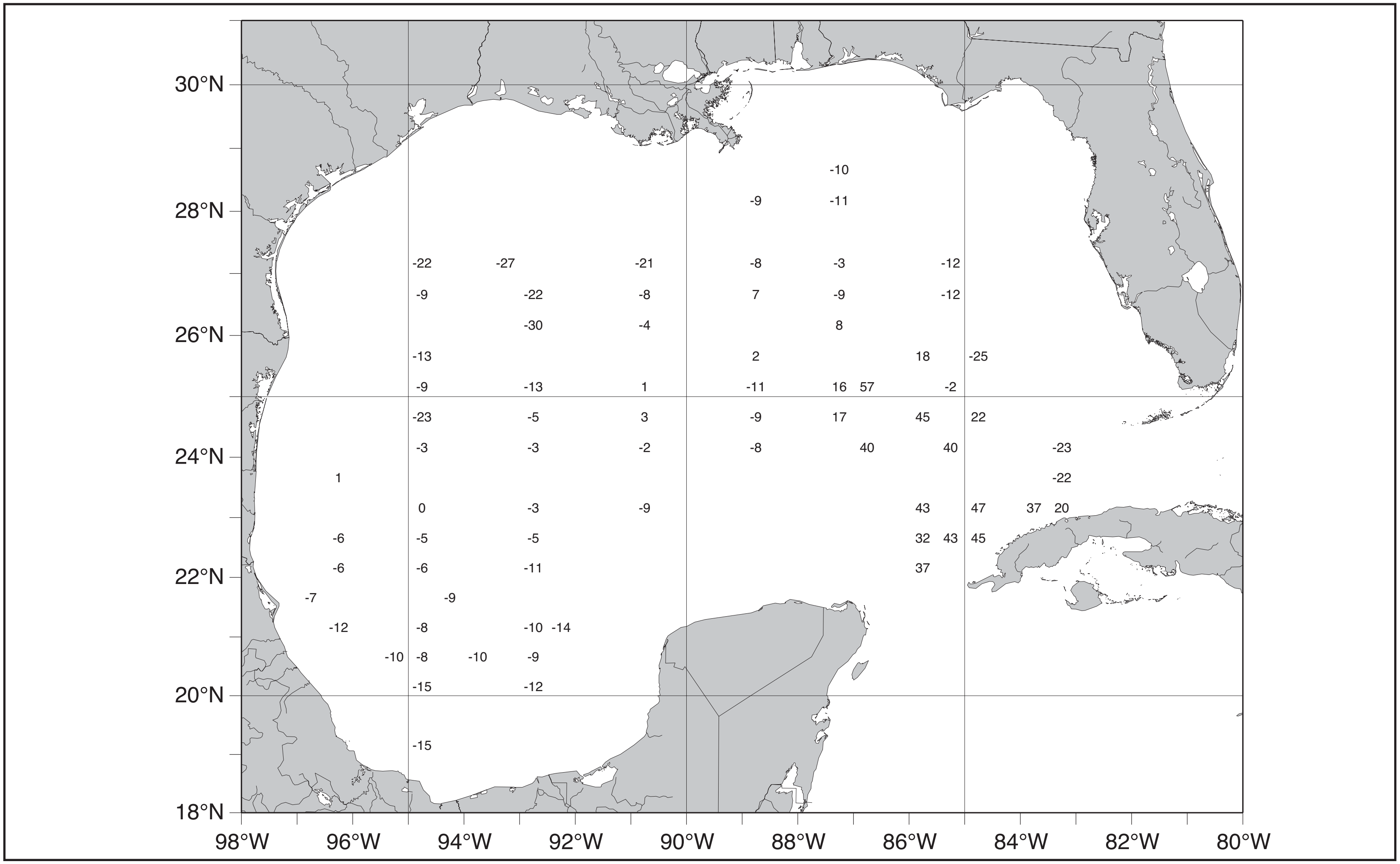

Figure 5.1-8. Dynamic height values (dyn cm) for the sea surface relative to 800 db based on data from *Hidalgo* cruise 62-H-3 in February-March 1962. An area average of 114.6 dyn cm was removed from all values.

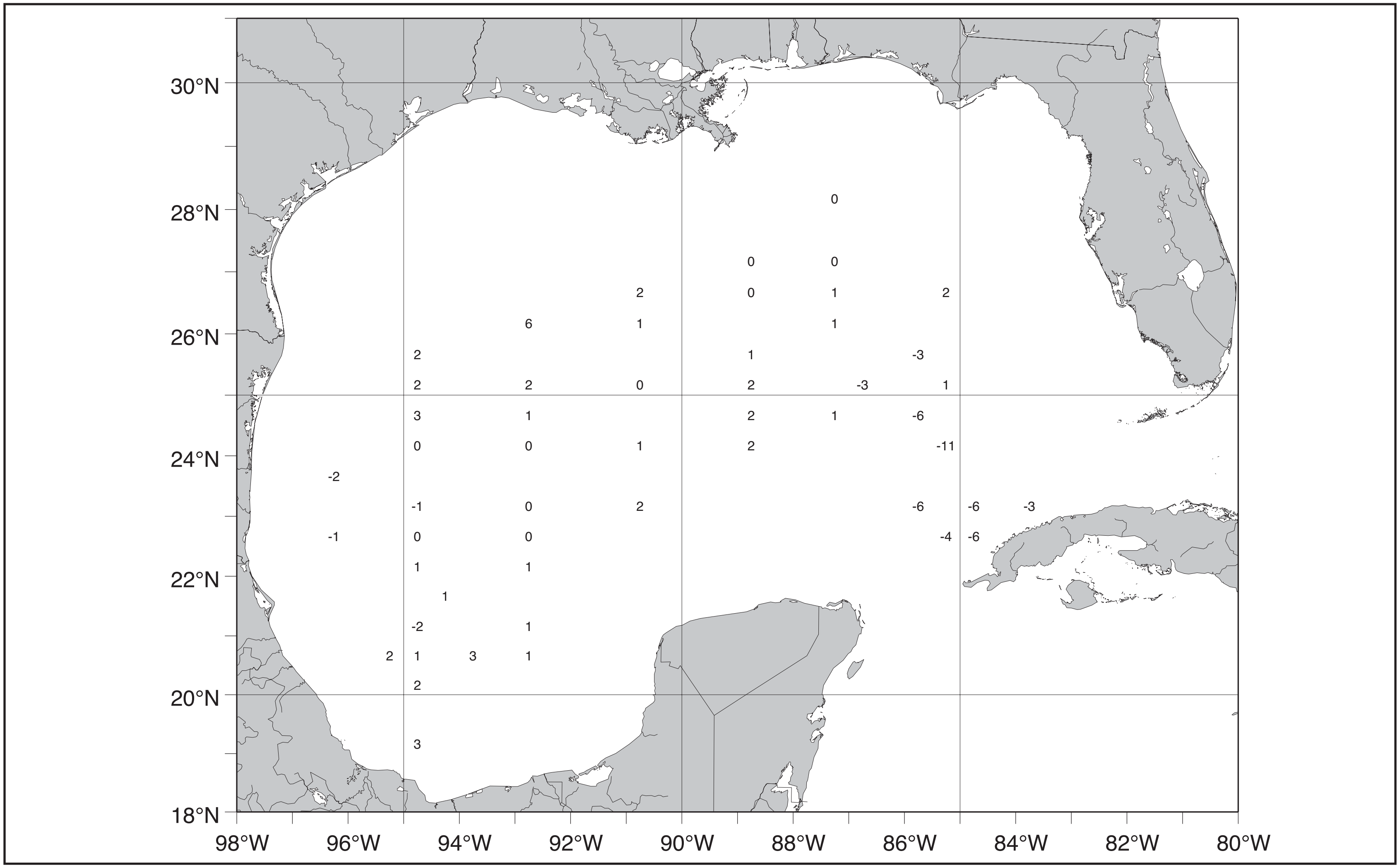

Figure 5.1-9. Dynamic height values (dyn cm) for 1500 db relative to 800 db based on data from *Hidalgo* cruise 62-H-3 in February-March 1962. An area average of 40.3 dyn cm was removed from all values.

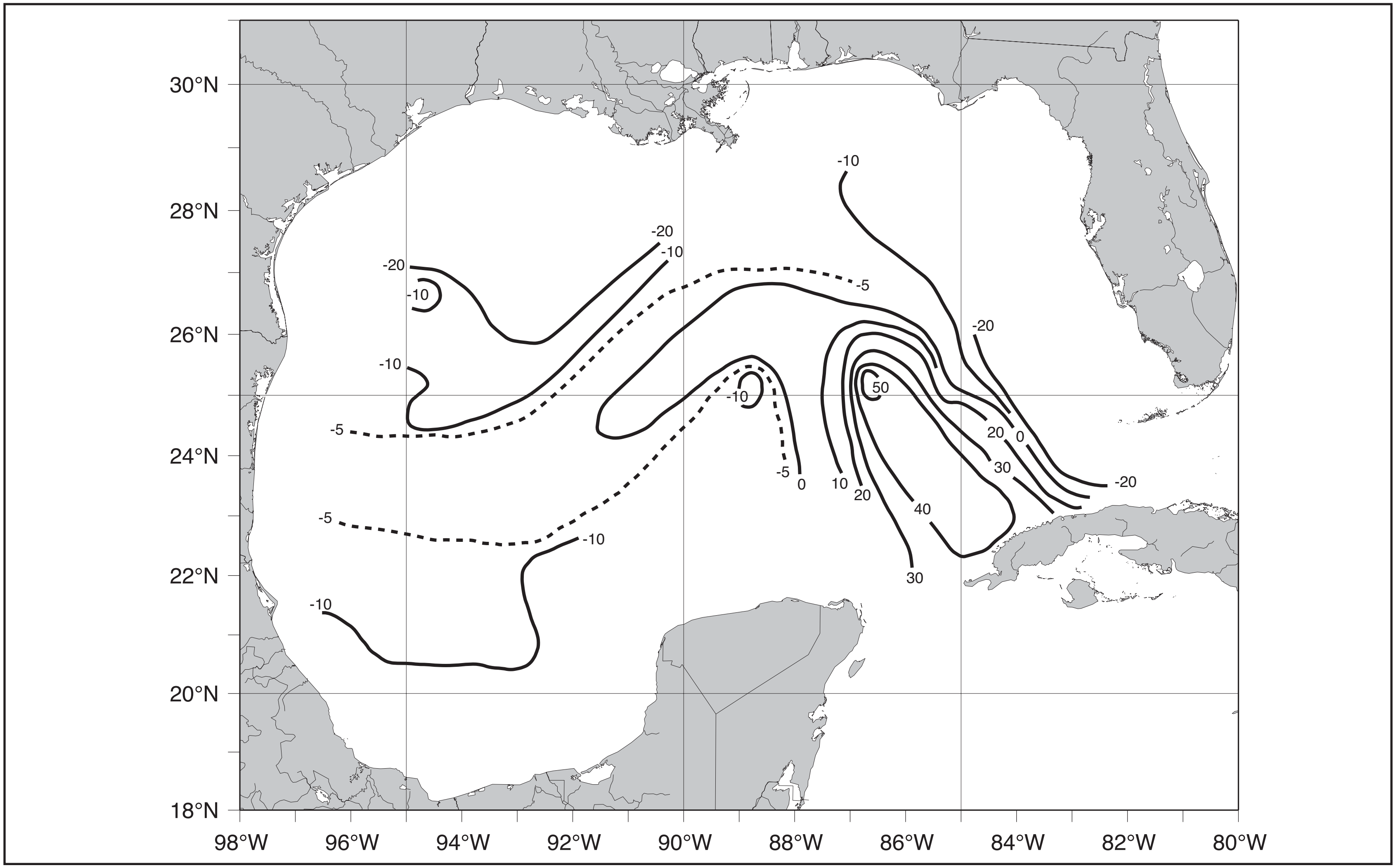

Figure 5.1-10. Hand-contoured field of dynamic topography (dyn cm) of the sea surface relative to 800 db using values shown in Figure 5.1-8.

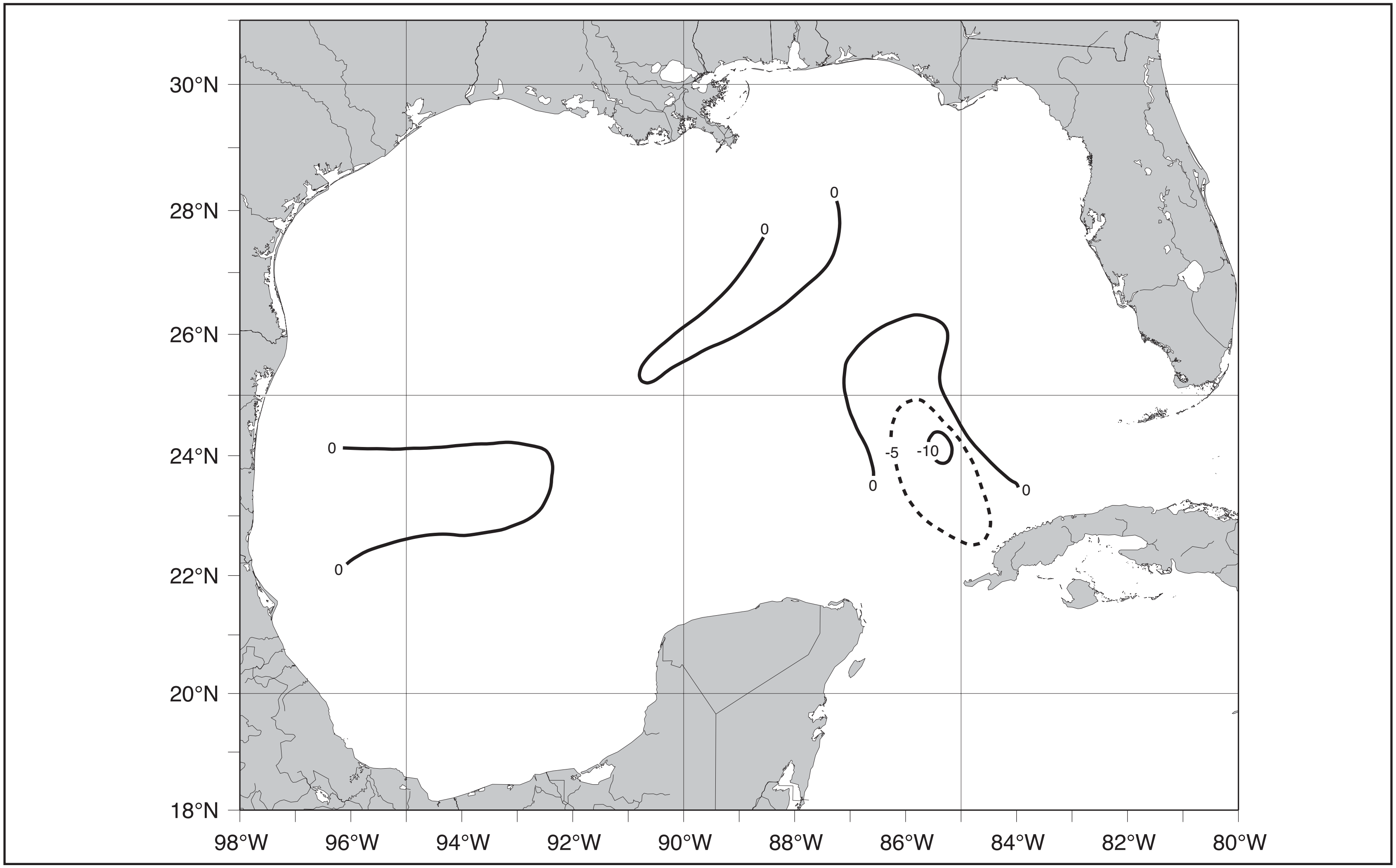

Figure 5.1-11. Hand-contoured field of dynamic topography (dyn cm) of 1500 db relative to 800 db using values shown in Figure 5.1-9.

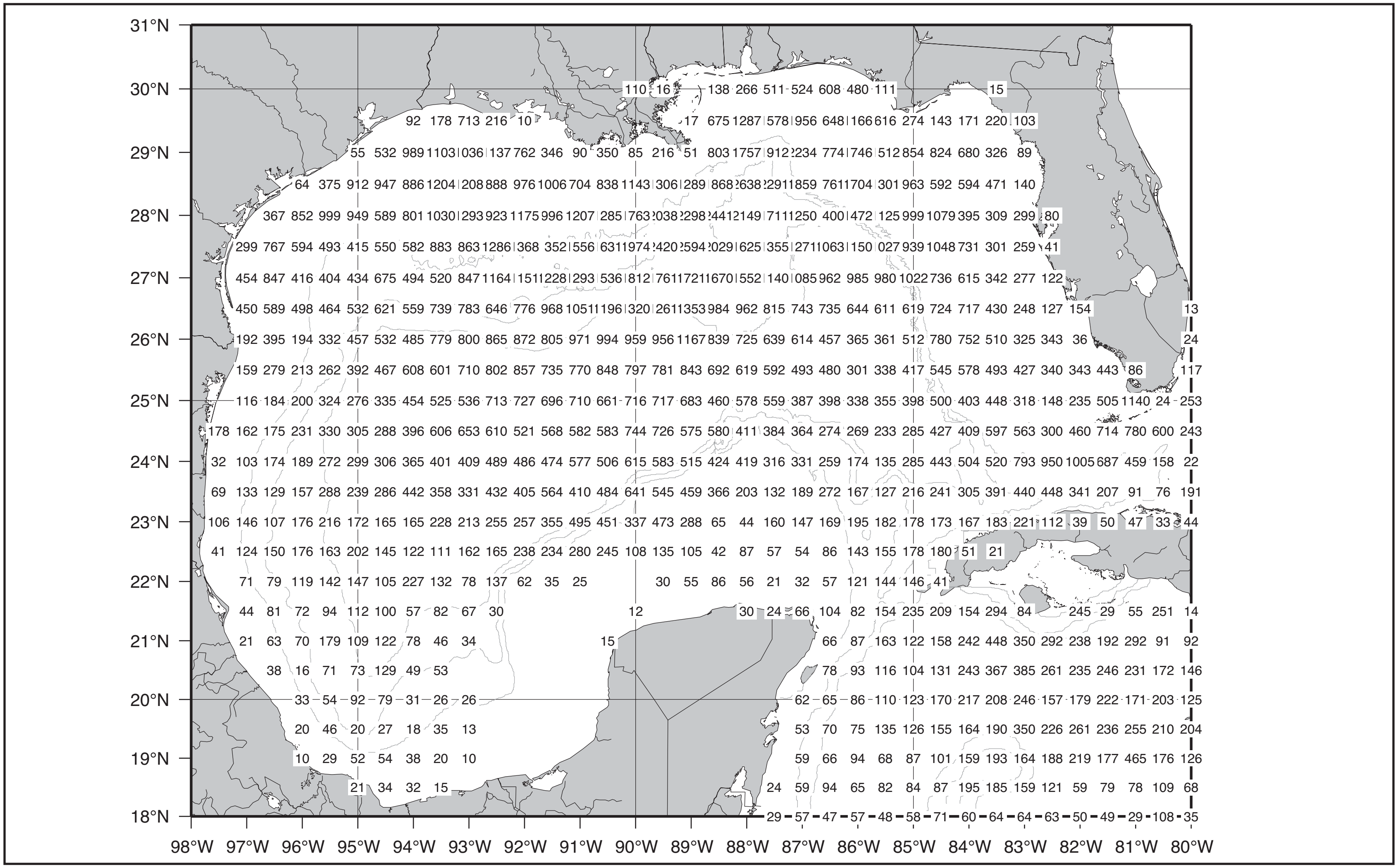

Figure 5.2-1. Numbers of near-surface velocity estimates in each 0.5° x 0.5° bin from spline-fit positions of drifters drogued at depths between 6 and 200 m during the period 1989-1999. Shown are the 200-, 1000-, and 3000-m isobaths.

represents the information associated with the oceanic portion of the box. The orientation angle and magnitudes of the major and minor principal axes of the variance ellipses are estimated from the variances of the vector velocity fluctuations in each gridded bin according to the method given in Emery and Thompson (1997).

Before presenting the results, there are several caveats that should be noted. First, drifters tend to undersample the high current core of the Loop Current and rings since most curl away from these regions and are never trapped in the core. Second, drifters are usually deployed in the northern Gulf, not the southern Gulf. Third, during the early years of monitoring in the Gulf of Mexico, more drifters were deployed in the summer when AVHRR imagery was poor than in other seasons. Finally, the year-to-year buoy sampling has varied widely. These factors can lead to temporal and/or spatial sampling biases.

The fields of vector velocity and variance ellipses are shown in Figures 5.2-2 and 5.2-3, respectively. Seen is a westward intensification of the Yucatan Current in the western Cayman basin with strong inflow to the Gulf through the Yucatan Channel. Variance ellipses are elongated in the direction of mean flow in this current regime. Some outflow is seen just west of Cape San Antonio. Energetic westward flow is seen in the zonal band between 22° and 24°N extending to the Mexican shelf. South of that flow a cyclonic circulation is seen in the Bay of Campeche. Large variances are seen over the Campeche Shelf and shelf south of the Bay of Campeche. Evidence appears for an anticyclonic feature in the west-central Gulf—centered about 24.5°N, 94.5°W with westward intensification. There also is anticyclonic circulation over the central deep Gulf, centered near 25.5°N, 90°W. The outflowing limb of the Loop Current leading into the Straits of Florida shows large speeds and variances, elongated more in the mean flow direction as one moves into the straits. Variances are large in the deep water region of the Gulf, especially to the east, where the mean currents are greatest. In the long-term average vector field, the lack of closure between inflowing and outflowing limbs of the Loop Current likely results from the separation of eddies from that current.

Seasonal patterns were prepared and studied. We show in Figures 5.2-4 and 5.2-5 the average vectors for summer (June—August) and winter (December—February) seasons, Figures 5.2-6 and 5.2-7 show the numbers of drifter velocity estimates in each bin used to produce the averages in Figures 5.2-4 and 5.2-5, respectively. With this information the reader can estimate the standard error of the estimate of seasonal sample vectors, assuming the data are random realizations from a Gaussian estimate. The individual variance ellipses by season are all similar and are merely small sample size versions of the ellipses based on all seasons (Figure 5.2-3) and are not shown. Fall is September—November; Spring is March—May.

The velocity estimates in summer (Figure 5.2-4) in the Yucatan Current and in the Bay of Campeche are sparse relative to other seasons (exemplified by Figure 5.2-5). In fact the Loop Current in summer seems confined to an outflow. Clearly this must be the artifact of the limited sample size. The rendition of the inflowing part of the Loop Current is vulnerable to bias for a small sample of drifter realizations that may coincide with an eddy separation event.

Only for the winter season do the average vectors illustrate the classic picture of continuous Loop Current through the eastern Gulf (Figure 5.2-5). Loop Current representations in the spring and fall vector fields are similar to the long-term mean shown in Figure 5.2-2. As seen in Table 6.2-1, Sturges and Leben (2000) detailed Loop Current eddy separation events for a period that included this 1989-1999 drifter data set. For that period, they estimated five eddy separations each in summer and fall, four in spring, but none in winter. We speculate that the long-term mean picture and the seasonal pictures for spring, summer, and fall do not show the classic continuous Loop Current because of eddy separations; whereas the winter picture does

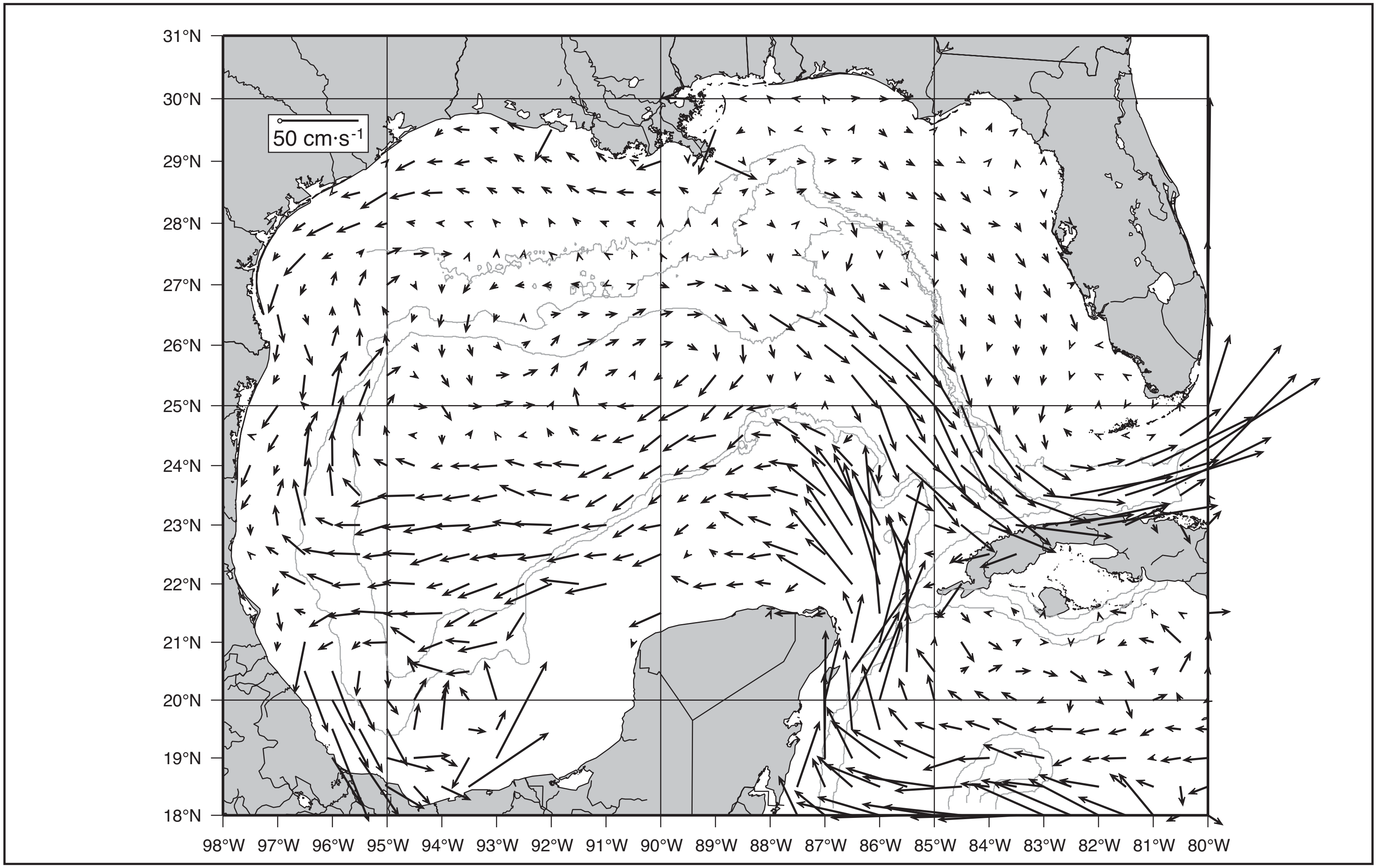

Figure 5.2-2. Near-surface velocity estimates for each 0.5°x 0.5° bin based on averaging all drifter velocity estimates in that bin for the period 1989-1999. Shown are the 200-, 1000-, and 3000-m isobaths.

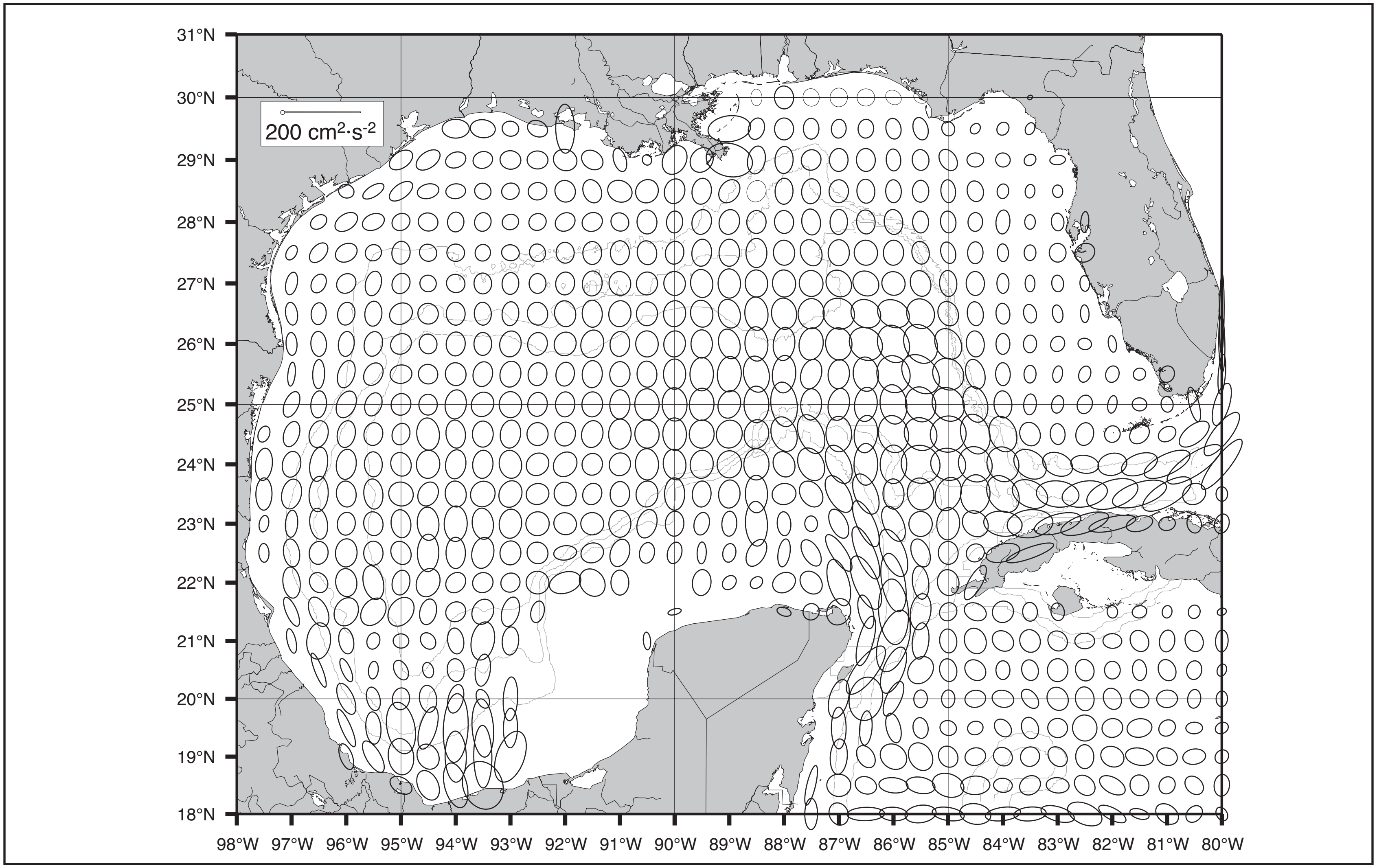

Figure 5.2-3. Variance ellipses corresponding to the long-term near-surface velocity estimates shown in Figure 5.2-2.

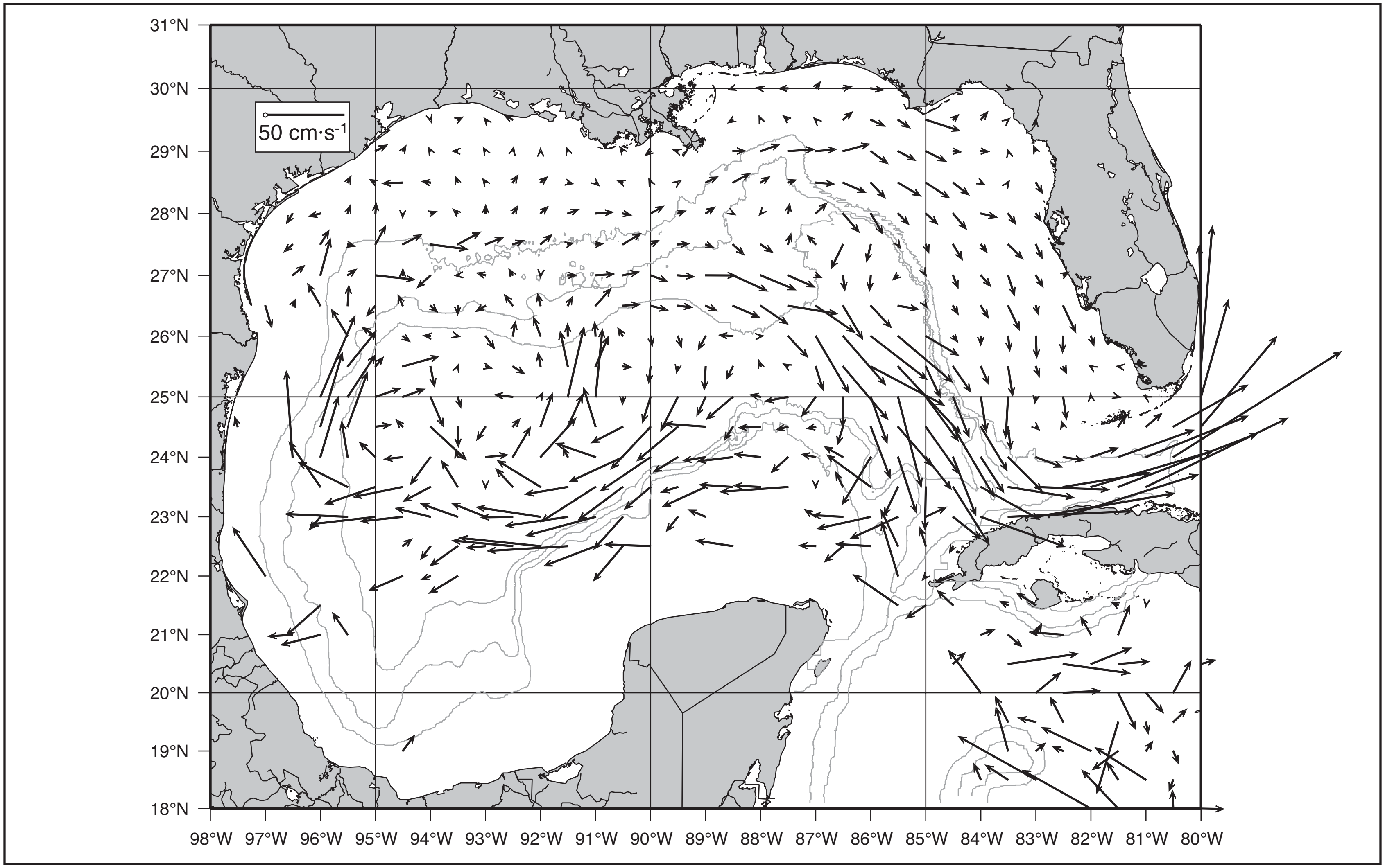

Figure 5.2-4. Summer near-surface velocity estimates for each 0.5°x 0.5° bin based on averaging all drifter velocity estimates in that bin during summers of 1989-1999. Shown are the 200-, 1000-, and 3000-m isobaths.

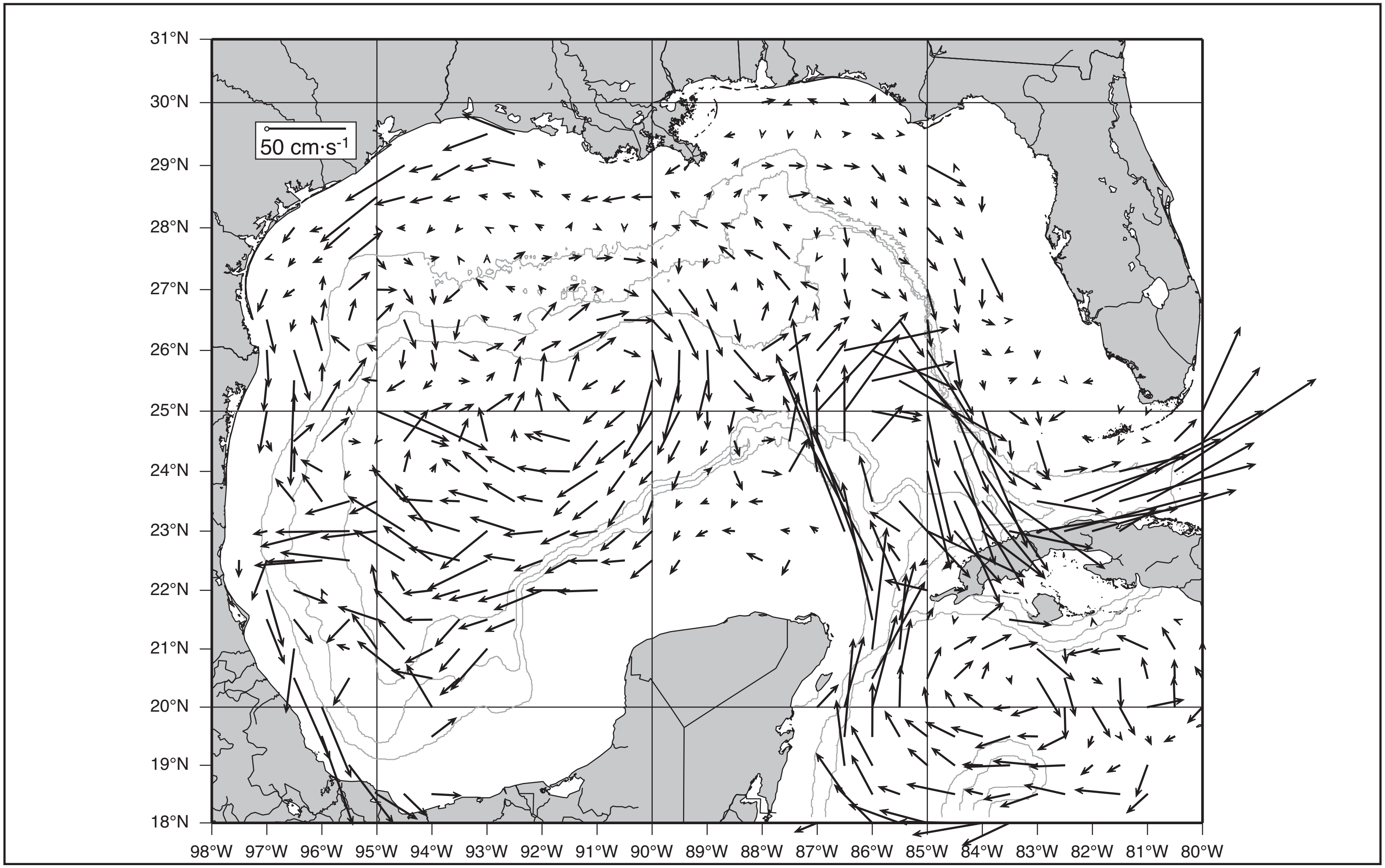

Figure 5.2-5. Winter near-surface velocity estimates for each 0.5°x 0.5° bin based on averaging all drifter velocity estimates in that bin during winters of 1989-1999. Shown are the 200-, 1000-, and 3000-m isobaths.

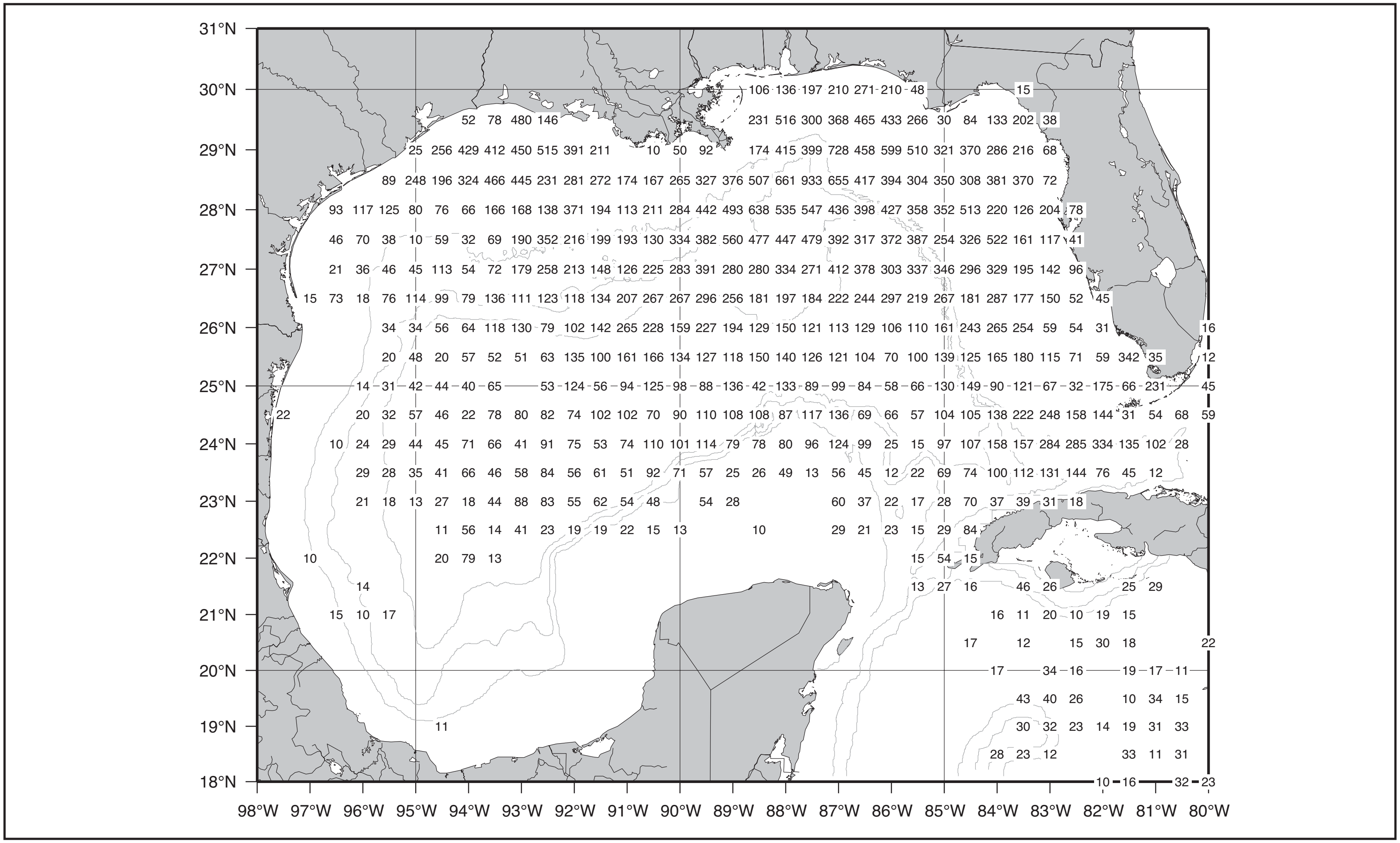

Figure 5.2-6. Numbers of summer near-surface velocity estimates in each 0.5°x 0.5° bin from spline-fit positions of drifters drogued at depths between 6 and 200 m during the summers of 1989-1999. Shown are the 200-, 1000-, and 3000-m isobaths.

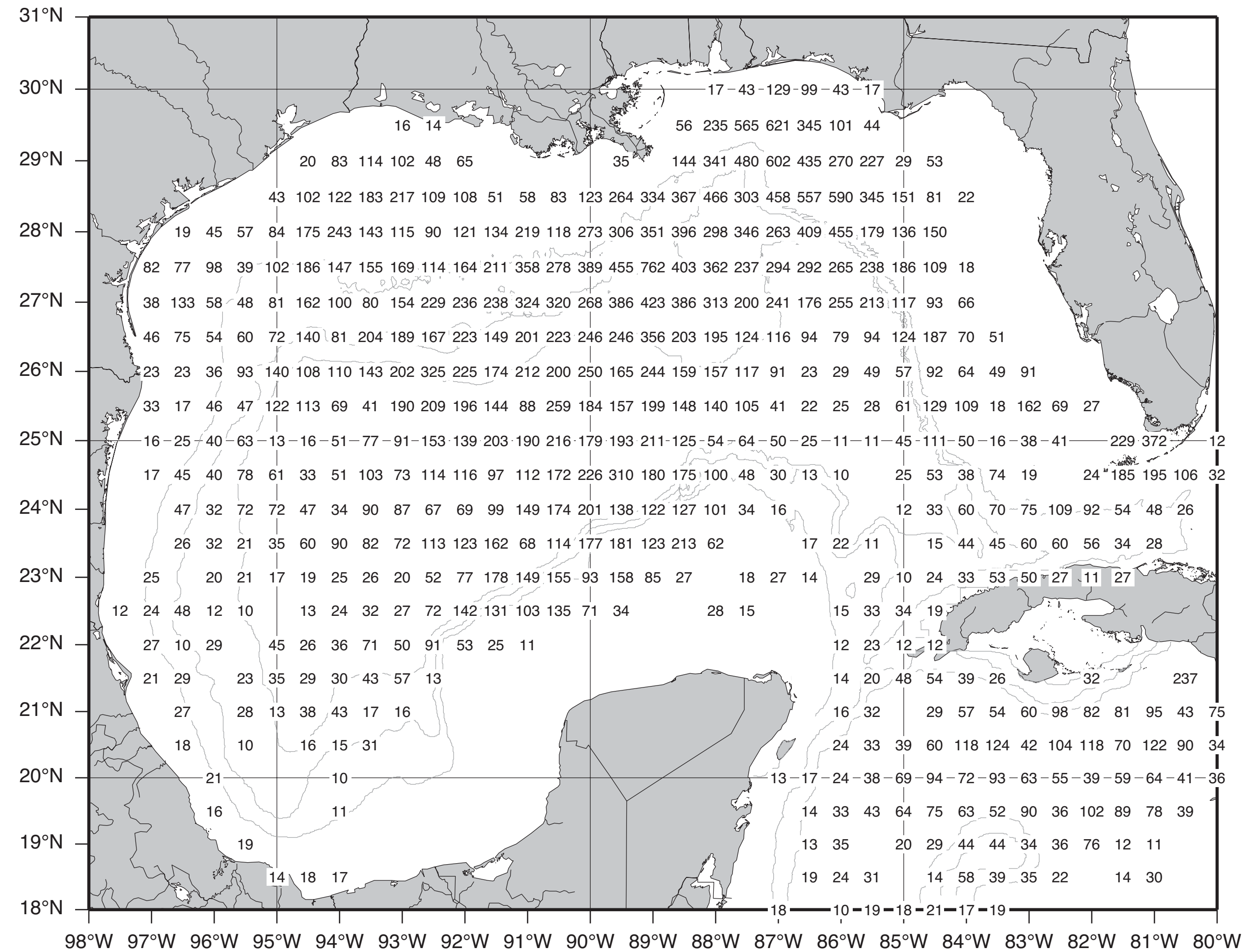

Figure 5.2-7. Numbers of winter near-surface velocity estimates for each 0.5°x 0.5° bin from spline-fit positions of drifters drogued at depths between 6 and 200 m during winters of 1989-1999. Shown are the 200-, 1000-, and 3000-m isobaths.

because of the absence of eddy separations during that season for the period studied. Because there was no deep penetration of the Loop Current into the Gulf during the winters considered, the northern limb of the Loop Current in Figure 5.2-5 is seen at about 26°N.

The strong westward flow across the Gulf in the band 22°-24°N is seen in the summer and fall (exemplified by Figure 5.2-4) but not in winter and spring (exemplified by Figure 5.2-5), even though the numbers of velocity estimates are similar. In winter and spring the circulation regimes of eastern and western Gulf seem more separated than in summer and fall. This might be related to the annual cycle of wind stress curl over the Gulf. Or it might be related to the fact that there were more Loop Current eddy separations in summer and fall (five in each season) for the period examined, but only four in spring and none in winter, which shows the most separation between eastern and western circulation regimes.

The western boundary current is strongest in summer (Figure 5.2-4) and weakest in winter (Figure 5.2-5). This tends to support the wind-driven signal proposed by Sturges (1993) who found strongest currents in July and weakest in October. Despite the small sample sizes for summer and winter in the western boundary current region, it can be shown that the boundary current strengths for summer and winter are significantly different at the 95 percent confidence level.

The fall vector representation (not shown) appears to have the best overall coverage, it is similar to a less smooth version of the long-term mean (Figure 5.2-2). The fall picture is the only one with sufficient data to give a definitive cyclone in the Bay of Campeche. It seems likely that because of seasonal variability of that feature (Vazquez 1993) the long-term mean may not exhibit as clear a picture of the Campeche cyclone as good seasonal pictures would. Because most drifters were deployed north of 25°N, the relative paucity of observations along the Mexican coast and the Bay of Campeche in summer may be an indication of the strong northward flow along the western Gulf boundary in summer (i.e., there is no conduit from the northern to the southern Gulf in that season).

Downcoast flow (Mississippi River toward Mexico) occurs along the northwestern shelf region of the Gulf for non-summer (exemplified by winter). In summer, the shelf flow derived from drifter data is very weak, in agreement with the SCULP drifter data (Herring et al. 1999). Current meter and hydrographic data on the other hand show significant upcoast flow in the summer (Nowlin et al. 1998a). The drifter-derived results for summer and winter are based on comparable sample sizes (Figures 5.2-6 and -7).

Near-surface flow over the West Florida shelf is strongly southward during summer. During fall and spring it is relatively weak and non-uniform in direction. The winter picture shows relatively strong southward flow over the outer part of the northern shelf, weaker and less uniform flow over the outer part of the southern shelf.

5.3 Statistical Descriptions of Circulation from CUPOM Output

Based on model outputs from the University of Colorado Princeton Ocean Model (CUPOM), developed and operated by the Colorado Center for Astrodynamic Research, we have examined the circulation of the deepwater region of the Gulf of Mexico. In this section we present features of the mean circulation as deduced from model output. Further use of the model mean circulation is made in section 5.4 and comparisons with other estimates of the circulation are found throughout the document. In section 8, we present deductions regarding the deep circulations based on animated time series of CUPOM velocity fields at different levels within the deepwater Gulf.

Based on CUPOM output for the model years 1993-1999, we produced maps of currents and their variance ellipses at selected levels: sea surface, 500 m, 1000 m, 2000 m, and the first sigma level above the sea bed. The principal feature shown in the surface field is the Loop Current (Figure 5.3-1). The isobaths shown in these figures are for 200, 1000, 2000, and 3000 m. Within the loop there is a closed anticyclone just northwest of Cuba. Unlike observations, no southward flow to the Caribbean is seen west of Cape San Antonio, Cuba, because the model boundary conditions just to the south specify only flow into the Gulf. Strong flow is also seen over the continental shelves of the southern and western Gulf as well as within the deepwater portion of the western basin. As expected the variance ellipses for the surface currents (Figure 5.3-2) are largest for the region of the Loop Current. Compare Figures 5.2-2 and 5.2-3 for drifters. At the edges of the current, the semi-major axes of variance are oriented parallel to the record-length flow. Along the center axis of that current they are more nearly circular and appear oriented NE-SW, indicating highest variability in a direction normal to the inflowing and outflowing limbs of the current regime. Variance ellipses are more nearly circular elsewhere in the deep water regions of the Gulf; they decrease in size westward and southward, indicating a path of high variability from the Loop Current into the north-central Gulf. Ellipses over the shelves tend to be elongate, with major axes oriented along shelf. Highest variability is indicated along the western shelves.

As at the surface, record-length currents at the 500-m level (Figure 5.3-3) are weaker at the maximum extent of penetration of the Loop Current into the Gulf than the currents within the inflow or outflow limbs of that current, probably because of intermittent intrusion of the loop into the Gulf and the shedding of eddies. Again there is a closed anticyclone within the loop. There is strong clockwise flow intensified offshore of the continental shelves extending from the Campeche Bay to near DeSoto Canyon. In the north-central Gulf just offshore of the 3000-m isobath and in the northwest between the 2000 and 3000-m isobaths the record-length flow at 500 m is seen to be counterclockwise, resulting in a shear zone on its inshore side. Centered near 23.5°N, 94°W in the central western Gulf is an anticyclone. Variance ellipses for the 500-m level flow (Figure 5.3-4) show strongest variability in the deepwater regions of the Gulf, as expected due to the presence of surface-intensified eddies. Near the 500-m isobath the strong effect of bathymetry on the directionality of the variability is seen.

At 1000 m the record-length model currents (Figure 5.3-5) do not show a Loop Current. The strongest feature seen in the eastern Gulf at that level is an intense cyclone centered near 24°N, 85°W. This is the location at which lower level cyclones are seen to form in animations of the model output during the separation of Loop Current eddies. A weaker cyclone is seen to the northwest, centered near 27°N, 86°W. The directions of record-length currents along the boundary of the Campeche Shelf change with location, unlike those at 500 m which are essentially westward. Other than that, the pattern of record-length circulation in the western Gulf is very similar at 1000 m to that at 500 m. There is an anticyclone in the west central Gulf, centered near 23.5°N, 94°W, which is more prominent, relative to other background circulation, than at 500 m. Also clearly seen at 1000 m is a counterclockwise current directed westward and then southward situated between the anticyclone in the central western Gulf and the clockwise flow near the 1000-m isobath in the west and north. In the central Gulf there is some evidence of cyclonic flow in the deep basin (within the 3000-m contour). Variances at 1000 m (Figure 5.3-6) are largest within the 3000-m contour. They decrease westward from maxima in the region of the cyclones under the Loop Current. The effect of bathymetry on directionality of variability is apparent near the 1000-m isobath.

Record-length model currents at 2000 m are clearly intensified as a cyclonic flow around the basin near the 3000-m isobath (Figure 5.3-7). These flow directions agree rather well with those of currents at 1000 m, and even at 500 m. As in the upper layers, an anticyclone is seen over the

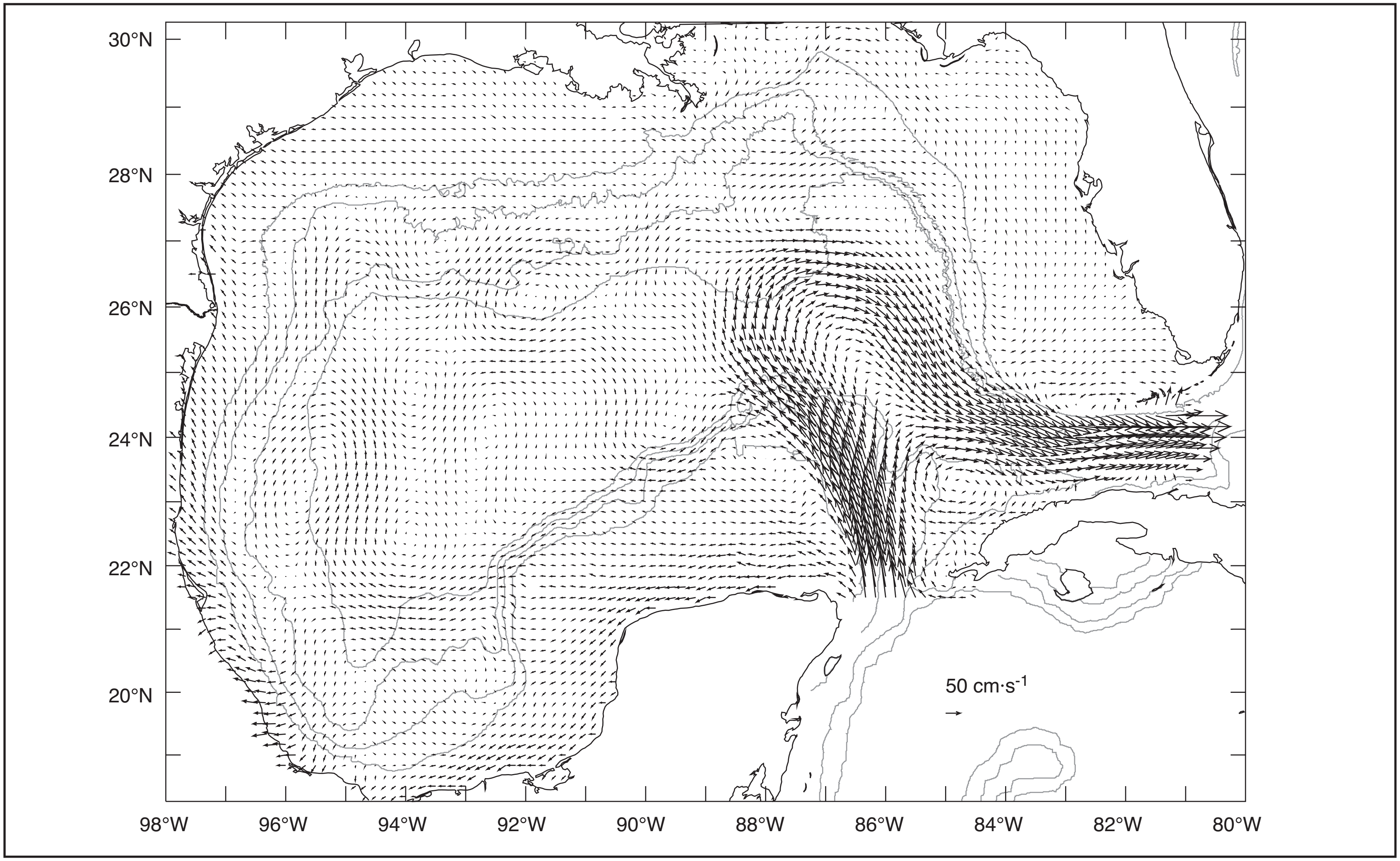

Figure 5.3-1. Record-length mean surface current vectors constructed from University of Colorado Princeton Ocean Model output for the years 1993-1999. Shown are the 200-, 1000-, 2000-, and 3000-m isobaths.

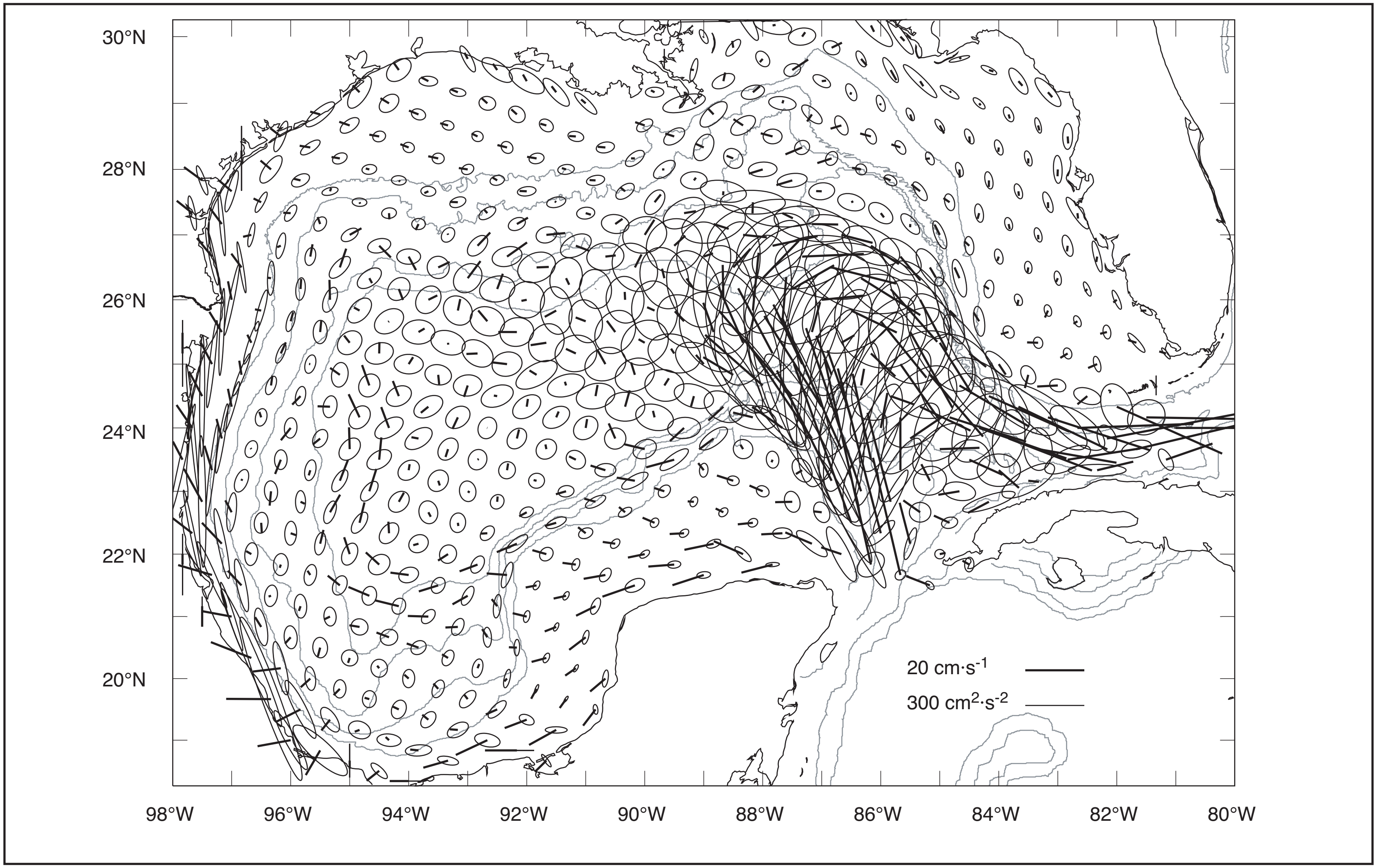

Figure 5.3-2. Variance ellipses and record-length current vectors for the sea surface constructed from University of Colorado Princeton Ocean Model output for the years 1993-1999. Shown are the 200-, 1000-, 2000-, and 3000-m isobaths.

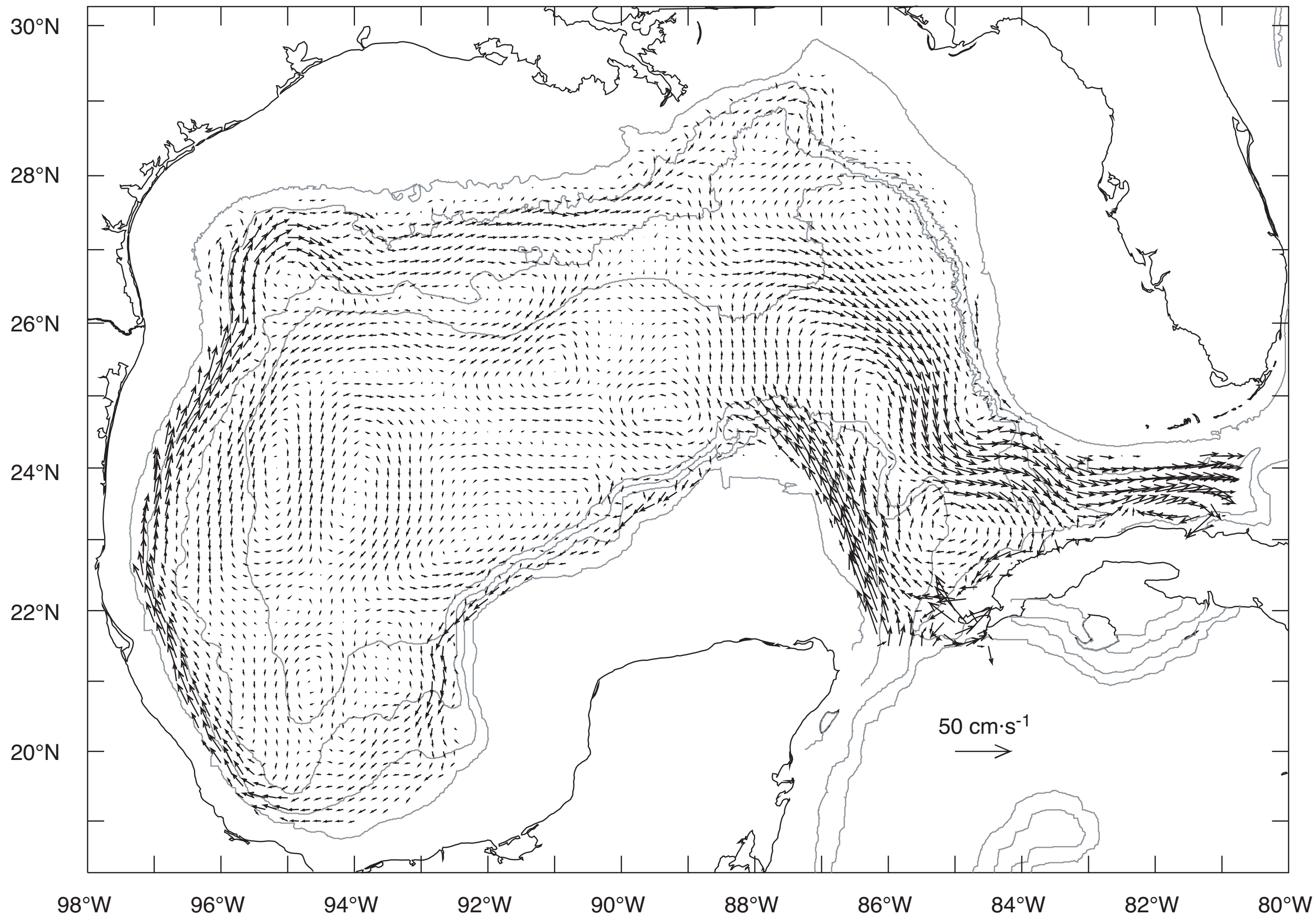

Figure 5.3-3. Record-length mean current vectors at 500 m constructed from University of Colorado Princeton Ocean Model output for the years 1993-1999. Shown are the 200-, 1000-, 2000-, and 3000-m isobaths.

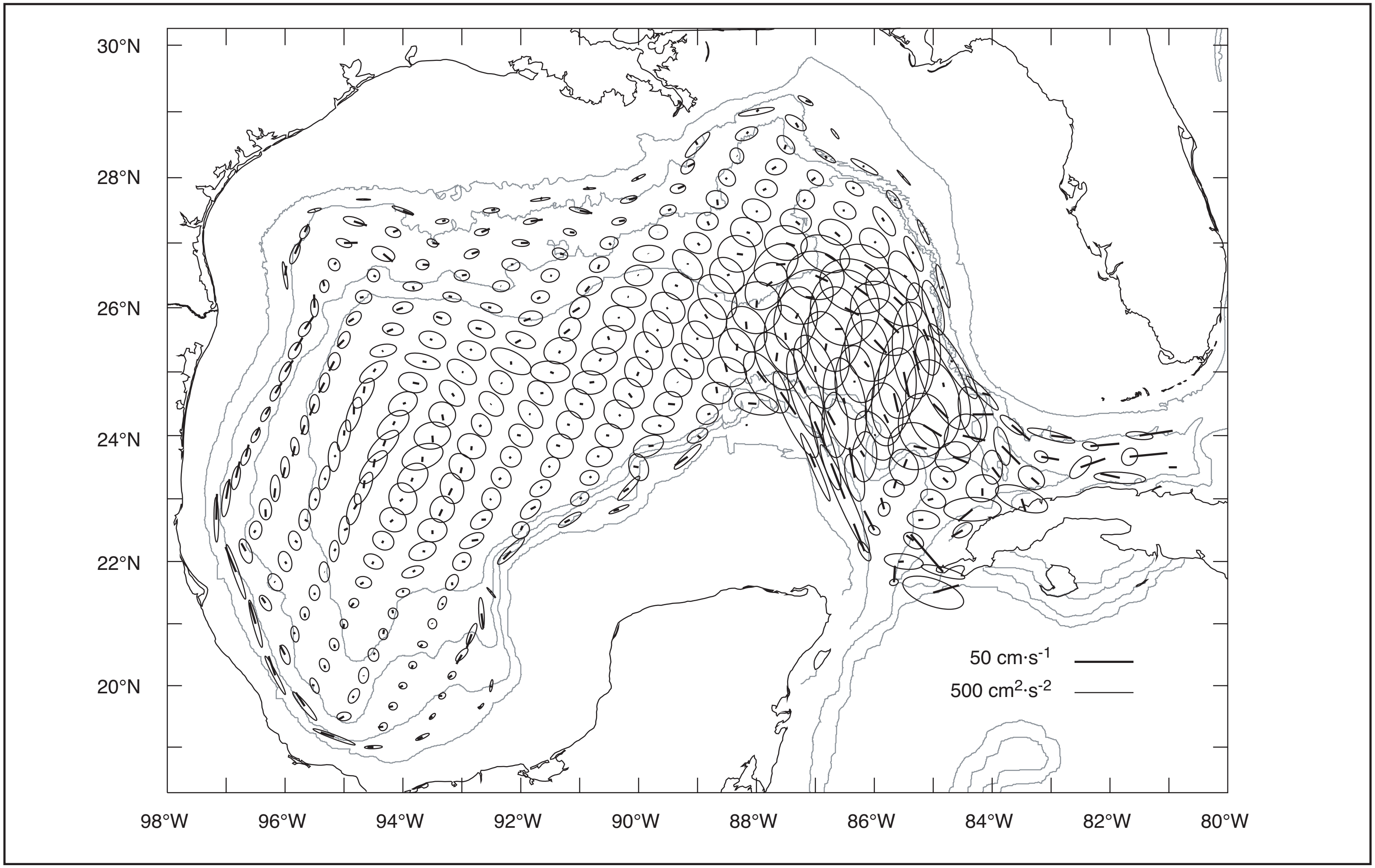

Figure 5.3-4. Variance ellipses and record-length current vectors for 500 m constructed from University of Colorado Princeton Ocean Model output for the years 1993-1999. Shown are the 200-, 1000-, 2000-, and 3000-m isobaths.

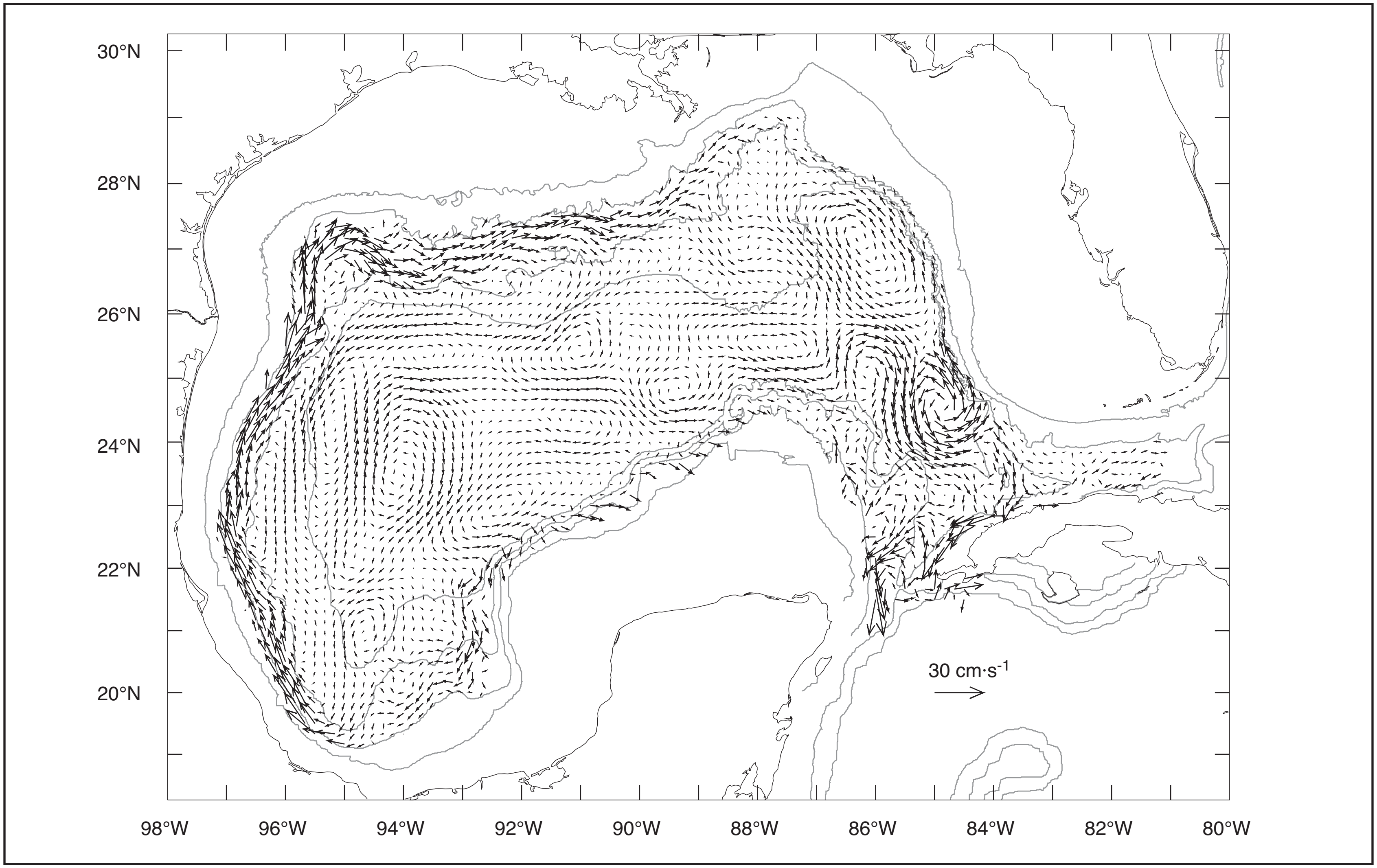

Figure 5.3-5. Record-length mean current vectors at 1000 m constructed from University of Colorado Princeton Ocean Model output for the years 1993-1999. Shown are the 200-, 1000-, 2000-, and 3000-m isobaths.

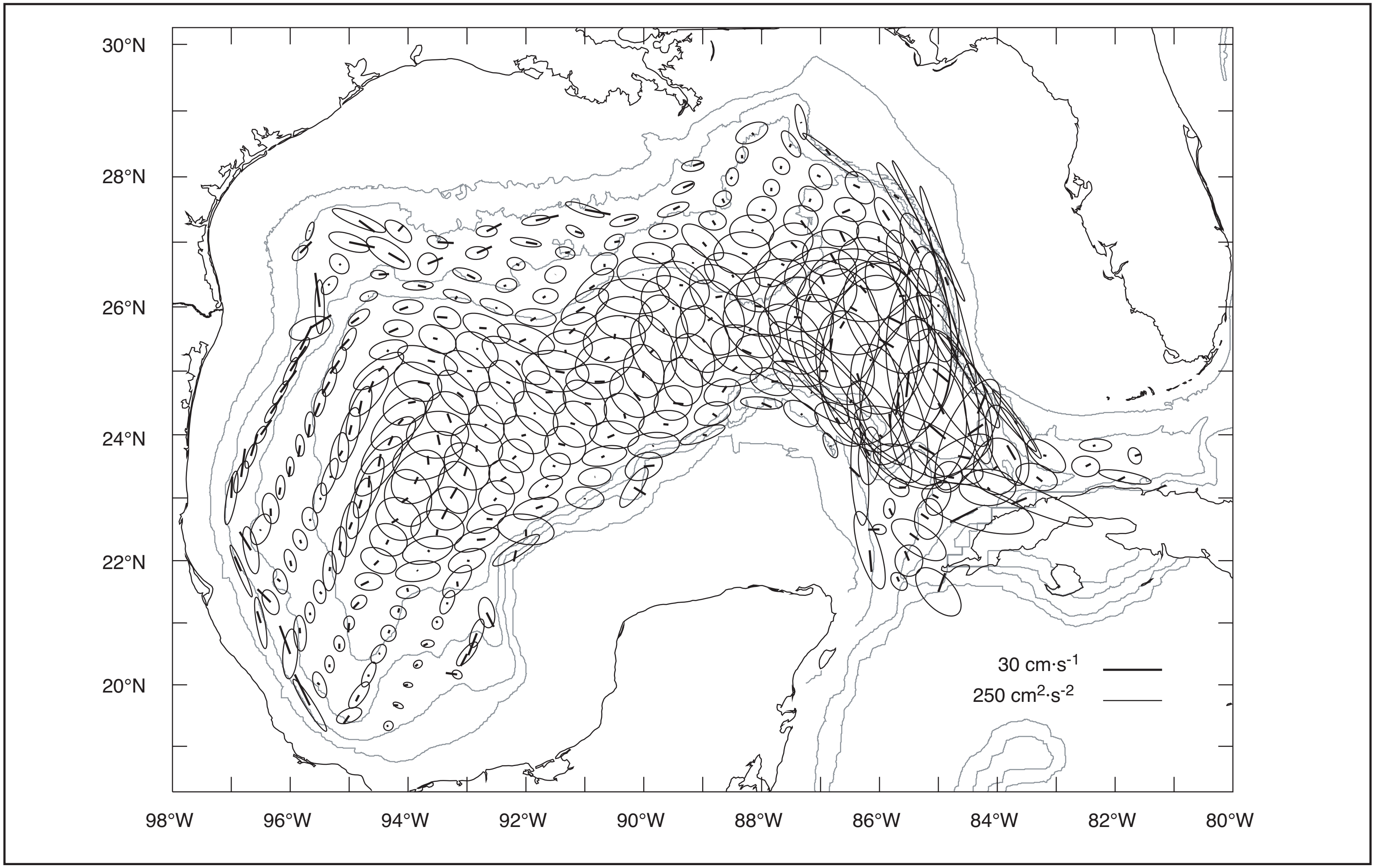

Figure 5.3-6. Variance ellipses and record-length current vectors for 1000 m constructed from University of Colorado Princeton Ocean Model output for the years 1993-1999. Shown are the 200-, 1000-, 2000-, and 3000-m isobaths.

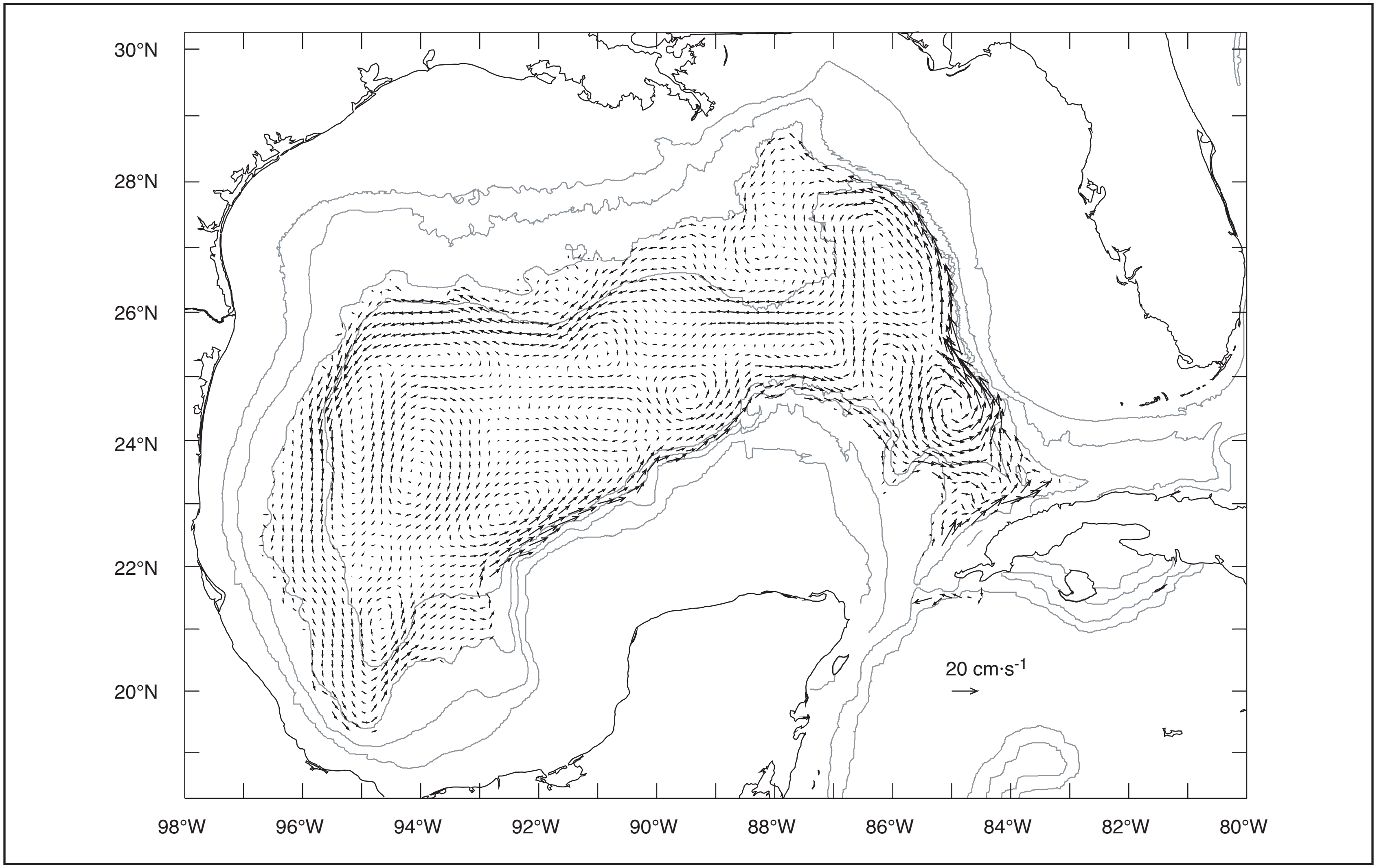

Figure 5.3-7. Record-length mean current vectors at 2000 m constructed from University of Colorado Princeton Ocean Model output for the years 1993-1999. Shown are the 200-, 1000-, 2000-, and 3000-m isobaths.

central western basin, though it is relatively weak, and the cyclones are still seen beneath the Loop Current region. The pattern of variability at 2000 m (not shown) is quite similar to that at 1000 m.

In Figure 5.3-8 are shown the record-length model currents at the first sigma level above the bottom. The clear pattern is of cyclonic flow around the basin intensified near the 3000-m isobath, in close correspondence with the currents at the same locations on the 1000 and 2000-m levels. This direction and intensification is consonant with the long-term bottom currents needed to produce the mega-furrows described in Section 6.1.3. The variance ellipses for the slope and rise region of the north, central Gulf are shown in Figure 5.3-9. Seen is an intensification of currents along the offshore edge of the Sigsbee Escarpment. The flow is directed westward along isobaths with little cross-isobath component to the variance. This is the flow regime expected for the furrows and fluke marks present in the bottom sediments of this region.

We obtained hourly model output from CUPOM on seven vertical sections extending over the continental slope in the northern Gulf of Mexico. The positions of those sections are shown in Figure 5.3-10. The mean flow normal to each of those sections was computed for the output for model years 1993-1999. Contoured fields of speed normal to each section are shown in Figures 5.3-11 through 5.3-17. Positive values indicate flow in a cyclonic direction around the basin.

In each section the mean flow is seen to be intensified in a cyclonic direction for increasing depth at the base of the slope. Of course this is in agreement with the previous results shown on level surfaces, but these figures illustrate the lateral and vertical shear over the margins of the deep Gulf. This feature is not clearly seen in Figure 5.3-15 because this section at 92°W does not extend south of the Sigsbee Escarpment.

Through section 1 there is northward flow in the upper layers over the upper slope. Further offshore the influence of the Loop Current anticyclonic flow is clearly seen in the upper ocean. Likewise, sections 3-7 show some mean cyclonic (westward) flow in the upper layers over the upper slope with anticyclonic flow further offshore. The cyclonic flow near the shelf break seems enhanced toward the as one moves to the southwest along the Texas shelf (sections 5-7).

Finally as a means of summarizing the mean circulation patterns in the CUPOM output, we produced fields of relative vorticity from the mean model circulation fields at each level. Figure 5.3-18 shows the vorticity field for the record-length horizontal velocity field at 2000 m. The truly remarkable, and heretofore unknown (if real), feature of the field is the large area of cyclonic vorticity in the eastern Gulf just southwest of the Florida continental slope. In the animated time series of circulation from the model, a deep cyclone is seen in this region most of the time; such cyclones are centered at different positions within the region of cyclonic vorticity—sometimes far to the southeast, sometimes to the north.

We also examined such statistics as variance of the vorticity fields and correlation between fields at different levels. Figure 5.3-19 shows the smoothed correlation (at zero lag) between the record-length vorticity fields at 500 m and 2000 m. The highest correlations are seen for the west-central Gulf, in particular for a rather large region centered near 23°N, 94°W. As seen in Figure 5.3-18, that is a region of anticyclonic flow. Clearly the anticyclonic flow regime, described for the surface layers by Sturges (1993), extends throughout the water column in the mean flow.

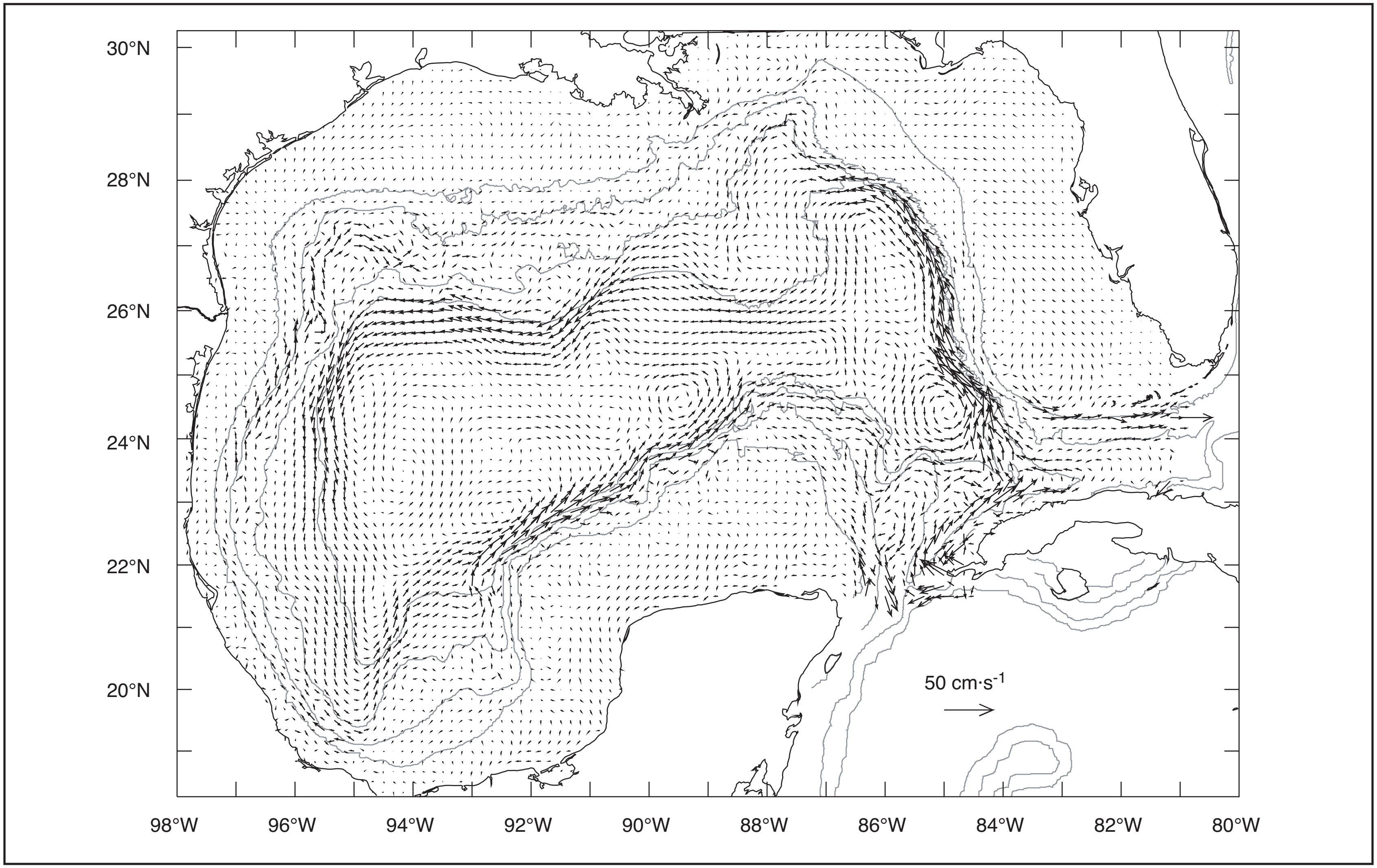

Figure 5.3-8. Record-length mean current vectors at the first sigma level above the bottom constructed from University of Colorado Princeton Ocean Model output for the years 1993-1999. Shown are the 200-, 1000-, 2000-, and 3000-m isobaths.

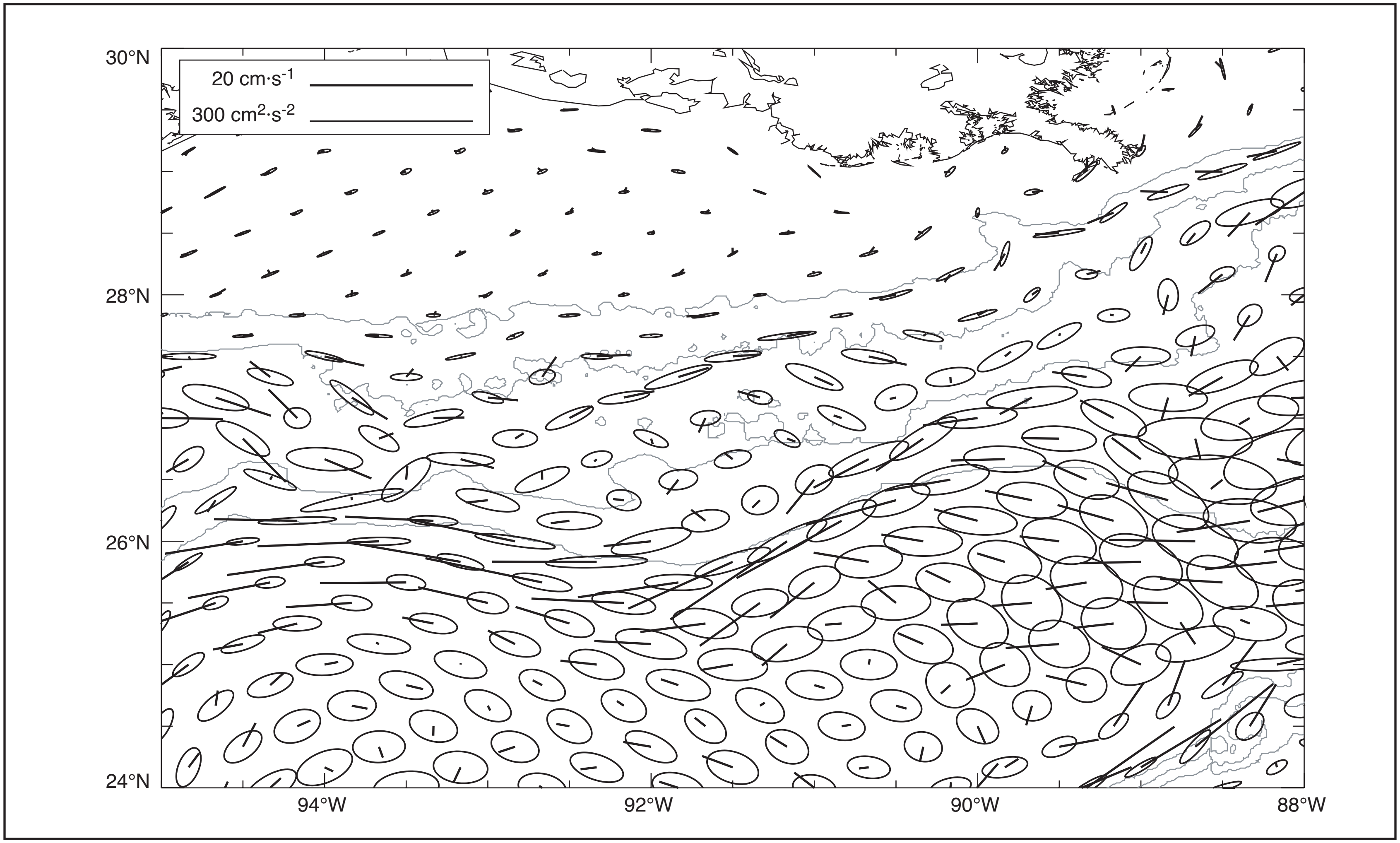

Figure 5.3-9. Variance ellipses and record-length mean current vectors at the first sigma level above the bottom constructed from University of Colorado Princeton Ocean Model output for the years 1993-1999. Shown are the 200-, 1000-, 2000-, and 3000-m isobaths.

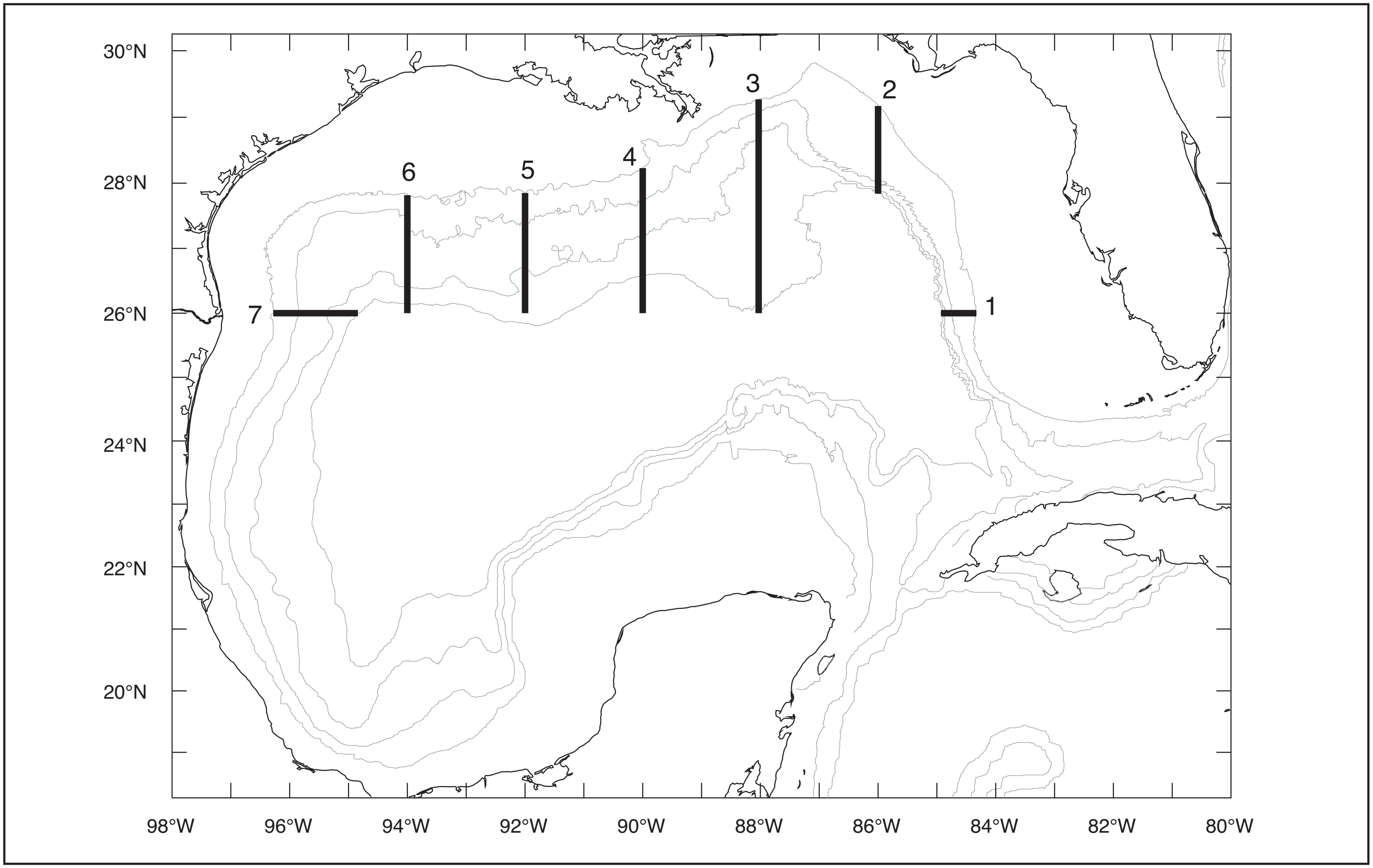

Figure 5.3-10. Locations of vertical sections from which CUPOM output was extracted hourly for the years 1993-1999. Shown are the 200-, 1000-, 2000-, and 3000-m isobaths.

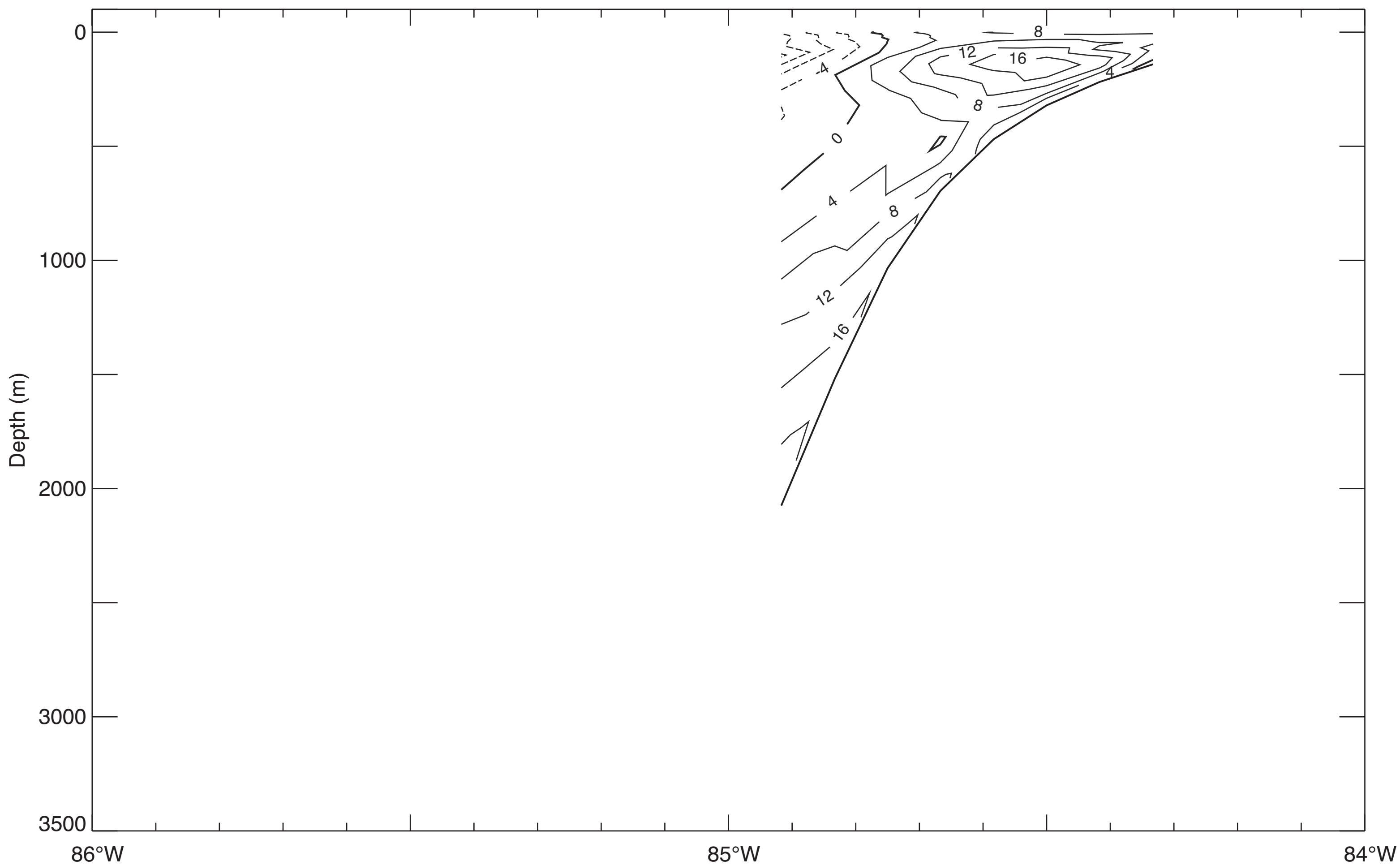

Figure 5.3-11. Mean flow ($cm \cdot s^{-1}$) normal to section 1 in Figure 5.3-10 from CUPOM output for years 1993-1999. Positive values are northward.

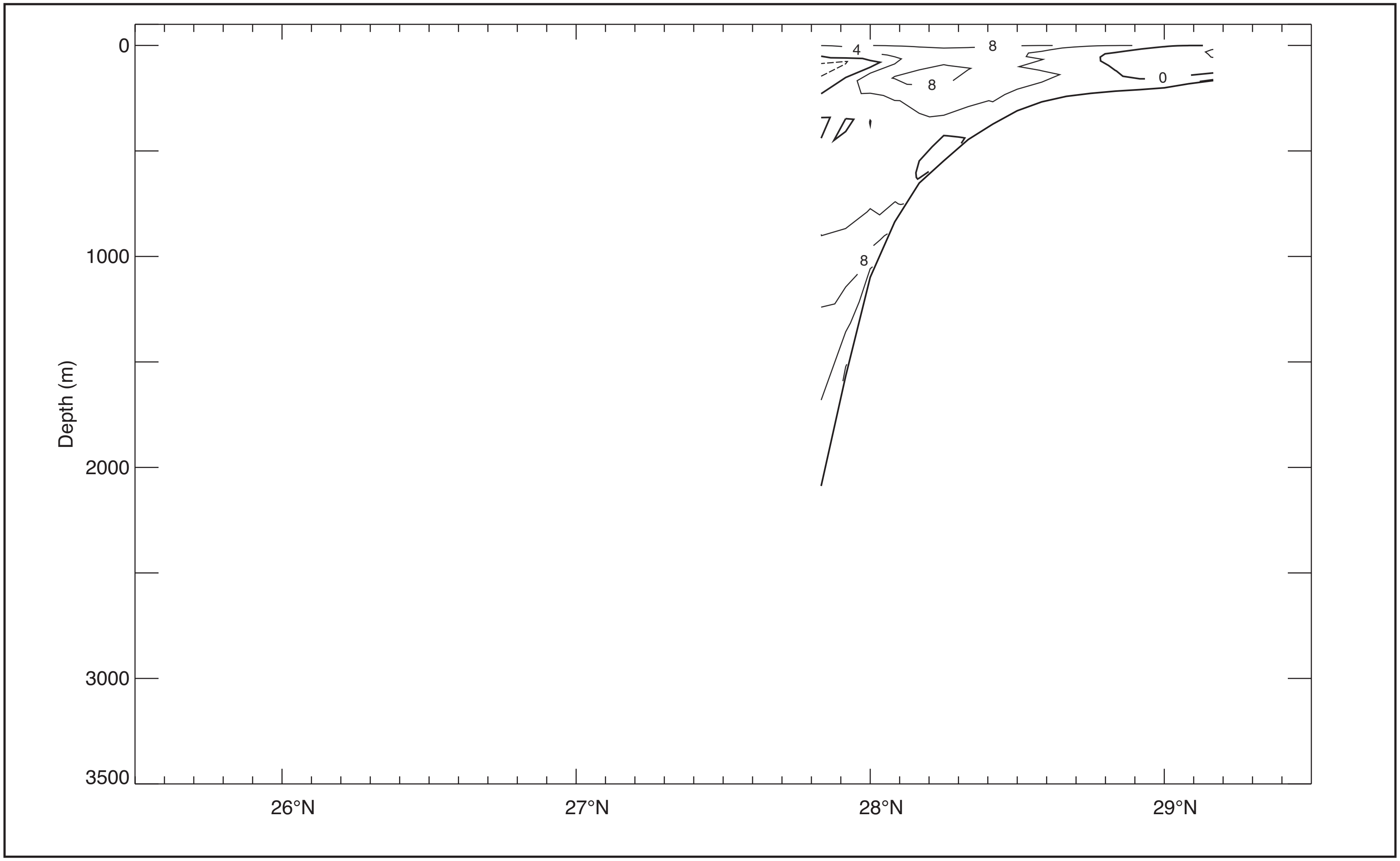

Figure 5.3-12. Mean flow (cm·s^{-1}) normal to section 2 in Figure 5.3-10 from CUPOM output for years 1993-1999. Positive values are westward.

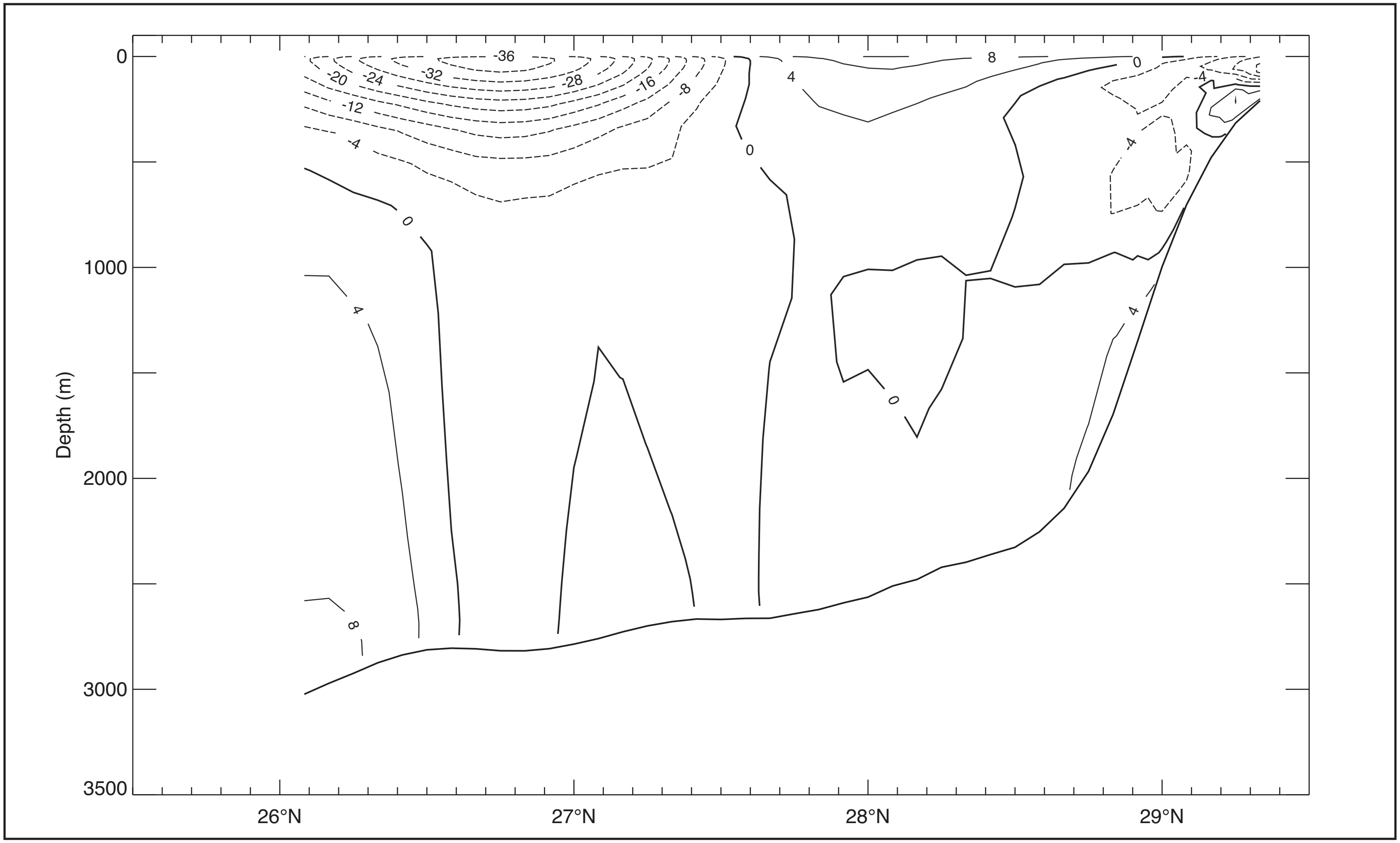

Figure 5.3-13. Mean flow (cm·s^{-1}) normal to section 3 in Figure 5.3-10 from CUPOM output for years 1993-1999. Positive values are westward.

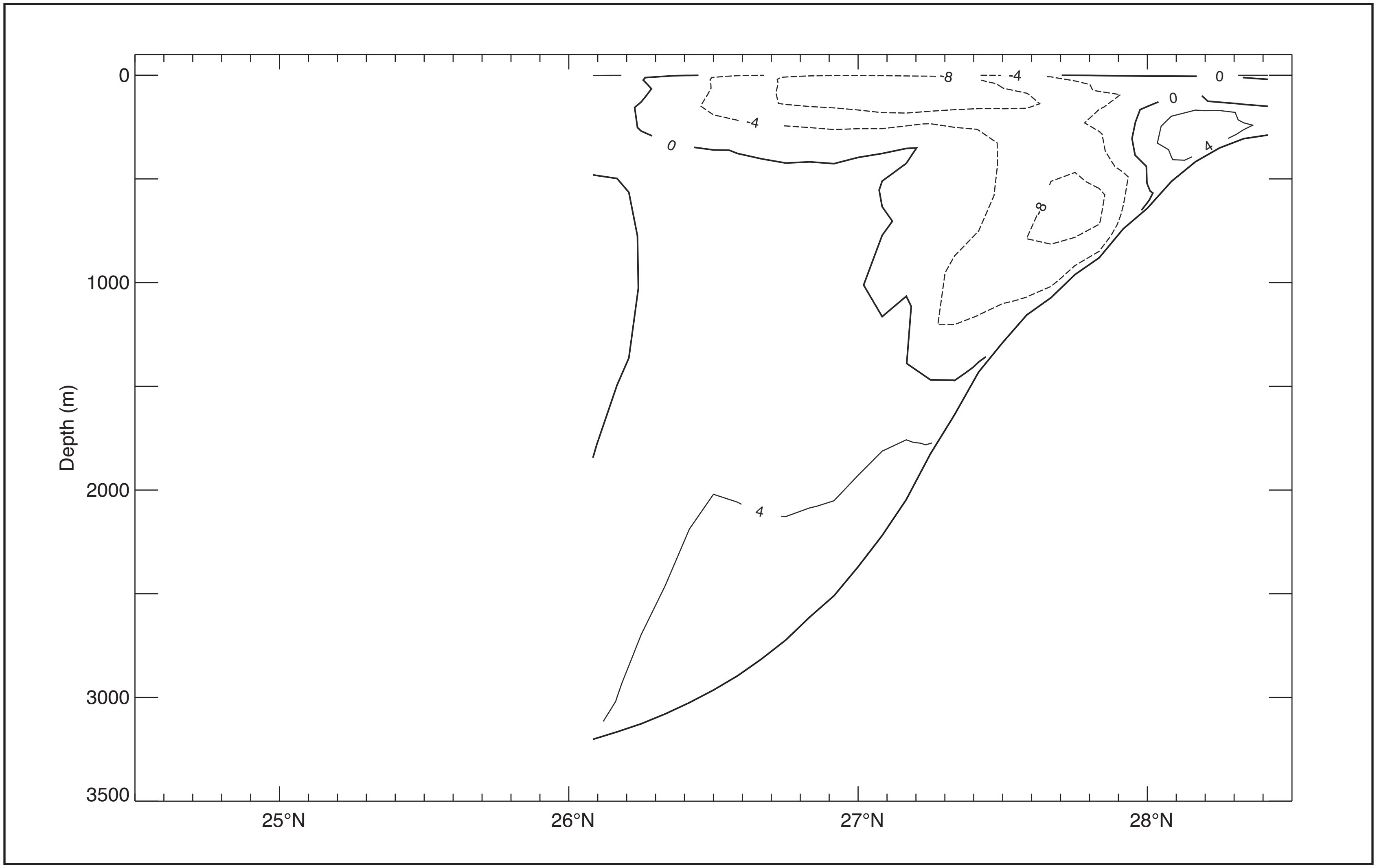

Figure 5.3-14. Mean flow ($cm \cdot s^{-1}$) normal to section 4 in Figure 5.3-10 from CUPOM output for years 1993-1999. Positive values are westward.

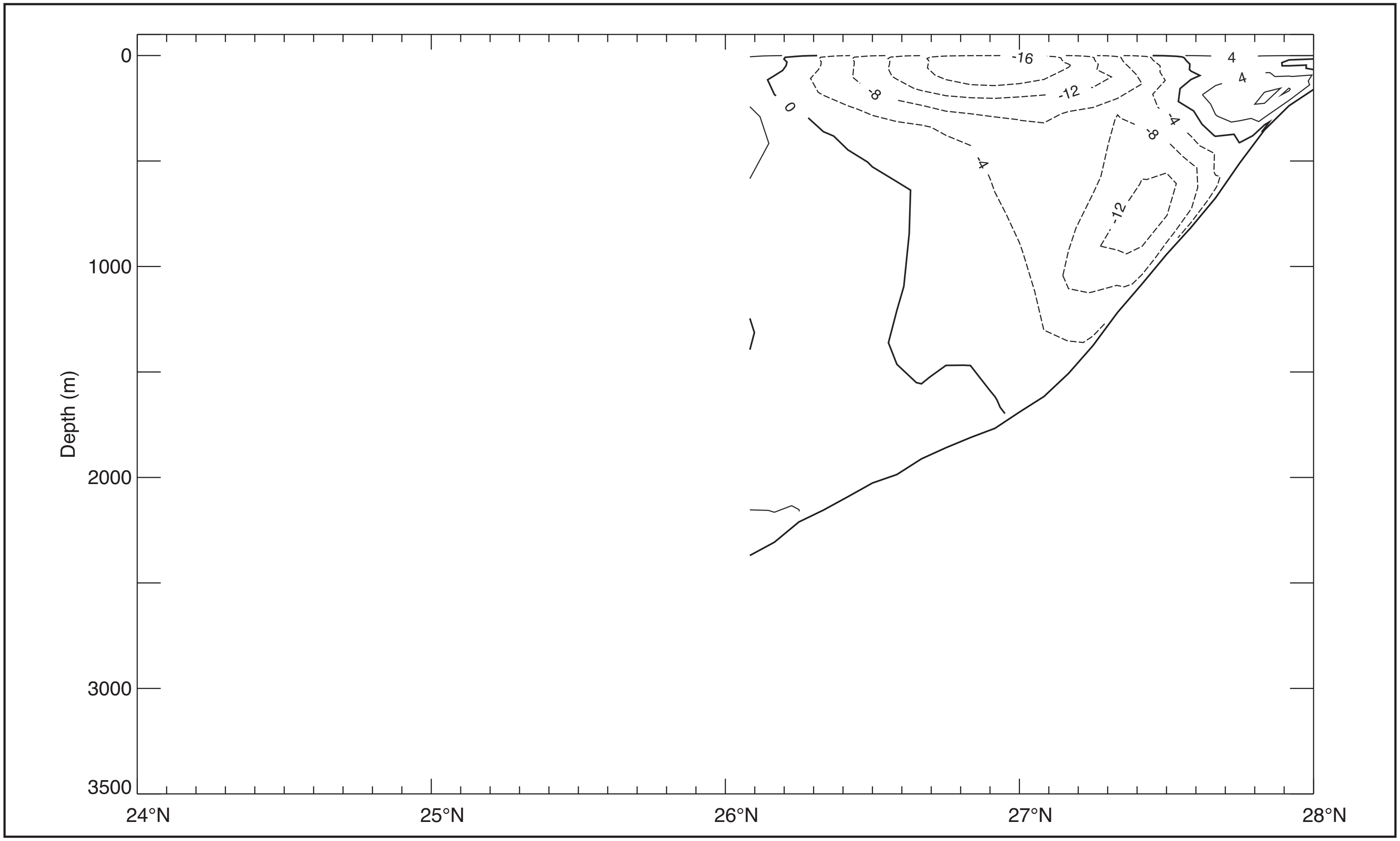

Figure 5.3-15. Mean flow (cm·s^{-1}) normal to section 5 in Figure 5.3-10 from CUPOM output for years 1993-1999. Positive values are westward.

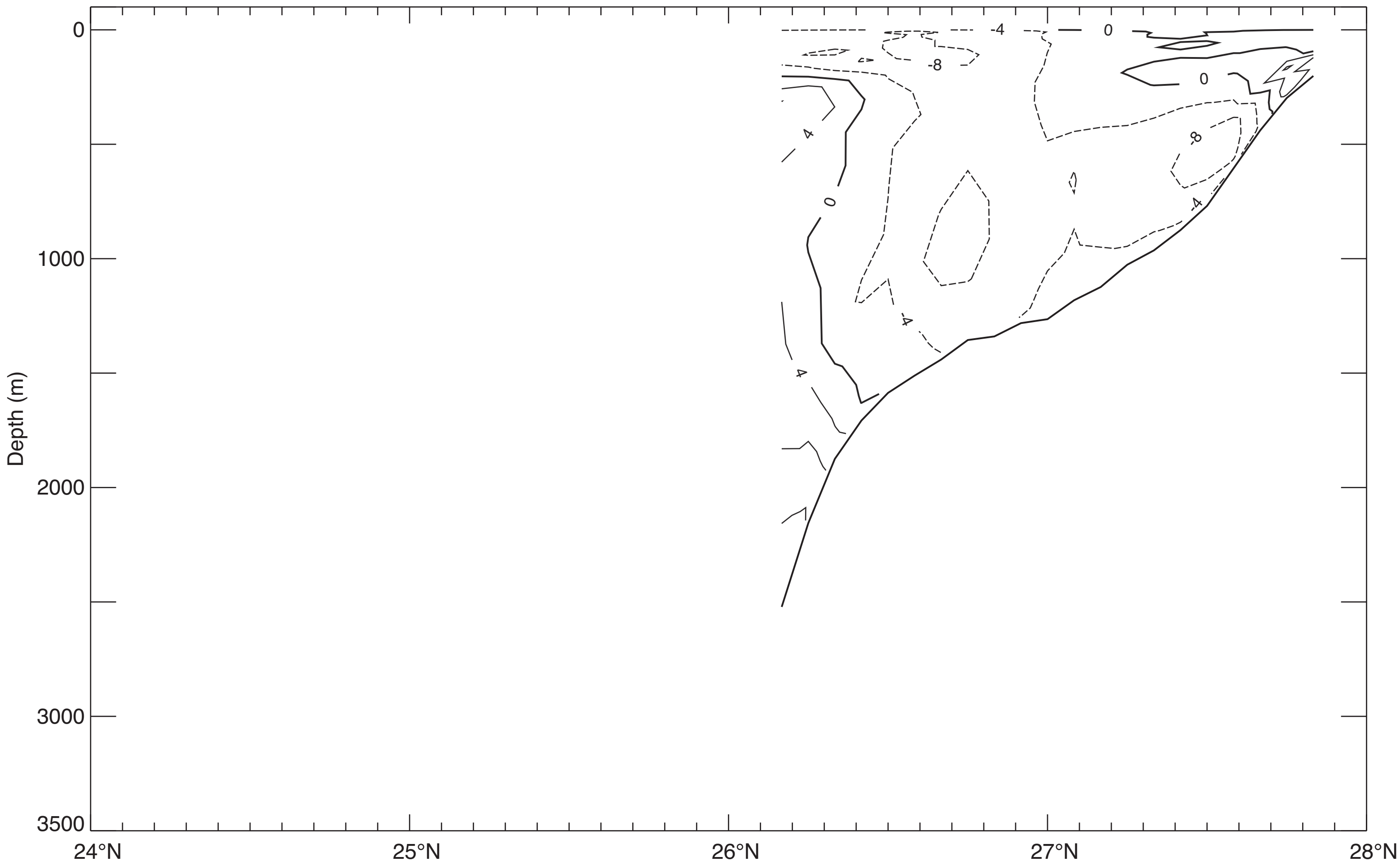

Figure 5.3-16. Mean flow (cm·s^{-1}) normal to section 6 in Figure 5.3-10 from CUPOM output for years 1993-1999. Positive values are westward.

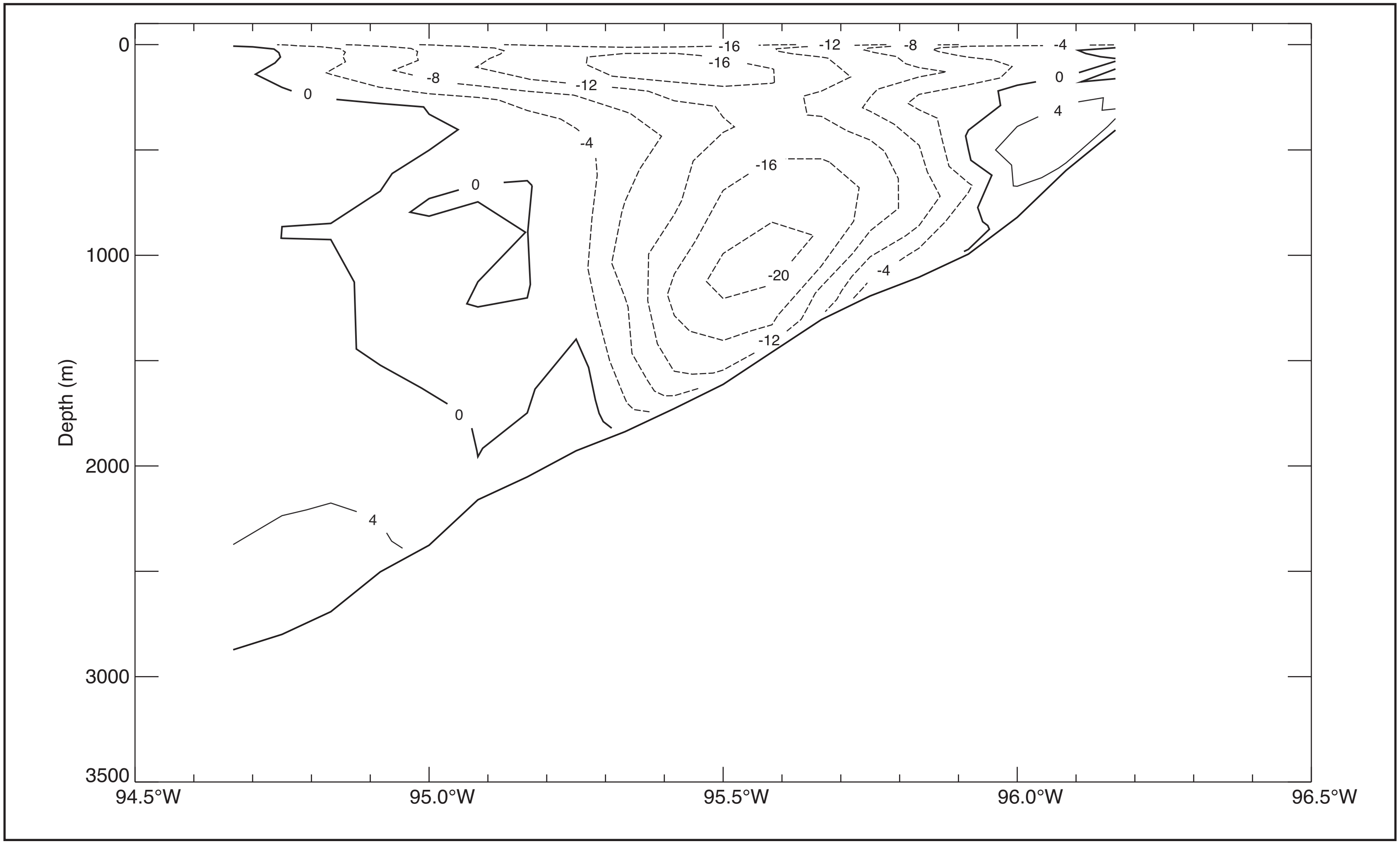

Figure 5.3-17. Mean flow (cm·s^{-1}) normal to section 7 in Figure 5.3-10 from CUPOM output for years 1993-1999. Positive values are southward.

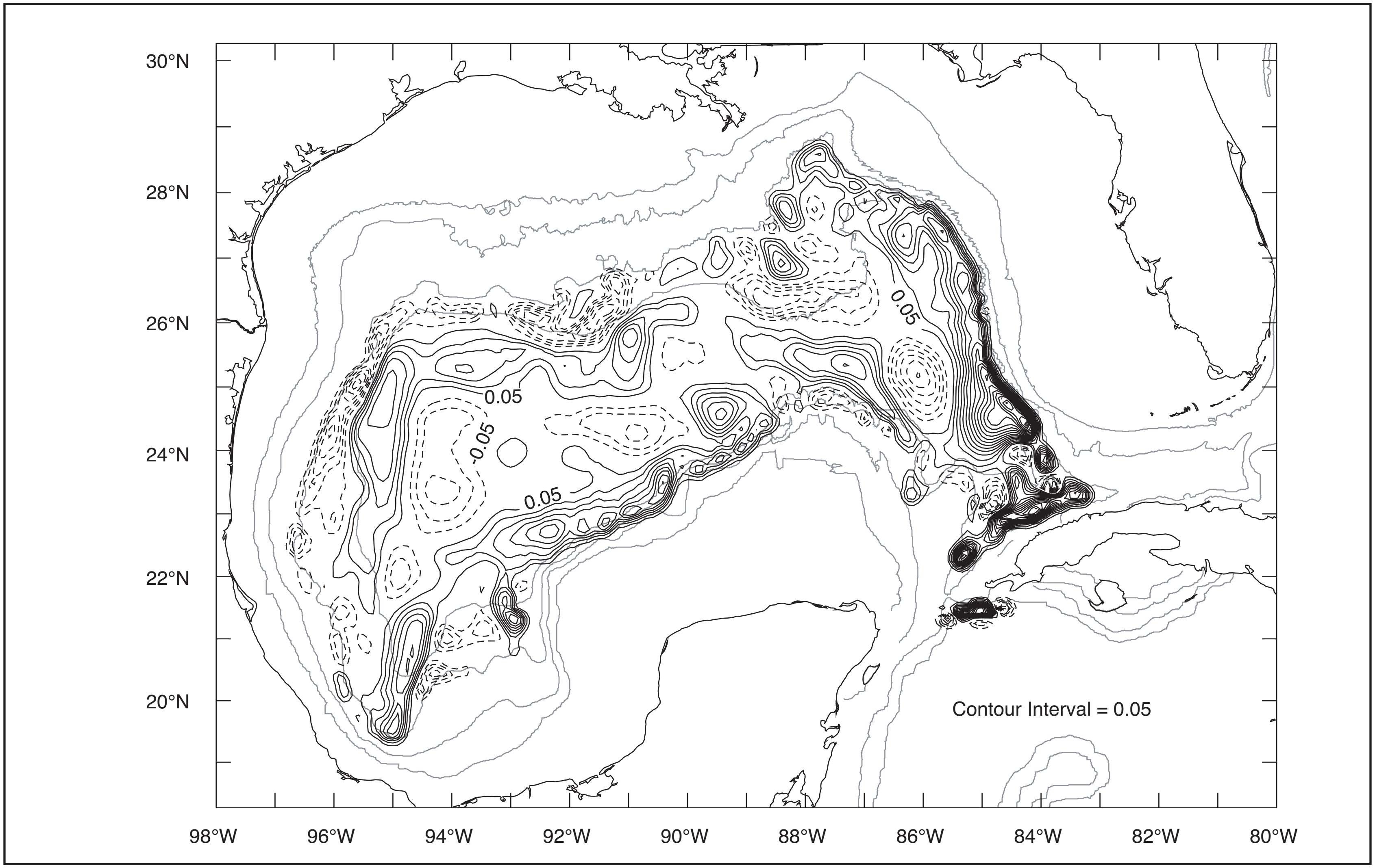

Figure 5.3-18. Relative vorticity (10^{-5} s^{-1}; positive cyclonic) based on record-length average horizontal velocity for model years 1993-1999 from CUPOM at 2000-m level (Figure 5.3-7). Shown are the 200-, 1000-, 2000-, and 3000-m isobaths. The zero contour has been omitted for clarity.

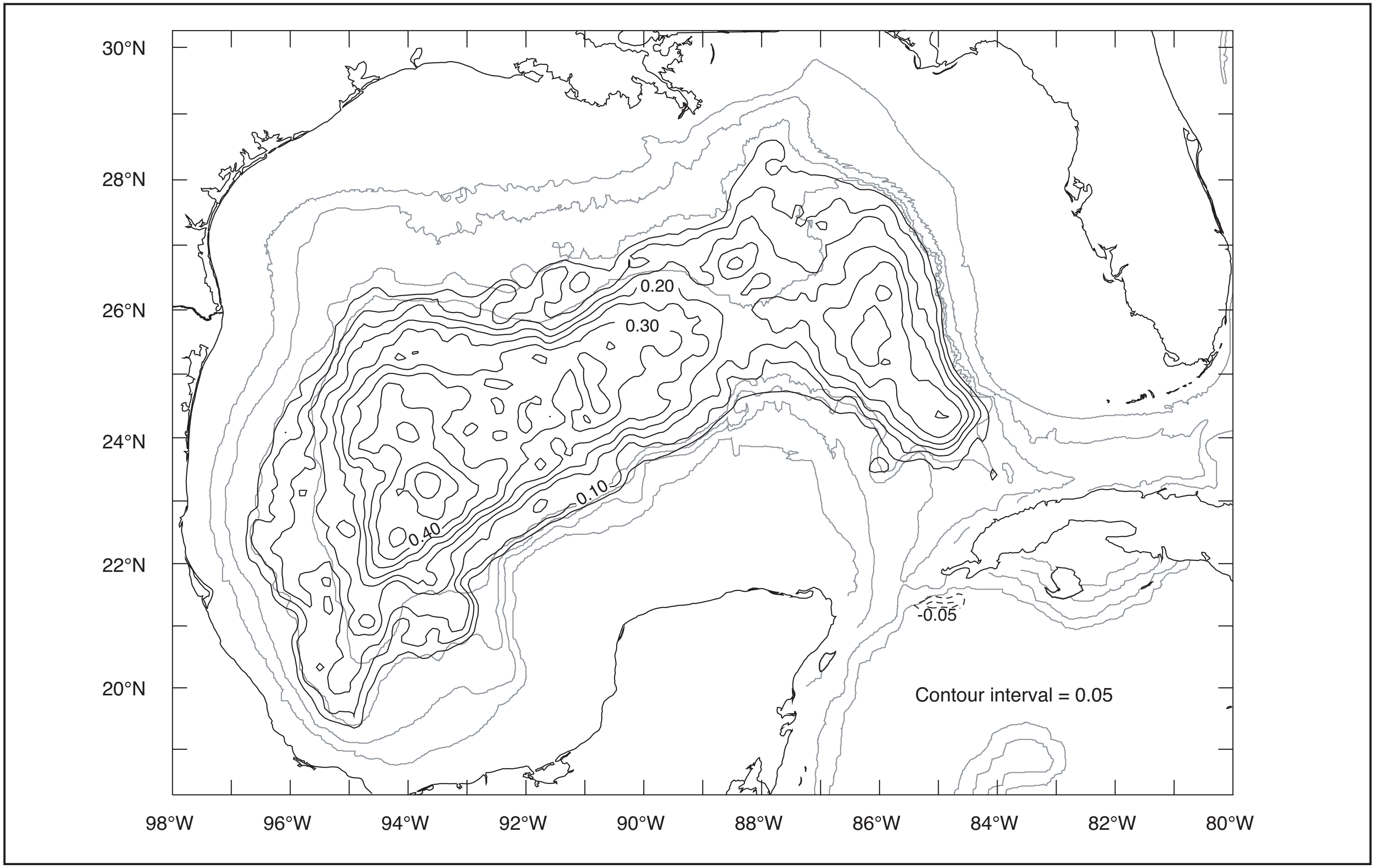

Figure 5.3-19. Smoothed correlation coefficient (zero lag) between average vorticity fields at 500 m and 2000 m based on record-length mean velocities from CUPOM output for model years 1993-1999. Shown are the 200-, 1000-, 2000-, and 3000-m isobaths.

5.4 Mean and Variability of SSH and SSHA

In this section, we consider sea surface height of the Gulf of Mexico as obtained from satellite altimetry and model output. In Figure 5.4-1 is shown the mean sea surface height (SSH) computed by averaging surface height output from the CUPOM hindcast run for the model years 1993-1999 (data courtesy of Robert Leben, CCAR). This field represents a best estimate of the mean SSH associated with ocean circulation over the time period. We also present time series of SSH fields to describe the formation, separation, and subsequent behavior of Eddy Juggernaut.

Mean and standard deviation. The most significant feature seen is the Loop Current, with a surface height range of approximately 60 cm. Off northwest Cuba is a closed anticyclonic circulation within the loop having an amplitude of near 10 cm. A slight lowering of sea level appears around the margins of the Gulf relative to the center, suggestive of a slight anticyclonic circulation. The marginal depression in SSH is of order 5 cm. The average dynamic topography of the sea surface relative to 800 db (shown in Figure 5.1-4) evidences a similar pattern, although not nearly as smooth. This is to be expected because of the large difference in numbers of values used to prepare the two fields. The extent of intrusion of the Loop Current into the Gulf is approximately the same for the two fields. The maximum dynamic range of features seen in the dynamic height field constructed from station data is greater than 40 dyn cm, in contrast to approximately 60 dyn cm for the mean model output. Like the SSH field from the model, the dynamic topography shows a lowering of sea level around the margins of the basin.

Geostrophic surface speeds were derived from mean model SSH field and are shown in Figure 5.4-2. Maximum speeds are seen to exceed 100 $cm \cdot s^{-1}$ in the core of the Loop Current as seen in synoptic realizations, e.g., Section 6.1.1. Maximum speeds exceed those average values shown in Figure 5.2-2 which is based on drifter observations. Moreover, the patterns differ in that the drifter observations do not show clear closure of the Loop Current. It should be remembered that the two fields are not expected to agree because the drifter observations are from a range of near-surface depths, are not uniformly distributed in time and space, and reflect Ekman as well as geostrophic components of the circulation.

Sea surface height anomaly (SSHA) fields were prepared by Robert Leben (CCAR) by blending altimeter data from TOPEX/POSEIDON with ERS-1 or ERS-2 (Sturges and Leben 2000; Lillibridge et al. 1997) and removing the Ohio State University Mean Sea Level (OSU MSL) (Yi 1995). The OSU MSL is a best estimate of the geoid plus an unknown mean sea level departure from the geoid due to ocean circulation. Daily maps of SSHA were created using an objective analysis procedure with spatial and temporal decorrelation scales of (approximately) 100 km and 12 d, respectively (Sturges and Leben 2000; Hamilton et al. 2000). Shown in Figure 5.4-3 is the resulting SSHA field for 1 January 1993.

Adding the SSHA field in Figure 5.4-3 to the model mean SSH in Figure 5.4-1 would give the sea surface height relative to the geoid on 1 January 1993 provided that (1) the model mean gives a true mean SSH relative to the geoid and (2) the OSU MSL accurately represents the effect of mean circulation. We have no means of examining the first supposition. However, to some extent, we can examine the second. If we average the daily SSHA values over a long period, the resulting average is a measure of departure of the OSU MSL from the mean sea level for that period. It should be noted that because of the large low-frequency variability in the Gulf caused by the Loop Current and the LCEs, many years of data (more than the seven years available for use here) would be needed to determine an effective mean.

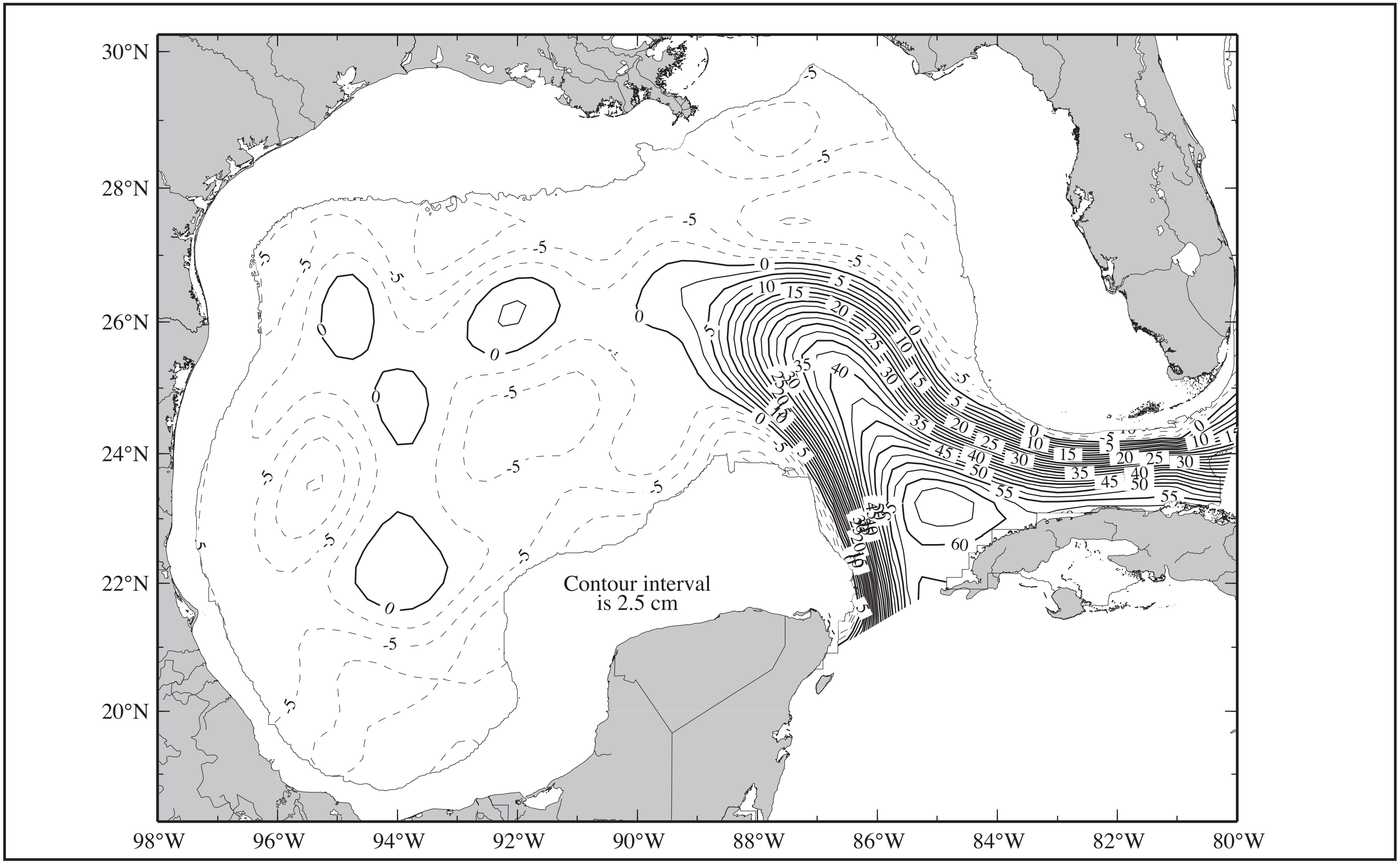

Figure 5.4-1. Mean sea surface height for the Gulf of Mexico based on averaging sea surface height from the University of Colorado Princeton Ocean Model output for the years 1993-1999 (data courtesy of Robert Leben, CCAR). Values are not shown for water depths less than 200 m.

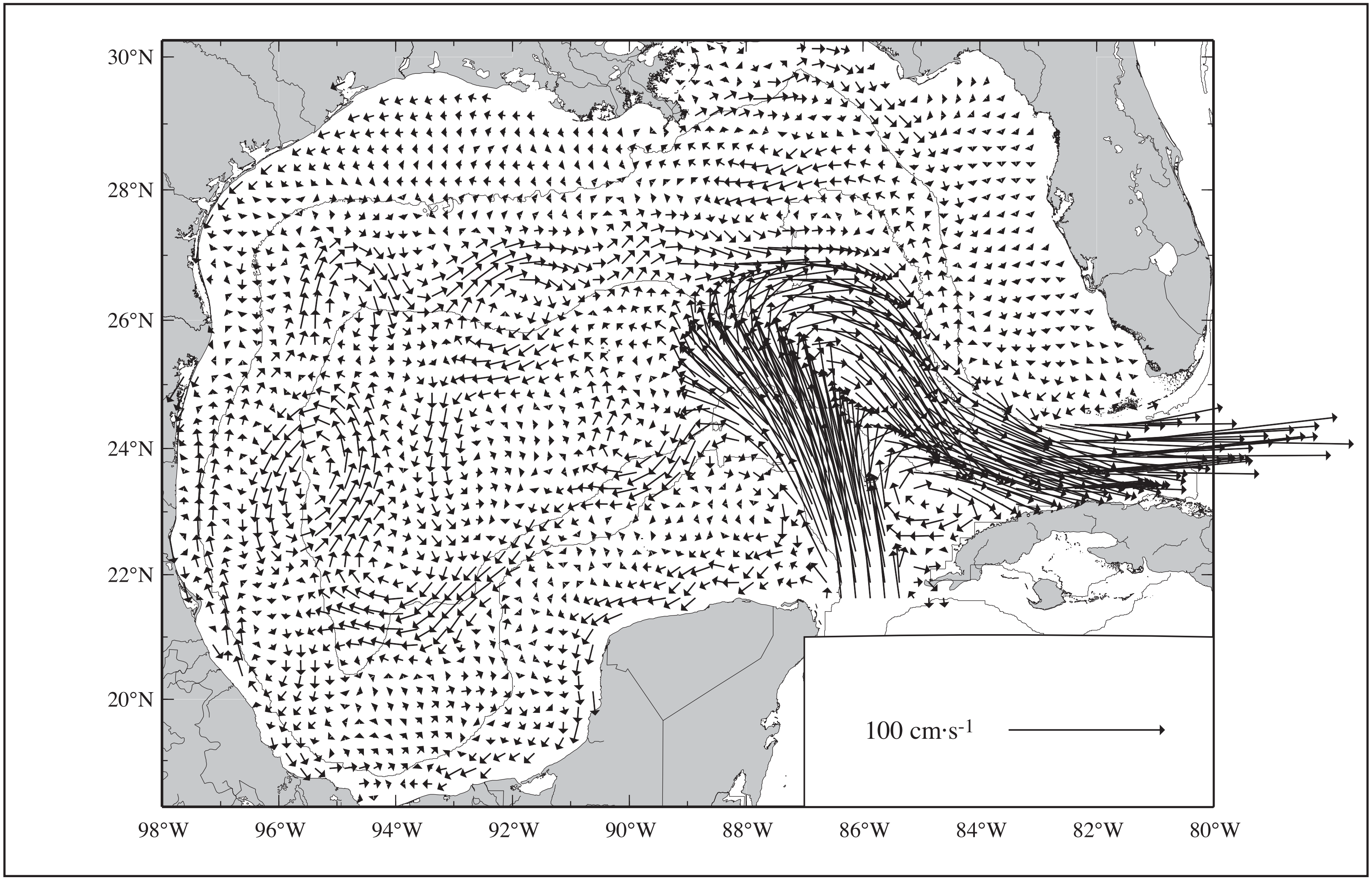

Figure 5.4-2. Geostrophic surface current vectors derived from the mean model SSH field shown in Figure 5.4-1. The 200-m and 3000-m bathymetric contours are shown.

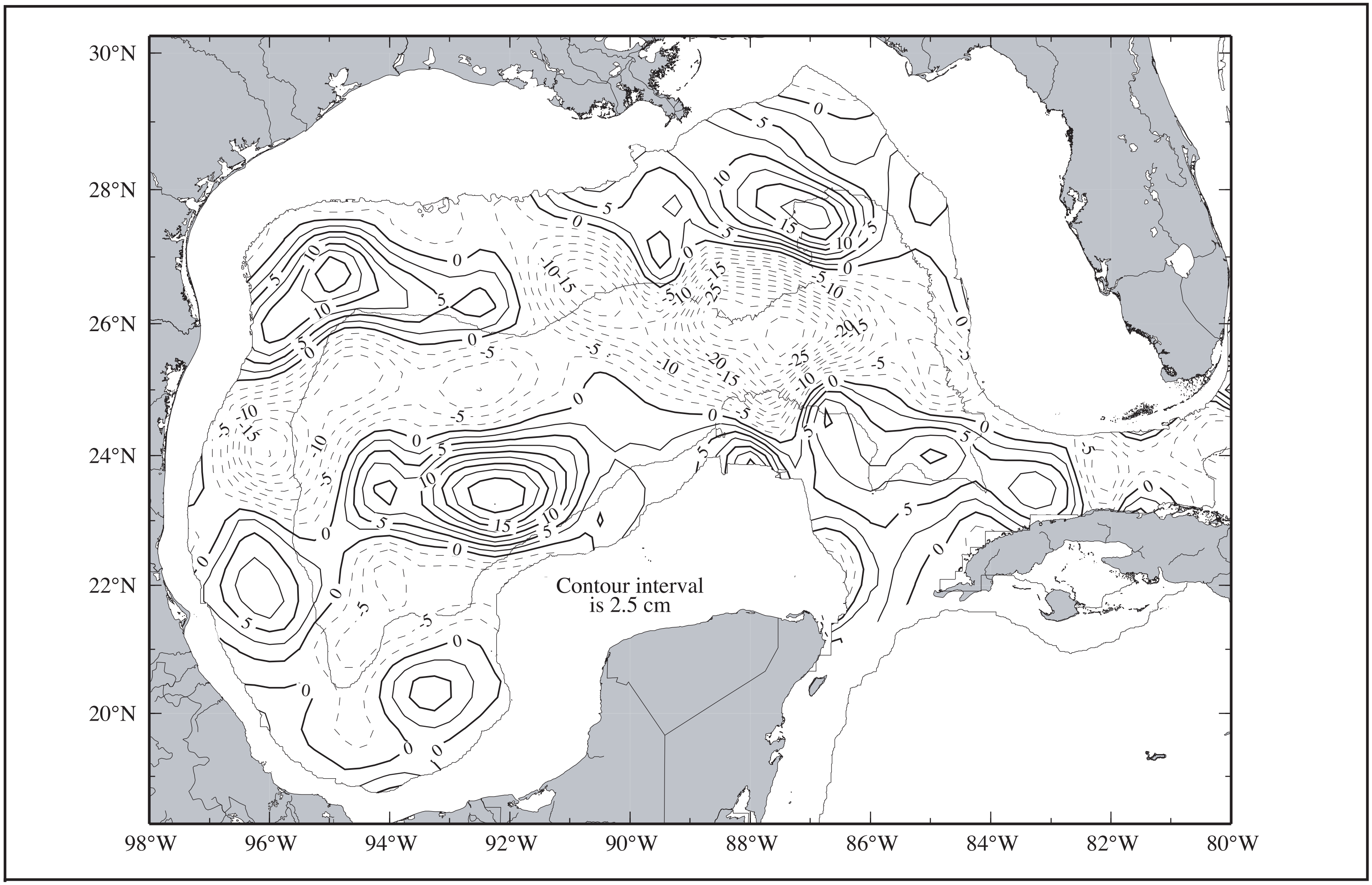

Figure 5.4-3. Sea surface height anomaly field for 1 January 1993. Bathymetric contours are shown for 200 and 3000 m.

In Figure 5.4-4 is shown the mean of daily SSHA fields averaged for the period 1993-1999. The mean is seen to depart from zero by isolated values in excess of 7.5 cm, although values generally are ± 2.5 to 5 cm. To obtain a best estimate of the SSH due to ocean circulation (i.e., relative to the geoid) for a given day, we subtract from the SSHA relative to the OSU MSL for that day the mean SSHA field for 1993-1999 and then add the model mean SSH for 1993-1999. The resulting SSH for 1 January 1993 is shown in Figure 5.4-5.

On 1 January 1993, the Loop Current is seen to have extended into the Gulf to about 25.5°N, based on the location of the 17-cm height contour. That contour has been shown by Hamilton et al. (2000) to closely match the maximum horizontal surface gradient for meso-scale circulation features in the Gulf. As in the mean picture, a closed circulation, with strength in excess of 6.5 cm is seen within the Loop Current just northwest of Cuba. North-northwest of the Loop Current near DeSoto Canyon was an anticyclone, centered near 28°N, 87°W with maximum surface elevation of only about 12 cm. In the western Gulf were remnants of three LCEs. Centered near 26.5°N, 95°W was Eddy Vazquez moving into the northwestern corner of the deep water Gulf. The large oblong eddy centered near 23.5°N, 92°W was Eddy Unchained, moving westward. The motions of both of those eddies were confirmed by drifters. To the west of, and perhaps connected with, Eddy Unchained was a weak anticyclone believed to be the decaying remnant of Eddy Triton. The cyclone located against the western continental slope between Eddy Triton and Eddy Vazquez was strong and had been in that position for quite some time.

To quantify the variability in sea surface height, we show in Figure 5.4-6 the standard deviation in SSHA fields for the period 1993-1999. As expected, the largest values (in excess of 22.5 cm) are found in the region of normal Loop Current intrusion and eddy formation, centered near 26°N, 87°W. Along the shelf edge in the central and western Gulf, standard deviation values are less than 5 cm, indicating that about 95% of the time variations of sea surface height are less than 10 cm. This field of standard deviations for the satellite-derived SSHA is in quite good agreement with the standard deviation field for SSH derived from the CUPOM for model years 1993-1999 (Figure 5.4-7). This good comparison is expected because the SSHA data are assimilated into CUPOM.

The standard deviations of satellite-derived SSHA shown in Fig. 5.4-6 also compare rather well with standard deviations for the 0/800 db dynamic topography (Figure 5.1-3). Of course, the values for the hydrographic estimation are much less smooth, because of the sparse and non-uniform numbers of realizations of dynamic topography. For both fields, values within the Loop Current region and for an extension into the western central Gulf exceed 10 dyn cm. Values within the Loop Current are typically near 20, but may exceed 25 dyn cm.

We noted, in Section 5.1, that the field of 0/800 db dynamic topography from hydrographic stations agrees well with the mean SSH field from the CUPOM. That is evidence that 800 db is a good reference level for the geostrophic flow in the Gulf of Mexico, assuming that the model gives realistic results. The fact that there is fair agreement between the standard deviation fields for the 0/800 db dynamic topography and for SSH derived from satellite altimetry is further evidence of the reasonableness of the 0/800 db geostrophic shear as a measure of the geostrophic surface circulation.

To show the information available from time series of SSH fields and to provide background information for discussions of data sets in Section 6, a brief examination is made of one large LCE, named Eddy Juggernaut. Eddy Juggernaut separated from the Loop Current in late 1999 following a long period during which the Loop Current extended into the Gulf of Mexico far enough that the nascent ring was over the continental slope and rise just west of the Mississippi

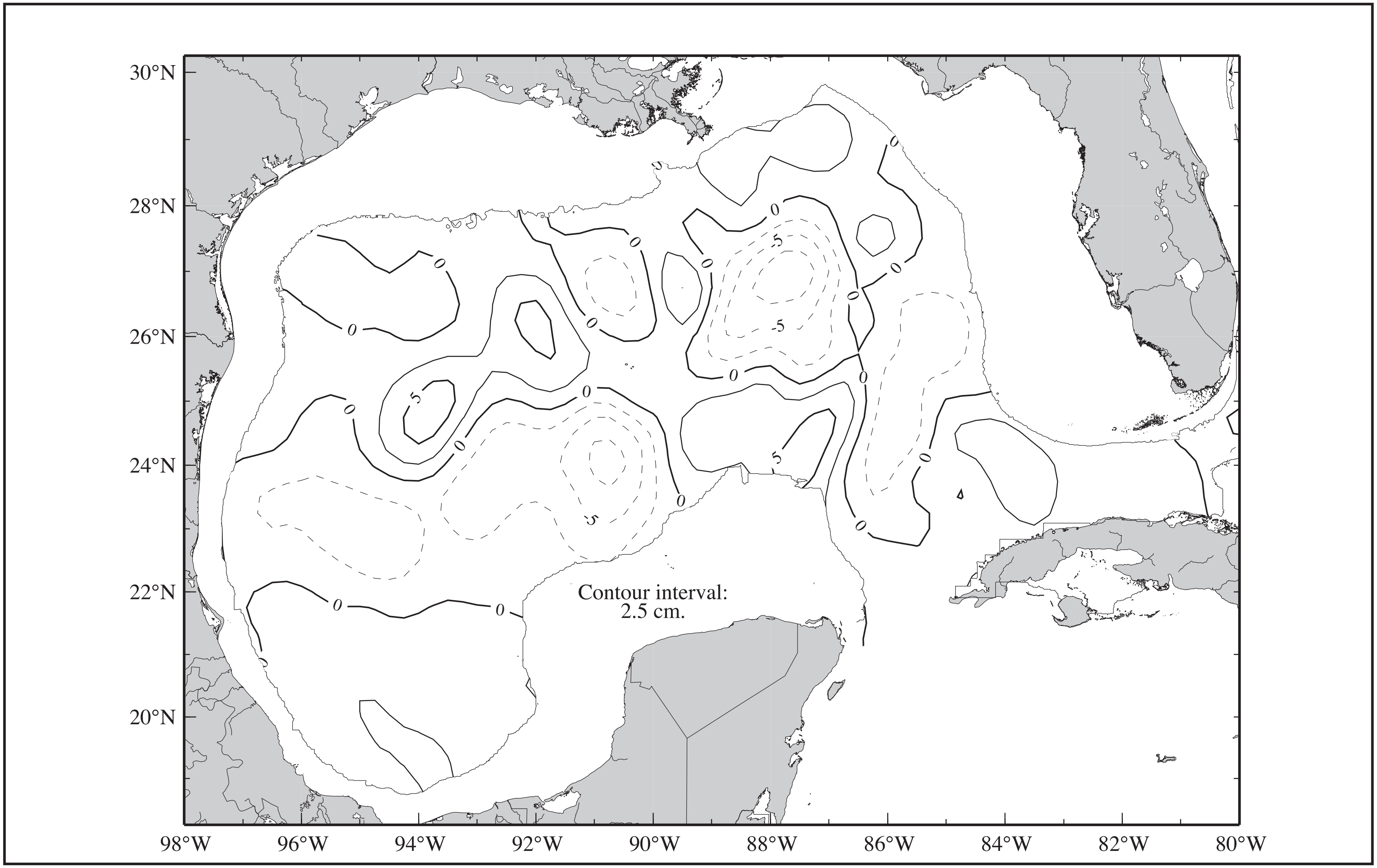

Figure 5.4-4. The mean of daily SSHA fields averaged for the period 1993-1999. The 200-m bathymetric contour is shown.

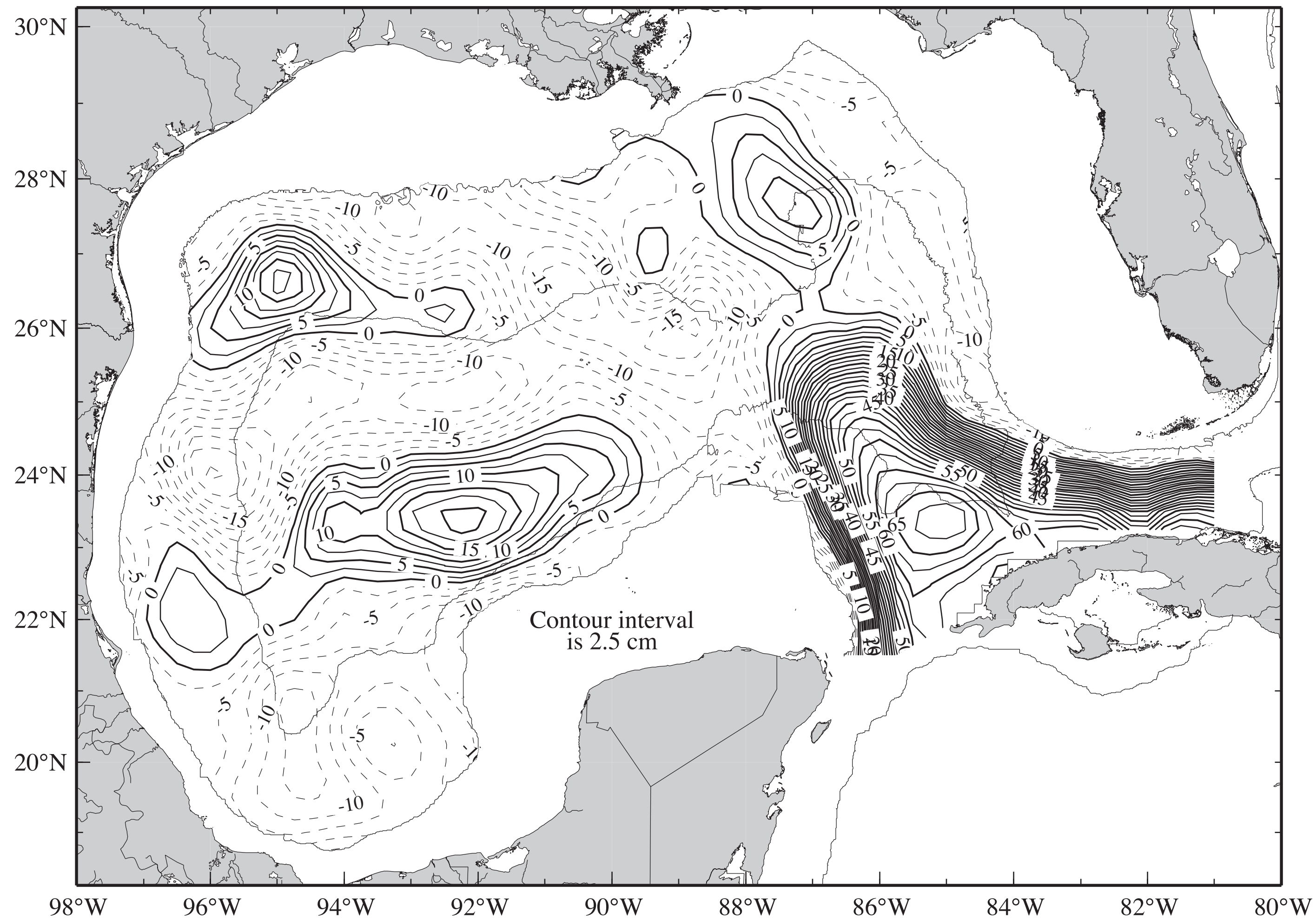

Figure 5.4-5. Estimate of SSH for 1 January 1993 obtained by subtracting Figure 5.4-4 from the sum of the fields shown in Figures 5.4-1 and -3. Shown is the 200-m bathymetric contour.

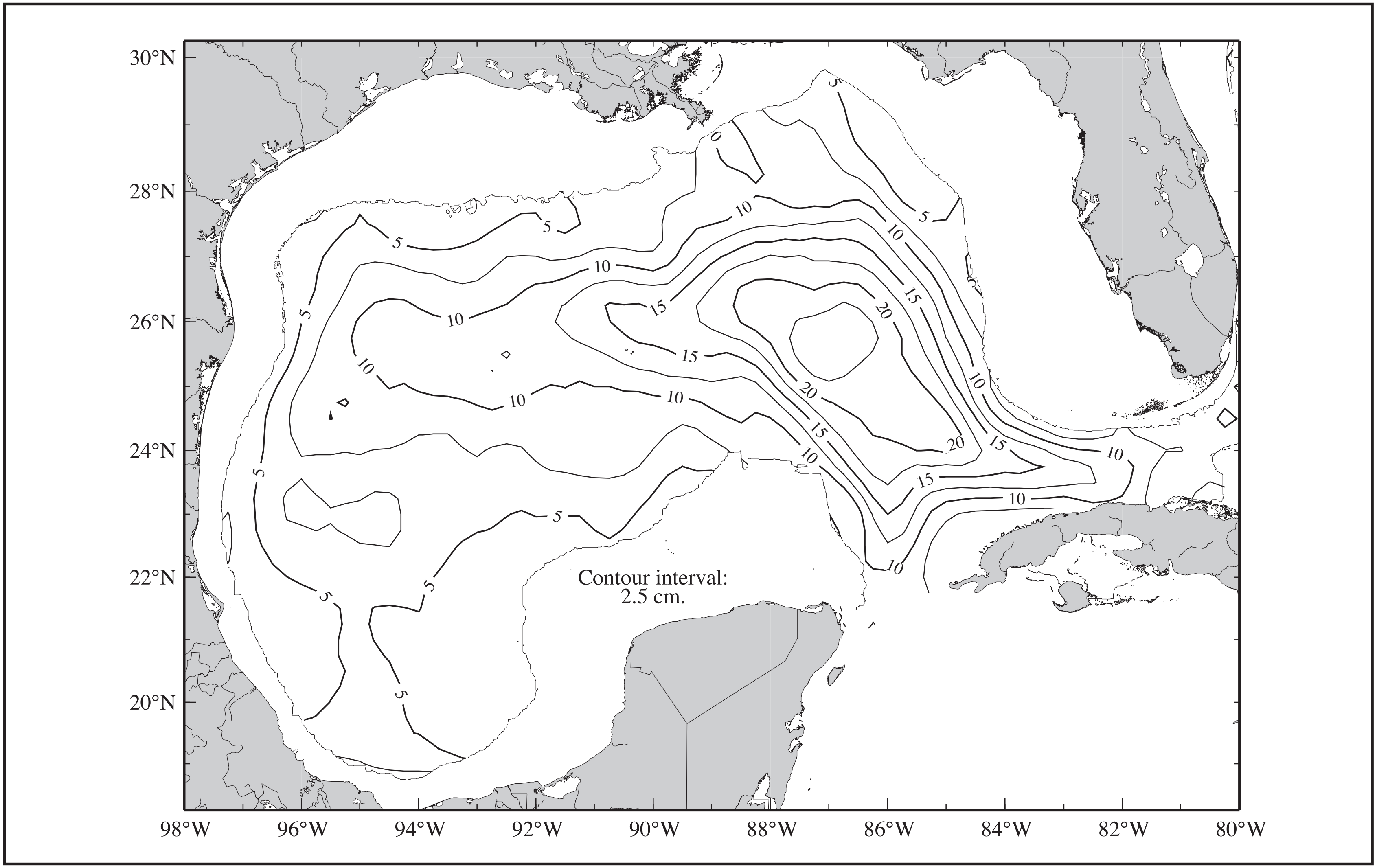

Figure 5.4-6. Standard deviation of sea surface height based on SSHA anomaly fields for the period 1993-1999. Bathymetric contour shown is 200 m.

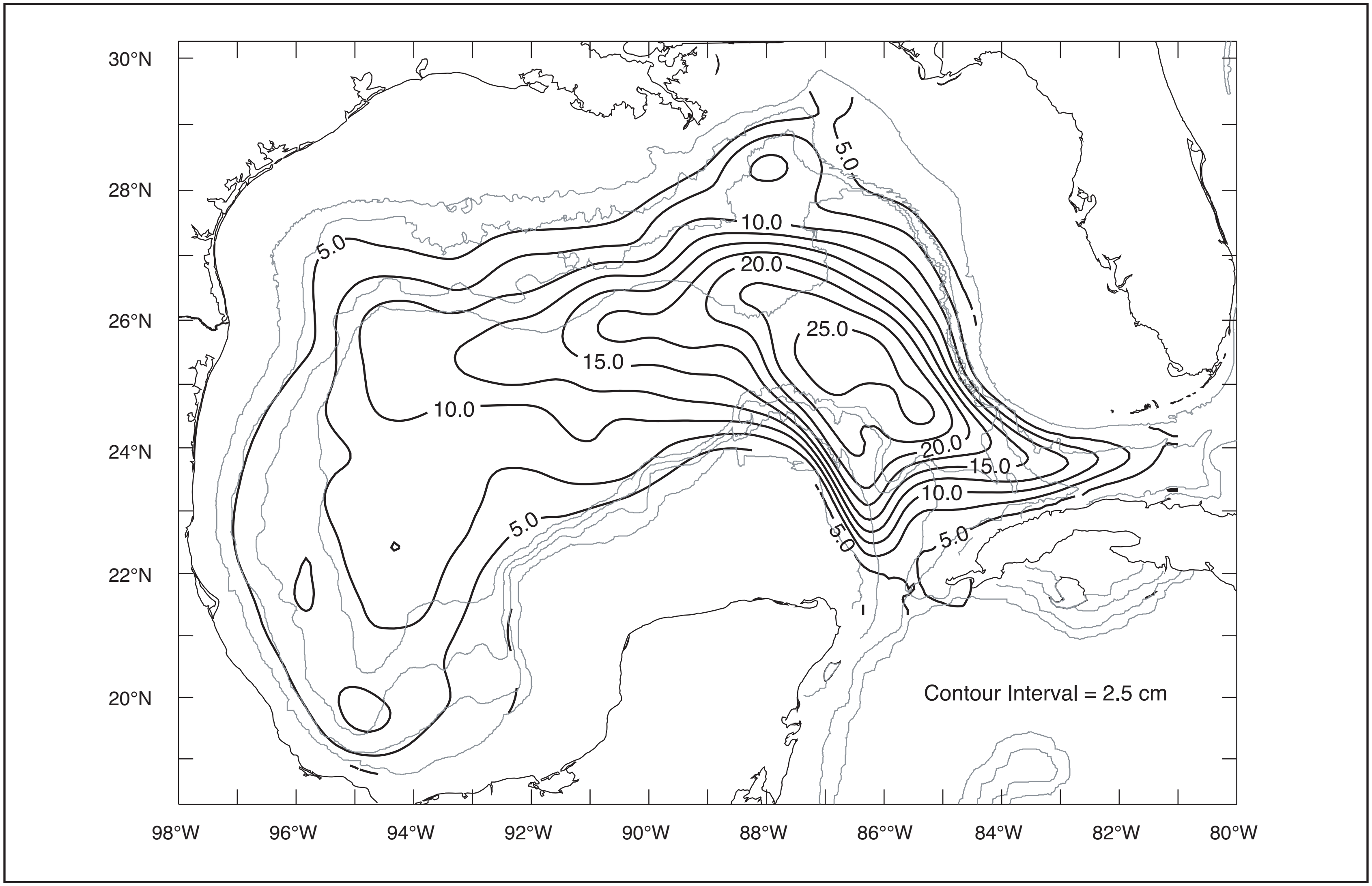

Figure 5.4-7. Standard deviation (cm) of SSH based on the CUPOM output for model years 1993-1999.

Delta. Following its separation, Eddy Juggernaut remained in the north-central Gulf for a considerable time. The size and intensity of Juggernaut is judged to be that of a 10-year event; the previous LCE of similar size, power, and influence was Eddy Nelson, which separated in 1989.

We examined a sequence of SSH fields for the period July 1999 through January 2000 to describe the formation and subsequent behavior of Eddy Juggernaut. The description which follows is arranged into time periods in which notable changes occurred. The narrative is brief, but is supplemented by illustrations of the SSH fields at key times.

2-27 July 1999 The northern front of the Loop Current extended northwestward past 27°N, 89.5°W (Figure 5.4-8) until it was impinging on the outer continental shelf by 1 August (Figure 5.4-9).

1-21 August 1999 Interaction of the Loop Current with the bathymetry seems to have led to near separation of a ring and withdrawal of the Loop Current away from the shelf to the southeast. During this period an anticyclonic bulge of the Loop Current developed toward the southwest from approximately 26°N, 88°W (Figure 5.4-10).

21-26 August 1999 It is possible that a small new ring separated from the Loop Current and began to move toward the south-southwest from a center near 24.5°N, 90.5°W (Figure 5.4-11). This separation took place 22 August according to Sturges and Leben (2000). However, the time sequence of SSH fields during July and August is subject to an alternative interpretation. During July there was in the western Gulf just northwest of the Campeche Platform an elongated, relatively weak high oriented southwest-northeast. During early July it appeared weakly connected with the Loop Current. It separated from the Loop Current in mid July and reconnected in early August when its eastern end was considerably intensified. Thereafter, just after 21 August, the high ridge again was separated from the Loop Current, but at that time the anticyclonic circulation in its eastern end was strong enough that it might be considered as a separate eddy. (The LCE separation of Eddy Juggernaut took place in October of 1999.)

26 August - 20 September 1999 The Loop Current strengthened and again extended northwestward until its northern front was over the continental slope (Figure 5.4-12).

25 September - 10 October 1999 The neck between the closed circulation in the northwest extension of the Loop Current and Loop Current main body narrowed to form a large anticyclonic ring. During this same period the developing Eddy Juggernaut attached to the ring that had formed in late August (Figure 5.4-13). The separation of Eddy Juggernaut was complete by 15 October (Figure 5.4-14). Loop Current statistics prepared by Leben (personal communication; compiled as part of the DeSoto Canyon Eddy Intrusion Study) show the maximum area of the Loop Current and maximum extent of northward intrusion of the Loop Current both ending approximately in the first week of October, in agreement with the formation of a large LCE at that time. Shown in Figure 5.4-15 are (upper) a time series of the surface area in the Gulf of Mexico bounded by the Loop Current as found by integration of the area within the 17-cm SSH contour and (lower) a time series of the northward penetration of the Loop Current within the Gulf based on the northward extent of the 17-cm SSH contour. Clearly seen is the long period of northward penetration and or large surface area prior to the time (about 22 August) of the separation of Eddy Juggernaut. This figure was prepared by Robert Leben using techniques described in Hamilton et al. (2000).

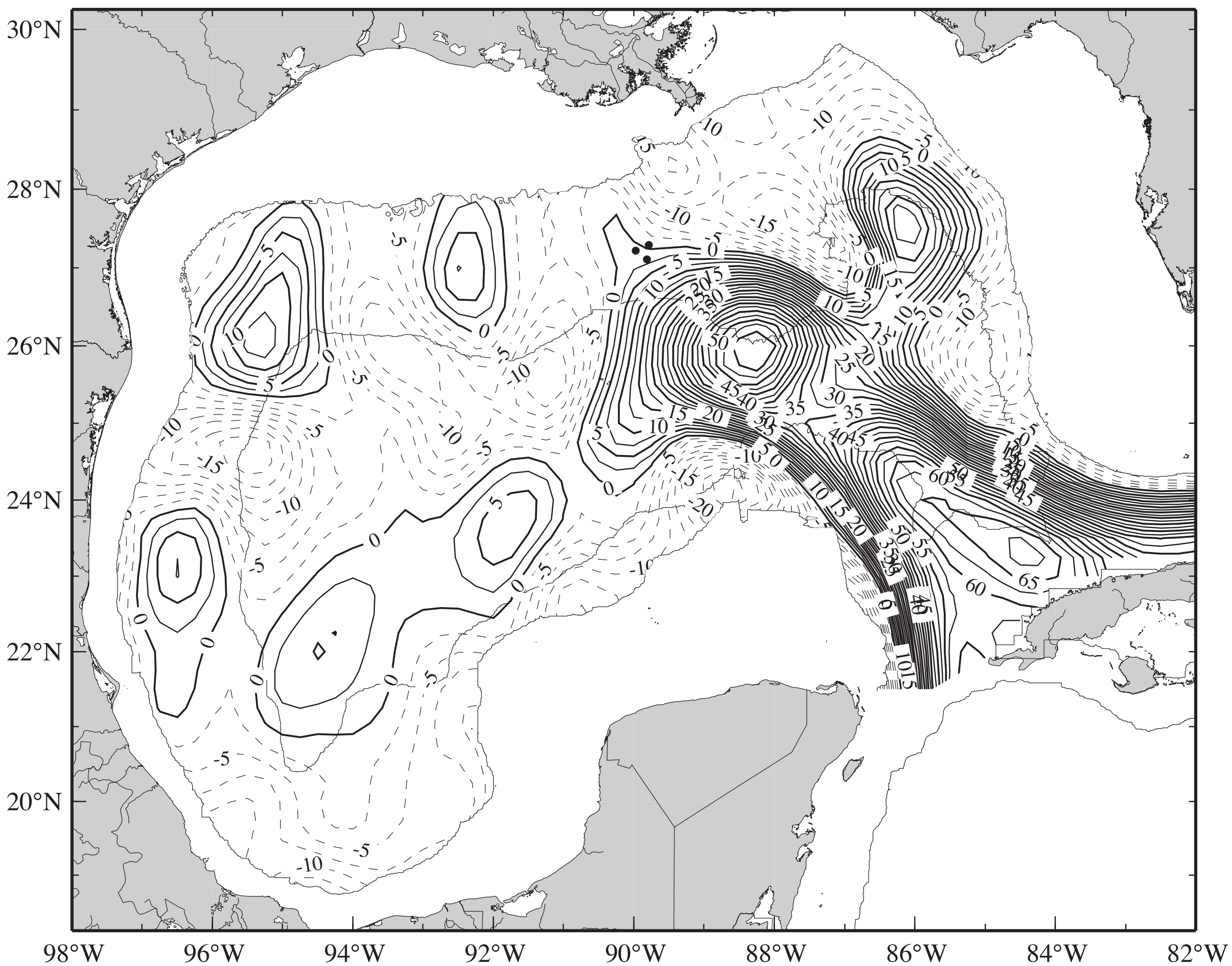

Figure 5.4-8. Sea surface height field for 2 July 1999 prepared in the same manner as the field in Figure 5.4-5. Bathymetric contours are 200 and 3000 m. SSH contour interval is 2.5 cm. Dots show locations of MMS current meter moorings.

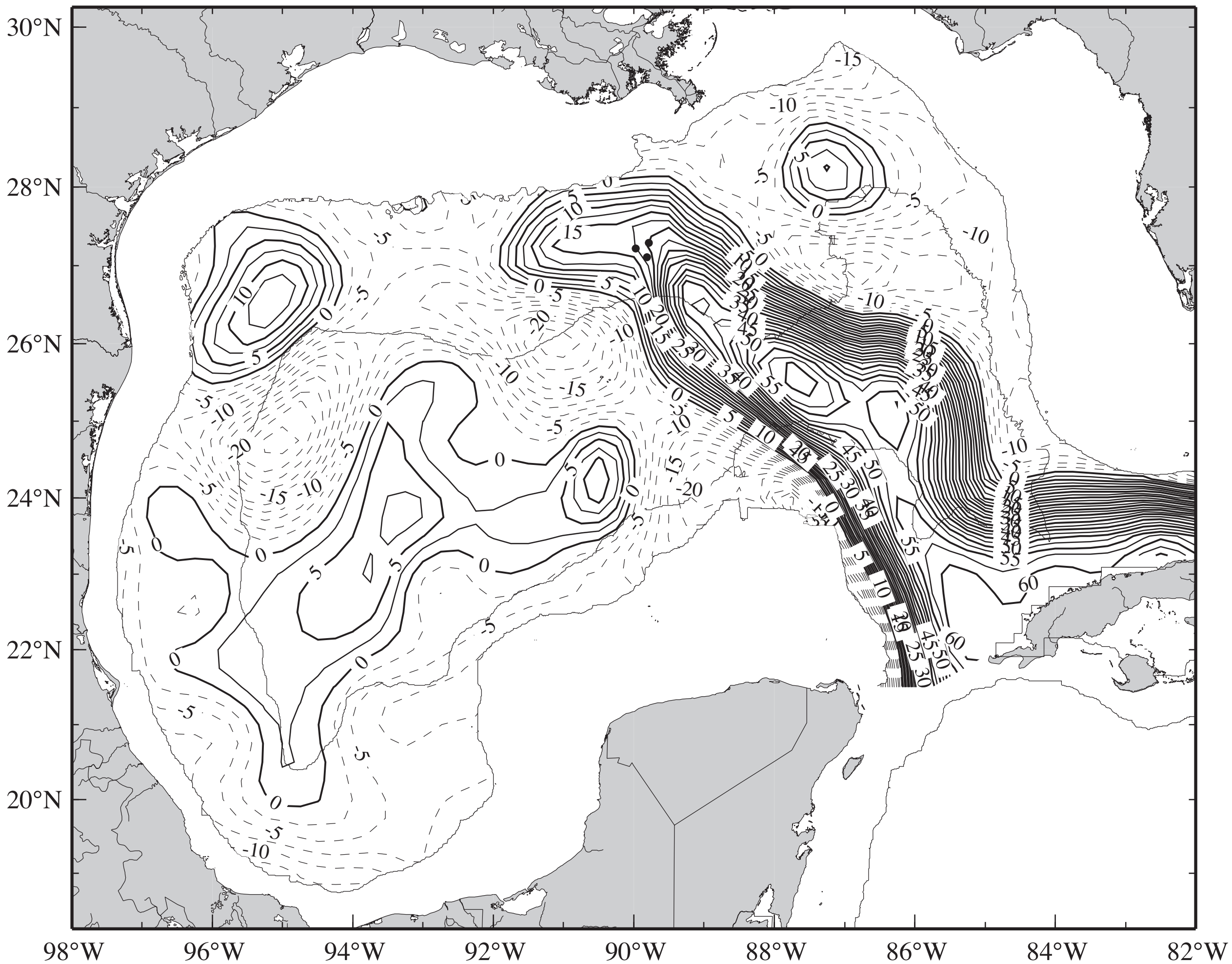

Figure 5.4-9. Sea surface height field for 1 August 1999 prepared in the same manner as the field in Figure 5.4-5. Bathymetric contours are 200 and 3000 m. SSH contour interval is 2.5 cm. Dots show locations of MMS current meter moorings.

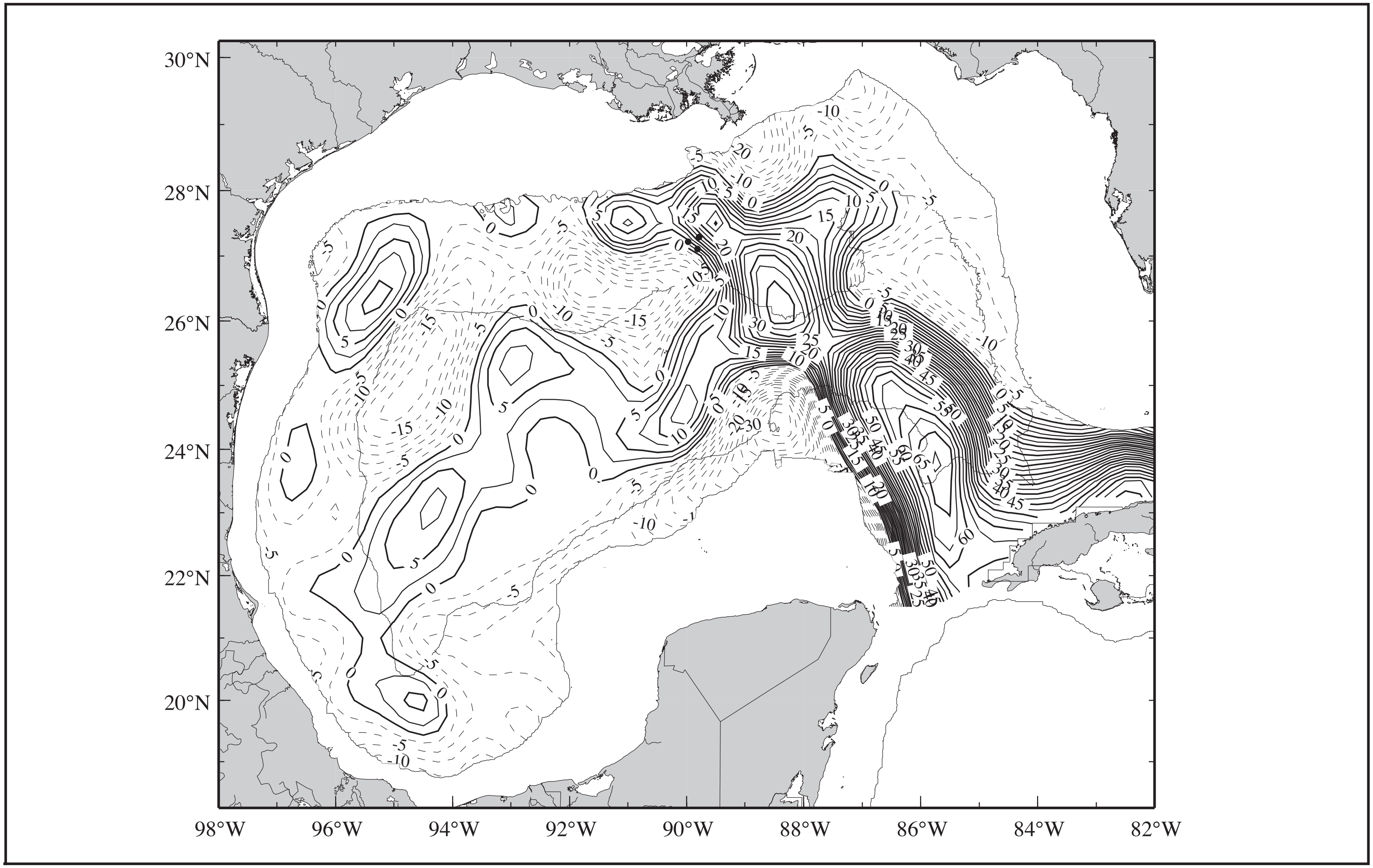

Figure 5.4-10. Sea surface height field for 16 August 1999 prepared in the same manner as the field in Figure 5.4-5. Bathymetric contours are 200 and 3000 m. SSH contour interval is 2.5 cm. Dots show locations of MMS current meter moorings.

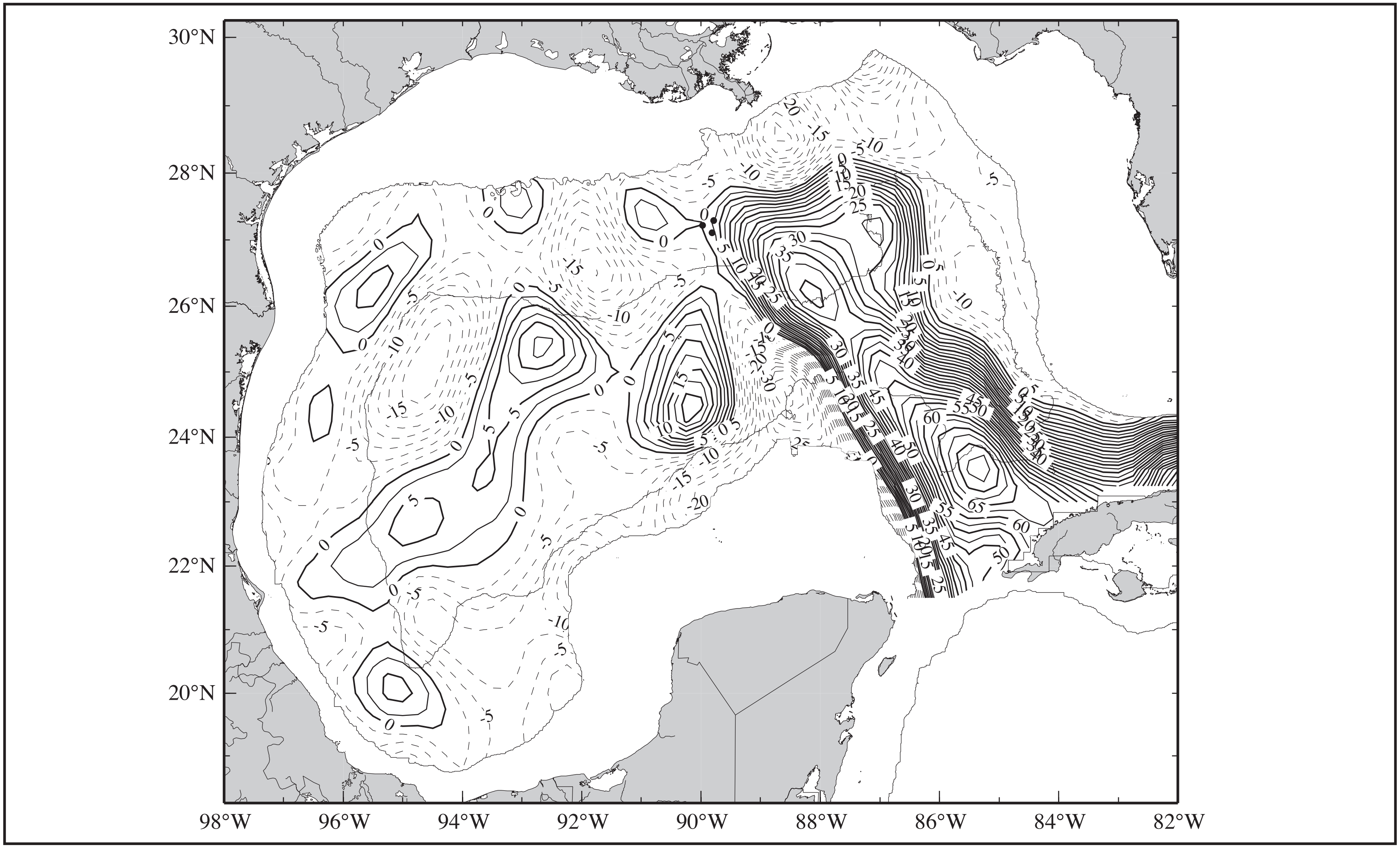

Figure 5.4-11. Sea surface height field for 26 August 1999 prepared in the same manner as the field in Figure 5.4-5. Bathymetric contours are 200 and 3000 m. SSH contour interval is 2.5 cm. Dots show locations of MMS current meter moorings.

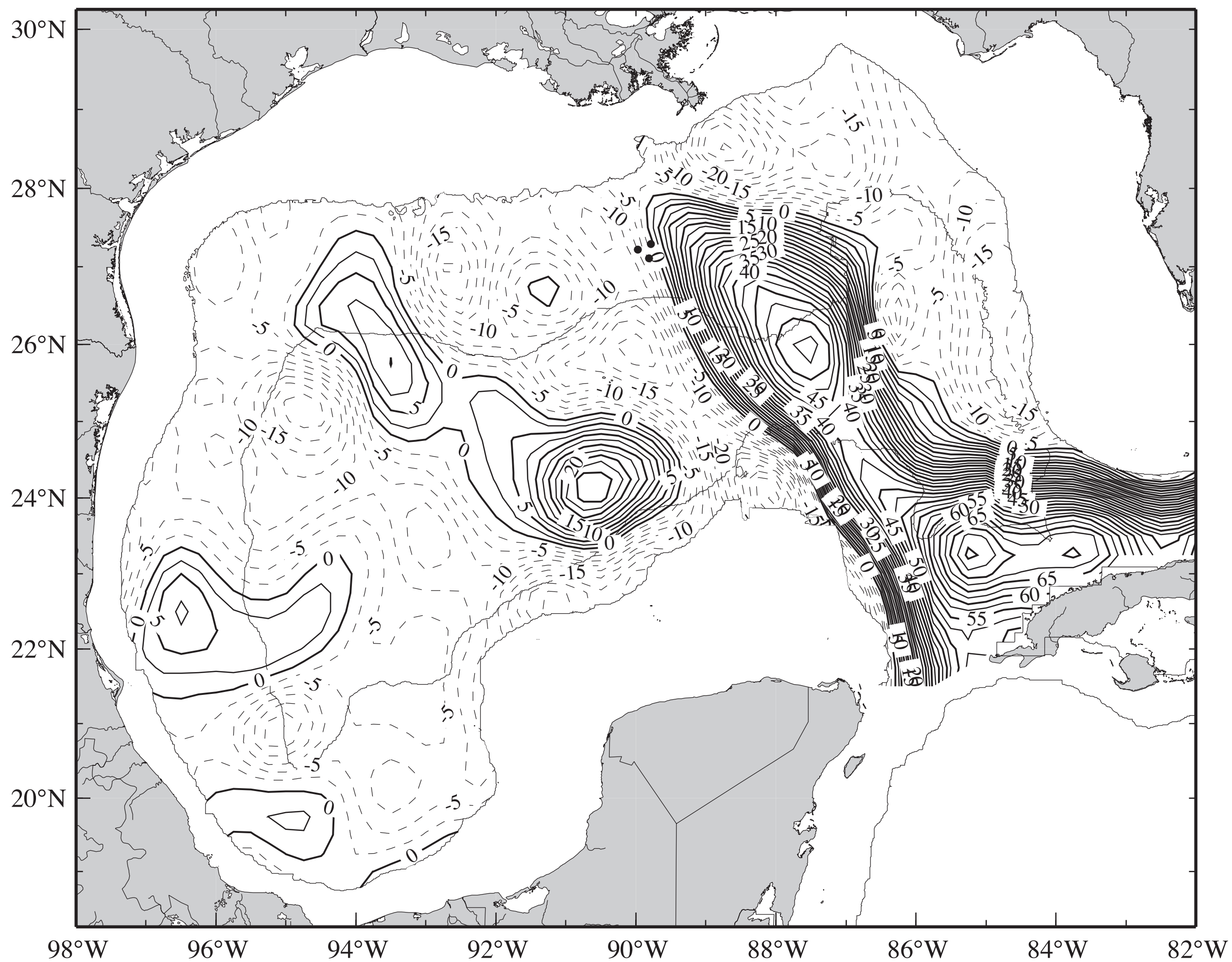

Figure 5.4-12. Sea surface height field for 20 September 1999 prepared in the same manner as the field in Figure 5.4-5. Bathymetric contours are 200 and 3000 m. SSH contour interval is 2.5 cm. Dots show locations of MMS current meter moorings.

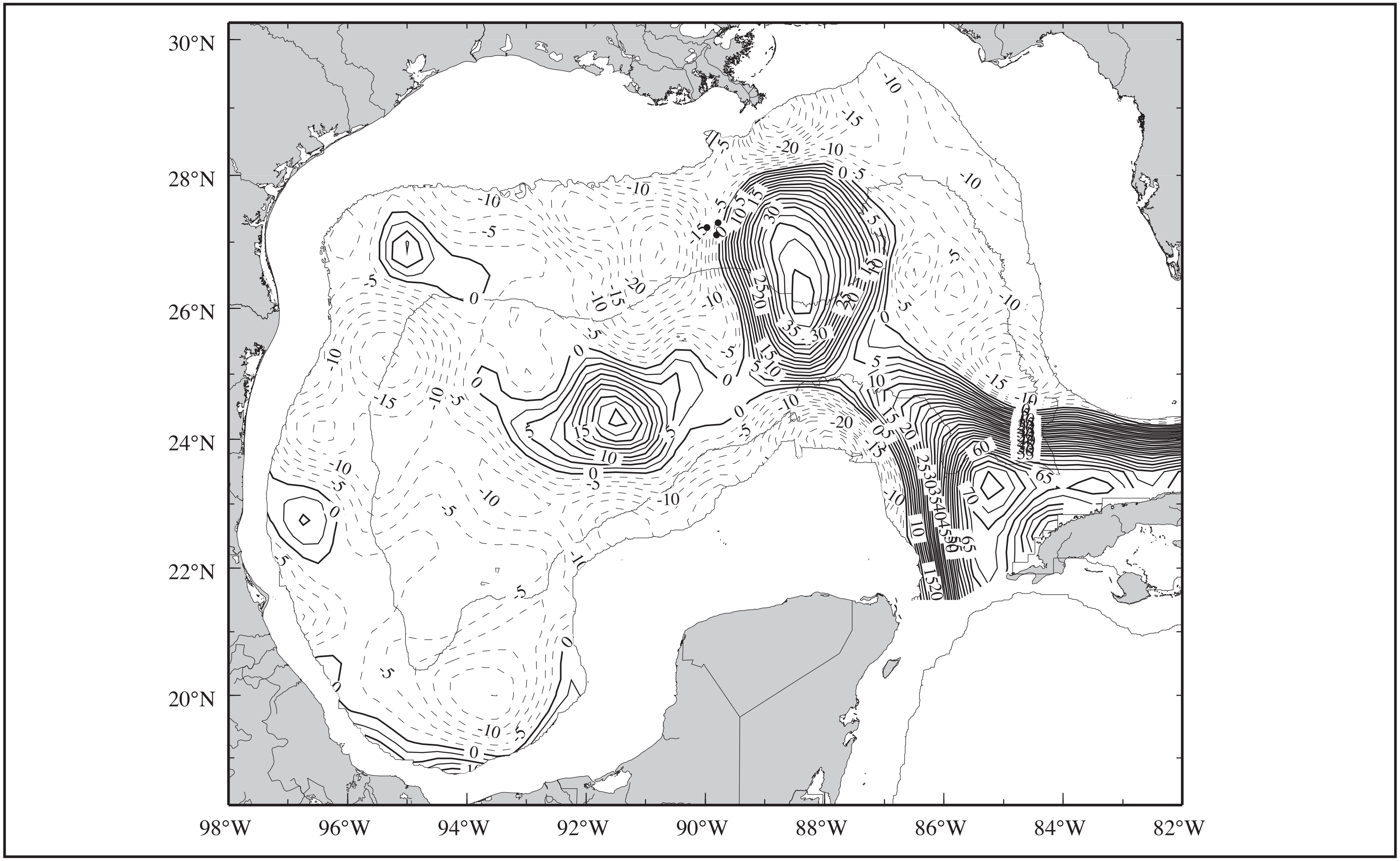

Figure 5.4-13. Sea surface height field for 5 October 1999 prepared in the same manner as the field in Figure 5.4-5. Bathymetric contours are 200 and 3000 m. SSH contour interval is 2.5 cm. Dots show locations of MMS current meter moorings.

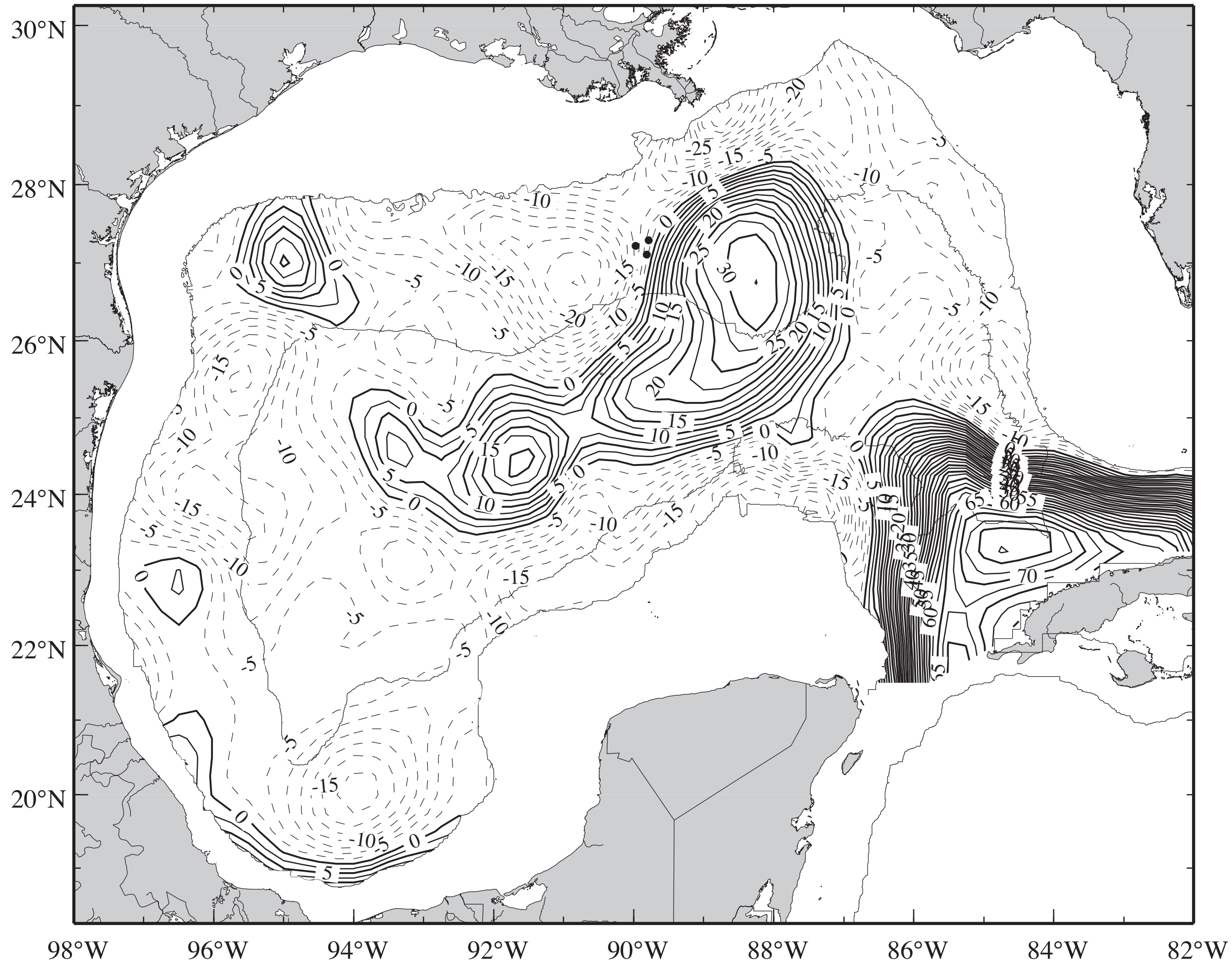

Figure 5.4-14. Sea surface height field for 15 October 1999 prepared in the same manner as the field in Figure 5.4-5. Bathymetric contours are 200 and 3000 m. SSH contour interval is 2.5 cm. Dots show locations of MMS current meter moorings.

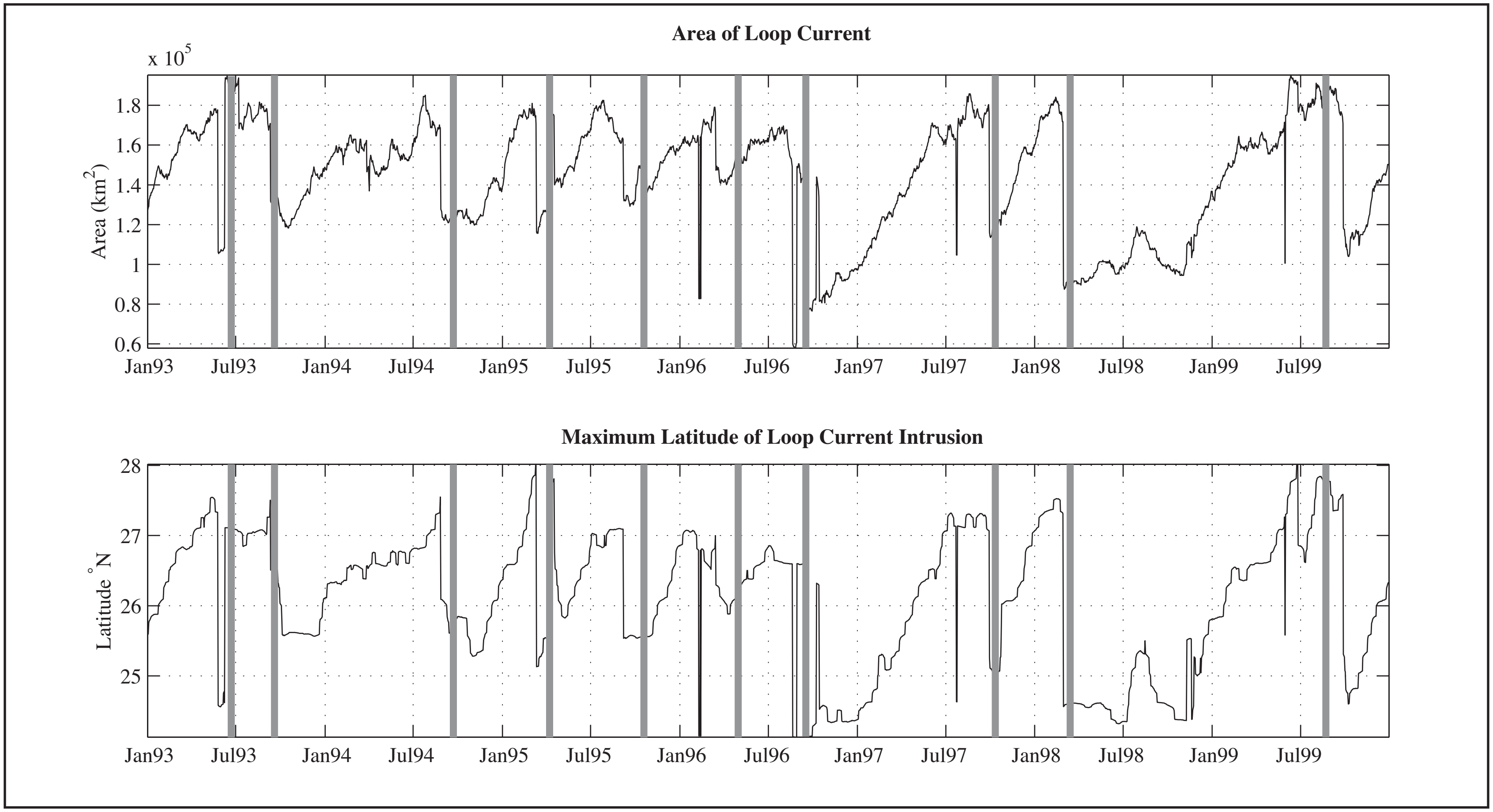

Figure 5.4-15. (Upper) a time series of the surface area in the Gulf of Mexico bounded by the Loop Current as found by integration of the area within the 17-cm SSH contour; and (lower) a time series of the northward penetration of the Loop Current within the Gulf based on the northward extent of the 17-cm SSH contour. Computations courtesy of Robert Leben using techniques described in Hamilton et al. (2000).

15 October - 14 November 1999 Eddy Juggernaut and its appendage ring appear to have strengthened with a center SSH increasing from ~ 35 cm to ~ 45 cm. By 14 November (Figure 5.4-16), the center lay near 26.2°N, 89.5°W. Juggernaut elongated in an approximate east-west orientation to an extension of approximately 550 km.

19 November - 14 December 1999 The southeast front of Juggernaut interacted with the renewed northward extension of the Loop Current (Figure 5.4-17). Its center moved somewhat west of 90°W. It coalesced more firmly with the ring to its west resulting in an elongated anticyclonic circulation reaching the continental slope from 24.5 to 26.5°N.

14-29 December 1999 Eddy Juggernaut again withdrew from the Loop Current and assumed a more circular shape. The "appendage" ring to its west intensified (Figure 5.4-18).

January 2000 — By 3 January, Juggernaut was nearly circular with a diameter ~300 km and SSH at its center of ~35 cm. During most of the month it remained in nearly the same position (Figure 5.4-19). Its connection with the western ring weakened but persisted. It still appeared to be drawing fluid and energy from the Loop Current.

Because of its size, Juggernaut was unique in its dominance of the western Gulf circulation and relation to the Loop Current. (The only comparable LCE to have been observed was Nelson Eddy in 1989.) Its size is clear from the SSH fields. ADCP measurements from a survey through Juggernaut were presented in Section 6.1.1. To further characterize its current field, we present in Figure 5.4-20 the vector time series of currents observed at 106 m and 198 m on MMS mooring I1 located at 29.293°N, 88.795°W in water of depth 2001 m. This mooring and I2 and I3 were part of the DeSoto Canyon Eddy Intrusion Study Extension. The locations of the three moorings are shown as dots in the figures showing the SSH fields. Beginning 29 August 1999, mooring I1 had current measurements extending from 52 m to 1989 m while moorings I2 and I3 each had current measurements at three depths from 1600 m or greater. We show only two near-surface records from I1 because it is representative of the currents in the upper 800 m, and because the deep currents are not correlated with those in the upper ocean, and so not characteristic of the eddy. Additional information regarding currents from MMS moorings I1-I3 are presented in Section 7.1.1 (joint probability distributions, current roses, and persistence tables) and Section 7.1.2 (record-length current vectors and variance ellipses).

When MMS current record I1 began on 29 August 1999, near-surface currents were strongly toward the north-northeast (Figure 5.4-20), in agreement with the SSH field for 26 August (Figure 5.4-11), which shows the outer edge of the northwesternmost extension of the Loop Current situated over the mooring location. The maximum extension of the Loop Current remained near the mooring location throughout September. During that period there was a regular low-frequency oscillation of the surface current between north-northeastward and northwestward. At the end of September, the nascent ring moved somewhat southwestward, resulting in a northerly surface current at mooring I1 by the beginning of October. Figure 5.4-13 shows the SSH field for 5 October. By about 15 October Juggernaut had separated from the Loop Current and begun to move southwestward to pass south of mooring I1. That resulted in a clockwise rotation of surface currents at the mooring, turning from north to east to southeast with time.

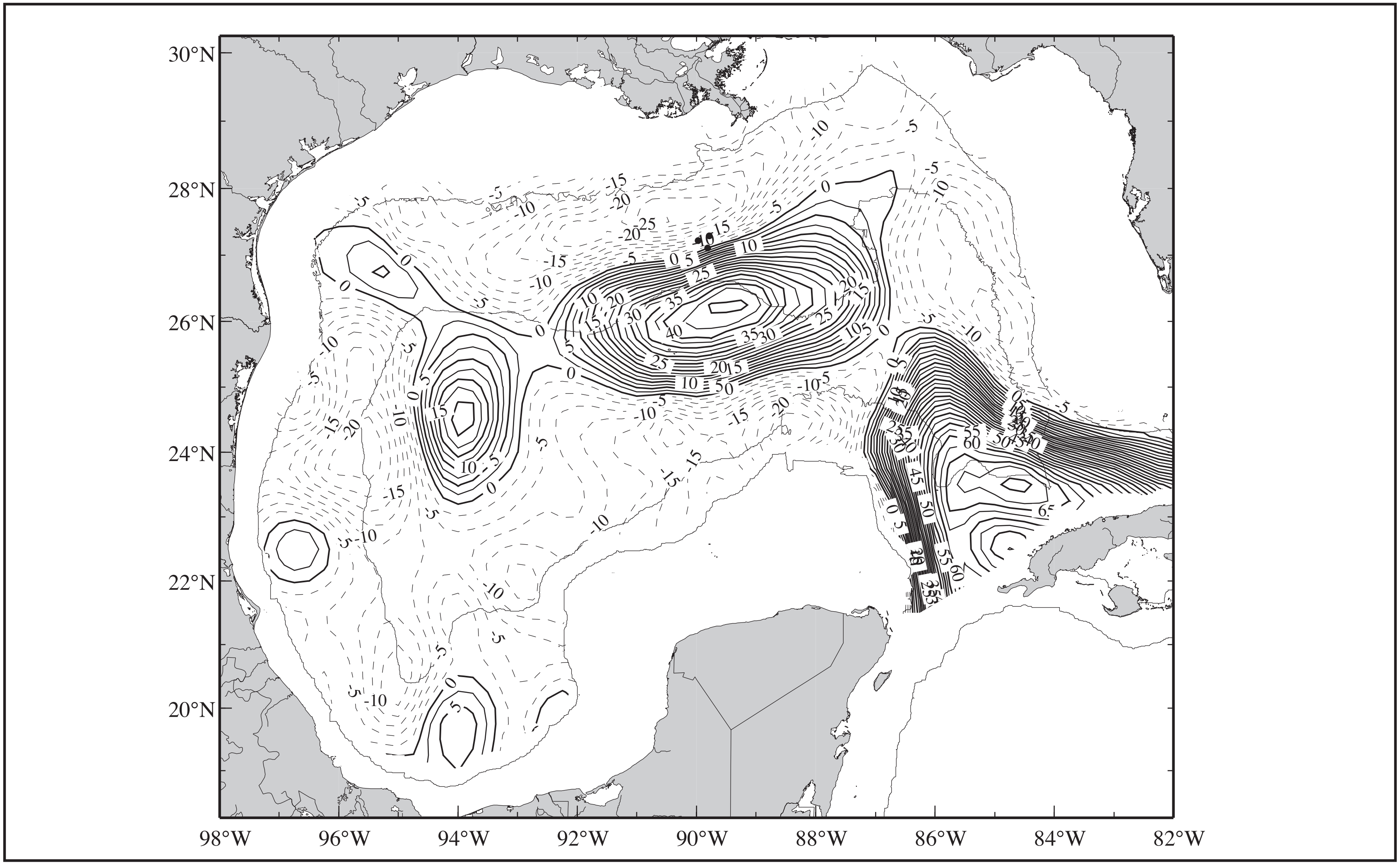

Figure 5.4-16. Sea surface height field for 14 November 1999 prepared in the same manner as the field in Figure 5.4-5. Bathymetric contours are 200 and 3000 m. SSH contour interval is 2.5 cm. Dots show locations of MMS current meter moorings.

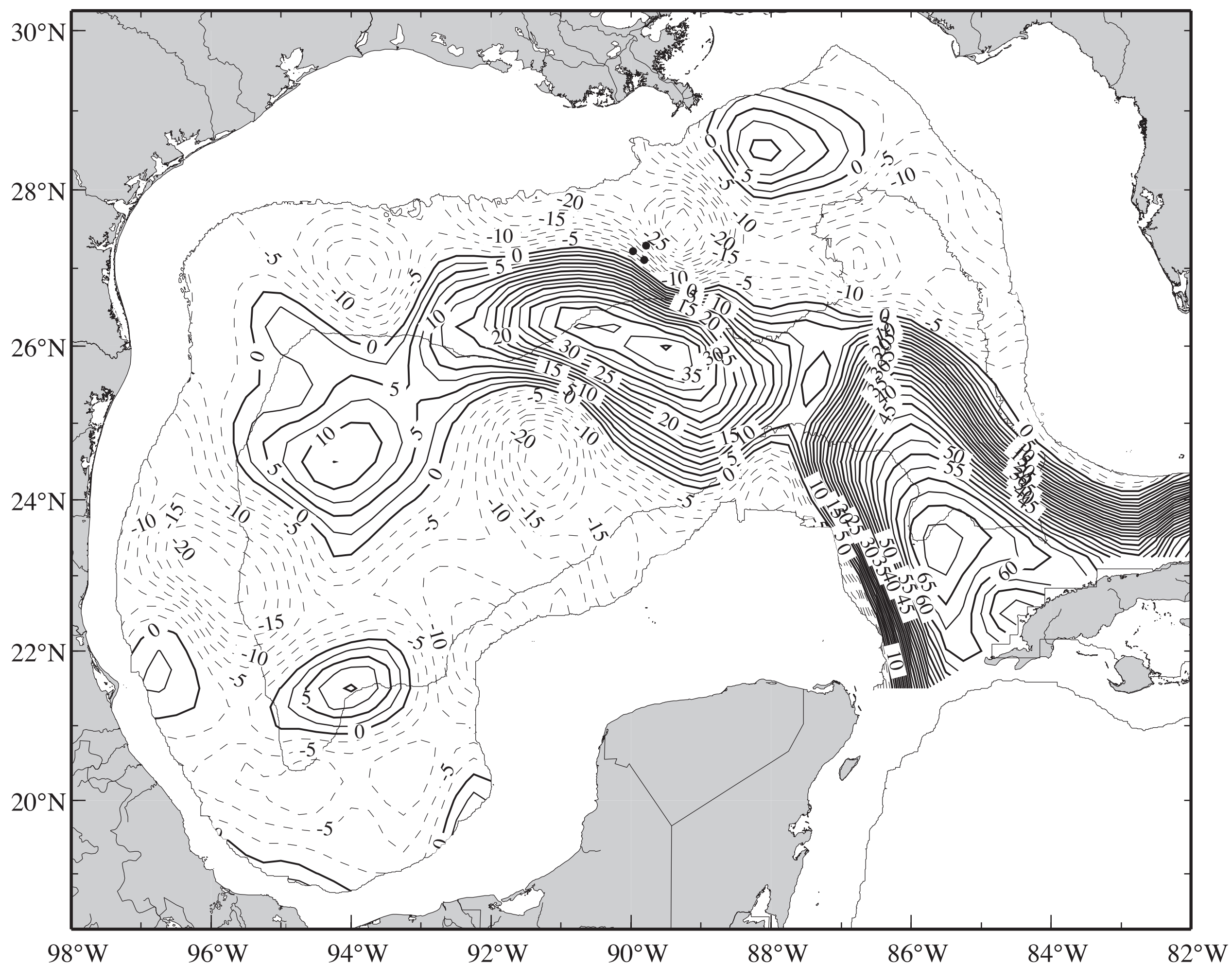

Figure 5.4-17. Sea surface height field for 9 December 1999 prepared in the same manner as the field in Figure 5.4-5. Bathymetric contours are 200 and 3000 m. SSH contour interval is 2.5 cm. Dots show locations of MMS current meter moorings.

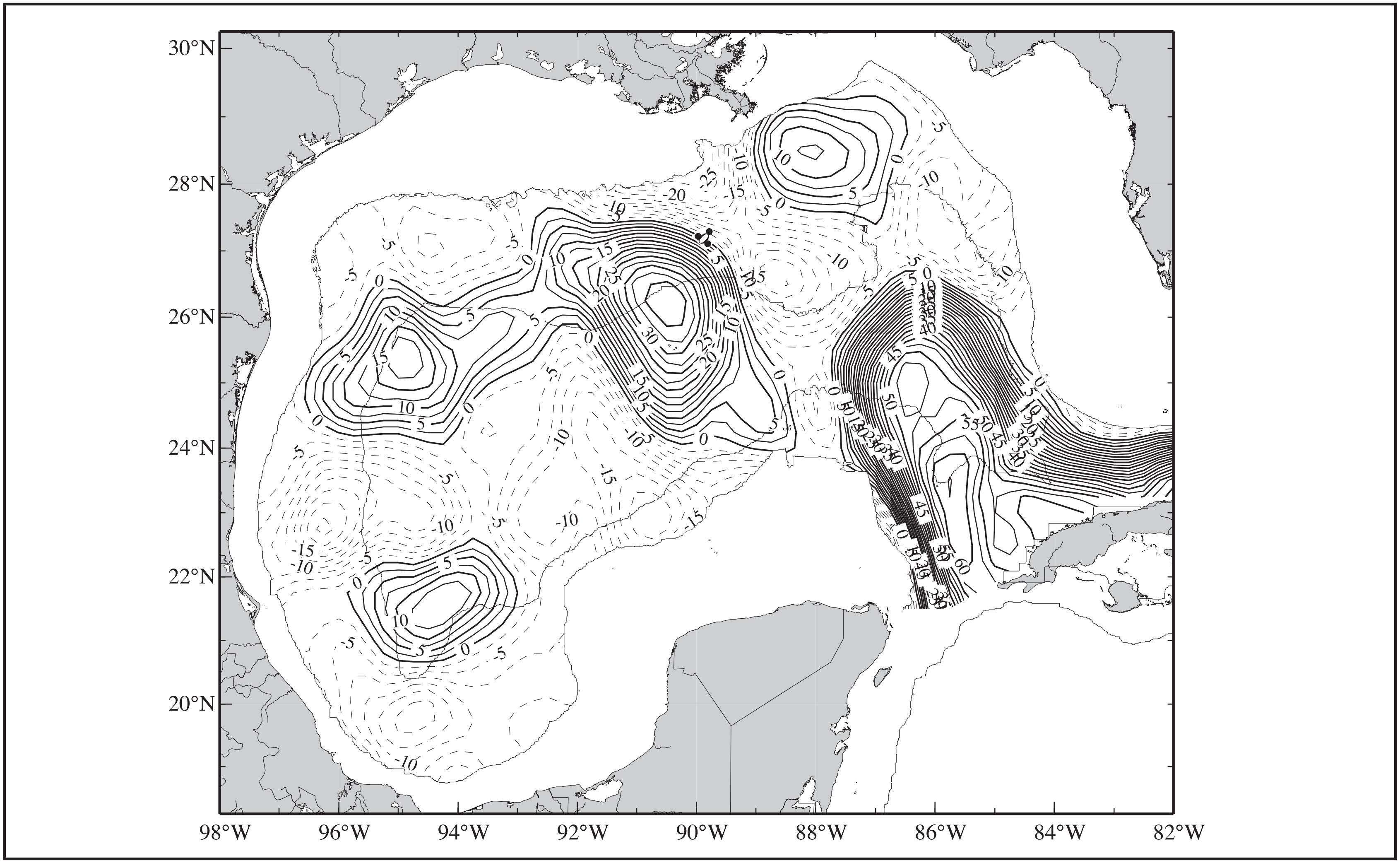

Figure 5.4-18. Sea surface height field for 29 December 1999 prepared in the same manner as the field in Figure 5.4-5. Bathymetric contours are 200 and 3000 m. SSH contour interval is 2.5 cm. Dots show locations of MMS current meter moorings.

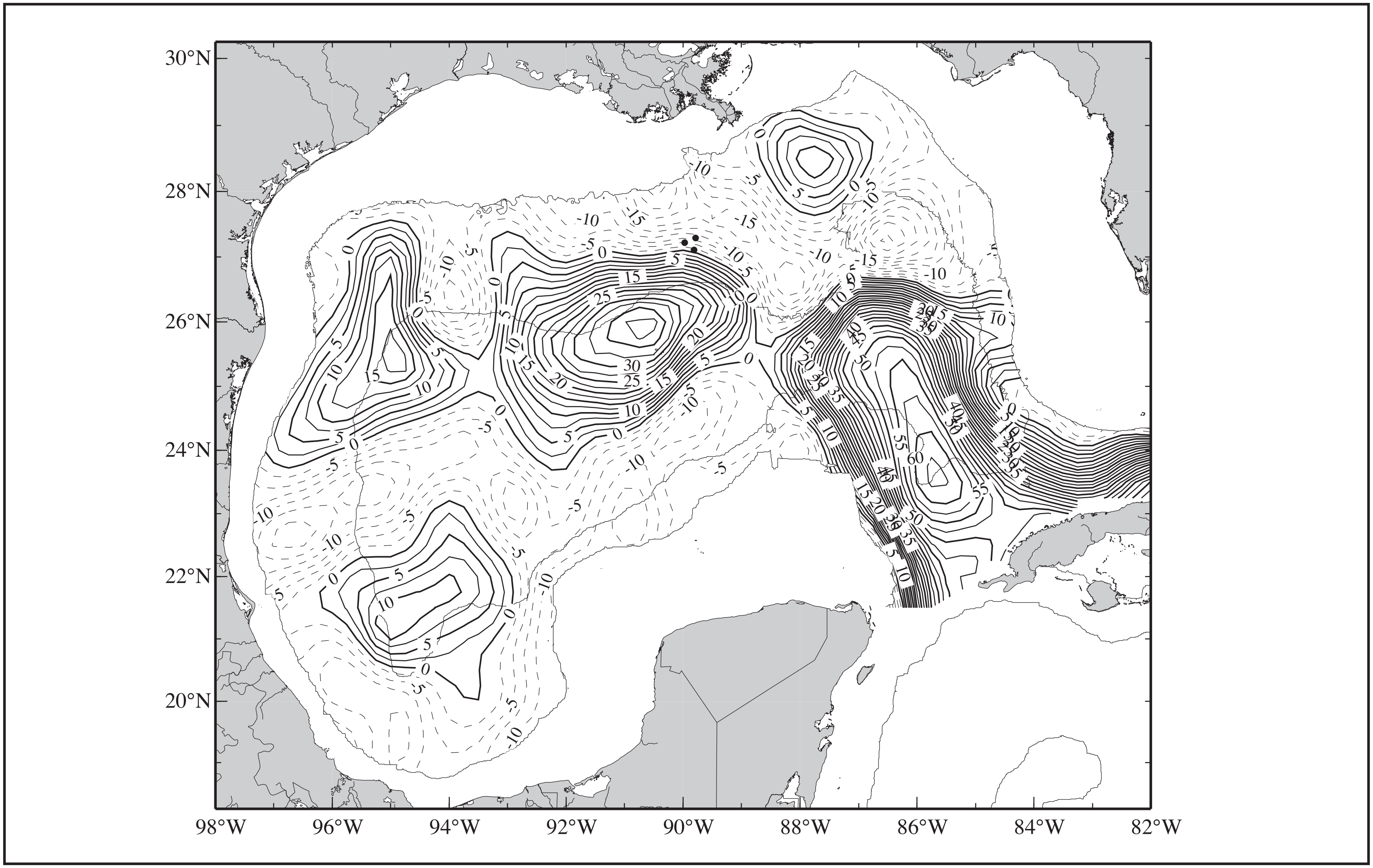

Figure 5.4-19. Sea surface height field for 18 January 2000 prepared in the same manner as the field in Figure 5.4-5. Bathymetric contours are 200 and 3000 m. SSH contour interval is 2.5 cm. Dots show locations of MMS current meter moorings.

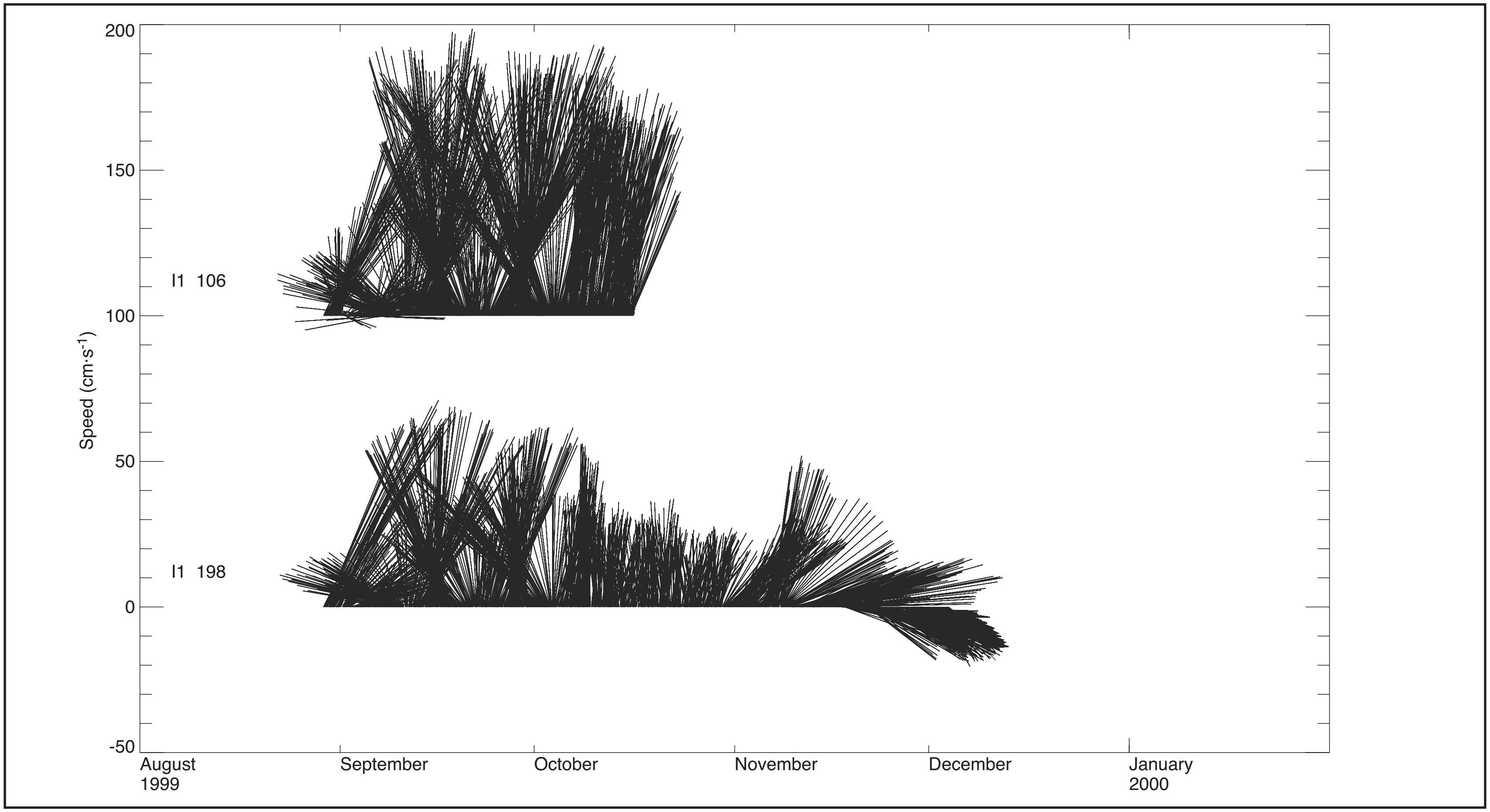

Figure 5.4-20. Vector time series of currents observed at 106 and 198 m on MMS mooring I1 located at 29.293°N, 88.795°W in water of depth 2001 m. North is upward.

6 IDENTIFICATION OF ENERGETIC CURRENT EVENTS

In this section are considered energetic current events observed to occur in the deepwater portion of the Gulf of Mexico. These include surface-intensified eddies; deep barotropic motions, sometimes with bottom intensification; atmospheric storm generated motions, internal waves generated by topographic influence, and mid-water current jets. The identification of such events is based solely on a search of current measurements and numerical model output. Our search has been for situations where the magnitudes of currents over the period of an event are considerably greater than the background currents for the region and/or for situations where the currents had characteristics known to be associated with the particular class of event.

6.1 General Description of Energetic Current Events in the Deepwater Gulf

6.1.1 Loop Current and Surface-Intensified Current Rings

The most energetic current phenomenon found in the deep water Gulf of Mexico is the Loop Current. Figure 6.1.1-1 shows shipboard 150 kHz ADCP current vectors from 4- or 8-m vertical bins centered at 17-m depth for a section across the Yucatan Channel collected during October 1999 on a National Ocean Partnership Program (NOPP) Gulf of Mexico Ocean Monitoring System (GOMOMS) survey. On this section most of the surface flow was northward to northeastward, with speeds exceeding 100 $cm \cdot s^{-1}$ over the width of the main inflow to the Gulf. However, near the Yucatan Peninsula on the west and off the west coast of Cuba to the east, there was surface flow from the Gulf toward the Caribbean Sea.

Figure 6.1.1-2 shows contours of smoothed ADCP (38 kHz) current components normal to the same vertical section pictured in Figure 6.1.1-1. The section shows the southward flow off western Cuba extended to at least the 600-m depth of the observations and the northward, energetic currents ($\geq$ 40 $cm \cdot s^{-1}$) of the Loop Current reached below the 600-m depth. The southward near-surface flow off the Yucatan Peninsula is seen only as a subsurface feature, because the 38 kHz data did not extend as far west as the 150 kHz data, which show southward flow in the upper 250 m. For comparison, Figure 6.1.1-3 shows a vertical section of the normal component of geostrophic speed relative to 800 m (or the deepest sampled depth) along the same section. As with the ADCP currents, a small region of southward current is seen at the western side of the channel and a large region of southward flow is seen to the east off Cuba. The total northward transport estimated from these speeds is 17 Sv for the section shallower than 800 m.

In Figure 6.1.1-4 are shown surface current vectors from geomagnetic electrokinetograph (GEK) measurements and geopotential anomaly of the sea surface for the eastern Gulf of Mexico showing the Loop Current and a newly detached ring as observed in 1967 (after Nowlin and Hubertz 1972). For the hydrographic stations across the Loop Current and ring along the lines shown in Figure 6.1.1-4 (right), vertical sections of geostrophic current relative to 1350 m are shown in Figure 6.1.1-5, along with GEK surface current components normal to the sections. The GEK measurements show currents in the cores of these features in excess of 1.5 $m \cdot s^{-1}$, considerably greater than the relative geostrophic surface current, which represents an average between stations.

Another prominent class of energetic current events in the Gulf is represented by anticyclonic eddies that separate from the Loop Current, referred to here as Loop Current Eddies (LCEs). This class includes also other surface-intensified current rings both cyclonic and anticyclonic.

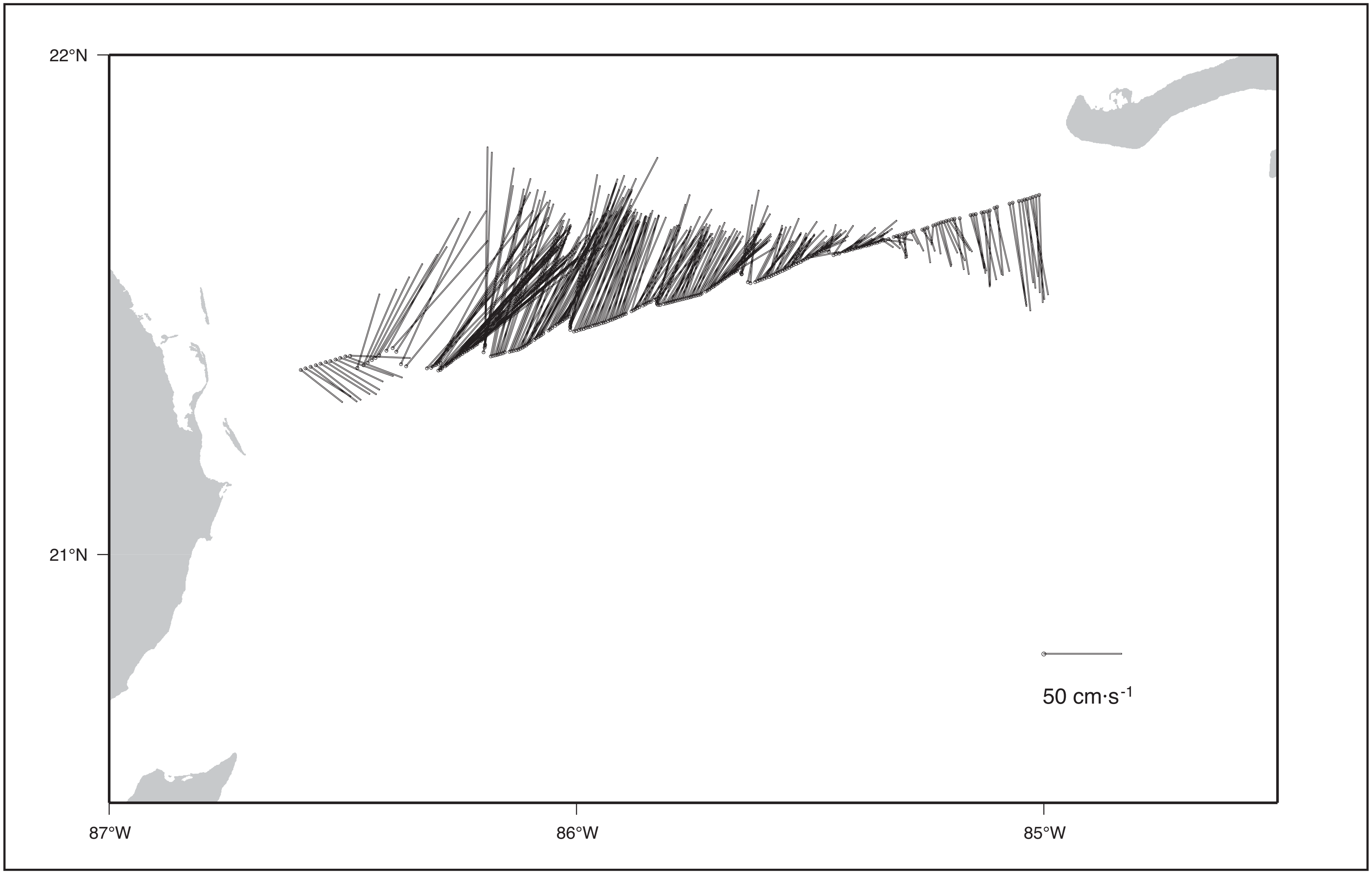

Figure 6.1.1-1. Shipboard 150 kHz ADCP currents from 4- or 8-m depth bins centered at approximately 17 m along a section made during October 1999 on a cruise across the Yucatan Channel. (Courtesy of the NOPP-sponsored GOMOMS project.)

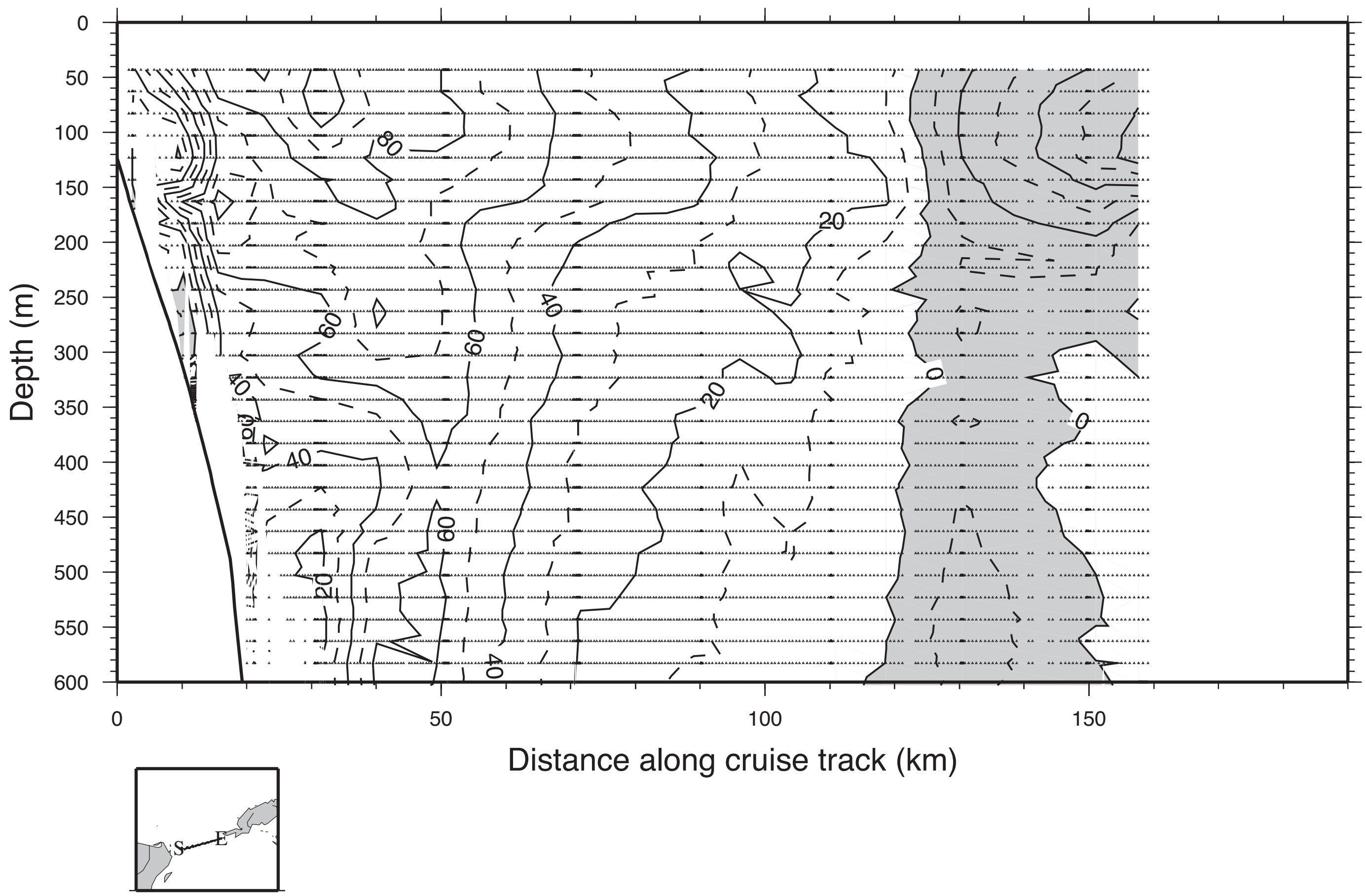

Figure 6.1.1-2. Vertical section of shipboard 38 kHz ADCP current component normal to the same transect across the Yucatan Channel shown in Figure 6.1.1-1. Currents were averaged for 5 minutes over 20-m vertical bins, and then smoothed over 8 km in the horizontal. Shading indicates southward flow.

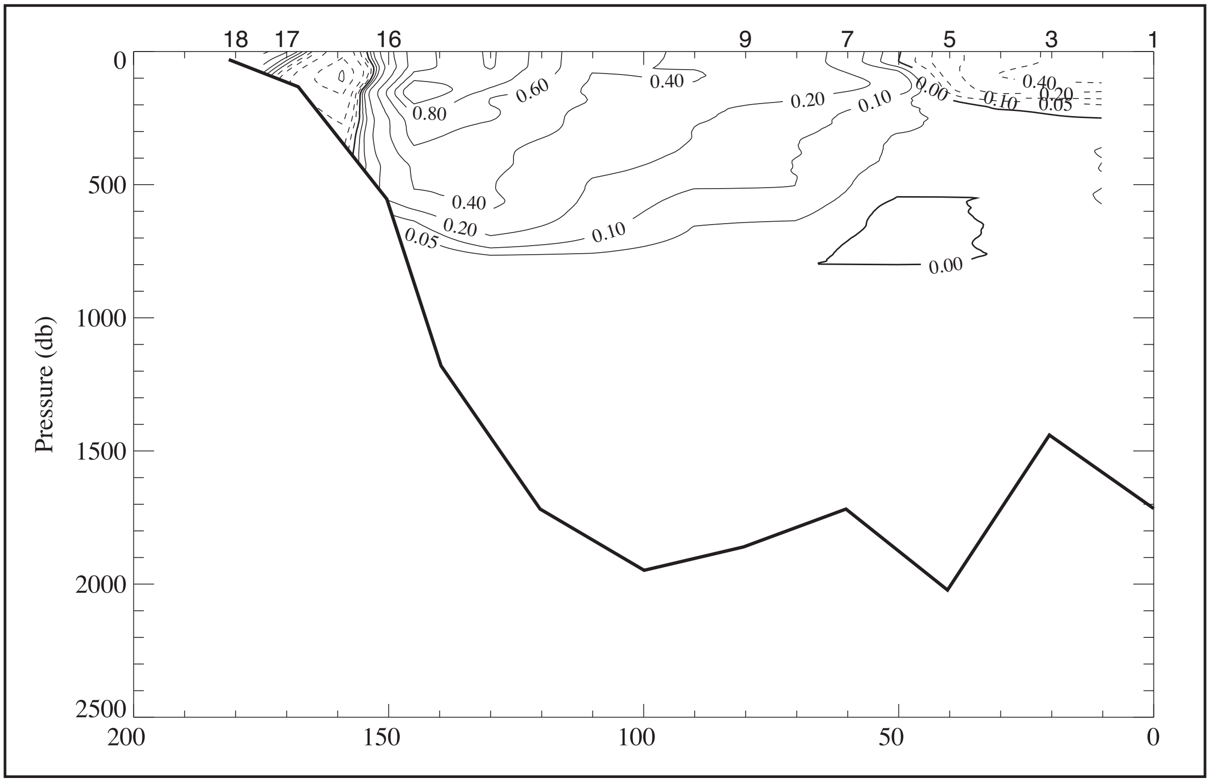

Figure 6.1.1-3. Geostrophic speed relative to 800 db or greatest depth sampled, normal to section across Yucatan Channel shown in Figure 6.1.1-1. Results are based on CTD casts made during the October 1999 NOPP cruise to the Cayman Sea. Isotachs are in $m \cdot s^{-1}$. Broken lines indicate southward flow. Total northward transport estimated at 17 Sv.

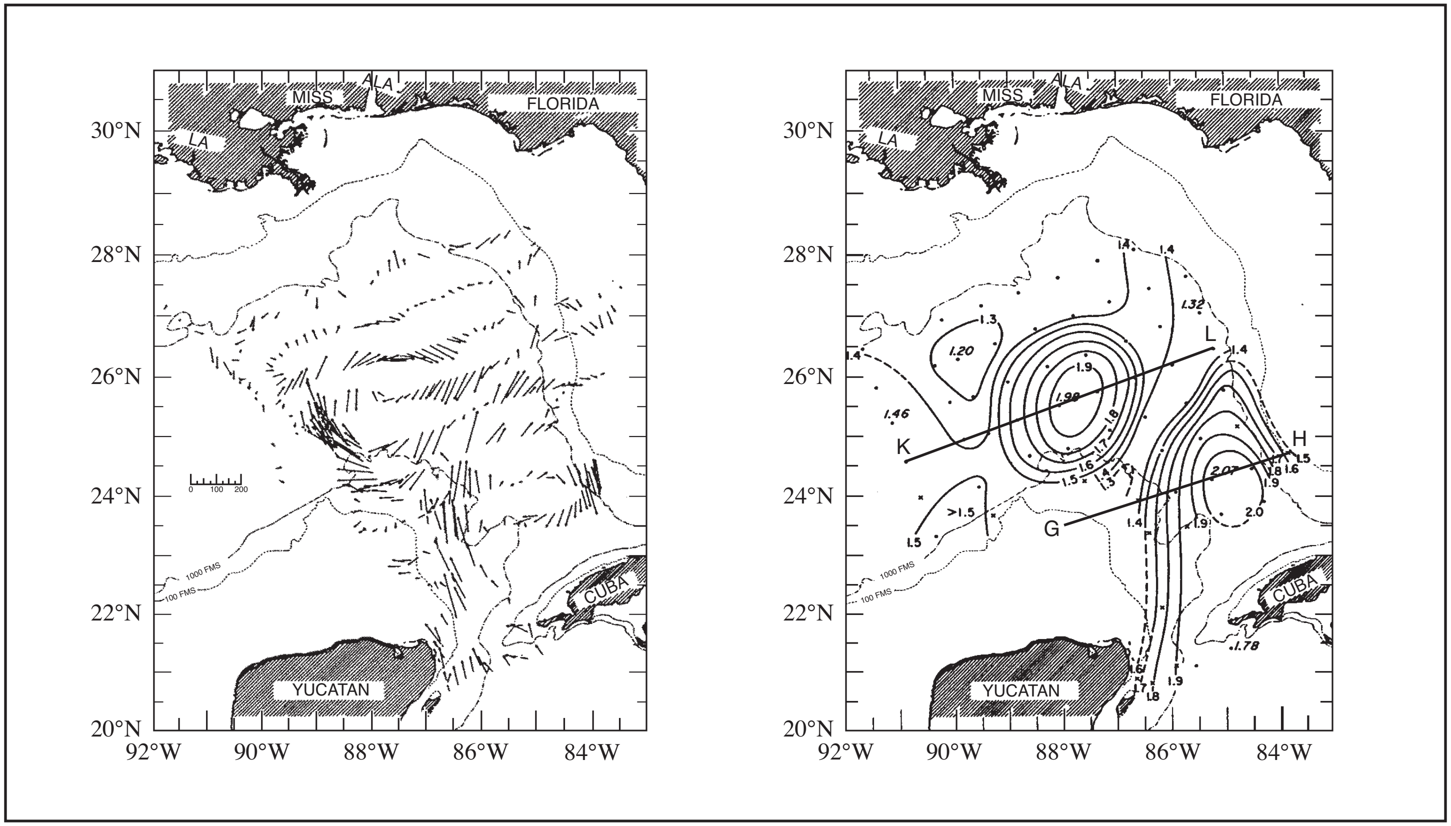

Figure 6.1.1-4. GEK vectors and geopotential anomaly (dynamic m) of the sea surface relative to 1350 db for *Alaminos* cruise 67-A-4 during June 1967. Station positions are shown. A newly separated anticyclonic ring is seen northwest of the Loop Current.

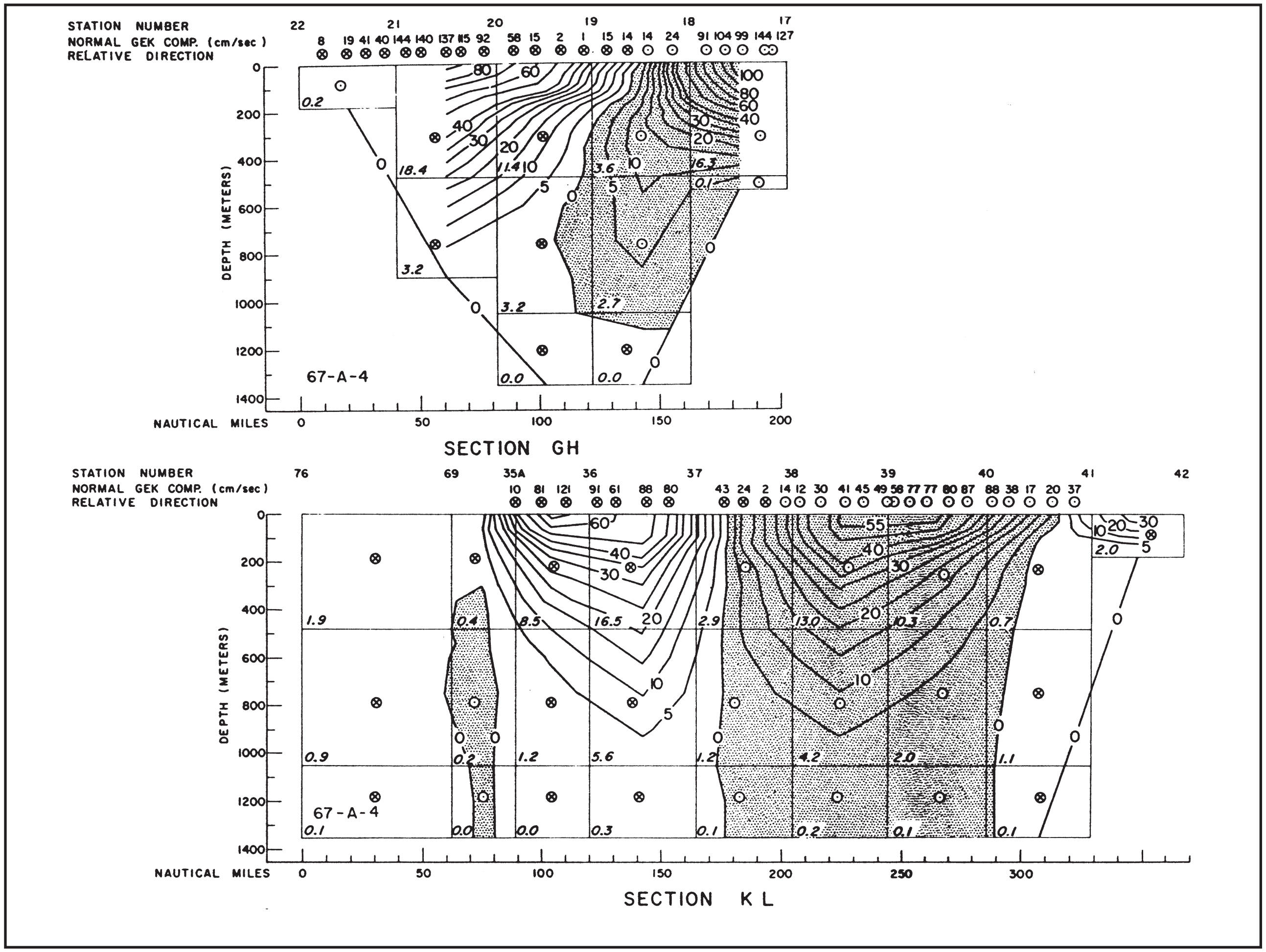

Figure 6.1.1-5. Isotachs of geostrophic speed ($cm \cdot s^{-1}$) relative to 1350 db, normal to section GH which passes southwest-northeast through both limbs of the Loop Current and section KL which passes southwest-northeast through the ring center. Also shown are normal components of GEK surface velocities measured along each section and relative volume transport ($10^6\ m^3 \cdot s^{-1}$) for indicated depth intervals between adjacent stations. A circled dot indicates flow toward the reader. Data are from Alaminos 67-A-4, June 1967. Locations of sections are shown in Figure 6.1.1-4.

Figure 6.1.1-6 (after Forristall et al. 1992) shows swirl speeds in excess of 100 $cm \cdot s^{-1}$ through a relatively strong LCE, called Fast Eddy, during August 1985.

Another extremely strong eddy, called Juggernaut, was surveyed 27-29 October 1999 as it was separating from the Loop Current. In Figures 6.1.1-7 through 6.1.1-9 are shown: (a) shipboard ADCP (150 kHz) vectors averaged over 4-m vertical bins centered approximately at 41 m overlaid on sea surface height anomaly from satellite altimeter data nowcast to 28 October; (b) ADCP vectors from the 17-m level, and (c) ADCP vectors from the 96-m level. Clearly the kinematic field is well represented by the SSHA field. The developing eddy had maximum current speeds of ~150 $cm \cdot s^{-1}$ near-surface and ~100 $cm \cdot s^{-1}$ at 100 m. In November, after Juggernaut had detached and moved to the central Gulf, the high speeds persisted, near-surface and penetrating to depth, and the eddy was elongated with a semi-major axis diameter of about 450 km.

6.1.2 Currents Generated by Energetic Wind Events

Strong, episodic wind events that force the Gulf include tropical cyclones (especially hurricanes), extratropical cyclones, and cold air outbreaks. Such wind events can result in extreme waves and cause currents with speeds of 100-150 $cm \cdot s^{-1}$ over the continental shelves. Examples for the shelf and upper slope off Texas and Louisiana are given in Nowlin et al. (1998a). Others (e.g., Brooks 1983, 1984; Molinari and Mayer 1982) have reported the effects of such phenomena down to depths of 700 and 980 m over the continental slopes in the northwestern and northeastern Gulf, respectively.

Tropical conditions normally prevail over the Gulf from May or June until October or November. During that time the region is dominated by moist, warm tropical air masses, and the atmospheric circulation is influenced by the northeast trade winds. This leads to fewer frontal passages in summer than in winter, but also results in tropical storm systems entering or developing within the Gulf. A review of the meteorological data base and climatology of the Gulf is given by Florida A&M University (1988). The nominal hurricane season is 1 June through 30 November.

A number of studies consider the effects of hurricanes on ocean currents and thermal (and density) structures. Those with a focus on hurricanes in the Gulf of Mexico include Leipper (1967), O'Brien and Reid (1967), O'Brien (1967), Forristall (1974), Forristall (1980), and Cooper and Thompson (1989a, 1989b). Although the three hurricanes studied were not in the Gulf, Sanford et al. (1987) and Price et al. (1994) gave results of direct current observations within hurricanes accompanied by model hindcasting and comparisons that should be applicable to the Gulf. They measured currents in the upper 200 m by deploying aircraft expendable current profilers (AXCP) in a pattern through each hurricane using a weather reconnaissance plane from which meteorological observations were taken. They separated surface mixed layer (50 m) and surface wave currents. The maximum surface currents from combining these two components were estimated at 133 to 346 $cm \cdot s^{-1}$. These results are consistent with their model results. The mixed layer currents showed patterns of divergence centered behind the eyes of the storms; these lead to upwelling at the base of that layer and a lowering of sea level above. The mixed layer divergence and the associated distortion of the thermal and density fields occurred on near-inertial periods, giving rise to inertial waves with wave lengths of several hundred km and decay scales of 5-10 d, e.g., see results of Brooks (1983) later in this section. Following the initial response of the ocean to energetic atmospheric events, there is the response of inertial oscillations as the ocean once again is restored to equilibrium.

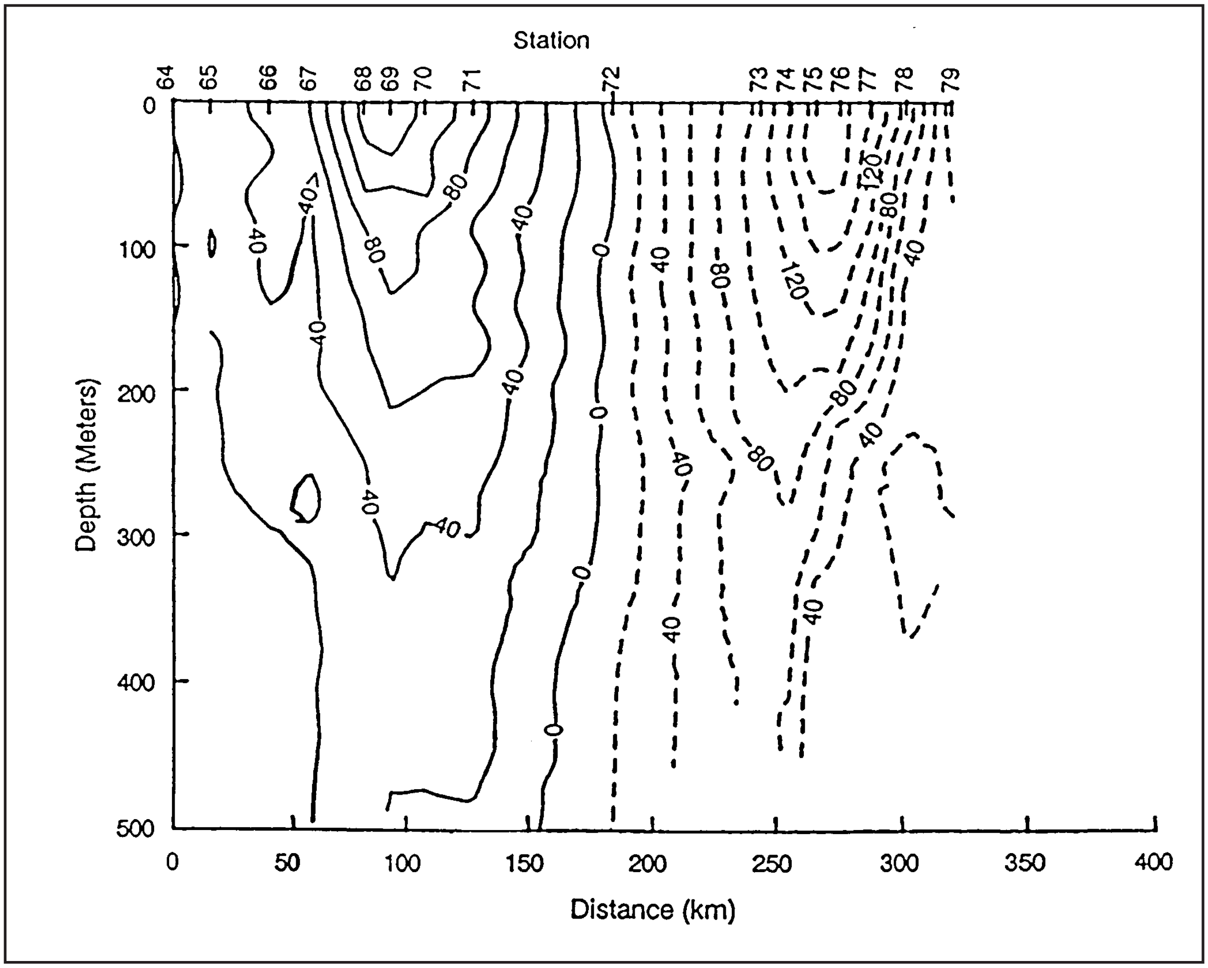

Figure 6.1.1-6. Components of velocity (cm·s^{-1}) normal to a section extending from approximately 27.4°N, 90.6°W (station 64) to 24.8°N, 89.4°W (station 78). Measurements were made by Forristall et al. (1992) using a lowered Neil Brown acoustic current meter; ship motion was estimated using Loran-C and motion of the instrument relative to the ship was measured with an ultra-short baseline acoustic system. This section crossed the LCE called Fast Eddy during August 1985, and components are taken to represent azimuthal swirl speeds of the eddy. Positive components are directed toward 65°.

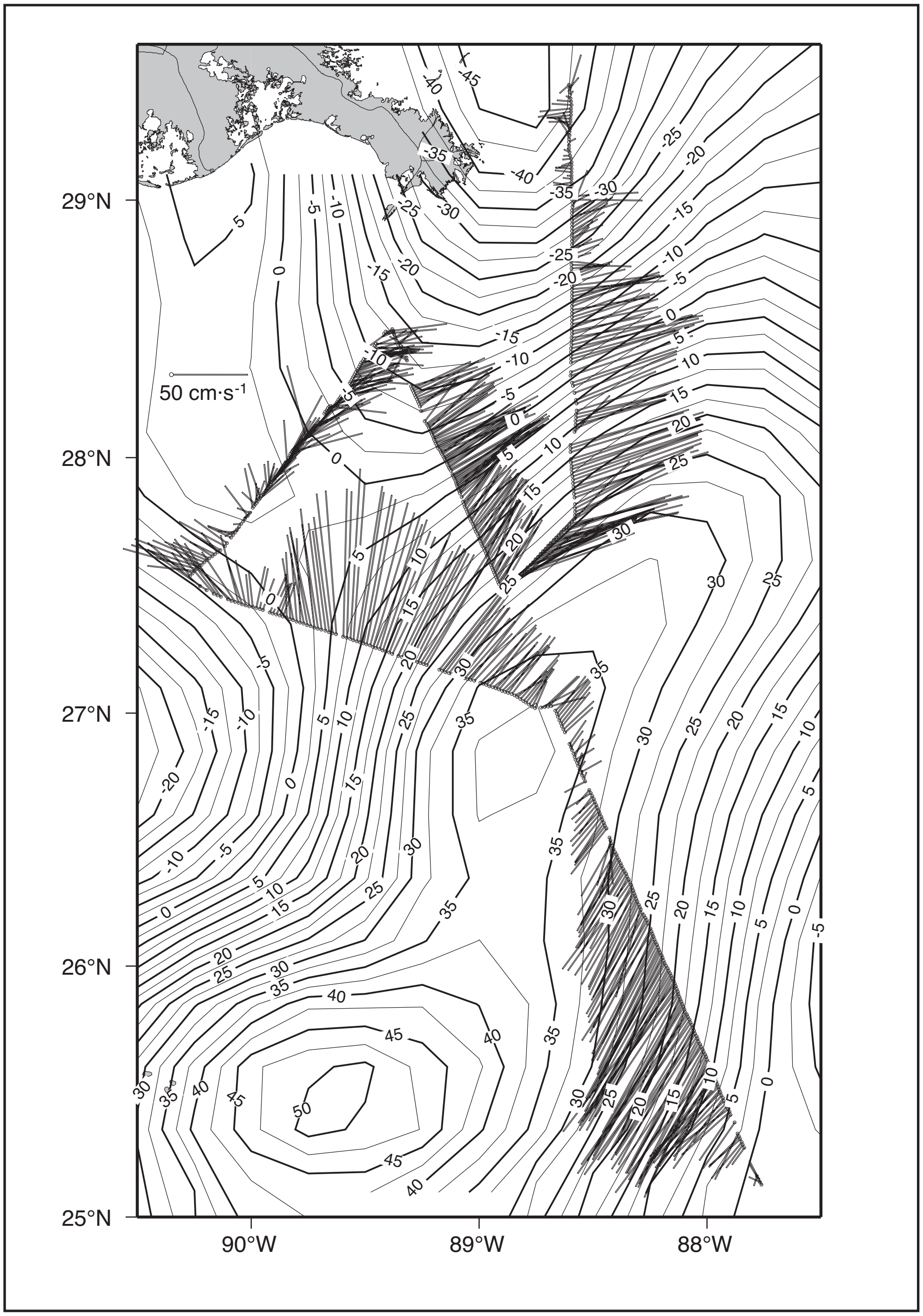

Figure 6.1.1-7. ADCP (150 kHz) current vectors averaged over 4-m vertical bins centered approximately at 41 m on the NOPP-sponsored GOMOMS cruise, 27-29 October 1999. Track crosses LCE Juggernaut during a period when that LCE was detaching from the Loop Current. The sea surface height anomaly field (contour interval 2.5 cm) is from satellite altimeter nowcast data for 28 October 1999.

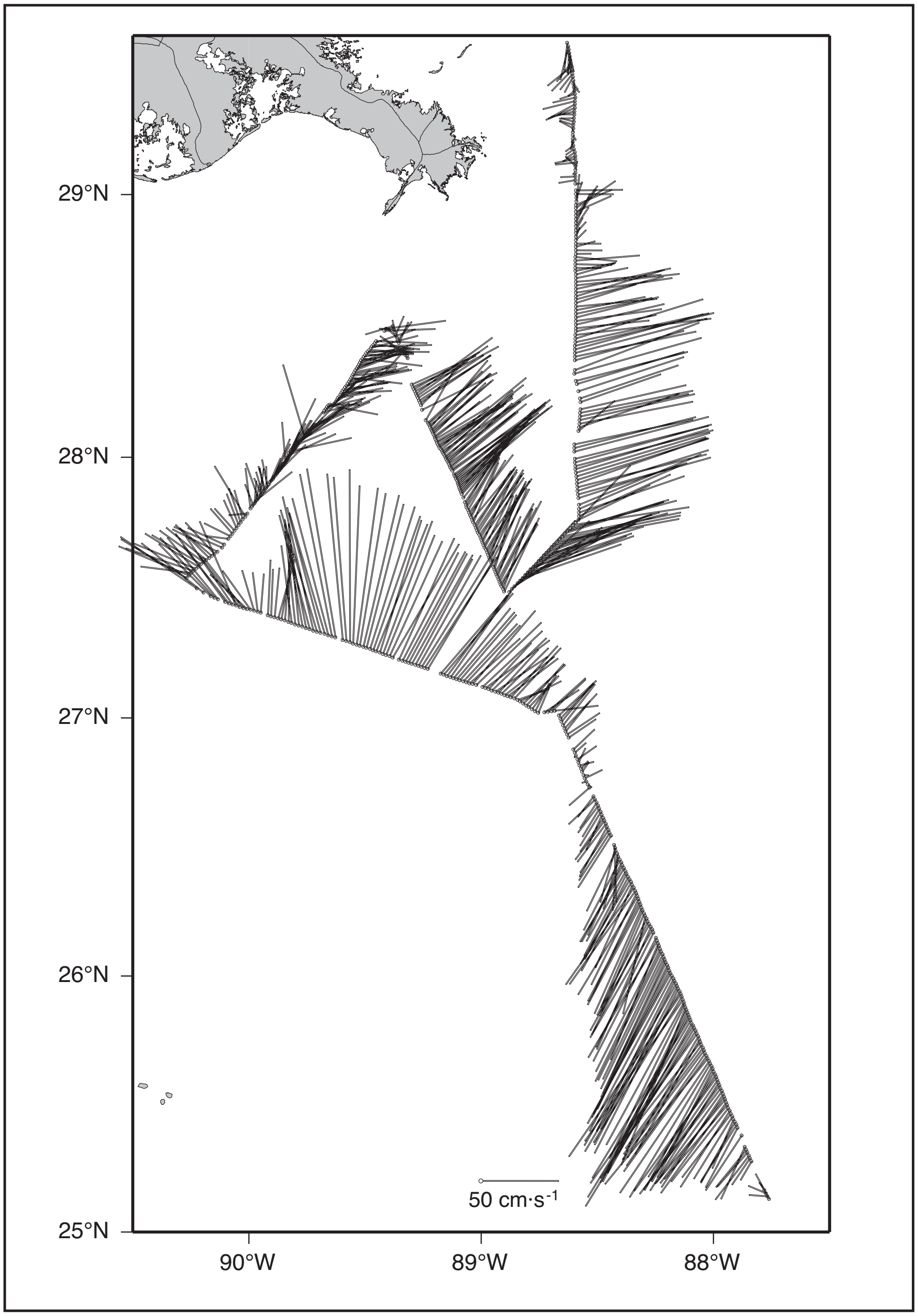

Figure 6.1.1-8. ADCP (150 kHz) current vectors averaged over 4-m vertical bins centered at 17 m on the NOPP-sponsored GOMOMS cruise, 27-29 October 1999.

Figure 6.1.1-9. ADCP (150 kHz) current vectors averaged over 4-m vertical bins centered at 97 m on the NOPP-sponsored GOMOMS cruise, 27-29 October 1999.

Figure 6.1.2-1 shows horizontal current vectors (hourly values from 3-hr low-passed records) during late August 1992 from two locations off Louisiana at approximately 90.5°W on the shelf edge and upper slope (see Section 6.3.4). Moorings 13 and 12 were located in water depths of 200 and 504 m, respectively. Current meter depths are indicated on the figure. The eye of Hurricane Andrew passed on a northwestward track about 85 km north of mooring 13 at 0000 UTC on 26 August. Near-surface instruments recorded a large surge of water directed to the left of the storm's track just before the passage of the eye; maximum values at 10 m on mooring 13 reached 163 $cm \cdot s^{-1}$. Following the initial surge, an oscillation with near-inertial period was set up which penetrated, with diminished amplitude, to the deepest instrument on mooring 13 approximately 24 hours after the initial surge. Some time delay and considerable decrease in amplitude with depth is seen, although the maximum speed at 190 m exceeded 100 $cm \cdot s^{-1}$. There was a coherent but weak response at 490 m at mooring 12 (note change in velocity scale). The inertial oscillation continued for about a week with diminishing amplitudes. A review of shallow currents associated with Andrew is presented by Keen and Glenn (1999).

Figure 6.1.2-2 shows hourly current components (u positive to the east and v positive to the north) measured at indicated depths from 200 to 700 m on moorings S (26°N, 96.28°W) and C (55 km north of S). Both moorings were approximately on the 730-m isobath. About 0000 UTC on 10 August 1980, the eye of Hurricane Allen passed some 65 km WSW of mooring S on a track toward the NNW. (See Figure 6.3.2-1.) The effects of the hurricane passage were reported by Brooks (1983). Currents were stronger at mooring C than at S, although currents at both were affected—even to within 20 m of the bottom. A strong southward, along-shelf current occurred with the landward passage of the hurricane; maximum speeds exceeded 90 $cm \cdot s^{-1}$ in the thermocline at 200 m and 15 $cm \cdot s^{-1}$ at 700 m. This surge triggered a series of internal waves with near inertial period; these elliptical motions had maximum speeds along shore which reached a range of 50 $cm \cdot s^{-1}$ within about 3 days and then lasted for about 5 days with decreasing amplitudes. These oscillations were coherent over the scale of mooring separation (55 km) and with depth.

From October or November until March or April the Gulf experiences intrusions of cold, dry continental air masses. These result in the formation of extratropical cyclones and cold air outbreaks, both of which can cause quite energetic surface currents. On average about 10-12 extratropical cyclones are formed over the northern Gulf per year; the number of frontal passages varies from 0-2 per month in summer to order 10 per month in winter months. To illustrate the effects of an extreme extratropical cyclone, Figure 6.1.2-3 shows eastward (u) and northward (v) components of currents (hourly values from 3-hr low-passed records) from two moorings located off Louisiana at approximately 90.5°W. Mooring 13 was in water of depth 200 m; mooring 12 was in water depth of 504 m. (See Figure 6.3.4-1 for location.) On 12 March 1993, a class 5 extratropical cyclone moved from west to east across the Texas-Louisiana shelf with its center approximately over the 1500-m isobath. (A class 5 extratropical cyclone is one that approaches hurricane strength; see Nowlin et al. 1998b and Hsu 1993 for discussion.) Initially the flow over the outer shelf and slope was toward the northeast as part of an induced cyclonic circulation over the Texas-Louisiana shelf. Following the passage of the storm out of the area, on 13 March, there occurred a surge to the southwest followed by a period (14-17 March) of strong motion toward the northeast, with diurnal modulation. This was followed by an energetic near-inertial oscillation with decreasing amplitude lasting for over a week. Maximum observed speeds associated with this event were: 65, 22, 67, 41, and 35 $cm \cdot s^{-1}$ at mooring/depth (m) 12/12, 12/100, 13/10, 13/100, and 13/190, respectively.

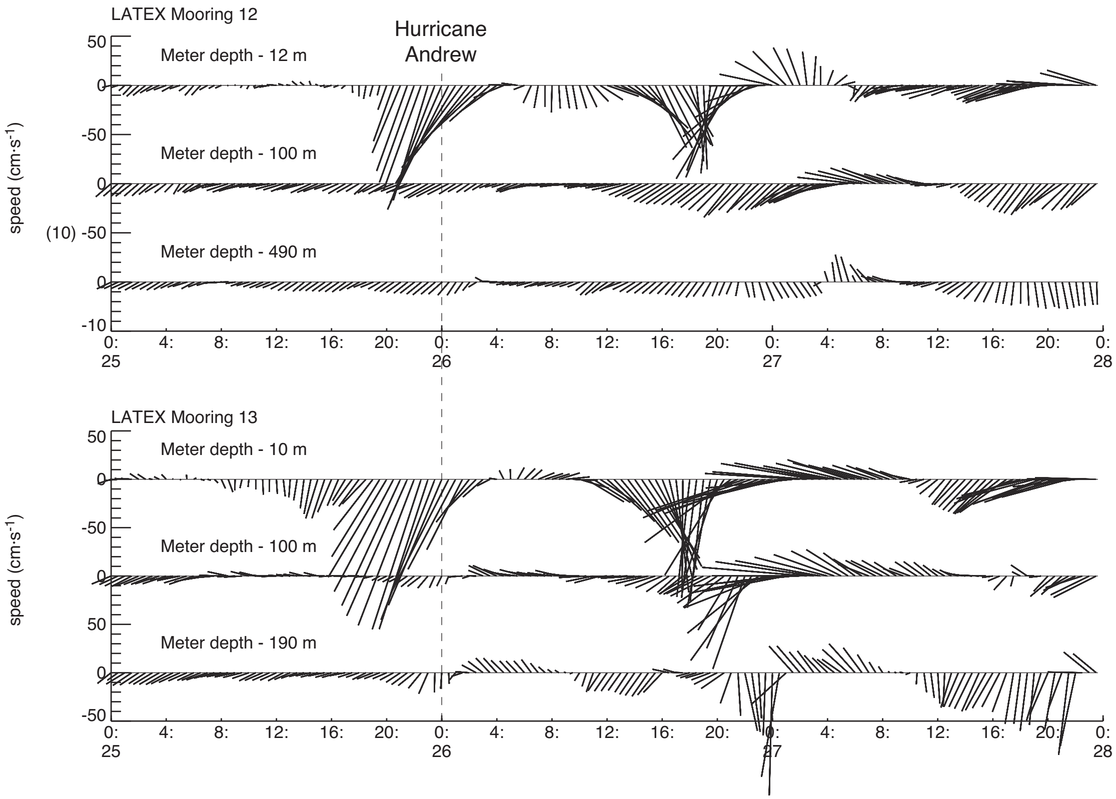

Figure 6.1.2-1. Horizontal current vectors (hourly values from 3-hr low-passed records) during late August 1992 from two locations off Louisiana at approximately 90.5°W on the shelf edge and upper slope. The cross-shelf components are oriented up and down (up is on shore) and alongshelf components are oriented across the figure (generally eastward to the right). Moorings 13 and 12 were located in water depths of 200 and 504 m; current meter depths are indicated. The eye of Hurricane Andrew passed on a northwestward track approximately 85 km north of mooring 13 at about 0000 UTC on 26 August (Figure 6.3.4-1).

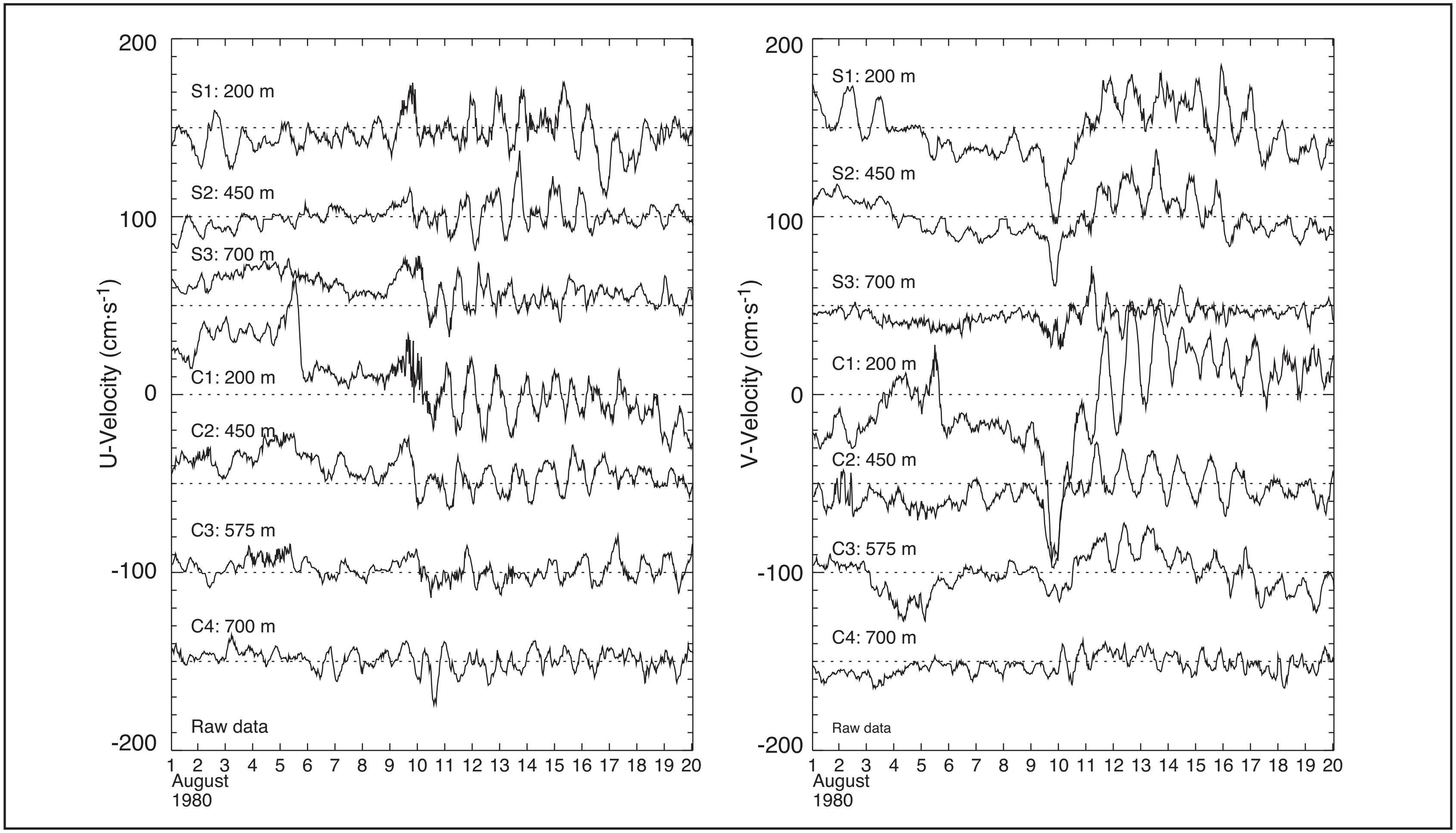

Figure 6.1.2-2. Components (u positive to the east and v positive to the north) of hourly currents at indicated depths on moorings S (26°N, 96.28°W) and C (55 km north of S). Both moorings are approximately on the 730-m isobath. The eye of Hurricane Allen, on a track toward the NNW, passed about 65 km WSW of mooring S at 0000 UTC on 10 August 1980 (Figure 6.3.2-1). Tick marks denote the start of the day.

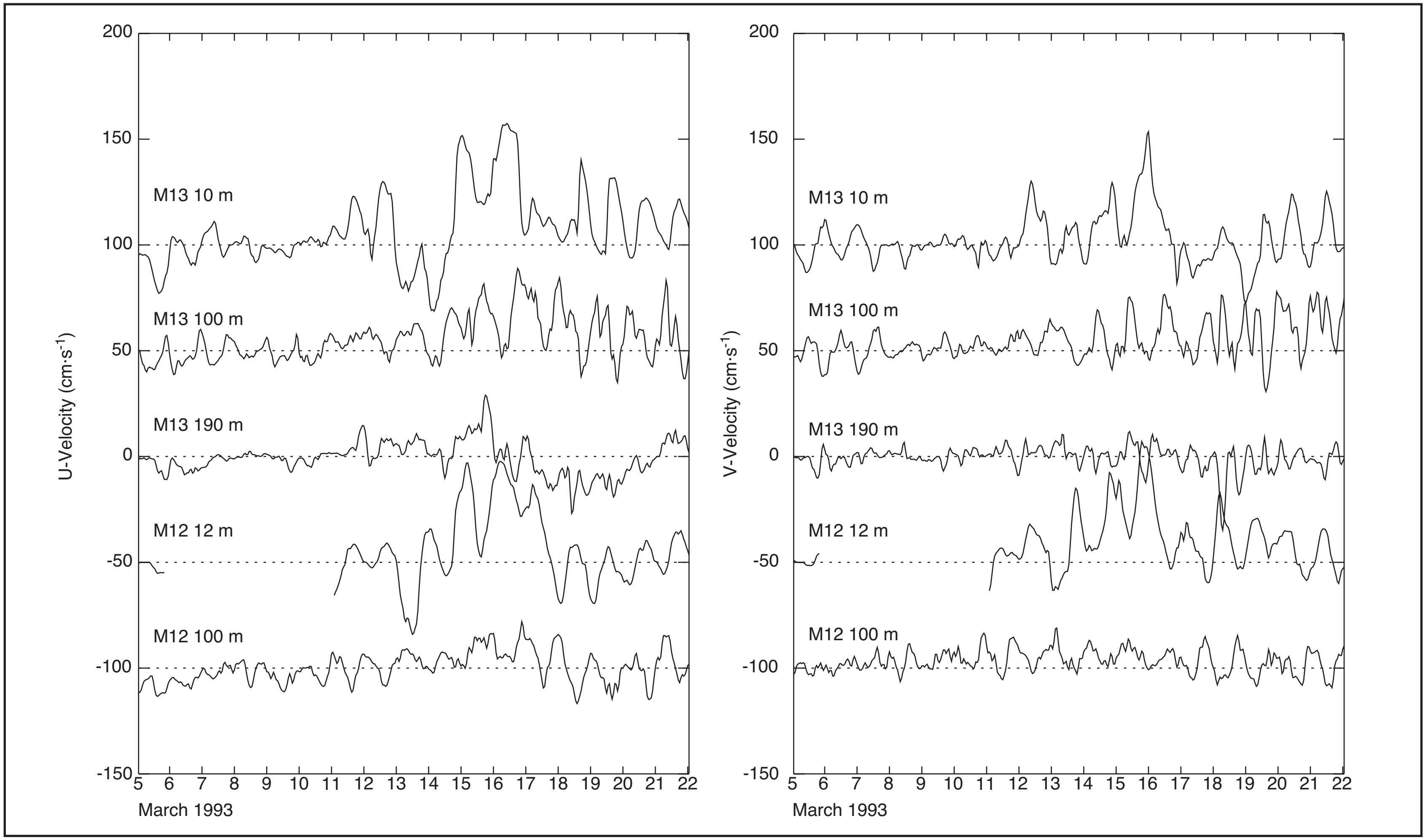

Figure 6.1.2-3. Eastward (u) and northward (v) components of currents (hourly values from 3-hr low-passed records) from moorings located off Louisiana at approximately 90.5°W. Mooring 13 was in water depth of 200 m; mooring 12 was in water depth of 504 m. On 12 March 1993, a class 5 extratropical cyclone moved from west to east across the Texas-Louisiana shelf with its center approximately over the 1500-m isobath. Tick marks denote the start of the day.

Clearly episodic wind events can cause major currents in the deep water Gulf. The initial currents give rise to inertial oscillations lasting for up to about ten days with decreasing amplitudes, superimposed on longer period signals.

In Figure 6.1.2-4 is shown a weather map for 1200 UCT on 16 February 1998. The center of a strong extratropical cyclone is seen near the eastern border of Arkansas; its track from the Gulf to that position is also shown. During the time of this cyclone, moorings of the DeSoto Canyon Eddy Intrusion Study were in place (see Figure 6.3.5-1 for locations). The 3- to 50-hr band-passed current components from mooring C3 of that study are shown in Figure 6.1.2-5 for the period 2 February to 9 March 1998. Shown is the effect of the storm on generating inertial and near-inertial oscillations in the upper layer. Also shown is the subsequent passage of packets of intertial waves laterally and downward into the water column at least to 500 m, but not to 1290 m.

DiMarco et al. (2000) described over the Texas and Louisiana shelves a class of energetic surface currents previously unreported in the Gulf of Mexico. To illustrate, Figure 6.1.2-6 shows eastward (u) and northward (v) components of currents from 3- to 40-hr band-passed records made in July and December 1992 at mooring 10 located off Louisiana at 27.94°N, 92.75°W in water of depth 200 m. The July sequence shows maximum amplitudes of 40-60 $cm \cdot s^{-1}$ at depth of 12 m for the situation of light winds. The period of diminished amplitudes followed an atmospheric frontal passage. These are near-circular, clockwise-rotating oscillations with period near 24.0 hr. They seem to be an illustration of thermally induced cycling (Price et al. 1986) in which large amplitude rotary currents can exist in thin mixed layers typical of summer. By contrast, the corresponding current sequence shown for December shows no such behavior. Many examples of such currents, in phase at distinct locations, exist for the Texas-Louisiana shelf. These currents also have been observed over the slope in the northeast Gulf. By implication they exist further offshore.

6.1.3 Deep Barotropic and Bottom-Trapped Motions

During the mid-1980s, barotropic (depth independent) currents were observed to extend from depths near 1000 m to the bottom. Shown in Figure 6.1.3-1 are 40-hr low passed current vectors from SAIC mooring G maintained in the eastern Gulf as part of an MMS-sponsored physical oceanography program (SAIC 1987). As described by Hamilton (1990), the northern edge (eastward currents) of the Loop Current was affecting the array during December 1984. Then, from January to March 1985 the mooring was influenced by the southward flow of the eastern limb of the Loop Current as it extended further into the Gulf. Note that currents above 1000 m were affected in a coherent, surface-intensified manner, but currents below 1000 m were not affected. During the period April-June an eddy separated from the LC. At that time considerable energy appeared in the lower water column and vertical coherence with slight near-bottom intensification is seen.

Based on sparse current meter arrays of the MMS-sponsored physical oceanography program, Hamilton (1990) inferred that low-frequency fluctuations with periods greater than 10 d propagate from east to west in the deep Gulf with group speeds near 9 $km \cdot d^{-1}$, faster than typical observed westward travel speeds for LCEs. These deep motions were observed to be highly coherent in the vertical with bottom intensification and have been attributed to topographic Rossby waves. Speeds within these deep motions are observed to be as great as 30 $cm \cdot s^{-1}$ beneath the Loop Current, but less in the central and western Gulf. There is evidence that these deep perturbations are excited by the Loop Current, perhaps when LCEs separate.

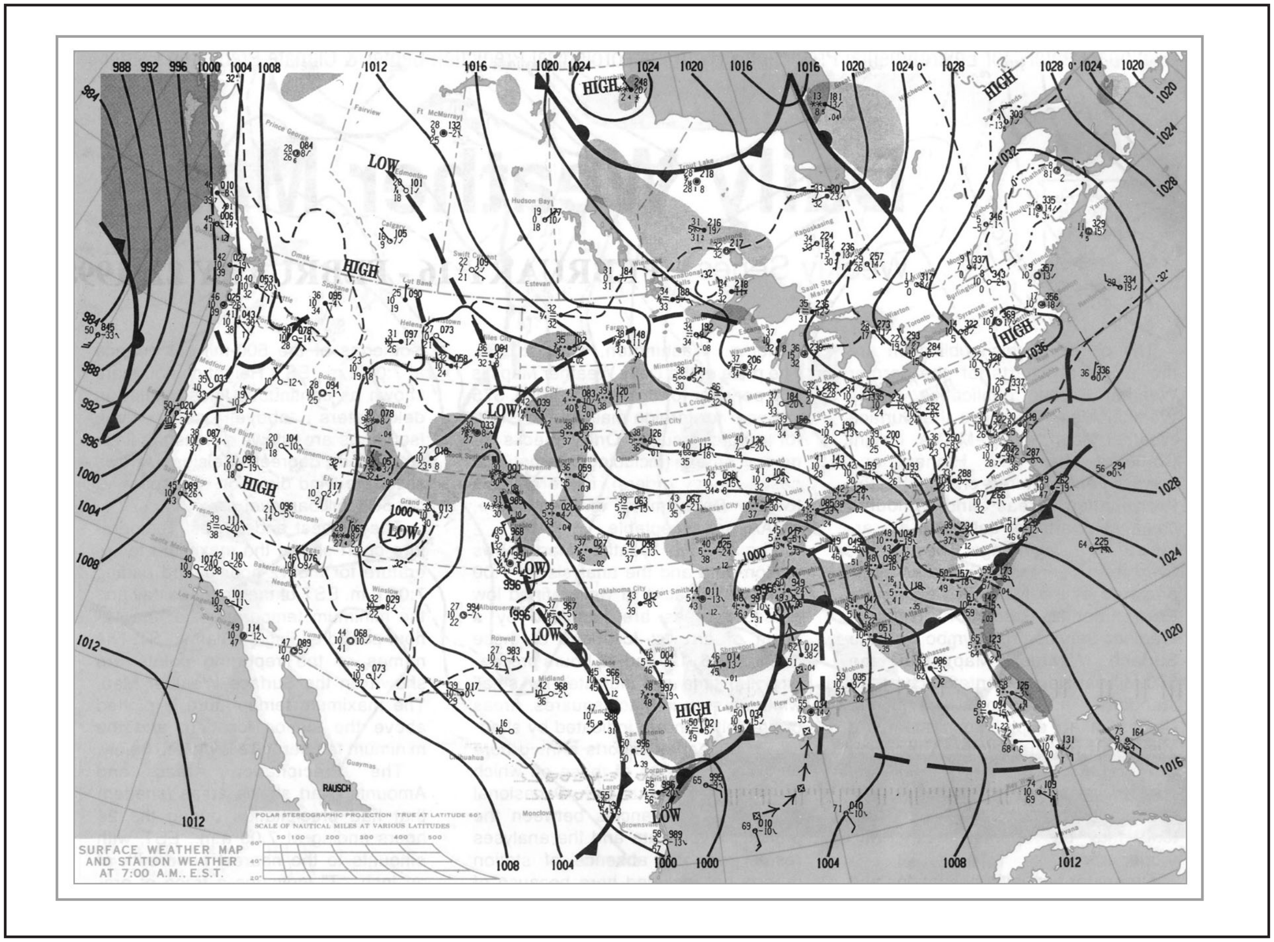

Figure 6.1.2-4. Weather map for 1200 UTC on 16 February 1998 (from *Daily Weather Maps*, weekly series February 16-February 22, 1998, NOAA). Shown is track and present center of an extratropical cyclone that passed from the Gulf of Mexico to the lower mid-western United States.

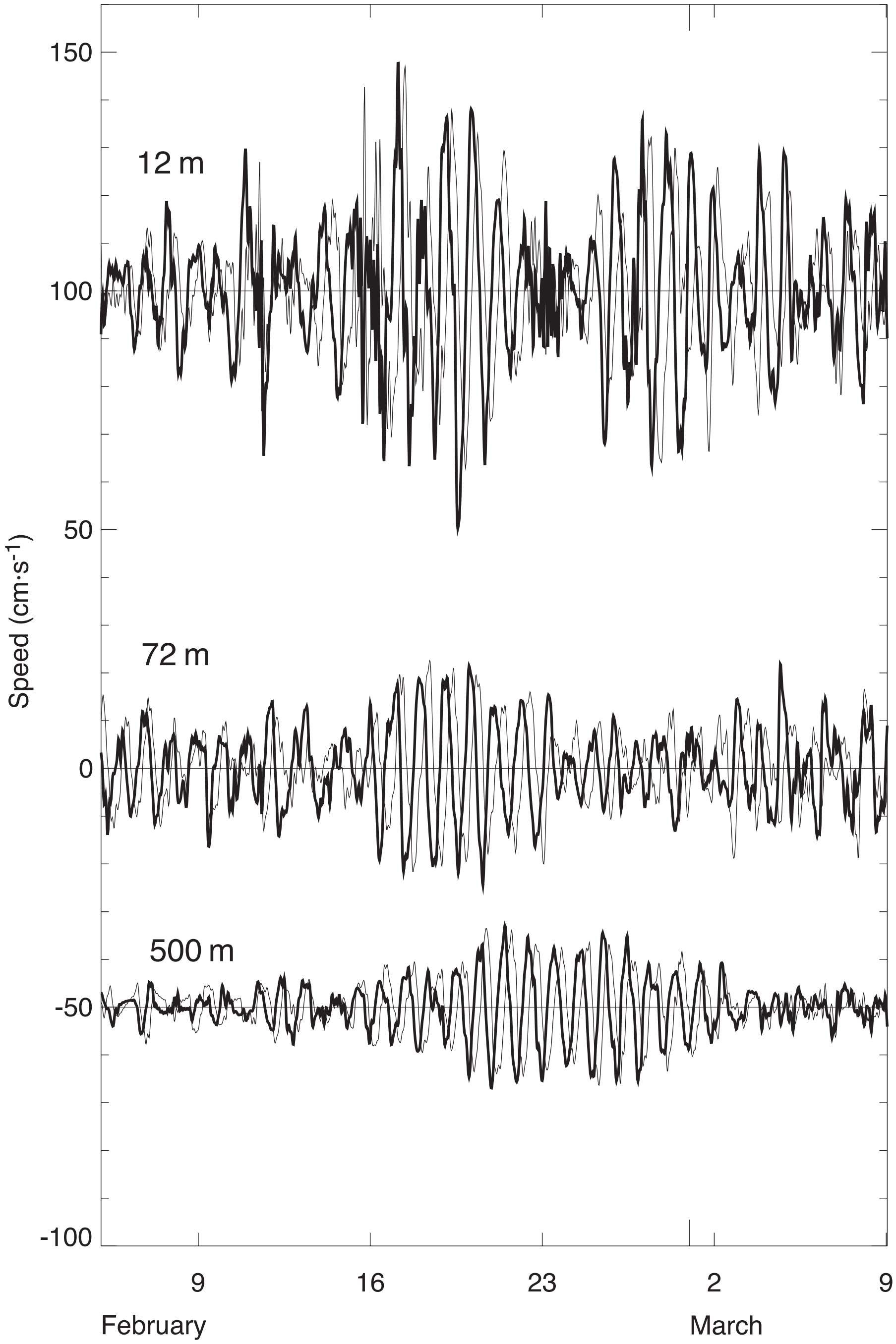

Figure 6.1.2-5. Band-passed (3-50 hr) current components from DeSoto Canyon Eddy Intrusion Study mooring C3 for 2 February - 9 March 1998. This period includes the time of northward passage of an extratropical cyclone (Figure 6.1.2-4) to the west of this mooring. Tick marks denote start of the day.

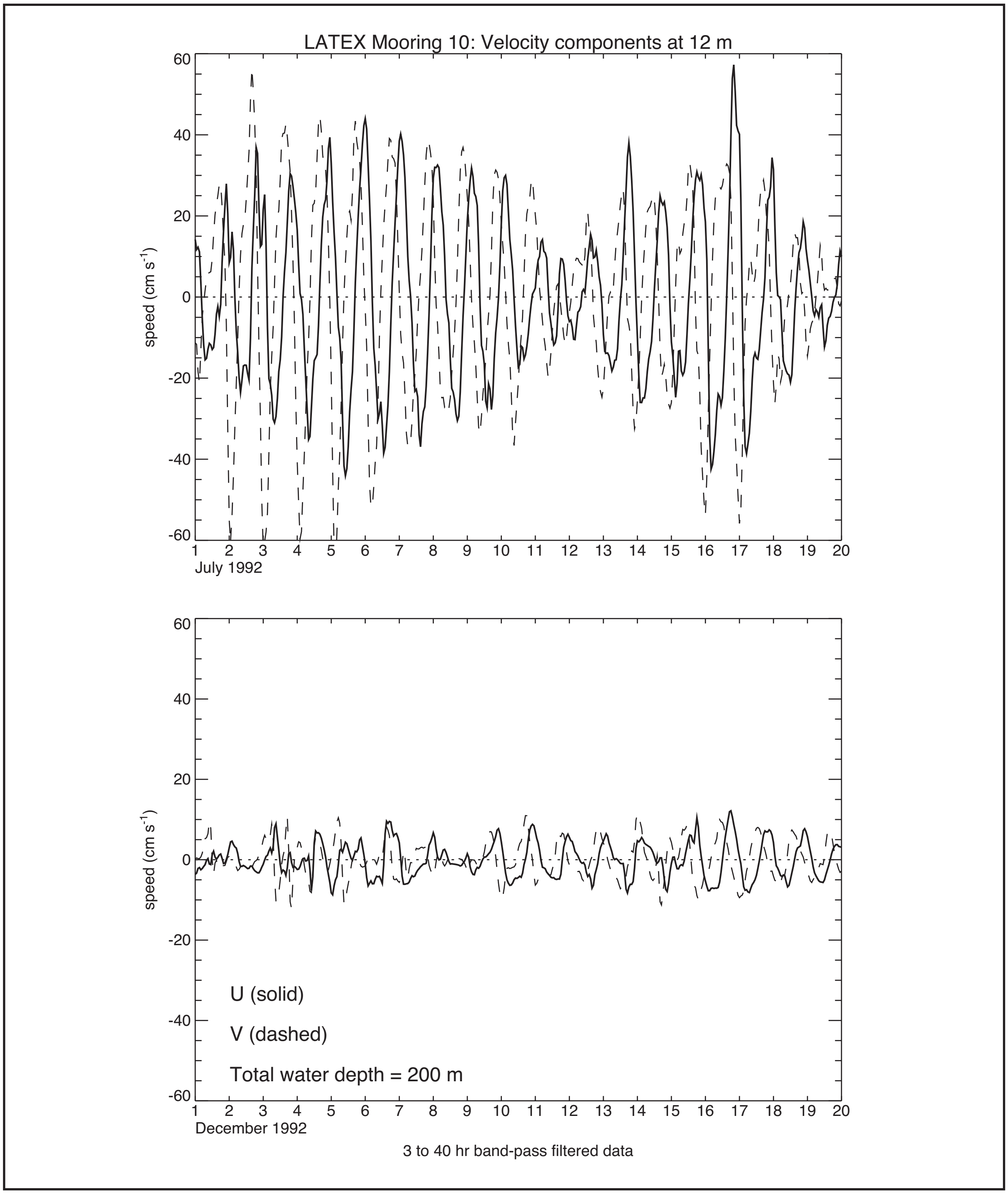

Figure 6.1.2-6. Eastward (u) and northward (v) components of currents from 3- to 40-hr band-passed records made in July and December 1992 at mooring 10 located off Louisiana at 27.94°N, 92.75°W in water depth of 200 m. Tick marks denote the start of the day.

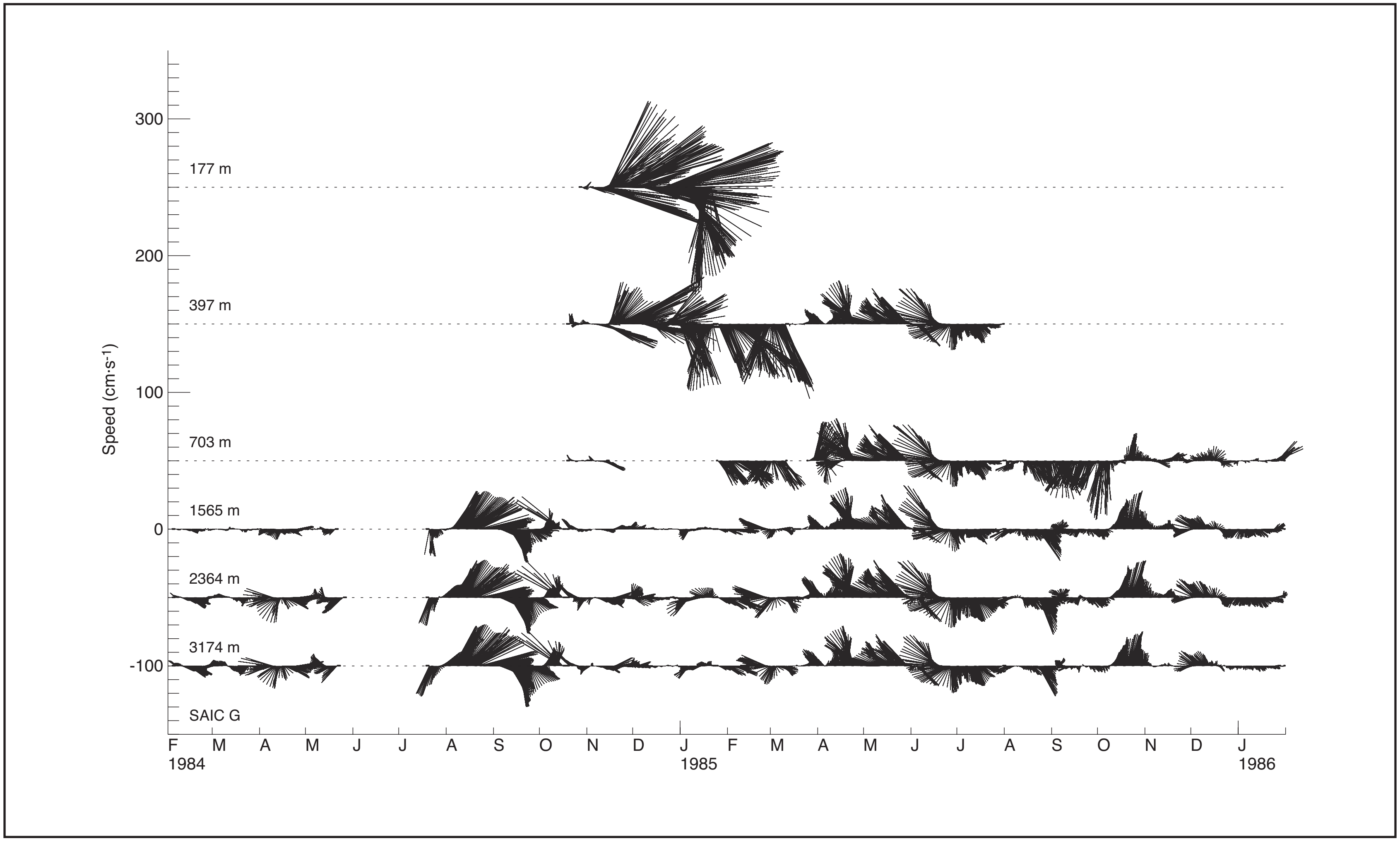

Figure 6.1.3-1. Current vectors (40-hr low-passed; north directed upward) from SAIC mooring G located in 3200 m water depth at 25.60°N, 85.50°W off the southern West Florida Shelf. Position is shown in Figure 6.3.1-1. Tick marks denote the start of the month.

Proprietary oil company measurements show similar barotropic currents with maximum speeds near 40 $cm \cdot s^{-1}$ and periods of weeks. Moreover, data give some indication of bottom current intensification. Figure 6.1.3-2 shows current vectors from five current meters deployed on mooring R by SAIC as part of the MMS-sponsored physical oceanography program. (See Figures 6.3.3-7 and 8 for the location of mooring and time lines of records.) As seems typically to be the case, current records for 1000 m and below are quite coherent. Note the bottom intensification, as discussed by Hamilton (1990). For some periods upper ocean currents show coherence with those in the deep basin (e.g., during early August in this case), but at other times the upper ocean and deep currents are not coherent.

High resolution numerical circulation models of the Gulf evidence both cyclonic and anticyclonic eddies in the deep basin waters. They form in the eastern Gulf under the Loop Current regime and propagate into the western Gulf guided by topography. In at least three models deep eddies appear to form as LCEs are formed: Sturges et al. (1993); Inoue and Welsh (1997); Welsh and Inoue (2000); and the CUPOM output. Deep circulation patterns distinct from those associated with the surface-intensified eddies were seen in numerical model studies by Sturges et al. (1993) and Inoue and Welsh (1997). Welsh and Inoue (2000) suggested that an anticyclone and a stronger cyclone are form in the lower layer in response to a westward moving newly formed anticyclonic LCE in the upper layer. Evidence from their model is that the deep eddy pair remains coupled with the upper ring, although the two deep rings rotate cyclonically as a pair, and that the deep anticyclone decays more rapidly than the deep cyclone.

In early 1999, William Bryant of Texas A&M University discovered and mapped, using a deep towed acoustic system, a previously unexplored bedform just offshore of the Sigsbee Escarpment in the northwestern Gulf of Mexico. A small area of the sea floor covered by furrows is shown in Figure 6.1.3-3. The location is at the mouth of Bryant Canyon (~92°W). The upper panel shows the surface expression from deep tow measurements; the lower panel gives the sub-bottom profile along the track (center of upper panel). These large, long furrows are eroded into the Holocene deposits blanketing this region. These furrows have depths of 5 to 10 m, widths of several 10s of meters, are spaced on the order of 100 m apart, and extend unbroken for distances of many 10s of km. Generally they are oriented nearly along depth contours. Bryant has observed them in the region of 90°W just off the Sigsbee Escarpment and near the Bryant Fan south of Bryant Canyon from 91°W to 92.5°W. Depths in those regions range from 2000 to 3000 m. More recently, the existence of these features has been corroborated and they have been mapped more extensively in the area of Green's Knoll by offshore oil and gas operators. Observations of furrows demonstrate that such bedforms are widespread and important features in regions with cohesive, fine-grained sediments and directionally stable currents (Flood 1983).

It seems likely that the processes responsible for these furrows are active at present. Based on the change in character of these features from offshore toward the escarpment, and on the rather good agreement of that change with changes observed in published laboratory studies of submarine erosion (e.g., Allen 1969; Dzulynski 1965), the tentative conclusion is that bottom currents responsible for these features have along-isobath components and increase in strength toward the escarpment. Such work attributes the furrows to rows of counter-rotating helical currents generally directed along the furrows with rising parts of the helixes over the furrows (see Table 1 in Allen 1969 and Figure 28 in Dzulynski 1965). No direct measurements have been reported to test this concept. The laboratory experiments indicate that furrows of different separation, wavelengths, and fundamental character occur for different flow rates. However, it is difficult to scale these model results to field conditions. Speculation is that near-bottom speeds of currents responsible for the inshore furrows might

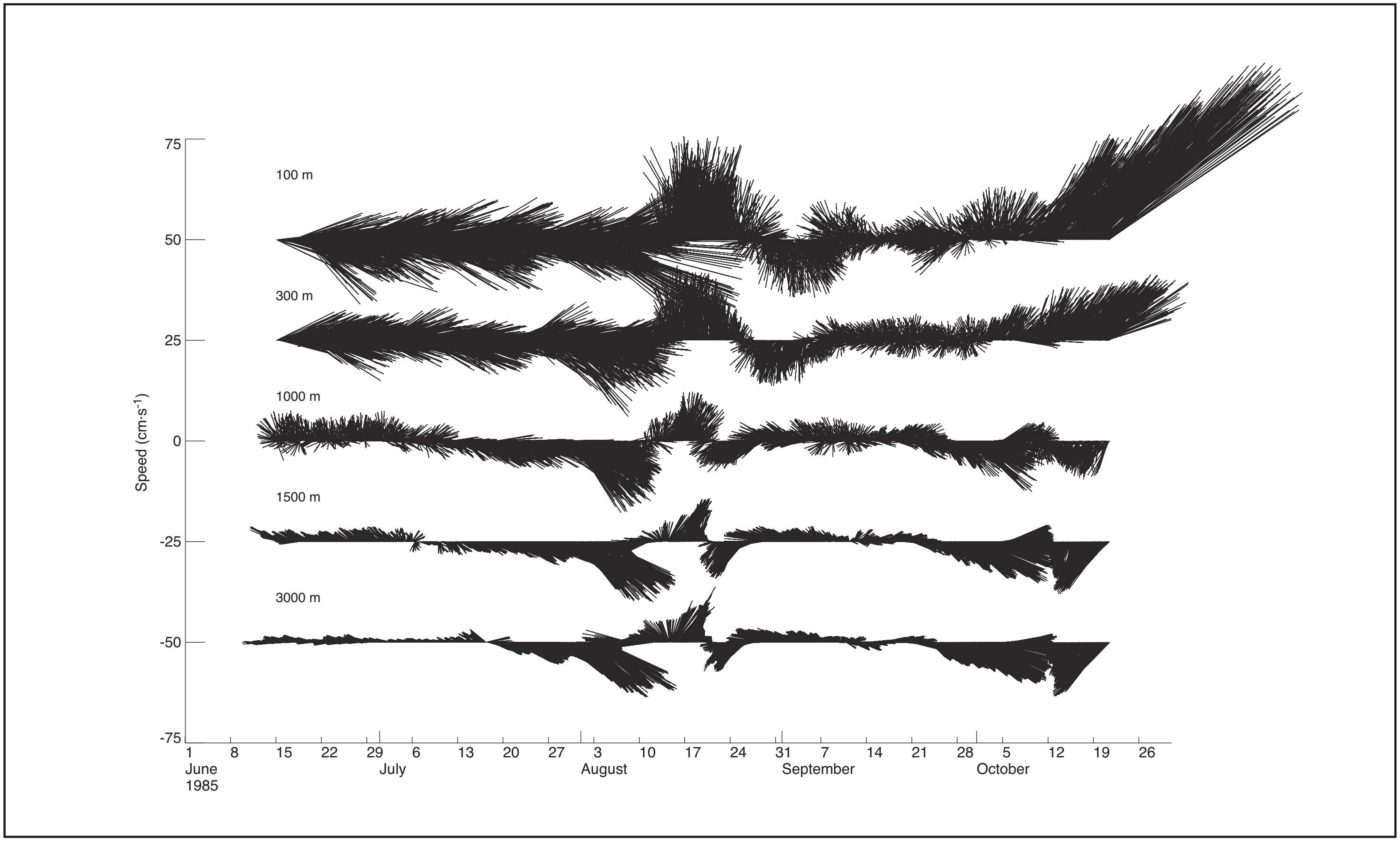

Figure 6.1.3-2. Current vectors (unfiltered; north directed upward) from SAIC mooring R located in 3500 m water depth at 25.49°N, 94.16°W south of the east Texas shelf. Position is shown in Figure 6.3.3-4. Tick marks denote the start of the day indicated.

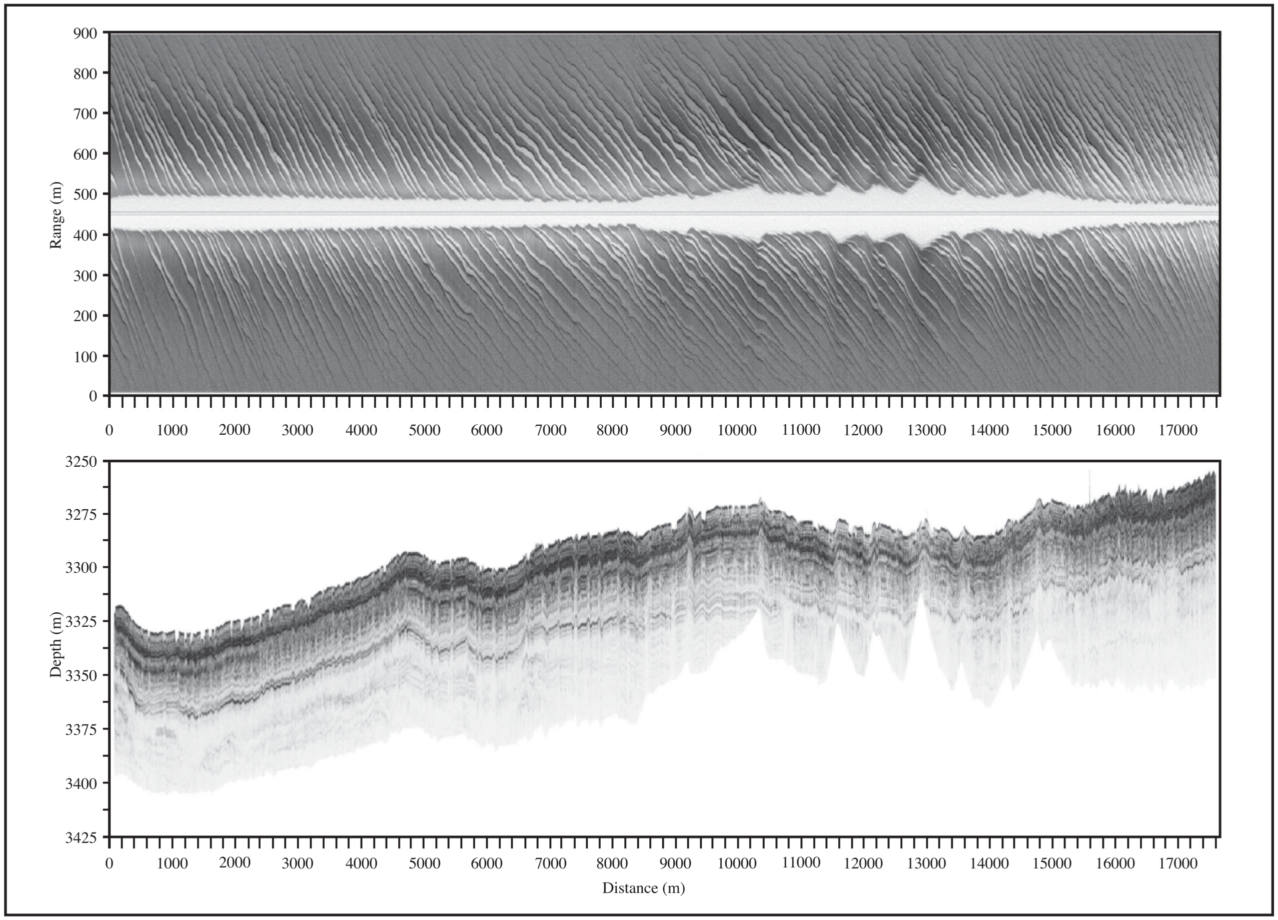

Figure 6.1.3-3. Bottom topography of small area in region of mega-furrows at the mouth of Bryant Canyon in north central Gulf of Mexico (near 25.8°N, 92°W) (Courtesy of William Bryant, Texas A&M University).

be 50 cm·s^{-1} or even in excess of 100 cm·s^{-1}. These furrows and the currents responsible for them may also exist over a considerable part of the yet unexplored base of the continental slope in the Gulf of Mexico.

Figure 6.1.3-4 gives an example of currents from a deep mooring located somewhat east of the main known region of mega-furrows. Shown are unfiltered current vectors from three deep instruments on a mooring in water depth of 1998 m. These records made by SAIC for the MMS show very energetic currents reaching 100 cm·s^{-1}. Reversals in direction occur on order of 10 d with much stronger flow oriented west-southwest than east-northeast. Those are the predominant orientation of the furrows in this area. Note the marked vertical coherence and some hint of bottom intensification between 1800 and 1989 m. Other deep currents seen (proprietary) above the region of mega-furrows are weaker and of distinctly different character.

As was discussed in Section 5, the mean circulation deeper than 1000 m, as deduced from model output and geostrophic calculations, is generally counterclockwise in the Gulf basin. Moreover, near the bottom it is intensified offshore of regions of steep bathymetry, such as the Sigsbee Escarpment. Thus, the currents responsible for the mega-furrows may be sporadic or quasi-permanent. They also could be a distinctly different phenomenon than the other classes of currents examined to date.

6.1.4 Subsurface, Mid-Water Column Motions

Several deep water oil and gas operators have reported observing very high-speed, subsurface-intensified currents lasting of the order of a day at locations over the upper continental slopes. Such currents may have vertical extents of less than 100 m, with maxima generally observed within the depth range of 100 to 300 m. Maximum speeds exceeding 150 cm·s^{-1} have been reported. Figure 6.1.4-1 shows time-averaged current profiles before, during, and after the occurrence of such a subsurface jet in Mississippi Canyon in 1997. Total water depth at the location is estimated to be 800-900 m. The profiles in the upper 100 m are similar, showing a strong surface current with average speeds of about 30 cm·s^{-1} at the surface decreasing to roughly 12 cm·s^{-1} at 100 m. Below 100 m the profiles for the periods before and after the jet event were essentially barotropic at 8-10 cm·s^{-1}. The profile during the event shows a strong current at mid-depth with maximum averaged speeds greater than 30 cm·s^{-1} near 300 m. Analyses of individual profiles show that peak currents generally occurred between 250-300 m with a maximum speed of 56 cm·s^{-1}.

We have examined data from locations over the northern continental slope and observed currents with subsurface maximum speeds of 50 cm·s^{-1} lasting for about one day with bursts of speed peaking at more than 100 cm·s^{-1}. Some higher speed currents appear to propagate upward, characteristic of baroclinic waves (either sub- or super-inertial); others are clearly downward propagating motions. An example is shown in Figure 6.1.4-2. Results from the CCAR numerical model also show short-period, subsurface-intensified currents over the Gulf slopes—but with maximum speeds approaching only 50 cm·s^{-1}. It seems possible that such phenomena could be intensified near topography. Causal mechanisms are being sought.

6.1.5 Topographically Generated Near-Inertial Motion

Near-inertial motion in the upper layer is commonly seen in Gulf current meter records during passage of storms. Downward-propagating wave packets of near inertial motion reaching well below the thermocline is also common, but upward-propagating waves that

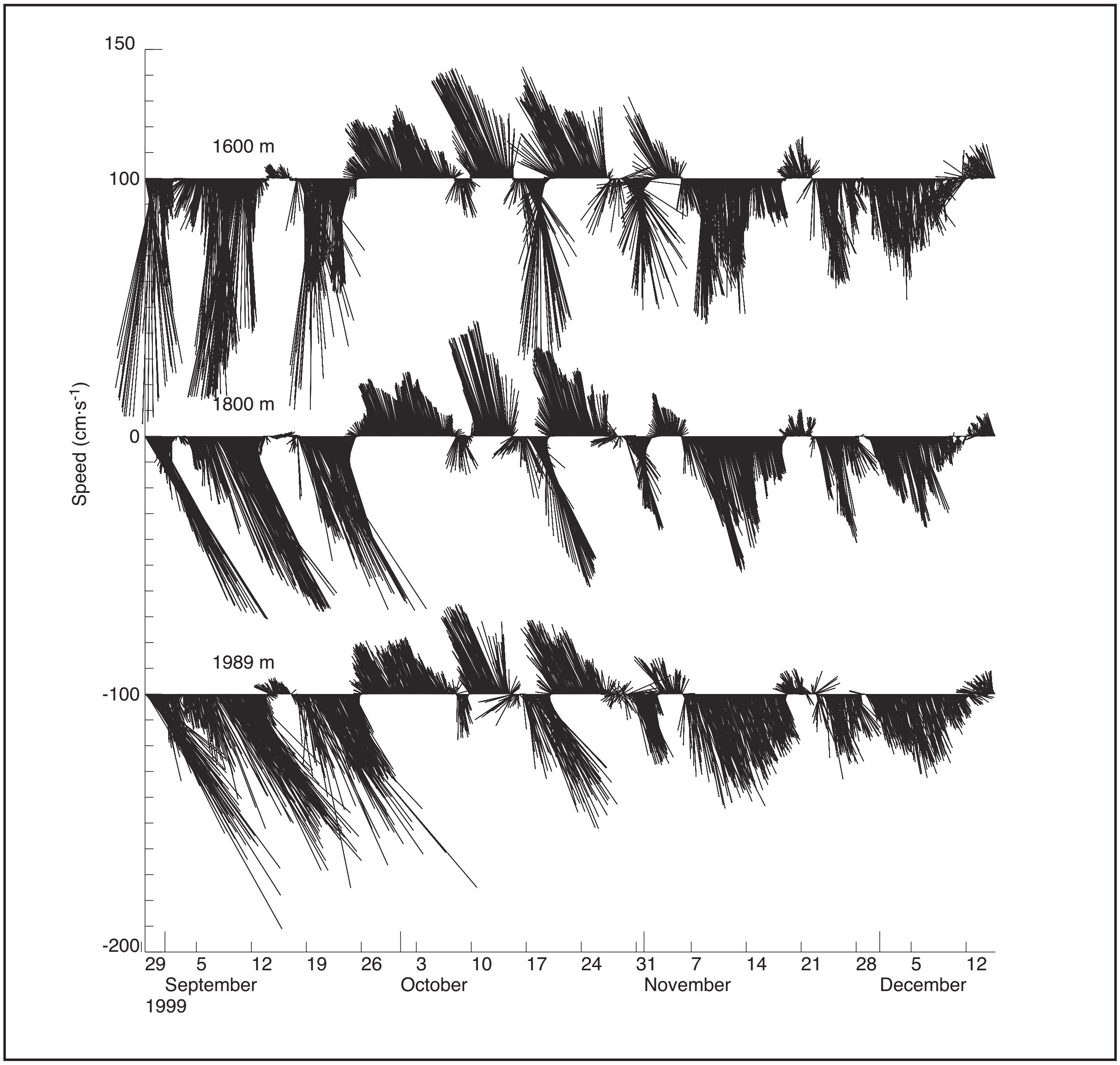

Figure 6.1.3-4. Current vectors (unfiltered; east directed upward) from MMS mooring I2 located in 1998 m water depth at 27.23°N, 89.97°W. Tick marks denote start of day indicated.

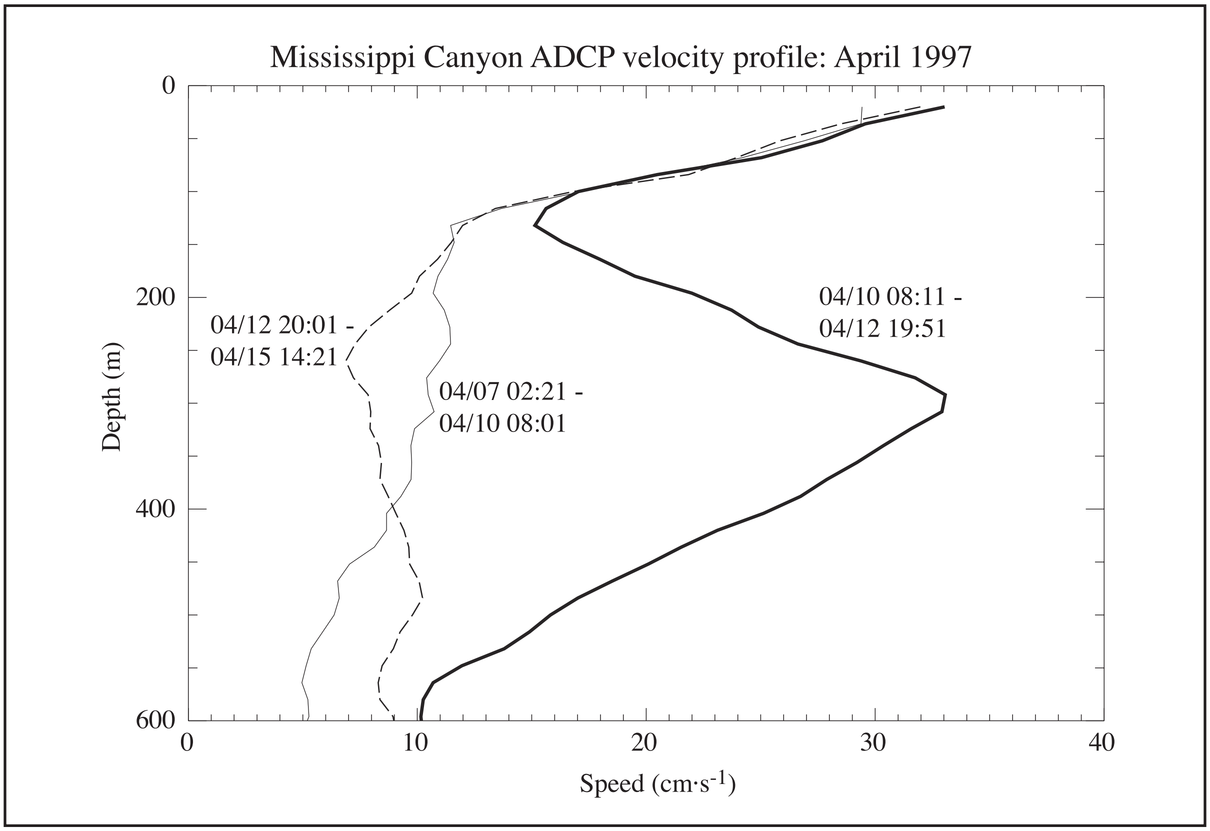

Figure 6.1.4-1. Average current profiles before (thin line), during (thick line), and after (dashed line) a subsurface jet event in Mississippi Canyon (data courtesy of Chevron).

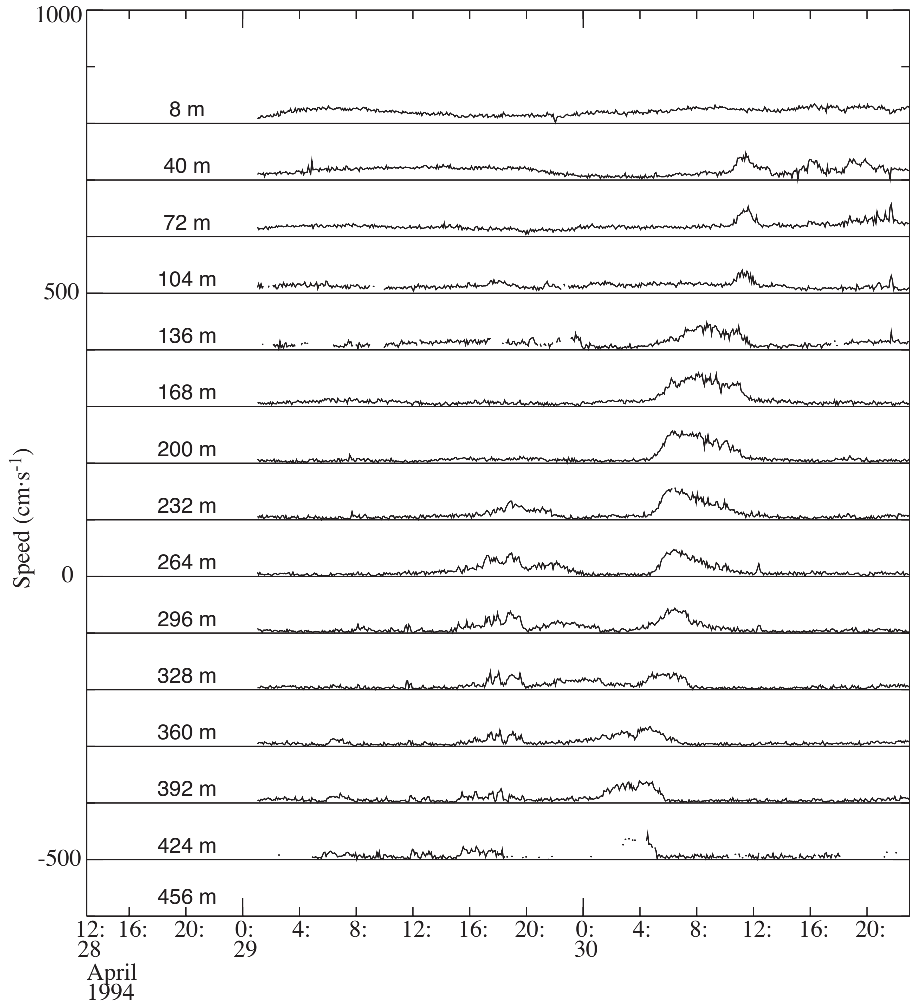

Figure 6.1.4-2. ADCP current speed in Green Canyon block 200 from 29 April through 30 April 1994 showing 50 $cm \cdot s^{-1}$ current event propagating upwards in the water column beginning about 30 April. Distances shown are in meters from the instrument, which was close to the surface. Data provided courtesy of Marathon.

might be generated at the sea bed are rare in the records we have examined. A possible example of such an event that occurred during the passage of a hurricane is described here.

During late September and early October 1998 an interesting sequence occurred during the time of passage of Hurricane Georges over mooring C3 located in the DeSoto Canyon region in 1300-m water depth (see Figure 6.3.5-1 for mooring location). Georges caused surface currents in excess of 200 $cm \cdot s^{-1}$ (see Table 6.3.5-1 for further details). As seen in Figure 6.1.5-1, speeds of unfiltered currents at 52 m had diminished to approximately 75 $cm \cdot s^{-1}$. Filtering the records with an 18-29 hr bandpass, resulted in Figure 6.1.5-2. Very tight groups of inertial oscillations are seen to propagate downward through the thermocline, with vertical propagation speed of about 40 $m \text{-} d^{-1}$. Amplitudes decreased from about 50 $cm \cdot s^{-1}$ at 12 m to 25 $cm \cdot s^{-1}$ at 500 m. Inertial waves were not seen at 1290 m. However, filtering the records with a 29-50 hr bandpass Figure 6.1.5-3 reveals a 40 hr signal with a maximum amplitude of 25 $cm \cdot s^{-1}$ at 1290 m (in 1300-m depth). This sub-inertial wave packet was initiated approximately 2 days after the hurricane-initiated inertial oscillations in the near surface water and continued for two weeks. It is not clear whether the much shorter groups of sub-inertial oscillations at 52 m and 500 m are related to that near the seabed, and there is no information at depths between 500 m and 1290 m. The sub-inertial frequency would suggest that the motion is a bottom trapped evanescent phenomenon whose amplitude decays with distance above the bottom, rather than an upward-propagating wave.

Because of the paucity of unequivocal cases of topographically produced near-inertial motion seen in the Gulf current records, we have not pursued this subject further in this synthesis report.

6.2 Methodology Used in Identification of Events

As a guide to identifying and understanding the nature of energetic current events, including processes and causal factors, we used various types of information describing the forcing and surface fields. As background to the identification of LCEs, we began with the list of LCE separation times, since 1973, developed by Sturges and Leben (2000), and presented here as Table 6.2-1. Then, to track LCEs within the Gulf we used EddyWatch charts prepared by Horizon Marine, Inc., and provided to us by industry subscribers. As further confirmation of the locations of LCEs, as well as the locations of other current rings in the Gulf, we used the compilation of GeoSat SSHA maps prepared by Berger et al. (1996b) and the SSH and SSHA maps prepared by Robert Leben (University of Colorado, personal communication) for the period April 1992 through 1999 using TOPEX/POSEIDON and/or ERS-1 or ERS-2 altimetry data.

Table 6.2-2 gives a summary of individual tropical cyclones that entered the Gulf of Mexico from 1977 through 1999. The source of this information is UNISYS Corporation Weather (http://weather.unisys.com/hurricane/index.html). The tracks of tropical cyclones presented in Section 6.3 with general descriptions of the current meter arrays were derived from the same source. The Saffir-Simpson index is given in Table 6.2-3. Table 6.2-4 gives a summary of extratropical cyclones in the Gulf of Mexico for the period December 1966 through February 1996. These data were provided by Dr. Jeffrey Hardy, East Stroudsburg University and Dr. S. A. Hsu, Louisiana State University (personal communication). They were based on examination of the 30-year record of NOAA series *Daily Weather Maps* for a winter season defined as November through May (Nowlin et al. 1998b; Hardy and Hsu 1997).

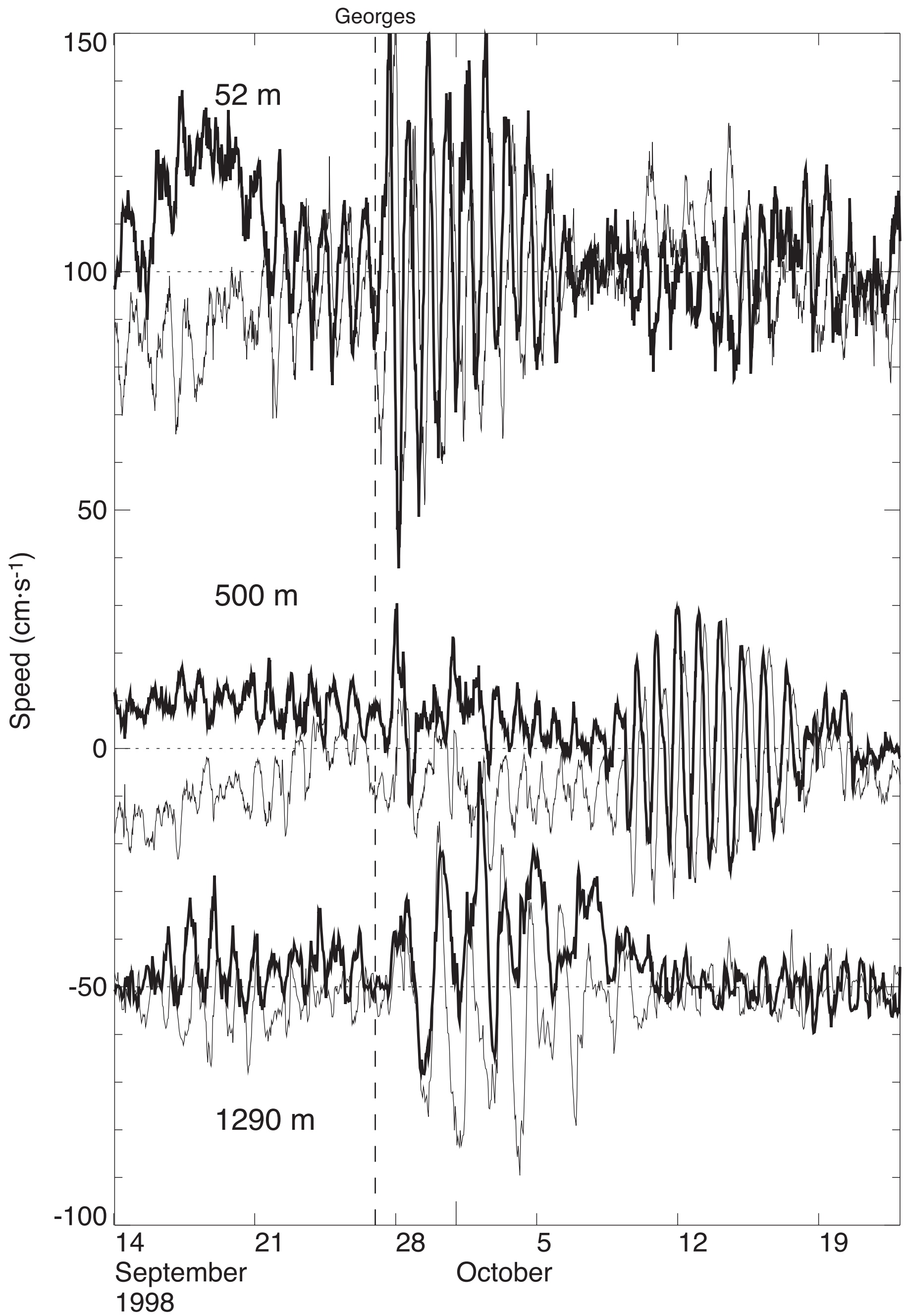

Figure 6.1.5-1. Unfiltered velocity components at 52, 500, and 1290 m at the MMS-sponsored Eddy Intrusion Study mooring C3 in DeSoto Canyon. Thick line denotes the v-component (north-south); thin line the u-component (east-west). See Figure 6.3.5-1 for mooring location. Hurricane Georges passed over the region on 27 September 1998. Tick marks denote start of day indicated.

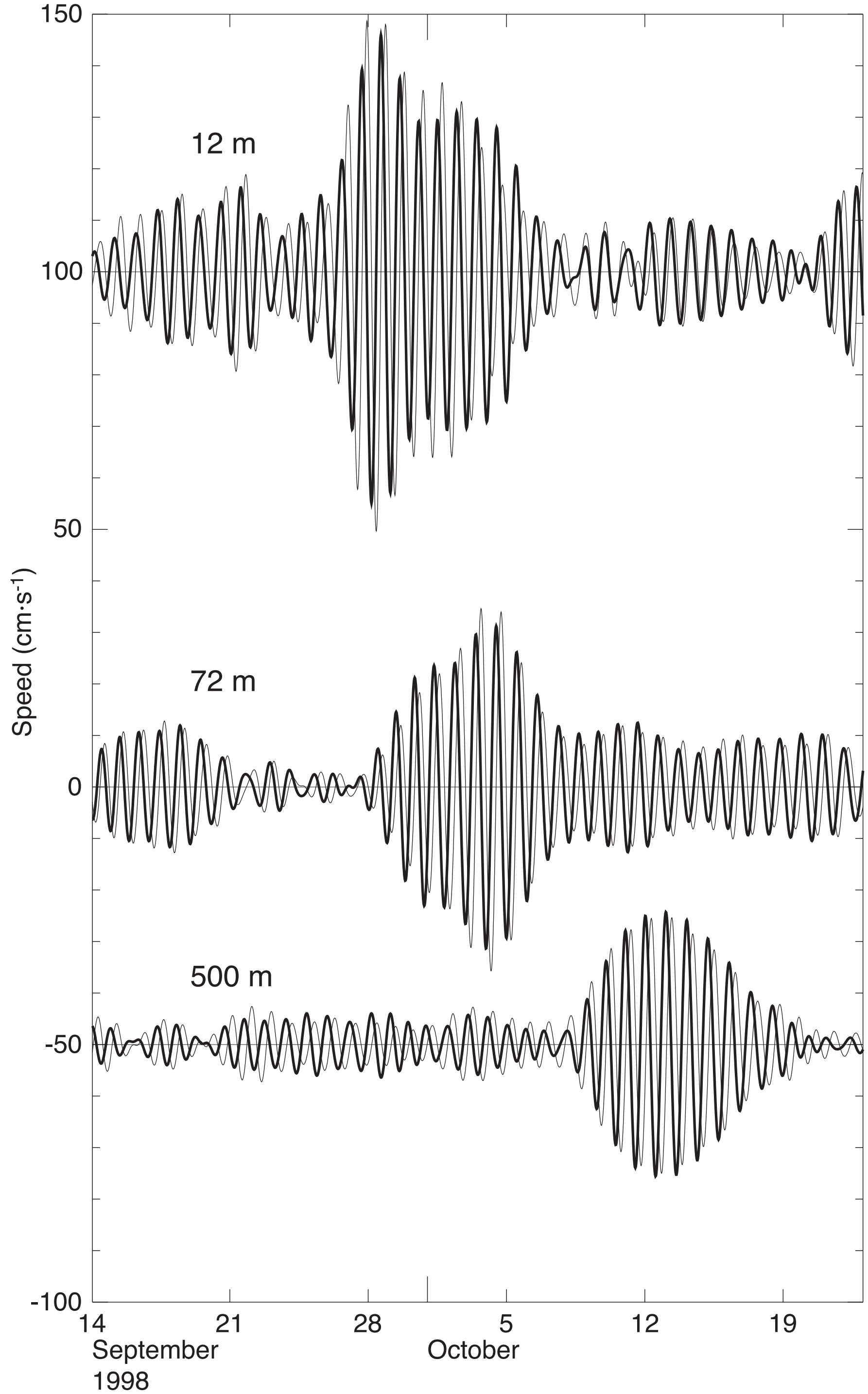

Figure 6.1.5-2. Current components from 18-29 hr band-passed records from the same mooring described in Figure 6.1.5-1. Thick line denotes the v-component (north-south); thin line the u-component (east-west). Tick marks denote start of the day indicated.

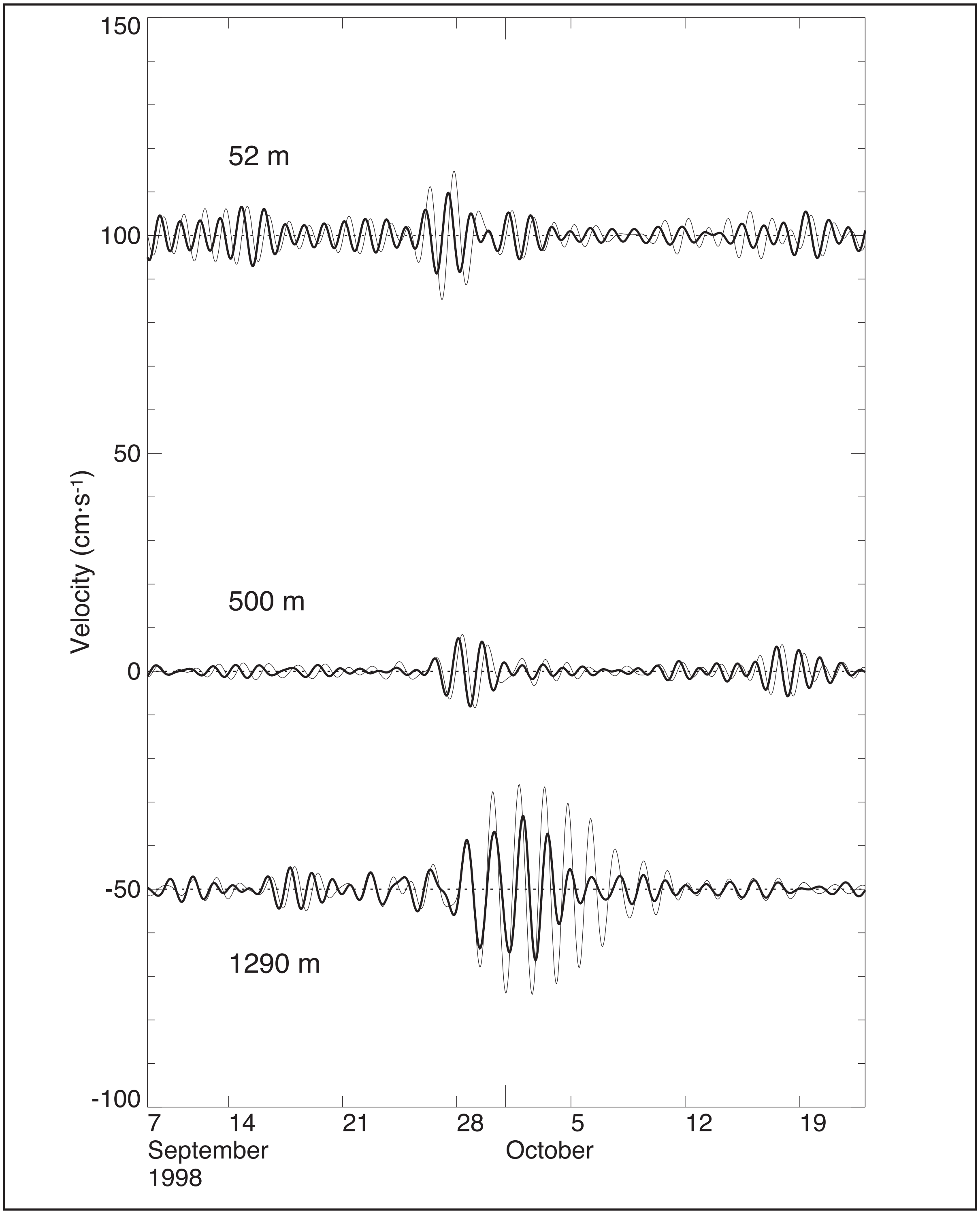

Figure 6.1.5-3. Current components from 29-50 hr band-passed records from the same mooring described in Figure 6.1.5-1. Thick line denotes the v-component (north-south), thin line the u-component (east-west). Tick marks denote start of the day indicated.

Table 6.2-1. Separation times of Loop Current eddies based on times when data were available to reliably show a ring separating from the Loop Current (from Sturges and Leben 2000). Entries through October 1986 are from Vukovich (1988); other entries prior to July 1992 are from Table 1 of Sturges (1994) using corrections based on Berger (1993). Data beginning in 1992 are based on satellite altimetry. Separation time for Eddy Juggernaut has been added.

Year	Month	Separation Period (months)	Estimated uncertainty (weeks)	Eddy Name
1973	July			
1974	April	9		
1975	January	9		
1975	July	6		
1976	August	13		
1977	March	7		
1978	June	15		
1979	April	10		
1980	January	9		
1981	March	14		
1981	November	8		
1982	May	6		
1983	March	10		
1984	February	11		
1984	August	6		Arnold
1985	July	11		Fast
1986	January	6		Hot Core
1986	October	9		
1987	September	11		Kathleen ?
1988	May	8		Murphy
1989	May-June (?)	12.5		Nelson
1990	August	14.5		Quiet
1991	August-September	12.5		Triton
1992	July 19	11.5	4	Unchained
1993	June 22	11	4	Whopper
1993	September 19	3	1	X-tra
1994	September 22	12	4	Yucatan
1995	April 8	7	4	Zapp
1995	October 18	6	4	Aggie
1996	April 30	6	5	Biloxi
1996	September	5	4	Creole
1997	October 11	13	3	El Dorado
1998	March 14	5	2.5	Fourchon
1999	August 22	17	2	Indigo ?
1999	October 15	2	1	Juggernaut

Table 6.2-2. Summary of individual tropical storms that entered the Gulf of Mexico from 1977 through 2000. Pressures are in millibars and winds are in knots where one knot is equal to 1.15 mph. The storm number is the sequential number of Atlantic tropical depression/storms for the season. The source of this information is UNISYS Corporation Weather. Storm category is based on the Saffir-Simpson scale, explained in Table 6.2-3.

Year	Storm #	Name	Dates	Wind	Pres.	Cat.
1977	1	Hurricane ANITA	29 AUG-3 SEP	150	926	5
	2	Hurricane BABE	3-9 SEP	65	995	1
1978	2	Tropical Storm AMELIA	30 JUL-1 AUG	45	1005	TS
	3	Tropical Storm BESS	5-8 AUG	45	1005	TS
	5	Tropical Storm DEBRA	26-29 AUG	50	1000	TS
1979	2	Hurricane BOB	9-16 JUL	65	986	1
	3	Tropical Storm CLAUDETTE	15-29 JUL	45	997	TS
	5	Tropical Storm ELENA	30 AUG-2 SEP	35	1004	TS
	6	Hurricane FREDERIC	29 AUG-15 SEP	115	943	4
	8	Hurricane HENRI	15-24 SEP	75	983	1
1980	1	Hurricane ALLEN	31 JUL-11 AUG	165	899	5
	4	Tropical Storm DANIELLE	4-7 SEP	50	1004	TS
	8	Tropical Storm HERMINE	20-26 SEP	60	993	TS
	10	Hurricane JEANNE	7-16 NOV	85	986	2
1981	4	Hurricane DENNIS	7-22 AUG	70	995	1
1982	2	Subtropical Storm 1	18-20 JUN	60	984	TS
	4	Tropical Storm CHRIS	9-12 SEP	55	994	TS
1983	1	Hurricane ALICIA	15-21 AUG	100	963	3
	2	Hurricane BARRY	23-29 AUG	70	986	1
1984	6	Tropical Storm EDOUARD	14-15 SEP	55	998	TS
1985	2	Hurricane BOB	21-26 JUL	65	1002	1
	4	Hurricane DANNY	12-20 AUG	80	988	1
	5	Hurricane ELENA	28 AUG- 4 SEP	110	953	3
	10	Hurricane JUAN	26 OCT- 1 NOV	75	971	1
	11	Hurricane KATE	15-23 NOV	105	954	3
1986	2	Hurricane BONNIE	23-28 JUN	75	992	1
1987	1	Tropical Storm #1	9-17 AUG	40	1007	TS
	7	Hurricane FLOYD	9-14 OCT	65	993	1
1988	2	Tropical Storm BERYL	8-10 AUG	45	1001	TS
	4	Hurricane DEBBY	31 AUG-8 SEP	65	987	1
	7	Hurricane FLORENCE	7-11 SEP	70	983	1
	8	Hurricane GILBERT	8-20 SEP	160	888	5
	12	Tropical Storm KEITH	17-26 NOV	65	945	TS
1989	1	Tropical Storm ALLISON	24 JUN-1 JUL	45	999	TS
	3	Hurricane CHANTAL	30 JUL-3 AUG	70	984	1
	10	Hurricane JERRY	12-16 OCT	75	983	1
1990	4	Hurricane DIANA	4-9 AUG	85	980	2
	13	Tropical Storm MARCO	9-13 OCT	55	989	TS
1991	1	Tropical Storm ANA	29 JUN-5 JUL	45	1000	TS
1992	2	Hurricane ANDREW	16-28 AUG	135	922	5
1993	1	Tropical Storm ARLENE	18-21 JUN	35	1000	TS
	7	Hurricane GERT	14-21 SEP	85	970	2
1994	1	Tropical Storm ALBERTO	30 JUN-7 JUL	55	993	TS
	2	Tropical Storm BERYL	14-19 AUG	50	1000	TS

Table 6.2-2. Summary of individual tropical storms that entered the Gulf of Mexico from 1977 through 2000 (continued).

Year	Storm #	Name	Dates	Wind	Pres.	Cat.
1994	7	Hurricane GORDON	8-21 NOV	75	980	1
1995	1	Hurricane ALLISON	03-06 JUN	65	987	1
	4	Tropical Storm DEAN	28-31 JUL	40	999	TS
	5	Hurricane ERIN	31 JUL-03 AUG	75	975	1
	6	Tropical Depression #6	05-07 AUG	30	1001	TD
	8	Tropical Storm GABRIELLE	09-12 AUG	60	988	TS
	11	Tropical Storm JERRY	22-25 AUG	35	1003	TS
	17	Hurricane OPAL	27 SEP-05 OCT	130	916	4
	19	Hurricane ROXANNE	07-20 OCT	100	958	3
1996	4	Hurricane DOLLY	19-23 AUG	70	987	1
	10	Tropical Storm JOSEPHINE	04-08 OCT	60	981	TS
1997	4	Hurricane DANNY	16-26 JUL	70		1
1998	3	Tropical Storm CHARLEY	21-22 AUG	50	1003	TS
	5	Hurricane EARL	31 AUG-03 SEP	85	986	2
	6	Tropical Storm FRANCES	08-12 SEP	55	990	TS
	7	Hurricane GEORGES	15-29 SEP	130	938	4
	8	Tropical Storm HERMINE	17-20 SEP	40	999	TS
	13	Hurricane MITCH	22 OCT-05 NOV	155		5
1999	2	Tropical Depression TWO	03-03 JUL	30	1004	TD
	3	Hurricane BRET	18-23 AUG	120	945	4
	7	Tropical Depression SEVEN	05-07 SEP	30	1005	TD
	10	Tropical Storm HARVEY	19-22 SEP	50	995	TS
	11	Tropical Depression ELEVEN	04-06 OCT	30	1002	TD
	13	Hurricane IRENE	13-19 OCT	90	958	2
	15	Tropical Storm KATRINA	28 OCT-01 NOV	35	999	TS
2000	5	Tropical Storm BERYL	13-15 AUG	45	1007	TS
	9	Tropical Depression NINE	09-09 SEP	30		TD
	11	Hurricane GORDON	14-18 SEP	65	981	1
	12	Tropical Storm HELENE	15-22 SEP	55	996	TS
	15	Hurricane KEITH	28 SEP-06 OCT	115	942	4

Table 6.2-3. Saffir-Simpson Scale for tropical storms.

Type	Category	Pressure (mb)	Winds (knots)	Winds (mph)	Surge (ft)
Depression	TD	--	< 34	< 39	
Tropical Storm	TS	--	34-63	39-73	
Hurricane	1	> 980	64-82	74-95	4-5
Hurricane	2	965-980	83-95	96-110	6-8
Hurricane	3	945-965	96-113	111-130	9-12
Hurricane	4	920-945	114-135	131-155	13-18
Hurricane	5	< 920	>135	>155	>18

Table 6.2-4. Summary of extratropical cyclones in the Gulf of Mexico during the 1966 through 1996 winter cyclogenesis season (unpublished data from Hardy and Hsu 1997, personal communication; Nowlin et al. 1998b). Given are dates of cyclones that reached a minimum pressure of ≤ 1012 mb, which corresponds to class 2, weak cyclogenesis (Hsu 1993).

Winter Years	**Dates mm dd yy**	**Winter Years**	**Dates mm dd yy**	**Winter Years**	**Dates mm dd yy**
1966-1967	12 30 66	1978-1979	01 12 79	1990-1991	11 08 90
	01 13 67		01 27 79		01 18 91
	02 12 67		01 30 79		01 29 91
1967-1968	12 17 67		02 06 79		03 17 91
	12 27 67		04 22 79		05 18 91
	12 30 67	1979-1980	01 26 80	1991-1992	11 30 91
	02 21 68		03 01 80		01 05 92
	03 06 68		04 13 80		01 12 92
1968-1969	02 21 69		05 19 80		01 18 92
	03 16 69	1980-1981	11 26 80		02 04 92
	04 12 69		01 20 81		02 22 92
1969-1970	12 06 69	1981-1982	03 24 82	1992-1993	11 04 92
	12 09 69	1982-1983	01 19 83		11 24 92
	01 05 70		02 05 83		12 09 92
	01 17 70		02 15 83		12 15 92
1970-1971	none		02 20 83		02 21 93
1971-1972	12 05 71		02 26 83		03 12 93
	02 01 72		03 16 83		04 08 93
	02 16 72		03 23 83		05 12 93
	03 30 72	1983-1984	01 09 84	1993-1994	12 20 93
	05 11 72		01 26 84		12 22 93
1972-1973	11 18 72	1984-1985	02 01 85		02 10 94
	12 21 72		05 18 85		03 01 94
	01 25 73	1985-1986	02 08 86		04 22 94
	02 18 73	1986-1987	7 events		05 02 94
1973-1974	none				05 13 94
1974-1975	none				05 16 94
1975-1976	11 26 75			1994-1995	12 03 94
	12 29 75				12 31 94
	03 07 76				01 17 95
	05 22 76				03 29 95
1976-1977	11 14 76	1987-1988	2 events		04 04 95
	01 02 77				04 20 95
1977-1978	11 25 77	1988-1989	none		05 31 95
	11 30 77	1989-1990	1 event	1995-1996	12 22 95
	04 12 78				12 31 95
					02 01 96

To obtain estimates of the background currents in the Gulf of Mexico, we extracted the maximum, record-length mean, and standard deviation for each current time series in our data inventory. These were then sorted by longitude into three groups before plotting versus depth: locations east of 89°W, 89° to 93°W, and west of 93°W. Results are presented in Section 7.1.

As a group, we then examined vector stick plots of all current meter records in our inventory. We searched for energetic events and attempted to identify each event as to type of phenomena and to relate each to possible forcing. In the next section (6.3) are presented general notes made during that examination for non-proprietary data sets. In Section 6.4 are presented inventories of the energetic events that were identified, grouped by type of phenomena.

6.3 General Description of Data Sets

General descriptions and notes regarding the non-proprietary current meter and moored or suspended ADCP data sets are presented here. The description of each data set follows this general outline:

- Basic description of data set including a map showing mooring locations, time lines with instrument depths and start/stop times, total water depth, type of instruments (i.e., ADCP, single point current meter, other), source of records, and references to published descriptions. The data quality codes of the files are given. Note that each storm tracked on the base map is given its own line type as an aid to differentiating between multiple tracks.
- Environmental background including information on tropical and extratropical cyclones, eddy separations, and major mesoscale features in the vicinity of the measurements during deployment.
- Basic statistics including maximum and mean speed and standard deviation for record-length data at selected depths and plots of these versus depth. The unfiltered data were used unless otherwise noted.
- General description of records examining both low-frequency (40-hr low-passed) and high-frequency (40-hr high-passed) records; attention was focused on energetic events.

For each set of data, three figures are shown. One is a map with the locations of the moorings and the tracks of tropical storms and hurricanes that passed through the Gulf during the deployment period. The second gives the time lines in the form of vector stick plots of the data sets. For each tropical storm or hurricane that was in the Gulf during an instrument deployment, the first day of storm tracking given in the UNISYS Corporation Weather storm summary (http://weather.unisys.com/hurricane/index.html) is noted on this figure. For the vectors, north is upward unless otherwise noted. To determine the vector magnitudes, the interval between the lines of individual mooring data is 50 $cm \cdot s^{-1}$. The third plot shows the record-length maximum speed, mean speed and standard deviation versus depth for all instruments with quality of A, B, C, or D (quality codes are indicated). The names for the LCEs are those given by Horizon Marine, Inc., as part of the EddyWatch program (see Section 3.2) or those found in the literature.

Few of the measured time series of currents available from the Gulf of Mexico are long enough to enable estimation with certainty of statistical measures of the currents. This applies to means, variances, maxima, and all such measures. Knowing this, we nevertheless have estimated such statistical measures and included them in this report. The reader is cautioned to remember this caveat when using such measures.

6.3.1 Molinari and Mayer Eastern Gulf Moorings, 1977-1979

Basic description of data set. These data were collected by scientists from the Atlantic Oceanographic and Meteorological Laboratories, NOAA, in support of a Department of Energy Ocean Thermal Energy Conversion study. The records were obtained from NODC. The currents are described in Molinari and Mayer (1982). There were four moorings in this data set. Three (M1, M2, and M3) were sited off Mobile, AL, on the northwest slope of the DeSoto Canyon and one (T1) was sited off Tampa, FL (Figure 6.3.1-1). Data were collected at the Mobile site from July 1977 through August 1978. For three months, July through October 1977, M1 and M2 were deployed simultaneously. Only one mooring was deployed at the Mobile site for the remainder of the sampling period. Data were collected at the Tampa site from June 1978 through June 1979, overlapping in time with M3 by approximately two months (June to August 1978). Figure 6.3.1-2 shows the time lines and vector stick plots for the moorings. The nominal water depth at all four sites was 1050 m. Instrument depths varied by mooring and are shown in Table 6.3.1-1. The quality code for these data is A. File names for the current records in the database are

- M1: VK770717.C01-C02
- M2: VK770717.C03-C05
- M3: DD771018.C01-C02; DD771019.C01; DD780227.C01-C03
- M3: DD780617.C01-C03 (second location)
- T1: EL780612.C01-C03; EL781026.C01-C03; EL790213.C01-C03.

Environmental background. Two hurricanes passed through the Gulf during these deployments: Anita (23 August–3 September 1977) and Babe (3–9 September 1977). These hurricanes passed south and/or west of moorings M1 and M2 as indicated by the tracks shown in Figure 6.3.1-1. Three tropical storms (Amelia, Bess, and Debra) were in the Gulf during 1978. Their tracks were mainly outside the northeast Gulf location of the moorings (Figure 6.3.1-1). Tropical Storm Amelia (30 July–1 August 1978) was entirely in the far western Gulf. Moorings M3 and T1 were deployed during passage of Amelia and Bess; T1 was in the water also during Debra (Figure 6.3.1-2). At least 10 cold front passages were identified as affecting the T1 and M3 moorings from December 1977 through February 1978.

There are no Eddy Watch charts, sea surface height anomaly, or GEOSAT maps available for these mooring deployments. However, Molinari and Mayer (1982) noted that the Loop Current or a detached eddy was near the Mobile site in summer 1978 and that the Loop Current was adjacent to the Tampa site in fall 1978 and winter 1979. Based on available data, no LCE separations occurred during the deployment period (Sturges and Leben 2000).

Basic statistics. Record-length mean, standard deviation, and maximum speeds for the moorings are shown in Table 6.3.1-1. Figure 6.3.1-3 shows the statistics versus depth for all instrument depths. Mean speeds decreased with depth at all mooring locations. The standard deviations were less than the means and decreased with increasing depth. Maximum speeds in the upper 300 m generally were 50 $cm \cdot s^{-1}$ or more, but none exceeded 70 $cm \cdot s^{-1}$. Below 900 m, maximum speeds were ~30 $cm \cdot s^{-1}$ or less.

General description of records. For both M2 and M3, the current record from the deepest instrument had a much different character, in terms of energetic periodicities, amplitudes, and direction, than did the top or middle instruments. There was no significant visual coherence between the deep and upper records. There was, however, coherence in the data from the two upper instruments. The records from the two M1 instruments, which were within the upper 215 m, show significant coherence. At T1, the records from 150, 250, and

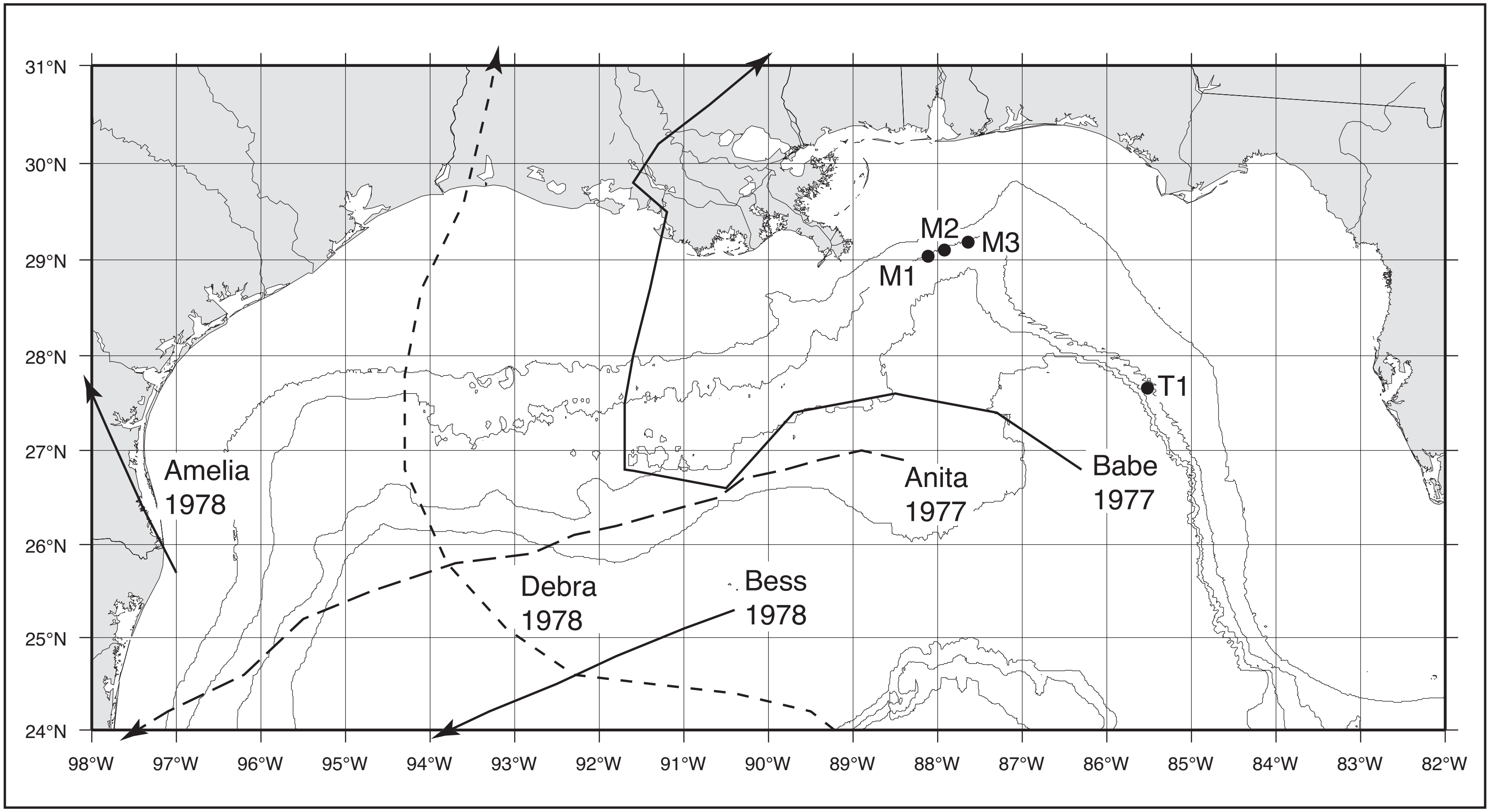

Figure 6.3.1-1. Location map for the Molinari and Mayer eastern Gulf moorings. The tracks of tropical storms and hurricanes in the Gulf during the deployment period are shown. Shown are the 200-, 1000-, 2000-, and 3000-m isobaths.

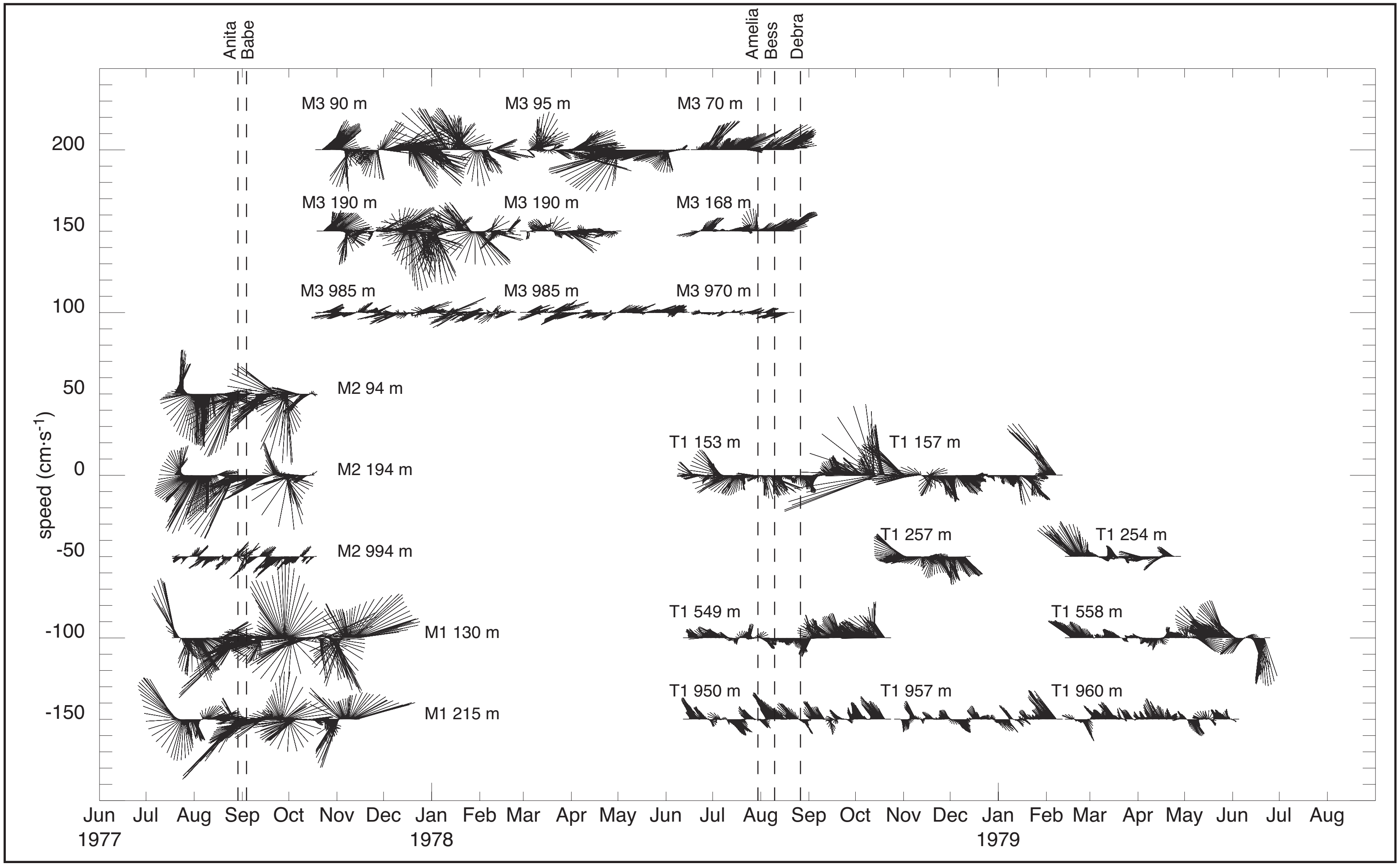

Figure 6.3.1-2. Time lines and vector stick plots for the Molinari and Mayer eastern Gulf moorings. The first day of tracking for tropical storms and hurricanes in the Gulf during the deployment period is indicated by the vertical dashed line with the storm name given above it. North is upward. Tick marks denote start of the month.

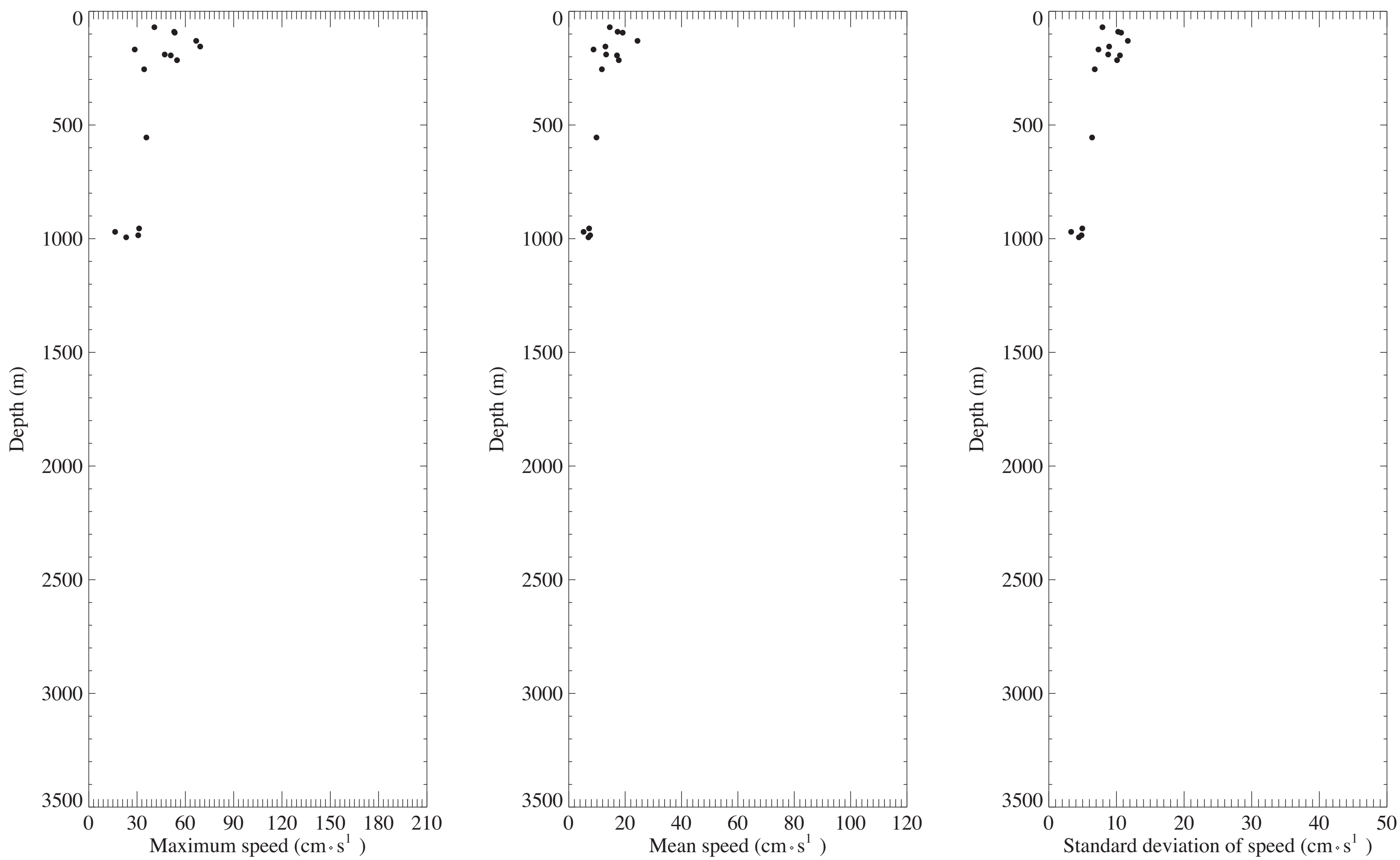

Figure 6.3.1-3. Observed speed (a) maximum, (b) mean, and (c) standard deviation versus instrument depth for unfiltered records from Molinari and Mayer eastern Gulf moorings (npts = 15). Quality codes: A or B (dot), C (square), D (plus).

Table 6.3.1-1. Record-length mean, standard deviation, and maximum speed for Molinari and Mayer 1977-1979 eastern Gulf data. Instruments were current meters.

Mooring	**Instrument Depth (m)**	**Mean Speed ($cm{\cdot}s^{-1}$)**	**Standard Deviation ($cm{\cdot}s^{-1}$)**	**Maximum Speed ($cm{\cdot}s^{-1}$)**
M1	130	24.4	11.7	66.8
	215	17.8	10.1	54.8
M2	94	19.1	10.7	53.4
	194	17.1	10.5	51.0
	994	7.0	4.5	23.3
M3	90	17.3	10.3	53.1
(1^{st})	190	13.3	8..8	47.2
	985	7.6	4.8	30.7
M3	70	14.6	7.9	40.8
(2^{nd})	168	8.8	7.3	28.6
	970	5.3	3.3	16.4
T1	150	13.0	8.9	69.2
	250	11.8	6.8	34.4
	550	9.8	6.4	35.8
	950	7.2	5.0	31.3

550 m were significantly correlated, but there was not significant coherence between records at 550 and 950 m. For the limited-duration periods of pairs of overlapping records, Molinari and Mayer (1982) determined there was no significant coherence between M1 and M2 and between M3 and T1 for the frequencies that could be resolved.

In considering both data from these sites and historical data mainly from drift bottles, Molinari and Mayer (1982) found summer flows in the upper 200 m at the Mobile site to be generally westward, likely in response to the mean wind stress, but nonsummer flows to be eastward. They found the mean flow to be generally westward and in the direction of the wind at the Tampa site. At both sites, they noted that effects of the Loop Current or LCEs could significantly alter the mean flow patterns that they found. One such event was in summer 1978 at M3, where the currents were eastward, rather than the expected westward flow of summertime, in response to an intrusion of the Loop Current into the Mobile site (Figure 6.3.1-2). The Loop Current also resulted in energetic currents at T1 during October 1978 (Figure 6.3.1-2). Frontal passages were marked by an increase in wind forced inertial oscillations. Molinari and Mayer (1982) also examined the tidal forcing exhibited in the records.

6.3.2 Brooks Western Gulf Moorings, 1980-1981

Basic description of data set. These data were collected by D. A. Brooks of Texas A&M University as part of a National Science Foundation-sponsored study of the circulation and hydrography of the western Gulf. Data were obtained from NODC. Aspects of the current meter records were described in Brooks (1983, 1984). Three current meter moorings were placed along the 730-m isobath on the slope in the western Gulf: North (N), Central (C), and

South (S). Mooring locations are shown in Figure 6.3.2-1. The moorings were separated by approximately 55 km. Instrument depths are given in Table 6.3.2-1. The records extend from July 1980 through February 1981. Time lines as vector stick plots are given in Figure 6.3.2-2. The instruments at 200 and 450 m on mooring N failed less than 1 month after deployment. The quality code for these data is A. File names for the current records in the database are

- N: CC800717.C01-C03
- C: PI800717.C04-C07
- S: PI800717.C01-C03

Environmental background. Four tropical cyclones passed through the Gulf during these measurements: Hurricane Allen (31 July–11 August 1980), Tropical Storm Danielle (4–7 September 1980), Tropical Storm Hermine (20–26 September 1980), and Hurricane Jeanne (7–16 November 1980). Hurricane Allen, a very powerful storm, was most notable and passed approximately 60 km to the south of mooring S; the track is shown in Figure 6.3.2-1. The track of Hermine was entirely south of 20°N.

There are no Eddy Watch charts, sea surface height anomaly, or GEOSAT maps available during the measurement period. Based on satellite sea surface temperature images, Brooks (1984) described the presence of one or more LCEs to the southeast of the moorings during much of the deployment period (see also Brooks and Legeckis 1982). He also mentioned that two LCEs had separated from the Loop Current in January and May 1980. The January separation is consistent with the separations listed by Sturges and Leben (2000); the May separation is not.

Basic statistics. Record-length mean, standard deviation, and maximum speeds for the moorings are shown in Table 6.3.2-1. Figure 6.3.2-3 shows the statistics versus depth for all instrument depths. Mean speeds decreased with depth. Standard deviations also decreased with depth and were smaller than associated means. Mooring N had smaller maximum speeds at all depths than moorings C and S, but the upper two records were of short duration. Moorings C and S had comparable speeds at each depth. Maximum speeds at the top meters of those moorings exceeded 90 $cm \cdot s^{-1}$.

General description of records. Hurricane Allen passed 60 km south of mooring S on 9 August 1980. The maximum speed during the hurricane at mooring C at 200 m was southward at 93.9 $cm \cdot s^{-1}$; currents at 450 m approached 50 $cm \cdot s^{-1}$, while at 575 and 700 m there was a 10-15 $cm \cdot s^{-1}$ perturbation in the background current velocities. At mooring S, the effects of the hurricane were less pronounced. Current speeds at 200 m peaked at 50-55 $cm \cdot s^{-1}$ and 40 $cm \cdot s^{-1}$ at 450 m. At 700 m there was a 10-15 $cm \cdot s^{-1}$ perturbation in the background current velocities. The strong currents were accompanied by a large temperature and salinity increase at 200 m which produced T-S oscillations that persisted for about one week after the storm. The upwelling displacement depth at the mid-thermocline (200-300 m) was estimated by Brooks (1983) to be about 20 m. Large amplitude inertial currents at all measurement depths also followed the storm's passage. The amplitude of these oscillations was approximately 25 $cm \cdot s^{-1}$ at 200 m and 10-15 $cm \cdot s^{-1}$ at 450 m.

From mid-September through October 1980 there was a strong persistent northward current at mooring S. Hydrographic data indicated that an anticyclonic LCE had migrated across the Gulf during spring 1980 and was centered near 24.4°N, 95.5°W in July 1980 when the moorings were deployed (Brooks 1984; Brooks and Legeckis 1982). The eddy had a diameter of approximately 220 km and an estimated drift speed of 5 $km \cdot d^{-1}$. Hydrographic data taken during July 1980 revealed this eddy to be of Loop Current origin. The nearly

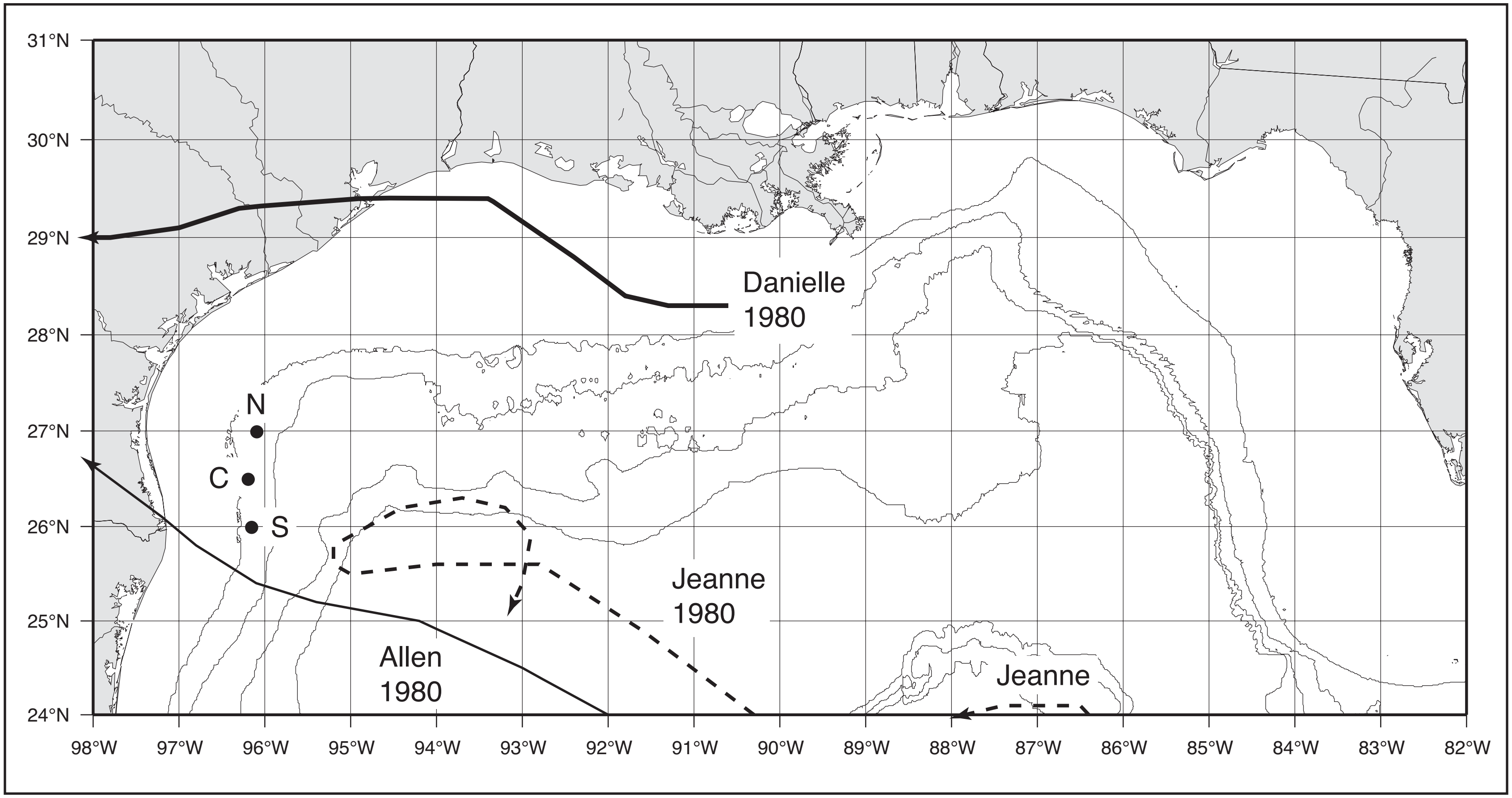

Figure 6.3.2-1. Location map for the Brooks western Gulf moorings. The tracks of tropical storms and hurricanes in the Gulf for the deployment period are shown. Shown are the 200-, 1000-, 2000-, and 3000-m isobaths.

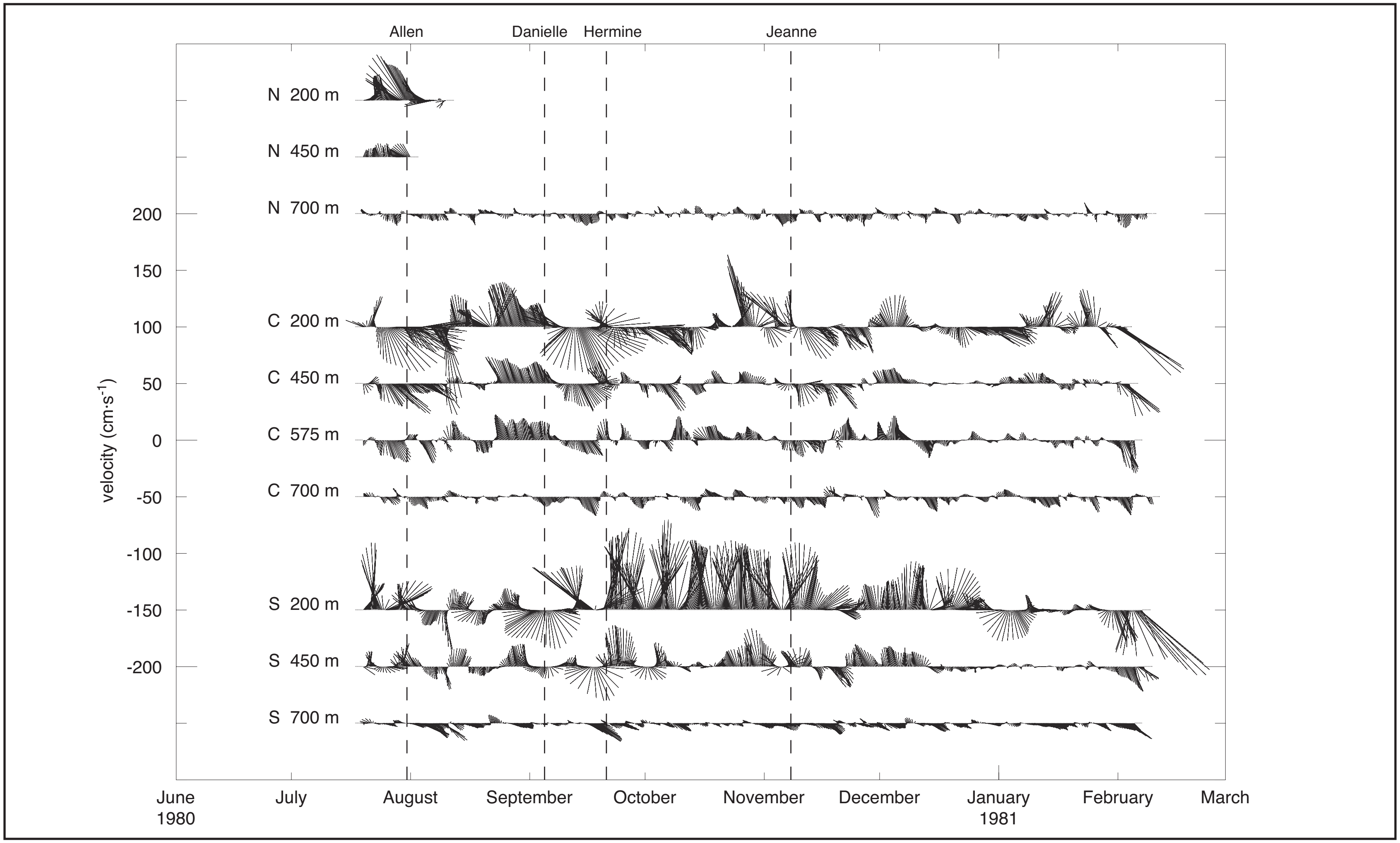

Figure 6.3.2-2. Time lines and vector stick plots for the Brooks western Gulf moorings. The first day of tracking for tropical storms and hurricanes in the Gulf during the deployment period is indicated by the vertical dashed line with the storm name given above it. North is upward. Tick marks denote start of the month.

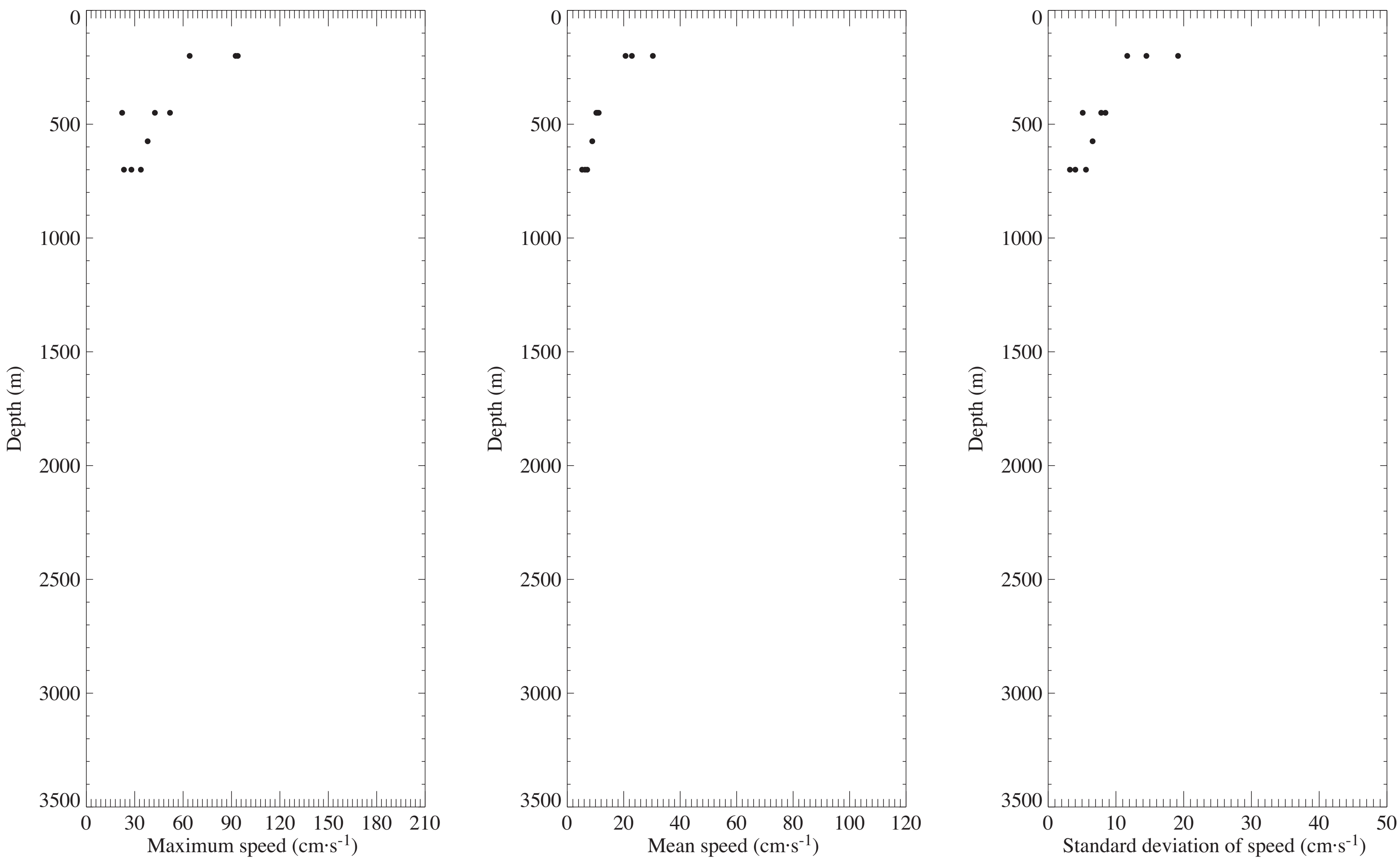

Figure 6.3.2-3. Observed speed (a) maximum, (b) mean, and (c) standard deviation versus instrument depth for unfiltered records from Brooks western Gulf moorings (npts = 10). Quality codes: A or B (dot), C (square), D (plus).

Table 6.3.2-1. Record-length mean, standard deviation, and maximum speed for the Brooks 1980-1981 western Gulf data. Instruments were current meters.

Mooring	Instrument Depth (m)	Mean Speed ($cm \cdot s^{-1}$)	Standard Deviation ($cm \cdot s^{-1}$)	Maximum Speed ($cm \cdot s^{-1}$)
N	200	20.7	11.7	64.1
	450	10.3	5.1	22.2
	700	5.3	3.2	23.3
C	200	22.9	14.5	93.9
	450	10.7	8.5	51.9
	575	8.9	6.6	38.0
	700	6.3	4.0	28.0
S	200	30.3	19.2	92.6
	450	11.2	7.8	42.5
	700	7.1	5.6	33.8

symmetric temperature profile suggests that the eddy had just arrived in the western Gulf. The eddy drifted north over the next several weeks and ultimately moved over mooring S in late September 1980. Currents at 200 m on S exceeded 70 $cm \cdot s^{-1}$ several times between 21 September–25 October 1980 with a mean speed of roughly 50 $cm \cdot s^{-1}$.

These strong currents were only seen at the 200-m instrument (not at the 450-m instrument) and are indicative of a baroclinic event. However, it should be noted that by October 1980 this eddy was relatively old and the lack of energetic currents at 450 m may have resulted from repeated interaction of the eddy with the slope. Strong currents were not seen at C except for brief intermittent northward pulses at 200 m caused by northward displacements of the anticyclone as suggested by a hydrographic survey done between 26 October and 8 November 1980 (Brooks 1984).

The large amplitude oscillations (~20 $cm \cdot s^{-1}$) with a 7-10 day period in the east-west currents at 200 m on mooring S from mid-September through October may have resulted from a slope vorticity wave. The gravest vorticity mode for the Gulf of Mexico is about 5 days (R. O. Reid, personal communication).

6.3.3 SAIC Five-Year Physical Oceanography Study, 1983-1988

During 1983-1988, current meter measurements were made in three regions over the continental slope and deep basin of the Gulf of Mexico. We refer to these regions as eastern Gulf (under or adjacent to the Loop Current), central Gulf (along 92°W across the Texas-Louisiana continental slope), and western Gulf (over the Rio Grande slope, rise and basin off south Texas). These moorings were deployed by Science Applications International Corporation (SAIC) as part of the MMS-funded five-year Gulf of Mexico Physical Oceanography Program. The data files were obtained from the NODC. The west moorings were deployed simultaneously with the east moorings for approximately six months; the central moorings were independent. The currents and evidence for deep topographic Rossby waves were described by Hamilton (1990) using data from all three regions. Hamilton (1992) described cyclonic eddies along the lower continental slope using data from the central region. The currents also were examined in a series of technical reports (SAIC 1986, 1987, 1988, 1989). Each region is considered separately below. Only moorings in water depths greater than 200 m are discussed.

6.3.3.1 Eastern Gulf Moorings, 1983-1986

Basic description of data set. Two current meter moorings were deployed in water depths greater than 200 m in the eastern Gulf: mooring A in water depth of 1696 m and mooring G in water depth of 3200 m. Locations are shown in Figure 6.3.3-1. Instrument depths are given in Table 6.3.3-1. The current meter deployments extended from January 1983 through February 1986. Time lines and vector stick plots are shown in Figure 6.3.3-2. The quality codes for these data are A, B, and C. File names for the current records in the database are

- A: HH830127.C01-C03; HH830127.T01-T02; HH830729,C01; HH830730.C01-C02; HH840426.C01-C02; HH840718.C01-C04; HH841018.C01-C05; HH850124.C01-C05; HH850731.C01-C-2; HH850801.C01-C02
- G: HH840203.C01-C03; HH840718.C05-C07; HH841018.C06-C10; HH841028.C01; HH850124.C06-C10; HH850312.C01-C02; HH850801.C03-C06.

Environmental background. A total of eight severe tropical cyclones were present in the Gulf during the deployment of these moorings: hurricanes Alicia (15–21 August 1983) and Barry (23–29 August 1983); Tropical Storm Edouard (14–15 September 1984); hurricanes Bob (15–26 July 1985), Danny (12–20 August 1985), Elena (28 August–4 September 1985), Juan (26 October–1 November 1985), and Kate (15–23 November 1985). During hurricanes Alicia and Barry, only mooring A was deployed (Figure 6.3.3-2).

The two moorings were located in a region where the Loop Current passes over or near them. Five LCE separations took place during the deployment (Sturges and Leben 2000): Eddy Arnold (August 1984), Fast Eddy (July 1985), Hot Eddy (January 1986), and two unnamed eddies in March 1983 and February 1984. Hamilton (1990) described the effects of the formation of Fast Eddy and Hot Eddy, which he called eddy B and C respectively, on the deep currents at these moorings. The separation of Fast Eddy from the Loop Current and its movement out of the eastern Gulf are described in Lewis and Kirwan (1987), Forristall et al. (1992), and Lewis et al. (1989).

Basic statistics. Record-length mean, standard deviation, and maximum speeds for the moorings are shown in Table 6.3.3-1. Figure 6.3.3-3 shows the statistics versus depth for all instrument depths. Standard deviations and mean speeds generally decreased with depth to 1600 m at both locations. Mean speeds at the lower two instruments on G, however, were higher than those at ~1600 m. At comparable depths, mean speeds were higher at G than at A, due most likely to the closer proximity of the Loop Current to G. Mean speed and standard deviation were generally of the same order at depth, but mean speeds were 1.5-2 times higher than the standard deviations at the top instrument.

General description of records. At 1100- and 1600-m depths on mooring A the currents were consistently oriented along the slope and northward with infrequent current reversals to the south. Deep currents were coherent, but with smaller magnitude at 1600 m. The currents above 1000 m were considerably more variable and energetic owing to the direct influence of the Loop Current. At G, currents deeper than 1000 m also were strongly coherent in depth,

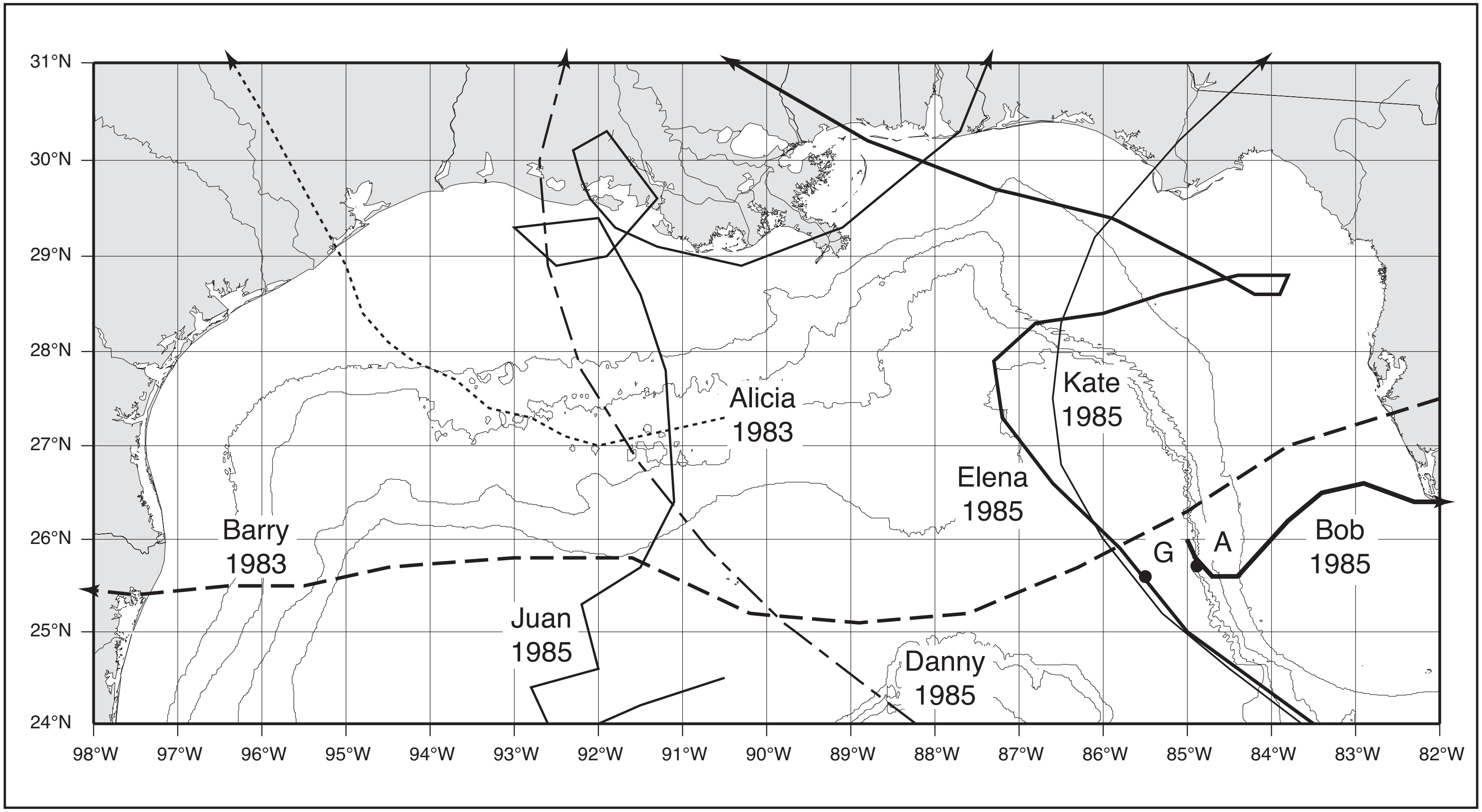

Figure 6.3.3-1. Location map for the eastern Gulf SAIC 5-year moorings in water depths greater than 200 m. The tracks of tropical storms and hurricanes in the Gulf for the deployment period are shown. Shown are the 200-, 1000-, 2000-, and 3000-m isobaths.

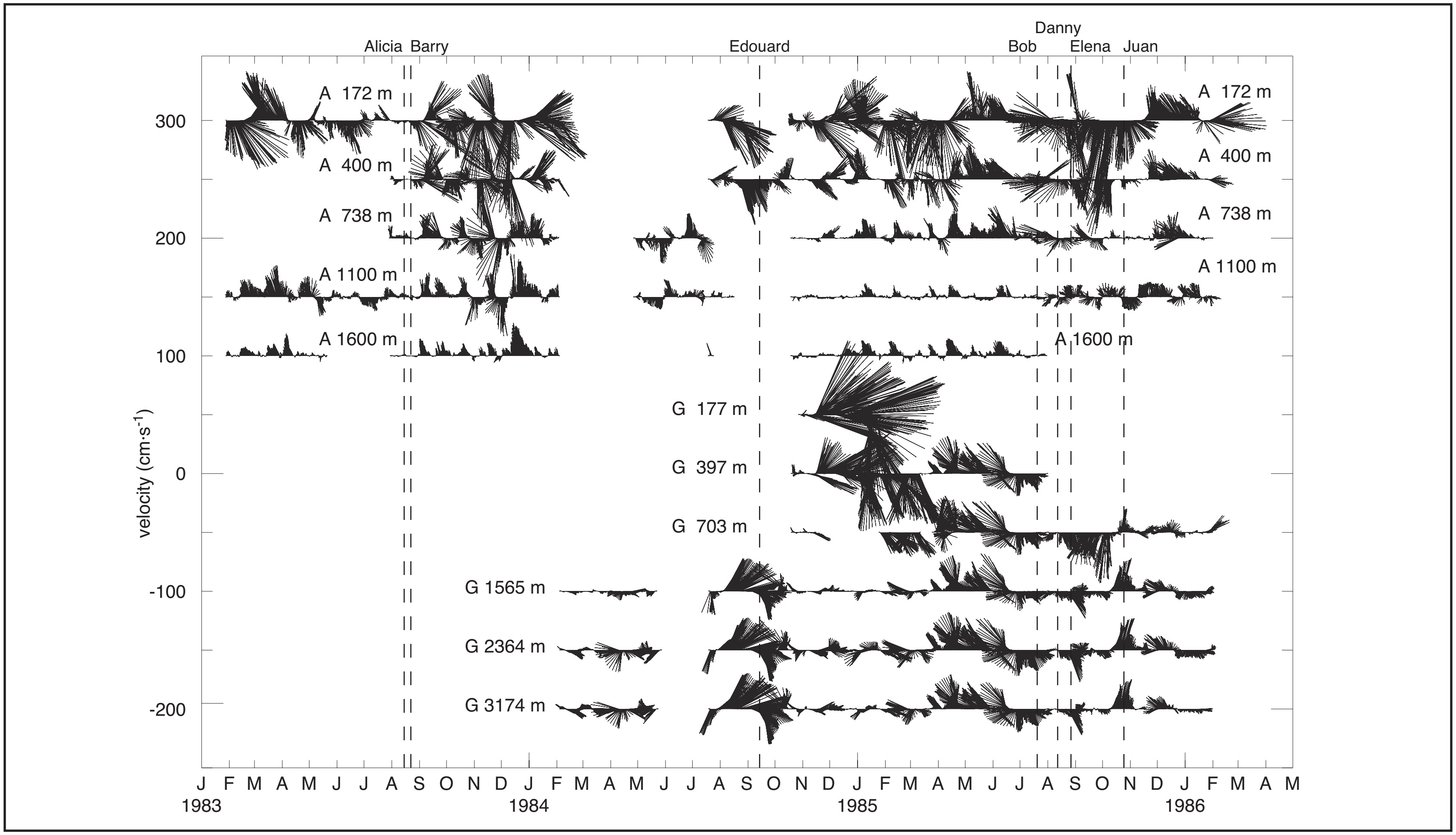

Figure 6.3.3-2. Time lines and vector stick plots for the eastern Gulf SAIC 5-year moorings in water depths greater than 200 m. The first day of tracking for tropical storms and hurricanes in the Gulf during the deployment period is indicated by the vertical dashed line with the storm name given above it. North is upward. Tick marks denote start of the month.

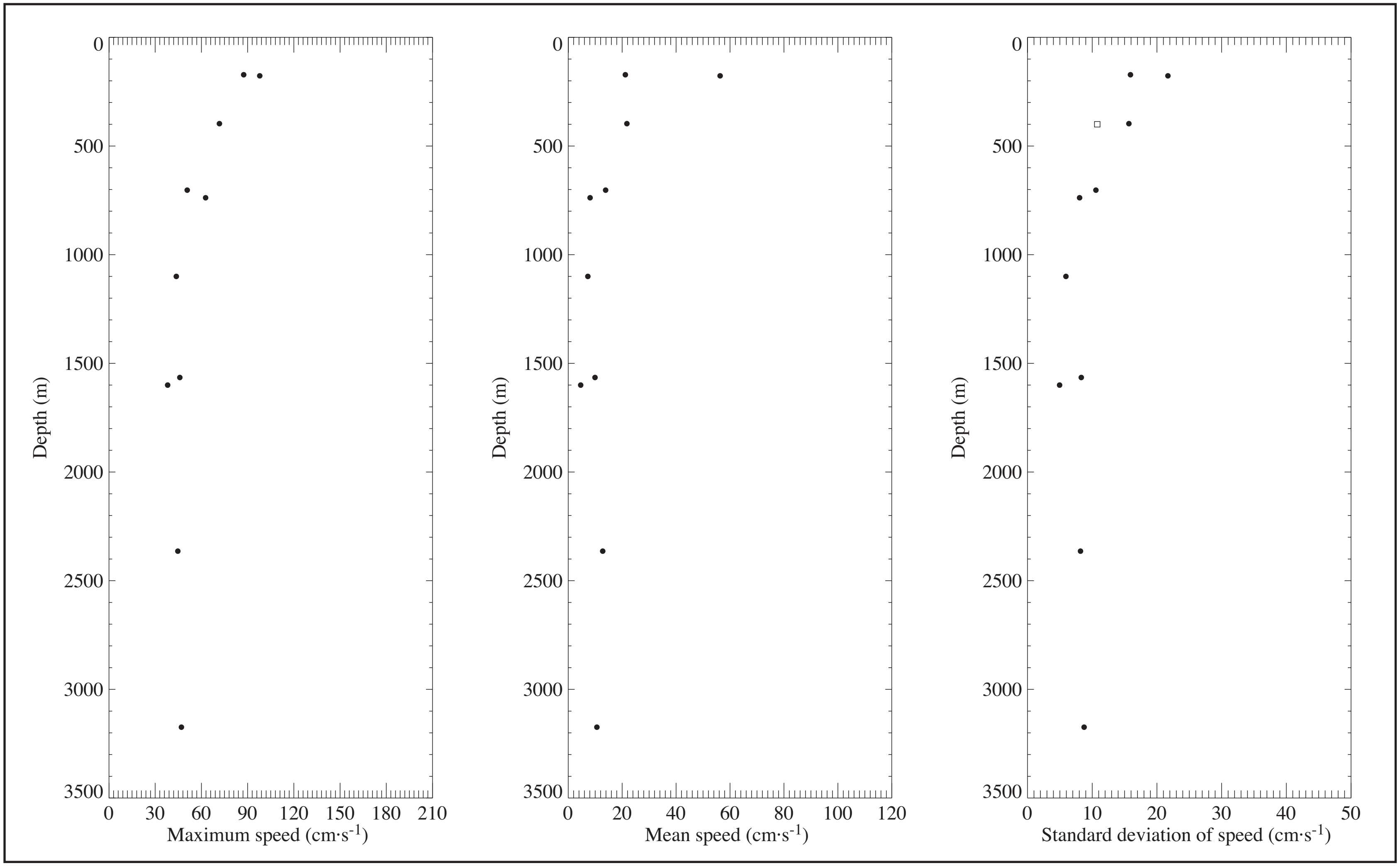

Figure 6.3.3-3. Observed speed (a) maximum, (b) mean, and (c) standard deviation versus instrument depth for unfiltered records from SAIC 5-year eastern Gulf moorings (npts = 11). Quality codes: A or B (dot), C (square), D (plus).

Table 6.3.3-1. Record-length mean, standard deviation, and maximum speed for data from the eastern Gulf in the SAIC 1983-1988 five-year physical oceanography study. Instruments were current meters.

Mooring	Instrument Depth (m)	Mean Speed ($cm \cdot s^{-1}$)	Standard Deviation ($cm \cdot s^{-1}$)	Maximum Speed ($cm \cdot s^{-1}$)
A	172	21.2	15.9	87.5
	400	12.2	10.8	73.0
	738	8.1	8.1	62.7
	1100	7.3	5.9	43.7
	1600	4.6	5.0	38.1
G	177	56.3	21.7	97.9
	397	21.8	15.7	71.7
	703	13.9	10.6	50.8
	1565	9.9	8.3	46.0
	2364	12.8	8.2	44.7
	3174	10.6	8.8	47.0

with evidence of intensification at 3174 m during large current events. The record from 177 m was only about two months long, but currents during that period appear surface intensified and coherent among the 177, 397, and 703-m records. During the six-month period beginning March 1985 currents at mooring G were coherent from 397 m to the bottom instrument at 3174 m; from September 1985 to the end of the record (when there was no data from the 397-m meter), currents generally were coherent from 703 m to bottom.
During August 1984, currents at mooring G changed direction clockwise from northeastward to southward with constant speeds of about 35 $cm \cdot s^{-1}$. This event was coherent at the three deep (1565, 2364, and 3174 m) instruments, and there is evidence of bottom intensification at 3174 m (almost a 25% increase in speed). A similar rotation is seen in the upper 172- and 400-m records at A; however, the currents at A led those at G by about two weeks. This resulted in the strong shear seen between A and G, possibly as the western edge of a cyclone pushed from the slope at A into the deeper waters at G. The Loop Current was well south of the moorings during this current event.

There were two Loop Current intrusions at A, during March-April 1985 and October 1985. Both were marked by strong sustained southward flow in the upper 1000 m. During the October 1985 intrusion, currents at 172 m on A reached 150 $cm \cdot s^{-1}$. During the eddy separation events that occurred during the deployment period of moorings A and G, there seemed to be increased current variability in the lower 1000 m; the cause has not been determined.

During October 1985, there was a strong pulse of northward current at 700 m on mooring G that lasted about 2 weeks and had an amplitude of ~20 $cm \cdot s^{-1}$; deeper currents were also northward directed but stronger at ~30 $cm \cdot s^{-1}$. During the same period at mooring A, currents at 1100 m were directed southward with amplitudes of less than 20 $cm \cdot s^{-1}$, suggesting a bottom-intensified anticyclonic feature at depth.

Tropical storms and hurricanes affected the surface currents during Hurricane Barry (August 1983) and Hurricanes Bob, Danny, and Elena (August - September 1985). The low-passed currents showed increased variability during these periods.

6.3.3.2 Western Gulf Moorings, 1985-1986

Basic description of data set. The western group consisted of five moorings located as shown in Figure 6.3.3-4. Instrument depths are given in Table 6.3.3-2. The deployments covered the period from June 1985 through May 1986. Time lines and vector stick plots are shown in Figure 6.3.3-5. The quality codes for these data are A and B. File names for the current records in the database are

- P: AC850611.C01-C03
- Q: MC850615.C01-C04; MC851020.C01
- R: MG850615.C06-C09
- S: MG850612.C01-C03; MG851102.C01
- T: MG850613.C01-C03.

Environmental background. Five hurricanes crossed the Gulf during this deployment: Bob, Danny, Elena, Juan, and Kate. None passed directly over the moorings. Hurricanes Danny (12–20 August 1985) and Juan (26 October–1 November 1985) passed closest and to the east of the moorings (Figure 6.3.3-4). During Hurricane Juan, mooring R was not deployed and no data were available from the upper three instruments on mooring S (Figure 6.3.3-5).

Two LCEs separated from the Loop Current during the period of the deployment (Sturges and Leben 2000): Fast Eddy in July 1985 and Hot Eddy in January 1986. Of these, Fast Eddy reached the western Gulf during the deployment period. Additionally, from the EddyWatch charts and GEOSAT SSHA maps, a second anticyclonic eddy, Ghost Eddy, was in the vicinity of the moorings during the deployment. Ghost Eddy had not separated directly from the Loop Current, but rather likely was formed from the interaction of a cyclone with the western perimeter of Fast Eddy (Berger et al. 1996a) or by the splitting of Fast Eddy into two pieces (Forristall et al. 1992). A strong cyclone, situated between Fast Eddy and Ghost Eddy, may have been over moorings Q and S during August and early September 1985. Hamilton (1990) describes the effects on the currents of the arrival of Fast Eddy, which he calls eddy B. Lewis et al. (1989), Forristall et al. (1992), and Berger et al. (1996a) discuss Fast Eddy and Ghost Eddy.

Basic statistics. Record-length mean, standard deviation, and maximum speeds for the moorings are shown in Table 6.3.3-2. Figure 6.3.3-6 shows the statistics versus depth for all instrument depths. Mean speeds were generally smaller than those seen in the Eastern and Central mooring groups. The mean and standard deviation decreased with depth, and the standard deviation was smaller than the mean. The highest maximum speeds were seen at the upper two meters of mooring T. They exceeded 100 $cm \cdot s^{-1}$ and likely were in response to LCE activity.

General description of records. Except at mooring T, which was under the influence of a strong cyclone, current speeds and variability generally were small from June to early August 1985 in the western Gulf. Examination of the time series of unfiltered u- and v-

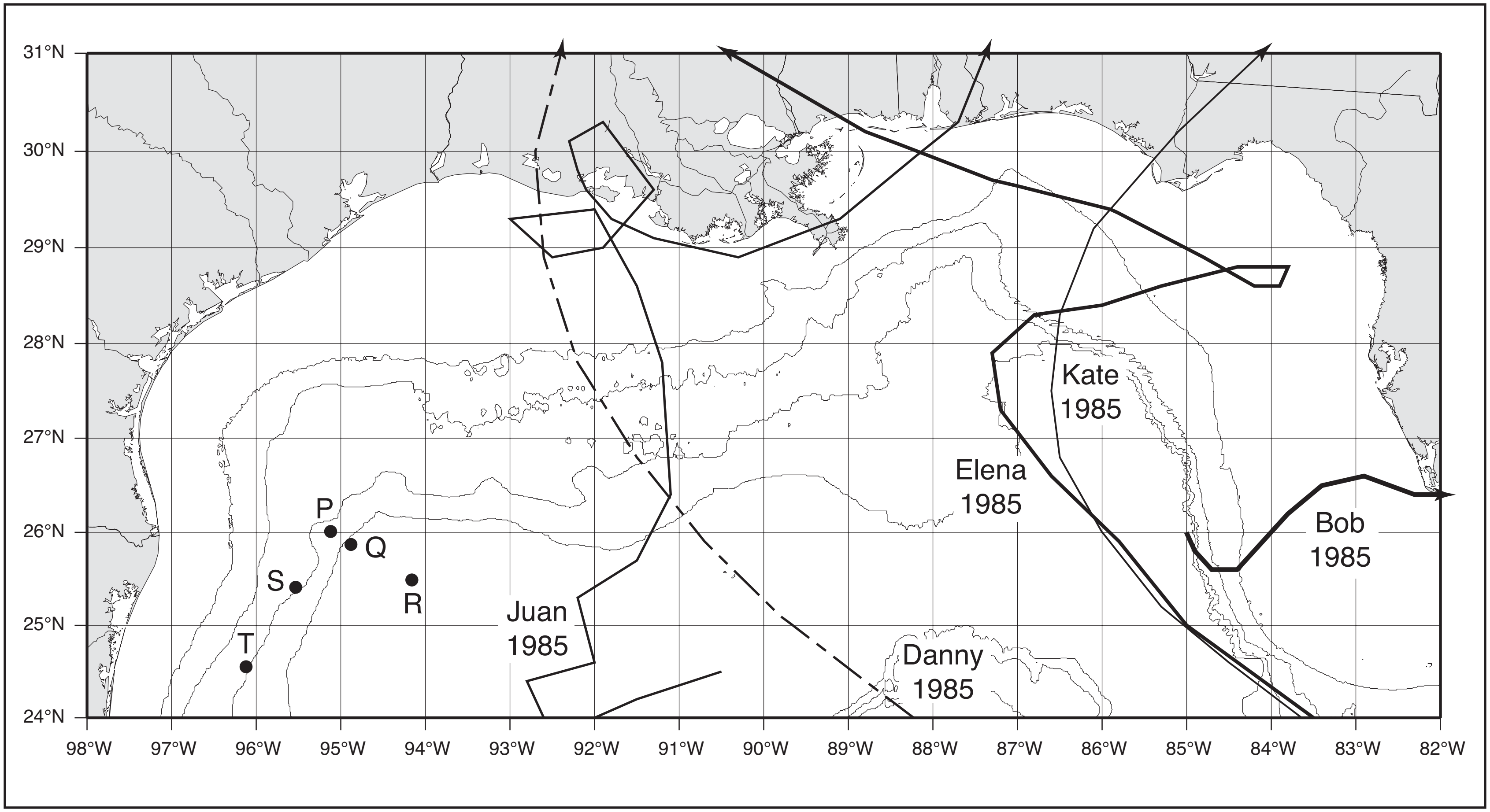

Figure 6.3.3-4. Location map for the western Gulf SAIC 5-year moorings in water depths greater than 200 m. The tracks of tropical storms and hurricanes in the Gulf for the deployment period are shown. Shown are the 200-, 1000-, 2000-, and 3000-m isobaths.

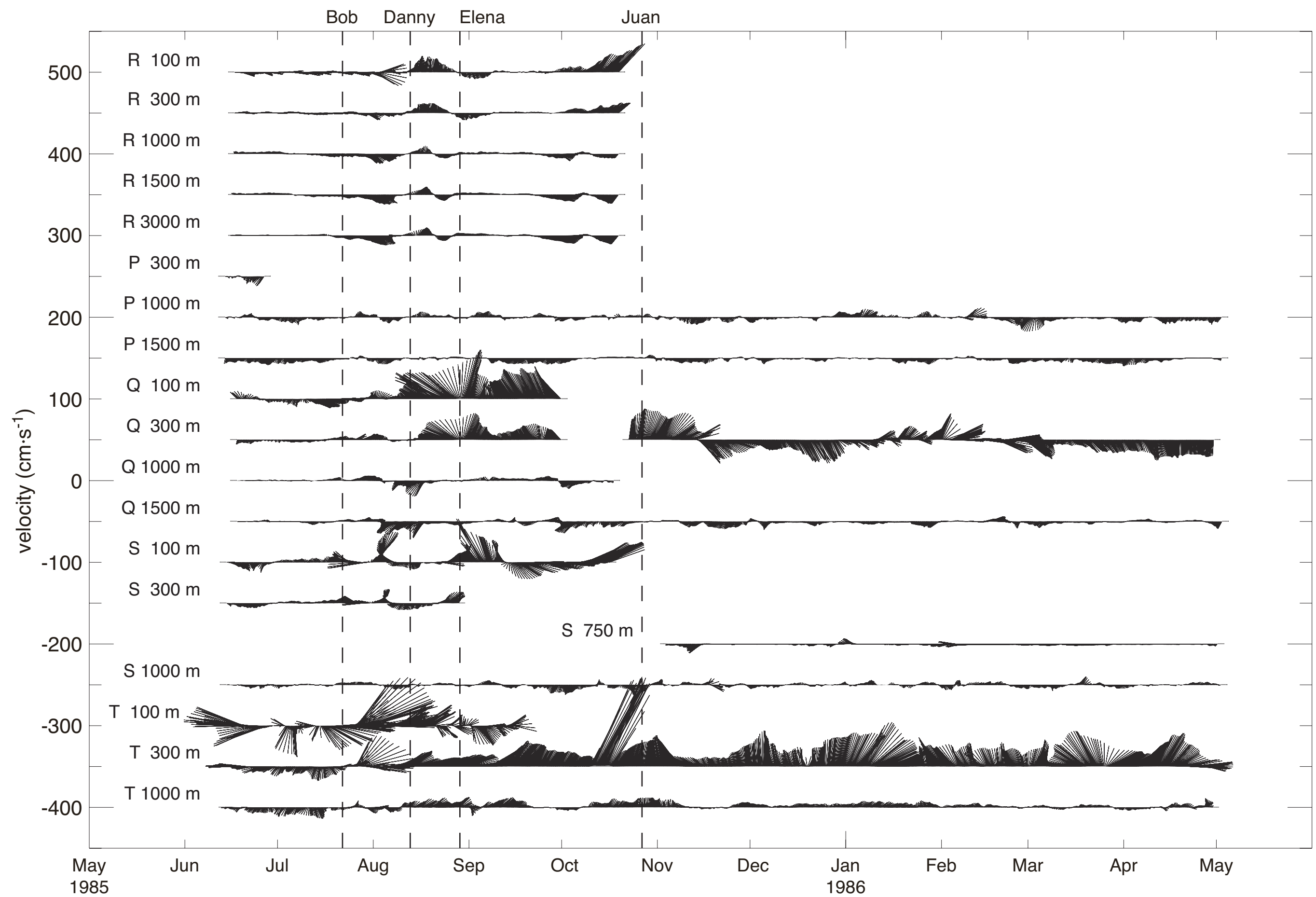

Figure 6.3.3-5. Time lines and vector stick plots for the western Gulf SAIC 5-year moorings in water depths greater than 200 m. The first day of tracking for tropical storms and hurricanes in the Gulf during the deployment period is indicated by the vertical dashed line with the storm name given above it. North is upward. Tick marks denote start of the month.

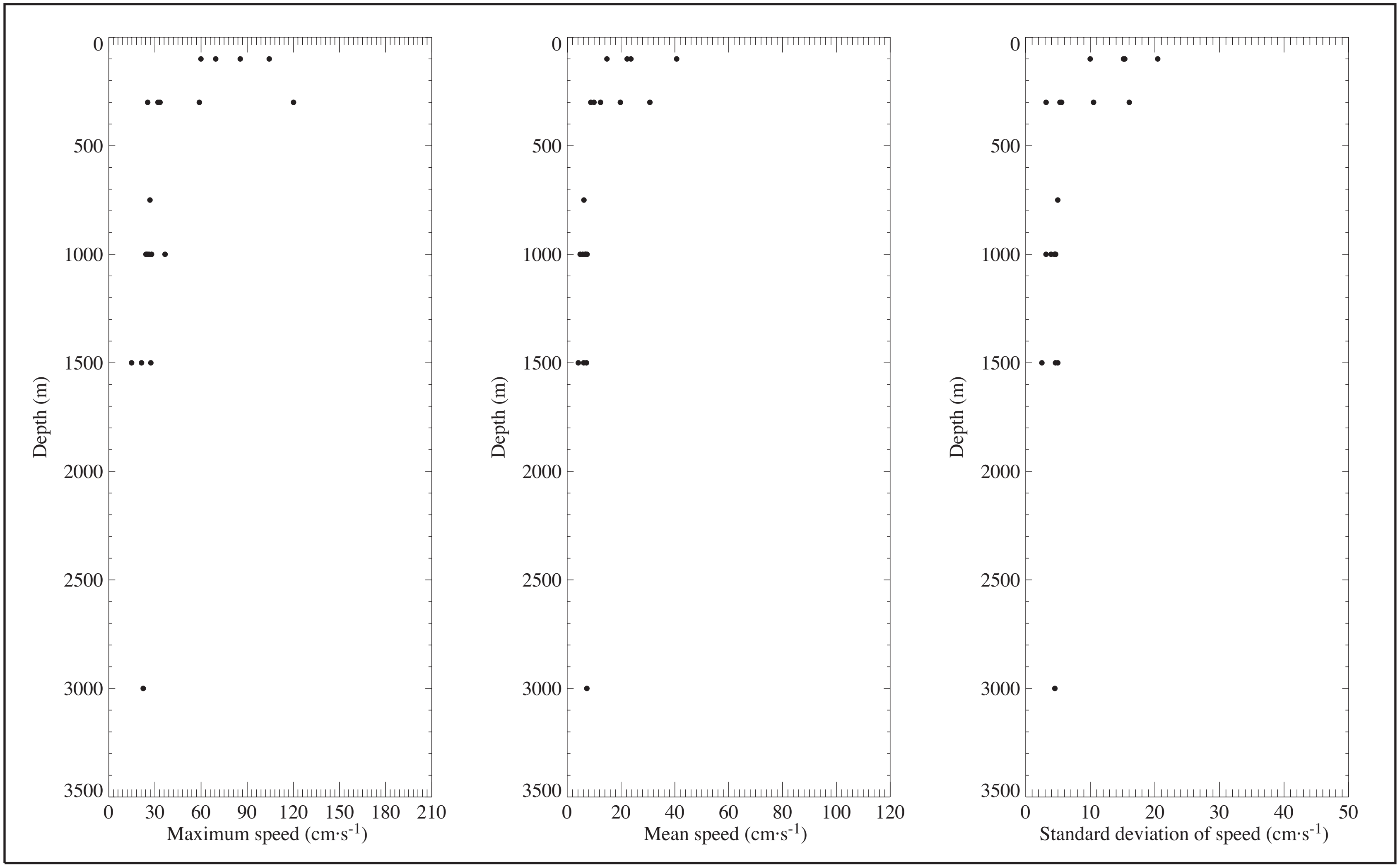

Figure 6.3.3-6. Observed speed (a) maximum, (b) mean, and (c) standard deviation versus instrument depth for unfiltered records from SAIC 5-year western Gulf moorings (npts = 19). Quality codes: A or B (dot), C (square), D (plus).

Table 6.3.3-2. Record-length mean, standard deviation, and maximum speed for data from the western Gulf in the SAIC 1983-1988 five-year physical oceanography study. Instruments were current meters.

Mooring	Instrument Depth (m)	Mean Speed ($cm{\cdot}s^{-1}$)	Standard Deviation ($cm{\cdot}s^{-1}$)	Maximum Speed ($cm{\cdot}s^{-1}$)
P	300	12.4	3.2	25.3
	1000	6.8	4.6	36.6
	1500	4.1	2.5	14.9
Q	100	23.7	15.3	85.5
	300	19.8	10.5	58.9
	1000	5.8	4.5	25.0
	1500	6.1	5.0	27.4
R	100	14.8	10.0	59.9
	300	9.9	5.3	33.3
	1000	6.7	3.9	24.2
	1500	7.1	4.6	21.3
	3000	7.3	4.5	22.4
S	100	22.3	15.2	69.5
	300	8.8	5.6	32.0
	750	6.2	5.0	26.8
	1000	4.8	3.2	27.8
T	100	40.7	20.4	104.4
	300	30.7	16.0	120.1
	1000	7.4	4.5	26.1

components of velocity for this period reveals information about inertial oscillations. Currents at 100 and 300 m on mooring Q exhibited inertial oscillations with amplitudes of 10-20 $cm{\cdot}s^{-1}$. Smaller amplitude oscillations of 5-10 $cm{\cdot}s^{-1}$ were observed at 1000 m; inertial oscillations were not discernable at 1500 m. Mooring R also exhibited inertial motions during June and July as well as intermittently to the end of the record. In general, 1000-m currents had much different character (spectra, amplitude, direction) than the upper layer currents at 100 and 300 m, which were highly coherent and surface-intensified.

Strong northward currents at mooring R in mid-August 1985 coincided with Hurricane Danny which passed to the east of the mooring; the storm was centered at about 92.5°W at closest passage to the mooring. Otherwise the hurricanes and tropical storms, which were located well to the east of the moorings, did not appear to affect the currents in the western Gulf.

During June to September 1985, mooring T was influenced by a strong cyclone located to the west of Fast Eddy as that LCE moved into the western Gulf. The cyclone center fluctuated about 24.5°N 96°W. An older anticyclonic eddy, Ghost Eddy, was located to the south of the cyclone. Currents at 300 m were generally southward when the western limb of the cyclone was located in the vicinity of the mooring and northeastward in association with the southern limb of the cyclone. From September through November, mooring T was variously under the eastern limb of the cyclone, the western limb of Fast Eddy, and the northwestern limb of

Ghost Eddy. The resulting currents were directed northward. From December to the end of the record in April 1986, mooring T was generally located under the western limb of Fast Eddy; currents were directed northward. As Fast Eddy decayed, the current speeds diminished. During most of the deployment period, the current speeds at 1000 m on mooring T are much smaller, but show coherence with the currents at 300-m.

The record at mooring Q also shows the effects of the eddies present in the western Gulf during the deployment period. During August 1985, currents speeds at 100 m on mooring Q increased to a peak of 65 $cm{\cdot}s^{-1}$ to the northwest and rotated clockwise to the north. These strong currents were not associated with Hurricane Elena, which passed through the far eastern Gulf at that time, but rather with the influence of a cyclonic eddy located to the west of the LCE Fast Eddy. From mid-August to October, mooring Q was in the vicinity of the eastern limb of the cyclone, which induced the northward and rotating currents seen at 300-m depth. There is a one-month data gap in the 300-m record which coincides with the arrival time of Fast Eddy in the vicinity of the mooring location. When measurements continued in late October, the western limb of the eddy was over mooring Q and directing persistent currents at 300 m to the north with a 40-50 $cm{\cdot}s^{-1}$ amplitude. From mid-November 1985 to February 1986, mooring Q was influenced by the eastern limb of the eddy, resulting in southward currents. Currents decreased in magnitude during the second week in January 1986, with magnitudes between 10-20 $cm{\cdot}s^{-1}$. Subsequently, the predominant current direction was eastward with north-south oscillations having periods of 7-10 days. This likely was due to the varying influence of Fast Eddy and a cyclone to its north as they moved back and forth over the mooring. From early March currents were persistently toward the south until the end of the record in April 1986, reflecting the mooring location in the western limb of the cyclone at that time.

Currents at 1500 m on Q were weak and not strongly coherent with those at 300 m. A bottom event is seen at Q just prior to arrival of the cyclone preceding Fast Eddy in August 1985 with speeds of 20-25 $cm{\cdot}s^{-1}$ directed to the southwest. Currents also changed direction about 1 October 1985; this coincided with the movement of the western cyclone out of the mooring vicinity and the arrival of Fast Eddy. There was another direction change about 15 November, presumably when the center of the eddy passed nearest to mooring Q. Deep currents at Q (1000- and 1500-m) in general were not correlated with currents above 1000 m, but showed high coherence with each other.

At mooring S, upper currents during late August and early September were variable with current speeds increasing to 60 $cm{\cdot}s^{-1}$ (40-hr low-passed; 70 $cm{\cdot}s^{-1}$, raw) and oriented to the northwest. They rotated counterclockwise during September and into October 1985 (when the record ends). These currents were related to the strong cyclone that passed over the moorings and was situated between Fast Eddy (freshly broken off the LC) and Ghost Eddy in the southwestern Gulf.

Currents at mooring R were barotropic from mid-July through mid-September 1985, with instruments at all depths (100 to 3000 m) showing similar changes in direction and speeds. There is some subsurface intensification between 300 and 3000 m. This was followed by a baroclinic, two-layer event from mid-September through late October, where the upper layer (100 to 300 m) currents were northward and the lower layer (1000 to 3000 m) currents were southward. In early August 1985, there was evidence at 1000 m of an anticyclonic circulation with southward currents at R, northward at S, northeastward at P, and east-northeastward at Q.

Mooring P showed weak coherence between 1000 and 1500 m. The two-week record at 300 m was dominated by inertial oscillations and internal waves of very high frequency during mid-June 1985.

6.3.3.3 Central Gulf Moorings, 1987-1988

Basic description of data set. The central moorings consisted of three moorings, EE, FF, and GG, located along 92°W across the central Texas-Louisiana slope; locations are shown in Figure 6.3.3-7. The deployments were from April 1987 through November 1988. Total water depths were 825 m (EE), 1750 m (FF), 2500 m (GG). Instrument depths are given in Table 6.3.3-3. Time lines and vector stick plots are shown in Figure 6.3.3-8. The quality codes for these data are A, B, and C. File names for the current records in the database are

- EE: GB870405.C03-C05; GB871108.C01-C02; GB871202.C01
- FF: KC870406.C01-C04; KC871108.C01-C03; KC871109.C01; KC880414.C01
- GG: AB870406.C01-C03; AB871109.C01-C03; AB871110.C01; AB880409.C01-C02.

Environmental background. During these deployments, tropical storm #1 (9–17 August 1987), hurricane Floyd (9–14 October 1987), tropical storm Beryl (8–10 August 1988), tropical storm Keith (17–26 November 1988), and hurricanes Debby (31 August–8 September 1988), Florence, (7–11 September 1988), and Gilbert (8–20 September 1988) passed through the Gulf. The cyclones passing closest to the moorings were tropical storm #1, which passed to the west, and hurricane Florence, which passed to the east (Figure 6.3.3-7). Only the bottom instruments were operating during tropical storm #1 and hurricane Floyd (Figure 6.3.3-8).

During the deployment, LCE separations occurred in September 1987 and May 1988 (Sturges and Leben 2000). EddyWatch charts and GEOSAT SSHA indicate these were Eddy Kathleen and Eddy Murphy, respectively (named E and F in SAIC 1989, Hamilton 1990, and Berger et al. 1996a). Both eddies prominently affected the records. In October 1986, GEOSAT SSHA maps showed the separation of an LCE called eddy D or Krazy Eddy (Hamilton 1990; Berger et al. 1996a, 1996b). This eddy was transiting the central Gulf from mid-December 1986 through April 1987; but only the near-bottom instruments on the moorings produced data during that time. A number of slope cyclonic eddies passed through the central Gulf at the time of the deployments (Hamilton 1992).

Basic statistics. Record-length mean, standard deviation, and maximum speeds for the moorings are shown in Table 6.3.3-3. Figure 6.3.3-9 shows the statistics versus depth for all instrument depths. Mean currents and standard deviations decreased with increasing depth. Standard deviations were less than associated means. At common depths, the mean currents increased with increasing distance offshore. The maximum speed at the top meter of mooring GG exceeded 100 $cm{\cdot}s^{-1}$.

General description of records. A total of 14 current meters were deployed at the beginning of April 1987 at three mooring locations (EE, FF, and GG). Of these, only three instruments produced valid data for the entire deployment period ending in November 1987, seven produced data for approximately 1 week, and four instruments failed completely. The three working instruments were located at 725 m on EE, at 1650 m on FF, and at 1650 m on GG. These instruments are generally below depths directly influenced by wind forcing and LCEs as well. The 40-hr low-passed records showed variable current with 5-10 day periods and

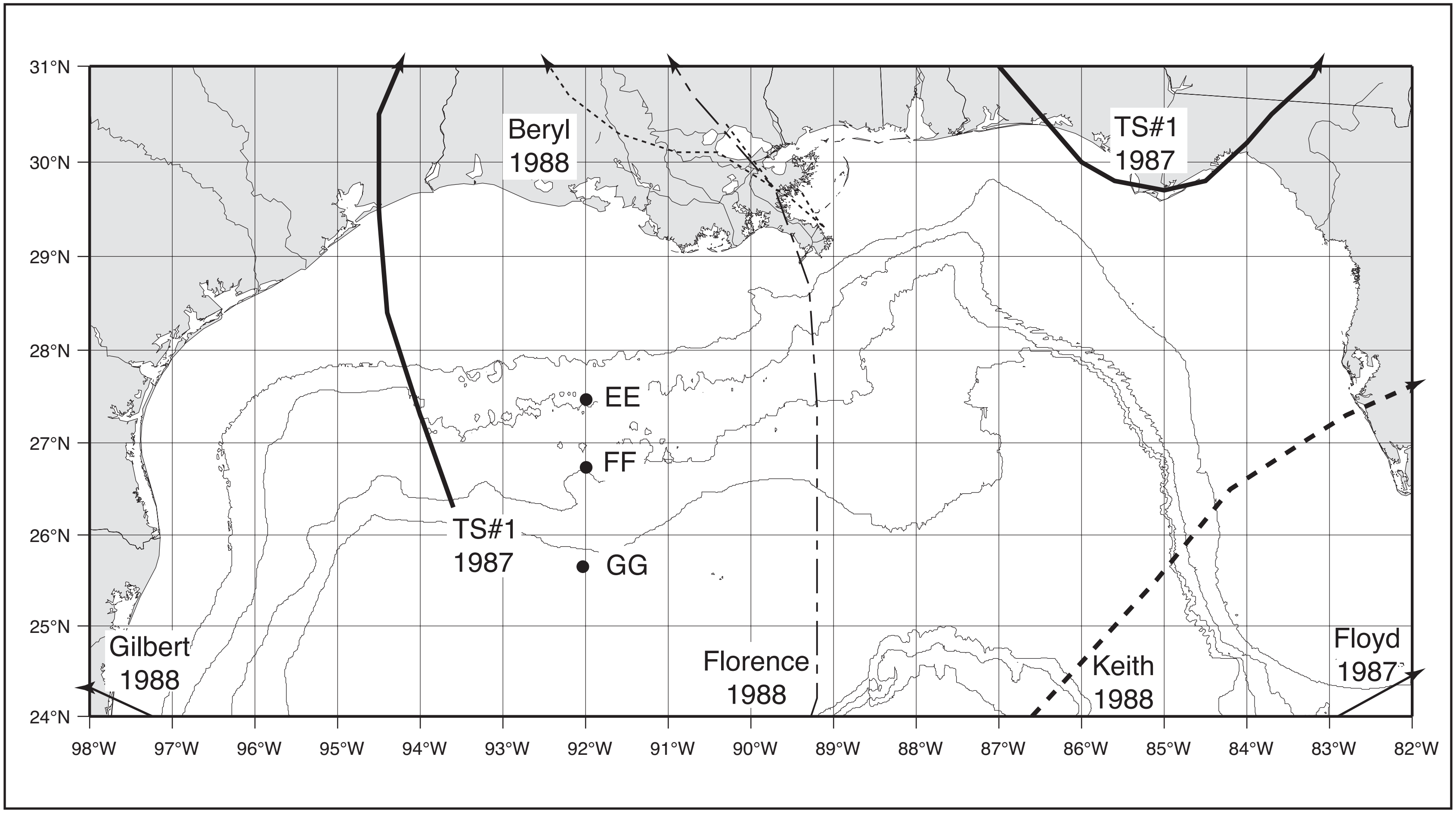

Figure 6.3.3-7. Location map for the central Gulf SAIC 5-year moorings in water depths greater than 200 m. The tracks of tropical storms and hurricanes in the Gulf for the deployment period are shown. Shown are the 200-, 1000-, 2000-, and 3000-m isobaths.

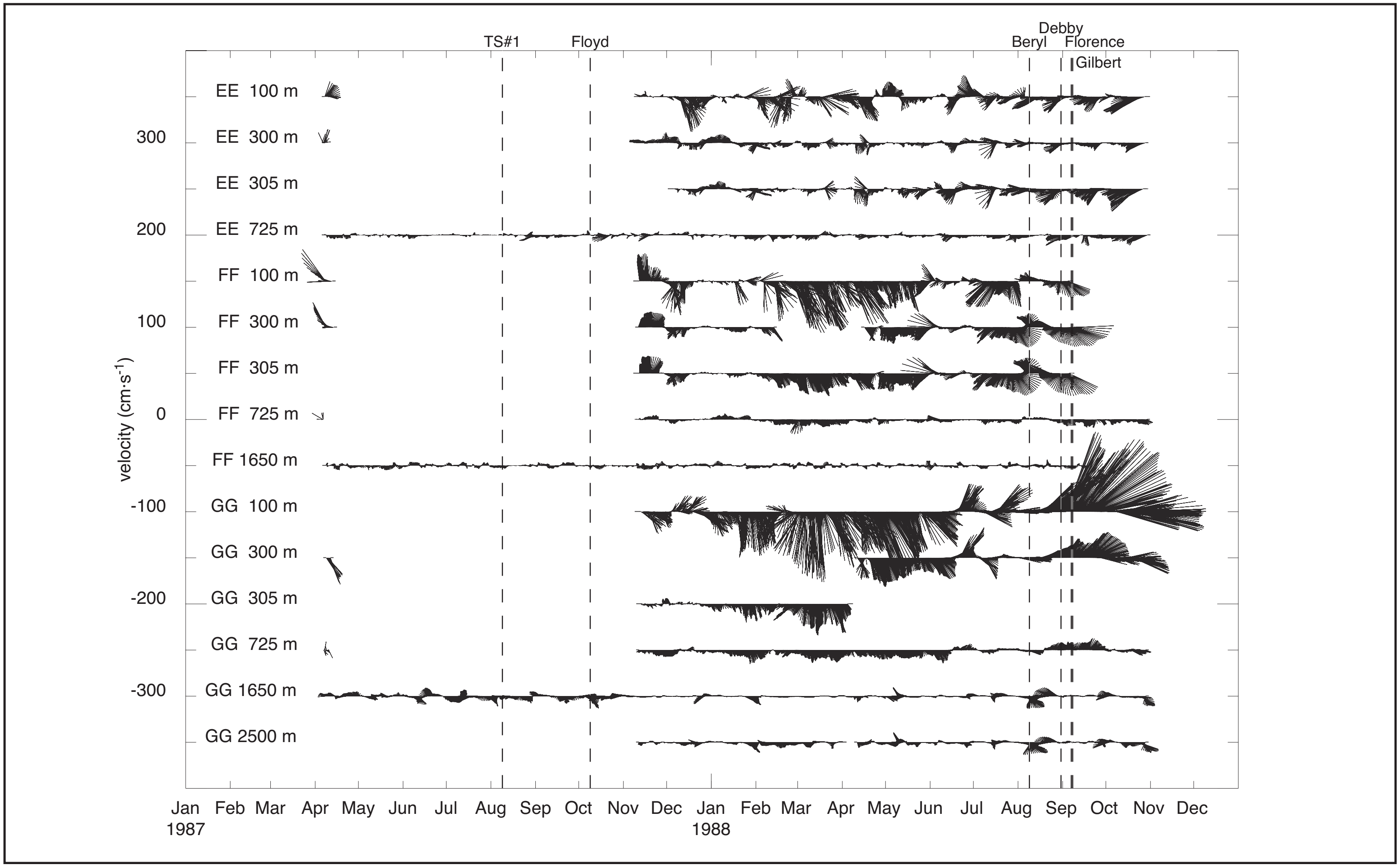

Figure 6.3.3-8. Time lines and vector stick plots for the central Gulf SAIC 5-year moorings in water depths greater than 200 m. The first day of tracking for tropical storms and hurricanes in the Gulf during the deployment period is indicated by the vertical dashed line with the storm name given above it. North is upward. Tick marks denote start of the month.

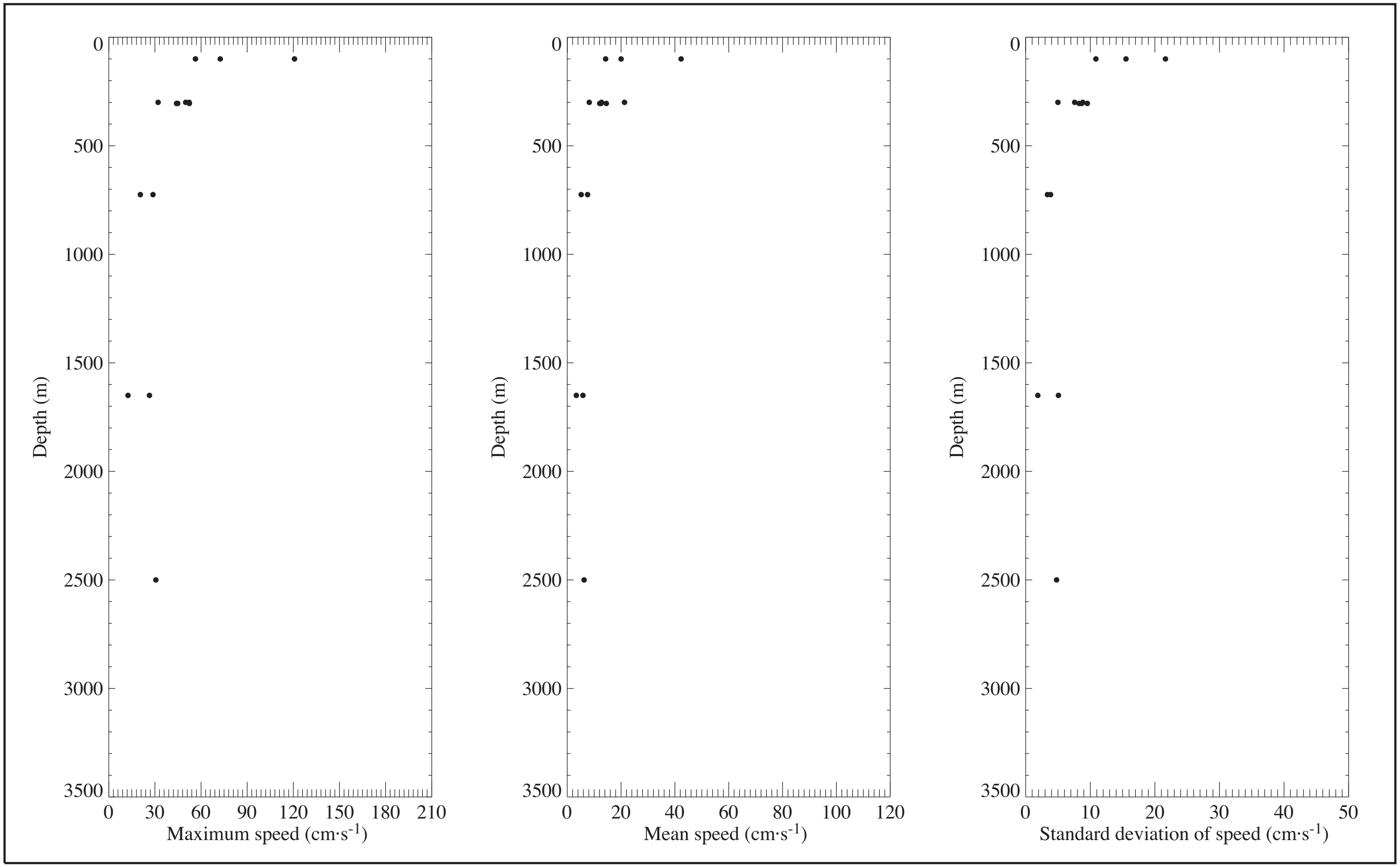

Figure 6.3.3-9. Observed speed (a) maximum, (b) mean, and (c) standard deviation versus instrument depth for unfiltered records from SAIC 5-year central Gulf moorings (npts = 15). Quality codes: A or B (dot), C (square), D (plus).

Table 6.3.3-3. Record-length mean, standard deviation, and maximum speed for data from the central Gulf in the SAIC 1983-1988 five-year physical oceanography study. Instruments were current meters.

Mooring	Instrument Depth (m)	Mean Speed ($cm \cdot s^{-1}$)	Standard Deviation ($cm \cdot s^{-1}$)	Maximum Speed ($cm \cdot s^{-1}$)
EE	100	14.3	10.9	56.4
	300	8.2	5.0	32.1
	305	12.6	8.3	44.1
	725	5.2	4.6	31.9
FF	100	20.0	15.5	72.5
	300	12.7	7.6	52.3
	305	14.5	8.7	52.4
	725	5.2	3.4	20.5
	1650	3.4	1.9	12.5
GG	100	42.3	21.6	120.8
	300	21.3	8.8	50.0
	305	12.1	9.5	44.8
	725	7.6	3.9	28.8
	1650	5.8	5.1	26.5
	2500	6.3	4.8	30.6

small amplitudes (about 5 $cm \cdot s^{-1}$). The record at 1650 m on GG was slightly more energetic than the other two with amplitudes in the range of 5-10 $cm \cdot s^{-1}$.

All 15 instruments deployed in November 1987 returned good data for the deployment period ending in November 1988. In late January 1988 a small diameter anticyclonic eddy strengthened to the west of moorings FF and GG. South and southwestward currents persisted until mid-March when Eddy Kathleen migrated westward and coalesced with the small eddy. Eddy Kathleen then moved south and west of the moorings. Currents at the 100-m instrument on GG remained steady toward the south and strong, with speeds of 75 $cm \cdot s^{-1}$, until June and then rapidly diminished in amplitude and turned counterclockwise to the east. In mid-May, a powerful cyclone moved into the region from the east as Eddy Kathleen moved west past mooring GG. By July, mooring GG was between the cyclone-anticyclone pair which produced two large amplitude north-south oscillations of about 30 $cm \cdot s^{-1}$ and 15-day period at 100 m. At FF the currents were southwestward and turned cyclonically to the south, east, north, and northwest, before turning anticyclonically back to the south just prior to the arrival of Eddy Murphy.

By late August 1988, only mooring GG was recording data. In September 1988, Eddy Murphy produced strong (80-90 $cm \cdot s^{-1}$ at 100 m, 30-40 $cm \cdot s^{-1}$ at 300 m, and 10-20 $cm \cdot s^{-1}$ at 725 m) north-eastward currents. By late October, Eddy Murphy was south of GG and currents there were strong and steady to the east with speeds of 70-80 $cm \cdot s^{-1}$ at 100 m. Currents decreased with depth with no indication of the energetic surface motions at the 1650- and 2500-m levels.

Currents at the upper slope mooring FF were more variable and did not show the persistently strong currents present at the other two locations. This was probably due in part to the broadness of the Texas-Louisiana slope at 92°W. The bathymetry here seems to steer eddies to the south, away from the shelf. The slope narrows again west of 93°W, and the region between 25°N and 28°N, 94°W and 96°W is sometimes referred to as the eddy graveyard because old eddies are frequently found in that area. This was confirmed by the LATEX A data set, where instruments along the 200-m isobath at the edge of the Texas-Louisiana shelf showed much less mesoscale (eddy forced, low frequency) energy between 92°W and 93°W than further to the west (Nowlin et al. 1998a, 1998b).

Other events of note include: a 3-week period from mid-December 1987 to mid-January 1988 of low speed currents at all depths on mooring FF. During this period SSHA maps showed virtually no SSHA gradient. In general, currents below 1000 m at the same mooring were coherent with depth and generally independent of surface motions. Energetic bottom events at GG occurred approximately 1-3 months after the reported eddy separation dates. Given that eddy separation dates can be subjective, the proximity of these events to the separations is under further study to determine if there is a causal relation. These may be related to the topographic Rossby wave propagation mechanism discussed by Hamilton (1990). There were three events of bottom-intensified barotropic current at GG during January, May, and August 1988. The May event, in particular, had no surface expression or variability during the time of the event. At FF, there also were two subsurface-intensified events where the 300-m currents were stronger than those at 100 m: a short event at the beginning of June and a longer event from August 1988 through the end of the record in September 1988.

6.3.4 TAMU Northwest Gulf LATEX A Moorings, 1992-1994

Basic description of data set. Scientists at Texas A&M University (TAMU) collected current meter data at the 500-m isobath as part of the Texas-Louisiana Shelf Circulation and Transport Processes Study of the Louisiana-Texas Shelf Physical Oceanography Program (LATEX A) sponsored by the MMS. Data were obtained from TAMU. DiMarco and Reid (1998) present the tidal currents associated with these and the other LATEX data. Cho et al. (1998) describe the horizontally nondivergent part of the near-surface, shelf-wide scale, low-frequency circulation from the LATEX moorings. Nowlin et al. (1998a) discuss the low-frequency currents at all measured depths, together with possible causation, for the LATEX current measurements. The two moorings deployed off the shelf were M12 and M49; they were deployed at 90.5°W and 95.9°W, respectively. None of the shelf moorings are presented here. Locations are shown in Figure 6.3.4-1 (note mooring 13, which is in water depth less than 200 m, is also shown because it is discussed in section 6.1.2). Each mooring consisted of three instruments which recorded current velocity, temperature, and salinity. Instrument depths are given in Table 6.3.4-1. The deployment period for M12 was April 1992 to December 1993; that for M49 was April 1992 through December 1994. Time lines and vector stick plots are shown in Figure 6.3.4-2. The quality codes for these data are A, B, and C. File names for the current records in the database are

- M12: GC920415.C01; GC930112.C01; GC920415.C02; GC930112.C02; GC920415.C03; GC930112.T01; GC921022.C01; GC930718.C01; GC921023.C01; GC930718.C02; GC921023.C02; GC930718.T01

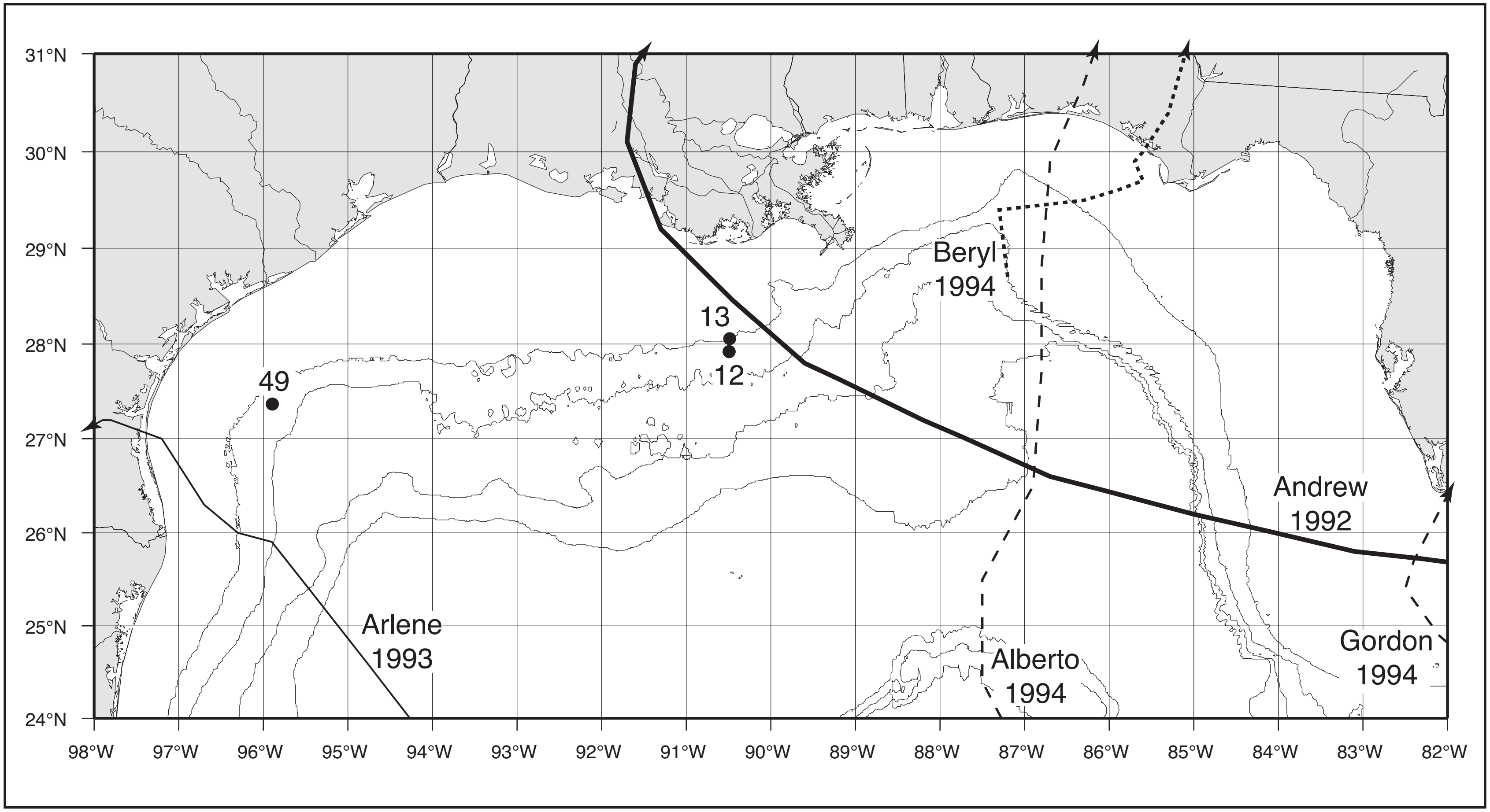

Figure 6.3.4-1. Location map for the TAMU LATEX A northwestern Gulf moorings in water depths greater than 200 m. The tracks of tropical storms and hurricanes in the Gulf for the deployment period are shown. Shown are the 200-, 1000-, 2000-, and 3000-m isobaths.

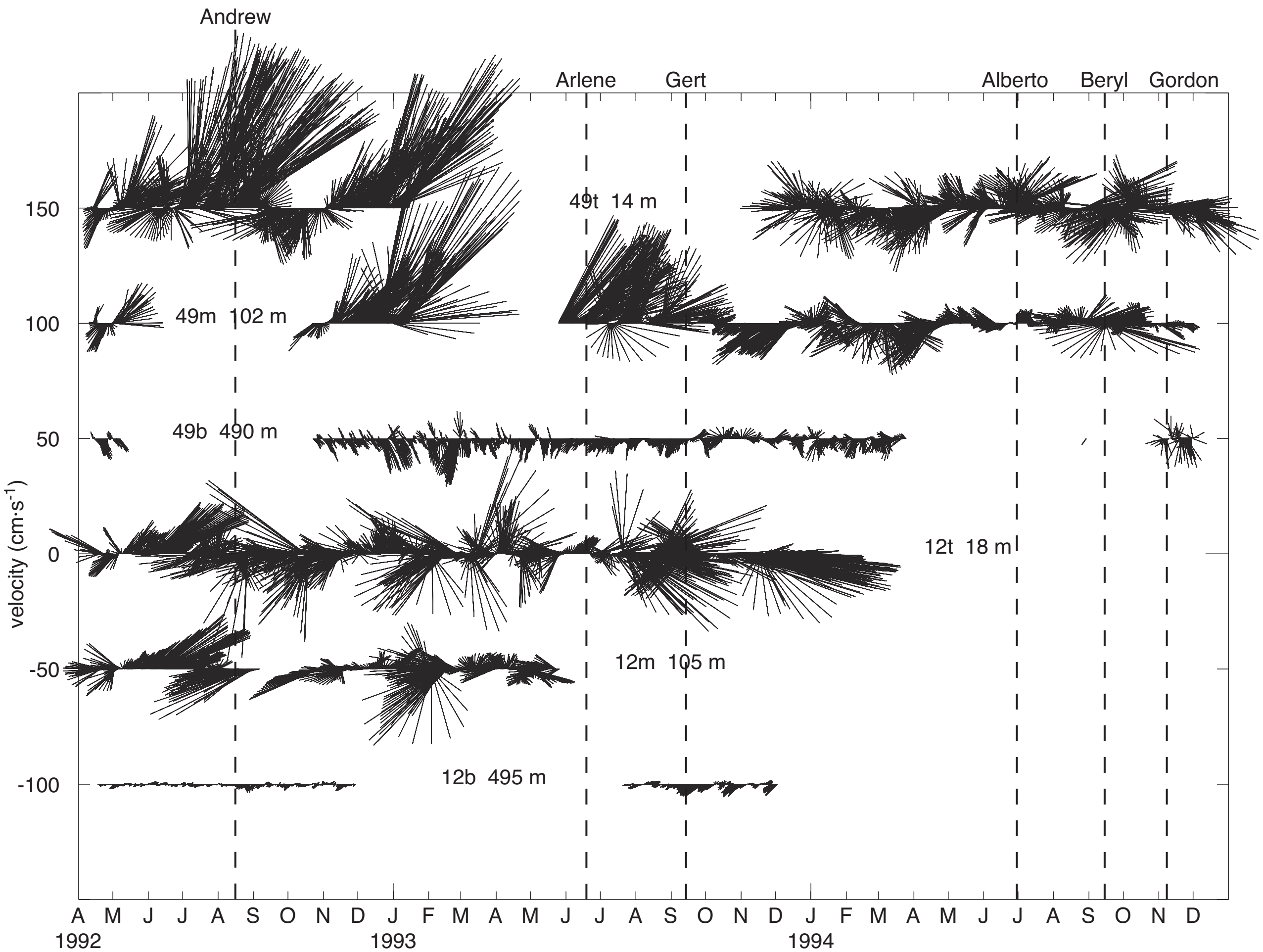

Figure 6.3.4-2. Time lines and vector stick plots for the TAMU LATEX A northwestern Gulf moorings in water depths greater than 200 m. The first day of tracking for tropical storms and hurricanes in the Gulf during the deployment period is indicated by the vertical dashed line with the storm name given above it. North is upward. Tick marks denote start of the month.

Table 6.3.4-1. Record-length mean, standard deviation, and maximum speed for data from the northwestern Gulf in the TAMU 1992-1993 LATEX A study. Instruments were current meters.

Mooring	Instrument Depth (m)	Mean Speed ($cm{\cdot}s^{-1}$)	Standard Deviation ($cm{\cdot}s^{-1}$)	Maximum Speed ($cm{\cdot}s^{-1}$)
M12	15	18.9	14.0	138.7
	100	13.8	9.8	69.7
	495	2.7	1.5	10.0
M49	15	24.0	17.7	100.0
	100	15.9	14.1	87.4
	495	5.4	3.8	27.5

- M49: EB920409.C01; EB930119.C01; EB931212.C03; EB920409.C02; EB930520.C01; EB940330.C01; EB920409.C03; EB930520.C02; EB940330.C02; EB921018.C01; EB930520.T01; EB940730.C01; EB921018.C02; EB931212.C01; EB940730.C02; EB921018.C03; EB931212.C02; EB940730.C03.

Environmental background. During the period April 1992 through December 1994, a total of six tropical cyclones passed through the Gulf of Mexico: hurricanes Andrew (16–2 August 1992), Gert (14–21 September 1993), and Gordon (8–12 November 1994), and tropical storms Arlene (18–21 June 1993), Alberto (30 June–7 July 1994), and Beryl (14–19 August 1994). Hurricane Andrew passed near M12 (Figure 6.3.4-1).

There were a total of four LCE separations during the deployment period (Sturges and Leben 2000). These were Eddy Unchained (July 1992), Eddy Whopper (June 1993), Xtra Eddy (September 1993), and Eddy Yucatan (September 1994). Two additional LCEs were in the northwestern Gulf during the deployment period: Eddy Triton and Eddy Vazquez. These eddies are described in Berger et al. (1996a, 1996b), Biggs et al. (1996), Hamilton et al. (1999), and Nowlin et al. (1998a, 1998b).

Basic statistics. Record-length mean, standard deviation, and maximum speeds for the moorings are shown in Table 6.3.4-1. Figure 6.3.4-3 shows the statistics versus depth for all instrument depths. Mean speeds and standard deviations decreased with depth and standard deviations were less than associated means. Maximum near-surface and 100-m current speeds at M12 were recorded at the time of the passage of Hurricane Andrew. Those at M49 were associated with a nearby LCE.

General description of records.
Mooring 12: From the SSHA maps of May-June 1992, an anticyclonic slope eddy moved over and past the mooring location. That slope eddy may have been influenced by Eddy Unchained which was about to separate from the Loop Current (in July 1992). Maximum

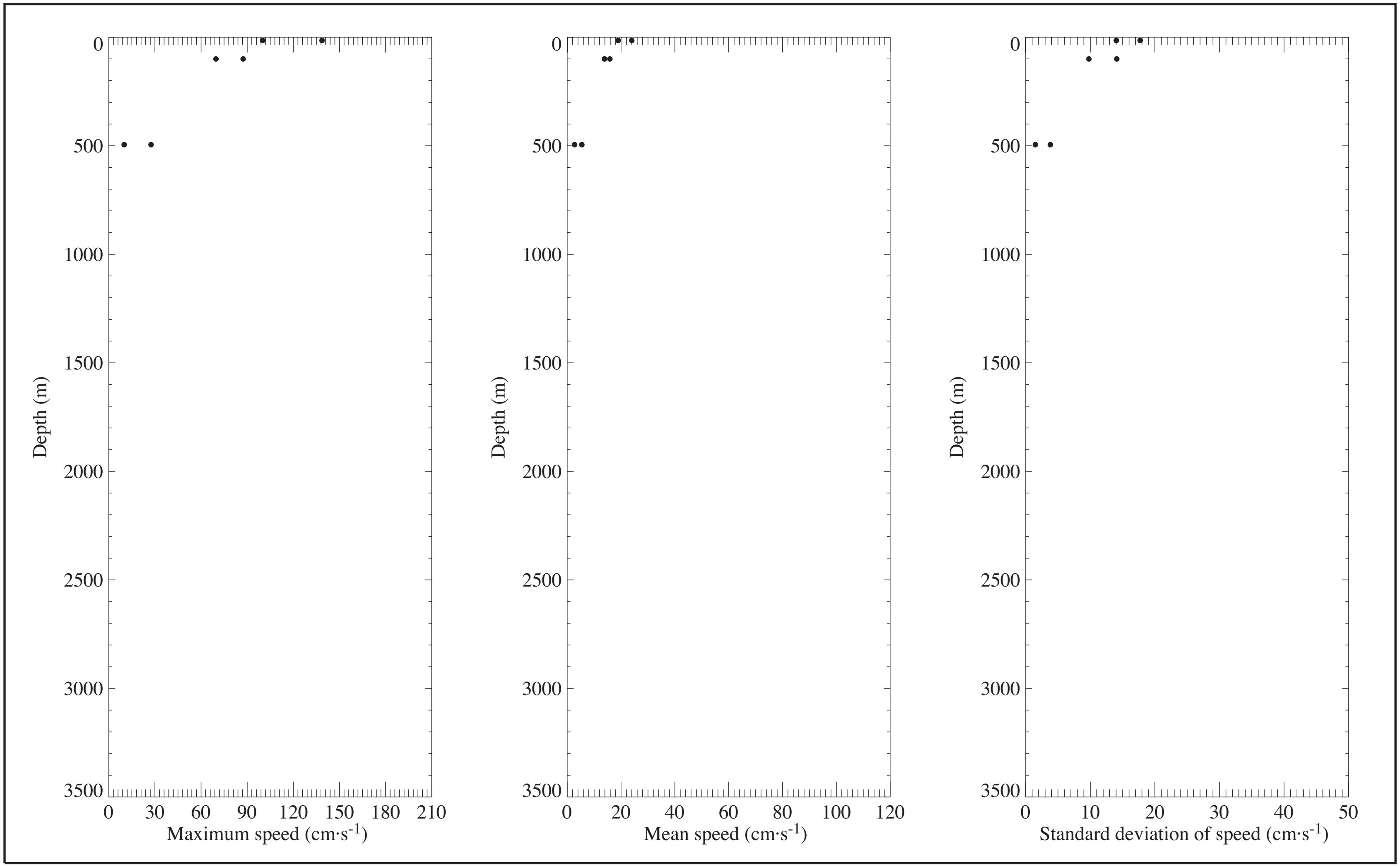

Figure 6.3.4-3. Observed speed (a) maximum, (b) mean, and (c) standard deviation versus instrument depth for unfiltered records from TAMU LATEX A northwestern Gulf moorings (npts = 6). Quality codes: A or B (dot), C (square), D (plus).

surface speeds during period were of order 25 $cm \cdot s^{-1}$. The near-surface and mid-water currents were coherent and with very little attenuation with depth.

In late August 1992, Hurricane Andrew passed less than 50 km to the north of this location. Maximum 3-hr low-passed current speeds during this passage reached 105, 62, and 5 $cm \cdot s^{-1}$ at the top, middle, and bottom instruments. The maximum current speeds were then followed by strong inertial oscillations near-surface and at 100 m. Near-bottom there was approximately a 24-hour delay between maximum surface currents and maximum near-bottom currents. The effects of this storm on the general circulation of the Texas-Louisiana shelf are given in Nowlin et al. (1998b).

From September 1992 through January 1993, a weak cold core (cyclonic) eddy influenced the mooring and produced variable, mostly westward currents.

During 12–14 March 1993, a strong winter cyclone generated over the northwestern Gulf and moved eastward, passing the mooring location before turning northeastward. The size and strength of this storm, which swept the eastern seaboard burying it in a blanket of snow, caused it to be known at the time as the 'Storm of the Century'. Maximum near-surface speeds during the storm reached 48 $cm \cdot s^{-1}$ with 100-m speeds of 20.5 $cm \cdot s^{-1}$. No bottom speeds were reported. The circulation effects of this storm are also given in Nowlin et al. (1998b).

During April 1993, the eastern and northern limb of an anticyclonic slope eddy moved past the mooring. The effects of this eddy are clear in the data as currents turn clockwise from northward to southeastward. From late April to June 1993, currents in this region were weak speeds of 10-15 $cm \cdot s^{-1}$ and predominately eastward.
In late July and early August 1993, the newly separated LCE Eddy Whopper moved westward to the south of the mooring. It produced southeastward currents at the mooring with maximum speeds of 73 $cm \cdot s^{-1}$ and average near-surface speeds of 35-40 $cm \cdot s^{-1}$. In November 1993, Xtra Eddy produced east-southeast currents with speeds of 45-55 $cm \cdot s^{-1}$ lasting 2-3 weeks. There were no 100 m currents available during this event. However, bottom currents were generally small (less than 5 $cm \cdot s^{-1}$) and directed to the southwest from July to December 1993.

In general, near-bottom currents were small during the entire deployment, even during the hurricane event, leading to speculation that local topographic features shielded this mooring from larger current activity.

Mooring 49: Data collected at mooring 49 were strikingly different from those collected at mooring 12. While mooring 12 was situated in a location where freshly separated LCEs could migrate past, mooring 49 was situated in a location to which old eddies are known to migrate and spend considerable time—perhaps weeks in essentially the same location.

From June to early September 1992, the northwest limb of Eddy Triton directed currents at mooring 49 toward the north-northwest with mean speeds of about 60 $cm \cdot s^{-1}$ and peak speeds approaching 100 $cm \cdot s^{-1}$. These currents persisted for several weeks. No 100- or 490-m records were available during this period. The effect of Hurricane Andrew on the shelf circulation was to turn the shelf edge currents toward the west. However, the effect of Andrew on the already strong eastward currents at mooring 49 was to decrease the eastward component.

From mid-September to October 1992, currents at mooring 49 were in a calm period as the effects of Eddy Triton waned and another eddy, Eddy Vazquez, migrated into the region. Currents during this time were weak (~10 $cm{\cdot}s^{-1}$) and southward.

From November 1992 through January 1993, Eddy Vazquez caused currents to the northeast with speeds between 20-30 $cm{\cdot}s^{-1}$. The near-surface and 100-m currents were strongly coherent. The near-bottom currents were of very different character. This was probably due to the interaction of the eddies with the bottom and shoaling which tend to shear off the deeper parts of the eddy. No records were available from M49 during the March 1993 Storm of the Century. In June 1993, Eddy Vazquez was in the vicinity of mooring 49. It generated intense northward and north-northeastward currents at 100 m. From August through December 1993, currents were dominated by a weak cyclone producing southwestward currents of 20 $cm{\cdot}s^{-1}$. From January through December 1994, there were no major eddy impacts in this region, currents were variable and slow with average speeds of 10-20 $cm{\cdot}s^{-1}$. Spectra during this period show weekly periodicity with virtually no energy at periods longer than 10 days.

6.3.5 SAIC DeSoto Canyon Eddy Intrusion Study Moorings, 1997-1999

Basic description of data set. Science Applications International Corporation deployed an extensive current meter array as part of the MMS-sponsored DeSoto Canyon Eddy Intrusion Study (EIS). Data were obtained from SAIC. Of the 13 moorings arranged into four cross-slope lines, seven were located in water depths greater than 200 m. The moorings were deployed from March 1997 through April 1999. Each mooring included an upward looking ADCP at a depth of approximately 90 m. Mooring locations are shown in Figure 6.3.5-1. ADCPs were configured to measure current velocity in four meter bins between 8 and 80-m depth at half-hour intervals. Depending on water depth, one to three single point current meters were moored below the ADCP. The nominal depths of the single point current meters are given in Table 6.3.5-1. Time lines of the deployments and vector stick plots are shown in Figure 6.3.5-2. The quality codes for these data are A and B. File names for the current records in the database are

- A2: VK970320.A01-A19; VK970321.C01-C03; VK970710.A01-A18; VK970710.C01-C03; VK971113.A01-A18; VK97113.C01-C03; VK980402.A01-A33; VK990402.C01-C03; VK980806.A01-A19; VK980806.C01-C03; VK981213.A01-A18; VK981213.C01-C03
- A3: MC970320.A01-A20; MC970320.C01-C02;MC970710.A01-A18; MC970710.C01-C02; MC971113.A01-A18; MC97114.C01-C02; MC980402.A01-A18; MC980401.C01-C02; MC980806.A01-A17; MC980806.C01-C02; MC981203.A01-A17; MC981203.C01
- B2: VK970327.A01-A18; VK970328.C01; VK970328.C02; VK970328.C03; VK970712.A01-A18; VK970712.C01; VK970712.C02; VK970712.C03; VK971115.A01-A19; VK971115.C01; VK971115.C02; VK971115.C03; VK980404.A01; VK980404.C01; VK980404.C02; VK980404.C03; VK980807.A01-A19; VK980807.A19; VK980807.C01; VK980807.C02; VK980807.C03; VK981205.A01-A19; VK981205.C01; VK981205.C02; VK981205.C03
- B3: VK970322.A01-A16; VK970322.C01; VK970322.C02; VK970712.A19-A34; VK970712.C04; VK970822.C01; VK971115.A20-A36; VK971115.C04; VK971115.C05; VK980403.A01-A36; VK980403.C01; VK980403.C02; VK980807.A20-A36; VK980807.C04; VK980808.C01; VK981204.A01-A16; VK981204.C01

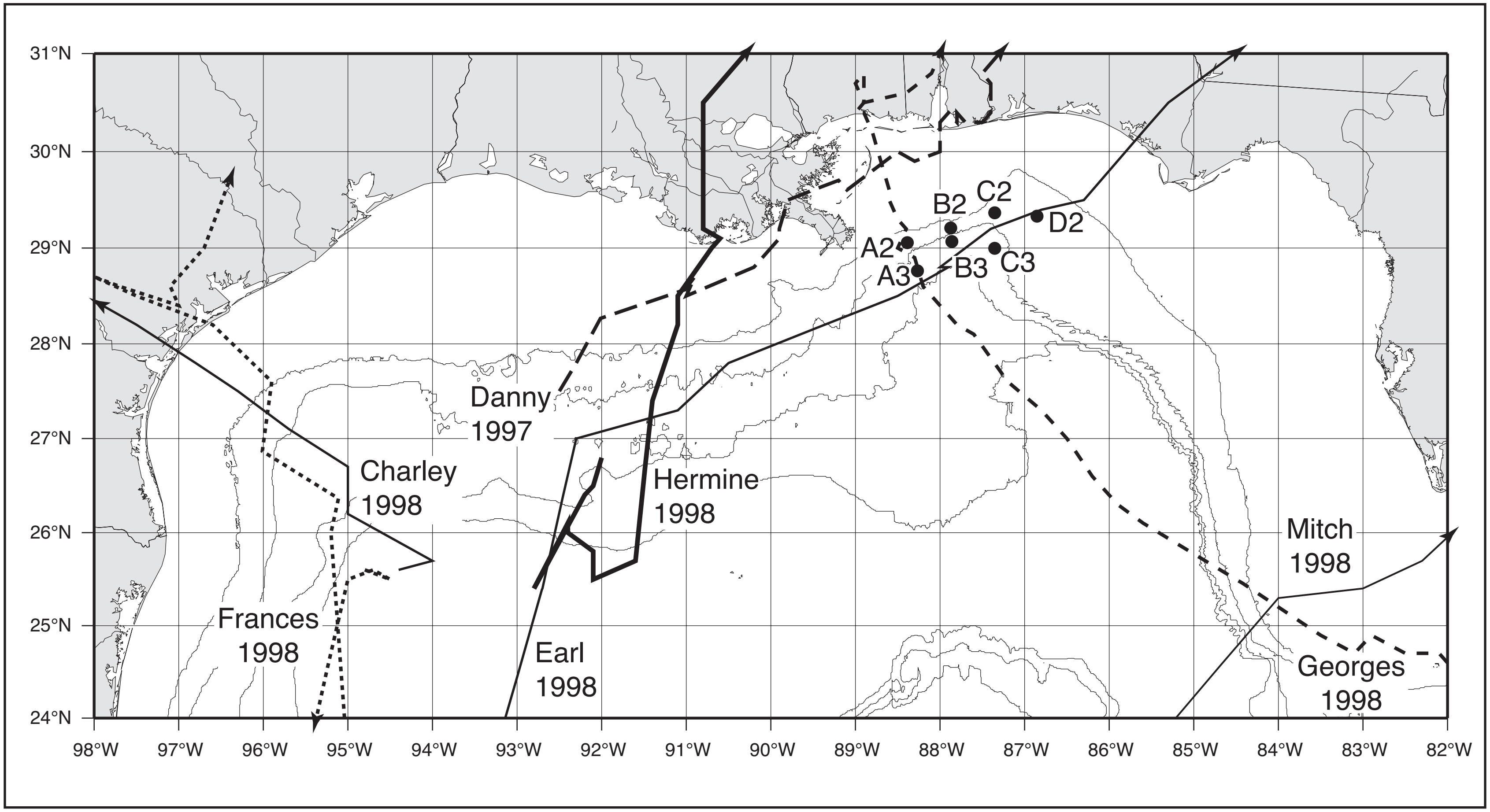

Figure 6.3.5-1. Location map for the SAIC DeSoto Canyon moorings in water depths greater than 200 m. The tracks of tropical storms and hurricanes in the Gulf for the deployment period are shown. Shown are the 200-, 1000-, 2000-, and 3000-m isobaths.

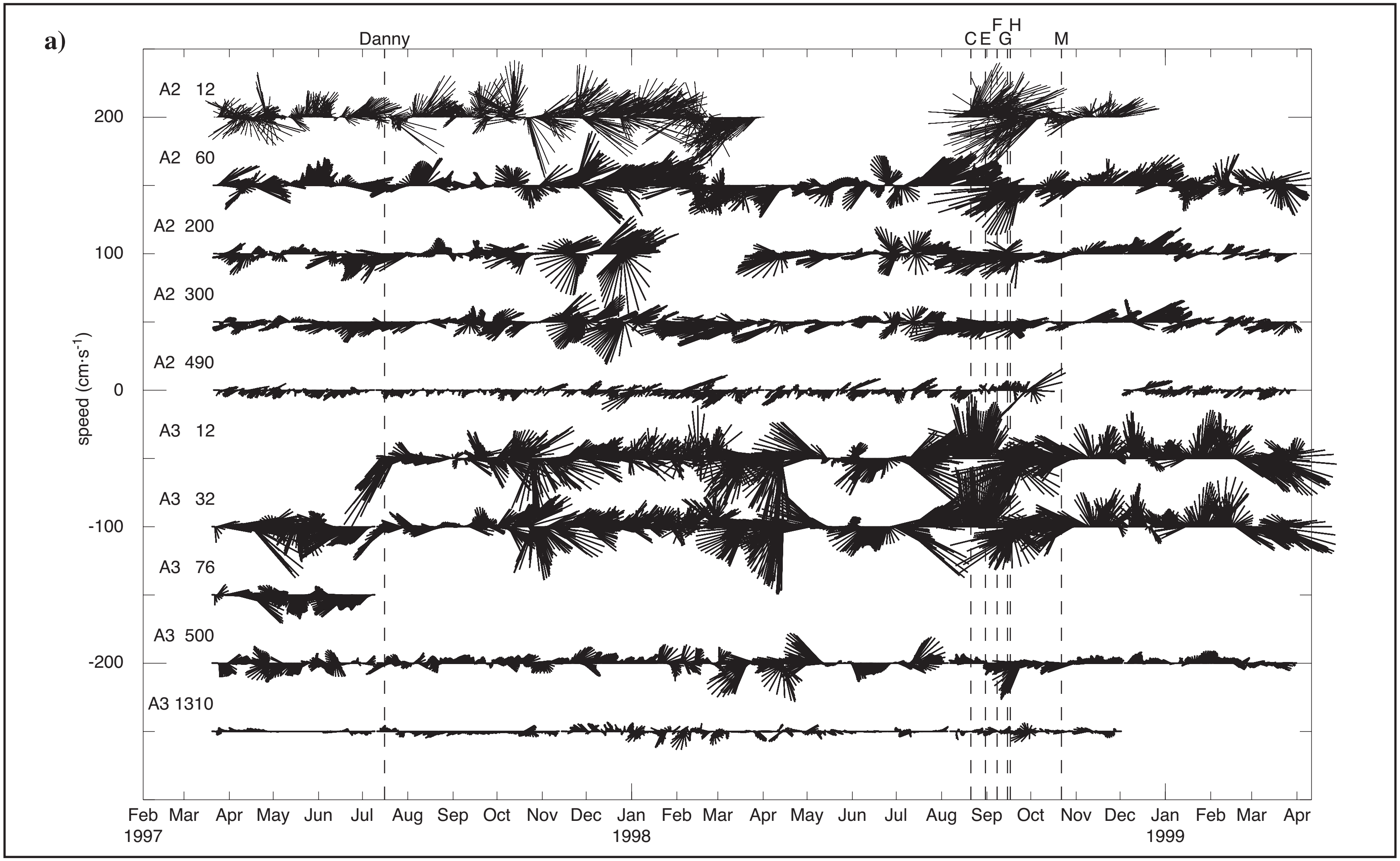

Figure 6.3.5-2. Time lines and vector stick plots for SAIC DeSoto Canyon moorings in water depths greater than 200 m. First day of tracking for tropical storms and hurricanes in the Gulf during the deployment period is indicated by vertical dashed lines with storm names given above. C= Charley; E = Earl; F = Frances; G = Georges; H = Hermine and M = Mitch. North is upward. Tick marks indicate start of the month.

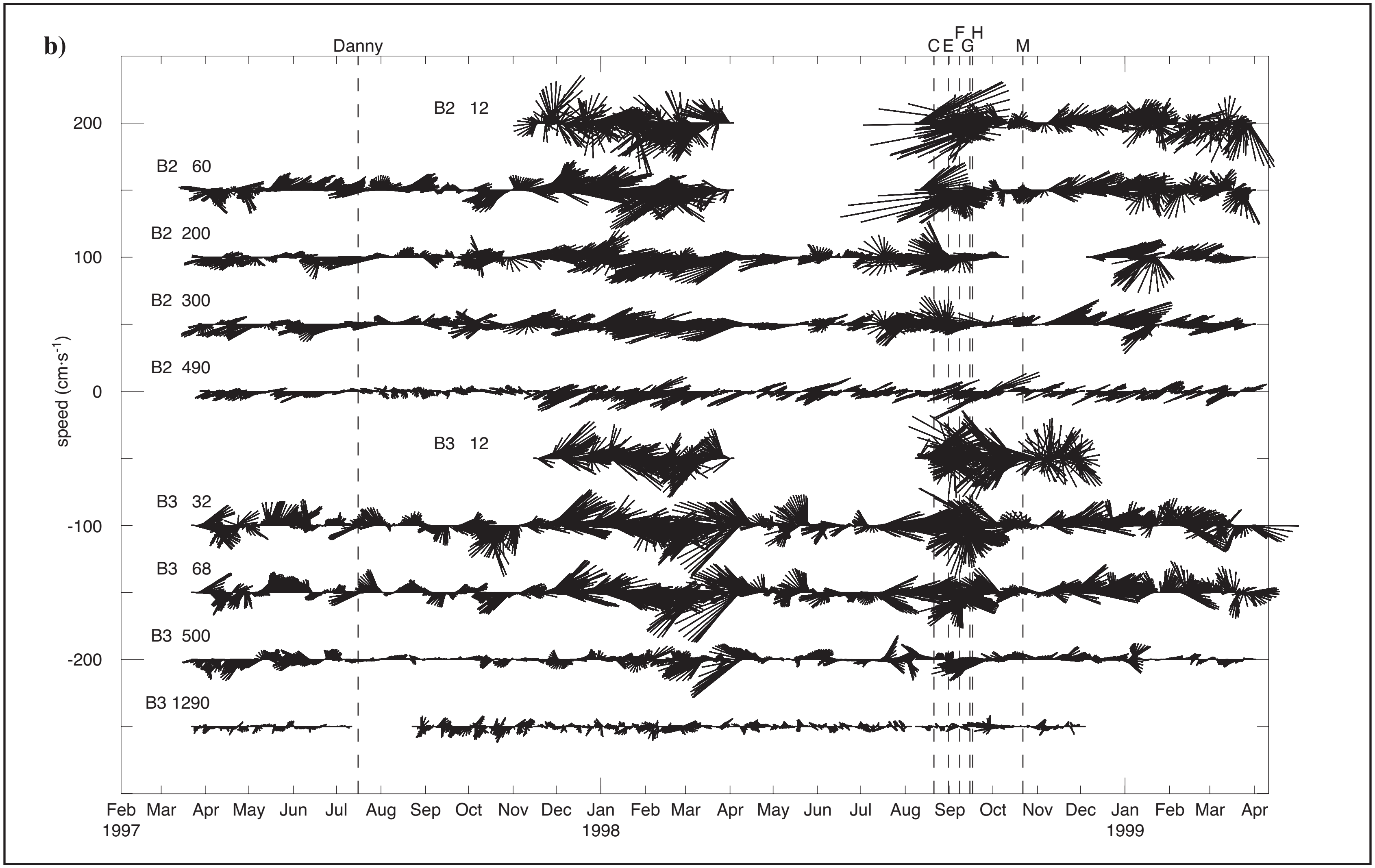

Figure 6.3.5-2. Time lines and vector stick plots for SAIC DeSoto Canyon moorings in water depths greater than 200 m. (continued)

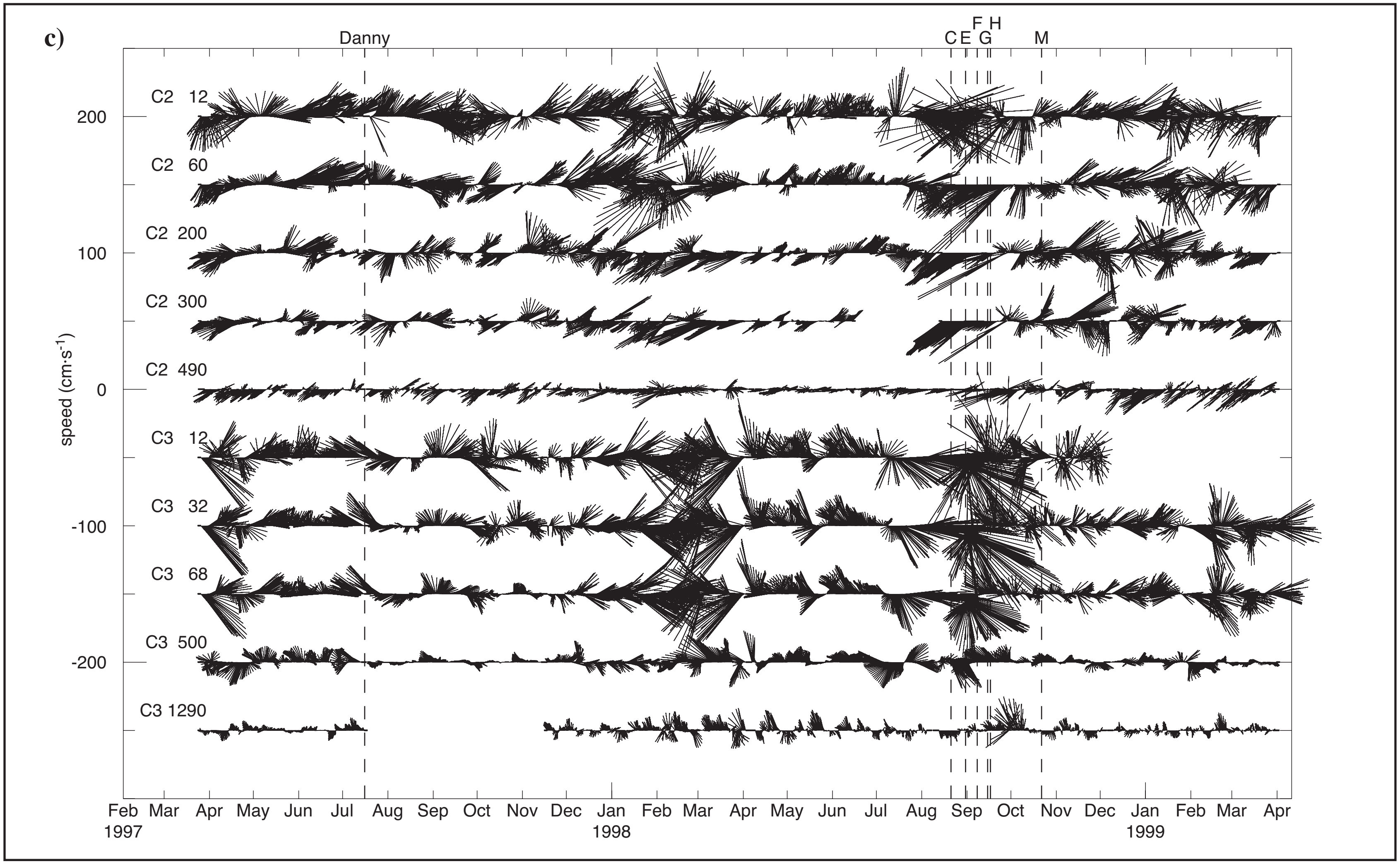

Figure 6.3.5-2. Time lines and vector stick plots for SAIC DeSoto Canyon moorings in water depths greater than 200 m. (continued)

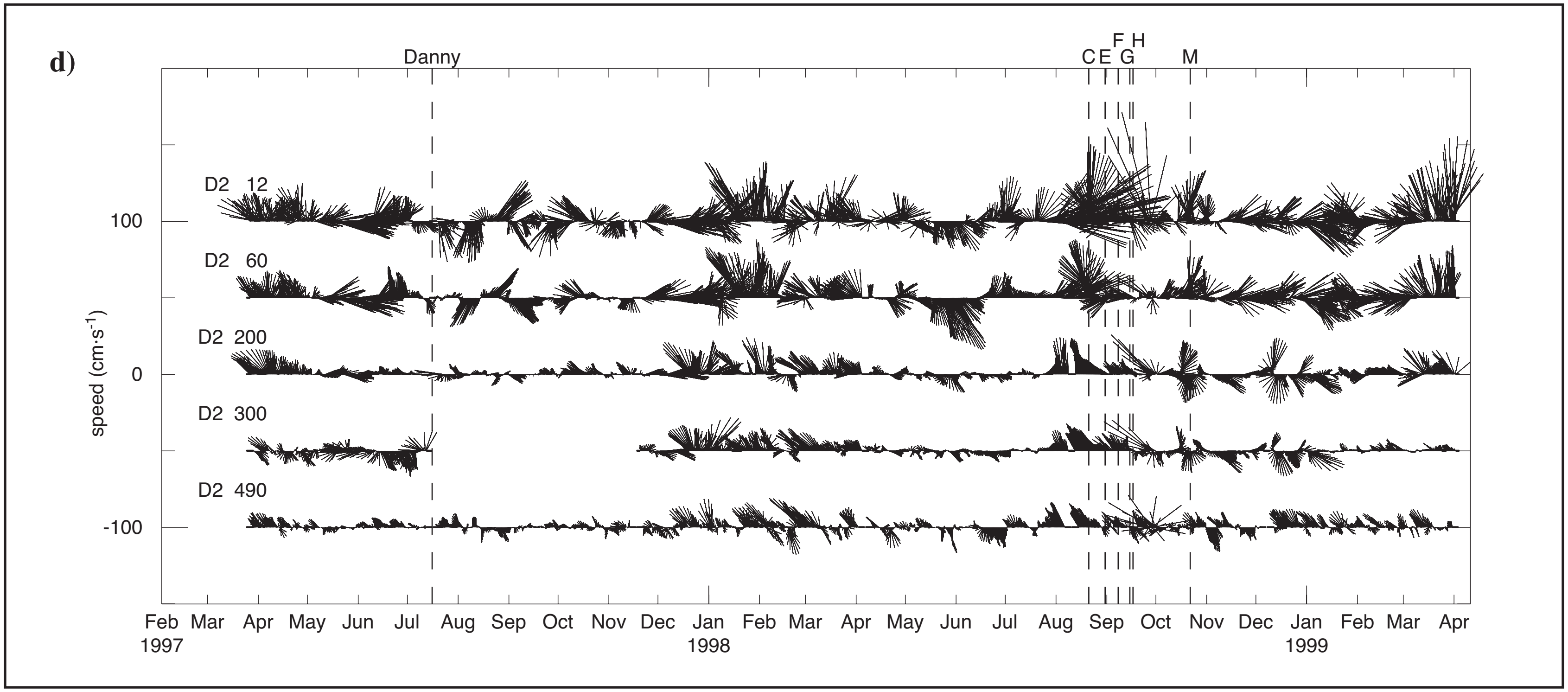

Figure 6.3.5-2. Time lines and vector stick plots for SAIC DeSoto Canyon moorings in water depths greater than 200 m. (continued)

Table 6.3.5-1. Record-length mean, standard deviation, and maximum speed for data from the northeastern Gulf in the SAIC 1997-1999 DeSoto Canyon Eddy Intrusion Study. The asterisk denotes the instrument was a current meter; others are selected depths from a moored ADCP.

Mooring	Instrument Depth (m)	Mean Speed ($cm \cdot s^{-1}$)	Standard Deviation ($cm \cdot s^{-1}$)	Maximum Speed ($cm \cdot s^{-1}$)
A2	12	24.8	15.0	161.0
	60	18.2	10.7	119.3
	200*	13.0	9.1	89.2
	300*	12.6	9.4	90.6
	490*	6.5	5.2	48.0
A3	12	24.6	14.4	143.6
	32	22.4	12.3	120.9
	76	14.7	7.7	47.0
	500*	8.9	6.6	39.5
	1310*	4.0	3.1	29.3
B2	12	24.4	15.0	153.1
	60	19.7	12.5	138.2
	200*	16.2	12.5	128.4
	300*	16.3	11.7	97.0
	490*	9.4	6.4	65.1
B3	12	26.5	14.5	161.8
	32	20.5	12.4	110.4
	68	17.4	11.0	76.3
	500*	7.8	6.5	54.3
	1290*	4.6	3.5	27.7
C2	12	23.9	13.9	179.4
	60	18.0	10.7	117.9
	200*	14.2	9.4	110.1
	300*	11.8	9.3	85.7
	490*	8.2	5.8	72.0
C3	12	25.4	15.8	202.8
	32	21.2	13.8	141.3
	68	17.8	11.2	74.2
	500*	8.4	6.0	38.6
	1290*	5.3	4.4	48.6
D2	12	22.4	13.5	156.8
	60	16.8	8.9	59.9
	200*	9.0	7.0	49.1
	300*	8.2	5.9	52.8
	490*	6.8	4.9	39.6

- C2: DD970324.A01-A20; DD970324.C01; DD970324.C02; DD970324.C03; DD970717.A01-A19; DD970717.C01; DD970717.C02; DD970717.C03; DD971120.A19-A36; DD971120.C02; DD971120.C03; DD971120.C04; DD980409.A19-A37; DD980409.C02; DD980409.C03; DD980409.C04; DD980812.A01-A19; DD980812.C01; DD980812.C02; DD980812.C03; DD981209.A01-A19; DD981209.C01; DD981209.C02; DD981209.C03
- C3: DD970324.A21-A37; DD970324.C04; DD970324.C05; DD970718.A19-A35; DD970718.C01; DD971116.A01-A17; DD971116.C01; DD971116.C02; DD980405.A01-A18; DD980405.C01; DD980405.C02; DD980808.A01-A17; DD980808.C01; DD980808.C02; DD981205.A01-A16; DD981205.C01; DD981206.C01
- D2: DD970324.A38-A57; DD970324.C06; DD970324.C07; DD970324.C08; DD970716.A01-A20; DD970716.C01; DD970716.C02; DD971118.A01-A19; DD971118.C01; DD971118.C02; DD971118.C03; DD980406.A01-A18; DD980406.C01; DD980406.C02; DD980406.C03; DD980810.A01-A19; DD980810.C01; DD980810.C02; DD980810.C03; DD981207.A01-A19; DD981207.C01; DD981207.C02; DD981207.C03

Environmental background. Tropical cyclone activity in the Gulf of Mexico during the deployment period consisted of hurricanes Danny (16–26 July 1997), Earl (31 August–3 September 1998), Georges (15–29 September 1998), and Mitch (22 October–5 November 1998) as well as tropical storms Charley (21–26 August 1997), Frances (8–12 September 1997), and Hermine (17–20 September 1998). Hurricanes Earl and Georges passed over the moorings (Figure 6.3.5-1).

SSHA fields indicate the Loop Current did not extend into the mooring locations and was located south of 28°N (and often south of 26°N) throughout the deployment period. Two LCEs separated from the Loop Current during the deployment period: Eddy El Dorado in October 1997 and Eddy Fourchon in March 1998 (Sturges and Leben 2000). These also were located south of 28°N. A high in SSHA, indicative of anticyclonic circulation, persisted in the DeSoto Canyon region from March through June 1997, November 1997 through January 1998, and May 1998 through May 1999. As Eddy Fourchon moved westward in late summer 1998, the anticyclone over the slope in the DeSoto Canyon region intensified.

Basic Statistics. Record-length mean, standard deviation, and maximum speeds for the moorings are shown in Table 6.3.5-1. Figure 6.3.5-3 shows the statistics versus depth for all instrument depths. Because of the large number of files associated with the upward-looking ADCPs, only statistics for the bins included on Figure 6.3.5-2 and a near-bottom bin are shown. The other statistics reported are from the Aanderaa single-point meters deployed below the ADCPs. In general, the upward-looking ADCPs showed that mean speeds varied quasi-linearly with depth at each location. Average speeds for ADCP measurements in the depth range of 8-20 m was 22 $cm \cdot s^{-1}$, for 20-40 m it was 19 $cm \cdot s^{-1}$, for 40-60 m it was 16 $cm \cdot s^{-1}$, and for 60-80 m it was 15 $cm \cdot s^{-1}$. As seen with other measurements, the mean speeds and associated standard deviations decreased with depth, and the standard deviations were smaller than the means. Maximum speeds depended on location and proximity to severe weather, particularly during September 1998 when four storms passed over the region. The intense surface wave action caused by severe weather, including breaking waves and large fluctuations of sea surface level, likely make the extreme current velocity estimates in the upper 20 m unreliable by introducing signal contamination in the upper bins of the ADCP data. Data from the upper bins, however, are retained in the data set because the data are reliable in the absence of such extreme conditions. Data in the upper bins during extreme weather should be used with caution and closely compared with data below those bins.

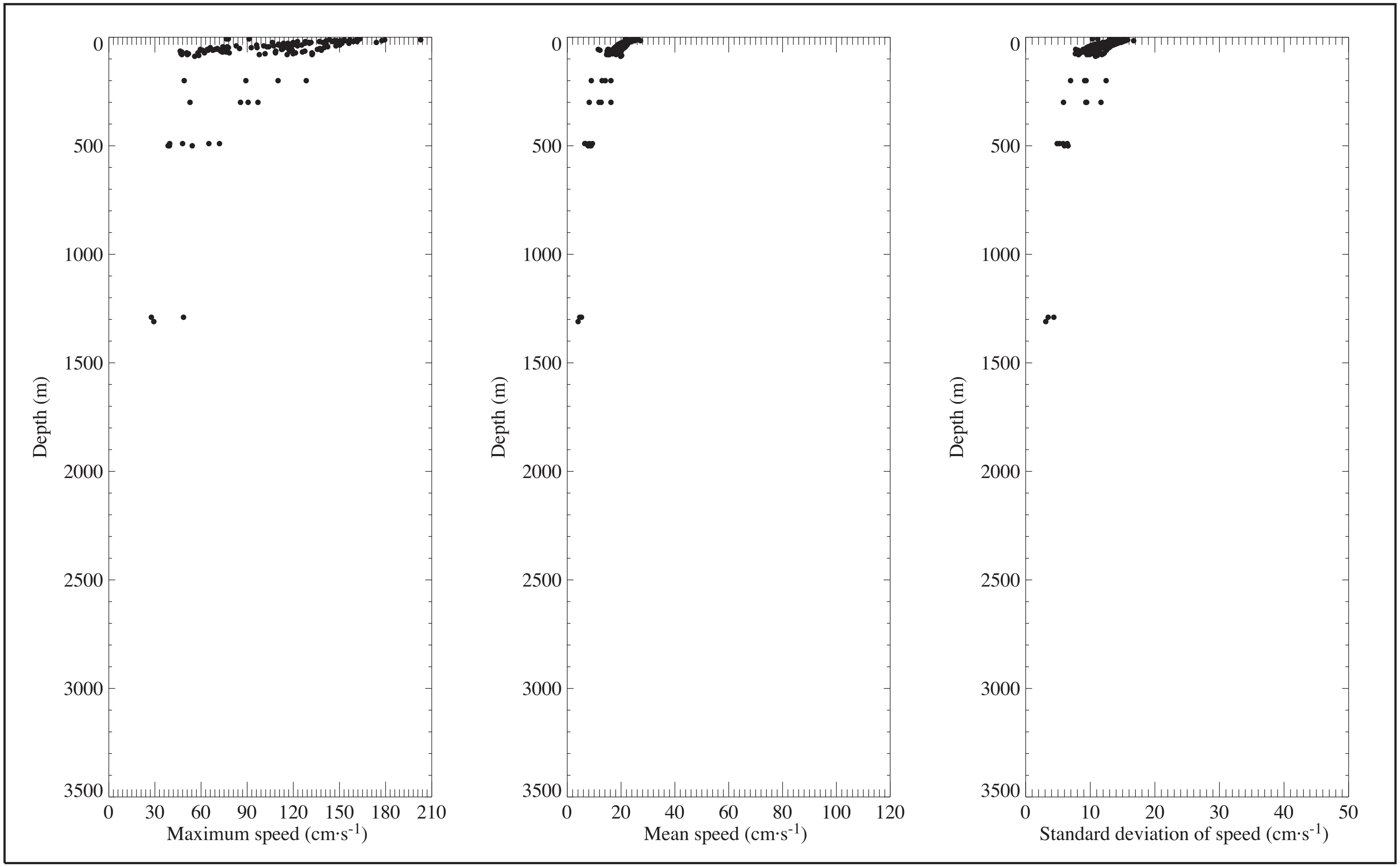

Figure 6.3.5-3. Observed speed (a) maximum, (b) mean, and (c) standard deviation versus instrument depth for unfiltered records from SAIC DeSoto Canyon moorings (npts = 146). Quality codes: A or B (dot), C (square), D (plus).

<u>General description of records.</u> A strong oblong anticyclone, with major axis oriented along the bathymetry and center near 28°N, 88.25°W, was present in the SSHA maps of April 1997. It affected the regional circulation when the EIS moorings were first deployed. This eddy was not an LCE, but rather resulted from coalescence of a number of smaller anticyclones. It was named Eddy Deviant in the EddyWatch charts. The influence of Eddy Deviant is most clearly seen in the deep moorings (A3, B3, and C3) along the DeSoto Canyon slope. At A3, the currents reflected the northern limb of the anticyclone, with persistent eastward currents with speeds greater than 50 $cm \cdot s^{-1}$ in the upper 100 m. Near-surface currents at B3, which was closer to the center of rotation for this anticyclone, were weaker with eastward direction and 25 $cm \cdot s^{-1}$ speeds. At C3, near-surface currents were strong (45-55 $cm \cdot s^{-1}$) but southeastward, corresponding to the northeastern limb of the eddy. At 500 m and below, currents were weak (< 10 $cm \cdot s^{-1}$) and variable in direction, particularly at1290 m on C3.

In May 1997, Eddy Deviant moved westward, away from the current moorings. Surface currents turned southward and then southwestward and weakened considerably. In June, a small diameter (50 km) anticyclone appeared over line A. Northeastward currents were seen over A1 and A2 on the shelf (not shown), while at A3 the flow was southwestward. Near the surface at C1 on the shelf, strong northeastward currents persisted for about two weeks. The eastern limb of the anticyclone was seen at E1on the shelf with persistent southeastward currents of 10-30 $cm \cdot s^{-1}$ into July.

From July through October 1997, currents over the northeastern Gulf slope were affected indirectly by Eddy El Dorado. SSHA maps indicated a cyclone was located north of Eddy El Dorado; that cyclone dominated circulation in the DeSoto Canyon region. The northern limb of the cyclone generated cyclonic currents as evidenced by the westward currents in the upper 100 m at A3 during August. The deep current records offshore were highly variable in both amplitude and direction with periods of 7-10 days.

From November 1997 to January 1998, a weak anticyclone centered south of the moorings at 28°N, 88°W forced the near-surface circulation with predominately eastward currents at A3, B3, and C3. That anticyclone strengthened during December and January. In February (according to EddyWatch) or March (according to Sturges and Leben), Eddy Fourchon separated from the Loop Current. Negative SSHA covered the DeSoto Canyon region, and a small diameter cyclone was positioned over the DeSoto Canyon slope. In February, the near surface currents at A3 were variable and at B3 and C3 they were eastward. At all three locations, they turned predominately toward the west in March. In April, as Eddy Fourchon moved away from the region toward the west, currents at C3 turned northward but remained westward at A3 and B3.

From May through September 1998, a strong anticyclone (Eddy Gyre) developed over the slope. The largest associated SSHA gradient is seen for September. Currents were strongest at C3, reaching100 $cm \cdot s^{-1}$, while at A3 and B3 they were greater than 50 $cm \cdot s^{-1}$. Directions were mostly toward the east; however, at A3 the current turned counterclockwise from eastward to northward in the beginning of the month. Some of the large currents in September may be attributed to the unusually large number (4) of tropical storms during that month.

From October 1998 through March 1999, Eddy Gyre remained poised over the shelf and slope regions of DeSoto Canyon. Currents were generally variable as the eddy moved on and off the slope. SSHA maps show the eddy retreating offshore in December 1998 and moving west in April 1999.

Inertial energy is ubiquitous in the EIS records. There are indications of summer diurnal oscillations (DiMarco et al. 2000) at 12-m depths at A3 and C3, as well as shelf edge moorings C2 and D2. The amplitudes can be seen to decrease with depth, but there is some indication that they extended below the main thermocline to depths of 70 m and deeper. By far the largest amplitudes and most persistent (long lasting) inertial band energy was during September 1998, when hurricanes and tropical weather dominated the forcing of this region. Tables 6.3.5-2 and 6.3.5-3 show the maximum speeds from the surface and fourth depth bins, respectively, at each mooring location. These are the maximum speeds for the unfiltered near-surface records during September 1998.

Modulated envelopes of deep (500 m) inertial band energy occurred at A3, B3, and C3. These currents are similar to those seen in proprietary industry records in the central Gulf. Current hodographs for these packets are circular and have anticyclonic rotation with amplitudes of 15-20 $cm \cdot s^{-1}$. Packet envelopes generally span 7-10 days. There are multiple examples of inertial band energy associated with extratropical cyclones and frontal passages. They are short lived, decaying rapidly in time and depth.

During late September and early October 1998, a very interesting bottom event occurred simultaneous with the passage of Hurricane Georges. This is discussed in Section 6.1.5.

Table 6.3.5-2. Dates and maximum speeds of unfiltered currents during September 1998 at depth bin 1 on each DeSoto Canyon mooring in water depths of greater than 200 m.

Mooring	**Depth (m)**	**Speed ($cm \cdot s^{-1}$)**	**Date (mm/dd/yyyy hh:mm)**
A2	12	161.0	09/27/1998 17:30
A3	8	163.2	09/27/1998 13:00
B2	12	153.1	09/27/1998 12:00
C2	12	179.4	09/03/1998 01:00
C3	12	202.8	09/27/1998 17:30
D2	12	156.8	09/27/1998 13:30

Table 6.3.5-3. Dates and maximum speeds of unfiltered currents during September 1998 at depth bin 4 on each DeSoto Canyon mooring in water depths of greater than 200 m.

Mooring	**Depth (m)**	**Speed ($cm \cdot s^{-1}$)**	**Date (mm/dd/yyyy hh:mm)**
A2	24	119.9	9/27/98 19:30
A3	20	137.1	9/27/98 13:00
B2	24	148.4	9/27/98 00:30
C2	24	106.4	9/03/98 03:30
C3	24	174.0	9/27/98 15:00
D2	24	139.4	9/27/98 10:30

6.3.6 MMS Moorings I1, 12, and I3, 1999-2000

Basic description of data. SAIC deployed three moorings in the central Gulf in water depths of approximately 2000 m for the MMS. One mooring each was deployed in lease blocks Atwater 663 (I1), Green Canyon 744 (I2), and Atwater 838 (I3). Data were obtained from SAIC. The locations of the moorings are shown in Figure 6.3.6-1. On mooring I1, seven current meters and six ADCPs (upward-looking at 90, 240, and 600 m; downward-looking at 100, 250, and 650 m) were used on the first deployment and eight current meters and five ADCPs (upward-looking at 90 and 240 m; downward-looking at 100, 250, and 650 m) on the second. The mooring was deployed from 29 August 1999 through 26 August 2000 in water depth of 2001 m. Three instruments were deployed on mooring I2 from 29 August 1999 through 27 August 2000. The water depth was 1998 m. Three current meters were deployed on I3 between 29 August 1999 and 26 August 2000 in water depth of 2175 m. Current meter instrument depths for the three moorings are given in Table 6.3.6-1, together with a few depths from the ADCPs. Time lines and vector stick plots for the data are shown in Figures 6.3.6-2 (data from water depths greater than 1500 m) and 6.3.6-3 (data from I1). The quality codes for these data are A and C. File names for the current records in the database are

- I1: AT990829.A01-A84; AT990829.A85-A99; AT990829.Aa0-Aa9; AT990829.Ab0-Ab5; AT990829.Ab6-Ab9; AT990829.Ac0-Ac9; AT990829.Ad0-Ad9; AT990829.Ae0-Ae9; AT990829.Af0-Af9; AT990829.Ag0-Ag9; AT990829.Ah0-Ah5; AT000225.A01-A99; AT000225.Aa0-Aa9; AT000225.Ab0-Ab9; AT000225.Ac0-Ac9; AT000225.Ad0-Ad3; AT990829.C01-C07; AT000225. C01-C08
- I2: GC990829.C01-C03; GC000223.C01-C03
- I3: AT990829.C08-C10; AT000224.C01-C03

Environmental background. Six tropical cyclones passed through the Gulf of Mexico during the deployment period: hurricane Irene (13-19 October 1999); tropical storms Harvey (19–22 September 1999), Katrina (28 October–1 November 1999), and Beryl (13-15 August 2000); and tropical depressions #7 (5–7 September 1999) and #11 (4–6 October 1999). None of the storms passed over the moorings and most were in the southern Gulf (Figure 6.3.6-1).

Eddy Juggernaut detached from the Loop Current near the beginning of the deployment of the moorings. SSHA fields show that this LCE and/or an associated cyclone to its west were south of the moorings throughout 1999. By February 2000, the eddy had passed the mooring locations. Weak lows in SSHA were present in the vicinity of the moorings into June 2000, after which weak highs in SSHA were present.

Basic statistics. Record-length mean, standard deviation, and maximum speeds for the moorings are given in Table 6.3.6-1. Figure 6.3.6-4 shows the statistics versus depth for all instrument depths. Mean speeds for the deep currents below 1500 m were of order 20 $cm \cdot s^{-1}$ at I2 and 12 $cm \cdot s^{-1}$ at I1 and I3, with standard deviations of ~14 and ~9 $cm \cdot s^{-1}$, respectively. The maximum speeds at I2, reaching over 90 $cm \cdot s^{-1}$, were some of the highest seen in the 1500-2000 m water depths. Mean speeds decreased with depth to approximately 1000 m. Deeper currents then increased with depth.

General description of records. At the beginning of the records for the three moorings there were several large current events below 1500 m (Figure 6.3.6-2, east is up). The largest were at I2 with speeds in excess of 80 $cm \cdot s^{-1}$. These events persisted for periods of 5-10 days and recurred after a 4-5 day period of weak currents in essentially the opposite direction. Currents at I2 accelerated from 0 to 80^{+} $cm \cdot s^{-1}$ in just a few hours. Strongest currents were oriented

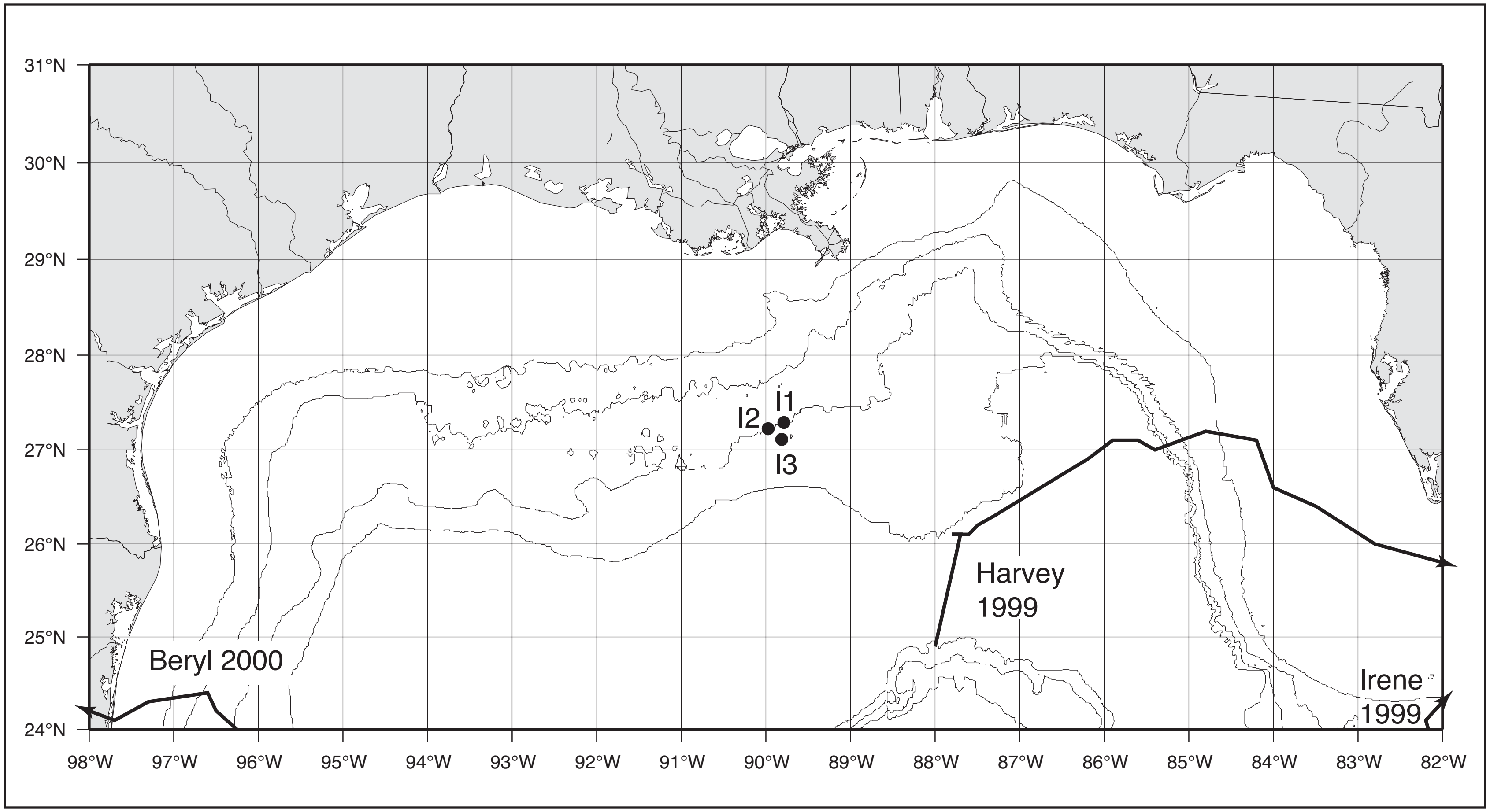

Figure 6.3.6-1. Location map for MMS central Gulf moorings. The tracks of tropical storms and hurricanes in the Gulf during the deployment period are shown. Shown are the 200-, 1000-, 2000-, and 3000-m isobaths.

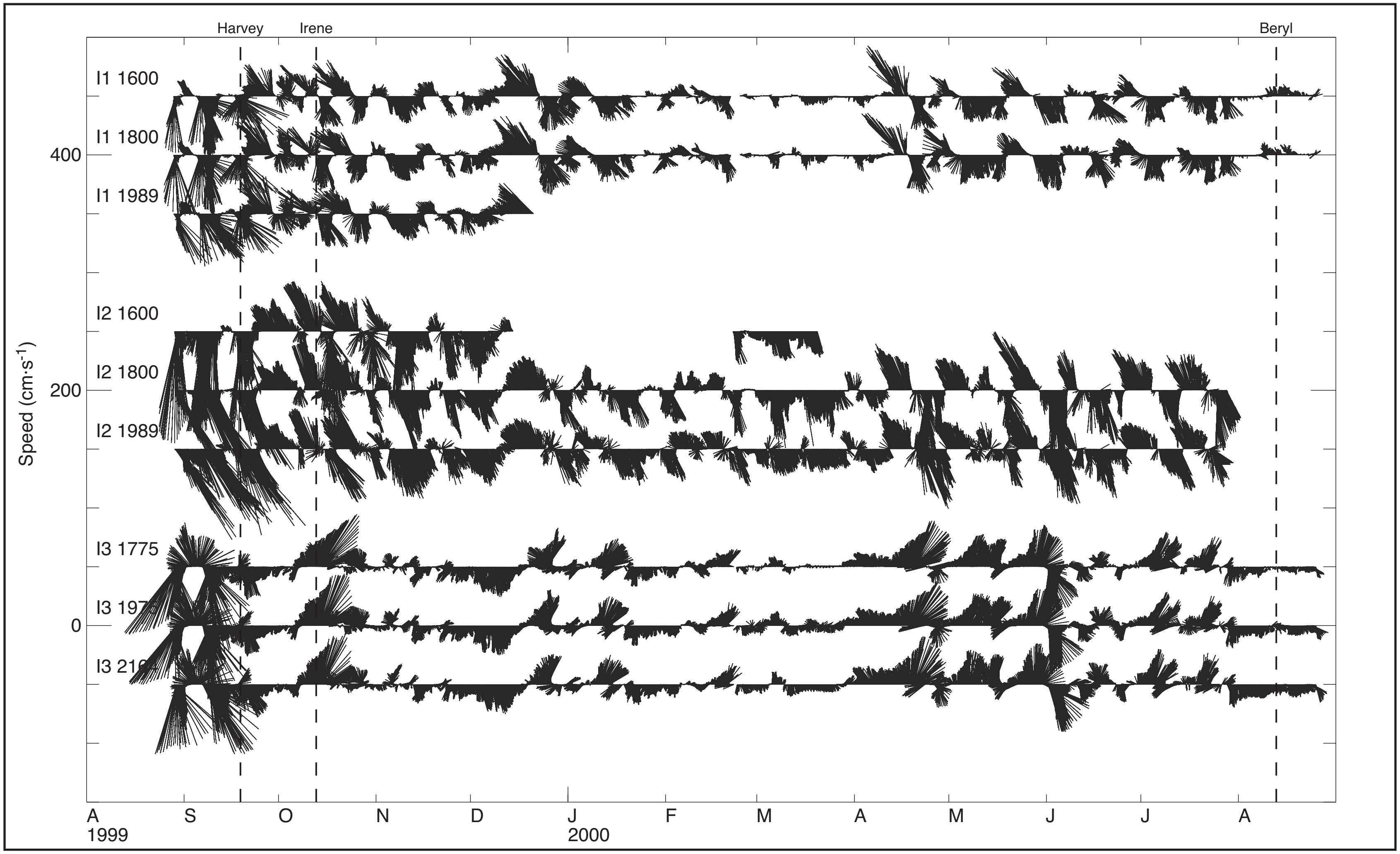

Figure 6.3.6-2. Time lines and vector stick plots for instruments at 1600 m or deeper for MMS moorings in the central northern Gulf. The first day of tracking for tropical storms and hurricanes in the Gulf during the deployment period is indicated by the vertical dashed line with the storm name given above it. East is upward. Tick marks denote start of the month.

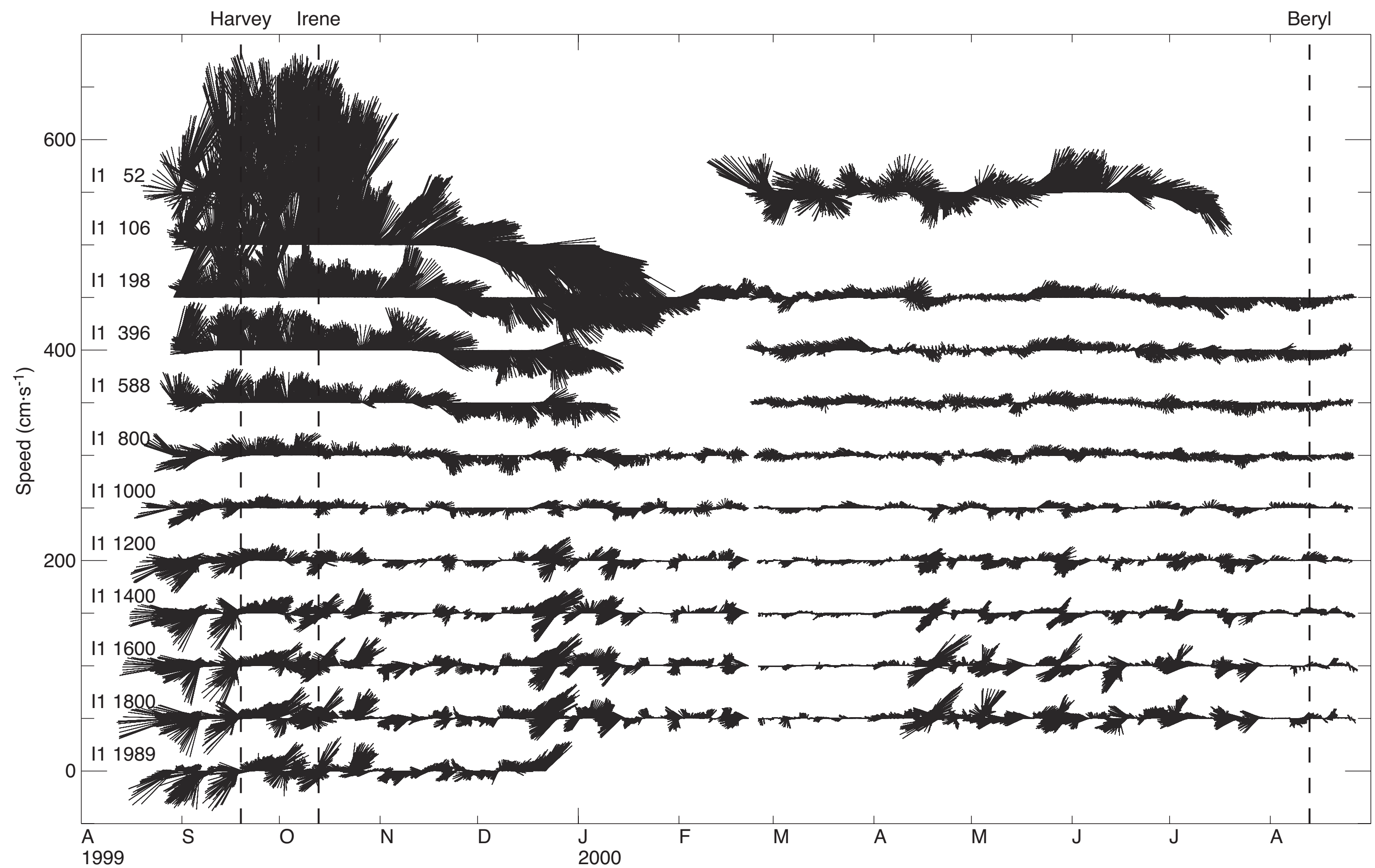

Figure 6.3.6-3. Time lines and vector stick plots for MMS mooring I1 in the central northern Gulf. The first day of tracking for tropical storms and hurricanes in the Gulf during the deployment period is indicated by vertical dashed lines with storm names given above. North is upward. Tick marks denote start of the month.

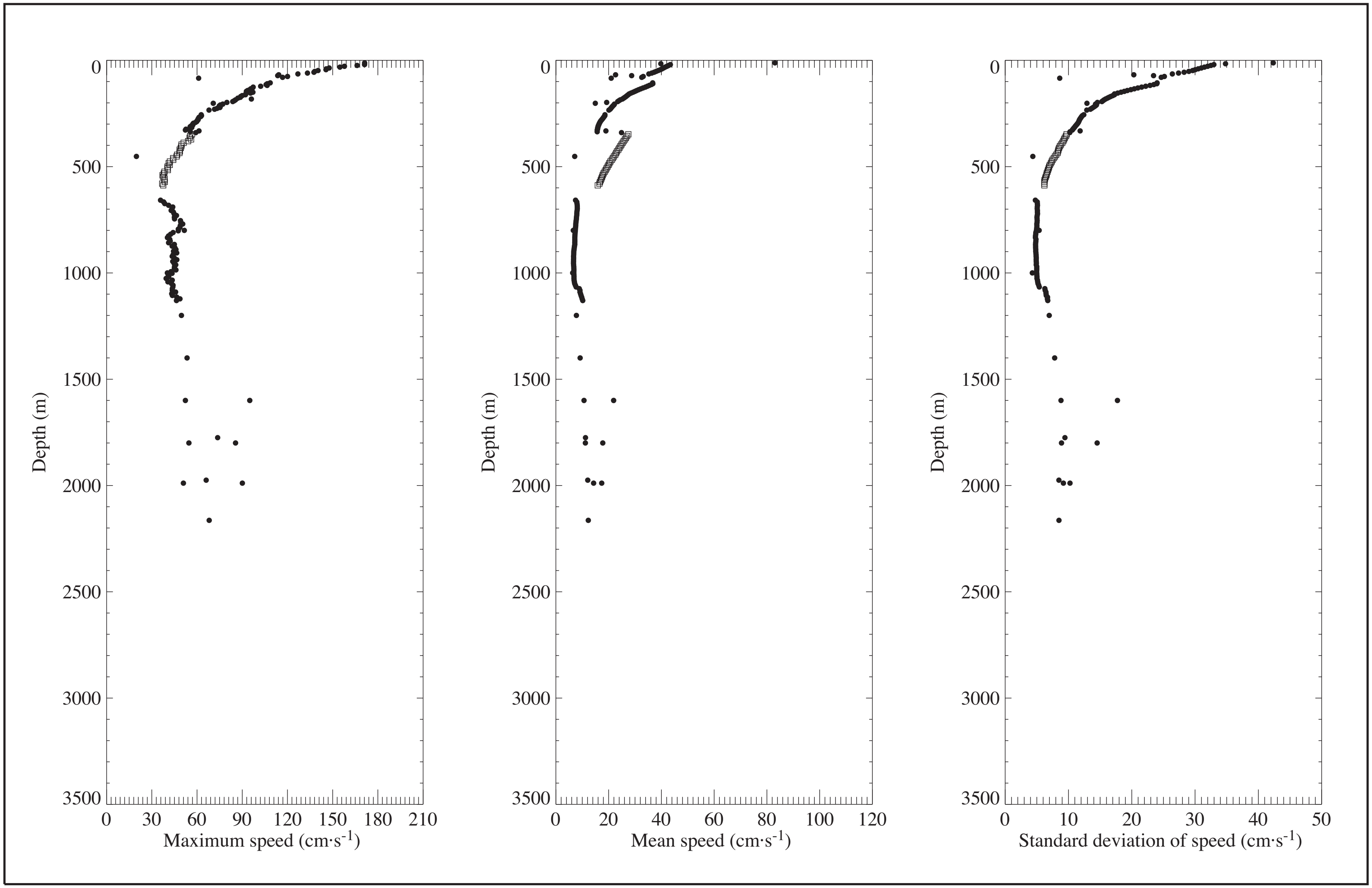

Figure 6.3.6-4. Observed speed (a) maximum, (b) mean, and (c) standard deviation versus instrument depth for unfiltered records from MMS central Gulf moorings (npts = 179). Quality codes: A or B (dot), C (square), D (plus).

Table 6.3.6-1. Record-length mean, standard deviation, and maximum speed for data from the 1999 MMS moorings in the central Gulf. The asterisk denotes the instrument was a current meter; others are selected depths from a moored ADCP.

Mooring	Instrument Depth (m)	Mean Speed ($cm{\cdot}s^{-1}$)	Standard Deviation ($cm{\cdot}s^{-1}$)	Maximum Speed ($cm{\cdot}s^{-1}$)
I1	12	83.1	42.4	171.2
	52	38.0	29.0	138.1
	106	36.7	24.0	108.6
	198	19.3	14.6	79.8
	396	24.9	8.8	49.7
	588	15.9	6.2	37.6
	800*	6.6	5.4	51.6
	1000*	6.4	4.3	40.3
	1200*	7.8	7.0	49.7
	1400*	9.2	7.8	53.4
	1600*	10.7	8.8	52.3
	1800*	11.2	8.9	54.6
	1989*	14.3	9.2	51.0
I2	1600*	21.9	17.7	95.0
	1800*	17.8	14.5	85.6
	1989*	17.4	10.2	90.1
I3	1775*	11.2	9.4	73.7
	1975*	12.1	8.5	66.1
	2164*	12.3	8.5	68.1

along the bathymetry and flowed to the west and southwest, with I3 also having northwest currents. The records are highly coherent. These large currents occurred when the extension of the Loop Current (soon to separate as Eddy Juggernaut) was adjacent to and approximately south of the moorings. The upper currents during this time at I1 show the strong northward flows associated with the northwest side of the anticyclonic eddy (Figure 6.3.6-3, north is up) and the rotation of the flows to the east as the north side of the eddy passes the mooring and to the southeast as the northeast side of the eddy passes. It should be noted that each large deep current event in the records occurs during a period when a tropical storm is in the Gulf, but this likely is coincidental because no storm passed particularly close to the mooring sites and the upper currents at I1 do not indicate a response to a storm. During the last half of the records, when the eddy had moved past the moorings, both the deep and upper currents are weaker. on each mooring, the currents at 1000 m or deeper are coherent. At mooring I1, there is indication of bottom intensification of the currents.

6.3.7 TAMU Mississippi Canyon Mooring, 1998

Basic description of data. These data were collected by C. Burden from TAMU as part of National Science Foundation-funded research and were described in her M.S. thesis (Burden 1999). The data were obtained from TAMU. One mooring was deployed near the head of Mississippi Canyon in a water depth of 300 m. Figure 6.3.7-1 shows the location of the

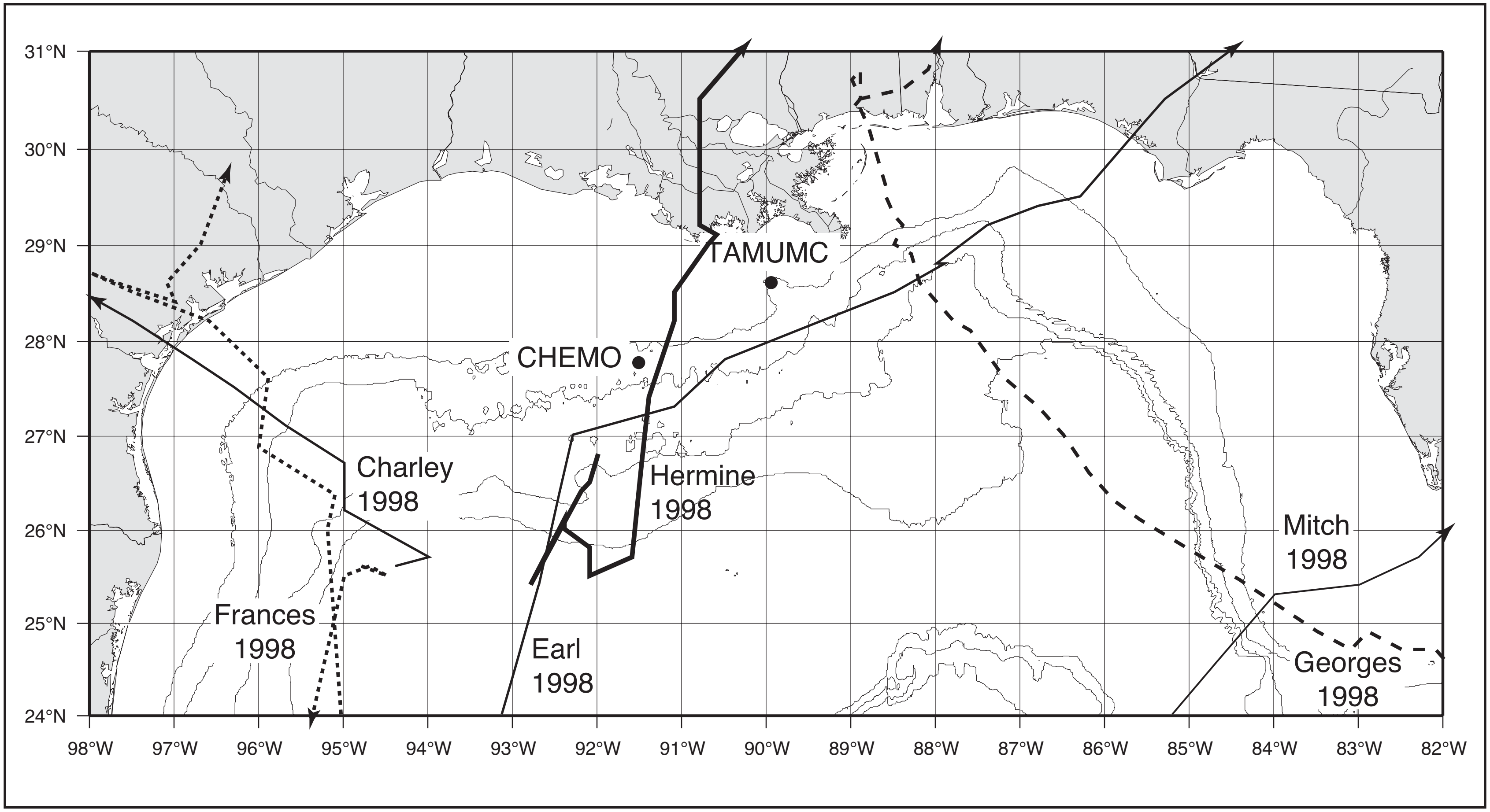

Figure 6.3.7-1. Location map for the TAMU Mississippi Canyon and GERG Chemosynthetic study moorings. The tracks of tropical storms and hurricanes in the Gulf for the deployment period are shown. Shown are the 200-, 1000-, 2000-, and 3000-m isobaths.

mooring. There were two deployments. The first was from 18 May through 25 July 1998 and consisted of two instruments deployed at 3.5 m and 50 m above bottom. Instrument depths are given in Table 6.3.7-1. The second deployment, which consisted of only the bottom instrument, began two weeks after the first and extended from 6 August through 12 November 1998. Time lines and vector stick plots for the two instruments are shown in Figure 6.3.7-2. The quality codes for these data are A and C. File names for the current records in the database are

- TAMUMC: EW980518.C01; EW980518.C02; EW980806.C01

Environmental background. Six tropical cyclones were present in the Gulf of Mexico during the second deployment: hurricanes Earl (31 August–3 September 1998), Georges (15–29 September 1998), and Mitch (22 October–5 November 1998), and tropical storms Charley (21–26 August 1997), Frances (8–12 September 1997), and Hermine (17–20 September 1998). Hurricane Earl passed near the mooring (Figure 6.3.7-1).

There were no Loop Current eddy separations during this deployment (Sturges and Leben 2000). SSHA fields indicate no LCEs or major anticyclonic or cyclonic eddies were over or adjacent to the mooring. From May through September 1998, the region was in a SSHA low and in a high during October and November.

Basic statistics. Record-length mean, standard deviation, and maximum speeds for the moorings are shown in Table 6.3.7-1. Figure 6.3.7-3 shows the statistics versus depth for all instrument depths. The highest statistics were at the bottom instrument, which was 3 m above the sea floor.

General description of records. The record at 250 m was dominated by inertial oscillations with amplitudes of 10-15 $cm \cdot s^{-1}$, particularly during June. The semi-major axis of the variability ellipse was aligned along the canyon axis. At 297 m, the inertial oscillation amplitudes were larger during the first deployment (summer) than in the late summer-fall second deployment. Peak speeds during the September storms reached 40 $cm \cdot s^{-1}$, particularly during Hurricane Georges. Currents near bottom (297 m) were generally more energetic than at 250 m.

6.3.8 GERG Chemosynthetic Mooring, 1997-1998

Basic description of data. The Geochemical and Environmental Research Group (GERG) of TAMU deployed a single mooring in lease block Green Canyon 185 as part of a chemosynthetic study for the MMS (Guinasso 2000). Data were obtained from GERG. The location of the mooring is shown in Figure 6.3.7-1. The two Aanderaa current meters were deployed in the mid-water column and near bottom in 545-m water depth from 8 August 1997 through 22 May 1998. Instrument depths are given in Table 6.3.8-1. Time lines and vector stick plots for the data are shown in Figure 6.3.7-2. The quality codes for these data are B and C. File names for the current records in the database are

- CHEMO: GC970808.C01; GC970809.C01

Environmental background. There were no tropical cyclones present in the Gulf of Mexico during this deployment. LCE El Dorado separated from the Loop Current during October 1997, and Eddy Fourchon separated in March 1998. SSHA fields indicate the mooring was generally under a low in SSHA and that Eddy El Dorado passed about 50 km to the south of the mooring during December 1997 through March-April 1998.

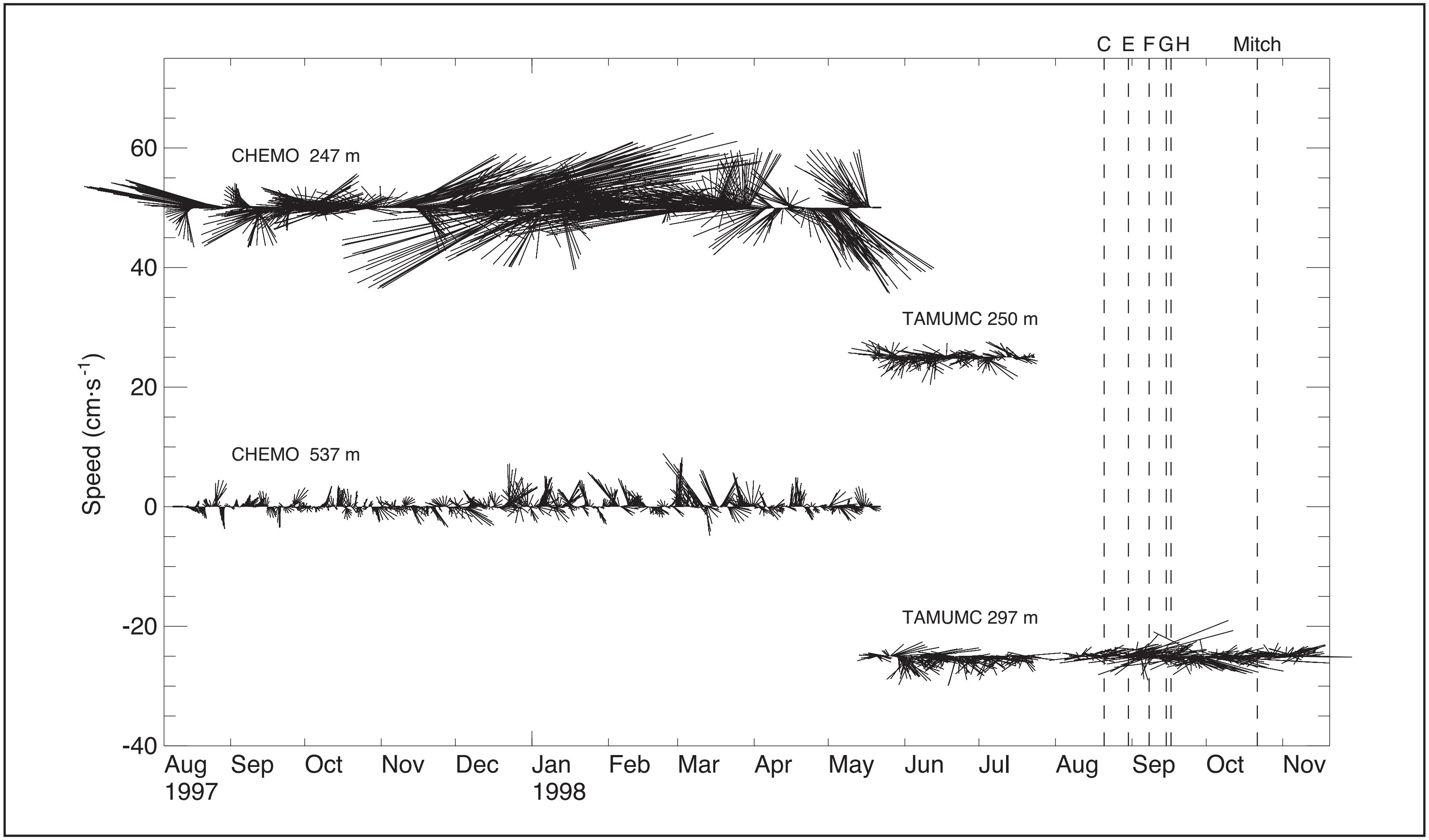

Figure 6.3.7-2. Time lines and vector stick plots for the TAMU Mississippi Canyon and GERG Chemosynthetic study moorings. The first day of tracking for tropical storms and hurricanes in the Gulf during the deployment period is indicated by the vertical dashed line with the storm name given above it. C= Charley; E = Earl; F = Frances; G = Georges; and H = Hermine. North is upward. Tick marks denote start of the month.

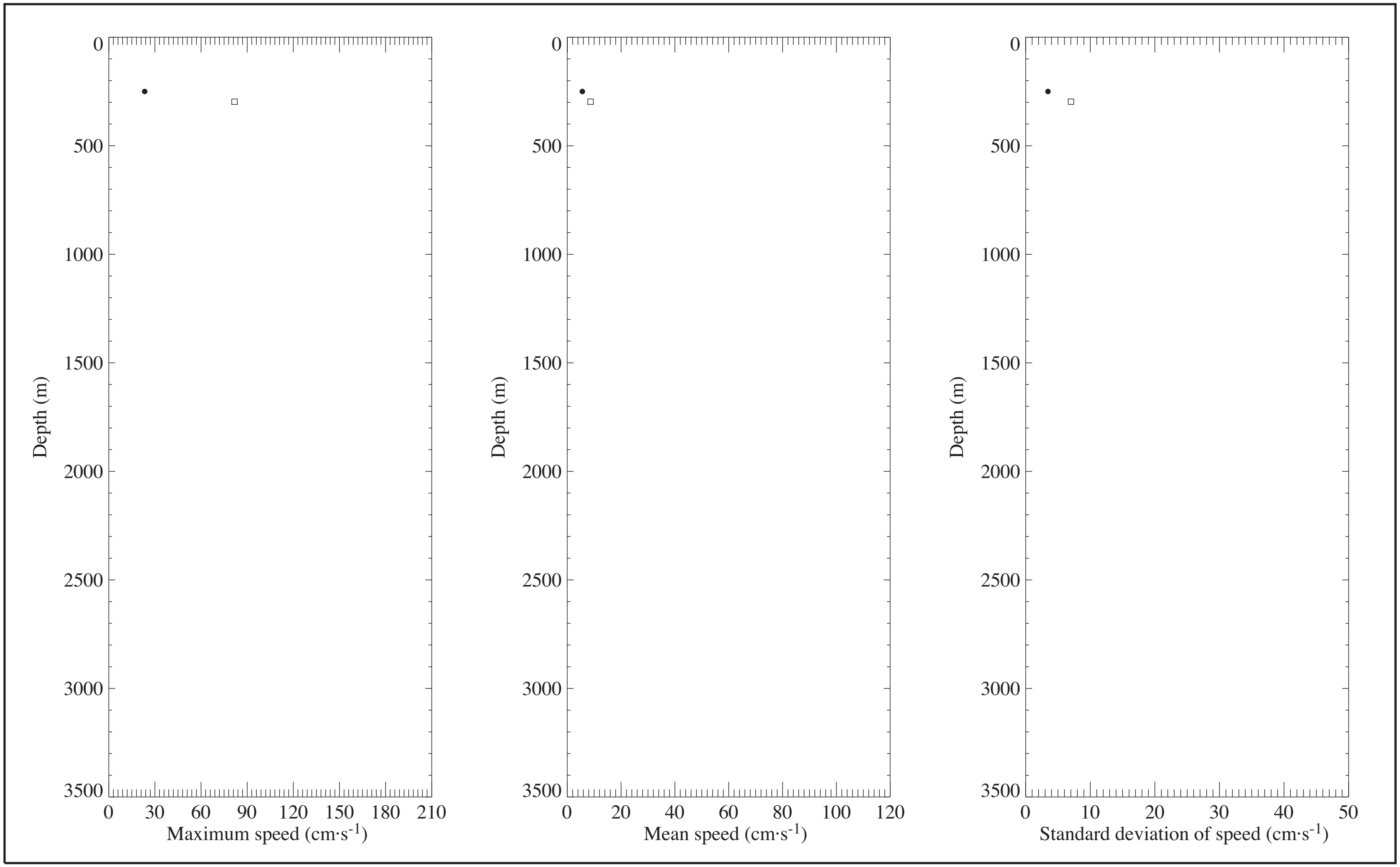

Figure 6.3.7-3. Observed speed (a) maximum, (b) mean, and (c) standard deviation versus instrument depth for unfiltered records from TAMU Mississippi Canyon mooring (npts = 2). Quality codes: A or B (dot), C (square), D (plus).

Table 6.3.7-1. Record-length mean, standard deviation, and maximum speed for data from the TAMU 1998 Mississippi Canyon mooring. Instruments were current meters.

Mooring	Instrument Depth (m)	Mean Speed ($cm \cdot s^{-1}$)	Standard Deviation ($cm \cdot s^{-1}$)	Maximum Speed ($cm \cdot s^{-1}$)
MC	250	5.6	3.5	23.4
	297	8.7	7.0	81.8

Table 6.3.8-1. Record-length mean, standard deviation, and maximum speed for data from the north central Gulf in the GERG 1997-1998 Chemosynthetic study. Instruments were current meters.

Mooring	Instrument Depth (m)	Mean Speed ($cm \cdot s^{-1}$)	Standard Deviation ($cm \cdot s^{-1}$)	Maximum Speed ($cm \cdot s^{-1}$)
CHEMO	247	12.0	9.1	55.5
	537	3.8	3.6	22.5

Basic statistics. Record-length mean, standard deviation, and maximum speeds for the moorings are shown in Table 6.3.8-1. Figure 6.3.8-1 shows the statistics versus depth for all instrument depths. The speed statistics decrease with depth.

General description of records. The bottom record was much less energetic than the mid-column record. As expected, spectra show the inertial band to be clockwise rotating. During August through October 1997, there was a cyclonic feature in the vicinity of the mooring, located between Eddy Deviant to its west and the newly forming Eddy El Dorado to its east. Currents at the mid-column instrument appear to be influenced by this cyclone, e.g., westward speeds of ~20 $cm \cdot s^{-1}$ in August correspond to when the northern limb of the cyclone was adjacent to the mooring. From November 1997 through January 1998, mid-column currents were affected by Eddy El Dorado, as it moved westward to the south of the mooring, and by a cyclone to the north of Eddy El Dorado. The strong (40-50 $cm \cdot s^{-1}$) pulses of eastward and westward currents during this period were related to these two eddy features. Low-frequency oscillations with periods of about 10 days tended to dominate the east-west current component at the mid-column instrument after Eddy El Dorado had moved west and no longer was located south of the mooring (February to the end of the record). These low-frequency oscillations were not seen in the 537-m record.

6.3.9 MAMES Moorings, 1987-1990

Basic description of data. The Geochemical and Environmental Research Group (GERG) of TAMU deployed a number of current moorings as part of the MMS Mississippi-Alabama

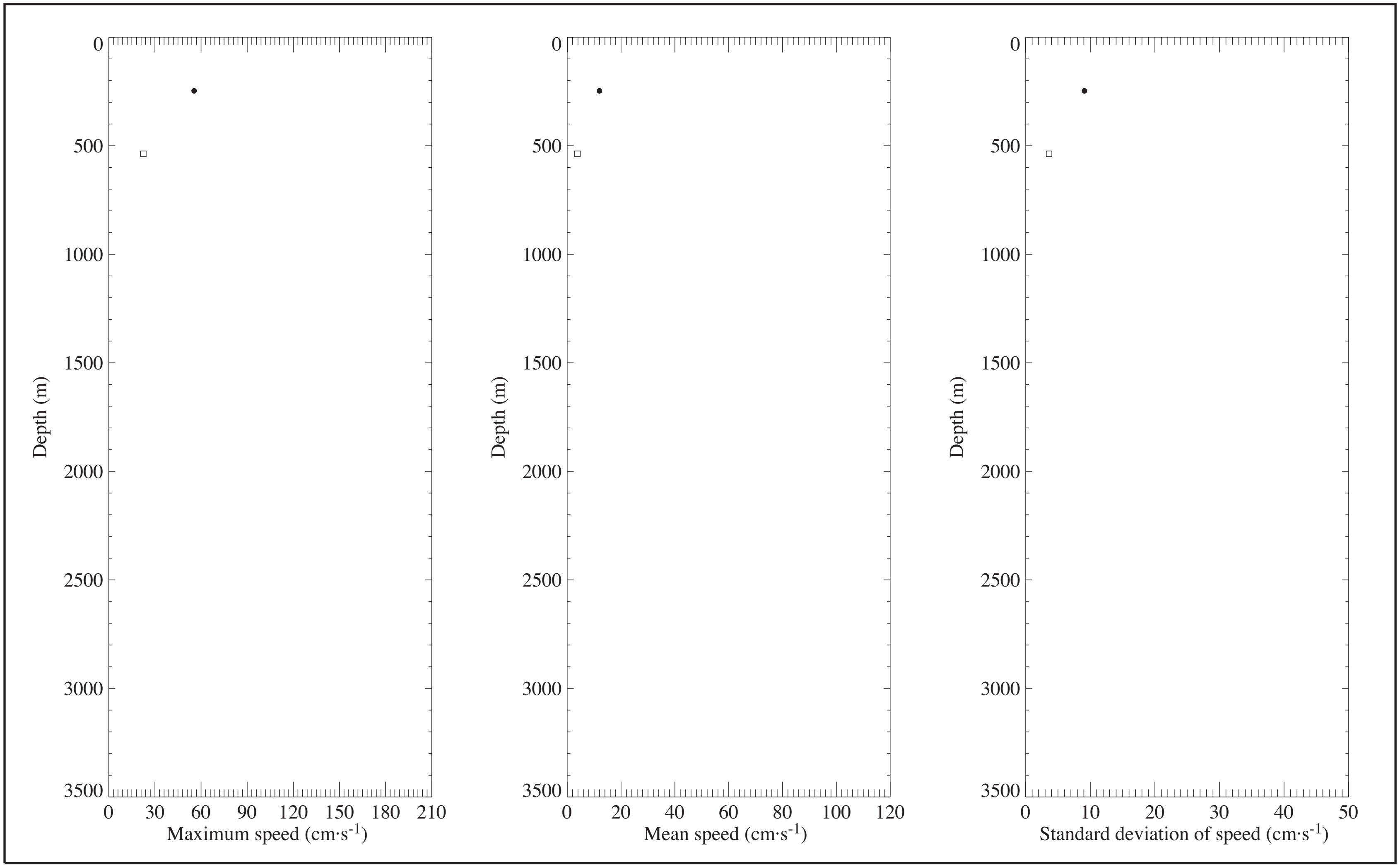

Figure 6.3.8-1. Observed speed (a) maximum, (b) mean, and (c) standard deviation versus instrument depth for unfiltered records from GERG Chemosynthetic central Gulf moorings (npts = 2). Quality codes: A or B (dot), C (square), D (plus).

Continental Shelf Ecosystem Study (MAMES). The results from this study are presented in Brooks (1991). Two of the moorings were located in water depths greater than 200 m and are described here. Data were obtained from GERG. The locations of the moorings are shown in Figure 6.3.9-1. Mooring C was deployed between 30 December 1987 and 10 February 1990, with three- and one-month gaps in, respectively, June–August 1988 and January/February 1989. Mooring E was deployed from 15 February–22 October 1989. Both moorings were in 430-m water depth. Instrument depths are given in Table 6.3.9-1. Time lines and vector stick plots for the data are shown in Figure 6.3.9-2. The quality codes for these data are A, B, C, and D. File names for the current records in the database are

- C: DD871230.C01-C02; DD880825.C01-C02; DD890216.C01-C03; DD890621.C01-C03; DD891023.C01-C03
- E: VK890215.C01-C03; VK890623.C01-C02

Environmental background. There were seven tropical cyclones during the deployment periods: hurricanes Debby (31 August–8 September 1988), Florence (7-11 September 1988), Gilbert (8-20 September 1988), Chantal (30 July–3 August 1989), and Jerry (12-16 October 1989), and tropical storms Keith (17–26 November 1988) and Allison (24 June–1 July 1989). Most were far to the west or south of the mooring. Hurricane Florence came closest. Tropical storm Beryl (8–10 August 1988) was near the moorings, but occurred about two weeks prior to the mooring deployment. There were two extratropical cyclones during the deployment period. Two LCE separations, May 1988 and May-June 1989, occurred during the deployments. The May-June 1989 separation was of Nelson Eddy, which was a particularly large and energetic LCE.

Basic statistics. Record-length mean, standard deviation, and maximum speeds for the moorings are shown in Table 6.3.9-1. Figure 6.3.9-3 shows the statistics versus depth for all instrument depths. The speed statistics show a decrease with depth. Standard deviations are about half of the means. Maximum speeds do not exceed 80 $cm \cdot s^{-1}$.

General description of records. Chapters 10 (physical oceanography/water mass characterization) and 11 (satellite oceanography) of Brooks (1991) provide a detailed discussion of the forcing factors present in the study area and their effects on the currents. Some of these results are summarized here. Of the tropical cyclones, hurricane Gilbert had the most impact, even though its track was in the southern Gulf. While hurricane Gilbert was in the Gulf, currents at all depths on mooring C flowed southwestward. Peak speeds were reached about 15 September 1988. This current response to Gilbert was attributed as being partly a result of basin-scale horizontal pressure gradients set up by the hurricane (Brooks 1991). Other than when the hurricane effects dominated, the flows at 20 m on mooring C were primarily eastward or northeastward. Currents at 426 m were persistently southwestward. At mooring E, predominant flow directions were comparable to those at C, except that at the 20- and 150-m depths the flows were persistently westward or southwestward in October and November 1989. The coherence between the 20- and 426-m records at both C and E was not significant, while that between the 20- and 150-m records was significant in a number of frequency bands. The influence of the intrusion of Loop Current filaments on the water masses and circulation in the study area is examined in Brooks (1991). Intrusions were noted in satellite AVHRR imagery during December 1987, January, March, and May 1988, and February, March, and May 1989 (see Brooks for details). The data from C and E show the influence of intrusions on temperature, but do not show clear changes in the currents. GEOSAT fields (Berger et al. 1996b) show that the developing LCE Nelson during 1989 was substantially south of the moorings.

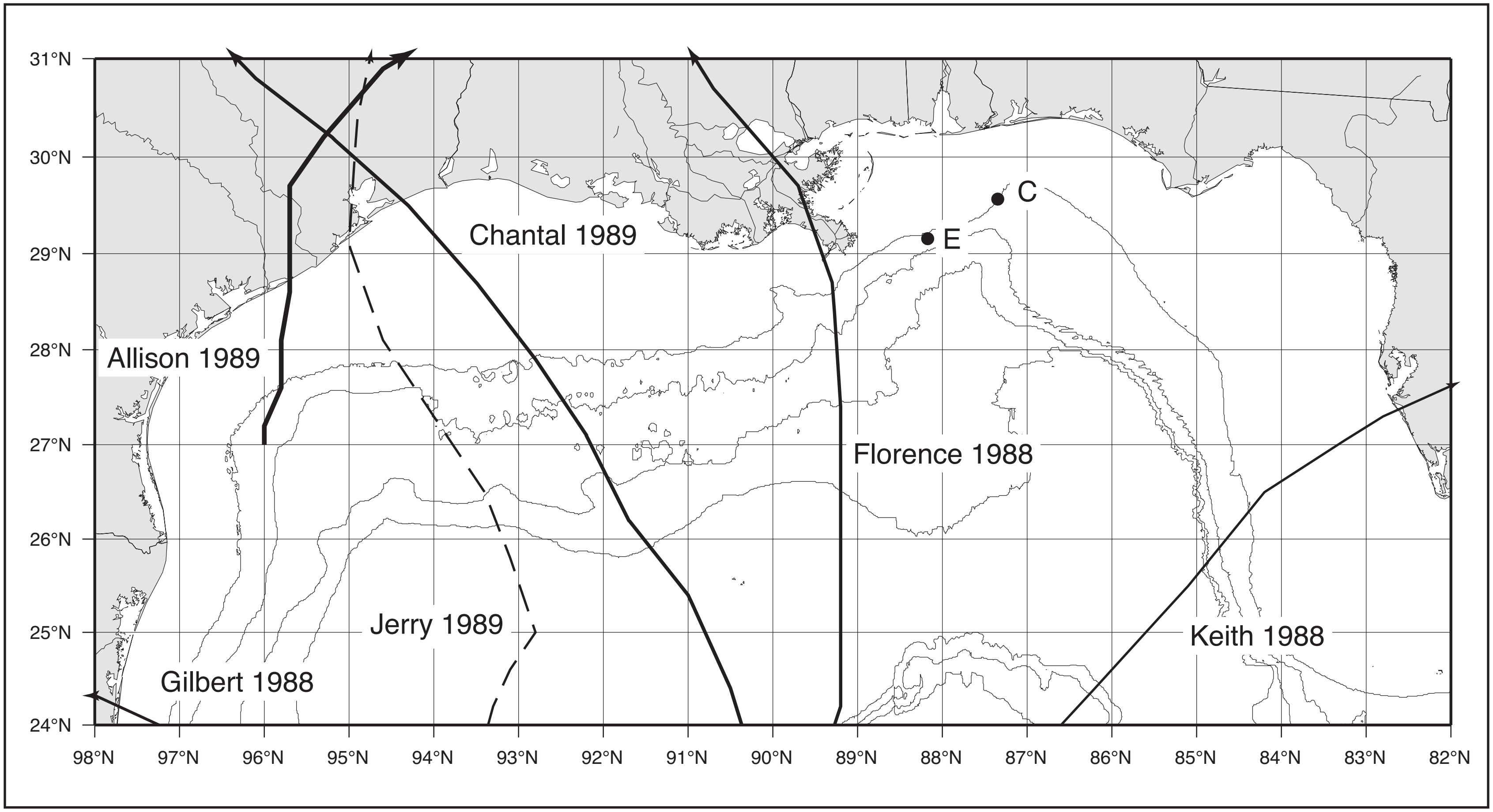

Figure 6.3.9-1. Location map for the 1987-1990 MAMES study moorings. The tracks of tropical storms and hurricanes in the Gulf for the deployment period are shown. Shown are the 200-, 1000-, 2000-, and 3000-m isobaths.

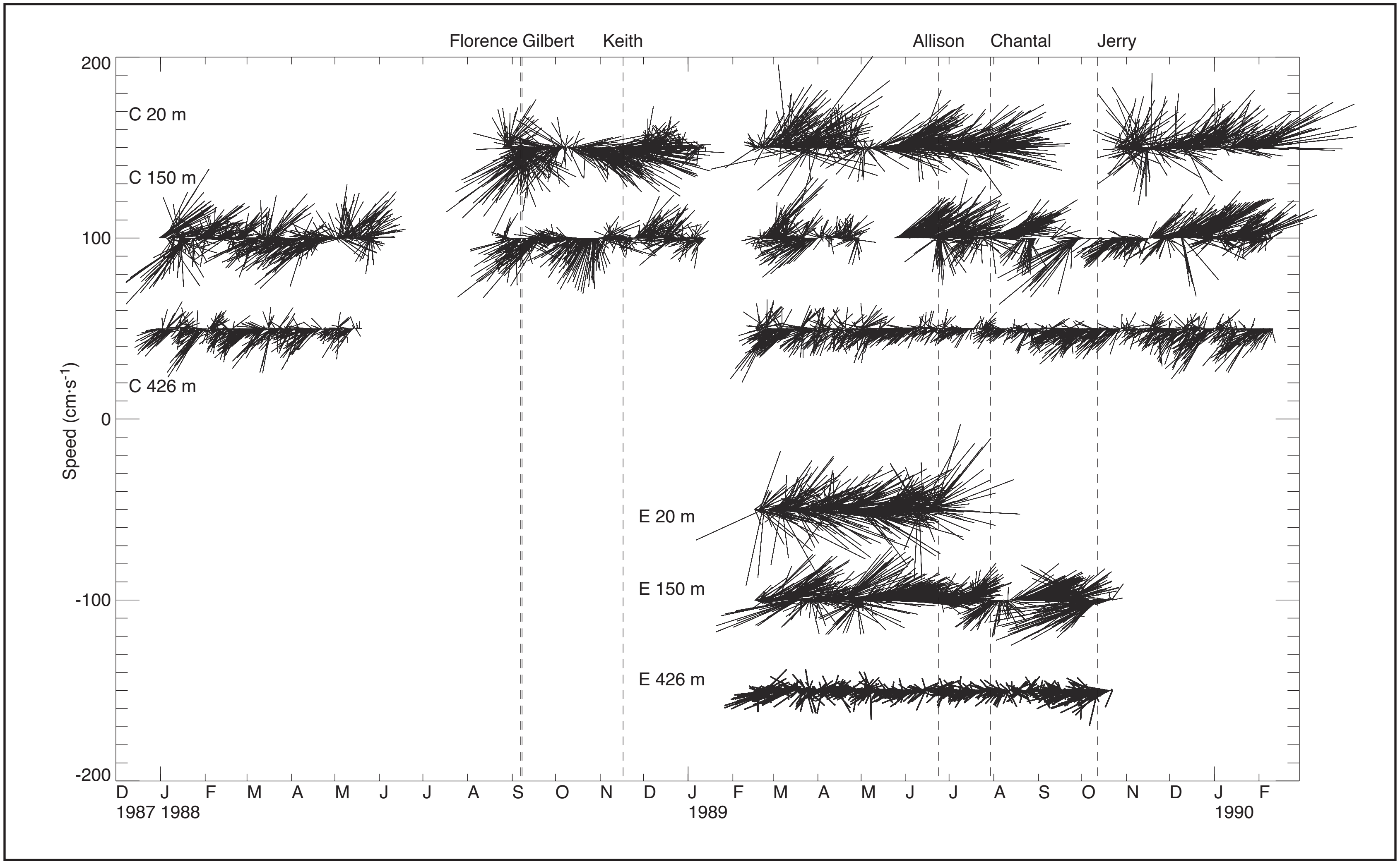

Figure 6.3.9-2. Time lines and vector stick plots for 1987-1990 MAMES moorings in the northeastern Gulf. The first day of tracking for tropical storms and hurricanes in the Gulf during the deployment period is indicated by vertical dashed lines with storm names above. North is upward. Tick marks denote start of the month.

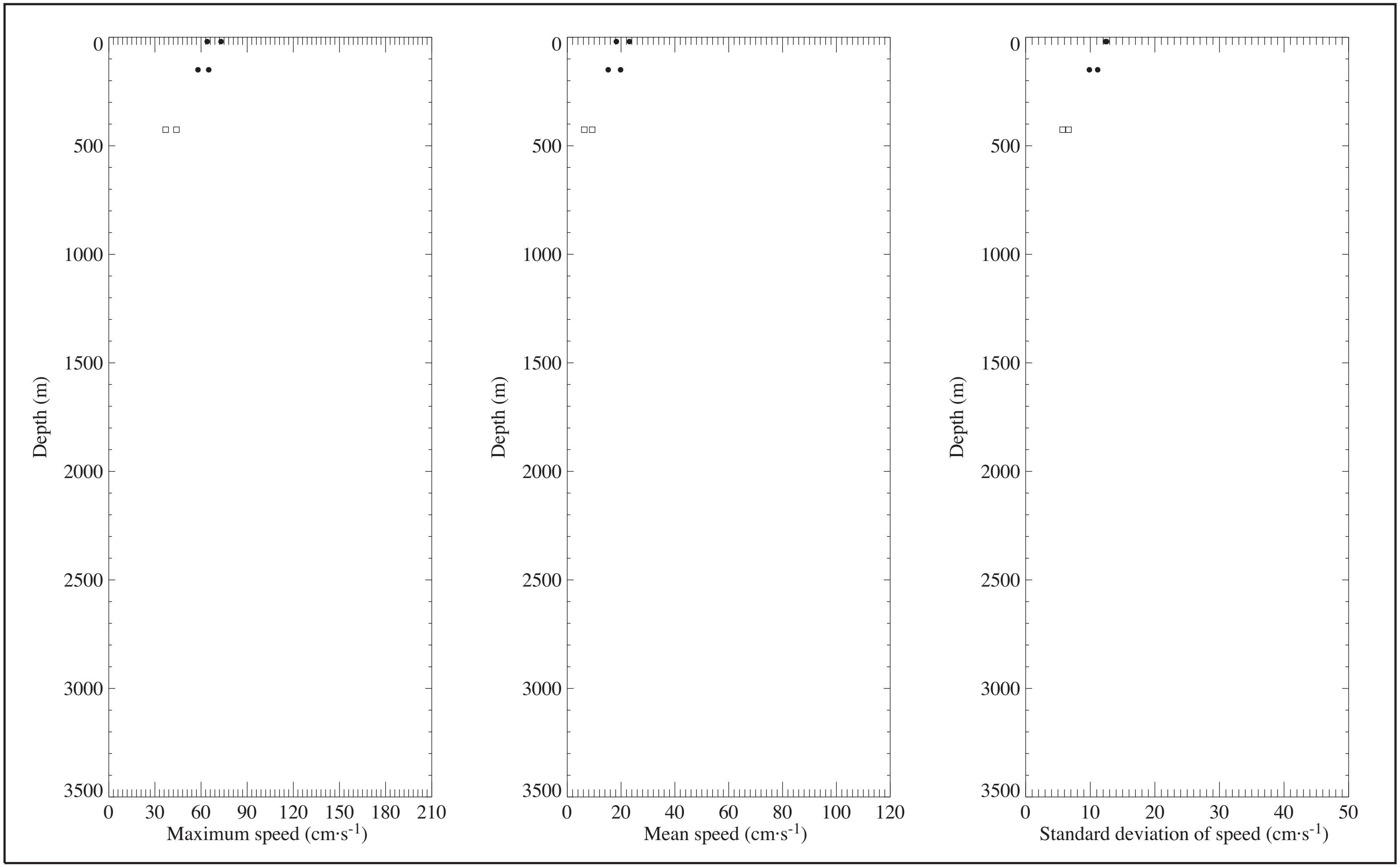

Figure 6.3.9-3. Observed speed (a) maximum, (b) mean, and (c) standard deviation versus instrument depth for unfiltered records from MAMES northeastern Gulf moorings (npts = 6). Quality codes: A or B (dot), C (square), D (plus).

Table 6.3.9-1. Record-length mean, standard deviation, and maximum speed for data from the northeastern Gulf in the GERG 1987-1990 MAMES study. Instruments were current meters.

Mooring	Instrument Depth (m)	Mean Speed ($cm\cdot s^{-1}$)	Standard Deviation ($cm\cdot s^{-1}$)	Maximum Speed ($cm\cdot s^{-1}$)
C	20	18.3	12.5	73.0
	150	15.2	9.9	58.0
	426	9.3	6.6	44.0
E	20	23.1	12.4	64.0
	150	19.8	11.2	65.0
	426	6.4	5.7	37.0

6.3.10 Yucatan Sill Moorings, 1977-1980

Basic description of data. NOAA deployed a mooring halfway between Mexico and Cuba in the Yucatan Channel from 29 October 1977 through 22 November 1980 (Maul et al. 1985). It had two current meters, located 10 m apart, that were approximately 145 m above the sill depth of 2040 m. Because of gaps in the records of both instruments, the data were merged into a single continuous time series. The raw data are not available. Instead, the data file contains the 40-hr low-pass filtered data, decimated to six-hourly intervals, for 3 November 1977 through 19 October 1980. The location of the mooring is shown in Figure 6.3.10-1. The average instrument depth is shown in Table 6.3.10-1. Time lines and vector stick plots for the data are shown in Figure 6.3.10-2. The quality code for the data is A. The file name for the current record in the database is

- YS771103.C01

Environmental background. During the deployment period there were twelve tropical cyclones present in the Gulf of Mexico: hurricanes Bob (9–19 July 1979), Frederic (29 August–15 September 1979), Henri (15–24 September 1979), Allen (31 July–11 August 1980), and Jeanne (7–16 November 1980), and tropical storms Amelia (30 July–1 August 1978), Bess (5–8 August 1978), Debra (26–29 August 1978), Claudette (15–19 July 1979), Elena (30 August–2 September 1979), Danielle (4–7 September 1980), and Hermine (20–26 September 1980). Five of these storms, hurricanes Frederic, Henri, Allen, and Jeanne, and tropical storm Claudette, moved from the Caribbean or Atlantic northward into the Gulf through the Yucatan Channel. The Saffir-Simpson categories of these storms when they moved by the mooring location were hurricane (Allen category 4 and 5, Frederic category 1), tropical storm (Jeanne) and tropical depression (Claudette, Henri). Only these five storms are shown on Figures 6.3.10-1 and 6.3.10-2. There were twelve extratropical cyclones in the Gulf during the deployment period (Table 6.2-4). Three separations of Loop Current eddies from the Loop Current occurred during the deployment: June 1978, April 1979, and January 1980 (Sturges and Leben 2000; see also Table 6.2-1).

Basic statistics. Record-length mean, standard deviation, and maximum speeds for the mooring are shown in Table 6.3.10-1. Figure 6.3.10-3 shows the statistics versus depth for all

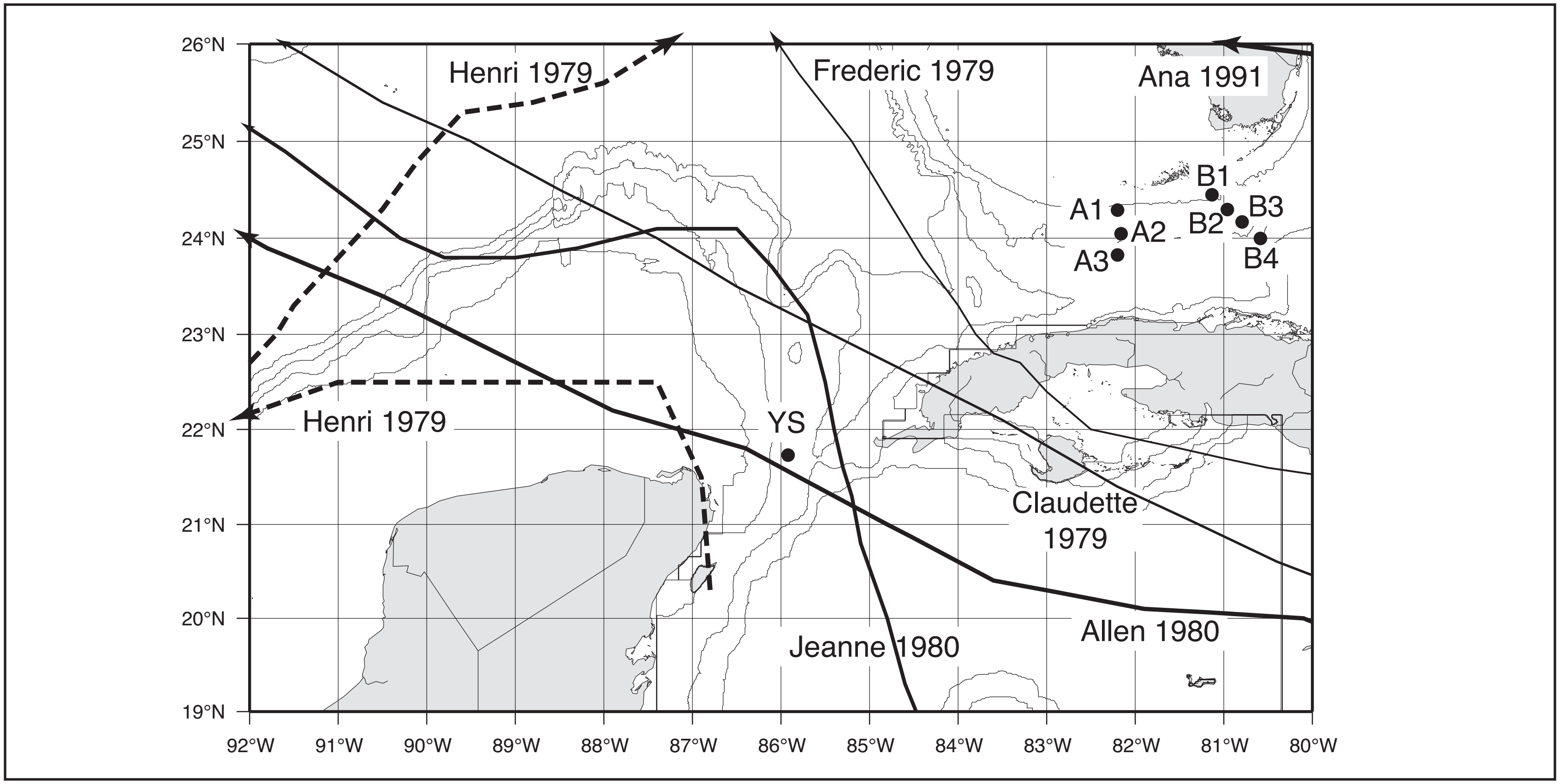

Figure 6.3.10-1. Location map for the NOAA 1977-1980 Yucatan Sill mooring and the 1990-1991 Straits of Florida moorings. The tracks of tropical storms and hurricanes in the Gulf for the deployment periods are shown. Shown are the 200-, 1000-, 2000-, and 3000-m isobaths.

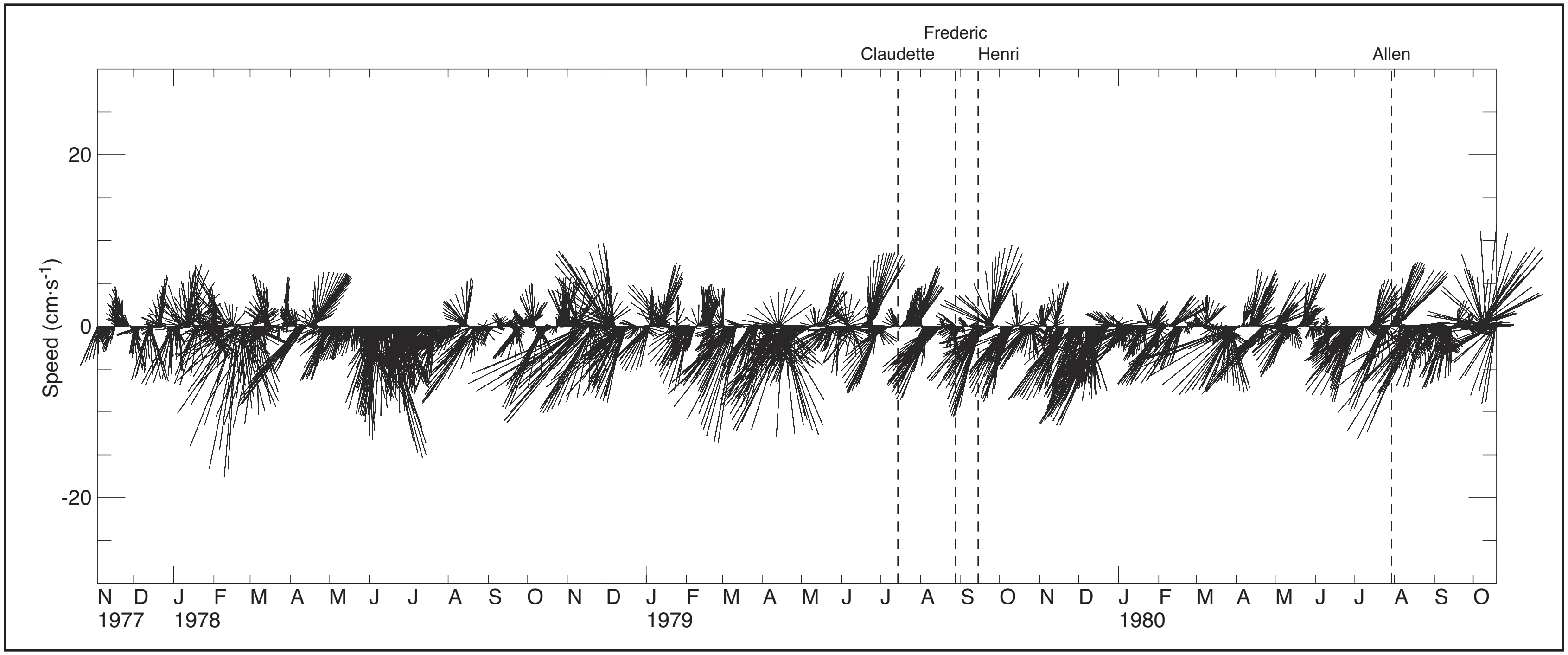

Figure 6.3.10-2. Time line and vector stick plot for the NOAA 1977-1980 Yucatan Sill mooring in the Yucatan Channel. Data are 40-hour low-pass filtered, decimated to six-hourly intervals. The first day of tracking for tropical storms and hurricanes in the Gulf during the deployment is indicated by the vertical dashed line with the storm name given above it. North is upward. Tick marks denote start of the month.

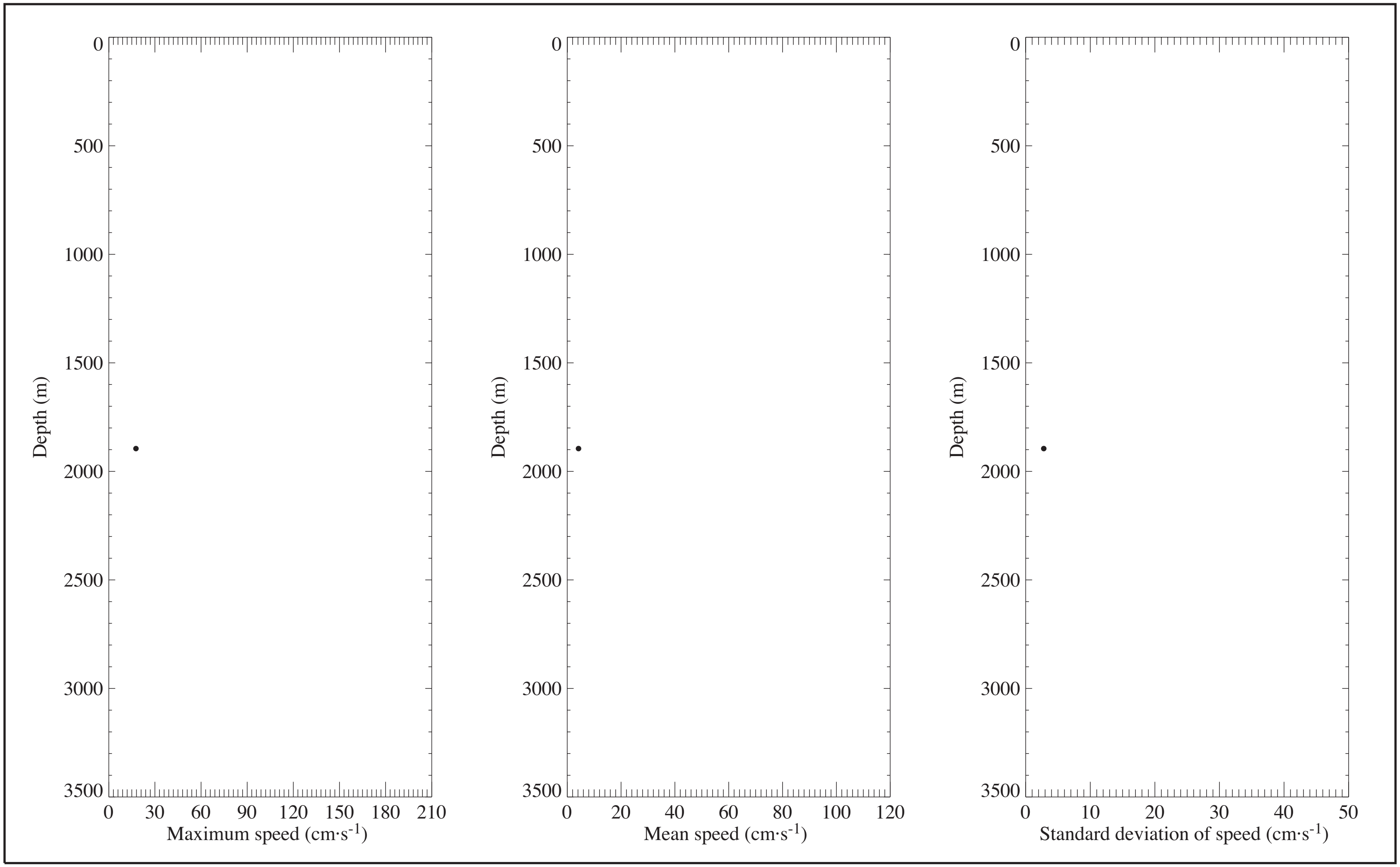

Figure 6.3.10-3. Observed speed (a) maximum, (b) mean, and (c) standard deviation versus instrument depth for unfiltered records for NOAA Yucatan Sill mooring (npts = 1). Quality codes: A or B (dot), C (square), D (plus).

Table 6.3.10-1. Record-length mean, standard deviation, and maximum speed for data from the 1977-1980 Yucatan Sill mooring. These statistics were from the 40-hour low-passed data record, decimated to six-hourly intervals; raw data were not available. Instruments were current meters.

Mooring	Instrument Depth (m)	Mean Speed ($cm \cdot s^{-1}$)	Standard Deviation ($cm \cdot s^{-1}$)	Maximum Speed ($cm \cdot s^{-1}$)
YS	1895	4.2	2.8	17.7

instrument depths. The speed at this deep instrument did not exceed 20 $cm \cdot s^{-1}$. The maximum speed was just over four times the mean speed.

General description of records. The filtered data allow description only of low-frequency currents in the middle of the Yucatan channel. Maul et al. (1985), however, had the raw data available and provided a description of both low-frequency and high-frequency currents. They found the low-frequency (< 14^{-1} $cycles \cdot d^{-1}$) motions were oriented approximately parallel to the isobaths with an average velocity of 1.8 $cm \cdot s^{-1}$. At intervals of approximately 8 months, sustained southward flows, with averages of 5 $cm \cdot s^{-1}$ and bursts up to 15 $cm \cdot s^{-1}$, were observed. Maul et al. (1985) also found the deep Yucatan Channel currents did not have measurable inertial energy from three hurricanes (one of which was category 5) that passed over the mooring. They determined the principal tidal motions were diurnal and oriented approximately northwest, across isobaths, and found no semidiurnal, inertial, or fortnightly energy was present above the noise.

6.3.11 Florida Straits Moorings, 1990-1991

Basic description of data. Seven current moorings deployed in the Florida Straits by SAIC as part of an MMS-sponsored study of the variability of the Florida Current were in water depths greater than 200 m and within the Gulf of Mexico region. See SAIC (1992) for more information. Lee et al. (1995) present results from analysis of these and other data. Four moorings were located across the strait at about 81°W and three at approximately 82°W. The locations are shown in Figure 6.3.10-1. Total water depths were 245 m at A1, 820 m at A2, 1500 m at A3, 200 m at B1, 320 m at B2, 850 m at B3, and 1080 m at B4. The instrument depths are shown in Table 6.3.11-1. The moorings were deployed between 25 November 1990 and 19 August 1991. Time lines and vector stick plots for the data are given in Figure 6.3.11-1. The quality codes for the data are A and B. The file names for the current records in the data base are

- A1: FS901128.C01-C02; FS910216.C01-C02; FS910503.C01
- A2: FS910502.C01-C03; FS910217.C01-C02
- A3: FS910217.C03-C07; FS910504.C01-5
- B1: FS901127.C01-C02; FS910216.C03-C04; FS910502.C04-C05

Table 6.3.11-1. Record-length mean, standard deviation, and maximum speed for data from the 1990-1991 Florida Straits moorings. Instruments were current meters.

Mooring	Instrument Depth (m)	Mean Speed ($cm \cdot s^{-1}$)	Standard Deviation ($cm \cdot s^{-1}$)	Maximum Speed ($cm \cdot s^{-1}$)
A1	75	42.0	38.2	146.5
	150	30.2	25.7	115.9
A2	145	28.2	25.2	101.1
	300	23.2	16.4	78.9
	600	8.8	7.8	45.1
A3	145	55.6	20.8	123.8
	300	34.6	15.0	76.2
	600	9.9	8.9	49.3
	1000	8.2	6.6	39.5
	1400	6.2	4.2	31.1
B1	75	72.9	36.9	180.0
	150	34.2	15.8	90.5
B2	75	104.1	31.9	198.1
	200	54.9	27.6	135.4
B3	30	105.8	22.1	184.4
	48	115.0	18.4	192.4
	66	110.9	16.8	185.5
	84	105.2	16.2	170.6
	102	100.2	15.5	163.4
	120	95.9	14.7	151.7
	138	91.7	13.8	145.4
	156	87.6	12.9	138.0
	174	83.8	13.4	148.6
	192	80.4	13.8	143.3
	210	77.6	13.6	132.0
	228	74.7	13.4	127.3
	246	72.0	13.6	129.9
	273	68.8	13.1	117.3
	300	61.1	14.6	120.1
	600	32.0	15.9	82.3
	805	9.8	6.5	40.3
B4	145	70.8	15.0	158.7
	300	52.4	12.2	105.1
	600	26.3	10.4	58.0
	1000	9.3	5.2	34.6

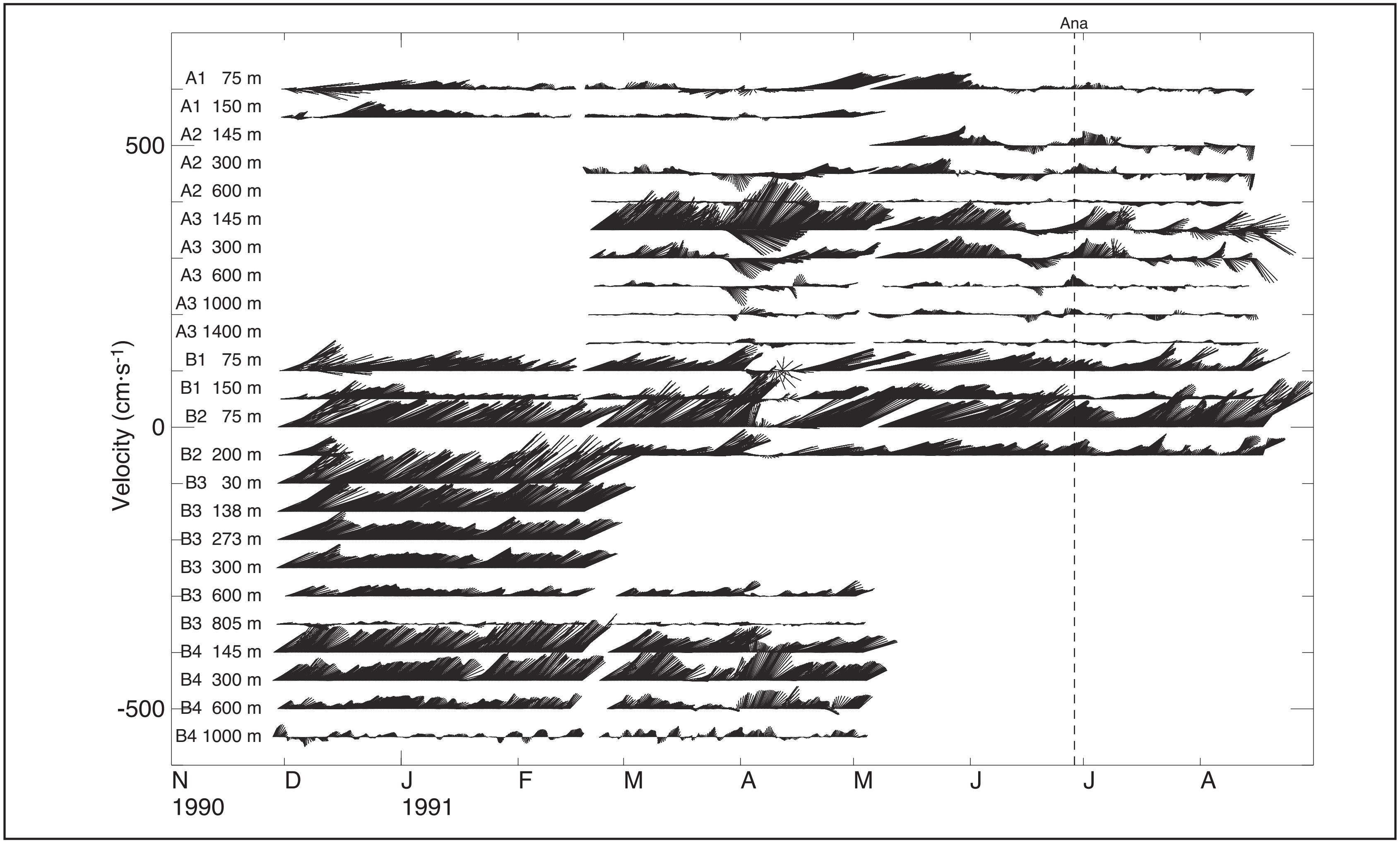

Figure 6.3.11-1. Time lines and vector stick plots for the 1990-1991 Straits of Florida moorings. The first day of tracking for tropical storms and hurricanes in the Gulf during the deployment period is indicated by the vertical dashed line with the storm name given above it. North is upward. Tick marks denote start of the month.

- B2: FS901127.C03-C04; FS910219.C01-C02; FS910505.C01-C02
- B3: FS901126.C01-C17; FS910222.C01-C03
- B4: FS901125.C01-C04; FS910220.C01-C04

Environmental background. One tropical cyclone, which barely entered the Gulf, occurred during the deployment of the Straits of Florida current moorings: Tropical Storm Ana (29 June–5 July 1991). Five extratropical cyclones occurred during the deployment period (Table 6.2-4). Eddy Triton separated from the Loop Current in August-September 1991, which was near the end of the deployment period.

Basic statistics. Record-length mean, standard deviation, and maximum speeds for the mooring are shown in Table 6.3.11-1. Figure 6.3.11-2 shows the statistics versus depth for all instrument depths. The speed statistics decrease with depth. The greatest maximum speeds reach 200 $cm \cdot s^{-1}$. Highest mean values are in the upper 100 m and are excess of 100 $cm \cdot s^{-1}$. Even down to the ~500-m depth, mean speeds are in excess of 50 $cm \cdot s^{-1}$. These show the presence of the Florida Current in the vicinity of the moorings.

General description of records. These currents show the influence of the Florida Current. Currents generally have an eastward component and often exceed 100 $cm \cdot s^{-1}$. Flows are vertically coherent at ~600 m and above. Lee et al. (1995) discuss the effects of meanders of the Florida Current and of a cold, cyclonic recirculation that develops off the Dry Tortugas. Onshore meanders of the Florida Current front lead to intensified (≥ 100 cms^{-1}) eastward flows (e.g., see mooring A1 at 75 m in January 1991 in Figure 6.3.11-1). Offshore shifts of the front can weaken (~30 $cm \cdot s^{-1}$) and reverse the currents to westward (e.g., see mooring A1 at 75 m in March 1991 in Figure 6.3.11-1). The meander and gyre features can propagate eastward.

6.3.12 Industry Moorings

The petroleum industry made a number of their current data sets available for use in the Deepwater Study. Those sets that were provided as proprietary are not included on the CD-ROM and are not described here. The non-proprietary data sets, however, are included on the CD-ROM and, for records with lengths of a few days or more, are described below. When no actual location is unavailable, the measurement location is given as the center of the lease block and a notation is made in the metadata. Several instruments were freely suspended in the upper 20 m from a drill rig. For a few of these, the exact instrument depth is unknown. Measurement depths from these instruments are estimated, and a notation is made in the metadata. Users of these data should note: (1) these data and any analyses therefrom were provided without any warranty of any kind, either express or implied, by the study participants, sponsors, or contributors of data, and (2) the entire risk of use of the data or analyses is with the user.

6.3.12.1 Industry Moorings, 1980-1981

Basic description of data. Moored current meters were deployed in lease blocks GC137 and GC184. Data were collected by Conoco. Locations of the moorings are shown in Figure 6.3.12-1. Five current meters were deployed in GC137 in 350 m water depth from 16 December 1980 through 18 January 1981. Six current meters were deployed in GC184 in a water depth of 435 m from 19 January through 22 April 1981. Five returned acceptable current data. Currents for the 300-m instrument were bad, so only the temperature data (file not listed) are provided on the CD-ROM. The 100-m record at GC184 behaves oddly, with extended periods of low current speeds (~1 $cm \cdot s^{-1}$) and pulses where the current velocity goes

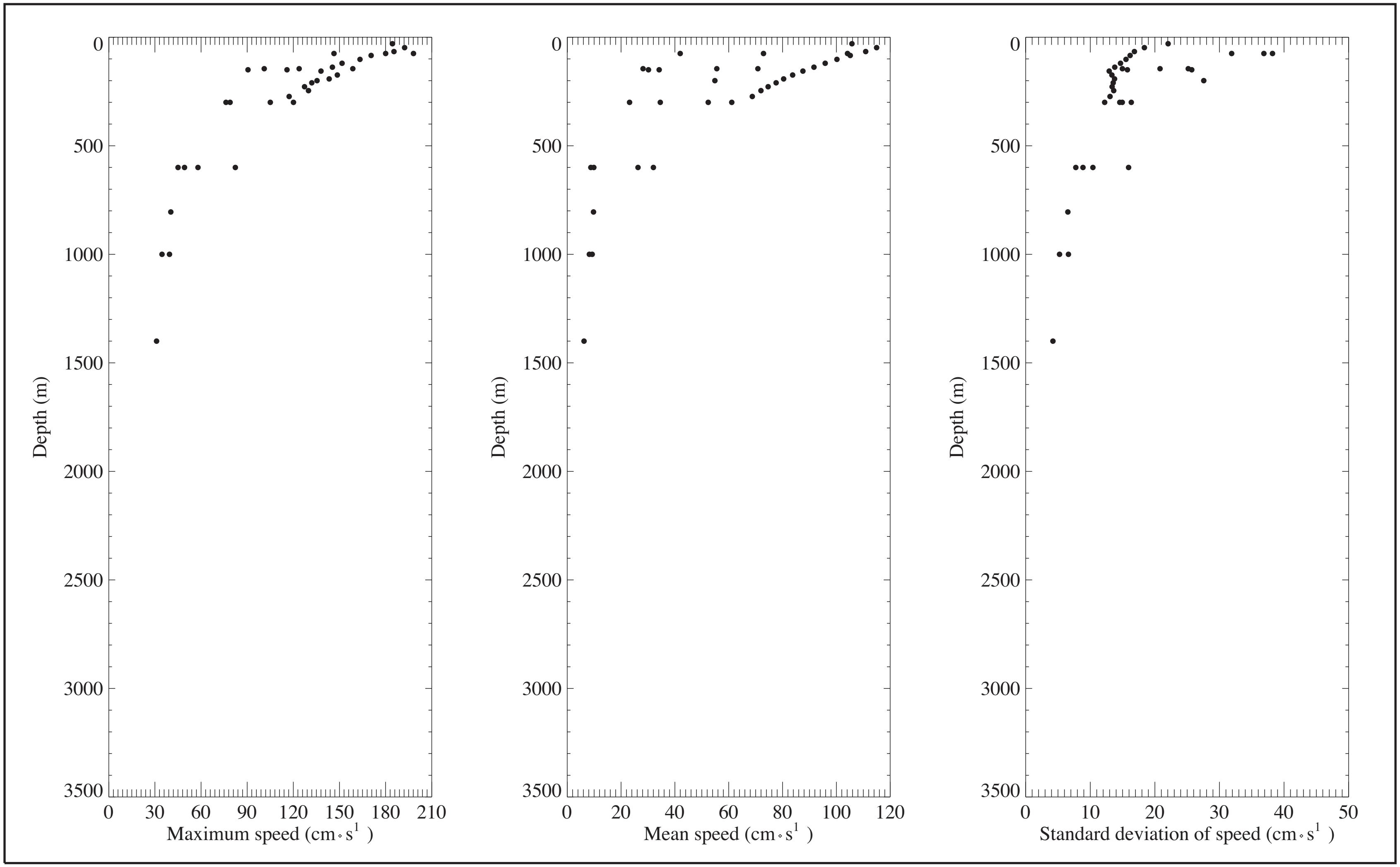

Figure 6.3.11-2. Observed speed (a) maximum, (b) mean, and (c) standard deviation versus instrument depth for unfiltered records from SAIC Straits of Florida moorings (npts = 35). Quality codes: A or B (dot), C (square), D (plus).

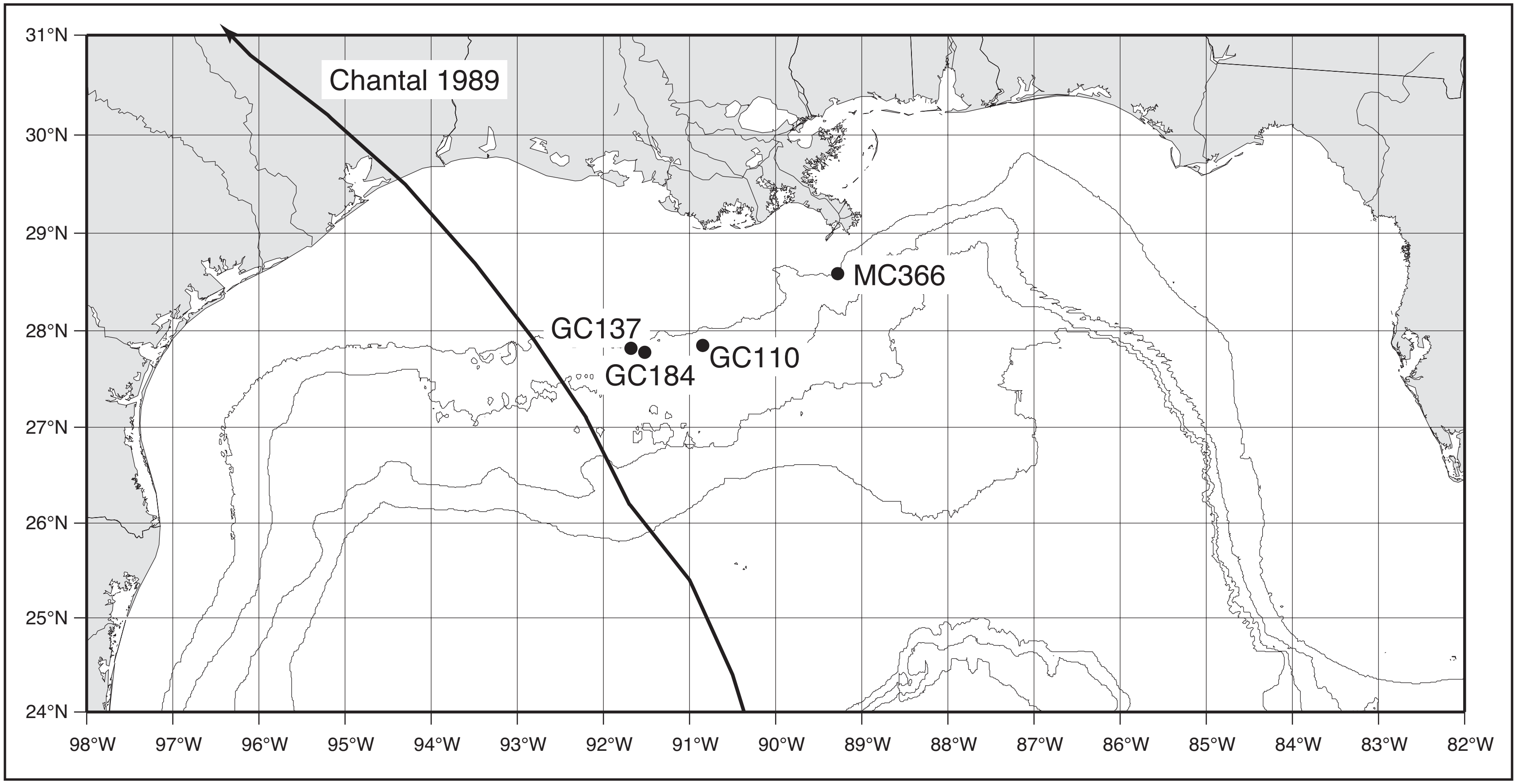

Figure 6.3.12-1. Location map for non-proprietary industry moorings, deployed during 1980, 1981, and 1984, in water depths greater than 200 m. The tracks of tropical storms and hurricanes in the Gulf for the deployment periods are shown. Shown are the 200-, 1000-, 2000-, and 3000-m isobaths.

from low to higher (20 $cm \cdot s^{-1}$) speeds at nearly uniform intervals; this record should be used with caution. Instrument depths are given in Table 6.3.12-1. Figure 6.3.12-2 shows the time lines and vector stick plots for the moorings. The quality codes for these data are B and C at GC137 and B and D at GC184. File name for the current records in the data base are

- GC137 GC801216.C01; GC801217.C01-C04
- GC184 GC810119.C01-C02; GC810119.C03; GC810119.C04-C05

Environmental background. There were no tropical cyclones during these deployments. One extratropical cyclone occurred on 20 January 1981, during deployment of the GC184 mooring. There were no eddy separations during these deployments.

Basic Statistics. Record-length mean, standard deviation, and maximum speeds for the moorings are shown in Table 6.3.12-1. Figure 6.3.12-3 shows the statistics versus depth for all instrument depths. The speed statistics generally decrease with increasing depth at both locations. Maximum speeds in the upper 200 m at GC184 were 40-50 $cm \cdot s^{-1}$; these were associated with the extratropical cyclone.

General description of records.
GC137: Currents were generally northward during this one-month deployment. Near bottom currents were mostly southward and very weak. Currents in the upper 100 m were basically coherent for low frequencies, but deeper instruments had less coherence at low frequencies. Low amplitude inertial oscillations existed at all depths. A current event in excess of 40 $cm \cdot s^{-1}$ and persisting more than one day occurred in the 38 and 79 m records around 3 January 1981.

Table 6.3.12-1. Record-length mean, standard deviation, and maximum speed for data from the 1980-1981 industry moorings. Instruments were current meters.

Mooring	**Instrument Depth (m)**	**Mean Speed ($cm \cdot s^{-1}$)**	**Standard Deviation ($cm \cdot s^{-1}$)**	**Maximum Speed ($cm \cdot s^{-1}$)**
GC137	38	16.3	8.0	48.0
	79	14.7	7.0	39.0
	107	9.9	7.8	31.7
	156	10.6	4.3	23.9
	306	3.1	1.6	9.1
GC184	35	17.5	9.4	48.1
	65	15.9	8.9	51.5
	100	12.3	9.4	41.6
	150	12.3	7.4	42.8
	400	5.5	4.4	27.6

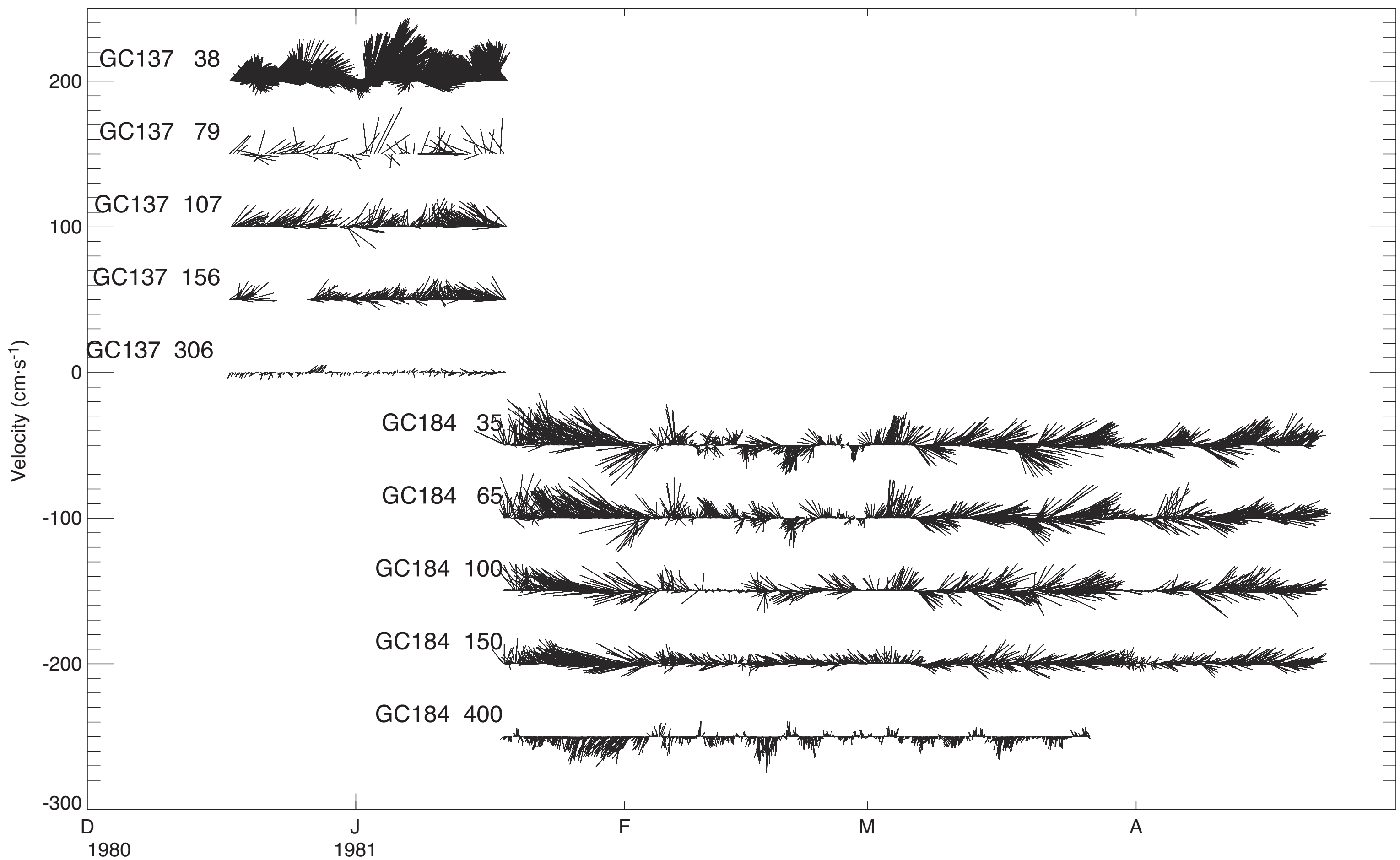

Figure 6.3.12-2. Time lines and vector stick plots for non-proprietary industry moorings, deployed during 1980 and 1981, in water depths greater than 200 m. There were no tropical storms or hurricanes in the Gulf for the deployment periods. North is upward. Tick marks denote start of the month.

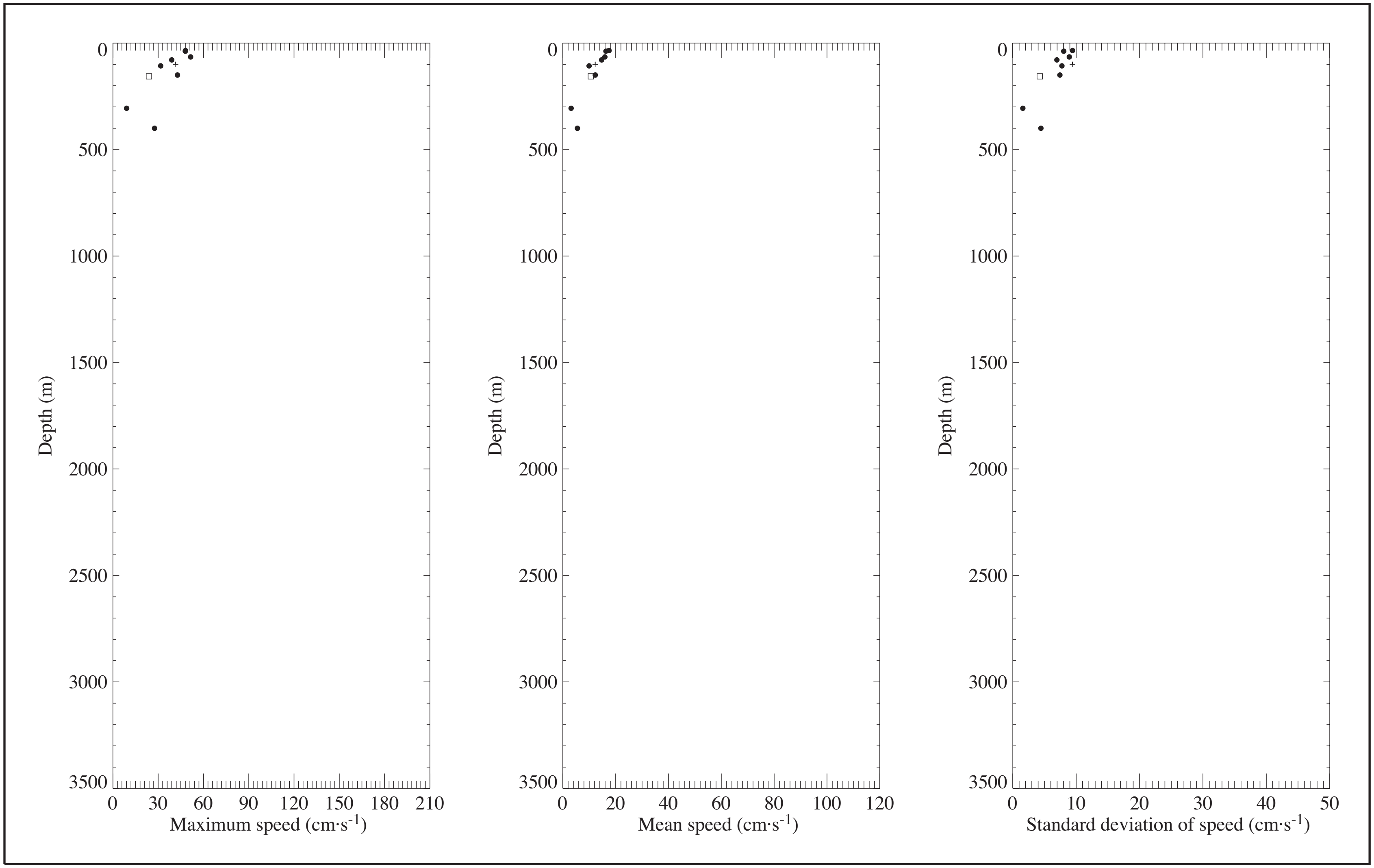

Figure 6.3.12-3. Observed speed (a) maximum, (b) mean, and (c) standard deviation versus instrument depth for unfiltered records from 1980-1981 industry moorings (npts = 10). Quality codes: A or B (dot), C (square), D (plus).

GC184: Currents were generally variable during this three-month deployment. They were westward during the first half and eastward during the second. The 35- and 65-m records were highly coherent throughout the deployment. Coherence of the mid-water records (100 and 150 m) with upper records decreased with depth and was highest during the March and April 1981 period of the deployment. The 400-m record showed no low-frequency coherence with the records above it. Strongest currents occurred about the time of the extratropical cyclone. Low amplitude inertial oscillations were present at all depths.

6.3.12.2 Industry Moorings, 1984

Basic description of data. Industry current moorings were deployed in 1984 in lease blocks GC110 and MC366. Data were provided by Marathon Oil. Locations of the moorings are shown on Figure 6.3.12-1.

The GC110 deployment was from 21 March through 4 July 1984. Two current meters, placed at 213 and 305 m, were moored approximately 1.5 miles southeast of a drill ship. These data were supplemented with current profiler data obtained by lowering a current meter from the drill ship through the water column. The results for each 20-m bin were averaged and then interpolated to the hourly intervals given in the data set. The 20-m bins were centered on the depths reported in the file as the instrument depth (see also Table 6.3.12-2). Twelve time series were created with two depths from moored current meters and ten depths from the profiling.

Measurements were made at MC366 from 17–26 December 1984. The technique used was to lower the current meter through the water column and then average the results within 20-m bins centered at the depths given in the files and shown in Table 6.3.12-2. Time series at nine different depths were formed and the hourly values, reported in the files, were produced by interpolation.

Water depths at the moorings were 489 m at GC110 and 222 m at MC366. Instrument depths are given in Table 6.3.12-2. Figure 6.3.12-4 shows the time lines and vector stick plots for these moorings. The quality codes for these data are B and D at GC110 and A at MC366. File names for the current records in the data base are

- GC110 GC840321.C01-C02; GC840326.C01-C10
- MC366 MC841217.C01-C09

Environmental background. There were no tropical storms, hurricanes, extratropical cyclones, or eddy separations during these deployments.

Basic statistics. Record-length mean, standard deviation, and maximum speeds for the mooring are shown in Table 6.3.12-2. Figure 6.3.12-5 shows the statistics versus depth for all instrument depths. Speed statistics generally decrease with depth. There is an indication of bottom intensification at GC110, but this may be due to the spatial separation of moored current meter data (the bottom two measurements) from profiling current meter data (averaged over 20-m bins from the remainder of the water column) or to the difference in measurement techniques.

General description of records.
GC110: The most energetic flows began 29 May 1984 and persisted throughout June to the end of the record. No currents exceeded 50 $cm \cdot s^{-1}$. Flow is somewhat coherent with depth, with speeds diminishing with depth in the upper 200 m. The flows measured by the deeper,

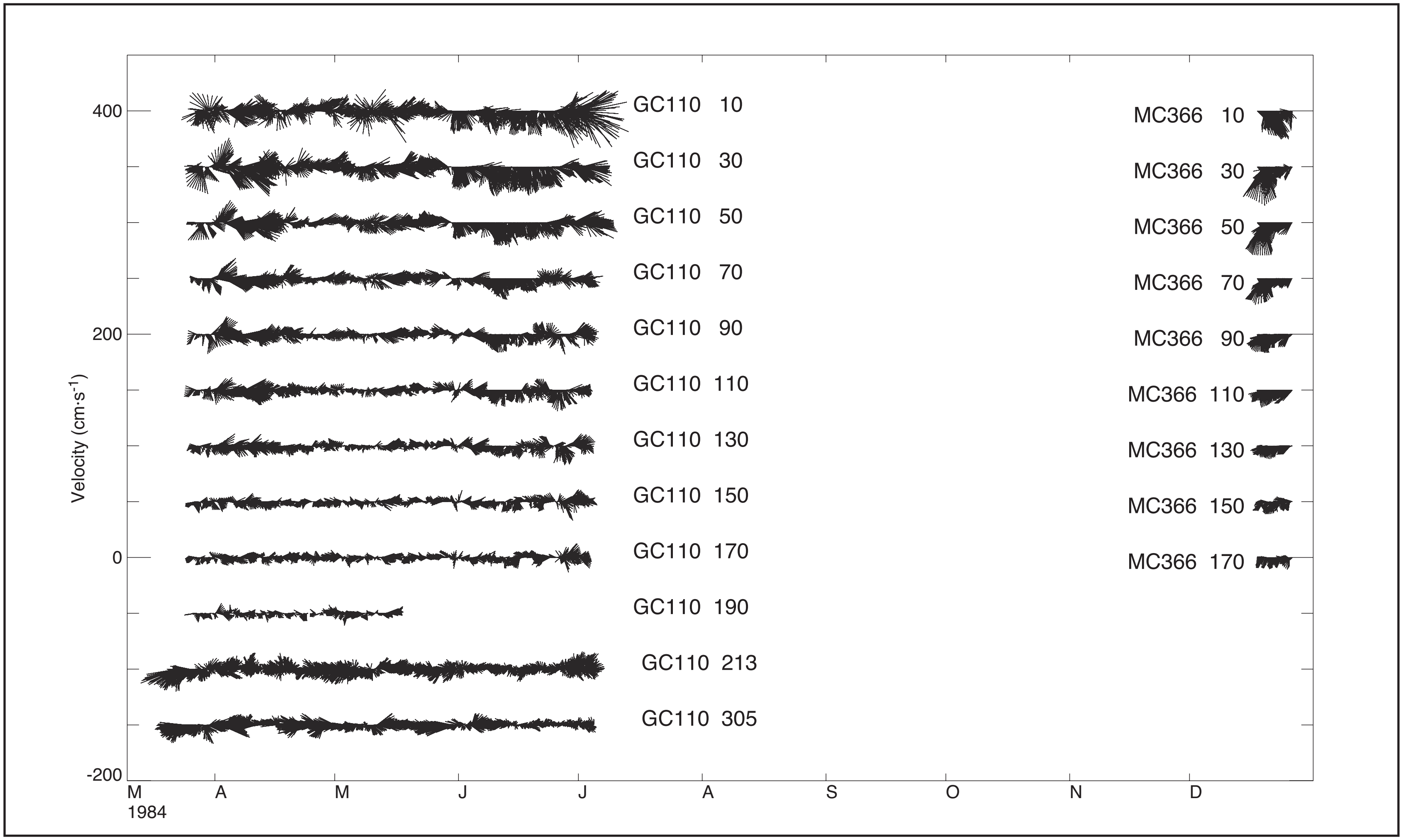

Figure 6.3.12-4. Time lines and vector stick plots for non-proprietary industry moorings, deployed during 1984, in water depths greater than 200 m. There were no tropical storms or hurricanes in the Gulf for the deployment periods. North is upward. Tick marks denote start of the month.

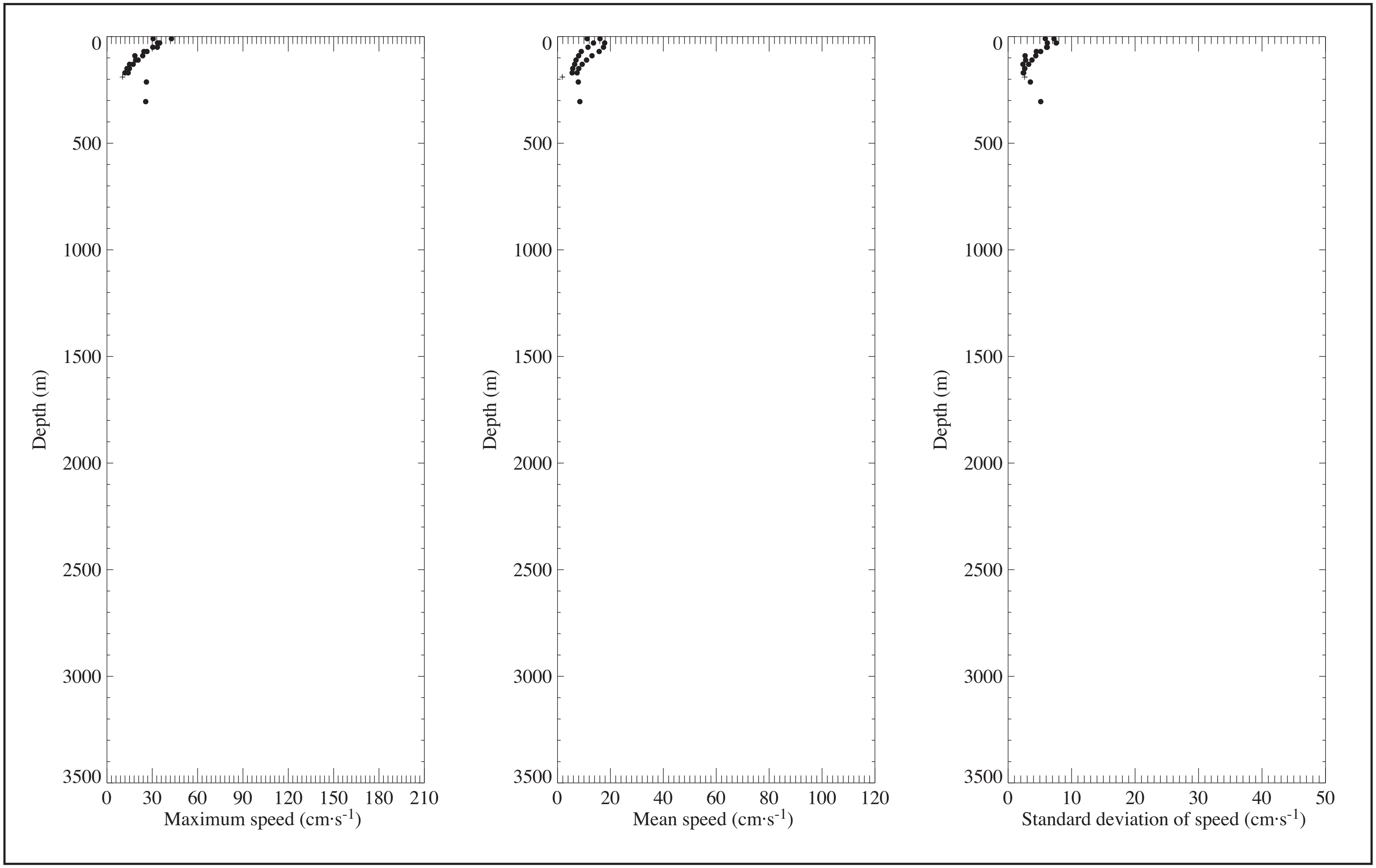

Figure 6.3.12-5. Observed speed (a) maximum, (b) mean, and (c) standard deviation versus instrument depth for unfiltered records from 1984 industry moorings (npts = 21). Quality codes: A or B (dot), C (square), D (plus).

Table 6.3.12-2. Record-length mean, standard deviation, and maximum speed for data from the 1984 industry moorings. Instruments were current meters.

Mooring	Instrument Depth (m)	Mean Speed ($cm \cdot s^{-1}$)	Standard Deviation ($cm \cdot s^{-1}$)	Maximum Speed ($cm \cdot s^{-1}$)
GC110	10	11.2	5.9	42.7
	30	13.6	6.2	33.5
	50	11.5	6.2	33.4
	70	9.0	5.1	26.5
	90	8.0	4.4	23.7
	110	7.0	3.8	20.7
	130	6.5	3.2	17.4
	150	5.8	2.6	14.9
	170	5.6	2.5	14.1
	190	1.8	2.6	10.3
	213	7.9	3.5	26.1
	305	8.5	5.1	25.7
MC366	10	16.1	7.2	30.6
	30	17.8	7.6	34.9
	50	17.4	6.1	30.4
	70	15.8	4.5	24.5
	90	13.0	2.7	18.5
	110	11.0	2.8	19.0
	130	9.3	2.3	15.0
	150	8.0	2.6	13.3
	170	7.4	2.4	11.9

moored current meters were more energetic than those between ~100 and 200 m. The lack of near-surface speeds in excess of 50 $cm \cdot s^{-1}$ suggests that no major events influenced the site during the deployment period.

MC366: Currents during the nine days of the deployment generally had a southward component throughout the water column. The most energetic period was near the beginning of the record with speeds of ~35 $cm \cdot s^{-1}$ at 30 m (20- to 40-m depth interval). This suggests that no major events influenced the currents at the site during the deployment period.

6.3.12.3 Industry Moorings, 1991-1994

Basic description of data. Industry moorings deployed during 1991-1994 were in EW873, EW1006, and GC200. There were four deployments at EW873, three in 1991 and one in 1994. Data were provided by Marathon Oil. Figure 6.3.12-6 shows the locations of the moorings (GC200A notes the location of the 1994 GC200 mooring). Estimated instrument depths are given in Table 6.3.12-3. The first bin in the database for these sites consists of temperature only; this file is not listed below.

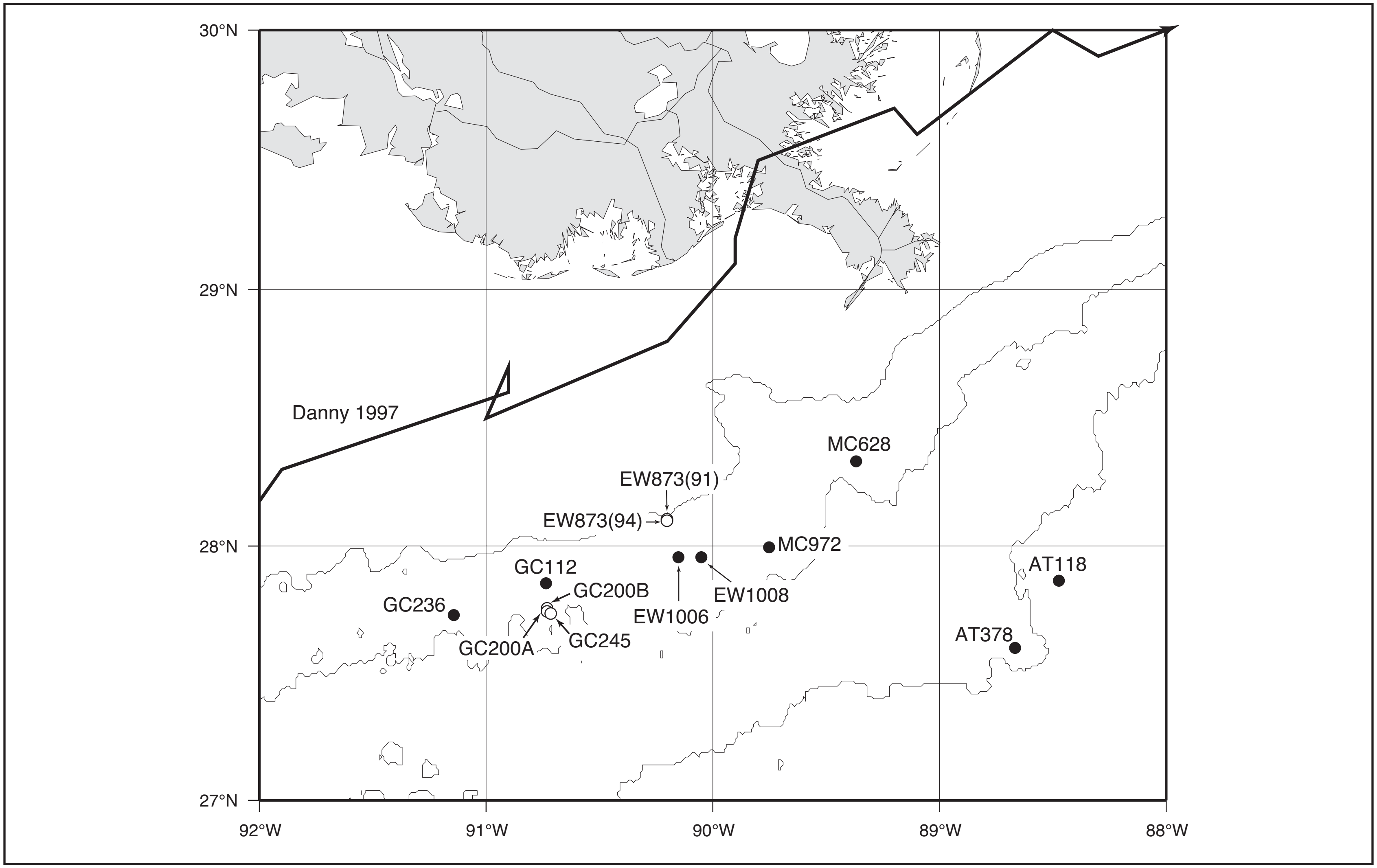

Figure 6.3.12-6. Location map for non-proprietary industry moorings, deployed during 1991-1998, in water depths greater than 200 m. The tracks of tropical storms and hurricanes in the Gulf for the deployment periods are shown. Shown are the 200-, 1000-, and 2000-m isobaths.

Table 6.3.12-3. Record-length mean, standard deviation, and maximum speed for data from the 1991-1994 industry moorings. The asterisk indicates the instrument was a current meter; others are selected depths from a suspended ADCP. Depths are estimated.

Mooring	Instrument Depth (m)	Mean Speed ($cm \cdot s^{-1}$)	Standard Deviation ($cm \cdot s^{-1}$)	Maximum Speed ($cm \cdot s^{-1}$)
EW873 (1991)	20*	43.7	29.9	199.9
	31	22.0	17.5	87.9
	63	20.1	16.8	91.2
	95	17.1	14.5	74.1
	127	12.6	10.0	66.0
	199	7.1	3.8	26.5
EW1006	20	28.9	13.3	70.1
	52	25.3	12.7	64.2
	84	18.6	8.9	44.7
	116	15.9	9.9	42.6
	404	21.0	9.0	53.9
GC200	31	16.9	9.3	48.5
	63	14.8	8.1	42.2
	95	14.6	7.9	44.6
	127	11.9	6.5	41.5
	447	10.4	5.8	36.6
EW873 (1994)	31	23.3	11.8	54.9
	63	18.4	10.5	47.9
	95	13.0	8.4	40.6
	127	15.1	8.1	40.0
	223	13.8	8.0	36.2

The first deployment at EW873 occurred from 30 June–2 September 1991 and consisted of a single current meter suspended from a drill ship in the upper 20 m (EW873A). The instrument was deployed near-surface, but the actual depth is uncertain; a nominal depth of 20 m is given in Table 6.3.12-3. A short ADCP deployment was made at the same location from 6–13 September 1991 (EW873B), followed by a longer ADCP deployment from 20 September through 24 December 1991 (EW873C). The ADCP also was suspended from a drill ship in the upper 20 m. The depth range for both ADCP deployments covers approximately 23 to 231 m in 8-m bins. The total water depth at this location was 236 m. On Figure 6.3.12-6, these three deployments were located at the mooring labeled EW873 (91).

From 15 September through 8 December 1993, a suspended ADCP was deployed for Marathon Oil by Evans-Hamilton, Inc., at EW1006. Water depth at this site was 584 m. Data coverage extended from approximately 12 to 460 m in 8-m bins.

The 1994 deployment in EW873 (EW873C) was a suspended ADCP deployed by Evans-Hamilton, Inc., for Marathon Oil. The total water depth at the site was 236 m. The deployment began 21 May 1994 and ended 2 June 1994. The vertical range of data is 23 to 223 m in 8-m bins.

The 1994 GC200 deployment was from 12 February through 2 June 1994. The estimated vertical range of data coverage was 23 to 463 m in 8-m bins. Total water depth was 895 m.

Figure 6.3.12-7 shows the time lines and vector stick plots for these moorings. The quality codes for these data are C and D. File names for the current records in the data base are

- EW873A EW910630.C01
- EW873B/C EW910906.A01-A31; EW910920.A01-A26
- EW1006 EW930915.A01-A56
- EW873 (94) EW940521.A01-A28
- GC20094 GC940212.A01-A55

Environmental background. During the 1991 deployments at EW873, Tropical Storm Ana passed through the Gulf (29 June–5 July 1991) well east of the site. Eddy Triton separated during August-September 1991. One extratropical cyclone occurred on 30 November 1991. During the 1993 deployment at EW1006, Hurricane Gert (14–21 September 1993) passed through the Gulf of Mexico well south of the site. No extratropical cyclones developed. Loop Current Eddy X-tra separated from the Loop Current during September 1993. During the period of the 1994 GC200 deployment, no tropical cyclones were present in the Gulf of Mexico during this deployment. Extratropical cyclones passed through the Gulf on 1 March, 22 April, and 3 May 1994. A slope eddy passed over the mooring in April. During the 1994 deployment at EW873, no tropical or extratropical cyclones were present in the Gulf. A slope eddy was present at the site in late May 1994.
Basic statistics. Record-length mean, standard deviation, and maximum speeds for the mooring are shown in Table 6.3.12-3. The time series for EW873B and EW873C were merged to compute the basics statistics. Figure 6.3.12-8 shows the statistics versus depth for all instrument depths. The speed statistics generally decrease with depth. There is indication of bottom intensification at EW1006.

General description of records.
EW873 (91): The current meter at an estimated 20-m depth measured high northward currents during much of its deployment. During this time, the Loop Current was extended northwestward to near the site. Maximum speeds measured by the ADCPs exceeded 50 $cm \cdot s^{-1}$ in the upper 150 m in September, when Eddy Triton separated from the Loop Current and moved by the mooring site. These currents were northeastward, consistent with the influence of the passage of the north side of an LCE by a site.

EW1006: During September 1993, currents in the upper 400 m were persistent and southwestward. During this time, the measurement site was located on the north side of a small cyclone that was north of and between LCE Whopper and LCE X-tra. Amplitudes during this period were 20-25 $cm \cdot s^{-1}$ with a subsurface maximum near 200-250 m. Hurricane Gert (September 14-21) turned the near-surface records toward the north. After the storm, these currents resumed a southwestward direction. In October, X-tra Eddy passed south of the site. Near-surface (0-100 m) currents were southeastward at about 50 $cm \cdot s^{-1}$. After the eddy moved farther west away from the site, currents below 75 m were more variable, with 7- to 10-d period oscillations during November and December.

GC200 (1994): Low-frequency currents were generally weak (less than 40 $cm \cdot s^{-1}$) with an oscillation period of about 10 d. There were no significant events until late April when a peanut-shaped slope anticyclone passed the site. Currents rotated clockwise from southwest

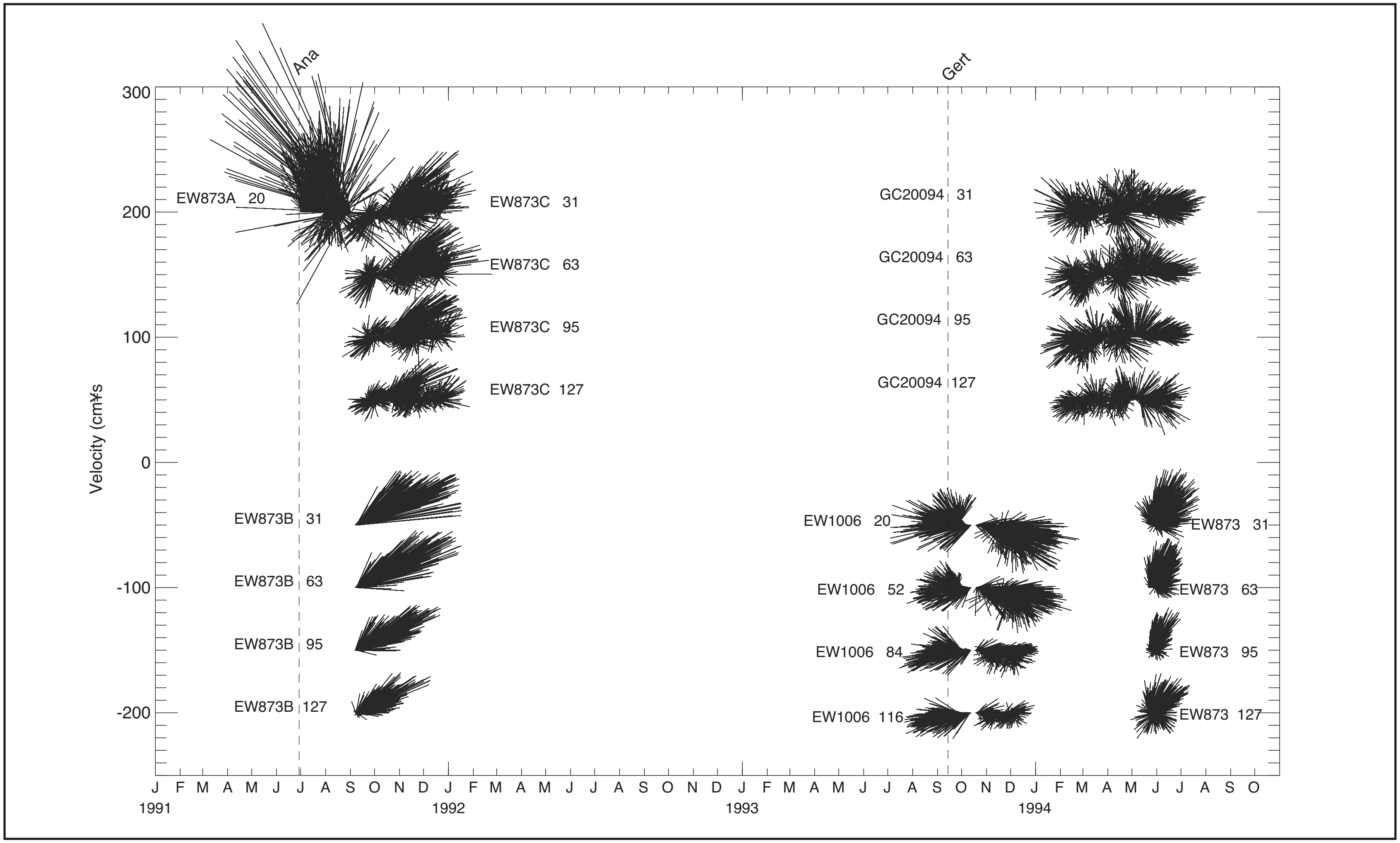

Figure 6.3.12-7. Time lines and vector stick plots for non-proprietary industry moorings, deployed during 1991-1994, in water depths greater than 200 m. The first day of tracking for tropical storms and hurricanes in the Gulf during the deployment periods is indicated by the vertical dashed line with the storm name given above it. North is upward. Tick marks denote start of the month.

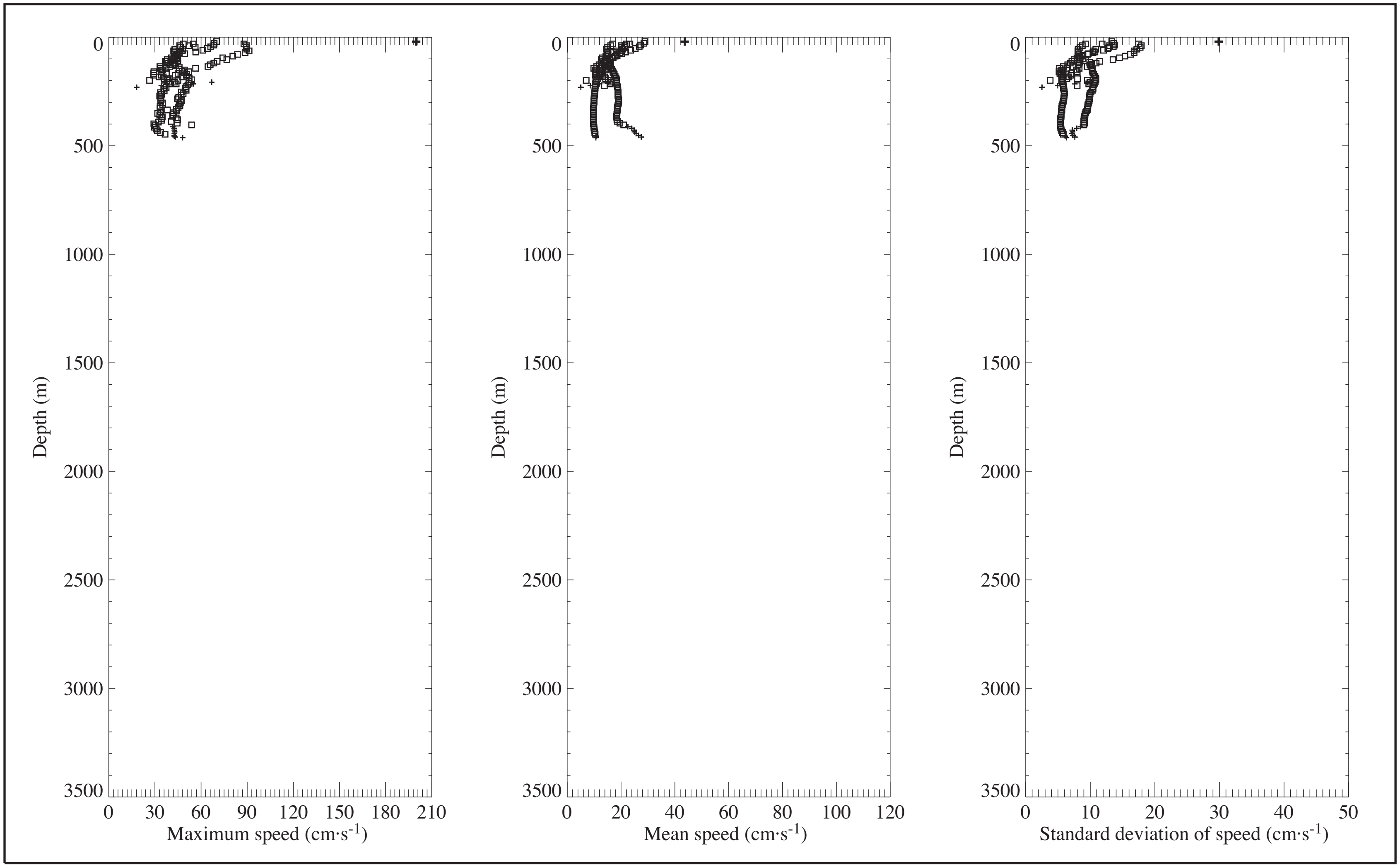

Figure 6.3.12-8. Observed speed (a) maximum, (b) mean, and (c) standard deviation versus instrument depth for unfiltered records from 1991-1994 industry moorings (npts = 163). Quality codes: A or B (dot), C (square), D (plus).

to east where they persisted at approximately 25 cm·s^{-1} for a period of six weeks. These currents were surface-intensified and coherent throughout the vertical measurement range. Inertial oscillations of varying amplitudes were present throughout the deployment. The raw data have substantial high-frequency signals, particularly at depths between 150 and 300 m. These motions might be related to high-speed sub-surface jets. However, there are insufficient data to distinguish these events from interference with acoustic energy by the drill string or drilling platform.

EW873 (94): This was a very short record during a time when slope anticyclones were influencing the currents at this site, resulting in predominantly northeastward flows near surface for most of the deployment. Although the currents at all depths during the beginning of the record were predominantly northeastward, the last half of the records show increasing tendency toward southeastward flow with depth. At 200 m the currents were approximately 20 cm·s^{-1} and oriented in the direction opposite that of the near-surface currents. Strong inertial currents with amplitudes of 20-25 cm·s^{-1} dominated the near-surface records and are superimposed on a mean speed of ~20 cm·s^{-1}.

6.3.12.4 Industry Moorings, 1995

Basic description of data. Industry moorings deployed during 1995 were in GC200, GC245, and MC972. Data were provided by Marathon Oil. Figure 6.3.12-6 shows the locations of the moorings (GC200B notes the location of the 1995 GC200 mooring). Estimated instrument depths are given in Table 6.3.12-4. Data collected at all four sites were from a suspended ADCP deployed by Evans-Hamilton, Inc., for Marathon Oil. The first bin in the database for these sites consists of temperature only; this file is not listed below.

The 1995 GC200 deployment was from 25 June through 16 July 1995. The estimated depth range of the data was 21 to 741 m in 8-m bins. Total water depth was 877 m.

The GC245 deployment occurred between 7 September and 13 November 1995. The estimated depth range was 21 to 733 m in 8-m bins. Total water depth was 889 m. Data have large temporal gaps that split the deployment into basically three sub-deployments lasting on the order of 7-14 days each.

The deployment at MC972 began 17 November 1995 and ended 18 December 1995. Estimated vertical range of data coverage was 21 to 445 m in 8-m bins. Total water depth was 769 m.

Figure 6.3.12-9 shows the time lines and vector stick plots for these moorings. The quality code for these data is C, except the bottom few bins which are rated D. File names for the current records in the data base are

- GC20095 GC950625.A01-A90
- GC245 GC950907.A01-A89
- MC972 MC951117.A01-A53

Environmental background. During the period of the 1995 deployment at GC200, no tropical or extratropical cyclones were present in the Gulf of Mexico. Loop Current Eddy Zapp influenced this region during time the instrument was deployed. No Loop Current eddies detached during this deployment. During the period of the deployment at GC245, hurricane Roxanne (7–21 October 1995) was present in the Bay of Campeche. Although hurricane Opal (27 September–6 October 1995) occurred within the time range of the deployment, no

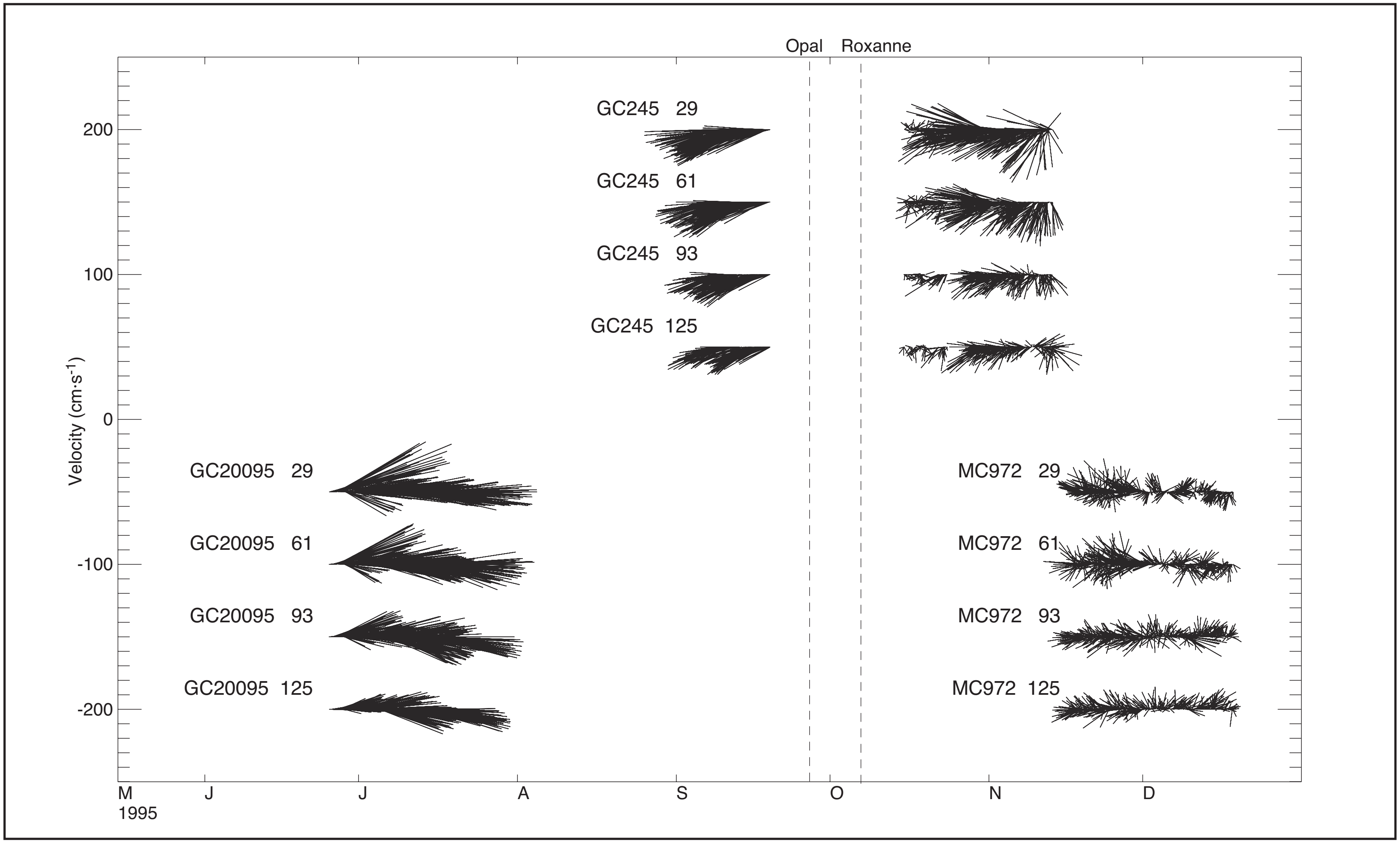

Figure 6.3.12-9. Time lines and vector stick plots for non-proprietary industry moorings, deployed during 1995, in water depths greater than 200 m. The first day of tracking for tropical storms and hurricanes in the Gulf during the deployment period is indicated by the vertical dashed line with the storm name given above it. North is upward. Tick marks denote start of the month.

Table 6.3.12-4. Record-length mean, standard deviation, and maximum speed for data from the 1995 industry moorings. The instruments were suspended ADCPs so only selected depths are shown. Depths are estimated.

Mooring	Instrument Depth (m)	Mean Speed ($cm \cdot s^{-1}$)	Standard Deviation ($cm \cdot s^{-1}$)	Maximum Speed ($cm \cdot s^{-1}$)
GC200	29	48.5	12.5	86.4
	61	46.4	10.5	69.5
	93	43.6	10.4	64.8
	125	38.2	9.6	56.0
	205	27.7	8.9	50.3
	501	6.4	3.4	16.9
	725	4.7	2.7	14.6
GC245	29	33.0	11.9	57.1
	61	26.5	11.1	52.6
	93	18.8	9.5	40.8
	125	16.7	8.8	34.7
	205	16.1	9.0	37.4
	501	7.9	3.4	18.1
	701	5.8	3.1	16.8
MC972	29	9.8	5.3	31.6
	61	11.0	6.4	32.2
	93	9.2	5.0	31.3
	125	9.5	4.5	24.4
	205	10.3	6.3	36.5
	421	6.5	3.8	22.5

data were collected during that storm. No extratropical cyclones were present in the Gulf. Loop Current Eddy Aggie detached during this deployment (September 1995). At MC972, no tropical or extratropical cyclones were present in the Gulf of Mexico during this deployment. No LCEs detached.

Basic statistics. Record-length mean, standard deviation, and maximum speeds for the mooring are shown in Table 6.3.12-4. Figure 6.3.12-10 shows the statistics versus depth for all instrument depths. The speed statistics generally decrease with depth. Mean currents in the upper 200 m at MC972 are of order 10 $cm \cdot s^{-1}$. Mean currents in the upper 100 m at GC200 are of order 45 $cm \cdot s^{-1}$. The maximum speeds at GC200 are associated with passage of an LCE.

General description of records.
GC200 (1995): The dominant event during this deployment was the influence of Eddy Zapp as it passed to the south of the mooring. Surface currents were predominantly eastward with magnitudes larger than 50 $cm \cdot s^{-1}$ in the upper 200 m. Below approximately 150 m, currents began to exhibit oscillations with periods of several days. The oscillatory character of the records intensified deeper in the water column and the eastward forcing from the eddy influence decreased. Currents below 450 m were not coherent with those at the surface. The

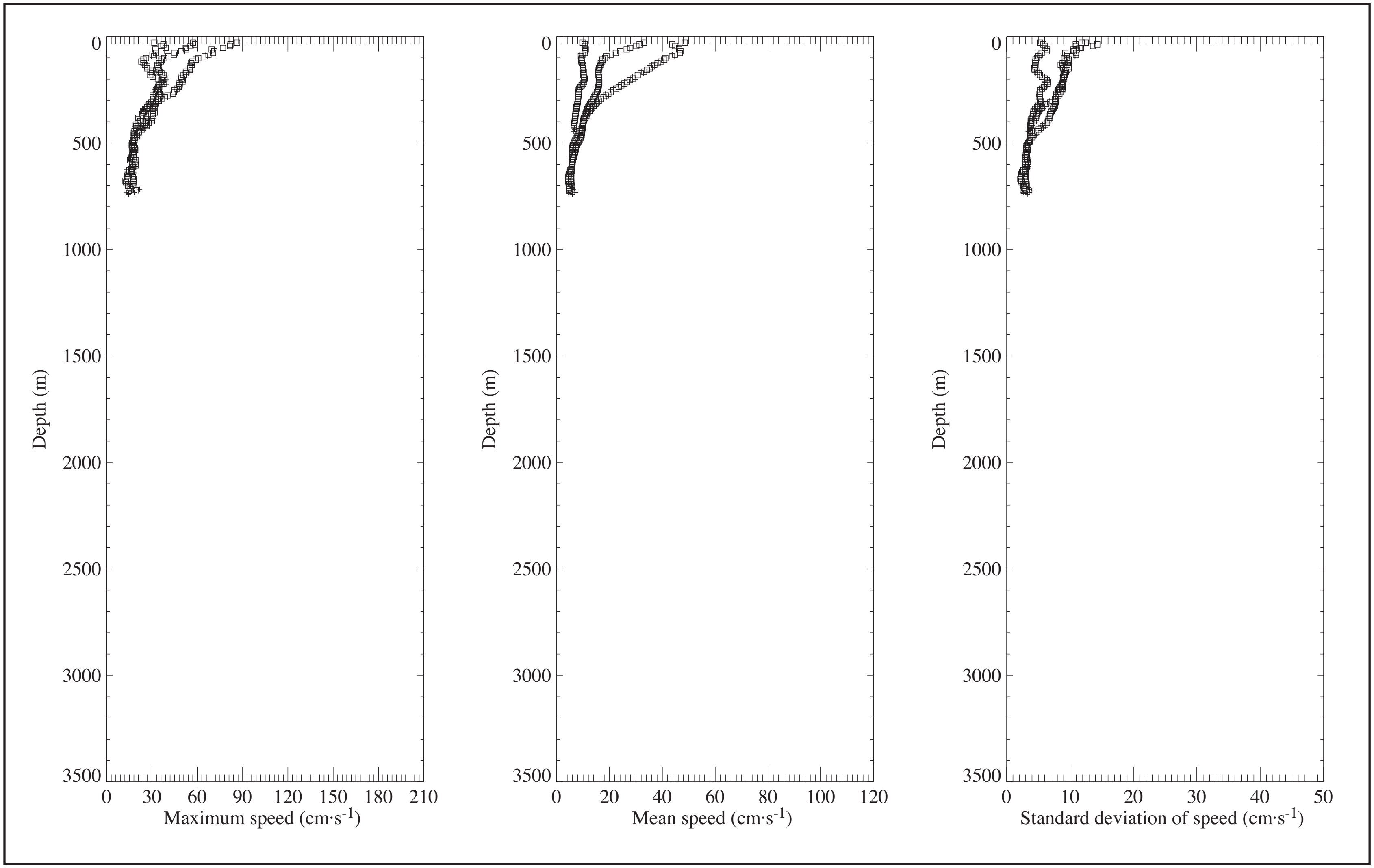

Figure 6.3.12-10. Observed speed (a) maximum, (b) mean, and (c) standard deviation versus instrument depth for unfiltered records from 1995 industry moorings (npts = 232). Quality codes: A or B (dot), C (square), D (plus).

deep currents were weak (<10 cm·s^{-1}), cycled generally between southward and northward in direction, and had principal oscillation periods of several days.

GC245: This site was between the southern limb of a slope anticyclone and the northern limb of a weak cyclone during the deployment. In mid-September, the near-surface (29-m) currents were greater than 50 cm·s^{-1} and to the southwest. Currents rapidly diminished in amplitude with depth. Below 500-m depth, currents were weak (< 10 cm·s^{-1}) with variable direction. During October and November, 29-m currents were westward and southwestward with amplitudes of 40-50 cm·s^{-1}. Currents above 100 m were generally greater than 10 cm·s^{-1}, while those below were weaker. Inertial oscillations were present near-surface throughout the deployment and were strongest during November.

MC972: Near-surface (29-m) currents were highly variable with strong inertial oscillations. Low-frequency motions were about 10 cm·s^{-1} with oscillation periods of 5-7 d. Below 100 m, currents were less variable and more coherent. The site was influenced by a slope anticyclone during the short, 4-week deployment. The raw data have substantial, high-frequency signals, particularly at depths between 150 and 300 m during 6–8 December. These motions have been associated with high-speed sub-surface jets; however, there is insufficient data to distinguish these events from interference with acoustic energy by the drill string or drilling platform.

6.3.12.5 Industry Moorings, Set 1, 1997-1998

Basic description of data. Industry moorings deployed for Marathon Oil during 1997-1998 were in EW1008 and GC112. There were two deployments at one site in GC112. Data were provided by Marathon Oil. Figure 6.3.12-6 shows the locations of the moorings. Estimated instrument depths are given in Table 6.3.12-5. Data collected were from a suspended ADCP deployed by Evans-Hamilton, Inc. The first bin in the database for these sites consists of temperature only; this file is not listed below.

The deployment in EW1008 began 22 October 1997 and ended 15 December 1997. The estimated vertical range of data coverage was 23 to 583 m in 8-m bins. Total water depth was 1172 m. The first deployment in lease block GC112 occurred between 28 December 1997 and 28 January 1998. Total water depth was 536 m. The estimated depth range was from 23 to 535 m in 8-m bins. The second deployment in lease block GC112 was from 28 January through 26 February 1998. Total water depth was 536 m. The estimated vertical range of data coverage was between 23 and 535 m in 8-m bins.

Timelines and vector stick plots are shown in Figure 6.3.12-11. The quality code for these data is C, except the bottom few bins at GC112 are D. File names for the current records in the data base are

- EW1008 EW971022.A01-A70
- GC112 GC971228.A01-A64; GC980128.A01-A64

Environmental background. No tropical cyclones were present in the Gulf of Mexico during these deployments. Loop Current Eddy El Dorado detached during the EW1008 deployment (October 1997).

Basic statistics. Record-length mean, standard deviation, and maximum speeds for the mooring are shown in Table 6.3.12-5. The time series for GC112A and GC112B were merged to compute the basics statistics. Figure 6.3.12-12 shows the statistics versus depth for

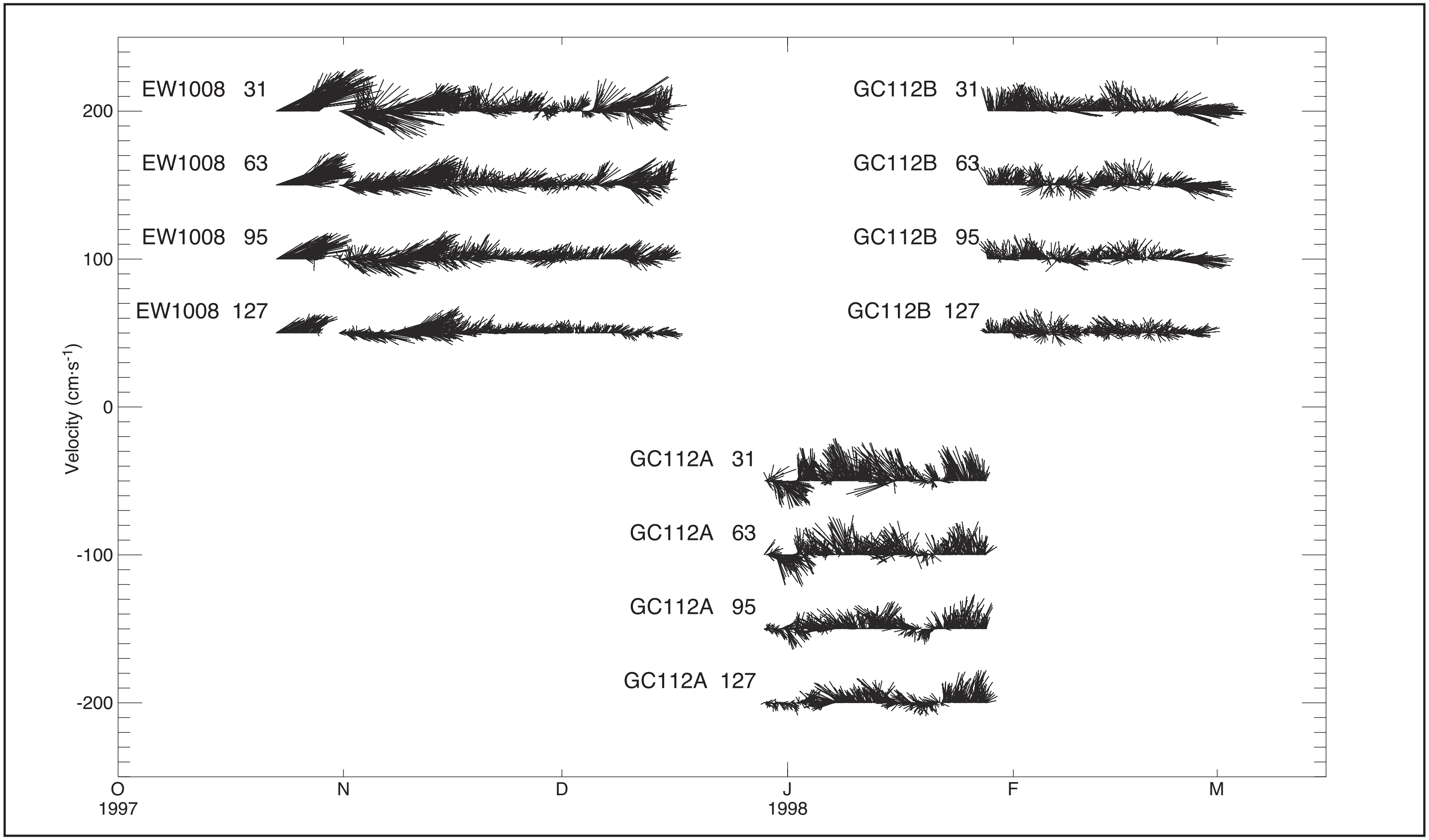

Figure 6.3.12-11. Time lines and vector stick plots for non-proprietary industry moorings (set 1), deployed during 1997-1998, in water depths greater than 200 m. There were no tropical storms or hurricanes in the Gulf for the deployment periods. North is upward. Tick marks denote start of the month.

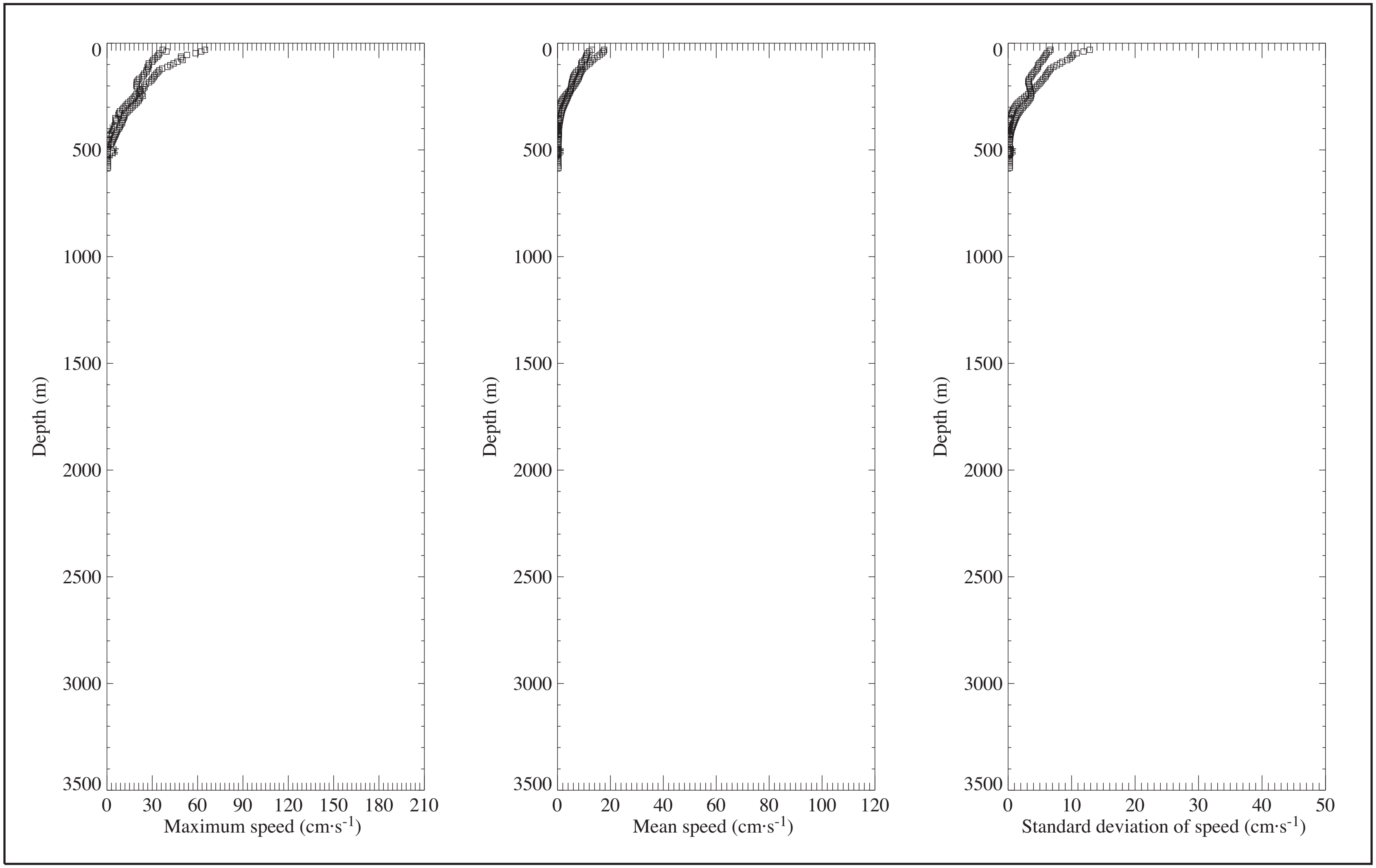

Figure 6.3.12-12. Observed speed (a) maximum, (b) mean, and (c) standard deviation versus instrument depth for unfiltered records from 1997-1998 set 1 industry moorings (npts = 134). Quality codes: A or B (dot), C (square), D (plus).

Table 6.3.12-5. Record-length mean, standard deviation, and maximum speed for data from the 1997-1998 industry moorings, set 1. The instruments were suspended ADCPs so only selected depths are shown. Depths are estimated.

Mooring	Instrument Depth (m)	Mean Speed ($cm \cdot s^{-1}$)	Standard Deviation ($cm \cdot s^{-1}$)	Maximum Speed ($cm \cdot s^{-1}$)
EW1008	31	17.6	12.9	64.9
	63	15.1	10.0	49.0
	95	12.1	8.2	44.1
	127	9.2	6.5	34.7
	207	5.8	4.4	24.9
	503	0.3	0.3	0.7
	583	0.4	0.3	0.7
GC112	31	13.0	6.7	36.9
	63	10.8	5.8	33.2
	95	9.0	4.9	27.6
	127	7.9	4.4	26.3
	207	5.1	3.4	19.9
	479	0.4	0.3	2.6

all instrument depths. There is a decrease in the speed statistics with depth. Values below 250-300 m are extremely small (< 2 $cm \cdot s^{-1}$).

General description of records.
EW1008: There was substantial data dropout with depth in this ADCP record. Surface currents have inertial oscillations throughout the deployment. Super-inertial oscillations are also present throughout the deployment. Data quality is suspect.

GC112A: There was substantial data dropout with depth in this ADCP record. Surface currents had inertial oscillations throughout the deployment. Super-inertial oscillations were also present throughout the deployment. Data quality is suspect. The site was positioned in space and time between LCEs El Dorado and Fourchon. Currents in the upper 100 m were predominantly northward at 10-20 $cm \cdot s^{-1}$.

GC112B: There was substantial data dropout with depth in this ADCP record. Surface currents had inertial oscillations throughout the deployment. Super-inertial oscillations were also present throughout the deployment. Data quality is suspect. Because the two sites are close in space, this deployment essentially is a continuation of GC112A. Weak (15 $cm \cdot s^{-1}$) currents were mostly to north early in the record; they turn east during the last quarter of the record. Below 370 m, currents were generally less than 1 $cm \cdot s^{-1}$.

6.3.12.6 Industry Moorings, Set 2, 1997-1998

Basic description of data. These data from Chevron consist of four ADCP deployments at four different sites: MC628 (21 January through 3 July 3 1997); AT378 (11 July through 6 December 1997); GC236 (9 April through 14 May 1998); and AT118 (14 August through 3 December 1998). Figure 6.3.12-6 shows the locations of the measurements. Total water depths were 838 m, 1843 m, 674 m, and 2371 m for MC628, AT378, GC236, and AT118, respectively. The instruments were suspended directly over the side of the drill ship and placed roughly 20-25 m below the surface. Vertical coverage ranged from 20 m to ~800 m. Selected estimated depths are given in Table 6.3.12-6. Timelines and vector stick plots are shown in Figure 6.3.12-13. The quality code for these data is generally B with that for the last few bins being C or D. File names for the current records in the data base are

- MC628 MC970121.A01-A50 (estimated instrument depths 20–804 m)
- AT378 AT970711.A01-A48 (estimated instrument depths 20–772 m)
- GC236 GC980409.A01-A39 (estimated instrument depths 20–628 m)
- AT118 AT980814.A01-A46 (estimated instrument depths 20–740 m)

Environmental background. No tropical cyclones or Loop Current eddy separations occurred during the deployments at MC628 and GC238. Hurricane Danny (16–26 July 1997) occurred during the deployment at AT378, but there were no Loop Current eddy separations. During the deployment at AT118, two tropical cyclones passed through the Gulf: tropical storm Charley (21-24 August 1998) and hurricane Mitch (22 October–9 November 1998).

Basic statistics. Record-length mean, standard deviation, and maximum speeds for the mooring are shown in Table 6.3.12-6. For multiple deployments at a site, the time series were merged for computation of the statistics. Figure 6.3.12-14 shows the statistics versus depth for all instrument depths. The general pattern of decreasing mean speed and standard deviation with increasing depth holds for the data collected at these four locations. The statistics for AT378 are generally greater than those at the other three moorings for any given depth. This reflects the presence of a large current event at AT378 in August 1997; no such large current event occurred at the other three locations or times.

General description of records.
MC628: Slope eddy Deviant strongly influenced the circulation at this site. Near-surface currents exceeded 75 $cm \cdot s^{-1}$ and persisted for 6-8 weeks with generally northeastward directions. The currents above 275-m during this time exceeded 50 $cm \cdot s^{-1}$. Currents turned clockwise from northeastward to eastward to southward as the slope eddy passed this site. Currents were coherent in the upper 400 m. Below that, the northeastward pattern was weakly present, but current directions were highly variable. The clockwise turn in the currents was coherent with increasing depth.

AT378: In July 1997, The AT378 site was located in July 1997 between Eddy Deviant, which was to the west of the site, and the Loop Current to the southeast. Currents were generally southward throughout the water column, reflecting the greater influence of the southward forcing of the currents by Eddy Deviant. They had magnitudes of order 50 $cm \cdot s^{-1}$ in the upper 100 m decreasing to order 10 $cm \cdot s^{-1}$ at 400 m. In August 1997, LCE El Dorado was beginning to form from the Loop Current. To its north was a strong cyclone. The AT378 site was now located near the region of the eastward flowing jet between the nascent LCE and the cyclone. The measurements show strong currents shifted toward the southeast when the western edge of that cyclone, as seen in sea surface height fields, influenced the circulation. Currents in the upper 100 m were greater than 100 $cm \cdot s^{-1}$ and currents below also were relatively strong. As the cyclone-nascent LCE pair moved westward, the currents turned counter-clockwise to the northeast. Speeds were ≥ 120 $cm \cdot s^{-1}$ in the upper 100 m, with maxima in excess of 50 $cm \cdot s^{-1}$ throughout the upper 500 m. In the mid-November 1997 deployment at AT378, strong southwestward currents, with near-surface speeds in excess of 75 $cm \cdot s^{-1}$, occurred during the westward passage of a slope anticyclonic eddy to the north of the site. Currents were stronger than 50 $cm \cdot s^{-1}$ to depths of about 700 m during this event.

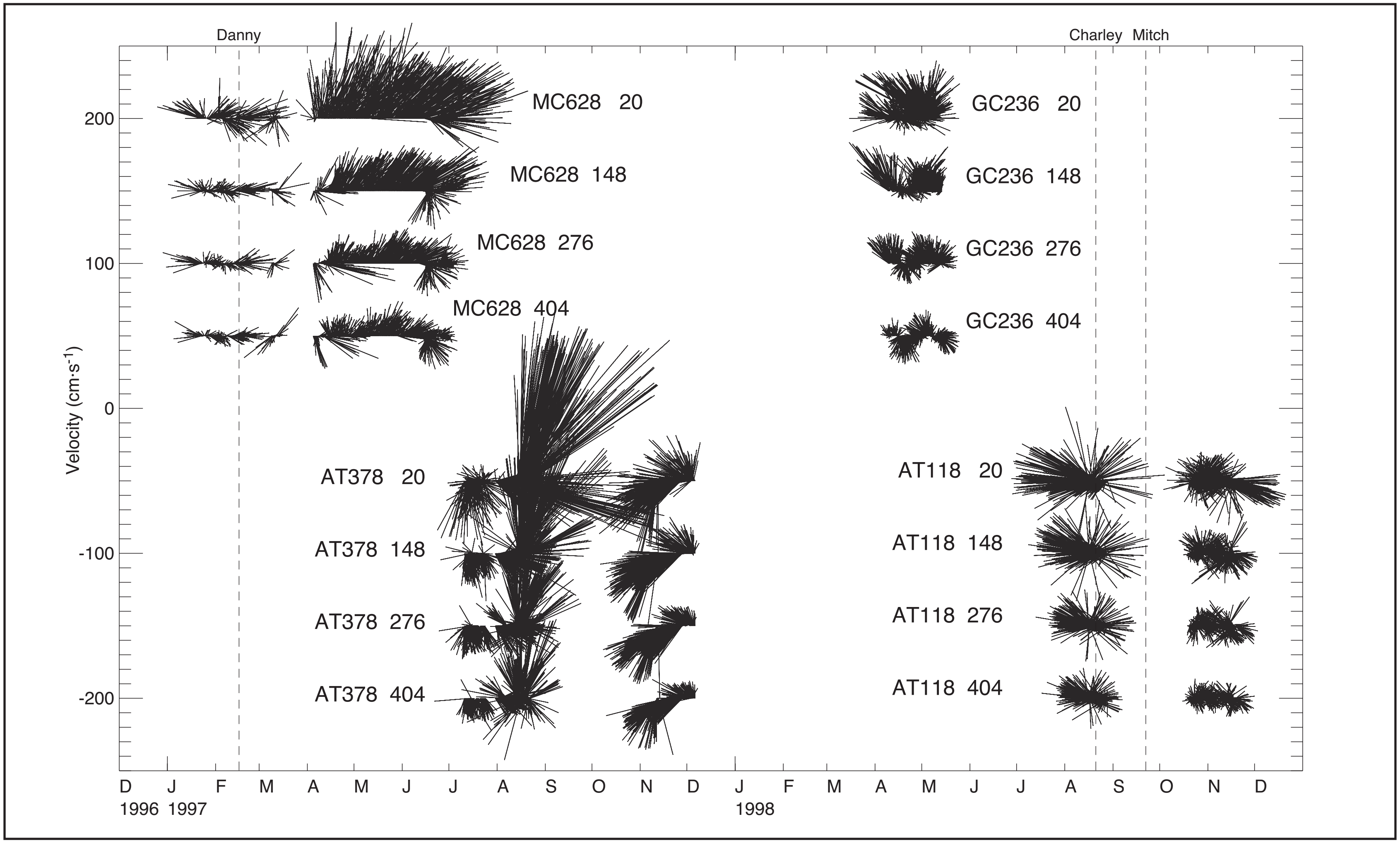

Figure 6.3.12-13. Time lines and vector stick plots for non-proprietary industry moorings (set 2), deployed during 1997-1998, in water depths greater than 200 m. The first day of tracking for tropical storms and hurricanes in the Gulf during the deployment periods is indicated by the vertical dashed line with the storm name given above it. North is upward. Tick marks denote start of the month.

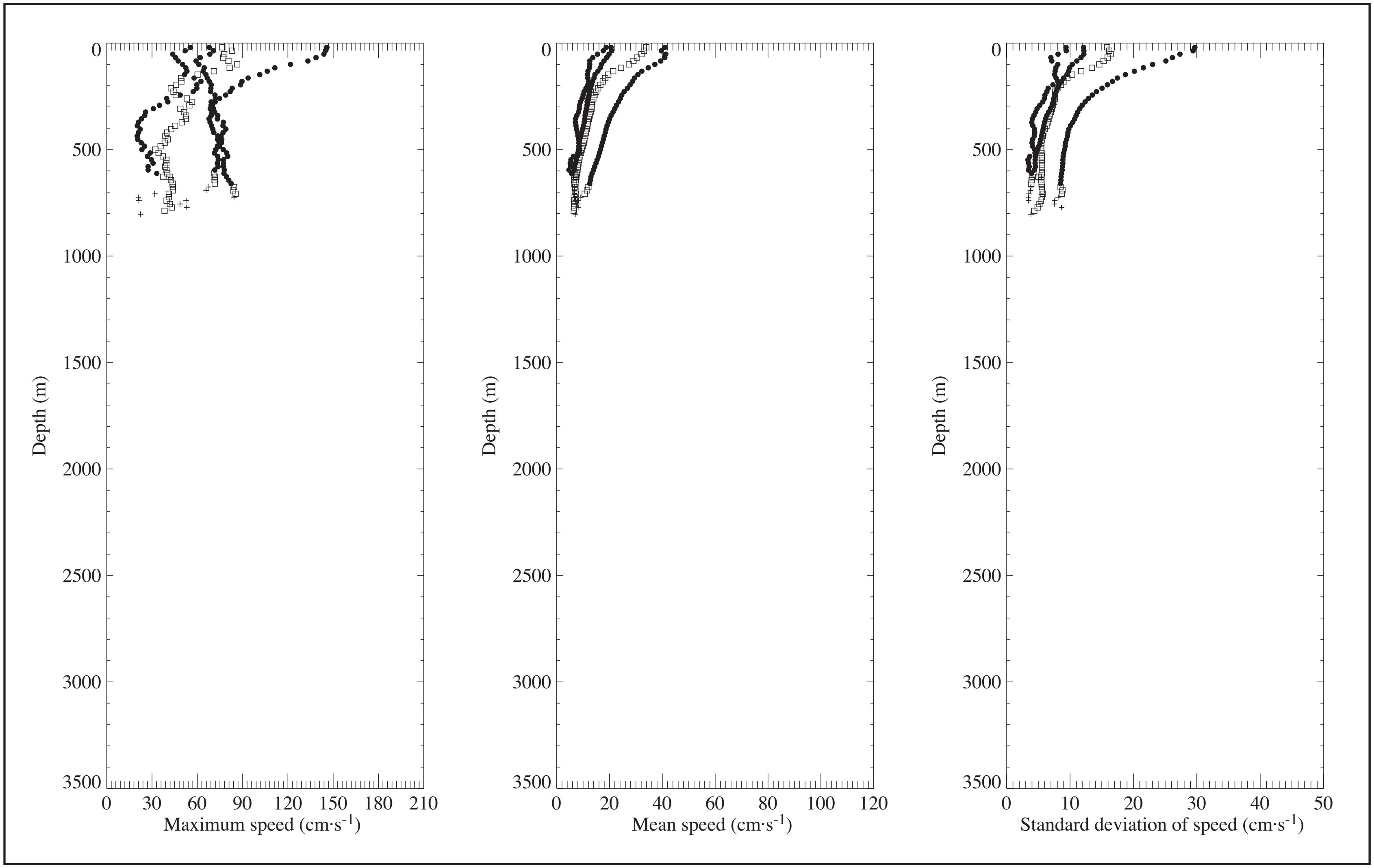

Figure 6.3.12-14. Observed speed (a) maximum, (b) mean, and (c) standard deviation versus instrument depth for unfiltered records from 1997-1998 set 2 industry moorings (npts = 183). Quality codes: A or B (dot), C (square), D (plus).

Table 6.3.12-6. Record-length mean, standard deviation, and maximum speed for data from the 1997-1998 industry moorings, set 2. The instruments were suspended ADCPs so only selected depths are shown. Depths are estimated.

Mooring	**Instrument**	**Mean Speed**	**Standard**	**Maximum**
MC628	20	33.9	15.9	76.6
	148	19.5	10.3	60.2
	276	13.5	7.5	56.5
	404	11.4	6.0	42.7
	500	9.5	5.4	32.2
	788	6.5	4.4	38.3
AT378	20	41.0	29.7	145.8
	148	30.8	18.7	101.4
	276	23.4	12.4	71.9
	404	18.7	9.8	70.3
	500	16.6	9.1	77.2
	660	12.5	8.5	82.4
GC236	20	18.8	9.4	55.3
	148	11.6	7.6	51.5
	276	9.0	5.7	40.5
	404	7.5	4.4	22.2
	500	8.6	4.4	23.3
	612	5.6	3.9	33.2
AT118	20	20.6	12.1	67.9
	148	14.5	9.5	65.7
	276	11.5	7.4	69.2
	404	9.8	5.8	78.9
	500	8.2	4.9	72.3
	596	6.7	4.4	71.6

GC238: Currents were predominantly northward and surface-intensified for the duration of this record. As seen in sea surface height fields, a cold-core cyclonic eddy passed over this site during the deployment. Currents below 300 m were more variable than those at shallower depths.

AT118: This record is from two deployments: August 1998 and October-November 1998. During August, the site was in the jet region between a slope eddy (Eddy Gyre) to the northeast and a deepwater cyclone to the southwest. Currents were predominantly westward and surface-intensified. Maxima exceeded 50 $cm \cdot s^{-1}$ down to about 700 m. During the second deployment, there was a cyclonic eddy to the south of the site and an anticyclonic slope eddy to the north. Currents were variable with oscillations periods of about 10 d. Near-surface currents reached speeds of order 50 $cm \cdot s^{-1}$, while below ~300 m currents were of order 10 $cm \cdot s^{-1}$. Current direction during this deployment is suspect.

6.4 Inventory of Current Records During Energetic Processes and Phenomena

The inventory of identified processes and phenomena was carried out in three steps: identification of energetic currents, identification of possible processes/phenomena, and categorization of currents by category. Each time series of currents was examined for the occurrence of energetic currents, as discussed in Section 6.2. The possible processes and phenomena were identified from the literature and from the character of the energetic currents observed. The current records then were compared and, where appropriate, matched in time and space to the known occurrences of the Loop Current, LCEs, other anticyclonic or cyclonic rings, tropical storms, hurricanes, winter cyclones, frontal passages, and other energetic wind events. Those portions of each record, for which the following categories of physical processes of phenomena (events) were present (occurred), were identified and placed in the inventory to be used in compiling statistics of energetic current events:

- Loop Current eddy separations
- Presence in the Gulf of extratropical cyclones identified by Hardy and Hsu (1997)
- Presence in the Gulf of tropical cyclones
- Presence of eddy near mooring
- Presence of Loop Current near mooring
- Deep barotropic motions, sometimes with bottom intensification
- Inertial and near-inertial motions
- Subsurface, mid-water column motions

Note that some of these categories are not independent (e.g., the decay process following initial currents forced by atmospheric disturbances almost always involve inertial oscillations). For some categories of energetic phenomena or processes in which we have interest there were few or only poor examples of currents in the available records.

The resulting inventory is given as Table A-1. The organization is by year, beginning with 1977. The second level of organization within the table is by event and date of event. For each event, each current record listing consists of: data set name, mooring name, instrument depth (m), and data directory/filename. Our holdings are divided into five data directories:

TAMU: contains TAMU, LATEX, MAMES, and GERG data sets
NODC-DEEP: contains NODC holdings from deepwater Gulf of Mexico, including Straits of Florida
MMS: contains DeSoto Canyon EIS and Extension study data
INDUSTRY: contains non-proprietary industry holdings
YUCATAN: contains data from Yucatan Channel

7 CLIMATOLOGY OF PROCESSES AND PHENOMENA

7.1 General Current Statistics

The Deepwater current meter archive includes 4608 current meter records. Many records have time series of temperature, and sometimes of salinity as well. This archive includes both proprietary and non-proprietary records. As a function of quality code the current and temperature records are divided as follows:

Quality code	No. of records
A	1824
B	368
C	1669
D	343
F	404

Table 7.1-1 shows in the aggregate for all unfiltered current meter records of quality codes A, B, or C the percentage of time currents exceeded various speed thresholds as a function of depth ranges. The total number of files used was 3654 which results in 8.508 million hours of current records. It seems noteworthy that currents above 200 m exceed 75 $cm{\cdot}s^{-1}$ 2% of the time, and 100 $cm{\cdot}s^{-1}$ almost 1% of the time. Our collection of records includes instruments set over the full range of depths in the Gulf of Mexico—extending below 3000 m. Clearly, the fastest currents are near surface and percents for all speed bins decrease rapidly with depth above 800 m. As shown in Section 7.1.2, currents below 800 m are normally rather coherent in the vertical, sometimes with bottom intensification. We have provided two groupings for the deep records: all records below 800 m, and all records below 1200 m. As seen there is some evidence for intensification below 1200 m relative to the depth interval 800-1200 m.

Table 7.1-1. Percentage of time currents exceeded threshold speeds arranged by depth range. Total number of current records examined for this calculation was 3654. Also given is the number of records for each depth range and the number of instrument hours of collected data for that depth range. Each bin in which ADCP data were available was counted. Data from the entire deepwater Gulf of Mexico were included. A 0 denotes that no currents in that speed range were found in that depth range.

Depth Range (m)	Percent time with speeds > 40 $cm{\cdot}s^{-1}$	> 75 $cm{\cdot}s^{-1}$	> 100 $cm{\cdot}s^{-1}$	> 150 $cm{\cdot}s^{-1}$	> 200 $cm{\cdot}s^{-1}$	Number of Records	Instrument hours x 1000 hr
0 - 200	10.30	2.03	0.710	0.024	0.00001	1694	4258
200 - 400	4.66	0.40	0.046	0	0	754	1493
400 - 800	0.23	0.0002	0	0	0	958	1874
below 800	0.34	0.013	0.00006	0	0	248	883
below 1200	0.61	0.028	0.0001	0	0	125	408

For all current records, we produced persistence tables, showing lengths of time during which speeds were within various ranges, and current roses. The current records were aggregated to produce vertical profiles of mean and maximum speeds and standard deviations, by area. Various other statistical products were produced using the ensemble of current records. These results are introduced or presented in this section.

7.1.1 Current Roses and Persistence Tables

For each current meter record we produced current roses, based on joint distributions of speed and direction, and persistence tables. An example current rose, with joint distribution table, is shown in Figure 7.1.1-1. The current rose was constructed using the information in the table and the scale shown. White and stipples segments indicate, from the rose center outward, the percentage of time the current was in the indicated speed bins 1-5 $cm \cdot s^{-1}$, 5-10 $cm \cdot s^{-1}$, ..., >75 $cm \cdot s^{-1}$. The length of each segment corresponds to the percentage of time the current was in that speed bin. If the percentage was less than 1% for a particular bin, the corresponding segment was not shown. Calms are indicated in the center of the rose. DiMarco et al. (1997) provides further details on these products. For all non-proprietary data sets these products are included in the data report to accompany the data CD-ROM resulting from this study (DiMarco et al. 2001). Here we give some examples of the current roses and persistence tables to illustrate what they contain and potential uses.

In August 1999, the Minerals Management Service had three current meter arrays installed in the north-central Gulf just south of the Sigsbee Escarpment. These three moorings, referred to here as I1, I2, and I3, were located at 29.293°N, 88.795°W; 27.228°N, 89.971°W; and 27.116°N, 89.814°W, respectively. A site map (Figure 6.3-23) and additional information are available in Section 6.3.6. In Figure 7.1.1-1 is shown the current rose for the 16-m depth bin for the initial period of deployment, 29 August 1999 to 25 October 1999 of mooring I1, in water depth of 2001 m. The record was dominated by strong northward flow 71% of the time with an average speed of 97 $cm \cdot s^{-1}$. For 17% of the record length the current was toward the northeast with average speed of 83 $cm \cdot s^{-1}$. This remarkably strong and unidirectional flow resulted because during the deployment period the western limb of Eddy Juggernaut was over the mooring (e.g., Figure 5.4-10). For contrast, Figure 7.1.1-2 pictures the current rose for the same mooring and depth for the period 25 February 2000 to 26 August 2000. Currents are seen to be almost equally divided in terms of direction around the compass with average speeds from 20 to 30 $cm \cdot s^{-1}$. No dominant surface intensified feature was present during the period.

For the initial deployment period of mooring I1, Figures 7.1.1-3 and 7.1.1-4 show the current roses for records from 800 and 1800 m. This includes the period for which the currents at the 16-m level averaged 97 $cm \cdot s^{-1}$ toward the north for 71% of the time. Note that at 800 m (Figure 7.1.1-3) the currents were almost evenly distributed in direction and average speeds did not exceed 13 $cm \cdot s^{-1}$ toward any quadrant. In fact, the average speeds recorded at this level were the smallest for any depth on I1 during this period. It is not atypical for the minimum speeds in the water column to be found in the depth range 800-1000 m. From Figure 7.1.1-4 it is seen that currents nearer the bottom (at 1800 m) were greater than at 800 m and had dominant directions westward and northeastward. The orientation of the Sigsbee Escarpment, located just north-northwest of mooring I1, is approximately east-northeast. We have seen in Section 5.3 that model results show the variance in deep water near the escarpment to be oriented strongly along the direction of the escarpment. The observations confirm this result. Note that the average speeds in those directions were of order 15 $cm \cdot s^{-1}$.

Filename : AT990829.A02
Version : 21-Nov-2000
Latitude : 27.2933 N
Longitude : 89.7845 W
Lease Block : AT0663
Instrument Depth : 16.0 M
Total Water Depth : 2001.0 M
Start Time : 08/29/1999 11:00:00
Stop Time : 10/25/1999 05:00:00
Sampling Interval : 60 MIN 0 SEC
Total Data : 1363
Valid Data : 1363

Mooring Name : I1

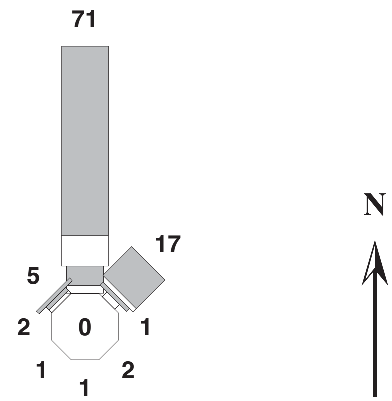

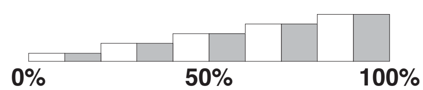

Dir	Current Speed Range (cm·s^{-1})											Avg.
	1-5	5-10	10-15	15-25	25-35	35-45	45-55	55-65	65-75	>75	Total	Speed
N	0.2	0.8	0.7	0.2	0.3	0.7	2.1	5.4	8.4	52.5	71.3	97.0
NE	0.1	0.8	1.8	0.2	0.0	0.3	0.2	1.2	1.3	11.3	17.2	83.5
E	0.0	0.0	0.1	0.2	0.4	0.0	0.0	0.0	0.0	0.0	0.7	23.5
SE	0.0	0.0	0.1	0.6	0.5	0.2	0.0	0.0	0.0	0.0	1.5	26.6
S	0.1	0.1	0.0	0.1	0.5	0.4	0.0	0.0	0.0	0.0	1.2	28.2
SW	0.0	0.0	0.1	0.4	0.1	0.2	0.0	0.0	0.0	0.0	0.9	25.6
W	0.0	0.2	0.1	0.9	0.1	0.1	0.1	0.1	0.0	0.0	1.7	25.2
NW	0.1	0.1	0.4	0.3	1.1	1.1	0.8	0.2	0.1	1.1	5.4	54.8
Total	0.6	2.1	3.3	3.0	3.1	3.2	3.3	6.8	9.8	64.9	100.0	88.1
Calm											0.0	

Figure 7.1.1-1. Current rose for the unfiltered record at depth bin centered at 16 m on mooring I1 for the period 29 August-25 October 1999.

Filename : AT000225.A01
Version : 21-Nov-2000
Latitude : 27.2925 N
Longitude : 89.7852 W
Lease Block : AT0663
Instrument Depth : 16.0 M
Total Water Depth : 2001.0 M
Start Time : 02/25/2000 09:00:00
Stop Time : 08/26/2000 04:00:00
Sampling Interval : 60 MIN 0 SEC
Total Data : 4388
Valid Data : 4388

Mooring Name : I1

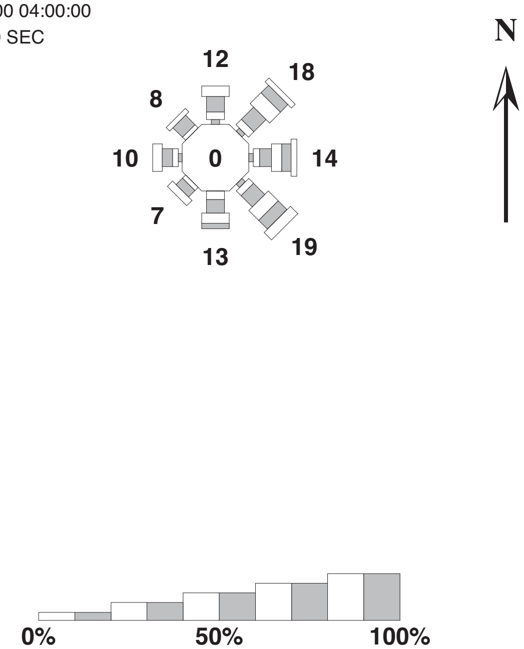

Dir	Current Speed Range (cm·s^{-1})											Avg. Speed
	1-5	5-10	10-15	15-25	25-35	35-45	45-55	55-65	65-75	>75	Total	
N	0.5	1.3	2.1	4.3	2.9	0.9	0.1	0.0	0.0	0.0	12.1	20.7
NE	0.2	1.2	2.1	4.8	4.3	2.9	1.5	0.5	0.0	0.0	17.5	27.1
E	0.4	1.2	1.8	3.3	2.8	2.6	1.6	0.1	0.0	0.0	13.9	27.0
SE	0.3	1.3	1.9	4.4	3.9	3.4	2.9	0.6	0.1	0.0	18.8	29.8
S	0.4	0.9	2.4	3.7	2.8	1.5	0.6	0.1	0.0	0.0	12.6	23.3
SW	0.3	0.7	1.2	2.5	2.1	0.5	0.0	0.0	0.0	0.0	7.3	20.9
W	0.4	1.0	1.6	2.9	2.6	0.8	0.1	0.1	0.0	0.0	9.5	21.6
NW	0.3	0.9	1.2	3.7	1.4	0.3	0.3	0.0	0.0	0.0	8.3	20.4
Total	2.7	8.6	14.4	29.6	22.9	12.9	7.1	1.5	0.1	0.0	99.9	24.8
Calm											0.1	

Figure 7.1.1-2. Current rose for the unfiltered record at depth bin centered at 16 m on mooring I1 for the period 25 February-26 August 2000.

Filename : AT990829.C01
Version : 21-Nov-2000
Latitude : 27.2933 N
Longitude : 89.7845 W
Lease Block : AT0663
Instrument Depth : 800.0 M
Total Water Depth : 2001.0 M
Start Time : 08/29/1999 09:00:00
Stop Time : 02/22/2000 12:00:00
Sampling Interval : 60 MIN 0 SEC
Total Data : 4252
Valid Data : 4252

Mooring Name : I1

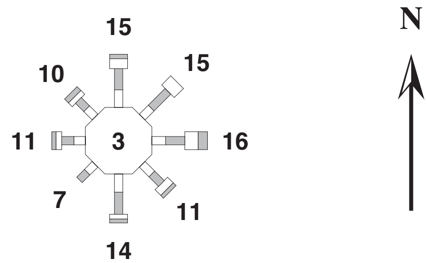

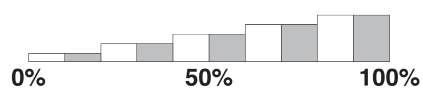

Dir	Current Speed Range (cm·s⁻¹)											Avg.
	1-5	5-10	10-15	15-25	25-35	35-45	45-55	55-65	65-75	>75	Total	Speed
N	4.8	5.9	2.7	1.3	0.0	0.0	0.0	0.0	0.0	0.0	14.7	7.8
NE	3.5	6.6	3.6	0.9	0.2	0.0	0.0	0.0	0.0	0.0	14.8	8.6
E	3.8	5.3	3.7	2.6	0.1	0.0	0.0	0.0	0.0	0.0	15.5	9.6
SE	3.8	3.7	2.2	1.1	0.0	0.0	0.0	0.0	0.0	0.0	10.7	7.8
S	5.0	6.1	1.4	1.0	0.0	0.0	0.0	0.0	0.0	0.0	13.5	7.0
SW	3.1	3.0	0.4	0.3	0.1	0.0	0.0	0.0	0.0	0.0	6.9	6.6
W	3.2	3.3	1.6	1.2	0.7	0.7	0.4	0.0	0.0	0.0	11.0	12.9
NW	3.3	3.2	1.5	1.5	0.4	0.0	0.0	0.0	0.0	0.0	9.8	9.2
Total	30.5	37.1	17.0	9.8	1.5	0.7	0.4	0.0	0.0	0.0	96.9	8.7
Calm											3.1	

Figure 7.1.1-3. Current rose for unfiltered record at 800 m on mooring I1 for the period 28 August 1999-22 February 2000.

Filename : AT990829.C06
Version : 21-Nov-2000
Latitude : 27.2933 N
Longitude : 89.7845 W
Lease Block : AT0663
Instrument Depth : 1800.0 M
Total Water Depth : 2001.0 M
Start Time : 08/29/1999 10:00:00
Stop Time : 02/22/2000 12:00:00
Sampling Interval : 60 MIN 0 SEC
Total Data : 4251
Valid Data : 4251

Mooring Name : I1

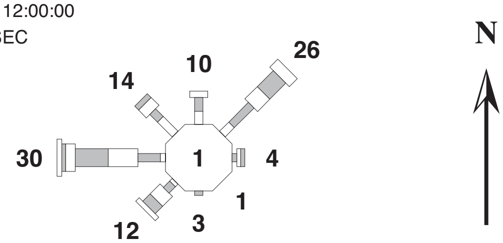

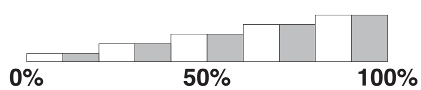

Dir	Current Speed Range (cm·s^{-1})											Avg.
	1-5	5-10	10-15	15-25	25-35	35-45	45-55	55-65	65-75	>75	Total	Speed
N	3.6	3.8	1.8	0.4	0.0	0.0	0.0	0.0	0.0	0.0	9.6	7.1
NE	3.6	7.7	4.8	6.3	3.1	0.7	0.0	0.0	0.0	0.0	26.1	13.9
E	0.8	1.3	1.1	1.1	0.0	0.0	0.0	0.0	0.0	0.0	4.3	10.7
SE	0.6	0.4	0.4	0.0	0.0	0.0	0.0	0.0	0.0	0.0	1.4	6.4
S	0.3	1.2	0.8	0.1	0.0	0.0	0.0	0.0	0.0	0.0	2.5	9.5
SW	1.0	2.5	3.9	2.8	1.4	0.2	0.1	0.0	0.0	0.0	11.8	14.7
W	1.4	6.2	8.2	9.2	2.6	1.1	1.3	0.0	0.0	0.0	29.9	17.1
NW	5.8	3.0	3.1	1.5	0.2	0.0	0.0	0.0	0.0	0.0	13.7	8.0
Total	17.0	26.1	24.1	21.5	7.4	2.0	1.4	0.0	0.0	0.0	99.5	13.1
Calm											0.5	

Figure 7.1.1-4. Current rose for the unfiltered record at 1800 m on mooring I1 for the period 28 August 1999-22 February 2000.

As final examples we show in Figures 7.1.1-5 and 7.1.1-6 the current roses from 1600 m at mooring I2 (water depth 1998 m) and 1975 m from mooring I3 (water depth 2175 m), respectively. The results are strikingly similar to those from 200 m above the bottom at mooring I1, with dominant currents in the direction of orientation of the escarpment. However, it should be noted that mooring I2 is located closer to the escarpment and further west, while mooring I3 is located east of mooring I1 and further south of the escarpment. We may expect stronger currents closer to the base of the escarpment (see Section 6.1.3). This is confirmed also by the CUPOM output.

As illustrations, we include as Tables 7.1.1-1 through 7.1.1-6 persistance tables corresponding to the current roses for records from MMS moorings I1, I2, and I3 shown in Figures 7.1.1-1 through 7.1.1-6. Of course, all persistence records to be included in the data report to accompany the data CD-ROM were prepared from unfiltered records. Speed ranges used are 0-25, 25-50,..., 175-200, and >200 $cm \cdot s^{-1}$; duration limits used are 0-0.5, 0.5-1, 1-2, 2-4, 4-8, 8-16, and >16 d. These ranges were selected to emphasize large speeds, particularly those lasting for extended periods.

7.1.2 Current Speed Versus Depth by Region of the Gulf of Mexico

To obtain estimates of the background currents in the Gulf of Mexico, we extracted the maximum, record-length mean, and standard deviation of current speed for unfiltered current time series in our data inventory. These include both proprietary and non-proprietary records, but only records with quality control rating of A, B, or C were included in this analysis. For records made at the same location and depth, all gaps were removed, including gaps during which instruments were being replaced. Next, records were sorted into three groups by record length: $\geq$ 100 d, less than 100 but at least 20 d, and < 20 d. For each time series the maximum, record-length mean, and standard deviation were calculated. Finally, results were sorted by longitude into three groups before plotting versus depth: locations east of 89°W, 89° to 93°W, and west of 93°W.

The plots of maximum speeds are given in Figures 7.1.2-1 through 7.1.2-3. The numbers of records from the western Gulf is small for all record lengths, and likely are not adequate to allow meaningful characterization of currents for that region. The same is true for short records from the eastern Gulf. Overall patterns of maximum speed versus depth are similar in the eastern and central regions. Maxima in the upper 100 m are greater than those below, with the maxima in the eastern Gulf (up to ~200 $cm \cdot s^{-1}$) being generally higher than those in the central Gulf. Maxima then decrease with depth to near 1000 m; throughout that range greater maxima are found in the eastern than in the central Gulf. Maxima at depths below 1000 m are generally 10-50 $cm \cdot s^{-1}$, but for the central region can approach ~100 $cm \cdot s^{-1}$. In that region, the maximum speeds appear to be smallest near 1000 m. For records in the western region the maxima in the upper 100 m reach ~100 $cm \cdot s^{-1}$ and decrease to < 35 $cm \cdot s^{-1}$ below 1000 m.

Record-length mean speeds, shown in Figures 7.1.2-4 through 7.1.2-6, generally are a factor of three to four less than maximum speeds. The exception is the upper ocean in the eastern Gulf (region of DeSoto Canyon) where means reach half the maximum values in some cases. As for maximum speeds, the largest mean speeds are near the sea surface and there is a tendency toward a minimum near 1000 m with some increase with depth below that level. Several energetic events lead to mean speeds in excess of 10 $cm \cdot s^{-1}$ at depth in the eastern and central sectors. The standard deviations of speed versus depth are shown for each region in Figures 7.1.2-7 through 7.1.2-9. The standard deviations are seen to be generally less than

Filename : GC990829.C01
Version : 21-Nov-2000
Latitude : 27.2280 N
Longitude : 89.9710 W
Lease Block : GC0744
Instrument Depth : 1600.0 M
Total Water Depth : 1998.0 M
Start Time : 08/29/1999 18:00:00
Stop Time : 12/15/1999 09:00:00
Sampling Interval : 60 MIN 0 SEC
Total Data : 2584
Valid Data : 2584

Mooring Name : I2

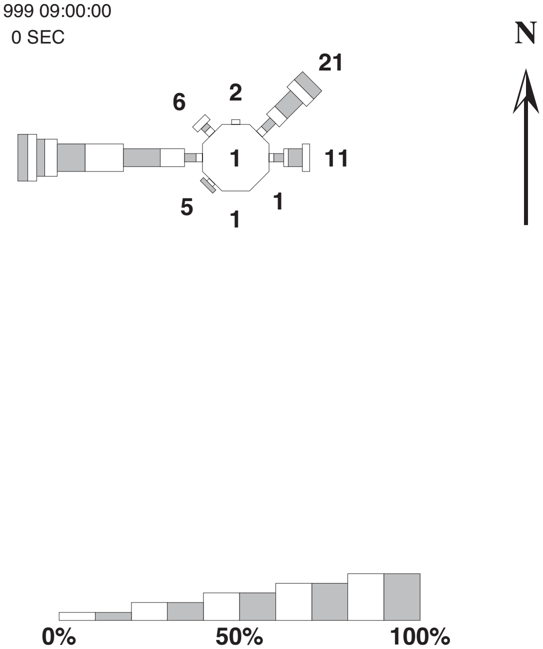

Dir	Current Speed Range (cm·s^{-1})											Avg. Speed
	1-5	5-10	10-15	15-25	25-35	35-45	45-55	55-65	65-75	>75	Total	
N	1.3	0.2	0.7	0.2	0.0	0.0	0.0	0.0	0.0	0.0	2.3	6.7
NE	1.9	3.4	3.2	6.1	2.9	3.2	0.5	0.0	0.0	0.0	21.2	20.5
E	1.3	2.7	1.3	3.9	2.0	0.2	0.0	0.0	0.0	0.0	11.4	16.1
SE	0.5	0.3	0.0	0.0	0.0	0.0	0.0	0.0	0.0	0.0	0.9	4.7
S	0.3	0.1	0.1	0.0	0.0	0.0	0.0	0.0	0.0	0.0	0.5	6.3
SW	1.0	0.7	0.7	1.2	0.9	0.6	0.0	0.0	0.0	0.0	5.1	18.0
W	1.7	3.2	6.8	10.2	10.6	7.7	3.5	2.2	2.5	2.7	51.1	32.1
NW	1.8	1.4	2.0	0.9	0.1	0.0	0.0	0.0	0.0	0.0	6.1	9.3
Total	9.8	12.1	14.8	22.4	16.5	11.7	3.9	2.2	2.5	2.7	98.7	24.6
Calm											1.3	

Figure 7.1.1-5. Current rose for the unfiltered record at 1600 m on mooring I2 for the period 28 August-15 December 1999.

Filename : AT990829.C09
Version : 21-Nov-2000
Latitude : 27.1160 N
Longitude : 89.8138 W
Lease Block : AT0838
Instrument Depth : 1975.0 M
Total Water Depth : 2175.0 M
Start Time : 08/29/1999 14:00:00
Stop Time : 02/23/2000 13:00:00
Sampling Interval : 60 MIN 0 SEC
Total Data : 4272
Valid Data : 4272

Mooring Name : I3

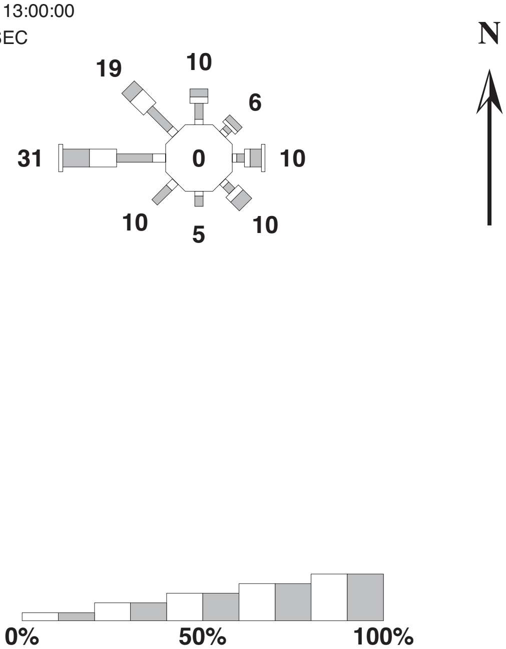

Dir	Current Speed Range (cm·s^{-1})											Avg.
	1-5	5-10	10-15	15-25	25-35	35-45	45-55	55-65	65-75	>75	Total	Speed
N	1.5	4.4	1.8	2.2	0.0	0.0	0.0	0.0	0.0	0.0	9.9	10.0
NE	1.2	1.3	1.0	1.7	0.5	0.0	0.0	0.0	0.0	0.0	5.8	13.2
E	1.2	2.1	1.6	3.1	1.0	0.4	0.1	0.0	0.0	0.0	9.6	15.8
SE	1.3	2.4	1.9	3.4	0.5	0.1	0.1	0.0	0.0	0.0	9.6	13.8
S	1.3	2.8	0.4	0.2	0.3	0.0	0.0	0.0	0.0	0.0	5.0	8.5
SW	2.4	5.7	0.6	0.4	0.1	0.1	0.2	0.0	0.0	0.0	9.5	8.5
W	3.6	9.9	7.6	7.3	1.2	0.7	0.3	0.4	0.1	0.0	31.1	13.9
NW	2.0	8.0	5.2	3.3	0.1	0.1	0.2	0.3	0.0	0.0	19.3	11.8
Total	14.5	36.6	20.1	21.6	3.7	1.4	0.9	0.7	0.1	0.0	99.7	12.4
Calm											0.3	

Figure 7.1.1-6. Current rose for the unfiltered record at 1975 m on mooring I3 for the period 28 August 1999 - 23 February 2000.

Table 7.1.1-1. Persistence table for the unfiltered record at depth bin centered at 16 m on mooring I1 for the period 29 August 1999 - 25 October 1999.

Filename	:	AT990829.A02	Mooring Name	:	I1
Version	:	21-Nov-2000	Instrument Depth	:	16 M
Latitude	:	27.2933°N	Total Water Depth	:	2001 M
Longitude	:	89.7845°W	Start Time	:	08/29/1999 11:00:00
Lease Block	:	AT0663	Stop Time	:	10/25/1999 05:00:00
Quality Code	:	B			

Speed (S)	Duration limits (hours)							Duration statistics (hours)		
$cm \cdot s^{-1}$	0	12	24	48	96	100	total	max	mean	std.dev
0 ≤ S < 25	4	0	0	0	1		5	100.0	24.4	37.9
25 ≤ S < 50	10	3	1	0	0		14	32.0	8.0	7.8
50 ≤ S < 75	31	4	2	0	0		37	27.0	6.6	6.3
75 ≤ S < 100	43	6	1	0	0		50	31.0	6.7	6.4
100 ≤ S < 125	28	6	1	1	0		36	50.0	7.9	9.4
125 ≤ S < 150	14	6	2	0	0		22	40.0	10.3	10.2
150 ≤ S < 172	8	0	0	0	0		8	11.0	5.0	3.5
Data gaps	0	0	0	0	0		0	0.0	0.0	

Table 7.1.1-2. Persistence table for the unfiltered record at depth bin centered at 16 m on mooring I1 for the period 25 February 2000 - 26 August 2000.

Filename	:	AT990829.A01	Mooring Name	:	I1
Version	:	21-Nov-2000	Instrument Depth	:	16 M
Latitude	:	27.2925°N	Total Water Depth	:	2001 M
Longitude	:	89.7852°W	Start Time	:	02/25/2000 09:00:00
Lease Block	:	AT0663	Stop Time	:	08/26/2000 04:00:00
Quality Code	:	B			

Speed (S)	Duration limits (hours)							Duration statistics (hours)		
$cm \cdot s^{-1}$	0	12	24	48	96	111	total	max	mean	std.dev
0 ≤ S < 25	76	40	15	13	1		145	111.0	16.8	19.7
25 ≤ S < 50	124	39	11	3	0		177	74.0	10.0	10.7
50 ≤ S < 71	29	4	0	0	0		33	15.0	5.5	3.9
Data gaps	0	0	0	0	0		0	0.0	0.0	

Table 7.1.1-3. Persistence table for unfiltered record at 800 m on mooring I1 for the period 28 August 1999 - 22 February 2000.

Filename	:	AT990829.C01	Mooring Name	:	I1
Version	:	21-Nov-2000	Instrument Depth	:	800 M
Latitude	:	27.2933°N	Total Water Depth	:	2001 M
Longitude	:	89.7845°W	Start Time	:	08/29/1999 09:00:00
Lease Block	:	AT0663	Stop Time	:	02/22/2000 12:00:00
Quality Code	:	A			

Speed (S)	Duration limits (hours)								Duration statistics (hours)		
$cm \cdot s^{-1}$	0	12	24	48	96	192	384 2239	total	max	mean	std.dev
0 ≤ S < 25	6	1	1	0	1	2	2	13	2239.0	318.7	626.1
25 ≤ S < 50	11	1	0	1	0	0	0	13	49.0	8.2	12.7
50 ≤ S < 52	1	0	0	0	0	0	0	1	2.0	2.0	0.0
Data gaps	0	0	0	0	0	0	0	0	0.0	0.0	

Table 7.1.1-4. Persistence table for unfiltered record at 1800 m on mooring I1 for the period 28 August 1999 - 22 February 2000.

Filename	:	AT990829.C06	Mooring Name	:	I1
Version	:	21-Nov-2000	Instrument Depth	:	1800 M
Latitude	:	27.2933°N	Total Water Depth	:	2001 M
Longitude	:	89.7845°W	Start Time	:	08/29/1999 10:00:00
Lease Block	:	AT0663	Stop Time	:	02/22/2000 12:00:00
Quality Code	:	A			

Speed (S)	Duration limits (hours)								Duration statistics (hours)		
$cm \cdot s^{-1}$	0	12	24	48	96	192	384 1273	total	max	mean	std.dev
0 ≤ S < 25	15	0	2	1	3	2	3	26	1273.0	145.8	299.3
25 ≤ S < 50	17	5	4	2	0	0	0	28	74.0	15.8	18.4
50 ≤ S < 55	3	0	0	0	0	0	0	3	9.5	5.8	3.1
Data gaps	0	0	0	0	0	0	0	0	0.0	0.0	

Table 7.1.1-5. Persistence table for unfiltered record at 1600 m on mooring I2 for the period 28 August 1999 - 15 December 1999.

Filename	:	GC990829.C01	Mooring Name	:	I2
Version	:	21-Nov-2000	Instrument Depth	:	1600 M
Latitude	:	27.2280°N	Total Water Depth	:	1998 M
Longitude	:	89.9710°W	Start Time	:	08/29/1999 18:00:00
Lease Block	:	GC0744	Stop Time	:	12/15/1999 09:00:00
Quality Code	:	A			

Speed (S)	Duration limits (hours)							Duration statistics (hours)		
$cm \cdot s^{-1}$	0	12	24	48	96	192 213	total	max	mean	std.dev
0 ≤ S < 25	21	4	4	3	5	2	39	213.0	40.0	59.2
25 ≤ S < 50	33	11	7	2	1	0	54	98.0	14.7	20.0
50 ≤ S < 75	18	2	2	0	0	0	22	32.0	7.2	8.4
75 ≤ S < 95	3	2	1	0	0	0	6	30.0	11.7	10.2
Data gaps	0	0	0	0	0	0	0	0.0	0.0	

Table 7.1.1-6. Persistence table for unfiltered record at 1975 m on mooring I3 for the period 28 August 1999 - 23 February 2000.

Filename	:	AT990829.C09	Mooring Name	:	I3
Version	:	21-Nov-2000	Instrument Depth	:	1975 M
Latitude	:	27.1160°N	Total Water Depth	:	2175 M
Longitude	:	89.8138°W	Start Time	:	08/29/1999 14:00:00
Lease Block	:	AT0838	Stop Time	:	02/23/2000 13:00:00
Quality Code	:	A			

Speed (S)	Duration limits (hours)								Duration statistics (hours)		
$cm \cdot s^{-1}$	0	12	24	48	96	192	384 1246	total	max	mean	std.dev
0 ≤ S < 25	3	4	1	1	0	2	4	15	1246.0	265.2	378.8
25 ≤ S < 50	12	2	1	2	0	0	0	17	66.0	14.4	17.5
50 ≤ S < 67	0	1	1	0	0	0	0	2	29.0	24.5	4.5
Data gaps	0	0	0	0	0	0	0	0	0.0	0.0	

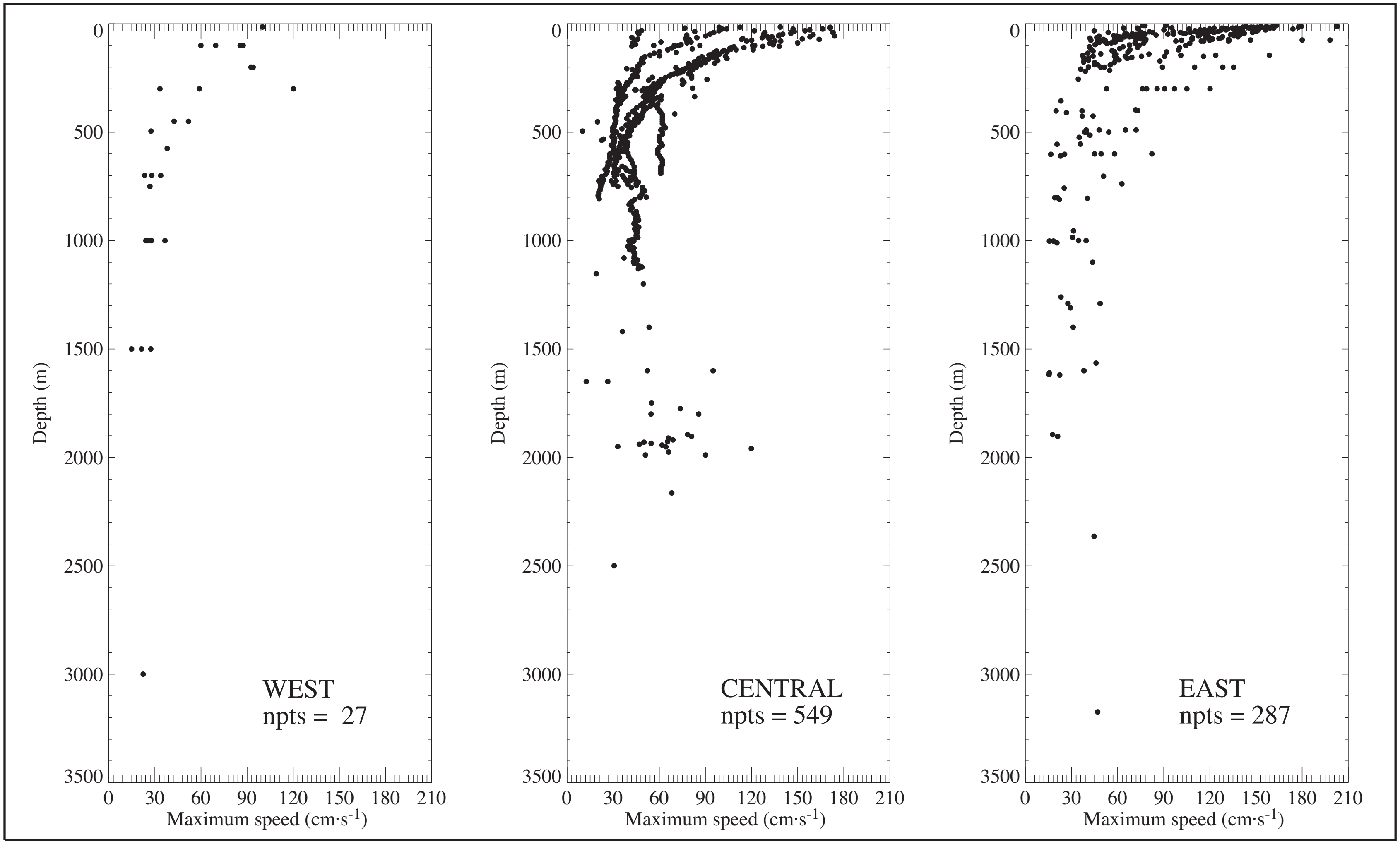

Figure 7.1.2-1. Maximum observed speed versus depth for unfiltered records of at least 100-d duration for (left) west of 93°W, (center) 89° to 93°W, and (right) east of 89°W. All records have quality control grade of A, B, or C.

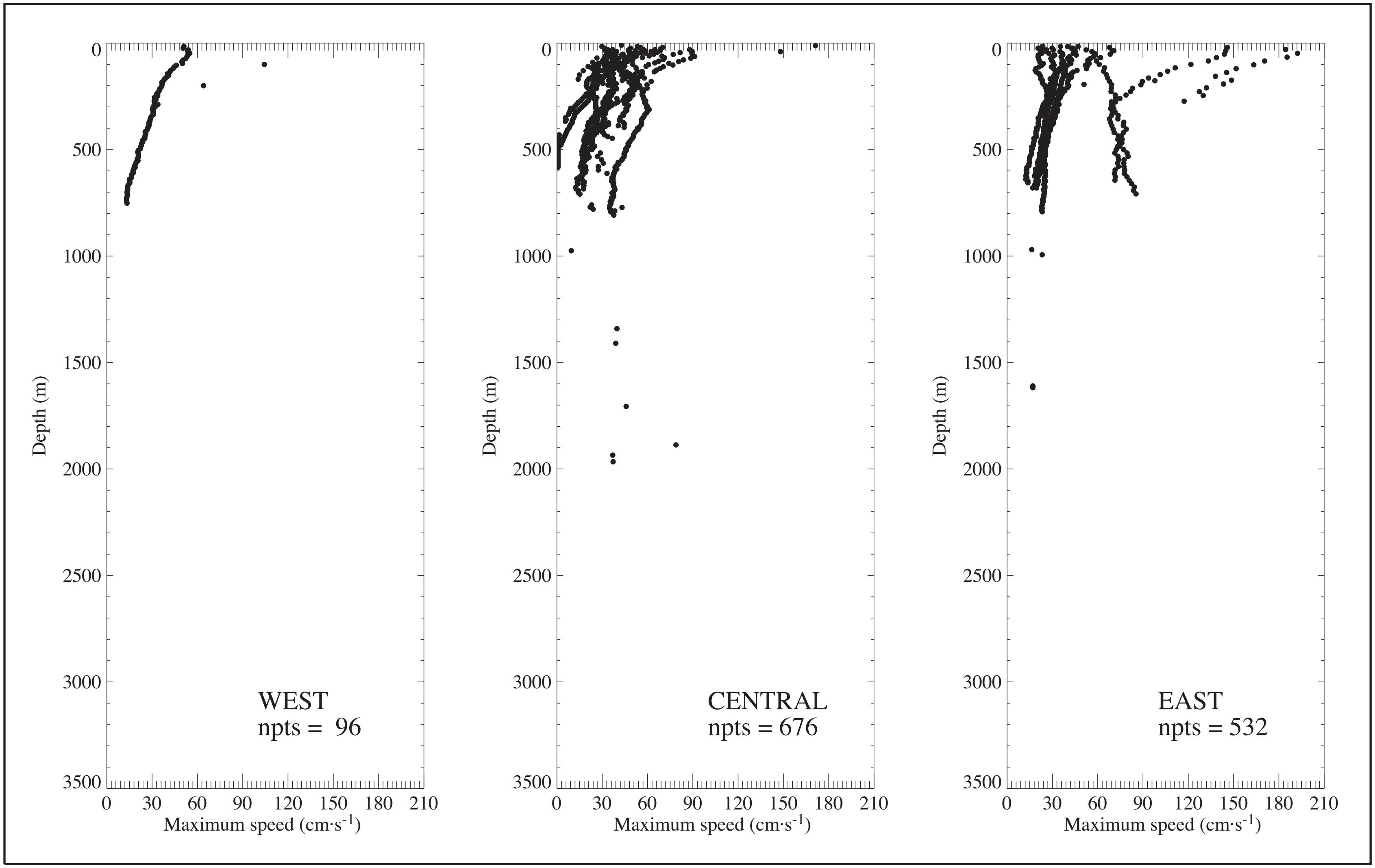

Figure 7.1.2-2. Maximum observed speed versus depth for unfiltered records of duration between 20 and 100 d for (left) west of 93°W, (center) 89° to 93°W, and (right) east of 89°W. All records have quality control grade of A, B, or C.

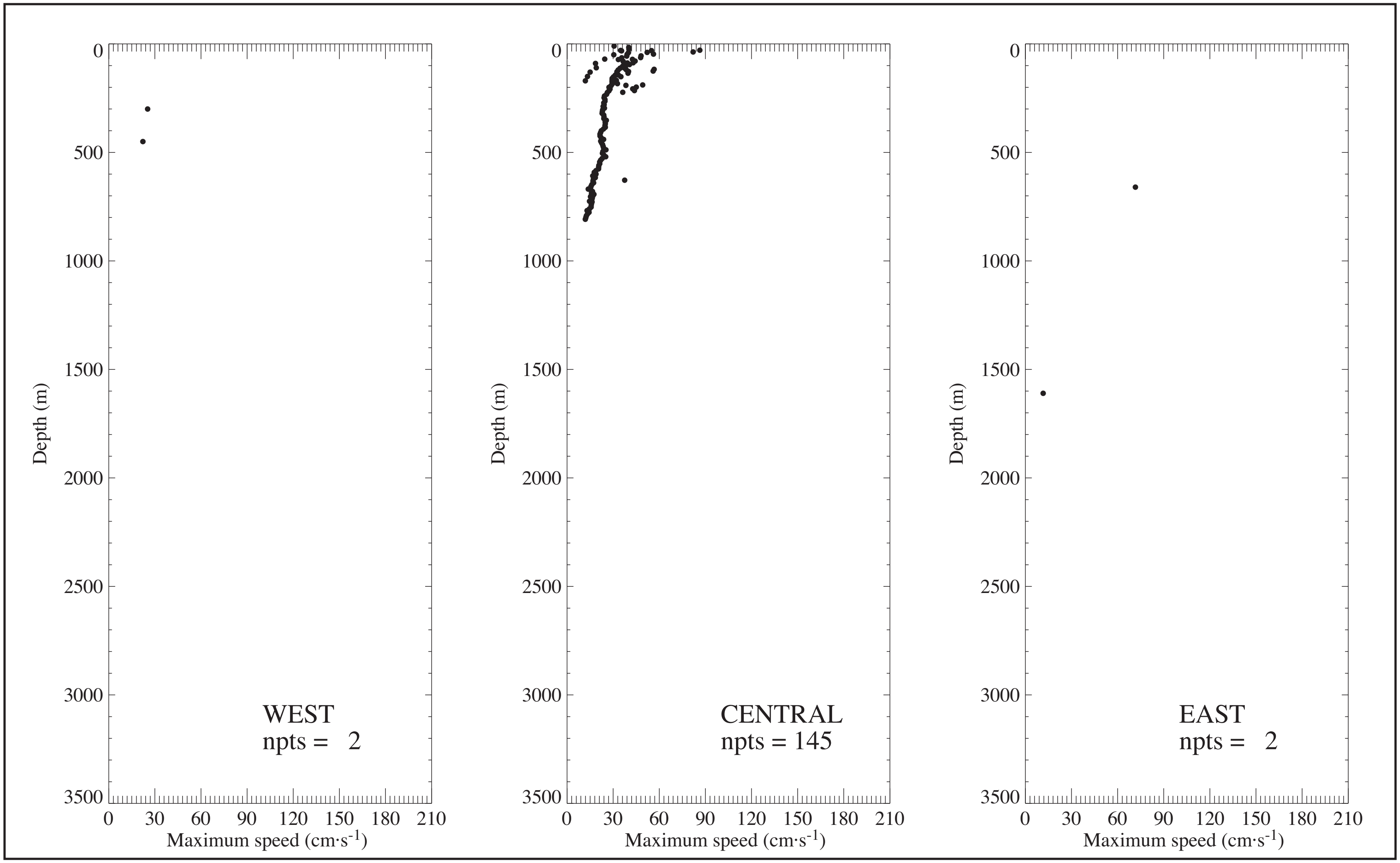

Figure 7.1.2-3. Maximum observed speed versus depth for unfiltered records of less than 20-d duration for (left) west of 93°W, (center) 89° to 93°W, and (right) east of 89°W. All records have quality control grade of A, B, or C.

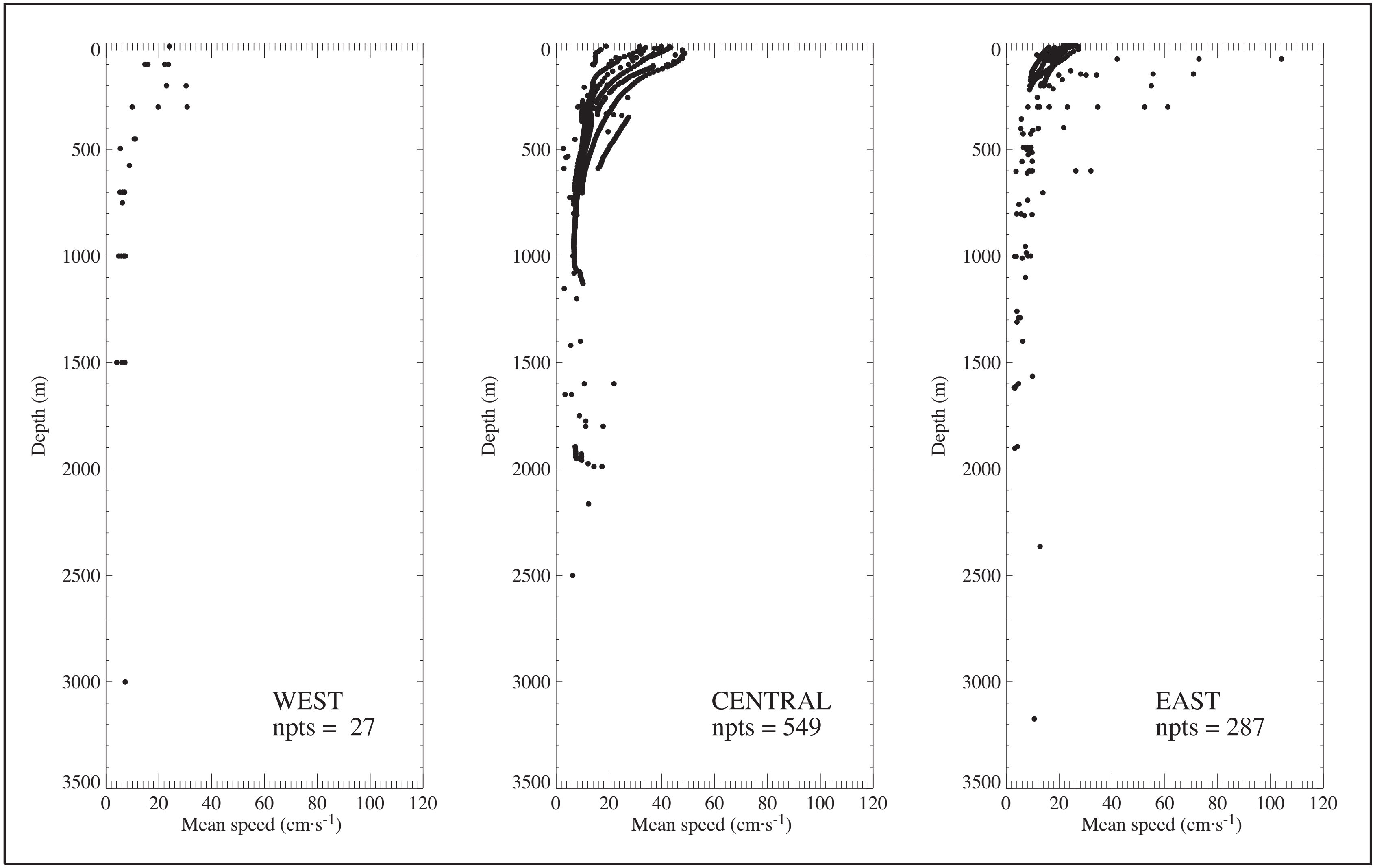

Figure 7.1.2-4. Mean record-length speed versus depth for unfiltered records of at least 100-d duration for (left) west of 93°W, (center) 89° to 93°W, and (right) east of 89°W. All records have quality control grade of A, B, or C.

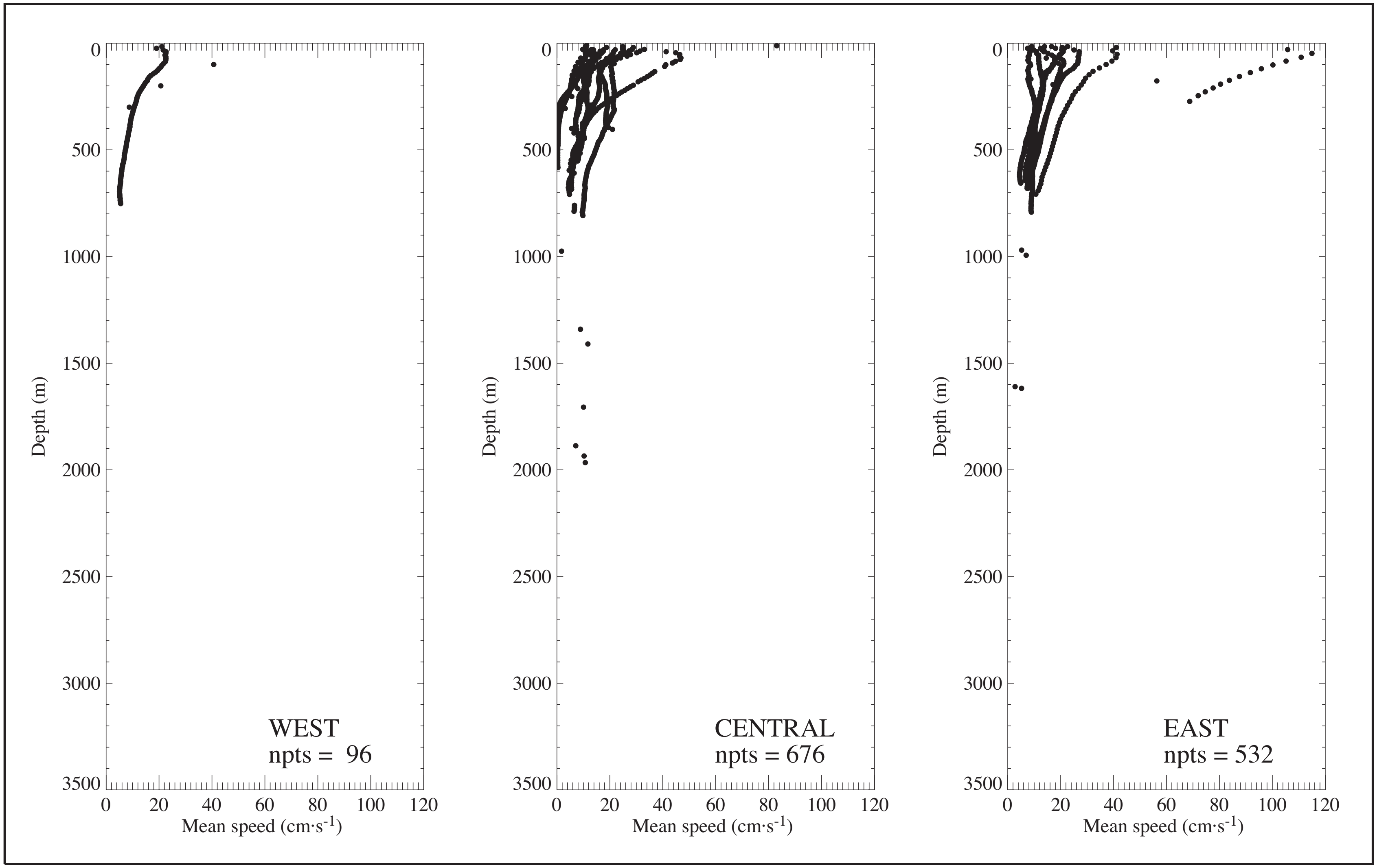

Figure 7.1.2-5. Mean record-length speed versus depth for unfiltered records of duration between 20 and 100 d for (left) west of 93°W, (center) 89° to 93°W, and (right) east of 89°W. All records have quality control grade of A, B, or C.

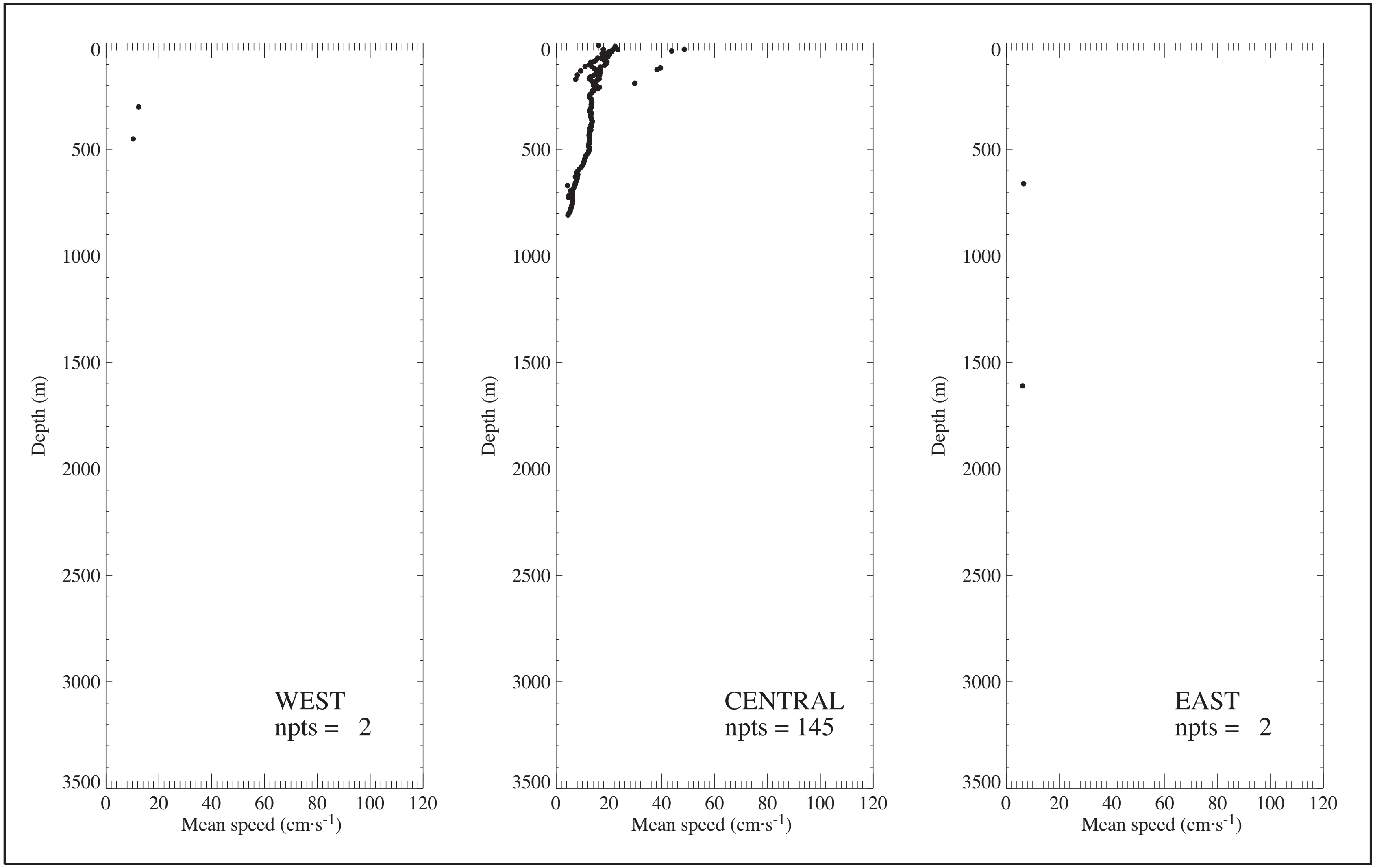

Figure 7.1.2-6. Mean record-length speed versus depth for unfiltered records of less than 20-d duration for (left) west of 93°W, (center) 89° to 93°W, and (right) east of 89°W. All records have quality control grade of A, B, or C.

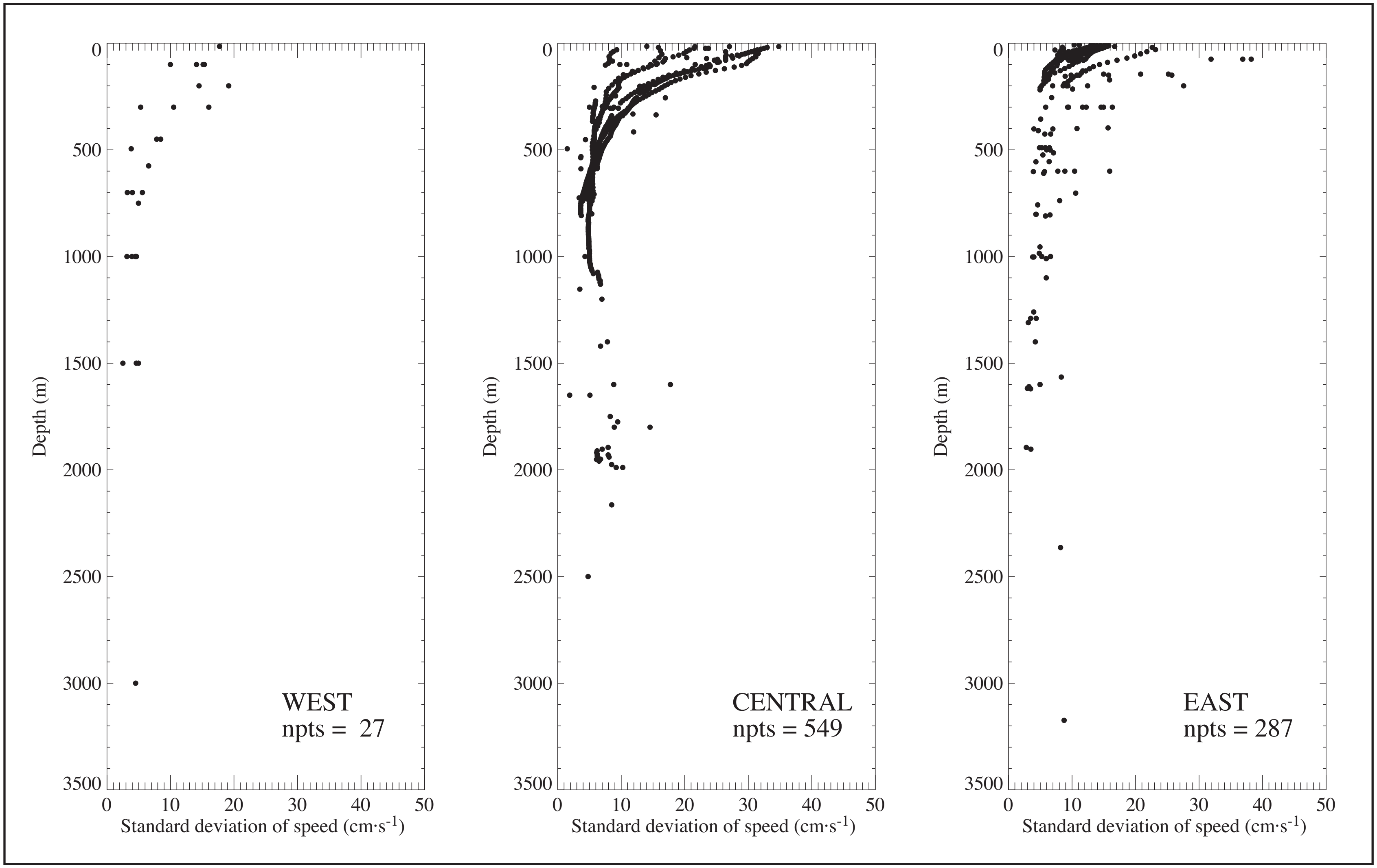

Figure 7.1.2-7. Standard deviation of speed versus depth for unfiltered records of at least 100-d duration for (left) west of 93°W, (center) 89° to 93°W, and (right) east of 89°W. All records have quality control grade of A, B, or C.

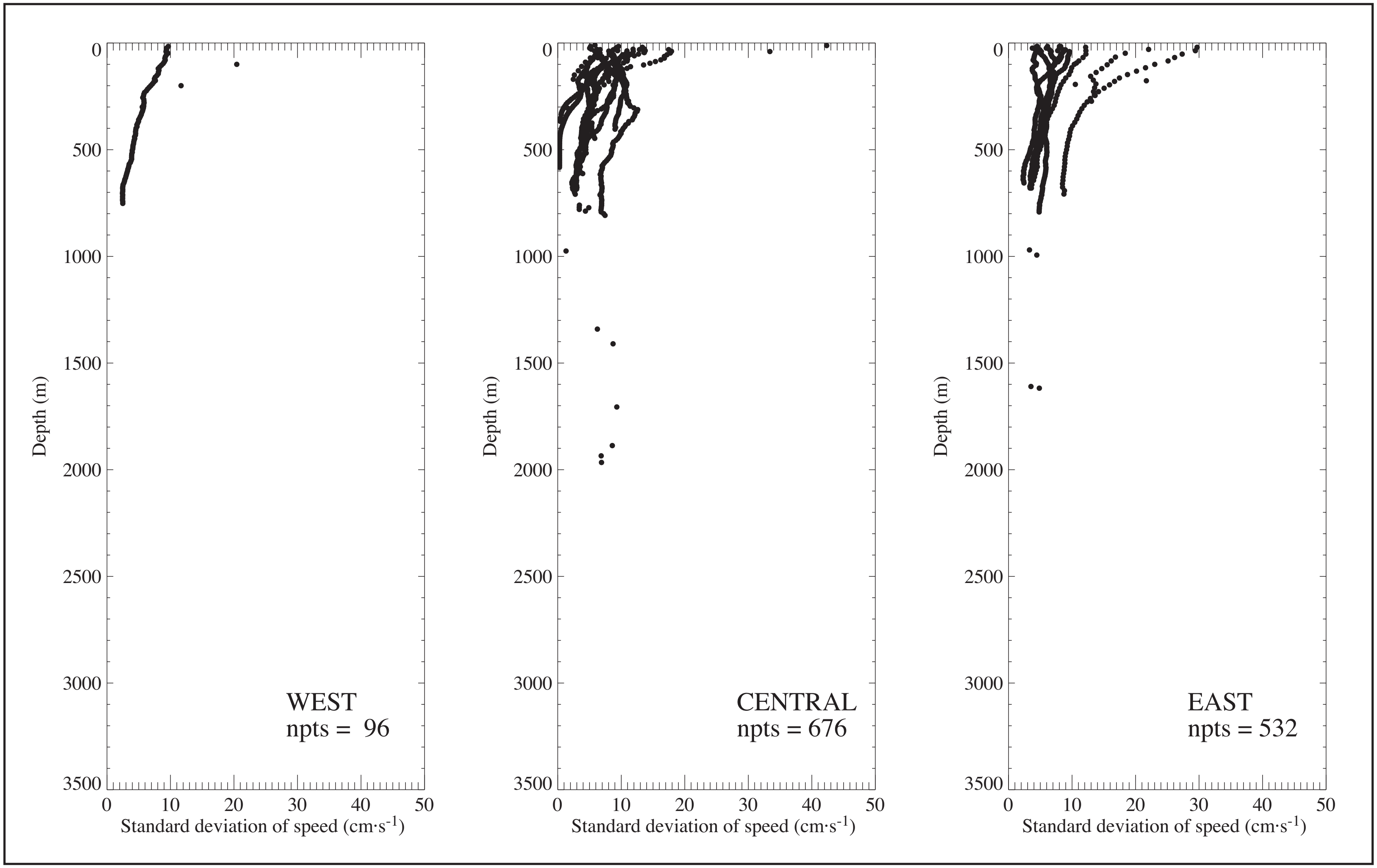

Figure 7.1.2-8. Standard deviation of speed versus depth for unfiltered records of duration between 20 and 100 d for (left) west of 93°W, (center) 89° to 93°W, and (right) east of 89°W. All records have quality control grade of A, B, or C.

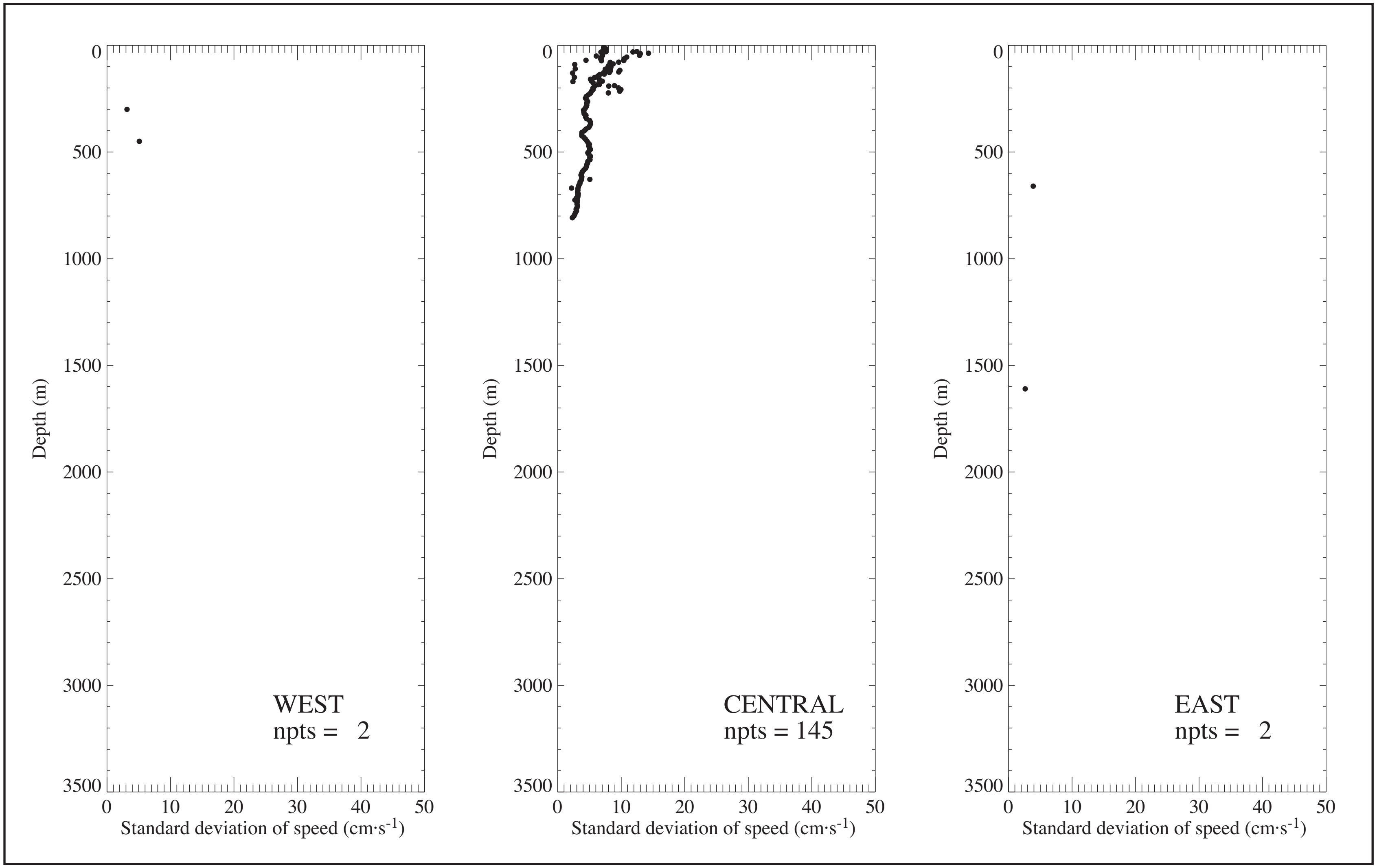

Figure 7.1.2-9. Standard deviation of speed versus depth for unfiltered records of less than 20-d duration for (left) west of 93°W, (center) 89° to 93°W, and (right) east of 89°W. All records have quality control grade of A, B, or C.

the means. Relatively large values at depth, particularly in the central region, are indicative of energetic events.

Averaged speeds and standard deviation were also examined versus normalized depth. The records from each mooring were binned according to instrument depth divided by water depth at the mooring. Then values of speed and standard deviation were averaged by bin. In Figure 7.1.2-10 are shown for western, central, and eastern Gulf the vertical profiles of binned average speeds and standard deviations for normalized depth bins of 0.05. Only unfiltered current records with quality control ratings of A or B and of at least 100-d duration were used to produce this result. Surface intensification and indication of bottom intensification due to energetic events are seen. It is noteworthy that the bottom intensification of the mean and standard deviation is most evident in the central region of the Gulf. Figure 7.1.2-11 shows the analogous result for all records of at least 20-d duration. Both record-length means and standard deviations for the upper and deep ocean generally are reduced relative to the records of at least 100-d duration. Shorter records are less likely to contain very energetic events.

7.1.3 Record-Length Velocities and Variances

We examined record-length current vectors and variance ellipses for all current meter records in water depths of at least 200 m in the Gulf of Mexico. Shown first are a few interesting examples of plots combining the vectors and ellipses as a function of depth for specific moorings. As a follow up to our discussion of current roses in section 7.1.1, we show in Figures 7.1.3-1, 7.1.3-2, and 7.1.3-3 record-length current vectors and variance ellipses for records of duration greater than 100 d from MMS mooring I1, I2, and I3. The records used are rated as grade A quality control and are at least 100-d duration. The ADCP records from the upper part of mooring I1 have been decimated to approximate 20-m intervals to facilitate viewing. The features expected on the basis of foregoing discussions are clearly seen here. At mooring I1: there were strong surface intensified currents and variability due to Eddy Juggernaut; the minimum vectors and variance are seen to occur in the depth interval of 800-1000 m; and there is intensification of currents and variance with depth below that interval. Near-bottom currents on mooring I2 were stronger than on moorings I1 or I3 and the variability was strongly oriented along the isobaths. There was less bottom intensification at mooring I3 but the variability was less constrained in direction by the bathymetry because the mooring was located further from the escarpment.

Figure 7.1.3-4 shows record-length current vectors and variance ellipses from a 1994 Marathon mooring in lease block EW1006. The records were from a suspended ADCP and were of duration between 20 and 100 d. During this deployment, LCEs Whopper and Xtra passed near the mooring resulting in a generally southwestward flow. Near surface there was considerable decrease in variance and clockwise rotation of the mean vector with depth. From near 100 to 400 m the mean vector and variance remained almost uniform, but in the lowest 40 m of the record the mean vector increased dramatically and the variance decreased with depth.

We compiled record-length current vectors and variance ellipses within depth intervals of 10% of water depths 50, 500, 1000, and 2000 m. Used were all current records with quality control grades of A or B. For ADCP data only the bin closest to the target depth was used. We considered results in three groups depending on duration: longer than 100 d, 20 to 100 d, and less than 20 d.

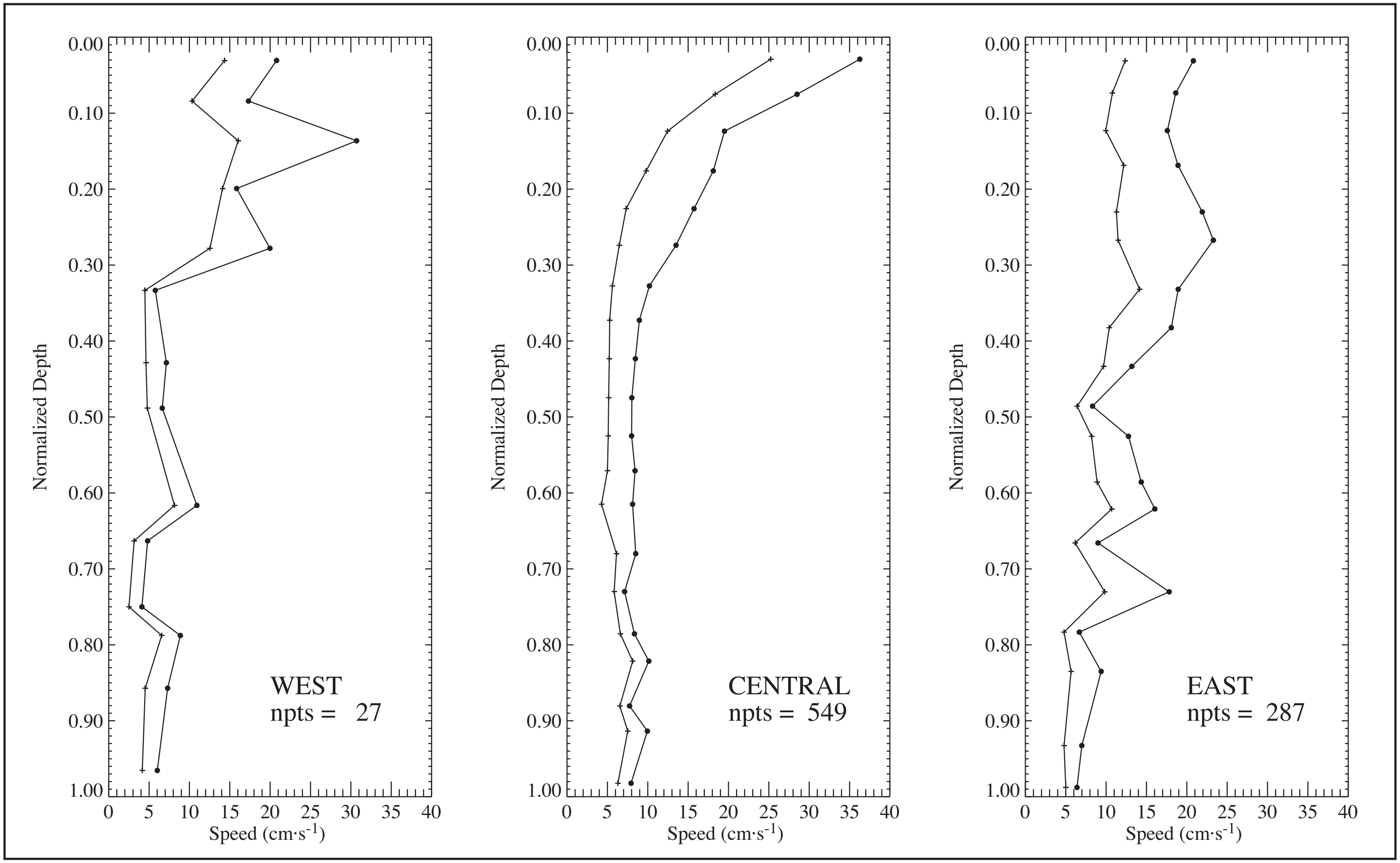

Figure 7.1.2-10. Bin averages of mean record-length speed (dots) and standard deviations (crosses) versus normalized depth (normalized bin depth 0.05) for deepwater Gulf of Mexico (left) west of 93°W, (center) 89° to 93°W, and (right) east of 89°W. All unfiltered current records with quality control ratings of A, B, or C and lengths of at least 100 d were used.

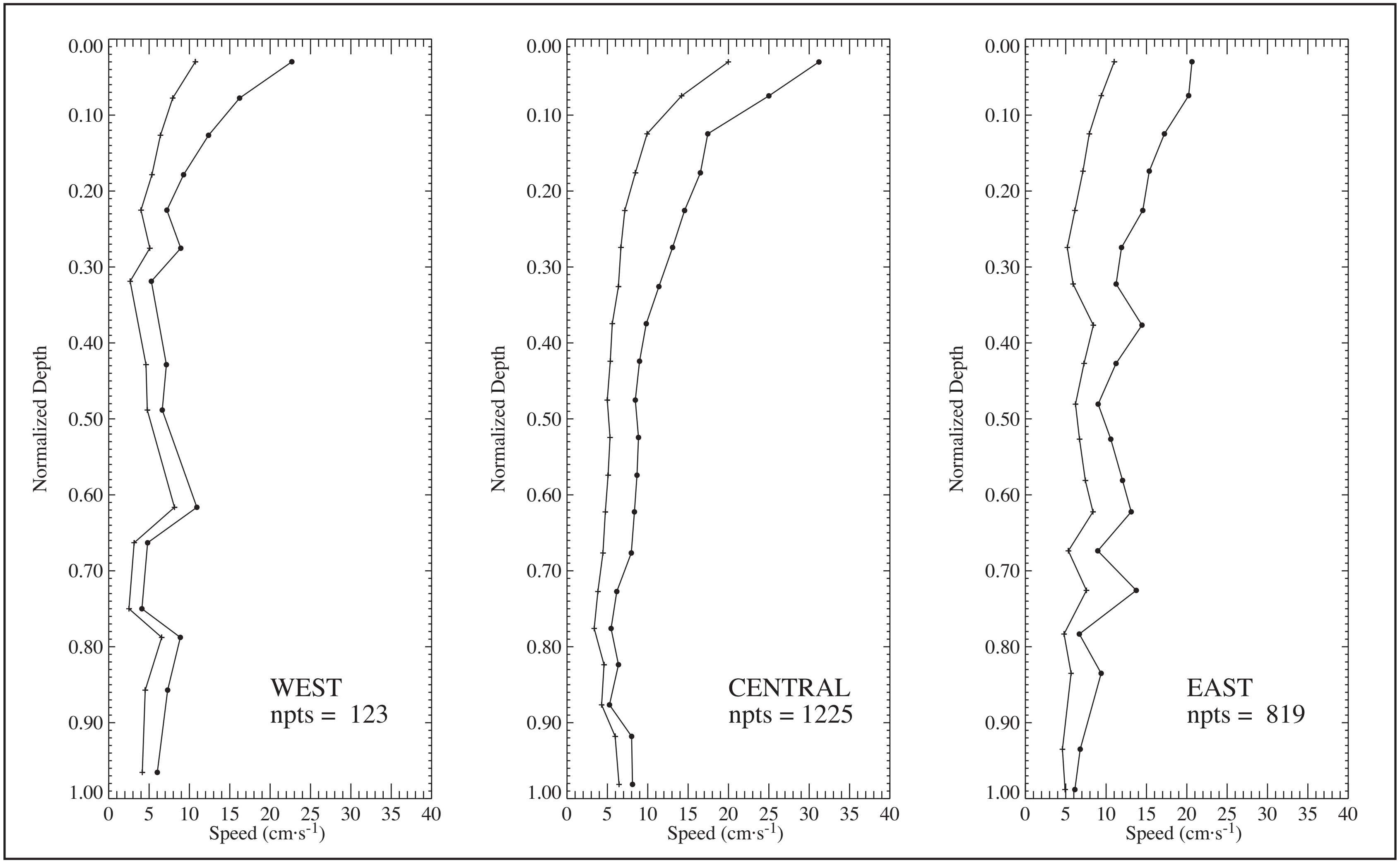

Figure 7.1.2-11. Bin averages of mean record-length speed (dots) and standard deviations (crosses) versus normalized depth (normalized bin depth 0.05) for deepwater Gulf of Mexico (left) west of 93°W, (center) 89° to 93°W, and (right) east of 89°W. All unfiltered current records with quality control ratings of A, B, or C and lengths of at least 20 d were used.

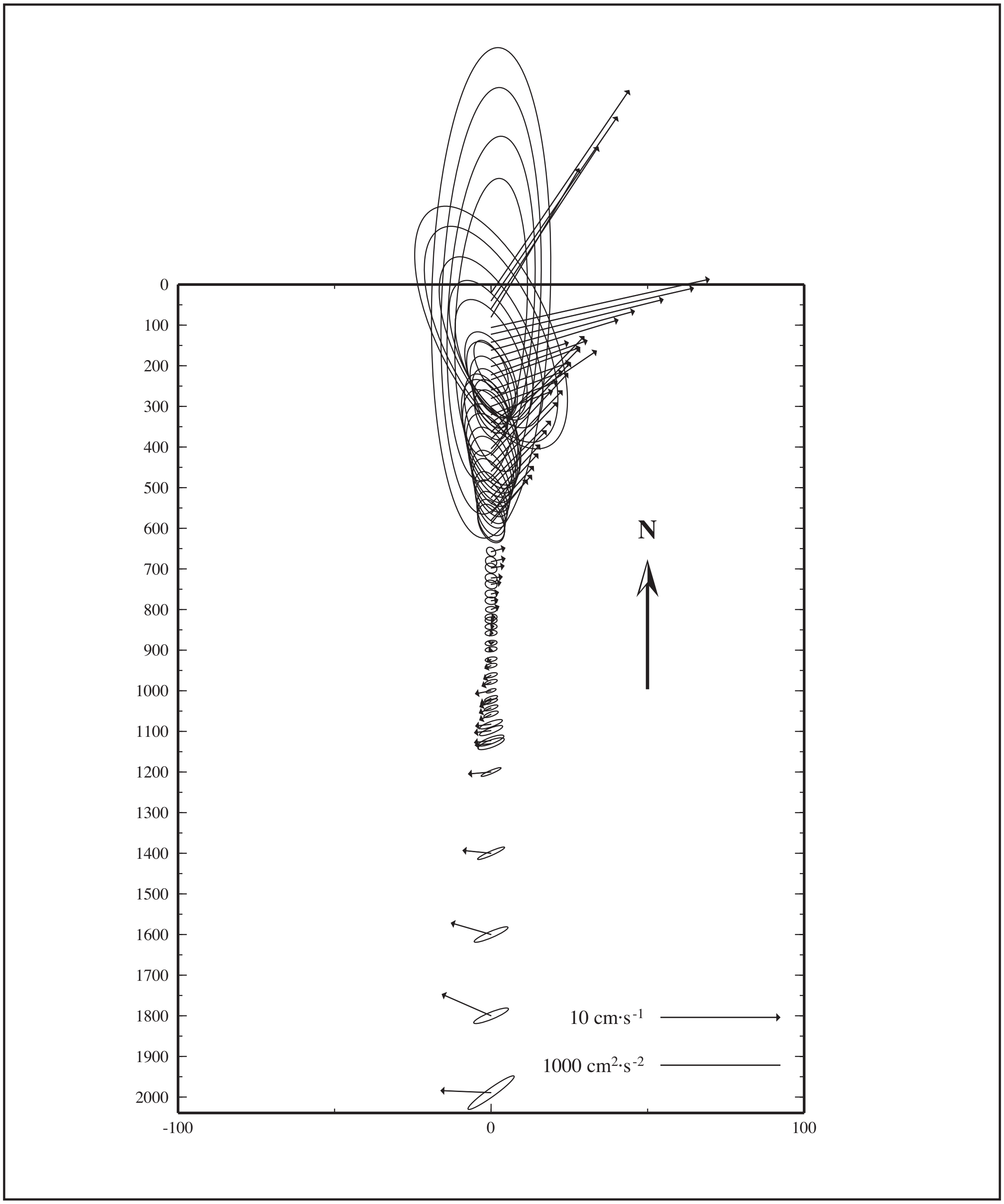

Figure 7.1.3-1. Record-length current vectors and variance ellipses for records of duration greater than 100 d from MMS mooring I1 at 89.784°W, 27.293°N. Records are quality control grade A or C; ADCP data on upper mooring has been decimated to ~20-m intervals.

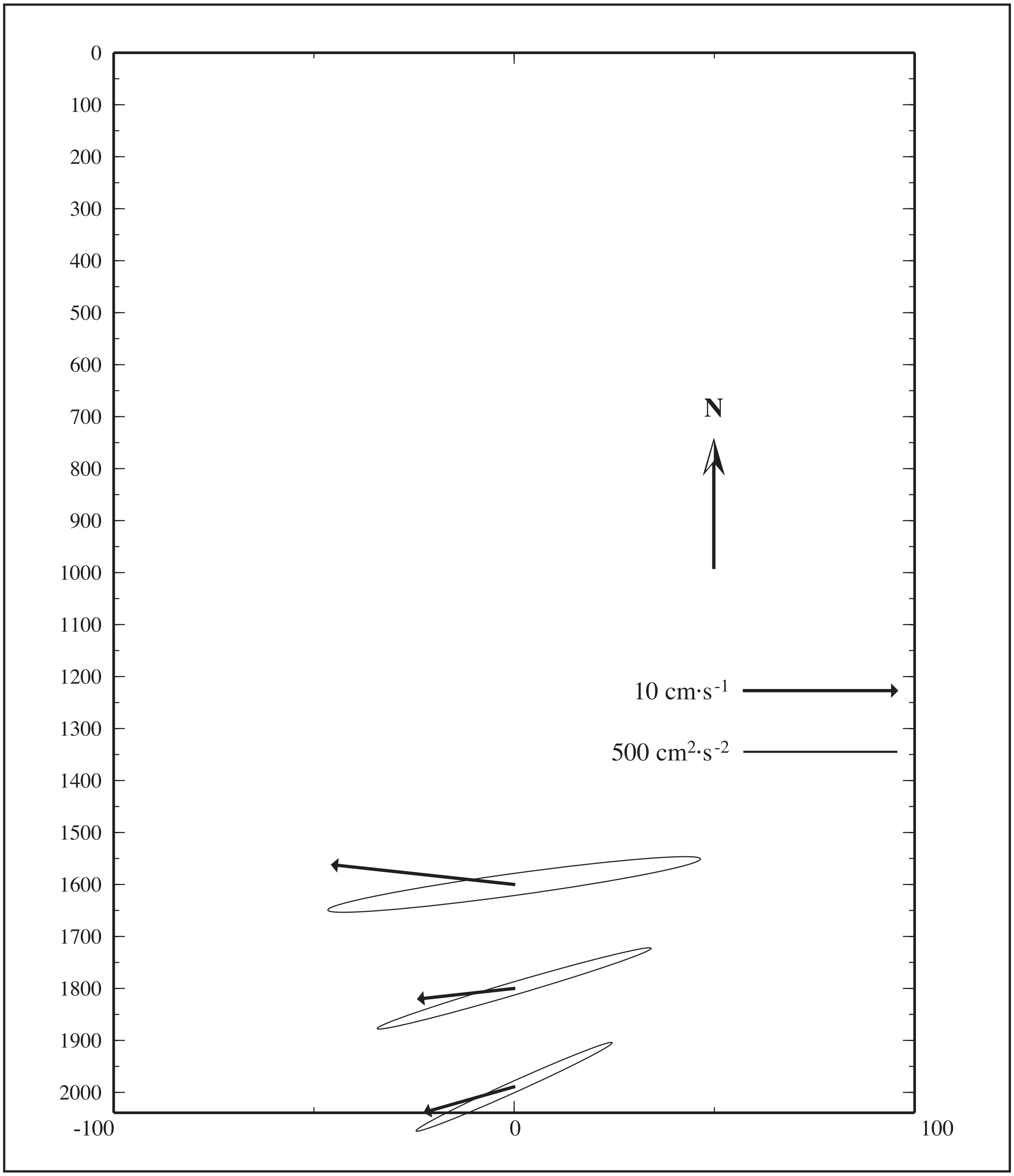

Figure 7.1.3-2. Record-length current vectors and variance ellipses for records of duration greater than 100 d from MMS mooring I2 at 89.971°W, 27.228°N. Records are quality control grade A.

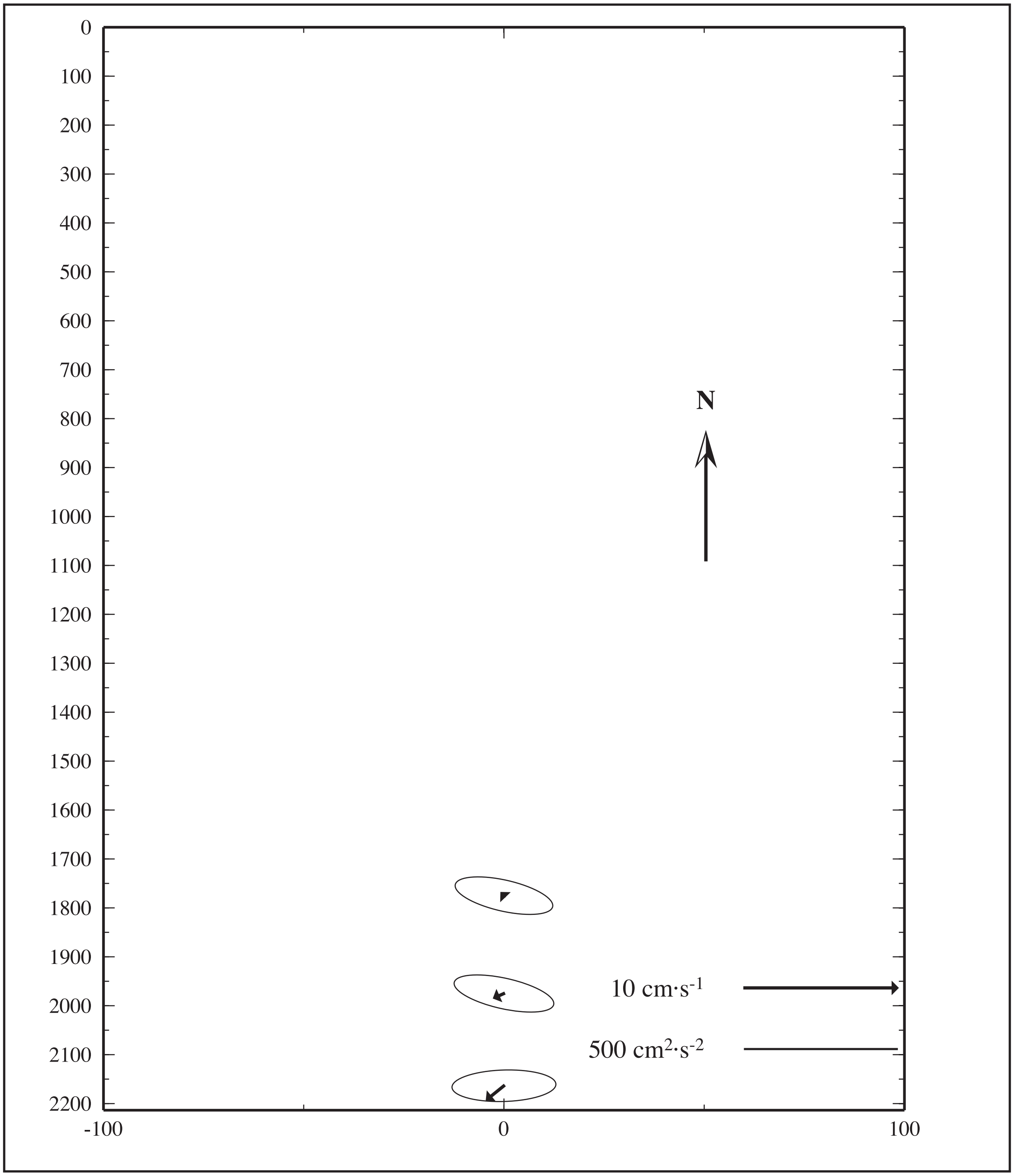

Figure 7.1.3-3. Record-length current vectors and variance ellipses for records of duration greater than 100 d from MMS mooring I3 at 89.814°W, 27.116°N. Records are quality control grade A.

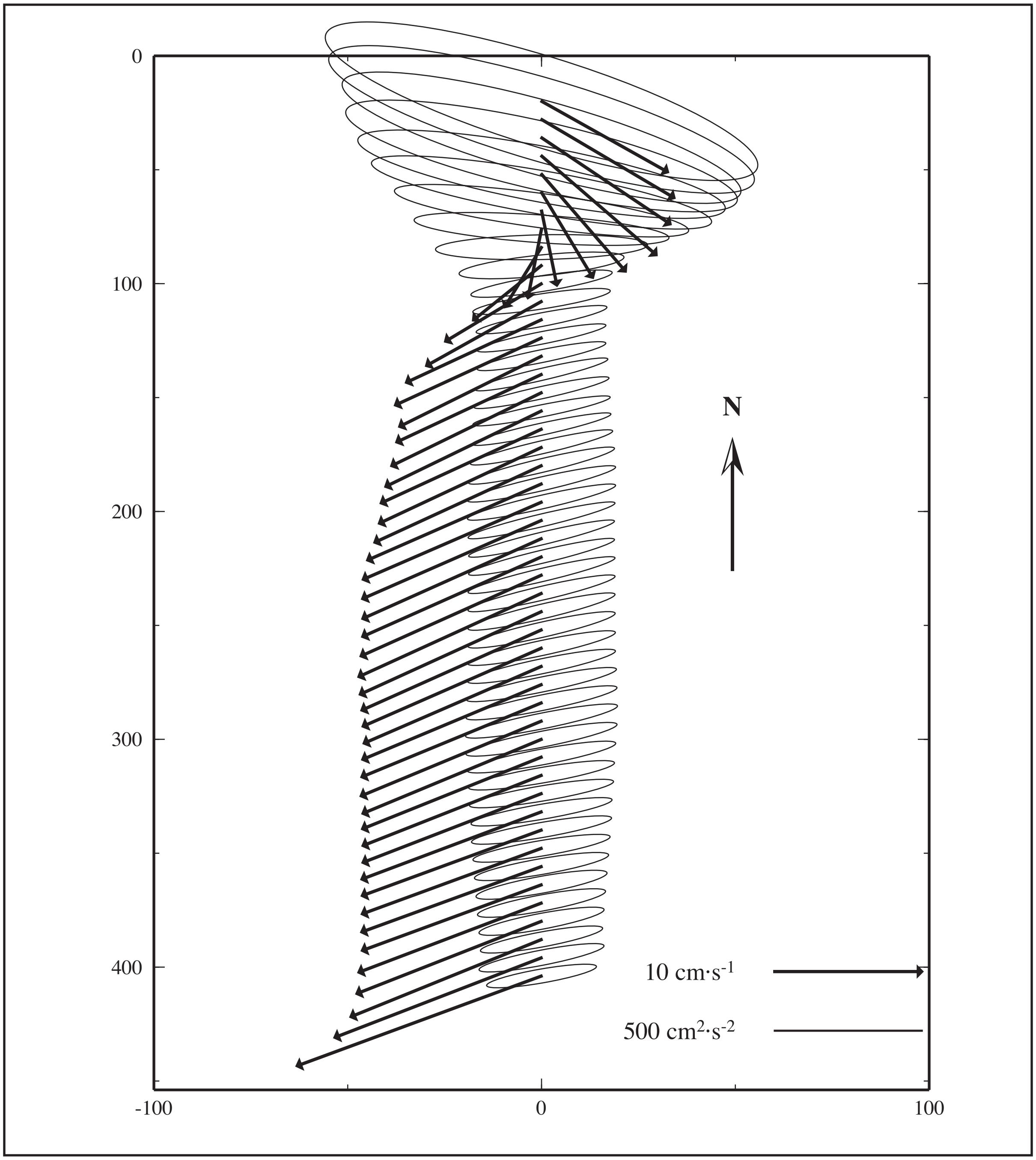

Figure 7.1.3-4. Record-length current vectors and variance ellipses for records of duration between 20 and 100 d for 1994 Marathon mooring in lease block EW1006 at 90.151°W, 27.958°N. Records are quality control C because the ADCP was suspended.

Shown in Figures 7.1.3-5 and 7.1.3-6 are mean vectors and variance ellipses for records of duration 100 d or more from instruments within ± 5 m of 50 m depth and within ± 50 m of 500 m depth, respectively. There are few such records, most coming from the DeSoto Canyon Eddy Intrusion Study. The mean flow and ellipses over the continental slope generally are oriented along bathymetry. For shorter records near 50-m depth this orientation was not so clear.

Mean vectors and variance ellipses for records of at least 100-d duration and from within ±100 m of 1000 m depth are shown in Figure 7.1.3-7. The mean directions and orientations of variance ellipses for the two records in the entrance to the Straits of Florida are along-isobath and toward the Atlantic, as expected. For records over the continental slope and rise, the mean currents are commensurate with cyclonic mean flow (with two exceptions) and all variance ellipses are elongated along the bathymetric contours. This result is in agreement with mean currents and variances from the CUPOM output (Section 5.3). Observed currents and variances within ± 200 m of 2000 m depth, shown in Figure 7.1.3-8, also show this pattern.

7.1.4 Eddy Kinetic Energy Distributions

As part of our study of energy levels, we computed the eddy kinetic energy (per unit mass) for four period bands and examined the distributions in space—depth and location within the Gulf. The spectral energy density was calculated (using the Fast Fourier Transform of the individual velocity components) for all current records of duration at least 100 d and quality grades A-D. Then, the energy densities for the following bins were obtained: high frequency band (≤ 2 d), weather band (2 to 10 d), mesoscale band (10 to 100 d), and sub-mesoscale band (>100 d). The eddy kinetic energy for each period band is then defined as the integrated spectral energy density over that band. See DiMarco et al. (2001) for more descriptions of kinetic energy spectrum calculation.

As an overview, Figure 7.1.4-1 shows eddy kinetic energy plotted as a function of instrument depth and by frequency band for all records as long as 100 d from the Gulf, regardless of location. Several features are clearly seen. First, the near-surface (say < 400 m) energy levels are smallest for the weather band, followed closely by the high-frequency band. Near-surface energy levels for the mesoscale band are generally greater. This is commensurate with results found over the outer shelf and upper slope of Louisiana and Texas during the LATEX program (Nowlin et al. 1998a). The highest eddy kinetic energy levels in the upper 800 m are found in the sub-mesoscale band and are associated with the Loop Current in the Florida Straits.

At depths below 800 m there is little indication of elevated energy in the high-frequency band. However, for the other three bands, energy levels increase with depth below that level. An apparent maximum is reached near 1600 m for all three bands, but, as we have seen elsewhere, this is likely because the most energetic currents at depth are found over the continental rise with water depths of 1000 to 2000 m. The mesoscale band has the greatest deep energy levels.

To provide more detail on the vertical distributions of eddy kinetic energy by band and document the differences in these distributions among the western, central, and eastern Gulf, Figures 7.1.4-2 through 7.1.4-5 are presented. Each figure shows for one energy band the vertical distributions west of 93°W, 89° to 93°W, and east of 89°W. It is of interest to note that in the central Gulf both the weather band and the mesoscale bands show pronounced increase in energy in the depth range of 1600-2000 m. The relative paucity of data from the

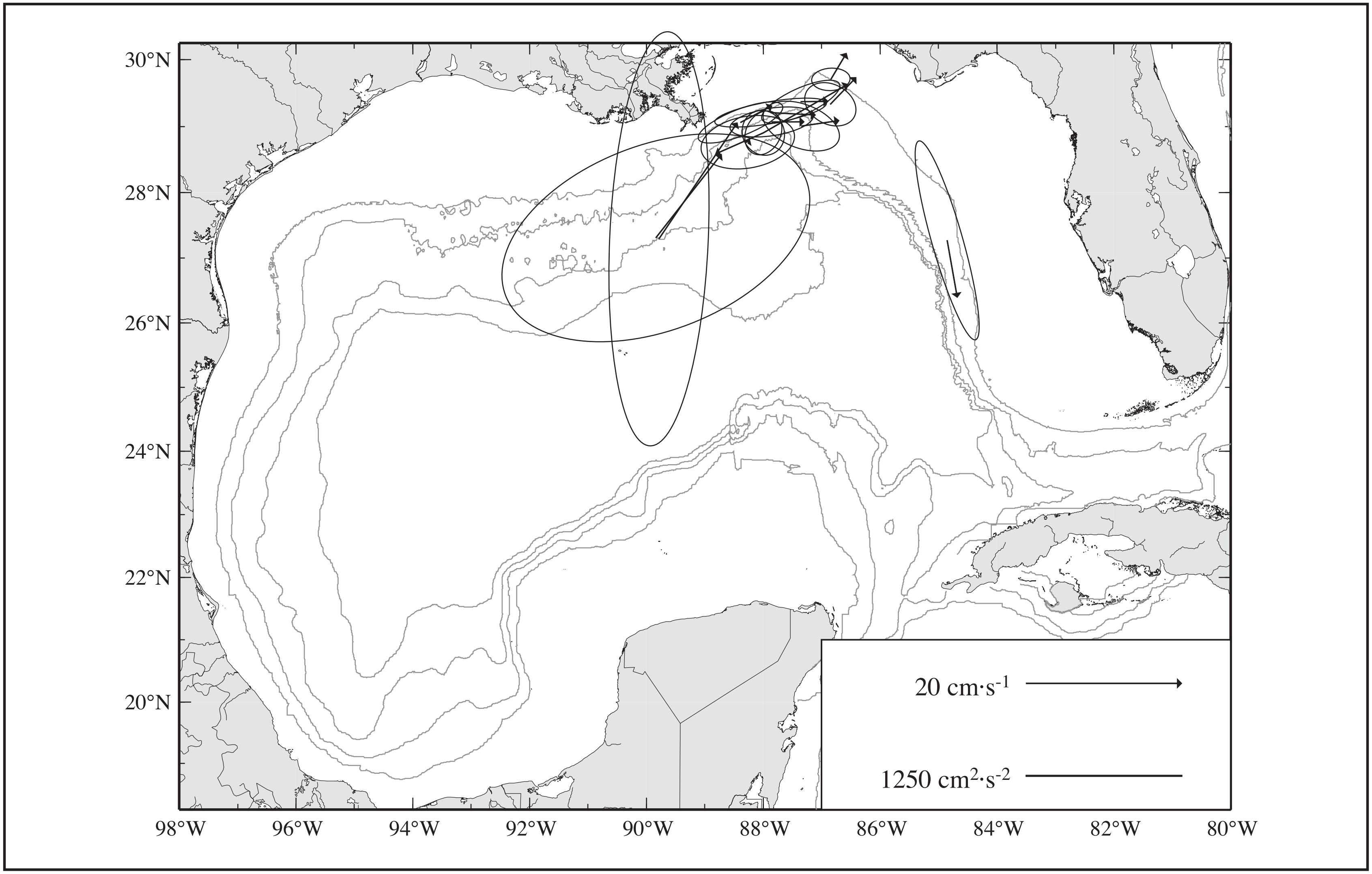

Figure 7.1.3-5. Record-length current vectors and variance ellipses at depth fo 50 m ± 5 m for records of quality control grades A or B and durations of at least 100 d in water depths of at least 200 m in the Gulf of Mexico. Bathymetric contours are 200, 1000, 2000, and 3000 m.

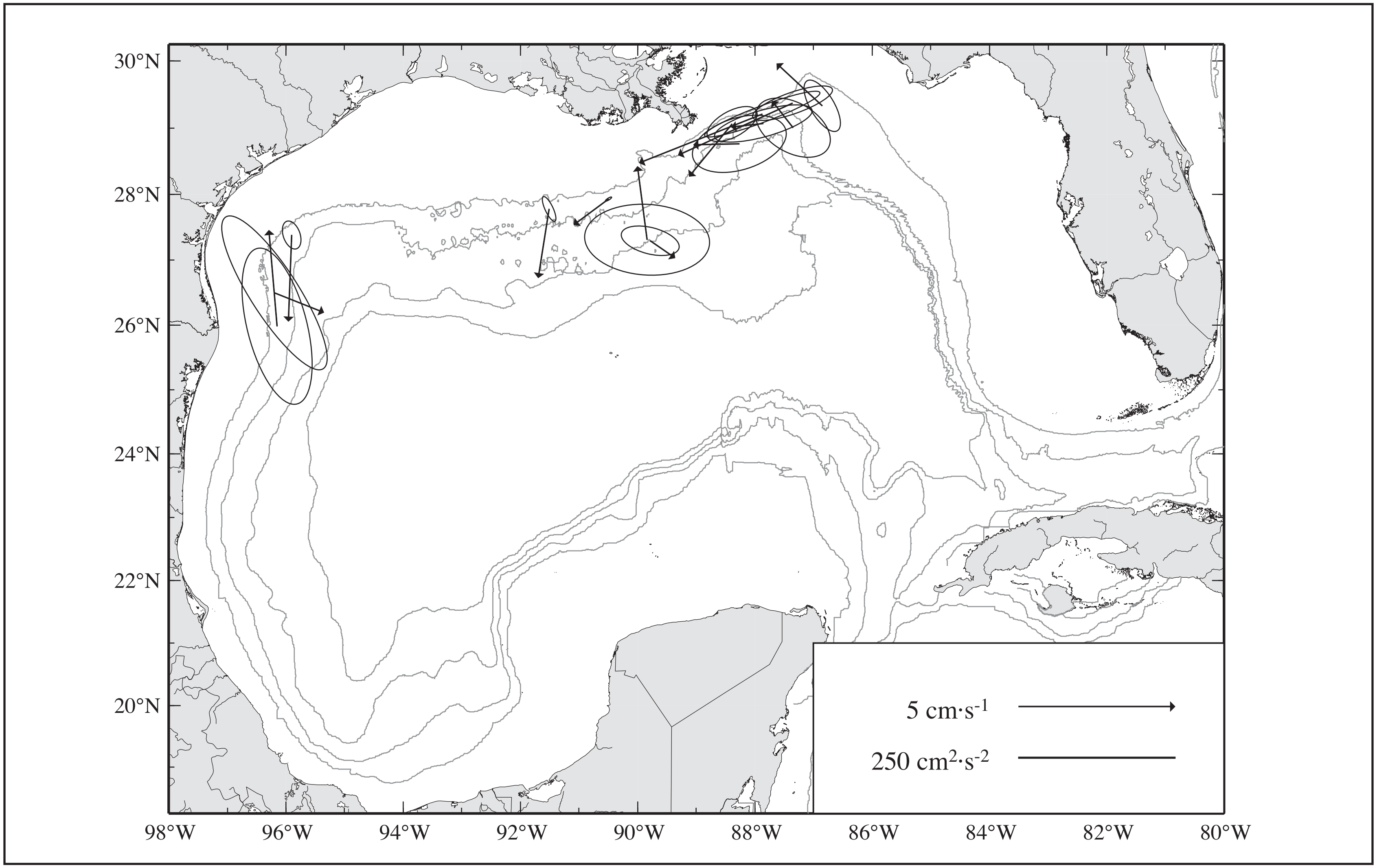

Figure 7.1.3-6. Record-length current vectors and variance ellipses at depth of 500 m ± 50 m for records of quality control grades A or B and durations of at least 100 d in water depths of at least 200 m in the Gulf of Mexico. Bathymetric contours are 200, 1000, 2000, and 3000 m.

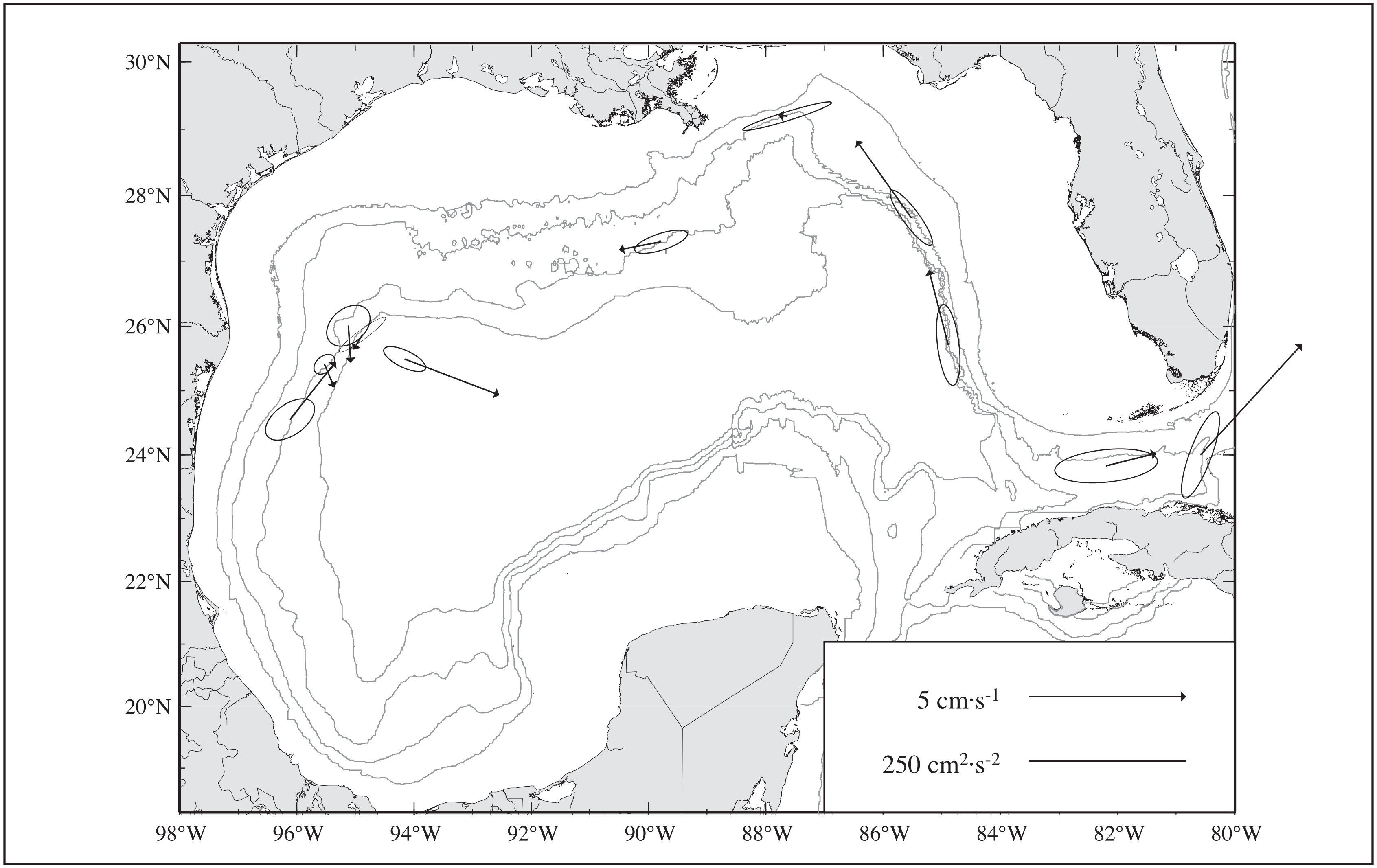

Figure 7.1.3-7. Record-length current vectors and variance ellipses at depth of 1000 m ± 100 m for records of quality control grades A or B and durations of at least 100 d in water depths of at least 200 m in the Gulf of Mexico. Bathymetric contours are 200, 1000, 2000, and 3000 m.

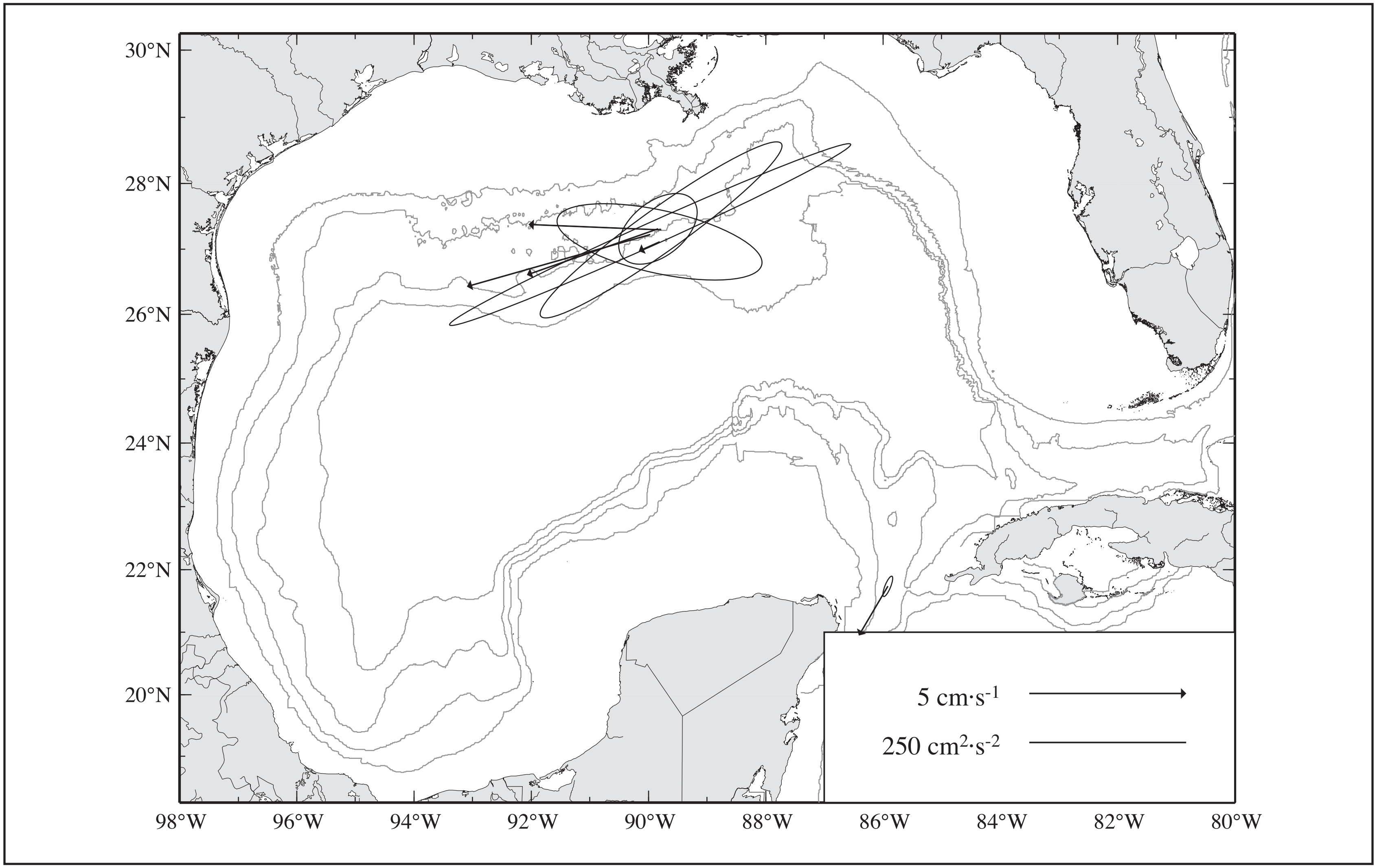

Figure 7.1.3-8. Record-length current vectors and variance ellipses at depth of 2000 m ± 200 m for records of quality control grade A or B and durations of at least 100 d in water depths of at least 2000 m in the Gulf of Mexico. Bathymetric contours are 200, 1000, 2000, and 3000 m.

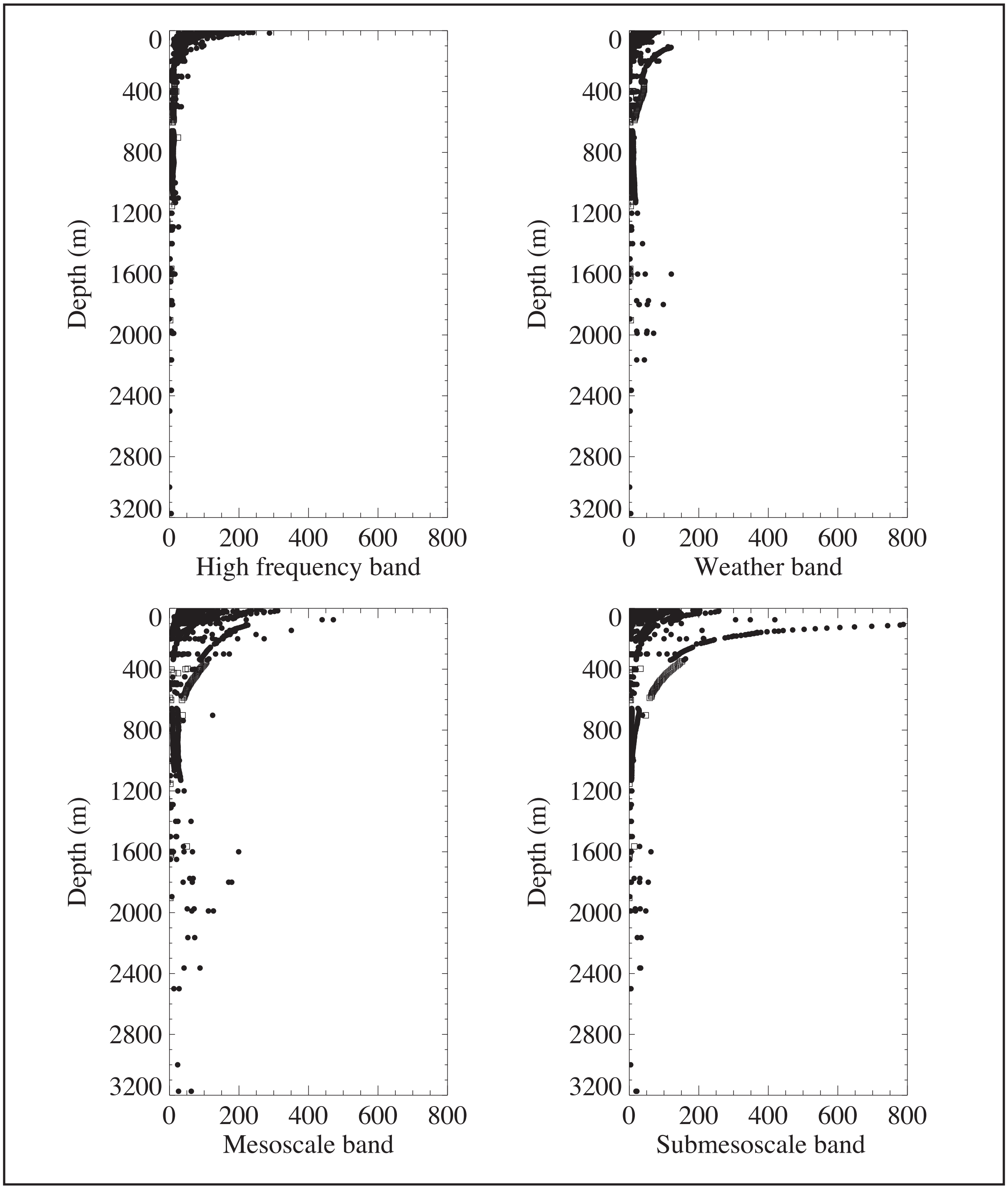

Figure 7.1.4-1. Eddy kinetic energy ($cm^2 \cdot s^{-2}$) versus instrument depth for current records of at least 100 d duration. The total number of records used was 1079. Data quality codes are: circle for A and B, square for C, and plus for D. Bands are high-frequency (≤ 2 d), weather band (2 to 10 d), mesoscale band (10 to 100 d), and sub-mesoscale band (> 100 d).

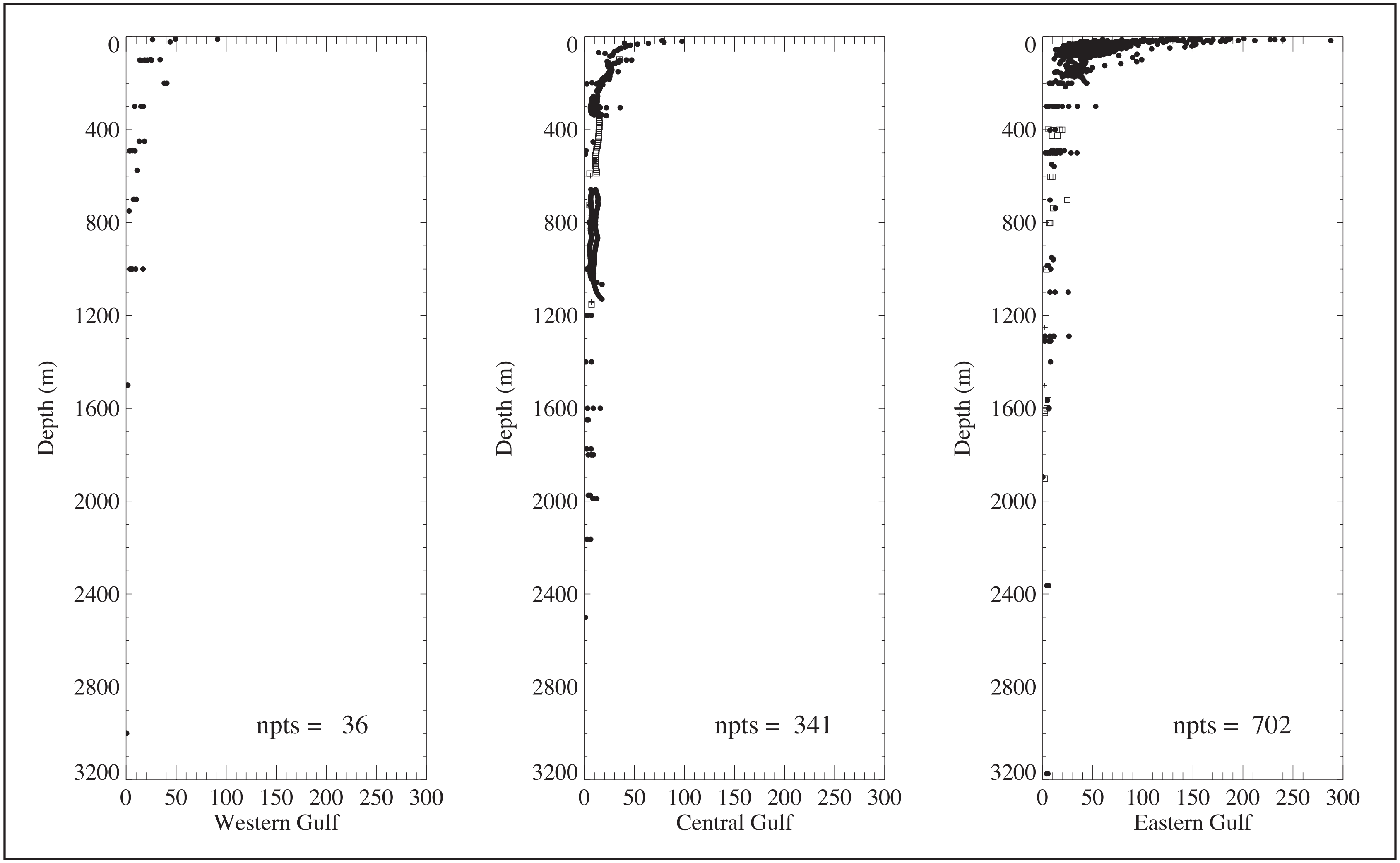

Figure 7.1.4-2. High-frequency band (period ≤ 2 d) eddy kinetic energy ($cm^2 \cdot s^{-2}$) versus instrument depth for records of duration for at least 100 d for (left) west of 93°W, (center) 89° to 93°W, and (right) east of 89°W. Data quality codes are: circle for A and B, square for C, and plus for D. The number of records (npts) is shown for each panel.

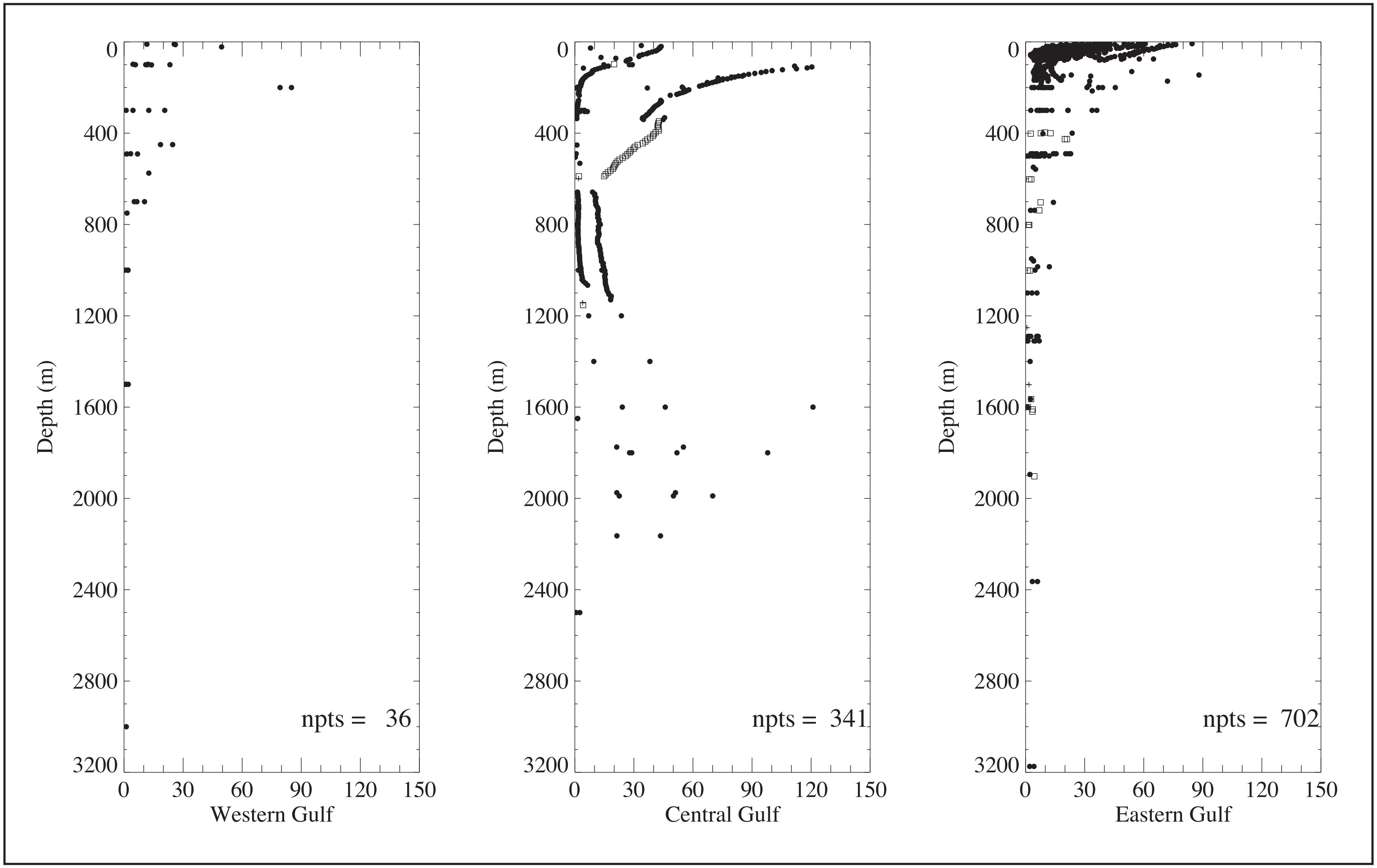

Figure 7.1.4-3. Weather band (2 to 10 d period) eddy kinetic energy ($cm^2 \cdot s^{-2}$) versus instrument depth for records of duration for at least 100 d for (left) west of 93°W, (center) 89° to 93°W, and (right) east of 89°W. Data quality codes are: circle for A and B, square for C, and plus for D. The number of records (npts) is shown for each panel.

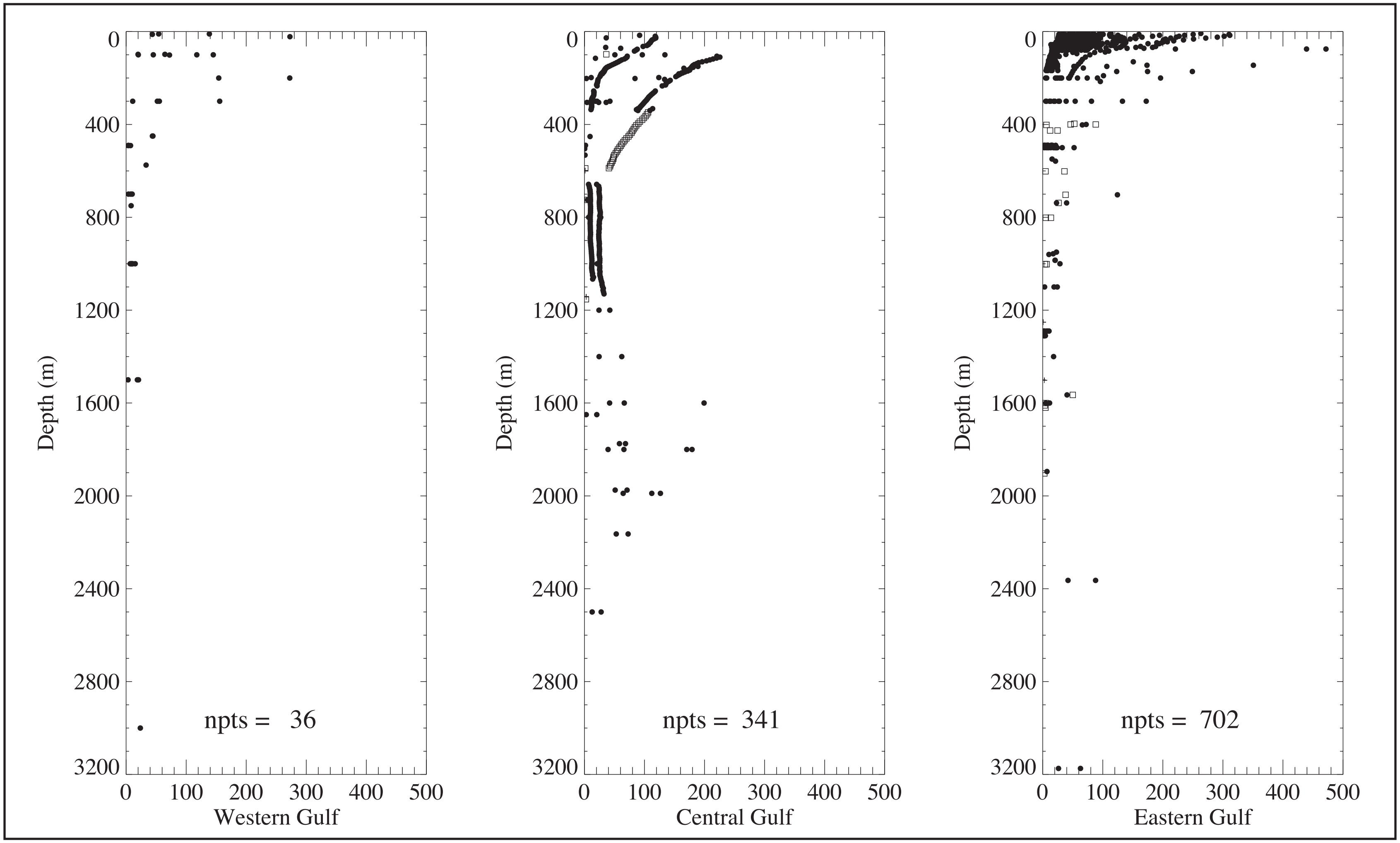

Figure 7.1.4-4. Mesoscale band (10 to 100 d period) eddy kinetic energy ($cm^2 \cdot s^{-2}$) versus instrument depth for records of duration for at least 100 d for (left) west of 93°W, (center) 89° to 93°W, and (right) east of 89°W. Data quality codes are: circle for A and B, square for C, and plus for D. The number of records (npts) is shown for each panel.

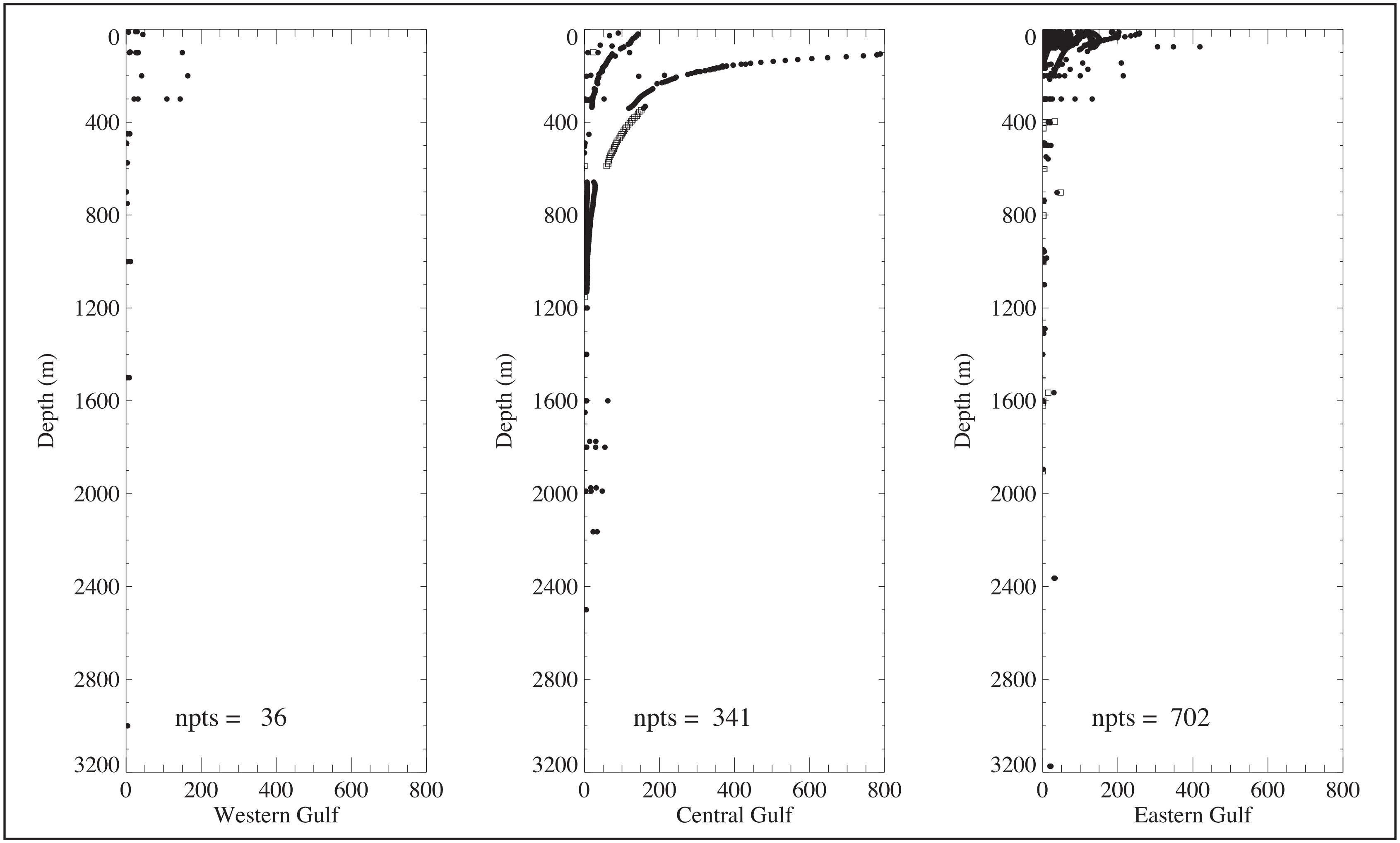

Figure 7.1.4-5. Submesoscale band (period > 100 d) eddy kinetic energy ($cm^2 \cdot s^{-2}$) versus instrument depth for records of duration for at least 100 d for (left) west of 93°W, (center) 89° to 93°W, and (right) east of 89°W. Data quality codes are: circle for A and B, square for C, and plus for D. The number of records (npts) is shown for each panel.

western Gulf limits comparisons with the eastern and central Gulf to only the broadest features. Moreover, comments on bottom intensification must be viewed with the understanding that the number of deep records is relatively small. With these caveats, we offer a few general conclusions.

The greatest high-frequency EKE in water depths of 800 m or less was in the eastern Gulf, with values well over twice those of the central or western Gulf (Figure 7.1.4-2). From Figure 7.1.4-3 it is seen that below 100 m the largest weatherband kinetic energy is found in the central Gulf, and the bottom intensification of energy in that band also is greatest in the central Gulf. By contrast, mesoscale band kinetic energy (Figure 7.1.4-4) within the upper 1000 m is greatest in the eastern Gulf. For this band also the bottom intensification is greatest for the central Gulf, but intensification toward the bottom is seen in the eastern Gulf as well. Finally, the largest sub-mesoscale kinetic energy values (Figure 7.1.4-5) are found near 100 m in the central Gulf. (These values are from MMS mooring I1, consistent with the long presence of Eddy Juggernaut in the area.) Again for this band the most pronounced bottom intensification is in the central Gulf.

7.1.5 Energy Spectra

Energy spectra from long current records throughout the deepwater Gulf were examined. Shown in Figure 7.1.5-1 are representative spectra from long records at a range of depths from the western, central, and eastern Gulf. Table 7.1.5-1 identifies the records used in constructing Figure 7.1.5-1 and gives locations, times, and record lengths. Note that several mooring locations were used for each region. Only publicly available data were used. Unfiltered records were used when available. All records used were given quality ratings of A or B.

At the lowest frequencies (periods greater than ~30 d) minimum energy values are found in the range 700-1000 m. This is consonant with the result that record-length mean speeds reach relative minimum values in the depth range 800-1000 m shown in Section 7.1.2.

For periods of 1-10 d there is less variation of energy with depth in the eastern region than within the central and western regions. This excitation of more higher frequency motions in the eastern Gulf than elsewhere could result from the presence of the Loop Current and its variabiabity.

The diurnal peaks in the eastern region are probably due mainly to diurnal tides. The location is in the southeast Gulf and there are large diurnal fluxes through the two straits connecting the Gulf to the Atlantic and Caribbean. The diurnal energy levels at depth in the central and western Gulf are small (much smaller than for the eastern Gulf). The more energetic near-diurnal energy levels in the upper layers of the western and central Gulf are probably due to inertial motion.

7.1.6 Vertical Empirical Orthogonal Function Analyses

Empirical orthogonal function (EOF) analysis, also known as principal component analysis, has become an accepted tool to quantify patterns of variability present in large sets of time-series data (Emery and Thomson 1997). We employed EOF analysis on current meter data taken from several long-term deep Gulf of Mexico mooring locations in which data were available from at least 5 depth levels distributed throughout the water column.

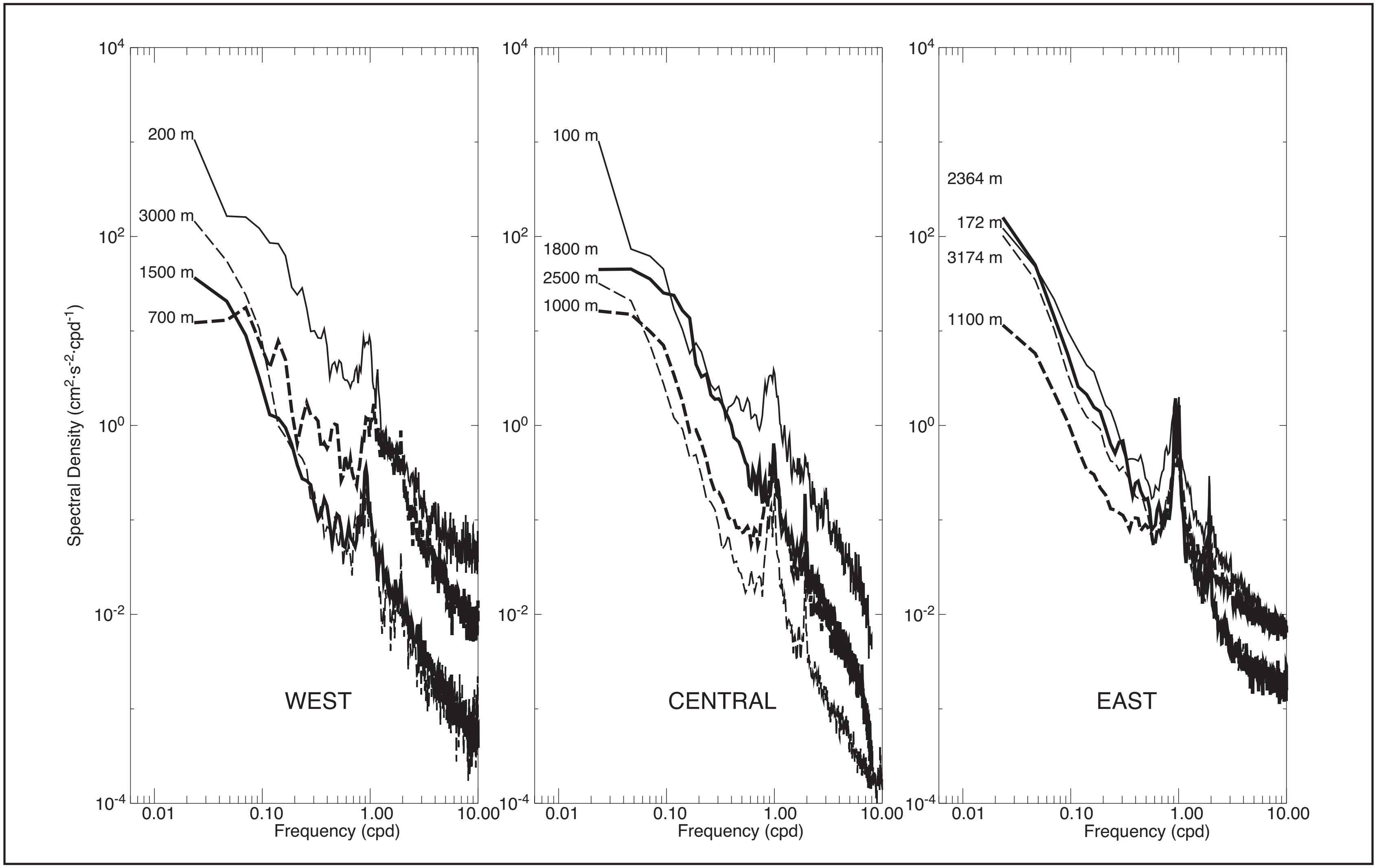

Figure 7.1.5-1. Energy spectra from selected long current records in the western (west of 93°W), central (89° to 93°W), and eastern (east of 89°W) deep water Gulf of Mexico. Table 7.1.5-1 identifies the moorings used and gives dates and duration of sampling. The depth of the instrument is shown.

Table 7.1.5-1. Locations, times, and durations of current time series used in constructing Figure 7.1.5-1, grouped by region of Gulf of Mexico.

Region	Depth (m)	Name	Dates (m/d/y)	Duration
West	200	Brooks S	7/17/1980–2/9/1981	~ 7 months
	700	Brooks C	7/17/1980–2/11/1981	~ 7 months
	1500	SAIC Q	6/15/1985–5/4/1986	11 months
	3000	SAIC R	6/15/1985–10/21/1985	4 months
Central	100	I1	8/29/1999–8/26/2000	12 months
	1000	I1	8/29/1999–8/26/2000	12 months
	1800	I1	8/29/1999–8/26/2000	12 months
	2500	GG	11/8/1987–10/30/1988	12 months
East	172	A	1/27/1984–2/1/1986	15 months (9 month gap not included)
	1100	A	1/27/1984–1/31/1986	19 months (5 month gap not included)
	2364	A	2/3/1984–1/31/1986	21 months (3 month gap not included)
	3174	A	2/3/1984–1/31/1986	21 months (3 month gap not included)

The EOF analyses were done first on the raw unfiltered data at locations from the eastern (SAIC A), central (SAIC GG), and western (SAIC R) regions of the Gulf of Mexico. Each mooring consisted of 5 instruments which spanned the water column. The length of the time series analyzed at each location varied depending on deployment length and gaps at each level. Analyses were performed using those data that were available at all depth levels, i.e., irrespective of any temporal gaps. For SAIC A, the time-series duration was roughly 13 months, for SAIC GG 12 months, and for SAIC R it was 5 months. To facilitate analysis of the EOF modal time series, singular value decomposition (SVD) was used to provide both the modal amplitudes and principal component time series.

Figure 7.1.6-1 shows the vertical structure of the first three EOF modes at each mooring location. All three panels show roughly the same modal structure. Mode 1, containing the largest percentage of total variance, has a surface maximum that decreases exponentially with depth. At the central location (SAIC GG) mode 1 is zero at depth. Mode 2, containing the second largest percentage of variance, is bottom-intensified with a zero-crossing or minimum in the upper 500 meters with a barotropic (nearly constant) span at depth. Mode 3 has two zero-crossings in the upper 1000 m. Below 1000 m, mode 3 resembles mode 2 with a deep barotropic span. These patterns are typical of EOF analyses performed at other locations which had less than four instruments and did not span the entire water column.

The results of these analyses are consistent with our interpretation of a dominant surface-intensified mode exponentially decaying with depth and a deep barotropic mode below 1000 m. Because the depth levels of the three cases depicted in Figure 7.1.6-1 are not the same, a direct comparison of the variance of each mode is not prudent. However, the percentage of variance in the first (surface-intensified) mode is substantially greater than that of mode 2. This is a general characteristic seen in the EOF analysis performed on all locations in the Gulf of Mexico that had full water column coverage.

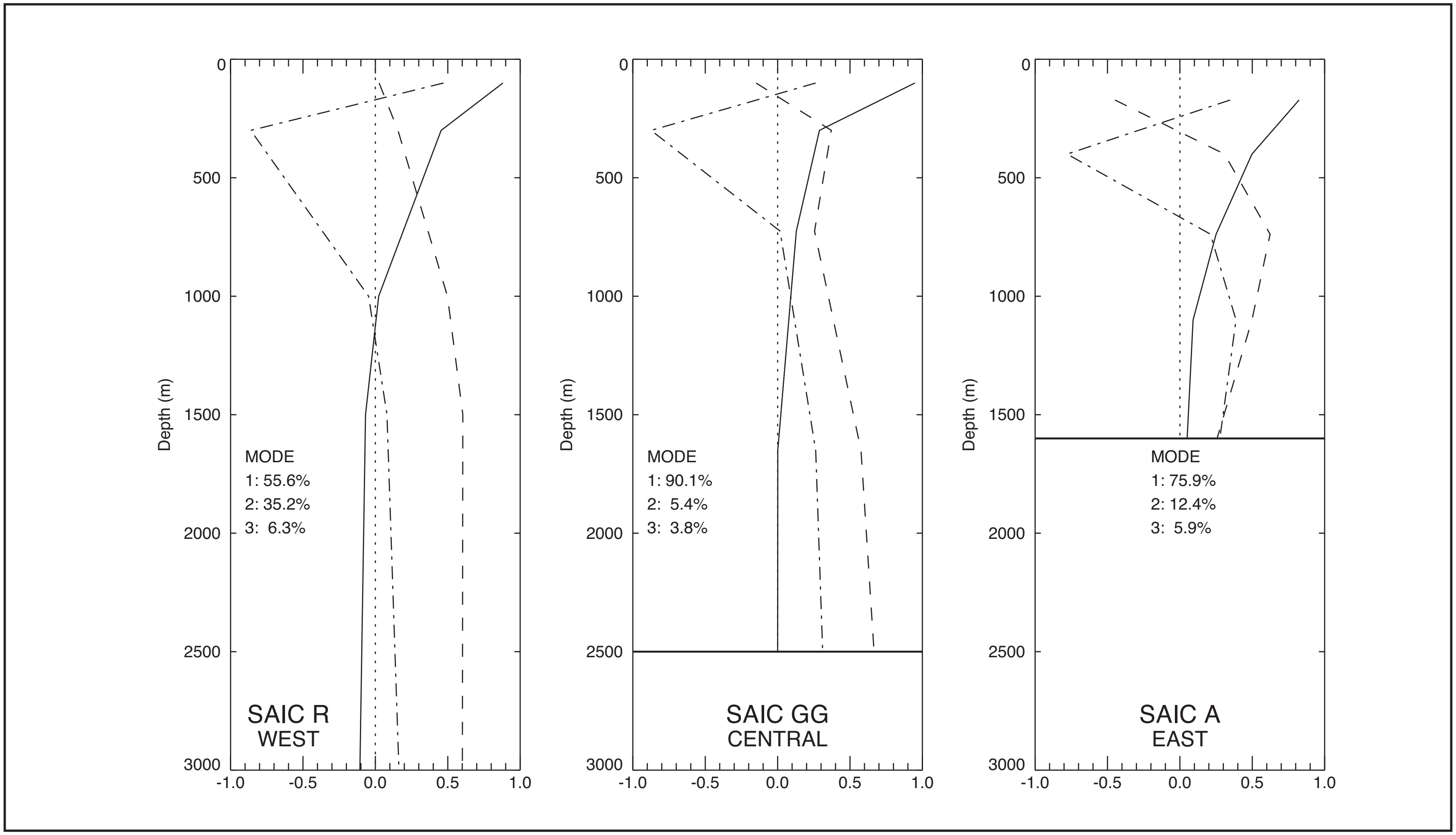

Figure 7.1.6-1. EOF modes 1-3 for deep Gulf of Mexico stations SAIC R in the western Gulf (left panel), SAIC GG in the central Gulf (center panel), and SAIC A in the eastern Gulf (right panel). Water depths at SAIC R, GG, and A were 3500, 3000, and 1697 m, respectively. Mode 1 is solid, mode 2 is dashed, and mode 3 is dot-dash. Percentages of variance in each mode are shown. Data used were raw and unfiltered. Five depth levels were used for each location.

Recently, a full water column deployment in the north central Gulf at the edge of the Sigsbee Escarpment (MMS-sponsored SAIC EIS extension mooring I1) containing multiple ADCP and RCM7/8 current meters afforded unprecedented spatial resolution during 1999 and 2000. The vertical modal structure of the first three EOF modes from year-long, hourly, unfiltered records at 11 depth levels between 100 and 1800 m is shown in the right panel of Figure 7.1.6-2. The structure is remarkably similar to those found from the 5 level locations described previously. The dominant mode 1 is surface intensified and exponentially decreases with depth. Mode 2 has a zero-crossing at about 300 m, increasing slowly to 1000 m, then more rapidly before leveling below 1500 m. Mode 3 has the most variability in the upper 1000 m with two zero-crossings and small values below 1000 m. The percentage of variance accounted for in each mode is shown in the figure.

The left panel of Figure 7.1.6-2 shows the modal structure from 17 levels of CUPOM model data at a grid point close to the SAIC I1 location. The data used in this EOF analysis spanned the model years 1993 through 1998 and was 40-hr low-pass filtered and then decimated to one point per 48 hours due to computer limitations imposed by the SVD procedures. Again the structure of the first three modes is remarkably similar to that found from the I1, A, GG, and R observations. Mode 1 is surface-intensified and exponentially decreases with depth. Mode 2 is a deep barotropic mode. Mode 3 is variable in the upper 1000 m and small below.

Since EOF modes are statistical constructs and do not represent physical modes, it is useful to decompose the EOF modes into dynamic modes. The discussion of dynamic mode decomposition of the CUPOM output and observations is given in Section 8.3.

7.2 Statistical Measures of Energetic Events

Current records were treated in three basic ways to identify segments containing energetic events. Records that matched in time the occurrence of Loop Current eddy separations, tropical cyclones, hurricanes, and extratropical (winter) cyclones were identified and examined for the period of interest. Records from mooring locations in the vicinity of the Loop Current Eddies, other anticyclonic eddies, or cyclonic eddies, as located in SSH fields or EddyWatch charts during the deployment period, were identified and examined. Two documented cases of a Loop Current intrusion were examined. Finally, energetic current events not attributable to these phenomena were visually identified and then characterized by their similarity to the characteristics of other types of phenomena, such as deep barotropic motions. Below are described the statistics of the energetic events by type: Loop Current and surface-intensified eddies, currents generated by energetic wind events, deep barotropic and bottom-trapped motions, and subsurface mid-water column motions.

The maximum speed, mean speed, and standard deviation of speed for each energetic current event identified in a non-proprietary record are provided by type of phenomenon in the Appendix, together with information on the file name, dates of event, mooring location, instrument depth, and total water depth. The Appendix also contains figures showing details of several events. Note the event statistics discussed below cover only the non-proprietary data sets.

7.2.1 Loop Current and Surface-Intensified Eddies

There were a number of cases where a mooring was directly influenced by the Loop Current. Most notably, the moorings deployed in the Straits of Florida and moorings A and G of the SAIC 5-year study were impacted by the Loop Current. These are described further in Section 6.3. Other events associated with the Loop Current and surface-intensified eddies

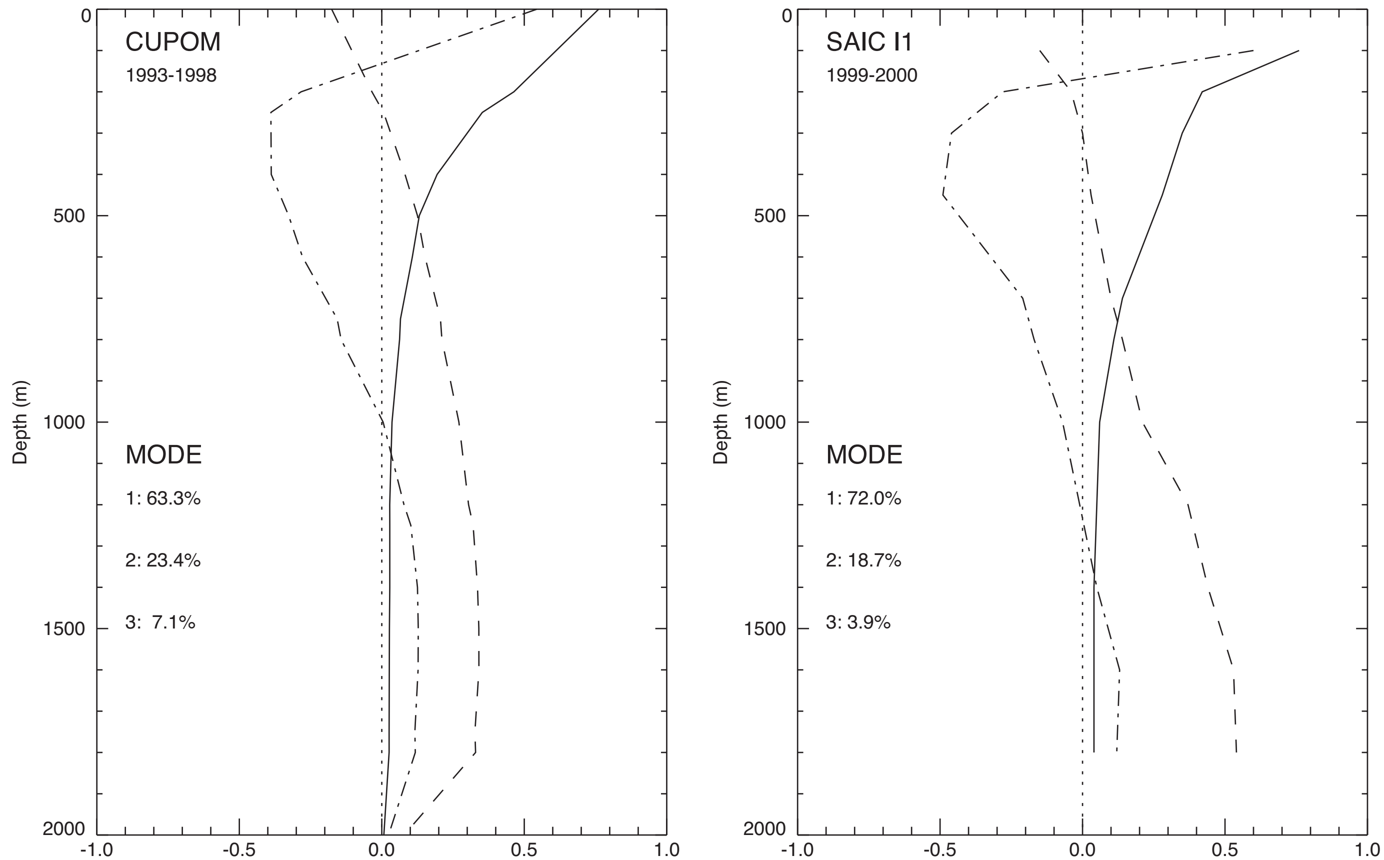

Figure 7.1.6-2. EOF modes 1-3 for MMS EIS extension mooring I1 (right panel) and for CUPOM output for grid point near that mooring in the north-central Gulf of Mexico near Sigsbee Escarpment. For mooring I1, eleven depth levels of unfiltered data spanning the period from August 1999 through August 2000 were used. CUPOM hindcast currents at 17 levels for the model years 1993-1998 were used. They were 40-hr low-pass filtered and then decimated to 1 point per 48 hours. Mode 1 is solid, mode 2 is dashed, and mode 3 is dot-dash. Percentages of variance in each mode are shown.

were identified as Loop Current intrusions, Loop Current Eddy separations, Loop Current Eddies, cyclonic eddies, and slope eddies. Speed statistics for each of these types are given in, respectively, Tables B-1 through B-5 of Appendix B.

Molinari and Meyer (1982) give details of two cases of an intrusion of the Loop Current over a current meter mooring located on the northeastern Gulf slope. Speed statistics of the events are given in Table B-1. Near-surface currents are intensified relative to deeper currents. Maximum speed at 150 m depth was 69 $cm \cdot s^{-1}$.

Loop Current Eddy separation events were determined by searching the database for current records occurring during the month of eddy separation that is given in Sturges and Leben (2000). Between 1977 and 1999, there were 30 eddy separation events. Of these, 20 occurred when at least one instrument was in the water. Each record was examined to determine whether there were energetic currents occurring during the eddy separation. There were 10 such cases. The remaining 10 had no unusual or significant effects during the separation. The effects consisted mainly of internal wave packets at depth. The deep inertial oscillations seemed to be produced particularly in the eastern Gulf locations during the months in which separations occurred. Because corroborative data are not available, there is no conclusive evidence that these packets are the direct result of the Loop Current eddy separations. Speed statistics of the events are given in Table B-2. Figure 7.2.1-1 shows the maximum speed, mean speed, and standard deviation of speed for all occurrences of energetic currents during an eddy separation. In general, the currents are intensified near the surface with some indication of intensification near the bottom as well.

Loop Current eddies are ubiquitous in the Gulf of Mexico, and it is generally acknowledged that at least one LCE is present somewhere in the Gulf at any given time. Additionally, anticyclonic and/or cyclonic eddies spun up through eddy-eddy interaction or eddy-slope interaction can also exist in the Gulf simultaneous with LCEs. This makes the identification of events associated with particular eddies dependent on information giving the location of the eddies relative to the moorings. Where available, the SSH fields from GEOSAT for 1985-1989 (Berger et al. 1996b) and blended from TOPEX, ERS-1, and ERS-2 (data provided by Robert Leben of CU) for mid-1992 through 1999, as well as available EddyWatch charts from 1984-1999, were used to establish the proximity of moorings to eddies. When no SSH fields or EddyWatch charts were available, the literature on the mooring deployments was consulted.

To identify energetic currents associated with LCEs, each mooring location was compared to the locations of LCEs in the Gulf during the deployment period. Records from moorings near LCEs were examined for energetic current events for the time period when the LCE was nearby. Note that when the LCE was in a part of the Gulf away from a mooring, currents were not affected by the LCE. Because of the sparseness of the data sets, no systematic analysis was made of how close an LCE must be to a mooring location to affect the currents. During the years 1977 to 2000, there were 14 LCEs that affected the currents at moorings. Speed statistics of the events are given in Table B-3, with the LCE identified by the names noted in Table 6.2-1. Note that the current statistics associated with Eddy Juggernaut are included in Table B-3 as event 16. Figure 7.2.1-2 shows the maximum speed, mean speed, and standard deviation of speed for all occurrences of energetic currents associated with an LCE. In general, the currents are intensified near the surface with some indication of intensification near the bottom as well. Maximum speeds can be 100 $cm \cdot s^{-1}$ or more. The mean speed has a minimum near 1000 m.

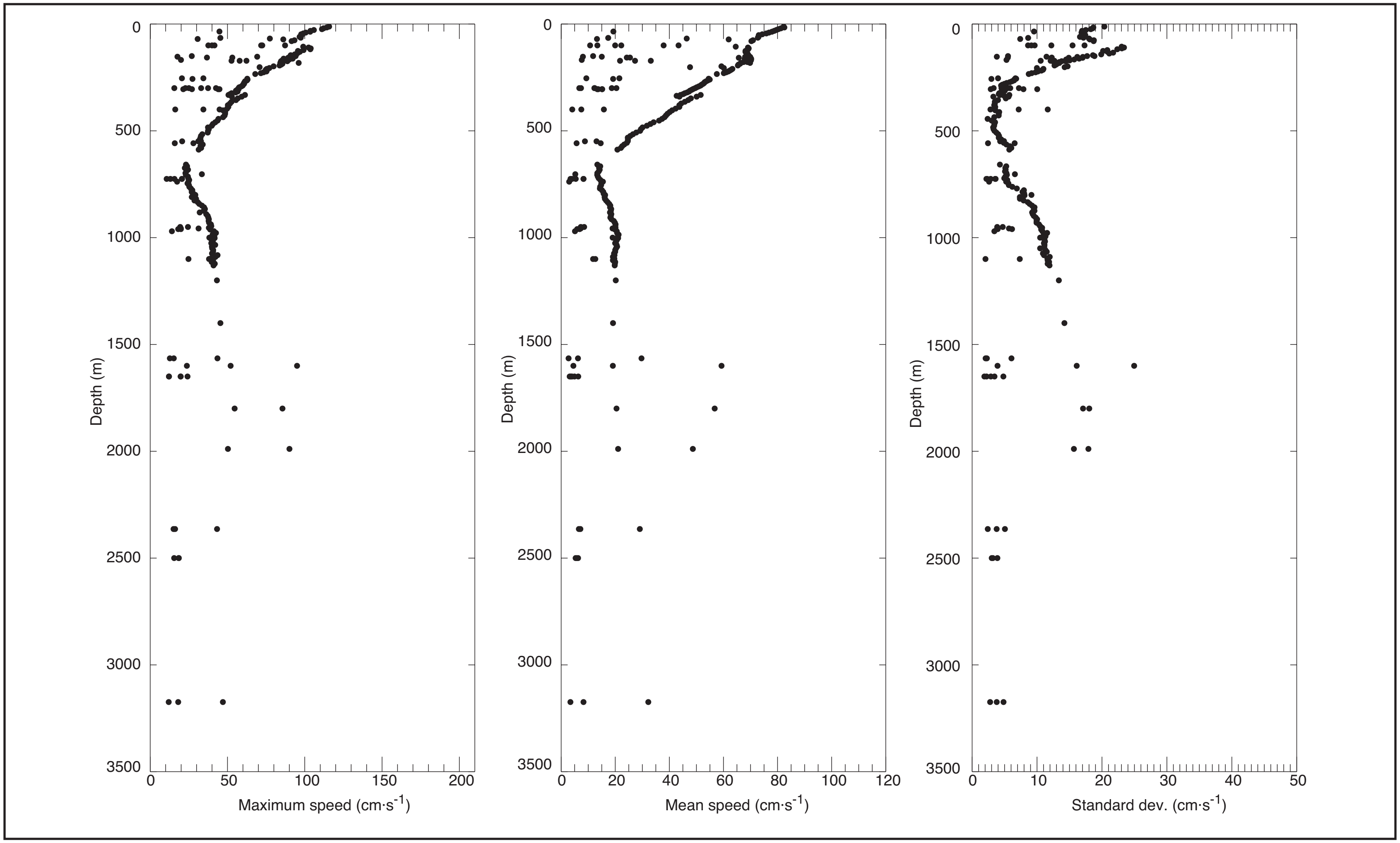

Figure 7.2.1-1. Maximum speed, mean speed, and standard deviation of speed for all occurrences of energetic currents during Loop Current eddy separations.

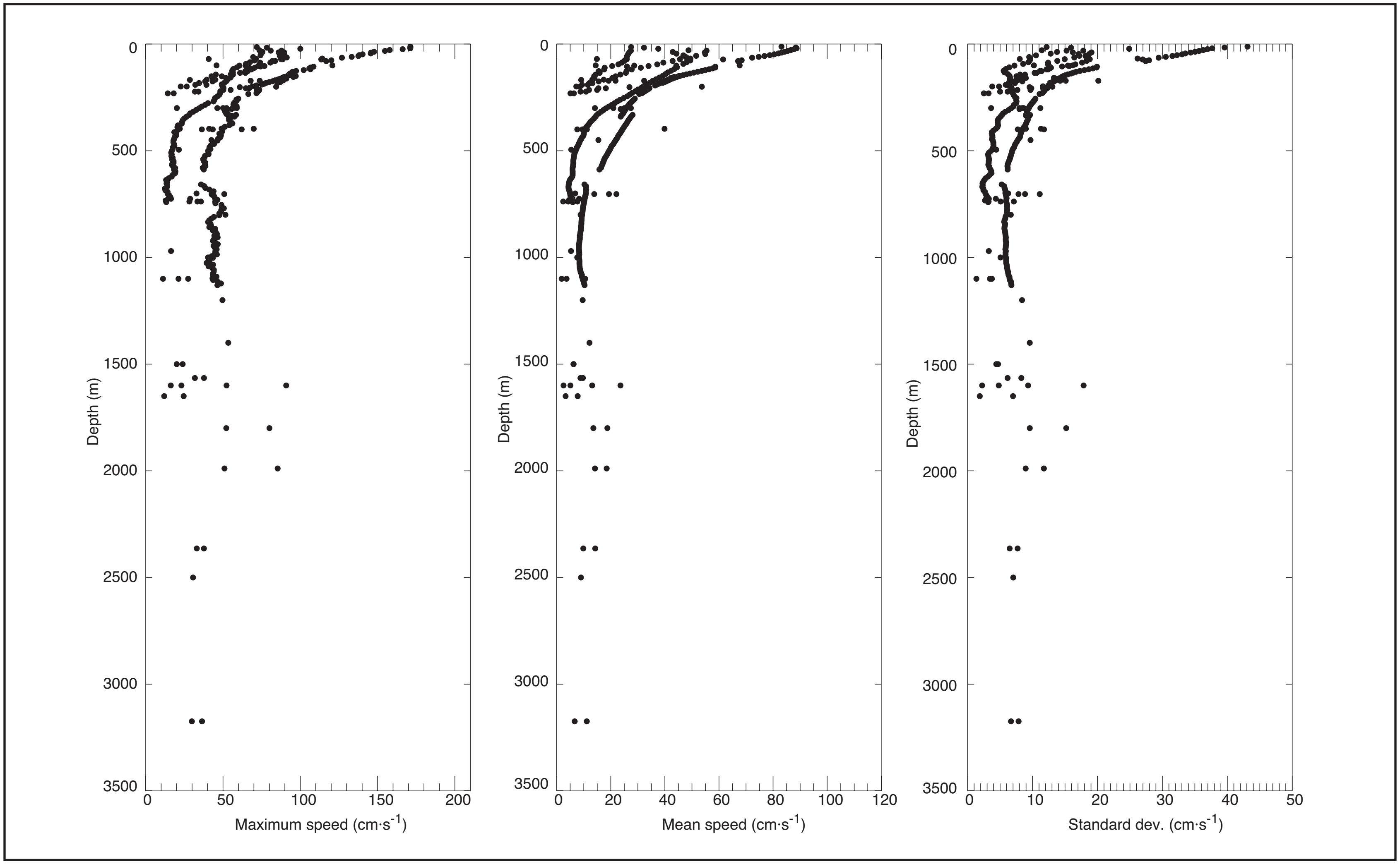

Figure 7.2.1-2. Maximum speed, mean speed, and standard deviation of speed for all occurrences of energetic currents associated with Loop Current eddies.

Energetic current events associated with anticyclonic slope eddies were identified in a manner similar to that used for the LCEs. Seven energetic current events were associated with these eddies. Speed statistics of the events are given in Table B-4. At least two of these eddies (Deviant Eddy and Eddy Gyre) were of such a significant size as to warrant naming by Horizon Marine. A high in SSH appeared to be a semi-permanent feature on the northwest slope of the DeSoto Canyon; it often resulted in energetic current events as measured by the SAIC EIS data. The anticyclonic slope eddies tend to be of much smaller radial and vertical scale than Loop Current Eddies. Figure 7.2.1-3 shows the maximum speed, mean speed, and standard deviation of speed for the occurrences of energetic currents associated with anticyclonic slope eddies. Generally, mean currents and standard deviations are less than those associated with LCEs. Maximum speeds can reach 100 $cm \cdot s^{-1}$. Note the observations of slope eddies are limited mainly to the upper 1000 m, i.e., to water depths associated with the slope regions of the Gulf.

Energetic current events associated with cyclonic eddies also were identified in a manner similar to that used for the LCEs. A total of 12 energetic current events associated with cyclonic eddies were measured between 1984 and 1999. The total non-overlapping duration of these events lasted roughly 30 months. Speed statistics of these events are given in Table B-5. Figure 7.2.1-4 shows the maximum speed, mean speed, and standard deviation of speed for all occurrences of energetic currents associated with cyclonic eddies. Generally, mean currents and standard deviations are less than those associated with LCEs, but comparable to those associated with the anticyclonic slope eddies. Maximum speeds can reach 100 $cm \cdot s^{-1}$.

The major conclusions regarding measurement of energetic current events associated with the Loop Current and surface-intensified eddies are that the mooring must be in relative close proximity to the eddy for the currents to be impacted and that the currents are surface intensified, with maximum speeds near-surface of order 100 $cm \cdot s^{-1}$.

7.2.2 Currents Generated by Energetic Wind Events

The current records were examined for the dates during which tropical cyclones, which include hurricanes, tropical storms, and tropical depressions, were present in the Gulf of Mexico (Table 6.2-2). During 1977-2000, 60 tropical cyclones were present in the Gulf while at least one current meter was deployed. Of these, 50 had no appreciable affect on measured currents. This was due mainly to the fact that the storm tracks were far from the instrument locations. Often these storms passed through Mexican waters of the Gulf of Mexico, where no current measurements were available. The 10 remaining tropical cyclones did affect the measured currents. Speed statistics of these events are given in Table B-6. Statistics were computed for the period during which the storm affected the currents, as determined by visual examination of the current record. Figure 7.2.2-1 shows the maximum speed, mean speed, and standard deviation of speed for all occurrences of energetic currents associated with tropical cyclones. Currents are surface-intensified, with maximum speeds reaching up to 200 $cm \cdot s^{-1}$. Maximum speeds down to 500 m depth also are high, exceeding 50 $cm \cdot s^{-1}$ in many cases. Mean currents near-surface can be energetic with standard deviations of order half the mean. These current events show little, if any, bottom trapping as occurred in Figure 7.2.1-1. An exception is Hurricane Georges of 1998, which produced substantial, bottom-intensified, sub-inertial oscillations at depth, in addition to the 200^{+} $cm \cdot s^{-1}$ surface currents.

To determine the effect of extratropical (winter) cyclones on the currents, the current records were searched for the dates of storms listed in Table 6.2-4 (unpublished data from Hardy and Hsu 1997; see also Nowlin et al. 1998b). A total of 50 storms occurred when at least one

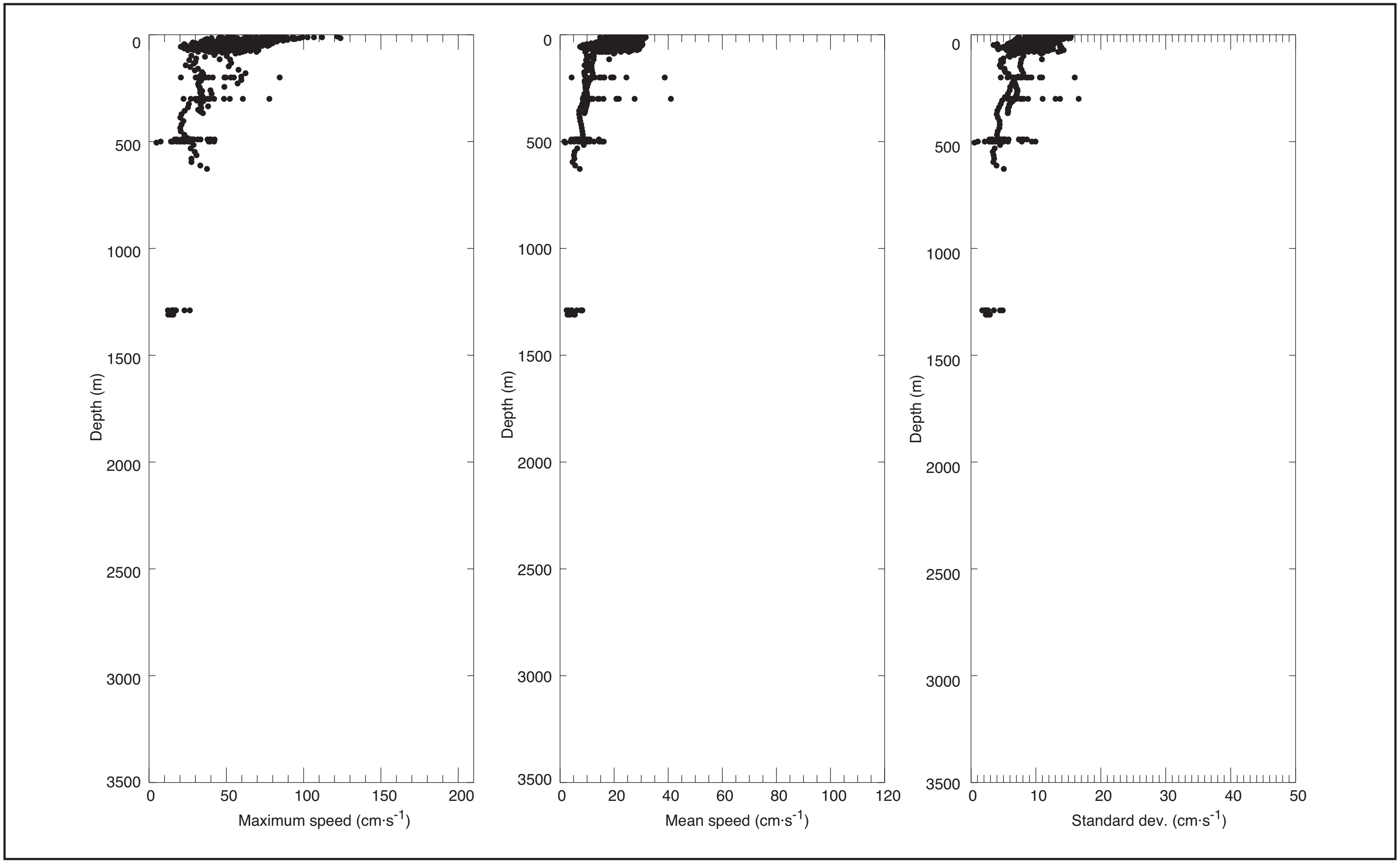

Figure 7.2.1-3. Maximum speed, mean speed, and standard deviation of speed for all occurrences of energetic currents associated with anticyclonic slope eddies.

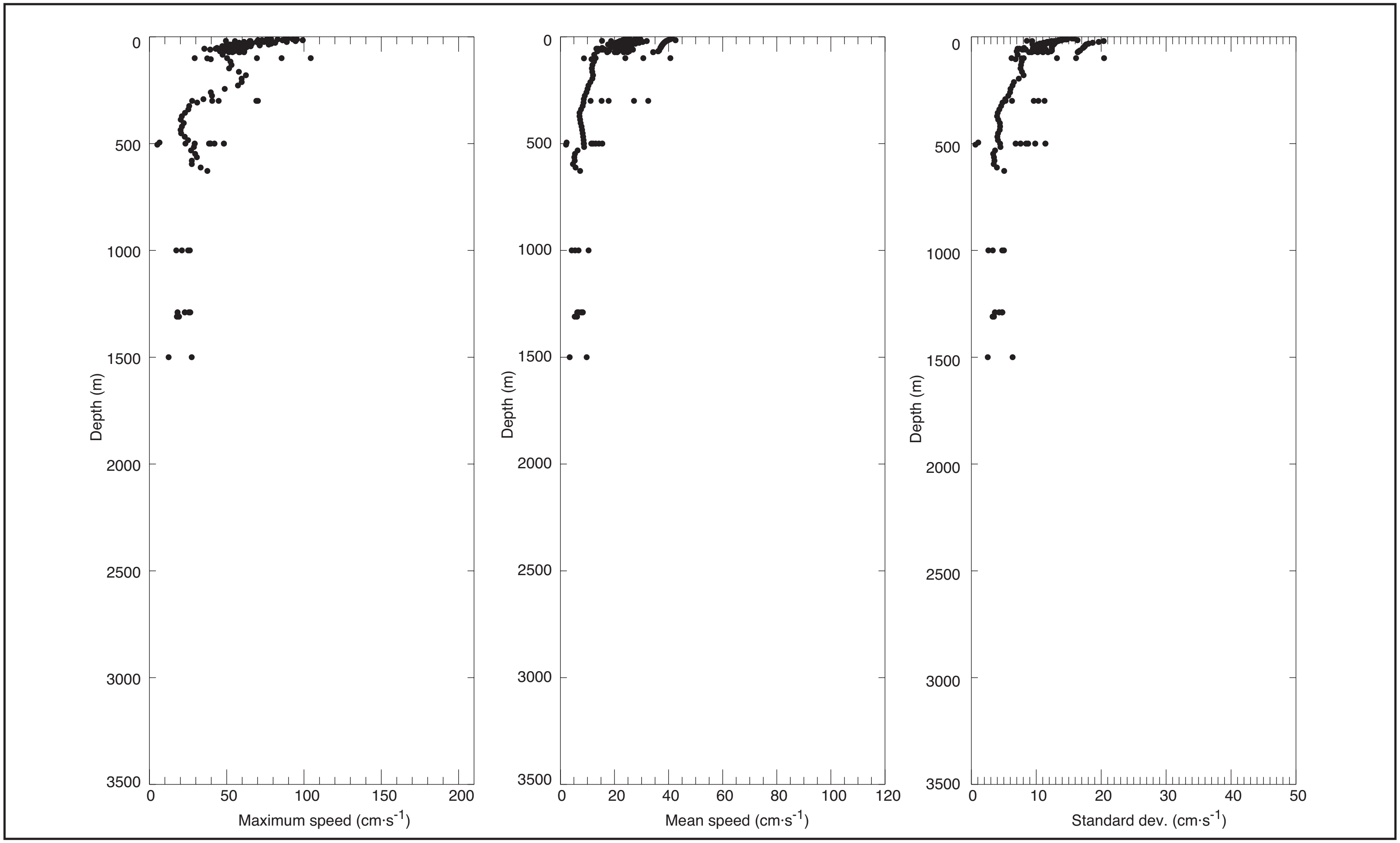

Figure 7.2.1-4. Maximum speed, mean speed, and standard deviation of speed for all occurrences of energetic currents associated with cyclonic eddies.

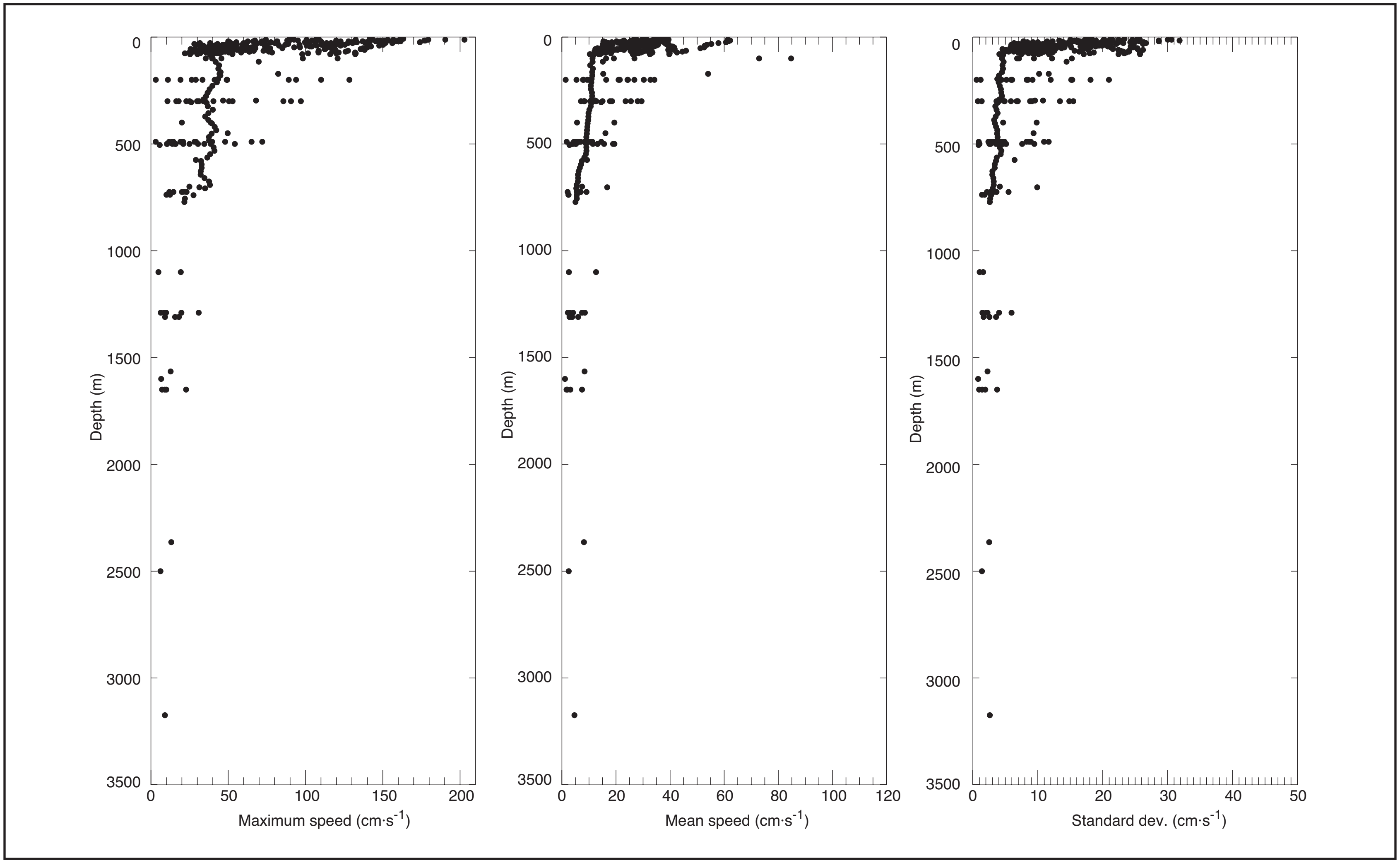

Figure 7.2.2-1. Maximum speed, mean speed, and standard deviation of speed for all occurrences of energetic currents during tropical cyclones.

mooring was deployed (Table A-1). Most of these had no effect on the measured currents. Twenty had an effect, with most producing only modest (10-20 $cm \cdot s^{-1}$) inertial oscillations. One notable exception was the so-called "Storm of the Century" of 12 March 12 1993, which originated over the western Gulf off south Texas and traveled east-northeast over the Texas-Louisiana shelf before bringing historic amounts of snow to the eastern seaboard. Speed statistics of these events are given in Table B-7. Statistics were computed for the period during which the storm affected the currents, as determined by visual examination of the current record. Storms with effects that occurred within 3 days of each other were concatenated into one set of statistics. Figure 7.2.2-2 shows the maximum speed, mean speed, and standard deviation of speed for all occurrences of energetic currents associated with extratropical cyclones. These statistics show that the extratropical cyclones have a relatively small impact on the currents when compared to the impact of tropical cyclones. As in Figure 7.2.2-1, the winter cyclones do not produce any bottom trapping.

The major conclusions regarding measurement of energetic current events associated with energetic wind events are that the mooring must be in close proximity to the storm for there to be an appreciable effect on currents and that the currents are surface intensified and can be very energetic when associated with strong tropical cyclones.

7.2.3 Deep Barotropic and Bottom-Trapped Motions

Events such as energetic deep barotropic motions (e.g., topographic Rossby waves or deep eddies), sometimes with bottom intensification, were found by examining the deep current records by eye. No independent verification of these events is available. A total of 7 deep barotropic or bottom intensified events were identified in the current meter archive. It is notable that an additional 8 events were found in the proprietary data. One of these events was identified as a deep anticyclonic eddy. Speed statistics of the deep barotropic motions, including bottom intensification, are given in Table B-8. Figure 7.2.3-1 shows the maximum speed, mean speed, and standard deviation of speed for all occurrences of these motions. Table B-9 gives the statistics associated with the one deep anticyclonic eddy that was identified from the records. Figure 7.2.3-2 shows the maximum speed, mean speed, and standard deviation of speed for that event.

In general, these deep events showed no surface expression and were confined to water depths of 1000 m and below. By far the most intense of these events was the large amplitude, 7-10 day period jets that occurred during August to October 1999 at the SAIC EIS Extension moorings I1, I2, and I3. This event seems to be related to the interaction of Eddy Juggernaut with the continental slope. The current speed at I2 approached 100 $cm \cdot s^{-1}$ in depths 1600 to 2000 m. The one example of a deep anticyclonic eddy was found at the SAIC 5-year study moorings S, P, Q, and R by the characteristic anticyclonic circulation pattern of current vectors found at those moorings.

7.2.4 Subsurface, Mid-Water Column Motions

Subsurface jets are extremely elusive. Early evidence for their existence was often anecdotal. The jets tended to be short lived (order of 1 day or less), which made it difficult to mobilize and deploy an instrument in time to measure the event. The increased spatial and temporal resolution afforded by an ADCP greatly increased the potential ability to characterize an event. Unfortunately, the data quality of many of the early occurrences is seriously in doubt. Three potential events have been identified in the non-proprietary records. The first two events are from ADCP measurements made by industry and are discussed in Section 6.1.4. The third example occurs after the passage of Hurricane Georges in 1998 and, as discussed in

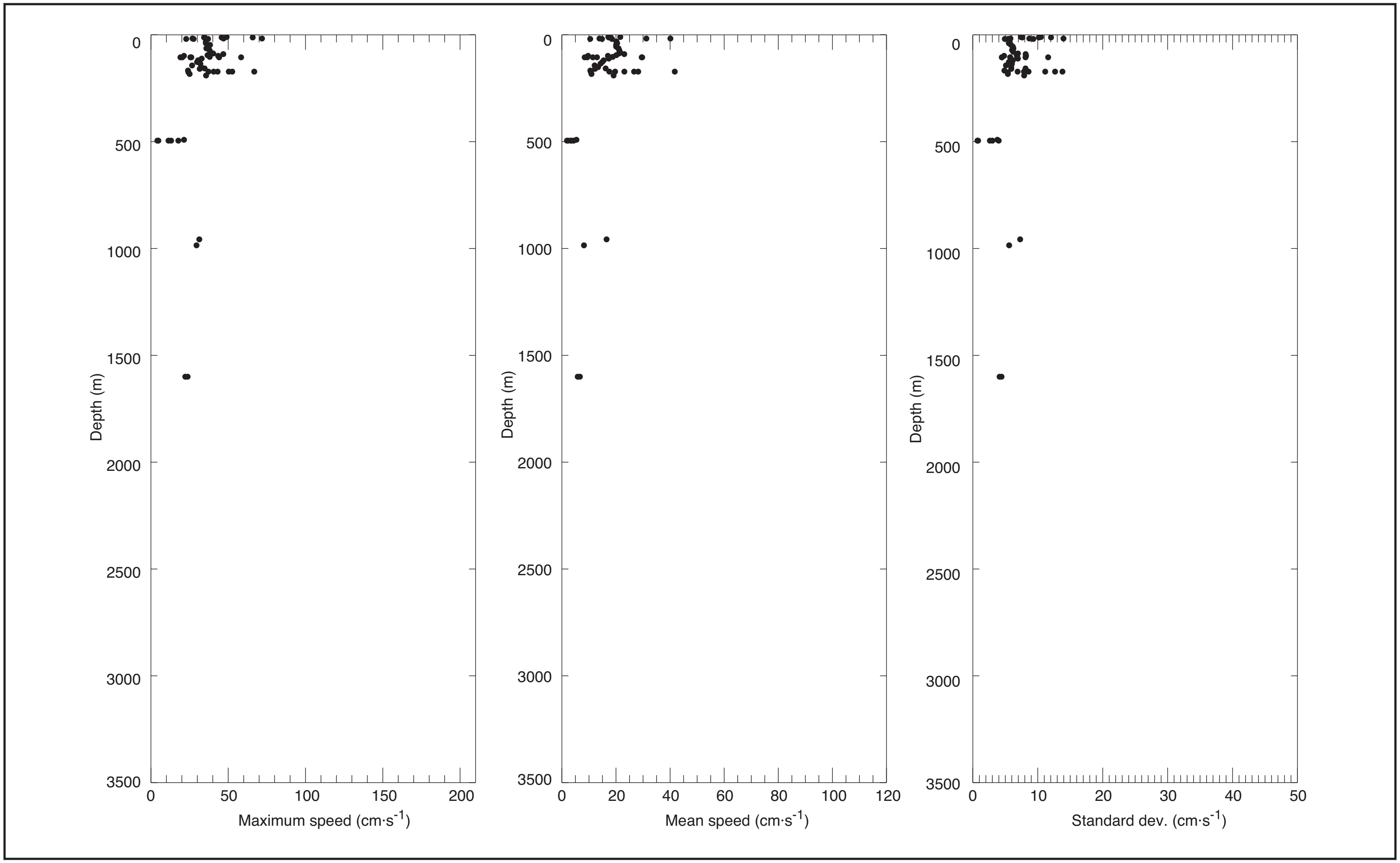

Figure 7.2.2-2. Maximum speed, mean speed, and standard deviation of speed for all occurrences of energetic currents during extratropical (winter) cyclones.

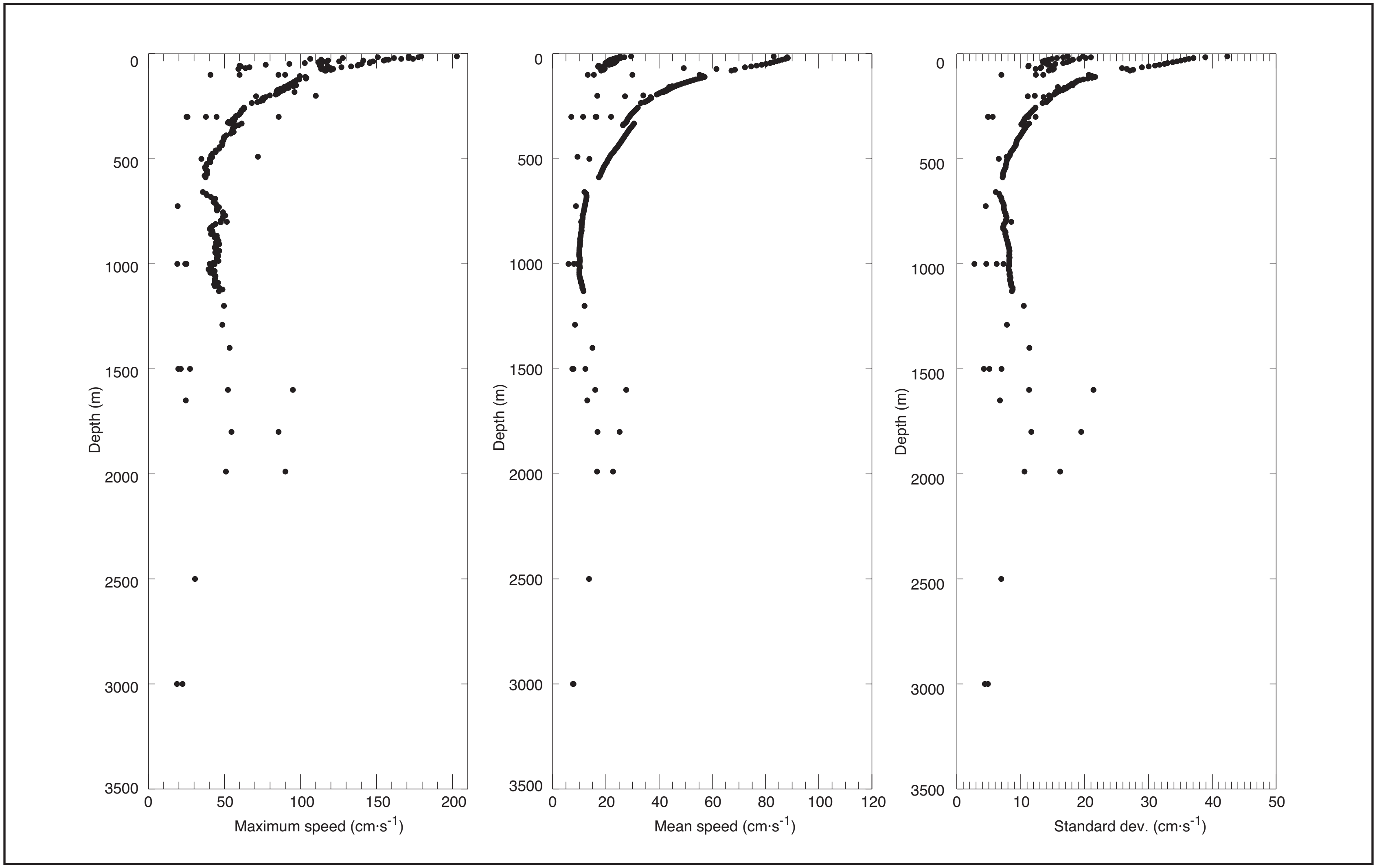

Figure 7.2.3-1. Maximum speed, mean speed, and standard deviation of speed for all occurrences of energetic deep barotropic motions, including bottom intensification.

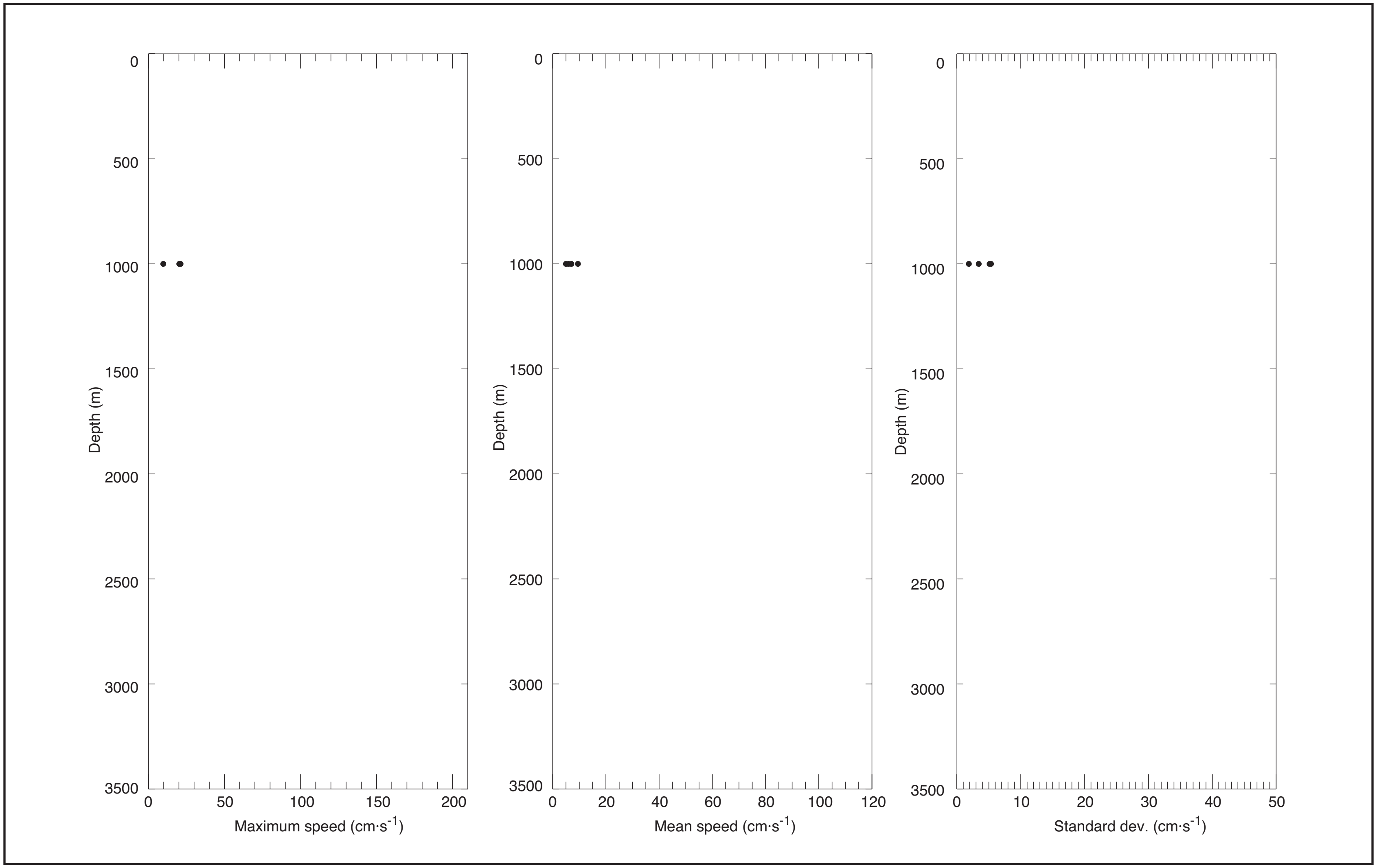

Figure 7.2.3-2. Maximum speed, mean speed, and standard deviation of speed for all occurrences of energetic currents associated with deep anticyclonic eddies.

Section 6.1.5, may help to explain some of the anecdotal occurrences from the past. Speed statistics of these events are given in Table B-10. Note: The maximum speed is the only statistic that is pertinent to the jets climatology. The jet event is relatively short-lived (< 1 day), but the statistics were computed over 2-3 days. Although the mean and standard deviation are given, they represent the statistics for the period before, during, and after the jet events. Figure 7.2.4-1 shows the maximum speed for all occurrences of subsurface jets in non-proprietary data sets. Note first that there is surface intensification in the upper 100 m that likely is associated with energetic wind events. Indeed the maximum speeds in the upper 100 m are associated with Hurricane Georges (compare Figure 7.2.2-1). The maximum speed statistics show a relatively high subsurface maxima at about 250-400 m depth with associated high variability as evidenced by the standard deviation statistics. This pattern is a likely characteristic of the subsurface jet phenomenon.

7.3 Prioritization of Data Needs for Energetic Processes and Phenomena

A goal of this study is to prioritize the physical processes and phenomena as to the need for additional data for improved understanding, simulation, and prediction of slope and subsurface circulation. The steps toward this prioritization are to identify the processes and phenomena of interest, to determine a set of criteria to use in the prioritization, and to determine the priority of the processes and phenomena.

7.3.1 Categories of Physical Processes and Phenomena for Prioritization

Sections 5 and 6 identified physical processes and phenomena associated with the large scale circulation and energetic current events. For purposes of prioritization, these processes and phenomena are subdivided into ten categories. These are defined as:

1. General surface-intensified circulation due to local wind forcing (e.g., Sturges 1993); Section 5
2. General deep circulation; Section 5
3. Loop Current; Sections 6.1.1, 6.4.1, and 7.2.1
4. Surface-intensified eddy-induced currents, including mesoscale cyclonic and anticyclonic rings and Loop Current eddies; Sections 6.1.1, 6.4.1, and 7.2.1
5. Motions induced by hurricanes and tropical storms (Qi et al. 1995); Sections 6.1.2, 6.4.2, and 7.2.2
6. Motions induced by winter cyclones, frontal passages, and other energetic wind events (Qi et al. 1995); Sections 6.1.2, 6.4.2, and 7.2.2
7. Deep barotropic and bottom-trapped motions, including topographic Rossby waves and deep cyclonic and anticyclonic eddies and eddy-pairs (e.g., Welsh and Inoue 2000); Sections 6.1.3, 6.4.3, and 7.2.3
8. Currents associated with furrows; Sections 6.1.3 and 6.4.3
9. Subsurface, mid-water column motions; Sections 6.1.4, 6.4.4, and 7.2.4
10. Topographically generated near-inertial motion; Section 6.1.5.

Currents associated with these processes/phenomena may not be distinct. For example, class 2 or class 7 may in fact be responsible for furrows (class 8).

7.3.2 Criteria Used to Prioritize

Three major criteria were selected for use in determining the priority of the need to obtain additional data regarding the physical processes and phenomena. These are: improved level of understanding, improved ability to simulate and predict, and ability to observe.

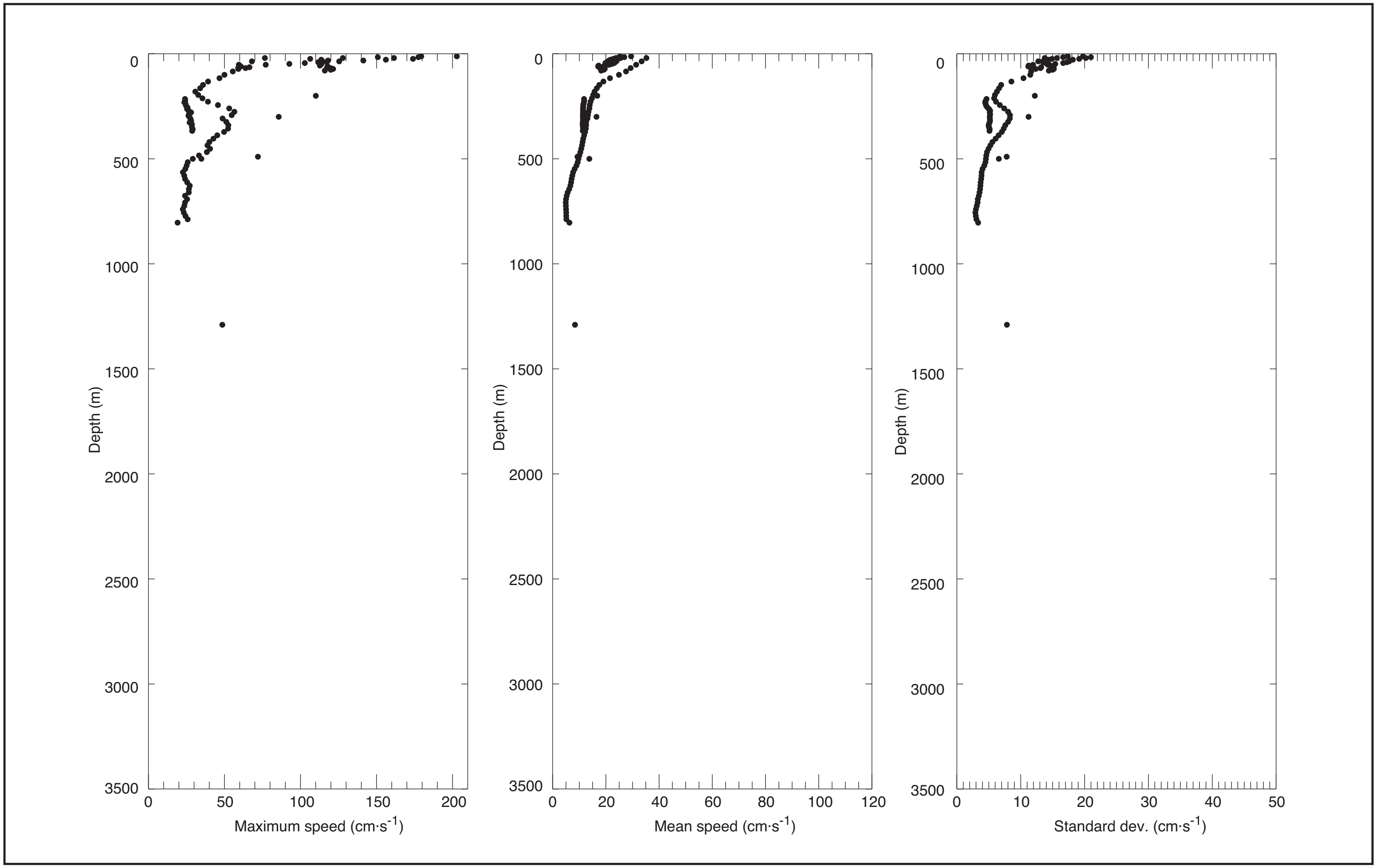

Figure 7.2.4-1. Maximum speed, mean speed, and standard deviation of speed for all occurrences of subsurface, mid-water column jets. Mean and standard deviation represent smoothed statistics for before, during, and after the jet event.

The first criterion is the need to improve our level of understanding of the process/phenomena. For this criterion, a numerical rating was determined by weighting five factors, consisting of the level of general description of the process/phenomenon that is available and four event-specific physical characteristics. The first factor considers the present ability to provide a general description of the process/phenomenon and its causation. The four event-specific physical factors are: frequency of occurrence, energy level, duration, and spatial extent. The frequency of occurrence criterion considers how often an event occurs. The energy level is based on how strong the associated currents are. Duration considers the temporal extent or how long the motions typically last. The spatial extent considers the size of the area over which the motions occur. These five factors then identify the relative need to improve our understanding. Table 7.3.2-1 provides the rating for each motion by the five factors and gives the overall weighted rating for the understanding criterion.

The second criterion is the need to improve our ability to simulate and/or predict the motion in numerical models. This criterion addresses the question of whether enhancements are needed in the data base to reasonably model the occurrence and nature of the motion. It does not address the issue of whether improvements are needed in the modeling code or computing hardware. Four factors were used to determine the ratings for this criterion. These are the importance of additional data for (1) improving skill assessments, (2) making accurate predictions of impacts to structures/vessels/other human activities, (3) making accurate assessments of pollutant transports, and (4) enhancing the ability to parameterize the motion in a deterministic model. Table 7.3.2-2 provides the ratings by motion of these four factors and gives the overall rating for the simulate/predict criterion.

The third criterion, ability to observe, also was considered. This criterion examined the issue of whether there are reasonable measurement systems that could be designed to capture the motion. Except for the mid-water column motions, it was determined that systems could be designed to measure the other identified events. It should be noted that, to capture the motion, costs associated with the deep and bottom water column motions (categories 6, 7, and 8) might be relatively expensive and measurement of currents associated with tropical storms and hurricanes would depend on whether a storm occurred during the measurement period. It was determined that the weight of this criterion should be less than the first two. This factor was weighed as half that of each of the other factors.

7.3.3 Priority Determination

Each identified category of physical process or phenomenon was rated according to the criteria discussed in Section 7.3.2. Table 7.3.3-1 shows the ratings by criteria and gives the overall priority ranking. The emphasis in the ratings has been on assessing the need for additional data to improve our ability to understand and simulate/predict the motions generated by the physical processes and phenomena. Ability to observe was given only half the weight of the other two criteria in preparing the total rating. The motions with the highest ranking are those about which the least is known or which are relatively high in energy for periods lasting on the order of weeks to months.

Table 7.3.2-1. Rating of motions by factors to determine the need to improve understanding of the motion. Ratings are little (5), medium (3), and much (1) is known about the process and its causes. In the total event-specific average, the energy level was weighted three times the weight of the frequency, duration, and spatial extent factors. The rating for the need to improve understanding criterion is an average of the ratings for the total event-specific average and the general description level.

Type of Current or Motion	Frequency of Occurrence	Energy Level	Duration of Motion	Spatial Extent	Total Event-Specific Average	Level of General Description	Need to Improve Understanding
General circulation currents-surface	5	3	5	5	4.0	1	2.5
General circulation currents-deep	5	3	5	5	4.0	5	4.5
Loop Current	5	5	5	3	4.7	2	3.3
Eddy induced currents	3	5	5	3	4.3	3	3.7
Hurricane/tropical storm induced motions	1	5	1	3	3.3	2	2.7
Other energetic wind event induced motions	3	3	1	3	2.7	1	1.8
Deep barotropic & bottom-intensified motions	3	3	3	5	3.3	4	3.7
Currents associated with furrows	3	3	5	3	3.3	5	4.2
Subsurface, mid-water column motions	1	3	1	1	2.0	5	3.5
Topographically generated near-inertial motion	3	1	1	5	2.0	3	2.5

Table 7.3.2-2. Rating of motions by factors to determine the need to improve simulation and prediction of the motion. Ratings are high (5), medium (3), low (1). In determining the average, all factors were weighted equally.

Type of Current or Motion	Need for Improved Skill Assessment	Need for Improved Impact Prediction	Need for Improved Transport Assessment	Ability to Model Deterministically	Need to Improve Simulation/ Prediction
General circulation currents-surface	1	3	5	5	3.5
General circulation currents-deep	4	3	3	4	3.5
Loop Current	2	4	4	3	3.3
Eddy induced currents	3	5	5	3	4.0
Hurricane/tropical storm induced motions	2	2	1	3	2.0
Other energetic wind event induced motions	2	1	1	2	1.5
Deep barotropic & bottom-intensified motions	5	5	3	5	4.5
Currents associated with furrows	4	5	3	3	3.8
Subsurface, mid-water column motions	3	4	2	1	2.5
Topographically generated near-inertial motion	3	1	1	1	1.5

Table 7.3.3-1. Ratings of motions on basis of need to improve understanding, need to improve simulation/prediction, and ability to observe. Ratings are high (5), medium (3), or low (1). The priority rank is based on all criteria, giving ability to observe half the weight of the other two criteria.

Type of Current or Motion	Need to Improve Under-standing	Need to Improve Simulation/ Prediction	Ability to Observe	Total Rating	Priority Rank
General circulation currents-surface	2.5	3.5	5.0	3.4	6
General circulation currents-deep	4.5	3.5	3.0	3.8	2
Loop Current	3.3	3.3	5.0	3.6	5
Eddy induced currents	3.7	4.0	3.0	3.7	4
Hurricane/tropical storm induced motions	2.7	2.0	2.0	2.3	8
Other energetic wind event induced motions	1.8	1.5	3.0	1.9	9
Deep barotropic & bottom-intensified motions	3.7	4.5	4.0	4.1	1
Currents associated with furrows	4.2	3.8	3.0	3.8	3
Subsurface, mid-water column motions	3.5	2.5	2.0	2.8	7
Topographically generated near-inertial motion	2.5	1.5	1.0	1.8	10

8 MEASUREMENT SYSTEM DESIGN CRITERIA

8.1 Location Focus

The primary region of interest for gathering further data to characterize energetic phenomena and processes in the Gulf of Mexico is the north-central slope and rise and northwest corner of the deepwater Gulf. This deepwater area is the likely principal focus within the Gulf of petroleum exploration and production for the foreseeable future. It also is a region frequently visited by energetic surface-intensified currents, as well as by moderately energetic deep phenomena and processes for which we have only sparse information. Knowledge of these currents is required for efficient and safe designs and operations within the oil and gas industry and for regulation of these operations by the federal government. This region also is the site of newly discovered mega-furrows and associated deep currents near the base of the Sigsbee Escarpment; these phenomena pose significant challenges to the efficient and safe extraction of hydrocarbons from beneath and near the major salt sheet forming the Escarpment.

Although the focus is on the north-central slope and rise and northwest corner of the deepwater Gulf, observations are needed in other Gulf regions as well, if the recommended measurement program is to meet the criteria used in Section 7.3 to prioritize the classes of energetic current events in the Gulf.

8.2 Physical Phenomena and Processes to be Characterized and Studied

The highest priority phenomena/processes are considered to be the low-frequency currents in deep water. These include: (1) deep anticyclonic-cyclonic eddy pairs and associated topographic Rossby waves (TRWs); (2) the deep general circulation; and (3) currents associated with furrows (Table 7.3.3-1). Next in priority are the currents associated with surface-intensified eddies. Recommended measurement projects should be focused on these classes of currents, although the resulting observations may aid in characterizing and understanding other classes as well.

Limited observations, numerical simulations, and theoretical considerations tell us that TRWs (very energetic motions extending through the water column below the main thermocline with periods of order 10 - 100 d) are excited in the eastern Gulf and propagate cyclonically along the continental slope and rise, passing the region of most intense oil and gas development in the north-central Gulf. See Section 6.1.3 for more discussion.

We have examined the CUPOM hindcast currents from 1993-1998 for occurrences of large variability in deep water passing westward from the eastern Gulf along the continental slope and rise of the north-central Gulf. Here we illustrate with an example. According to Sturges and Leben (2000), the surface-intensified, anticyclonic Eddy Zapp separated from the Loop Current on about 8 April 1995. Examination of the CUPOM surface current output for the period showed that during February 1995 the Loop Current's intrusion northward into the eastern Gulf of Mexico was increasing. Its maximum extension into the Gulf, before beginning to form a ring, appeared to be on February 23, for which surface currents are shown in Figure 8.2-1a. Following that date, the weak cyclone seen in Figure 8.2-1a off the west Florida shelf intensified and moved southwestward, forcing a neck to be formed in the Loop Current. This is illustrated in Figure 8.2-1b showing surface currents on 7 March 1995. It appears in the CUPOM output that by March 14 the LCE Zapp was completely separated from the main body of the Loop Current by an elongated cyclone (Figure 8.2-1c). Shown in Figure 8.2-1d is the model hindcast for surface currents on 8 April 1995, the date of Eddy

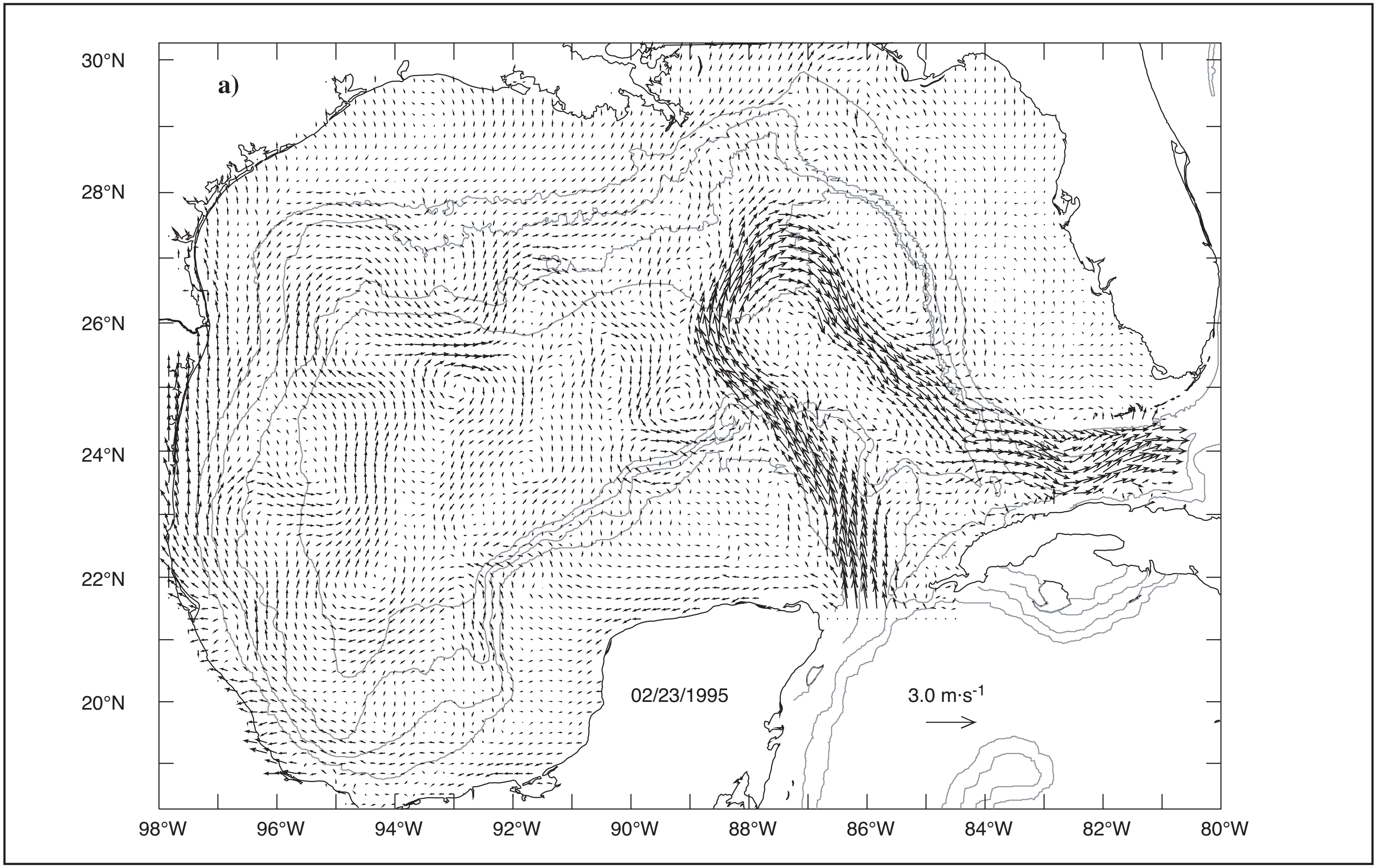

Figure 8.2-1. CUPOM hindcast surface currents for selected model dates in 1995. Shown are a) 23 February 1995; b) 7 March 1995; c) 14 March 1995; d) 8 April 1995, and e) 4 May 1995.

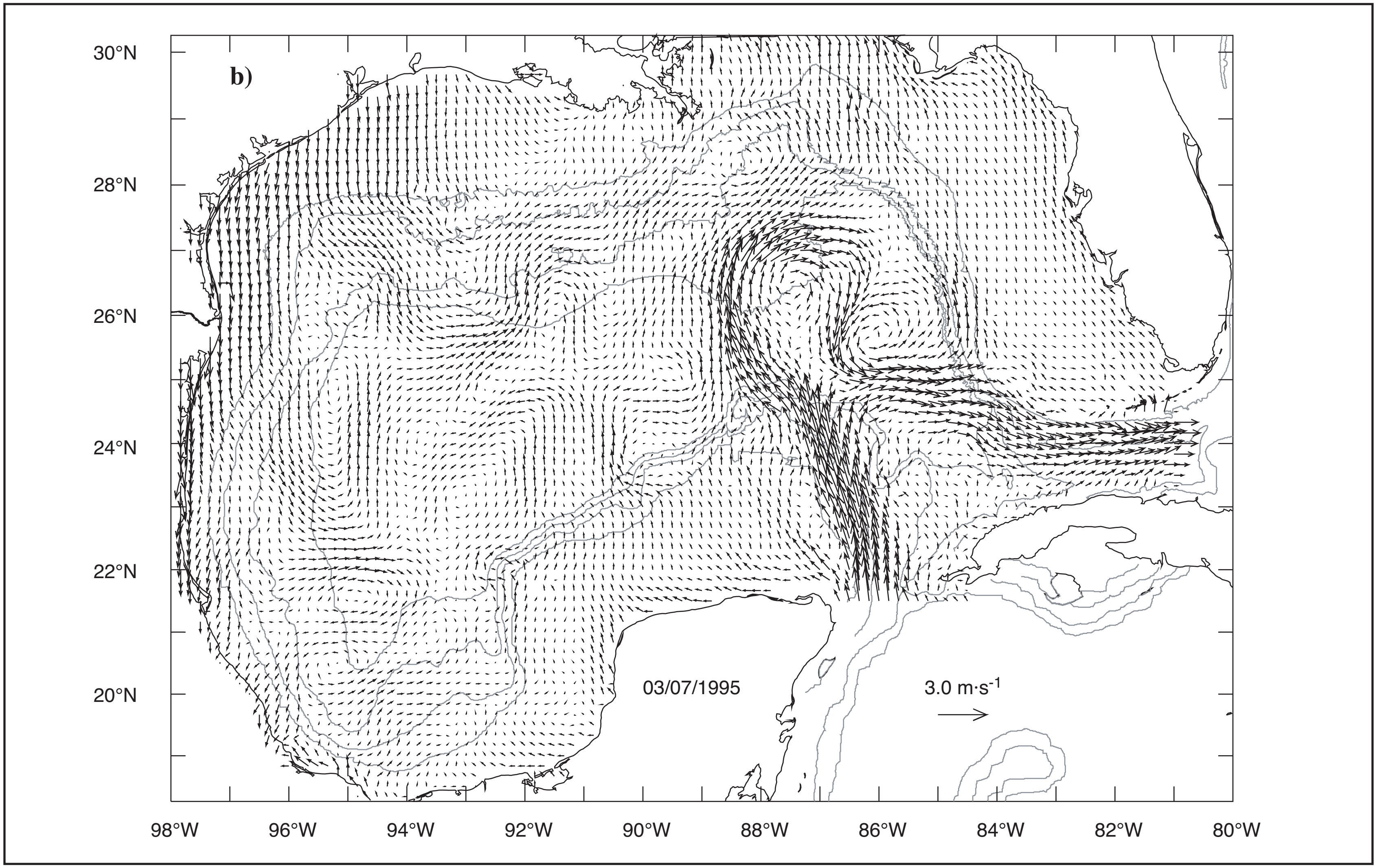

Figure 8.2-1. CUPOM hindcast surface currents for selected model dates in 1995. (continued)

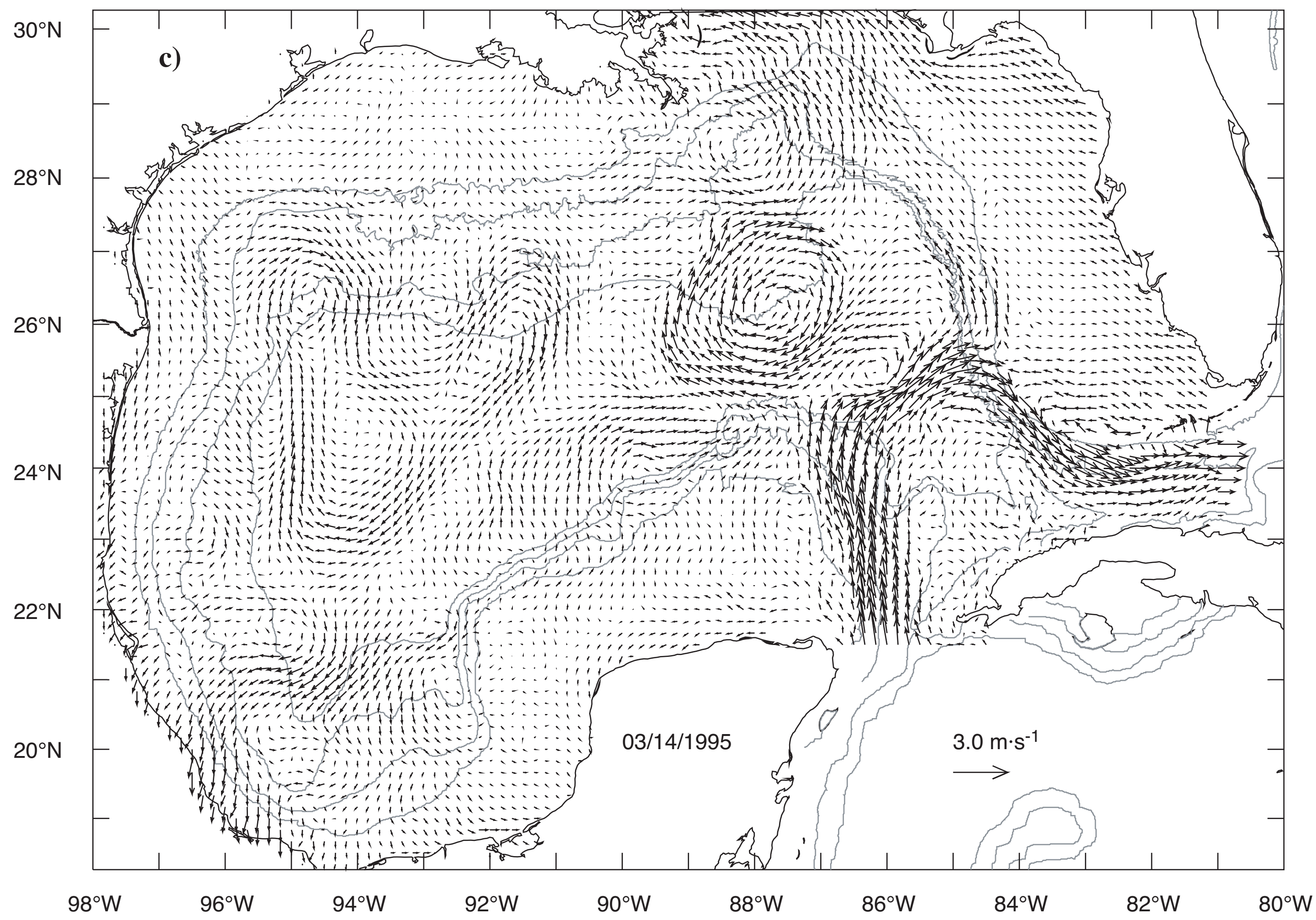

Figure 8.2-1. CUPOM hindcast surface currents for selected model dates in 1995. (continued)

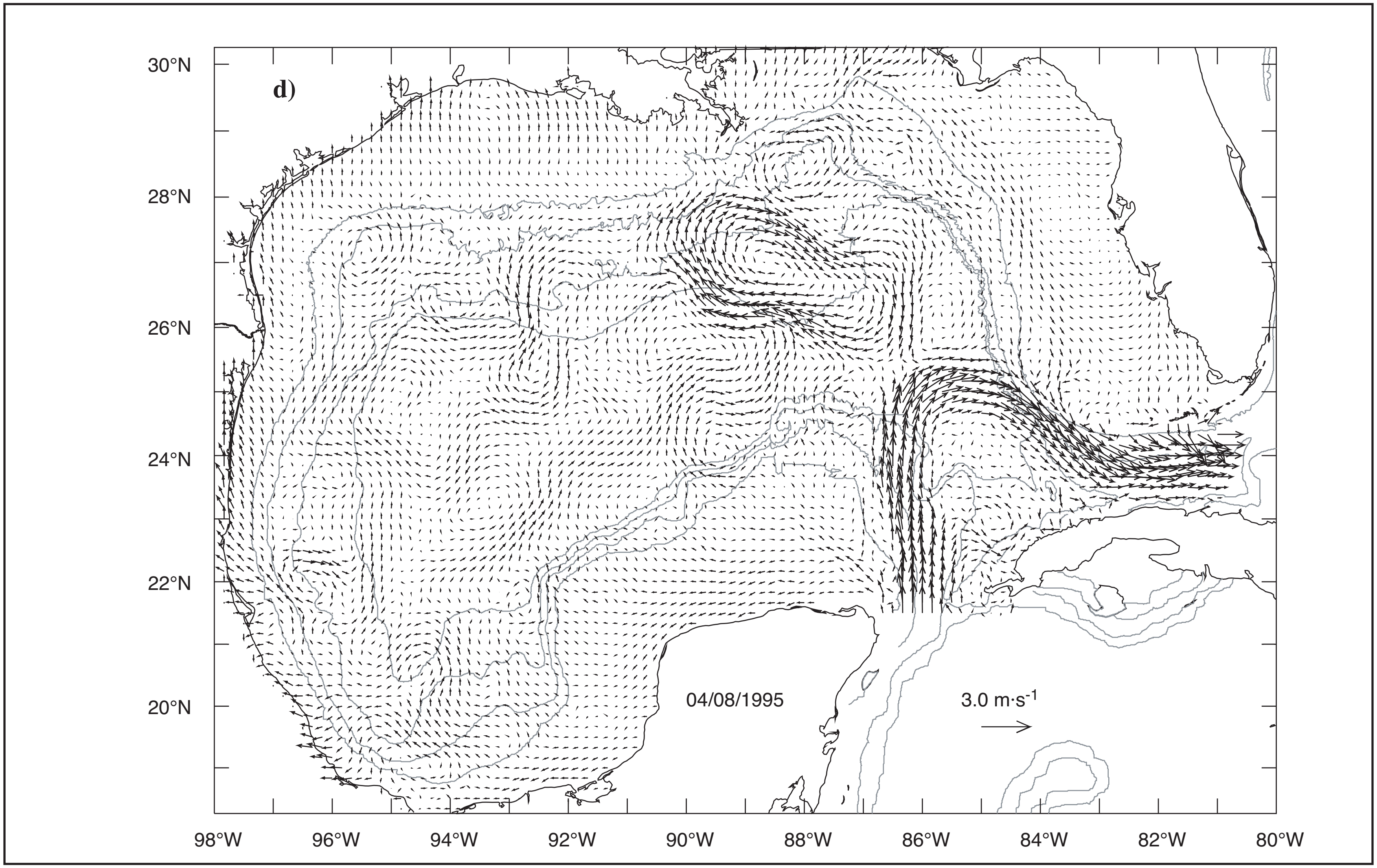

Figure 8.2-1. CUPOM hindcast surface currents for selected model dates in 1995. (continued)

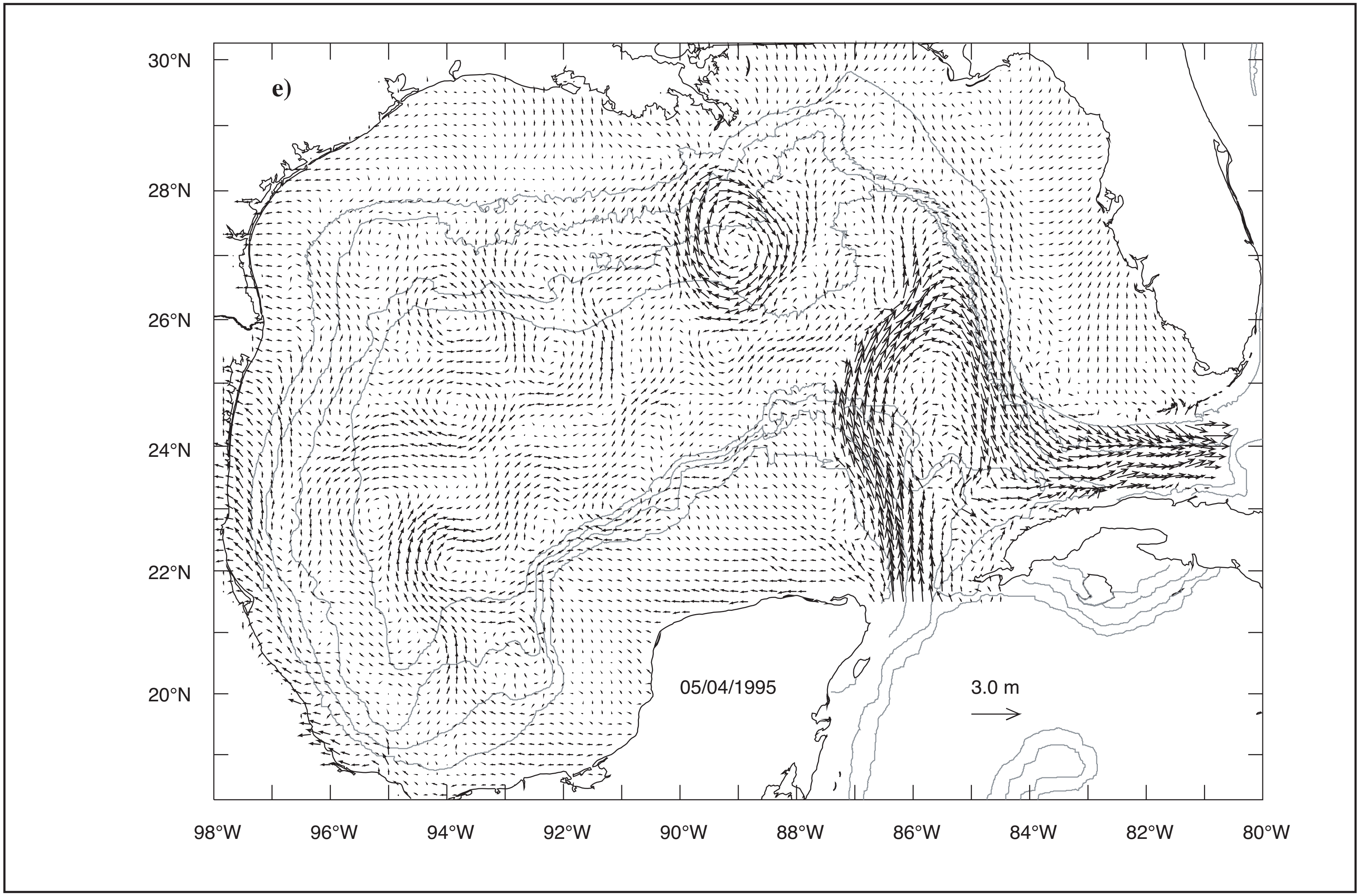

Figure 8.2-1. CUPOM hindcast surface currents for selected model dates in1995. (continued)

Zapp's separation according to the estimate of Sturges and Leben (2000) based on data. The separated LCE continued to move northwestward while decreasing in size. It became quite circular in shape by about 4 May 1995 as it reached a position just off the continental shelf south of the Mississippi Delta (Figure 8.2-1e). After that time this LCE appeared to begin to lose coherence and strength, perhaps because of its interaction with the continental slope. The ultimate fate of Eddy Zapp was to move west along the Louisiana-Texas slope into the northwest corner of the Gulf, finally dissipating in December 1995.

We also examined the CUPOM hindcast currents at 2000 m and near-bottom for the period of formation of Eddy Zapp. During 7-9 March 1995, when the surface currents showed that a LCE was in the formation stage, a small cyclone formed at 2000 m with its center near 25°N, 87°W. Another larger, but less coherent cyclone was seen to develop to the southeast off the Florida shelf. In the period March 20-29 the small cyclone dissipated while the larger cyclone strengthened. From March 29 through April 8, the larger cyclone continued to strengthen while moving northwestward just off the Florida slope. Figure 8.2-2(a-g) shows a sequence of CUPOM model currents at 2000 m beginning 8 April 1995. In the first figure the 2000-m circulation shows an energetic cyclone centered near 26°N, 86°W. Along the north-central Gulf slope there was westward, wavelike flow intensified near the 3000-m isobath. In subsequent pictures the deep cyclone appeared to elongate westward while a series of smaller cyclones and anticyclones were formed and moved westward (see Figure 8.2-2b, c, and d). There was considerable strengthening of the wavelike flow at 2000-m over the lower slope and rise in the north-central Gulf. The cyclone was seen to move westward and begin to separate into two parts (see Figure 8.2-2e for 20 April 1995). The eastern part of the cyclone appeared to stay centered off the west Florida Shelf, while the western part separated and moved westward to ultimately be dissipated against the northern slope. By May 5 the 2000-m currents along the 2000- to 3000-m isobaths had lessened, but both the east and west cyclones were still evident (Figure 8.2-2f). By May 13 the west cyclone had essentially dissipated (center of remaining structure at 26.5°N 90°W) and an anticyclone had appeared nearby (Figure 8.2-2g). A small new cyclone had appeared in the original location of the now dissipated cyclone (25°N, 87.5°W).

The result of this event was the formation of a cyclonic current field intensified along the base of the escarpment and extending westward to the continental slope and rise off Mexico. Shown in Figure 8.2-3 (a-g) are a sequence of CUPOM near-bottom currents. On 1 March 1995, when a neck was just forming in the Loop Current and before the formation of cyclonic eddies at the 2000-m level, there were no pronounced energetic currents along the Sigsbee Escarpment in the north-central Gulf (Figure 8.2-3a). During the period 7-20 March 1995, a small cyclone near 26.5°N, 87°W intensified and a larger one formed and intensified to its southeast. The situation on March 14 is shown in Figure 8.2-3b; the current pattern in the eastern Gulf is quite similar to that seen in currents at the 2000-m level for the same time (not shown). Note that between March 1 and March 14 the cyclonic flow around the lower slope and rise in the western Gulf intensified, especially along the northern slope and rise. By March 30 the smaller near-bottom cyclone in the northeastern Gulf had dissipated and the larger cyclone had strengthened and moved somewhat northwestward (Figure 8.2-3c). Figures 8.2-3d-f show near-bottom currents on April 8, 14, and 20, corresponding to the situation at 2000 m shown in Figures 8.2-2a, c, and e. This sequence shows the cyclone in the deep northeastern Gulf move to the northwest and elongate west-east into a peanut shape, much like the cyclone at the 2000-m level. Meanwhile the westward wavelike current along the Sigsbee Escarpment in the northern Gulf intensified, reaching what appear to be maximum currents about April 15. As the cyclone near 26°N, 88°W in the 2000-m circulation formed into a tight circular pattern on May 5 (Figure 8.2-2f), the cyclone in the near-bottom current field did likewise (Figure 8.2-3g). And, the near-bottom and 2000-m

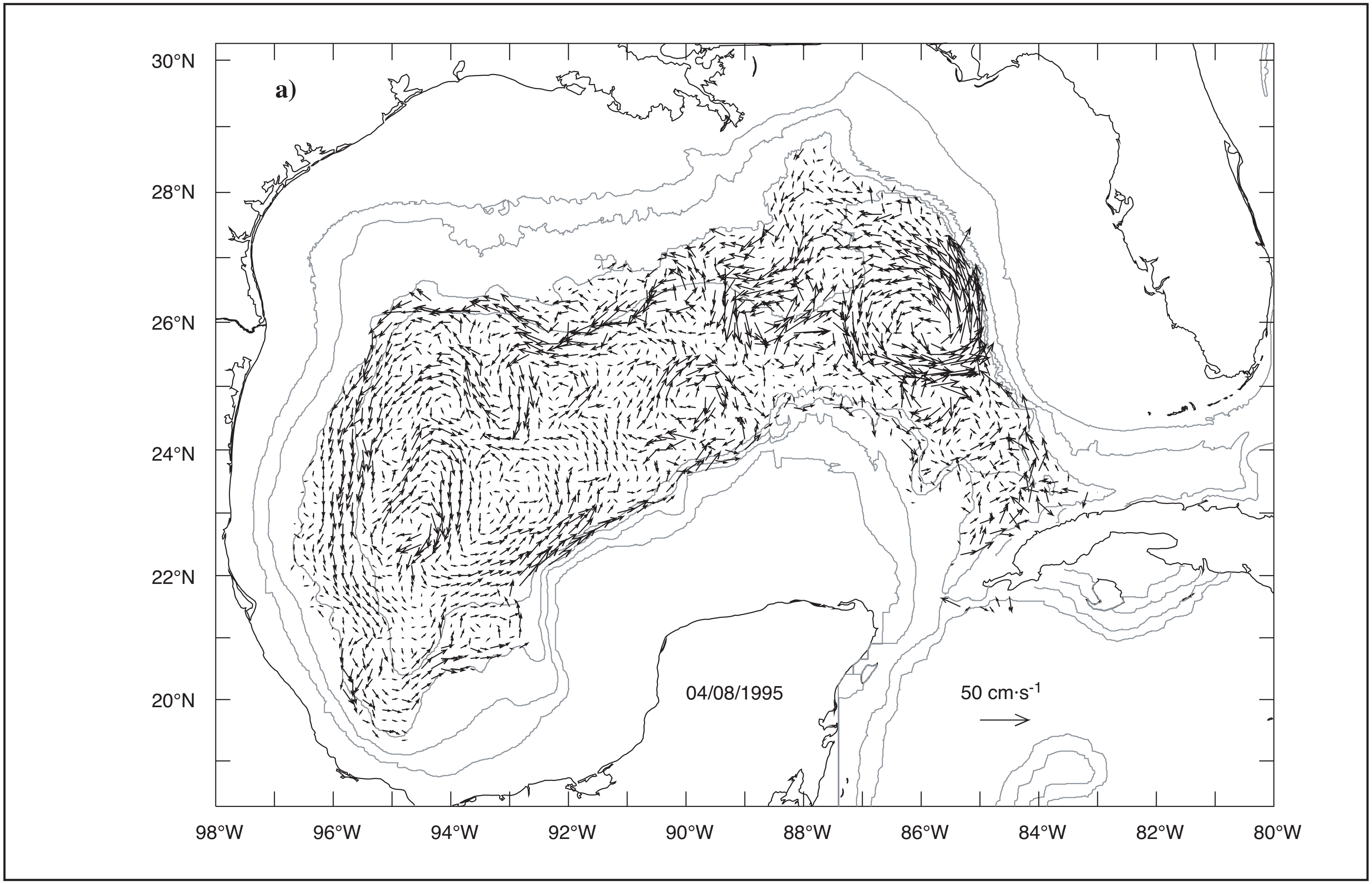

Figure 8.2-2. CUPOM hindcast currents at 2000 m for selected model dates in 1995. Shown are a) 8 April 1995; b) 11 April 1995; c) 14 April 1995; d) 17 April 1995; e) 20 April 1995; f) 5 May 1995; and g) 13 May 1995.

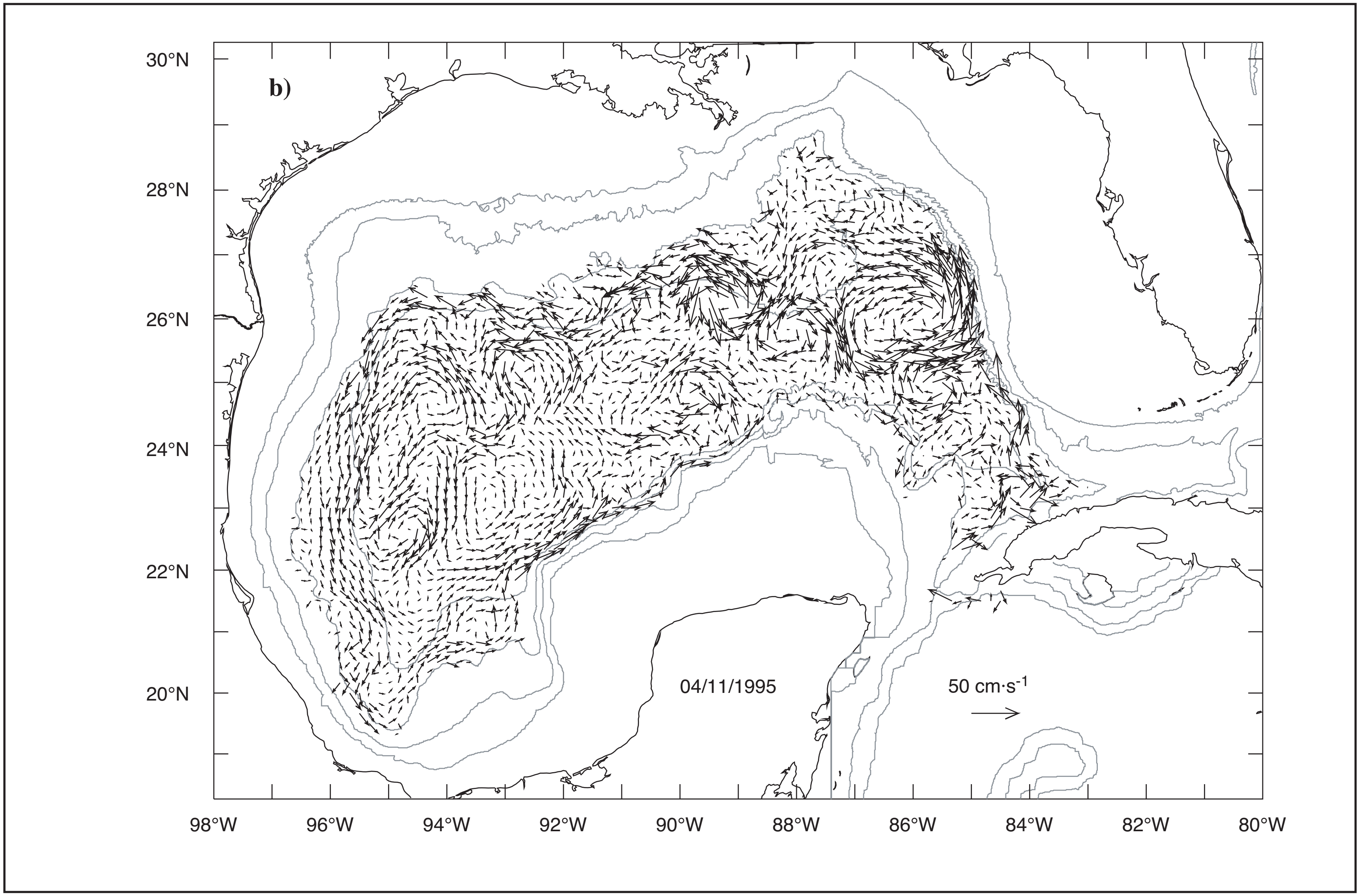

Figure 8.2-2. CUPOM hindcast currents at 2000 m for selected model dates in 1995. (continued)

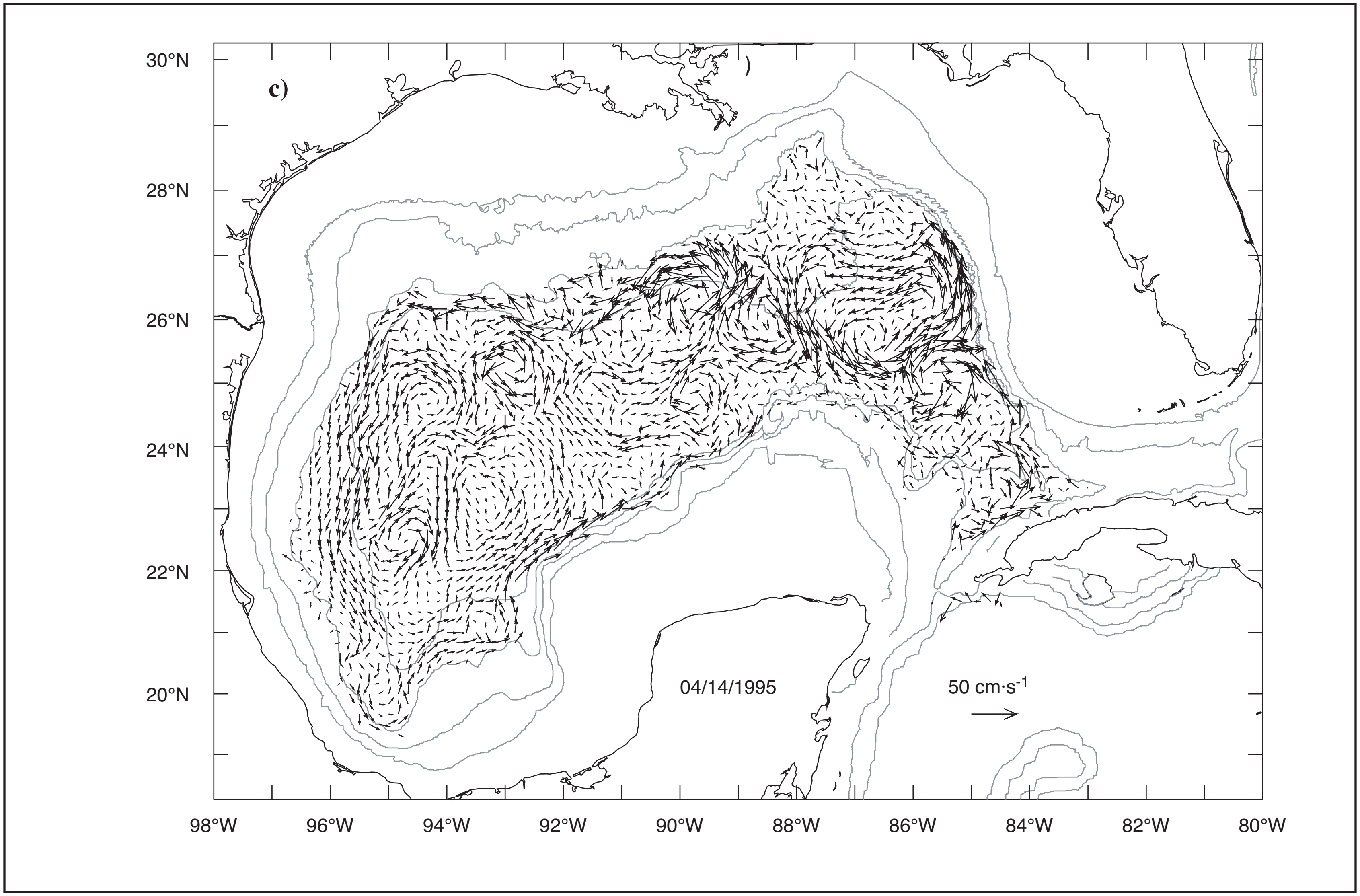

Figure 8.2-2. CUPOM hindcast currents at 2000 m for selected model dates in 1995. (continued)

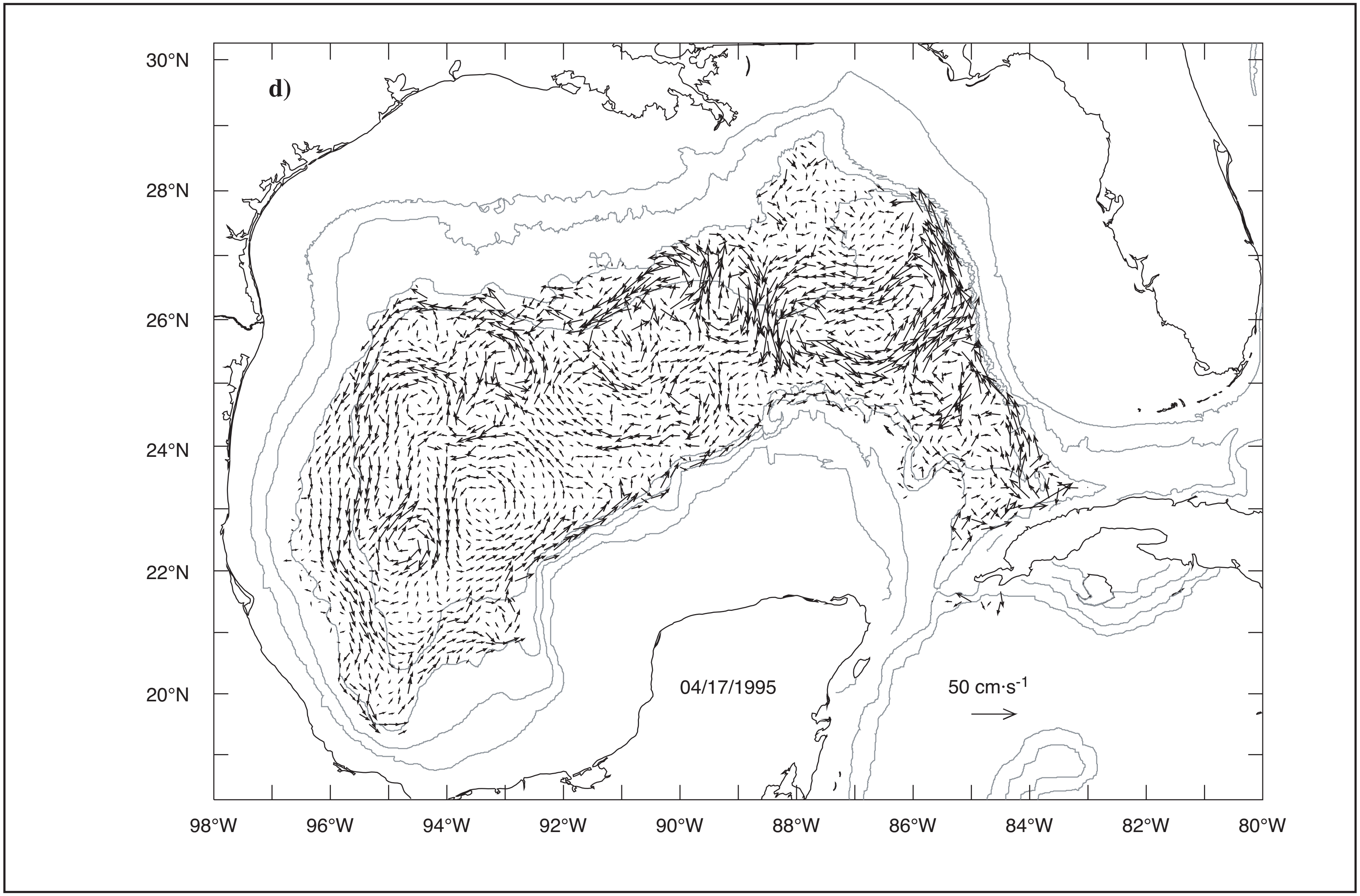

Figure 8.2-2. CUPOM hindcast currents at 2000 m for selected model dates in 1995. (continued)

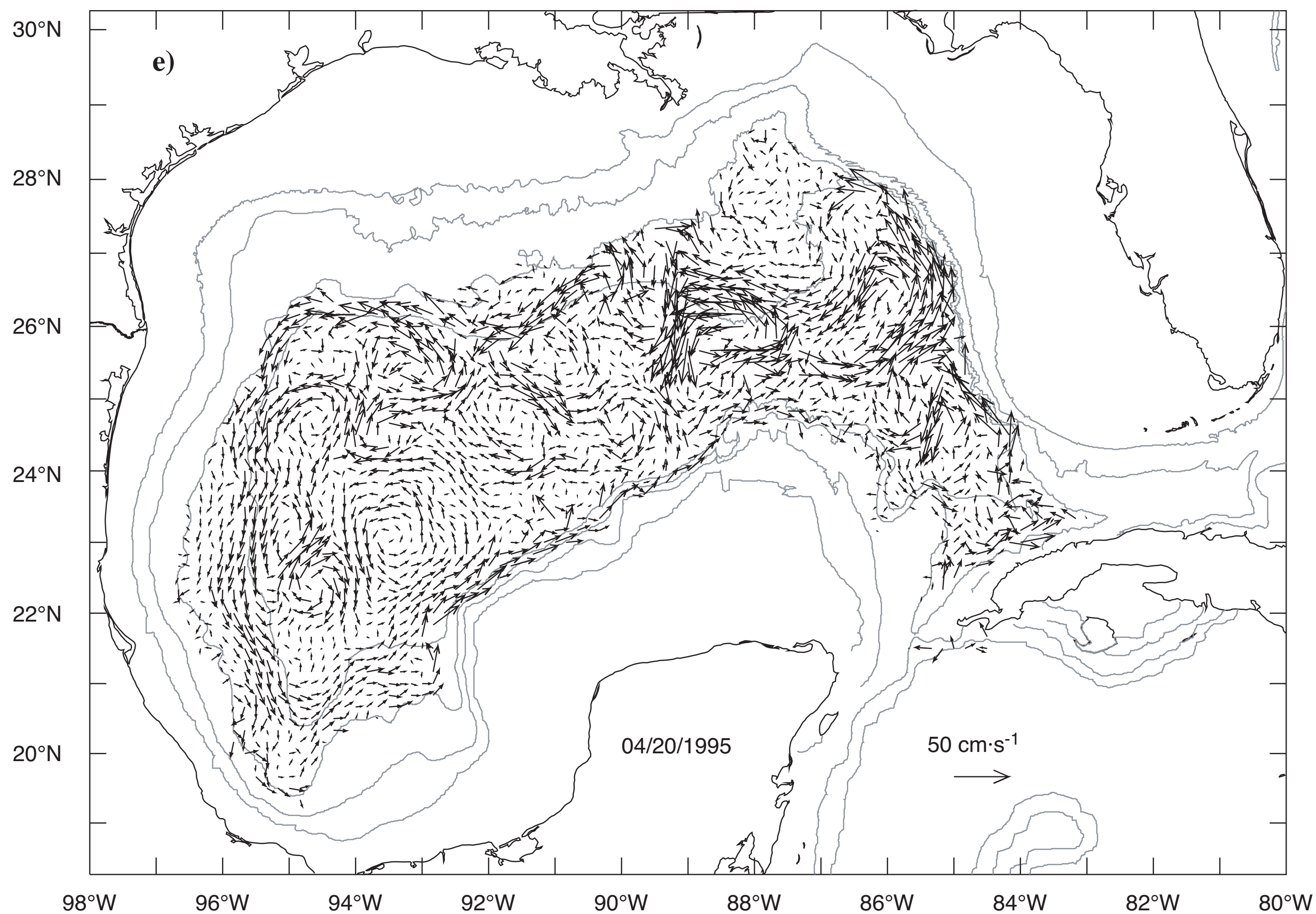

Figure 8.2-2. CUPOM hindcast currents at 2000 m for selected model dates in 1995. (continued)

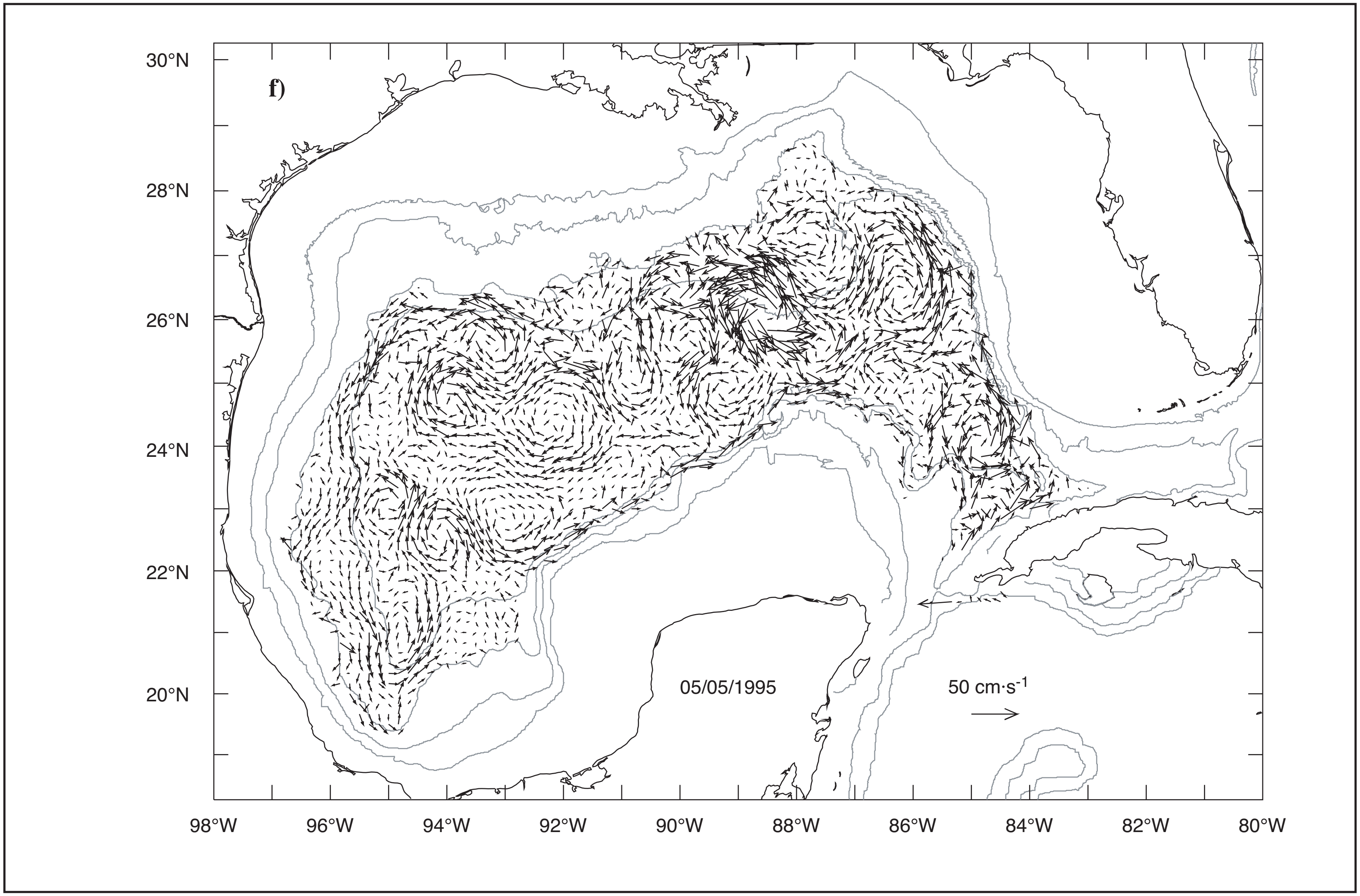

Figure 8.2-2. CUPOM hindcast currents at 2000 m for selected model dates in 1995. (continued)

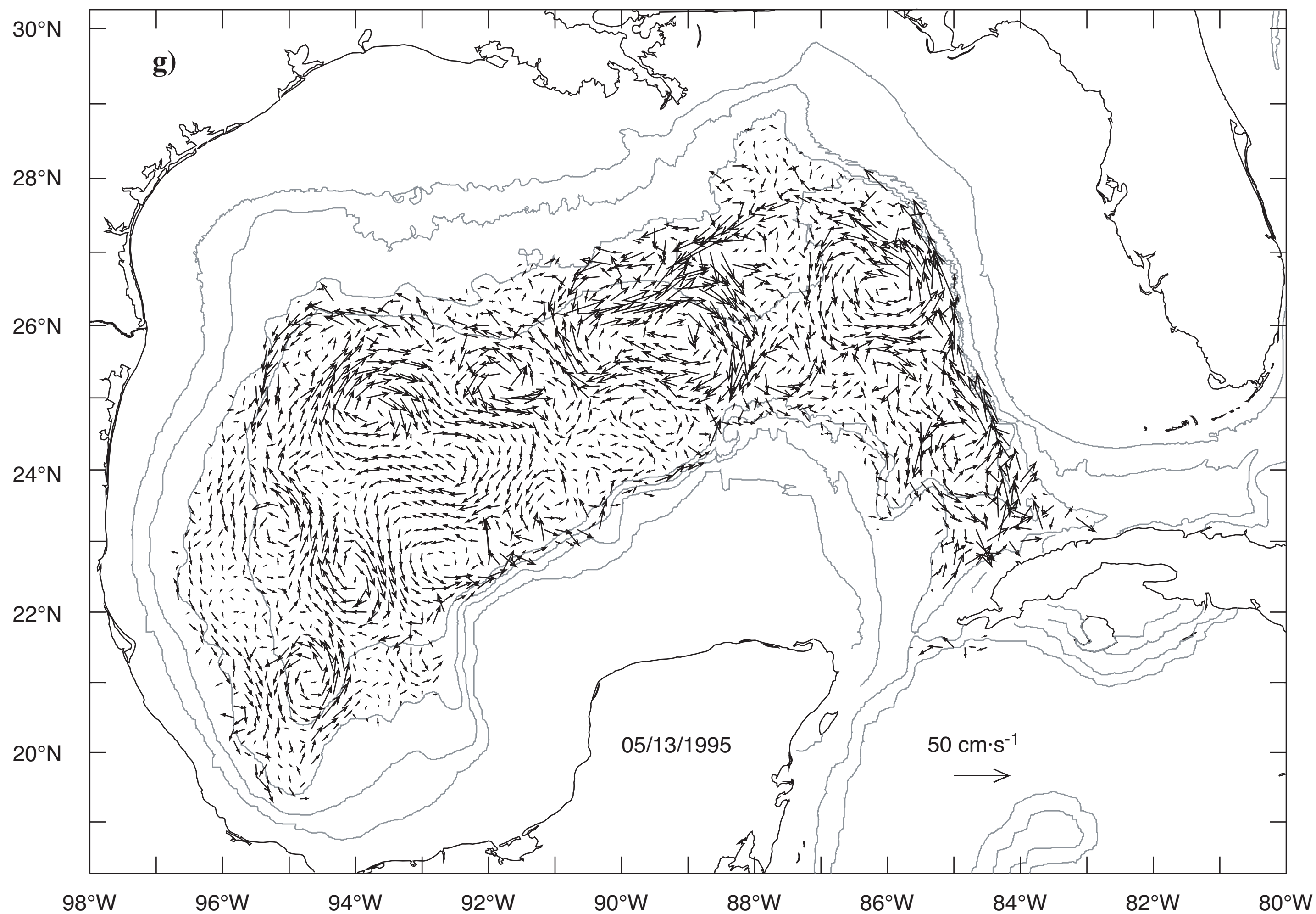

Figure 8.2-2. CUPOM hindcast currents at 2000 m for selected model dates in 1995. (continued)

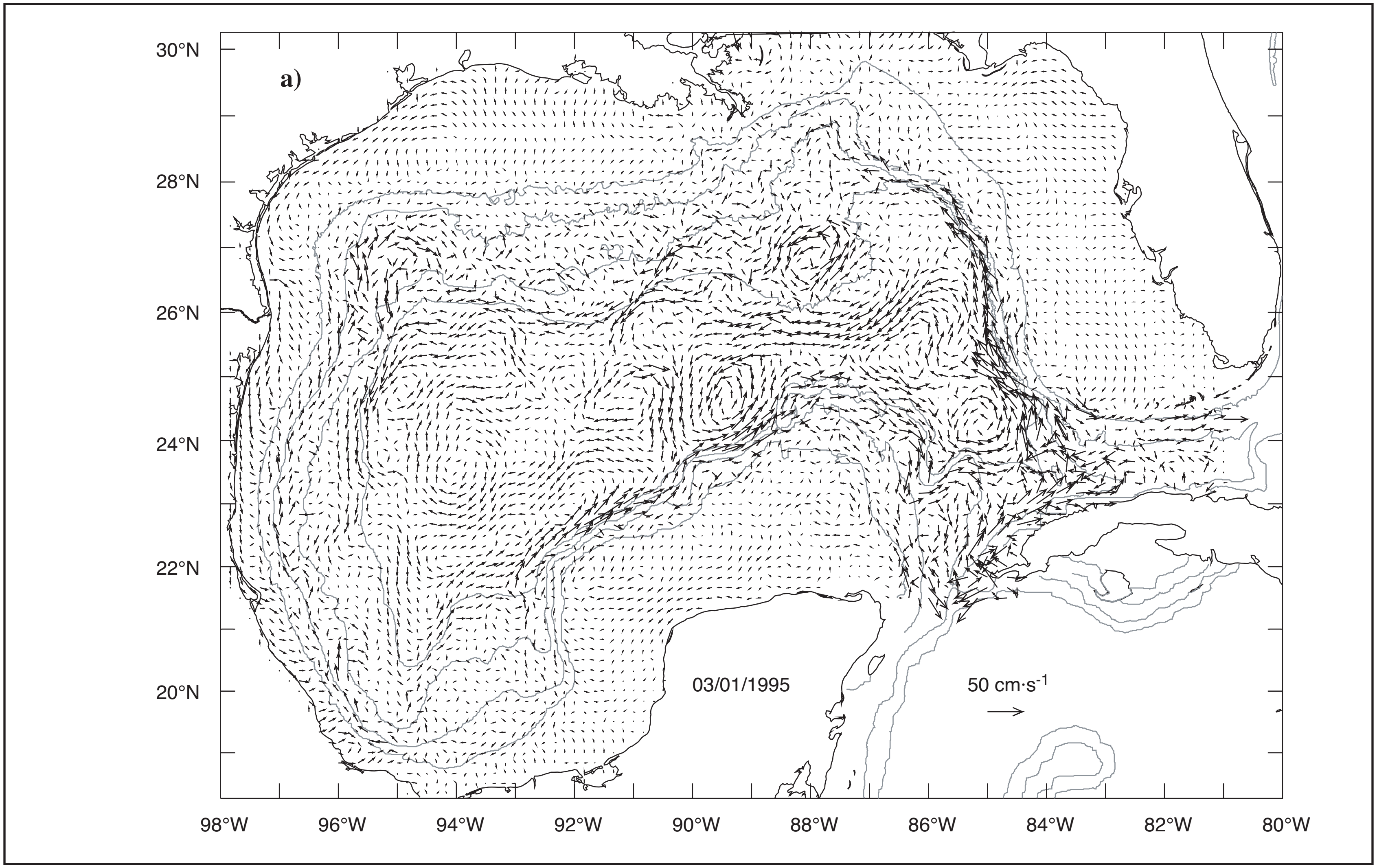

Figure 8.2-3. CUPOM hindcast currents from first sigma level above the bottom for selected model dates in 1995. Shown are a) 1 March 1995; b) 14 March 1995; c) 30 March 1995; d) 8 April 1995; e) 14 April 1995; f) 20 April 1995; and g) 5 May 1995.

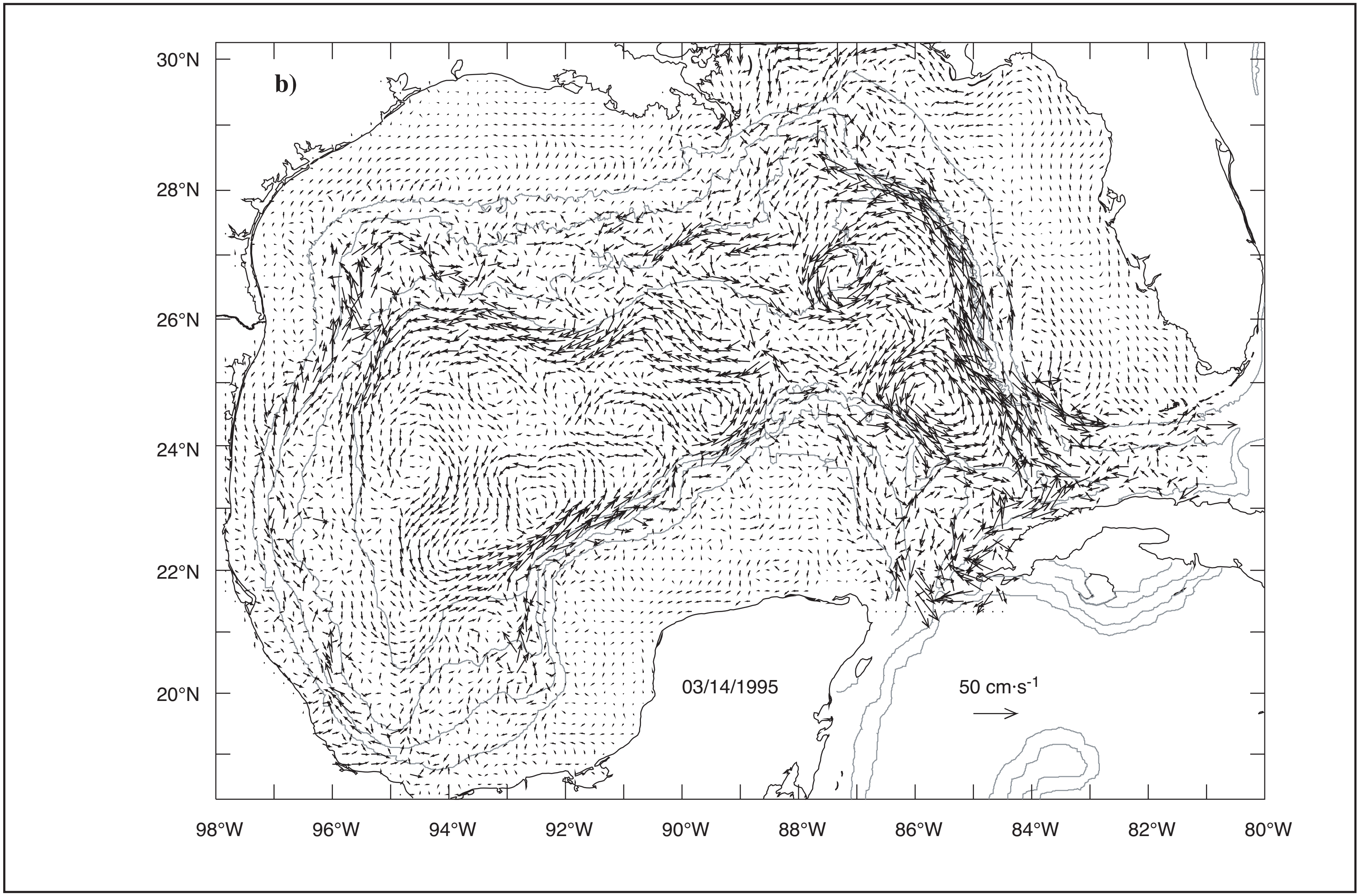

Figure 8.2-3. CUPOM hindcast currents from first sigma level above the bottom for selected model dates in 1995. (continued)

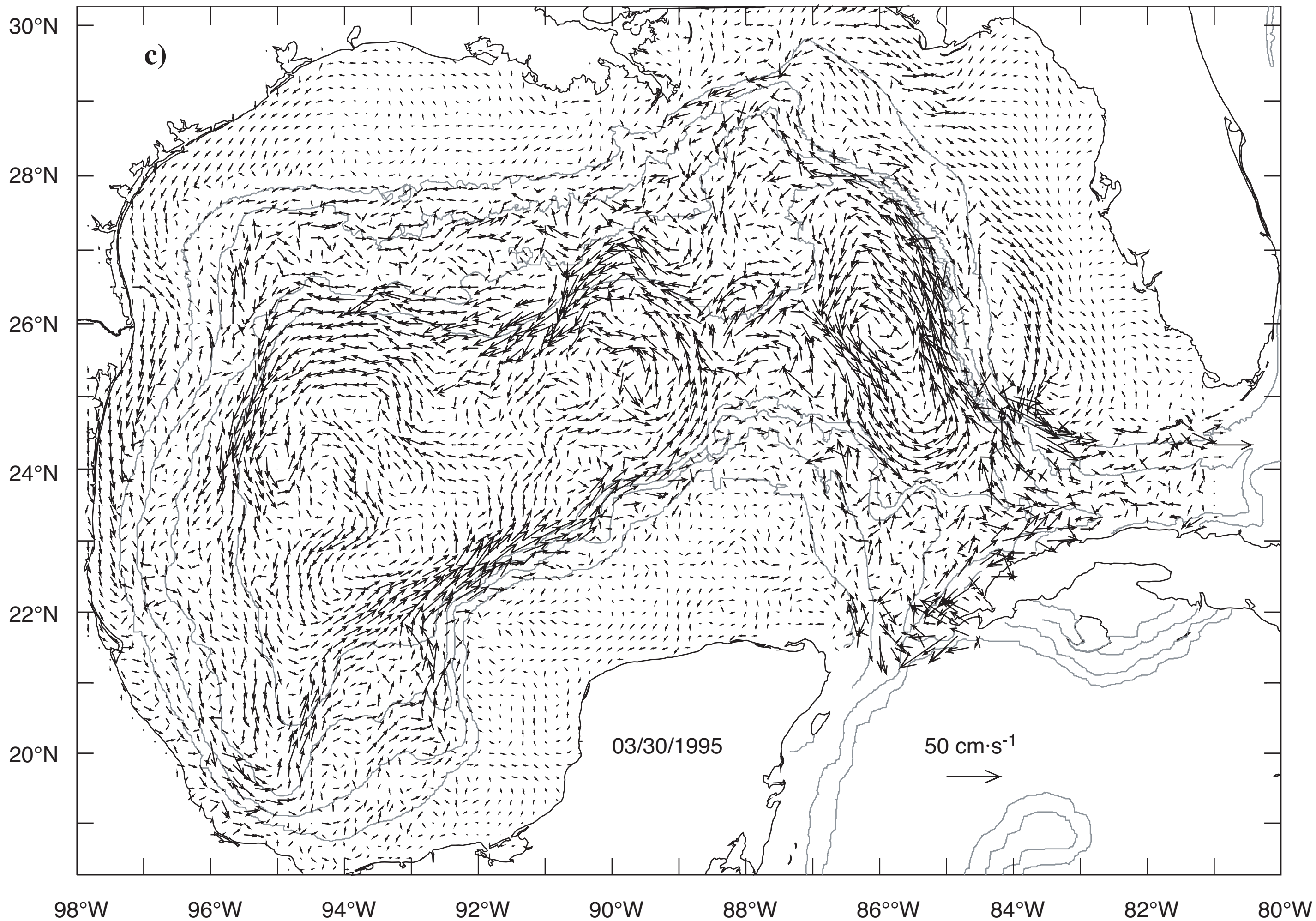

Figure 8.2-3. CUPOM hindcast currents from first sigma level above the bottom for selected model dates in 1995. (continued)

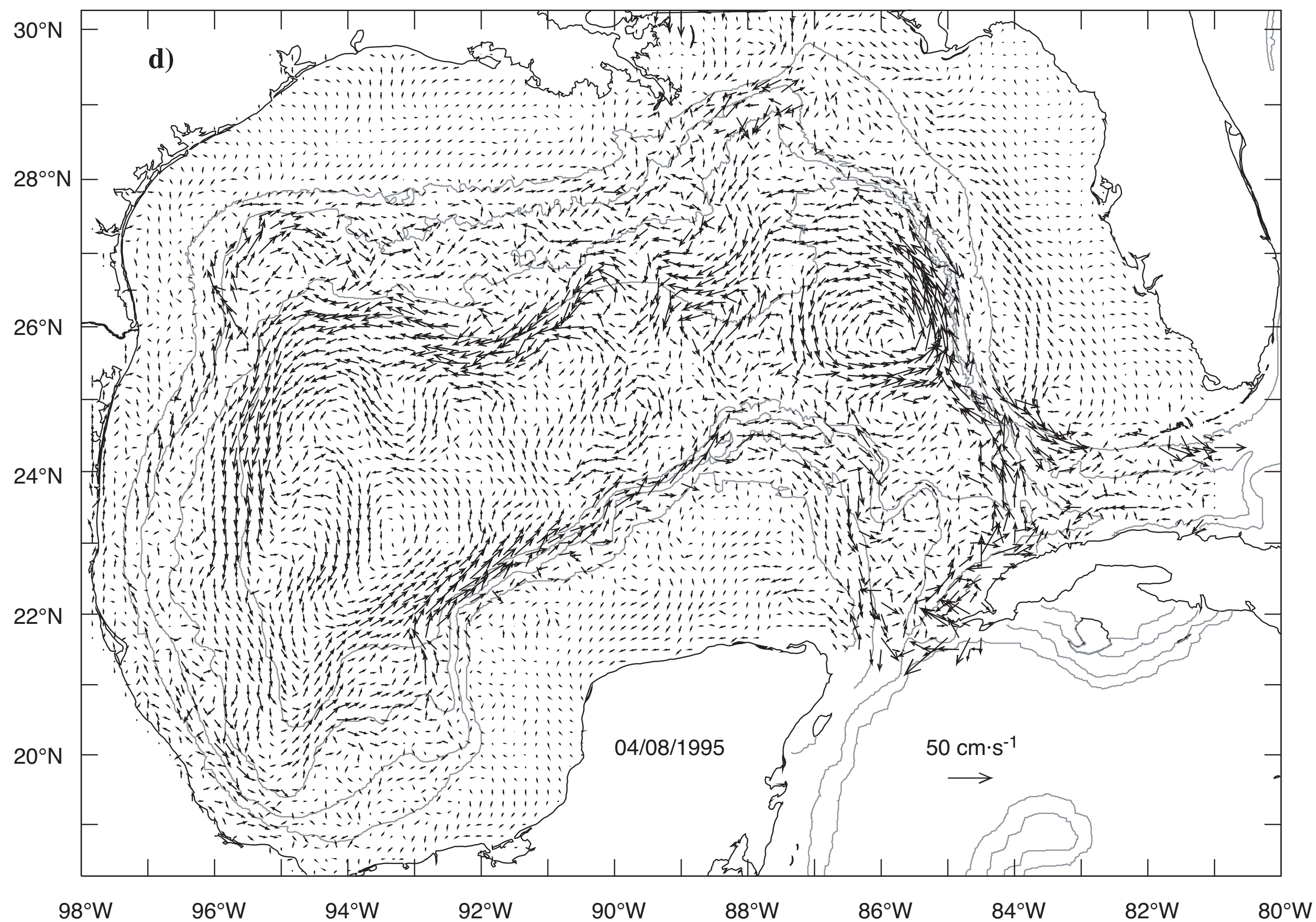

Figure 8.2-3. CUPOM hindcast currents from first sigma level above the bottom for selected model dates in 1995. (continued)

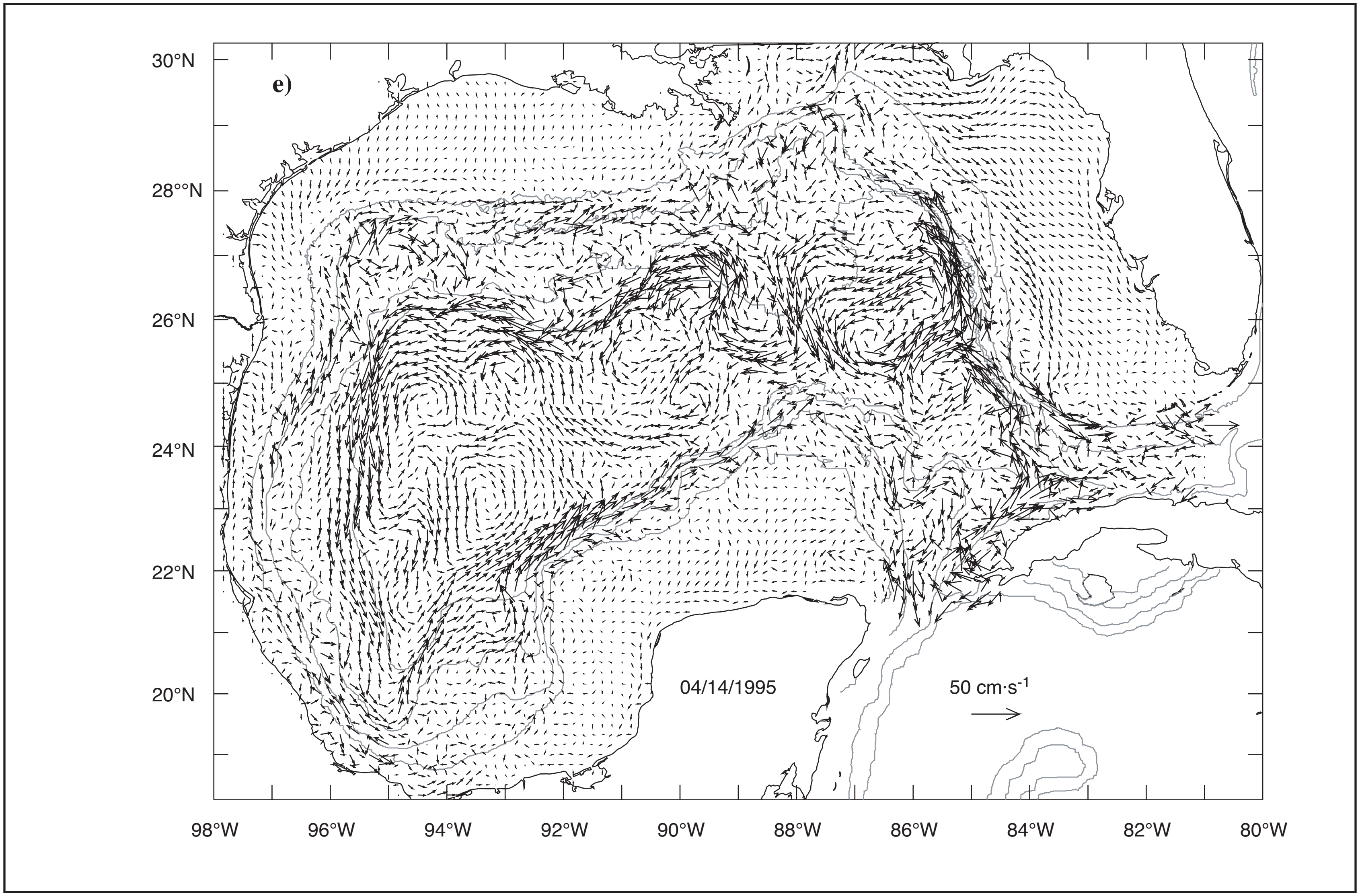

Figure 8.2-3. CUPOM hindcast currents from first sigma level above the bottom for selected model dates in 1995. (continued)

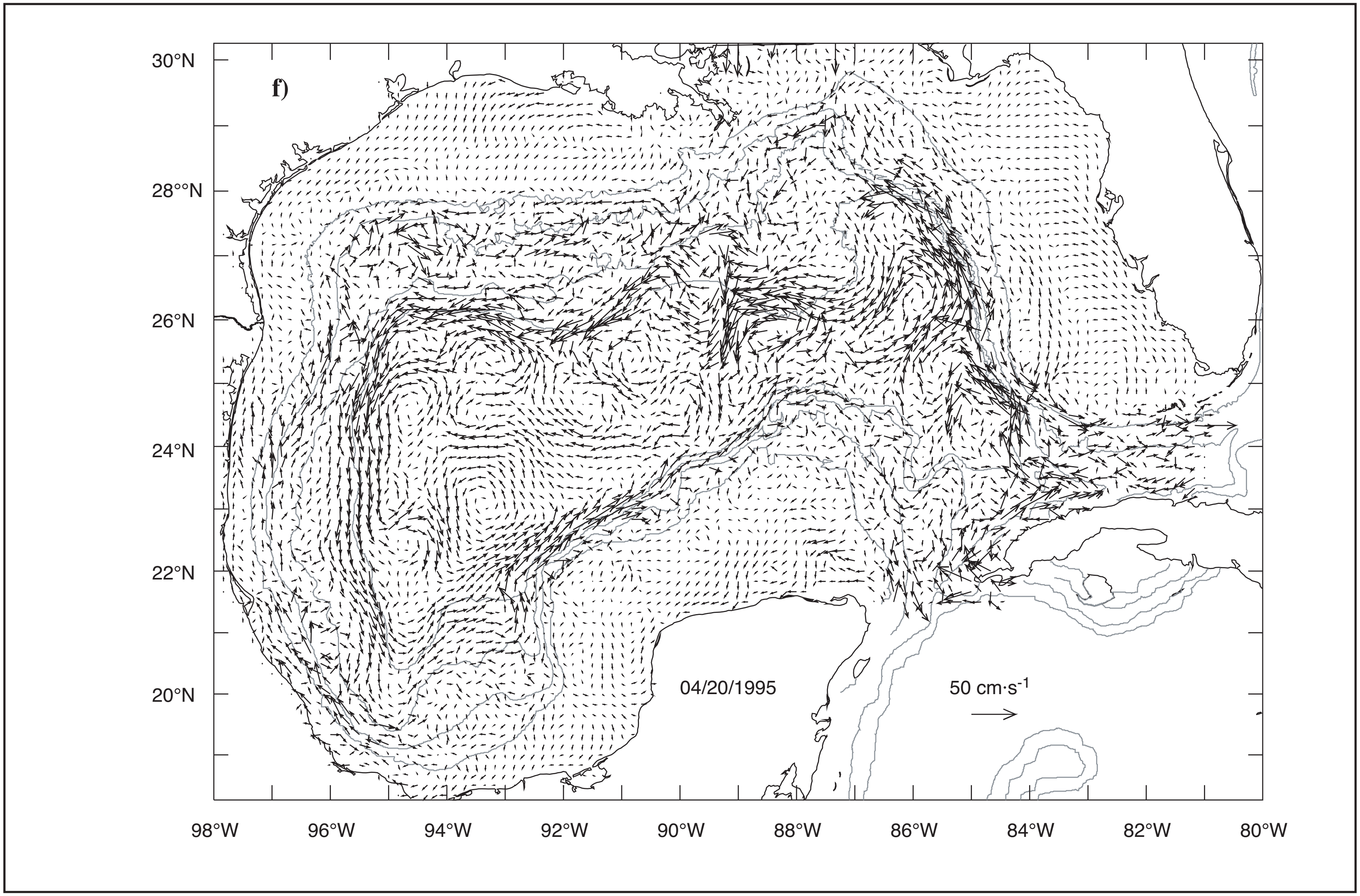

Figure 8.2-3. CUPOM hindcast currents from first sigma level above the bottom for selected model dates in 1995. (continued)

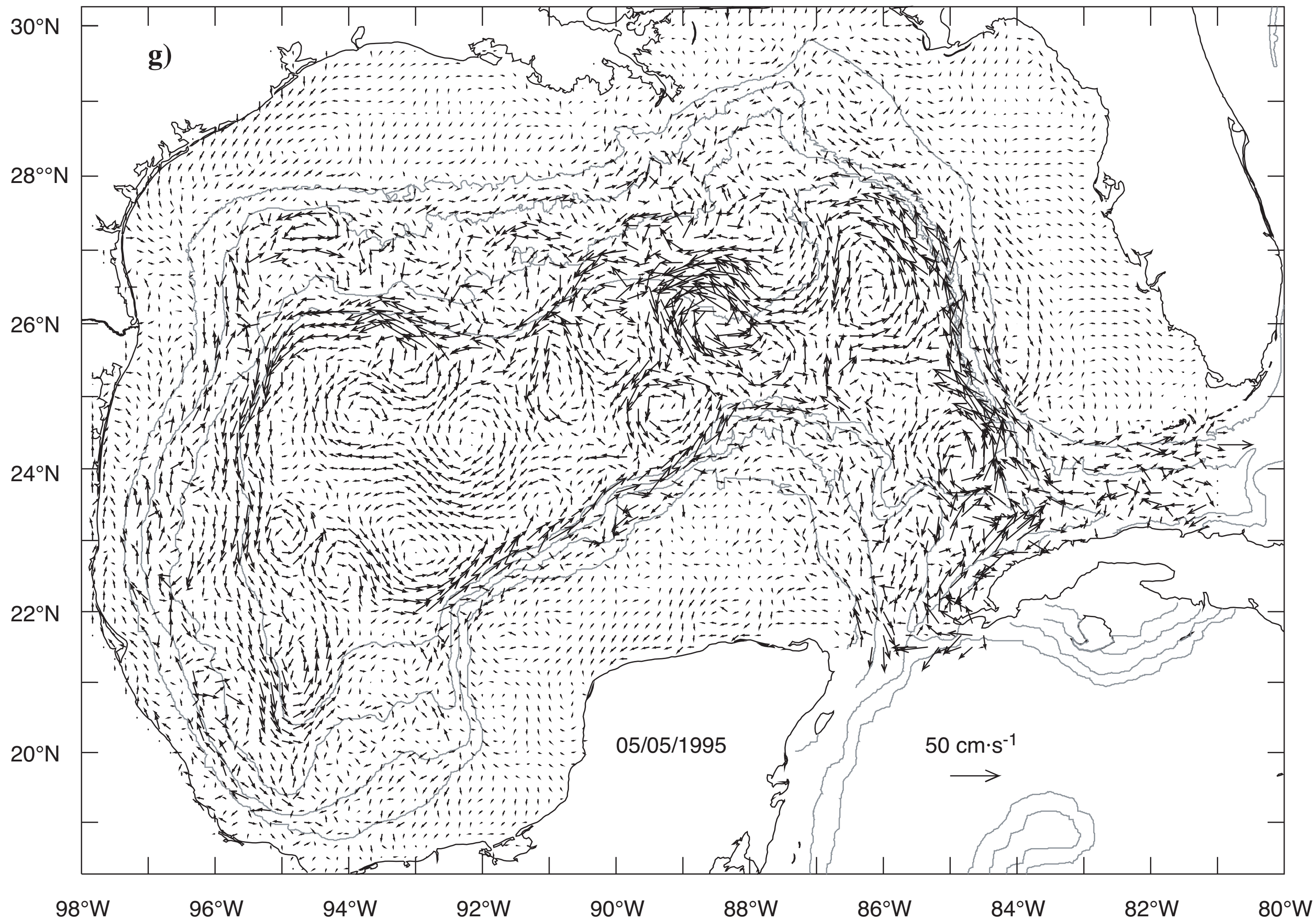

Figure 8.2-3. CUPOM hindcast currents from first sigma level above the bottom for selected model dates in 1995. (continued)

flow continued to track closely as the currents decreased in strength over the following weeks.

We know that large and very energetic, surface-intensified eddies propagate across the deepwater Gulf to its western boundary (see Section 4). Published results of studies of outputs from Gulf of Mexico circulation models (Sturges et al. 1993; Welsh and Inoue 2000) indicate the existence of deep cyclonic and anticyclonic eddies, sometimes in pairs, but more often as cyclones, that propagate westward over the abyssal plain. The present wisdom is that such deep eddies are triggered in the eastern Gulf of Mexico as a result of surface-intensified rings and then move to the west.

Based on our examination of the CUPOM hindcast circulation, it is our tentative conclusion that most of the cyclones formed in the northeastern Gulf are trapped against the northern slope and rise leading to a sequence of events such as seen in Figures 8.2-2 and 8.2-3. Examination of the 2000-m current fields from the 1993-1998 CUPOM hindcasts, revealed only *one* clear example of an energetic deep ring formed in the northeastern Gulf, passing the relatively narrow north-south extent of deep water for longitudes 88°-89° W, and continuing to move westward over the abyssal plain. That example is described in the next paragraph. Other deep cyclones passing these narrows seemed to have become trapped against the northern slope and rise, moving westward and dissipating as discussed previously.

About the second week in February 1998, a large anticyclonic ring began to separate from the Loop Current as seen in the CUPOM hindcast surface currents. Sturges and Leben (2000) assigned a separation date of 14 March 1998 to Eddy Fourchon. Indeed the hindcast results indicated separation of a ring during the second week in March 1998. However, that ring remained in contact with the Loop Current as it moved westward, resulting in the formation of a second anticyclonic feature between the initial LCE and the Loop Current. This situation for 28 May 1998 is pictured in Figure 8.2-4a. The initial anticyclonic core continued to move west-northwestward, but appeared to maintain its connection with the Loop Current as seen in Figure 8.2-4b for 17 June 1998. By 29 June 1998 the principal anticyclone seemed to be distinctly separated, but a secondary ring remained connected to the Loop Current and between the other two features. This is pictured for 7 July 1998 in Figure 8.2-4c. The two rings then moved westward. They coalesced with one another, and then with another LCE that had separated in 1997 (11 October 1997 according to Sturges and Leben 2000). The result is seen in Figure 8.2-4d for 22 August 1998. That ring remained approximately stationary through October, after which it moved southward along the slope and still was weakly present at the end of the year.

Within that setting, the hindcast currents at the 2000-m level indicate that in late May 1998 a deep cyclone formed in the eastern Gulf and moved westward along the northern slope of the Campeche Bank. The situation on 28 May 1998 is seen in Figure 8.2-5a with the cyclone centered about 25.5°N, 87°W. This cyclone moved westward along the northern flank of Campeche Bank and passed through the deep constriction. Figure 8.2-5b shows 2000-m currents on 17 June 1998 with the cyclone now centered about 25.5°N, 88.5°W (compare the surface circulation in Figure 8.2-4b). (There was a second cyclone to the west; the two appeared to have interacted briefly in early June. See Figure 8.2-4b.) The cyclone of interest then moved slightly north of west, leaving the southern slope region and crossing the abyssal plain. On 7 July it was seen to be approaching the northern rise/slope in the central Gulf (Figure 8.2-5c). (By that time the western cyclone had weakened greatly and was centered about 25°N, 93°W.) The cyclone of interest continued to move westward (Figure 8.2-5d shows the situation on 13 August 1998 when it was centered about 25°N, 92°W) into the northwest corner of the deep gulf where it dissipated in the September-October time frame.

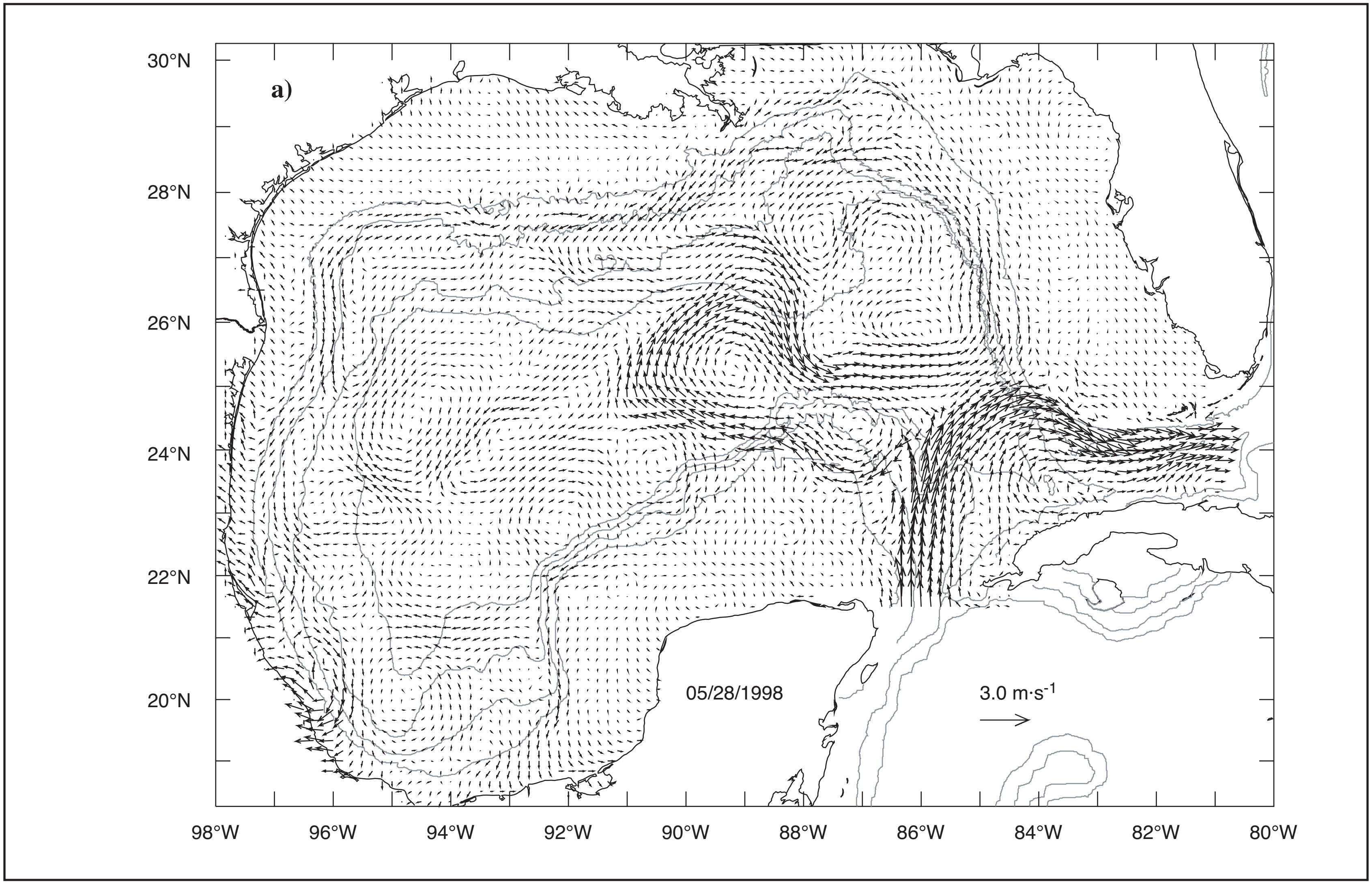

Figure 8.2-4. CUPOM hindcast surface currents for selected model dates in 1998. Shown are a) 28 May 1998, b) 17 June 1998, c) 7 July 1998, and d) 22 August 1998.

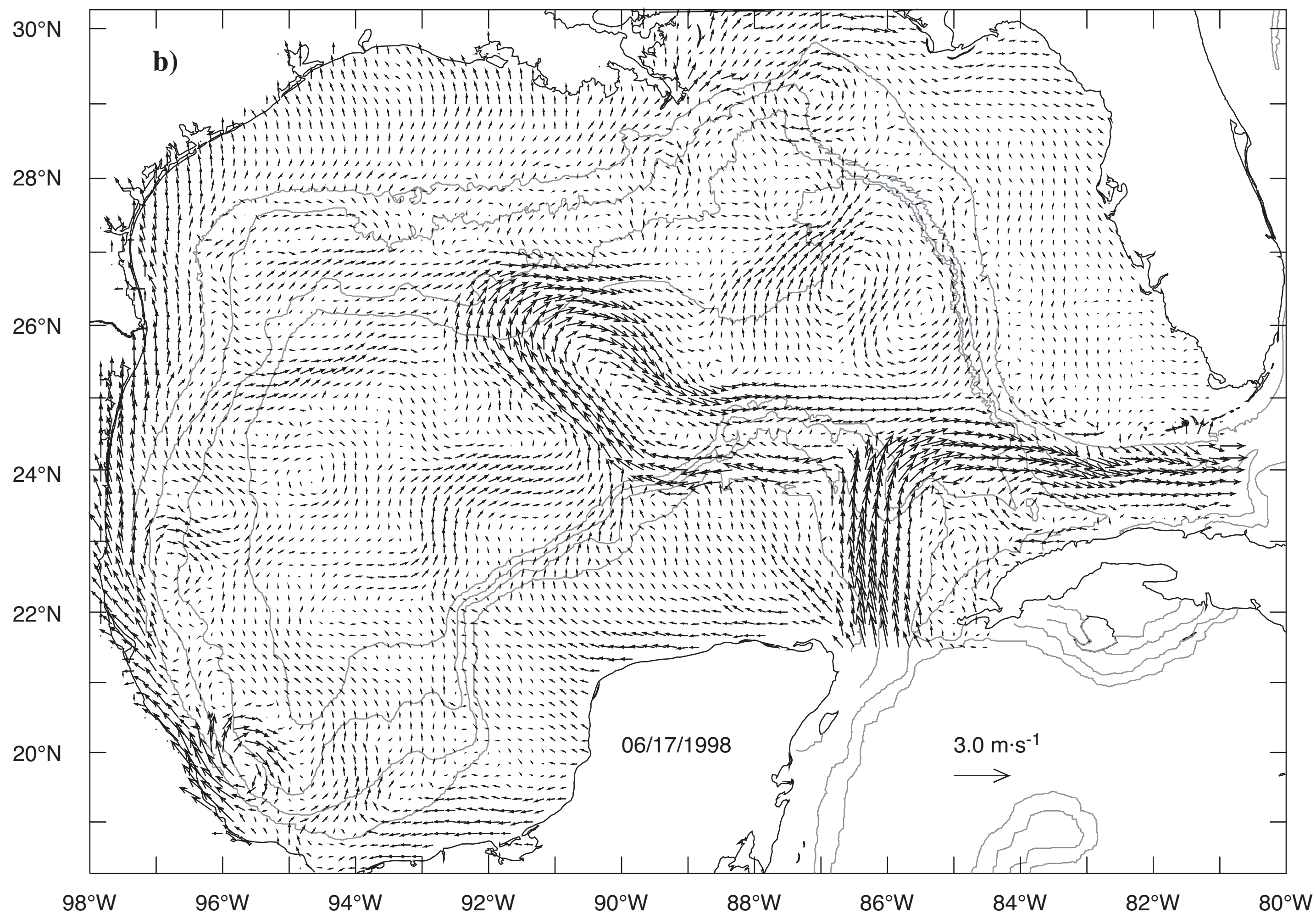

Figure 8.2-4. CUPOM hindcast surface currents for selected model dates in 1998. (continued)

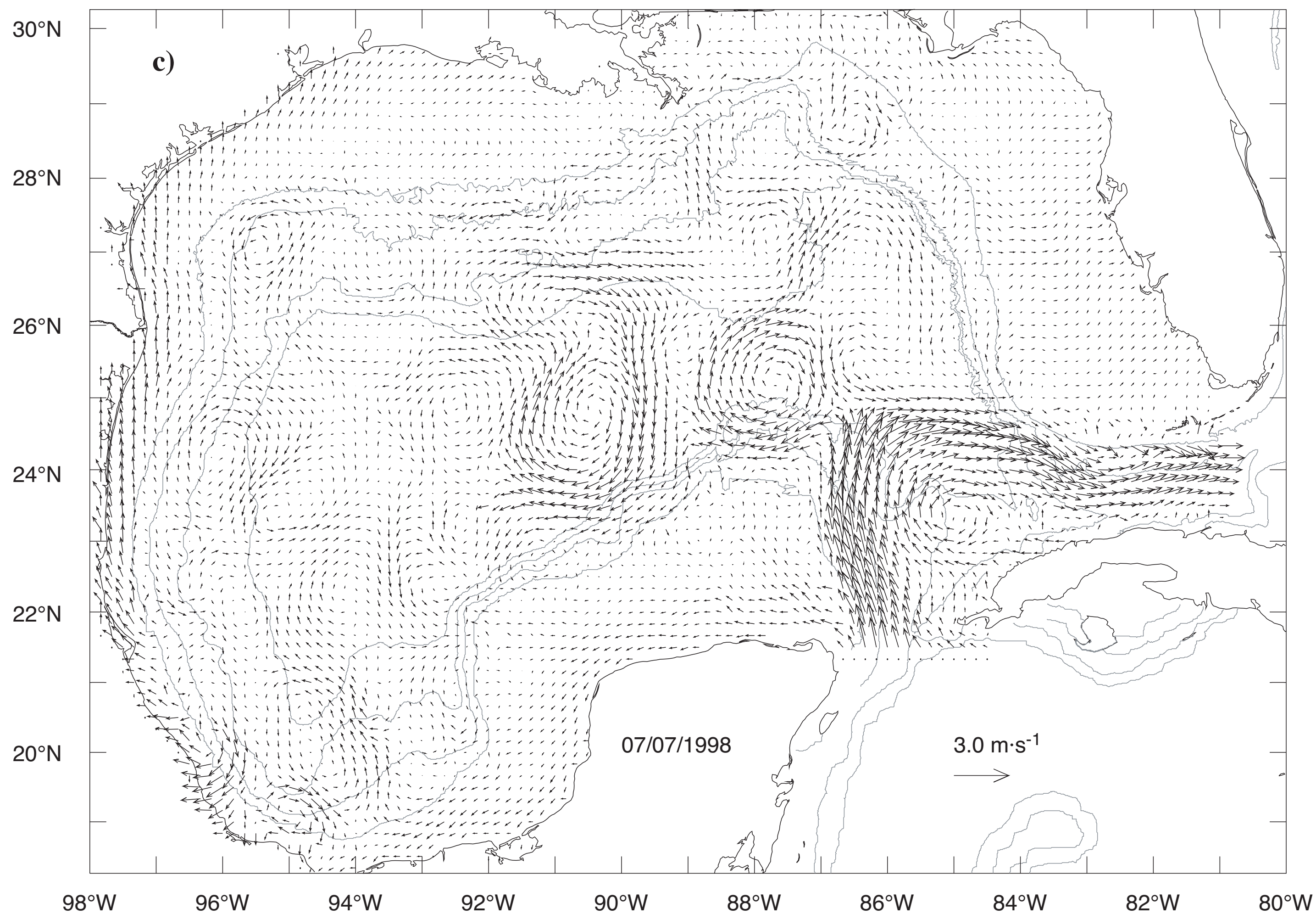

Figure 8.2-4. CUPOM hindcast surface currents for selected model dates in 1998. (continued)

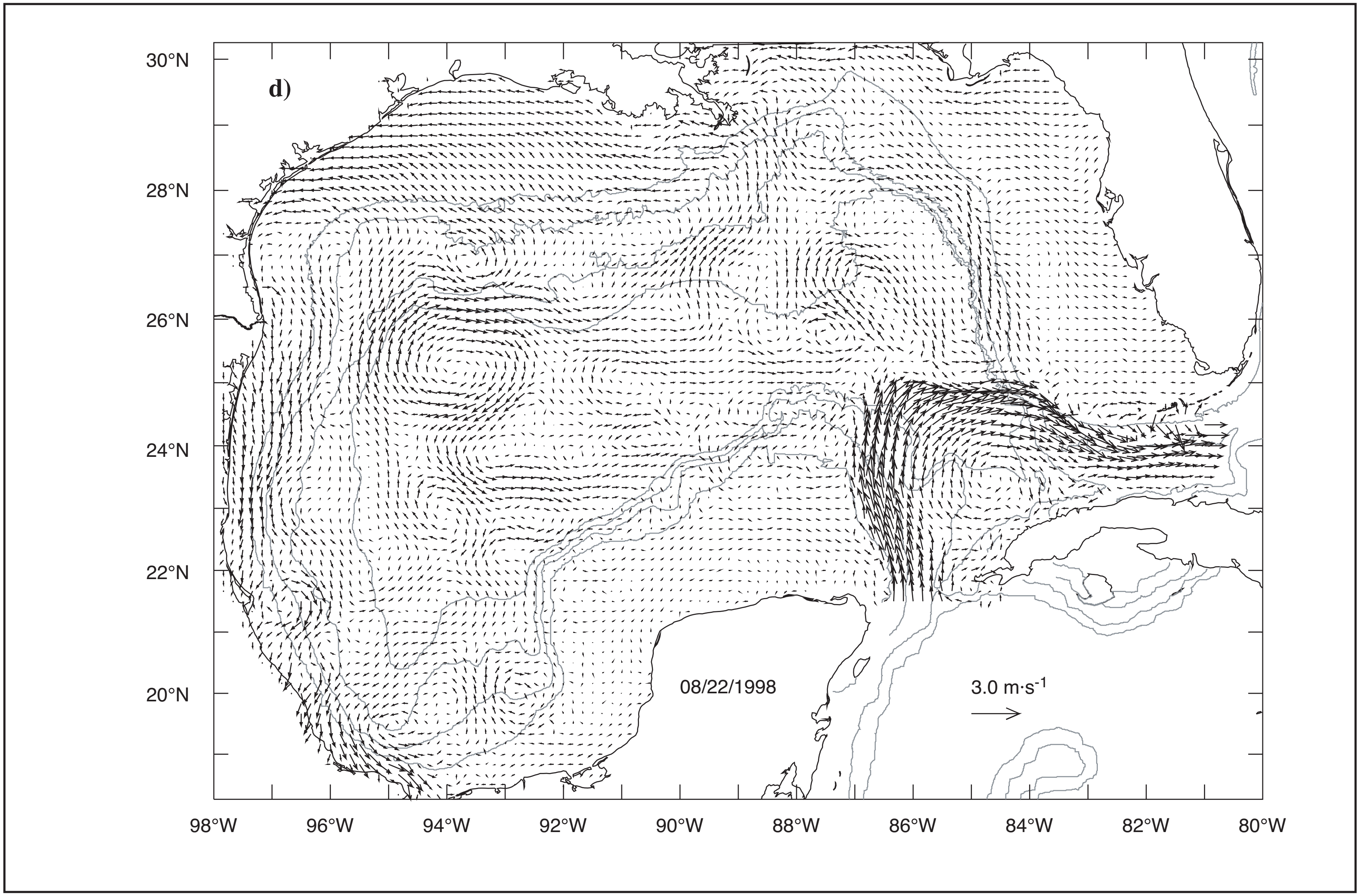

Figure 8.2-4. CUPOM hindcast surface currents for selected model dates in 1998. (continued)

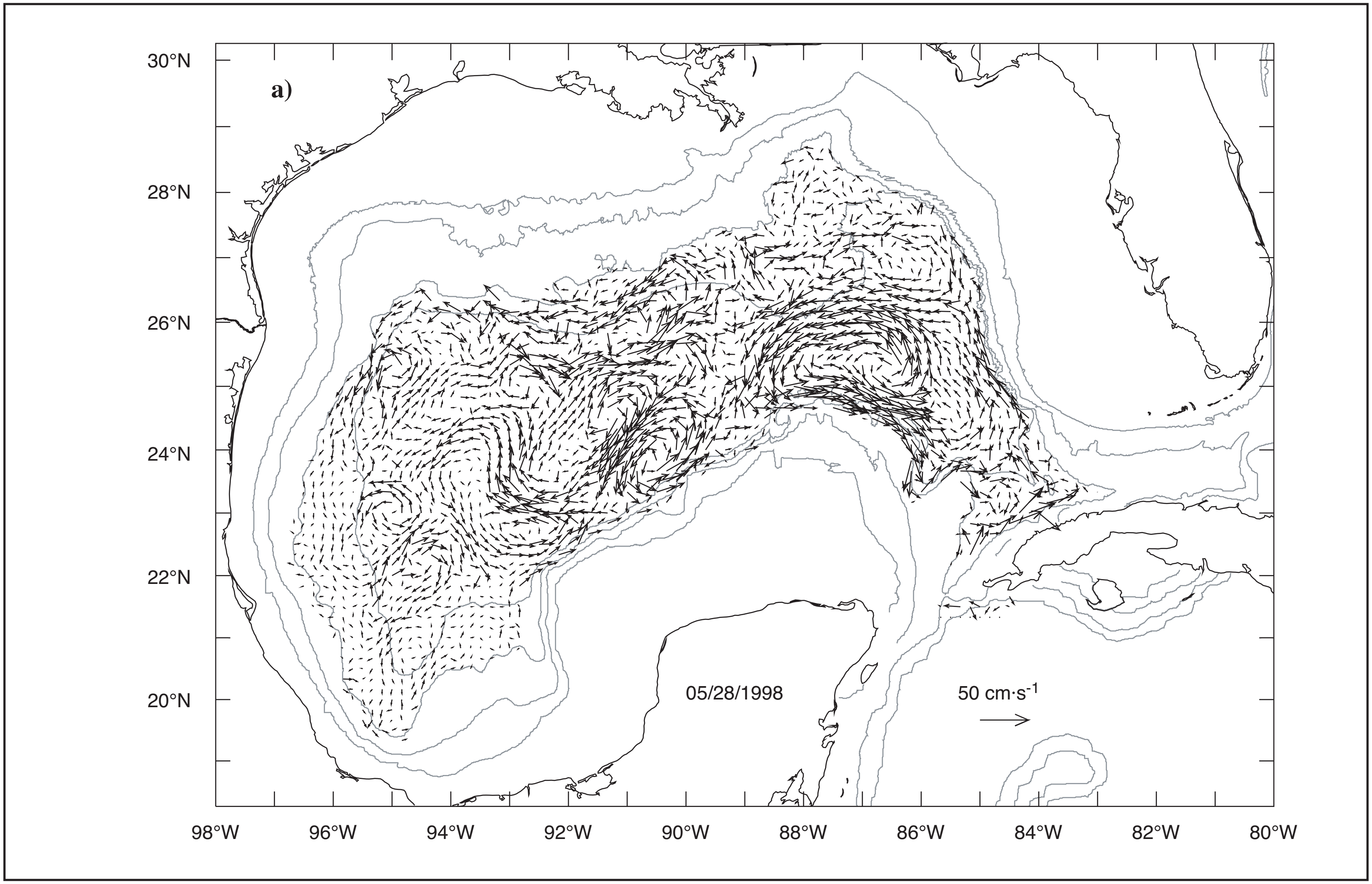

Figure 8.2-5. CUPOM hindcast currents at 2000 m for selected model dates in 1998. Shown are a) 28 May 1998, b) 17 June 1998, c) 7 July 1998, and d) 13 August 1998.

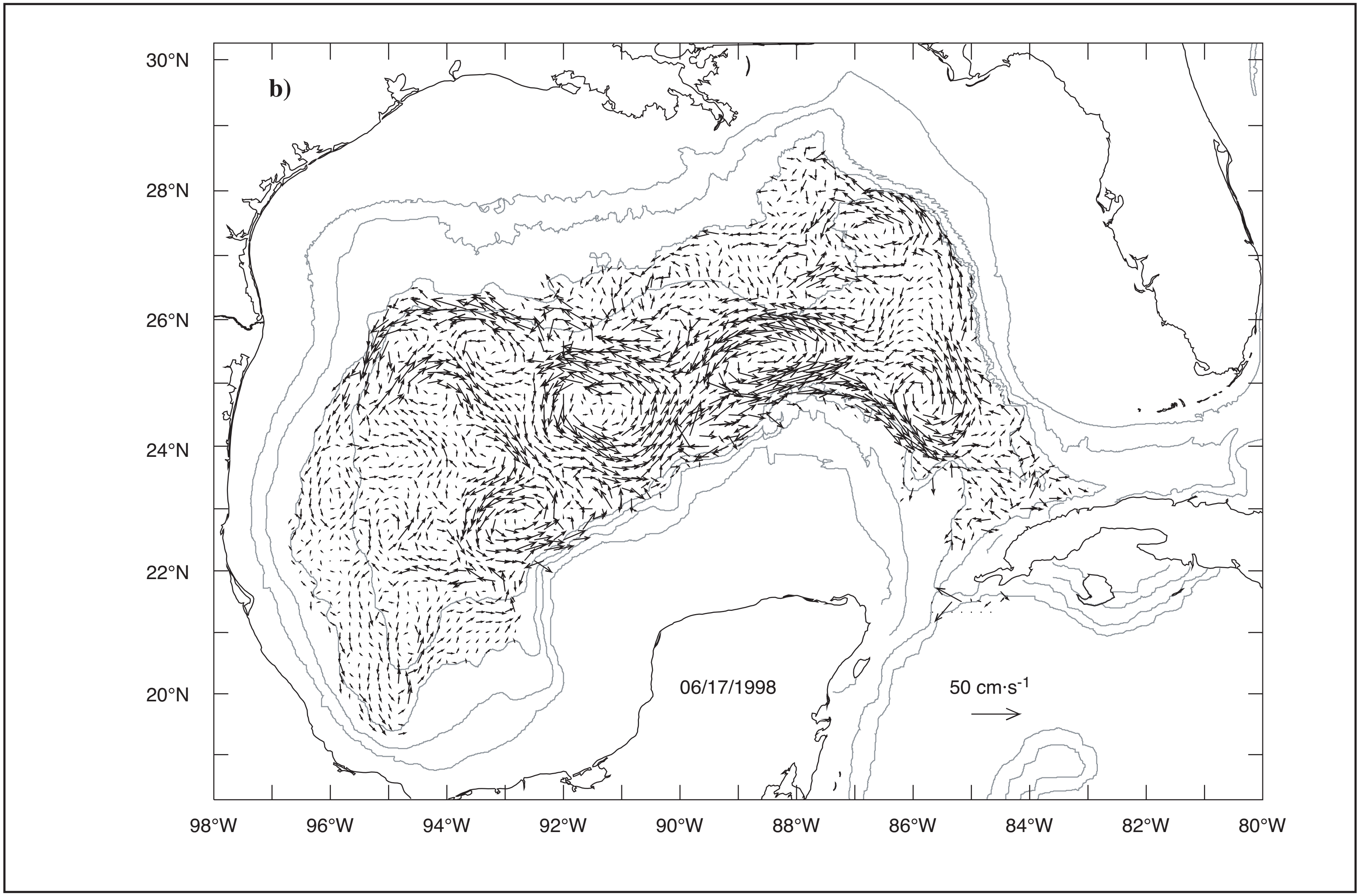

Figure 8.2-5. CUPOM hindcast currents at 2000 m for selected model dates in 1998. (continued)

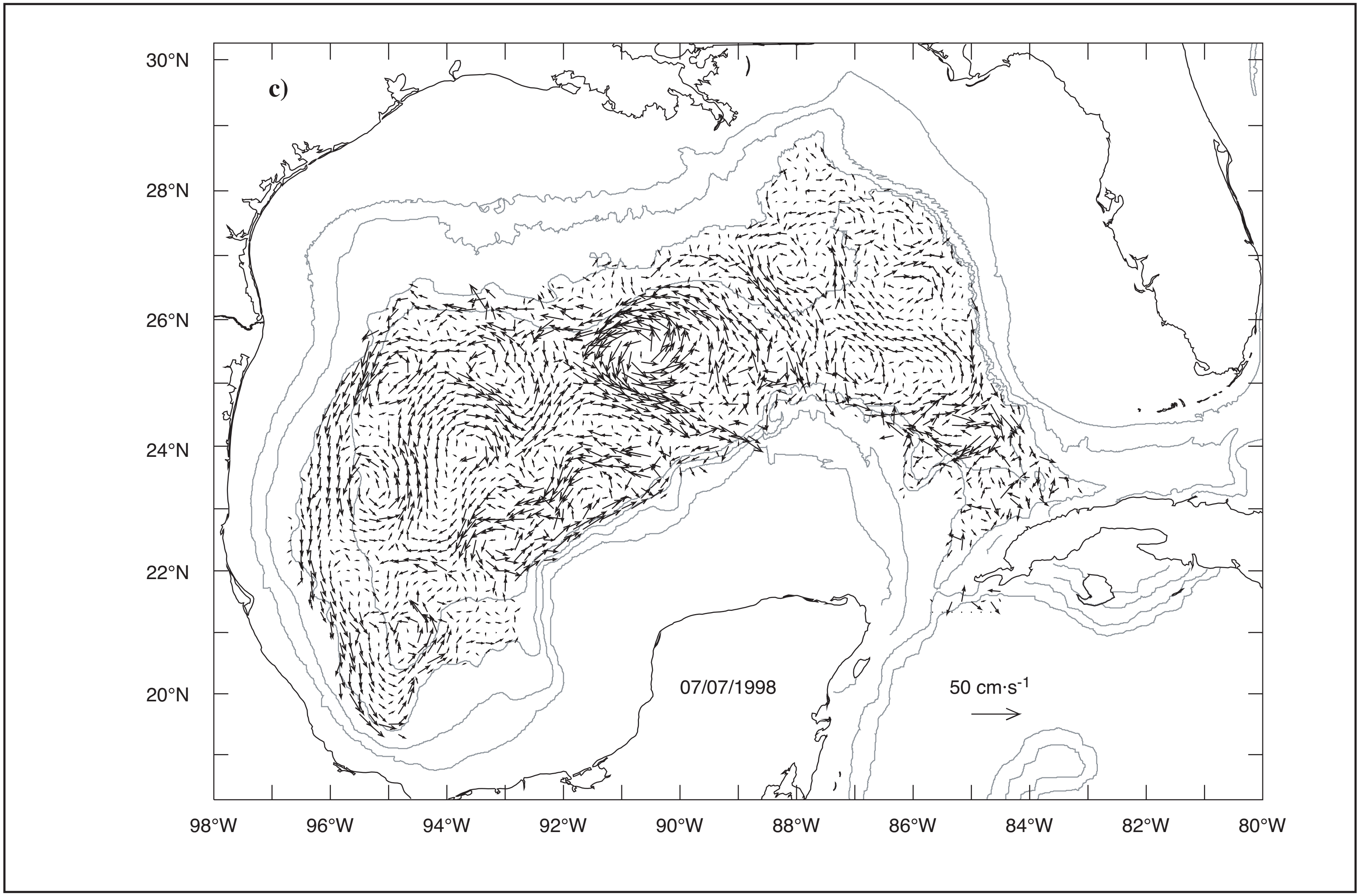

Figure 8.2-5. CUPOM hindcast currents at 2000 m for selected model dates in 1998. (continued)

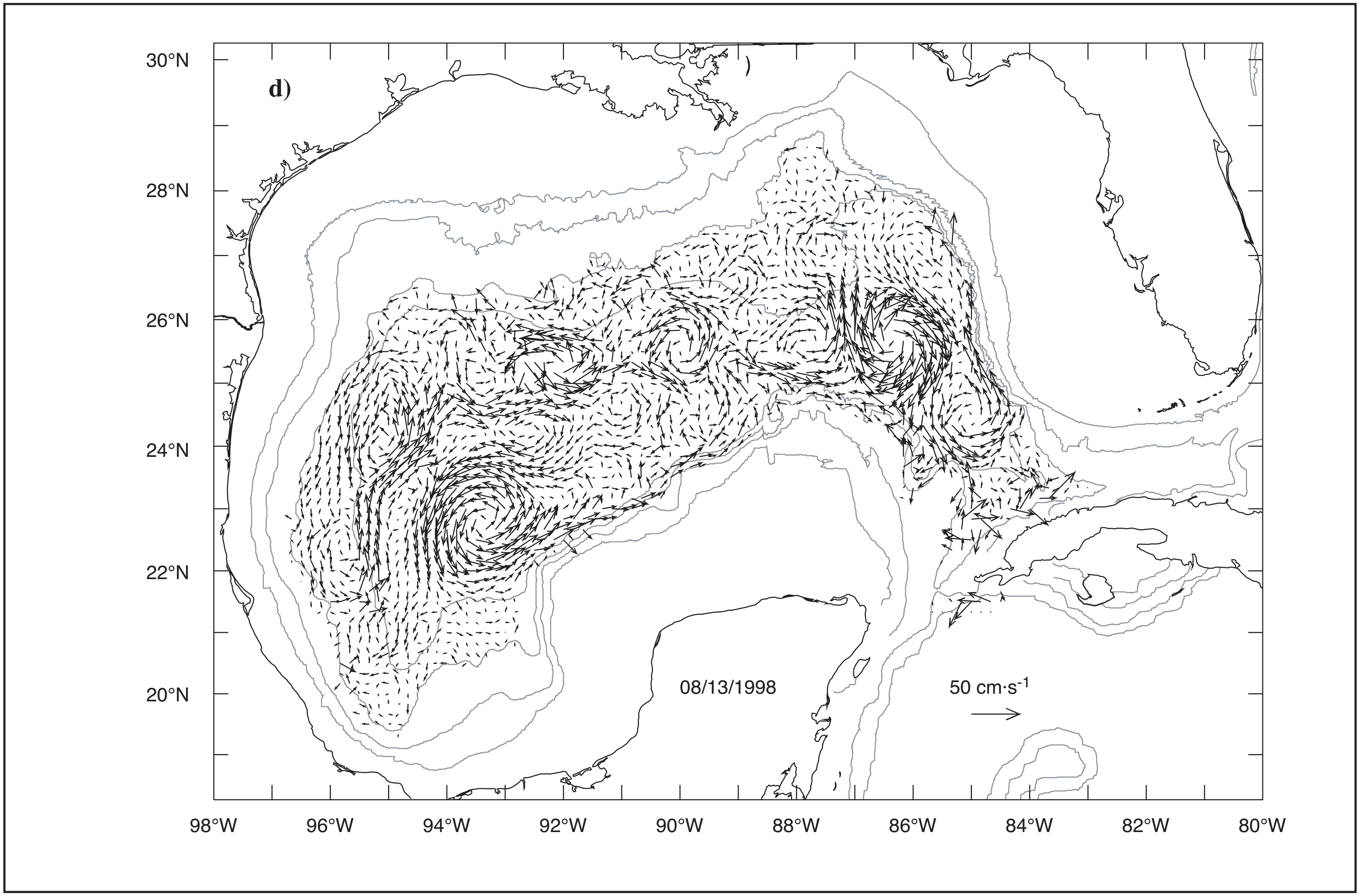

Figure 8.2-5. CUPOM hindcast currents at 2000 m for selected model dates in 1998. (continued)

The formation of rings, particularly cyclones, in the 2000-m hindcast currents over the abyssal plain to the west of 89°-90°W was not at all uncommon. Many of these cyclones persisted for long periods and moved westward. They were often accompanied by the formation of anticyclones and/or coalesced with other deep rings.

One notable example occurred in July 1996. There was no appreciable activity in the deep western Gulf during the last half of June 1996. By June 30 (Figure 8.2-6a) there was evidence of a cyclone near 24°N, 91°W with an anticyclone to the southwest and another cyclone further west. By 7 July 1996 (Figure 8.2-6b) these features had strengthened considerably. The stronger, eastern cyclone was moving westward, and by July 17 is seen centered near 92.5°W (Figure 8.2-6c). The cyclone-anticyclone pair rotated counterclockwise, as seen in the situation for July 22 (Figure 8.2-6d) and for August 16 (Figure 8.2-6e). Note that during this process another cyclone intensified in the central Gulf west of the deep narrows. In Figure 8.2-7a-b are shown hindcast surface currents for 2 and 17 July 1996. There are in the western Gulf two old anticyclonic rings moving westward. They were located north of the two deep cyclones in early July when the latter were seen to strengthen. In August and September these two surface anticyclones appeared to coalesce.

Another example of deep rings moving westward over the abyssal plain of the Gulf occurred in the CUPOM hindcast fields during late 1997. During April through June of 1997 the Loop Current was relatively well developed with strong closed interior circulation. It extended northwestward during the first two weeks of July. Then a neck begin to form about July 15 and by 22 October 1997 a ring was fully separated (Figure 8.2-8a) with cyclonic flow separating the LCE from the Loop Current. According to Sturges and Leben (2000) Eddy El Dorado separated on 11 October 1997, which agrees rather well with these results. The LCE drifted westward, past 90°W by December 9 (Figure 8.2-8b). During the next month the ring moved west-northwestward, its center reaching 92°W by mid January 1998 (Figure 8.2-8c). Perhaps it was beginning to interact with the northern slope because during the next month it became elongated east-west over the north-central slope and rise (Figure 8.2-8d shows the situation on 11 February 1998). Meanwhile another ring—Eddy Fourchon—had begun to separate from the Loop Current, as discussed earlier. Eddy El Dorado was still in the western Gulf, centered about 25°N, 92°W, and the initial separation of Eddy Fouchron was essentially complete by 23 February 1998 (shown in Figure 8.2-8e).

During the time of neck and ring development of Eddy El Dorado, August and September 1997, a strong cyclone in the 2000-m current field was seen to develop under the northern edge of the Loop Current. During the second week in October, while El Dorado was separating, a second deep cyclone was formed with center about 25°N, 89°W. A deep anticyclone was seen between them near 25.5°N, 86.5°W. These features are seen in the 2000-m current field for 11 October 1997 (Figure 8.2-9a). Also seen in the western Gulf are two cyclone-anticyclone pairs centered about 23.5°N, 94°W and 24.5°N, 91.5°W. The smaller eastern cyclone near the deep bathymetric neck moved westward over the abyssal plain and in the picture for October 25 (Figure 8.2-9b) had moved to 25°N, 90°W and an anticyclone had formed on its eastern flank and was interacting. The cyclone-anticyclone pairs in the eastern Gulf and near 94°W remained nearly in place, although a new cyclone was strengthening at 22.5°N, 93°W and squeezing the western anticyclone to its northwest. The cyclone-anticyclone pair that in Figure 8.2-9a was centered near 91.5°W had largely dissipated and was seen in Figure 9.2-9b as a small disturbance near 25°N, 93°W.

During the next three weeks the cyclone-anticyclone pair in the eastern Gulf moved southward; we will not further describe features in the eastern Gulf. The pair of cyclones in the far western Gulf continued to bracket the anticyclone in the 2000-m field for 15

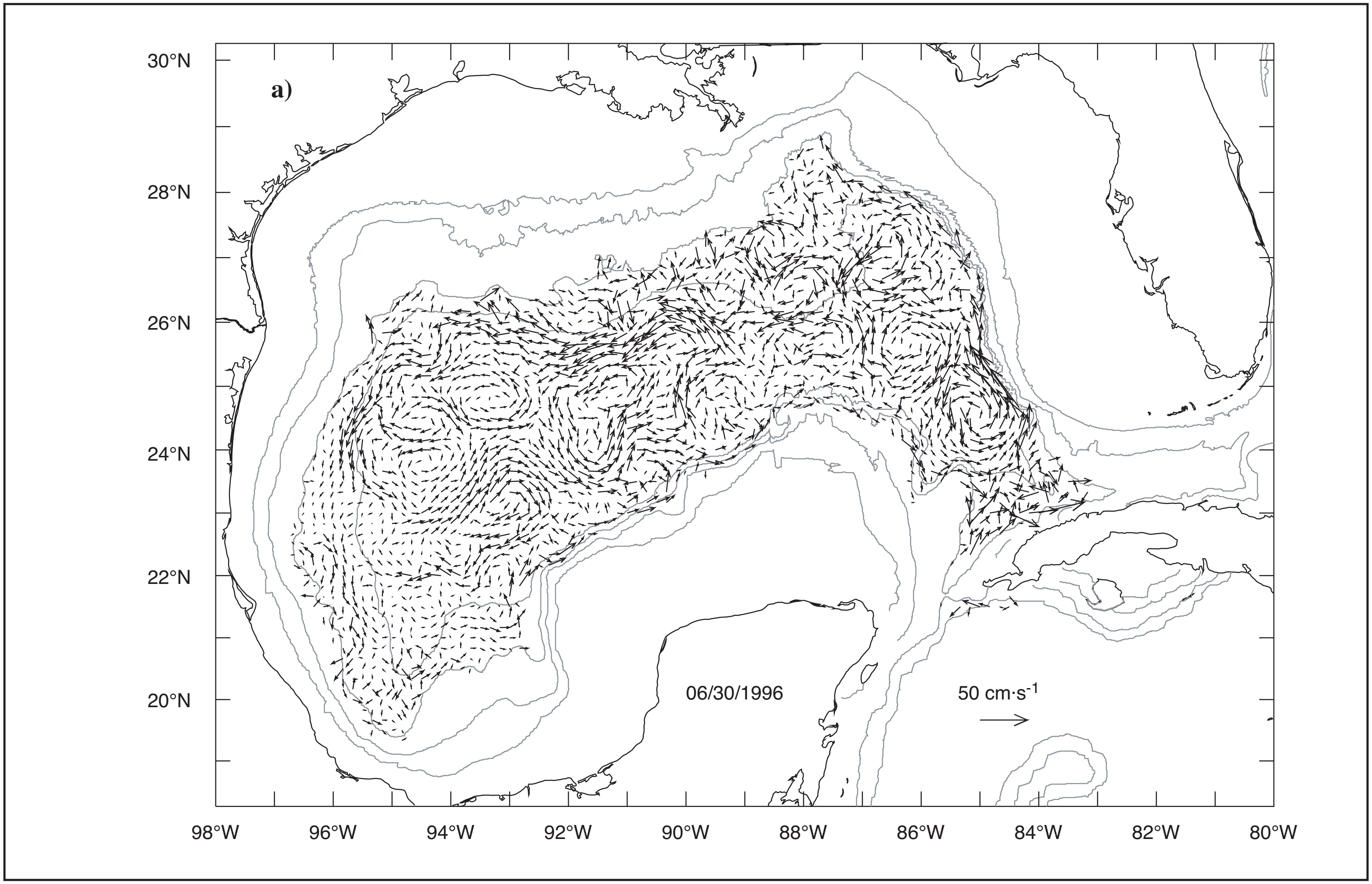

Figure 8.2-6. CUPOM hindcast currents at 2000 m for selected model dates in 1996. Shown are a) 30 June 1996, b) 7 July 1996, c) 17 July 1996, d) 22 July 1996, and e) 16 August 1996.

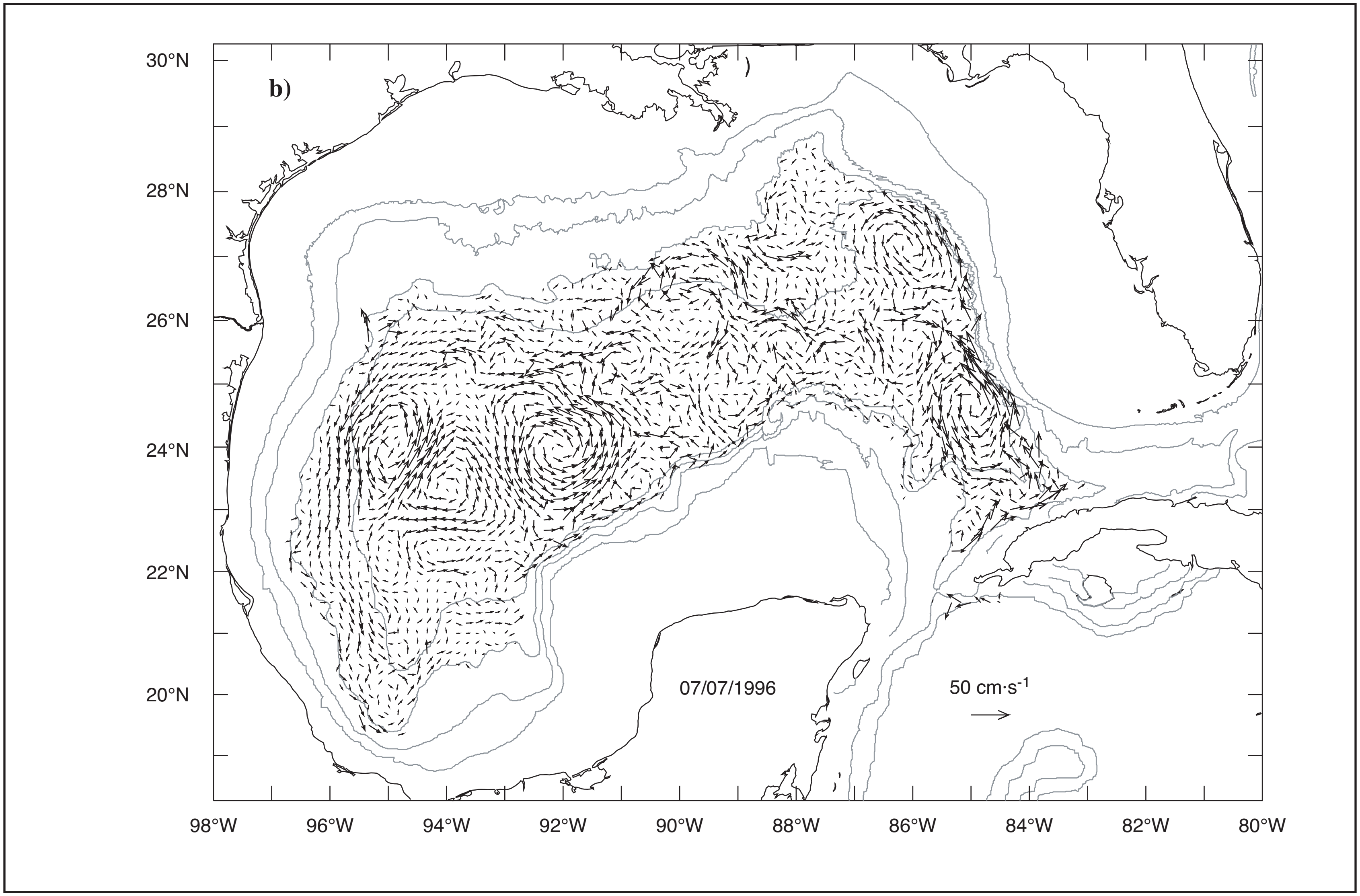

Figure 8.2-6. CUPOM hindcast currents at 2000 m for selected model dates in 1996. (continued)

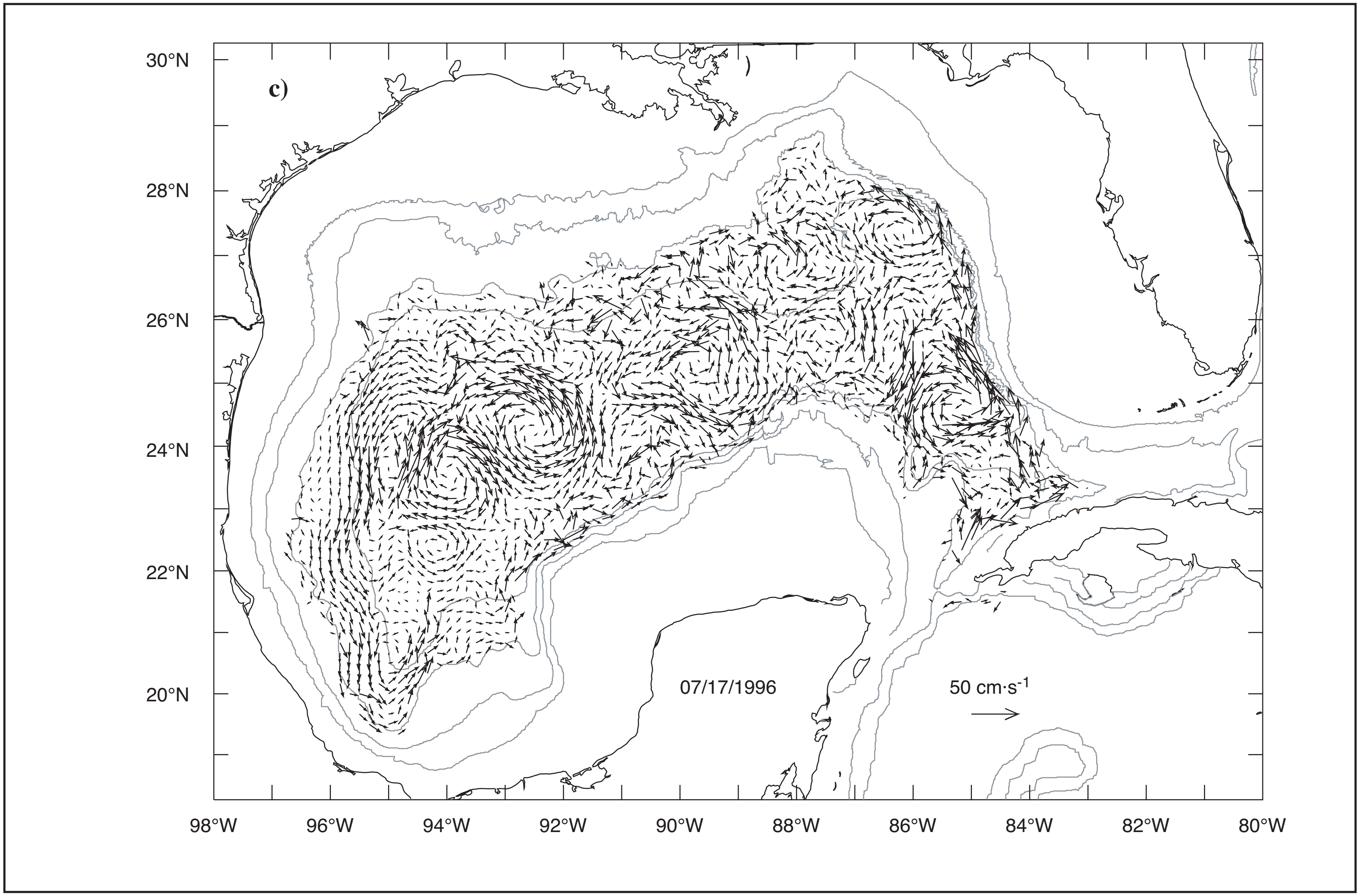

Figure 8.2-6. CUPOM hindcast currents at 2000 m for selected model dates in 1996. (continued)

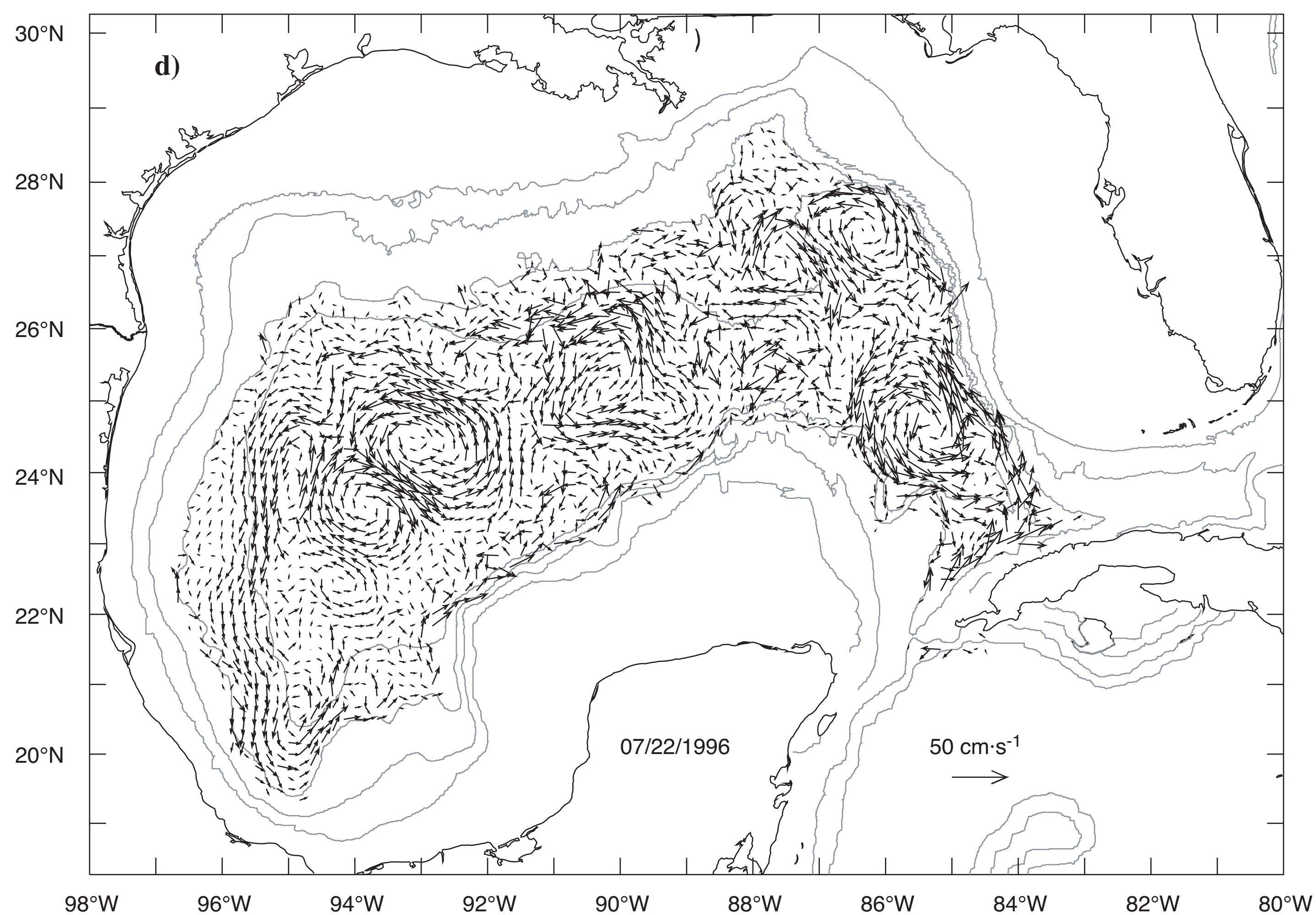

Figure 8.2-6. CUPOM hindcast currents at 2000 m for selected model dates in 1996. (continued)

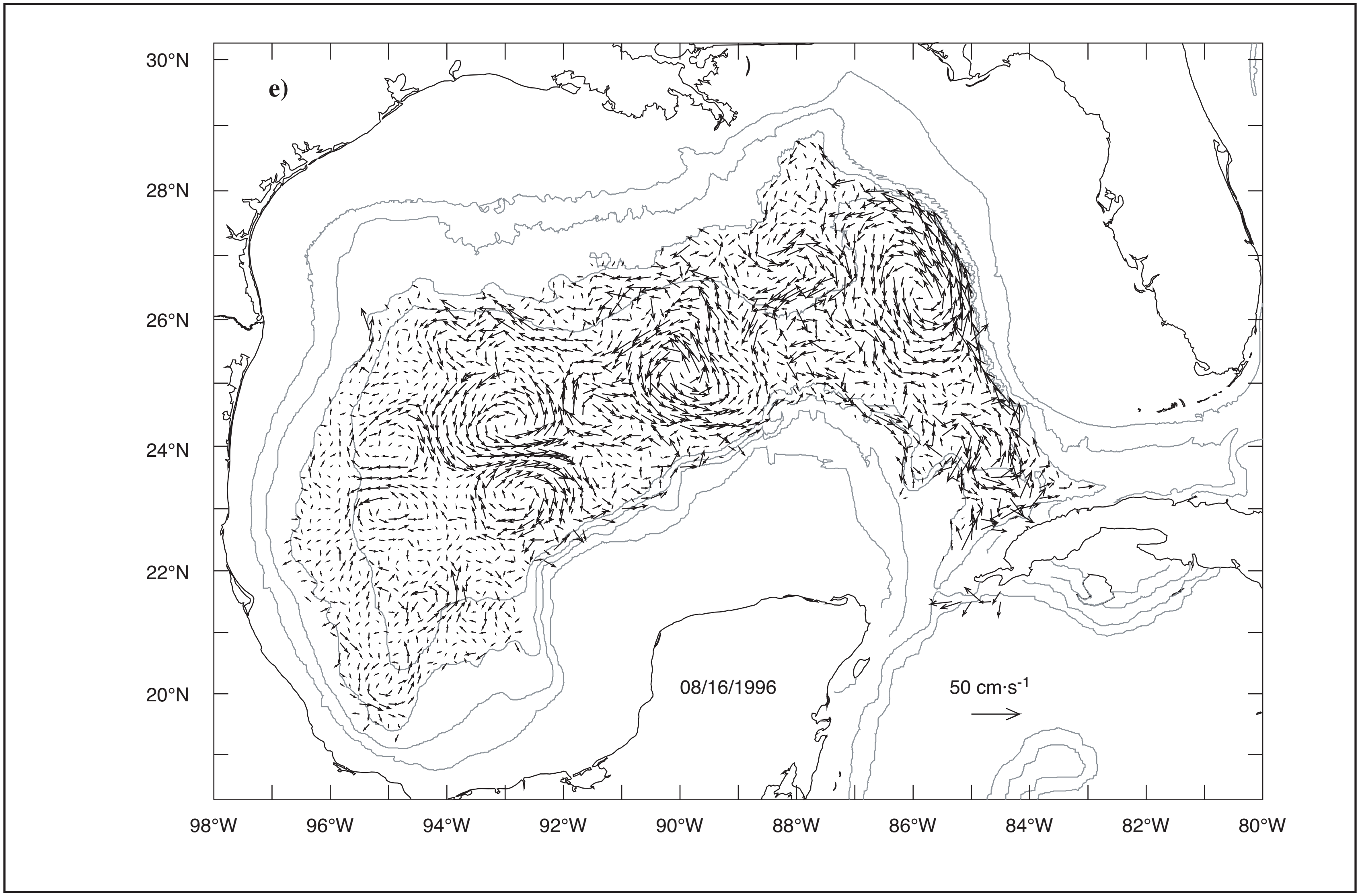

Figure 8.2-6. CUPOM hindcast currents at 2000 m for selected model dates in 1996. (continued)

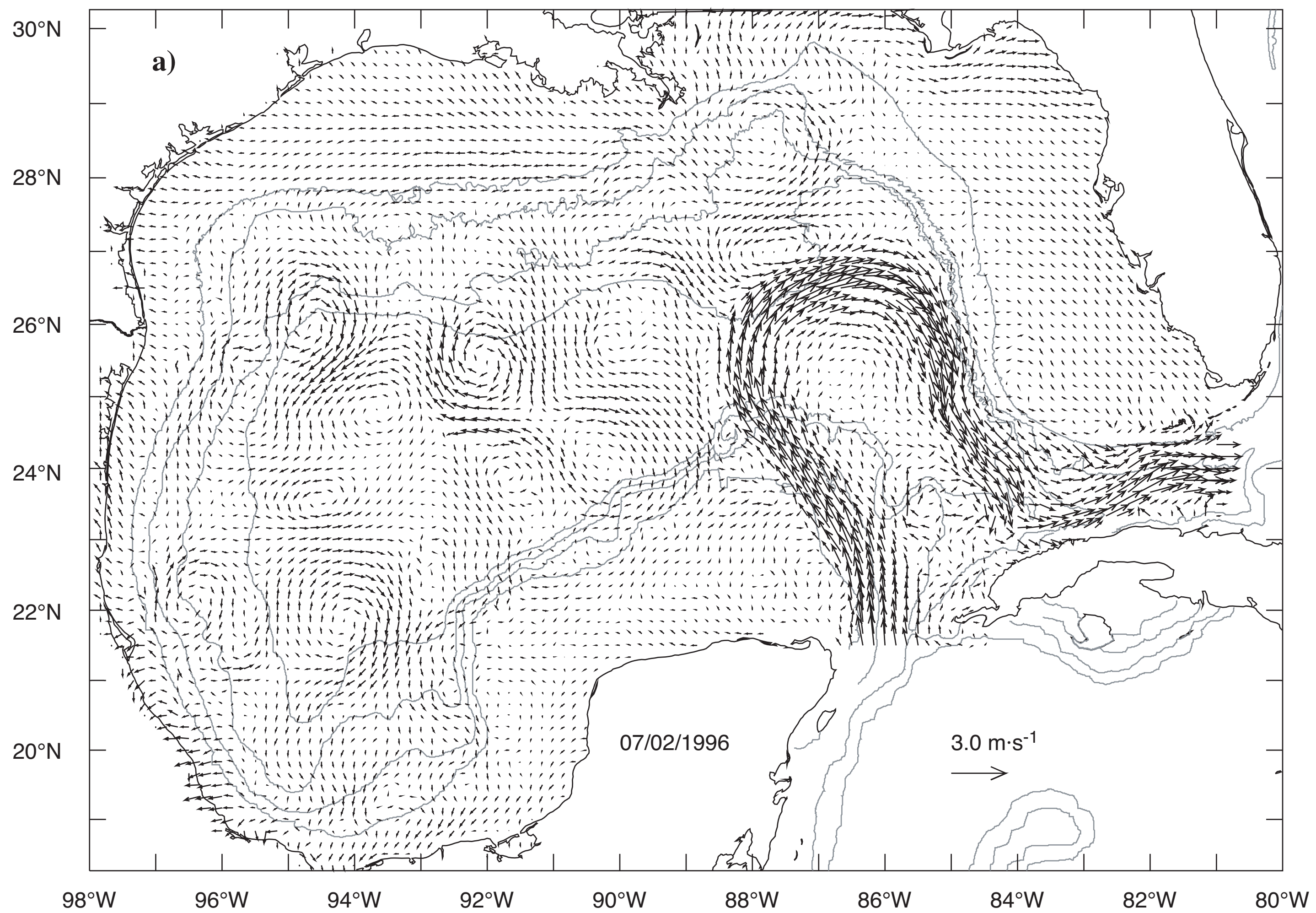

Figure 8.2-7. CUPOM hindcast surface currents for selected model dates in 1996. Shown are a) 2 July 1996 and b) 17 July 1996.

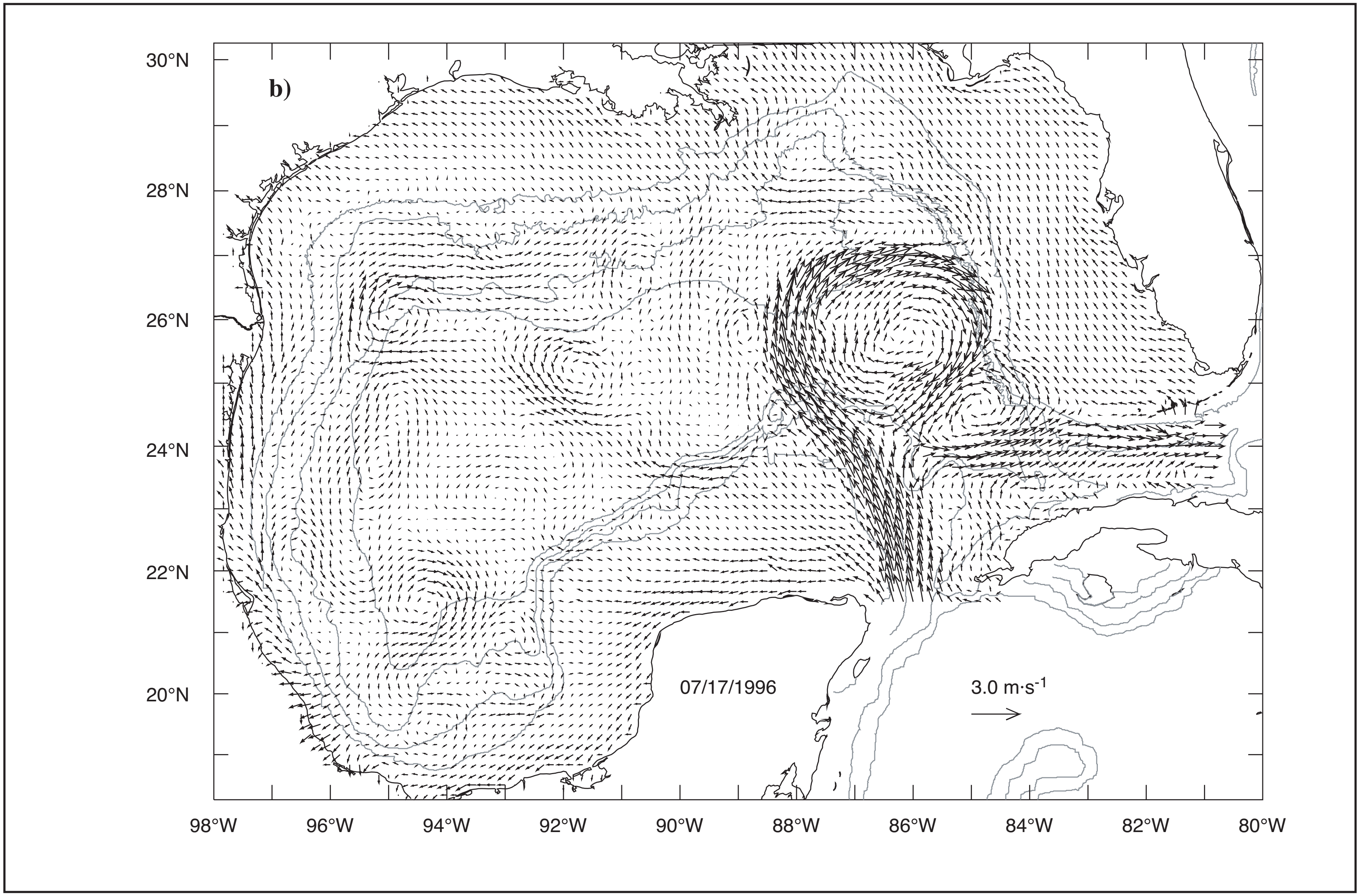

Figure 8.2-7. CUPOM hindcast surface currents for selected model dates in 1996. (continued)

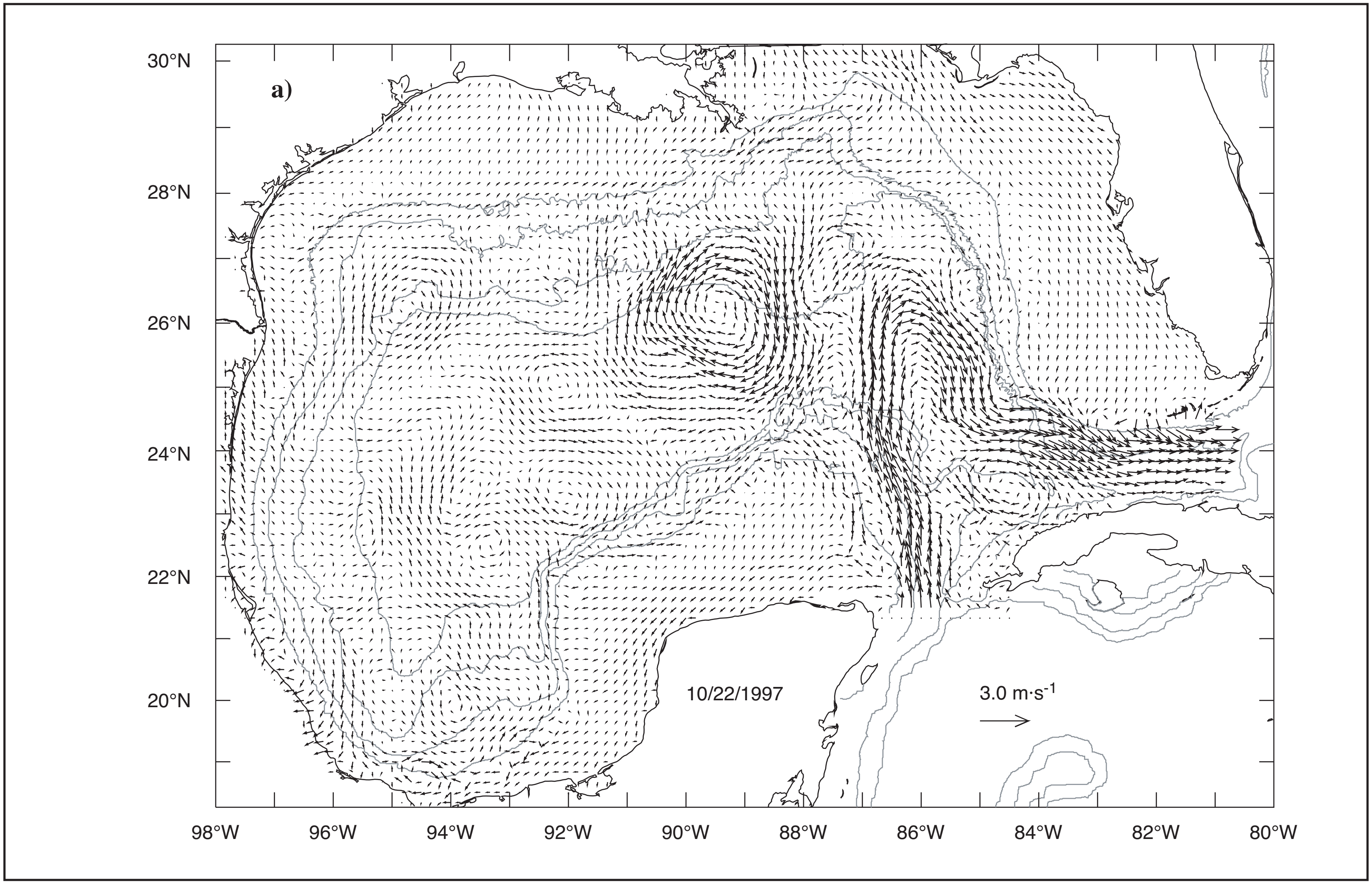

Figure 8.2-8. CUPOM hindcast surface currents for selected model dates in 1997-1998. Shown are a) 22 October 1997, b) 9 December 1997, c) 10 January 1998, d) 11 February 1998, and e) 23 February 1998.

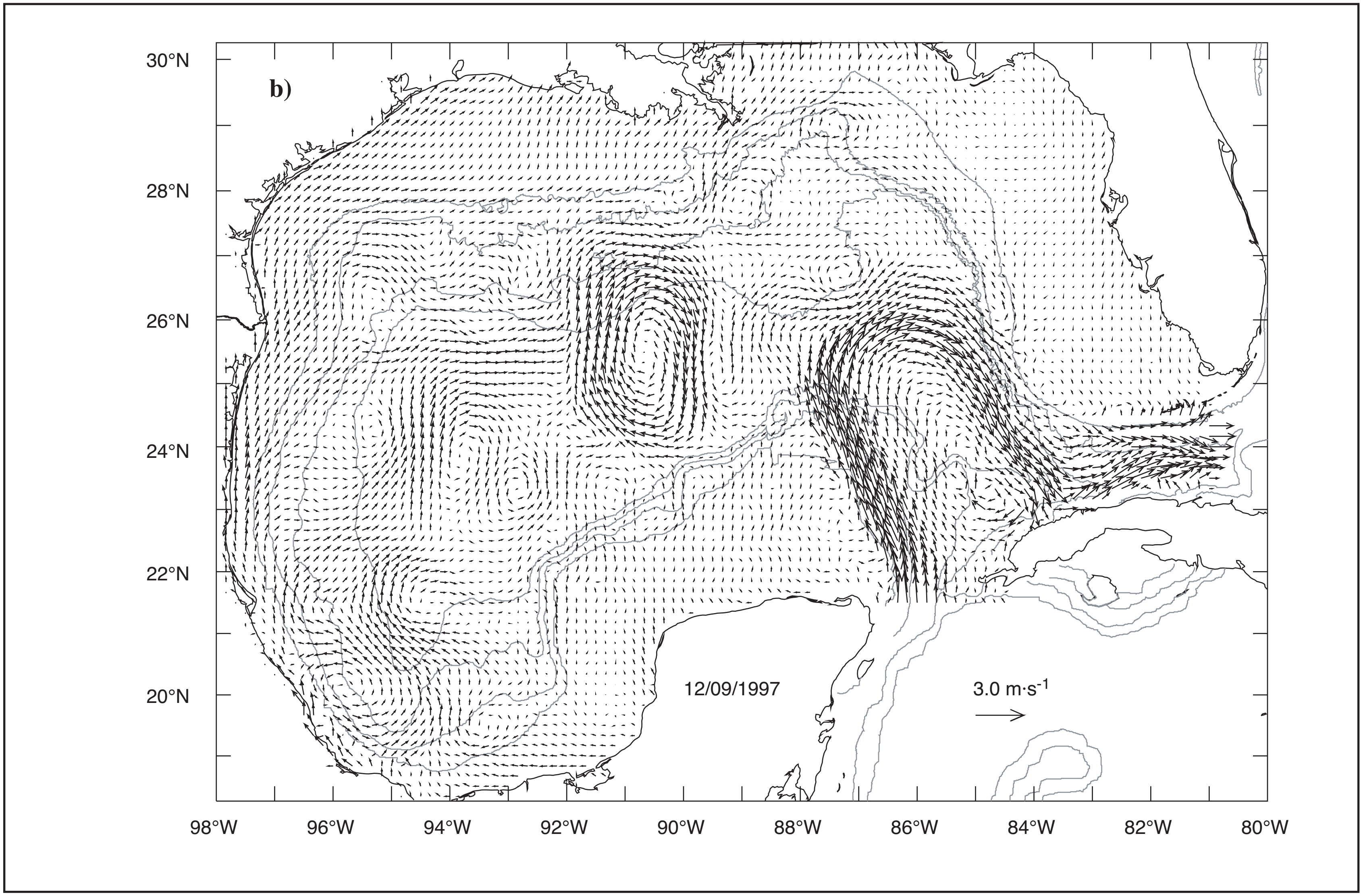

Figure 8.2-8. CUPOM hindcast surface currents for selected model dates in 1997-1998. (continued)

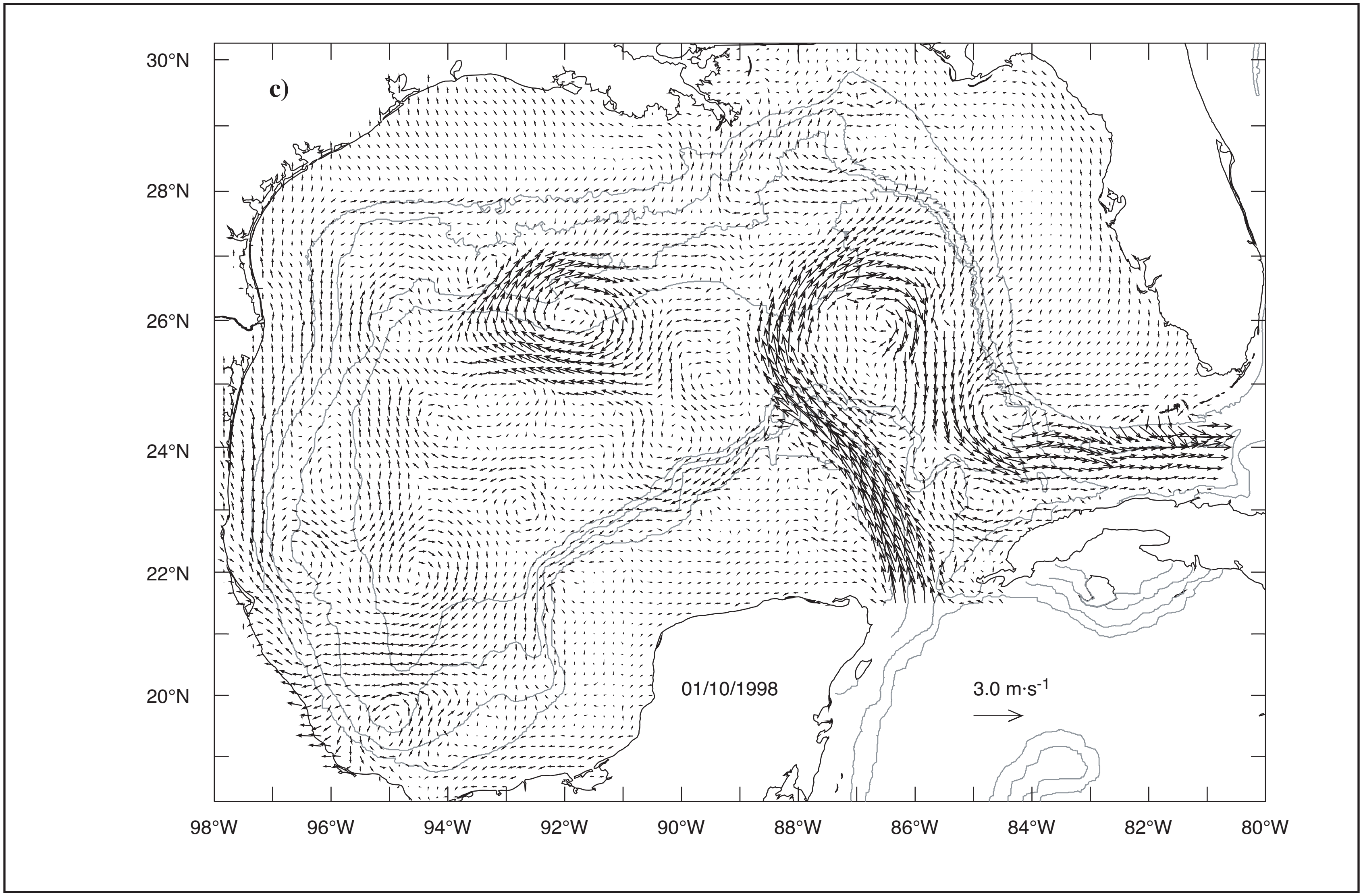

Figure 8.2-8. CUPOM hindcast surface currents for selected model dates in 1997-1998. (continued)

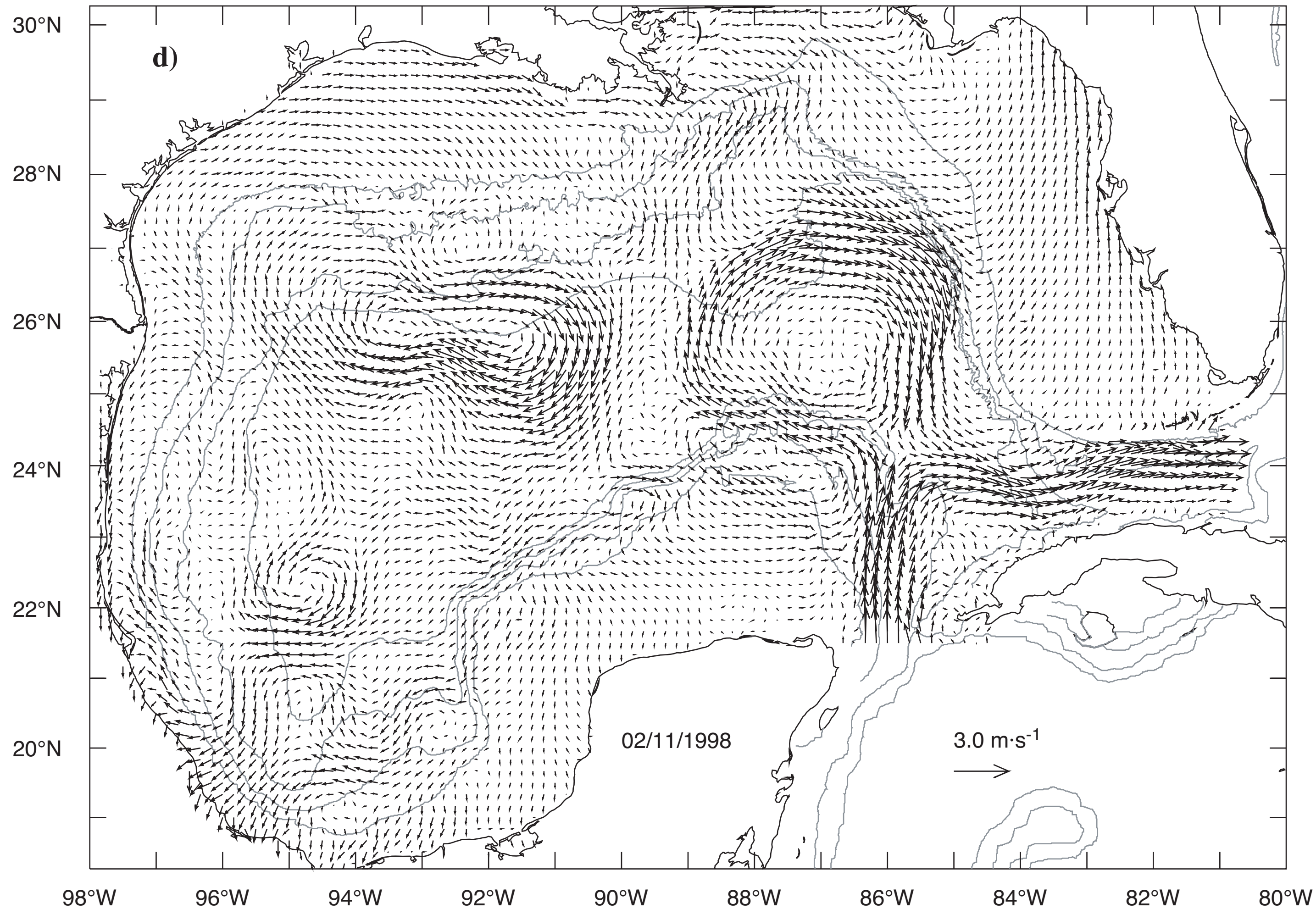

Figure 8.2-8. CUPOM hindcast surface currents for selected model dates in 1997-1998. (continued)

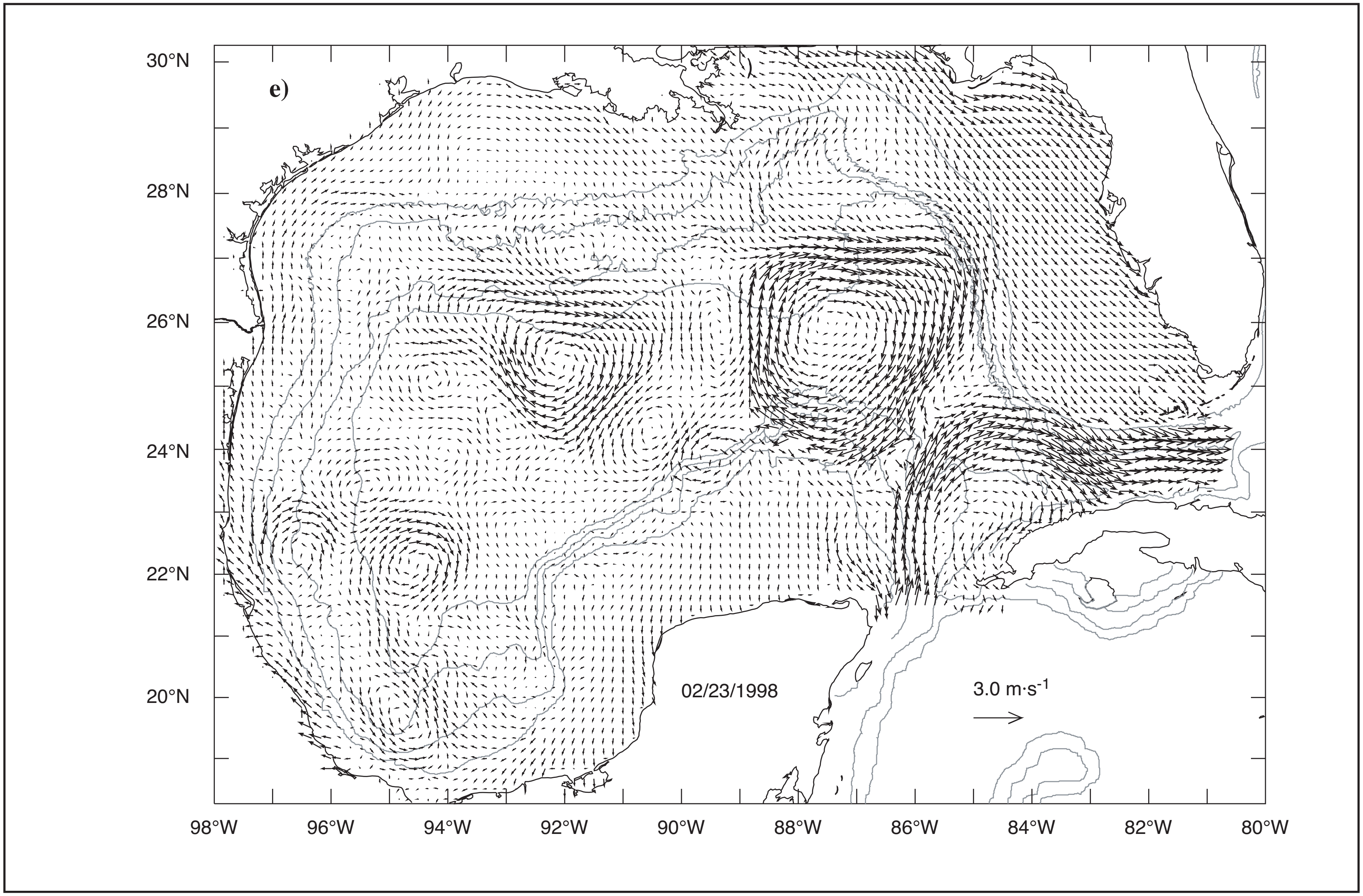

Figure 8.2-8. CUPOM hindcast surface currents for selected model dates in 1997-1998. (continued)

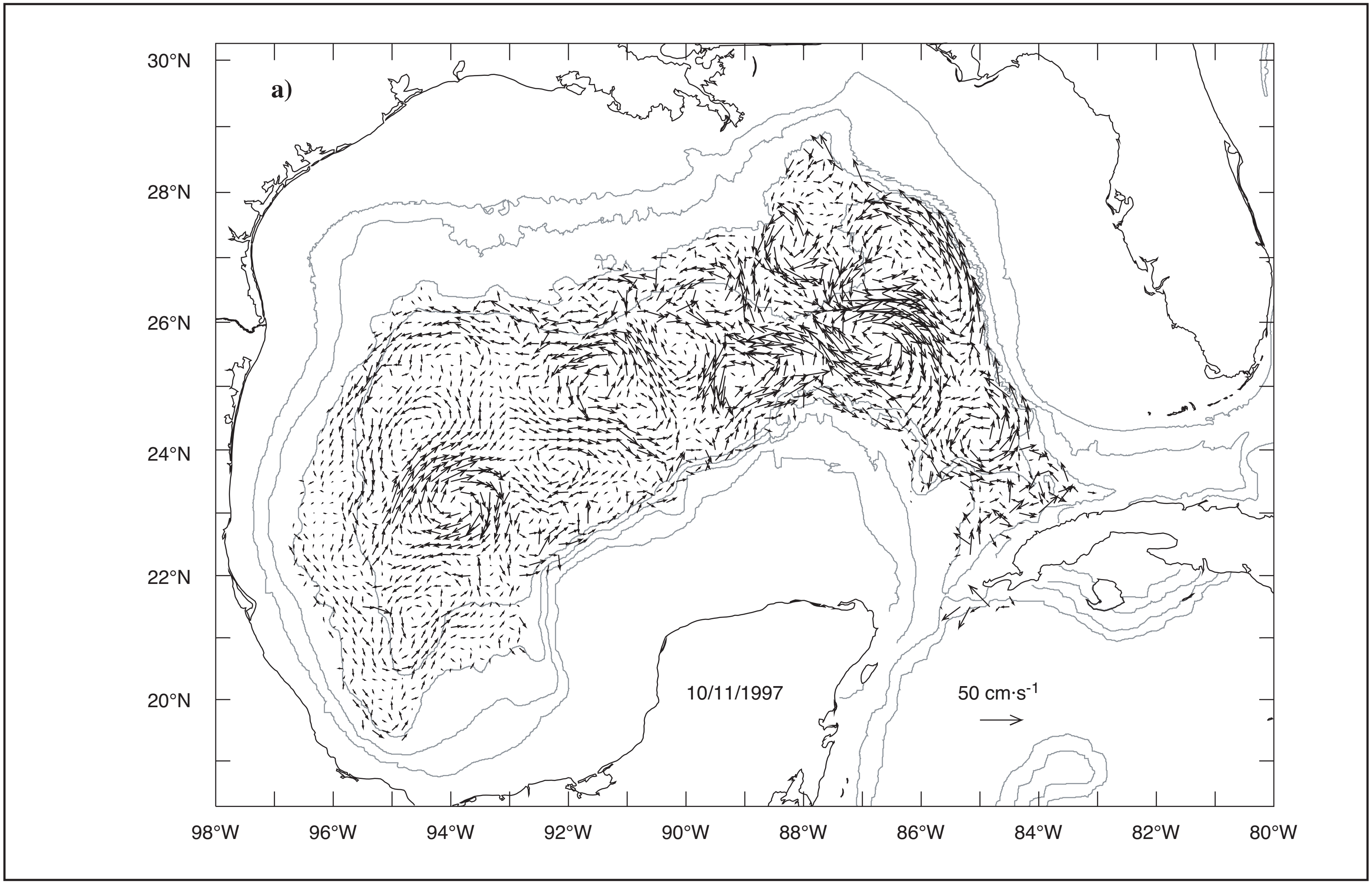

Figure 8.2-9. CUPOM hindcast currents at 2000 m for selected model dates in 1997-1998. Shown are a) 11 October 1997, b) 25 October 1997, c) 15 November 1997, d) 16 December 1997, e) 1 January 1998, and f) 10 January 1998.

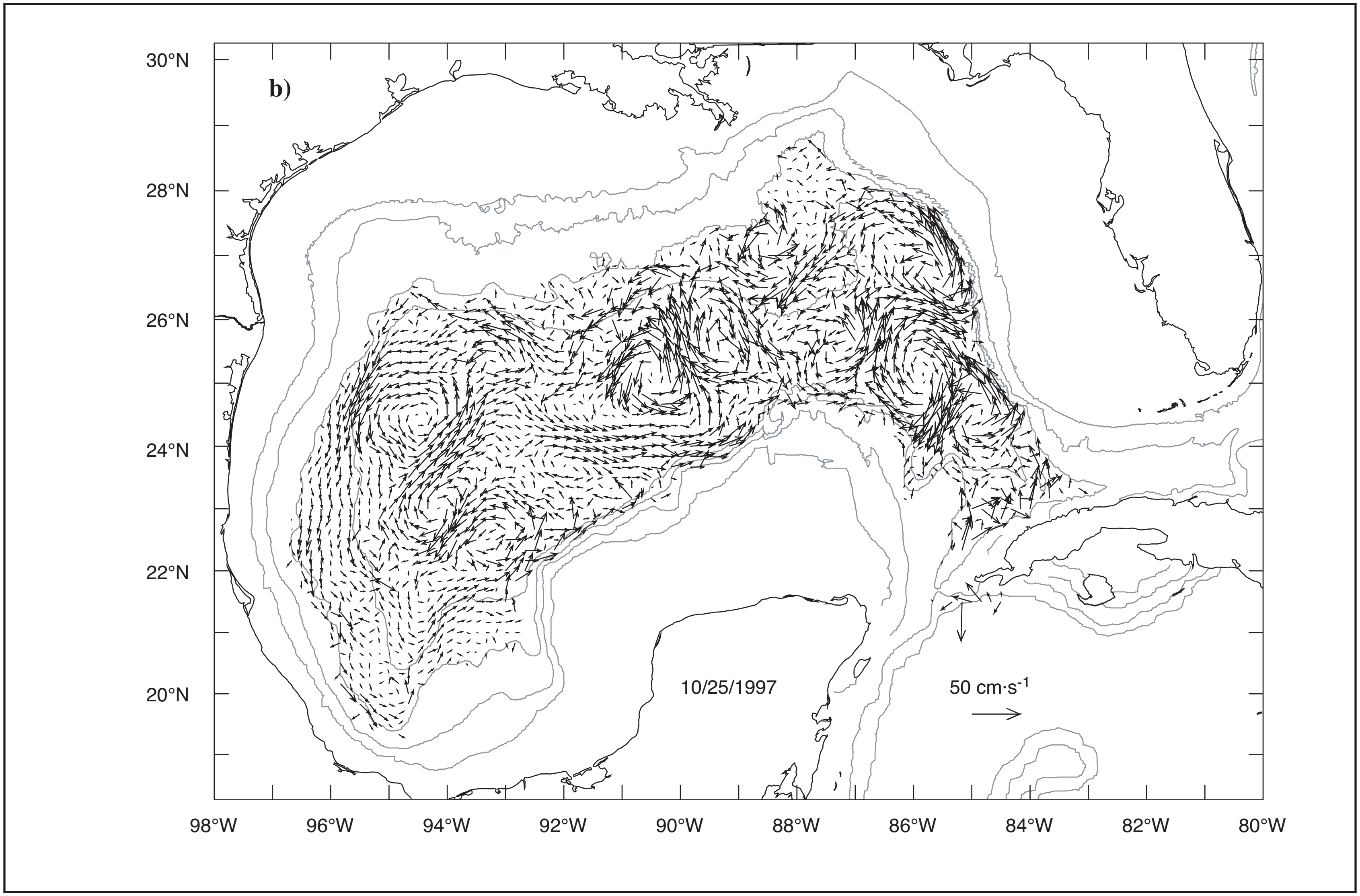

Figure 8.2-9. CUPOM hindcast currents at 2000 m for selected model dates in 1997-1998. (continued)

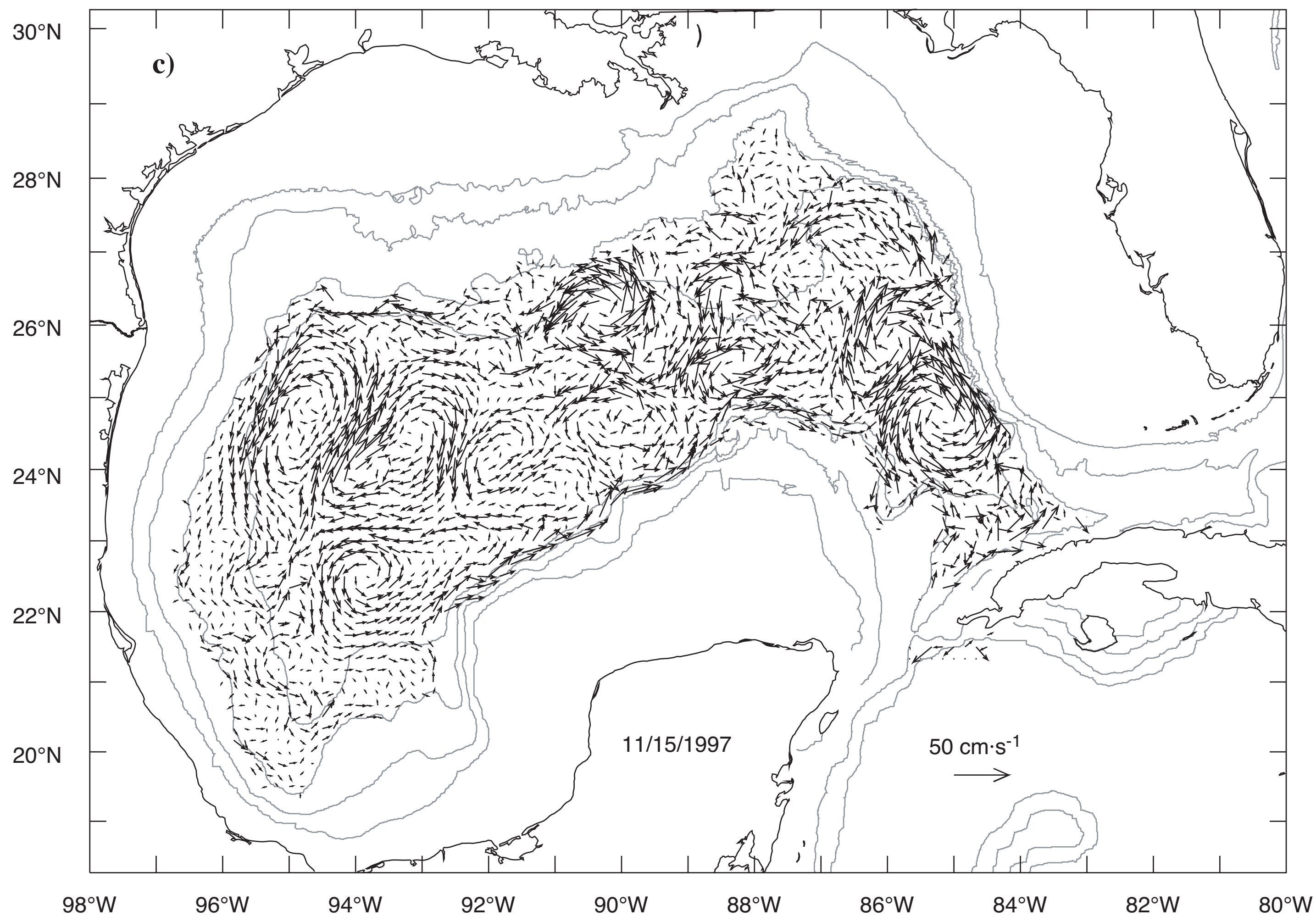

Figure 8.2-9. CUPOM hindcast currents at 2000 m for selected model dates in 1997-1998. (continued)

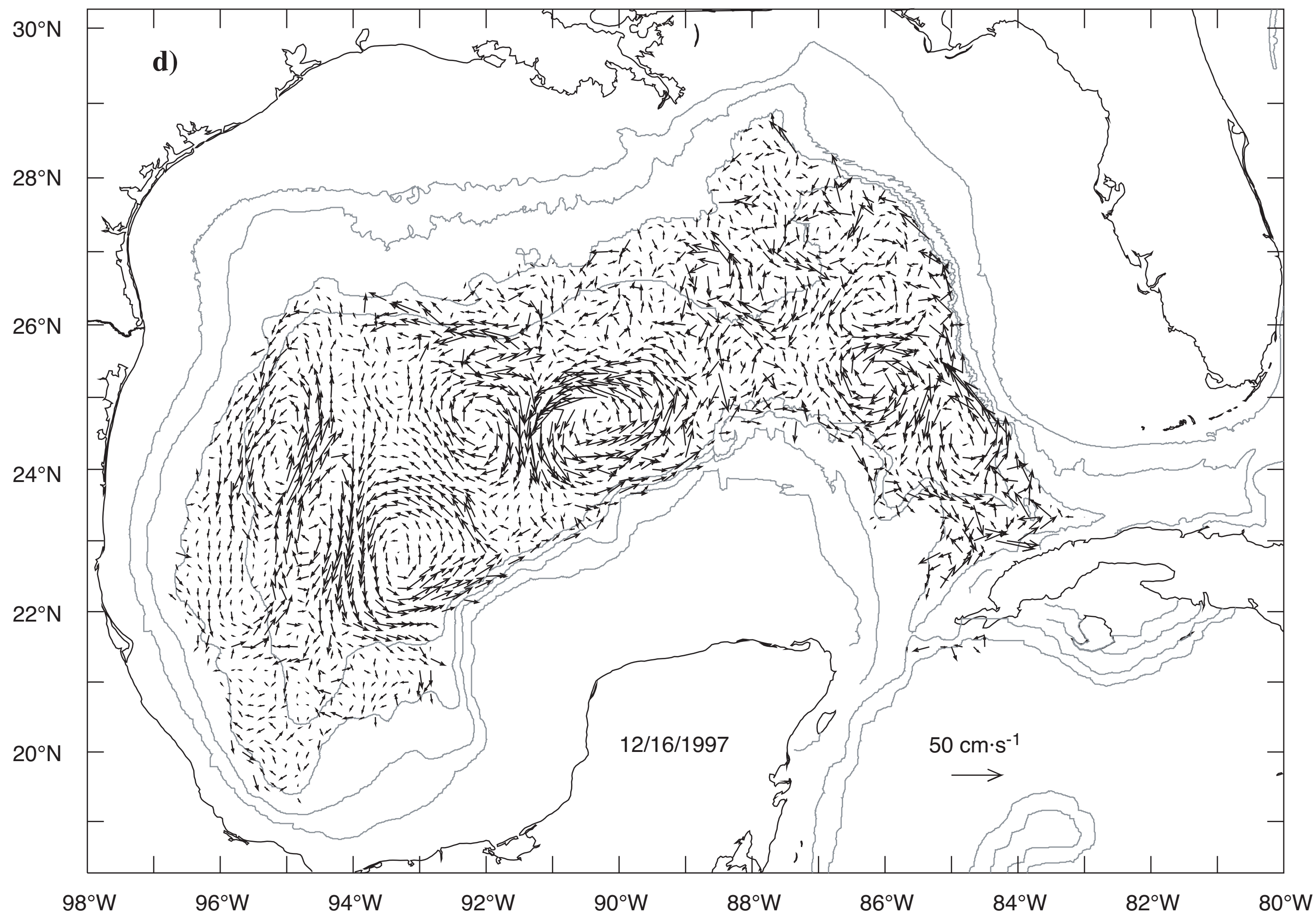

Figure 8.2-9. CUPOM hindcast currents at 2000 m for selected model dates in 1997-1998. (continued)

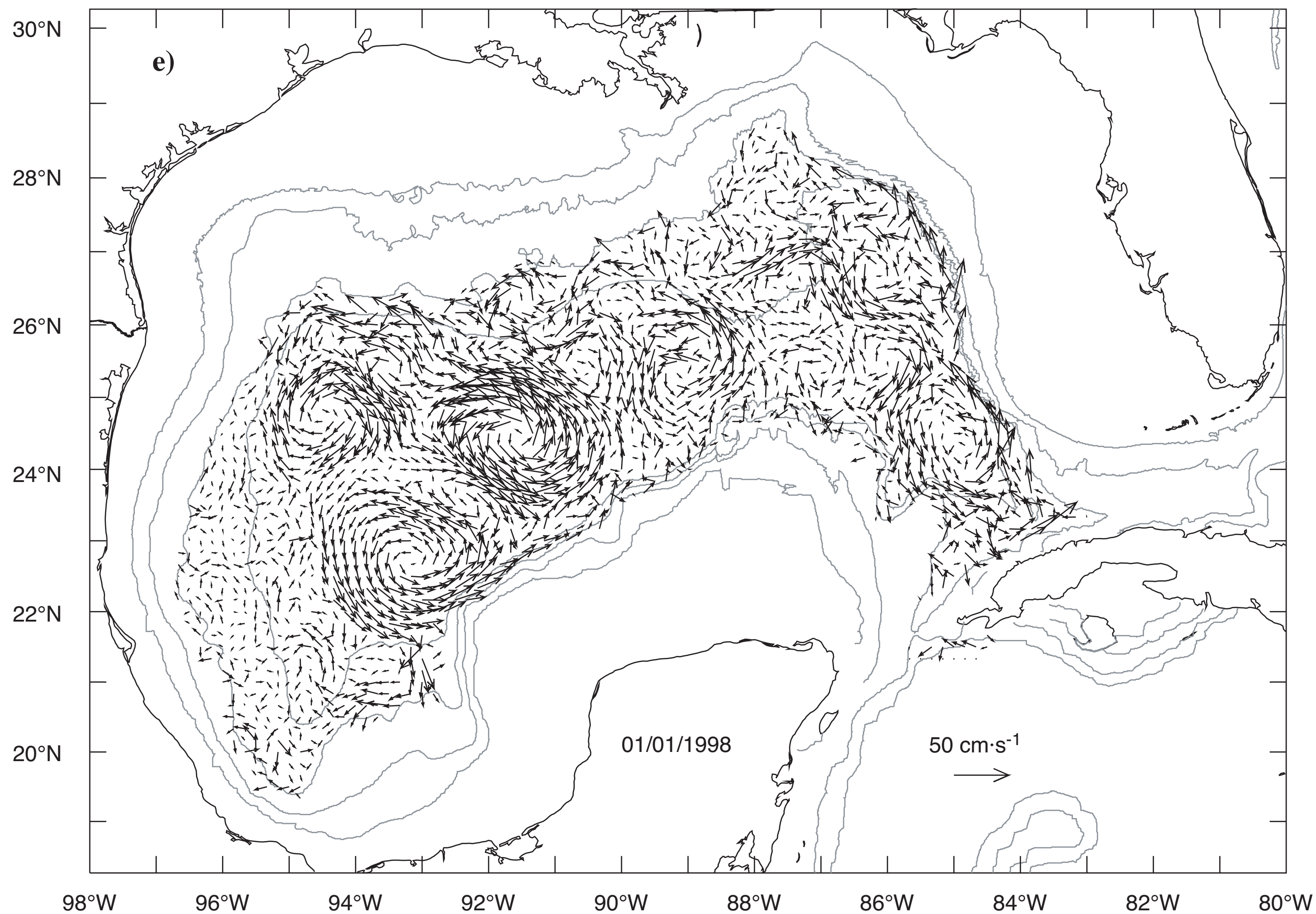

Figure 8.2-9. CUPOM hindcast currents at 2000 m for selected model dates in 1997-1998. (continued)

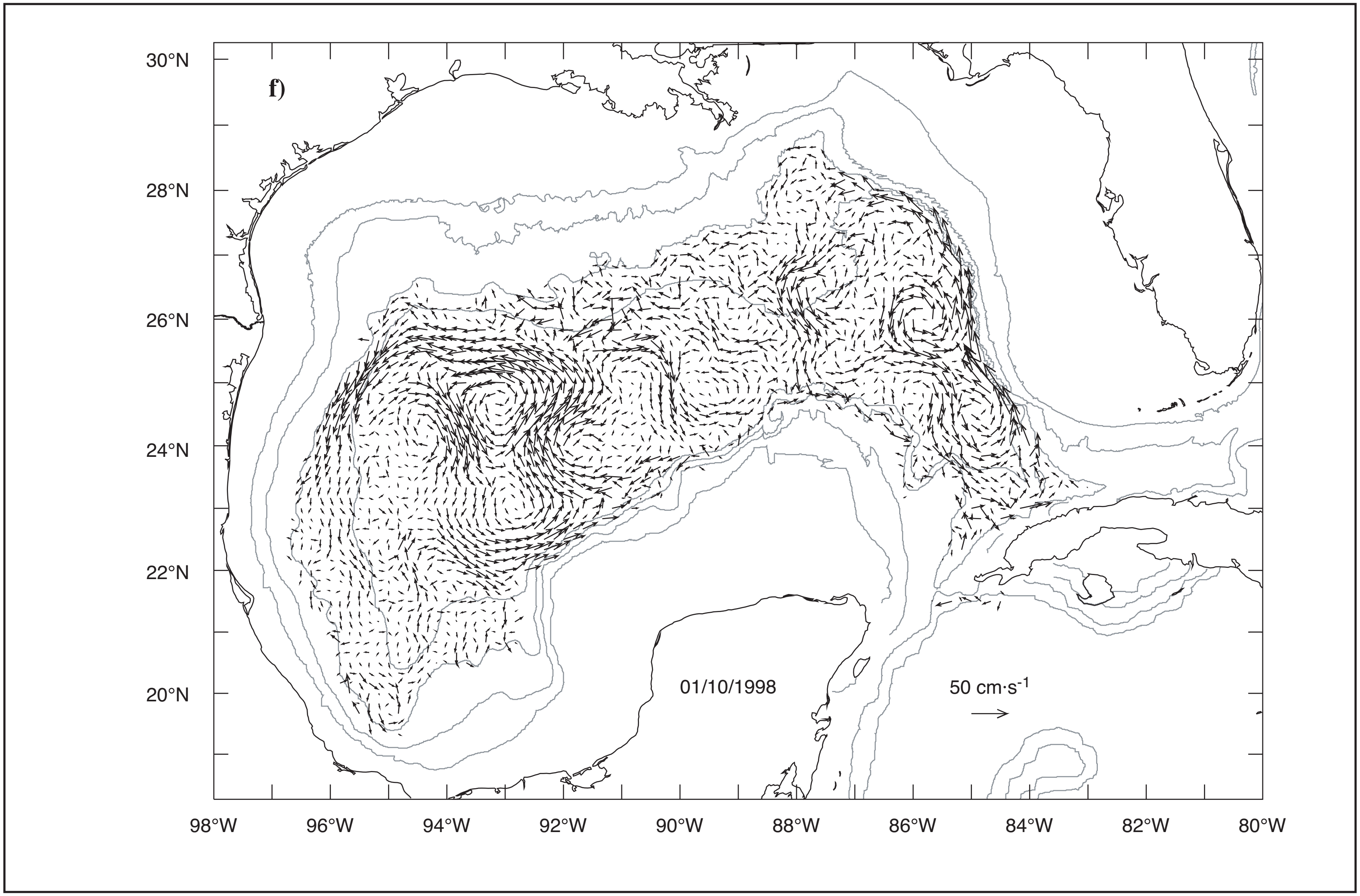

Figure 8.2-9. CUPOM hindcast currents at 2000 m for selected model dates in 1997-1998. (continued)

November (Figure 8.2-9c). During that period, another cyclone spun up east of and in association with the cyclone-anticyclone pair seen centered near 25°N, 90°W on 25 October. The new cyclone strengthened, while the pair moved northwestward and dissipated over the slope regime. In Figure 8.2-9c the new cyclone is centered near 26°N, 90.5°W. During the next month, this new cyclone also moved northwestward and dissipated over the slope near 92-94°W. At the same time a new cyclone-anticyclone pair was formed and is seen centered near 24.5°N, 91°W in the 2000-m current field for 16 December (Figure 8.2-9d). The deep ring triad was still seen in the western Gulf, where the southeastern cyclone seems much the stronger of the three. By 1 January 1998 (Figure 8.2-9e) the new ring pair in the central Gulf had transformed essentially into a strong cyclone centered about 24°N, 91.5. The triad in the west had transformed by the disappearance of the western cyclone, strengthening of the anticyclone and clockwise rotation of remaining pair. The result was a triad of three relatively strong deep rings centered about 24°N, 93°W in Figure 8.2-9e. These three major deep rings continued to move and by 10 January 1998 are in the process of coalescence (Figure 8.2-9f), resulting in a general cyclonic flow around the deep western Gulf.

Hydrographic observations together with limited long, deep current observations give some evidence for mean cyclonic circulation beneath 800 m in the Gulf basin. Circulation models are the main source of evidence for such circulation. As an example, see Figure 5.3-7 based on CUPOM output. Strong collaborative evidence is lacking.

There is, on the other hand, proof of mega-furrows seaward of the Sigsbee Escarpment (see Sections 4 and 6.1.3) and of strong currents in and above those furrows as observed on recent submersible dives (William Bryant, personal communication 2000). Moreover, the CUPOM model shows that the near bottom mean currents (Figure 5.3-9) are intensified near the base of the escarpment and that the principal variability is oriented along the isobaths, as essentially are the furrows, though they move down slope slightly to the west. Some measurements have been made within and between the furrows using an ADCP mounted on ALVIN. Current components measured within a furrow near Green Knoll gave components slightly greater than 10 $cm \cdot s^{-1}$ with an orientation along the furrow to the southwest. Analysis of ADCP backscatter intensity data shows pronounced increase in the backscatter acoustic signal as one approaches and enters a furrow. It is inferred that a moderate (~25 $cm \cdot s^{-1}$) is needed to sustain the sediment loading. However, the process responsible for these furrows is not known.

All of the priority phenomena need further study via measurements because of their potential importance coupled with poor knowledge of their statistics and causal mechanisms. The topographic Rossby waves and deep eddies have time scales of 10 to 100 days, and spatial scales of hundreds of kilometers. All are quasi-geostrophic phenomena, with the possible exception of flow in furrows. Desired are observational systems for quantifying the spatial structure and time evolution associated with these priority events. The detection of flow associated with TRWs and with deep anticyclonic-cyclonic eddy pairs clearly requires a moored array for monitoring of currents. The topic of flow in furrows while representing a sea bed problem requires information about flow within the deep water column for complete understanding of the phenomenon. Hence a moored array, if appropriately located, could serve two purposes. On the other hand, knowledge of deep circulation of the Gulf is more easily obtained via continual release of deep-water floats that can cover the deep Gulf as a whole. Since each of the three priority phenomena has certain distinct requirements for its measurement, these are considered separately in Section 8.3 dealing with measurement systems.

8.3 Measurement Systems

8.3.1 A North-Central Gulf Array for Mesoscale Motions

The CUPOM hindcast results for 1993-1999 show significant current variability in the deep water over the north-central slope region in the form of cyclonic and anticyclonic eddies (Figure 8.2-2) as well as waves in the deep circulation. Existing current measurements over this region, especially the recent MMS-sponsored Eddy Intrusion Study extension mooring data in 2000-m water depth near 90˚W, confirm that significant bottom-trapped energy exists based on EOF analyses of these data (see Section 7.1.6). Figure 5.3-9 shows variance ellipses and record-length mean currents near the sea bed in the north-central Gulf based on the CUPOM output. As discussed by Hamilton (1984, 1990), the variability ellipses on the slope and rise provide an index for possible TRW activity, particularly for those regions where the major axes are aligned along the isobaths. In this figure a potential corridor of TRW propagation is apparent in the narrow swath of elongated ellipses passing near 90˚W and 27˚N and southwestwards to near 92˚W and 25.5˚N. This corridor lies essentially between the 2000- and 3000-m isobaths, passing along a portion of the Sigsbee Escarpment. It is a possible location for a current measurement array to detect TRWs and associated deep eddies.

To determine propagation characteristics, several moorings oriented along-isobath are needed from which the phase lags as well as the energy of the coherent parts of the frequency cross-spectra can be evaluated for the 10- to 100-d period bands. In addition, the cross-slope pattern of TRW events requires cross-shelf arrays of moorings at one or more locations along the slope. A recommended array that could capture and quantify the energetics and propagation characteristics of bottom-trapped signals is shown in Figure 8.3.1-1. It consists of nine current measurement moorings. The distances between the moorings should be consistent with those scales that allow significant coherence between the current signals at all mooring pairs. We have estimated transverse and longitudinal decorrelation scales for along- and across-isobath separations using the results from the CUPOM hindcasts. The results given in Table 8.3.1-1 indicate that the total along-isobath mooring separation ought to be no more than 160 km to have coherent along-isobath currents, but less than 50 km for coherent cross-isobath currents, in depths of about 2000 m. The total separation of the cross-isobath moorings ought to be no more than 50 km in order to have coherent signals for either current component for comparable depths. The array shown in Figure 8.3.1-1 will allow estimation of phase changes for coherent signals in the along-slope current between moorings 80 and 160 km apart along the slope. It also will allow coherent cross-slope patterns for both current components at each of the three cross-slope sections. The array has some deliberate redundancy in terms of cross-shelf pattern detection and along shelf phase changes for two reasons. One is to minimize the expected problem of data gaps caused by instrument malfunction. The other is to enhance the statistical robustness of estimated patterns and phase change for periods when data gaps are minimal.

Although for the detection of TRW signals, single-point and/or acoustic Doppler current meters in the lowest 1000 m of water column might be sufficient, the inclusion of current measurements throughout the water column will allow the monitoring of energetic near-surface signals as well. This may enable a better analysis of the relationship between energetic near-surface currents and deep motions. Moreover, measurements over the whole water column will allow a quantitative decomposition of the signals into distinct vertical modes. One option is to employ EOF modes as in Section 7.1.6, using single value decomposition methodology for determination of both modal profiles and time sequences of

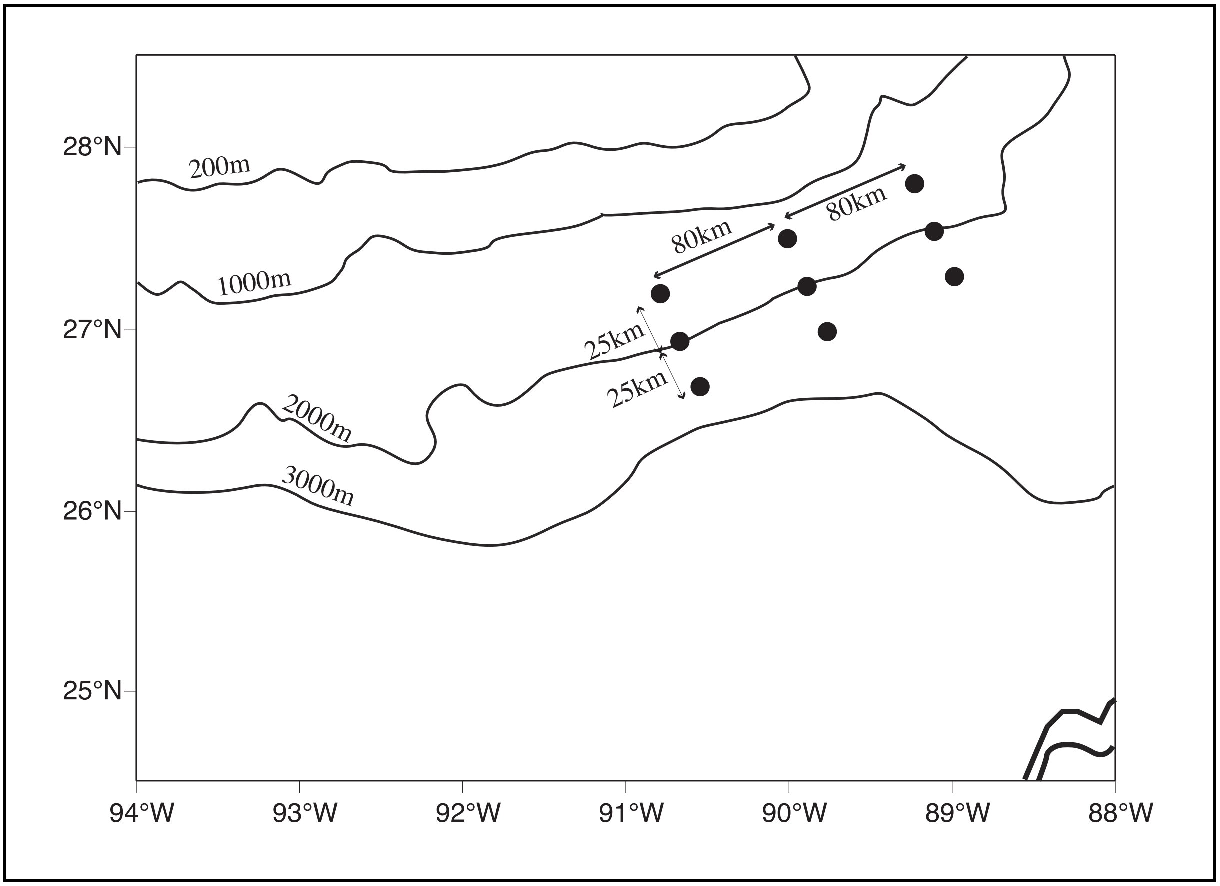

Figure 8.3.1-1. Proposed north-central Gulf array for deep mesoscale motions.

the amplitudes of current vectors. Another option is to employ dynamic mode profiles over a sloping seabed using the methodology of Charney and Flierl (1981). The TRW signals are those associated with true bottom-trapped modes, whose vertical profile is approximately exponential with maximum value at the bottom. They are the generalization over a slope of the uniform flat-bottom barotropic mode. The decomposition into bottom-trapped and surface-trapped modes requires measurements with reasonable resolution through the entire water column.

The CUPOM output is useful in testing the detection ability of a design array, assuming that the model is reasonably accurate in its simulation of certain statistics of the current structure. An important measure of the model skill is its capability of reproducing the observed relative distribution of variance of dynamic modes over the slope. Thus, as a test of CUPOM, we carried out a dynamic mode decomposition of the 1993-1998 hindcasts of currents for a grid location near 90˚W in water depth of about 2000 m and slope of about 1/100. The stability profile employed was an average for the Gulf of Mexico shown in Arango and Reid (1991, figure 4) and based on climatological data in Levitus (1982). The modal profiles for the bottom-trapped (mode 0) and the first three baroclinic modes are shown in Figure 8.3.1-2. The variances of each of these modes and the residual are given in Table 8.3.1-2 as a percent

Table 8.3.1-1. Spatial scale analyses from model output. We estimated longitudinal (C_L) and transverse (C_T) decorrelation scales using CUPOM output along- and cross-isobaths in the region near Green Knoll. Estimated spatial scales are small.

Cross-Isobath Separations		
C_L	Surface layers	~ 200 km
	200 m	~ 100 km
	1000 m	~ 50 km
C_T	All depths	~ 50 km

Along-Isobath Separations						
			Depths			
Isobath	**Surface**	**50 m**	**200 m**	**500 m**	**1000 m**	**2000 m**
			C_L (km)			
500 m	75	35	25	75	—	—
1000 m	100	75	60	20	10	—
2000 m	60	60	30	70	100	160
			C_T (km)			
500 m	50	25	15	15	—	—
1000 m	60	35	20	10	15	—
2000 m	30	25	15	15	10	25

of the total. We also carried out a dynamic mode decomposition of data from the MMS-sponsored SAIC EIS extension mooring I1, whose location during the 1999-2000 measurement period was almost the same. The percent distribution by dynamic mode also is shown in Table 8.3.1-2. The chi-square test of the two distributions gives a value close to the median value of chi-square using 5 degrees of freedom, so there is definitely no significant difference. This and other model skill assessments provide some confidence in use of CUPOM hindcasts in tests of the array design.

Using CUPOM hindcasts as a surrogate for measured data we have tested a hypothetical array even more redundant than the array design (Figure 8.3.1-1) recommended here. These tests included single value decomposition determination of time sequences of bottom-trapped current amplitude for nine simulated moorings along the 2000-m isobath at distances of 10, 30, 80, and 160 km east and west of a central mooring near 90˚W. Cross-spectra of the bottom trapped modes from each mooring with the central mooring were calculated from these time sequences to estimate coherence, phase, gain, and energy versus frequency. It was found that reasonable estimates of phase change for the along-slope current were determined for moorings at 80 km east and west of the central mooring. It was also found that cross-slope arrays of three moorings with total separation of 50 km gave coherent patterns of the along- and cross-slope current components in the 10- to 100-d period band. Based on the information derived from these cross-spectra, the spatial scale, energy and propagation rates can be determined for bottom-trapped TRWs. Similar information for isolated eddy events

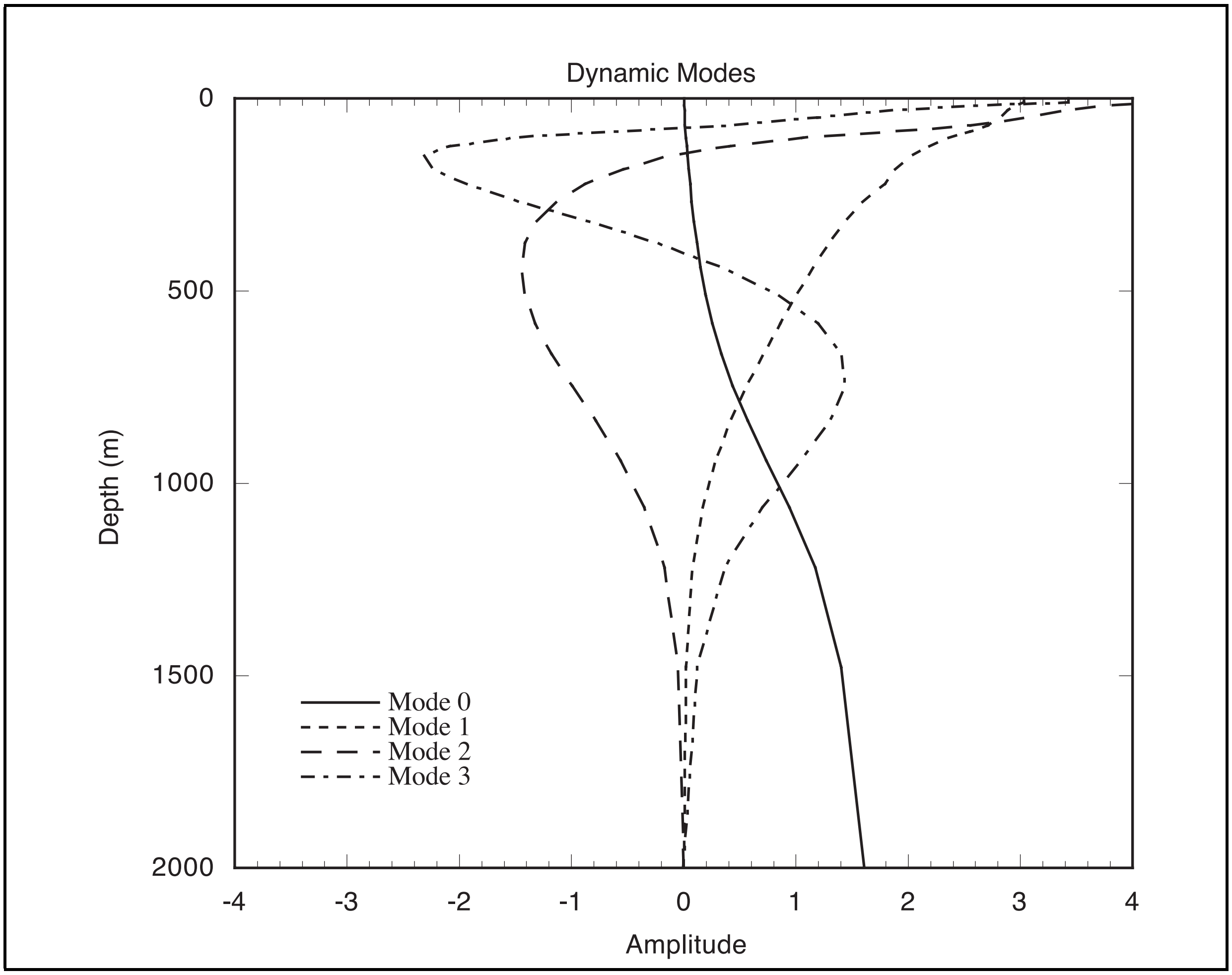

Figure 8.3.1-2. Dynamic modes for currents over a sea bed having slope of 1/100 in water depth of 2000 m for eddies of scale 100 km as determined by the method of Charney and Flierl (1981).

Table 8.3.1-2. Relative variances of dynamic modes based on CUPOM current hindcasts for 1993-1998 at 90°W in water depth of 2000 m, using the method of Charney and Flierl (1981). Comparison is made to the relative variances of dynamic modes based on data from the MMS-sponsored EIS extension mooring I1 near the same location. All variances are expressed as percents of the total variance.

Dynamic Mode	0	1	2	3	4	Residual
CUPOM 1993-98	23.4	61.3	6.9	3.0	1.4	4.0
MMS mooring I1	18.7	70.7	4.6	1.4	1.0	3.6

over the abyssal plain can be determined from analyses of current vectors on the spatial arrays shown in Figure 8.3.1-1.

Using CUPOM hindcasts as a surrogate for measured data we have tested a hypothetical array even more redundant than the array design (Figure 8.3.1-1) recommended here. These tests included single value decomposition determination of time sequences of bottom-trapped current amplitude for nine simulated moorings along the 2000-m isobath at distances of 10, 30, 80, and 160 km east and west of a central mooring near 90˚W. Cross-spectra of the bottom trapped modes from each mooring with the central mooring were calculated from these time sequences to estimate coherence, phase, gain, and energy versus frequency. It was found that reasonable estimates of phase change for the along-slope current were determined for moorings at 80 km east and west of the central mooring. It was also found that cross-slope arrays of three moorings with total separation of 50 km gave coherent patterns of the along- and cross-slope current components in the 10- to 100-d period band. Based on the information derived from these cross-spectra, the spatial scale, energy and propagation rates can be determined for bottom-trapped TRWs. Similar information for isolated eddy events over the abyssal plain can be determined from analyses of current vectors on the spatial arrays shown in Figure 8.3.1-1.

A north-central Gulf array would be most useful in obtaining added characterization of both surface and bottom-trapped current if kept in place for one or more years. This is based on the knowledge that considerable interannual variability exists in surface LCE fields as inferred from the satellite-derived SSH, and from the hindcasts from CUPOM of the deep-water energetics. This is also confirmed by the recent current measurements at the MMS-funded mooring I1 in 2000-m depth just east of 90˚W longitude.

While the proposed array is intended mainly to gather much needed information on low-frequency motions throughout the water column, it could also be used to study upward and downward propagating near-inertial motions as in Hamilton (1984). Near-inertial waves tend to propagate with a very slight angle to the horizontal. A multi-mooring array as in Figure 8.3.1-1 would provide the means to detect wave groups at a given mooring that originated earlier in time and at a different level from one of the other moorings. It might also provide added information on the phenomena of subsurface-intensified midwater column jets. Thus there can be a wealth of added information on current processes other than bottom-trapped, low-frequency TRWs and eddies from the recommended array.

8.3.2 Deep Circulation and Eddy Measurements

Eulerian array for eddy characterization and study. Numerical circulation models tell us that large, energetic eddies propagate across the deep water region of the Gulf of Mexico to the western boundary, but we have almost no data to verify this, or to tell us what the levels of energy are. See in Figure 8.3.2-1 the locations of existing public current meter records, most collected non-simultaneously, from the deep water regime of the Gulf. Therefore, we propose a moored current meter array in the abyssal plain of the Gulf to verify and describe the deep eddies. According to model results of Welsh and Inoue (2000), the deep cyclones have diameters of some 250-300 km in the central Gulf of Mexico and migration speeds of order 5 $cm \cdot s^{-1}$. Deep cyclones seen in the CUPOM output have a larger range of diameters, encompassing the range reported by Welsh and Inoue, with smaller diameters for rings passing through the narrower north-south deep bathymetry near 88°-89°W.

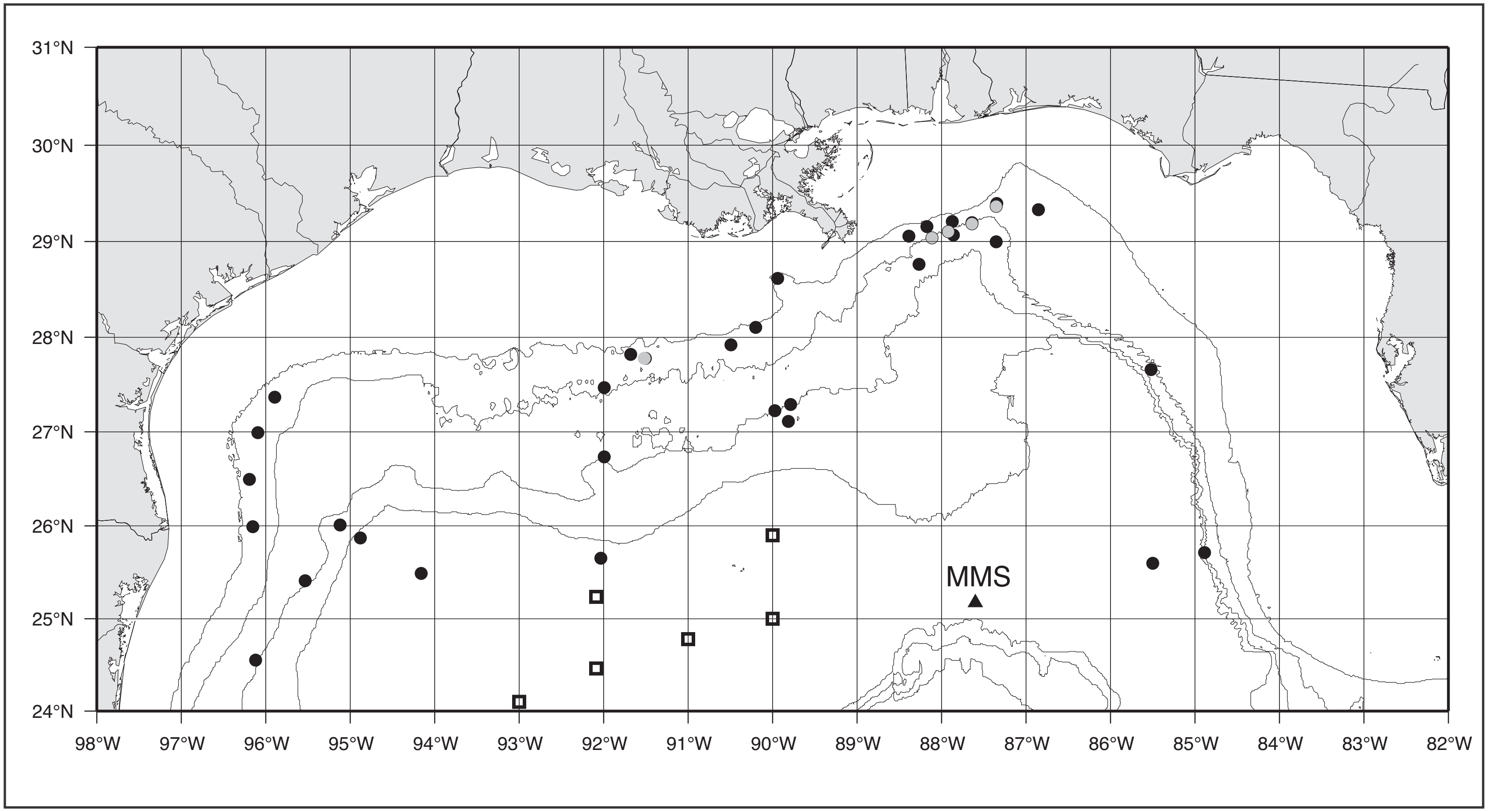

Figure 8.3.2-1. Proposed current meter array to observe deep eddies in the central Gulf abyssal plain (squares). The existing MMS mooring, shown as a triangle, would be an important part of this array. Mooring locations of publicly available current records from the deep Gulf are shown as dots (shaded dots indicate locations of second moorings from essentially the same location). The 200-, 1000-, 2000-, and 3000-m isobaths are shown.

Shown in Figure 8.3.2-1 are the suggested locations of six moorings in the central abyssal Gulf of Mexico to measure for the first time the propagation of deep eddies into the western Gulf. The MMS mooring now in place north of the Campeche Shelf should be continued and used as a part of this array. This array consists of two triangular current meter arrays resulting in four moorings oriented along the probable direction of travel and two moorings to the north. The mooring separation is of order 100 km, which is less than half of the expected eddy diameter and should result in measurements that will allow characterization of propagation as well as energy levels. The upstream MMS mooring is well positioned to detect the existence of deep cyclones as they approach the deep bathymetric constriction. These locations are subject to refinement based on further study of model output and observations.

It is suggested that currents and temperatures be measured throughout the water column on these moorings. Such data also will capture other energetic current events in the central Gulf. Measurements from the upper layers (say above 800 m) can be used to describe for the first time from a fixed array of adequate spatial extent the propagation of surface-intensified eddies in the Gulf. The propagation and decay of those features remain subjects of some speculation. Data from the deep part of this array, combined with the Lagrangian observations described next in this section, will contribute to the first substantial data set to elucidate deep flow climatology, here considered to include not only mean fields but measures of the variability. Coupling the deep measurements with the upper measurements also may allow us to better relate the surface-intensified eddies to the deep eddies and circulation, contributing to a better understanding of the causal mechanisms of the deep currents.

All moorings must be deployed together. The deployments should be for at least one year and preferably two years. Follow-on re-deployments are recommended to ensure record lengths adequate to measure multiple events, and thus result in meaningful statistics.

<u>Lagrangian deep circulation array.</u> Numerical model simulations indicate that the deep flow regime in the Gulf of Mexico is complex and energetic, with boundary intensification and major bathymetric effects on both mean flow and variability, but observations are inadequate for verification. Rudimentary current measurements and general physical considerations suggest that the deep flow between the Gulf and the Caribbean Sea is extremely energetic and variable in direction, with transports of the same order as the surface-intensified Loop Current.

Proposed is a Lagrangian float experiment in the deep Gulf Basin designed to obtain statistics regarding the deep circulation and its variability, and to give indications of deep flow through the Yucatan Channel. This would provide for the first time information regarding the interchange of deep organisms and properties between the Gulf and the Caribbean.

Suggested is a deployment for two years of approximately 60 RAFOS floats distributed between the 2500-m and 1500-m levels. Floats at 2500 m will be confined within the Gulf Basin, because the deepest sill depth at Yucatan Channel is approximately 2000 m. Floats at 1500 m would be free to move through the Yucatan Channel, but not to leave the Gulf via the Straits of Florida with its sill depth of about 800 m. Sound sources must be positioned in the Cayman Sea as well as in the Gulf, and some of the floats should be deployed south of Yucatan Channel. Seven to eight sound sources would be needed.

A subset of these floats might be deployed so as to provide estimates of dispersion within the deep Gulf. This information could be of interest in considering the effects of deep release of oil or of dispersion of other materials.

8.3.3 Characterizing Currents Responsible for Mega-Furrows

Off the mouth of Bryant Canyon, near 92°W, deep tow measurements showed the mega-furrow regime to vary in character in the cross-isobath direction. Beginning as linear parallel features, they change toward the Sigsbee Escarpment progressively from parallel trenches, to trenches with undulating wave forms, to flukes, and finally to features with wave crests almost cross-isobath or even complete erosion of the weakly consolidated upper sediment layer. Three-dimensional seismic measurements have shown these features to extend along the base of the escarpment from near 90.83°W (close to Farnella Canyon) to 90°W (east of Green Knoll). Thus they represent a gigantic land form caused by erosion and deposition due to bottom currents.

To understand the processes responsible for these furrows, it is important to describe the horizontal flow regime as a function of character of the furrow regime. This should include measurements very near the sea bed, both within and between the furrows, and within the overlying free flow regime. Proposed as initial measurements are near-bottom current measurements with temperature and perhaps optical backscatter sensors. Each should be mounted quite near the sea bed.

The mega-furrow regime appears to extend some 30-35 km offshore from the base of the Sigsbee Escarpment in the region near Green Knoll. Therefore, assuming there are several sub-regimes in which the character of the furrows differ, and which may result from currents of different character or at least speed, we recommend that some eight current meter moorings be located across the furrow regime and kept in place for durations totaling at least a year. Five of these locations should be offshore from the escarpment with final spacing/locations determined from examination of geological information and further study of preliminary data. One mooring should be located on the face of the escarpment and two atop the escarpment. This would result in estimates of the background circulation and its spatial variability in relation to the furrow field and escarpment.

Description of the details of currents in the furrows and improved understanding of the dynamics of interactions between currents and furrows would require three-dimensional measurements of currents coupled with geological measurements.

9 CONCLUSIONS AND RECOMMENDATIONS

9.1 Data

The amount of physical data from the deepwater Gulf of Mexico is considerable (e.g., we have over 8 million hours (1000 yr) of time series records on currents and temperature from water depths of 200 m or more, and over 6500 oceanographic stations with bottle, CTD, or STD observations). On close examination, however, the usefulness and adequacy for study of important processes and phenomena are limited for several reasons.

- Data from many ocean stations are judged of bad or suspect quality and few cruises provide good regional coverage.
- Quality of the time series records varies greatly.
- Metadata are commonly inadequate to allow quality assurance, and sometimes to allow use, even for data derived from the National Oceanographic Data Center.
- Many time series are of too short duration or offer too limited spatial coverage to allow characterization of many important processes.
- Some synoptic survey data taken since about 1980 are available only as descriptions in proprietary reports.
- Many data sets, particularly recent current meter observations, are proprietary.

9.2 Energetic Events

We have described by example, and characterized with the available data sets, those classes of energetic current events thought to occur in the deepwater Gulf of Mexico. Here we summarize our findings from a general perspective.

- The general surface circulation for the Gulf is rather well described and understood in terms of forcing and response.
- There appear to be adequate data to characterize surface features such as the Loop Current and anticyclonic eddies, but not to understand the processes of eddy evolution and decay. Moreover, models and their inflow conditions are not yet adequate to hindcast or forecast them with the needed degree of skill.
- There are inadequate data to fully characterize the deep subsurface processes, which include barotropic deep events in the form of topographic Rossby waves or deep eddies, or to determine the influence of surface processes, such as LCE separation events, on such deep processes.
- The verification of mid-water jets remains problematical; a few (perhaps 8) events have been documented, but the data quality remains in doubt.
- There is no convincing evidence of topographically generated near-inertial motion in the Gulf.
- Knowledge of the general deep Gulf circulation is based principally on model output and physical speculation. However, the sparse, existing data sets tend to confirm the speculation and model results.
- The processes responsible for the mega-furrows near the Sigsbee Escarpment in the north-central Gulf are not understood.

We have prioritized the need for additional measurements related to ten classes of energetic events in the Gulf. The prioritization is based on the need to improve understanding, need to improve simulation/prediction, and ability to observe. Rankings, with 1 being the highest rated in terms of additional measurements needed, are:

1. Deep barotropic & bottom-intensified motions
2. General circulation—deep currents
3. Currents associated with furrows
4. Eddy induced currents
5. Loop Current
6. General circulation—surface currents
7, Subsurface, mid-water column motions
8. Hurricane/tropical storm-induced motions
9. Other energetic wind event induced motions
10. Topographically generated near-inertial motion

9.3 Recommended Measurements

Recommended are two general classes of observations. We suggest several carefully considered measurement programs designed to characterize and understand specific processes/phenomena. We also suggest the development of a systematic program of monitoring data for use in models to provide nowcasts and forecasts with improved skill. Section 8.1 gives the rationale for the focus of the recommendations on the north-central Gulf region.

9.3.1 Specific Measurement Programs

We recommend specific measurement programs.

- A moored array near the Sigsbee Escarpment in the north-central Gulf designed to measure barotropic deep motions propagated along this boundary. This array would be specific to topographic Rossby waves, but also would identify and characterize other deep motions, surface-intensified eddies (whether slope eddies or larger surface rings or cyclones), and less common, episodic phenomena (e.g., mid-water jets and effects of energetic atmospheric events) as might occur during the deployment period.

- A thin array of current moorings over the abyssal plain to detect and describe deep eddy pairs and surface-intensified eddies propagating across the Gulf. This array also would supplement the description of the general deep Gulf circulation.

- A Lagrangian float (RAFOS) experiment in the deep basin designed to obtain statistics regarding the deep circulation and its variability and to give indications of deep flow through the Yucatan Channel. This would provide for the first time information regarding the interchange mechanisms for deep organisms and material between the Gulf and the Caribbean. The deployment of a properly designed sub-array would enable estimations to be made of dispersion in the deep Gulf waters. This information might be most useful in considering potential environmental impacts.

- An experiment to determine the processes responsible for the mega-furrows in the north-central Gulf.

9.3.2 Systematic Monitoring

The number of systematic observations being made in the Gulf is increasing, although most are still over the continental shelves. First we recommend a program to enhance the environmental observations obtained on the drill vessels and production platforms of the petroleum industry. Data gathered from exploratory drill vessels can be used to advance knowledge at sites of future production platforms. Second, we encourage the establishment of long-term observations extending into the deepwater region of the Gulf. These might be considered as part of the Global Ocean Observing System (GOOS).

- Measurements from industry platforms. Although there are some current measurements from the slope and rise of the north-central Gulf, the region of most active petroleum exploration and recovery, most records are short (months) and few deployments cover the vertical extent of the water column. In addition, most are proprietary and the metadata quality is highly variable. In this environmentally critical region we have inadequate observations to statistically describe the energetic current events known to exist. At any given time there can be 10-20 drilling or production platforms in the deepwater region of the north-central Gulf. Available are electricity and personnel to power and service instruments. These platforms regularly acquire current measurements from downward looking ADCPs suspended near the surface. However, the data are not necessarily quality controlled or saved. With modest additional expenditures, additional instruments could be added to obtain vertical resolution of currents, tides at platforms, and perhaps biogeochemical measurements as well, and the quality control of the observations could be enhanced substantially. Clearly, this is a potentially cost effective method of building a climatology of energetic current events over the continental slope and rise—including both barotropic deep and surface-intensified motions. Moreover, such data should be transmitted in real time for use in monitoring and simulations.

- GOOS developments. It is now possible to monitor surface currents with pairs of CODARs (HF radars) that have useful ranges of order 200-300 km and resolution of order 10 km. These could be installed now on Cuba, the Yucatan Peninsula, and Key West to monitor the surface inflow and outflow to the Gulf.

  Over-the-horizon radar capability is developing. It seems likely that within a very short time it will be possible to monitor surface currents over the entire Gulf with two to three units and achieve resolution of order 15 km.

  Using automated sea level and meteorological stations on both sides of the Yucatan Channel and between Cuba and Key West, it would be possible to monitor the transport of the inflow and outflow. This might also be accomplished by the installation of a conducting cable. Either of these techniques would require an experiment to directly monitor the flow for a limited time to calibrate the system.

  To obtain regular surface estimates of velocity and temperature and subsurface measurements of temperature and salinity, the Gulf of Mexico could be included in the operational surface drifter and ship-of-opportunity XBT programs of NOAA. It also could be added to the Argo program of profiling float deployments so as to obtain systematic estimates of vertical profiles of salinity and temperature over the upper 2000 m as well as estimates of the 2000-m velocity.

9.4 Regarding Circulation Modeling of the Gulf of Mexico

Because the Gulf contains such a wide variety of energetic events, many of which are of relatively small scale, it is likely that needed environmental information will be obtained in considerable measure from numerical circulation models, constrained by a thin suite of observations. There are some half dozen models configured for the Gulf that have/are producing outputs. These outputs do not always agree, even on main issues such as whether deep barotropic eddies are "locked" to surface-intensified Loop Current eddies as they move into the western Gulf. Periodic, careful comparisons should be made between results from these various models, corroborated by available observations.

Improvements to Gulf of Mexico circulation modeling are needed. These include notably better boundary conditions for the regional models. Needed is a full Atlantic circulation model with synoptic winds to drive a joint Caribbean Sea and Gulf of Mexico model. Data discussed in Section 9.3.2 then could be assimilated into such a model to improve both the exchange between the Caribbean and Gulf and the circulation within the Gulf. Various techniques, including nudging and inverse methodology, should be used for the regular assimilation of the growing numbers of quasi-operational, and serendipitous data sets.

10 LITERATURE CITED

Allen, J. R. L., 1969: Erosional current marks of weakly cohesive mud beds. *J. Sedimentary Petrology*, **39**, 607–623.

Arango, H. G. and R. O. Reid, 1991: A generalized reduced-gravity ocean model. *Atmosphere-Ocean*, **29**, 256–287.

Bender, L. C. III and F. J. Kelly, 1998: LATEX Shelf Data Report: Acoustic Doppler current profiler, July 1992 through December 1994. Texas A&M University Dept. of Oceanography, College Station TX. Reference No. 96-3-T. 249 pp. [Available with the data through NODC on CD-ROM NODC-92, Texas-Louisiana Shelf Circulation and Transport Processes Study, Hydrography, Drifters, ADCP, and Miscellaneous Sensors Data and Reports, 1992-1994.]

Berger, T., 1993: Loop Current eddy shedding cycle. *LATEX Program Newsletter*, **2**(24). [Available from Department of Oceanography, Texas A&M University, College Station, TX.]

Berger, T. J., P. Hamilton, J. J. Singer, R. R. Leben, G. H. Born, and C. A. Fox, 1996a: Louisiana/Texas shelf physical oceanography program: eddy circulation study, final synthesis report. Volume I: Technical Report. OCS Study MMS 96-0051. U. S. Department of the Interior, Minerals Management Service, Gulf of Mexico OCS Region, New Orleans, LA, 324 pp.

Berger, T. J., P. Hamilton, J. J. Singer, R. R. Leben, G. H. Born, and C. A. Fox, 1996b: Louisiana/Texas shelf physical oceanography program: eddy circulation study, final synthesis report. Volume II: Appendices. OCS Study MMS 96-0052. U. S. Department of the Interior, Minerals Management Service, Gulf of Mexico OCS Region, New Orleans, LA, 151 pp.

Biggs, D. C., G. S. Fargion, P. Hamilton, and R. R. Leben, 1996: Cleavage of a Gulf of Mexico Loop Current eddy by a deep water cyclone. *J. Geophys. Res.*, **101**, 20,629–20,641.

Brooks, D. A., 1983: The wake of Hurricane Allen in the western Gulf of Mexico. *J. Phys. Oceanogr.*, **13**, 117–129.

Brooks, D. A., 1984: Current and hydrographic variability in the northwestern Gulf of Mexico. *J. Geophys. Res.*, **89**, 8,022–8,032.

Brooks, D. A., and R. V. Legeckis, 1982: A ship and satellite view of hydrographic features in the western Gulf of Mexico. *J. Geophys. Res.*, **87**, 4,195–4,206.

Brooks, J. M., 1991: Mississippi-Alabama Continental Shelf Ecosystem Study: Data Summary and Synthesis. Volume II. Technical Narrative. OCS Study MMS 91-0063. U. S. Department of the Interior. Minerals Management Service. Gulf of Mexico OCS Region, New Orleans, LA. 862 pp.

Bryant, W., D. Bean, N. Slowey, and E. Scott, 2000a: Mega-Furrows on the Continental Rise South of the Sigsbee Escarpment, Northwest Gulf of Mexico. Abstract, American Association of Petroleum Geologists Annual Meeting, May 2000, New Orleans, Louisiana.

Bryant, W., D. Bean, N. Slowey, and E. Scott, 2000b: Mega-Furrows on the Continental Rise South of the Sigsbee Escarpment, Northwest Gulf of Mexico. Abstract, Gulf Coast Association of Geological Societies, October 2000, Houston, Texas.

Bryant, W., D. Bean, N. Slowey, and E. Scott, 2001: Sediment Furrows of the Northwest Gulf of Mexico. Abstract, AGU Chapman Conference, June 2001, Ponce, Puerto Rico.

Burden, C. A., 1999: Sediment transport in the Mississippi Canyon: the role of currents and storm events on optical variability. Master's Thesis, Department of Oceanography, Texas A&M University.

Carney, R. S., 1997: Workshop on environmental issues surrounding deepwater oil and gas development: Final report. OCS Study MMS 98-0022. U. S. Department of the Interior, Minerals Management Service, Gulf of Mexico OCS Region, New Orleans, LA. 163 pp.

Carruthers, J. W., 1972: Water Masses at intermediate depths. *Contributions on the Physical Oceanography of the Gulf of Mexico*, L. R. A. Capurro and J. L. Reid, eds., Gulf Publ. Co., pp. 53-64.

Charney, J. G. and G. R. Flierl, 1981: Evolution of Physical oceanography. *Oceanic analogues of Atmospheric Motions*, B. A. Warren and C. Wunsch, eds., MIT Press, 504–548.

Cho, K., R. O. Reid, and W. D. Nowlin, Jr., 1998: Objectively mapped stream function fields on the Texas-Louisiana shelf based on 32 months of moored current meter data. *J. Geophys. Res.*, **103**, 10,377–10,390.

Clifford, M., C. Horton, J. Schmitz, and L. Kantha, 1997: An oceanographic nowcast/forecast system for the Red Sea. *J. Geophys. Res.*, **102**, 25,101–25,122.

Cochrane, J. D., 1969: Water and circulation on Campeche Bank in May. Papers in Dedication to Professor Michitaka Uda, November 1969, Tokyo, Japan. *Special Bulletin of the Japanese Soc. Fish. Oceanogr.*, 123-129.

Continental Shelf Associates, Inc., 2000: Deepwater Gulf of Mexico environmental and socioeconomic data search and literature synthesis. Volume I: Narrative Report, OCS Study MMS 2000-049. Volume II: Annotated bibliography, OCS Study MMS 2000-050. U.S. Department of the Interior, Minerals Management Service, Gulf of Mexico OCS Region, New Orleans.

Cooper, C., and J. D. Thompson, 1989a: Hurricane-generated currents on the outer continental shelf, 1. Model formations and verifications. *J. Geophys. Res.*, **94**, 12,513–12,539.

Cooper, C., and J. D. Thompson, 1989b: Hurricane-generated currents on the outer continental shelf, 2. Model sensitivity studies. *J. Geophys. Res.*, **94**, 12,540–12,554.

DiMarco, S. F., A. E. Jochens, and M. K. Howard, 1997: LATEX Shelf Data Report: Current meters, April 1992 through December 1994. TAMU Oceanography Tech. Rpt. No. 97-1-T. Texas A&M University, College Station, TX. 10 volumes. [Available with the data through NODC on CD-ROM NODC-88, Texas-Louisiana Shelf Circulation and Transport Processes Study, Current Meter, Meteorological Buoy, XBT/XSV/XCP/CTD/IES Data and Reports, 1992-1994.]

DiMarco, S. F., and R. O. Reid, 1998: Characterization of the principal tidal current constituents on the Texas-Louisiana shelf. *J. Geophys. Res.*, **103**, 3,093–3,109.

DiMarco, S. F., M. K. Howard, and A. E. Jochens, 2001: Deepwater Gulf of Mexico Historical Physical Oceanography Data Report. TAMU Oceanography Tech. Rpt. No. 01-01-D. Texas A&M University, College Station, TX.

DiMarco, S. F., M. K. Howard, and R. O. Reid, 2000: Seasonal variation of wind-driven diurnal current cycling on the Texas-Louisiana Continental Shelf. *Geophys. Res. Lett.*, **27**, 1,017–1,020.

Dzulynski, S., 1965: New data on experimental production of sedimentary structures. *J. Sed. Pet.*, **35**, 196–212.

Elliott, B. A., 1982: Anticyclonic rings in the Gulf of Mexico. *J. Phys. Oceanogr.*, **12**, 1,292–1,309.

Emery, W. J., and R. E. Thomson, 1997: *Data Analysis Methods in Physical Oceanography*. Pergamon, 650 pp.

Flood, R. D., 1983: Classification of sedimentary furrows and a model for furrow initiation and evolution. *Geol. Soc. Amer. Bull.*, **94**, 630–639.

Florida A&M University, 1988: Meteorological database and synthesis for the Gulf of Mexico. OCS Study MMS 83-0064. Dept of the Interior, Minerals Management Service, New Orleans. 486 pp.

Forristall, G. Z., 1974: Three-dimensional structure of storm-generated currents, *J. Geophys. Res.*, **79**, 2,721–2,729.

Forristall, G. Z., 1980: A two-layer model for hurricane-driven currents on an irregular grid. *J. Phys. Oceanogr.*, **10**, 1,417–1,438.

Forristall, G. Z., K. J. Schaudt, and C. K. Cooper, 1992: Evolution and kinematics of a Loop Current eddy in the Gulf of Mexico during 1985. *J. Geophys. Res.*, **97**, 2173–2184.

Guinasso, N. L., Jr., ed., 2000: Final Report: Stability and Change in Chemosynthetic Communities. OCS Study MMS 2000-xxx. U. S. Department of the Interior, Minerals Management Service, Gulf of Mexico OCS Region, New Orleans, LA, xxx pp.

Hamilton, P., 1984: Topographic and inertial waves on the continental rise of the Mid-Atlantic Bight. *J. Geophys. Res.*, **89**, 695–710.

Hamilton, P., 1990: Deep currents in the Gulf of Mexico. *J. Phys. Oceanogr.*, **20**, 1,087–1,104.

Hamilton, P., 1992: Lower continental slope eddies in the central Gulf of Mexico. *J. Geophys. Res.*, **97**, 2,185–2,200.

Hamilton, P., G. S. Fargion, and D. C. Biggs, 1999: Loop Current eddy paths in the western Gulf of Mexico. *J. Phys. Oceanorg.*, **29**, 1,180–1,207.

Hamilton, P., T. J. Berger, J. H. Churchill, R. R. Leben, T. N. Lee, J. J. Singer, W. Sturges, and E. Waddell, 2000: Desoto Canyon Eddy Intrusion Study; Final Report, Volume II: Technical Report. OCS Study MMS 2000-XXX. U.S. Dept. of the Interior, Minerals Management Service, Gulf of Mexico OCS Region, New Orleans, LA. 269 pp.

Hardy, J.W, and S.A. Hsu, 1997: A climatology of winter cyclogenesis intensity in the northwest Gulf of Mexico. *Natl. Wea. Dig.*, **22**, 3–7.

Herring, H. J., M. Inoue, G. L. Mellor, C. N. K. Mooers, P. P. Niiler, L.-Y. Oey, R. C. Patchen, F. M. Vukovich, and W. J. Wiseman, Jr., 1999: Coastal Ocean Modelling Program for the Gulf of Mexico, Final Report, Volume 2. Prepared for Minerals Management Service Environmental Division, Technical Analysis Group. Report No. 115.2, 194 pp.

Hofmann, E. E., and S. J. Worley, 1986: An investigation of the circulation of the Gulf of Mexico. *J. Geophys. Res.*, **91**, 14,221–14,326.

Horton, C., M. Clifford, and J. Schmitz, 1997: A real-time oceanographic nowcast/ forecast system for the Mediterranean Sea. *J. Geophys. Res.*, **102**, 25,123–25,156.

Howard, M. K., and S. F. DiMarco, 1998: LATEX A Data Report: Drifter and Miscellaneous Instruments. TAMU Oceanography Tech. Rpt. No. 98-2-T. Texas A&M University, College Station, TX. 181 pp. [Available with the data through NODC on CD-ROM NODC-92, Texas-Louisiana Shelf Circulation and Transport Processes Study, Hydrography, Drifters, ADCP, and Miscellaneous Sensors Data and Reports, 1992-1994.]

Hsu, S. A., 1993: The Gulf of Mexico—a breeding ground for winter storms. *Mar. Wea. Log*, **37**, 4–11.

Inoue, M., and S. E. Welsh, 1997: Numerical Simulation of Gulf of Mexico Circulation under Present and Glacial Climatic Conditions, New Orleans, LA: U.S. Dept. of the Interior, Minerals Management Service, OCS Study MMS 96-0067. 147 pp.

Jochens, A. E., and W. D. Nowlin, Jr., eds., 2000: Northeastern Gulf of Mexico Chemical Oceanography and Hydrography Study Annual Report: Year 3. OCS Study MMS 2000-078, U.S. Dept. of the Interior, Minerals Management Service, Gulf of Mexico OCS Region, New Orleans, LA. 89 pp.

Jochens, A. E., D. A. Wiesenburg, L. E. Sahl, C. N. Lyons, and D. A. DeFreitas, 1998: LATEX Shelf Data Report: Hydrography, April 1992 through November 1994. TAMU Oceanography Tech. Rpt. No. 96-6-T. Texas A&M University, College Station TX. 6 volumes. [Available with the data through NODC on CD-ROM NODC-92, Texas-

Louisiana Shelf Circulation and Transport Processes Study, Hydrography, Drifters, ADCP, and Miscellaneous Sensors Data and Reports, 1992-1994.]

Kantha, L., J.-K. Choi, R. Leben, C. Cooper, M. Vogel, and J. Feeney, 1999: Hindcasts and real-time nowcast/forecasts of currents in the Gulf of Mexico. Offshore Technology Conference (OTC ’99), May 3-6, 1999, Houston, TX.

Keen, T. R., and S. M. Glenn, 1999: Shallow water currents during Hurricane Andrew. *J. Geophys. Res.*, **104**, 23,443–23,458.

Lee, T. N., K. Leaman, E. Williams, T. Berger, and L. Atkinson, 1995: Florida Current meanders and gyre formation in the southern Straits of Florida. *J. Geophys. Res.*, **100**, 8,607–8,620.

Leipper, D. F., 1967: Observed ocean conditions and Hurricane Hilda, 1964. *J. Atmos. Sci.*, **24**, 182–196.

Levitus, S., 1982: Climatological Atlas of the World Ocean, NOAA, Prof. Papers, No. 13, U. S. Government Printing Office, 173 pp.

Lewis, J. K., A. D. Kirwan, Jr., and G. Z. Forristall, 1989: Evolution of a warm-core ring in the Gulf of Mexico: Lagrangian observations. *J. Geophys. Res.*, **94**, 8,163–8,178.

Lewis, J. K., and A. D. Kirwan, Jr., 1987: Genesis of a Gulf of Mexico ring as determined from kinematic analysis. *J. Geophys. Res.*, **92**, 11,727–11,740.

Lillibridge, J., R. Leben, and F Vossepoel, 1997: Real-time processing from ERS-2. Proc. Third ERS Symp., Vol. 3, Florence, Italy, European Space Agency, SP414, 1,449–1,453.

Maul, G. A., D. A. Mayer, and S. R. Baig, 1985: Comparisons between a continuous 3-year current-meter observation at the sill of the Yucatan Strait, satellite measurements of Gulf Loop Current area, and regional sea level. *J. Geophys. Res.*, **90**, 9,089–9,096.

McLellan, H. J., and W. D. Nowlin, Jr., 1963: Some features of the deep water in the Gulf of Mexico. *J. Mar. Res.*, **21**, 233–245.

Molinari, R. L., and D. A. Mayer, 1982: Current meter observations on the continental slope at two sites in the eastern Gulf of Mexico. *J. Phys. Oceanogr.*, **12**, 1,480–1,492.

Nowlin, W. D., Jr., A. E. Jochens, R. O. Reid, and S. F. DiMarco, 1998a: Texas-Louisiana shelf circulation and transport processes study: Synthesis Report, Volume I: Technical Report. OCS Study MMS 98-0035. U. S. Department of the Interior, Minerals Management Service, Gulf of Mexico OCS Region, New Orleans, 502 pp.

Nowlin, W. D., Jr., A. E. Jochens, R. O. Reid, and S. F. DiMarco, 1998b: Texas-Louisiana shelf circulation and transport processes study: Synthesis Report, Volume II: Appendices. OCS Study MMS 98-0036. U. S. Department of the Interior, Minerals Management Service, Gulf of Mexico OCS Region, New Orleans, 288 pp.

Nowlin, W. D., Jr., and H. J. McLellan, 1967: A characterization of the Gulf of Mexico waters in winter. *J. Mar. Res.*, **25**, 25–59.

Nowlin, W. D., Jr., and J. M. Hubertz, 1972: Contrasting summer circulation patterns for the eastern Gulf. *Contributions on the Physical Oceanography of the Gulf of Mexico*, L. R. A. Capurro and J. L. Reid, eds., Gulf Publ. Co., pp. 119-137.

O'Brien, J. J., 1967: The non-linear response of a two-layer, baroclinic ocean to a stationary, axially-symetric hurricane: Part II. Upwelling and mixing induced by momentum transfer. *J. Atmos. Sci.*, **24**, 208–215.

O'Brien, J. J., and R. O. Reid, 1967: The non-linear response of a two-layer, baroclinic ocean to a stationary, axially-symmetric hurricane: Part I: Upwelling induced by momentum transfer. *J. Atmos. Sci.*, **24**, 197–207.

Price, J. F., T. B. Sanford, and G. Z. Forristall, 1994: Forced stage response to a moving hurricane. *J. Phys. Oceanogr.*, **24**, 233–260.

Price, J. R., R. A. Weller, and R. Pinkel, 1986: Diurnal cycling: observations and models of the upper ocean response to diurnal heating, cooling, and wind mixing. *J. Geophys. Res.*, **91**, 8,411–8,427.

Qi, B., R. A. deSzoeke, and C. A. Paulson, 1995: The structure of near-inertial waves during ocean storms. *J. Phys. Oceanogr.*, **25**, 2,853–2,871.

Sanford, T. B., P. G. Black, J. R. Haustein, J. W. Feeney, G. Z. Forristall, and J. F. Price, 1987: Ocean Response to a Hurricane. Part I: Observations. *J. Phys. Oceanogr.*, **17**, 2,065–2,083.

Science Applications International Corporation, 1986: Gulf of Mexico physical oceanography program, Final Report: Years 1 and 2, Volume II: Technical Report. OCS Study MMS 85-0094, U.S. Dept. of the Interior, Minerals Management Service, Gulf of Mexico OCS Region, New Orleans, 403 pp.

Science Applications International Corporation, 1987: Gulf of Mexico physical oceanography program, Final Report: Year 4, Volume II: Technical Report. OCS Study MMS 87-0007, U.S. Dept. of the Interior, Minerals Management Service, Gulf of Mexico OCS Region, New Orleans, 315 pp.

Science Applications International Corporation, 1988: Gulf of Mexico physical oceanography program, Final Report: Year 3, Volume II: Technical Report. OCS Study MMS 88-0046, U.S. Dept. of the Interior, Minerals Management Service, Gulf of Mexico OCS Region, New Orleans, 266 pp.

Science Applications International Corporation, 1989: Gulf of Mexico physical oceanography program, Final Report: Year 5, Volume II: Technical Report. OCS Study MMS 89-0068, U.S. Dept. of the Interior, Minerals Management Service, Gulf of Mexico OCS Region, New Orleans, 333 pp.

Science Applications International Corporation, 1992: Straits of Florida physical oceanographic field study, final interpretive report. Volume II. OCS Study MMS 92-0024. U. S. Department of the Interior. Minerals Management Service. Gulf of Mexico OCS Region, New Orleans, 174 pp.

Scott, E., F. Peel, C. Taylor, W. Bryant, and D. Bean, 2001: Deepwater Gulf of Mexico Seafloor Features Revealed Through 3D Seismic, Offshore Technology Conference, April 30-May 2, 2001, Houston, TX. Paper OTC 12961, p. 1-8.

Sturges, W., 1993: The annual cycle of the western boundary current in the Gulf of Mexico. *J. Geophys. Res.*, **98**, 18,053–18,068.

Sturges, W., 1994: The frequency of ring separations from the Loop Current. *J. Phys. Oceanogr.*, **24**, 1,647–1,651.

Sturges, W., and R. Leben, 2000: Frequency of ring separations from the Loop Current in the Gulf of Mexico: a revised estimate. *J. Phys. Oceanogr.*, **30**, 1,814–1,819.

Sturges, W., J. Evans, S. Welsh, and W. Holland, 1993: Separation of warm-core rings in the Gulf of Mexico. *J. Phys. Oceanogr.*, **23**, 250–268.

Vazquez De la Cerda, A. M., 1993: Bay of Campeche Cyclone. Ph.D. Dissertation, Texas A&M University, 91 pp.

Vukovich, F. M., 1988: Loop Current boundary variations. *J. Geophys. Res.*, **93**, 15,585–15,591.

Welsh, S. E., and M. Inoue, 2000: Loop Current rings and the deep circulation in the Gulf of Mexico. *J. Geophys. Res.*, **105**, 16,951–16,959.

Yi, Y. 1995. Determination of gridded mean sea surface from altimeter data of TOPEX, ERS-1, and GEOSAT. Ph.D. Thesis, Department of Geodetic Science and Surveying, The Ohio State University, 140 pp.

APPENDIX A: INVENTORY OF CURRENT RECORDS DURING ENERGETIC PROCESSES AND PHENOMENA

The inventory of identified processes and phenomena was carried out in three steps: identification of energetic currents, identification of possible processes/phenomena, and categorization of currents by category. Each time series of currents was examined for the occurrence of energetic currents, as discussed in Section 6.2. The possible processes and phenomena were identified from the literature and from the character of the energetic currents observed. The current records then were compared and, where appropriate, matched in time and space to the known occurrences of the Loop Current, LCEs, other anticyclonic or cyclonic rings, tropical storms, hurricanes, winter cyclones, frontal passages, and other energetic wind events. Those portions of each record, for which the following categories of physical processes of phenomena (events) were present (occurred), were identified and placed in the inventory to be used in compiling statistics of energetic current events:

- Loop Current eddy separations
- Presence in the Gulf of extratropical cyclones identified by Hardy and Hsu (1997)
- Presence in the Gulf of tropical cyclones
- Presence of eddy near mooring
- Presence of Loop Current near mooring
- Deep barotropic motions, sometimes with bottom intensification
- Inertial and near-inertial motions
- Subsurface, mid-water column motions

Note that some of these categories are not independent (e.g., the decay process following initial currents forced by atmospheric disturbances almost always involve inertial oscillations). For some categories of energetic phenomena or processes in which we have interest there were few or only poor examples of currents in the available records.

The resulting inventory is given as Table A-1. The organization is by year, beginning with 1977. The second level of organization within the table is by event and date of event. For each event, each current record listing consists of: data set name, mooring name, instrument depth (m), and data directory/filename. Our holdings are divided into five data directories:

TAMU: contains TAMU, LATEX, MAMES, and GERG data sets
NODC-DEEP: contains NODC holdings from deepwater Gulf of Mexico, including Straits of Florida
MMS: contains DeSoto Canyon EIS and Extension study data
INDUSTRY: contains non-proprietary industry holdings
YUCATAN: contains data from Yucatan Channel

Table A-1. Inventory of portions of current records from the Gulf of Mexico during which energetic physical processes or phenomena were present in the Gulf. Basic arrangement is by year, beginning with 1977. For each year, arrangement is by type of event that occurred. Each current record listing consists of: data set name, mooring name, instrument depth (m), and data directory/filename.

1977

Data sets: NODC_DEEP NOAA M1, M2
YUCATAN Yucatan Straits

Tropical Cyclones
Hurricane ANITA 29 AUG - 3 SEP
NOAA M1 130 NODC_DEEP/VK770717.C01
NOAA M1 215 NODC_DEEP/VK770717.C02
NOAA M2 94 NODC_DEEP/VK770717.C03
NOAA M2 194 NODC_DEEP/VK770717.C04
NOAA M2 994 NODC_DEEP/VK770717.C05

Hurricane BABE 3 - 9 SEP
NOAA M1 130 NODC_DEEP/VK770717.C01
NOAA M1 215 NODC_DEEP/VK770717.C02
NOAA M2 94 NODC_DEEP/VK770717.C03
NOAA M2 194 NODC_DEEP/VK770717.C04
NOAA M2 994 NODC_DEEP/VK770717.C05

Extra-tropical Cyclones
December 25
NOAA M3 90 NODC_DEEP/DD771018.C01
NOAA M3 190 NODC_DEEP/DD771019.C01
NOAA M3 985 NODC_DEEP/DD771018.C02

1978

Data sets: NODC_DEEP NOAA M1, M3
YUCATAN Yucatan Straits

Tropical Cyclones
Tropical Storm AMELIA 30 JUL-1 AUG
NOAA M3 70 NODC_DEEP/DD780617.C01
NOAA M3 168 NODC_DEEP/DD780617.C02
NOAA M3 970 NODC_DEEP/DD780617.C03
NOAA T1 153 NODC_DEEP/EL780612.C01
NOAA T1 549 NODC_DEEP/EL780612.C02
NOAA T1 950 NODC_DEEP/EL780612.C03

Tropical Storm BESS 5-8 AUG
NOAA M3 70 NODC_DEEP/DD780617.C01
NOAA M3 168 NODC_DEEP/DD780617.C02
NOAA M3 970 NODC_DEEP/DD780617.C03
NOAA T1 153 NODC_DEEP/EL780612.C01
NOAA T1 549 NODC_DEEP/EL780612.C02
NOAA T1 950 NODC_DEEP/EL780612.C03

Tropical Storm DEBRA 26-29 AUG
NOAA T1 153 NODC_DEEP/EL780612.C01
NOAA T1 549 NODC_DEEP/EL780612.C02
NOAA T1 950 NODC_DEEP/EL780612.C03

Table A-1. Inventory of portions of current records from the Gulf of Mexico during which energetic physical processes or phenomena were present in the Gulf. (continued)

Loop Current Eddy separations
June
NOAA M3 70 NODC_DEEP/DD780617.C01
NOAA M3 168 NODC_DEEP/DD780617.C02
NOAA M3 970 NODC_DEEP/DD780617.C03
NOAA T1 153 NODC_DEEP/EL780612.C01
NOAA T1 549 NODC_DEEP/EL780612.C02
NOAA T1 950 NODC_DEEP/EL780612.C03
NOAA YS 1895 YUCATAN/YS771103.C01

Extra-tropical Cyclones
January 1
NOAA M3 90 NODC_DEEP/DD771018.C01
NOAA M3 190 NODC_DEEP/DD771019.C01
NOAA M3 985 NODC_DEEP/DD771018.C02

January 2
NOAA M3 90 NODC_DEEP/DD771018.C01
NOAA M3 190 NODC_DEEP/DD771019.C01
NOAA M3 985 NODC_DEEP/DD771018.C02

January 9
NOAA M3 90 NODC_DEEP/DD771018.C01
NOAA M3 190 NODC_DEEP/DD771019.C01
NOAA M3 985 NODC_DEEP/DD771018.C02

January 13
NOAA M3 90 NODC_DEEP/DD771018.C01
NOAA M3 190 NODC_DEEP/DD771019.C01
NOAA M3 985 NODC_DEEP/DD771018.C02

January 18
NOAA M3 90 NODC_DEEP/DD771018.C01
NOAA M3 190 NODC_DEEP/DD771019.C01
NOAA M3 985 NODC_DEEP/DD771018.C02

January 20
NOAA M3 90 NODC_DEEP/DD771018.C01
NOAA M3 190 NODC_DEEP/DD771019.C01
NOAA M3 985 NODC_DEEP/DD771018.C02

January 25
NOAA M3 90 NODC_DEEP/DD771018.C01
NOAA M3 190 NODC_DEEP/DD771019.C01
NOAA M3 985 NODC_DEEP/DD771018.C02

February 5
NOAA M3 90 NODC_DEEP/DD771018.C01
NOAA M3 190 NODC_DEEP/DD771019.C01
NOAA M3 985 NODC_DEEP/DD771018.C02

February 13
NOAA M3 90 NODC_DEEP/DD771018.C01
NOAA M3 190 NODC_DEEP/DD771019.C01
NOAA M3 985 NODC_DEEP/DD771018.C02

February 18
NOAA M3 90 NODC_DEEP/DD771018.C01
NOAA M3 190 NODC_DEEP/DD771019.C01
NOAA M3 985 NODC_DEEP/DD771018.C02

Table A-1. Inventory of portions of current records from the Gulf of Mexico during which energetic physical processes or phenomena were present in the Gulf. (continued)

Extra-tropical Cyclones (continued)
April 12
NOAA M3 90 NODC_DEEP/DD771018.C01
NOAA M3 190 NODC_DEEP/DD771019.C01
NOAA M3 985 NODC_DEEP/DD771018.C02

Loop Current Eddies
July-August: Unnamed
NOAA M3 70 NODC_DEEP/DD780617.C01
NOAA M3 168 NODC_DEEP/DD780617.C02
NOAA M3 970 NODC_DEEP/DD780617.C03

Loop Current intrusions
Early September - Early November
NOAA T1 153 NODC_DEEP/EL780612.C01
NOAA T1 157 NODC_DEEP/EL781026.C01
NOAA T1 257 NODC_DEEP/EL781026.C02
NOAA T1 549 NODC_DEEP/EL780612.C02
NOAA T1 950 NODC_DEEP/EL780612.C03
NOAA T1 957 NODC_DEEP/EL781026.C03

1979

Data sets: NODC_DEEP NOAA T1
YUCATAN Yucatan Straits

Loop Current Eddy separations
April
NOAA T1 254 NODC_DEEP/EL790213.C01
NOAA T1 558 NODC_DEEP/EL790213.C02
NOAA T1 960 NODC_DEEP/EL790213.C03
NOAA YS 1895 YUCATAN/YS771103.C01

Extra-tropical Cyclones
January 12
NOAA T1 157 NODC_DEEP/EL781026.C01
NOAA T1 957 NODC_DEEP/EL781026.C03

January 27
NOAA T1 157 NODC_DEEP/EL781026.C01
NOAA T1 957 NODC_DEEP/EL781026.C03

January 30
NOAA T1 157 NODC_DEEP/EL781026.C01
NOAA T1 957 NODC_DEEP/EL781026.C03

February 6
NOAA T1 157 NODC_DEEP/EL781026.C01
NOAA T1 957 NODC_DEEP/EL781026.C03

April 22
NOAA T1 254 NODC_DEEP/EL790213.C01
NOAA T1 558 NODC_DEEP/EL790213.C02
NOAA T1 960 NODC_DEEP/EL790213.C03

Loop Current intrusions
February
NOAA T1 157 NODC_DEEP/EL781026.C01
NOAA T1 254 NODC_DEEP/EL790213.C01
NOAA T1 558 NODC_DEEP/EL790213.C02
NOAA T1 957 NODC_DEEP/EL781026.C03
NOAA T1 960 NODC_DEEP/EL790213.C03

Table A-1. Inventory of portions of current records from the Gulf of Mexico during which energetic physical processes or phenomena were present in the Gulf. (continued)

1980

Data sets: INDUSTRY GC137
NODC_DEEP Brooks N, S, C

Tropical Cyclones
Hurricane ALLEN 31 JUL-11 AUG
Brooks N 700 NODC_DEEP/CC800717.C03
Brooks C 200 NODC_DEEP/PI800717.C04
Brooks C 450 NODC_DEEP/PI800717.C05
Brooks C 575 NODC_DEEP/PI800717.C06
Brooks C 700 NODC_DEEP/PI800717.C07
Brooks S 200 NODC_DEEP/PI800717.C01
Brooks S 450 NODC_DEEP/PI800717.C02
Brooks S 700 NODC_DEEP/PI800717.C03

Tropical Storm DANIELLE 4-7 SEP
Brooks N 700 NODC_DEEP/CC800717.C03
Brooks C 200 NODC_DEEP/PI800717.C04
Brooks C 450 NODC_DEEP/PI800717.C05
Brooks C 575 NODC_DEEP/PI800717.C06
Brooks C 700 NODC_DEEP/PI800717.C07
Brooks S 200 NODC_DEEP/PI800717.C01
Brooks S 450 NODC_DEEP/PI800717.C02
Brooks S 700 NODC_DEEP/PI800717.C03

Tropical Storm HERMINE 20-26 SEP
Brooks N 700 NODC_DEEP/CC800717.C03
Brooks C 200 NODC_DEEP/PI800717.C04
Brooks C 450 NODC_DEEP/PI800717.C05
Brooks C 575 NODC_DEEP/PI800717.C06
Brooks C 700 NODC_DEEP/PI800717.C07
Brooks S 200 NODC_DEEP/PI800717.C01
Brooks S 450 NODC_DEEP/PI800717.C02
Brooks S 700 NODC_DEEP/PI800717.C03

Hurricane JEANNE 7-16 NOV
Brooks N 700 NODC_DEEP/CC800717.C03
Brooks C 200 NODC_DEEP/PI800717.C04
Brooks C 450 NODC_DEEP/PI800717.C05
Brooks C 575 NODC_DEEP/PI800717.C06
Brooks C 700 NODC_DEEP/PI800717.C07
Brooks S 200 NODC_DEEP/PI800717.C01
Brooks S 450 NODC_DEEP/PI800717.C02
Brooks S 700 NODC_DEEP/PI800717.C03

Extra-tropical Cyclones
November 26
Brooks C 200 NODC_DEEP/PI800717.C04
Brooks C 450 NODC_DEEP/PI800717.C05
Brooks C 575 NODC_DEEP/PI800717.C06
Brooks C 700 NODC_DEEP/PI800717.C07
Brooks S 200 NODC_DEEP/PI800717.C01
Brooks S 450 NODC_DEEP/PI800717.C02
Brooks S 700 NODC_DEEP/PI800717.C03

Loop Current Eddies
Mid-September - October
Brooks S 200 NODC_DEEP/PI800717.C01
Brooks S 450 NODC_DEEP/PI800717.C02
Brooks S 700 NODC_DEEP/PI800717.C03

- -

Table A-1. Inventory of portions of current records from the Gulf of Mexico during which energetic physical processes or phenomena were present in the Gulf. (continued)

1981

Data sets: INDUSTRY GC137, GC184

Loop Current Eddy separations
March
INDUSTRY GC184 35 INDUSTRY/GC810119.C01
INDUSTRY GC184 65 INDUSTRY/GC810119.C02
INDUSTRY GC184 100 INDUSTRY/GC810119.C03
INDUSTRY GC184 150 INDUSTRY/GC810119.C04
INDUSTRY GC184 400 INDUSTRY/GC810119.C05

1982

No data during events

1983

Data sets: NODC_DEEP SAIC 5YR A, G

Tropical Cyclones
Hurricane ALICIA 15-21 AUG
SAIC A 172 NODC_DEEP/HH830127.C01
SAIC A 400 NODC_DEEP/HH830729.C01
SAIC A 738 NODC_DEEP/HH830730.C01
SAIC A 1100 NODC_DEEP/HH830127.C02
SAIC A 1600 NODC_DEEP/HH830730.C02

Hurricane BARRY 23-29 AUG
SAIC A 172 NODC_DEEP/HH830127.C01
SAIC A 400 NODC_DEEP/HH830729.C01
SAIC A 738 NODC_DEEP/HH830730.C01
SAIC A 1100 NODC_DEEP/HH830127.C02
SAIC A 1600 NODC_DEEP/HH830730.C02

Loop Current Eddy separations
March: Unnamed
SAIC A 172 NODC_DEEP/HH830127.C01
SAIC A 1100 NODC_DEEP/HH830127.C02
SAIC A 1600 NODC_DEEP/HH830127.C03

Extra-tropical Cyclones
February 5
SAIC A 172 NODC_DEEP/HH830127.C01
SAIC A 1100 NODC_DEEP/HH830127.C02
SAIC A 1600 NODC_DEEP/HH830127.C03

February 15
SAIC A 172 NODC_DEEP/HH830127.C01
SAIC A 1100 NODC_DEEP/HH830127.C02
SAIC A 1600 NODC_DEEP/HH830127.C03

February 20
SAIC A 172 NODC_DEEP/HH830127.C01
SAIC A 1100 NODC_DEEP/HH830127.C02
SAIC A 1600 NODC_DEEP/HH830127.C03

February 26
SAIC A 172 NODC_DEEP/HH830127.C01
SAIC A 1100 NODC_DEEP/HH830127.C02
SAIC A 1600 NODC_DEEP/HH830127.C03

Table A-1. Inventory of portions of current records from the Gulf of Mexico during which energetic physical processes or phenomena were present in the Gulf. (continued)

Extra-tropical Cyclones (continued)
March 16
SAIC A 172 NODC_DEEP/HH830127.C01
SAIC A 1100 NODC_DEEP/HH830127.C02
SAIC A 1600 NODC_DEEP/HH830127.C03

March 23
SAIC A 172 NODC_DEEP/HH830127.C01
SAIC A 1100 NODC_DEEP/HH830127.C02
SAIC A 1600 NODC_DEEP/HH830127.C03

1984

Data sets: INDUSTRY GC110
NODC_DEEP SAIC 5YR A, G

Tropical Cyclones
Tropical Storm EDOUARD 14-15 SEP
SAIC A 400 NODC_DEEP/HH840718.C02
SAIC G 1565 NODC_DEEP/HH840718.C05
SAIC G 2364 NODC_DEEP/HH840718.C06
SAIC G 3174 NODC_DEEP/HH840718.C07

Loop Current Eddy separations
February: Unnamed
SAIC G 1565 NODC_DEEP/HH840203.C01
SAIC G 2364 NODC_DEEP/HH840203.C02
SAIC G 3174 NODC_DEEP/HH840203.C03

August: Slim Chance Eddy (aka Eddy Arnold)
SAIC A 172 NODC_DEEP/HH840718.C01
SAIC A 400 NODC_DEEP/HH840718.C02
SAIC G 1565 NODC_DEEP/HH840718.C05
SAIC G 2364 NODC_DEEP/HH840718.C06
SAIC G 3174 NODC_DEEP/HH840718.C07

Loop Current Eddies
18 October - 31 December
SAIC A 172 NODC_DEEP/HH841018.C01 (Loop current over mooring)
SAIC A 400 NODC_DEEP/HH841018.C02
SAIC A 738 NODC_DEEP/HH841018.C03
SAIC A 1100 NODC_DEEP/HH841018.C04
SAIC A 1600 NODC_DEEP/HH841018.C05

1985

Data sets: NODC_DEEP SAIC 5YR A, G, P, Q, R, S, T

Tropical Cyclones
Hurricane BOB 21-26 JUL
SAIC A 172 NODC_DEEP/HH850124.C01
SAIC A 400 NODC_DEEP/HH850124.C02
SAIC A 738 NODC_DEEP/HH850124.C03
SAIC A 1100 NODC_DEEP/HH850124.C04
SAIC A 1600 NODC_DEEP/HH850124.C05
SAIC G 703 NODC_DEEP/HH850312.C02
SAIC G 1565 NODC_DEEP/HH850124.C08
SAIC G 2364 NODC_DEEP/HH850124.C09
SAIC G 3174 NODC_DEEP/HH850124.C10
SAIC P 1000 NODC_DEEP/AC850611.C02
SAIC P 1500 NODC_DEEP/AC850611.C03

Table A-1. Inventory of portions of current records from the Gulf of Mexico during which energetic physical processes or phenomena were present in the Gulf. (continued)

Tropical Cyclones (continued)

Hurricane BOB (continued) 21-26 JUL

SAIC Q 100 NODC_DEEP/MG850615.C01
SAIC Q 300 NODC_DEEP/MG850615.C02
SAIC Q 1000 NODC_DEEP/MG850615.C03
SAIC Q 1500 NODC_DEEP/MG850615.C04
SAIC R 100 NODC_DEEP/MG850615.C05
SAIC R 300 NODC_DEEP/MG850615.C06
SAIC R 1000 NODC_DEEP/MG850615.C07
SAIC R 1500 NODC_DEEP/MG850615.C08
SAIC S 100 NODC_DEEP/MG850612.C01
SAIC S 300 NODC_DEEP/MG850612.C02
SAIC S 1000 NODC_DEEP/MG850612.C03
SAIC T 100 NODC_DEEP/MG850613.C01
SAIC T 300 NODC_DEEP/MG850613.C02
SAIC T 1000 NODC_DEEP/MG850613.C03

Hurricane DANNY 12-20 AUG

SAIC A 172 NODC_DEEP/HH850801.C01
SAIC A 400 NODC_DEEP/HH850801.C02
SAIC A 738 NODC_DEEP/HH850731.C01
SAIC A 1100 NODC_DEEP/HH850731.C02
SAIC G 703 NODC_DEEP/HH850801.C03
SAIC G 1565 NODC_DEEP/HH850801.C04
SAIC G 2364 NODC_DEEP/HH850801.C05
SAIC G 3174 NODC_DEEP/HH850801.C06
SAIC P 1000 NODC_DEEP/AC850611.C02
SAIC P 1500 NODC_DEEP/AC850611.C03
SAIC Q 100 NODC_DEEP/MG850615.C01
SAIC Q 300 NODC_DEEP/MG850615.C02
SAIC Q 1000 NODC_DEEP/MG850615.C03
SAIC Q 1500 NODC_DEEP/MG850615.C04
SAIC R 100 NODC_DEEP/MG850615.C05
SAIC R 300 NODC_DEEP/MG850615.C06
SAIC R 1000 NODC_DEEP/MG850615.C07
SAIC R 1500 NODC_DEEP/MG850615.C08
SAIC S 100 NODC_DEEP/MG850612.C01
SAIC S 1000 NODC_DEEP/MG850612.C03
SAIC T 100 NODC_DEEP/MG850613.C01
SAIC T 300 NODC_DEEP/MG850613.C02
SAIC T 1000 NODC_DEEP/MG850613.C03

Hurricane ELENA 28 AUG- 4 SEP

SAIC A 172 NODC_DEEP/HH850801.C01
SAIC A 400 NODC_DEEP/HH850801.C02
SAIC A 738 NODC_DEEP/HH850731.C01
SAIC A 1100 NODC_DEEP/HH850731.C02
SAIC G 703 NODC_DEEP/HH850801.C03
SAIC G 1565 NODC_DEEP/HH850801.C04
SAIC G 2364 NODC_DEEP/HH850801.C05
SAIC G 3174 NODC_DEEP/HH850801.C06
SAIC P 1000 NODC_DEEP/AC850611.C02
SAIC P 1500 NODC_DEEP/AC850611.C03
SAIC Q 100 NODC_DEEP/MG850615.C01
SAIC Q 300 NODC_DEEP/MG850615.C02
SAIC Q 1000 NODC_DEEP/MG850615.C03
SAIC Q 1500 NODC_DEEP/MG850615.C04
SAIC R 100 NODC_DEEP/MG850615.C05
SAIC R 300 NODC_DEEP/MG850615.C06
SAIC R 1000 NODC_DEEP/MG850615.C07
SAIC R 1500 NODC_DEEP/MG850615.C08
SAIC S 100 NODC_DEEP/MG850612.C01
SAIC S 1000 NODC_DEEP/MG850612.C03
SAIC T 100 NODC_DEEP/MG850613.C01

Table A-1. Inventory of portions of current records from the Gulf of Mexico during which energetic physical processes or phenomena were present in the Gulf. (continued)

Tropical Cyclones (continued)

Hurricane ELENA (continued) 28 AUG- 4 SEP

SAIC T 300 NODC_DEEP/MG850613.C02
SAIC T 1000 NODC_DEEP/MG850613.C03

Hurricane JUAN 26 OCT- 1 NOV

SAIC A 172 NODC_DEEP/HH850801.C01
SAIC A 400 NODC_DEEP/HH850801.C02
SAIC A 738 NODC_DEEP/HH850731.C01
SAIC A 1100 NODC_DEEP/HH850731.C02
SAIC G 703 NODC_DEEP/HH850801.C03
SAIC G 1565 NODC_DEEP/HH850801.C04
SAIC G 2364 NODC_DEEP/HH850801.C05
SAIC G 3174 NODC_DEEP/HH850801.C06
SAIC P 1000 NODC_DEEP/AC850611.C02
SAIC P 1500 NODC_DEEP/AC850611.C03
SAIC Q 300 NODC_DEEP/MG851020.C01
SAIC Q 1500 NODC_DEEP/MG850615.C04
SAIC S 1000 NODC_DEEP/MG850612.C03
SAIC T 300 NODC_DEEP/MG850613.C02
SAIC T 1000 NODC_DEEP/MG850613.C03

Hurricane KATE 15-23 NOV

SAIC A 172 NODC_DEEP/HH850801.C01
SAIC A 400 NODC_DEEP/HH850801.C02
SAIC A 738 NODC_DEEP/HH850731.C01
SAIC A 1100 NODC_DEEP/HH850731.C02
SAIC G 703 NODC_DEEP/HH850801.C03
SAIC G 1565 NODC_DEEP/HH850801.C04
SAIC G 2364 NODC_DEEP/HH850801.C05
SAIC G 3174 NODC_DEEP/HH850801.C06
SAIC P 1000 NODC_DEEP/AC850611.C02
SAIC P 1500 NODC_DEEP/AC850611.C03
SAIC Q 300 NODC_DEEP/MG851020.C01
SAIC Q 1500 NODC_DEEP/MG850615.C04
SAIC S 750 NODC_DEEP/MG851102.C01
SAIC S 1000 NODC_DEEP/MG850612.C03
SAIC T 300 NODC_DEEP/MG850613.C02
SAIC T 1000 NODC_DEEP/MG850613.C03

Loop Current Eddy separations

July: Fast Eddy (aka Eddy B)

SAIC A 172 NODC_DEEP/HH850124.C01
SAIC A 400 NODC_DEEP/HH850124.C02
SAIC A 738 NODC_DEEP/HH850124.C03
SAIC A 738 NODC_DEEP/HH850731.C01
SAIC A 1100 NODC_DEEP/HH850124.C04
SAIC A 1100 NODC_DEEP/HH850731.C02
SAIC A 1600 NODC_DEEP/HH850124.C05
SAIC G 703 NODC_DEEP/HH850312.C02
SAIC G 1565 NODC_DEEP/HH850124.C08
SAIC G 2364 NODC_DEEP/HH850124.C09
SAIC G 3174 NODC_DEEP/HH850124.C10
SAIC P 1000 NODC_DEEP/AC850611.C02
SAIC P 1500 NODC_DEEP/AC850611.C03
SAIC Q 100 NODC_DEEP/MG850615.C01
SAIC Q 300 NODC_DEEP/MG850615.C02
SAIC Q 1000 NODC_DEEP/MG850615.C03
SAIC Q 1500 NODC_DEEP/MG850615.C04
SAIC R 100 NODC_DEEP/MG850615.C05
SAIC R 300 NODC_DEEP/MG850615.C06
SAIC R 1000 NODC_DEEP/MG850615.C07
SAIC R 1500 NODC_DEEP/MG850615.C08
SAIC S 100 NODC_DEEP/MG850612.C01

Table A-1. Inventory of portions of current records from the Gulf of Mexico during which energetic physical processes or phenomena were present in the Gulf. (continued)

Loop Current Eddy separations (continued)
July: Fast Eddy (aka Eddy B) (continued)

SAIC S 300 NODC_DEEP/MG850612.C02
SAIC S 1000 NODC_DEEP/MG850612.C03
SAIC T 100 NODC_DEEP/MG850613.C01
SAIC T 300 NODC_DEEP/MG850613.C02
SAIC T 1000 NODC_DEEP/MG850613.C03

Extra-tropical Cyclones
February 1

SAIC A 172 NODC_DEEP/HH850124.C01
SAIC A 400 NODC_DEEP/HH850124.C02
SAIC A 738 NODC_DEEP/HH850124.C03
SAIC A 1100 NODC_DEEP/HH850124.C04
SAIC A 1600 NODC_DEEP/HH850124.C05
SAIC G 397 NODC_DEEP/HH850124.C06
SAIC G 703 NODC_DEEP/HH850124.C07
SAIC G 1565 NODC_DEEP/HH850124.C08
SAIC G 2364 NODC_DEEP/HH850124.C09
SAIC G 3174 NODC_DEEP/HH850124.C10

May 18

SAIC A 172 NODC_DEEP/HH850124.C01
SAIC A 400 NODC_DEEP/HH850124.C02
SAIC A 738 NODC_DEEP/HH850124.C03
SAIC A 1100 NODC_DEEP/HH850124.C04
SAIC A 1600 NODC_DEEP/HH850124.C05
SAIC G 397 NODC_DEEP/HH850312.C01
SAIC G 703 NODC_DEEP/HH850312.C02
SAIC G 1565 NODC_DEEP/HH850124.C08
SAIC G 2364 NODC_DEEP/HH850124.C09
SAIC G 3174 NODC_DEEP/HH850124.C10

Loop Current Eddies
24 January - 30 April

SAIC A 172 NODC_DEEP/HH850124.C01 (LC over mooring)
SAIC A 400 NODC_DEEP/HH850124.C02
SAIC A 738 NODC_DEEP/HH850124.C03
SAIC A 1100 NODC_DEEP/HH850124.C04
SAIC A 1600 NODC_DEEP/HH850124.C05
SAIC G 397 NODC_DEEP/HH850124.C06
SAIC G 397 NODC_DEEP/HH850312.C01
SAIC G 703 NODC_DEEP/HH850124.C07
SAIC G 703 NODC_DEEP/HH850312.C02
SAIC G 1565 NODC_DEEP/HH850124.C08
SAIC G 2364 NODC_DEEP/HH850124.C09
SAIC G 3174 NODC_DEEP/HH850124.C10

September - November

SAIC A 172 NODC_DEEP/HH850801.C01 (LC over mooring)
SAIC A 400 NODC_DEEP/HH850801.C02
SAIC A 738 NODC_DEEP/HH850731.C01
SAIC A 1100 NODC_DEEP/HH850731.C02
SAIC G 703 NODC_DEEP/HH850801.C03
SAIC G 1565 NODC_DEEP/HH850801.C04
SAIC G 2364 NODC_DEEP/HH850801.C05
SAIC G 3174 NODC_DEEP/HH850801.C06

October - December: Fast Eddy

SAIC Q 300 NODC_DEEP/MG850615.C02
SAIC Q 300 NODC_DEEP/MG851020.C01
SAIC Q 1500 NODC_DEEP/MG850615.C04

Table A-1. Inventory of portions of current records from the Gulf of Mexico during which energetic physical processes or phenomena were present in the Gulf. (continued)

Cyclonic Eddies
August - September
SAIC Q 100 NODC_DEEP/MG850615.C01
SAIC Q 300 NODC_DEEP/MG850615.C02
SAIC Q 1000 NODC_DEEP/MG850615.C03
SAIC Q 1500 NODC_DEEP/MG850615.C04
SAIC S 100 NODC_DEEP/MG850612.C01
SAIC S 300 NODC_DEEP/MG850612.C02
SAIC S 1000 NODC_DEEP/MG850612.C03
June - September
SAIC T 100 NODC_DEEP/MG850613.C01
SAIC T 300 NODC_DEEP/MG850613.C02
SAIC T 1000 NODC_DEEP/MG850613.C03
December - Next April
SAIC T 300 NODC_DEEP/MG850613.C02
SAIC T 1000 NODC_DEEP/MG850613.C03

Deep barotropic events
July - August
SAIC R 100 NODC_DEEP/MG850615.C05
SAIC R 300 NODC_DEEP/MG850615.C06
SAIC R 1000 NODC_DEEP/MG850615.C07
SAIC R 1500 NODC_DEEP/MG850615.C08
SAIC R 3000 NODC_DEEP/MG850615.C09

August
SAIC Q 100 NODC_DEEP/MG850615.C01
SAIC Q 300 NODC_DEEP/MG850615.C02
SAIC Q 1000 NODC_DEEP/MG850615.C03
SAIC Q 1500 NODC_DEEP/MG850615.C04

September - October
SAIC R 100 NODC_DEEP/MG850615.C05
SAIC R 300 NODC_DEEP/MG850615.C06
SAIC R 1000 NODC_DEEP/MG850615.C07
SAIC R 1500 NODC_DEEP/MG850615.C08
SAIC R 3000 NODC_DEEP/MG850615.C09

Deep anticyclonic eddy
Early August
SAIC R 1000 NODC_DEEP/MG850615.C07
SAIC S 1000 NODC_DEEP/MG850612.C03
SAIC P 1000 NODC_DEEP/AC850611.C02
SAIC Q 1000 NODC_DEEP/MG850615.C03

Inertial oscillations and internal waves
11 - 28 June
SAIC P 300 NODC_DEEP/AC850611.C01

1986

Data sets: NODC_DEEP SAIC 5YR A, G, P, Q, R, S, T

Loop Current Eddy separations
January: Hot Core Eddy
SAIC P 1000 NODC_DEEP/AC850611.C02
SAIC P 1500 NODC_DEEP/AC850611.C03
SAIC Q 300 NODC_DEEP/MG851020.C01
SAIC Q 1500 NODC_DEEP/MG850615.C04
SAIC S 750 NODC_DEEP/MG851102.C01
SAIC S 1000 NODC_DEEP/MG850612.C03

Table A-1. Inventory of portions of current records from the Gulf of Mexico during which energetic physical processes or phenomena were present in the Gulf. (continued)

Loop Current Eddy separations (continued)
January: Hot Core Eddy (continued)
SAIC T 300 NODC_DEEP/MG850613.C02
SAIC T 1000 NODC_DEEP/MG850613.C03
SAIC A 172 NODC_DEEP/HH850801.C01
SAIC A 400 NODC_DEEP/HH850801.C02
SAIC A 738 NODC_DEEP/HH850731.C01
SAIC A 1100 NODC_DEEP/HH850731.C02
SAIC G 703 NODC_DEEP/HH850801.C03
SAIC G 1565 NODC_DEEP/HH850801.C04
SAIC G 2364 NODC_DEEP/HH850801.C05
SAIC G 3174 NODC_DEEP/HH850801.C06

Extra-tropical Cyclones
February 6
SAIC P 1000 NODC_DEEP/AC850611.C02
SAIC P 1500 NODC_DEEP/AC850611.C03
SAIC Q 300 NODC_DEEP/MG851020.C01
SAIC Q 1500 NODC_DEEP/MG850615.C04
SAIC S 750 NODC_DEEP/MG851102.C01
SAIC S 1000 NODC_DEEP/MG850612.C03
SAIC T 300 NODC_DEEP/MG850613.C02
SAIC T 1000 NODC_DEEP/MG850613.C03

Loop Current Eddies
January - February: Fast Eddy
SAIC Q 300 NODC_DEEP/MG851020.C01
SAIC Q 1500 NODC_DEEP/MG850615.C04

Cyclonic Eddy
March - April
SAIC Q 300 NODC_DEEP/MG851020.C01
SAIC Q 1500 NODC_DEEP/MG850615.C04

1987

Data sets: NODC_DEEP SAIC 5YR EE, FF, GG
TAMU MAMES C, E

Tropical Cyclones
Tropical Depression ONE 9-17 AUG
SAIC EE 725 NODC_DEEP/GB870405.C05
SAIC FF 1650 NODC_DEEP/KC870406.C04
SAIC GG 1650 NODC_DEEP/AB870406.C03

Hurricane FLOYD 9-14 OCT
SAIC EE 725 NODC_DEEP/GB870405.C05
SAIC FF 1650 NODC_DEEP/KC870406.C04
SAIC GG 1650 NODC_DEEP/AB870406.C03

Loop Current Eddy separations
September: Kathleen
SAIC EE 725 NODC_DEEP/GB870405.C05
SAIC FF 1650 NODC_DEEP/KC870406.C04
SAIC GG 1650 NODC_DEEP/AB870406.C03

Extra-tropical Cyclones
No extra-tropical cyclones identified by Hardy and Hsu (1997)

Table A-1. Inventory of portions of current records from the Gulf of Mexico during which energetic physical processes or phenomena were present in the Gulf. (continued)

1988

Data sets: NODC_DEEP SAIC 5YR EE, FF, GG
TAMU MAMES

Tropical Cyclones
Tropical Storm BERYL 8-10 AUG
SAIC EE 100 NODC_DEEP/GB871108.C01
SAIC EE 300 NODC_DEEP/GB871108.C02
SAIC EE 305 NODC_DEEP/GB871202.C01
SAIC EE 725 NODC_DEEP/GB870405.C05
SAIC FF 100 NODC_DEEP/KC871108.C01
SAIC FF 300 NODC_DEEP/KC880414.C01
SAIC FF 305 NODC_DEEP/KC871108.C02
SAIC FF 725 NODC_DEEP/KC871108.C03
SAIC FF 1650 NODC_DEEP/KC870406.C04
SAIC GG 100 NODC_DEEP/AB871109.C01
SAIC GG 300 NODC_DEEP/AB880409.C01
SAIC GG 725 NODC_DEEP/AB871109.C02
SAIC GG 1650 NODC_DEEP/AB870406.C03
SAIC GG 2500 NODC_DEEP/AB880409.C02

Hurricane DEBBY 31 AUG- 8 SEP
SAIC EE 100 NODC_DEEP/GB871108.C01
SAIC EE 300 NODC_DEEP/GB871108.C02
SAIC EE 305 NODC_DEEP/GB871202.C01
SAIC EE 725 NODC_DEEP/GB870405.C05
SAIC FF 100 NODC_DEEP/KC871108.C01
SAIC FF 300 NODC_DEEP/KC880414.C01
SAIC FF 305 NODC_DEEP/KC871108.C02
SAIC FF 725 NODC_DEEP/KC871108.C03
SAIC FF 1650 NODC_DEEP/KC870406.C04
SAIC GG 100 NODC_DEEP/AB871109.C01
SAIC GG 300 NODC_DEEP/AB880409.C01
SAIC GG 725 NODC_DEEP/AB871109.C02
SAIC GG 1650 NODC_DEEP/AB870406.C03
SAIC GG 2500 NODC_DEEP/AB880409.C02
MAMES C 20 TAMU/DD880825.C01
MAMES C 150 TAMU/DD880825.C02

Hurricane FLORENCE 7-11 SEP
SAIC EE 100 NODC_DEEP/GB871108.C01
SAIC EE 300 NODC_DEEP/GB871108.C02
SAIC EE 305 NODC_DEEP/GB871202.C01
SAIC EE 725 NODC_DEEP/GB870405.C05
SAIC FF 100 NODC_DEEP/KC871108.C01
SAIC FF 300 NODC_DEEP/KC880414.C01
SAIC FF 305 NODC_DEEP/KC871108.C02
SAIC FF 725 NODC_DEEP/KC871108.C03
SAIC FF 1650 NODC_DEEP/KC870406.C04
SAIC GG 100 NODC_DEEP/AB871109.C01
SAIC GG 300 NODC_DEEP/AB880409.C01
SAIC GG 725 NODC_DEEP/AB871109.C02
SAIC GG 1650 NODC_DEEP/AB870406.C03
SAIC GG 2500 NODC_DEEP/AB880409.C02
MAMES C 20 TAMU/DD880825.C01
MAMES C 150 TAMU/DD880825.C02

Hurricane GILBERT 8-20 SEP
SAIC EE 100 NODC_DEEP/GB871108.C01
SAIC EE 300 NODC_DEEP/GB871108.C02
SAIC EE 305 NODC_DEEP/GB871202.C01
SAIC EE 725 NODC_DEEP/GB870405.C05
SAIC FF 725 NODC_DEEP/KC871108.C03

Table A-1. Inventory of portions of current records from the Gulf of Mexico during which energetic physical processes or phenomena were present in the Gulf. (continued)

Tropical Cyclones (continued)
Hurricane GILBERT (continued) 8-20 SEP
SAIC FF 1650 NODC_DEEP/KC870406.C04
SAIC GG 100 NODC_DEEP/AB871109.C01
SAIC GG 300 NODC_DEEP/AB880409.C01
SAIC GG 725 NODC_DEEP/AB871109.C02
SAIC GG 1650 NODC_DEEP/AB870406.C03
SAIC GG 2500 NODC_DEEP/AB880409.C02
MAMES C 20 TAMU/DD880825.C01
MAMES C 150 TAMU/DD880825.C02

Tropical Storm KEITH 17-26 NOV
MAMES C 20 TAMU/DD880825.C01
MAMES C 150 TAMU/DD880825.C02

Loop Current Eddy separations
May: Eddy Murphy
SAIC EE 100 NODC_DEEP/GB871108.C01
SAIC EE 300 NODC_DEEP/GB871108.C02
SAIC EE 305 NODC_DEEP/GB871202.C01
SAIC EE 725 NODC_DEEP/GB870405.C05
SAIC FF 100 NODC_DEEP/KC871108.C01
SAIC FF 300 NODC_DEEP/KC880414.C01
SAIC FF 305 NODC_DEEP/KC871108.C02
SAIC FF 725 NODC_DEEP/KC871108.C03
SAIC FF 1650 NODC_DEEP/KC870406.C04
SAIC GG 100 NODC_DEEP/AB871109.C01
SAIC GG 300 NODC_DEEP/AB880409.C01
SAIC GG 725 NODC_DEEP/AB871109.C02
SAIC GG 1650 NODC_DEEP/AB870406.C03
SAIC GG 2500 NODC_DEEP/AB880409.C02
MAMES C 20 TAMU/DD871230.C01
MAMES C 150 TAMU/DD871230.C02

Extra-tropical Cyclones
No extra-tropical cyclones identified by Hardy and Hsu (1997)

Loop Current Eddies
January - June: Eddy Kathleen
SAIC FF 100 NODC_DEEP/KC871108.C01
SAIC FF 300 NODC_DEEP/KC871109.C01
SAIC FF 300 NODC_DEEP/KC880414.C01
SAIC FF 305 NODC_DEEP/KC871108.C02
SAIC FF 725 NODC_DEEP/KC871108.C03
SAIC FF 1650 NODC_DEEP/KC870406.C04
SAIC GG 100 NODC_DEEP/AB871109.C01
SAIC GG 300 NODC_DEEP/AB880409.C01
SAIC GG 305 NODC_DEEP/AB871110.C01
SAIC GG 725 NODC_DEEP/AB871109.C02
SAIC GG 1650 NODC_DEEP/AB870406.C03
SAIC GG 2500 NODC_DEEP/AB871109.C03
SAIC GG 2500 NODC_DEEP/AB880409.C02

August - October: Eddy Murphy
SAIC FF 100 NODC_DEEP/KC871108.C01
SAIC FF 300 NODC_DEEP/KC880414.C01
SAIC FF 305 NODC_DEEP/KC871108.C02
SAIC FF 725 NODC_DEEP/KC871108.C03
SAIC FF 1650 NODC_DEEP/KC870406.C04
SAIC GG 100 NODC_DEEP/AB871109.C01
SAIC GG 300 NODC_DEEP/AB880409.C01
SAIC GG 725 NODC_DEEP/AB871109.C02
SAIC GG 1650 NODC_DEEP/AB870406.C03
SAIC GG 2500 NODC_DEEP/AB880409.C02

Table A-1. Inventory of portions of current records from the Gulf of Mexico during which energetic physical processes or phenomena were present in the Gulf. (continued)

Deep barotropic events
August
SAIC GG 100 NODC_DEEP/AB871109.C01
SAIC GG 300 NODC_DEEP/AB880409.C01
SAIC GG 725 NODC_DEEP/AB871109.C02
SAIC GG 1650 NODC_DEEP/AB870406.C03
SAIC GG 2500 NODC_DEEP/AB880409.C02

Sub-surface event
July - September
SAIC FF 100 NODC_DEEP/KC871108.C01
SAIC FF 300 NODC_DEEP/KC880414.C01
SAIC FF 305 NODC_DEEP/KC871108.C02
SAIC FF 725 NODC_DEEP/KC871108.C03
SAIC FF 1650 NODC_DEEP/KC870406.C04

1989

Data sets: TAMU MAMES C, E
Additional proprietary data

Tropical Cyclones
Tropical Storm ALLISON 24 JUN - 1 JUL
MAMES C 20 TAMU/DD890621.C01
MAMES C 150 TAMU/DD890621.C02
MAMES C 426 TAMU/DD890621.C03
MAMES E 20 TAMU/VK890623.C01
MAMES E 150 TAMU/VK890623.C02
MAMES E 426 TAMU/VK890623.C03
Additional proprientary data

Hurricane CHANTAL 30 JUL - 3 AUG
MAMES C 20 TAMU/DD890621.C01
MAMES C 150 TAMU/DD890621.C02
MAMES C 426 TAMU/DD890621.C03
MAMES E 150 TAMU/VK890623.C02
MAMES E 426 TAMU/VK890623.C03
Additional proprientary data

Hurricane JERRY 12-16 OCT
MAMES C 150 TAMU/DD890621.C02
MAMES C 426 TAMU/DD890621.C03
MAMES E 150 TAMU/VK890623.C02
MAMES E 426 TAMU/VK890623.C03
Additional proprientary data

Loop Current Eddy separations
May-June Nelson
MAMES C 20 TAMU/DD890216.C01
MAMES C 20 TAMU/DD890621.C01
MAMES C 150 TAMU/DD890216.C02
MAMES C 150 TAMU/DD890621.C02
MAMES C 426 TAMU/DD890216.C03
MAMES C 426 TAMU/DD890621.C03
MAMES E 20 TAMU/VK890623.C01
MAMES E 150 TAMU/VK890623.C02
MAMES E 426 TAMU/VK890623.C03
Additional proprientary data

Extra-tropical Cyclones
No extra-tropical cyclones identified by Hardy and Hsu (1997)

Table A-1. Inventory of portions of current records from the Gulf of Mexico during which energetic physical processes or phenomena were present in the Gulf. (continued)

---

1 9 9 0

Data set: NODC Florida Straits A1, A2, A3, B1, B2, B3, B4

No events

- -

1 9 9 1

Data sets: INDUSTRY EW873A, EW873B, EW873CM
NODC_DEEP Florida Straits A1, A2, A3, B1, B2, B3, B4

Tropical Cyclones
Tropical Storm ANA 29 JUN- 5 JUL
INDUSTRY EW873CM SFC INDUSTRY/EW910630.C01
NODC FS A2 145 NODC_DEEP/FS910502.C01
NODC FS A2 300 NODC_DEEP/FS910502.C02
NODC FS A2 600 NODC_DEEP/FS910502.C03
NODC FS B1 75 NODC_DEEP/FS910502.C04
NODC FS B1 150 NODC_DEEP/FS910502.C05
NODC FS A1 75 NODC_DEEP/FS910503.C01
NODC FS A3 145 NODC_DEEP/FS910504.C01
NODC FS A3 300 NODC_DEEP/FS910504.C02
NODC FS A3 600 NODC_DEEP/FS910504.C03
NODC FS A3 1000 NODC_DEEP/FS910504.C04
NODC FS A3 1000 NODC_DEEP/FS910504.C05
NODC FS B2 75 NODC_DEEP/FS910505.C01
NODC FS B2 200 NODC_DEEP/FS910505.C02

Loop Current Eddy separations
September: Eddy Triton
INDUSTRY EW873A 31-231 INDUSTRY/EW910906.A01-EW910906.A20
INDUSTRY EW873B 23-231 INDUSTRY/EW910920.A01-EW910920.A26

Extra-tropical Cyclones
November 30
INDUSTRY EW873B 23-231 INDUSTRY/EW910920.A01-EW910920.A26

Loop Current Eddies
September - October
INDUSTRY EW873A 31-231 INDUSTRY/EW910906.A01-EW910906.A20
INDUSTRY EW873B 23-231 INDUSTRY/EW910920.A01-EW910920.A26

- -

1 9 9 2

Data sets: TAMU LATEX M12, M49

Tropical Cyclones
Hurricane ANDREW 16-28 AUG
LATEX M12 27 LATEX/GC920415.C01
LATEX M12 115 LATEX/GC920415.C02
LATEX M12 505 LATEX/GC920415.C03
LATEX M49 22 LATEX/EB920409.C01

Loop Current Eddy separations
July: Unchained Eddy
LATEX M12 27 LATEX/GC920415.C01
LATEX M12 115 LATEX/GC920415.C02
LATEX M12 505 LATEX/GC920415.C03
LATEX M49 22 LATEX/EB920409.C01

Table A-1. Inventory of portions of current records from the Gulf of Mexico during which energetic physical processes or phenomena were present in the Gulf. (continued)

Loop Current Eddies
Proprietary data only

Extra-tropical Cyclones
November 4
LATEX M12 19 LATEX/GC921023.C01
LATEX M12 105 LATEX/GC921023.C02
LATEX M12 495 LATEX/GC921022.C01
LATEX M49 17 LATEX/EB921018.C01
LATEX M49 105 LATEX/EB921018.C02
LATEX M49 495 LATEX/EB921018.C03

November 24
LATEX M12 19 LATEX/GC921023.C01
LATEX M12 105 LATEX/GC921023.C02
LATEX M12 495 LATEX/GC921022.C01
LATEX M49 17 LATEX/EB921018.C01
LATEX M49 105 LATEX/EB921018.C02
LATEX M49 495 LATEX/EB921018.C03

December 9
LATEX M12 19 LATEX/GC921023.C01
LATEX M12 105 LATEX/GC921023.C02
LATEX M49 17 LATEX/EB921018.C01
LATEX M49 105 LATEX/EB921018.C02
LATEX M49 495 LATEX/EB921018.C03

December 15
LATEX M12 19 LATEX/GC921023.C01
LATEX M12 105 LATEX/GC921023.C02
LATEX M49 17 LATEX/EB921018.C01
LATEX M49 105 LATEX/EB921018.C02
LATEX M49 495 LATEX/EB921018.C03

Loop Current Eddies
June - September: Eddy Triton
LATEX M49 22 LATEX/EB920409.C01

November - December: Eddy Vazquez
LATEX M49 17 LATEX/EB921018.C01
LATEX M49 105 LATEX/EB921018.C02
LATEX M49 495 LATEX/EB921018.C03

Slope Eddy
May - June
LATEX M12 27 LATEX/GC920415.C01
LATEX M12 115 LATEX/GC920415.C02
LATEX M12 505 LATEX/GC920415.C03

Cyclonic Eddy
October - December
LATEX M12 27 LATEX/GC920415.C01
LATEX M12 505 LATEX/GC920415.C03
LATEX M12 19 LATEX/GC921023.C01
LATEX M12 105 LATEX/GC921023.C02
LATEX M12 495 LATEX/GC921022.C01

Table A-1. Inventory of portions of current records from the Gulf of Mexico during which energetic physical processes or phenomena were present in the Gulf. (continued)

---

1 9 9 3

Data sets: TAMU LATEX M12, M49
INDUSTRY EW1006

Tropical Cyclones
Tropical Storm ARLENE 18-21 JUN
LATEX M12 12 LATEX/GC930112.C01
LATEX M49 101 LATEX/EB930520.C01
LATEX M49 491 LATEX/EB930520.C02

Hurricane GERT 14-21 SEP
LATEX M12 14 LATEX/GC930718.C01
LATEX M12 490 LATEX/GC930718.C02
LATEX M49 101 LATEX/EB930520.C01
LATEX M49 491 LATEX/EB930520.C02
INDUSTRY EW1006 20-460 INDUSTRY/EW930915.A01-EW930915.A56 (15-30 September only)

Loop Current Eddy separations
June: Eddy Whopper
LATEX M12 12 LATEX/GC930112.C01
LATEX M49 101 LATEX/EB930520.C01
LATEX M49 491 LATEX/EB930520.C02

September: X-tra Eddy
LATEX M12 14 LATEX/GC930718.C01
LATEX M12 490 LATEX/GC930718.C02
LATEX M49 101 LATEX/EB930520.C01
LATEX M49 491 LATEX/EB930520.C02
INDUSTRY EW1006 20-460 INDUSTRY/EW930915.A01-EW930915.A56 (15-30 September only)

Extra-tropical Cyclones
February 21
LATEX M12 12 LATEX/GC930112.C01
LATEX M49 491 LATEX/EB930119.C01

March 12 (Storm of the Century)
LATEX M12 12 LATEX/GC930112.C01
LATEX M49 491 LATEX/EB930119.C01

April 8
LATEX M12 12 LATEX/GC930112.C01
LATEX M49 491 LATEX/EB930119.C01

May 12
LATEX M12 12 LATEX/GC930112.C01
LATEX M49 491 LATEX/EB930119.C01

December 20
LATEX M49 12 LATEX/EB931212.C01
LATEX M49 100 LATEX/EB931212.C02
LATEX M49 490 LATEX/EB931212.C03

December 22
LATEX M49 12 LATEX/EB931212.C01
LATEX M49 100 LATEX/EB931212.C02
LATEX M49 490 LATEX/EB931212.C03

Loop Current Eddies
June - August: Eddy Vazquez (north)
LATEX M49 101 LATEX/EB930520.C01
LATEX M49 491 LATEX/EB930520.C02

Table A-1. Inventory of portions of current records from the Gulf of Mexico during which energetic physical processes or phenomena were present in the Gulf. (continued)

Loop Current Eddies (continued)
August Eddy: Eddy Whopper
LATEX M12 14 LATEX/GC930718.C01
LATEX M12 490 LATEX/GC930718.C02

Cyclonic Eddy
September - December
LATEX M49 101 LATEX/EB930520.C01
LATEX M49 100 LATEX/EB931212.C02

Slope Eddy
April
LATEX M12 12 LATEX/GC930112.C01
LATEX M12 98 LATEX/GC930112.C02

- -

1994

Data sets: TAMU LATEX M12, M49
INDUSTRY EW873, GC200
Additional proprietary data

Tropical Cyclones
Tropical Storm ALBERTO 30 JUN- 7 JUL
LATEX M49 10 LATEX/EB940330.C01
LATEX M49 98 LATEX/EB940330.C02

Tropical Storm BERYL 14-19 AUG
LATEX M49 10 LATEX/EB940730.C01
LATEX M49 98 LATEX/EB940730.C02
Additional proprietary data

Hurricane GORDON 8-21 NOV
LATEX M49 10 LATEX/EB940730.C01
LATEX M49 98 LATEX/EB940730.C02
LATEX M49 488 LATEX/EB940730.C03

Loop Current Eddy separations
September: Eddy Yucatan
LATEX M49 10 LATEX/EB940730.C01
LATEX M49 98 LATEX/EB940730.C02

Extra-tropical Cyclones
February 10
LATEX M49 12 LATEX/EB931212.C01
LATEX M49 100 LATEX/EB931212.C02
LATEX M49 490 LATEX/EB931212.C03

March 1
LATEX M49 12 LATEX/EB931212.C01
LATEX M49 100 LATEX/EB931212.C02
LATEX M49 490 LATEX/EB931212.C03
INDUSTRY GC200 31-463 INDUSTRY/GC940212.A01-GC940212.A55

April 22
LATEX M49 10 LATEX/EB940330.C01
LATEX M49 98 LATEX/EB940330.C02
INDUSTRY GC200 31-463 INDUSTRY/GC940212.A01-GC940212.A55

May 3
LATEX M49 10 LATEX/EB940330.C01
LATEX M49 98 LATEX/EB940330.C02
INDUSTRY GC200 31-463 INDUSTRY/GC940212.A01-GC940212.A55

Table A-1. Inventory of portions of current records from the Gulf of Mexico during which energetic physical processes or phenomena were present in the Gulf. (continued)

Extra-tropical Cyclones (continued)
May 13
LATEX M49 10 LATEX/EB940330.C01
LATEX M49 98 LATEX/EB940330.C02

May 16
LATEX M49 10 LATEX/EB940330.C01
LATEX M49 98 LATEX/EB940330.C02

Loop Current Eddies
September - October: Eddy Yucatan
Proprietary data only

Slope Eddies
April
INDUSTRY GC200 31-463 INDUSTRY/GC940212.A01-GC940212.A55

May
INDUSTRY EW873 31-215 INDUSTRY/EW940521.A01-EW940521.A25

Low-frequency Mid-water Intensification
September
Proprietary data only

Subsurface Jets
May
INDUSTRY GC200 31-463 INDUSTRY/GC940212.A01-GC940212.A55

- -

1995

Data sets: INDUSTRY GC200, GC245, MC972
Additional proprietary data

Tropical Cyclones
Hurricane ALLISON 03-06 JUN
Proprietary data only

Tropical Storm DEAN 28-31 JUL
Proprietary data only

Hurricane ERIN 31 JUL-03 AUG
Proprietary data only

Tropical Depression SIX 05-07 AUG
Proprietary data only

Tropical Storm GABRIELLE 09-12 AUG
Proprietary data only

Tropical Storm JERRY 22-25 AUG
Proprietary data only

Hurricane OPAL 27 SEP-05 OCT
Proprietary data only

Hurricane ROXANNE 07-20 OCT
Proprietary data only

Table A-1. Inventory of portions of current records from the Gulf of Mexico during which energetic physical processes or phenomena were present in the Gulf. (continued)

Loop Current Eddy separations
April: Eddy Zapp
Proprietary data only

October: Eddy Aggie
INDUSTRY GC245 29-733 INDUSTRY/GC950907.A01-GC950907.A89
Additional proprietary data

Extra-tropical Cyclones
January 17
Proprietary data only

March 29
Proprietary data only

April 4
Proprietary data only

April 20
Proprietary data only

May 31
Proprietary data only

December 22
Proprietary data only

December 31
Proprietary data only

Loop Current Eddies
April - June: Eddy Zapp
Proprietary data only

July: Eddy Zapp
INDUSTRY GC200 29-941 INDUSTRY/GC950625.A01-GC950625.A90

September-November: Eddy Aggie
Proprietary data only

1996

Data sets: Proprietary data only

Tropical Cyclones
Hurricane DOLLY 19-23 AUG
Proprietary data only

Tropical Storm JOSEPHINE 04-08 OCT
Proprietary data only

Loop Current Eddy separations
April: Biloxi Eddy
Proprietary data only

September: Eddy Creole
Proprietary data only

Table A-1. Inventory of portions of current records from the Gulf of Mexico during which energetic physical processes or phenomena were present in the Gulf. (continued)

Loop Current Eddies
April - July: Eddy Aggie
Proprietary data only
March - May: Biloxi Eddy
Proprietary data only

Slope Eddy
March - July
Proprietary data only

- - -

1997

Data sets: MMS SAIC EIS A2, A3, B2, B3, C2, C3, D2
INDUSTRY AT378, CHEMO, EW1008, GC112A, MC628
Additional proprietary data

Tropical Cyclones
Hurricane DANNY 16-26 JUL
SAICEIS A2 12-76 MMS/VK970710.A01-VK970710.A17
SAICEIS A2 200 MMS/VK970710.C01
SAICEIS A2 300 MMS/VK970710.C02
SAICEIS A2 490 MMS/VK970710.C03
SAICEIS A3 8-72 MMS/MC970710.A01-MC970710.A17
SAICEIS A3 500 MMS/MC970710.C01
SAICEIS A3 1310 MMS/MC970710.C02
SAICEIS B2 16-80 MMS/VK970712.A01-VK970712.A17
SAICEIS B2 200 MMS/VK970712.C01
SAICEIS B2 300 MMS/VK970712.C02
SAICEIS B2 490 MMS/VK970712.C03
SAICEIS B3 16-72 MMS/VK970712.A18-VK970712.A32
SAICEIS B3 500 MMS/VK970712.C04
SAICEIS C2 12-80 MMS/DD970717.A01-DD970717.A18
SAICEIS C2 200 MMS/DD970717.C01
SAICEIS C2 300 MMS/DD970717.C02
SAICEIS C2 490 MMS/DD970717.C03
SAICEIS C3 8-68 MMS/DD970718.A18-DD970718.A33
SAICEIS C3 500 MMS/DD970324.C04
SAICEIS C3 500 MMS/DD970718.C01
SAICEIS C3 1290 MMS/DD970324.C05
SAICEIS D2 8-80 MMS/DD970716.A01-DD970716.A19
SAICEIS D2 200 MMS/DD970324.C07
SAICEIS D2 200 MMS/DD970716.C01
SAICEIS D2 300 MMS/DD970324.C08
SAICEIS D2 490 MMS/DD970324.C09
SAICEIS D2 490 MMS/DD970716.C02
CHEVRON AT378 20-788 INDUSTRY/AT970711.A01-AT970711.A48
Additional proprietary data

Loop Current Eddy separations
October: Eddy El Dorado
SAICEIS A2 12-76 MMS/VK970710.A01-VK970710.A17
SAICEIS A2 200 MMS/VK970710.C01
SAICEIS A2 300 MMS/VK970710.C02
SAICEIS A2 490 MMS/VK970710.C03
SAICEIS A3 8-72 MMS/MC970710.A01-MC970710.A17
SAICEIS A3 500 MMS/MC970710.C01
SAICEIS A3 1310 MMS/MC970710.C02
SAICEIS B2 16-80 MMS/VK970712.A01-VK970712.A17
SAICEIS B2 200 MMS/VK970712.C01
SAICEIS B2 300 MMS/VK970712.C02
SAICEIS B2 490 MMS/VK970712.C03
SAICEIS B3 16-72 MMS/VK970712.A18-VK970712.A32

Table A-1. Inventory of portions of current records from the Gulf of Mexico during which energetic physical processes or phenomena were present in the Gulf. (continued)

Loop Current Eddy separations (continued)
October: Eddy El Dorado (continued)
SAICEIS B3 500 MMS/VK970712.C04
SAICEIS B3 1290 MMS/VK970822.C01
SAICEIS C2 12-80 MMS/DD970717.A01-DD970717.A18
SAICEIS C2 200 MMS/DD970717.C01
SAICEIS C2 300 MMS/DD970717.C02
SAICEIS C2 490 MMS/DD970717.C03
SAICEIS C3 8-68 MMS/DD970718.A18-DD970718.A33
SAICEIS C3 500 MMS/DD970718.C01
SAICEIS D2 8-80 MMS/DD970716.A01-DD970716.A19
SAICEIS D2 490 MMS/DD970324.C09
SAICEIS D2 490 MMS/DD970716.C02
TAMU CHEMO 247 TAMU/GC970809.C01
TAMU CHEMO 537 TAMU/GC970808.C01
INDUSTRY EW1008 31-583 INDUSTRY/EW971022.A01-EW971022.A70
Additional proprietary data

Loop Current Eddies
Eddy: El Dorado
August - December
Proprietary data only

Slope Eddies
Deviant: Eddy
March - August
SAICEIS A2 12-80 MMS/VK970320.A01-VK970320.A18
SAICEIS A2 12-76 MMS/VK970710.A01-VK970710.A17
SAICEIS A2 200 MMS/VK970321.C01
SAICEIS A2 200 MMS/VK970710.C01
SAICEIS A2 300 MMS/VK970321.C02
SAICEIS A2 300 MMS/VK970710.C02
SAICEIS A2 490 MMS/VK970321.C03
SAICEIS A2 490 MMS/VK970710.C03
SAICEIS A3 16-88m MMS/MC970320.A01-MC970320.A19
SAICEIS A3 8-72m MMS/MC970710.A01-MC970710.A17
SAICEIS A3 500 MMS/MC970320.C01
SAICEIS A3 500 MMS/MC970710.C01
SAICEIS A3 1310 MMS/MC970320.C02
SAICEIS A3 1310 MMS/MC970710.C02
SAICEIS B2 16-80 MMS/VK970327.A01-VK970327.A17
SAICEIS B2 16-80 MMS/VK970712.A01-VK970712.A17
SAICEIS B2 200 MMS/VK970328.C01
SAICEIS B2 200 MMS/VK970712.C01
SAICEIS B2 300 MMS/VK970328.C02
SAICEIS B2 300 MMS/VK970712.C02
SAICEIS B2 490 MMS/VK970328.C03
SAICEIS B2 490 MMS/VK970712.C03
SAICEIS B3 16-72 MMS/VK970322.A01-VK970322.A15
SAICEIS B3 16-72 MMS/VK970712.A18-VK970712.A32
SAICEIS B3 500 MMS/VK970322.C01
SAICEIS B3 500 MMS/VK970712.C04
SAICEIS B3 1290 MMS/VK970322.C02
SAICEIS B3 1290 MMS/VK970822.C01
SAICEIS C2 8-80 MMS/DD970324.A01-DD970324.A19
SAICEIS C2 12-80 MMS/DD970717.A01-DD970717.A18
SAICEIS C2 200 MMS/DD970324.C01
SAICEIS C2 200 MMS/DD970717.C01
SAICEIS C2 300 MMS/DD970324.C02
SAICEIS C2 300 MMS/DD970717.C02
SAICEIS C2 490 MMS/DD970324.C03
SAICEIS C2 490 MMS/DD970717.C03
SAICEIS C3 12-72 MMS/DD970324.A20-DD970324.A35
SAICEIS C3 8-68 MMS/DD970718.A18-DD970718.A33

Table A-1. Inventory of portions of current records from the Gulf of Mexico during which energetic physical processes or phenomena were present in the Gulf. (continued)

Slope Eddies (continued)
Deviant: Eddy
March - August (continued)
SAICEIS C3 500 MMS/DD970324.C04
SAICEIS C3 500 MMS/DD970718.C01
SAICEIS C3 1290 MMS/DD970324.C05
Additional proprietary data

April - June
CHEVRON MC628 20-788 INDUSTRY/MC970121.A01-MC970121.A50
Additional proprietary data

April - July
Proprietary data onlyJuly
Proprietary data only

August
Proprietary data only

November - December
SAICEIS A2 12-76 MMS/VK970710.A01-VK970710.A17
SAICEIS A2 12-76 MMS/VK971113.A01-VK971113.A17
SAICEIS A2 200 MMS/VK970710.C01
SAICEIS A2 200 MMS/VK971113.C01
SAICEIS A2 300 MMS/VK970710.C02
SAICEIS A2 300 MMS/VK971113.C02
SAICEIS A2 490 MMS/VK970710.C03
SAICEIS A2 490 MMS/VK971113.C03
SAICEIS A3 8-72 MMS/MC970710.A01-MC970710.A17
SAICEIS A3 8-72 MMS/MC971113.A01-MC971113.A17
SAICEIS A3 500 MMS/MC971114.C01
SAICEIS A3 500 MMS/MC970710.C01
SAICEIS A3 1310 MMS/MC971114.C02
SAICEIS A3 1310 MMS/MC970710.C02
SAICEIS B2 16-80 MMS/VK970712.A01-VK970712.A17
SAICEIS B2 12-80 MMS/VK971115.A01-VK971115.A18
SAICEIS B2 200 MMS/VK970712.C01
SAICEIS B2 200 MMS/VK971115.C01
SAICEIS B2 300 MMS/VK970712.C02
SAICEIS B2 300 MMS/VK971115.C02
SAICEIS B2 490 MMS/VK970712.C03
SAICEIS B2 490 MMS/VK971115.C03
SAICEIS B3 16-72 MMS/VK970712.A18-VK970712.A32
SAICEIS B3 12-72 MMS/VK971115.A19-VK971115.A34
SAICEIS B3 500 MMS/VK970712.C04
SAICEIS B3 500 MMS/VK971115.C04
SAICEIS B3 1290 MMS/VK970822.C01
SAICEIS B3 1290 MMS/VK971115.C05
SAICEIS C2 12-80 MMS/DD970717.A01-DD970717.A18
SAICEIS C2 12-76 MMS/DD971120.A18-DD971120.A34
SAICEIS C2 200 MMS/DD970717.C01
SAICEIS C2 200 MMS/DD971120.C02
SAICEIS C2 300 MMS/DD970717.C02
SAICEIS C2 300 MMS/DD971120.C03
SAICEIS C2 490 MMS/DD970717.C03
SAICEIS C2 490 MMS/DD971120.C04
SAICEIS C3 8-68 MMS/DD970718.A18-DD970718.A33
SAICEIS C3 12-72 MMS/DD971116.A01-DD971116.A16
SAICEIS C3 500 MMS/DD970718.C01
SAICEIS C3 500 MMS/DD971116.C01
SAICEIS C3 1290 MMS/DD971116.C02
SAICEIS D2 8-80 MMS/DD970716.A01-DD970716.A19
SAICEIS D2 12-80 MMS/DD971118.A01-DD971118.A18
SAICEIS D2 490 MMS/DD970324.C09

Table A-1. Inventory of portions of current records from the Gulf of Mexico during which energetic physical processes or phenomena were present in the Gulf. (continued)

Slope Eddies (continued)
Deviant: Eddy
November - December (continued)
SAICEIS D2 490 MMS/DD970716.C02
SAICEIS D2 200 MMS/DD970324.C09
SAICEIS D2 200 MMS/DD971118.C01
SAICEIS D2 300 MMS/DD970324.C09
SAICEIS D2 300 MMS/DD971118.C02
SAICEIS D2 490 MMS/DD970324.C09
SAICEIS D2 490 MMS/DD971118.C03
INDUSTRY EW1008 31-583 INDUSTRY/EW971022.A01-EW971022.A70

Bottom Intensification
Proprietary data only

Cyclonic Eddy
February
Proprietary data only

Low-frequency Mid-water Intensification
July
Proprietary data only
September
Proprietary data only
October
Proprietary data only

Subsurface Jets
February
Proprietary data only
April
CHEVRON MC628 20-788 INDUSTRY/MC970121.A01-MC970121.A50
November
Proprietary data only

1998

Data sets: INDUSTRY AT118, GC112A, GC112B, GC236
MMS SAIC EIS A2, A3, B2, B3, C2, C3, D2
TAMU TAMUMC
Additional proprietary data

Tropical Cyclones
Tropical Storm CHARLEY 21-22 AUG
SAICEIS A2 0-80 MMS/VK980806.A01-VK980806.A18
SAICEIS A2 200 MMS/VK980806.C01
SAICEIS A2 300 MMS/VK980806.C02
SAICEIS A2 490 MMS/VK980806.C03
SAICEIS A3 0-80 MMS/MC980806.A01-MC980806.A16
SAICEIS A3 500 MMS/MC980806.C01
SAICEIS A3 1310 MMS/MC980806.C02
SAICEIS B2 0-80 MMS/VK980807.A01-VK980807.A18
SAICEIS B2 200 MMS/VK980807.C01
SAICEIS B2 300 MMS/VK980807.C02
SAICEIS B2 490 MMS/VK980807.C03
SAICEIS B3 0-80 MMS/VK980807.A19-VK980807.A34
SAICEIS B3 500 MMS/VK980807.C04
SAICEIS B3 1290 MMS/VK980807.C01
SAICEIS C2 0-80 MMS/DD980812.A01-DD980812.A18
SAICEIS C2 200 MMS/DD980812.C01
SAICEIS C2 300 MMS/DD980812.C02
SAICEIS C2 490 MMS/DD980812.C03

Table A-1. Inventory of portions of current records from the Gulf of Mexico during which energetic physical processes or phenomena were present in the Gulf. (continued)

Tropical Cyclones (continued)
Tropical Storm CHARLEY (continued) 21-22 AUG
SAICEIS C3 0-80 MMS/DD980808.A01-DD980808.A16
SAICEIS C3 500 MMS/DD980808.C01
SAICEIS C3 1290 MMS/DD980808.C02
SAICEIS D2 0-80 MMS/DD980810.A01-DD980810.A18
SAICEIS D2 200 MMS/DD980810.C01
SAICEIS D2 300 MMS/DD980810.C02
SAICEIS D2 490 MMS/DD980810.C03
INDUSTRY TAMUMC 297 TAMU/EW980806.C01
CHEVRON AT118 0-786 INDUSTRY/AT980814.A01-AT980814.A42
Additional proprietary data

Hurricane EARL 31 AUG-03 SEP
SAICEIS A2 0-80 MMS/VK980806.A01-VK980806.A18
SAICEIS A2 200 MMS/VK980806.C01
SAICEIS A2 300 MMS/VK980806.C02
SAICEIS A2 490 MMS/VK980806.C03
SAICEIS A3 0-80 MMS/MC980806.A01-MC980806.A16
SAICEIS A3 500 MMS/MC980806.C01
SAICEIS A3 1310 MMS/MC980806.C02
SAICEIS B2 0-80 MMS/VK980807.A01-VK980807.A18
SAICEIS B2 200 MMS/VK980807.C01
SAICEIS B2 300 MMS/VK980807.C02
SAICEIS B2 490 MMS/VK980807.C03
SAICEIS B3 0-80 MMS/VK980807.A19-VK980807.A34
SAICEIS B3 500 MMS/VK980807.C04
SAICEIS B3 1290 MMS/VK980807.C01
SAICEIS C2 0-80 MMS/DD980812.A01-DD980812.A18
SAICEIS C2 200 MMS/DD980812.C01
SAICEIS C2 300 MMS/DD980812.C02
SAICEIS C2 490 MMS/DD980812.C03
SAICEIS C3 0-80 MMS/DD980808.A01-DD980808.A16
SAICEIS C3 500 MMS/DD980808.C01
SAICEIS C3 1290 MMS/DD980808.C02
SAICEIS D2 0-80 MMS/DD980810.A01-DD980810.A18
SAICEIS D2 200 MMS/DD980810.C01
SAICEIS D2 300 MMS/DD980810.C02
SAICEIS D2 490 MMS/DD980810.C03
TAMU TAMUMC 297 TAMU/EW980806.C01
Additional proprietary data

Tropical Storm FRANCES 08-12 SEP
SAICEIS A2 0-80 MMS/VK980806.A01-VK980806.A18
SAICEIS A2 200 MMS/VK980806.C01
SAICEIS A2 300 MMS/VK980806.C02
SAICEIS A2 490 MMS/VK980806.C03
SAICEIS A3 0-80 MMS/MC980806.A01-MC980806.A16
SAICEIS A3 500 MMS/MC980806.C01
SAICEIS A3 1310 MMS/MC980806.C02
SAICEIS B2 0-80 MMS/VK980807.A01-VK980807.A18
SAICEIS B2 200 MMS/VK980807.C01
SAICEIS B2 300 MMS/VK980807.C02
SAICEIS B2 490 MMS/VK980807.C03
SAICEIS B3 0-80 MMS/VK980807.A19-VK980807.A34
SAICEIS B3 500 MMS/VK980807.C04
SAICEIS B3 1290 MMS/VK980807.C01
SAICEIS C2 0-80 MMS/DD980812.A01-DD980812.A18
SAICEIS C2 200 MMS/DD980812.C01
SAICEIS C2 300 MMS/DD980812.C02
SAICEIS C2 490 MMS/DD980812.C03
SAICEIS C3 0-80 MMS/DD980808.A01-DD980808.A16
SAICEIS C3 500 MMS/DD980808.C01
SAICEIS C3 1290 MMS/DD980808.C02

Table A-1. Inventory of portions of current records from the Gulf of Mexico during which energetic physical processes or phenomena were present in the Gulf. (continued)

Tropical Cyclones (continued)
Tropical Storm FRANCES (continued) 08-12 SEP
SAICEIS D2 0-80 MMS/DD980810.A01-DD980810.A18
SAICEIS D2 200 MMS/DD980810.C01
SAICEIS D2 300 MMS/DD980810.C02
SAICEIS D2 490 MMS/DD980810.C03
TAMU TAMUMC 297 TAMU/EW980806.C01
Additional proprietary data

Hurricane GEORGES 15-29 SEP
SAICEIS A2 0-80 MMS/VK980806.A01-VK980806.A18
SAICEIS A2 200 MMS/VK980806.C01
SAICEIS A2 300 MMS/VK980806.C02
SAICEIS A2 490 MMS/VK980806.C03
SAICEIS A3 0-80 MMS/MC980806.A01-MC980806.A16
SAICEIS A3 500 MMS/MC980806.C01
SAICEIS A3 1310 MMS/MC980806.C02
SAICEIS B2 0-80 MMS/VK980807.A01-VK980807.A18
SAICEIS B2 200 MMS/VK980807.C01
SAICEIS B2 300 MMS/VK980807.C02
SAICEIS B2 490 MMS/VK980807.C03
SAICEIS B3 0-80 MMS/VK980807.A19-VK980807.A34
SAICEIS B3 500 MMS/VK980807.C04
SAICEIS B3 1290 MMS/VK980807.C01
SAICEIS C2 0-80 MMS/DD980812.A01-DD980812.A18
SAICEIS C2 200 MMS/DD980812.C01
SAICEIS C2 300 MMS/DD980812.C02
SAICEIS C2 490 MMS/DD980812.C03
SAICEIS C3 0-80 MMS/DD980808.A01-DD980808.A16
SAICEIS C3 500 MMS/DD980808.C01
SAICEIS C3 1290 MMS/DD980808.C02
SAICEIS D2 0-80 MMS/DD980810.A01-DD980810.A18
SAICEIS D2 200 MMS/DD980810.C01
SAICEIS D2 300 MMS/DD980810.C02
SAICEIS D2 490 MMS/DD980810.C03
TAMU TAMUMC 297 TAMU/EW980806.C01
Additional proprietary data

Tropical Storm HERMINE 17-20 SEP
SAICEIS A2 0-80 MMS/VK980806.A01-VK980806.A18
SAICEIS A2 200 MMS/VK980806.C01
SAICEIS A2 300 MMS/VK980806.C02
SAICEIS A2 490 MMS/VK980806.C03
SAICEIS A3 0-80 MMS/MC980806.A01-MC980806.A16
SAICEIS A3 500 MMS/MC980806.C01
SAICEIS A3 1310 MMS/MC980806.C02
SAICEIS B2 0-80 MMS/VK980807.A01-VK980807.A18
SAICEIS B2 200 MMS/VK980807.C01
SAICEIS B2 300 MMS/VK980807.C02
SAICEIS B2 490 MMS/VK980807.C03
SAICEIS B3 0-80 MMS/VK980807.A19-VK980807.A34
SAICEIS B3 500 MMS/VK980807.C04
SAICEIS B3 1290 MMS/VK980807.C01
SAICEIS C2 0-80 MMS/DD980812.A01-DD980812.A18
SAICEIS C2 200 MMS/DD980812.C01
SAICEIS C2 300 MMS/DD980812.C02
SAICEIS C2 490 MMS/DD980812.C03
SAICEIS C3 0-80 MMS/DD980808.A01-DD980808.A16
SAICEIS C3 500 MMS/DD980808.C01
SAICEIS C3 1290 MMS/DD980808.C02
SAICEIS D2 0-80 MMS/DD980810.A01-DD980810.A18
SAICEIS D2 200 MMS/DD980810.C01
SAICEIS D2 300 MMS/DD980810.C02
SAICEIS D2 490 MMS/DD980810.C03

Table A-1. Inventory of portions of current records from the Gulf of Mexico during which energetic physical processes or phenomena were present in the Gulf. (continued)

Tropical Cyclones (continued)
Tropical Storm HERMINE (continued) 17-20 SEP
TAMU TAMUMC 297 TAMU/EW980806.C01
Additional proprietary data

Hurricane MITCH 22 OCT-05 NOV
SAICEIS A2 0-80 MMS/VK980806.A01-VK980806.A18
SAICEIS A2 200 MMS/VK980806.C01
SAICEIS A2 300 MMS/VK980806.C02
SAICEIS A2 490 MMS/VK980806.C03
SAICEIS A3 0-80 MMS/MC980806.A01-MC980806.A16
SAICEIS A3 500 MMS/MC980806.C01
SAICEIS A3 1310 MMS/MC980806.C02
SAICEIS B2 0-80 MMS/VK980807.A01-VK980807.A18
SAICEIS B2 300 MMS/VK980807.C02
SAICEIS B2 490 MMS/VK980807.C03
SAICEIS B3 0-80 MMS/VK980807.A19-VK980807.A34
SAICEIS B3 500 MMS/VK980807.C04
SAICEIS B3 1290 MMS/VK980807.C01
SAICEIS C2 0-80 MMS/DD980812.A01-DD980812.A18
SAICEIS C2 200 MMS/DD980812.C01
SAICEIS C2 300 MMS/DD980812.C02
SAICEIS C2 490 MMS/DD980812.C03
SAICEIS C3 0-80 MMS/DD980808.A01-DD980808.A16
SAICEIS C3 500 MMS/DD980808.C01
SAICEIS C3 1290 MMS/DD980808.C02
SAICEIS D2 0-80 MMS/DD980810.A01-DD980810.A18
SAICEIS D2 200 MMS/DD980810.C01
SAICEIS D2 300 MMS/DD980810.C02
SAICEIS D2 490 MMS/DD980810.C03
TAMU TAMUMC 297 TAMU/EW980806.C01
CHEVRON AT118 0-786 INDUSTRY/AT980814.A01-AT980814.A46
Additional proprietary data

Loop Current Eddy separations
March: Eddy Fourchon
TAMU CHEMO 247 TAMU/GC970809.C01
TAMU CHEMO 537 TAMU/GC970808.C01
SAICEIS A2 0-80 MMS/VK971113.A01-VK971113.A17
SAICEIS A2 300 MMS/VK971113.C02
SAICEIS A2 490 MMS/VK971113.C03
SAICEIS A3 0-80 MMS/MC971113.A01-MC971113.A17
SAICEIS A3 500 MMS/MC971114.C01
SAICEIS A3 1310 MMS/MC971114.C02
SAICEIS B2 0-80 MMS/VK971115.A01-VK971115.A18
SAICEIS B2 200 MMS/VK971115.C01
SAICEIS B2 300 MMS/VK971115.C02
SAICEIS B2 490 MMS/VK971115.C03
SAICEIS B3 0-80 MMS/VK971115.A19-VK971115.A34
SAICEIS B3 500 MMS/VK971115.C04
SAICEIS B3 1290 MMS/VK971115.C05
SAICEIS C2 0-80 MMS/DD971120.A18-DD971120.A34
SAICEIS C2 200 MMS/DD971120.C02
SAICEIS C2 300 MMS/DD971120.C03
SAICEIS C2 490 MMS/DD971120.C04
SAICEIS C3 0-80 MMS/DD971116.A01-DD971116.A16
SAICEIS C3 500 MMS/DD971116.C01
SAICEIS C3 1290 MMS/DD971116.C02
SAICEIS D2 0-80 MMS/DD971118.A01-DD971118.A18
SAICEIS D2 200 MMS/DD971118.C01
SAICEIS D2 300 MMS/DD971118.C02
SAICEIS D2 490 MMS/DD971118.C03
Additional proprietary data

Table A-1. Inventory of portions of current records from the Gulf of Mexico during which energetic physical processes or phenomena were present in the Gulf. (continued)

Loop Current Eddies
Eddy Fourchon
March - April
Proprietary data only
May - June
Proprietary data only
May - July
Proprietary data only

Slope Eddies
January
SAICEIS A3 0-80 MMS/MC971113.A01-MC971113.A17
SAICEIS A3 500 MMS/MC971114.C01
SAICEIS A3 1310 MMS/MC971114.C02
SAICEIS B3 0-80 MMS/VK971115.A19-VK971115.A34
SAICEIS B3 500 MMS/VK971115.C04
SAICEIS B3 1290 MMS/VK971115.C05
SAICEIS C3 0-80 MMS/DD971116.A01-DD971116.A16
SAICEIS C3 500 MMS/DD971116.C01
SAICEIS C3 1290 MMS/DD971116.C02
INDUSTRY GC112A 31-535 INDUSTRY/GC971228.A01-GC971228.A64
INDUSTRY GC112B 31-535 INDUSTRY/GC980128.A01-GC980128.A64

April - September: Eddy Gyre
SAICEIS A3 0-80 MMS/MC971113.A01-MC971113.A17
SAICEIS A3 0-80 MMS/MC980402.A01-MC980402.A17
SAICEIS A3 0-80 MMS/MC980806.A01-MC980806.A16
SAICEIS A3 500 MMS/MC971114.C01
SAICEIS A3 500 MMS/MC980402.C01
SAICEIS A3 500 MMS/MC980806.C01
SAICEIS A3 1310 MMS/MC971114.C02
SAICEIS A3 1310 MMS/MC980402.C02
SAICEIS A3 1310 MMS/MC980806.C02
SAICEIS B3 0-80 MMS/VK971115.A19-VK971115.A34
SAICEIS B3 0-80 MMS/VK980403.A01-VK980403.A16
SAICEIS B3 0-80 MMS/VK980807.A19-VK980807.A34
SAICEIS B3 500 MMS/VK971115.C04
SAICEIS B3 500 MMS/VK980403.C01
SAICEIS B3 500 MMS/VK980807.C04
SAICEIS B3 1290 MMS/VK971115.C05
SAICEIS B3 1290 MMS/VK980403.C02
SAICEIS B3 1290 MMS/VK980807.C01
SAICEIS C3 0-80 MMS/DD971116.A01-DD971116.A16
SAICEIS C3 0-80 MMS/DD980405.A01-DD980405.A17
SAICEIS C3 0-80 MMS/DD980808.A01-DD980808.A16
SAICEIS C3 500 MMS/DD971116.C01
SAICEIS C3 500 MMS/DD980405.C01
SAICEIS C3 500 MMS/DD980808.C01
SAICEIS C3 1290 MMS/DD971116.C02
SAICEIS C3 1290 MMS/DD980405.C02
SAICEIS C3 1290 MMS/DD980808.C02
August
CHEVRON AT118 0-786 INDUSTRY/AT980814.A01-AT980814.A46

Cyclonic Eddies
February - April
SAICEIS A3 0-80 MMS/MC971113.A01-MC971113.A17
SAICEIS A3 0-80 MMS/MC980402.A01-MC980402.A17
SAICEIS A3 500 MMS/MC971114.C01
SAICEIS A3 500 MMS/MC980402.C01
SAICEIS A3 1310 MMS/MC971114.C02
SAICEIS A3 1310 MMS/MC980402.C02

Table A-1. Inventory of portions of current records from the Gulf of Mexico during which energetic physical processes or phenomena were present in the Gulf. (continued)

Cyclonic Eddies (continued)
February–April (continued)
SAICEIS B3 0-80 MMS/VK971115.A19-VK971115.A34
SAICEIS B3 0-80 MMS/VK980403.A01-VK980403.A16
SAICEIS B3 500 MMS/VK971115.C04
SAICEIS B3 500 MMS/VK980403.C01
SAICEIS B3 1290 MMS/VK971115.C05
SAICEIS B3 1290 MMS/VK980403.C02
SAICEIS C3 0-80 MMS/DD971116.A01-DD971116.A16
SAICEIS C3 0-80 MMS/DD980405.A01-DD980405.A17
SAICEIS C3 500 MMS/DD971116.C01
SAICEIS C3 500 MMS/DD980405.C01
SAICEIS C3 1290 MMS/DD971116.C02
SAICEIS C3 1290 MMS/DD980405.C02
April - May
CHEVRON GC236 0-788 INDUSTRY/GC980409.A01-39
July - October
Proprietary data only
August - October
Proprietary data only
October - November
CHEVRON AT118 0-788 INDUSTRY/AT980814.A01-AT980814.A46

Bottom Intensification
September - October
SAICEIS C2 0-80 MMS/DD980812.A01-DD980812.A18
SAICEIS C2 200 MMS/DD980812.C01
SAICEIS C2 300 MMS/DD980812.C02
SAICEIS C2 490 MMS/DD980812.C03
SAICEIS C3 0-80 MMS/DD980808.A01-DD980808.A16
SAICEIS C3 500 MMS/DD980808.C01
SAICEIS C3 1310 MMS/DD980808.C02
May
Proprietary data only

Low-frequency Mid-water Intensification
August - September
Proprietary data only
November
Proprietary data only

Subsurface Jets
September
SAICEIS C3 0-80 MMS/DD980808.A01-DD980808.A16
SAICEIS C3 500 MMS/DD980808.C01
SAICEIS C3 1310 MMS/DD980808.C02
Additional proprietary data

1999

Data sets: TAMU CHEMO
MMS SAIC EIS A2, A3, B2, B3, C2, C3, D2
MMS EIS Extension Study I1, I2, I3
Additional proprietary data

Tropical Cyclones
Hurricane BRET 18-23 AUG
EISEXT I1 16-1130 MMS/AT990829.A01-AT990829.Ah5
EISEXT I1 800 MMS/AT990829.C01
EISEXT I1 1000 MMS/AT000225.C02
EISEXT I1 1200 MMS/AT990829.C03
EISEXT I1 1400 MMS/AT990829.C04

Table A-1. Inventory of portions of current records from the Gulf of Mexico during which energetic physical processes or phenomena were present in the Gulf. (continued)

Tropical Cyclones (continued)
Hurricane BRET (continued) 18-23 AUG
EISEXT I1 1600 MMS/AT990829.C05
EISEXT I1 1800 MMS/AT990829.C06
EISEXT I1 1989 MMS/AT990829.C07
EISEXT I3 1775 MMS/AT990829.C08
EISEXT I3 1975 MMS/AT990829.C09
EISEXT I3 2164 MMS/AT990829.C10
EISEXT I2 1600 MMS/GC990829.C01
EISEXT I2 1800 MMS/GC990829.C02
EISEXT I2 1989 MMS/GC990829.C03
Additional proprietary data

Tropical Depression SEVEN 05-07 SEP
EISEXT I1 16-1130 MMS/AT990829.A01-AT990829.Ah5
EISEXT I1 800 MMS/AT990829.C01
EISEXT I1 1000 MMS/AT000225.C02
EISEXT I1 1200 MMS/AT990829.C03
EISEXT I1 1400 MMS/AT990829.C04
EISEXT I1 1600 MMS/AT990829.C05
EISEXT I1 1800 MMS/AT990829.C06
EISEXT I1 1989 MMS/AT990829.C07
EISEXT I3 1775 MMS/AT990829.C08
EISEXT I3 1975 MMS/AT990829.C09
EISEXT I3 2164 MMS/AT990829.C10
EISEXT I2 1600 MMS/GC990829.C01
EISEXT I2 1800 MMS/GC990829.C02
EISEXT I2 1989 MMS/GC990829.C03

Tropical Storm HARVEY 19-22 SEP
EISEXT I1 16-1130 MMS/AT990829.A01-AT990829.Ah5
EISEXT I1 800 MMS/AT990829.C01
EISEXT I1 1000 MMS/AT000225.C02
EISEXT I1 1200 MMS/AT990829.C03
EISEXT I1 1400 MMS/AT990829.C04
EISEXT I1 1600 MMS/AT990829.C05
EISEXT I1 1800 MMS/AT990829.C06
EISEXT I1 1989 MMS/AT990829.C07
EISEXT I3 1775 MMS/AT990829.C08
EISEXT I3 1975 MMS/AT990829.C09
EISEXT I3 2164 MMS/AT990829.C10
EISEXT I2 1600 MMS/GC990829.C01
EISEXT I2 1800 MMS/GC990829.C02
EISEXT I2 1989 MMS/GC990829.C03

Tropical Depression ELEVEN 04-06 OCT
EISEXT I1 16-1130 MMS/AT990829.A01-AT990829.Ah5
EISEXT I1 800 MMS/AT990829.C01
EISEXT I1 1000 MMS/AT000225.C02
EISEXT I1 1200 MMS/AT990829.C03
EISEXT I1 1400 MMS/AT990829.C04
EISEXT I1 1600 MMS/AT990829.C05
EISEXT I1 1800 MMS/AT990829.C06
EISEXT I1 1989 MMS/AT990829.C07
EISEXT I3 1775 MMS/AT990829.C08
EISEXT I3 1975 MMS/AT990829.C09
EISEXT I3 2164 MMS/AT990829.C10
EISEXT I2 1600 MMS/GC990829.C01
EISEXT I2 1800 MMS/GC990829.C02
EISEXT I2 1989 MMS/GC990829.C03

Table A-1. Inventory of portions of current records from the Gulf of Mexico during which energetic physical processes or phenomena were present in the Gulf. (continued)

Tropical Cyclones (continued)

Hurricane IRENE 13-19 OCT

EISEXT I1 16-1130 MMS/AT990829.A01-AT990829.Ah5
EISEXT I1 800 MMS/AT990829.C01
EISEXT I1 1000 MMS/AT000225.C02
EISEXT I1 1200 MMS/AT990829.C03
EISEXT I1 1400 MMS/AT990829.C04
EISEXT I1 1600 MMS/AT990829.C05
EISEXT I1 1800 MMS/AT990829.C06
EISEXT I1 1989 MMS/AT990829.C07
EISEXT I3 1775 MMS/AT990829.C08
EISEXT I3 1975 MMS/AT990829.C09
EISEXT I3 2164 MMS/AT990829.C10
EISEXT I2 1600 MMS/GC990829.C01
EISEXT I2 1800 MMS/GC990829.C02
EISEXT I2 1989 MMS/GC990829.C03

Tropical Storm KATRINA 28 OCT-01 NOV

EISEXT I1 16-1130 MMS/AT990829.A01-AT990829.Ah5
EISEXT I1 800 MMS/AT990829.C01
EISEXT I1 1000 MMS/AT000225.C02
EISEXT I1 1200 MMS/AT990829.C03
EISEXT I1 1400 MMS/AT990829.C04
EISEXT I1 1600 MMS/AT990829.C05
EISEXT I1 1800 MMS/AT990829.C06
EISEXT I1 1989 MMS/AT990829.C07
EISEXT I3 1775 MMS/AT990829.C08
EISEXT I3 1975 MMS/AT990829.C09
EISEXT I3 2164 MMS/AT990829.C10
EISEXT I2 1600 MMS/GC990829.C01
EISEXT I2 1800 MMS/GC990829.C02
EISEXT I2 1989 MMS/GC990829.C03

Loop Current Eddy separations

August: Indigo

EISEXT I1 16-1130 MMS/AT990829.A01-AT990829.Ah5
EISEXT I1 800 MMS/AT990829.C01
EISEXT I1 1000 MMS/AT000225.C02
EISEXT I1 1200 MMS/AT990829.C03
EISEXT I1 1400 MMS/AT990829.C04
EISEXT I1 1600 MMS/AT990829.C05
EISEXT I1 1800 MMS/AT990829.C06
EISEXT I1 1989 MMS/AT990829.C07
EISEXT I3 1775 MMS/AT990829.C08
EISEXT I3 1975 MMS/AT990829.C09
EISEXT I3 2164 MMS/AT990829.C10
EISEXT I2 1600 MMS/GC990829.C01
EISEXT I2 1800 MMS/GC990829.C02
EISEXT I2 1989 MMS/GC990829.C03
Additional proprietary data

October: Juggernaut

EISEXT I1 16-1130 MMS/AT990829.A01-AT990829.Ah5
EISEXT I1 800 MMS/AT990829.C01
EISEXT I1 1000 MMS/AT000225.C02
EISEXT I1 1200 MMS/AT990829.C03
EISEXT I1 1400 MMS/AT990829.C04
EISEXT I1 1600 MMS/AT990829.C05
EISEXT I1 1800 MMS/AT990829.C06
EISEXT I1 1989 MMS/AT990829.C07
EISEXT I3 1775 MMS/AT990829.C08
EISEXT I3 1975 MMS/AT990829.C09
EISEXT I3 2164 MMS/AT990829.C10
EISEXT I2 1600 MMS/GC990829.C01

Table A-1. Inventory of portions of current records from the Gulf of Mexico during which energetic physical processes or phenomena were present in the Gulf. (continued)

Loop Current Eddy separations (continued)
October: Juggernaut (continued)
EISEXT I2 1800 MMS/GC990829.C02
EISEXT I2 1989 MMS/GC990829.C03

Loop Current Eddies
Juggernaut
EISEXT I1 16-1130 MMS/AT990829.A01-AT990829.Ah5
EISEXT I1 800 MMS/AT990829.C01
EISEXT I1 1000 MMS/AT000225.C02
EISEXT I1 1200 MMS/AT990829.C03
EISEXT I1 1400 MMS/AT990829.C04
EISEXT I1 1600 MMS/AT990829.C05
EISEXT I1 1800 MMS/AT990829.C06
EISEXT I1 1989 MMS/AT990829.C07
EISEXT I3 1775 MMS/AT990829.C08
EISEXT I3 1975 MMS/AT990829.C09
EISEXT I3 2164 MMS/AT990829.C10
EISEXT I2 1600 MMS/GC990829.C01
EISEXT I2 1800 MMS/GC990829.C02
EISEXT I2 1989 MMS/GC990829.C03
Additional proprietary data

2000

Data Sets: MMS EIS Extension Study I1, I2, I3

Tropical Cyclones
Tropical Depression ONE 07-08 JUN
EISEXT I1 16-1066 MMS/AT000225.A01-AT000225.Ad3
EISEXT I1 452 MMS/AT000225.C01
EISEXT I1 800 MMS/AT000225.C02
EISEXT I1 1000 MMS/AT000225.C03
EISEXT I1 1200 MMS/AT000225.C04
EISEXT I1 1400 MMS/AT000225.C05
EISEXT I1 1600 MMS/AT000225.C06
EISEXT I1 1800 MMS/AT000225.C07
EISEXT I2 1600 MMS/GC000203.C01
EISEXT I2 1800 MMS/GC000203.C02
EISEXT I2 1989 MMS/GC000203.C03
EISEXT I3 1775 MMS/AT000224.C01
EISEXT I3 1975 MMS/AT000224.C02
EISEXT I3 2164 MMS/AT000224.C03

Tropical Storm BERYL 13-15 AUG
EISEXT I1 16-1066 MMS/AT000225.A01-AT000225.Ad3
EISEXT I1 452 MMS/AT000225.C01
EISEXT I1 800 MMS/AT000225.C02
EISEXT I1 1000 MMS/AT000225.C03
EISEXT I1 1200 MMS/AT000225.C04
EISEXT I1 1400 MMS/AT000225.C05
EISEXT I1 1600 MMS/AT000225.C06
EISEXT I1 1800 MMS/AT000225.C07
EISEXT I2 1600 MMS/GC000203.C01
EISEXT I2 1800 MMS/GC000203.C02
EISEXT I2 1989 MMS/GC000203.C03
EISEXT I3 1775 MMS/AT000224.C01
EISEXT I3 1975 MMS/AT000224.C02
EISEXT I3 2164 MMS/AT000224.C03

APPENDIX B: SPEED STATISTICS FOR ENERGETIC CURRENT EVENTS

This appendix contains tables that give the specific data files, time periods, locations, and speed statistics for each energetic current event identified in the non-proprietary current measurement data sets. Speed statistics are maximum speed, mean speed, and standard deviation of speed for the time period over which the event was occurring. Event duration was determined mainly in a subjective fashion by examination of the unfiltered (when available) current records. Also given are brief discussions of the characteristics of the event. Events are illustrated by references to the main body of this report and/or by new figures showing vector time series.

The energetic current events are classed into ten categories. One table is given for each event category. The categories and associated tables are:

Loop Current intrusion	Table B-1
Loop Current eddy separations	Table B-2
Loop Current eddies	Table B-3
Anticyclonic slope eddies	Table B-4
Cyclonic eddies	Table B-5
Tropical cyclones	Table B-6
Extratropical cyclones	Table B-7
Deep barotropic/bottom intensified motions	Table B-8
Deep anticyclonic eddy	Table B-9
Subsurface mid-water column jets	Table B-10

Energetic current events associated with the Loop Current itself are discussed in Section 6.3 as part of the Straits of Florida moorings and SAIC 5-year study moorings A and G.

Each table lists in chronological order the statistics for every event of the category type. The filename of the record containing the data of interest and the directory in which the file can be found are keyed to the CD-ROM database. The time period used to calculate the statistics are given by the event start and end dates. These are followed by the three speed statistics, the measurement location, the depth of the measurement, and the total water depth at the site.

Table B-1. Speed statistics for energetic current events associated with intrusions of the Loop Current. Given are the name of the file containing the event (keyed to the directory on the CD-ROM database), the start and stop dates used to characterize the event, maximum speed, mean speed, standard deviation of speed, mooring location, depth of the instrument, and total water depth. Comments on the event, keyed by the event number, are given in the notes below the table.

Event No.	Year	Filename	Directory	Event start date (m/d/y)	Event end date (m/d/y)	Maximum speed ($cm \cdot s^{-1}$)	Mean speed ($cm \cdot s^{-1}$)	Stand. dev. of speed ($cm \cdot s^{-1}$)	Latitude (°N)	Longitude (°W)	Depth (m)	Total water depth (m)
1	1978	EL780612.C01	/NODC_DEEP/	09/01/1978	10/25/1978	69.220	15.021	11.459	27.6633	85.5167	153.0	1050.0
	1978	EL780612.C02	/NODC_DEEP/	09/01/1978	10/25/1978	31.091	13.067	4.321	27.6633	85.5167	549.0	1050.0
	1978	EL780612.C03	/NODC_DEEP/	09/01/1978	10/25/1978	24.424	7.264	4.715	27.6633	85.5167	950.0	1050.0
	1978	EL781026.C01	/NODC_DEEP/	11/01/1978	11/10/1978	36.704	25.445	5.499	27.6633	85.5217	157.0	1050.0
	1978	EL781026.C02	/NODC_DEEP/	11/01/1978	11/10/1978	27.347	19.209	2.971	27.6650	85.5217	257.0	1050.0
	1978	EL781026.C03	/NODC_DEEP/	11/01/1978	11/10/1978	19.841	7.230	3.855	27.6633	85.5217	957.0	1050.0
2	1979	EL781026.C01	/NODC_DEEP/	02/01/1979	02/12/1979	53.131	24.264	12.266	27.6633	85.5217	157.0	1050.0
	1979	EL790213.C01	/NODC_DEEP/	02/13/1979	02/28/1979	34.408	21.516	6.674	27.6633	85.5217	254.0	1050.0
	1979	EL790213.C02	/NODC_DEEP/	02/13/1979	02/28/1979	27.953	14.619	6.552	27.6650	85.5217	558.0	1050.0
	1979	EL781026.C03	/NODC_DEEP/	02/01/1979	02/12/1979	31.286	19.000	5.673	27.6633	85.5217	957.0	1050.0
	1979	EL790213.C03	/NODC_DEEP/	02/13/1979	02/28/1979	19.841	6.821	6.145	27.6633	85.5217	960.0	1050.0

Notes by event number

1 1978: Early September - Early November

Large amplitude, surface-intensified currents occur during this event with peak speeds of 69 $cm \cdot s^{-1}$ at NOAA T1, 153 m, from October 14-20. Data from NOAA T1 are plotted in Figures 6.3.1-2.

2 1979: February

Northwest flow persists at NOAA T1. Winds are to the south. The cause of the flow may be a jet related to impingement of the LC on the West Florida shelf (see Molinari and Meyer, 1982). Data from NOAA T1 are plotted in Figure 6.3.1-2.

Table B-2. Speed statistics for energetic current events associated with Loop Current eddy separations. Given are the name of the file containing the event (keyed to the directory on the CD-ROM database), the start and stop dates used to characterize the event, maximum speed, mean speed, standard deviation of speed, mooring location, depth of the instrument, and total water depth. Comments on the event, keyed by the event number, are given in the notes below the table.

Event No.	Year	Filename	Directory	Event start date (m/d/y)	Event end date (m/d/y)	Maximum speed ($cm \cdot s^{-1}$)	Mean speed ($cm \cdot s^{-1}$)	Stand. dev. of speed ($cm \cdot s^{-1}$)	Latitude (°N)	Longitude (°W)	Depth (m)	Total water depth (m)
1	1978	DD780617.C01	/NODC_DEEP/	06/17/1978	06/30/1978	30.694	13.238	7.407	29.1983	87.6383	70.0	1033.0
	1978	DD780617.C02	/NODC_DEEP/	06/17/1978	06/30/1978	19.911	7.611	5.294	29.1983	87.6383	168.0	1033.0
	1978	DD780617.C03	/NODC_DEEP/	06/17/1978	06/30/1978	14.041	5.104	3.426	29.1983	87.6383	970.0	1033.0
	1978	YS771103.C01	/YUCATAN/	06/01/1978	06/30/1978	15.933	7.765	2.691	21.7333	85.9167	1895.0	2040.0
	1978	EL780612.C01	/NODC_DEEP/	06/20/1978	06/30/1978	17.628	8.042	3.804	27.6633	85.5167	153.0	1050.0
	1978	EL780612.C02	/NODC_DEEP/	06/20/1978	06/30/1978	20.671	8.783	4.881	27.6633	85.5167	549.0	1050.0
	1978	EL780612.C03	/NODC_DEEP/	06/20/1978	06/30/1978	19.409	8.503	3.864	27.6633	85.5167	950.0	1050.0
2	1979	EL790213.C01	/NODC_DEEP/	04/01/1979	04/29/1979	20.516	9.306	3.994	27.6633	85.5217	254.0	1050.0
	1979	EL790213.C02	/NODC_DEEP/	04/01/1979	04/30/1979	15.900	5.701	2.446	27.6650	85.5217	558.0	1050.0
	1979	EL790213.C03	/NODC_DEEP/	04/01/1979	04/30/1979	18.123	5.913	3.940	27.6633	85.5217	960.0	1050.0
	1979	YS771103.C01	/YUCATAN/	04/01/1979	04/30/1979	13.729	6.840	3.229	21.7333	85.9167	1895.0	2040.0
3	1981	GC810119.C01	/INDUSTRY/	03/01/1981	03/31/1981	44.801	19.298	9.531	27.7780	91.5213	35.0	435.0
	1981	GC810119.C02	/INDUSTRY/	03/01/1981	03/31/1981	45.399	17.393	8.631	27.7780	91.5213	65.0	435.0
	1981	GC810119.C03	/INDUSTRY/	03/01/1981	03/31/1981	41.598	13.382	9.131	27.7780	91.5213	100.0	435.0
	1981	GC810119.C04	/INDUSTRY/	03/01/1981	03/31/1981	26.904	11.807	5.526	27.7780	91.5213	150.0	435.0
	1981	GC810119.C05	/INDUSTRY/	03/01/1981	03/27/1981	16.202	4.103	2.822	27.7780	91.5213	400.0	435.0
4	1983	HH830127.C01	/NODC_DEEP/	03/01/1983	03/31/1983	52.608	27.306	12.093	25.7150	84.8850	172.0	1697.0
	1983	HH830127.C02	/NODC_DEEP/	03/01/1983	03/31/1983	38.055	11.800	7.340	25.7150	84.8850	1100.0	1697.0
	1983	HH830127.C03	/NODC_DEEP/	03/01/1983	03/31/1983	23.722	4.519	3.913	25.7150	84.8850	1600.0	1697.0
5	1984	HH840203.C01	/NODC_DEEP/	02/03/1984	02/29/1984	15.251	2.743	2.268	25.6003	85.4995	1565.0	3200.0
	1984	HH840203.C02	/NODC_DEEP/	02/03/1984	02/29/1984	16.095	6.546	3.778	25.6003	85.4995	2364.0	3200.0
	1984	HH840203.C03	/NODC_DEEP/	02/03/1984	02/29/1984	18.110	8.258	3.790	25.6003	85.4995	3174.0	3200.0
6	1984	HH840718.C01	/NODC_DEEP/	08/01/1984	08/26/1984	57.874	33.143	10.560	25.7150	84.8850	172.0	1697.0
	1984	HH840718.C02	/NODC_DEEP/	08/01/1984	08/31/1984	44.879	15.791	11.649	25.7150	84.8850	400.0	1697.0
	1984	HH840718.C05	/NODC_DEEP/	08/01/1984	08/31/1984	43.506	29.697	6.061	25.6003	85.4995	1565.0	3200.0
	1984	HH840718.C06	/NODC_DEEP/	08/01/1984	08/31/1984	43.242	29.081	5.053	25.6003	85.4995	2364.0	3200.0
	1984	HH840718.C07	/NODC_DEEP/	08/01/1984	08/31/1984	47.026	32.218	4.836	25.6003	85.4995	3174.0	3200.0
7	1986	HH850801.C01	/NODC_DEEP/	01/01/1986	01/31/1986	62.271	21.763	12.670	25.7150	84.8850	172.0	1697.0
	1986	HH850801.C02	/NODC_DEEP/	01/01/1986	01/31/1986	34.409	7.451	7.173	25.7150	84.8850	400.0	1697.0
	1986	HH850731.C01	/NODC_DEEP/	01/01/1986	01/31/1986	17.393	2.969	2.610	25.7150	84.8850	738.0	1697.0

Table B-2. Speed statistics for energetic current events associated with Loop Current eddy separations. (continued)

Event No.	Year	Filename	Directory	Event start date (m/d/y)	Event end date (m/d/y)	Maximum speed (cm·s^{-1})	Mean speed (cm·s^{-1})	Stand. dev. of speed (cm·s^{-1})	Latitude (°N)	Longitude (°W)	Depth (m)	Total water depth (m)
7	1986	HH850731.C02	/NODC_DEEP/	01/01/1986	01/31/1986	24.751	12.628	2.056	25.7150	84.8850	1100.0	1697.0
	1986	HH850801.C03	/NODC_DEEP/	01/01/1986	01/31/1986	33.425	5.221	6.589	25.6003	85.4995	703.0	3200.0
	1986	HH850801.C04	/NODC_DEEP/	01/01/1986	01/31/1986	12.714	6.211	2.078	25.6003	85.4995	1565.0	3200.0
	1986	HH850801.C05	/NODC_DEEP/	01/01/1986	01/31/1986	15.101	7.107	2.409	25.6003	85.4995	2364.0	3200.0
	1986	HH850801.C06	/NODC_DEEP/	01/01/1986	01/31/1986	11.977	3.424	2.775	25.6003	85.4995	3174.0	3200.0
8	1987	AB870406.C03	/NODC_DEEP/	09/01/1987	09/30/1987	24.142	6.314	2.881	25.6532	92.0333	1650.0	3000.0
9	1988	GB871108.C01	/NODC_DEEP/	05/01/1988	05/31/1988	37.600	10.701	8.611	27.4683	91.9932	100.0	845.0
	1988	GB871108.C02	/NODC_DEEP/	05/01/1988	05/31/1988	15.595	6.706	3.317	27.4683	91.9932	300.0	845.0
	1988	GB871202.C01	/NODC_DEEP/	05/01/1988	05/31/1988	21.394	13.349	2.867	27.4683	91.9932	305.0	845.0
	1988	GB870405.C05	/NODC_DEEP/	05/01/1988	05/31/1988	10.646	4.042	2.312	27.4683	91.9932	725.0	845.0
	1988	KC871108.C01	/NODC_DEEP/	05/01/1988	05/31/1988	39.989	19.963	9.635	26.7400	91.9950	100.0	1750.0
	1988	KC880414.C01	/NODC_DEEP/	05/01/1988	05/31/1988	25.016	12.413	4.522	26.7400	91.9950	300.0	1750.0
	1988	KC871108.C02	/NODC_DEEP/	05/01/1988	05/31/1988	27.016	15.143	4.613	26.7400	91.9950	305.0	1750.0
	1988	KC871108.C03	/NODC_DEEP/	05/01/1988	05/31/1988	13.073	3.451	2.857	26.7400	91.9950	725.0	1750.0
	1988	KC870406.C04	/NODC_DEEP/	05/01/1988	05/31/1988	12.144	4.013	2.223	26.7400	91.9950	1650.0	1750.0
	1988	AB871109.C01	/NODC_DEEP/	05/01/1988	05/31/1988	71.777	43.395	12.204	25.6532	92.0333	100.0	3000.0
	1988	AB880409.C01	/NODC_DEEP/	05/01/1988	05/31/1988	32.948	18.709	5.481	25.6532	92.0333	300.0	3000.0
	1988	AB871109.C02	/NODC_DEEP/	05/01/1988	05/31/1988	15.689	8.260	2.200	25.6532	92.0333	725.0	3000.0
	1988	AB870406.C03	/NODC_DEEP/	05/01/1988	05/31/1988	19.701	4.933	4.814	25.6532	92.0333	1650.0	3000.0
	1988	AB880409.C02	/NODC_DEEP/	05/01/1988	05/31/1988	18.490	6.250	3.891	25.6532	92.0333	2500.0	3000.0
10	1998	VK971113.A01	/MMS/	03/01/1998	03/31/1998	75.190	30.691	13.395	29.0592	88.3900	12.0	500.0
	1998	VK971113.A02	/MMS/	03/01/1998	03/31/1998	63.084	29.136	12.145	29.0592	88.3900	16.0	500.0
	1998	VK971113.A03	/MMS/	03/01/1998	03/31/1998	62.359	27.613	11.659	29.0592	88.3900	20.0	500.0
	1998	VK971113.A04	/MMS/	03/01/1998	03/31/1998	60.779	26.121	11.849	29.0592	88.3900	24.0	500.0
	1998	VK971113.A05	/MMS/	03/01/1998	03/31/1998	62.208	24.878	12.167	29.0592	88.3900	28.0	500.0
	1998	VK971113.A06	/MMS/	03/01/1998	03/31/1998	62.517	23.776	12.283	29.0592	88.3900	32.0	500.0
	1998	VK971113.A07	/MMS/	03/01/1998	03/31/1998	61.683	22.849	12.447	29.0592	88.3900	36.0	500.0
	1998	VK971113.A08	/MMS/	03/01/1998	03/31/1998	64.265	22.439	12.520	29.0592	88.3900	40.0	500.0
	1998	VK971113.A09	/MMS/	03/01/1998	03/31/1998	64.798	22.454	12.441	29.0592	88.3900	44.0	500.0
	1998	VK971113.A10	/MMS/	03/01/1998	03/31/1998	62.231	22.516	12.224	29.0592	88.3900	48.0	500.0
	1998	VK971113.A11	/MMS/	03/01/1998	03/31/1998	60.440	22.657	11.884	29.0592	88.3900	52.0	500.0
	1998	VK971113.A12	/MMS/	03/01/1998	03/31/1998	60.444	22.636	11.581	29.0592	88.3900	56.0	500.0
	1998	VK971113.A13	/MMS/	03/01/1998	03/31/1998	61.546	22.564	11.530	29.0592	88.3900	60.0	500.0
	1998	VK971113.A14	/MMS/	03/01/1998	03/31/1998	57.103	18.191	9.916	29.0592	88.3900	64.0	500.0

Table B-2. Speed statistics for energetic current events associated with Loop Current eddy separations. (continued)

Event No.	Year	Filename	Directory	Event start date (m/d/y)	Event end date (m/d/y)	Maximum speed (cm·s^{-1})	Mean speed (cm·s^{-1})	Stand. dev. of speed (cm·s^{-1})	Latitude (°N)	Longitude (°W)	Depth (m)	Total water depth (m)
10	1998	VK971113.A15	/MMS/	03/01/1998	03/31/1998	59.882	19.334	10.455	29.0592	88.3900	68.0	500.0
	1998	VK971113.A16	/MMS/	03/01/1998	03/31/1998	65.169	22.796	11.822	29.0592	88.3900	72.0	500.0
	1998	VK971113.A17	/MMS/	03/01/1998	03/31/1998	62.115	22.723	11.844	29.0592	88.3900	76.0	500.0
	1998	VK971113.C02	/MMS/	03/01/1998	03/31/1998	60.675	27.579	13.722	29.0592	88.3900	300.0	500.0
	1998	VK971113.C03	/MMS/	03/01/1998	03/31/1998	37.806	10.047	7.379	29.0592	88.3900	490.0	500.0
	1998	MC971113.A01	/MMS/	03/01/1998	03/31/1998	87.433	30.460	15.397	28.7662	88.2650	8.0	1300.0
	1998	MC971113.A02	/MMS/	03/01/1998	03/31/1998	78.743	29.580	14.703	28.7662	88.2650	12.0	1300.0
	1998	MC971113.A03	/MMS/	03/01/1998	03/31/1998	67.426	28.117	14.068	28.7662	88.2650	16.0	1300.0
	1998	MC971113.A04	/MMS/	03/01/1998	03/31/1998	63.954	27.316	13.226	28.7662	88.2650	20.0	1300.0
	1998	MC971113.A05	/MMS/	03/01/1998	03/31/1998	61.186	26.706	12.716	28.7662	88.2650	24.0	1300.0
	1998	MC971113.A06	/MMS/	03/01/1998	03/31/1998	61.221	26.435	12.560	28.7662	88.2650	28.0	1300.0
	1998	MC971113.A07	/MMS/	03/01/1998	03/31/1998	61.157	26.391	12.428	28.7662	88.2650	32.0	1300.0
	1998	MC971113.A08	/MMS/	03/01/1998	03/31/1998	60.952	26.317	12.285	28.7662	88.2650	36.0	1300.0
	1998	MC971113.A09	/MMS/	03/01/1998	03/31/1998	58.134	26.216	12.223	28.7662	88.2650	40.0	1300.0
	1998	MC971113.A10	/MMS/	03/01/1998	03/31/1998	55.547	26.065	12.073	28.7662	88.2650	44.0	1300.0
	1998	MC971113.A11	/MMS/	03/01/1998	03/31/1998	53.181	25.951	11.853	28.7662	88.2650	48.0	1300.0
	1998	MC971113.A12	/MMS/	03/01/1998	03/31/1998	51.108	25.915	11.687	28.7662	88.2650	52.0	1300.0
	1998	MC971113.A13	/MMS/	03/01/1998	03/31/1998	35.547	16.978	7.733	28.7662	88.2650	56.0	1300.0
	1998	MC971113.A14	/MMS/	03/01/1998	03/31/1998	39.309	18.658	8.482	28.7662	88.2650	60.0	1300.0
	1998	MC971113.A15	/MMS/	03/01/1998	03/31/1998	53.003	25.564	11.296	28.7662	88.2650	64.0	1300.0
	1998	MC971113.A16	/MMS/	03/01/1998	03/31/1998	52.800	25.166	11.194	28.7662	88.2650	68.0	1300.0
	1998	MC971113.A17	/MMS/	03/01/1998	03/31/1998	51.416	24.619	10.891	28.7662	88.2650	72.0	1300.0
	1998	MC971114.C01	/MMS/	03/01/1998	03/31/1998	39.462	14.544	9.375	28.7662	88.2650	500.0	1300.0
	1998	MC971114.C02	/MMS/	03/01/1998	03/31/1998	14.705	5.484	2.656	28.7662	88.2650	1310.0	1320.0
	1998	VK971115.A01	/MMS/	03/01/1998	03/31/1998	75.195	29.930	13.420	29.2120	87.8722	12.0	500.0
	1998	VK971115.A02	/MMS/	03/01/1998	03/31/1998	70.464	29.325	15.305	29.2120	87.8722	16.0	500.0
	1998	VK971115.A03	/MMS/	03/01/1998	03/31/1998	67.121	27.410	14.208	29.2120	87.8722	20.0	500.0
	1998	VK971115.A04	/MMS/	03/01/1998	03/31/1998	66.633	25.696	13.493	29.2120	87.8722	24.0	500.0
	1998	VK971115.A05	/MMS/	03/01/1998	03/31/1998	63.394	24.394	13.252	29.2120	87.8722	28.0	500.0
	1998	VK971115.A06	/MMS/	03/01/1998	03/31/1998	61.289	23.286	13.248	29.2120	87.8722	32.0	500.0
	1998	VK971115.A07	/MMS/	03/01/1998	03/31/1998	61.795	22.360	13.481	29.2120	87.8722	36.0	500.0
	1998	VK971115.A08	/MMS/	03/01/1998	03/31/1998	61.166	21.937	13.581	29.2120	87.8722	40.0	500.0
	1998	VK971115.A09	/MMS/	03/01/1998	03/31/1998	60.560	21.936	13.648	29.2120	87.8722	44.0	500.0
	1998	VK971115.A10	/MMS/	03/01/1998	03/31/1998	61.326	22.022	13.696	29.2120	87.8722	48.0	500.0

Table B-2. Speed statistics for energetic current events associated with Loop Current eddy separations. (continued)

Event No.	Year	Filename	Directory	Event start date (m/d/y)	Event end date (m/d/y)	Maximum speed (cm·s^{-1})	Mean speed (cm·s^{-1})	Stand. dev. of speed (cm·s^{-1})	Latitude (°N)	Longitude (°W)	Depth (m)	Total water depth (m)
10	1998	VK971115.A11	/MMS/	03/01/1998	03/31/1998	61.652	22.081	13.721	29.2120	87.8722	52.0	500.0
	1998	VK971115.A12	/MMS/	03/01/1998	03/31/1998	63.244	22.312	13.737	29.2120	87.8722	56.0	500.0
	1998	VK971115.A13	/MMS/	03/01/1998	03/31/1998	64.018	22.493	13.961	29.2120	87.8722	60.0	500.0
	1998	VK971115.A14	/MMS/	03/01/1998	03/31/1998	58.272	17.104	11.849	29.2120	87.8722	64.0	500.0
	1998	VK971115.A15	/MMS/	03/01/1998	03/31/1998	64.107	18.583	12.647	29.2120	87.8722	68.0	500.0
	1998	VK971115.A16	/MMS/	03/01/1998	03/31/1998	70.743	23.076	14.278	29.2120	87.8722	72.0	500.0
	1998	VK971115.A17	/MMS/	03/01/1998	03/31/1998	69.604	22.830	13.868	29.2120	87.8722	76.0	500.0
	1998	VK971115.A18	/MMS/	03/01/1998	03/31/1998	69.528	22.497	13.447	29.2120	87.8722	80.0	500.0
	1998	VK971115.C01	/MMS/	03/01/1998	03/31/1998	84.509	38.715	15.983	29.2120	87.8722	200.0	500.0
	1998	VK971115.C02	/MMS/	03/01/1998	03/31/1998	77.827	40.985	16.587	29.2120	87.8722	300.0	500.0
	1998	VK971115.C03	/MMS/	03/01/1998	03/31/1998	42.399	14.382	8.618	29.2120	87.8722	490.0	500.0
	1998	VK971115.A19	/MMS/	03/01/1998	03/31/1998	81.799	28.571	13.259	29.0705	87.8568	12.0	1300.0
	1998	VK971115.A20	/MMS/	03/01/1998	03/31/1998	78.976	29.707	12.169	29.0705	87.8568	16.0	1300.0
	1998	VK971115.A21	/MMS/	03/01/1998	03/31/1998	75.801	29.314	11.490	29.0705	87.8568	20.0	1300.0
	1998	VK971115.A22	/MMS/	03/01/1998	03/31/1998	74.150	28.901	10.951	29.0705	87.8568	24.0	1300.0
	1998	VK971115.A23	/MMS/	03/01/1998	03/31/1998	70.345	28.262	10.698	29.0705	87.8568	28.0	1300.0
	1998	VK971115.A24	/MMS/	03/01/1998	03/31/1998	66.286	27.625	10.564	29.0705	87.8568	32.0	1300.0
	1998	VK971115.A25	/MMS/	03/01/1998	03/31/1998	64.005	26.864	10.751	29.0705	87.8568	36.0	1300.0
	1998	VK971115.A26	/MMS/	03/01/1998	03/31/1998	58.071	26.236	11.008	29.0705	87.8568	40.0	1300.0
	1998	VK971115.A27	/MMS/	03/01/1998	03/31/1998	57.904	25.629	11.228	29.0705	87.8568	44.0	1300.0
	1998	VK971115.A28	/MMS/	03/01/1998	03/31/1998	56.600	25.201	11.321	29.0705	87.8568	48.0	1300.0
	1998	VK971115.A29	/MMS/	03/01/1998	03/31/1998	54.700	24.867	11.306	29.0705	87.8568	52.0	1300.0
	1998	VK971115.A30	/MMS/	03/01/1998	03/31/1998	44.102	18.332	8.192	29.0705	87.8568	56.0	1300.0
	1998	VK971115.A31	/MMS/	03/01/1998	03/31/1998	46.865	19.226	8.522	29.0705	87.8568	60.0	1300.0
	1998	VK971115.A32	/MMS/	03/01/1998	03/31/1998	53.778	24.911	11.382	29.0705	87.8568	64.0	1300.0
	1998	VK971115.A33	/MMS/	03/01/1998	03/31/1998	54.730	24.661	11.555	29.0705	87.8568	68.0	1300.0
	1998	VK971115.A34	/MMS/	03/01/1998	03/31/1998	53.703	24.012	11.546	29.0705	87.8568	72.0	1300.0
	1998	VK971115.C04	/MMS/	03/01/1998	03/31/1998	42.077	16.173	9.936	29.0705	87.8568	500.0	1300.0
	1998	VK971115.C05	/MMS/	03/01/1998	03/31/1998	26.396	6.187	4.481	29.0705	87.8568	1290.0	1300.0
	1998	DD971120.A18	/MMS/	03/01/1998	03/31/1998	99.220	19.768	13.926	29.3712	87.3563	12.0	500.0
	1998	DD971120.A19	/MMS/	03/01/1998	03/31/1998	94.071	18.984	13.311	29.3712	87.3563	16.0	500.0
	1998	DD971120.A20	/MMS/	03/01/1998	03/31/1998	89.114	18.287	12.907	29.3712	87.3563	20.0	500.0
	1998	DD971120.A21	/MMS/	03/01/1998	03/31/1998	84.228	17.727	12.508	29.3712	87.3563	24.0	500.0
	1998	DD971120.A22	/MMS/	03/01/1998	03/31/1998	78.381	17.247	12.146	29.3712	87.3563	28.0	500.0

Table B-2. Speed statistics for energetic current events associated with Loop Current eddy separations. (continued)

Event No.	Year	Filename	Directory	Event start date (m/d/y)	Event end date (m/d/y)	Maximum speed ($cm \cdot s^{-1}$)	Mean speed ($cm \cdot s^{-1}$)	Stand. dev. of speed ($cm \cdot s^{-1}$)	Latitude (°N)	Longitude (°W)	Depth (m)	Total water depth (m)
10	1998	DD971120.A23	/MMS/	03/01/1998	03/31/1998	73.051	16.836	11.702	29.3712	87.3563	32.0	500.0
	1998	DD971120.A24	/MMS/	03/01/1998	03/31/1998	65.122	16.473	11.252	29.3712	87.3563	36.0	500.0
	1998	DD971120.A25	/MMS/	03/01/1998	03/31/1998	59.095	16.166	10.874	29.3712	87.3563	40.0	500.0
	1998	DD971120.A26	/MMS/	03/01/1998	03/31/1998	51.847	15.937	10.619	29.3712	87.3563	44.0	500.0
	1998	DD971120.A27	/MMS/	03/01/1998	03/31/1998	49.645	15.852	10.570	29.3712	87.3563	48.0	500.0
	1998	DD971120.A28	/MMS/	03/01/1998	03/31/1998	51.367	15.959	10.692	29.3712	87.3563	52.0	500.0
	1998	DD971120.A29	/MMS/	03/01/1998	03/31/1998	57.164	16.188	10.875	29.3712	87.3563	56.0	500.0
	1998	DD971120.A30	/MMS/	03/01/1998	03/31/1998	59.540	16.301	11.102	29.3712	87.3563	60.0	500.0
	1998	DD971120.A31	/MMS/	03/01/1998	03/31/1998	58.149	16.080	11.108	29.3712	87.3563	64.0	500.0
	1998	DD971120.A32	/MMS/	03/01/1998	03/31/1998	59.748	16.013	11.309	29.3712	87.3563	68.0	500.0
	1998	DD971120.A33	/MMS/	03/01/1998	03/31/1998	59.953	16.010	11.301	29.3712	87.3563	72.0	500.0
	1998	DD971120.A34	/MMS/	03/01/1998	03/31/1998	58.904	16.110	11.158	29.3712	87.3563	76.0	500.0
	1998	DD971120.C02	/MMS/	03/01/1998	03/31/1998	49.632	19.775	10.619	29.3712	87.3563	200.0	500.0
	1998	DD971120.C03	/MMS/	03/01/1998	03/31/1998	52.249	20.847	13.020	29.3712	87.3563	300.0	500.0
	1998	DD971120.C04	/MMS/	03/01/1998	03/31/1998	39.396	9.830	8.123	29.3712	87.3563	490.0	500.0
	1998	DD971116.A01	/MMS/	03/01/1998	03/31/1998	92.853	31.684	14.732	29.0032	87.3532	12.0	1300.0
	1998	DD971116.A02	/MMS/	03/01/1998	03/31/1998	86.230	31.181	14.406	29.0032	87.3532	16.0	1300.0
	1998	DD971116.A03	/MMS/	03/01/1998	03/31/1998	79.067	30.799	14.101	29.0032	87.3532	20.0	1300.0
	1998	DD971116.A04	/MMS/	03/01/1998	03/31/1998	72.439	30.475	13.727	29.0032	87.3532	24.0	1300.0
	1998	DD971116.A05	/MMS/	03/01/1998	03/31/1998	64.519	30.141	13.502	29.0032	87.3532	28.0	1300.0
	1998	DD971116.A06	/MMS/	03/01/1998	03/31/1998	64.213	29.810	13.284	29.0032	87.3532	32.0	1300.0
	1998	DD971116.A07	/MMS/	03/01/1998	03/31/1998	63.637	29.546	13.111	29.0032	87.3532	36.0	1300.0
	1998	DD971116.A08	/MMS/	03/01/1998	03/31/1998	61.502	29.319	12.802	29.0032	87.3532	40.0	1300.0
	1998	DD971116.A09	/MMS/	03/01/1998	03/31/1998	60.210	29.135	12.662	29.0032	87.3532	44.0	1300.0
	1998	DD971116.A10	/MMS/	03/01/1998	03/31/1998	60.909	28.960	12.631	29.0032	87.3532	48.0	1300.0
	1998	DD971116.A11	/MMS/	03/01/1998	03/31/1998	58.718	28.782	12.625	29.0032	87.3532	52.0	1300.0
	1998	DD971116.A12	/MMS/	03/01/1998	03/31/1998	53.043	25.335	11.124	29.0032	87.3532	56.0	1300.0
	1998	DD971116.A13	/MMS/	03/01/1998	03/31/1998	53.684	26.743	11.478	29.0032	87.3532	60.0	1300.0
	1998	DD971116.A14	/MMS/	03/01/1998	03/31/1998	59.136	29.298	12.484	29.0032	87.3532	64.0	1300.0
	1998	DD971116.A15	/MMS/	03/01/1998	03/31/1998	59.829	29.180	12.469	29.0032	87.3532	68.0	1300.0
	1998	DD971116.A16	/MMS/	03/01/1998	03/31/1998	58.393	28.464	12.084	29.0032	87.3532	72.0	1300.0
	1998	DD971116.C01	/MMS/	03/01/1998	03/31/1998	38.590	15.525	7.829	29.0032	87.3532	500.0	1300.0
	1998	DD971116.C02	/MMS/	03/01/1998	03/31/1998	22.898	7.980	4.891	29.0032	87.3532	1290.0	1300.0
	1998	DD971118.A01	/MMS/	03/01/1998	03/31/1998	69.335	19.490	10.869	29.3348	86.8520	12.0	500.0

Table B-2. Speed statistics for energetic current events associated with Loop Current eddy separations. (continued)

Event No.	Year	Filename	Directory	Event start date (m/d/y)	Event end date (m/d/y)	Maximum speed (cm·s-1)	Mean speed (cm·s-1)	Stand. dev. of speed (cm·s-1)	Latitude (°N)	Longitude (°W)	Depth (m)	Total water depth (m)
10	1998	DD971118.A02	/MMS/	03/01/1998	03/31/1998	66.731	18.401	10.185	29.3348	86.8520	16.0	500.0
	1998	DD971118.A03	/MMS/	03/01/1998	03/31/1998	53.959	17.746	9.696	29.3348	86.8520	20.0	500.0
	1998	DD971118.A04	/MMS/	03/01/1998	03/31/1998	48.462	17.282	9.126	29.3348	86.8520	24.0	500.0
	1998	DD971118.A05	/MMS/	03/01/1998	03/31/1998	49.559	16.967	8.685	29.3348	86.8520	28.0	500.0
	1998	DD971118.A06	/MMS/	03/01/1998	03/31/1998	48.735	16.766	8.354	29.3348	86.8520	32.0	500.0
	1998	DD971118.A07	/MMS/	03/01/1998	03/31/1998	48.485	16.579	8.181	29.3348	86.8520	36.0	500.0
	1998	DD971118.A08	/MMS/	03/01/1998	03/31/1998	47.646	16.529	8.071	29.3348	86.8520	40.0	500.0
	1998	DD971118.A09	/MMS/	03/01/1998	03/31/1998	48.638	16.649	7.960	29.3348	86.8520	44.0	500.0
	1998	DD971118.A10	/MMS/	03/01/1998	03/31/1998	47.981	16.961	7.866	29.3348	86.8520	48.0	500.0
	1998	DD971118.A11	/MMS/	03/01/1998	03/31/1998	49.821	17.164	7.863	29.3348	86.8520	52.0	500.0
	1998	DD971118.A12	/MMS/	03/01/1998	03/31/1998	48.721	17.288	7.817	29.3348	86.8520	56.0	500.0
	1998	DD971118.A13	/MMS/	03/01/1998	03/31/1998	47.535	17.362	7.962	29.3348	86.8520	60.0	500.0
	1998	DD971118.A14	/MMS/	03/01/1998	03/31/1998	46.105	16.112	7.331	29.3348	86.8520	64.0	500.0
	1998	DD971118.A15	/MMS/	03/01/1998	03/31/1998	44.959	16.650	7.873	29.3348	86.8520	68.0	500.0
	1998	DD971118.A16	/MMS/	03/01/1998	03/31/1998	50.681	17.915	8.833	29.3348	86.8520	72.0	500.0
	1998	DD971118.A17	/MMS/	03/01/1998	03/31/1998	51.830	17.845	9.005	29.3348	86.8520	76.0	500.0
	1998	DD971118.A18	/MMS/	03/01/1998	03/31/1998	51.103	17.425	8.832	29.3348	86.8520	80.0	500.0
	1998	DD971118.C01	/MMS/	03/01/1998	03/31/1998	35.687	11.684	8.471	29.3348	86.8520	200.0	500.0
	1998	DD971118.C02	/MMS/	03/01/1998	03/31/1998	31.908	11.578	6.076	29.3348	86.8520	300.0	500.0
	1998	DD971118.C03	/MMS/	03/01/1998	03/31/1998	28.002	8.851	5.787	29.3348	86.8520	490.0	500.0
11	1999	AT990829.A01	/MMS/	08/29/1999	08/31/1999	115.753	82.265	20.367	27.2933	89.7845	12.0	2001.0
	1999	AT990829.A02	/MMS/	08/29/1999	08/31/1999	114.228	82.512	18.667	27.2933	89.7845	16.0	2001.0
	1999	AT990829.A03	/MMS/	08/29/1999	08/31/1999	112.177	81.242	18.558	27.2933	89.7845	20.0	2001.0
	1999	AT990829.A04	/MMS/	08/29/1999	08/31/1999	111.116	80.301	18.277	27.2933	89.7845	24.0	2001.0
	1999	AT990829.A05	/MMS/	08/29/1999	08/31/1999	105.879	79.538	17.511	27.2933	89.7845	28.0	2001.0
	1999	AT990829.A06	/MMS/	08/29/1999	08/31/1999	103.645	78.750	16.936	27.2933	89.7845	32.0	2001.0
	1999	AT990829.A07	/MMS/	08/29/1999	08/31/1999	103.518	77.909	16.969	27.2933	89.7845	36.0	2001.0
	1999	AT990829.A08	/MMS/	08/29/1999	08/31/1999	100.617	76.843	16.851	27.2933	89.7845	40.0	2001.0
	1999	AT990829.A09	/MMS/	08/29/1999	08/31/1999	99.016	75.846	17.106	27.2933	89.7845	44.0	2001.0
	1999	AT990829.A10	/MMS/	08/29/1999	08/31/1999	97.674	74.357	17.312	27.2933	89.7845	48.0	2001.0
	1999	AT990829.A11	/MMS/	08/29/1999	08/31/1999	97.946	73.052	17.430	27.2933	89.7845	52.0	2001.0
	1999	AT990829.A12	/MMS/	08/29/1999	08/31/1999	97.453	73.008	16.858	27.2933	89.7845	56.0	2001.0
	1999	AT990829.A13	/MMS/	08/29/1999	08/31/1999	96.661	72.972	16.613	27.2933	89.7845	60.0	2001.0
	1999	AT990829.A14	/MMS/	08/29/1999	08/31/1999	97.399	72.713	17.149	27.2933	89.7845	64.0	2001.0

Table B-2. Speed statistics for energetic current events associated with Loop Current eddy separations. (continued)

Event No.	Year	Filename	Directory	Event start date (m/d/y)	Event end date (m/d/y)	Maximum speed ($cm \cdot s^{-1}$)	Mean speed ($cm \cdot s^{-1}$)	Stand. dev. of speed ($cm \cdot s^{-1}$)	Latitude (°N)	Longitude (°W)	Depth (m)	Total water depth (m)
11	1999	AT990829.A15	/MMS/	08/29/1999	08/31/1999	77.407	46.411	18.005	27.2933	89.7845	68.0	2001.0
	1999	AT990829.A16	/MMS/	08/29/1999	08/31/1999	86.100	61.926	18.131	27.2933	89.7845	72.0	2001.0
	1999	AT990829.A17	/MMS/	08/29/1999	08/31/1999	93.334	70.905	18.755	27.2933	89.7845	76.0	2001.0
	1999	AT990829.A18	/MMS/	08/29/1999	08/31/1999	91.480	70.331	18.716	27.2933	89.7845	80.0	2001.0
	1999	AT990829.A19	/MMS/	08/29/1999	08/31/1999	98.990	64.533	23.032	27.2933	89.7845	106.0	2001.0
	1999	AT990829.A20	/MMS/	08/29/1999	08/31/1999	102.492	69.054	23.393	27.2933	89.7845	110.0	2001.0
	1999	AT990829.A21	/MMS/	08/29/1999	08/31/1999	103.837	69.328	23.062	27.2933	89.7845	114.0	2001.0
	1999	AT990829.A22	/MMS/	08/29/1999	08/31/1999	103.598	69.127	22.362	27.2933	89.7845	118.0	2001.0
	1999	AT990829.A23	/MMS/	08/29/1999	08/31/1999	99.214	68.707	20.821	27.2933	89.7845	122.0	2001.0
	1999	AT990829.A24	/MMS/	08/29/1999	08/31/1999	95.564	68.141	20.169	27.2933	89.7845	126.0	2001.0
	1999	AT990829.A25	/MMS/	08/29/1999	08/31/1999	96.813	68.130	20.851	27.2933	89.7845	130.0	2001.0
	1999	AT990829.A26	/MMS/	08/29/1999	08/31/1999	95.635	68.403	21.721	27.2933	89.7845	134.0	2001.0
	1999	AT990829.A27	/MMS/	08/29/1999	08/31/1999	94.996	68.859	21.125	27.2933	89.7845	138.0	2001.0
	1999	AT990829.A28	/MMS/	08/29/1999	08/31/1999	93.561	69.030	19.885	27.2933	89.7845	142.0	2001.0
	1999	AT990829.A29	/MMS/	08/29/1999	08/31/1999	90.899	69.235	18.612	27.2933	89.7845	146.0	2001.0
	1999	AT990829.A30	/MMS/	08/29/1999	08/31/1999	90.823	69.465	17.714	27.2933	89.7845	150.0	2001.0
	1999	AT990829.A39	/MMS/	08/29/1999	08/31/1999	94.083	69.094	18.851	27.2933	89.7845	150.0	2001.0
	1999	AT990829.A31	/MMS/	08/29/1999	08/31/1999	92.712	69.881	17.054	27.2933	89.7845	154.0	2001.0
	1999	AT990829.A40	/MMS/	08/29/1999	08/31/1999	90.294	67.996	16.198	27.2933	89.7845	154.0	2001.0
	1999	AT990829.A32	/MMS/	08/29/1999	08/31/1999	92.334	69.908	17.018	27.2933	89.7845	158.0	2001.0
	1999	AT990829.A41	/MMS/	08/29/1999	08/31/1999	89.214	65.669	14.881	27.2933	89.7845	158.0	2001.0
	1999	AT990829.A33	/MMS/	08/29/1999	08/31/1999	92.129	70.220	16.487	27.2933	89.7845	162.0	2001.0
	1999	AT990829.A42	/MMS/	08/29/1999	08/31/1999	86.335	67.847	14.884	27.2933	89.7845	162.0	2001.0
	1999	AT990829.A34	/MMS/	08/29/1999	08/31/1999	89.990	70.228	15.724	27.2933	89.7845	166.0	2001.0
	1999	AT990829.A43	/MMS/	08/29/1999	08/31/1999	87.003	68.993	14.478	27.2933	89.7845	166.0	2001.0
	1999	AT990829.A35	/MMS/	08/29/1999	08/31/1999	87.848	70.150	15.028	27.2933	89.7845	170.0	2001.0
	1999	AT990829.A44	/MMS/	08/29/1999	08/31/1999	85.435	68.281	14.690	27.2933	89.7845	170.0	2001.0
	1999	AT990829.A36	/MMS/	08/29/1999	08/31/1999	88.728	69.514	14.385	27.2933	89.7845	174.0	2001.0
	1999	AT990829.A45	/MMS/	08/29/1999	08/31/1999	84.641	67.921	13.795	27.2933	89.7845	174.0	2001.0
	1999	AT990829.A37	/MMS/	08/29/1999	08/31/1999	84.633	68.856	12.596	27.2933	89.7845	178.0	2001.0
	1999	AT990829.A46	/MMS/	08/29/1999	08/31/1999	84.481	67.434	13.442	27.2933	89.7845	178.0	2001.0
	1999	AT990829.A38	/MMS/	08/29/1999	08/31/1999	96.058	69.836	13.410	27.2933	89.7845	182.0	2001.0
	1999	AT990829.A47	/MMS/	08/29/1999	08/31/1999	84.193	66.445	13.440	27.2933	89.7845	182.0	2001.0
	1999	AT990829.A48	/MMS/	08/29/1999	08/31/1999	85.535	66.128	13.101	27.2933	89.7845	186.0	2001.0

Table B-2. Speed statistics for energetic current events associated with Loop Current eddy separations. (continued)

Event No.	Year	Filename	Directory	Event start date (m/d/y)	Event end date (m/d/y)	Maximum speed ($cm \cdot s^{-1}$)	Mean speed ($cm \cdot s^{-1}$)	Stand. dev. of speed ($cm \cdot s^{-1}$)	Latitude (°N)	Longitude (°W)	Depth (m)	Total water depth (m)
11	1999	AT990829.A49	/MMS/	08/29/1999	08/31/1999	84.710	65.558	12.914	27.2933	89.7845	190.0	2001.0
	1999	AT990829.A50	/MMS/	08/29/1999	08/31/1999	83.707	65.328	12.692	27.2933	89.7845	194.0	2001.0
	1999	AT990829.A51	/MMS/	08/29/1999	08/31/1999	79.819	59.247	14.711	27.2933	89.7845	198.0	2001.0
	1999	AT990829.A52	/MMS/	08/29/1999	08/31/1999	70.778	47.640	14.252	27.2933	89.7845	202.0	2001.0
	1999	AT990829.A53	/MMS/	08/29/1999	08/31/1999	77.092	60.142	9.976	27.2933	89.7845	206.0	2001.0
	1999	AT990829.A54	/MMS/	08/29/1999	08/31/1999	75.477	63.301	10.982	27.2933	89.7845	210.0	2001.0
	1999	AT990829.A55	/MMS/	08/29/1999	08/31/1999	74.805	62.848	10.919	27.2933	89.7845	214.0	2001.0
	1999	AT990829.A56	/MMS/	08/29/1999	08/31/1999	75.402	62.328	10.668	27.2933	89.7845	218.0	2001.0
	1999	AT990829.A57	/MMS/	08/29/1999	08/31/1999	75.181	61.783	10.133	27.2933	89.7845	222.0	2001.0
	1999	AT990829.A58	/MMS/	08/29/1999	08/31/1999	73.324	61.009	9.768	27.2933	89.7845	226.0	2001.0
	1999	AT990829.A59	/MMS/	08/29/1999	08/31/1999	71.603	60.128	9.170	27.2933	89.7845	230.0	2001.0
	1999	AT990829.A60	/MMS/	08/29/1999	08/31/1999	67.959	57.545	8.719	27.2933	89.7845	234.0	2001.0
	1999	AT990829.A61	/MMS/	08/29/1999	08/31/1999	62.784	54.540	6.788	27.2933	89.7845	256.0	2001.0
	1999	AT990829.A62	/MMS/	08/29/1999	08/31/1999	62.966	54.926	6.497	27.2933	89.7845	260.0	2001.0
	1999	AT990829.A63	/MMS/	08/29/1999	08/31/1999	62.535	54.224	6.456	27.2933	89.7845	264.0	2001.0
	1999	AT990829.A64	/MMS/	08/29/1999	08/31/1999	61.366	53.601	6.151	27.2933	89.7845	268.0	2001.0
	1999	AT990829.A65	/MMS/	08/29/1999	08/31/1999	61.079	53.067	5.817	27.2933	89.7845	272.0	2001.0
	1999	AT990829.A66	/MMS/	08/29/1999	08/31/1999	60.691	52.862	5.337	27.2933	89.7845	276.0	2001.0
	1999	AT990829.A67	/MMS/	08/29/1999	08/31/1999	60.701	52.457	4.983	27.2933	89.7845	280.0	2001.0
	1999	AT990829.A68	/MMS/	08/29/1999	08/31/1999	60.076	51.920	4.652	27.2933	89.7845	284.0	2001.0
	1999	AT990829.A69	/MMS/	08/29/1999	08/31/1999	59.825	51.536	4.462	27.2933	89.7845	288.0	2001.0
	1999	AT990829.A70	/MMS/	08/29/1999	08/31/1999	58.963	50.868	4.765	27.2933	89.7845	292.0	2001.0
	1999	AT990829.A71	/MMS/	08/29/1999	08/31/1999	57.607	50.147	4.897	27.2933	89.7845	296.0	2001.0
	1999	AT990829.A72	/MMS/	08/29/1999	08/31/1999	57.191	49.554	5.122	27.2933	89.7845	300.0	2001.0
	1999	AT990829.A73	/MMS/	08/29/1999	08/31/1999	57.243	48.820	5.044	27.2933	89.7845	304.0	2001.0
	1999	AT990829.A74	/MMS/	08/29/1999	08/31/1999	56.230	48.236	5.033	27.2933	89.7845	308.0	2001.0
	1999	AT990829.A75	/MMS/	08/29/1999	08/31/1999	55.473	47.618	5.031	27.2933	89.7845	312.0	2001.0
	1999	AT990829.A76	/MMS/	08/29/1999	08/31/1999	56.540	47.274	4.776	27.2933	89.7845	316.0	2001.0
	1999	AT990829.A77	/MMS/	08/29/1999	08/31/1999	55.336	46.605	4.410	27.2933	89.7845	320.0	2001.0
	1999	AT990829.A78	/MMS/	08/29/1999	08/31/1999	52.659	45.708	4.171	27.2933	89.7845	324.0	2001.0
	1999	AT990829.A79	/MMS/	08/29/1999	08/31/1999	51.727	45.095	4.104	27.2933	89.7845	328.0	2001.0
	1999	AT990829.A80	/MMS/	08/29/1999	08/31/1999	50.641	44.133	4.309	27.2933	89.7845	332.0	2001.0
	1999	AT990829.A83	/MMS/	08/29/1999	08/31/1999	61.304	51.582	5.732	27.2933	89.7845	332.0	2001.0
	1999	AT990829.A81	/MMS/	08/29/1999	08/31/1999	52.371	42.687	4.941	27.2933	89.7845	336.0	2001.0

Table B-2. Speed statistics for energetic current events associated with Loop Current eddy separations. (continued)

Event No.	Year	Filename	Directory	Event start date (m/d/y)	Event end date (m/d/y)	Maximum speed ($cm \cdot s^{-1}$)	Mean speed ($cm \cdot s^{-1}$)	Stand. dev. of speed ($cm \cdot s^{-1}$)	Latitude (°N)	Longitude (°W)	Depth (m)	Total water depth (m)
11	1999	AT990829.A82	/MMS/	08/29/1999	08/31/1999	52.814	43.717	3.266	27.2933	89.7845	340.0	2001.0
	1999	AT990829.A84	/MMS/	08/29/1999	08/31/1999	59.197	50.081	5.613	27.2933	89.7845	340.0	2001.0
	1999	AT990829.A85	/MMS/	08/29/1999	08/31/1999	56.640	47.947	5.188	27.2933	89.7845	348.0	2001.0
	1999	AT990829.A86	/MMS/	08/29/1999	08/31/1999	55.472	46.987	3.985	27.2933	89.7845	356.0	2001.0
	1999	AT990829.A87	/MMS/	08/29/1999	08/31/1999	52.601	45.712	3.496	27.2933	89.7845	364.0	2001.0
	1999	AT990829.A88	/MMS/	08/29/1999	08/31/1999	51.626	44.360	3.503	27.2933	89.7845	372.0	2001.0
	1999	AT990829.A89	/MMS/	08/29/1999	08/31/1999	50.231	43.686	3.399	27.2933	89.7845	380.0	2001.0
	1999	AT990829.A90	/MMS/	08/29/1999	08/31/1999	50.540	43.698	3.559	27.2933	89.7845	388.0	2001.0
	1999	AT990829.A91	/MMS/	08/29/1999	08/31/1999	49.742	42.323	3.508	27.2933	89.7845	396.0	2001.0
	1999	AT990829.A92	/MMS/	08/29/1999	08/31/1999	47.124	41.031	3.579	27.2933	89.7845	404.0	2001.0
	1999	AT990829.A93	/MMS/	08/29/1999	08/31/1999	48.484	40.126	4.169	27.2933	89.7845	412.0	2001.0
	1999	AT990829.A94	/MMS/	08/29/1999	08/31/1999	48.450	39.326	4.096	27.2933	89.7845	420.0	2001.0
	1999	AT990829.A95	/MMS/	08/29/1999	08/31/1999	48.128	38.753	4.093	27.2933	89.7845	428.0	2001.0
	1999	AT990829.A96	/MMS/	08/29/1999	08/31/1999	47.151	38.235	3.413	27.2933	89.7845	436.0	2001.0
	1999	AT990829.A97	/MMS/	08/29/1999	08/31/1999	44.157	37.318	2.385	27.2933	89.7845	444.0	2001.0
	1999	AT990829.A98	/MMS/	08/29/1999	08/31/1999	43.572	36.213	3.016	27.2933	89.7845	452.0	2001.0
	1999	AT990829.A99	/MMS/	08/29/1999	08/31/1999	42.090	34.190	3.530	27.2933	89.7845	460.0	2001.0
	1999	AT990829.Aa0	/MMS/	08/29/1999	08/31/1999	40.564	33.007	3.420	27.2933	89.7845	468.0	2001.0
	1999	AT990829.Aa1	/MMS/	08/29/1999	08/31/1999	39.839	31.702	3.390	27.2933	89.7845	476.0	2001.0
	1999	AT990829.Aa2	/MMS/	08/29/1999	08/31/1999	37.386	30.089	3.239	27.2933	89.7845	484.0	2001.0
	1999	AT990829.Aa3	/MMS/	08/29/1999	08/31/1999	37.916	29.500	3.300	27.2933	89.7845	492.0	2001.0
	1999	AT990829.Aa4	/MMS/	08/29/1999	08/31/1999	37.403	29.179	3.444	27.2933	89.7845	500.0	2001.0
	1999	AT990829.Aa5	/MMS/	08/29/1999	08/31/1999	37.234	27.751	3.728	27.2933	89.7845	508.0	2001.0
	1999	AT990829.Aa6	/MMS/	08/29/1999	08/31/1999	33.698	26.551	4.007	27.2933	89.7845	516.0	2001.0
	1999	AT990829.Aa7	/MMS/	08/29/1999	08/31/1999	32.840	25.565	4.147	27.2933	89.7845	524.0	2001.0
	1999	AT990829.Aa8	/MMS/	08/29/1999	08/31/1999	32.560	24.621	4.101	27.2933	89.7845	532.0	2001.0
	1999	AT990829.Aa9	/MMS/	08/29/1999	08/31/1999	32.122	24.676	4.473	27.2933	89.7845	540.0	2001.0
	1999	AT990829.Ab0	/MMS/	08/29/1999	08/31/1999	32.820	24.634	4.910	27.2933	89.7845	548.0	2001.0
	1999	AT990829.Ab1	/MMS/	08/29/1999	08/31/1999	32.770	24.281	4.876	27.2933	89.7845	556.0	2001.0
	1999	AT990829.Ab2	/MMS/	08/29/1999	08/31/1999	33.976	23.299	5.282	27.2933	89.7845	564.0	2001.0
	1999	AT990829.Ab3	/MMS/	08/29/1999	08/31/1999	32.514	22.549	5.823	27.2933	89.7845	572.0	2001.0
	1999	AT990829.Ab4	/MMS/	08/29/1999	08/31/1999	32.969	22.086	6.040	27.2933	89.7845	580.0	2001.0
	1999	AT990829.Ab5	/MMS/	08/29/1999	08/31/1999	31.369	20.794	5.727	27.2933	89.7845	588.0	2001.0
	1999	AT990829.Ab6	/MMS/	08/29/1999	08/31/1999	23.139	13.371	4.282	27.2933	89.7845	658.0	2001.0

Table B-2. Speed statistics for energetic current events associated with Loop Current eddy separations. (continued)

Event No.	Year	Filename	Directory	Event start date (m/d/y)	Event end date (m/d/y)	Maximum speed ($cm \cdot s^{-1}$)	Mean speed ($cm \cdot s^{-1}$)	Stand. dev. of speed ($cm \cdot s^{-1}$)	Latitude (°N)	Longitude (°W)	Depth (m)	Total water depth (m)
11	1999	AT990829.Ab7	/MMS/	08/29/1999	08/31/1999	23.855	14.449	5.255	27.2933	89.7845	666.0	2001.0
	1999	AT990829.Ab8	/MMS/	08/29/1999	08/31/1999	22.406	14.026	5.117	27.2933	89.7845	674.0	2001.0
	1999	AT990829.Ab9	/MMS/	08/29/1999	08/31/1999	24.461	14.241	5.163	27.2933	89.7845	682.0	2001.0
	1999	AT990829.Ac0	/MMS/	08/29/1999	08/31/1999	23.345	13.889	5.066	27.2933	89.7845	690.0	2001.0
	1999	AT990829.Ac1	/MMS/	08/29/1999	08/31/1999	22.792	13.369	5.285	27.2933	89.7845	698.0	2001.0
	1999	AT990829.Ac2	/MMS/	08/29/1999	08/31/1999	23.066	13.327	5.356	27.2933	89.7845	706.0	2001.0
	1999	AT990829.Ac3	/MMS/	08/29/1999	08/31/1999	24.369	13.559	5.119	27.2933	89.7845	714.0	2001.0
	1999	AT990829.Ac4	/MMS/	08/29/1999	08/31/1999	24.642	13.882	4.954	27.2933	89.7845	722.0	2001.0
	1999	AT990829.Ac5	/MMS/	08/29/1999	08/31/1999	25.214	14.496	5.414	27.2933	89.7845	730.0	2001.0
	1999	AT990829.Ac6	/MMS/	08/29/1999	08/31/1999	24.767	15.439	5.243	27.2933	89.7845	738.0	2001.0
	1999	AT990829.Ac7	/MMS/	08/29/1999	08/31/1999	24.144	14.851	5.582	27.2933	89.7845	746.0	2001.0
	1999	AT990829.Ac8	/MMS/	08/29/1999	08/31/1999	25.036	14.785	5.656	27.2933	89.7845	754.0	2001.0
	1999	AT990829.Ac9	/MMS/	08/29/1999	08/31/1999	25.333	14.397	6.194	27.2933	89.7845	762.0	2001.0
	1999	AT990829.Ad0	/MMS/	08/29/1999	08/31/1999	26.311	14.323	6.891	27.2933	89.7845	770.0	2001.0
	1999	AT990829.Ad1	/MMS/	08/29/1999	08/31/1999	27.245	15.084	7.978	27.2933	89.7845	778.0	2001.0
	1999	AT990829.Ad2	/MMS/	08/29/1999	08/31/1999	26.846	15.570	7.758	27.2933	89.7845	786.0	2001.0
	1999	AT990829.Ad3	/MMS/	08/29/1999	08/31/1999	27.927	15.699	8.022	27.2933	89.7845	794.0	2001.0
	1999	AT990829.Ad4	/MMS/	08/29/1999	08/31/1999	27.633	16.198	8.073	27.2933	89.7845	802.0	2001.0
	1999	AT990829.Ad5	/MMS/	08/29/1999	08/31/1999	26.897	16.063	7.351	27.2933	89.7845	810.0	2001.0
	1999	AT990829.Ad6	/MMS/	08/29/1999	08/31/1999	29.653	16.170	7.358	27.2933	89.7845	818.0	2001.0
	1999	AT990829.Ad7	/MMS/	08/29/1999	08/31/1999	28.622	16.621	7.933	27.2933	89.7845	826.0	2001.0
	1999	AT990829.Ad8	/MMS/	08/29/1999	08/31/1999	30.761	17.194	8.570	27.2933	89.7845	834.0	2001.0
	1999	AT990829.Ad9	/MMS/	08/29/1999	08/31/1999	31.749	17.749	8.863	27.2933	89.7845	842.0	2001.0
	1999	AT990829.Ae0	/MMS/	08/29/1999	08/31/1999	33.467	18.167	9.231	27.2933	89.7845	850.0	2001.0
	1999	AT990829.Ae1	/MMS/	08/29/1999	08/31/1999	34.823	18.078	9.611	27.2933	89.7845	858.0	2001.0
	1999	AT990829.Ae2	/MMS/	08/29/1999	08/31/1999	35.394	18.501	9.504	27.2933	89.7845	866.0	2001.0
	1999	AT990829.Ae3	/MMS/	08/29/1999	08/31/1999	34.627	18.378	9.605	27.2933	89.7845	874.0	2001.0
	1999	AT990829.Ae4	/MMS/	08/29/1999	08/31/1999	32.025	18.042	9.244	27.2933	89.7845	882.0	2001.0
	1999	AT990829.Ae5	/MMS/	08/29/1999	08/31/1999	36.270	18.536	9.340	27.2933	89.7845	890.0	2001.0
	1999	AT990829.Ae6	/MMS/	08/29/1999	08/31/1999	37.180	18.378	9.508	27.2933	89.7845	898.0	2001.0
	1999	AT990829.Ae7	/MMS/	08/29/1999	08/31/1999	37.591	18.186	9.804	27.2933	89.7845	906.0	2001.0
	1999	AT990829.Ae8	/MMS/	08/29/1999	08/31/1999	37.947	18.620	10.013	27.2933	89.7845	914.0	2001.0
	1999	AT990829.Ae9	/MMS/	08/29/1999	08/31/1999	37.794	19.450	9.924	27.2933	89.7845	922.0	2001.0
	1999	AT990829.Af0	/MMS/	08/29/1999	08/31/1999	38.081	19.840	9.921	27.2933	89.7845	930.0	2001.0

Table B-2. Speed statistics for energetic current events associated with Loop Current eddy separations. (continued)

Event No.	Year	Filename	Directory	Event start date (m/d/y)	Event end date (m/d/y)	Maximum speed ($cm \cdot s^{-1}$)	Mean speed ($cm \cdot s^{-1}$)	Stand. dev. of speed ($cm \cdot s^{-1}$)	Latitude (°N)	Longitude (°W)	Depth (m)	Total water depth (m)
11	1999	AT990829.Af1	/MMS/	08/29/1999	08/31/1999	39.273	20.112	10.292	27.2933	89.7845	938.0	2001.0
	1999	AT990829.Af2	/MMS/	08/29/1999	08/31/1999	39.524	20.023	10.475	27.2933	89.7845	946.0	2001.0
	1999	AT990829.Af3	/MMS/	08/29/1999	08/31/1999	37.943	20.086	10.783	27.2933	89.7845	954.0	2001.0
	1999	AT990829.Af4	/MMS/	08/29/1999	08/31/1999	38.821	19.908	10.639	27.2933	89.7845	962.0	2001.0
	1999	AT990829.Af5	/MMS/	08/29/1999	08/31/1999	41.226	20.552	10.828	27.2933	89.7845	970.0	2001.0
	1999	AT990829.Af6	/MMS/	08/29/1999	08/31/1999	42.546	20.684	11.553	27.2933	89.7845	978.0	2001.0
	1999	AT990829.Af7	/MMS/	08/29/1999	08/31/1999	40.363	21.236	11.032	27.2933	89.7845	986.0	2001.0
	1999	AT990829.Af8	/MMS/	08/29/1999	08/31/1999	41.482	20.993	11.300	27.2933	89.7845	994.0	2001.0
	1999	AT990829.Af9	/MMS/	08/29/1999	08/31/1999	41.685	21.059	11.131	27.2933	89.7845	1002.0	2001.0
	1999	AT990829.Ag0	/MMS/	08/29/1999	08/31/1999	39.672	20.622	11.142	27.2933	89.7845	1010.0	2001.0
	1999	AT990829.Ag1	/MMS/	08/29/1999	08/31/1999	40.523	20.292	11.227	27.2933	89.7845	1018.0	2001.0
	1999	AT990829.Ag2	/MMS/	08/29/1999	08/31/1999	39.498	19.954	11.058	27.2933	89.7845	1026.0	2001.0
	1999	AT990829.Ag3	/MMS/	08/29/1999	08/31/1999	42.049	20.493	11.149	27.2933	89.7845	1034.0	2001.0
	1999	AT990829.Ag4	/MMS/	08/29/1999	08/31/1999	39.916	20.688	11.120	27.2933	89.7845	1042.0	2001.0
	1999	AT990829.Ag5	/MMS/	08/29/1999	08/31/1999	40.084	20.290	10.473	27.2933	89.7845	1050.0	2001.0
	1999	AT990829.Ag6	/MMS/	08/29/1999	08/31/1999	40.743	19.989	11.284	27.2933	89.7845	1058.0	2001.0
	1999	AT990829.Ag7	/MMS/	08/29/1999	08/31/1999	40.647	19.970	11.498	27.2933	89.7845	1066.0	2001.0
	1999	AT990829.Ag9	/MMS/	08/29/1999	08/31/1999	43.567	19.716	11.073	27.2933	89.7845	1082.0	2001.0
	1999	AT990829.Ah0	/MMS/	08/29/1999	08/31/1999	42.208	19.129	11.953	27.2933	89.7845	1090.0	2001.0
	1999	AT990829.Ah1	/MMS/	08/29/1999	08/31/1999	39.124	19.662	11.600	27.2933	89.7845	1098.0	2001.0
	1999	AT990829.Ah2	/MMS/	08/29/1999	08/31/1999	40.660	19.135	11.633	27.2933	89.7845	1106.0	2001.0
	1999	AT990829.Ah3	/MMS/	08/29/1999	08/31/1999	39.765	19.978	11.856	27.2933	89.7845	1114.0	2001.0
	1999	AT990829.Ah4	/MMS/	08/29/1999	08/31/1999	41.775	19.861	11.631	27.2933	89.7845	1122.0	2001.0
	1999	AT990829.Ah5	/MMS/	08/29/1999	08/31/1999	40.962	19.795	11.920	27.2933	89.7845	1130.0	2001.0
	1999	AT990829.C01	/MMS/	08/29/1999	08/31/1999	29.196	16.229	9.138	27.2933	89.7845	800.0	2001.0
	1999	AT990829.C02	/MMS/	08/29/1999	08/31/1999	38.253	19.030	10.477	27.2933	89.7845	1000.0	2001.0
	1999	AT990829.C03	/MMS/	08/29/1999	08/31/1999	43.167	20.185	13.359	27.2933	89.7845	1200.0	2001.0
	1999	AT990829.C04	/MMS/	08/29/1999	08/31/1999	45.421	19.166	14.217	27.2933	89.7845	1400.0	2001.0
	1999	AT990829.C05	/MMS/	08/29/1999	08/31/1999	52.032	19.109	16.110	27.2933	89.7845	1600.0	2001.0
	1999	AT990829.C06	/MMS/	08/29/1999	08/31/1999	54.617	20.463	18.042	27.2933	89.7845	1800.0	2001.0
	1999	AT990829.C07	/MMS/	08/29/1999	08/31/1999	50.284	21.051	15.677	27.2933	89.7845	1989.0	2001.0
	1999	GC990829.C01	/MMS/	08/29/1999	08/31/1999	95.005	59.281	24.958	27.2280	89.9710	1600.0	1998.0
	1999	GC990829.C02	/MMS/	08/29/1999	08/31/1999	85.574	56.750	17.087	27.2280	89.9710	1800.0	1998.0
	1999	GC990829.C03	/MMS/	08/29/1999	08/31/1999	90.082	48.683	17.913	27.2280	89.9710	1989.0	1998.0

Table B-2. Speed statistics for energetic current events associated with Loop Current eddy separations. (continued)

Notes by event number

1 1978: June

A packet of inertial oscillations occurs at NOAA M3 at 168 m (amplitudes of ~10 cm·s^{-1}). A packet of inertial oscillations occurs at NOAA T1 at 550 m (amplitudes of ~20 cm·s^{-1}). Data from NOAA M3 and T1 are plotted in Figure 6.3.1-2.

2 1979: April

Inertial oscillation packets seen at NOAA T1 960 m. Data from NOAA M3 and T1 are plotted in Figure 6.3.1-2.

3 1981: March

A surface intensified feature is present most of the month in Industry GC184, although there are no SST, SSH, or drifter data available to confirm whether this event is an LCE, cyclone, or a small slope anticyclonic eddy. Data from Industry GC184 are plotted in Figure 6.3.12-2.

4 1983: March, Unnamed LCE

Increased high-frequency current variability (super-inertial) at SAIC A at 1600 m, but data quality is suspect. Some low-frequency energy at SAIC A, 172 m, with currents to the northwest. Data from SAIC A are plotted in Figure 6.3.3-2.

5 1984: February, Unnamed LCE

Low-frequency, bottom-intensified motions at SAIC G at 2364 and 3174 m. Data from SAIC G are plotted in Figure 6.3.3-2.

6 1984: August, Slim Chance Eddy (also called Eddy Arnold)

Coherent and bottom-intensified currents of significant amplitude (~45 cm·s^{-1}). This event also is seen at the SAIC G 1565, 2364, and 3175 m instruments. However, it is not seen in the upper (< 700 m) instruments. Data from SAIC G are plotted in Figure 6.3.3-2.

7 1986: January, Hot Core Eddy

Inertial-period energy is in the deep records of SAIC A and G, particularly at 1000 m. Data from SAIC A and G are plotted in Figure 6.3.3-2.

8 1987: September, Eddy Kathleen

Some low-frequency motions are at SAIC GG (amplitudes of ~25 cm·s^{-1}) at 1650 m. Data from SAIC GG are plotted in Figure 6.3.3-8.

9 1988: May, Eddy Murphy

The upper records from the SAIC central Gulf locations are dominated by inertial oscillations. The deep records at SAIC GG show a 15 cm·s^{-1} low-frequency wave on May 1-16. Note at the same time, the effects of Eddy Kathleen are seen at SAIC GG at 100 and 300 m. Data from SAIC EE, FF, and GG are plotted in Figure 6.3.3-8.

10 1998: March, Eddy Fourchon

Slope eddy Gyre begins to influence DeSoto Canyon during March when Eddy Fourchon separates from the Loop Current. There is no way to separate the causal effects of separation from the direct influence of the slope eddy. See Slope Eddy Gyre statistics in Table A-4. Data from SAIC EIS are plotted in Figure 6.3.5-2.

Table B-2. Speed statistics for energetic current events associated with Loop Current eddy separations. (continued)

Notes by event number (continued)

11 1999: August, Eddy Indigo

Strong bottom-intensified oscillations occur at SAIC EISEXT locations (I1, I2, I3). Speeds approach 100 $cm \cdot s^{-1}$ at I2 bottom instruments. This is a major event at SAIC EISEXT locations and represents some of the strongest bottom currents measured in the Gulf of Mexico. See bottom-intensified motions in Table A-8 for more information. Data from SAIC EIS Extension are plotted in Figures 6.3.6-2 and 6.3.6-3.

Table B-3. Speed statistics for energetic current events associated with Loop Current eddies. Given are the name of the file containing the event (keyed to the directory on the CD-ROM database), the start and stop dates used to characterize the event, maximum speed, mean speed, standard deviation of speed, mooring location, depth of the instrument, and total water depth. Comments on the event, keyed by the event number, are given in the notes below the table.

Event No.	Year	Filename	Directory	Event start date (m/d/y)	Event end date (m/d/y)	Maximum speed ($cm \cdot s^{-1}$)	Mean speed ($cm \cdot s^{-1}$)	Stand. dev. of speed ($cm \cdot s^{-1}$)	Latitude (°N)	Longitude (°W)	Depth (m)	Total water depth (m)
1	1978	DD780617.C01	/NODC_DEEP/	07/01/1978	08/23/1978	40.764	14.866	8.029	29.1983	87.6383	70.0	1033.0
	1978	DD780617.C02	/NODC_DEEP/	07/01/1978	08/23/1978	28.571	9.061	7.727	29.1983	87.6383	168.0	1033.0
	1978	DD780617.C03	/NODC_DEEP/	07/01/1978	08/23/1978	16.381	5.301	3.267	29.1983	87.6383	970.0	1033.0
2	1980	PI800717.C01	/NODC_DEEP/	09/15/1980	10/31/1980	84.384	53.672	13.054	25.9900	96.1517	200.0	730.0
	1980	PI800717.C02	/NODC_DEEP/	09/15/1980	10/31/1980	42.518	15.424	9.687	25.9900	96.1517	450.0	730.0
	1980	PI800717.C03	/NODC_DEEP/	09/15/1980	10/31/1980	32.858	6.846	6.254	25.9900	96.1517	700.0	730.0
3	1984	HH841018.C01	/NODC_DEEP/	10/18/1984	12/31/1984	73.755	19.204	14.259	25.7150	84.8850	172.0	1697.0
	1984	HH841018.C02	/NODC_DEEP/	10/18/1984	12/31/1984	36.319	7.610	7.728	25.7150	84.8850	400.0	1697.0
	1984	HH841018.C03	/NODC_DEEP/	10/18/1984	12/31/1984	28.262	2.409	3.231	25.7150	84.8850	738.0	1697.0
	1984	HH841018.C04	/NODC_DEEP/	10/18/1984	12/31/1984	11.182	1.849	1.349	25.7150	84.8850	1100.0	1697.0
	1984	HH841018.C05	/NODC_DEEP/	10/18/1984	12/31/1984	16.225	2.540	2.230	25.7150	84.8850	1600.0	1697.0
4	1985	HH850124.C01	/NODC_DEEP/	01/24/1985	04/30/1985	67.900	21.772	15.111	25.7150	84.8850	172.0	1697.0
	1985	HH850124.C02	/NODC_DEEP/	01/24/1985	04/30/1985	43.371	9.516	8.522	25.7150	84.8850	400.0	1697.0
	1985	HH850124.C03	/NODC_DEEP/	01/24/1985	04/30/1985	35.738	7.663	7.116	25.7150	84.8850	738.0	1697.0
	1985	HH850124.C04	/NODC_DEEP/	01/24/1985	04/30/1985	27.461	3.650	3.736	25.7150	84.8850	1100.0	1697.0
	1985	HH850124.C05	/NODC_DEEP/	01/24/1985	04/30/1985	23.097	5.089	4.796	25.7150	84.8850	1600.0	1697.0
	1985	HH850124.C06	/NODC_DEEP/	01/24/1985	03/11/1985	69.864	39.874	8.968	25.6003	85.4995	397.0	3200.0
	1985	HH850312.C01	/NODC_DEEP/	03/12/1985	04/30/1985	41.053	10.478	11.293	25.6003	85.4995	397.0	3200.0
	1985	HH850124.C07	/NODC_DEEP/	01/24/1985	03/11/1985	42.666	19.338	7.834	25.6003	85.4995	703.0	3200.0
	1985	HH850312.C02	/NODC_DEEP/	03/24/1985	04/30/1985	42.709	22.085	8.845	25.6003	85.4995	703.0	3200.0
	1985	HH850124.C08	/NODC_DEEP/	01/24/1985	04/30/1985	37.700	8.797	8.273	25.6003	85.4995	1565.0	3200.0
	1985	HH850124.C09	/NODC_DEEP/	01/24/1985	04/30/1985	37.670	14.255	7.700	25.6003	85.4995	2364.0	3200.0
	1985	HH850124.C10	/NODC_DEEP/	01/24/1985	04/30/1985	36.431	11.131	7.850	25.6003	85.4995	3174.0	3200.0
5	1985	HH850801.C01	/NODC_DEEP/	09/01/1985	11/30/1985	87.464	32.344	20.129	25.7150	84.8850	172.0	1697.0
	1985	HH850801.C02	/NODC_DEEP/	09/01/1985	11/30/1985	62.076	11.164	11.768	25.7150	84.8850	400.0	1697.0
	1985	HH850731.C01	/NODC_DEEP/	09/01/1985	11/30/1985	33.443	4.285	5.077	25.7150	84.8850	738.0	1697.0
	1985	HH850731.C02	/NODC_DEEP/	09/01/1985	11/30/1985	21.200	10.566	3.435	25.7150	84.8850	1100.0	1697.0
	1985	HH850801.C03	/NODC_DEEP/	09/01/1985	11/30/1985	50.809	13.885	11.106	25.6003	85.4995	703.0	3200.0
	1985	HH850801.C04	/NODC_DEEP/	09/01/1985	11/30/1985	31.802	9.683	6.158	25.6003	85.4995	1565.0	3200.0
	1985	HH850801.C05	/NODC_DEEP/	09/01/1985	11/30/1985	33.035	9.850	6.474	25.6003	85.4995	2364.0	3200.0

Table B-3. Speed statistics for energetic current events associated with Loop Current eddies. (continued)

Event No.	Year	Filename	Directory	Event start date (m/d/y)	Event end date (m/d/y)	Maximum speed (cm·s^{-1})	Mean speed (cm·s^{-1})	Stand. dev. of speed (cm·s^{-1})	Latitude (°N)	Longitude (°W)	Depth (m)	Total water depth (m)
5	1985	HH850801.C06	/NODC_DEEP/	09/01/1985	11/30/1985	29.865	6.661	6.681	25.6003	85.4995	3174.0	3200.0
6	1985	MG850615.C02	/NODC_DEEP/	10/01/1985	10/02/1985	20.165	14.146	3.615	25.8717	94.8800	300.0	3000.0
	1985	MG851020.C01	/NODC_DEEP/	10/20/1985	12/31/1985	46.296	25.557	8.412	25.8717	94.8800	300.0	3000.0
	1985	MG850615.C04	/NODC_DEEP/	10/01/1985	12/31/1985	23.905	6.241	4.689	25.8717	94.8800	1500.0	3000.0
7	1986	MG851020.C01	/NODC_DEEP/	01/01/1986	02/28/1986	58.901	27.427	11.207	25.8717	94.8800	300.0	3000.0
	1986	MG850615.C04	/NODC_DEEP/	01/01/1986	02/28/1986	20.072	6.227	4.410	25.8717	94.8800	1500.0	3000.0
8	1988	KC871108.C01	/NODC_DEEP/	01/01/1988	06/30/1988	72.504	22.224	17.314	26.7400	91.9950	100.0	1750.0
	1988	KC871109.C01	/NODC_DEEP/	01/01/1988	02/15/1988	22.783	7.333	4.659	26.7400	91.9950	300.0	1750.0
	1988	KC880414.C01	/NODC_DEEP/	04/14/1988	06/30/1988	37.435	12.273	5.875	26.7400	91.9950	300.0	1750.0
	1988	KC871108.C02	/NODC_DEEP/	01/01/1988	06/30/1988	43.979	13.728	7.908	26.7400	91.9950	305.0	1750.0
	1988	KC871108.C03	/NODC_DEEP/	01/01/1988	06/30/1988	20.539	5.392	3.550	26.7400	91.9950	725.0	1750.0
	1988	KC870406.C04	/NODC_DEEP/	01/01/1988	06/30/1988	12.144	3.527	1.887	26.7400	91.9950	1650.0	1750.0
	1988	AB871109.C01	/NODC_DEEP/	01/01/1988	06/30/1988	87.250	37.882	15.469	25.6532	92.0333	100.0	3000.0
	1988	AB880409.C01	/NODC_DEEP/	04/09/1988	06/30/1988	42.561	20.430	7.208	25.6532	92.0333	300.0	3000.0
	1988	AB871110.C01	/NODC_DEEP/	01/01/1988	04/08/1988	44.817	15.151	10.029	25.6532	92.0333	305.0	3000.0
	1988	AB871109.C02	/NODC_DEEP/	01/01/1988	06/30/1988	20.536	8.262	3.618	25.6532	92.0333	725.0	3000.0
	1988	AB870406.C03	/NODC_DEEP/	01/01/1988	06/30/1988	19.701	3.153	3.447	25.6532	92.0333	1650.0	3000.0
	1988	AB871109.C03	/NODC_DEEP/	01/01/1988	04/03/1988	15.495	5.760	3.021	25.6532	92.0333	2500.0	3000.0
	1988	AB880409.C02	/NODC_DEEP/	04/09/1988	06/30/1988	18.490	5.344	3.193	25.6532	92.0333	2500.0	3000.0
9	1988	KC871108.C01	/NODC_DEEP/	08/01/1988	09/09/1988	45.801	14.422	10.208	26.7400	91.9950	100.0	1750.0
	1988	KC880414.C01	/NODC_DEEP/	08/01/1988	09/10/1988	52.269	20.967	8.627	26.7400	91.9950	300.0	1750.0
	1988	KC871108.C02	/NODC_DEEP/	08/01/1988	09/10/1988	52.406	23.628	7.987	26.7400	91.9950	305.0	1750.0
	1988	KC871108.C03	/NODC_DEEP/	08/01/1988	10/31/1988	16.340	5.877	3.266	26.7400	91.9950	725.0	1750.0
	1988	KC870406.C04	/NODC_DEEP/	08/01/1988	09/20/1988	11.953	3.299	1.867	26.7400	91.9950	1650.0	1750.0
	1988	AB871109.C01	/NODC_DEEP/	08/01/1988	10/30/1988	120.767	67.649	16.181	25.6532	92.0333	100.0	3000.0
	1988	AB880409.C01	/NODC_DEEP/	08/01/1988	10/30/1988	50.033	25.068	7.983	25.6532	92.0333	300.0	3000.0
	1988	AB871109.C02	/NODC_DEEP/	08/01/1988	10/30/1988	28.754	8.313	4.346	25.6532	92.0333	725.0	3000.0
	1988	AB870406.C03	/NODC_DEEP/	08/01/1988	10/30/1988	24.554	7.770	6.992	25.6532	92.0333	1650.0	3000.0
	1988	AB880409.C02	/NODC_DEEP/	08/01/1988	10/30/1988	30.619	8.984	7.028	25.6532	92.0333	2500.0	3000.0
10	1991	EW910906.A01	/INDUSTRY/	09/06/1991	09/13/1991	87.878	55.412	15.236	28.1064	90.2020	31.0	236.0
	1991	EW910920.A01	/INDUSTRY/	09/20/1991	10/31/1991	80.872	27.430	17.813	28.1064	90.2020	31.0	236.0
	1991	EW910906.A02	/INDUSTRY/	09/06/1991	09/13/1991	89.554	54.788	16.210	28.1064	90.2020	39.0	236.0
	1991	EW910920.A02	/INDUSTRY/	09/20/1991	10/31/1991	86.001	26.807	19.080	28.1064	90.2020	39.0	236.0
	1991	EW910906.A03	/INDUSTRY/	09/06/1991	09/13/1991	89.359	54.943	17.090	28.1064	90.2020	47.0	236.0

Table B-3. Speed statistics for energetic current events associated with Loop Current eddies. (continued)

Event No.	Year	Filename	Directory	Event start date (m/d/y)	Event end date (m/d/y)	Maximum speed (cm·s^{-1})	Mean speed (cm·s^{-1})	Stand. dev. of speed (cm·s^{-1})	Latitude (°N)	Longitude (°W)	Depth (m)	Total water depth (m)
10	1991	EW910920.A03	/INDUSTRY/	09/20/1991	10/31/1991	88.955	26.424	18.708	28.1064	90.2020	47.0	236.0
	1991	EW910906.A04	/INDUSTRY/	09/06/1991	09/13/1991	86.770	51.552	17.204	28.1064	90.2020	55.0	236.0
	1991	EW910920.A04	/INDUSTRY/	09/20/1991	10/31/1991	89.762	26.071	18.160	28.1064	90.2020	55.0	236.0
	1991	EW910906.A05	/INDUSTRY/	09/06/1991	09/13/1991	91.236	47.997	16.433	28.1064	90.2020	63.0	236.0
	1991	EW910920.A05	/INDUSTRY/	09/20/1991	10/31/1991	89.332	25.858	18.294	28.1064	90.2020	63.0	236.0
	1991	EW910906.A06	/INDUSTRY/	09/06/1991	09/13/1991	88.640	45.584	14.952	28.1064	90.2020	71.0	236.0
	1991	EW910920.A06	/INDUSTRY/	09/20/1991	10/31/1991	87.573	25.918	18.816	28.1064	90.2020	71.0	236.0
	1991	EW910906.A07	/INDUSTRY/	09/06/1991	09/13/1991	82.002	42.855	13.811	28.1064	90.2020	79.0	236.0
	1991	EW910920.A07	/INDUSTRY/	09/20/1991	10/31/1991	83.744	24.988	18.335	28.1064	90.2020	79.0	236.0
	1991	EW910906.A08	/INDUSTRY/	09/06/1991	09/13/1991	74.035	39.426	12.396	28.1064	90.2020	87.0	236.0
	1991	EW910920.A08	/INDUSTRY/	09/20/1991	10/31/1991	80.654	24.116	17.631	28.1064	90.2020	87.0	236.0
	1991	EW910906.A09	/INDUSTRY/	09/06/1991	09/13/1991	73.866	37.174	12.379	28.1064	90.2020	95.0	236.0
	1991	EW910920.A09	/INDUSTRY/	09/20/1991	10/31/1991	74.138	22.818	16.603	28.1064	90.2020	95.0	236.0
	1991	EW910906.A10	/INDUSTRY/	09/06/1991	09/13/1991	76.781	33.959	12.554	28.1064	90.2020	103.0	236.0
	1991	EW910920.A10	/INDUSTRY/	09/20/1991	10/31/1991	72.707	20.506	15.664	28.1064	90.2020	103.0	236.0
	1991	EW910906.A11	/INDUSTRY/	09/06/1991	09/13/1991	70.436	31.100	12.836	28.1064	90.2020	111.0	236.0
	1991	EW910920.A11	/INDUSTRY/	09/20/1991	10/31/1991	66.994	17.748	12.465	28.1064	90.2020	111.0	236.0
	1991	EW910906.A12	/INDUSTRY/	09/06/1991	09/13/1991	65.531	27.739	12.397	28.1064	90.2020	119.0	236.0
	1991	EW910920.A12	/INDUSTRY/	09/20/1991	10/31/1991	68.347	17.550	12.139	28.1064	90.2020	119.0	236.0
	1991	EW910906.A13	/INDUSTRY/	09/06/1991	09/13/1991	64.413	25.819	11.387	28.1064	90.2020	127.0	236.0
	1991	EW910920.A13	/INDUSTRY/	09/20/1991	10/31/1991	65.964	15.539	11.105	28.1064	90.2020	127.0	236.0
	1991	EW910906.A14	/INDUSTRY/	09/06/1991	09/13/1991	61.057	25.590	10.629	28.1064	90.2020	135.0	236.0
	1991	EW910920.A14	/INDUSTRY/	09/20/1991	10/31/1991	64.498	15.897	10.318	28.1064	90.2020	135.0	236.0
	1991	EW910906.A15	/INDUSTRY/	09/06/1991	09/13/1991	45.393	23.536	8.076	28.1064	90.2020	143.0	236.0
	1991	EW910920.A15	/INDUSTRY/	09/20/1991	10/31/1991	56.436	14.387	8.832	28.1064	90.2020	143.0	236.0
	1991	EW910906.A16	/INDUSTRY/	09/06/1991	09/13/1991	42.547	21.787	7.522	28.1064	90.2020	151.0	236.0
	1991	EW910920.A16	/INDUSTRY/	09/20/1991	10/31/1991	49.244	13.846	8.458	28.1064	90.2020	151.0	236.0
	1991	EW910906.A17	/INDUSTRY/	09/06/1991	09/13/1991	43.489	20.587	7.962	28.1064	90.2020	159.0	236.0
	1991	EW910920.A17	/INDUSTRY/	09/20/1991	10/31/1991	51.935	13.997	8.962	28.1064	90.2020	159.0	236.0
	1991	EW910906.A18	/INDUSTRY/	09/06/1991	09/13/1991	39.424	17.404	7.813	28.1064	90.2020	167.0	236.0
	1991	EW910920.A18	/INDUSTRY/	09/20/1991	10/31/1991	45.069	13.161	7.579	28.1064	90.2020	167.0	236.0
	1991	EW910906.A19	/INDUSTRY/	09/06/1991	09/13/1991	38.471	15.527	8.436	28.1064	90.2020	175.0	236.0
	1991	EW910920.A19	/INDUSTRY/	09/20/1991	10/31/1991	43.267	12.948	7.203	28.1064	90.2020	175.0	236.0
	1991	EW910906.A20	/INDUSTRY/	09/06/1991	09/13/1991	34.482	13.240	7.287	28.1064	90.2020	183.0	236.0

Table B-3. Speed statistics for energetic current events associated with Loop Current eddies. (continued)

Event No.	Year	Filename	Directory	Event start date (m/d/y)	Event end date (m/d/y)	Maximum speed ($cm \cdot s^{-1}$)	Mean speed ($cm \cdot s^{-1}$)	Stand. dev. of speed ($cm \cdot s^{-1}$)	Latitude (°N)	Longitude (°W)	Depth (m)	Total water depth (m)
10	1991	EW910920.A20	/INDUSTRY/	09/20/1991	10/31/1991	34.533	12.069	6.513	28.1064	90.2020	183.0	236.0
	1991	EW910906.A21	/INDUSTRY/	09/06/1991	09/13/1991	32.070	9.375	5.873	28.1064	90.2020	191.0	236.0
	1991	EW910920.A21	/INDUSTRY/	09/20/1991	10/31/1991	39.275	11.521	6.359	28.1064	90.2020	191.0	236.0
	1991	EW910906.A22	/INDUSTRY/	09/06/1991	09/13/1991	26.519	8.674	4.836	28.1064	90.2020	199.0	236.0
	1991	EW910920.A22	/INDUSTRY/	09/20/1991	10/31/1991	22.655	7.266	3.790	28.1064	90.2020	199.0	236.0
	1991	EW910906.A23	/INDUSTRY/	09/06/1991	09/13/1991	66.922	18.177	12.248	28.1064	90.2020	207.0	236.0
	1991	EW910920.A23	/INDUSTRY/	09/20/1991	10/31/1991	64.771	15.427	9.812	28.1064	90.2020	207.0	236.0
	1991	EW910906.A24	/INDUSTRY/	09/06/1991	09/13/1991	54.939	14.946	9.687	28.1064	90.2020	215.0	236.0
	1991	EW910920.A24	/INDUSTRY/	09/20/1991	10/31/1991	50.210	11.958	7.668	28.1064	90.2020	215.0	236.0
	1991	EW910906.A25	/INDUSTRY/	09/06/1991	09/13/1991	34.125	10.835	6.161	28.1064	90.2020	223.0	236.0
	1991	EW910920.A25	/INDUSTRY/	09/20/1991	10/31/1991	31.851	8.824	5.002	28.1064	90.2020	223.0	236.0
	1991	EW910906.A26	/INDUSTRY/	09/06/1991	09/13/1991	18.118	6.359	3.232	28.1064	90.2020	231.0	236.0
	1991	EW910920.A26	/INDUSTRY/	09/20/1991	10/31/1991	14.300	5.089	2.504	28.1064	90.2020	231.0	236.0
11	1992	EB920409.C01	/TAMU/	06/01/1992	09/30/1992	100.011	37.560	24.883	27.3690	95.8940	22.0	510.0
12	1992	EB921018.C01	/TAMU/	11/01/1992	12/31/1992	78.365	32.284	15.921	27.3690	95.8940	17.0	505.0
	1992	EB921018.C02	/TAMU/	11/01/1992	12/31/1992	74.301	25.974	14.547	27.3690	95.8940	105.0	505.0
	1992	EB921018.C03	/TAMU/	11/01/1992	12/31/1992	21.446	5.386	4.399	27.3690	95.8940	495.0	505.0
13	1993	EB930520.C01	/TAMU/	06/01/1993	08/31/1993	64.692	28.679	15.432	27.3860	95.8990	101.0	501.0
14	1993	GC930718.C01	/TAMU/	08/01/1993	08/31/1993	71.867	27.507	12.167	27.9280	90.4970	14.0	500.0
15	1995	GC950625.A01	/INDUSTRY/	07/01/1995	07/16/1995	73.561	48.728	11.428	27.7569	90.7301	29.0	876.8
	1995	GC950625.A02	/INDUSTRY/	07/01/1995	07/16/1995	75.515	42.901	13.768	27.7569	90.7301	37.0	876.8
	1995	GC950625.A03	/INDUSTRY/	07/01/1995	07/16/1995	74.560	44.266	12.794	27.7569	90.7301	45.0	876.8
	1995	GC950625.A04	/INDUSTRY/	07/01/1995	07/16/1995	74.285	46.828	10.531	27.7569	90.7301	53.0	876.8
	1995	GC950625.A05	/INDUSTRY/	07/01/1995	07/16/1995	69.516	47.738	9.479	27.7569	90.7301	61.0	876.8
	1995	GC950625.A06	/INDUSTRY/	07/01/1995	07/16/1995	71.253	48.912	9.634	27.7569	90.7301	69.0	876.8
	1995	GC950625.A07	/INDUSTRY/	07/01/1995	07/16/1995	70.401	49.390	9.572	27.7569	90.7301	77.0	876.8
	1995	GC950625.A08	/INDUSTRY/	07/01/1995	07/16/1995	67.418	48.046	9.363	27.7569	90.7301	85.0	876.8
	1995	GC950625.A09	/INDUSTRY/	07/01/1995	07/16/1995	64.817	46.810	8.547	27.7569	90.7301	93.0	876.8
	1995	GC950625.A10	/INDUSTRY/	07/01/1995	07/16/1995	60.638	44.229	7.209	27.7569	90.7301	101.0	876.8
	1995	GC950625.A11	/INDUSTRY/	07/01/1995	07/16/1995	59.064	44.467	6.418	27.7569	90.7301	109.0	876.8
	1995	GC950625.A12	/INDUSTRY/	07/01/1995	07/16/1995	56.641	43.475	5.886	27.7569	90.7301	117.0	876.8
	1995	GC950625.A13	/INDUSTRY/	07/01/1995	07/16/1995	56.004	42.346	5.547	27.7569	90.7301	125.0	876.8
	1995	GC950625.A14	/INDUSTRY/	07/01/1995	07/16/1995	56.396	41.084	5.676	27.7569	90.7301	133.0	876.8
	1995	GC950625.A15	/INDUSTRY/	07/01/1995	07/16/1995	55.109	40.209	6.197	27.7569	90.7301	141.0	876.8

Table B-3. Speed statistics for energetic current events associated with Loop Current eddies. (continued)

Event No.	Year	Filename	Directory	Event start date (m/d/y)	Event end date (m/d/y)	Maximum speed (cm·s^{-1})	Mean speed (cm·s^{-1})	Stand. dev. of speed (cm·s^{-1})	Latitude (°N)	Longitude (°W)	Depth (m)	Total water depth (m)
15	1995	GC950625.A16	/INDUSTRY/	07/01/1995	07/16/1995	55.340	39.250	6.458	27.7569	90.7301	149.0	876.8
	1995	GC950625.A17	/INDUSTRY/	07/01/1995	07/16/1995	54.893	37.997	6.540	27.7569	90.7301	157.0	876.8
	1995	GC950625.A18	/INDUSTRY/	07/01/1995	07/16/1995	52.842	36.736	6.530	27.7569	90.7301	165.0	876.8
	1995	GC950625.A19	/INDUSTRY/	07/01/1995	07/16/1995	52.369	35.448	6.512	27.7569	90.7301	173.0	876.8
	1995	GC950625.A20	/INDUSTRY/	07/01/1995	07/16/1995	50.934	34.507	6.361	27.7569	90.7301	181.0	876.8
	1995	GC950625.A21	/INDUSTRY/	07/01/1995	07/16/1995	49.186	33.604	6.359	27.7569	90.7301	189.0	876.8
	1995	GC950625.A22	/INDUSTRY/	07/01/1995	07/16/1995	49.601	32.510	6.445	27.7569	90.7301	197.0	876.8
	1995	GC950625.A23	/INDUSTRY/	07/01/1995	07/16/1995	50.344	31.344	6.738	27.7569	90.7301	205.0	876.8
	1995	GC950625.A24	/INDUSTRY/	07/01/1995	07/16/1995	50.142	30.061	6.885	27.7569	90.7301	213.0	876.8
	1995	GC950625.A25	/INDUSTRY/	07/01/1995	07/16/1995	48.283	29.106	6.877	27.7569	90.7301	221.0	876.8
	1995	GC950625.A26	/INDUSTRY/	07/01/1995	07/16/1995	48.231	27.895	6.940	27.7569	90.7301	229.0	876.8
	1995	GC950625.A27	/INDUSTRY/	07/01/1995	07/16/1995	47.668	26.990	7.074	27.7569	90.7301	237.0	876.8
	1995	GC950625.A28	/INDUSTRY/	07/01/1995	07/16/1995	46.487	26.074	7.197	27.7569	90.7301	245.0	876.8
	1995	GC950625.A29	/INDUSTRY/	07/01/1995	07/16/1995	44.847	24.789	7.521	27.7569	90.7301	253.0	876.8
	1995	GC950625.A30	/INDUSTRY/	07/01/1995	07/16/1995	44.478	23.463	7.475	27.7569	90.7301	261.0	876.8
	1995	GC950625.A31	/INDUSTRY/	07/01/1995	07/16/1995	43.821	22.403	7.533	27.7569	90.7301	269.0	876.8
	1995	GC950625.A32	/INDUSTRY/	07/01/1995	07/16/1995	40.262	21.437	7.464	27.7569	90.7301	277.0	876.8
	1995	GC950625.A33	/INDUSTRY/	07/01/1995	07/16/1995	38.451	20.393	7.136	27.7569	90.7301	285.0	876.8
	1995	GC950625.A34	/INDUSTRY/	07/01/1995	07/16/1995	36.184	19.290	7.035	27.7569	90.7301	293.0	876.8
	1995	GC950625.A35	/INDUSTRY/	07/01/1995	07/16/1995	34.562	18.247	6.692	27.7569	90.7301	301.0	876.8
	1995	GC950625.A36	/INDUSTRY/	07/01/1995	07/16/1995	32.596	17.320	6.323	27.7569	90.7301	309.0	876.8
	1995	GC950625.A37	/INDUSTRY/	07/01/1995	07/16/1995	30.761	16.431	5.832	27.7569	90.7301	317.0	876.8
	1995	GC950625.A38	/INDUSTRY/	07/01/1995	07/16/1995	28.779	15.531	5.456	27.7569	90.7301	325.0	876.8
	1995	GC950625.A39	/INDUSTRY/	07/01/1995	07/16/1995	27.951	14.831	5.273	27.7569	90.7301	333.0	876.8
	1995	GC950625.A40	/INDUSTRY/	07/01/1995	07/16/1995	26.315	14.278	5.036	27.7569	90.7301	341.0	876.8
	1995	GC950625.A41	/INDUSTRY/	07/01/1995	07/16/1995	24.885	13.779	4.787	27.7569	90.7301	349.0	876.8
	1995	GC950625.A42	/INDUSTRY/	07/01/1995	07/16/1995	23.964	13.119	4.625	27.7569	90.7301	357.0	876.8
	1995	GC950625.A43	/INDUSTRY/	07/01/1995	07/16/1995	23.505	12.458	4.636	27.7569	90.7301	365.0	876.8
	1995	GC950625.A44	/INDUSTRY/	07/01/1995	07/16/1995	23.324	12.022	4.641	27.7569	90.7301	373.0	876.8
	1995	GC950625.A45	/INDUSTRY/	07/01/1995	07/16/1995	20.887	11.558	4.677	27.7569	90.7301	381.0	876.8
	1995	GC950625.A46	/INDUSTRY/	07/01/1995	07/16/1995	20.500	10.959	4.598	27.7569	90.7301	389.0	876.8
	1995	GC950625.A47	/INDUSTRY/	07/01/1995	07/16/1995	22.051	10.467	4.343	27.7569	90.7301	397.0	876.8
	1995	GC950625.A48	/INDUSTRY/	07/01/1995	07/16/1995	20.359	10.233	3.995	27.7569	90.7301	405.0	876.8
	1995	GC950625.A49	/INDUSTRY/	07/01/1995	07/16/1995	18.507	10.095	3.728	27.7569	90.7301	413.0	876.8

Table B-3. Speed statistics for energetic current events associated with Loop Current eddies. (continued)

Event No.	Year	Filename	Directory	Event start date (m/d/y)	Event end date (m/d/y)	Maximum speed ($cm \cdot s^{-1}$)	Mean speed ($cm \cdot s^{-1}$)	Stand. dev. of speed ($cm \cdot s^{-1}$)	Latitude (°N)	Longitude (°W)	Depth (m)	Total water depth (m)
15	1995	GC950625.A50	/INDUSTRY/	07/01/1995	07/16/1995	19.698	10.042	3.717	27.7569	90.7301	421.0	876.8
	1995	GC950625.A51	/INDUSTRY/	07/01/1995	07/16/1995	19.609	9.877	3.803	27.7569	90.7301	429.0	876.8
	1995	GC950625.A52	/INDUSTRY/	07/01/1995	07/16/1995	18.682	9.401	3.828	27.7569	90.7301	437.0	876.8
	1995	GC950625.A53	/INDUSTRY/	07/01/1995	07/16/1995	18.385	9.048	3.734	27.7569	90.7301	445.0	876.8
	1995	GC950625.A54	/INDUSTRY/	07/01/1995	07/16/1995	17.923	8.697	3.885	27.7569	90.7301	453.0	876.8
	1995	GC950625.A55	/INDUSTRY/	07/01/1995	07/16/1995	17.923	8.427	3.963	27.7569	90.7301	461.0	876.8
	1995	GC950625.A56	/INDUSTRY/	07/01/1995	07/16/1995	18.337	8.118	3.966	27.7569	90.7301	469.0	876.8
	1995	GC950625.A57	/INDUSTRY/	07/01/1995	07/16/1995	18.561	7.849	3.987	27.7569	90.7301	477.0	876.8
	1995	GC950625.A58	/INDUSTRY/	07/01/1995	07/16/1995	17.493	7.438	3.918	27.7569	90.7301	485.0	876.8
	1995	GC950625.A59	/INDUSTRY/	07/01/1995	07/16/1995	17.393	7.276	3.840	27.7569	90.7301	493.0	876.8
	1995	GC950625.A60	/INDUSTRY/	07/01/1995	07/16/1995	16.867	6.984	3.581	27.7569	90.7301	501.0	876.8
	1995	GC950625.A61	/INDUSTRY/	07/01/1995	07/16/1995	16.508	6.709	3.288	27.7569	90.7301	509.0	876.8
	1995	GC950625.A62	/INDUSTRY/	07/01/1995	07/16/1995	16.808	6.507	3.147	27.7569	90.7301	517.0	876.8
	1995	GC950625.A63	/INDUSTRY/	07/01/1995	07/16/1995	16.621	6.397	3.190	27.7569	90.7301	525.0	876.8
	1995	GC950625.A64	/INDUSTRY/	07/01/1995	07/16/1995	17.443	6.309	3.247	27.7569	90.7301	533.0	876.8
	1995	GC950625.A65	/INDUSTRY/	07/01/1995	07/16/1995	17.066	6.202	3.293	27.7569	90.7301	541.0	876.8
	1995	GC950625.A66	/INDUSTRY/	07/01/1995	07/16/1995	18.028	6.150	3.253	27.7569	90.7301	549.0	876.8
	1995	GC950625.A67	/INDUSTRY/	07/01/1995	07/16/1995	18.028	6.169	3.246	27.7569	90.7301	557.0	876.8
	1995	GC950625.A68	/INDUSTRY/	07/01/1995	07/16/1995	16.919	6.088	3.186	27.7569	90.7301	565.0	876.8
	1995	GC950625.A69	/INDUSTRY/	07/01/1995	07/16/1995	17.678	6.009	3.306	27.7569	90.7301	573.0	876.8
	1995	GC950625.A70	/INDUSTRY/	07/01/1995	07/16/1995	19.039	5.881	3.387	27.7569	90.7301	581.0	876.8
	1995	GC950625.A71	/INDUSTRY/	07/01/1995	07/16/1995	18.337	5.859	3.543	27.7569	90.7301	589.0	876.8
	1995	GC950625.A72	/INDUSTRY/	07/01/1995	07/16/1995	19.235	5.915	3.646	27.7569	90.7301	597.0	876.8
	1995	GC950625.A73	/INDUSTRY/	07/01/1995	07/16/1995	19.039	5.908	3.678	27.7569	90.7301	605.0	876.8
	1995	GC950625.A74	/INDUSTRY/	07/01/1995	07/16/1995	17.557	5.908	3.389	27.7569	90.7301	613.0	876.8
	1995	GC950625.A75	/INDUSTRY/	07/01/1995	07/16/1995	16.771	5.767	3.142	27.7569	90.7301	621.0	876.8
	1995	GC950625.A76	/INDUSTRY/	07/01/1995	07/16/1995	14.866	5.322	2.775	27.7569	90.7301	629.0	876.8
	1995	GC950625.A77	/INDUSTRY/	07/01/1995	07/16/1995	13.200	4.904	2.573	27.7569	90.7301	637.0	876.8
	1995	GC950625.A78	/INDUSTRY/	07/01/1995	07/16/1995	13.901	4.657	2.407	27.7569	90.7301	645.0	876.8
	1995	GC950625.A79	/INDUSTRY/	07/01/1995	07/16/1995	13.463	4.599	2.292	27.7569	90.7301	653.0	876.8
	1995	GC950625.A80	/INDUSTRY/	07/01/1995	07/16/1995	13.901	4.415	2.325	27.7569	90.7301	661.0	876.8
	1995	GC950625.A81	/INDUSTRY/	07/01/1995	07/16/1995	13.793	4.356	2.259	27.7569	90.7301	669.0	876.8
	1995	GC950625.A82	/INDUSTRY/	07/01/1995	07/16/1995	12.420	4.413	2.411	27.7569	90.7301	677.0	876.8
	1995	GC950625.A83	/INDUSTRY/	07/01/1995	07/16/1995	12.728	4.593	2.434	27.7569	90.7301	685.0	876.8

Table B-3. Speed statistics for energetic current events associated with Loop Current eddies. (continued)

Event No.	Year	Filename	Directory	Event start date (m/d/y)	Event end date (m/d/y)	Maximum speed (cm·s^{-1})	Mean speed (cm·s^{-1})	Stand. dev. of speed (cm·s^{-1})	Latitude (°N)	Longitude (°W)	Depth (m)	Total water depth (m)
15	1995	GC950625.A84	/INDUSTRY/	07/01/1995	07/16/1995	14.160	4.855	2.678	27.7569	90.7301	693.0	876.8
	1995	GC950625.A85	/INDUSTRY/	07/01/1995	07/16/1995	14.142	4.961	2.753	27.7569	90.7301	701.0	876.8
	1995	GC950625.A86	/INDUSTRY/	07/01/1995	07/16/1995	15.240	5.058	2.885	27.7569	90.7301	709.0	876.8
	1995	GC950625.A87	/INDUSTRY/	07/01/1995	07/16/1995	15.945	5.187	3.066	27.7569	90.7301	717.0	876.8
	1995	GC950625.A88	/INDUSTRY/	07/01/1995	07/16/1995	14.603	5.011	2.835	27.7569	90.7301	725.0	876.8
	1995	GC950625.A89	/INDUSTRY/	07/01/1995	07/16/1995	12.903	4.474	2.682	27.7569	90.7301	733.0	876.8
	1995	GC950625.A90	/INDUSTRY/	07/01/1995	07/15/1995	13.285	5.934	3.168	27.7569	90.7301	741.0	876.8
16	1999	AT990829.A01	/MMS/	09/01/1999	10/25/1999	171.219	83.101	43.110	27.2933	89.7845	12.0	2001.0
	1999	AT990829.A02	/MMS/	09/01/1999	10/25/1999	171.224	88.406	39.580	27.2933	89.7845	16.0	2001.0
	1999	AT990829.A03	/MMS/	09/01/1999	10/25/1999	171.168	88.713	37.663	27.2933	89.7845	20.0	2001.0
	1999	AT990829.A04	/MMS/	09/01/1999	10/25/1999	166.227	87.763	36.940	27.2933	89.7845	24.0	2001.0
	1999	AT990829.A05	/MMS/	09/01/1999	10/25/1999	157.818	86.587	36.299	27.2933	89.7845	28.0	2001.0
	1999	AT990829.A06	/MMS/	09/01/1999	10/25/1999	154.805	85.401	35.659	27.2933	89.7845	32.0	2001.0
	1999	AT990829.A07	/MMS/	09/01/1999	10/25/1999	147.711	84.273	35.038	27.2933	89.7845	36.0	2001.0
	1999	AT990829.A08	/MMS/	09/01/1999	10/25/1999	145.756	83.165	34.358	27.2933	89.7845	40.0	2001.0
	1999	AT990829.A09	/MMS/	09/01/1999	10/25/1999	145.566	81.997	33.539	27.2933	89.7845	44.0	2001.0
	1999	AT990829.A10	/MMS/	09/01/1999	10/25/1999	140.295	80.471	33.032	27.2933	89.7845	48.0	2001.0
	1999	AT990829.A11	/MMS/	09/01/1999	10/25/1999	138.110	78.797	32.242	27.2933	89.7845	52.0	2001.0
	1999	AT990829.A12	/MMS/	09/01/1999	10/25/1999	137.582	76.807	31.541	27.2933	89.7845	56.0	2001.0
	1999	AT990829.A13	/MMS/	09/01/1999	10/25/1999	133.277	74.702	30.526	27.2933	89.7845	60.0	2001.0
	1999	AT990829.A14	/MMS/	09/01/1999	10/25/1999	126.931	72.260	29.424	27.2933	89.7845	64.0	2001.0
	1999	AT990829.A15	/MMS/	09/01/1999	10/25/1999	114.214	49.421	26.170	27.2933	89.7845	68.0	2001.0
	1999	AT990829.A16	/MMS/	09/01/1999	10/25/1999	113.559	61.536	26.955	27.2933	89.7845	72.0	2001.0
	1999	AT990829.A17	/MMS/	09/01/1999	10/25/1999	120.070	68.393	27.942	27.2933	89.7845	76.0	2001.0
	1999	AT990829.A18	/MMS/	09/01/1999	10/25/1999	116.759	67.059	27.430	27.2933	89.7845	80.0	2001.0
	1999	AT990829.A19	/MMS/	09/01/1999	01/31/2000	108.556	58.656	19.917	27.2933	89.7845	106.0	2001.0
	1999	AT990829.A20	/MMS/	09/01/1999	01/31/2000	106.637	58.616	19.853	27.2933	89.7845	110.0	2001.0
	1999	AT990829.A21	/MMS/	09/01/1999	01/31/2000	105.855	57.622	19.300	27.2933	89.7845	114.0	2001.0
	1999	AT990829.A22	/MMS/	09/01/1999	01/31/2000	106.533	56.340	18.665	27.2933	89.7845	118.0	2001.0
	1999	AT990829.A23	/MMS/	09/01/1999	01/31/2000	102.237	54.960	17.985	27.2933	89.7845	122.0	2001.0
	1999	AT990829.A24	/MMS/	09/01/1999	01/31/2000	97.265	53.620	17.298	27.2933	89.7845	126.0	2001.0
	1999	AT990829.A25	/MMS/	09/01/1999	01/31/2000	95.017	52.122	16.708	27.2933	89.7845	130.0	2001.0
	1999	AT990829.A26	/MMS/	09/01/1999	01/31/2000	94.539	50.650	16.291	27.2933	89.7845	134.0	2001.0
	1999	AT990829.A27	/MMS/	09/01/1999	01/31/2000	93.412	49.278	15.931	27.2933	89.7845	138.0	2001.0

Table B-3. Speed statistics for energetic current events associated with Loop Current eddies. (continued)

Event No.	Year	Filename	Directory	Event start date (m/d/y)	Event end date (m/d/y)	Maximum speed ($cm \cdot s^{-1}$)	Mean speed ($cm \cdot s^{-1}$)	Stand. dev. of speed ($cm \cdot s^{-1}$)	Latitude (°N)	Longitude (°W)	Depth (m)	Total water depth (m)
16	1999	AT990829.A28	/MMS/	09/01/1999	01/31/2000	92.806	47.946	15.437	27.2933	89.7845	142.0	2001.0
	1999	AT990829.A29	/MMS/	09/01/1999	01/31/2000	92.749	46.711	15.061	27.2933	89.7845	146.0	2001.0
	1999	AT990829.A30	/MMS/	09/01/1999	01/31/2000	91.603	45.491	14.748	27.2933	89.7845	150.0	2001.0
	1999	AT990829.A39	/MMS/	09/01/1999	01/31/2000	97.079	45.123	14.939	27.2933	89.7845	150.0	2001.0
	1999	AT990829.A31	/MMS/	09/01/1999	01/31/2000	89.545	44.455	14.505	27.2933	89.7845	154.0	2001.0
	1999	AT990829.A40	/MMS/	09/01/1999	01/31/2000	95.535	43.448	14.491	27.2933	89.7845	154.0	2001.0
	1999	AT990829.A32	/MMS/	09/01/1999	01/31/2000	89.076	43.541	14.273	27.2933	89.7845	158.0	2001.0
	1999	AT990829.A41	/MMS/	09/01/1999	01/31/2000	88.471	42.240	13.296	27.2933	89.7845	158.0	2001.0
	1999	AT990829.A33	/MMS/	09/01/1999	01/31/2000	86.991	42.711	14.102	27.2933	89.7845	162.0	2001.0
	1999	AT990829.A42	/MMS/	09/01/1999	01/31/2000	90.997	42.102	13.915	27.2933	89.7845	162.0	2001.0
	1999	AT990829.A34	/MMS/	09/01/1999	01/31/2000	86.273	41.999	13.862	27.2933	89.7845	166.0	2001.0
	1999	AT990829.A43	/MMS/	09/01/1999	01/31/2000	85.545	41.404	13.753	27.2933	89.7845	166.0	2001.0
	1999	AT990829.A35	/MMS/	09/01/1999	01/31/2000	89.019	41.332	13.560	27.2933	89.7845	170.0	2001.0
	1999	AT990829.A44	/MMS/	09/01/1999	01/31/2000	83.663	40.653	13.495	27.2933	89.7845	170.0	2001.0
	1999	AT990829.A36	/MMS/	09/01/1999	01/31/2000	87.573	40.615	13.366	27.2933	89.7845	174.0	2001.0
	1999	AT990829.A45	/MMS/	09/01/1999	01/31/2000	82.176	39.873	13.242	27.2933	89.7845	174.0	2001.0
	1999	AT990829.A37	/MMS/	09/01/1999	01/31/2000	87.077	39.967	13.110	27.2933	89.7845	178.0	2001.0
	1999	AT990829.A46	/MMS/	09/01/1999	01/31/2000	79.914	39.144	13.047	27.2933	89.7845	178.0	2001.0
	1999	AT990829.A38	/MMS/	09/01/1999	01/31/2000	85.373	39.158	12.687	27.2933	89.7845	182.0	2001.0
	1999	AT990829.A47	/MMS/	09/01/1999	01/31/2000	77.894	38.423	12.890	27.2933	89.7845	182.0	2001.0
	1999	AT990829.A48	/MMS/	09/01/1999	01/31/2000	76.697	37.706	12.745	27.2933	89.7845	186.0	2001.0
	1999	AT990829.A49	/MMS/	09/01/1999	01/31/2000	75.135	37.045	12.577	27.2933	89.7845	190.0	2001.0
	1999	AT990829.A50	/MMS/	09/01/1999	01/31/2000	71.509	36.411	12.438	27.2933	89.7845	194.0	2001.0
	1999	AT990829.A51	/MMS/	09/01/1999	01/31/2000	68.983	32.128	11.601	27.2933	89.7845	198.0	2001.0
	1999	AT990829.A52	/MMS/	09/01/1999	01/31/2000	60.897	26.907	9.536	27.2933	89.7845	202.0	2001.0
	1999	AT990829.A53	/MMS/	09/01/1999	01/31/2000	67.059	34.334	11.595	27.2933	89.7845	206.0	2001.0
	1999	AT990829.A54	/MMS/	09/01/1999	01/31/2000	71.796	34.011	11.989	27.2933	89.7845	210.0	2001.0
	1999	AT990829.A55	/MMS/	09/01/1999	01/31/2000	73.451	33.466	11.930	27.2933	89.7845	214.0	2001.0
	1999	AT990829.A56	/MMS/	09/01/1999	01/31/2000	73.262	32.969	11.844	27.2933	89.7845	218.0	2001.0
	1999	AT990829.A57	/MMS/	09/01/1999	01/31/2000	71.781	32.496	11.727	27.2933	89.7845	222.0	2001.0
	1999	AT990829.A58	/MMS/	09/01/1999	01/31/2000	72.172	32.030	11.611	27.2933	89.7845	226.0	2001.0
	1999	AT990829.A59	/MMS/	09/01/1999	01/31/2000	71.647	31.549	11.494	27.2933	89.7845	230.0	2001.0
	1999	AT990829.A60	/MMS/	09/01/1999	01/31/2000	66.376	30.529	11.083	27.2933	89.7845	234.0	2001.0
	1999	AT990829.A61	/MMS/	09/01/1999	01/31/2000	59.905	28.865	10.441	27.2933	89.7845	256.0	2001.0

Table B-3. Speed statistics for energetic current events associated with Loop Current eddies. (continued)

Event No.	Year	Filename	Directory	Event start date (m/d/y)	Event end date (m/d/y)	Maximum speed (cm·s^{-1})	Mean speed (cm·s^{-1})	Stand. dev. of speed (cm·s^{-1})	Latitude (°N)	Longitude (°W)	Depth (m)	Total water depth (m)
16	1999	AT990829.A62	/MMS/	09/01/1999	01/31/2000	58.682	28.603	10.371	27.2933	89.7845	260.0	2001.0
	1999	AT990829.A63	/MMS/	09/01/1999	01/31/2000	58.864	28.271	10.256	27.2933	89.7845	264.0	2001.0
	1999	AT990829.A64	/MMS/	09/01/1999	01/31/2000	58.548	27.948	10.166	27.2933	89.7845	268.0	2001.0
	1999	AT990829.A65	/MMS/	09/01/1999	01/31/2000	57.749	27.651	10.063	27.2933	89.7845	272.0	2001.0
	1999	AT990829.A66	/MMS/	09/01/1999	01/31/2000	57.217	27.315	9.939	27.2933	89.7845	276.0	2001.0
	1999	AT990829.A67	/MMS/	09/01/1999	01/31/2000	56.891	27.008	9.822	27.2933	89.7845	280.0	2001.0
	1999	AT990829.A68	/MMS/	09/01/1999	01/31/2000	56.746	26.728	9.739	27.2933	89.7845	284.0	2001.0
	1999	AT990829.A69	/MMS/	09/01/1999	01/31/2000	57.047	26.485	9.621	27.2933	89.7845	288.0	2001.0
	1999	AT990829.A70	/MMS/	09/01/1999	01/31/2000	58.826	26.262	9.543	27.2933	89.7845	292.0	2001.0
	1999	AT990829.A71	/MMS/	09/01/1999	01/31/2000	57.443	26.039	9.489	27.2933	89.7845	296.0	2001.0
	1999	AT990829.A72	/MMS/	09/01/1999	01/31/2000	56.657	25.809	9.418	27.2933	89.7845	300.0	2001.0
	1999	AT990829.A73	/MMS/	09/01/1999	01/31/2000	55.596	25.561	9.330	27.2933	89.7845	304.0	2001.0
	1999	AT990829.A74	/MMS/	09/01/1999	01/31/2000	52.795	25.330	9.255	27.2933	89.7845	308.0	2001.0
	1999	AT990829.A75	/MMS/	09/01/1999	01/31/2000	51.455	25.114	9.223	27.2933	89.7845	312.0	2001.0
	1999	AT990829.A76	/MMS/	09/01/1999	01/31/2000	51.326	24.941	9.194	27.2933	89.7845	316.0	2001.0
	1999	AT990829.A77	/MMS/	09/01/1999	01/31/2000	52.059	24.763	9.131	27.2933	89.7845	320.0	2001.0
	1999	AT990829.A78	/MMS/	09/01/1999	01/31/2000	51.977	24.594	9.117	27.2933	89.7845	324.0	2001.0
	1999	AT990829.A79	/MMS/	09/01/1999	01/31/2000	52.277	24.383	9.052	27.2933	89.7845	328.0	2001.0
	1999	AT990829.A80	/MMS/	09/01/1999	01/31/2000	53.760	24.066	8.982	27.2933	89.7845	332.0	2001.0
	1999	AT990829.A83	/MMS/	09/01/1999	01/05/2000	58.415	28.059	9.617	27.2933	89.7845	332.0	2001.0
	1999	AT990829.A81	/MMS/	09/01/1999	01/31/2000	55.555	23.772	8.996	27.2933	89.7845	336.0	2001.0
	1999	AT990829.A82	/MMS/	09/01/1999	01/31/2000	57.369	23.689	9.314	27.2933	89.7845	340.0	2001.0
	1999	AT990829.A84	/MMS/	09/01/1999	01/05/2000	55.613	27.499	9.437	27.2933	89.7845	340.0	2001.0
	1999	AT990829.A85	/MMS/	09/01/1999	01/05/2000	53.810	27.052	9.323	27.2933	89.7845	348.0	2001.0
	1999	AT990829.A86	/MMS/	09/01/1999	01/05/2000	53.920	26.578	9.250	27.2933	89.7845	356.0	2001.0
	1999	AT990829.A87	/MMS/	09/01/1999	01/05/2000	55.095	26.187	9.105	27.2933	89.7845	364.0	2001.0
	1999	AT990829.A88	/MMS/	09/01/1999	01/05/2000	56.048	25.832	9.015	27.2933	89.7845	372.0	2001.0
	1999	AT990829.A89	/MMS/	09/01/1999	01/05/2000	54.089	25.366	8.887	27.2933	89.7845	380.0	2001.0
	1999	AT990829.A90	/MMS/	09/01/1999	01/05/2000	51.121	24.927	8.699	27.2933	89.7845	388.0	2001.0
	1999	AT990829.A91	/MMS/	09/01/1999	01/05/2000	49.084	24.515	8.536	27.2933	89.7845	396.0	2001.0
	1999	AT990829.A92	/MMS/	09/01/1999	01/05/2000	49.590	24.134	8.399	27.2933	89.7845	404.0	2001.0
	1999	AT990829.A93	/MMS/	09/01/1999	01/05/2000	49.262	23.755	8.270	27.2933	89.7845	412.0	2001.0
	1999	AT990829.A94	/MMS/	09/01/1999	01/05/2000	47.645	23.370	8.177	27.2933	89.7845	420.0	2001.0
	1999	AT990829.A95	/MMS/	09/01/1999	01/05/2000	48.664	22.871	8.113	27.2933	89.7845	428.0	2001.0

Table B-3. Speed statistics for energetic current events associated with Loop Current eddies. (continued)

Event No.	Year	Filename	Directory	Event start date (m/d/y)	Event end date (m/d/y)	Maximum speed (cm·s^{-1})	Mean speed (cm·s^{-1})	Stand. dev. of speed (cm·s^{-1})	Latitude (°N)	Longitude (°W)	Depth (m)	Total water depth (m)
16	1999	AT990829.A96	/MMS/	09/01/1999	01/05/2000	48.333	22.539	8.052	27.2933	89.7845	436.0	2001.0
	1999	AT990829.A97	/MMS/	09/01/1999	01/05/2000	46.795	22.201	7.854	27.2933	89.7845	444.0	2001.0
	1999	AT990829.A98	/MMS/	09/01/1999	01/05/2000	46.435	21.731	7.672	27.2933	89.7845	452.0	2001.0
	1999	AT990829.A99	/MMS/	09/01/1999	01/05/2000	44.163	21.350	7.538	27.2933	89.7845	460.0	2001.0
	1999	AT990829.Aa0	/MMS/	09/01/1999	01/05/2000	44.194	20.984	7.353	27.2933	89.7845	468.0	2001.0
	1999	AT990829.Aa1	/MMS/	09/01/1999	01/05/2000	42.003	20.434	7.237	27.2933	89.7845	476.0	2001.0
	1999	AT990829.Aa2	/MMS/	09/01/1999	01/05/2000	41.244	20.078	7.153	27.2933	89.7845	484.0	2001.0
	1999	AT990829.Aa3	/MMS/	09/01/1999	01/05/2000	41.877	19.797	6.978	27.2933	89.7845	492.0	2001.0
	1999	AT990829.Aa4	/MMS/	09/01/1999	01/05/2000	40.400	19.400	6.865	27.2933	89.7845	500.0	2001.0
	1999	AT990829.Aa5	/MMS/	09/01/1999	01/05/2000	40.554	19.037	6.807	27.2933	89.7845	508.0	2001.0
	1999	AT990829.Aa6	/MMS/	09/01/1999	01/05/2000	40.663	18.738	6.724	27.2933	89.7845	516.0	2001.0
	1999	AT990829.Aa7	/MMS/	09/01/1999	01/05/2000	38.420	18.347	6.643	27.2933	89.7845	524.0	2001.0
	1999	AT990829.Aa8	/MMS/	09/01/1999	01/05/2000	37.999	17.941	6.547	27.2933	89.7845	532.0	2001.0
	1999	AT990829.Aa9	/MMS/	09/01/1999	01/05/2000	37.143	17.606	6.482	27.2933	89.7845	540.0	2001.0
	1999	AT990829.Ab0	/MMS/	09/01/1999	01/05/2000	37.488	17.386	6.358	27.2933	89.7845	548.0	2001.0
	1999	AT990829.Ab1	/MMS/	09/01/1999	01/05/2000	38.517	17.116	6.260	27.2933	89.7845	556.0	2001.0
	1999	AT990829.Ab2	/MMS/	09/01/1999	01/05/2000	38.336	16.912	6.173	27.2933	89.7845	564.0	2001.0
	1999	AT990829.Ab3	/MMS/	09/01/1999	01/05/2000	38.604	16.596	6.131	27.2933	89.7845	572.0	2001.0
	1999	AT990829.Ab4	/MMS/	09/01/1999	01/05/2000	36.912	16.392	6.166	27.2933	89.7845	580.0	2001.0
	1999	AT990829.Ab5	/MMS/	09/01/1999	01/05/2000	37.569	15.799	6.167	27.2933	89.7845	588.0	2001.0
	1999	AT990829.Ab6	/MMS/	09/01/1999	01/31/2000	35.798	10.272	5.245	27.2933	89.7845	658.0	2001.0
	1999	AT990829.Ab7	/MMS/	09/01/1999	01/31/2000	37.852	10.849	5.637	27.2933	89.7845	666.0	2001.0
	1999	AT990829.Ab8	/MMS/	09/01/1999	01/31/2000	38.585	10.898	5.684	27.2933	89.7845	674.0	2001.0
	1999	AT990829.Ab9	/MMS/	09/01/1999	01/31/2000	41.155	10.923	5.771	27.2933	89.7845	682.0	2001.0
	1999	AT990829.Ac0	/MMS/	09/01/1999	01/31/2000	43.901	10.826	5.830	27.2933	89.7845	690.0	2001.0
	1999	AT990829.Ac1	/MMS/	09/01/1999	01/31/2000	43.427	10.816	5.811	27.2933	89.7845	698.0	2001.0
	1999	AT990829.Ac2	/MMS/	09/01/1999	01/31/2000	42.844	10.708	5.880	27.2933	89.7845	706.0	2001.0
	1999	AT990829.Ac3	/MMS/	09/01/1999	01/31/2000	44.323	10.491	5.942	27.2933	89.7845	714.0	2001.0
	1999	AT990829.Ac4	/MMS/	09/01/1999	01/31/2000	44.804	10.411	6.004	27.2933	89.7845	722.0	2001.0
	1999	AT990829.Ac5	/MMS/	09/01/1999	01/31/2000	46.371	10.276	5.957	27.2933	89.7845	730.0	2001.0
	1999	AT990829.Ac6	/MMS/	09/01/1999	01/31/2000	44.976	10.142	5.953	27.2933	89.7845	738.0	2001.0
	1999	AT990829.Ac7	/MMS/	09/01/1999	01/31/2000	45.084	10.069	6.015	27.2933	89.7845	746.0	2001.0
	1999	AT990829.Ac8	/MMS/	09/01/1999	01/31/2000	49.036	9.912	6.082	27.2933	89.7845	754.0	2001.0
	1999	AT990829.Ac9	/MMS/	09/01/1999	01/31/2000	49.211	9.780	6.076	27.2933	89.7845	762.0	2001.0

Table B-3. Speed statistics for energetic current events associated with Loop Current eddies. (continued)

Event No.	Year	Filename	Directory	Event start date (m/d/y)	Event end date (m/d/y)	Maximum speed ($cm \cdot s^{-1}$)	Mean speed ($cm \cdot s^{-1}$)	Stand. dev. of speed ($cm \cdot s^{-1}$)	Latitude (°N)	Longitude (°W)	Depth (m)	Total water depth (m)
16	1999	AT990829.Ad0	/MMS/	09/01/1999	01/31/2000	50.525	9.659	6.062	27.2933	89.7845	770.0	2001.0
	1999	AT990829.Ad1	/MMS/	09/01/1999	01/31/2000	48.883	9.633	6.091	27.2933	89.7845	778.0	2001.0
	1999	AT990829.Ad2	/MMS/	09/01/1999	01/31/2000	48.685	9.564	6.055	27.2933	89.7845	786.0	2001.0
	1999	AT990829.Ad3	/MMS/	09/01/1999	01/31/2000	47.590	9.422	6.026	27.2933	89.7845	794.0	2001.0
	1999	AT990829.Ad4	/MMS/	09/01/1999	01/31/2000	47.566	9.360	5.950	27.2933	89.7845	802.0	2001.0
	1999	AT990829.Ad5	/MMS/	09/01/1999	01/31/2000	44.139	9.260	5.833	27.2933	89.7845	810.0	2001.0
	1999	AT990829.Ad6	/MMS/	09/01/1999	01/31/2000	42.503	9.226	5.792	27.2933	89.7845	818.0	2001.0
	1999	AT990829.Ad7	/MMS/	09/01/1999	01/31/2000	41.097	9.203	5.680	27.2933	89.7845	826.0	2001.0
	1999	AT990829.Ad8	/MMS/	09/01/1999	01/31/2000	40.359	9.138	5.634	27.2933	89.7845	834.0	2001.0
	1999	AT990829.Ad9	/MMS/	09/01/1999	01/31/2000	41.911	9.137	5.768	27.2933	89.7845	842.0	2001.0
	1999	AT990829.Ae0	/MMS/	09/01/1999	01/31/2000	42.230	9.084	5.744	27.2933	89.7845	850.0	2001.0
	1999	AT990829.Ae1	/MMS/	09/01/1999	01/31/2000	41.130	9.021	5.677	27.2933	89.7845	858.0	2001.0
	1999	AT990829.Ae2	/MMS/	09/01/1999	01/31/2000	44.967	9.010	5.668	27.2933	89.7845	866.0	2001.0
	1999	AT990829.Ae3	/MMS/	09/01/1999	01/31/2000	43.494	8.896	5.728	27.2933	89.7845	874.0	2001.0
	1999	AT990829.Ae4	/MMS/	09/01/1999	01/31/2000	45.346	8.772	5.775	27.2933	89.7845	882.0	2001.0
	1999	AT990829.Ae5	/MMS/	09/01/1999	01/31/2000	46.032	8.706	5.813	27.2933	89.7845	890.0	2001.0
	1999	AT990829.Ae6	/MMS/	09/01/1999	01/31/2000	44.413	8.545	5.844	27.2933	89.7845	898.0	2001.0
	1999	AT990829.Ae7	/MMS/	09/01/1999	01/31/2000	46.538	8.569	5.886	27.2933	89.7845	906.0	2001.0
	1999	AT990829.Ae8	/MMS/	09/01/1999	01/31/2000	44.202	8.553	5.867	27.2933	89.7845	914.0	2001.0
	1999	AT990829.Ae9	/MMS/	09/01/1999	01/31/2000	43.533	8.451	5.876	27.2933	89.7845	922.0	2001.0
	1999	AT990829.Af0	/MMS/	09/01/1999	01/31/2000	44.985	8.363	5.929	27.2933	89.7845	930.0	2001.0
	1999	AT990829.Af1	/MMS/	09/01/1999	01/31/2000	46.622	8.269	5.914	27.2933	89.7845	938.0	2001.0
	1999	AT990829.Af2	/MMS/	09/01/1999	01/31/2000	43.910	8.233	5.885	27.2933	89.7845	946.0	2001.0
	1999	AT990829.Af3	/MMS/	09/01/1999	01/31/2000	44.709	8.206	5.868	27.2933	89.7845	954.0	2001.0
	1999	AT990829.Af4	/MMS/	09/01/1999	01/31/2000	45.902	8.218	5.809	27.2933	89.7845	962.0	2001.0
	1999	AT990829.Af5	/MMS/	09/01/1999	01/31/2000	45.082	8.310	5.882	27.2933	89.7845	970.0	2001.0
	1999	AT990829.Af6	/MMS/	09/01/1999	01/31/2000	44.949	8.328	5.846	27.2933	89.7845	978.0	2001.0
	1999	AT990829.Af7	/MMS/	09/01/1999	01/31/2000	46.029	8.353	5.838	27.2933	89.7845	986.0	2001.0
	1999	AT990829.Af8	/MMS/	09/01/1999	01/31/2000	42.745	8.255	5.840	27.2933	89.7845	994.0	2001.0
	1999	AT990829.Af9	/MMS/	09/01/1999	01/31/2000	43.445	8.281	5.923	27.2933	89.7845	1002.0	2001.0
	1999	AT990829.Ag0	/MMS/	09/01/1999	01/31/2000	40.933	8.358	5.923	27.2933	89.7845	1010.0	2001.0
	1999	AT990829.Ag1	/MMS/	09/01/1999	01/31/2000	41.260	8.442	5.935	27.2933	89.7845	1018.0	2001.0
	1999	AT990829.Ag2	/MMS/	09/01/1999	01/31/2000	39.400	8.413	5.942	27.2933	89.7845	1026.0	2001.0
	1999	AT990829.Ag3	/MMS/	09/01/1999	01/31/2000	43.563	8.441	6.008	27.2933	89.7845	1034.0	2001.0

Table B-3. Speed statistics for energetic current events associated with Loop Current eddies. (continued)

Event No.	Year	Filename	Directory	Event start date (m/d/y)	Event end date (m/d/y)	Maximum speed (cm·s^{-1})	Mean speed (cm·s^{-1})	Stand. dev. of speed (cm·s^{-1})	Latitude (°N)	Longitude (°W)	Depth (m)	Total water depth (m)
16	1999	AT990829.Ag4	/MMS/	09/01/1999	01/31/2000	40.679	8.477	6.054	27.2933	89.7845	1042.0	2001.0
	1999	AT990829.Ag5	/MMS/	09/01/1999	01/31/2000	43.060	8.539	6.088	27.2933	89.7845	1050.0	2001.0
	1999	AT990829.Ag6	/MMS/	09/01/1999	01/31/2000	44.087	8.687	6.129	27.2933	89.7845	1058.0	2001.0
	1999	AT990829.Ag7	/MMS/	09/01/1999	01/31/2000	43.985	8.818	6.211	27.2933	89.7845	1066.0	2001.0
	1999	AT990829.Ag8	/MMS/	09/01/1999	01/31/2000	43.618	9.063	6.248	27.2933	89.7845	1074.0	2001.0
	1999	AT990829.Ag9	/MMS/	09/01/1999	01/31/2000	43.586	9.313	6.294	27.2933	89.7845	1082.0	2001.0
	1999	AT990829.Ah0	/MMS/	09/01/1999	01/31/2000	45.787	9.339	6.431	27.2933	89.7845	1090.0	2001.0
	1999	AT990829.Ah1	/MMS/	09/01/1999	01/31/2000	43.214	9.556	6.455	27.2933	89.7845	1098.0	2001.0
	1999	AT990829.Ah2	/MMS/	09/01/1999	01/31/2000	43.674	9.761	6.510	27.2933	89.7845	1106.0	2001.0
	1999	AT990829.Ah3	/MMS/	09/01/1999	01/31/2000	46.573	9.980	6.678	27.2933	89.7845	1114.0	2001.0
	1999	AT990829.Ah4	/MMS/	09/01/1999	01/31/2000	48.703	10.128	6.701	27.2933	89.7845	1122.0	2001.0
	1999	AT990829.Ah5	/MMS/	09/01/1999	01/31/2000	46.373	10.318	6.742	27.2933	89.7845	1130.0	2001.0
	1999	AT990829.C01	/MMS/	09/01/1999	01/31/2000	51.572	8.858	6.647	27.2933	89.7845	800.0	2001.0
	1999	AT990829.C02	/MMS/	09/01/1999	01/31/2000	40.315	7.598	5.064	27.2933	89.7845	1000.0	2001.0
	1999	AT990829.C03	/MMS/	09/01/1999	01/31/2000	49.663	9.607	8.385	27.2933	89.7845	1200.0	2001.0
	1999	AT990829.C04	/MMS/	09/01/1999	01/31/2000	53.401	12.132	9.570	27.2933	89.7845	1400.0	2001.0
	1999	AT990829.C05	/MMS/	09/01/1999	01/31/2000	52.290	13.122	9.316	27.2933	89.7845	1600.0	2001.0
	1999	AT990829.C06	/MMS/	09/01/1999	01/31/2000	52.116	13.570	9.575	27.2933	89.7845	1800.0	2001.0
	1999	AT990829.C07	/MMS/	09/01/1999	12/21/1999	50.959	14.155	8.939	27.2933	89.7845	1989.0	2001.0
	1999	GC990829.C01	/MMS/	09/01/1999	12/15/1999	90.883	23.583	17.863	27.2280	89.9710	1600.0	1998.0
	1999	GC990829.C02	/MMS/	09/01/1999	01/31/2000	80.057	18.744	15.184	27.2280	89.9710	1800.0	1998.0
	1999	GC990829.C03	/MMS/	09/01/1999	01/31/2000	85.362	18.485	11.747	27.2280	89.9710	1989.0	1998.0

Notes by event number

1 1978: July-August, Unnamed LCE

NOAA M3, 70 m and 168 m, northeast currents consistent with northern limb of Loop Current Eddy. No SST or SSHA data available to confirm eddy presence. Data from NOAA M3 are plotted in Figure 6.3.1-2.

2 1980: Mid-September - October, Unnamed LCE

Good example of a Loop Current eddy in the western Gulf of Mexico. Strong, persistent northward currents at Brooks mooring S. There were 7-10 oscillations superimposed on the currents that could indicate the presence of a vorticity wave. Data from Brooks S are plotted in Figure 6.3.2-2.

Table B-3. Speed statistics for energetic current events associated with Loop Current eddies. (continued)

Notes by event number (continued)

3 1984: 18 October - 31 December, most likely Eddy Arnold

Large amplitude (~50 $cm \cdot s^{-1}$), low-frequency, surface (SAIC A, 172 m) motions are superimposed on increased inertial period motions. The low-frequency motions are probably associated with the Loop Current passing over the mooring (see SAIC mooring G which show the influence of the Loop Current). Increased inertial motions are seen at SAIC A at 400 m and 1100 m, while the bottom instrument at 1600 m shows intensified inertial period events on October 29 and December 24. Data from SAIC A and G are plotted in Figure 6.3.3-2. A detail of the records at SAIC A and G for this time is shown in Figure A.3-1.

4 1985: 24 January - 30 April, most likely Eddy Arnold

The records from the upper (< 700 m) instruments at SAIC A and G show low-frequency motions. The records from the lower (1000 m) instruments at SAIC A also show low-frequency motions. Records at SAIC A and G have significant inertial period oscillations. Note the Loop Current passes over SAIC A during this time. Data from SAIC A and G are plotted in Figure 6.3.3-2.

5 1985: September - November, Fast Eddy

Low-frequency energy is seen in the records from the upper instruments at SAIC A and G. Records from SAIC A and G have significant inertial period oscillations. Note the Loop Current passes over SAIC A during this time. Data from SAIC A and G are plotted in Figure 6.3.3-2.

6 1985: October - December, Fast Eddy

Persistent southeastward currents occur at SAIC Q at 300 m. It is unclear whether the eddy is influencing currents at SAIC T as well. Data from SAIC Q and T are plotted in Figure 6.3.3-5.

7 1986: January - February, Fast Eddy

A good example of currents associated with LCE in the western Gulf. This case is a continuation of event number 6 during 1985. Currents are persistently eastward at 300 m with no notable effect below that depth. Data from SAIC P, Q R, S, and T are plotted in Figure 6.3.3-5.

8 1988: January - June, Eddy Kathleen

The January through March records show the presence of a small anticyclone prior to LCE Kathleen. During March through May, Eddy Kathleen, which coalesces with the small anticyclone, is heavily influencing currents at SAIC FF and GG. During June another small anticyclone from the east influences the currents at SAIC FF and GG. The directions of the upper currents are predominately south and southeastward, indicating the north and northeast limbs of the eddy. Two bottom (1650 and 2500 m) events occur at SAIC GG: one before the LCE arrives at the mooring and one after the LCE departs. Data from SAIC FF and GG are plotted in Figure 6.3.3-5. A detail of these records for this time is shown in Figure A.3-2.

9 1988: August - October, Eddy Murphy

Unfortunately the records at SAIC FF end just as Eddy Murphy approaches this mooring location. Northeast currents, which turn southeast and approach 100 $cm \cdot s^{-1}$, dominate the upper records at SAIC GG. Strong inertial oscillations also occur toward the end of September and into October. Data from SAIC FF and GG are plotted in Figure 6.3.3-5. A detail of these records for this time is shown in Figure A.3-2.

Table B-3. Speed statistics for energetic current events associated with Loop Current eddies. (continued)

Notes by event number (continued)

10 1991: September - October, Eddy Triton

Northeast currents dominate the currents at Industry EW873 during mid-October. Near-surface mean speeds are greater than 50 $cm \cdot s^{-1}$. Data from Industry EW873 are plotted in Figure 6.3.12-7.

11 1992: June - September, Eddy Triton

Near-surface (22 m) currents at LATEX 49 during Eddy Triton are persistent and to the northeast. Maximum speeds are greater than 100 $cm \cdot s^{-1}$. Data from LATEX 49 are plotted in Figure 6.3.4-2.

12 1992: November - December, Eddy Vazquez

The 14 and 100 m currents at LATEX 49 are strongly coherent and northeastward. The 500 m currents are weak (< 5 $cm \cdot s^{-1}$) with inertial period energy. A 20 $cm \cdot s^{-1}$ bottom event occurs around December 23. Data from LATEX 49 are plotted in Figure 6.3.4-2.

13 1993: June - August, Eddy Vazquez (north)

This record from LATEX 49 is a good example of an eddy/slope interaction. Currents are mostly north and northeast with large amplitude, low-frequency motions at 101 m. No effect is seen in the LATEX 49 bottom record at ~500 m. Data from LATEX 49 are plotted in Figure 6.3.4-2.

14 1993: August Eddy, Eddy Whopper

This record from LATEX 12 is a good example of eddy/slope interaction. Currents are mostly south and east-southeast with large amplitude, low-frequency motions at 14 m. No effect is seen in the LATEX 12 bottom record at ~500 m. Data from LATEX 12 are plotted in Figure 6.3.4-2.

15 1995: July, Eddy Zapp

Currents at Industry GC200 are coherent and east-northeast with mean speeds ~48 $cm \cdot s^{-1}$. Speeds diminish with depth. Data from Industry GC200 are plotted in Figure 6.2.12-7.

16 1999: September-January 2000, Eddy Juggernaut

Eddy Juggernaut has a major influence on currents measured at the SAIC EISEXT (I1, I2, and I3) locations, particularly during September-October 1999 through January 2000. Coherent motions to 800 m are apparent; they are due to the direct influence of the eddy. Bottom intensification and strong oscillations are evident at all three EISEXT locations. Mooring I2, being closest to the Sigsbee Escarpment, has the strongest currents of about 100 $cm \cdot s^{-1}$ at 1600-2000 m depth. Data from SAIC EIS Extension are plotted in Figures 6.3.6-2 and 6.3.6-3.

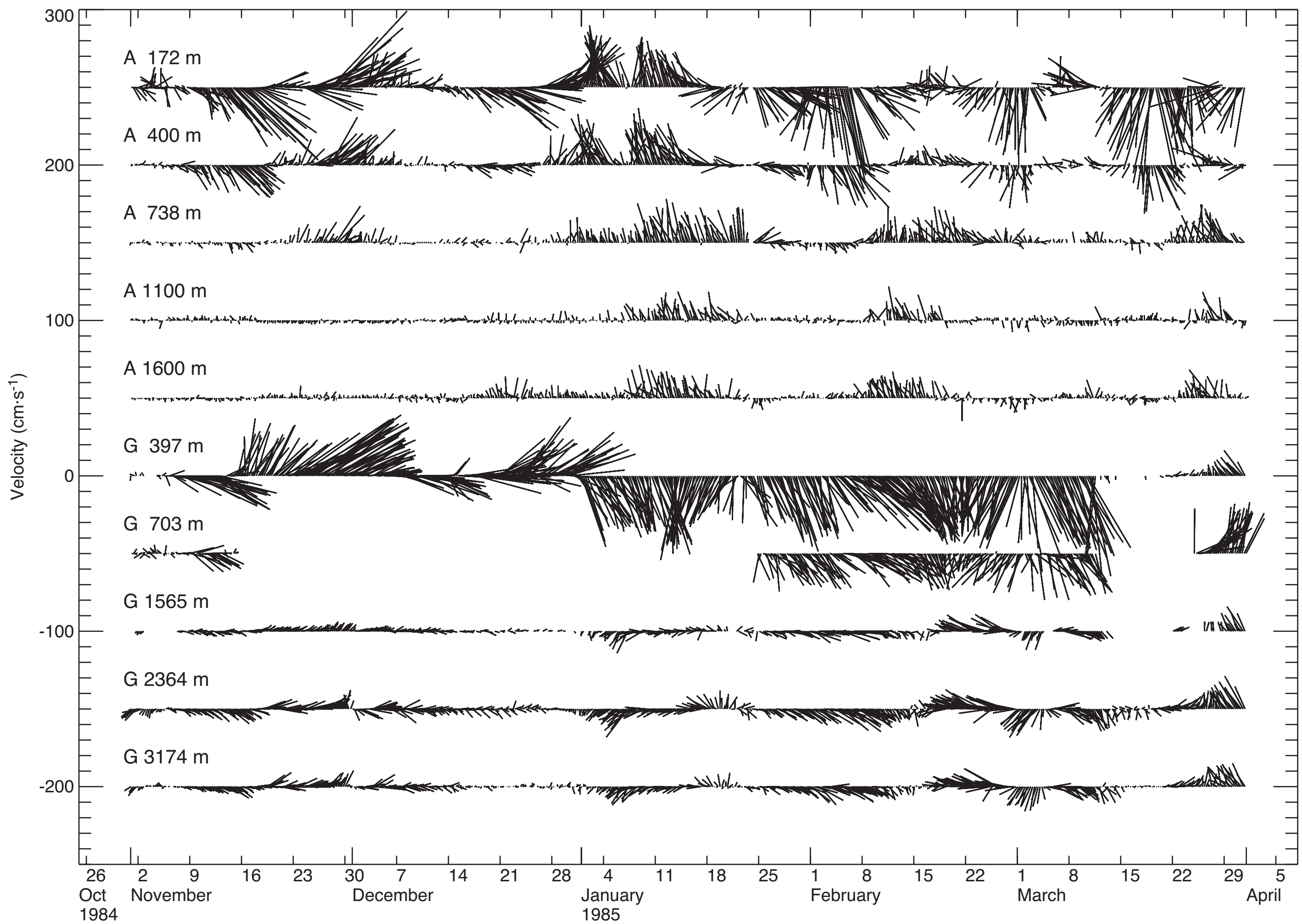

Figure B.3-1. Influence of the Loop Current and a Loop Current eddy on currents in the eastern Gulf at SAIC 5-year moorings A and G, October 1984 to April 1985. See also Table B-3, event 3.

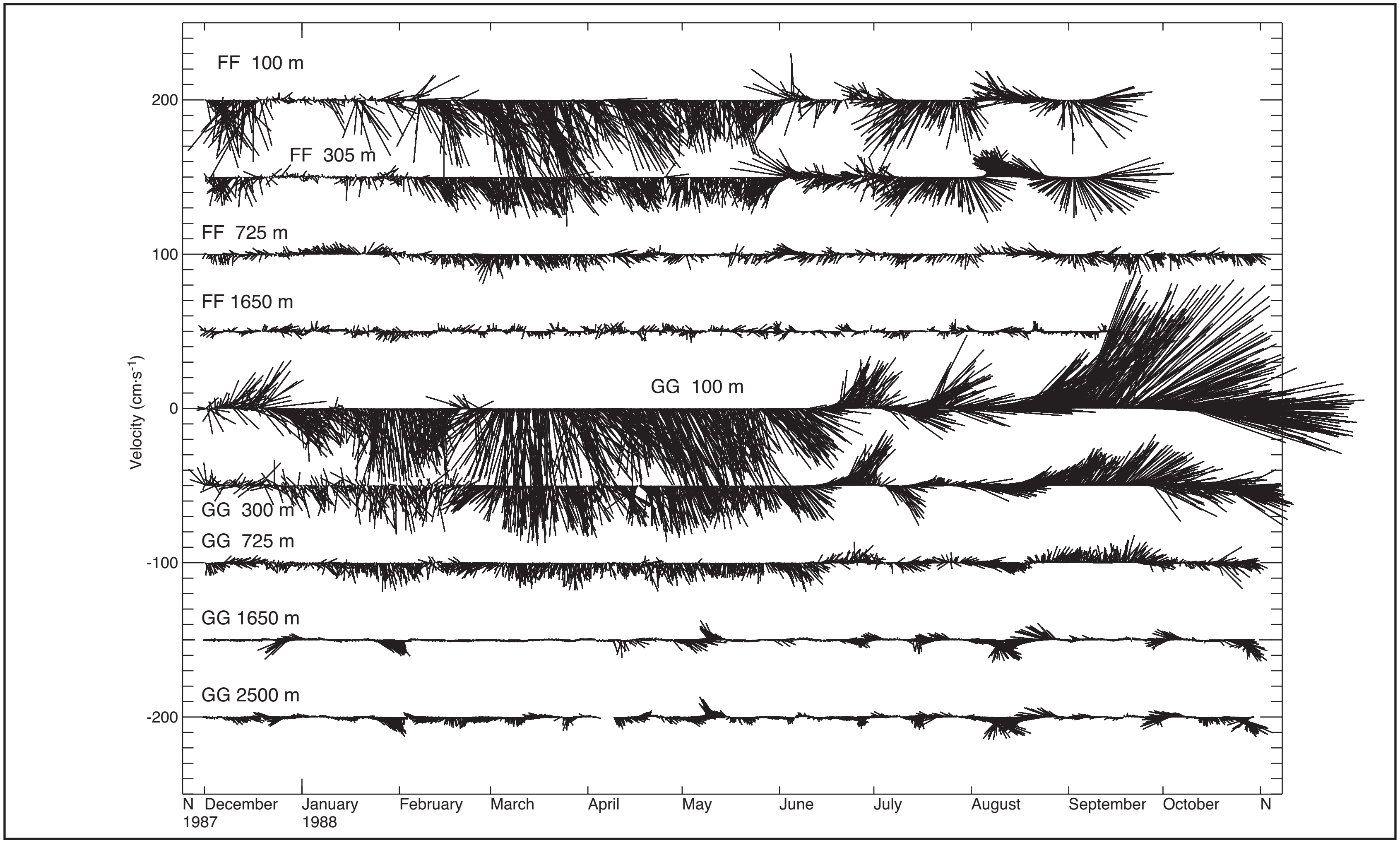

Figure B.3-2. Influence of Loop Current eddies Kathleen (December 1987 through July 1988) and Murphy (August to November 1988) on the currents in the central Gulf at SAIC 5-year moorings FF and GG. See also Table B-3, events 8 and 9.

Table B-4. Speed statistics for energetic current events associated with anticyclonic slope eddies. Given are the name of the file containing the event (keyed to the directory on the CD-ROM database), the start and stop dates used to characterize the event, maximum speed, mean speed, standard deviation of speed, mooring location, depth of the instrument, and total water depth. Comments on the event, keyed by the event number, are given in the notes below the table.

Event No.	Year	Filename	Directory	Event start date (m/d/y)	Event end date (m/d/y)	Maximum speed ($cm \cdot s^{-1}$)	Mean speed ($cm \cdot s^{-1}$)	Stand. dev. of speed ($cm \cdot s^{-1}$)	Latitude (°N)	Longitude (°W)	Depth (m)	Total water depth (m)
1	1992	GC920415.C01	/TAMU/	05/01/1992	06/30/1992	48.479	17.705	10.815	27.9240	90.4950	27.0	515.0
	1992	GC920415.C02	/TAMU/	05/01/1992	06/30/1992	45.664	18.169	10.925	27.9240	90.4950	115.0	515.0
	1992	GC920415.C03	/TAMU/	05/01/1992	06/30/1992	4.801	1.972	0.538	27.9240	90.4950	505.0	515.0
2	1993	GC930112.C01	/TAMU/	04/01/1993	04/30/1993	45.718	14.845	8.338	27.9290	90.4940	12.0	498.0
	1993	GC930112.C02	/TAMU/	04/01/1993	04/30/1993	27.331	9.918	5.775	27.9290	90.4940	98.0	498.0
3	1994	GC940212.A01	/INDUSTRY/	04/01/1994	04/30/1994	46.003	16.246	9.677	27.7457	90.7310	31.0	894.6
	1994	GC940212.A02	/INDUSTRY/	04/01/1994	04/30/1994	42.782	15.462	8.858	27.7457	90.7310	39.0	894.6
	1994	GC940212.A03	/INDUSTRY/	04/01/1994	04/30/1994	40.964	14.055	8.662	27.7457	90.7310	47.0	894.6
	1994	GC940212.A04	/INDUSTRY/	04/01/1994	04/30/1994	40.311	12.972	8.229	27.7457	90.7310	55.0	894.6
	1994	GC940212.A05	/INDUSTRY/	04/01/1994	04/30/1994	39.488	12.541	7.924	27.7457	90.7310	63.0	894.6
	1994	GC940212.A06	/INDUSTRY/	04/01/1994	04/30/1994	37.780	12.214	7.540	27.7457	90.7310	71.0	894.6
	1994	GC940212.A07	/INDUSTRY/	04/01/1994	04/30/1994	39.259	12.460	7.590	27.7457	90.7310	79.0	894.6
	1994	GC940212.A08	/INDUSTRY/	04/01/1994	04/30/1994	42.902	12.527	7.281	27.7457	90.7310	87.0	894.6
	1994	GC940212.A09	/INDUSTRY/	04/01/1994	04/30/1994	42.252	11.749	6.693	27.7457	90.7310	95.0	894.6
	1994	GC940212.A10	/INDUSTRY/	04/01/1994	04/30/1994	36.173	10.924	5.992	27.7457	90.7310	103.0	894.6
	1994	GC940212.A11	/INDUSTRY/	04/01/1994	04/30/1994	30.480	10.179	5.000	27.7457	90.7310	111.0	894.6
	1994	GC940212.A12	/INDUSTRY/	04/01/1994	04/30/1994	26.001	9.621	4.630	27.7457	90.7310	119.0	894.6
	1994	GC940212.A13	/INDUSTRY/	04/01/1994	04/30/1994	29.954	10.185	4.938	27.7457	90.7310	127.0	894.6
	1994	GC940212.A14	/INDUSTRY/	04/01/1994	04/30/1994	28.971	9.756	4.599	27.7457	90.7310	135.0	894.6
	1994	GC940212.A15	/INDUSTRY/	04/01/1994	04/30/1994	23.703	9.063	4.440	27.7457	90.7310	143.0	894.6
	1994	GC940212.A16	/INDUSTRY/	04/01/1994	04/30/1994	26.638	9.724	4.597	27.7457	90.7310	151.0	894.6
	1994	GC940212.A17	/INDUSTRY/	04/01/1994	04/30/1994	31.655	10.499	5.165	27.7457	90.7310	159.0	894.6
	1994	GC940212.A18	/INDUSTRY/	04/01/1994	04/30/1994	29.586	10.243	5.176	27.7457	90.7310	167.0	894.6
	1994	GC940212.A19	/INDUSTRY/	04/01/1994	04/30/1994	34.311	8.962	5.298	27.7457	90.7310	175.0	894.6
	1994	GC940212.A20	/INDUSTRY/	04/01/1994	04/30/1994	35.009	9.054	5.780	27.7457	90.7310	183.0	894.6
	1994	GC940212.A21	/INDUSTRY/	04/01/1994	04/30/1994	33.234	9.180	5.804	27.7457	90.7310	191.0	894.6
	1994	GC940212.A22	/INDUSTRY/	04/01/1994	04/30/1994	34.319	9.343	6.052	27.7457	90.7310	199.0	894.6
	1994	GC940212.A23	/INDUSTRY/	04/01/1994	04/30/1994	35.585	9.305	6.458	27.7457	90.7310	207.0	894.6
	1994	GC940212.A24	/INDUSTRY/	04/01/1994	04/30/1994	33.634	9.123	6.547	27.7457	90.7310	215.0	894.6
	1994	GC940212.A25	/INDUSTRY/	04/01/1994	04/30/1994	32.254	9.143	6.722	27.7457	90.7310	223.0	894.6

Table B-4. Speed statistics for energetic current events associated with anticyclonic slope eddies. (continued)

Event No.	Year	Filename	Directory	Event start date (m/d/y)	Event end date (m/d/y)	Maximum speed (cm·s^{-1})	Mean speed (cm·s^{-1})	Stand. dev. of speed (cm·s^{-1})	Latitude (°N)	Longitude (°W)	Depth (m)	Total water depth (m)
3	1994	GC940212.A26	/INDUSTRY/	04/01/1994	04/30/1994	31.726	9.350	6.815	27.7457	90.7310	231.0	894.6
	1994	GC940212.A27	/INDUSTRY/	04/01/1994	04/30/1994	32.106	9.463	6.916	27.7457	90.7310	239.0	894.6
	1994	GC940212.A28	/INDUSTRY/	04/01/1994	04/30/1994	32.802	9.368	6.953	27.7457	90.7310	247.0	894.6
	1994	GC940212.A29	/INDUSTRY/	04/01/1994	04/30/1994	33.025	9.506	7.131	27.7457	90.7310	255.0	894.6
	1994	GC940212.A30	/INDUSTRY/	04/01/1994	04/30/1994	34.355	9.667	7.183	27.7457	90.7310	263.0	894.6
	1994	GC940212.A31	/INDUSTRY/	04/01/1994	04/30/1994	33.077	9.901	7.076	27.7457	90.7310	271.0	894.6
	1994	GC940212.A32	/INDUSTRY/	04/01/1994	04/30/1994	33.868	9.974	7.062	27.7457	90.7310	279.0	894.6
	1994	GC940212.A33	/INDUSTRY/	04/01/1994	04/30/1994	33.898	10.027	6.929	27.7457	90.7310	287.0	894.6
	1994	GC940212.A34	/INDUSTRY/	04/01/1994	04/30/1994	33.773	10.112	6.849	27.7457	90.7310	295.0	894.6
	1994	GC940212.A35	/INDUSTRY/	04/01/1994	04/30/1994	35.000	10.166	6.628	27.7457	90.7310	303.0	894.6
	1994	GC940212.A36	/INDUSTRY/	04/01/1994	04/30/1994	35.046	10.159	6.431	27.7457	90.7310	311.0	894.6
	1994	GC940212.A37	/INDUSTRY/	04/01/1994	04/30/1994	33.364	10.018	6.117	27.7457	90.7310	319.0	894.6
	1994	GC940212.A38	/INDUSTRY/	04/01/1994	04/30/1994	33.400	9.894	5.895	27.7457	90.7310	327.0	894.6
	1994	GC940212.A39	/INDUSTRY/	04/01/1994	04/30/1994	38.185	9.708	5.892	27.7457	90.7310	335.0	894.6
	1994	GC940212.A40	/INDUSTRY/	04/01/1994	04/30/1994	33.765	9.497	5.734	27.7457	90.7310	343.0	894.6
	1994	GC940212.A41	/INDUSTRY/	04/01/1994	04/30/1994	31.766	9.341	5.689	27.7457	90.7310	351.0	894.6
	1994	GC940212.A42	/INDUSTRY/	04/01/1994	04/30/1994	33.110	9.275	5.727	27.7457	90.7310	359.0	894.6
	1994	GC940212.A43	/INDUSTRY/	04/01/1994	04/30/1994	34.829	9.023	5.670	27.7457	90.7310	367.0	894.6
	1994	GC940212.A44	/INDUSTRY/	04/01/1994	04/30/1994	34.221	8.848	5.479	27.7457	90.7310	375.0	894.6
	1994	GC940212.A45	/INDUSTRY/	04/01/1994	04/30/1994	34.221	8.802	5.446	27.7457	90.7310	383.0	894.6
	1994	GC940212.A46	/INDUSTRY/	04/01/1994	04/30/1994	32.222	8.706	5.366	27.7457	90.7310	391.0	894.6
	1994	GC940212.A47	/INDUSTRY/	04/01/1994	04/30/1994	29.288	8.472	5.187	27.7457	90.7310	399.0	894.6
	1994	GC940212.A48	/INDUSTRY/	04/01/1994	04/30/1994	29.288	8.476	5.008	27.7457	90.7310	407.0	894.6
	1994	GC940212.A49	/INDUSTRY/	04/01/1994	04/30/1994	28.112	8.524	4.933	27.7457	90.7310	415.0	894.6
	1994	GC940212.A50	/INDUSTRY/	04/01/1994	04/30/1994	27.370	8.439	4.798	27.7457	90.7310	423.0	894.6
	1994	GC940212.A51	/INDUSTRY/	04/01/1994	04/30/1994	26.223	8.494	4.719	27.7457	90.7310	431.0	894.6
	1994	GC940212.A52	/INDUSTRY/	04/01/1994	04/30/1994	24.771	8.656	4.666	27.7457	90.7310	439.0	894.6
	1994	GC940212.A53	/INDUSTRY/	04/01/1994	04/30/1994	28.829	8.656	4.742	27.7457	90.7310	447.0	894.6
	1994	GC940212.A54	/INDUSTRY/	04/01/1994	04/30/1994	26.202	8.653	5.110	27.7457	90.7310	455.0	894.6
	1994	GC940212.A55	/INDUSTRY/	04/01/1994	04/30/1994	25.142	7.075	3.968	27.7457	90.7310	463.0	894.6
4	1997	VK970320.A01	/MMS/	03/20/1997	07/09/1997	86.295	20.689	11.685	29.0592	88.3900	12.0	500.0
	1997	VK970710.A01	/MMS/	07/10/1997	08/31/1997	106.663	18.624	12.477	29.0592	88.3900	12.0	500.0
	1997	VK970320.A02	/MMS/	03/20/1997	07/09/1997	76.439	21.001	11.343	29.0592	88.3900	16.0	500.0
	1997	VK970710.A02	/MMS/	07/10/1997	08/31/1997	89.581	18.570	11.408	29.0592	88.3900	16.0	500.0

Table B-4. Speed statistics for energetic current events associated with anticyclonic slope eddies. (continued)

Event No.	Year	Filename	Directory	Event start date (m/d/y)	Event end date (m/d/y)	Maximum speed ($cm \cdot s^{-1}$)	Mean speed ($cm \cdot s^{-1}$)	Stand. dev. of speed ($cm \cdot s^{-1}$)	Latitude (°N)	Longitude (°W)	Depth (m)	Total water depth (m)
4	1997	VK970320.A03	/MMS/	03/20/1997	07/09/1997	64.771	18.937	9.846	29.0592	88.3900	20.0	500.0
	1997	VK970710.A03	/MMS/	07/10/1997	08/31/1997	62.689	18.371	10.054	29.0592	88.3900	20.0	500.0
	1997	VK970320.A04	/MMS/	03/20/1997	07/09/1997	62.221	17.597	9.162	29.0592	88.3900	24.0	500.0
	1997	VK970710.A04	/MMS/	07/10/1997	08/31/1997	55.260	16.384	8.356	29.0592	88.3900	24.0	500.0
	1997	VK970320.A05	/MMS/	03/20/1997	07/09/1997	67.801	16.785	8.676	29.0592	88.3900	28.0	500.0
	1997	VK970710.A05	/MMS/	07/10/1997	08/31/1997	39.599	15.671	7.429	29.0592	88.3900	28.0	500.0
	1997	VK970320.A06	/MMS/	03/20/1997	07/09/1997	62.849	16.330	8.662	29.0592	88.3900	32.0	500.0
	1997	VK970710.A06	/MMS/	07/10/1997	08/31/1997	43.089	15.727	7.991	29.0592	88.3900	32.0	500.0
	1997	VK970320.A07	/MMS/	03/20/1997	07/09/1997	58.104	16.195	8.623	29.0592	88.3900	36.0	500.0
	1997	VK970710.A07	/MMS/	07/10/1997	08/31/1997	42.314	15.463	8.217	29.0592	88.3900	36.0	500.0
	1997	VK970320.A08	/MMS/	03/20/1997	07/09/1997	55.030	16.140	8.519	29.0592	88.3900	40.0	500.0
	1997	VK970710.A08	/MMS/	07/10/1997	08/31/1997	39.623	14.995	7.644	29.0592	88.3900	40.0	500.0
	1997	VK970320.A09	/MMS/	03/20/1997	07/09/1997	52.240	15.935	8.323	29.0592	88.3900	44.0	500.0
	1997	VK970710.A09	/MMS/	07/10/1997	08/31/1997	37.420	14.825	7.006	29.0592	88.3900	44.0	500.0
	1997	VK970320.A10	/MMS/	03/20/1997	07/09/1997	50.741	15.691	8.254	29.0592	88.3900	48.0	500.0
	1997	VK970710.A10	/MMS/	07/10/1997	08/31/1997	37.510	14.459	6.603	29.0592	88.3900	48.0	500.0
	1997	VK970320.A11	/MMS/	03/20/1997	07/09/1997	44.006	15.468	8.084	29.0592	88.3900	52.0	500.0
	1997	VK970710.A11	/MMS/	07/10/1997	08/31/1997	32.336	14.171	6.634	29.0592	88.3900	52.0	500.0
	1997	VK970320.A12	/MMS/	03/20/1997	07/09/1997	42.495	15.156	7.952	29.0592	88.3900	56.0	500.0
	1997	VK970710.A12	/MMS/	07/10/1997	08/31/1997	35.007	14.292	6.877	29.0592	88.3900	56.0	500.0
	1997	VK970320.A13	/MMS/	03/20/1997	07/09/1997	42.746	14.942	7.856	29.0592	88.3900	60.0	500.0
	1997	VK970710.A13	/MMS/	07/10/1997	08/31/1997	37.173	14.252	7.188	29.0592	88.3900	60.0	500.0
	1997	VK970320.A14	/MMS/	03/20/1997	07/09/1997	37.987	13.652	7.174	29.0592	88.3900	64.0	500.0
	1997	VK970710.A14	/MMS/	07/10/1997	08/31/1997	37.989	12.622	6.831	29.0592	88.3900	64.0	500.0
	1997	VK970320.A15	/MMS/	03/20/1997	07/09/1997	37.772	13.734	7.283	29.0592	88.3900	68.0	500.0
	1997	VK970710.A15	/MMS/	07/10/1997	08/31/1997	38.828	12.617	7.287	29.0592	88.3900	68.0	500.0
	1997	VK970320.A16	/MMS/	03/20/1997	07/09/1997	41.564	14.372	7.798	29.0592	88.3900	72.0	500.0
	1997	VK970710.A16	/MMS/	07/10/1997	08/31/1997	39.885	13.398	8.022	29.0592	88.3900	72.0	500.0
	1997	VK970320.A17	/MMS/	03/20/1997	07/09/1997	42.300	14.278	7.758	29.0592	88.3900	76.0	500.0
	1997	VK970710.A17	/MMS/	07/10/1997	08/31/1997	42.405	12.973	7.724	29.0592	88.3900	76.0	500.0
	1997	VK970320.A18	/MMS/	03/20/1997	07/09/1997	41.141	14.302	7.863	29.0592	88.3900	80.0	500.0
	1997	VK970321.C01	/MMS/	03/21/1997	07/09/1997	35.974	9.950	6.575	29.0592	88.3900	200.0	500.0
	1997	VK970710.C01	/MMS/	07/10/1997	08/31/1997	35.690	12.815	7.851	29.0592	88.3900	200.0	500.0
	1997	VK970321.C02	/MMS/	03/21/1997	07/09/1997	38.884	9.727	7.760	29.0592	88.3900	300.0	500.0

Table B-4. Speed statistics for energetic current events associated with anticyclonic slope eddies. (continued)

Event No.	Year	Filename	Directory	Event start date (m/d/y)	Event end date (m/d/y)	Maximum speed (cm·s^{-1})	Mean speed (cm·s^{-1})	Stand. dev. of speed (cm·s^{-1})	Latitude (°N)	Longitude (°W)	Depth (m)	Total water depth (m)
4	1997	VK970710.C02	/MMS/	07/10/1997	08/31/1997	29.875	12.180	6.631	29.0592	88.3900	300.0	500.0
	1997	VK970321.C03	/MMS/	03/21/1997	07/09/1997	33.297	6.116	4.096	29.0592	88.3900	490.0	500.0
	1997	VK970710.C03	/MMS/	07/10/1997	08/31/1997	29.099	4.188	3.163	29.0592	88.3900	490.0	500.0
	1997	MC970320.C01	/MMS/	03/20/1997	07/09/1997	26.302	9.986	3.468	28.7662	88.2650	500.0	1300.0
	1997	MC970710.C01	/MMS/	07/10/1997	08/31/1997	20.902	9.092	3.177	28.7662	88.2650	500.0	1300.0
	1997	MC970320.C02	/MMS/	03/20/1997	07/09/1997	15.630	2.766	2.394	28.7662	88.2650	1310.0	1320.0
	1997	MC970710.C02	/MMS/	07/10/1997	08/31/1997	15.629	3.686	2.911	28.7662	88.2650	1310.0	1320.0
	1997	VK970328.C01	/MMS/	03/28/1997	07/11/1997	33.943	9.743	6.577	29.2120	87.8722	200.0	500.0
	1997	VK970712.C01	/MMS/	07/12/1997	08/31/1997	41.212	14.543	8.860	29.2120	87.8722	200.0	500.0
	1997	VK970328.C02	/MMS/	03/28/1997	07/11/1997	39.172	12.063	7.602	29.2120	87.8722	300.0	500.0
	1997	VK970712.C02	/MMS/	07/12/1997	08/31/1997	33.938	13.975	8.128	29.2120	87.8722	300.0	500.0
	1997	VK970328.C03	/MMS/	03/28/1997	07/11/1997	27.599	8.618	4.528	29.2120	87.8722	490.0	500.0
	1997	VK970712.C03	/MMS/	07/12/1997	08/31/1997	16.603	5.550	2.833	29.2120	87.8722	490.0	500.0
	1997	VK970322.C01	/MMS/	03/22/1997	07/11/1997	26.401	10.941	3.826	29.0705	87.8568	500.0	1300.0
	1997	VK970712.C04	/MMS/	07/12/1997	08/31/1997	14.469	3.894	2.980	29.0705	87.8568	500.0	1300.0
	1997	VK970322.C02	/MMS/	03/22/1997	07/11/1997	15.049	2.433	2.340	29.0705	87.8568	1290.0	1300.0
	1997	VK970822.C01	/MMS/	08/22/1997	08/31/1997	17.399	8.259	2.067	29.0705	87.8568	1290.0	1300.0
	1997	DD970324.C01	/MMS/	03/24/1997	07/16/1997	34.525	12.269	7.120	29.3712	87.3563	200.0	500.0
	1997	DD970717.C01	/MMS/	07/17/1997	08/31/1997	30.161	12.053	5.632	29.3712	87.3563	200.0	500.0
	1997	DD970324.C02	/MMS/	03/24/1997	07/16/1997	31.325	9.907	6.471	29.3712	87.3563	300.0	500.0
	1997	DD970717.C02	/MMS/	07/17/1997	08/31/1997	35.104	10.496	6.056	29.3712	87.3563	300.0	500.0
	1997	DD970324.C03	/MMS/	03/24/1997	07/16/1997	27.399	7.453	4.942	29.3712	87.3563	490.0	500.0
	1997	DD970717.C03	/MMS/	07/17/1997	08/31/1997	27.404	7.209	4.487	29.3712	87.3563	490.0	500.0
	1997	DD970324.C04	/MMS/	03/24/1997	07/17/1997	22.802	12.565	2.120	29.0032	87.3532	500.0	1300.0
	1997	DD970718.C01	/MMS/	07/18/1997	08/31/1997	15.635	3.954	2.813	29.0032	87.3532	500.0	1300.0
	1997	DD970324.C05	/MMS/	03/24/1997	07/17/1997	14.467	3.115	2.632	29.0032	87.3532	1290.0	1300.0
	1997	MC970710.A01	/MMS/	07/10/1997	08/31/1997	121.598	21.320	14.675	28.7662	88.2650	8.0	1300.0
	1997	MC970710.A02	/MMS/	07/10/1997	08/31/1997	111.884	20.417	13.524	28.7662	88.2650	12.0	1300.0
	1997	MC970320.A01	/MMS/	03/20/1997	07/09/1997	88.465	25.301	13.937	28.7662	88.2650	16.0	1300.0
	1997	MC970710.A03	/MMS/	07/10/1997	08/31/1997	97.270	19.746	12.104	28.7662	88.2650	16.0	1300.0
	1997	MC970320.A02	/MMS/	03/20/1997	07/09/1997	81.835	23.770	13.291	28.7662	88.2650	20.0	1300.0
	1997	MC970710.A04	/MMS/	07/10/1997	08/31/1997	78.462	18.769	10.715	28.7662	88.2650	20.0	1300.0
	1997	MC970320.A03	/MMS/	03/20/1997	07/09/1997	81.388	23.054	13.107	28.7662	88.2650	24.0	1300.0
	1997	MC970710.A05	/MMS/	07/10/1997	08/31/1997	63.106	17.889	9.919	28.7662	88.2650	24.0	1300.0

Table B-4. Speed statistics for energetic current events associated with anticyclonic slope eddies. (continued)

Event No.	Year	Filename	Directory	Event start date (m/d/y)	Event end date (m/d/y)	Maximum speed (cm·s^{-1})	Mean speed (cm·s^{-1})	Stand. dev. of speed (cm·s^{-1})	Latitude (°N)	Longitude (°W)	Depth (m)	Total water depth (m)
4	1997	MC970320.A04	/MMS/	03/20/1997	07/09/1997	79.763	22.848	13.008	28.7662	88.2650	28.0	1300.0
	1997	MC970710.A06	/MMS/	07/10/1997	08/31/1997	49.953	16.992	9.296	28.7662	88.2650	28.0	1300.0
	1997	MC970320.A05	/MMS/	03/20/1997	07/09/1997	76.601	22.695	12.759	28.7662	88.2650	32.0	1300.0
	1997	MC970710.A07	/MMS/	07/10/1997	08/31/1997	52.389	16.991	9.263	28.7662	88.2650	32.0	1300.0
	1997	MC970320.A06	/MMS/	03/20/1997	07/09/1997	70.577	22.678	12.488	28.7662	88.2650	36.0	1300.0
	1997	MC970710.A08	/MMS/	07/10/1997	08/31/1997	49.674	16.806	9.378	28.7662	88.2650	36.0	1300.0
	1997	MC970320.A07	/MMS/	03/20/1997	07/09/1997	68.700	22.742	12.380	28.7662	88.2650	40.0	1300.0
	1997	MC970710.A09	/MMS/	07/10/1997	08/31/1997	47.566	16.460	9.284	28.7662	88.2650	40.0	1300.0
	1997	MC970320.A08	/MMS/	03/20/1997	07/09/1997	72.340	22.773	12.297	28.7662	88.2650	44.0	1300.0
	1997	MC970710.A10	/MMS/	07/10/1997	08/31/1997	48.901	16.178	9.254	28.7662	88.2650	44.0	1300.0
	1997	MC970320.A09	/MMS/	03/20/1997	07/09/1997	74.142	22.656	12.253	28.7662	88.2650	48.0	1300.0
	1997	MC970710.A11	/MMS/	07/10/1997	08/31/1997	44.413	15.921	9.108	28.7662	88.2650	48.0	1300.0
	1997	MC970320.A10	/MMS/	03/20/1997	07/09/1997	73.185	22.451	12.221	28.7662	88.2650	52.0	1300.0
	1997	MC970710.A12	/MMS/	07/10/1997	08/31/1997	41.437	15.784	8.657	28.7662	88.2650	52.0	1300.0
	1997	MC970320.A11	/MMS/	03/20/1997	07/09/1997	69.153	22.200	12.219	28.7662	88.2650	56.0	1300.0
	1997	MC970710.A13	/MMS/	07/10/1997	08/31/1997	29.844	11.519	6.476	28.7662	88.2650	56.0	1300.0
	1997	MC970320.A12	/MMS/	03/20/1997	07/09/1997	60.930	21.948	12.106	28.7662	88.2650	60.0	1300.0
	1997	MC970710.A14	/MMS/	07/10/1997	08/31/1997	29.850	12.160	7.091	28.7662	88.2650	60.0	1300.0
	1997	MC970320.A13	/MMS/	03/20/1997	07/09/1997	58.434	21.630	11.976	28.7662	88.2650	64.0	1300.0
	1997	MC970710.A15	/MMS/	07/10/1997	08/31/1997	38.461	15.094	8.888	28.7662	88.2650	64.0	1300.0
	1997	MC970320.A14	/MMS/	03/20/1997	07/09/1997	57.177	21.338	11.789	28.7662	88.2650	68.0	1300.0
	1997	MC970710.A16	/MMS/	07/10/1997	08/31/1997	38.601	14.786	8.905	28.7662	88.2650	68.0	1300.0
	1997	MC970320.A15	/MMS/	03/20/1997	07/09/1997	57.563	20.934	11.576	28.7662	88.2650	72.0	1300.0
	1997	MC970710.A17	/MMS/	07/10/1997	08/31/1997	39.314	13.986	8.415	28.7662	88.2650	72.0	1300.0
	1997	MC970320.A16	/MMS/	03/20/1997	07/09/1997	46.973	14.741	7.691	28.7662	88.2650	76.0	1300.0
	1997	MC970320.A17	/MMS/	03/20/1997	07/09/1997	47.535	15.639	8.181	28.7662	88.2650	80.0	1300.0
	1997	MC970320.A18	/MMS/	03/20/1997	07/09/1997	58.549	20.242	11.100	28.7662	88.2650	84.0	1300.0
	1997	MC970320.A19	/MMS/	03/20/1997	07/09/1997	55.892	19.864	10.808	28.7662	88.2650	88.0	1300.0
	1997	VK970327.A01	/MMS/	03/27/1997	07/11/1997	93.014	22.444	12.911	29.2120	87.8722	16.0	500.0
	1997	VK970712.A01	/MMS/	07/12/1997	08/31/1997	88.172	20.565	10.081	29.2120	87.8722	16.0	500.0
	1997	VK970327.A02	/MMS/	03/27/1997	07/11/1997	80.006	20.018	11.217	29.2120	87.8722	20.0	500.0
	1997	VK970712.A02	/MMS/	07/12/1997	08/31/1997	61.574	19.529	8.839	29.2120	87.8722	20.0	500.0
	1997	VK970327.A03	/MMS/	03/27/1997	07/11/1997	64.622	18.842	9.476	29.2120	87.8722	24.0	500.0
	1997	VK970712.A03	/MMS/	07/12/1997	08/31/1997	48.953	19.499	9.014	29.2120	87.8722	24.0	500.0

Table B-4. Speed statistics for energetic current events associated with anticyclonic slope eddies. (continued)

Event No.	Year	Filename	Directory	Event start date (m/d/y)	Event end date (m/d/y)	Maximum speed ($cm \cdot s^{-1}$)	Mean speed ($cm \cdot s^{-1}$)	Stand. dev. of speed ($cm \cdot s^{-1}$)	Latitude (°N)	Longitude (°W)	Depth (m)	Total water depth (m)
4	1997	VK970327.A04	/MMS/	03/27/1997	07/11/1997	49.252	18.009	8.526	29.2120	87.8722	28.0	500.0
	1997	VK970712.A04	/MMS/	07/12/1997	08/31/1997	53.275	19.865	8.973	29.2120	87.8722	28.0	500.0
	1997	VK970327.A05	/MMS/	03/27/1997	07/11/1997	41.774	17.347	8.193	29.2120	87.8722	32.0	500.0
	1997	VK970712.A05	/MMS/	07/12/1997	08/31/1997	46.405	20.164	8.571	29.2120	87.8722	32.0	500.0
	1997	VK970327.A06	/MMS/	03/27/1997	07/11/1997	42.029	16.839	7.986	29.2120	87.8722	36.0	500.0
	1997	VK970712.A06	/MMS/	07/12/1997	08/31/1997	44.168	19.858	8.238	29.2120	87.8722	36.0	500.0
	1997	VK970327.A07	/MMS/	03/27/1997	07/11/1997	42.040	16.473	8.001	29.2120	87.8722	40.0	500.0
	1997	VK970712.A07	/MMS/	07/12/1997	08/31/1997	42.788	19.156	7.982	29.2120	87.8722	40.0	500.0
	1997	VK970327.A08	/MMS/	03/27/1997	07/11/1997	45.127	16.398	7.839	29.2120	87.8722	44.0	500.0
	1997	VK970712.A08	/MMS/	07/12/1997	08/31/1997	38.170	18.303	7.650	29.2120	87.8722	44.0	500.0
	1997	VK970327.A09	/MMS/	03/27/1997	07/11/1997	44.061	16.319	7.715	29.2120	87.8722	48.0	500.0
	1997	VK970712.A09	/MMS/	07/12/1997	08/31/1997	38.394	17.365	7.656	29.2120	87.8722	48.0	500.0
	1997	VK970327.A10	/MMS/	03/27/1997	07/11/1997	42.441	16.227	7.488	29.2120	87.8722	52.0	500.0
	1997	VK970712.A10	/MMS/	07/12/1997	08/31/1997	40.623	17.187	7.829	29.2120	87.8722	52.0	500.0
	1997	VK970327.A11	/MMS/	03/27/1997	07/11/1997	41.643	16.002	7.462	29.2120	87.8722	56.0	500.0
	1997	VK970712.A11	/MMS/	07/12/1997	08/31/1997	43.988	17.220	8.001	29.2120	87.8722	56.0	500.0
	1997	VK970327.A12	/MMS/	03/27/1997	07/11/1997	43.053	15.815	7.457	29.2120	87.8722	60.0	500.0
	1997	VK970712.A12	/MMS/	07/12/1997	08/31/1997	47.075	17.088	8.019	29.2120	87.8722	60.0	500.0
	1997	VK970327.A13	/MMS/	03/27/1997	07/11/1997	36.133	14.107	6.698	29.2120	87.8722	64.0	500.0
	1997	VK970712.A13	/MMS/	07/12/1997	08/31/1997	48.127	14.647	7.223	29.2120	87.8722	64.0	500.0
	1997	VK970327.A14	/MMS/	03/27/1997	07/11/1997	41.450	14.227	6.780	29.2120	87.8722	68.0	500.0
	1997	VK970712.A14	/MMS/	07/12/1997	08/31/1997	45.109	14.838	7.405	29.2120	87.8722	68.0	500.0
	1997	VK970327.A15	/MMS/	03/27/1997	07/11/1997	45.962	15.320	7.352	29.2120	87.8722	72.0	500.0
	1997	VK970712.A15	/MMS/	07/12/1997	08/31/1997	46.960	16.392	8.105	29.2120	87.8722	72.0	500.0
	1997	VK970327.A16	/MMS/	03/27/1997	07/11/1997	47.332	15.118	7.209	29.2120	87.8722	76.0	500.0
	1997	VK970712.A16	/MMS/	07/12/1997	08/31/1997	45.393	15.998	8.042	29.2120	87.8722	76.0	500.0
	1997	VK970327.A17	/MMS/	03/27/1997	07/11/1997	46.711	14.925	7.125	29.2120	87.8722	80.0	500.0
	1997	VK970712.A17	/MMS/	07/12/1997	08/31/1997	42.314	15.594	7.893	29.2120	87.8722	80.0	500.0
	1997	VK970322.A01	/MMS/	03/22/1997	07/11/1997	85.286	23.079	14.960	29.0705	87.8568	16.0	1300.0
	1997	VK970712.A18	/MMS/	07/12/1997	08/31/1997	123.846	17.652	11.736	29.0705	87.8568	16.0	1300.0
	1997	VK970322.A02	/MMS/	03/22/1997	07/11/1997	75.937	19.344	12.596	29.0705	87.8568	20.0	1300.0
	1997	VK970712.A19	/MMS/	07/12/1997	08/31/1997	94.519	16.077	10.094	29.0705	87.8568	20.0	1300.0
	1997	VK970322.A03	/MMS/	03/22/1997	07/11/1997	62.161	16.870	10.537	29.0705	87.8568	24.0	1300.0
	1997	VK970712.A20	/MMS/	07/12/1997	08/31/1997	66.707	16.198	8.710	29.0705	87.8568	24.0	1300.0

Table B-4. Speed statistics for energetic current events associated with anticyclonic slope eddies. (continued)

Event No.	Year	Filename	Directory	Event start date (m/d/y)	Event end date (m/d/y)	Maximum speed ($cm \cdot s^{-1}$)	Mean speed ($cm \cdot s^{-1}$)	Stand. dev. of speed ($cm \cdot s^{-1}$)	Latitude (°N)	Longitude (°W)	Depth (m)	Total water depth (m)
4	1997	VK970322.A04	/MMS/	03/22/1997	07/11/1997	54.675	15.633	9.023	29.0705	87.8568	28.0	1300.0
	1997	VK970712.A21	/MMS/	07/12/1997	08/31/1997	58.413	15.964	8.047	29.0705	87.8568	28.0	1300.0
	1997	VK970322.A05	/MMS/	03/22/1997	07/11/1997	52.225	14.597	8.250	29.0705	87.8568	32.0	1300.0
	1997	VK970712.A22	/MMS/	07/12/1997	08/31/1997	48.723	15.438	7.613	29.0705	87.8568	32.0	1300.0
	1997	VK970322.A06	/MMS/	03/22/1997	07/11/1997	48.674	13.992	7.737	29.0705	87.8568	36.0	1300.0
	1997	VK970712.A23	/MMS/	07/12/1997	08/31/1997	48.091	14.776	7.419	29.0705	87.8568	36.0	1300.0
	1997	VK970322.A07	/MMS/	03/22/1997	07/11/1997	42.602	13.529	7.574	29.0705	87.8568	40.0	1300.0
	1997	VK970712.A24	/MMS/	07/12/1997	08/31/1997	40.216	13.970	6.964	29.0705	87.8568	40.0	1300.0
	1997	VK970322.A08	/MMS/	03/22/1997	07/11/1997	39.502	13.197	7.483	29.0705	87.8568	44.0	1300.0
	1997	VK970712.A25	/MMS/	07/12/1997	08/31/1997	40.374	13.284	6.974	29.0705	87.8568	44.0	1300.0
	1997	VK970322.A09	/MMS/	03/22/1997	07/11/1997	42.849	13.011	7.440	29.0705	87.8568	48.0	1300.0
	1997	VK970712.A26	/MMS/	07/12/1997	08/31/1997	39.248	12.705	6.941	29.0705	87.8568	48.0	1300.0
	1997	VK970322.A10	/MMS/	03/22/1997	07/11/1997	44.588	12.866	7.478	29.0705	87.8568	52.0	1300.0
	1997	VK970712.A27	/MMS/	07/12/1997	08/31/1997	37.686	12.123	6.951	29.0705	87.8568	52.0	1300.0
	1997	VK970322.A11	/MMS/	03/22/1997	07/11/1997	25.111	7.413	4.225	29.0705	87.8568	56.0	1300.0
	1997	VK970712.A28	/MMS/	07/12/1997	08/31/1997	29.720	7.642	5.066	29.0705	87.8568	56.0	1300.0
	1997	VK970322.A12	/MMS/	03/22/1997	07/11/1997	28.545	7.949	4.777	29.0705	87.8568	60.0	1300.0
	1997	VK970712.A29	/MMS/	07/12/1997	08/31/1997	30.319	8.363	5.474	29.0705	87.8568	60.0	1300.0
	1997	VK970322.A13	/MMS/	03/22/1997	07/11/1997	47.105	12.600	7.734	29.0705	87.8568	64.0	1300.0
	1997	VK970712.A30	/MMS/	07/12/1997	08/31/1997	39.333	12.729	7.469	29.0705	87.8568	64.0	1300.0
	1997	VK970322.A14	/MMS/	03/22/1997	07/11/1997	45.558	12.310	7.713	29.0705	87.8568	68.0	1300.0
	1997	VK970712.A31	/MMS/	07/12/1997	08/31/1997	38.776	12.629	7.478	29.0705	87.8568	68.0	1300.0
	1997	VK970322.A15	/MMS/	03/22/1997	07/11/1997	42.991	12.087	7.596	29.0705	87.8568	72.0	1300.0
	1997	VK970712.A32	/MMS/	07/12/1997	08/31/1997	38.086	12.261	7.514	29.0705	87.8568	72.0	1300.0
	1997	DD970324.A01	/MMS/	03/24/1997	07/16/1997	76.517	21.589	11.147	29.3712	87.3563	8.0	500.0
	1997	DD970324.A02	/MMS/	03/24/1997	07/16/1997	76.827	24.218	11.889	29.3712	87.3563	12.0	500.0
	1997	DD970717.A01	/MMS/	07/17/1997	08/31/1997	69.199	29.245	13.412	29.3712	87.3563	12.0	500.0
	1997	DD970324.A03	/MMS/	03/24/1997	07/16/1997	68.432	23.424	11.409	29.3712	87.3563	16.0	500.0
	1997	DD970717.A02	/MMS/	07/17/1997	08/31/1997	62.329	28.231	13.216	29.3712	87.3563	16.0	500.0
	1997	DD970324.A04	/MMS/	03/24/1997	07/16/1997	64.855	22.733	11.252	29.3712	87.3563	20.0	500.0
	1997	DD970717.A03	/MMS/	07/17/1997	08/31/1997	62.720	28.376	13.024	29.3712	87.3563	20.0	500.0
	1997	DD970324.A05	/MMS/	03/24/1997	07/16/1997	59.760	22.013	10.933	29.3712	87.3563	24.0	500.0
	1997	DD970717.A04	/MMS/	07/17/1997	08/31/1997	56.260	27.254	12.011	29.3712	87.3563	24.0	500.0
	1997	DD970324.A06	/MMS/	03/24/1997	07/16/1997	54.502	21.300	10.538	29.3712	87.3563	28.0	500.0

Table B-4. Speed statistics for energetic current events associated with anticyclonic slope eddies. (continued)

Event No.	Year	Filename	Directory	Event start date (m/d/y)	Event end date (m/d/y)	Maximum speed ($cm \cdot s^{-1}$)	Mean speed ($cm \cdot s^{-1}$)	Stand. dev. of speed ($cm \cdot s^{-1}$)	Latitude (°N)	Longitude (°W)	Depth (m)	Total water depth (m)
4	1997	DD970717.A05	/MMS/	07/17/1997	08/31/1997	55.956	25.825	11.244	29.3712	87.3563	28.0	500.0
	1997	DD970324.A07	/MMS/	03/24/1997	07/16/1997	51.313	20.857	10.125	29.3712	87.3563	32.0	500.0
	1997	DD970717.A06	/MMS/	07/17/1997	08/31/1997	52.720	24.561	10.720	29.3712	87.3563	32.0	500.0
	1997	DD970324.A08	/MMS/	03/24/1997	07/16/1997	51.612	20.699	9.969	29.3712	87.3563	36.0	500.0
	1997	DD970717.A07	/MMS/	07/17/1997	08/31/1997	53.914	23.220	10.541	29.3712	87.3563	36.0	500.0
	1997	DD970324.A09	/MMS/	03/24/1997	07/16/1997	50.870	20.621	10.110	29.3712	87.3563	40.0	500.0
	1997	DD970717.A08	/MMS/	07/17/1997	08/31/1997	52.693	21.910	10.591	29.3712	87.3563	40.0	500.0
	1997	DD970324.A10	/MMS/	03/24/1997	07/16/1997	49.358	20.627	10.274	29.3712	87.3563	44.0	500.0
	1997	DD970717.A09	/MMS/	07/17/1997	08/31/1997	49.703	20.898	10.121	29.3712	87.3563	44.0	500.0
	1997	DD970324.A11	/MMS/	03/24/1997	07/16/1997	49.100	20.352	10.325	29.3712	87.3563	48.0	500.0
	1997	DD970717.A10	/MMS/	07/17/1997	08/31/1997	49.126	20.382	9.589	29.3712	87.3563	48.0	500.0
	1997	DD970324.A12	/MMS/	03/24/1997	07/16/1997	49.152	20.054	10.142	29.3712	87.3563	52.0	500.0
	1997	DD970717.A11	/MMS/	07/17/1997	08/31/1997	46.515	20.007	9.437	29.3712	87.3563	52.0	500.0
	1997	DD970324.A13	/MMS/	03/24/1997	07/16/1997	48.008	19.791	10.117	29.3712	87.3563	56.0	500.0
	1997	DD970717.A12	/MMS/	07/17/1997	08/31/1997	44.921	19.372	9.265	29.3712	87.3563	56.0	500.0
	1997	DD970324.A14	/MMS/	03/24/1997	07/16/1997	50.948	19.621	10.393	29.3712	87.3563	60.0	500.0
	1997	DD970717.A13	/MMS/	07/17/1997	08/31/1997	46.030	18.890	9.448	29.3712	87.3563	60.0	500.0
	1997	DD970324.A15	/MMS/	03/24/1997	07/16/1997	49.319	19.344	10.332	29.3712	87.3563	64.0	500.0
	1997	DD970717.A14	/MMS/	07/17/1997	08/31/1997	44.471	18.316	9.370	29.3712	87.3563	64.0	500.0
	1997	DD970324.A16	/MMS/	03/24/1997	07/16/1997	51.664	19.365	10.412	29.3712	87.3563	68.0	500.0
	1997	DD970717.A15	/MMS/	07/17/1997	08/31/1997	42.820	17.541	9.060	29.3712	87.3563	68.0	500.0
	1997	DD970324.A17	/MMS/	03/24/1997	07/16/1997	50.995	19.152	10.504	29.3712	87.3563	72.0	500.0
	1997	DD970717.A16	/MMS/	07/17/1997	08/31/1997	44.007	17.228	8.797	29.3712	87.3563	72.0	500.0
	1997	DD970324.A18	/MMS/	03/24/1997	07/16/1997	50.804	18.752	10.562	29.3712	87.3563	76.0	500.0
	1997	DD970717.A17	/MMS/	07/17/1997	08/31/1997	42.155	16.872	8.477	29.3712	87.3563	76.0	500.0
	1997	DD970324.A19	/MMS/	03/24/1997	07/16/1997	50.468	18.051	10.626	29.3712	87.3563	80.0	500.0
	1997	DD970717.A18	/MMS/	07/17/1997	08/31/1997	41.383	15.544	8.087	29.3712	87.3563	80.0	500.0
	1997	DD970718.A18	/MMS/	07/18/1997	08/31/1997	77.036	16.920	10.765	29.0032	87.3532	8.0	1300.0
	1997	DD970324.A20	/MMS/	03/24/1997	07/17/1997	84.682	22.869	12.697	29.0032	87.3532	12.0	1300.0
	1997	DD970718.A19	/MMS/	07/18/1997	08/31/1997	65.408	18.903	12.706	29.0032	87.3532	12.0	1300.0
	1997	DD970324.A21	/MMS/	03/24/1997	07/17/1997	83.104	21.431	12.011	29.0032	87.3532	16.0	1300.0
	1997	DD970718.A20	/MMS/	07/18/1997	08/31/1997	68.401	19.261	11.791	29.0032	87.3532	16.0	1300.0
	1997	DD970324.A22	/MMS/	03/24/1997	07/17/1997	81.484	19.873	11.466	29.0032	87.3532	20.0	1300.0
	1997	DD970718.A21	/MMS/	07/18/1997	08/31/1997	69.104	19.911	11.768	29.0032	87.3532	20.0	1300.0

Table B-4. Speed statistics for energetic current events associated with anticyclonic slope eddies. (continued)

Event No.	Year	Filename	Directory	Event start date (m/d/y)	Event end date (m/d/y)	Maximum speed (cm·s^{-1})	Mean speed (cm·s^{-1})	Stand. dev. of speed (cm·s^{-1})	Latitude (°N)	Longitude (°W)	Depth (m)	Total water depth (m)
4	1997	DD970324.A23	/MMS/	03/24/1997	07/17/1997	78.102	18.613	11.237	29.0032	87.3532	24.0	1300.0
	1997	DD970718.A22	/MMS/	07/18/1997	08/31/1997	60.317	19.457	10.675	29.0032	87.3532	24.0	1300.0
	1997	DD970324.A24	/MMS/	03/24/1997	07/17/1997	75.018	17.759	11.004	29.0032	87.3532	28.0	1300.0
	1997	DD970718.A23	/MMS/	07/18/1997	08/31/1997	51.779	18.086	8.943	29.0032	87.3532	28.0	1300.0
	1997	DD970324.A25	/MMS/	03/24/1997	07/17/1997	73.338	17.196	10.649	29.0032	87.3532	32.0	1300.0
	1997	DD970718.A24	/MMS/	07/18/1997	08/31/1997	46.169	16.153	8.059	29.0032	87.3532	32.0	1300.0
	1997	DD970324.A26	/MMS/	03/24/1997	07/17/1997	71.367	16.991	10.307	29.0032	87.3532	36.0	1300.0
	1997	DD970718.A25	/MMS/	07/18/1997	08/31/1997	47.461	15.306	8.078	29.0032	87.3532	36.0	1300.0
	1997	DD970324.A27	/MMS/	03/24/1997	07/17/1997	70.710	16.772	9.976	29.0032	87.3532	40.0	1300.0
	1997	DD970718.A26	/MMS/	07/18/1997	08/31/1997	47.981	15.308	8.048	29.0032	87.3532	40.0	1300.0
	1997	DD970324.A28	/MMS/	03/24/1997	07/17/1997	69.705	16.607	9.592	29.0032	87.3532	44.0	1300.0
	1997	DD970718.A27	/MMS/	07/18/1997	08/31/1997	47.528	15.656	7.660	29.0032	87.3532	44.0	1300.0
	1997	DD970324.A29	/MMS/	03/24/1997	07/17/1997	66.034	16.315	9.394	29.0032	87.3532	48.0	1300.0
	1997	DD970718.A28	/MMS/	07/18/1997	08/31/1997	45.675	15.793	7.629	29.0032	87.3532	48.0	1300.0
	1997	DD970324.A30	/MMS/	03/24/1997	07/17/1997	63.123	15.762	9.242	29.0032	87.3532	52.0	1300.0
	1997	DD970718.A29	/MMS/	07/18/1997	08/31/1997	44.704	15.385	7.775	29.0032	87.3532	52.0	1300.0
	1997	DD970324.A31	/MMS/	03/24/1997	07/17/1997	41.416	10.663	6.435	29.0032	87.3532	56.0	1300.0
	1997	DD970718.A30	/MMS/	07/18/1997	08/31/1997	40.501	12.243	6.999	29.0032	87.3532	56.0	1300.0
	1997	DD970324.A32	/MMS/	03/24/1997	07/17/1997	42.785	11.438	6.803	29.0032	87.3532	60.0	1300.0
	1997	DD970718.A31	/MMS/	07/18/1997	08/31/1997	36.152	11.967	7.460	29.0032	87.3532	60.0	1300.0
	1997	DD970324.A33	/MMS/	03/24/1997	07/17/1997	53.667	15.033	8.942	29.0032	87.3532	64.0	1300.0
	1997	DD970718.A32	/MMS/	07/18/1997	08/31/1997	37.938	13.318	8.175	29.0032	87.3532	64.0	1300.0
	1997	DD970324.A34	/MMS/	03/24/1997	07/17/1997	50.954	14.746	8.855	29.0032	87.3532	68.0	1300.0
	1997	DD970718.A33	/MMS/	07/18/1997	08/31/1997	35.920	12.928	7.665	29.0032	87.3532	68.0	1300.0
	1997	DD970324.A35	/MMS/	03/24/1997	07/17/1997	50.371	14.448	8.643	29.0032	87.3532	72.0	1300.0
5	1997	VK970710.A01	/MMS/	11/01/1997	11/12/1997	63.408	21.030	12.346	29.0592	88.3900	12.0	500.0
	1997	VK971113.A01	/MMS/	11/13/1997	12/31/1997	85.941	29.810	13.299	29.0592	88.3900	12.0	500.0
	1997	VK970710.A02	/MMS/	11/01/1997	11/12/1997	56.446	20.588	11.798	29.0592	88.3900	16.0	500.0
	1997	VK971113.A02	/MMS/	11/13/1997	12/31/1997	83.441	29.937	12.964	29.0592	88.3900	16.0	500.0
	1997	VK970710.A03	/MMS/	11/01/1997	11/12/1997	49.392	20.629	11.637	29.0592	88.3900	20.0	500.0
	1997	VK971113.A03	/MMS/	11/13/1997	12/31/1997	79.833	29.849	12.280	29.0592	88.3900	20.0	500.0
	1997	VK970710.A04	/MMS/	11/01/1997	11/12/1997	46.428	20.430	11.025	29.0592	88.3900	24.0	500.0
	1997	VK971113.A04	/MMS/	11/13/1997	12/31/1997	76.244	29.824	11.796	29.0592	88.3900	24.0	500.0
	1997	VK970710.A05	/MMS/	11/01/1997	11/12/1997	45.901	20.926	10.607	29.0592	88.3900	28.0	500.0

Table B-4. Speed statistics for energetic current events associated with anticyclonic slope eddies. (continued)

Event No.	Year	Filename	Directory	Event start date (m/d/y)	Event end date (m/d/y)	Maximum speed ($cm \cdot s^{-1}$)	Mean speed ($cm \cdot s^{-1}$)	Stand. dev. of speed ($cm \cdot s^{-1}$)	Latitude (°N)	Longitude (°W)	Depth (m)	Total water depth (m)
5	1997	VK971113.A05	/MMS/	11/13/1997	12/31/1997	71.906	29.893	11.507	29.0592	88.3900	28.0	500.0
	1997	VK970710.A06	/MMS/	11/01/1997	11/12/1997	44.346	21.341	10.645	29.0592	88.3900	32.0	500.0
	1997	VK971113.A06	/MMS/	11/13/1997	12/31/1997	68.370	30.044	11.275	29.0592	88.3900	32.0	500.0
	1997	VK970710.A07	/MMS/	11/01/1997	11/12/1997	42.682	21.665	10.630	29.0592	88.3900	36.0	500.0
	1997	VK971113.A07	/MMS/	11/13/1997	12/31/1997	65.935	30.143	11.072	29.0592	88.3900	36.0	500.0
	1997	VK970710.A08	/MMS/	11/01/1997	11/12/1997	45.131	21.693	11.042	29.0592	88.3900	40.0	500.0
	1997	VK971113.A08	/MMS/	11/13/1997	12/31/1997	62.274	30.304	11.001	29.0592	88.3900	40.0	500.0
	1997	VK970710.A09	/MMS/	11/01/1997	11/12/1997	48.069	21.666	11.180	29.0592	88.3900	44.0	500.0
	1997	VK971113.A09	/MMS/	11/13/1997	12/31/1997	60.178	30.484	10.875	29.0592	88.3900	44.0	500.0
	1997	VK970710.A10	/MMS/	11/01/1997	11/12/1997	50.736	21.066	10.608	29.0592	88.3900	48.0	500.0
	1997	VK971113.A10	/MMS/	11/13/1997	12/31/1997	60.564	30.394	10.801	29.0592	88.3900	48.0	500.0
	1997	VK970710.A11	/MMS/	11/01/1997	11/12/1997	46.618	19.960	9.935	29.0592	88.3900	52.0	500.0
	1997	VK971113.A11	/MMS/	11/13/1997	12/31/1997	60.395	30.014	10.769	29.0592	88.3900	52.0	500.0
	1997	VK970710.A12	/MMS/	11/01/1997	11/12/1997	41.332	19.676	8.222	29.0592	88.3900	56.0	500.0
	1997	VK971113.A12	/MMS/	11/13/1997	12/31/1997	61.877	29.502	10.671	29.0592	88.3900	56.0	500.0
	1997	VK970710.A13	/MMS/	11/01/1997	11/12/1997	39.750	19.264	7.778	29.0592	88.3900	60.0	500.0
	1997	VK971113.A13	/MMS/	11/13/1997	12/31/1997	63.824	28.816	10.377	29.0592	88.3900	60.0	500.0
	1997	VK970710.A14	/MMS/	11/01/1997	11/12/1997	34.129	17.376	6.777	29.0592	88.3900	64.0	500.0
	1997	VK971113.A14	/MMS/	11/13/1997	12/31/1997	49.956	22.649	8.713	29.0592	88.3900	64.0	500.0
	1997	VK970710.A15	/MMS/	11/01/1997	11/12/1997	33.247	17.620	6.486	29.0592	88.3900	68.0	500.0
	1997	VK971113.A15	/MMS/	11/13/1997	12/31/1997	51.272	22.925	8.956	29.0592	88.3900	68.0	500.0
	1997	VK970710.A16	/MMS/	11/01/1997	11/12/1997	35.451	18.578	7.137	29.0592	88.3900	72.0	500.0
	1997	VK971113.A16	/MMS/	11/13/1997	12/31/1997	62.017	26.071	10.169	29.0592	88.3900	72.0	500.0
	1997	VK970710.A17	/MMS/	11/01/1997	11/12/1997	36.898	18.101	7.537	29.0592	88.3900	76.0	500.0
	1997	VK971113.A17	/MMS/	11/13/1997	12/31/1997	56.327	25.075	9.886	29.0592	88.3900	76.0	500.0
	1997	VK970710.C01	/MMS/	11/01/1997	11/12/1997	38.585	18.859	6.979	29.0592	88.3900	200.0	500.0
	1997	VK971113.C01	/MMS/	11/13/1997	12/31/1997	54.865	24.540	10.959	29.0592	88.3900	200.0	500.0
	1997	VK970710.C02	/MMS/	11/01/1997	11/12/1997	37.719	21.741	6.443	29.0592	88.3900	300.0	500.0
	1997	VK971113.C02	/MMS/	11/13/1997	12/31/1997	38.886	16.068	8.794	29.0592	88.3900	300.0	500.0
	1997	VK970710.C03	/MMS/	11/01/1997	11/12/1997	23.501	5.896	4.831	29.0592	88.3900	490.0	500.0
	1997	VK971113.C03	/MMS/	11/13/1997	12/31/1997	31.503	6.516	5.181	29.0592	88.3900	490.0	500.0
	1997	MC970710.C01	/MMS/	11/01/1997	11/12/1997	19.801	9.840	3.314	28.7662	88.2650	500.0	1300.0
	1997	MC971114.C01	/MMS/	11/14/1997	12/31/1997	22.608	6.673	5.699	28.7662	88.2650	500.0	1300.0
	1997	MC970710.C02	/MMS/	11/01/1997	11/12/1997	13.887	3.281	2.737	28.7662	88.2650	1310.0	1320.0

Table B-4. Speed statistics for energetic current events associated with anticyclonic slope eddies. (continued)

Event No.	Year	Filename	Directory	Event start date (m/d/y)	Event end date (m/d/y)	Maximum speed (cm·s^{-1})	Mean speed (cm·s^{-1})	Stand. dev. of speed (cm·s^{-1})	Latitude (°N)	Longitude (°W)	Depth (m)	Total water depth (m)
5	1997	MC971114.C02	/MMS/	11/14/1997	12/31/1997	12.396	5.162	2.287	28.7662	88.2650	1310.0	1320.0
	1997	VK970712.C01	/MMS/	11/01/1997	11/14/1997	36.558	16.396	6.573	29.2120	87.8722	200.0	500.0
	1997	VK971115.C01	/MMS/	11/15/1997	12/31/1997	52.830	16.113	9.320	29.2120	87.8722	200.0	500.0
	1997	VK970712.C02	/MMS/	11/01/1997	11/14/1997	35.106	20.926	6.982	29.2120	87.8722	300.0	500.0
	1997	VK971115.C02	/MMS/	11/15/1997	12/31/1997	48.472	14.491	11.036	29.2120	87.8722	300.0	500.0
	1997	VK970712.C03	/MMS/	11/01/1997	11/14/1997	24.602	6.754	4.745	29.2120	87.8722	490.0	500.0
	1997	VK971115.C03	/MMS/	11/15/1997	12/31/1997	40.098	10.959	7.814	29.2120	87.8722	490.0	500.0
	1997	VK970712.C04	/MMS/	11/01/1997	11/11/1997	14.183	5.235	3.432	29.0705	87.8568	500.0	1300.0
	1997	VK971115.C04	/MMS/	11/15/1997	12/31/1997	17.953	7.045	3.287	29.0705	87.8568	500.0	1300.0
	1997	VK970822.C01	/MMS/	11/01/1997	11/14/1997	15.403	7.695	1.735	29.0705	87.8568	1290.0	1300.0
	1997	VK971115.C05	/MMS/	11/15/1997	12/31/1997	12.197	4.276	2.291	29.0705	87.8568	1290.0	1300.0
	1997	DD970717.C01	/MMS/	11/01/1997	11/19/1997	34.527	19.207	7.539	29.3712	87.3563	200.0	500.0
	1997	DD971120.C02	/MMS/	11/20/1997	12/31/1997	48.758	14.840	7.782	29.3712	87.3563	200.0	500.0
	1997	DD970717.C02	/MMS/	11/01/1997	11/19/1997	22.311	8.410	6.515	29.3712	87.3563	300.0	500.0
	1997	DD971120.C03	/MMS/	11/20/1997	12/31/1997	42.078	11.494	7.868	29.3712	87.3563	300.0	500.0
	1997	DD970717.C03	/MMS/	11/01/1997	11/19/1997	23.403	6.692	5.286	29.3712	87.3563	490.0	500.0
	1997	DD971120.C04	/MMS/	11/20/1997	12/31/1997	27.804	7.736	5.057	29.3712	87.3563	490.0	500.0
	1997	DD970718.C01	/MMS/	11/01/1997	11/15/1997	7.495	1.617	1.056	29.0032	87.3532	500.0	1300.0
	1997	DD971116.C01	/MMS/	11/16/1997	12/31/1997	25.512	7.299	5.022	29.0032	87.3532	500.0	1300.0
	1997	DD971116.C02	/MMS/	11/16/1997	12/31/1997	16.207	4.314	3.522	29.0032	87.3532	1290.0	1300.0
	1997	DD970716.C01	/MMS/	11/01/1997	11/17/1997	20.574	4.290	4.590	29.3348	86.8520	200.0	500.0
	1997	DD971118.C01	/MMS/	11/18/1997	12/31/1997	30.747	15.061	6.414	29.3348	86.8520	200.0	500.0
	1997	DD971118.C02	/MMS/	11/18/1997	12/31/1997	26.963	10.336	5.624	29.3348	86.8520	300.0	500.0
	1997	DD970716.C02	/MMS/	11/01/1997	11/17/1997	18.002	5.301	3.350	29.3348	86.8520	490.0	500.0
	1997	DD971118.C03	/MMS/	11/18/1997	12/31/1997	20.897	6.902	4.378	29.3348	86.8520	490.0	500.0
	1997	MC970710.A01	/MMS/	11/01/1997	11/12/1997	64.178	26.708	12.986	28.7662	88.2650	8.0	1300.0
	1997	MC971113.A01	/MMS/	11/13/1997	12/31/1997	77.089	19.708	10.239	28.7662	88.2650	8.0	1300.0
	1997	MC970710.A02	/MMS/	11/01/1997	11/12/1997	55.034	25.651	10.893	28.7662	88.2650	12.0	1300.0
	1997	MC971113.A02	/MMS/	11/13/1997	12/31/1997	62.221	20.145	9.771	28.7662	88.2650	12.0	1300.0
	1997	MC970710.A03	/MMS/	11/01/1997	11/12/1997	49.994	24.889	9.725	28.7662	88.2650	16.0	1300.0
	1997	MC971113.A03	/MMS/	11/13/1997	12/31/1997	55.238	19.848	9.372	28.7662	88.2650	16.0	1300.0
	1997	MC970710.A04	/MMS/	11/01/1997	11/12/1997	52.241	24.317	9.747	28.7662	88.2650	20.0	1300.0
	1997	MC971113.A04	/MMS/	11/13/1997	12/31/1997	52.398	19.597	9.082	28.7662	88.2650	20.0	1300.0
	1997	MC970710.A05	/MMS/	11/01/1997	11/12/1997	57.575	24.354	10.139	28.7662	88.2650	24.0	1300.0

Table B-4. Speed statistics for energetic current events associated with anticyclonic slope eddies. (continued)

Event No.	Year	Filename	Directory	Event start date (m/d/y)	Event end date (m/d/y)	Maximum speed ($cm \cdot s^{-1}$)	Mean speed ($cm \cdot s^{-1}$)	Stand. dev. of speed ($cm \cdot s^{-1}$)	Latitude (°N)	Longitude (°W)	Depth (m)	Total water depth (m)
5	1997	MC971113.A05	/MMS/	11/13/1997	12/31/1997	50.516	19.367	8.772	28.7662	88.2650	24.0	1300.0
	1997	MC970710.A06	/MMS/	11/01/1997	11/12/1997	60.091	24.767	9.848	28.7662	88.2650	28.0	1300.0
	1997	MC971113.A06	/MMS/	11/13/1997	12/31/1997	48.893	19.205	8.438	28.7662	88.2650	28.0	1300.0
	1997	MC970710.A07	/MMS/	11/01/1997	11/12/1997	60.890	25.053	10.079	28.7662	88.2650	32.0	1300.0
	1997	MC971113.A07	/MMS/	11/13/1997	12/31/1997	47.031	19.059	8.192	28.7662	88.2650	32.0	1300.0
	1997	MC970710.A08	/MMS/	11/01/1997	11/12/1997	59.712	24.809	9.852	28.7662	88.2650	36.0	1300.0
	1997	MC971113.A08	/MMS/	11/13/1997	12/31/1997	46.375	19.024	7.994	28.7662	88.2650	36.0	1300.0
	1997	MC970710.A09	/MMS/	11/01/1997	11/12/1997	55.466	24.281	9.825	28.7662	88.2650	40.0	1300.0
	1997	MC971113.A09	/MMS/	11/13/1997	12/31/1997	47.453	19.024	7.839	28.7662	88.2650	40.0	1300.0
	1997	MC970710.A10	/MMS/	11/01/1997	11/12/1997	54.968	23.778	9.442	28.7662	88.2650	44.0	1300.0
	1997	MC971113.A10	/MMS/	11/13/1997	12/31/1997	45.258	19.010	7.725	28.7662	88.2650	44.0	1300.0
	1997	MC970710.A11	/MMS/	11/01/1997	11/12/1997	51.442	22.771	8.458	28.7662	88.2650	48.0	1300.0
	1997	MC971113.A11	/MMS/	11/13/1997	12/31/1997	42.564	19.006	7.632	28.7662	88.2650	48.0	1300.0
	1997	MC970710.A12	/MMS/	11/01/1997	11/12/1997	49.418	21.200	8.598	28.7662	88.2650	52.0	1300.0
	1997	MC971113.A12	/MMS/	11/13/1997	12/31/1997	41.831	18.888	7.574	28.7662	88.2650	52.0	1300.0
	1997	MC970710.A13	/MMS/	11/01/1997	11/12/1997	32.793	16.123	6.692	28.7662	88.2650	56.0	1300.0
	1997	MC971113.A13	/MMS/	11/13/1997	12/31/1997	32.054	13.079	5.577	28.7662	88.2650	56.0	1300.0
	1997	MC970710.A14	/MMS/	11/01/1997	11/12/1997	32.795	16.506	6.570	28.7662	88.2650	60.0	1300.0
	1997	MC971113.A14	/MMS/	11/13/1997	12/31/1997	32.704	13.973	5.926	28.7662	88.2650	60.0	1300.0
	1997	MC970710.A15	/MMS/	11/01/1997	11/12/1997	39.713	19.290	7.355	28.7662	88.2650	64.0	1300.0
	1997	MC971113.A15	/MMS/	11/13/1997	12/31/1997	45.057	18.667	7.372	28.7662	88.2650	64.0	1300.0
	1997	MC970710.A16	/MMS/	11/01/1997	11/12/1997	42.580	18.405	7.405	28.7662	88.2650	68.0	1300.0
	1997	MC971113.A16	/MMS/	11/13/1997	12/31/1997	46.481	18.355	7.277	28.7662	88.2650	68.0	1300.0
	1997	MC970710.A17	/MMS/	11/01/1997	11/12/1997	43.834	17.794	7.475	28.7662	88.2650	72.0	1300.0
	1997	MC971113.A17	/MMS/	11/13/1997	12/31/1997	45.335	17.857	7.137	28.7662	88.2650	72.0	1300.0
	1997	VK971115.A01	/MMS/	11/15/1997	12/31/1997	72.770	24.331	11.922	29.2120	87.8722	12.0	500.0
	1997	VK970712.A01	/MMS/	11/01/1997	11/14/1997	54.965	24.406	10.645	29.2120	87.8722	16.0	500.0
	1997	VK971115.A02	/MMS/	11/15/1997	12/31/1997	66.796	29.157	11.905	29.2120	87.8722	16.0	500.0
	1997	VK970712.A02	/MMS/	11/01/1997	11/14/1997	49.510	23.982	10.385	29.2120	87.8722	20.0	500.0
	1997	VK971115.A03	/MMS/	11/15/1997	12/31/1997	63.960	29.141	11.309	29.2120	87.8722	20.0	500.0
	1997	VK970712.A03	/MMS/	11/01/1997	11/14/1997	51.514	23.704	10.703	29.2120	87.8722	24.0	500.0
	1997	VK971115.A04	/MMS/	11/15/1997	12/31/1997	64.439	29.444	10.773	29.2120	87.8722	24.0	500.0
	1997	VK970712.A04	/MMS/	11/01/1997	11/14/1997	56.290	23.137	11.147	29.2120	87.8722	28.0	500.0
	1997	VK971115.A05	/MMS/	11/15/1997	12/31/1997	64.396	29.772	10.501	29.2120	87.8722	28.0	500.0

Table B-4. Speed statistics for energetic current events associated with anticyclonic slope eddies. (continued)

Event No.	Year	Filename	Directory	Event start date (m/d/y)	Event end date (m/d/y)	Maximum speed (cm·s^{-1})	Mean speed (cm·s^{-1})	Stand. dev. of speed (cm·s^{-1})	Latitude (°N)	Longitude (°W)	Depth (m)	Total water depth (m)
5	1997	VK970712.A05	/MMS/	11/01/1997	11/14/1997	54.112	22.202	10.727	29.2120	87.8722	32.0	500.0
	1997	VK971115.A06	/MMS/	11/15/1997	12/31/1997	64.270	29.834	10.327	29.2120	87.8722	32.0	500.0
	1997	VK970712.A06	/MMS/	11/01/1997	11/14/1997	50.935	21.040	9.846	29.2120	87.8722	36.0	500.0
	1997	VK971115.A07	/MMS/	11/15/1997	12/31/1997	64.367	29.827	10.134	29.2120	87.8722	36.0	500.0
	1997	VK970712.A07	/MMS/	11/01/1997	11/14/1997	39.147	19.789	8.742	29.2120	87.8722	40.0	500.0
	1997	VK971115.A08	/MMS/	11/15/1997	12/31/1997	64.114	29.868	10.040	29.2120	87.8722	40.0	500.0
	1997	VK970712.A08	/MMS/	11/01/1997	11/14/1997	44.570	18.699	8.943	29.2120	87.8722	44.0	500.0
	1997	VK971115.A09	/MMS/	11/15/1997	12/31/1997	64.515	29.853	9.984	29.2120	87.8722	44.0	500.0
	1997	VK970712.A09	/MMS/	11/01/1997	11/14/1997	43.585	18.429	8.923	29.2120	87.8722	48.0	500.0
	1997	VK971115.A10	/MMS/	11/15/1997	12/31/1997	63.549	29.837	9.912	29.2120	87.8722	48.0	500.0
	1997	VK970712.A10	/MMS/	11/01/1997	11/14/1997	38.612	18.948	8.039	29.2120	87.8722	52.0	500.0
	1997	VK971115.A11	/MMS/	11/15/1997	12/31/1997	62.404	29.690	9.812	29.2120	87.8722	52.0	500.0
	1997	VK970712.A11	/MMS/	11/01/1997	11/14/1997	43.321	18.720	7.982	29.2120	87.8722	56.0	500.0
	1997	VK971115.A12	/MMS/	11/15/1997	12/31/1997	63.042	29.566	9.818	29.2120	87.8722	56.0	500.0
	1997	VK970712.A12	/MMS/	11/01/1997	11/14/1997	35.711	17.999	7.581	29.2120	87.8722	60.0	500.0
	1997	VK971115.A13	/MMS/	11/15/1997	12/31/1997	62.094	29.095	9.927	29.2120	87.8722	60.0	500.0
	1997	VK970712.A13	/MMS/	11/01/1997	11/14/1997	33.024	15.556	6.258	29.2120	87.8722	64.0	500.0
	1997	VK971115.A14	/MMS/	11/15/1997	12/31/1997	49.052	20.492	7.746	29.2120	87.8722	64.0	500.0
	1997	VK970712.A14	/MMS/	11/01/1997	11/14/1997	32.937	15.685	6.226	29.2120	87.8722	68.0	500.0
	1997	VK971115.A15	/MMS/	11/15/1997	12/31/1997	53.422	21.083	8.363	29.2120	87.8722	68.0	500.0
	1997	VK970712.A15	/MMS/	11/01/1997	11/14/1997	37.663	17.385	7.113	29.2120	87.8722	72.0	500.0
	1997	VK971115.A16	/MMS/	11/15/1997	12/31/1997	62.905	26.756	10.431	29.2120	87.8722	72.0	500.0
	1997	VK970712.A16	/MMS/	11/01/1997	11/14/1997	38.774	17.464	7.278	29.2120	87.8722	76.0	500.0
	1997	VK971115.A17	/MMS/	11/15/1997	12/31/1997	60.915	26.118	10.385	29.2120	87.8722	76.0	500.0
	1997	VK970712.A17	/MMS/	11/01/1997	11/14/1997	38.940	16.937	7.207	29.2120	87.8722	80.0	500.0
	1997	VK971115.A18	/MMS/	11/15/1997	12/31/1997	60.370	25.444	10.504	29.2120	87.8722	80.0	500.0
	1997	VK971115.A19	/MMS/	11/15/1997	12/31/1997	102.532	24.311	12.915	29.0705	87.8568	12.0	1300.0
	1997	VK970712.A18	/MMS/	11/01/1997	11/14/1997	57.266	20.319	10.139	29.0705	87.8568	16.0	1300.0
	1997	VK971115.A20	/MMS/	11/15/1997	12/31/1997	94.391	28.492	12.490	29.0705	87.8568	16.0	1300.0
	1997	VK970712.A19	/MMS/	11/01/1997	11/14/1997	45.943	18.753	8.792	29.0705	87.8568	20.0	1300.0
	1997	VK971115.A21	/MMS/	11/15/1997	12/31/1997	93.113	28.406	12.098	29.0705	87.8568	20.0	1300.0
	1997	VK970712.A20	/MMS/	11/01/1997	11/14/1997	38.495	17.347	7.726	29.0705	87.8568	24.0	1300.0
	1997	VK971115.A22	/MMS/	11/15/1997	12/31/1997	89.574	28.375	11.837	29.0705	87.8568	24.0	1300.0
	1997	VK970712.A21	/MMS/	11/01/1997	11/14/1997	36.936	16.021	7.005	29.0705	87.8568	28.0	1300.0

Table B-4. Speed statistics for energetic current events associated with anticyclonic slope eddies. (continued)

Event No.	Year	Filename	Directory	Event start date (m/d/y)	Event end date (m/d/y)	Maximum speed ($cm \cdot s^{-1}$)	Mean speed ($cm \cdot s^{-1}$)	Stand. dev. of speed ($cm \cdot s^{-1}$)	Latitude (°N)	Longitude (°W)	Depth (m)	Total water depth (m)
5	1997	VK971115.A23	/MMS/	11/15/1997	12/31/1997	86.829	28.198	11.538	29.0705	87.8568	28.0	1300.0
	1997	VK970712.A22	/MMS/	11/01/1997	11/14/1997	33.784	14.968	6.606	29.0705	87.8568	32.0	1300.0
	1997	VK971115.A24	/MMS/	11/15/1997	12/31/1997	82.651	28.118	11.196	29.0705	87.8568	32.0	1300.0
	1997	VK970712.A23	/MMS/	11/01/1997	11/14/1997	28.383	14.195	6.695	29.0705	87.8568	36.0	1300.0
	1997	VK971115.A25	/MMS/	11/15/1997	12/31/1997	80.002	28.082	10.887	29.0705	87.8568	36.0	1300.0
	1997	VK970712.A24	/MMS/	11/01/1997	11/14/1997	28.098	13.401	6.132	29.0705	87.8568	40.0	1300.0
	1997	VK971115.A26	/MMS/	11/15/1997	12/31/1997	79.857	28.086	10.546	29.0705	87.8568	40.0	1300.0
	1997	VK970712.A25	/MMS/	11/01/1997	11/14/1997	27.505	13.094	5.688	29.0705	87.8568	44.0	1300.0
	1997	VK971115.A27	/MMS/	11/15/1997	12/31/1997	76.976	28.053	10.281	29.0705	87.8568	44.0	1300.0
	1997	VK970712.A26	/MMS/	11/01/1997	11/14/1997	31.590	13.716	6.615	29.0705	87.8568	48.0	1300.0
	1997	VK971115.A28	/MMS/	11/15/1997	12/31/1997	77.824	27.985	10.061	29.0705	87.8568	48.0	1300.0
	1997	VK970712.A27	/MMS/	11/01/1997	11/14/1997	30.495	13.242	6.420	29.0705	87.8568	52.0	1300.0
	1997	VK971115.A29	/MMS/	11/15/1997	12/31/1997	76.685	27.831	9.758	29.0705	87.8568	52.0	1300.0
	1997	VK970712.A28	/MMS/	11/01/1997	11/14/1997	23.195	8.916	4.190	29.0705	87.8568	56.0	1300.0
	1997	VK971115.A30	/MMS/	11/15/1997	12/31/1997	71.185	20.400	8.211	29.0705	87.8568	56.0	1300.0
	1997	VK970712.A29	/MMS/	11/01/1997	11/14/1997	22.285	8.508	4.060	29.0705	87.8568	60.0	1300.0
	1997	VK971115.A31	/MMS/	11/15/1997	12/31/1997	67.652	21.184	8.422	29.0705	87.8568	60.0	1300.0
	1997	VK970712.A30	/MMS/	11/01/1997	11/14/1997	27.772	10.684	5.540	29.0705	87.8568	64.0	1300.0
	1997	VK971115.A32	/MMS/	11/15/1997	12/31/1997	67.268	27.880	9.374	29.0705	87.8568	64.0	1300.0
	1997	VK970712.A31	/MMS/	11/01/1997	11/14/1997	24.741	10.240	5.406	29.0705	87.8568	68.0	1300.0
	1997	VK971115.A33	/MMS/	11/15/1997	12/31/1997	63.781	27.083	9.031	29.0705	87.8568	68.0	1300.0
	1997	VK970712.A32	/MMS/	11/01/1997	11/14/1997	25.103	9.920	5.516	29.0705	87.8568	72.0	1300.0
	1997	VK971115.A34	/MMS/	11/15/1997	12/31/1997	61.917	26.265	8.814	29.0705	87.8568	72.0	1300.0
	1997	DD970717.A01	/MMS/	11/01/1997	11/19/1997	51.240	19.425	9.336	29.3712	87.3563	12.0	500.0
	1997	DD971120.A18	/MMS/	11/20/1997	12/31/1997	83.365	28.528	11.517	29.3712	87.3563	12.0	500.0
	1997	DD970717.A02	/MMS/	11/01/1997	11/19/1997	47.569	19.111	8.986	29.3712	87.3563	16.0	500.0
	1997	DD971120.A19	/MMS/	11/20/1997	12/31/1997	74.524	29.440	11.087	29.3712	87.3563	16.0	500.0
	1997	DD970717.A03	/MMS/	11/01/1997	11/19/1997	48.371	18.804	8.724	29.3712	87.3563	20.0	500.0
	1997	DD971120.A20	/MMS/	11/20/1997	12/31/1997	71.876	29.367	10.934	29.3712	87.3563	20.0	500.0
	1997	DD970717.A04	/MMS/	11/01/1997	11/19/1997	50.766	18.607	8.516	29.3712	87.3563	24.0	500.0
	1997	DD971120.A21	/MMS/	11/20/1997	12/31/1997	71.183	29.381	10.805	29.3712	87.3563	24.0	500.0
	1997	DD970717.A05	/MMS/	11/01/1997	11/19/1997	50.594	18.401	8.468	29.3712	87.3563	28.0	500.0
	1997	DD971120.A22	/MMS/	11/20/1997	12/31/1997	69.097	29.389	10.691	29.3712	87.3563	28.0	500.0
	1997	DD970717.A06	/MMS/	11/01/1997	11/19/1997	50.453	18.321	8.506	29.3712	87.3563	32.0	500.0

Table B-4. Speed statistics for energetic current events associated with anticyclonic slope eddies. (continued)

Event No.	Year	Filename	Directory	Event start date (m/d/y)	Event end date (m/d/y)	Maximum speed ($cm \cdot s^{-1}$)	Mean speed ($cm \cdot s^{-1}$)	Stand. dev. of speed ($cm \cdot s^{-1}$)	Latitude (°N)	Longitude (°W)	Depth (m)	Total water depth (m)
5	1997	DD971120.A23	/MMS/	11/20/1997	12/31/1997	67.543	29.408	10.591	29.3712	87.3563	32.0	500.0
	1997	DD970717.A07	/MMS/	11/01/1997	11/19/1997	51.185	18.135	8.463	29.3712	87.3563	36.0	500.0
	1997	DD971120.A24	/MMS/	11/20/1997	12/31/1997	67.248	29.391	10.419	29.3712	87.3563	36.0	500.0
	1997	DD970717.A08	/MMS/	11/01/1997	11/19/1997	46.384	17.957	8.044	29.3712	87.3563	40.0	500.0
	1997	DD971120.A25	/MMS/	11/20/1997	12/31/1997	66.731	29.465	10.354	29.3712	87.3563	40.0	500.0
	1997	DD970717.A09	/MMS/	11/01/1997	11/19/1997	40.548	17.517	7.976	29.3712	87.3563	44.0	500.0
	1997	DD971120.A26	/MMS/	11/20/1997	12/31/1997	66.369	29.502	10.529	29.3712	87.3563	44.0	500.0
	1997	DD970717.A10	/MMS/	11/01/1997	11/19/1997	43.971	17.680	8.278	29.3712	87.3563	48.0	500.0
	1997	DD971120.A27	/MMS/	11/20/1997	12/31/1997	65.901	29.391	10.672	29.3712	87.3563	48.0	500.0
	1997	DD970717.A11	/MMS/	11/01/1997	11/19/1997	46.605	17.177	8.853	29.3712	87.3563	52.0	500.0
	1997	DD971120.A28	/MMS/	11/20/1997	12/31/1997	65.681	29.107	10.674	29.3712	87.3563	52.0	500.0
	1997	DD970717.A12	/MMS/	11/01/1997	11/19/1997	45.971	17.035	8.170	29.3712	87.3563	56.0	500.0
	1997	DD971120.A29	/MMS/	11/20/1997	12/31/1997	67.825	28.847	10.612	29.3712	87.3563	56.0	500.0
	1997	DD970717.A13	/MMS/	11/01/1997	11/19/1997	43.108	17.263	7.859	29.3712	87.3563	60.0	500.0
	1997	DD971120.A30	/MMS/	11/20/1997	12/31/1997	69.838	28.343	10.559	29.3712	87.3563	60.0	500.0
	1997	DD970717.A14	/MMS/	11/01/1997	11/19/1997	37.677	17.155	8.234	29.3712	87.3563	64.0	500.0
	1997	DD971120.A31	/MMS/	11/20/1997	12/31/1997	67.205	27.443	10.380	29.3712	87.3563	64.0	500.0
	1997	DD970717.A15	/MMS/	11/01/1997	11/19/1997	38.105	17.205	8.746	29.3712	87.3563	68.0	500.0
	1997	DD971120.A32	/MMS/	11/20/1997	12/31/1997	67.211	26.807	10.460	29.3712	87.3563	68.0	500.0
	1997	DD970717.A16	/MMS/	11/01/1997	11/19/1997	38.420	17.283	9.154	29.3712	87.3563	72.0	500.0
	1997	DD971120.A33	/MMS/	11/20/1997	12/31/1997	66.011	26.187	10.532	29.3712	87.3563	72.0	500.0
	1997	DD970717.A17	/MMS/	11/01/1997	11/19/1997	38.980	17.246	9.503	29.3712	87.3563	76.0	500.0
	1997	DD971120.A34	/MMS/	11/20/1997	12/31/1997	65.655	25.345	10.505	29.3712	87.3563	76.0	500.0
	1997	DD970717.A18	/MMS/	11/01/1997	11/19/1997	40.377	17.048	9.727	29.3712	87.3563	80.0	500.0
	1997	DD970718.A18	/MMS/	11/01/1997	11/15/1997	52.682	16.859	8.898	29.0032	87.3532	8.0	1300.0
	1997	DD970718.A19	/MMS/	11/01/1997	11/15/1997	51.771	17.414	9.454	29.0032	87.3532	12.0	1300.0
	1997	DD971116.A01	/MMS/	11/16/1997	12/31/1997	81.692	18.489	9.050	29.0032	87.3532	12.0	1300.0
	1997	DD970718.A20	/MMS/	11/01/1997	11/15/1997	45.101	16.553	8.784	29.0032	87.3532	16.0	1300.0
	1997	DD971116.A02	/MMS/	11/16/1997	12/31/1997	64.459	18.007	8.557	29.0032	87.3532	16.0	1300.0
	1997	DD970718.A21	/MMS/	11/01/1997	11/15/1997	37.758	15.886	8.121	29.0032	87.3532	20.0	1300.0
	1997	DD971116.A03	/MMS/	11/16/1997	12/31/1997	57.455	17.606	8.198	29.0032	87.3532	20.0	1300.0
	1997	DD970718.A22	/MMS/	11/01/1997	11/15/1997	36.178	15.193	7.682	29.0032	87.3532	24.0	1300.0
	1997	DD971116.A04	/MMS/	11/16/1997	12/31/1997	51.438	17.337	7.982	29.0032	87.3532	24.0	1300.0
	1997	DD970718.A23	/MMS/	11/01/1997	11/15/1997	36.842	14.690	7.512	29.0032	87.3532	28.0	1300.0

Table B-4. Speed statistics for energetic current events associated with anticyclonic slope eddies. (continued)

Event No.	**Year**	**Filename**	**Directory**	**Event start date (m/d/y)**	**Event end date (m/d/y)**	**Maximum speed ($cm \cdot s^{-1}$)**	**Mean speed ($cm \cdot s^{-1}$)**	**Stand. dev. of speed ($cm \cdot s^{-1}$)**	**Latitude (°N)**	**Longitude (°W)**	**Depth (m)**	**Total water depth (m)**
5	1997	DD971116.A05	/MMS/	11/16/1997	12/31/1997	47.595	17.182	7.773	29.0032	87.3532	28.0	1300.0
	1997	DD970718.A24	/MMS/	11/01/1997	11/15/1997	35.970	14.237	7.637	29.0032	87.3532	32.0	1300.0
	1997	DD971116.A06	/MMS/	11/16/1997	12/31/1997	45.137	17.084	7.588	29.0032	87.3532	32.0	1300.0
	1997	DD970718.A25	/MMS/	11/01/1997	11/15/1997	34.714	13.243	7.247	29.0032	87.3532	36.0	1300.0
	1997	DD971116.A07	/MMS/	11/16/1997	12/31/1997	44.055	17.003	7.450	29.0032	87.3532	36.0	1300.0
	1997	DD970718.A26	/MMS/	11/01/1997	11/15/1997	30.377	11.540	5.961	29.0032	87.3532	40.0	1300.0
	1997	DD971116.A08	/MMS/	11/16/1997	12/31/1997	44.912	16.957	7.286	29.0032	87.3532	40.0	1300.0
	1997	DD970718.A27	/MMS/	11/01/1997	11/15/1997	22.756	9.862	4.038	29.0032	87.3532	44.0	1300.0
	1997	DD971116.A09	/MMS/	11/16/1997	12/31/1997	43.716	16.982	7.142	29.0032	87.3532	44.0	1300.0
	1997	DD970718.A28	/MMS/	11/01/1997	11/15/1997	23.489	8.536	3.475	29.0032	87.3532	48.0	1300.0
	1997	DD971116.A10	/MMS/	11/16/1997	12/31/1997	42.003	16.900	6.993	29.0032	87.3532	48.0	1300.0
	1997	DD970718.A29	/MMS/	11/01/1997	11/15/1997	21.775	8.126	4.063	29.0032	87.3532	52.0	1300.0
	1997	DD971116.A11	/MMS/	11/16/1997	12/31/1997	42.555	16.825	6.889	29.0032	87.3532	52.0	1300.0
	1997	DD970718.A30	/MMS/	11/01/1997	11/15/1997	20.541	9.050	4.119	29.0032	87.3532	56.0	1300.0
	1997	DD971116.A12	/MMS/	11/16/1997	12/31/1997	32.672	14.112	5.453	29.0032	87.3532	56.0	1300.0
	1997	DD970718.A31	/MMS/	11/01/1997	11/15/1997	22.945	10.219	4.236	29.0032	87.3532	60.0	1300.0
	1997	DD971116.A13	/MMS/	11/16/1997	12/31/1997	37.885	14.710	5.814	29.0032	87.3532	60.0	1300.0
	1997	DD970718.A32	/MMS/	11/01/1997	11/15/1997	22.812	10.574	4.346	29.0032	87.3532	64.0	1300.0
	1997	DD971116.A14	/MMS/	11/16/1997	12/31/1997	41.970	16.290	7.283	29.0032	87.3532	64.0	1300.0
	1997	DD970718.A33	/MMS/	11/01/1997	11/15/1997	24.573	9.266	4.201	29.0032	87.3532	68.0	1300.0
	1997	DD971116.A15	/MMS/	11/16/1997	12/31/1997	41.800	16.064	7.217	29.0032	87.3532	68.0	1300.0
	1997	DD970716.A01	/MMS/	11/01/1997	11/17/1997	53.326	20.969	8.688	29.3348	86.8520	8.0	500.0
	1997	DD970716.A02	/MMS/	11/01/1997	11/17/1997	46.831	17.945	7.418	29.3348	86.8520	12.0	500.0
	1997	DD971118.A01	/MMS/	11/18/1997	12/31/1997	73.913	21.710	10.713	29.3348	86.8520	12.0	500.0
	1997	DD970716.A03	/MMS/	11/01/1997	11/17/1997	40.429	17.613	7.157	29.3348	86.8520	16.0	500.0
	1997	DD971118.A02	/MMS/	11/18/1997	12/31/1997	69.065	21.286	10.348	29.3348	86.8520	16.0	500.0
	1997	DD970716.A04	/MMS/	11/01/1997	11/17/1997	37.401	17.296	6.974	29.3348	86.8520	20.0	500.0
	1997	DD971118.A03	/MMS/	11/18/1997	12/31/1997	64.828	20.963	10.046	29.3348	86.8520	20.0	500.0
	1997	DD970716.A05	/MMS/	11/01/1997	11/17/1997	36.020	17.052	6.836	29.3348	86.8520	24.0	500.0
	1997	DD971118.A04	/MMS/	11/18/1997	12/31/1997	64.316	20.660	9.902	29.3348	86.8520	24.0	500.0
	1997	DD970716.A06	/MMS/	11/01/1997	11/17/1997	35.560	16.899	6.681	29.3348	86.8520	28.0	500.0
	1997	DD971118.A05	/MMS/	11/18/1997	12/31/1997	61.531	20.441	9.821	29.3348	86.8520	28.0	500.0
	1997	DD970716.A07	/MMS/	11/01/1997	11/17/1997	34.607	16.619	6.531	29.3348	86.8520	32.0	500.0
	1997	DD971118.A06	/MMS/	11/18/1997	12/31/1997	61.425	20.270	9.739	29.3348	86.8520	32.0	500.0

Table B-4. Speed statistics for energetic current events associated with anticyclonic slope eddies. (continued)

Event No.	Year	Filename	Directory	Event start date (m/d/y)	Event end date (m/d/y)	Maximum speed ($cm \cdot s^{-1}$)	Mean speed ($cm \cdot s^{-1}$)	Stand. dev. of speed ($cm \cdot s^{-1}$)	Latitude (°N)	Longitude (°W)	Depth (m)	Total water depth (m)
5	1997	DD970716.A08	/MMS/	11/01/1997	11/17/1997	34.142	16.384	6.240	29.3348	86.8520	36.0	500.0
	1997	DD971118.A07	/MMS/	11/18/1997	12/31/1997	60.023	20.197	9.707	29.3348	86.8520	36.0	500.0
	1997	DD970716.A09	/MMS/	11/01/1997	11/17/1997	35.466	15.209	5.911	29.3348	86.8520	40.0	500.0
	1997	DD971118.A08	/MMS/	11/18/1997	12/31/1997	56.443	20.146	9.701	29.3348	86.8520	40.0	500.0
	1997	DD970716.A10	/MMS/	11/01/1997	11/17/1997	29.433	12.545	5.635	29.3348	86.8520	44.0	500.0
	1997	DD971118.A09	/MMS/	11/18/1997	12/31/1997	53.534	20.032	9.702	29.3348	86.8520	44.0	500.0
	1997	DD970716.A11	/MMS/	11/01/1997	11/17/1997	30.150	11.424	6.454	29.3348	86.8520	48.0	500.0
	1997	DD971118.A10	/MMS/	11/18/1997	12/31/1997	49.878	19.965	9.767	29.3348	86.8520	48.0	500.0
	1997	DD970716.A12	/MMS/	11/01/1997	11/17/1997	32.519	12.737	7.609	29.3348	86.8520	52.0	500.0
	1997	DD971118.A11	/MMS/	11/18/1997	12/31/1997	50.372	19.856	9.758	29.3348	86.8520	52.0	500.0
	1997	DD970716.A13	/MMS/	11/01/1997	11/17/1997	30.904	12.984	7.727	29.3348	86.8520	56.0	500.0
	1997	DD971118.A12	/MMS/	11/18/1997	12/31/1997	49.894	19.891	9.764	29.3348	86.8520	56.0	500.0
	1997	DD970716.A14	/MMS/	11/01/1997	11/17/1997	29.806	11.970	6.709	29.3348	86.8520	60.0	500.0
	1997	DD971118.A13	/MMS/	11/18/1997	12/31/1997	49.059	19.960	9.379	29.3348	86.8520	60.0	500.0
	1997	DD970716.A15	/MMS/	11/01/1997	11/17/1997	27.573	10.051	5.856	29.3348	86.8520	64.0	500.0
	1997	DD971118.A14	/MMS/	11/18/1997	12/31/1997	42.980	18.006	8.342	29.3348	86.8520	64.0	500.0
	1997	DD970716.A16	/MMS/	11/01/1997	11/17/1997	27.115	9.747	5.913	29.3348	86.8520	68.0	500.0
	1997	DD971118.A15	/MMS/	11/18/1997	12/31/1997	43.921	18.032	8.073	29.3348	86.8520	68.0	500.0
	1997	DD970716.A17	/MMS/	11/01/1997	11/17/1997	28.984	9.833	6.457	29.3348	86.8520	72.0	500.0
	1997	DD971118.A16	/MMS/	11/18/1997	12/31/1997	43.804	19.010	8.247	29.3348	86.8520	72.0	500.0
	1997	DD970716.A18	/MMS/	11/01/1997	11/17/1997	31.408	9.405	6.591	29.3348	86.8520	76.0	500.0
	1997	DD971118.A17	/MMS/	11/18/1997	12/31/1997	43.400	18.717	8.058	29.3348	86.8520	76.0	500.0
	1997	DD970716.A19	/MMS/	11/01/1997	11/17/1997	31.691	9.331	6.217	29.3348	86.8520	80.0	500.0
	1997	DD971118.A18	/MMS/	11/18/1997	12/31/1997	39.008	17.866	7.569	29.3348	86.8520	80.0	500.0
	1997	EW971022.A01	/INDUSTRY/	11/01/1997	12/15/1997	47.930	14.643	9.672	27.9567	90.0508	31.0	1172.0
	1997	EW971022.A02	/INDUSTRY/	11/01/1997	12/15/1997	45.478	14.809	9.312	27.9567	90.0508	39.0	1172.0
	1997	EW971022.A03	/INDUSTRY/	11/01/1997	12/15/1997	43.489	14.627	8.906	27.9567	90.0508	47.0	1172.0
	1997	EW971022.A04	/INDUSTRY/	11/01/1997	12/15/1997	41.355	14.028	8.492	27.9567	90.0508	55.0	1172.0
	1997	EW971022.A05	/INDUSTRY/	11/01/1997	12/15/1997	43.572	13.169	8.114	27.9567	90.0508	63.0	1172.0
	1997	EW971022.A06	/INDUSTRY/	11/01/1997	12/15/1997	42.953	12.137	7.749	27.9567	90.0508	71.0	1172.0
	1997	EW971022.A07	/INDUSTRY/	11/01/1997	12/15/1997	42.059	11.606	7.231	27.9567	90.0508	79.0	1172.0
	1997	EW971022.A08	/INDUSTRY/	11/01/1997	12/15/1997	39.803	11.084	6.642	27.9567	90.0508	87.0	1172.0
	1997	EW971022.A09	/INDUSTRY/	11/01/1997	12/15/1997	38.344	10.834	6.530	27.9567	90.0508	95.0	1172.0
	1997	EW971022.A10	/INDUSTRY/	11/01/1997	12/15/1997	38.243	10.064	6.386	27.9567	90.0508	103.0	1172.0

Table B-4. Speed statistics for energetic current events associated with anticyclonic slope eddies. (continued)

Event No.	Year	Filename	Directory	Event start date (m/d/y)	Event end date (m/d/y)	Maximum speed ($cm \cdot s^{-1}$)	Mean speed ($cm \cdot s^{-1}$)	Stand. dev. of speed ($cm \cdot s^{-1}$)	Latitude (°N)	Longitude (°W)	Depth (m)	Total water depth (m)
5	1997	EW971022.A11	/INDUSTRY/	11/01/1997	12/15/1997	40.056	9.551	6.346	27.9567	90.0508	111.0	1172.0
	1997	EW971022.A12	/INDUSTRY/	11/01/1997	12/15/1997	36.527	8.936	6.132	27.9567	90.0508	119.0	1172.0
	1997	EW971022.A13	/INDUSTRY/	11/01/1997	12/15/1997	34.731	8.560	6.118	27.9567	90.0508	127.0	1172.0
	1997	EW971022.A14	/INDUSTRY/	11/01/1997	12/15/1997	33.812	8.340	6.036	27.9567	90.0508	135.0	1172.0
	1997	EW971022.A15	/INDUSTRY/	11/01/1997	12/15/1997	32.696	8.143	5.920	27.9567	90.0508	143.0	1172.0
	1997	EW971022.A16	/INDUSTRY/	11/01/1997	12/15/1997	31.579	7.930	5.746	27.9567	90.0508	151.0	1172.0
	1997	EW971022.A17	/INDUSTRY/	11/01/1997	12/15/1997	31.121	7.782	5.779	27.9567	90.0508	159.0	1172.0
	1997	EW971022.A18	/INDUSTRY/	11/01/1997	12/15/1997	30.104	7.584	5.511	27.9567	90.0508	167.0	1172.0
	1997	EW971022.A19	/INDUSTRY/	11/01/1997	12/15/1997	29.334	7.322	5.332	27.9567	90.0508	175.0	1172.0
	1997	EW971022.A20	/INDUSTRY/	11/01/1997	12/15/1997	27.902	7.002	5.195	27.9567	90.0508	183.0	1172.0
	1997	EW971022.A21	/INDUSTRY/	11/01/1997	12/15/1997	25.812	6.700	5.034	27.9567	90.0508	191.0	1172.0
	1997	EW971022.A22	/INDUSTRY/	11/01/1997	12/15/1997	24.698	6.258	4.776	27.9567	90.0508	199.0	1172.0
	1997	EW971022.A23	/INDUSTRY/	11/01/1997	12/15/1997	24.870	5.835	4.568	27.9567	90.0508	207.0	1172.0
	1997	EW971022.A24	/INDUSTRY/	11/01/1997	12/15/1997	23.854	5.267	4.302	27.9567	90.0508	215.0	1172.0
	1997	EW971022.A25	/INDUSTRY/	11/01/1997	12/15/1997	22.389	4.641	4.020	27.9567	90.0508	223.0	1172.0
	1997	EW971022.A26	/INDUSTRY/	11/01/1997	12/15/1997	21.030	4.074	3.708	27.9567	90.0508	231.0	1172.0
	1997	EW971022.A27	/INDUSTRY/	11/01/1997	12/15/1997	19.558	3.514	3.316	27.9567	90.0508	239.0	1172.0
	1997	EW971022.A28	/INDUSTRY/	11/01/1997	12/15/1997	18.668	2.959	2.970	27.9567	90.0508	247.0	1172.0
	1997	EW971022.A29	/INDUSTRY/	11/01/1997	12/15/1997	17.755	2.459	2.646	27.9567	90.0508	255.0	1172.0
	1997	EW971022.A30	/INDUSTRY/	11/01/1997	12/15/1997	16.688	1.993	2.267	27.9567	90.0508	263.0	1172.0
	1997	EW971022.A31	/INDUSTRY/	11/01/1997	12/15/1997	15.628	1.616	1.959	27.9567	90.0508	271.0	1172.0
	1997	EW971022.A32	/INDUSTRY/	11/01/1997	12/15/1997	14.080	1.277	1.630	27.9567	90.0508	279.0	1172.0
	1997	EW971022.A33	/INDUSTRY/	11/01/1997	12/15/1997	13.086	1.020	1.390	27.9567	90.0508	287.0	1172.0
	1997	EW971022.A34	/INDUSTRY/	11/01/1997	12/15/1997	12.258	0.850	1.203	27.9567	90.0508	295.0	1172.0
	1997	EW971022.A35	/INDUSTRY/	11/01/1997	12/15/1997	11.102	0.698	0.988	27.9567	90.0508	303.0	1172.0
	1997	EW971022.A36	/INDUSTRY/	11/01/1997	12/15/1997	10.198	0.599	0.863	27.9567	90.0508	311.0	1172.0
	1997	EW971022.A37	/INDUSTRY/	11/01/1997	12/15/1997	8.631	0.528	0.728	27.9567	90.0508	319.0	1172.0
	1997	EW971022.A38	/INDUSTRY/	11/01/1997	12/15/1997	8.139	0.466	0.619	27.9567	90.0508	327.0	1172.0
	1997	EW971022.A39	/INDUSTRY/	11/01/1997	12/15/1997	7.649	0.431	0.562	27.9567	90.0508	335.0	1172.0
	1997	EW971022.A40	/INDUSTRY/	11/01/1997	12/15/1997	7.159	0.403	0.509	27.9567	90.0508	343.0	1172.0
	1997	EW971022.A41	/INDUSTRY/	11/01/1997	12/15/1997	5.590	0.393	0.461	27.9567	90.0508	351.0	1172.0
	1997	EW971022.A42	/INDUSTRY/	11/01/1997	12/15/1997	6.083	0.387	0.447	27.9567	90.0508	359.0	1172.0
	1997	EW971022.A43	/INDUSTRY/	11/01/1997	12/15/1997	5.590	0.368	0.402	27.9567	90.0508	367.0	1172.0
	1997	EW971022.A44	/INDUSTRY/	11/01/1997	12/15/1997	4.610	0.356	0.377	27.9567	90.0508	375.0	1172.0

Table B-4. Speed statistics for energetic current events associated with anticyclonic slope eddies. (continued)

Event No.	Year	Filename	Directory	Event start date (m/d/y)	Event end date (m/d/y)	Maximum speed ($cm \cdot s^{-1}$)	Mean speed ($cm \cdot s^{-1}$)	Stand. dev. of speed ($cm \cdot s^{-1}$)	Latitude (°N)	Longitude (°W)	Depth (m)	Total water depth (m)
5	1997	EW971022.A45	/INDUSTRY/	11/01/1997	12/15/1997	3.536	0.357	0.328	27.9567	90.0508	383.0	1172.0
	1997	EW971022.A46	/INDUSTRY/	11/01/1997	12/15/1997	3.536	0.326	0.310	27.9567	90.0508	391.0	1172.0
	1997	EW971022.A47	/INDUSTRY/	11/01/1997	12/15/1997	3.041	0.322	0.293	27.9567	90.0508	399.0	1172.0
	1997	EW971022.A48	/INDUSTRY/	11/01/1997	12/15/1997	2.550	0.304	0.288	27.9567	90.0508	407.0	1172.0
	1997	EW971022.A49	/INDUSTRY/	11/01/1997	12/15/1997	2.062	0.298	0.284	27.9567	90.0508	415.0	1172.0
	1997	EW971022.A50	/INDUSTRY/	11/01/1997	12/15/1997	1.500	0.296	0.284	27.9567	90.0508	423.0	1172.0
	1997	EW971022.A51	/INDUSTRY/	11/01/1997	12/15/1997	1.500	0.298	0.281	27.9567	90.0508	431.0	1172.0
	1997	EW971022.A52	/INDUSTRY/	11/01/1997	12/15/1997	1.500	0.291	0.280	27.9567	90.0508	439.0	1172.0
	1997	EW971022.A53	/INDUSTRY/	11/01/1997	12/15/1997	1.500	0.298	0.279	27.9567	90.0508	447.0	1172.0
	1997	EW971022.A54	/INDUSTRY/	11/01/1997	12/15/1997	1.000	0.303	0.278	27.9567	90.0508	455.0	1172.0
	1997	EW971022.A55	/INDUSTRY/	11/01/1997	12/15/1997	1.000	0.301	0.277	27.9567	90.0508	463.0	1172.0
	1997	EW971022.A56	/INDUSTRY/	11/01/1997	12/15/1997	1.000	0.292	0.278	27.9567	90.0508	471.0	1172.0
	1997	EW971022.A57	/INDUSTRY/	11/01/1997	12/15/1997	1.000	0.296	0.277	27.9567	90.0508	479.0	1172.0
	1997	EW971022.A58	/INDUSTRY/	11/01/1997	12/15/1997	0.707	0.298	0.277	27.9567	90.0508	487.0	1172.0
	1997	EW971022.A59	/INDUSTRY/	11/01/1997	12/15/1997	0.707	0.296	0.277	27.9567	90.0508	495.0	1172.0
	1997	EW971022.A60	/INDUSTRY/	11/01/1997	12/15/1997	0.707	0.293	0.279	27.9567	90.0508	503.0	1172.0
	1997	EW971022.A61	/INDUSTRY/	11/01/1997	12/15/1997	0.707	0.294	0.279	27.9567	90.0508	511.0	1172.0
	1997	EW971022.A62	/INDUSTRY/	11/01/1997	12/15/1997	0.707	0.293	0.278	27.9567	90.0508	519.0	1172.0
	1997	EW971022.A63	/INDUSTRY/	11/01/1997	12/15/1997	0.707	0.284	0.277	27.9567	90.0508	527.0	1172.0
	1997	EW971022.A64	/INDUSTRY/	11/01/1997	12/15/1997	0.707	0.290	0.277	27.9567	90.0508	535.0	1172.0
	1997	EW971022.A65	/INDUSTRY/	11/01/1997	12/15/1997	0.707	0.294	0.277	27.9567	90.0508	543.0	1172.0
	1997	EW971022.A66	/INDUSTRY/	11/01/1997	12/15/1997	0.707	0.300	0.278	27.9567	90.0508	551.0	1172.0
	1997	EW971022.A67	/INDUSTRY/	11/01/1997	12/15/1997	0.707	0.287	0.278	27.9567	90.0508	559.0	1172.0
	1997	EW971022.A68	/INDUSTRY/	11/01/1997	12/15/1997	0.707	0.291	0.277	27.9567	90.0508	567.0	1172.0
	1997	EW971022.A69	/INDUSTRY/	11/01/1997	12/15/1997	0.707	0.304	0.280	27.9567	90.0508	575.0	1172.0
	1997	EW971022.A70	/INDUSTRY/	11/01/1997	12/15/1997	0.707	0.392	0.264	27.9567	90.0508	583.0	1172.0
6	1998	MC971113.A01	/MMS/	01/01/1998	01/31/1998	67.807	18.942	10.347	28.7662	88.2650	8.0	1300.0
	1998	MC971113.A02	/MMS/	01/01/1998	01/31/1998	63.313	19.120	9.872	28.7662	88.2650	12.0	1300.0
	1998	MC971113.A03	/MMS/	01/01/1998	01/31/1998	58.259	18.661	9.471	28.7662	88.2650	16.0	1300.0
	1998	MC971113.A04	/MMS/	01/01/1998	01/31/1998	54.712	18.216	9.227	28.7662	88.2650	20.0	1300.0
	1998	MC971113.A05	/MMS/	01/01/1998	01/31/1998	51.752	17.883	9.134	28.7662	88.2650	24.0	1300.0
	1998	MC971113.A06	/MMS/	01/01/1998	01/31/1998	47.106	17.473	8.886	28.7662	88.2650	28.0	1300.0
	1998	MC971113.A07	/MMS/	01/01/1998	01/31/1998	42.134	17.043	8.613	28.7662	88.2650	32.0	1300.0
	1998	MC971113.A08	/MMS/	01/01/1998	01/31/1998	41.056	16.623	8.382	28.7662	88.2650	36.0	1300.0

Table B-4. Speed statistics for energetic current events associated with anticyclonic slope eddies. (continued)

Event No.	Year	Filename	Directory	Event start date (m/d/y)	Event end date (m/d/y)	Maximum speed ($cm \cdot s^{-1}$)	Mean speed ($cm \cdot s^{-1}$)	Stand. dev. of speed ($cm \cdot s^{-1}$)	Latitude (°N)	Longitude (°W)	Depth (m)	Total water depth (m)
6	1998	MC971113.A09	/MMS/	01/01/1998	01/31/1998	40.767	16.098	8.178	28.7662	88.2650	40.0	1300.0
	1998	MC971113.A10	/MMS/	01/01/1998	01/31/1998	39.608	15.725	7.905	28.7662	88.2650	44.0	1300.0
	1998	MC971113.A11	/MMS/	01/01/1998	01/31/1998	39.812	15.390	7.682	28.7662	88.2650	48.0	1300.0
	1998	MC971113.A12	/MMS/	01/01/1998	01/31/1998	39.801	15.046	7.507	28.7662	88.2650	52.0	1300.0
	1998	MC971113.A13	/MMS/	01/01/1998	01/31/1998	27.920	10.079	5.002	28.7662	88.2650	56.0	1300.0
	1998	MC971113.A14	/MMS/	01/01/1998	01/31/1998	29.314	10.795	5.446	28.7662	88.2650	60.0	1300.0
	1998	MC971113.A15	/MMS/	01/01/1998	01/31/1998	38.297	14.692	7.182	28.7662	88.2650	64.0	1300.0
	1998	MC971113.A16	/MMS/	01/01/1998	01/31/1998	37.505	14.482	7.004	28.7662	88.2650	68.0	1300.0
	1998	MC971113.A17	/MMS/	01/01/1998	01/31/1998	35.930	14.265	6.851	28.7662	88.2650	72.0	1300.0
	1998	MC971114.C01	/MMS/	01/01/1998	01/31/1998	33.944	8.583	7.489	28.7662	88.2650	500.0	1300.0
	1998	MC971114.C02	/MMS/	01/01/1998	01/31/1998	17.400	6.364	3.051	28.7662	88.2650	1310.0	1320.0
	1998	VK971115.A19	/MMS/	01/01/1998	01/31/1998	87.837	27.500	13.381	29.0705	87.8568	12.0	1300.0
	1998	VK971115.A20	/MMS/	01/01/1998	01/31/1998	94.790	30.980	13.944	29.0705	87.8568	16.0	1300.0
	1998	VK971115.A21	/MMS/	01/01/1998	01/31/1998	87.242	30.672	13.087	29.0705	87.8568	20.0	1300.0
	1998	VK971115.A22	/MMS/	01/01/1998	01/31/1998	78.208	30.704	12.318	29.0705	87.8568	24.0	1300.0
	1998	VK971115.A23	/MMS/	01/01/1998	01/31/1998	69.228	30.512	11.796	29.0705	87.8568	28.0	1300.0
	1998	VK971115.A24	/MMS/	01/01/1998	01/31/1998	69.274	30.316	11.441	29.0705	87.8568	32.0	1300.0
	1998	VK971115.A25	/MMS/	01/01/1998	01/31/1998	70.533	30.206	11.263	29.0705	87.8568	36.0	1300.0
	1998	VK971115.A26	/MMS/	01/01/1998	01/31/1998	68.679	29.746	11.067	29.0705	87.8568	40.0	1300.0
	1998	VK971115.A27	/MMS/	01/01/1998	01/31/1998	69.887	28.932	10.972	29.0705	87.8568	44.0	1300.0
	1998	VK971115.A28	/MMS/	01/01/1998	01/31/1998	69.560	28.002	10.904	29.0705	87.8568	48.0	1300.0
	1998	VK971115.A29	/MMS/	01/01/1998	01/31/1998	69.549	26.607	10.313	29.0705	87.8568	52.0	1300.0
	1998	VK971115.A30	/MMS/	01/01/1998	01/31/1998	48.172	18.140	7.267	29.0705	87.8568	56.0	1300.0
	1998	VK971115.A31	/MMS/	01/01/1998	01/31/1998	51.735	19.091	7.879	29.0705	87.8568	60.0	1300.0
	1998	VK971115.A32	/MMS/	01/01/1998	01/31/1998	65.709	26.892	11.145	29.0705	87.8568	64.0	1300.0
	1998	VK971115.A33	/MMS/	01/01/1998	01/31/1998	62.722	27.314	10.990	29.0705	87.8568	68.0	1300.0
	1998	VK971115.A34	/MMS/	01/01/1998	01/31/1998	58.533	26.377	10.805	29.0705	87.8568	72.0	1300.0
	1998	VK971115.C04	/MMS/	01/01/1998	01/31/1998	21.445	8.303	3.839	29.0705	87.8568	500.0	1300.0
	1998	VK971115.C05	/MMS/	01/01/1998	01/31/1998	14.797	4.751	2.748	29.0705	87.8568	1290.0	1300.0
	1998	DD971116.A01	/MMS/	01/01/1998	01/31/1998	83.550	32.060	13.333	29.0032	87.3532	12.0	1300.0
	1998	DD971116.A02	/MMS/	01/01/1998	01/31/1998	78.985	32.296	12.286	29.0032	87.3532	16.0	1300.0
	1998	DD971116.A03	/MMS/	01/01/1998	01/31/1998	74.797	32.535	11.767	29.0032	87.3532	20.0	1300.0
	1998	DD971116.A04	/MMS/	01/01/1998	01/31/1998	72.751	32.548	11.349	29.0032	87.3532	24.0	1300.0
	1998	DD971116.A05	/MMS/	01/01/1998	01/31/1998	70.516	32.434	11.004	29.0032	87.3532	28.0	1300.0

Table B-4. Speed statistics for energetic current events associated with anticyclonic slope eddies. (continued)

Event No.	Year	Filename	Directory	Event start date (m/d/y)	Event end date (m/d/y)	Maximum speed ($cm \cdot s^{-1}$)	Mean speed ($cm \cdot s^{-1}$)	Stand. dev. of speed ($cm \cdot s^{-1}$)	Latitude (°N)	Longitude (°W)	Depth (m)	Total water depth (m)
6	1998	DD971116.A06	/MMS/	01/01/1998	01/31/1998	68.142	32.178	10.783	29.0032	87.3532	32.0	1300.0
	1998	DD971116.A07	/MMS/	01/01/1998	01/31/1998	66.818	31.960	10.721	29.0032	87.3532	36.0	1300.0
	1998	DD971116.A08	/MMS/	01/01/1998	01/31/1998	66.537	31.756	10.824	29.0032	87.3532	40.0	1300.0
	1998	DD971116.A09	/MMS/	01/01/1998	01/31/1998	66.583	31.735	11.005	29.0032	87.3532	44.0	1300.0
	1998	DD971116.A10	/MMS/	01/01/1998	01/31/1998	64.635	31.721	11.164	29.0032	87.3532	48.0	1300.0
	1998	DD971116.A11	/MMS/	01/01/1998	01/31/1998	64.339	31.619	11.308	29.0032	87.3532	52.0	1300.0
	1998	DD971116.A12	/MMS/	01/01/1998	01/31/1998	51.349	24.619	9.100	29.0032	87.3532	56.0	1300.0
	1998	DD971116.A13	/MMS/	01/01/1998	01/31/1998	54.612	26.457	9.887	29.0032	87.3532	60.0	1300.0
	1998	DD971116.A14	/MMS/	01/01/1998	01/31/1998	58.927	31.575	11.384	29.0032	87.3532	64.0	1300.0
	1998	DD971116.A15	/MMS/	01/01/1998	01/31/1998	58.223	31.379	11.067	29.0032	87.3532	68.0	1300.0
	1998	DD971116.A16	/MMS/	01/01/1998	01/31/1998	57.078	31.015	10.743	29.0032	87.3532	72.0	1300.0
	1998	DD971116.C01	/MMS/	01/01/1998	01/31/1998	21.439	8.883	4.958	29.0032	87.3532	500.0	1300.0
	1998	DD971116.C02	/MMS/	01/01/1998	01/31/1998	16.507	5.748	4.110	29.0032	87.3532	1290.0	1300.0
7	1998	MC980402.A01	/MMS/	04/02/1998	08/05/1998	117.229	30.202	17.447	28.7662	88.2650	8.0	1300.0
	1998	MC980806.A01	/MMS/	08/06/1998	09/30/1998	163.238	32.084	18.736	28.7662	88.2650	8.0	1300.0
	1998	MC980402.A02	/MMS/	04/02/1998	08/05/1998	103.668	27.861	16.960	28.7662	88.2650	12.0	1300.0
	1998	MC980806.A02	/MMS/	08/06/1998	09/30/1998	143.560	30.895	17.605	28.7662	88.2650	12.0	1300.0
	1998	MC980402.A03	/MMS/	04/02/1998	08/05/1998	92.359	26.920	15.956	28.7662	88.2650	16.0	1300.0
	1998	MC980806.A03	/MMS/	08/06/1998	09/30/1998	153.638	30.704	16.823	28.7662	88.2650	16.0	1300.0
	1998	MC980402.A04	/MMS/	04/02/1998	08/05/1998	88.070	26.297	15.084	28.7662	88.2650	20.0	1300.0
	1998	MC980806.A04	/MMS/	08/06/1998	09/30/1998	137.061	30.657	16.222	28.7662	88.2650	20.0	1300.0
	1998	MC980402.A05	/MMS/	04/02/1998	08/05/1998	87.384	26.015	14.606	28.7662	88.2650	24.0	1300.0
	1998	MC980806.A05	/MMS/	08/06/1998	09/30/1998	130.133	30.380	15.882	28.7662	88.2650	24.0	1300.0
	1998	MC980402.A06	/MMS/	04/02/1998	08/05/1998	86.419	25.904	13.954	28.7662	88.2650	28.0	1300.0
	1998	MC980806.A06	/MMS/	08/06/1998	09/30/1998	127.429	30.375	15.547	28.7662	88.2650	28.0	1300.0
	1998	MC980402.A07	/MMS/	04/02/1998	08/05/1998	79.768	25.694	13.518	28.7662	88.2650	32.0	1300.0
	1998	MC980806.A07	/MMS/	08/06/1998	09/30/1998	120.877	30.312	15.285	28.7662	88.2650	32.0	1300.0
	1998	MC980402.A08	/MMS/	04/02/1998	08/05/1998	71.232	25.507	13.087	28.7662	88.2650	36.0	1300.0
	1998	MC980806.A08	/MMS/	08/06/1998	09/30/1998	112.485	29.904	14.957	28.7662	88.2650	36.0	1300.0
	1998	MC980402.A09	/MMS/	04/02/1998	08/05/1998	70.015	25.264	12.921	28.7662	88.2650	40.0	1300.0
	1998	MC980806.A09	/MMS/	08/06/1998	09/30/1998	107.307	29.157	14.450	28.7662	88.2650	40.0	1300.0
	1998	MC980402.A10	/MMS/	04/02/1998	08/05/1998	65.965	25.094	12.723	28.7662	88.2650	44.0	1300.0
	1998	MC980806.A10	/MMS/	08/06/1998	09/30/1998	104.066	28.464	14.012	28.7662	88.2650	44.0	1300.0
	1998	MC980402.A11	/MMS/	04/02/1998	08/05/1998	66.691	24.886	12.490	28.7662	88.2650	48.0	1300.0

Table B-4. Speed statistics for energetic current events associated with anticyclonic slope eddies. (continued)

Event No.	Year	Filename	Directory	Event start date (m/d/y)	Event end date (m/d/y)	Maximum speed (cm·s^{-1})	Mean speed (cm·s^{-1})	Stand. dev. of speed (cm·s^{-1})	Latitude (°N)	Longitude (°W)	Depth (m)	Total water depth (m)
7	1998	MC980806.A11	/MMS/	08/06/1998	09/30/1998	96.440	27.485	13.596	28.7662	88.2650	48.0	1300.0
	1998	MC980402.A12	/MMS/	04/02/1998	08/05/1998	66.725	24.532	12.425	28.7662	88.2650	52.0	1300.0
	1998	MC980806.A12	/MMS/	08/06/1998	09/30/1998	85.028	26.546	13.100	28.7662	88.2650	52.0	1300.0
	1998	MC980402.A13	/MMS/	04/02/1998	08/05/1998	47.724	15.331	8.174	28.7662	88.2650	56.0	1300.0
	1998	MC980806.A13	/MMS/	08/06/1998	09/30/1998	56.786	15.724	8.287	28.7662	88.2650	56.0	1300.0
	1998	MC980402.A14	/MMS/	04/02/1998	08/05/1998	50.932	16.920	8.981	28.7662	88.2650	60.0	1300.0
	1998	MC980806.A14	/MMS/	08/06/1998	09/30/1998	55.716	15.975	8.564	28.7662	88.2650	60.0	1300.0
	1998	MC980402.A15	/MMS/	04/02/1998	08/05/1998	60.624	24.097	12.404	28.7662	88.2650	64.0	1300.0
	1998	MC980806.A15	/MMS/	08/06/1998	09/30/1998	74.502	24.505	12.507	28.7662	88.2650	64.0	1300.0
	1998	MC980402.A16	/MMS/	04/02/1998	08/05/1998	59.992	23.667	12.202	28.7662	88.2650	68.0	1300.0
	1998	MC980806.A16	/MMS/	08/06/1998	09/30/1998	73.752	23.741	11.895	28.7662	88.2650	68.0	1300.0
	1998	MC980402.A17	/MMS/	04/02/1998	08/05/1998	57.991	22.886	11.581	28.7662	88.2650	72.0	1300.0
	1998	MC980402.C01	/MMS/	04/02/1998	08/05/1998	39.458	10.648	8.472	28.7662	88.2650	500.0	1300.0
	1998	MC980806.C01	/MMS/	08/06/1998	09/30/1998	34.522	9.290	7.780	28.7662	88.2650	500.0	1300.0
	1998	MC980402.C02	/MMS/	04/02/1998	08/05/1998	18.502	4.597	2.892	28.7662	88.2650	1310.0	1320.0
	1998	MC980806.C02	/MMS/	08/06/1998	09/30/1998	18.097	4.807	2.899	28.7662	88.2650	1310.0	1320.0
	1998	VK980807.A19	/MMS/	08/07/1998	09/30/1998	161.808	29.954	18.931	29.0705	87.8568	12.0	1300.0
	1998	VK980403.A01	/MMS/	04/03/1998	08/06/1998	102.140	43.764	17.730	29.0705	87.8568	16.0	1300.0
	1998	VK980807.A20	/MMS/	08/07/1998	09/30/1998	148.308	37.550	18.141	29.0705	87.8568	16.0	1300.0
	1998	VK980403.A02	/MMS/	04/03/1998	08/06/1998	94.561	29.979	16.498	29.0705	87.8568	20.0	1300.0
	1998	VK980807.A21	/MMS/	08/07/1998	09/30/1998	136.940	36.440	16.464	29.0705	87.8568	20.0	1300.0
	1998	VK980403.A03	/MMS/	04/03/1998	08/06/1998	88.819	25.254	15.036	29.0705	87.8568	24.0	1300.0
	1998	VK980807.A22	/MMS/	08/07/1998	09/30/1998	131.533	35.330	15.142	29.0705	87.8568	24.0	1300.0
	1998	VK980403.A04	/MMS/	04/03/1998	08/06/1998	81.354	22.911	14.669	29.0705	87.8568	28.0	1300.0
	1998	VK980807.A23	/MMS/	08/07/1998	09/30/1998	120.877	34.802	14.081	29.0705	87.8568	28.0	1300.0
	1998	VK980403.A05	/MMS/	04/03/1998	08/06/1998	78.814	21.777	14.645	29.0705	87.8568	32.0	1300.0
	1998	VK980807.A24	/MMS/	08/07/1998	09/30/1998	110.377	34.171	13.400	29.0705	87.8568	32.0	1300.0
	1998	VK980403.A06	/MMS/	04/03/1998	08/06/1998	77.191	21.001	14.595	29.0705	87.8568	36.0	1300.0
	1998	VK980807.A25	/MMS/	08/07/1998	09/30/1998	96.116	33.048	13.101	29.0705	87.8568	36.0	1300.0
	1998	VK980403.A07	/MMS/	04/03/1998	08/06/1998	71.363	20.472	14.304	29.0705	87.8568	40.0	1300.0
	1998	VK980807.A26	/MMS/	08/07/1998	09/30/1998	82.854	31.935	13.013	29.0705	87.8568	40.0	1300.0
	1998	VK980403.A08	/MMS/	04/03/1998	08/06/1998	63.725	20.065	13.776	29.0705	87.8568	44.0	1300.0
	1998	VK980807.A27	/MMS/	08/07/1998	09/30/1998	70.830	30.930	12.444	29.0705	87.8568	44.0	1300.0
	1998	VK980403.A09	/MMS/	04/03/1998	08/06/1998	62.595	19.484	13.178	29.0705	87.8568	48.0	1300.0

Table B-4. Speed statistics for energetic current events associated with anticyclonic slope eddies. (continued)

Event No.	Year	Filename	Directory	Event start date (m/d/y)	Event end date (m/d/y)	Maximum speed (cm·s^{-1})	Mean speed (cm·s^{-1})	Stand. dev. of speed (cm·s^{-1})	Latitude (°N)	Longitude (°W)	Depth (m)	Total water depth (m)
7	1998	VK980807.A28	/MMS/	08/07/1998	09/30/1998	70.241	29.938	12.115	29.0705	87.8568	48.0	1300.0
	1998	VK980403.A10	/MMS/	04/03/1998	08/06/1998	60.134	18.539	12.816	29.0705	87.8568	52.0	1300.0
	1998	VK980807.A29	/MMS/	08/07/1998	09/30/1998	68.101	29.161	12.258	29.0705	87.8568	52.0	1300.0
	1998	VK980403.A11	/MMS/	04/03/1998	08/06/1998	42.916	10.063	7.026	29.0705	87.8568	56.0	1300.0
	1998	VK980807.A30	/MMS/	08/07/1998	09/30/1998	55.704	19.610	9.564	29.0705	87.8568	56.0	1300.0
	1998	VK980403.A12	/MMS/	04/03/1998	08/06/1998	46.565	10.947	7.805	29.0705	87.8568	60.0	1300.0
	1998	VK980807.A31	/MMS/	08/07/1998	09/30/1998	61.059	20.236	9.553	29.0705	87.8568	60.0	1300.0
	1998	VK980403.A13	/MMS/	04/03/1998	08/06/1998	60.802	18.401	12.863	29.0705	87.8568	64.0	1300.0
	1998	VK980807.A32	/MMS/	08/07/1998	09/30/1998	72.827	28.014	11.692	29.0705	87.8568	64.0	1300.0
	1998	VK980403.A14	/MMS/	04/03/1998	08/06/1998	60.807	18.073	12.629	29.0705	87.8568	68.0	1300.0
	1998	VK980807.A33	/MMS/	08/07/1998	09/30/1998	76.287	27.464	11.484	29.0705	87.8568	68.0	1300.0
	1998	VK980403.A15	/MMS/	04/03/1998	08/06/1998	61.205	17.488	12.249	29.0705	87.8568	72.0	1300.0
	1998	VK980807.A34	/MMS/	08/07/1998	09/30/1998	78.339	25.669	11.198	29.0705	87.8568	72.0	1300.0
	1998	VK980403.C01	/MMS/	04/03/1998	08/06/1998	48.184	8.580	7.864	29.0705	87.8568	500.0	1300.0
	1998	VK980807.C04	/MMS/	08/07/1998	09/30/1998	54.281	11.858	8.681	29.0705	87.8568	500.0	1300.0
	1998	VK980403.C02	/MMS/	04/03/1998	08/06/1998	18.196	4.836	2.745	29.0705	87.8568	1290.0	1300.0
	1998	VK980808.C01	/MMS/	08/08/1998	09/30/1998	19.697	5.012	3.535	29.0705	87.8568	1290.0	1300.0
	1998	DD980405.A02	/MMS/	04/05/1998	08/08/1998	75.980	25.616	13.911	29.0032	87.3532	12.0	1300.0
	1998	DD980808.A01	/MMS/	08/08/1998	09/30/1998	202.837	44.704	25.243	29.0032	87.3532	12.0	1300.0
	1998	DD980405.A03	/MMS/	04/05/1998	08/08/1998	72.834	23.276	12.909	29.0032	87.3532	16.0	1300.0
	1998	DD980808.A02	/MMS/	08/08/1998	09/30/1998	177.568	47.762	27.444	29.0032	87.3532	16.0	1300.0
	1998	DD980405.A04	/MMS/	04/05/1998	08/08/1998	67.238	21.982	12.621	29.0032	87.3532	20.0	1300.0
	1998	DD980808.A03	/MMS/	08/08/1998	09/30/1998	161.485	46.359	27.445	29.0032	87.3532	20.0	1300.0
	1998	DD980405.A05	/MMS/	04/05/1998	08/08/1998	65.343	21.492	12.301	29.0032	87.3532	24.0	1300.0
	1998	DD980808.A04	/MMS/	08/08/1998	09/30/1998	174.001	45.370	26.753	29.0032	87.3532	24.0	1300.0
	1998	DD980405.A06	/MMS/	04/05/1998	08/08/1998	67.730	21.120	11.930	29.0032	87.3532	28.0	1300.0
	1998	DD980808.A05	/MMS/	08/08/1998	09/30/1998	156.170	44.673	25.037	29.0032	87.3532	28.0	1300.0
	1998	DD980405.A07	/MMS/	04/05/1998	08/08/1998	65.546	20.784	11.413	29.0032	87.3532	32.0	1300.0
	1998	DD980808.A06	/MMS/	08/08/1998	09/30/1998	141.319	43.954	23.195	29.0032	87.3532	32.0	1300.0
	1998	DD980405.A08	/MMS/	04/05/1998	08/08/1998	64.345	20.441	10.923	29.0032	87.3532	36.0	1300.0
	1998	DD980808.A07	/MMS/	08/08/1998	09/30/1998	125.455	42.896	21.729	29.0032	87.3532	36.0	1300.0
	1998	DD980405.A09	/MMS/	04/05/1998	08/08/1998	63.318	20.036	10.596	29.0032	87.3532	40.0	1300.0
	1998	DD980808.A08	/MMS/	08/08/1998	09/30/1998	117.282	41.585	20.536	29.0032	87.3532	40.0	1300.0
	1998	DD980405.A10	/MMS/	04/05/1998	08/08/1998	58.969	19.350	10.047	29.0032	87.3532	44.0	1300.0

Table B-4. Speed statistics for energetic current events associated with anticyclonic slope eddies. (continued)

Event No.	Year	Filename	Directory	Event start date (m/d/y)	Event end date (m/d/y)	Maximum speed (cm·s^{-1})	Mean speed (cm·s^{-1})	Stand. dev. of speed (cm·s^{-1})	Latitude (°N)	Longitude (°W)	Depth (m)	Total water depth (m)
7	1998	DD980808.A09	/MMS/	08/08/1998	09/30/1998	102.837	40.212	19.205	29.0032	87.3532	44.0	1300.0
	1998	DD980405.A11	/MMS/	04/05/1998	08/08/1998	56.106	18.815	9.369	29.0032	87.3532	48.0	1300.0
	1998	DD980808.A10	/MMS/	08/08/1998	09/30/1998	92.670	38.036	17.773	29.0032	87.3532	48.0	1300.0
	1998	DD980405.A12	/MMS/	04/05/1998	08/08/1998	51.065	18.341	9.096	29.0032	87.3532	52.0	1300.0
	1998	DD980808.A11	/MMS/	08/08/1998	09/30/1998	77.131	35.940	16.884	29.0032	87.3532	52.0	1300.0
	1998	DD980405.A13	/MMS/	04/05/1998	08/08/1998	48.264	15.698	8.478	29.0032	87.3532	56.0	1300.0
	1998	DD980808.A12	/MMS/	08/08/1998	09/30/1998	64.109	28.350	13.939	29.0032	87.3532	56.0	1300.0
	1998	DD980405.A14	/MMS/	04/05/1998	08/08/1998	48.811	16.392	8.776	29.0032	87.3532	60.0	1300.0
	1998	DD980808.A13	/MMS/	08/08/1998	09/30/1998	64.549	28.353	14.084	29.0032	87.3532	60.0	1300.0
	1998	DD980405.A15	/MMS/	04/05/1998	08/08/1998	51.202	18.020	9.328	29.0032	87.3532	64.0	1300.0
	1998	DD980808.A14	/MMS/	08/08/1998	09/30/1998	73.495	32.719	16.607	29.0032	87.3532	64.0	1300.0
	1998	DD980405.A16	/MMS/	04/05/1998	08/08/1998	48.964	17.564	9.311	29.0032	87.3532	68.0	1300.0
	1998	DD980808.A15	/MMS/	08/08/1998	09/30/1998	74.190	31.535	16.304	29.0032	87.3532	68.0	1300.0
	1998	DD980405.A17	/MMS/	04/05/1998	08/08/1998	48.110	16.824	9.070	29.0032	87.3532	72.0	1300.0
	1998	DD980808.A16	/MMS/	08/08/1998	09/30/1998	62.229	30.852	14.870	29.0032	87.3532	72.0	1300.0
	1998	DD980405.C01	/MMS/	04/05/1998	08/08/1998	29.292	9.299	5.646	29.0032	87.3532	500.0	1300.0
	1998	DD980808.C01	/MMS/	08/08/1998	09/30/1998	30.456	13.518	6.111	29.0032	87.3532	500.0	1300.0
	1998	DD980405.C02	/MMS/	04/05/1998	08/08/1998	25.500	6.149	3.971	29.0032	87.3532	1290.0	1300.0
	1998	DD980808.C02	/MMS/	08/08/1998	09/30/1998	43.701	7.060	5.405	29.0032	87.3532	1290.0	1300.0
	1998	DD980405.A01	/MMS/	04/05/1998	08/08/1998	77.737	25.695	13.835	29.0032	87.3532	8.0	1300.0

Notes by event number

1 1992: May - June

Low-frequency oscillations are in the 14- and 100-m records at LATEX 12. Currents rotate from southwestward to northeastward as the slope eddy slips past. Peak speeds of ~45 cm·s^{-1} occur. Data from LATEX 12 are plotted in Figure 6.3.4-2. A detail of this event is shown in Figure A.4-1.

2 1993: April

The currents turn from north to southeast as a slope eddy passes to the west of LATEX 12. An extratropical cyclone occurs during this time period. Data from LATEX 12 are plotted in Figure 6.3.4-2.

3 1994: April

Inertial oscillation packets occur during April 6-12 and are seen in the records from the surface to 367 m at Industry GC200. Data from Industry GC200 are plotted in Figure 6.3.12-7. A detail of this event is shown in Figure A.4-2.

Table B-4. Speed statistics for energetic current events associated with anticyclonic slope eddies. (continued)

Notes by event number (continued)

4 1997: March - August, Deviant Eddy

Low-frequency motions are prevalent as this named slope eddy influences the DeSoto Canyon region for several months. During this time, Hurricane Danny passes by the moorings, so caution should be used when analyzing these statistics. Data from SAIC EIS are plotted in Figure 6.3.5-2. A detail of this event is shown in Figure A.4-3.

5 1997: November - December

6 1998: January

Low-frequency motions at SAIC EIS locations, particularly at beginning of the month.

7 1998: April-September, Eddy Gyre

Low-frequency motions at SAIC EIS locations.

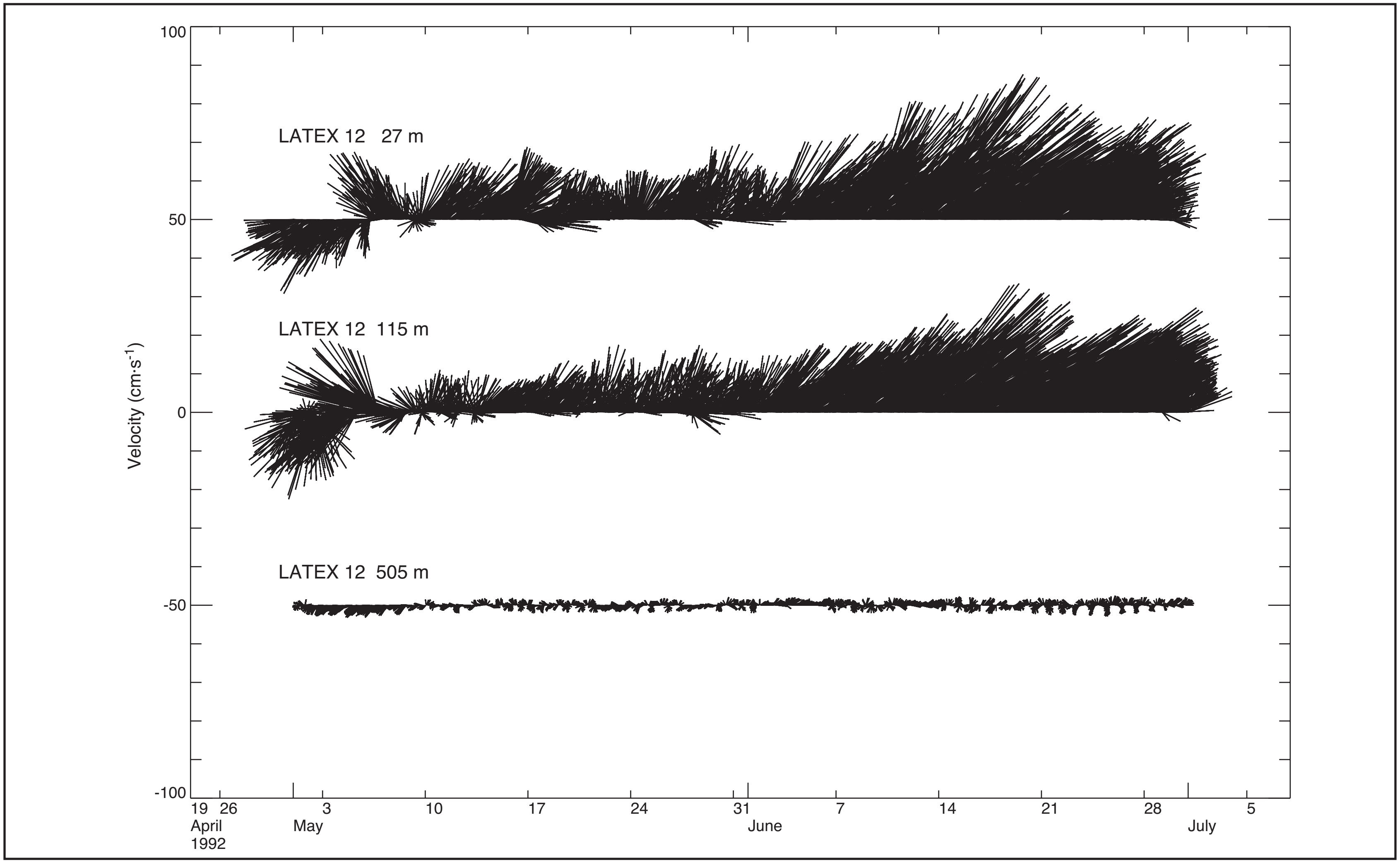

Figure B.4-1. Influence of an anticyclonic slope eddy on currents in the central Gulf at LATEX mooring 12, May and June 1992. See also Table B-4, event 1.

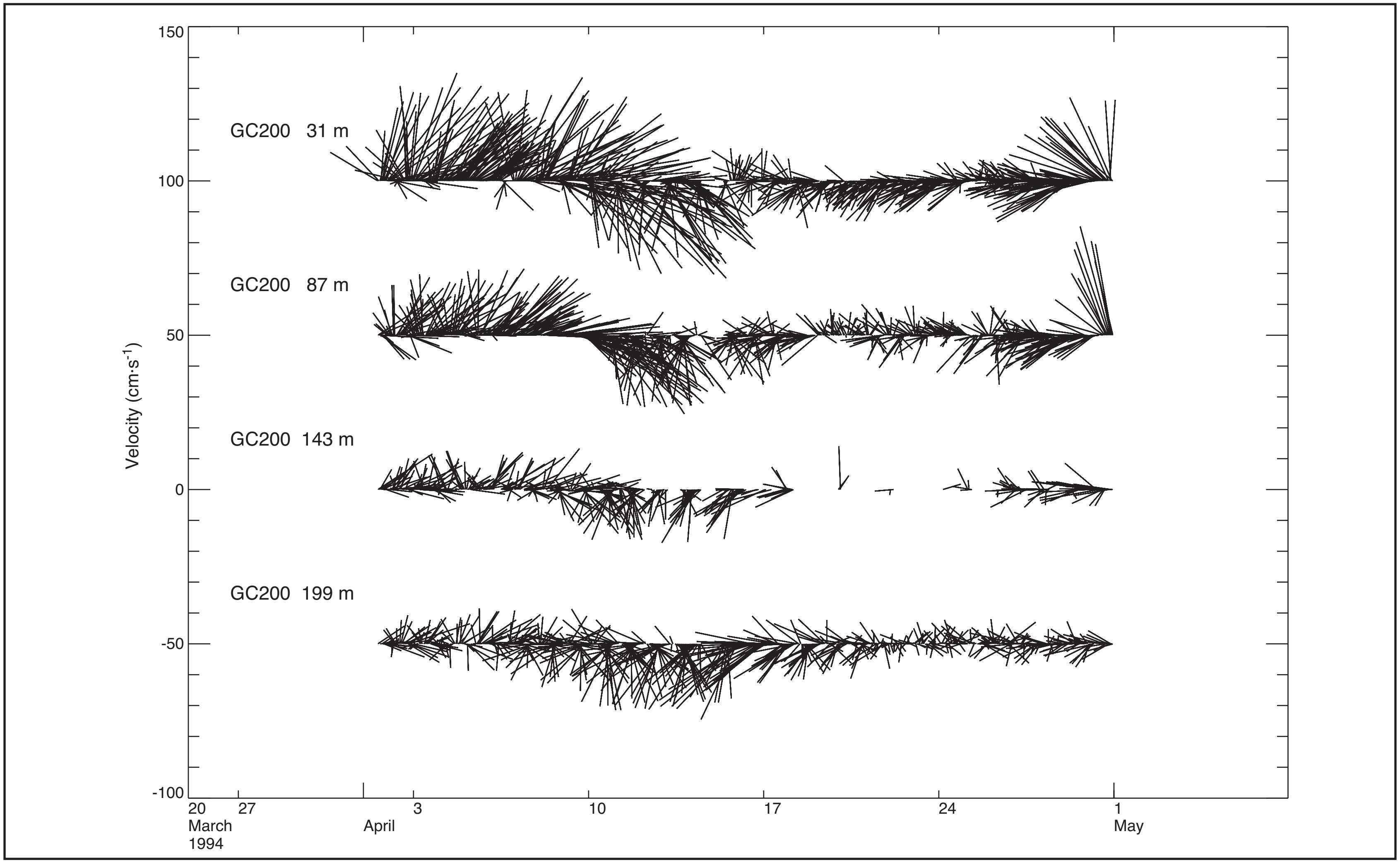

Figure B.4-2. Influence of an anticyclonic slope eddy on currents in the central Gulf at industry mooring GC200 during April 1994. See also Table B-4, event 3.

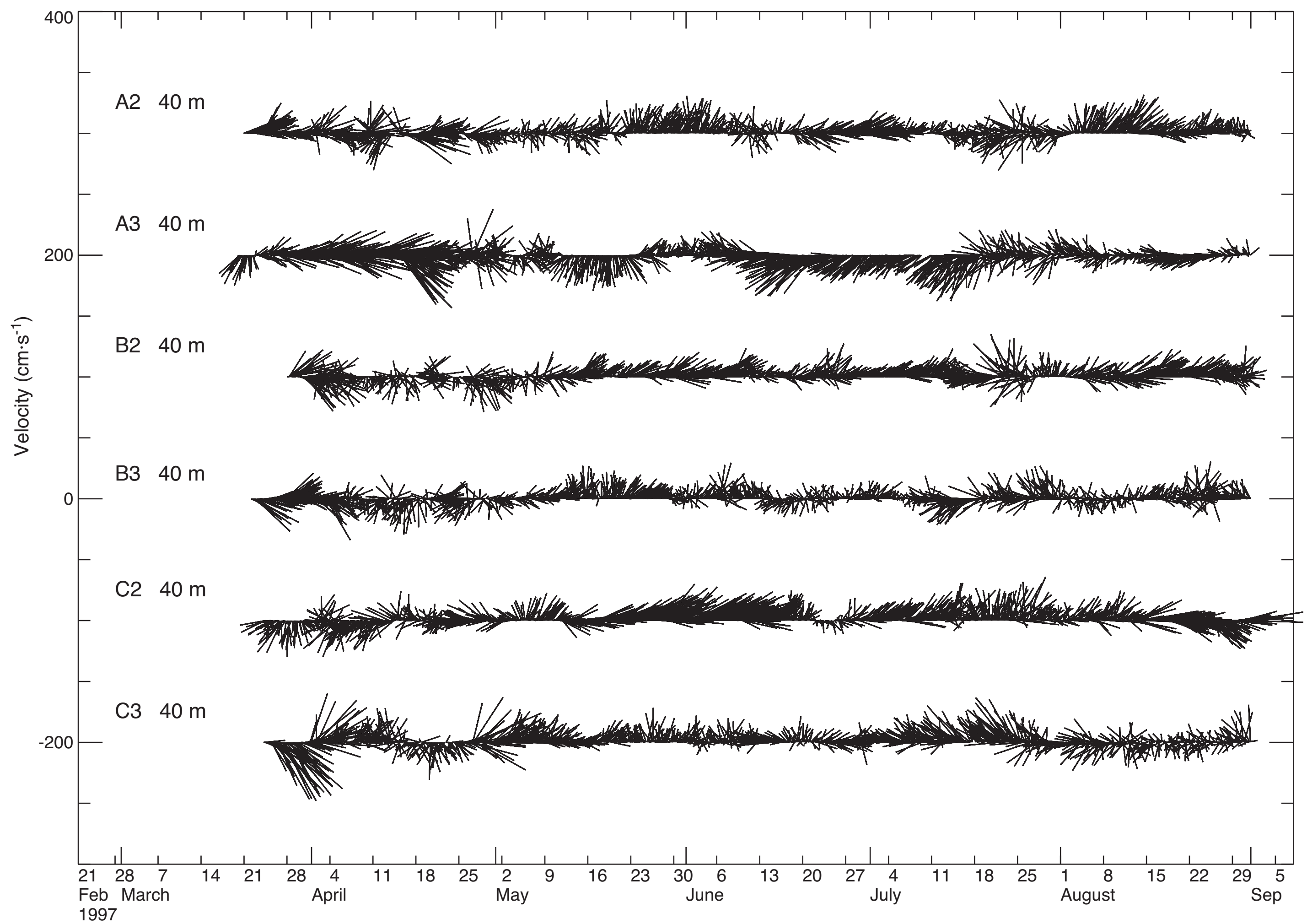

Figure B.4-3. Influence of anticyclonic slope eddy, Deviant Eddy, on currents at 40-m depth over DeSoto Canyon at SAIC EIS moorings, March through August 1997. See also Table B-4, event 4.

Table B-5. Speed statistics for energetic current events associated with cyclonic eddies. Given are the name of the file containing the event (keyed to the directory on the CD-ROM database), the start and stop dates used to characterize the event, maximum speed, mean speed, standard deviation of speed, mooring location, depth of the instrument, and total water depth. Comments on the event, keyed by the event number, are given in the notes below the table.

Event No.	Year	Filename	Directory	Event start date (m/d/y)	Event end date (m/d/y)	Maximum speed (cm·s^{-1})	Mean speed (cm·s^{-1})	Stand. dev. of speed (cm·s^{-1})	Latitude (°N)	Longitude (°W)	Depth (m)	Total water depth (m)
1	1985	MG850615.C01	/NODC_DEEP/	08/01/1985	09/30/1985	85.498	30.653	16.129	25.8717	94.8800	100.0	3000.0
	1985	MG850615.C02	/NODC_DEEP/	08/01/1985	09/30/1985	44.807	15.238	9.612	25.8717	94.8800	300.0	3000.0
	1985	MG850615.C03	/NODC_DEEP/	08/01/1985	09/30/1985	25.017	6.716	5.021	25.8717	94.8800	1000.0	3000.0
	1985	MG850615.C04	/NODC_DEEP/	08/01/1985	09/30/1985	27.352	9.715	6.356	25.8717	94.8800	1500.0	3000.0
	1985	MG850612.C01	/NODC_DEEP/	08/01/1985	09/30/1985	69.541	24.001	13.185	25.4115	95.5300	100.0	1503.0
	1985	MG850612.C02	/NODC_DEEP/	08/01/1985	08/30/1985	27.629	11.176	5.267	25.4115	95.5300	300.0	1503.0
	1985	MG850612.C03	/NODC_DEEP/	08/01/1985	09/30/1985	17.366	4.169	2.622	25.4115	95.5300	1000.0	1508.0
2	1985	MG850613.C01	/NODC_DEEP/	06/13/1985	09/18/1985	104.355	40.662	20.442	24.5532	96.1183	100.0	2200.0
	1985	MG850613.C02	/NODC_DEEP/	06/13/1985	09/30/1985	69.170	27.215	11.275	24.5532	96.1183	300.0	2200.0
	1985	MG850613.C03	/NODC_DEEP/	06/13/1985	09/30/1985	26.142	10.417	4.755	24.5532	96.1183	1000.0	2200.0
3	1985	MG850613.C02	/NODC_DEEP/	12/01/1985	04/30/1986	70.195	32.478	10.331	24.5532	96.1183	300.0	2200.0
	1985	MG850613.C03	/NODC_DEEP/	12/01/1985	04/30/1986	21.006	5.438	3.307	24.5532	96.1183	1000.0	2200.0
4	1986	MG851020.C01	/NODC_DEEP/	03/01/1986	04/30/1986	40.604	17.845	6.265	25.8717	94.8800	300.0	3000.0
	1986	MG850615.C04	/NODC_DEEP/	03/01/1986	04/30/1986	12.417	3.434	2.528	25.8717	94.8800	1500.0	3000.0
5	1992	GC921023.C01	/TAMU/	10/23/1992	12/31/1992	49.458	15.388	8.544	27.9240	90.4950	19.0	505.0
	1992	GC920415.C01	/TAMU/	10/01/1992	10/22/1992	61.533	23.880	11.719	27.9240	90.4950	27.0	515.0
	1992	GC921023.C02	/TAMU/	10/23/1992	12/31/1992	39.715	11.510	6.811	27.9240	90.4950	105.0	505.0
	1992	GC921022.C01	/TAMU/	10/22/1992	12/03/1992	6.530	2.301	1.063	27.9240	90.4950	495.0	505.0
	1992	GC920415.C03	/TAMU/	10/01/1992	10/22/1992	5.104	2.094	0.634	27.9240	90.4950	505.0	515.0
6	1993	EB930520.C01	/TAMU/	09/01/1993	12/12/1993	37.388	8.714	7.756	27.3860	95.8990	101.0	501.0
	1993	EB931212.C02	/TAMU/	12/12/1993	12/31/1993	29.275	13.023	6.187	27.3850	95.9020	100.0	500.0
7	1998	MC971113.A01	/MMS/	02/01/1998	04/01/1998	89.578	29.090	15.798	28.7662	88.2650	8.0	1300.0
	1998	MC980402.A01	/MMS/	04/02/1998	04/30/1998	87.945	41.265	15.516	28.7662	88.2650	8.0	1300.0
	1998	MC971113.A02	/MMS/	02/01/1998	04/01/1998	78.743	27.538	14.752	28.7662	88.2650	12.0	1300.0
	1998	MC980402.A02	/MMS/	04/02/1998	04/30/1998	82.925	40.527	14.585	28.7662	88.2650	12.0	1300.0
	1998	MC971113.A03	/MMS/	02/01/1998	04/01/1998	70.228	25.844	13.705	28.7662	88.2650	16.0	1300.0
	1998	MC980402.A03	/MMS/	04/02/1998	04/30/1998	78.013	39.796	13.722	28.7662	88.2650	16.0	1300.0
	1998	MC971113.A04	/MMS/	02/01/1998	04/01/1998	64.874	24.781	12.942	28.7662	88.2650	20.0	1300.0
	1998	MC980402.A04	/MMS/	04/02/1998	04/30/1998	73.082	39.121	12.781	28.7662	88.2650	20.0	1300.0
	1998	MC971113.A05	/MMS/	02/01/1998	04/01/1998	61.186	23.981	12.321	28.7662	88.2650	24.0	1300.0
	1998	MC980402.A05	/MMS/	04/02/1998	04/30/1998	69.366	38.690	11.816	28.7662	88.2650	24.0	1300.0

Table B-5. Speed statistics for energetic current events associated with cyclonic eddies. (continued)

Event No.	Year	Filename	Directory	Event start date (m/d/y)	Event end date (m/d/y)	Maximum speed (cm·s^{-1})	Mean speed (cm·s^{-1})	Stand. dev. of speed (cm·s^{-1})	Latitude (°N)	Longitude (°W)	Depth (m)	Total water depth (m)
7	1998	MC971113.A06	/MMS/	02/01/1998	04/01/1998	61.221	23.422	11.917	28.7662	88.2650	28.0	1300.0
	1998	MC980402.A06	/MMS/	04/02/1998	04/30/1998	65.906	38.344	11.101	28.7662	88.2650	28.0	1300.0
	1998	MC971113.A07	/MMS/	02/01/1998	04/01/1998	61.157	23.023	11.551	28.7662	88.2650	32.0	1300.0
	1998	MC980402.A07	/MMS/	04/02/1998	04/30/1998	61.100	38.053	10.539	28.7662	88.2650	32.0	1300.0
	1998	MC971113.A08	/MMS/	02/01/1998	04/01/1998	60.952	22.638	11.301	28.7662	88.2650	36.0	1300.0
	1998	MC980402.A08	/MMS/	04/02/1998	04/30/1998	61.887	37.793	10.178	28.7662	88.2650	36.0	1300.0
	1998	MC971113.A09	/MMS/	02/01/1998	04/01/1998	58.134	22.342	11.217	28.7662	88.2650	40.0	1300.0
	1998	MC980402.A09	/MMS/	04/02/1998	04/30/1998	63.873	37.569	10.123	28.7662	88.2650	40.0	1300.0
	1998	MC971113.A10	/MMS/	02/01/1998	04/01/1998	55.547	22.116	11.127	28.7662	88.2650	44.0	1300.0
	1998	MC980402.A10	/MMS/	04/02/1998	04/30/1998	65.500	37.368	10.009	28.7662	88.2650	44.0	1300.0
	1998	MC971113.A11	/MMS/	02/01/1998	04/01/1998	53.181	21.875	10.975	28.7662	88.2650	48.0	1300.0
	1998	MC980402.A11	/MMS/	04/02/1998	04/30/1998	63.008	37.202	9.750	28.7662	88.2650	48.0	1300.0
	1998	MC971113.A12	/MMS/	02/01/1998	04/01/1998	51.108	21.775	10.844	28.7662	88.2650	52.0	1300.0
	1998	MC980402.A12	/MMS/	04/02/1998	04/30/1998	61.914	36.999	9.516	28.7662	88.2650	52.0	1300.0
	1998	MC971113.A13	/MMS/	02/01/1998	04/01/1998	35.547	13.908	7.130	28.7662	88.2650	56.0	1300.0
	1998	MC980402.A13	/MMS/	04/02/1998	04/30/1998	47.724	24.319	7.418	28.7662	88.2650	56.0	1300.0
	1998	MC971113.A14	/MMS/	02/01/1998	04/01/1998	39.309	15.460	7.842	28.7662	88.2650	60.0	1300.0
	1998	MC980402.A14	/MMS/	04/02/1998	04/30/1998	50.932	26.809	7.934	28.7662	88.2650	60.0	1300.0
	1998	MC971113.A15	/MMS/	02/01/1998	04/01/1998	53.003	21.669	10.573	28.7662	88.2650	64.0	1300.0
	1998	MC980402.A15	/MMS/	04/02/1998	04/30/1998	60.624	36.513	9.797	28.7662	88.2650	64.0	1300.0
	1998	MC971113.A16	/MMS/	02/01/1998	04/01/1998	52.800	21.407	10.456	28.7662	88.2650	68.0	1300.0
	1998	MC980402.A16	/MMS/	04/02/1998	04/30/1998	59.992	36.139	9.720	28.7662	88.2650	68.0	1300.0
	1998	MC971113.A17	/MMS/	02/01/1998	04/01/1998	51.416	20.994	10.216	28.7662	88.2650	72.0	1300.0
	1998	MC980402.A17	/MMS/	04/02/1998	04/30/1998	57.991	34.297	8.901	28.7662	88.2650	72.0	1300.0
	1998	MC971114.C01	/MMS/	02/01/1998	04/01/1998	39.462	11.451	8.436	28.7662	88.2650	500.0	1300.0
	1998	MC980402.C01	/MMS/	04/02/1998	04/30/1998	39.458	14.236	9.839	28.7662	88.2650	500.0	1300.0
	1998	MC971114.C02	/MMS/	02/01/1998	04/01/1998	19.099	6.143	3.279	28.7662	88.2650	1310.0	1320.0
	1998	MC980402.C02	/MMS/	04/02/1998	04/30/1998	17.804	5.320	3.475	28.7662	88.2650	1310.0	1320.0
	1998	VK971115.A19	/MMS/	02/01/1998	04/03/1998	95.392	25.739	14.244	29.0705	87.8568	12.0	1300.0
	1998	VK971115.A20	/MMS/	02/01/1998	04/03/1998	86.079	27.410	13.413	29.0705	87.8568	16.0	1300.0
	1998	VK980403.A01	/MMS/	04/03/1998	04/30/1998	99.178	42.571	16.349	29.0705	87.8568	16.0	1300.0
	1998	VK971115.A21	/MMS/	02/01/1998	04/03/1998	75.801	26.474	12.351	29.0705	87.8568	20.0	1300.0
	1998	VK980403.A02	/MMS/	04/03/1998	04/30/1998	94.561	31.914	20.389	29.0705	87.8568	20.0	1300.0
	1998	VK971115.A22	/MMS/	02/01/1998	04/03/1998	74.150	25.523	11.662	29.0705	87.8568	24.0	1300.0

Table B-5. Speed statistics for energetic current events associated with cyclonic eddies. (continued)

Event No.	Year	Filename	Directory	Event start date (m/d/y)	Event end date (m/d/y)	Maximum speed ($cm \cdot s^{-1}$)	Mean speed ($cm \cdot s^{-1}$)	Stand. dev. of speed ($cm \cdot s^{-1}$)	Latitude (°N)	Longitude (°W)	Depth (m)	Total water depth (m)
7	1998	VK980403.A03	/MMS/	04/03/1998	04/30/1998	88.819	30.444	19.618	29.0705	87.8568	24.0	1300.0
	1998	VK971115.A23	/MMS/	02/01/1998	04/03/1998	70.345	24.515	11.341	29.0705	87.8568	28.0	1300.0
	1998	VK980403.A04	/MMS/	04/03/1998	04/30/1998	81.354	29.113	18.685	29.0705	87.8568	28.0	1300.0
	1998	VK971115.A24	/MMS/	02/01/1998	04/03/1998	66.286	23.698	11.109	29.0705	87.8568	32.0	1300.0
	1998	VK980403.A05	/MMS/	04/03/1998	04/30/1998	78.814	27.760	18.048	29.0705	87.8568	32.0	1300.0
	1998	VK971115.A25	/MMS/	02/01/1998	04/03/1998	64.005	22.938	11.009	29.0705	87.8568	36.0	1300.0
	1998	VK980403.A06	/MMS/	04/03/1998	04/30/1998	77.191	26.526	17.686	29.0705	87.8568	36.0	1300.0
	1998	VK971115.A26	/MMS/	02/01/1998	04/03/1998	58.071	22.303	11.047	29.0705	87.8568	40.0	1300.0
	1998	VK980403.A07	/MMS/	04/03/1998	04/30/1998	71.363	25.711	17.552	29.0705	87.8568	40.0	1300.0
	1998	VK971115.A27	/MMS/	02/01/1998	04/03/1998	57.904	21.748	11.102	29.0705	87.8568	44.0	1300.0
	1998	VK980403.A08	/MMS/	04/03/1998	04/30/1998	63.725	25.150	17.487	29.0705	87.8568	44.0	1300.0
	1998	VK971115.A28	/MMS/	02/01/1998	04/03/1998	56.600	21.262	11.153	29.0705	87.8568	48.0	1300.0
	1998	VK980403.A09	/MMS/	04/03/1998	04/30/1998	59.345	24.787	17.357	29.0705	87.8568	48.0	1300.0
	1998	VK971115.A29	/MMS/	02/01/1998	04/03/1998	54.700	20.837	11.023	29.0705	87.8568	52.0	1300.0
	1998	VK980403.A10	/MMS/	04/03/1998	04/30/1998	60.134	24.554	17.202	29.0705	87.8568	52.0	1300.0
	1998	VK971115.A30	/MMS/	02/01/1998	04/03/1998	44.102	15.096	7.968	29.0705	87.8568	56.0	1300.0
	1998	VK980403.A11	/MMS/	04/03/1998	04/30/1998	42.916	13.320	9.478	29.0705	87.8568	56.0	1300.0
	1998	VK971115.A31	/MMS/	02/01/1998	04/03/1998	46.865	15.724	8.378	29.0705	87.8568	60.0	1300.0
	1998	VK980403.A12	/MMS/	04/03/1998	04/30/1998	46.565	14.827	10.485	29.0705	87.8568	60.0	1300.0
	1998	VK971115.A32	/MMS/	02/01/1998	04/03/1998	53.778	20.664	11.138	29.0705	87.8568	64.0	1300.0
	1998	VK980403.A13	/MMS/	04/03/1998	04/30/1998	60.802	24.730	16.755	29.0705	87.8568	64.0	1300.0
	1998	VK971115.A33	/MMS/	02/01/1998	04/03/1998	54.730	20.488	11.191	29.0705	87.8568	68.0	1300.0
	1998	VK980403.A14	/MMS/	04/03/1998	04/30/1998	60.807	24.341	16.556	29.0705	87.8568	68.0	1300.0
	1998	VK971115.A34	/MMS/	02/01/1998	04/03/1998	53.703	20.123	11.030	29.0705	87.8568	72.0	1300.0
	1998	VK980403.A15	/MMS/	04/03/1998	04/30/1998	61.205	23.428	16.392	29.0705	87.8568	72.0	1300.0
	1998	VK971115.C04	/MMS/	02/01/1998	04/03/1998	42.077	12.071	8.745	29.0705	87.8568	500.0	1300.0
	1998	VK980403.C01	/MMS/	04/03/1998	04/30/1998	48.184	15.480	11.408	29.0705	87.8568	500.0	1300.0
	1998	VK971115.C05	/MMS/	02/01/1998	04/03/1998	26.396	6.673	4.279	29.0705	87.8568	1290.0	1300.0
	1998	VK980403.C02	/MMS/	04/03/1998	04/30/1998	18.196	6.250	3.635	29.0705	87.8568	1290.0	1300.0
	1998	DD980405.A01	/MMS/	04/05/1998	04/30/1998	77.737	24.592	14.008	29.0032	87.3532	8.0	1300.0
	1998	DD971116.A01	/MMS/	02/01/1998	04/04/1998	92.853	29.567	14.598	29.0032	87.3532	12.0	1300.0
	1998	DD980405.A02	/MMS/	04/05/1998	04/30/1998	75.980	23.768	14.345	29.0032	87.3532	12.0	1300.0
	1998	DD971116.A02	/MMS/	02/01/1998	04/04/1998	86.230	28.572	13.872	29.0032	87.3532	16.0	1300.0
	1998	DD980405.A03	/MMS/	04/05/1998	04/30/1998	72.834	23.002	13.913	29.0032	87.3532	16.0	1300.0

Table B-5. Speed statistics for energetic current events associated with cyclonic eddies. (continued)

Event No.	Year	Filename	Directory	Event start date (m/d/y)	Event end date (m/d/y)	Maximum speed ($cm \cdot s^{-1}$)	Mean speed ($cm \cdot s^{-1}$)	Stand. dev. of speed ($cm \cdot s^{-1}$)	Latitude (°N)	Longitude (°W)	Depth (m)	Total water depth (m)
7	1998	DD971116.A03	/MMS/	02/01/1998	04/04/1998	79.067	27.876	13.390	29.0032	87.3532	20.0	1300.0
	1998	DD980405.A04	/MMS/	04/05/1998	04/30/1998	65.398	22.033	13.036	29.0032	87.3532	20.0	1300.0
	1998	DD971116.A04	/MMS/	02/01/1998	04/04/1998	72.439	27.316	13.041	29.0032	87.3532	24.0	1300.0
	1998	DD980405.A05	/MMS/	04/05/1998	04/30/1998	61.179	21.360	12.140	29.0032	87.3532	24.0	1300.0
	1998	DD971116.A05	/MMS/	02/01/1998	04/04/1998	64.519	26.761	12.891	29.0032	87.3532	28.0	1300.0
	1998	DD980405.A06	/MMS/	04/05/1998	04/30/1998	58.065	20.529	11.309	29.0032	87.3532	28.0	1300.0
	1998	DD971116.A06	/MMS/	02/01/1998	04/04/1998	64.213	26.309	12.802	29.0032	87.3532	32.0	1300.0
	1998	DD980405.A07	/MMS/	04/05/1998	04/30/1998	56.243	19.636	10.733	29.0032	87.3532	32.0	1300.0
	1998	DD971116.A07	/MMS/	02/01/1998	04/04/1998	63.637	25.960	12.688	29.0032	87.3532	36.0	1300.0
	1998	DD980405.A08	/MMS/	04/05/1998	04/30/1998	53.875	19.333	10.411	29.0032	87.3532	36.0	1300.0
	1998	DD971116.A08	/MMS/	02/01/1998	04/04/1998	61.502	25.733	12.476	29.0032	87.3532	40.0	1300.0
	1998	DD980405.A09	/MMS/	04/05/1998	04/30/1998	49.541	19.239	10.019	29.0032	87.3532	40.0	1300.0
	1998	DD971116.A09	/MMS/	02/01/1998	04/04/1998	60.210	25.541	12.418	29.0032	87.3532	44.0	1300.0
	1998	DD980405.A10	/MMS/	04/05/1998	04/30/1998	47.182	19.181	9.756	29.0032	87.3532	44.0	1300.0
	1998	DD971116.A10	/MMS/	02/01/1998	04/04/1998	60.909	25.452	12.396	29.0032	87.3532	48.0	1300.0
	1998	DD980405.A11	/MMS/	04/05/1998	04/30/1998	48.734	19.057	9.669	29.0032	87.3532	48.0	1300.0
	1998	DD971116.A11	/MMS/	02/01/1998	04/04/1998	61.712	25.375	12.406	29.0032	87.3532	52.0	1300.0
	1998	DD980405.A12	/MMS/	04/05/1998	04/30/1998	49.283	18.404	9.830	29.0032	87.3532	52.0	1300.0
	1998	DD971116.A12	/MMS/	02/01/1998	04/04/1998	57.255	22.195	11.039	29.0032	87.3532	56.0	1300.0
	1998	DD980405.A13	/MMS/	04/05/1998	04/30/1998	48.264	15.774	9.736	29.0032	87.3532	56.0	1300.0
	1998	DD971116.A13	/MMS/	02/01/1998	04/04/1998	58.300	23.344	11.474	29.0032	87.3532	60.0	1300.0
	1998	DD980405.A14	/MMS/	04/05/1998	04/30/1998	48.811	16.438	9.750	29.0032	87.3532	60.0	1300.0
	1998	DD971116.A14	/MMS/	02/01/1998	04/04/1998	61.155	25.588	12.405	29.0032	87.3532	64.0	1300.0
	1998	DD980405.A15	/MMS/	04/05/1998	04/30/1998	49.258	17.998	9.795	29.0032	87.3532	64.0	1300.0
	1998	DD971116.A15	/MMS/	02/01/1998	04/04/1998	61.331	25.400	12.269	29.0032	87.3532	68.0	1300.0
	1998	DD980405.A16	/MMS/	04/05/1998	04/30/1998	48.314	17.771	9.711	29.0032	87.3532	68.0	1300.0
	1998	DD971116.A16	/MMS/	02/01/1998	04/04/1998	58.393	24.794	11.809	29.0032	87.3532	72.0	1300.0
	1998	DD980405.A17	/MMS/	04/05/1998	04/30/1998	47.653	17.316	9.280	29.0032	87.3532	72.0	1300.0
	1998	DD971116.C01	/MMS/	02/01/1998	04/04/1998	38.590	13.070	7.584	29.0032	87.3532	500.0	1300.0
	1998	DD980405.C01	/MMS/	04/05/1998	04/30/1998	29.292	8.679	6.826	29.0032	87.3532	500.0	1300.0
	1998	DD971116.C02	/MMS/	02/01/1998	04/04/1998	22.898	8.273	4.720	29.0032	87.3532	1290.0	1300.0
	1998	DD980405.C02	/MMS/	04/05/1998	04/30/1998	25.500	7.687	4.772	29.0032	87.3532	1290.0	1300.0
8	1998	GC980409.A01	/INDUSTRY/	04/09/1998	05/14/1998	55.340	18.752	9.370	27.7302	91.1419	20.0	674.3
	1998	GC980409.A02	/INDUSTRY/	04/09/1998	05/14/1998	52.002	17.624	9.414	27.7302	91.1419	36.0	674.3

Table B-5. Speed statistics for energetic current events associated with cyclonic eddies. (continued)

Event No.	Year	Filename	Directory	Event start date (m/d/y)	Event end date (m/d/y)	Maximum speed ($cm \cdot s^{-1}$)	Mean speed ($cm \cdot s^{-1}$)	Stand. dev. of speed ($cm \cdot s^{-1}$)	Latitude (°N)	Longitude (°W)	Depth (m)	Total water depth (m)
8	1998	GC980409.A03	/INDUSTRY/	04/09/1998	05/14/1998	43.729	15.446	8.114	27.7302	91.1419	52.0	674.3
	1998	GC980409.A04	/INDUSTRY/	04/09/1998	05/14/1998	45.607	13.688	6.981	27.7302	91.1419	68.0	674.3
	1998	GC980409.A05	/INDUSTRY/	04/09/1998	05/14/1998	47.321	12.505	7.127	27.7302	91.1419	84.0	674.3
	1998	GC980409.A06	/INDUSTRY/	04/09/1998	05/14/1998	50.249	12.488	8.069	27.7302	91.1419	100.0	674.3
	1998	GC980409.A07	/INDUSTRY/	04/09/1998	05/14/1998	52.402	12.419	7.758	27.7302	91.1419	116.0	674.3
	1998	GC980409.A08	/INDUSTRY/	04/09/1998	05/14/1998	53.106	11.847	7.648	27.7302	91.1419	132.0	674.3
	1998	GC980409.A09	/INDUSTRY/	04/09/1998	05/14/1998	51.539	11.631	7.574	27.7302	91.1419	148.0	674.3
	1998	GC980409.A10	/INDUSTRY/	04/09/1998	05/14/1998	57.873	11.784	7.795	27.7302	91.1419	164.0	674.3
	1998	GC980409.A11	/INDUSTRY/	04/09/1998	05/14/1998	62.426	12.074	8.048	27.7302	91.1419	180.0	674.3
	1998	GC980409.A12	/INDUSTRY/	04/09/1998	05/14/1998	59.641	11.821	7.303	27.7302	91.1419	196.0	674.3
	1998	GC980409.A13	/INDUSTRY/	04/09/1998	05/14/1998	59.701	11.087	6.554	27.7302	91.1419	212.0	674.3
	1998	GC980409.A14	/INDUSTRY/	04/09/1998	05/14/1998	57.273	10.378	6.342	27.7302	91.1419	228.0	674.3
	1998	GC980409.A15	/INDUSTRY/	04/09/1998	05/14/1998	48.708	10.031	6.036	27.7302	91.1419	244.0	674.3
	1998	GC980409.A16	/INDUSTRY/	04/09/1998	05/14/1998	39.699	9.631	5.966	27.7302	91.1419	260.0	674.3
	1998	GC980409.A17	/INDUSTRY/	04/09/1998	05/14/1998	40.475	9.023	5.695	27.7302	91.1419	276.0	674.3
	1998	GC980409.A18	/INDUSTRY/	04/09/1998	05/14/1998	34.918	8.649	5.226	27.7302	91.1419	292.0	674.3
	1998	GC980409.A19	/INDUSTRY/	04/09/1998	05/14/1998	30.887	8.548	4.799	27.7302	91.1419	308.0	674.3
	1998	GC980409.A20	/INDUSTRY/	04/09/1998	05/14/1998	25.739	8.247	4.586	27.7302	91.1419	324.0	674.3
	1998	GC980409.A21	/INDUSTRY/	04/09/1998	05/14/1998	25.164	7.627	4.312	27.7302	91.1419	340.0	674.3
	1998	GC980409.A22	/INDUSTRY/	04/09/1998	05/14/1998	23.005	7.081	4.064	27.7302	91.1419	356.0	674.3
	1998	GC980409.A23	/INDUSTRY/	04/09/1998	05/14/1998	20.988	7.073	3.957	27.7302	91.1419	372.0	674.3
	1998	GC980409.A24	/INDUSTRY/	04/09/1998	05/14/1998	20.248	7.291	4.136	27.7302	91.1419	388.0	674.3
	1998	GC980409.A25	/INDUSTRY/	04/09/1998	05/14/1998	22.204	7.485	4.394	27.7302	91.1419	404.0	674.3
	1998	GC980409.A26	/INDUSTRY/	04/09/1998	05/14/1998	21.030	7.825	4.427	27.7302	91.1419	420.0	674.3
	1998	GC980409.A27	/INDUSTRY/	04/09/1998	05/14/1998	20.156	8.031	4.373	27.7302	91.1419	436.0	674.3
	1998	GC980409.A28	/INDUSTRY/	04/09/1998	05/14/1998	20.506	8.246	4.110	27.7302	91.1419	452.0	674.3
	1998	GC980409.A29	/INDUSTRY/	04/09/1998	05/14/1998	22.853	8.415	4.004	27.7302	91.1419	468.0	674.3
	1998	GC980409.A30	/INDUSTRY/	04/09/1998	05/14/1998	25.005	8.581	4.093	27.7302	91.1419	484.0	674.3
	1998	GC980409.A31	/INDUSTRY/	04/09/1998	05/14/1998	23.286	8.630	4.424	27.7302	91.1419	500.0	674.3
	1998	GC980409.A32	/INDUSTRY/	04/09/1998	05/14/1998	28.779	8.774	4.485	27.7302	91.1419	516.0	674.3
	1998	GC980409.A33	/INDUSTRY/	04/09/1998	05/14/1998	26.926	6.367	3.651	27.7302	91.1419	532.0	674.3
	1998	GC980409.A34	/INDUSTRY/	04/09/1998	05/14/1998	29.568	5.388	3.356	27.7302	91.1419	548.0	674.3
	1998	GC980409.A35	/INDUSTRY/	04/09/1998	05/14/1998	30.700	5.142	3.481	27.7302	91.1419	564.0	674.3
	1998	GC980409.A36	/INDUSTRY/	04/09/1998	05/14/1998	27.409	5.302	3.562	27.7302	91.1419	580.0	674.3

Table B-5. Speed statistics for energetic current events associated with cyclonic eddies. (continued)

Event No.	Year	Filename	Directory	Event start date (m/d/y)	Event end date (m/d/y)	Maximum speed ($cm \cdot s^{-1}$)	Mean speed ($cm \cdot s^{-1}$)	Stand. dev. of speed ($cm \cdot s^{-1}$)	Latitude (°N)	Longitude (°W)	Depth (m)	Total water depth (m)
8	1998	GC980409.A37	/INDUSTRY/	04/09/1998	05/14/1998	27.409	4.639	3.444	27.7302	91.1419	596.0	674.3
	1998	GC980409.A38	/INDUSTRY/	04/09/1998	05/14/1998	33.155	5.598	3.933	27.7302	91.1419	612.0	674.3
	1998	GC980409.A39	/INDUSTRY/	04/09/1998	05/14/1998	37.477	7.294	5.057	27.7302	91.1419	628.0	674.3

Notes by event number

1 1985: August - September

A two-week lag occurs between the motions at SAIC Q and SAIC S, with SAIC Q leading. The currents are to the northwest, indicating the northeastern limb of the cyclone. Data from SAIC Q and S are plotted in Figure 6.3.3-5.

2 1985: June - September

The record at 100 m on SAIC T is suspicious; however, the record coincides with a cyclone passing through the region. West of Fast Eddy, a 60 $cm \cdot s^{-1}$ event occurs at 300 m on July 29 at SAIC T. Data from SAIC T are plotted in Figure 6.3.3-5.

3 1985: December 1985 - April 1986

A large low-frequency oscillation is seen at SAIC T. During this time a cyclone and Fast Eddy were adjacent to the mooring, with Fast Eddy to the east. The oscillation may be caused by the cyclone or by the western limb of Fast Eddy. It is unclear from the satellite data what is occurring. Data from SAIC T are plotted in Figure 6.3.3-5.

4 1986: March - April

The currents are south-southeast at SAIC Q in response to the western limb of a cyclone situated north of Fast Eddy. There is some slight indication that these cyclonic currents extend to 1500 m. Data from SAIC Q are plotted in Figure 6.3.3-5.

5 1992: October - December

Currents are westward, weak, and variable at LATEX 12 as a slope cyclone pushes past the mooring. Data from LATEX 12 are plotted in Figure 6.3.4-2. A detail of currents during this event is shown in Figure A.5-1.

6 1993: September - December

Predominantly southwestward currents, with peak speeds of ~30 $cm \cdot s^{-1}$, occur in November/December at 101 m on LATEX 49. Data from LATEX 49 are plotted in Figure 6.3.4-2. A detail of currents during this event is shown in Figure A.5-2.

7 1998: February - April

A small cyclone over the DeSoto Canyon region influenced the currents at the SAIC EIS moorings. Data from SAIC EIS are plotted in Figure 6.3.5-2. A detail of currents during this event is shown in Figure A.5-3.

Table B-5. Speed statistics for energetic current events associated with cyclonic eddies. (continued)

Notes by event number (continued)

8 1998: April - May

Although the record at Industry GC236 is short, coherent low-frequency oscillations are clear. The currents reach speeds of 50 $cm \cdot s^{-1}$ and are directed to the northwest in response to a cyclone. Data from Industry GC236 are plotted in Figure 6.3.12-13.

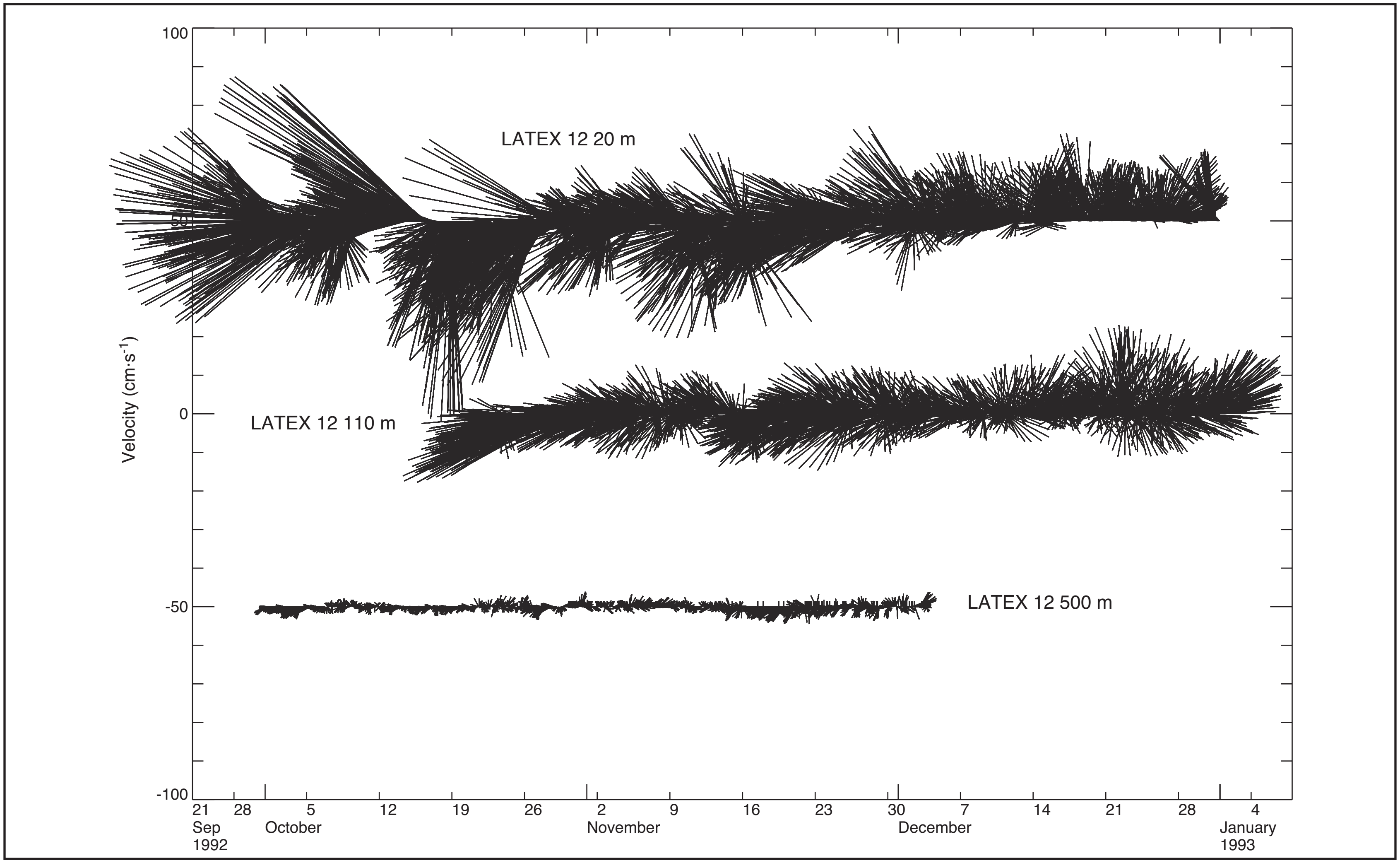

Figure B.5-1. Influence of a cyclonic eddy on currents in the central Gulf at LATEX mooring 12, October through December 1992. See also Table B-5, event 5.

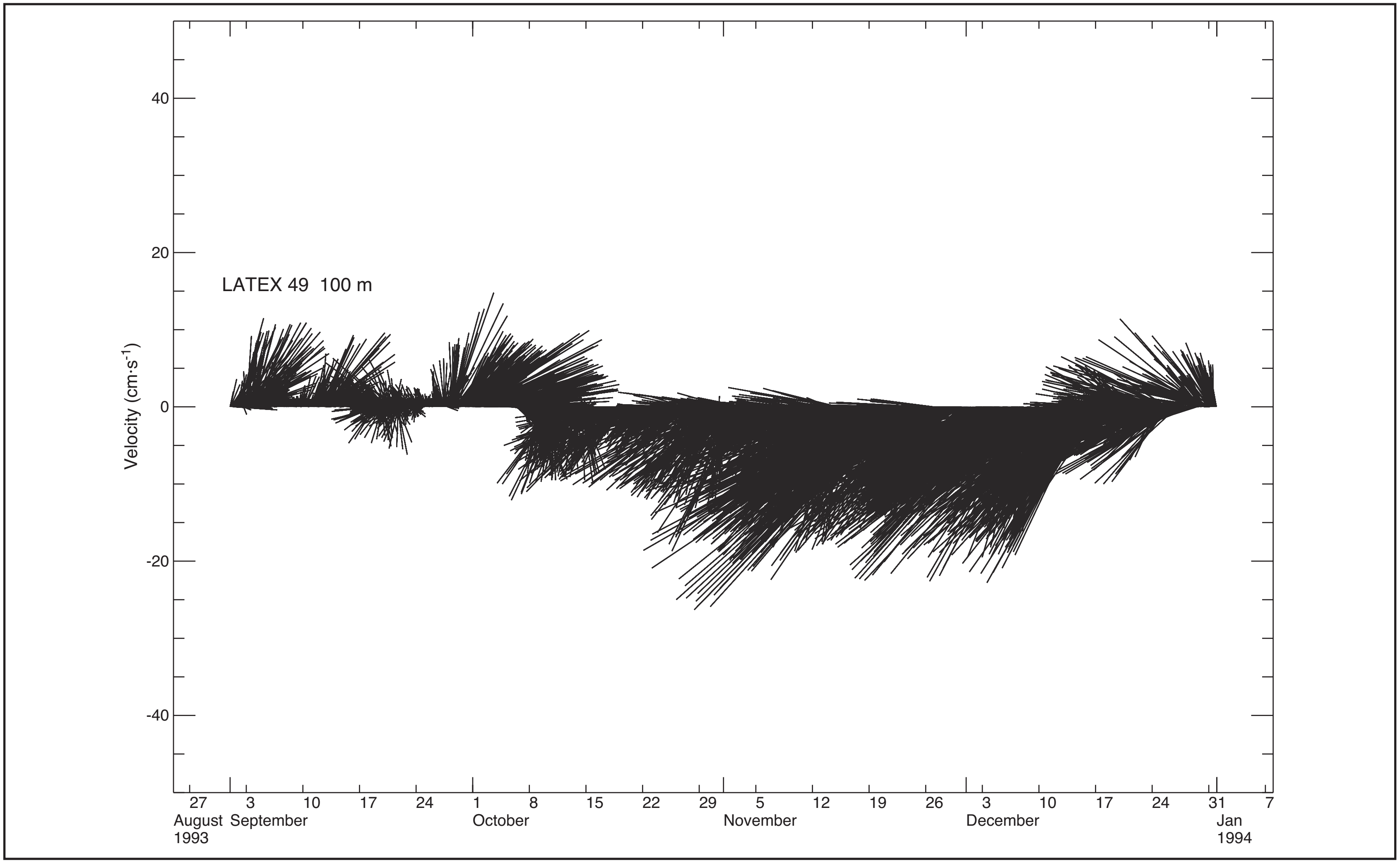

Figure B.5-2. Influence of a cyclonic eddy on currents at 100-m depth in the western Gulf at LATEX mooring 49, September through December 1993. See also Table B-5, event 6.

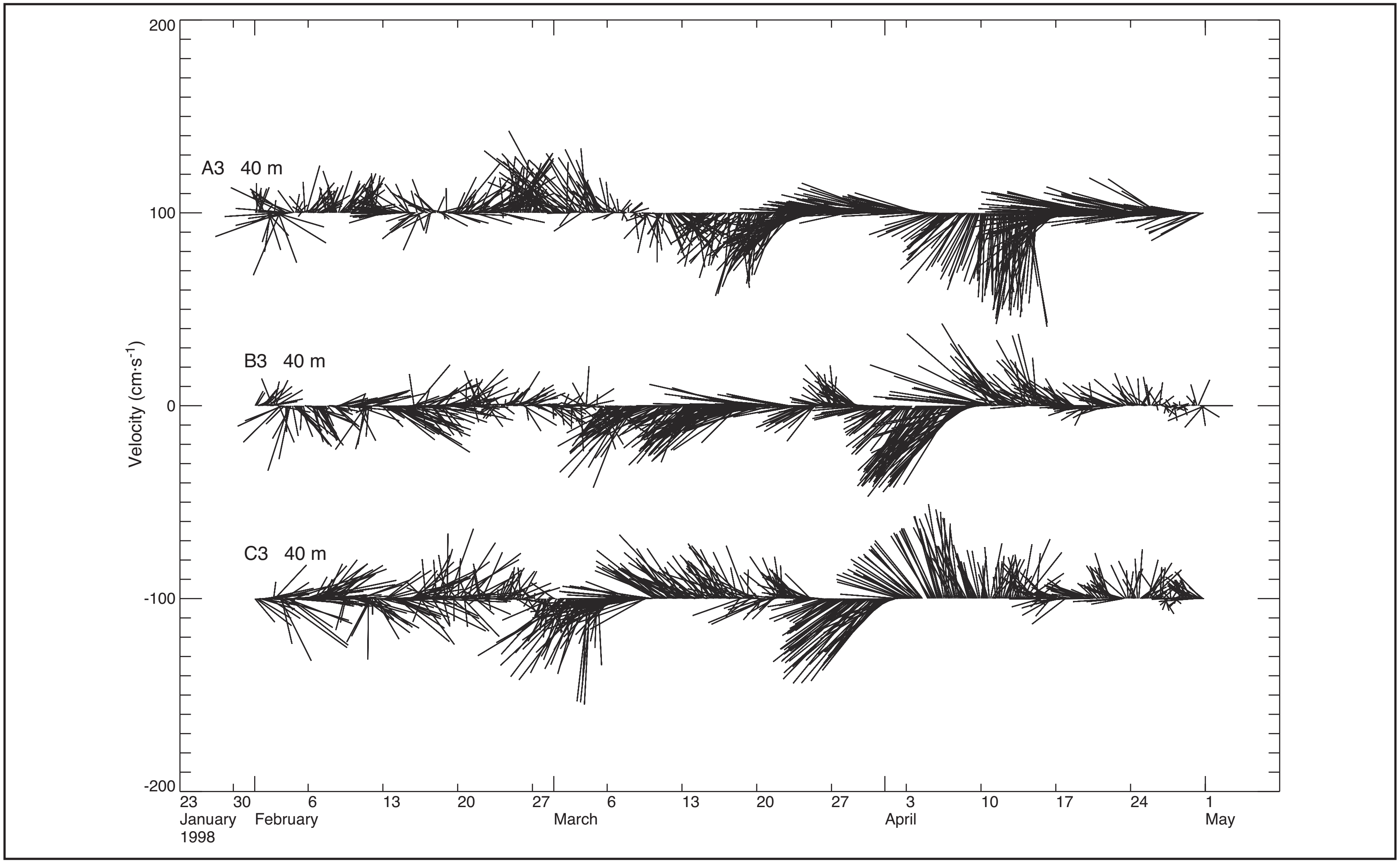

Figure B.5-3. Influence of a cyclonic eddy on currents at 40-m depth over DeSoto Canyon at SAIC EIS moorings, February through April 1998. See also Table B-5, event 7.

Table B-6. Speed statistics for energetic current events associated with tropical cyclones. Given are the name of the file containing the event (keyed to the directory on the CD-ROM database), the start and stop dates used to characterize the event, maximum speed, mean speed, standard deviation of speed, mooring location, depth of the instrument, and total water depth. Comments on the event, keyed by the event number, are given in the notes below the table.

Event No.	Year	Filename	Directory	Event start date (m/d/y)	Event end date (m/d/y)	Maximum speed ($cm \cdot s^{-1}$)	Mean speed ($cm \cdot s^{-1}$)	Stand. dev. of speed ($cm \cdot s^{-1}$)	Latitude (°N)	Longitude (°W)	Depth (m)	Total water depth (m)
1	1980	PI800717.C04	/NODC_DEEP/	08/09/1980	08/19/1980	93.898	27.451	17.260	26.5000	96.1917	200.0	730.0
	1980	PI800717.C05	/NODC_DEEP/	08/09/1980	08/19/1980	49.660	12.222	8.695	26.5000	96.1917	450.0	730.0
	1980	PI800717.C06	/NODC_DEEP/	08/09/1980	08/19/1980	27.819	11.627	5.746	26.5000	96.1917	575.0	730.0
	1980	PI800717.C07	/NODC_DEEP/	08/09/1980	08/19/1980	24.879	7.274	3.704	26.5000	96.1917	700.0	730.0
	1980	PI800717.C01	/NODC_DEEP/	08/09/1980	08/19/1980	56.801	18.894	10.425	25.9900	96.1517	200.0	730.0
	1980	PI800717.C02	/NODC_DEEP/	08/09/1980	08/19/1980	41.958	12.716	8.285	25.9900	96.1517	450.0	730.0
	1980	PI800717.C03	/NODC_DEEP/	08/09/1980	08/19/1980	33.839	10.128	7.082	25.9900	96.1517	700.0	730.0
2	1983	HH830127.C01	/NODC_DEEP/	08/23/1983	08/29/1983	44.383	15.276	10.203	25.7150	84.8850	172.0	1697.0
	1983	HH830729.C01	/NODC_DEEP/	08/23/1983	08/29/1983	20.006	5.600	4.661	25.7150	84.8850	400.0	1697.0
	1983	HH830730.C01	/NODC_DEEP/	08/23/1983	08/29/1983	12.333	2.466	1.405	25.7150	84.8850	738.0	1697.0
	1983	HH830127.C02	/NODC_DEEP/	08/23/1983	08/29/1983	4.855	2.596	1.047	25.7150	84.8850	1100.0	1697.0
	1983	HH830730.C02	/NODC_DEEP/	08/23/1983	08/29/1983	6.621	1.140	0.811	25.7150	84.8850	1600.0	1697.0
3	1985	HH850801.C01	/NODC_DEEP/	08/31/1985	09/02/1985	82.303	54.043	11.691	25.7150	84.8850	172.0	1697.0
	1985	HH850801.C02	/NODC_DEEP/	08/31/1985	09/02/1985	38.647	19.403	9.827	25.7150	84.8850	400.0	1697.0
	1985	HH850731.C01	/NODC_DEEP/	08/31/1985	09/02/1985	10.032	2.413	1.811	25.7150	84.8850	738.0	1697.0
	1985	HH850731.C02	/NODC_DEEP/	08/31/1985	09/02/1985	19.318	12.627	1.587	25.7150	84.8850	1100.0	1697.0
	1985	HH850801.C03	/NODC_DEEP/	08/31/1985	09/02/1985	31.327	16.749	9.911	25.6003	85.4995	703.0	3200.0
	1985	HH850801.C04	/NODC_DEEP/	08/31/1985	09/02/1985	12.741	8.379	2.257	25.6003	85.4995	1565.0	3200.0
	1985	HH850801.C05	/NODC_DEEP/	08/31/1985	09/02/1985	13.161	8.150	2.514	25.6003	85.4995	2364.0	3200.0
	1985	HH850801.C06	/NODC_DEEP/	08/31/1985	09/02/1985	9.048	4.639	2.610	25.6003	85.4995	3174.0	3200.0
4	1987	GB870405.C05	/NODC_DEEP/	08/09/1987	08/17/1987	11.890	2.119	2.176	27.4683	91.9932	725.0	845.0
	1987	KC870406.C04	/NODC_DEEP/	08/09/1987	08/17/1987	9.982	2.019	1.915	26.7400	91.9950	1650.0	1750.0
	1987	AB870406.C03	/NODC_DEEP/	08/09/1987	08/17/1987	22.743	7.444	3.739	25.6532	92.0333	1650.0	3000.0
5	1988	GB871108.C01	/NODC_DEEP/	09/07/1988	09/11/1988	35.433	19.214	7.111	27.4683	91.9932	100.0	845.0
	1988	KC871108.C01	/NODC_DEEP/	09/07/1988	09/09/1988	39.922	26.819	6.815	26.7400	91.9950	100.0	1750.0
	1988	AB871109.C01	/NODC_DEEP/	09/07/1988	09/11/1988	98.289	72.923	12.192	25.6532	92.0333	100.0	3000.0
6	1988	GB871108.C01	/NODC_DEEP/	09/15/1988	09/25/1988	45.615	18.179	9.560	27.4683	91.9932	100.0	845.0
	1988	GB871108.C02	/NODC_DEEP/	09/15/1988	09/25/1988	12.424	6.256	2.112	27.4683	91.9932	300.0	845.0
	1988	GB871202.C01	/NODC_DEEP/	09/15/1988	09/25/1988	25.524	15.413	3.335	27.4683	91.9932	305.0	845.0
	1988	GB870405.C05	/NODC_DEEP/	09/15/1988	09/25/1988	17.741	5.725	4.066	27.4683	91.9932	725.0	845.0

Table B-6. Speed statistics for energetic current events associated with tropical cyclones. (continued)

Event No.	Year	Filename	Directory	Event start date (m/d/y)	Event end date (m/d/y)	Maximum speed (cm·s^{-1})	Mean speed (cm·s^{-1})	Stand. dev. of speed (cm·s^{-1})	Latitude (°N)	Longitude (°W)	Depth (m)	Total water depth (m)
6	1988	KC871108.C03	/NODC_DEEP/	09/15/1988	09/25/1988	16.340	7.623	3.692	26.7400	91.9950	725.0	1750.0
	1988	KC870406.C04	/NODC_DEEP/	09/15/1988	09/20/1988	6.637	3.153	1.513	26.7400	91.9950	1650.0	1750.0
	1988	AB871109.C01	/NODC_DEEP/	09/15/1988	09/25/1988	120.767	91.085	13.223	25.6532	92.0333	100.0	3000.0
	1988	AB880409.C01	/NODC_DEEP/	09/15/1988	09/25/1988	44.903	34.747	3.819	25.6532	92.0333	300.0	3000.0
	1988	AB871109.C02	/NODC_DEEP/	09/15/1988	09/25/1988	20.068	10.668	3.689	25.6532	92.0333	725.0	3000.0
	1988	AB870406.C03	/NODC_DEEP/	09/15/1988	09/25/1988	5.050	1.540	0.263	25.6532	92.0333	1650.0	3000.0
	1988	AB880409.C02	/NODC_DEEP/	09/15/1988	09/25/1988	5.234	2.053	1.032	25.6532	92.0333	2500.0	3000.0
	1988	DD880825.C01	/TAMU/	09/15/1988	09/25/1988	61.999	29.076	13.327	29.3983	87.3450	20.0	430.0
	1988	DD880825.C02	/TAMU/	09/15/1988	09/25/1988	53.001	20.634	12.566	29.3983	87.3450	150.0	430.0
7	1992	GC920415.C01	/TAMU/	08/24/1992	09/06/1992	138.686	26.143	20.653	27.9240	90.4950	27.0	515.0
	1992	GC920415.C02	/TAMU/	08/24/1992	09/06/1992	69.720	32.215	13.171	27.9240	90.4950	115.0	515.0
	1992	GC920415.C03	/TAMU/	08/24/1992	09/06/1992	5.714	3.420	0.827	27.9240	90.4950	505.0	515.0
8	1997	VK970710.A01	/MMS/	07/16/1997	07/30/1997	106.663	23.135	18.360	29.0592	88.3900	12.0	500.0
	1997	VK970710.A02	/MMS/	07/16/1997	07/30/1997	89.581	20.391	15.476	29.0592	88.3900	16.0	500.0
	1997	VK970710.A03	/MMS/	07/16/1997	07/30/1997	62.689	18.597	12.157	29.0592	88.3900	20.0	500.0
	1997	VK970710.A04	/MMS/	07/16/1997	07/30/1997	55.260	15.620	8.520	29.0592	88.3900	24.0	500.0
	1997	VK970710.A05	/MMS/	07/16/1997	07/30/1997	38.308	16.429	7.338	29.0592	88.3900	28.0	500.0
	1997	VK970710.A06	/MMS/	07/16/1997	07/30/1997	43.089	17.361	8.930	29.0592	88.3900	32.0	500.0
	1997	VK970710.A07	/MMS/	07/16/1997	07/30/1997	42.314	16.922	9.245	29.0592	88.3900	36.0	500.0
	1997	VK970710.A08	/MMS/	07/16/1997	07/30/1997	38.342	15.863	8.317	29.0592	88.3900	40.0	500.0
	1997	VK970710.A09	/MMS/	07/16/1997	07/30/1997	37.420	15.160	7.731	29.0592	88.3900	44.0	500.0
	1997	VK970710.A10	/MMS/	07/16/1997	07/30/1997	37.510	15.321	7.352	29.0592	88.3900	48.0	500.0
	1997	VK970710.A11	/MMS/	07/16/1997	07/30/1997	32.336	15.796	7.446	29.0592	88.3900	52.0	500.0
	1997	VK970710.A12	/MMS/	07/16/1997	07/30/1997	35.007	16.774	7.738	29.0592	88.3900	56.0	500.0
	1997	VK970710.A13	/MMS/	07/16/1997	07/30/1997	37.173	17.625	8.098	29.0592	88.3900	60.0	500.0
	1997	VK970710.A14	/MMS/	07/16/1997	07/30/1997	37.989	16.110	7.771	29.0592	88.3900	64.0	500.0
	1997	VK970710.A15	/MMS/	07/16/1997	07/30/1997	38.828	16.596	8.456	29.0592	88.3900	68.0	500.0
	1997	VK970710.A16	/MMS/	07/16/1997	07/30/1997	39.885	18.001	9.426	29.0592	88.3900	72.0	500.0
	1997	VK970710.A17	/MMS/	07/16/1997	07/30/1997	42.405	17.670	9.246	29.0592	88.3900	76.0	500.0
	1997	VK970710.C01	/MMS/	07/16/1997	07/30/1997	33.362	20.809	4.229	29.0592	88.3900	200.0	500.0
	1997	VK970710.C02	/MMS/	07/16/1997	07/30/1997	29.875	19.000	3.741	29.0592	88.3900	300.0	500.0
	1997	VK970710.C03	/MMS/	07/16/1997	07/30/1997	29.099	5.740	4.053	29.0592	88.3900	490.0	500.0
	1997	MC970710.C01	/MMS/	07/16/1997	07/30/1997	20.902	10.817	3.717	28.7662	88.2650	500.0	1300.0
	1997	MC970710.C02	/MMS/	07/16/1997	07/30/1997	15.629	3.054	2.600	28.7662	88.2650	1310.0	1320.0

Table B-6. Speed statistics for energetic current events associated with tropical cyclones. (continued)

Event No.	Year	Filename	Directory	Event start date (m/d/y)	Event end date (m/d/y)	Maximum speed (cm·s^{-1})	Mean speed (cm·s^{-1})	Stand. dev. of speed (cm·s^{-1})	Latitude (°N)	Longitude (°W)	Depth (m)	Total water depth (m)
8	1997	VK970712.C01	/MMS/	07/16/1997	07/30/1997	41.212	24.289	5.339	29.2120	87.8722	200.0	500.0
	1997	VK970712.C02	/MMS/	07/16/1997	07/30/1997	33.938	22.559	4.743	29.2120	87.8722	300.0	500.0
	1997	VK970712.C03	/MMS/	07/16/1997	07/30/1997	15.597	5.621	3.499	29.2120	87.8722	490.0	500.0
	1997	VK970712.C04	/MMS/	07/16/1997	07/30/1997	14.469	5.323	3.527	29.0705	87.8568	500.0	1300.0
	1997	DD970324.C01	/MMS/	07/16/1997	07/16/1997	10.983	9.328	1.202	29.3712	87.3563	200.0	500.0
	1997	DD970717.C01	/MMS/	07/17/1997	07/30/1997	26.384	10.353	4.755	29.3712	87.3563	200.0	500.0
	1997	DD970324.C02	/MMS/	07/16/1997	07/16/1997	10.692	8.107	1.365	29.3712	87.3563	300.0	500.0
	1997	DD970717.C02	/MMS/	07/17/1997	07/30/1997	35.104	12.103	4.822	29.3712	87.3563	300.0	500.0
	1997	DD970324.C03	/MMS/	07/16/1997	07/16/1997	11.797	6.601	3.680	29.3712	87.3563	490.0	500.0
	1997	DD970717.C03	/MMS/	07/17/1997	07/30/1997	21.602	8.789	4.861	29.3712	87.3563	490.0	500.0
	1997	DD970324.C04	/MMS/	07/16/1997	07/17/1997	16.001	13.184	1.023	29.0032	87.3532	500.0	1300.0
	1997	DD970718.C01	/MMS/	07/18/1997	07/30/1997	15.635	4.154	2.865	29.0032	87.3532	500.0	1300.0
	1997	DD970324.C05	/MMS/	07/16/1997	07/17/1997	6.330	2.213	1.474	29.0032	87.3532	1290.0	1300.0
	1997	DD970324.C06	/MMS/	07/16/1997	07/16/1997	3.140	1.404	0.573	29.3348	86.8520	200.0	500.0
	1997	DD970716.C01	/MMS/	07/16/1997	07/30/1997	28.998	8.241	6.221	29.3348	86.8520	200.0	500.0
	1997	DD970324.C07	/MMS/	07/16/1997	07/16/1997	16.404	15.025	0.776	29.3348	86.8520	300.0	500.0
	1997	DD970324.C08	/MMS/	07/16/1997	07/16/1997	3.097	1.774	0.913	29.3348	86.8520	490.0	500.0
	1997	DD970716.C02	/MMS/	07/16/1997	07/30/1997	15.502	5.866	3.475	29.3348	86.8520	490.0	500.0
	1997	AT970711.A01	/INDUSTRY/	07/16/1997	07/30/1997	50.002	15.346	7.801	27.6019	88.6663	20.0	1843.4
	1997	AT970711.A02	/INDUSTRY/	07/16/1997	07/30/1997	43.546	16.535	8.293	27.6019	88.6663	36.0	1843.4
	1997	AT970711.A03	/INDUSTRY/	07/16/1997	07/30/1997	42.547	16.026	7.080	27.6019	88.6663	52.0	1843.4
	1997	AT970711.A04	/INDUSTRY/	07/16/1997	07/30/1997	42.711	14.594	5.986	27.6019	88.6663	68.0	1843.4
	1997	AT970711.A05	/INDUSTRY/	07/16/1997	07/30/1997	38.331	12.463	5.776	27.6019	88.6663	84.0	1843.4
	1997	AT970711.A06	/INDUSTRY/	07/16/1997	07/30/1997	39.579	11.957	5.378	27.6019	88.6663	100.0	1843.4
	1997	AT970711.A07	/INDUSTRY/	07/16/1997	07/30/1997	41.881	11.871	5.278	27.6019	88.6663	116.0	1843.4
	1997	AT970711.A08	/INDUSTRY/	07/16/1997	07/30/1997	44.102	10.973	5.106	27.6019	88.6663	132.0	1843.4
	1997	AT970711.A09	/INDUSTRY/	07/16/1997	07/30/1997	43.600	11.943	5.146	27.6019	88.6663	148.0	1843.4
	1997	AT970711.A10	/INDUSTRY/	07/16/1997	07/30/1997	45.069	11.506	4.681	27.6019	88.6663	164.0	1843.4
	1997	AT970711.A11	/INDUSTRY/	07/16/1997	07/30/1997	44.914	11.465	4.116	27.6019	88.6663	180.0	1843.4
	1997	AT970711.A12	/INDUSTRY/	07/16/1997	07/30/1997	43.500	11.195	3.887	27.6019	88.6663	196.0	1843.4
	1997	AT970711.A13	/INDUSTRY/	07/16/1997	07/30/1997	42.638	11.038	4.021	27.6019	88.6663	212.0	1843.4
	1997	AT970711.A14	/INDUSTRY/	07/16/1997	07/30/1997	39.756	10.798	4.121	27.6019	88.6663	228.0	1843.4
	1997	AT970711.A15	/INDUSTRY/	07/16/1997	07/30/1997	37.964	10.800	4.263	27.6019	88.6663	244.0	1843.4
	1997	AT970711.A16	/INDUSTRY/	07/16/1997	07/30/1997	36.705	11.044	4.325	27.6019	88.6663	260.0	1843.4

Table B-6. Speed statistics for energetic current events associated with tropical cyclones. (continued)

Event No.	Year	Filename	Directory	Event start date (m/d/y)	Event end date (m/d/y)	Maximum speed (cm·s^{-1})	Mean speed (cm·s^{-1})	Stand. dev. of speed (cm·s^{-1})	Latitude (°N)	Longitude (°W)	Depth (m)	Total water depth (m)
8	1997	AT970711.A17	/INDUSTRY/	07/16/1997	07/30/1997	35.700	11.079	4.472	27.6019	88.6663	276.0	1843.4
	1997	AT970711.A18	/INDUSTRY/	07/16/1997	07/30/1997	33.948	10.916	4.063	27.6019	88.6663	292.0	1843.4
	1997	AT970711.A19	/INDUSTRY/	07/16/1997	07/30/1997	36.062	10.866	3.709	27.6019	88.6663	308.0	1843.4
	1997	AT970711.A20	/INDUSTRY/	07/16/1997	07/30/1997	36.776	10.676	3.400	27.6019	88.6663	324.0	1843.4
	1997	AT970711.A21	/INDUSTRY/	07/16/1997	07/30/1997	40.028	10.239	3.607	27.6019	88.6663	340.0	1843.4
	1997	AT970711.A22	/INDUSTRY/	07/16/1997	07/30/1997	37.165	9.943	3.780	27.6019	88.6663	356.0	1843.4
	1997	AT970711.A23	/INDUSTRY/	07/16/1997	07/30/1997	35.089	9.878	3.482	27.6019	88.6663	372.0	1843.4
	1997	AT970711.A24	/INDUSTRY/	07/16/1997	07/30/1997	37.125	9.862	3.263	27.6019	88.6663	388.0	1843.4
	1997	AT970711.A25	/INDUSTRY/	07/16/1997	07/30/1997	39.437	9.677	3.447	27.6019	88.6663	404.0	1843.4
	1997	AT970711.A26	/INDUSTRY/	07/16/1997	07/30/1997	41.231	9.630	3.651	27.6019	88.6663	420.0	1843.4
	1997	AT970711.A27	/INDUSTRY/	07/16/1997	07/30/1997	42.252	9.483	3.822	27.6019	88.6663	436.0	1843.4
	1997	AT970711.A28	/INDUSTRY/	07/16/1997	07/30/1997	39.259	9.380	3.745	27.6019	88.6663	452.0	1843.4
	1997	AT970711.A29	/INDUSTRY/	07/16/1997	07/30/1997	37.500	9.158	3.799	27.6019	88.6663	468.0	1843.4
	1997	AT970711.A30	/INDUSTRY/	07/16/1997	07/30/1997	37.607	8.978	3.824	27.6019	88.6663	484.0	1843.4
	1997	AT970711.A31	/INDUSTRY/	07/16/1997	07/30/1997	38.710	8.981	3.762	27.6019	88.6663	500.0	1843.4
	1997	AT970711.A32	/INDUSTRY/	07/16/1997	07/30/1997	40.528	9.016	4.074	27.6019	88.6663	516.0	1843.4
	1997	AT970711.A33	/INDUSTRY/	07/16/1997	07/30/1997	41.110	9.040	4.326	27.6019	88.6663	532.0	1843.4
	1997	AT970711.A34	/INDUSTRY/	07/16/1997	07/30/1997	38.288	8.787	4.234	27.6019	88.6663	548.0	1843.4
	1997	AT970711.A35	/INDUSTRY/	07/16/1997	07/30/1997	36.459	8.199	3.651	27.6019	88.6663	564.0	1843.4
	1997	AT970711.A36	/INDUSTRY/	07/16/1997	07/30/1997	32.408	7.337	3.526	27.6019	88.6663	580.0	1843.4
	1997	AT970711.A37	/INDUSTRY/	07/16/1997	07/30/1997	32.802	7.103	3.316	27.6019	88.6663	596.0	1843.4
	1997	AT970711.A38	/INDUSTRY/	07/16/1997	07/30/1997	32.802	6.672	3.318	27.6019	88.6663	612.0	1843.4
	1997	AT970711.A39	/INDUSTRY/	07/16/1997	07/30/1997	32.222	6.209	2.962	27.6019	88.6663	628.0	1843.4
	1997	AT970711.A40	/INDUSTRY/	07/16/1997	07/30/1997	32.175	5.923	2.948	27.6019	88.6663	644.0	1843.4
	1997	AT970711.A41	/INDUSTRY/	07/16/1997	07/30/1997	34.655	5.954	3.112	27.6019	88.6663	660.0	1843.4
	1997	AT970711.A42	/INDUSTRY/	07/16/1997	07/30/1997	37.607	5.882	3.178	27.6019	88.6663	676.0	1843.4
	1997	AT970711.A43	/INDUSTRY/	07/16/1997	07/30/1997	38.184	5.453	3.167	27.6019	88.6663	692.0	1843.4
	1997	AT970711.A44	/INDUSTRY/	07/16/1997	07/30/1997	35.018	5.337	3.032	27.6019	88.6663	708.0	1843.4
	1997	AT970711.A45	/INDUSTRY/	07/16/1997	07/30/1997	21.077	5.417	2.750	27.6019	88.6663	724.0	1843.4
	1997	AT970711.A46	/INDUSTRY/	07/16/1997	07/30/1997	27.541	5.482	2.789	27.6019	88.6663	740.0	1843.4
	1997	AT970711.A47	/INDUSTRY/	07/16/1997	07/30/1997	21.983	5.527	2.673	27.6019	88.6663	756.0	1843.4
	1997	AT970711.A48	/INDUSTRY/	07/16/1997	07/30/1997	21.633	5.069	2.649	27.6019	88.6663	772.0	1843.4
	1997	MC970710.A01	/MMS/	07/16/1997	07/30/1997	121.598	29.884	21.578	28.7662	88.2650	8.0	1300.0
	1997	MC970710.A02	/MMS/	07/16/1997	07/30/1997	111.884	28.119	19.983	28.7662	88.2650	12.0	1300.0

Table B-6. Speed statistics for energetic current events associated with tropical cyclones. (continued)

Event No.	Year	Filename	Directory	Event start date (m/d/y)	Event end date (m/d/y)	Maximum speed ($cm{\cdot}s^{-1}$)	Mean speed ($cm{\cdot}s^{-1}$)	Stand. dev. of speed ($cm{\cdot}s^{-1}$)	Latitude (°N)	Longitude (°W)	Depth (m)	Total water depth (m)
8	1997	MC970710.A03	/MMS/	07/16/1997	07/30/1997	97.270	26.981	17.441	28.7662	88.2650	16.0	1300.0
	1997	MC970710.A04	/MMS/	07/16/1997	07/30/1997	78.462	25.091	14.553	28.7662	88.2650	20.0	1300.0
	1997	MC970710.A05	/MMS/	07/16/1997	07/30/1997	63.106	23.693	11.973	28.7662	88.2650	24.0	1300.0
	1997	MC970710.A06	/MMS/	07/16/1997	07/30/1997	49.953	22.157	9.973	28.7662	88.2650	28.0	1300.0
	1997	MC970710.A07	/MMS/	07/16/1997	07/30/1997	52.389	21.766	10.049	28.7662	88.2650	32.0	1300.0
	1997	MC970710.A08	/MMS/	07/16/1997	07/30/1997	49.674	21.373	10.328	28.7662	88.2650	36.0	1300.0
	1997	MC970710.A09	/MMS/	07/16/1997	07/30/1997	47.566	20.543	10.040	28.7662	88.2650	40.0	1300.0
	1997	MC970710.A10	/MMS/	07/16/1997	07/30/1997	48.901	19.983	9.806	28.7662	88.2650	44.0	1300.0
	1997	MC970710.A11	/MMS/	07/16/1997	07/30/1997	44.413	19.590	9.403	28.7662	88.2650	48.0	1300.0
	1997	MC970710.A12	/MMS/	07/16/1997	07/30/1997	38.998	18.971	8.695	28.7662	88.2650	52.0	1300.0
	1997	MC970710.A13	/MMS/	07/16/1997	07/30/1997	29.844	14.010	6.455	28.7662	88.2650	56.0	1300.0
	1997	MC970710.A14	/MMS/	07/16/1997	07/30/1997	29.824	14.636	6.845	28.7662	88.2650	60.0	1300.0
	1997	MC970710.A15	/MMS/	07/16/1997	07/30/1997	35.750	17.812	8.319	28.7662	88.2650	64.0	1300.0
	1997	MC970710.A16	/MMS/	07/16/1997	07/30/1997	35.724	17.194	8.077	28.7662	88.2650	68.0	1300.0
	1997	MC970710.A17	/MMS/	07/16/1997	07/30/1997	35.430	15.897	7.642	28.7662	88.2650	72.0	1300.0
	1997	VK970712.A01	/MMS/	07/16/1997	07/30/1997	88.172	17.822	12.467	29.2120	87.8722	16.0	500.0
	1997	VK970712.A02	/MMS/	07/16/1997	07/30/1997	61.574	17.022	8.950	29.2120	87.8722	20.0	500.0
	1997	VK970712.A03	/MMS/	07/16/1997	07/30/1997	39.655	17.052	7.717	29.2120	87.8722	24.0	500.0
	1997	VK970712.A04	/MMS/	07/16/1997	07/30/1997	44.294	17.880	8.451	29.2120	87.8722	28.0	500.0
	1997	VK970712.A05	/MMS/	07/16/1997	07/30/1997	41.347	19.492	8.715	29.2120	87.8722	32.0	500.0
	1997	VK970712.A06	/MMS/	07/16/1997	07/30/1997	44.168	20.771	8.869	29.2120	87.8722	36.0	500.0
	1997	VK970712.A07	/MMS/	07/16/1997	07/30/1997	40.529	19.875	8.624	29.2120	87.8722	40.0	500.0
	1997	VK970712.A08	/MMS/	07/16/1997	07/30/1997	37.541	17.621	7.660	29.2120	87.8722	44.0	500.0
	1997	VK970712.A09	/MMS/	07/16/1997	07/30/1997	38.394	15.592	8.167	29.2120	87.8722	48.0	500.0
	1997	VK970712.A10	/MMS/	07/16/1997	07/30/1997	40.623	15.714	8.510	29.2120	87.8722	52.0	500.0
	1997	VK970712.A11	/MMS/	07/16/1997	07/30/1997	43.988	16.743	8.962	29.2120	87.8722	56.0	500.0
	1997	VK970712.A12	/MMS/	07/16/1997	07/30/1997	47.075	17.523	9.576	29.2120	87.8722	60.0	500.0
	1997	VK970712.A13	/MMS/	07/16/1997	07/30/1997	48.127	16.180	9.387	29.2120	87.8722	64.0	500.0
	1997	VK970712.A14	/MMS/	07/16/1997	07/30/1997	45.109	16.584	9.881	29.2120	87.8722	68.0	500.0
	1997	VK970712.A15	/MMS/	07/16/1997	07/30/1997	46.960	17.697	10.510	29.2120	87.8722	72.0	500.0
	1997	VK970712.A16	/MMS/	07/16/1997	07/30/1997	45.393	17.008	10.095	29.2120	87.8722	76.0	500.0
	1997	VK970712.A17	/MMS/	07/16/1997	07/30/1997	42.314	16.531	9.315	29.2120	87.8722	80.0	500.0
	1997	VK970712.A18	/MMS/	07/16/1997	07/30/1997	123.846	22.014	15.507	29.0705	87.8568	16.0	1300.0
	1997	VK970712.A19	/MMS/	07/16/1997	07/30/1997	94.519	21.916	13.665	29.0705	87.8568	20.0	1300.0

Table B-6. Speed statistics for energetic current events associated with tropical cyclones. (continued)

Event No.	Year	Filename	Directory	Event start date (m/d/y)	Event end date (m/d/y)	Maximum speed ($cm \cdot s^{-1}$)	Mean speed ($cm \cdot s^{-1}$)	Stand. dev. of speed ($cm \cdot s^{-1}$)	Latitude (°N)	Longitude (°W)	Depth (m)	Total water depth (m)
8	1997	VK970712.A20	/MMS/	07/16/1997	07/30/1997	66.707	21.838	10.269	29.0705	87.8568	24.0	1300.0
	1997	VK970712.A21	/MMS/	07/16/1997	07/30/1997	46.551	21.131	7.804	29.0705	87.8568	28.0	1300.0
	1997	VK970712.A22	/MMS/	07/16/1997	07/30/1997	37.035	19.315	7.566	29.0705	87.8568	32.0	1300.0
	1997	VK970712.A23	/MMS/	07/16/1997	07/30/1997	35.797	17.991	7.431	29.0705	87.8568	36.0	1300.0
	1997	VK970712.A24	/MMS/	07/16/1997	07/30/1997	40.216	16.838	7.191	29.0705	87.8568	40.0	1300.0
	1997	VK970712.A25	/MMS/	07/16/1997	07/30/1997	40.374	15.723	7.784	29.0705	87.8568	44.0	1300.0
	1997	VK970712.A26	/MMS/	07/16/1997	07/30/1997	39.248	15.511	7.996	29.0705	87.8568	48.0	1300.0
	1997	VK970712.A27	/MMS/	07/16/1997	07/30/1997	37.686	15.687	8.161	29.0705	87.8568	52.0	1300.0
	1997	VK970712.A28	/MMS/	07/16/1997	07/30/1997	29.720	10.961	6.320	29.0705	87.8568	56.0	1300.0
	1997	VK970712.A29	/MMS/	07/16/1997	07/30/1997	30.319	12.155	6.624	29.0705	87.8568	60.0	1300.0
	1997	VK970712.A30	/MMS/	07/16/1997	07/30/1997	39.333	17.667	8.045	29.0705	87.8568	64.0	1300.0
	1997	VK970712.A31	/MMS/	07/16/1997	07/30/1997	38.776	17.953	7.804	29.0705	87.8568	68.0	1300.0
	1997	VK970712.A32	/MMS/	07/16/1997	07/30/1997	38.086	17.728	7.844	29.0705	87.8568	72.0	1300.0
	1997	DD970324.A02	/MMS/	07/16/1997	07/16/1997	28.265	17.431	6.324	29.3712	87.3563	12.0	500.0
	1997	DD970717.A01	/MMS/	07/17/1997	07/30/1997	69.199	25.220	14.436	29.3712	87.3563	12.0	500.0
	1997	DD970324.A03	/MMS/	07/16/1997	07/16/1997	20.706	14.754	4.651	29.3712	87.3563	16.0	500.0
	1997	DD970717.A02	/MMS/	07/17/1997	07/30/1997	55.166	21.745	12.941	29.3712	87.3563	16.0	500.0
	1997	DD970324.A04	/MMS/	07/16/1997	07/16/1997	19.362	12.401	3.693	29.3712	87.3563	20.0	500.0
	1997	DD970717.A03	/MMS/	07/17/1997	07/30/1997	54.602	22.723	12.570	29.3712	87.3563	20.0	500.0
	1997	DD970324.A05	/MMS/	07/16/1997	07/16/1997	21.967	12.506	5.555	29.3712	87.3563	24.0	500.0
	1997	DD970717.A04	/MMS/	07/17/1997	07/30/1997	54.693	23.200	12.439	29.3712	87.3563	24.0	500.0
	1997	DD970324.A06	/MMS/	07/16/1997	07/16/1997	24.151	14.147	6.052	29.3712	87.3563	28.0	500.0
	1997	DD970717.A05	/MMS/	07/17/1997	07/30/1997	53.562	21.955	10.952	29.3712	87.3563	28.0	500.0
	1997	DD970324.A07	/MMS/	07/16/1997	07/16/1997	30.815	14.985	7.536	29.3712	87.3563	32.0	500.0
	1997	DD970717.A06	/MMS/	07/17/1997	07/30/1997	49.003	20.030	10.033	29.3712	87.3563	32.0	500.0
	1997	DD970324.A08	/MMS/	07/16/1997	07/16/1997	36.882	15.693	8.183	29.3712	87.3563	36.0	500.0
	1997	DD970717.A07	/MMS/	07/17/1997	07/30/1997	43.290	18.012	8.665	29.3712	87.3563	36.0	500.0
	1997	DD970324.A09	/MMS/	07/16/1997	07/16/1997	36.444	16.662	7.326	29.3712	87.3563	40.0	500.0
	1997	DD970717.A08	/MMS/	07/17/1997	07/30/1997	39.418	16.741	7.560	29.3712	87.3563	40.0	500.0
	1997	DD970324.A10	/MMS/	07/16/1997	07/16/1997	34.519	17.548	6.926	29.3712	87.3563	44.0	500.0
	1997	DD970717.A09	/MMS/	07/17/1997	07/30/1997	34.974	16.420	6.913	29.3712	87.3563	44.0	500.0
	1997	DD970324.A11	/MMS/	07/16/1997	07/16/1997	22.916	17.287	4.497	29.3712	87.3563	48.0	500.0
	1997	DD970717.A10	/MMS/	07/17/1997	07/30/1997	33.217	16.548	6.720	29.3712	87.3563	48.0	500.0
	1997	DD970324.A12	/MMS/	07/16/1997	07/16/1997	31.525	17.308	5.496	29.3712	87.3563	52.0	500.0

Table B-6. Speed statistics for energetic current events associated with tropical cyclones. (continued)

Event No.	Year	Filename	Directory	Event start date (m/d/y)	Event end date (m/d/y)	Maximum speed (cm·s^{-1})	Mean speed (cm·s^{-1})	Stand. dev. of speed (cm·s^{-1})	Latitude (°N)	Longitude (°W)	Depth (m)	Total water depth (m)
8	1997	DD970717.A11	/MMS/	07/17/1997	07/30/1997	33.085	16.768	6.696	29.3712	87.3563	52.0	500.0
	1997	DD970324.A13	/MMS/	07/16/1997	07/16/1997	25.844	17.714	4.864	29.3712	87.3563	56.0	500.0
	1997	DD970717.A12	/MMS/	07/17/1997	07/30/1997	32.304	16.779	6.944	29.3712	87.3563	56.0	500.0
	1997	DD970324.A14	/MMS/	07/16/1997	07/16/1997	26.091	18.001	4.313	29.3712	87.3563	60.0	500.0
	1997	DD970717.A13	/MMS/	07/17/1997	07/30/1997	35.157	16.496	7.171	29.3712	87.3563	60.0	500.0
	1997	DD970324.A15	/MMS/	07/16/1997	07/16/1997	28.197	16.956	4.463	29.3712	87.3563	64.0	500.0
	1997	DD970717.A14	/MMS/	07/17/1997	07/30/1997	39.386	16.675	7.392	29.3712	87.3563	64.0	500.0
	1997	DD970324.A16	/MMS/	07/16/1997	07/16/1997	23.031	16.593	4.587	29.3712	87.3563	68.0	500.0
	1997	DD970717.A15	/MMS/	07/17/1997	07/30/1997	42.239	16.837	7.471	29.3712	87.3563	68.0	500.0
	1997	DD970324.A17	/MMS/	07/16/1997	07/16/1997	22.553	15.529	4.959	29.3712	87.3563	72.0	500.0
	1997	DD970717.A16	/MMS/	07/17/1997	07/30/1997	44.007	16.671	7.636	29.3712	87.3563	72.0	500.0
	1997	DD970324.A18	/MMS/	07/16/1997	07/16/1997	21.865	14.067	5.244	29.3712	87.3563	76.0	500.0
	1997	DD970717.A17	/MMS/	07/17/1997	07/30/1997	42.155	16.574	7.428	29.3712	87.3563	76.0	500.0
	1997	DD970324.A19	/MMS/	07/16/1997	07/16/1997	22.017	13.203	5.539	29.3712	87.3563	80.0	500.0
	1997	DD970717.A18	/MMS/	07/17/1997	07/30/1997	41.383	15.224	7.175	29.3712	87.3563	80.0	500.0
	1997	DD970718.A18	/MMS/	07/18/1997	07/30/1997	77.036	23.873	13.385	29.0032	87.3532	8.0	1300.0
	1997	DD970324.A20	/MMS/	07/16/1997	07/17/1997	36.676	23.874	6.275	29.0032	87.3532	12.0	1300.0
	1997	DD970718.A19	/MMS/	07/18/1997	07/30/1997	65.408	29.583	15.631	29.0032	87.3532	12.0	1300.0
	1997	DD970324.A21	/MMS/	07/16/1997	07/17/1997	36.840	24.525	6.058	29.0032	87.3532	16.0	1300.0
	1997	DD970718.A20	/MMS/	07/18/1997	07/30/1997	68.401	28.071	15.623	29.0032	87.3532	16.0	1300.0
	1997	DD970324.A22	/MMS/	07/16/1997	07/17/1997	37.306	25.597	5.465	29.0032	87.3532	20.0	1300.0
	1997	DD970718.A21	/MMS/	07/18/1997	07/30/1997	69.104	28.039	15.836	29.0032	87.3532	20.0	1300.0
	1997	DD970324.A23	/MMS/	07/16/1997	07/17/1997	38.729	25.301	7.522	29.0032	87.3532	24.0	1300.0
	1997	DD970718.A22	/MMS/	07/18/1997	07/30/1997	60.317	27.959	13.218	29.0032	87.3532	24.0	1300.0
	1997	DD970324.A24	/MMS/	07/16/1997	07/17/1997	40.733	23.624	6.643	29.0032	87.3532	28.0	1300.0
	1997	DD970718.A23	/MMS/	07/18/1997	07/30/1997	51.779	25.241	10.681	29.0032	87.3532	28.0	1300.0
	1997	DD970324.A25	/MMS/	07/16/1997	07/17/1997	39.806	23.272	6.777	29.0032	87.3532	32.0	1300.0
	1997	DD970718.A24	/MMS/	07/18/1997	07/30/1997	46.169	22.120	9.363	29.0032	87.3532	32.0	1300.0
	1997	DD970324.A26	/MMS/	07/16/1997	07/17/1997	40.092	24.182	7.535	29.0032	87.3532	36.0	1300.0
	1997	DD970718.A25	/MMS/	07/18/1997	07/30/1997	47.461	21.326	8.918	29.0032	87.3532	36.0	1300.0
	1997	DD970324.A27	/MMS/	07/16/1997	07/17/1997	42.008	24.239	7.919	29.0032	87.3532	40.0	1300.0
	1997	DD970718.A26	/MMS/	07/18/1997	07/30/1997	47.981	21.510	8.831	29.0032	87.3532	40.0	1300.0
	1997	DD970324.A28	/MMS/	07/16/1997	07/17/1997	42.396	23.273	8.521	29.0032	87.3532	44.0	1300.0
	1997	DD970718.A27	/MMS/	07/18/1997	07/30/1997	47.528	21.478	8.661	29.0032	87.3532	44.0	1300.0

Table B-6. Speed statistics for energetic current events associated with tropical cyclones. (continued)

Event No.	Year	Filename	Directory	Event start date (m/d/y)	Event end date (m/d/y)	Maximum speed ($cm \cdot s^{-1}$)	Mean speed ($cm \cdot s^{-1}$)	Stand. dev. of speed ($cm \cdot s^{-1}$)	Latitude (°N)	Longitude (°W)	Depth (m)	Total water depth (m)
8	1997	DD970324.A29	/MMS/	07/16/1997	07/17/1997	39.480	21.795	8.190	29.0032	87.3532	48.0	1300.0
	1997	DD970718.A28	/MMS/	07/18/1997	07/30/1997	45.675	21.714	8.642	29.0032	87.3532	48.0	1300.0
	1997	DD970324.A30	/MMS/	07/16/1997	07/17/1997	36.311	20.089	7.139	29.0032	87.3532	52.0	1300.0
	1997	DD970718.A29	/MMS/	07/18/1997	07/30/1997	44.704	22.112	8.610	29.0032	87.3532	52.0	1300.0
	1997	DD970324.A31	/MMS/	07/16/1997	07/17/1997	25.331	14.356	4.749	29.0032	87.3532	56.0	1300.0
	1997	DD970718.A30	/MMS/	07/18/1997	07/30/1997	40.501	18.658	7.799	29.0032	87.3532	56.0	1300.0
	1997	DD970324.A32	/MMS/	07/16/1997	07/17/1997	23.382	14.498	3.914	29.0032	87.3532	60.0	1300.0
	1997	DD970718.A31	/MMS/	07/18/1997	07/30/1997	36.152	18.942	8.002	29.0032	87.3532	60.0	1300.0
	1997	DD970324.A33	/MMS/	07/16/1997	07/17/1997	28.102	17.540	4.337	29.0032	87.3532	64.0	1300.0
	1997	DD970718.A32	/MMS/	07/18/1997	07/30/1997	37.938	20.934	8.480	29.0032	87.3532	64.0	1300.0
	1997	DD970324.A34	/MMS/	07/16/1997	07/17/1997	27.284	15.857	4.665	29.0032	87.3532	68.0	1300.0
	1997	DD970718.A33	/MMS/	07/18/1997	07/30/1997	35.920	19.775	8.314	29.0032	87.3532	68.0	1300.0
	1997	DD970324.A36	/MMS/	07/16/1997	07/16/1997	17.854	7.108	4.614	29.3348	86.8520	8.0	500.0
	1997	DD970716.A01	/MMS/	07/16/1997	07/30/1997	81.802	19.852	13.962	29.3348	86.8520	8.0	500.0
	1997	DD970324.A37	/MMS/	07/16/1997	07/16/1997	16.524	9.806	4.804	29.3348	86.8520	12.0	500.0
	1997	DD970716.A02	/MMS/	07/16/1997	07/30/1997	69.878	24.225	13.209	29.3348	86.8520	12.0	500.0
	1997	DD970324.A38	/MMS/	07/16/1997	07/16/1997	16.107	11.220	2.732	29.3348	86.8520	16.0	500.0
	1997	DD970716.A03	/MMS/	07/16/1997	07/30/1997	59.077	20.691	11.695	29.3348	86.8520	16.0	500.0
	1997	DD970324.A39	/MMS/	07/16/1997	07/16/1997	16.447	12.285	3.242	29.3348	86.8520	20.0	500.0
	1997	DD970716.A04	/MMS/	07/16/1997	07/30/1997	47.877	19.200	10.184	29.3348	86.8520	20.0	500.0
	1997	DD970324.A40	/MMS/	07/16/1997	07/16/1997	19.052	14.769	4.213	29.3348	86.8520	24.0	500.0
	1997	DD970716.A05	/MMS/	07/16/1997	07/30/1997	40.440	18.795	8.942	29.3348	86.8520	24.0	500.0
	1997	DD970324.A41	/MMS/	07/16/1997	07/16/1997	22.992	17.934	5.045	29.3348	86.8520	28.0	500.0
	1997	DD970716.A06	/MMS/	07/16/1997	07/30/1997	36.857	17.857	7.970	29.3348	86.8520	28.0	500.0
	1997	DD970324.A42	/MMS/	07/16/1997	07/16/1997	20.620	14.687	3.813	29.3348	86.8520	32.0	500.0
	1997	DD970716.A07	/MMS/	07/16/1997	07/30/1997	39.422	17.926	7.869	29.3348	86.8520	32.0	500.0
	1997	DD970324.A43	/MMS/	07/16/1997	07/16/1997	19.144	11.636	4.476	29.3348	86.8520	36.0	500.0
	1997	DD970716.A08	/MMS/	07/16/1997	07/30/1997	39.025	18.412	8.849	29.3348	86.8520	36.0	500.0
	1997	DD970324.A44	/MMS/	07/16/1997	07/16/1997	17.465	8.665	4.869	29.3348	86.8520	40.0	500.0
	1997	DD970716.A09	/MMS/	07/16/1997	07/30/1997	39.054	18.540	9.379	29.3348	86.8520	40.0	500.0
	1997	DD970324.A45	/MMS/	07/16/1997	07/16/1997	19.449	10.517	5.387	29.3348	86.8520	44.0	500.0
	1997	DD970716.A10	/MMS/	07/16/1997	07/30/1997	37.700	17.704	9.447	29.3348	86.8520	44.0	500.0
	1997	DD970324.A46	/MMS/	07/16/1997	07/16/1997	20.038	12.445	4.421	29.3348	86.8520	48.0	500.0
	1997	DD970716.A11	/MMS/	07/16/1997	07/30/1997	34.804	15.768	8.630	29.3348	86.8520	48.0	500.0

Table B-6. Speed statistics for energetic current events associated with tropical cyclones. (continued)

Event No.	Year	Filename	Directory	Event start date (m/d/y)	Event end date (m/d/y)	Maximum speed (cm·s^{-1})	Mean speed (cm·s^{-1})	Stand. dev. of speed (cm·s^{-1})	Latitude (°N)	Longitude (°W)	Depth (m)	Total water depth (m)
8	1997	DD970324.A47	/MMS/	07/16/1997	07/16/1997	21.932	11.852	4.993	29.3348	86.8520	52.0	500.0
	1997	DD970716.A12	/MMS/	07/16/1997	07/30/1997	31.313	14.141	7.533	29.3348	86.8520	52.0	500.0
	1997	DD970324.A48	/MMS/	07/16/1997	07/16/1997	16.227	11.920	3.444	29.3348	86.8520	56.0	500.0
	1997	DD970716.A13	/MMS/	07/16/1997	07/30/1997	28.640	13.060	6.576	29.3348	86.8520	56.0	500.0
	1997	DD970324.A49	/MMS/	07/16/1997	07/16/1997	12.678	7.807	2.948	29.3348	86.8520	60.0	500.0
	1997	DD970716.A14	/MMS/	07/16/1997	07/30/1997	27.921	12.116	5.978	29.3348	86.8520	60.0	500.0
	1997	DD970324.A50	/MMS/	07/16/1997	07/16/1997	10.922	4.630	2.781	29.3348	86.8520	64.0	500.0
	1997	DD970716.A15	/MMS/	07/16/1997	07/30/1997	27.042	11.110	5.881	29.3348	86.8520	64.0	500.0
	1997	DD970324.A51	/MMS/	07/16/1997	07/16/1997	10.990	5.433	2.904	29.3348	86.8520	68.0	500.0
	1997	DD970716.A16	/MMS/	07/16/1997	07/30/1997	27.051	11.055	6.152	29.3348	86.8520	68.0	500.0
	1997	DD970324.A52	/MMS/	07/16/1997	07/16/1997	13.462	7.444	3.211	29.3348	86.8520	72.0	500.0
	1997	DD970716.A17	/MMS/	07/16/1997	07/30/1997	27.432	10.965	5.867	29.3348	86.8520	72.0	500.0
	1997	DD970324.A53	/MMS/	07/16/1997	07/16/1997	13.086	8.432	2.904	29.3348	86.8520	76.0	500.0
	1997	DD970716.A18	/MMS/	07/16/1997	07/30/1997	23.577	9.879	4.888	29.3348	86.8520	76.0	500.0
	1997	DD970324.A54	/MMS/	07/16/1997	07/16/1997	13.551	8.446	3.480	29.3348	86.8520	80.0	500.0
	1997	DD970716.A19	/MMS/	07/16/1997	07/30/1997	23.983	9.307	4.370	29.3348	86.8520	80.0	500.0
9	1998	VK980806.A01	/MMS/	08/31/1998	09/03/1998	100.699	33.820	17.825	29.0592	88.3900	12.0	500.0
	1998	VK980806.A02	/MMS/	08/31/1998	09/03/1998	88.200	30.990	15.342	29.0592	88.3900	16.0	500.0
	1998	VK980806.A03	/MMS/	08/31/1998	09/03/1998	71.844	26.526	12.284	29.0592	88.3900	20.0	500.0
	1998	VK980806.A04	/MMS/	08/31/1998	09/03/1998	51.083	21.132	8.397	29.0592	88.3900	24.0	500.0
	1998	VK980806.A05	/MMS/	08/31/1998	09/03/1998	31.676	16.991	6.348	29.0592	88.3900	28.0	500.0
	1998	VK980806.A06	/MMS/	08/31/1998	09/03/1998	28.071	15.198	6.767	29.0592	88.3900	32.0	500.0
	1998	VK980806.A07	/MMS/	08/31/1998	09/03/1998	30.176	15.976	6.880	29.0592	88.3900	36.0	500.0
	1998	VK980806.A08	/MMS/	08/31/1998	09/03/1998	33.842	17.344	5.911	29.0592	88.3900	40.0	500.0
	1998	VK980806.A09	/MMS/	08/31/1998	09/03/1998	59.545	18.423	6.350	29.0592	88.3900	44.0	500.0
	1998	VK980806.A10	/MMS/	08/31/1998	09/03/1998	35.044	17.626	5.808	29.0592	88.3900	48.0	500.0
	1998	VK980806.A11	/MMS/	08/31/1998	09/03/1998	39.101	16.852	6.455	29.0592	88.3900	52.0	500.0
	1998	VK980806.A12	/MMS/	08/31/1998	09/03/1998	38.203	16.305	5.862	29.0592	88.3900	56.0	500.0
	1998	VK980806.A13	/MMS/	08/31/1998	09/03/1998	33.842	15.683	5.809	29.0592	88.3900	60.0	500.0
	1998	VK980806.A14	/MMS/	08/31/1998	09/03/1998	33.574	12.477	4.732	29.0592	88.3900	64.0	500.0
	1998	VK980806.A15	/MMS/	08/31/1998	09/03/1998	27.523	12.031	4.698	29.0592	88.3900	68.0	500.0
	1998	VK980806.A16	/MMS/	08/31/1998	09/03/1998	24.881	12.775	4.806	29.0592	88.3900	72.0	500.0
	1998	VK980806.A17	/MMS/	08/31/1998	09/03/1998	21.983	11.933	4.560	29.0592	88.3900	76.0	500.0
	1998	VK980806.A18	/MMS/	08/31/1998	09/03/1998	25.355	10.333	4.083	29.0592	88.3900	80.0	500.0

Table B-6. Speed statistics for energetic current events associated with tropical cyclones. (continued)

Event No.	Year	Filename	Directory	Event start date (m/d/y)	Event end date (m/d/y)	Maximum speed ($cm \cdot s^{-1}$)	Mean speed ($cm \cdot s^{-1}$)	Stand. dev. of speed ($cm \cdot s^{-1}$)	Latitude (°N)	Longitude (°W)	Depth (m)	Total water depth (m)
9	1998	VK980806.C01	/MMS/	08/31/1998	09/03/1998	42.076	21.410	11.993	29.0592	88.3900	200.0	500.0
	1998	VK980806.C02	/MMS/	08/31/1998	09/03/1998	31.039	11.112	8.812	29.0592	88.3900	300.0	500.0
	1998	VK980806.C03	/MMS/	08/31/1998	09/03/1998	14.503	6.306	2.394	29.0592	88.3900	490.0	500.0
	1998	MC980806.A01	/MMS/	08/31/1998	09/03/1998	89.755	36.629	18.304	28.7662	88.2650	8.0	1300.0
	1998	MC980806.A02	/MMS/	08/31/1998	09/03/1998	74.353	31.428	15.018	28.7662	88.2650	12.0	1300.0
	1998	MC980806.A03	/MMS/	08/31/1998	09/03/1998	67.296	30.433	13.298	28.7662	88.2650	16.0	1300.0
	1998	MC980806.A04	/MMS/	08/31/1998	09/03/1998	66.189	30.615	11.452	28.7662	88.2650	20.0	1300.0
	1998	MC980806.A05	/MMS/	08/31/1998	09/03/1998	68.027	29.580	10.008	28.7662	88.2650	24.0	1300.0
	1998	MC980806.A06	/MMS/	08/31/1998	09/03/1998	59.976	29.123	9.083	28.7662	88.2650	28.0	1300.0
	1998	MC980806.A07	/MMS/	08/31/1998	09/03/1998	52.900	29.568	7.086	28.7662	88.2650	32.0	1300.0
	1998	MC980806.A08	/MMS/	08/31/1998	09/03/1998	46.500	29.109	5.926	28.7662	88.2650	36.0	1300.0
	1998	MC980806.A09	/MMS/	08/31/1998	09/03/1998	48.552	29.026	6.175	28.7662	88.2650	40.0	1300.0
	1998	MC980806.A10	/MMS/	08/31/1998	09/03/1998	41.436	28.386	7.212	28.7662	88.2650	44.0	1300.0
	1998	MC980806.A11	/MMS/	08/31/1998	09/03/1998	41.726	27.754	7.392	28.7662	88.2650	48.0	1300.0
	1998	MC980806.A12	/MMS/	08/31/1998	09/03/1998	41.301	27.573	7.130	28.7662	88.2650	52.0	1300.0
	1998	MC980806.A13	/MMS/	08/31/1998	09/03/1998	25.684	16.401	4.562	28.7662	88.2650	56.0	1300.0
	1998	MC980806.A14	/MMS/	08/31/1998	09/03/1998	28.601	17.204	5.121	28.7662	88.2650	60.0	1300.0
	1998	MC980806.A15	/MMS/	08/31/1998	09/03/1998	42.539	27.564	7.422	28.7662	88.2650	64.0	1300.0
	1998	MC980806.A16	/MMS/	08/31/1998	09/03/1998	38.447	25.737	7.120	28.7662	88.2650	68.0	1300.0
	1998	MC980806.C01	/MMS/	08/31/1998	09/03/1998	10.395	4.092	2.738	28.7662	88.2650	500.0	1300.0
	1998	MC980806.C02	/MMS/	08/31/1998	09/03/1998	9.101	3.807	1.649	28.7662	88.2650	1310.0	1320.0
	1998	VK980807.A01	/MMS/	08/31/1998	09/03/1998	92.528	29.588	18.196	29.2120	87.8722	12.0	500.0
	1998	VK980807.A02	/MMS/	08/31/1998	09/03/1998	119.851	33.267	15.682	29.2120	87.8722	16.0	500.0
	1998	VK980807.A03	/MMS/	08/31/1998	09/03/1998	81.334	31.551	13.569	29.2120	87.8722	20.0	500.0
	1998	VK980807.A04	/MMS/	08/31/1998	09/03/1998	73.060	31.453	12.239	29.2120	87.8722	24.0	500.0
	1998	VK980807.A05	/MMS/	08/31/1998	09/03/1998	61.789	31.040	11.316	29.2120	87.8722	28.0	500.0
	1998	VK980807.A06	/MMS/	08/31/1998	09/03/1998	59.821	30.710	10.801	29.2120	87.8722	32.0	500.0
	1998	VK980807.A07	/MMS/	08/31/1998	09/03/1998	53.813	30.076	10.234	29.2120	87.8722	36.0	500.0
	1998	VK980807.A08	/MMS/	08/31/1998	09/03/1998	48.613	27.919	9.600	29.2120	87.8722	40.0	500.0
	1998	VK980807.A09	/MMS/	08/31/1998	09/03/1998	50.022	25.970	9.481	29.2120	87.8722	44.0	500.0
	1998	VK980807.A10	/MMS/	08/31/1998	09/03/1998	44.681	26.203	7.318	29.2120	87.8722	48.0	500.0
	1998	VK980807.A11	/MMS/	08/31/1998	09/03/1998	39.493	25.087	6.241	29.2120	87.8722	52.0	500.0
	1998	VK980807.A12	/MMS/	08/31/1998	09/03/1998	41.253	22.732	5.899	29.2120	87.8722	56.0	500.0
	1998	VK980807.A13	/MMS/	08/31/1998	09/03/1998	38.453	20.576	7.046	29.2120	87.8722	60.0	500.0

Table B-6. Speed statistics for energetic current events associated with tropical cyclones. (continued)

Event No.	Year	Filename	Directory	Event start date (m/d/y)	Event end date (m/d/y)	Maximum speed (cm·s^{-1})	Mean speed (cm·s^{-1})	Stand. dev. of speed (cm·s^{-1})	Latitude (°N)	Longitude (°W)	Depth (m)	Total water depth (m)
9	1998	VK980807.A14	/MMS/	08/31/1998	09/03/1998	35.277	13.750	6.832	29.2120	87.8722	64.0	500.0
	1998	VK980807.A15	/MMS/	08/31/1998	09/03/1998	32.583	13.731	6.295	29.2120	87.8722	68.0	500.0
	1998	VK980807.A16	/MMS/	08/31/1998	09/03/1998	37.892	15.268	9.385	29.2120	87.8722	72.0	500.0
	1998	VK980807.A17	/MMS/	08/31/1998	09/03/1998	37.787	12.794	10.463	29.2120	87.8722	76.0	500.0
	1998	VK980807.A18	/MMS/	08/31/1998	09/03/1998	38.729	14.107	10.123	29.2120	87.8722	80.0	500.0
	1998	VK980807.C01	/MMS/	08/31/1998	09/03/1998	49.347	26.791	8.498	29.2120	87.8722	200.0	500.0
	1998	VK980807.C02	/MMS/	08/31/1998	09/03/1998	22.894	10.977	5.869	29.2120	87.8722	300.0	500.0
	1998	VK980807.C03	/MMS/	08/31/1998	09/03/1998	28.196	11.246	8.262	29.2120	87.8722	490.0	500.0
	1998	VK980807.A19	/MMS/	08/31/1998	09/03/1998	132.474	30.659	25.301	29.0705	87.8568	12.0	1300.0
	1998	VK980807.A20	/MMS/	08/31/1998	09/03/1998	95.061	36.864	17.452	29.0705	87.8568	16.0	1300.0
	1998	VK980807.A21	/MMS/	08/31/1998	09/03/1998	109.995	35.445	16.538	29.0705	87.8568	20.0	1300.0
	1998	VK980807.A22	/MMS/	08/31/1998	09/03/1998	88.901	32.575	14.858	29.0705	87.8568	24.0	1300.0
	1998	VK980807.A23	/MMS/	08/31/1998	09/03/1998	80.199	30.160	13.506	29.0705	87.8568	28.0	1300.0
	1998	VK980807.A24	/MMS/	08/31/1998	09/03/1998	68.184	28.197	11.616	29.0705	87.8568	32.0	1300.0
	1998	VK980807.A25	/MMS/	08/31/1998	09/03/1998	53.117	25.354	9.882	29.0705	87.8568	36.0	1300.0
	1998	VK980807.A26	/MMS/	08/31/1998	09/03/1998	40.617	23.125	8.260	29.0705	87.8568	40.0	1300.0
	1998	VK980807.A27	/MMS/	08/31/1998	09/03/1998	42.448	22.341	7.878	29.0705	87.8568	44.0	1300.0
	1998	VK980807.A28	/MMS/	08/31/1998	09/03/1998	40.006	23.156	6.991	29.0705	87.8568	48.0	1300.0
	1998	VK980807.A29	/MMS/	08/31/1998	09/03/1998	37.844	23.398	7.103	29.0705	87.8568	52.0	1300.0
	1998	VK980807.A30	/MMS/	08/31/1998	09/03/1998	28.521	16.893	5.979	29.0705	87.8568	56.0	1300.0
	1998	VK980807.A31	/MMS/	08/31/1998	09/03/1998	41.941	18.895	6.369	29.0705	87.8568	60.0	1300.0
	1998	VK980807.A32	/MMS/	08/31/1998	09/03/1998	42.618	25.401	7.496	29.0705	87.8568	64.0	1300.0
	1998	VK980807.A33	/MMS/	08/31/1998	09/03/1998	48.203	26.731	8.372	29.0705	87.8568	68.0	1300.0
	1998	VK980807.A34	/MMS/	08/31/1998	09/03/1998	38.530	26.012	7.101	29.0705	87.8568	72.0	1300.0
	1998	VK980807.C04	/MMS/	08/31/1998	09/03/1998	10.402	5.006	2.545	29.0705	87.8568	500.0	1300.0
	1998	VK980808.C01	/MMS/	08/31/1998	09/03/1998	8.500	2.747	2.051	29.0705	87.8568	1290.0	1300.0
	1998	DD980812.A01	/MMS/	08/31/1998	09/03/1998	179.442	39.438	30.603	29.3712	87.3563	12.0	500.0
	1998	DD980812.A02	/MMS/	08/31/1998	09/03/1998	150.841	38.545	28.640	29.3712	87.3563	16.0	500.0
	1998	DD980812.A03	/MMS/	08/31/1998	09/03/1998	127.838	33.842	25.083	29.3712	87.3563	20.0	500.0
	1998	DD980812.A04	/MMS/	08/31/1998	09/03/1998	106.385	26.029	19.790	29.3712	87.3563	24.0	500.0
	1998	DD980812.A05	/MMS/	08/31/1998	09/03/1998	71.345	22.959	14.592	29.3712	87.3563	28.0	500.0
	1998	DD980812.A06	/MMS/	08/31/1998	09/03/1998	55.484	22.744	13.611	29.3712	87.3563	32.0	500.0
	1998	DD980812.A07	/MMS/	08/31/1998	09/03/1998	59.083	23.201	13.750	29.3712	87.3563	36.0	500.0
	1998	DD980812.A08	/MMS/	08/31/1998	09/03/1998	52.590	24.262	12.705	29.3712	87.3563	40.0	500.0

Table B-6. Speed statistics for energetic current events associated with tropical cyclones. (continued)

Event No.	Year	Filename	Directory	Event start date (m/d/y)	Event end date (m/d/y)	Maximum speed (cm·s^{-1})	Mean speed (cm·s^{-1})	Stand. dev. of speed (cm·s^{-1})	Latitude (°N)	Longitude (°W)	Depth (m)	Total water depth (m)
9	1998	DD980812.A09	/MMS/	08/31/1998	09/03/1998	50.894	24.970	11.950	29.3712	87.3563	44.0	500.0
	1998	DD980812.A10	/MMS/	08/31/1998	09/03/1998	50.982	25.068	12.338	29.3712	87.3563	48.0	500.0
	1998	DD980812.A11	/MMS/	08/31/1998	09/03/1998	53.891	25.497	12.536	29.3712	87.3563	52.0	500.0
	1998	DD980812.A12	/MMS/	08/31/1998	09/03/1998	51.335	26.130	12.611	29.3712	87.3563	56.0	500.0
	1998	DD980812.A13	/MMS/	08/31/1998	09/03/1998	53.451	26.615	12.447	29.3712	87.3563	60.0	500.0
	1998	DD980812.A14	/MMS/	08/31/1998	09/03/1998	50.340	26.198	12.007	29.3712	87.3563	64.0	500.0
	1998	DD980812.A15	/MMS/	08/31/1998	09/03/1998	50.276	26.187	11.991	29.3712	87.3563	68.0	500.0
	1998	DD980812.A16	/MMS/	08/31/1998	09/03/1998	50.472	26.308	11.637	29.3712	87.3563	72.0	500.0
	1998	DD980812.A17	/MMS/	08/31/1998	09/03/1998	52.626	26.405	11.690	29.3712	87.3563	76.0	500.0
	1998	DD980812.A18	/MMS/	08/31/1998	09/03/1998	52.703	26.209	11.741	29.3712	87.3563	80.0	500.0
	1998	DD980812.C01	/MMS/	08/31/1998	09/03/1998	49.057	30.292	8.293	29.3712	87.3563	200.0	500.0
	1998	DD980812.C02	/MMS/	08/31/1998	09/03/1998	50.505	29.457	6.927	29.3712	87.3563	300.0	500.0
	1998	DD980812.C03	/MMS/	08/31/1998	09/03/1998	19.400	6.995	4.630	29.3712	87.3563	490.0	500.0
	1998	DD980808.A01	/MMS/	08/31/1998	09/03/1998	190.439	61.350	30.019	29.0032	87.3532	12.0	1300.0
	1998	DD980808.A02	/MMS/	08/31/1998	09/03/1998	177.568	62.196	31.843	29.0032	87.3532	16.0	1300.0
	1998	DD980808.A03	/MMS/	08/31/1998	09/03/1998	156.497	61.546	28.656	29.0032	87.3532	20.0	1300.0
	1998	DD980808.A04	/MMS/	08/31/1998	09/03/1998	133.229	60.661	22.451	29.0032	87.3532	24.0	1300.0
	1998	DD980808.A05	/MMS/	08/31/1998	09/03/1998	102.604	57.865	17.247	29.0032	87.3532	28.0	1300.0
	1998	DD980808.A06	/MMS/	08/31/1998	09/03/1998	88.790	55.246	14.757	29.0032	87.3532	32.0	1300.0
	1998	DD980808.A07	/MMS/	08/31/1998	09/03/1998	86.901	53.625	14.007	29.0032	87.3532	36.0	1300.0
	1998	DD980808.A08	/MMS/	08/31/1998	09/03/1998	74.998	52.856	13.145	29.0032	87.3532	40.0	1300.0
	1998	DD980808.A09	/MMS/	08/31/1998	09/03/1998	73.779	52.676	10.966	29.0032	87.3532	44.0	1300.0
	1998	DD980808.A10	/MMS/	08/31/1998	09/03/1998	75.271	52.608	9.465	29.0032	87.3532	48.0	1300.0
	1998	DD980808.A11	/MMS/	08/31/1998	09/03/1998	74.195	51.199	8.240	29.0032	87.3532	52.0	1300.0
	1998	DD980808.A12	/MMS/	08/31/1998	09/03/1998	60.004	41.693	7.114	29.0032	87.3532	56.0	1300.0
	1998	DD980808.A13	/MMS/	08/31/1998	09/03/1998	60.784	41.507	7.592	29.0032	87.3532	60.0	1300.0
	1998	DD980808.A14	/MMS/	08/31/1998	09/03/1998	66.430	45.874	7.861	29.0032	87.3532	64.0	1300.0
	1998	DD980808.A15	/MMS/	08/31/1998	09/03/1998	63.861	44.540	7.883	29.0032	87.3532	68.0	1300.0
	1998	DD980808.A16	/MMS/	08/31/1998	09/03/1998	58.358	42.532	6.978	29.0032	87.3532	72.0	1300.0
	1998	DD980808.C01	/MMS/	08/31/1998	09/03/1998	24.932	15.596	4.654	29.0032	87.3532	500.0	1300.0
	1998	DD980808.C02	/MMS/	08/31/1998	09/03/1998	9.804	4.113	2.252	29.0032	87.3532	1290.0	1300.0
	1998	DD980810.A01	/MMS/	08/31/1998	09/03/1998	141.405	35.555	21.106	29.3348	86.8520	12.0	500.0
	1998	DD980810.A02	/MMS/	08/31/1998	09/03/1998	89.454	37.241	18.555	29.3348	86.8520	16.0	500.0
	1998	DD980810.A03	/MMS/	08/31/1998	09/03/1998	81.789	34.301	15.790	29.3348	86.8520	20.0	500.0

Table B-6. Speed statistics for energetic current events associated with tropical cyclones. (continued)

Event No.	Year	Filename	Directory	Event start date (m/d/y)	Event end date (m/d/y)	Maximum speed (cm·s^{-1})	Mean speed (cm·s^{-1})	Stand. dev. of speed (cm·s^{-1})	Latitude (°N)	Longitude (°W)	Depth (m)	Total water depth (m)
9	1998	DD980810.A04	/MMS/	08/31/1998	09/03/1998	77.634	28.502	13.944	29.3348	86.8520	24.0	500.0
	1998	DD980810.A05	/MMS/	08/31/1998	09/03/1998	81.913	26.834	11.838	29.3348	86.8520	28.0	500.0
	1998	DD980810.A06	/MMS/	08/31/1998	09/03/1998	73.997	26.116	11.370	29.3348	86.8520	32.0	500.0
	1998	DD980810.A07	/MMS/	08/31/1998	09/03/1998	48.056	24.455	9.852	29.3348	86.8520	36.0	500.0
	1998	DD980810.A08	/MMS/	08/31/1998	09/03/1998	50.139	23.863	9.287	29.3348	86.8520	40.0	500.0
	1998	DD980810.A09	/MMS/	08/31/1998	09/03/1998	51.435	22.542	11.136	29.3348	86.8520	44.0	500.0
	1998	DD980810.A10	/MMS/	08/31/1998	09/03/1998	51.509	21.912	12.254	29.3348	86.8520	48.0	500.0
	1998	DD980810.A11	/MMS/	08/31/1998	09/03/1998	50.317	21.674	12.838	29.3348	86.8520	52.0	500.0
	1998	DD980810.A12	/MMS/	08/31/1998	09/03/1998	47.794	20.389	11.401	29.3348	86.8520	56.0	500.0
	1998	DD980810.A13	/MMS/	08/31/1998	09/03/1998	43.506	18.488	10.166	29.3348	86.8520	60.0	500.0
	1998	DD980810.A14	/MMS/	08/31/1998	09/03/1998	33.365	15.450	7.722	29.3348	86.8520	64.0	500.0
	1998	DD980810.A15	/MMS/	08/31/1998	09/03/1998	31.636	15.143	8.072	29.3348	86.8520	68.0	500.0
	1998	DD980810.A16	/MMS/	08/31/1998	09/03/1998	35.612	15.901	8.906	29.3348	86.8520	72.0	500.0
	1998	DD980810.A17	/MMS/	08/31/1998	09/03/1998	31.801	14.437	8.586	29.3348	86.8520	76.0	500.0
	1998	DD980810.A18	/MMS/	08/31/1998	09/03/1998	30.085	13.729	7.495	29.3348	86.8520	80.0	500.0
	1998	DD980810.C01	/MMS/	08/31/1998	09/03/1998	19.122	5.393	5.889	29.3348	86.8520	200.0	500.0
	1998	DD980810.C02	/MMS/	08/31/1998	09/03/1998	17.954	10.481	3.797	29.3348	86.8520	300.0	500.0
	1998	DD980810.C03	/MMS/	08/31/1998	09/03/1998	19.099	4.446	4.253	29.3348	86.8520	490.0	500.0
	1998	EW980806.C01	/TAMU/	08/31/1998	09/03/1998	46.680	12.406	10.810	28.6190	89.9430	297.0	300.0
	1998	VK980806.A01	/MMS/	09/26/1998	10/19/1998	161.030	32.512	25.278	29.0592	88.3900	12.0	500.0
	1998	VK980806.A02	/MMS/	09/26/1998	10/19/1998	146.610	32.947	25.504	29.0592	88.3900	16.0	500.0
	1998	VK980806.A03	/MMS/	09/26/1998	10/19/1998	122.686	31.950	24.568	29.0592	88.3900	20.0	500.0
	1998	VK980806.A04	/MMS/	09/26/1998	10/19/1998	119.861	31.426	23.770	29.0592	88.3900	24.0	500.0
	1998	VK980806.A05	/MMS/	09/26/1998	10/19/1998	116.474	31.177	23.165	29.0592	88.3900	28.0	500.0
	1998	VK980806.A06	/MMS/	09/26/1998	10/19/1998	114.282	30.821	22.344	29.0592	88.3900	32.0	500.0
	1998	VK980806.A07	/MMS/	09/26/1998	10/19/1998	119.709	29.739	21.422	29.0592	88.3900	36.0	500.0
	1998	VK980806.A08	/MMS/	09/26/1998	10/19/1998	122.675	28.104	20.786	29.0592	88.3900	40.0	500.0
	1998	VK980806.A09	/MMS/	09/26/1998	10/19/1998	118.058	26.399	19.715	29.0592	88.3900	44.0	500.0
	1998	VK980806.A10	/MMS/	09/26/1998	10/19/1998	113.137	25.590	18.755	29.0592	88.3900	48.0	500.0
	1998	VK980806.A11	/MMS/	09/26/1998	10/19/1998	116.726	25.465	18.255	29.0592	88.3900	52.0	500.0
	1998	VK980806.A12	/MMS/	09/26/1998	10/19/1998	112.333	24.642	17.741	29.0592	88.3900	56.0	500.0
	1998	VK980806.A13	/MMS/	09/26/1998	10/19/1998	119.326	23.973	17.964	29.0592	88.3900	60.0	500.0
	1998	VK980806.A14	/MMS/	09/26/1998	10/19/1998	108.586	20.255	15.953	29.0592	88.3900	64.0	500.0
	1998	VK980806.A15	/MMS/	09/26/1998	10/19/1998	108.315	20.508	16.657	29.0592	88.3900	68.0	500.0

Table B-6. Speed statistics for energetic current events associated with tropical cyclones. (continued)

Event No.	Year	Filename	Directory	Event start date (m/d/y)	Event end date (m/d/y)	Maximum speed (cm·s^{-1})	Mean speed (cm·s^{-1})	Stand. dev. of speed (cm·s^{-1})	Latitude (°N)	Longitude (°W)	Depth (m)	Total water depth (m)
9	1998	VK980806.A16	/MMS/	09/26/1998	10/19/1998	108.411	23.181	18.826	29.0592	88.3900	72.0	500.0
	1998	VK980806.A17	/MMS/	09/26/1998	10/19/1998	101.636	23.109	18.329	29.0592	88.3900	76.0	500.0
	1998	VK980806.A18	/MMS/	09/26/1998	10/19/1998	97.878	22.948	17.567	29.0592	88.3900	80.0	500.0
	1998	VK980806.C01	/MMS/	09/26/1998	10/19/1998	89.164	16.592	14.652	29.0592	88.3900	200.0	500.0
	1998	VK980806.C02	/MMS/	09/26/1998	10/19/1998	90.610	14.165	14.493	29.0592	88.3900	300.0	500.0
	1998	VK980806.C03	/MMS/	09/26/1998	10/08/1998	47.999	11.125	10.925	29.0592	88.3900	490.0	500.0
	1998	MC980806.A01	/MMS/	09/26/1998	10/19/1998	163.238	37.410	23.409	28.7662	88.2650	8.0	1300.0
	1998	MC980806.A02	/MMS/	09/26/1998	10/19/1998	143.560	36.209	22.249	28.7662	88.2650	12.0	1300.0
	1998	MC980806.A03	/MMS/	09/26/1998	10/19/1998	153.638	35.035	21.252	28.7662	88.2650	16.0	1300.0
	1998	MC980806.A04	/MMS/	09/26/1998	10/19/1998	137.061	34.153	20.134	28.7662	88.2650	20.0	1300.0
	1998	MC980806.A05	/MMS/	09/26/1998	10/19/1998	130.133	33.583	19.231	28.7662	88.2650	24.0	1300.0
	1998	MC980806.A06	/MMS/	09/26/1998	10/19/1998	127.429	33.033	18.697	28.7662	88.2650	28.0	1300.0
	1998	MC980806.A07	/MMS/	09/26/1998	10/19/1998	120.877	32.597	18.329	28.7662	88.2650	32.0	1300.0
	1998	MC980806.A08	/MMS/	09/26/1998	10/19/1998	112.485	32.237	17.853	28.7662	88.2650	36.0	1300.0
	1998	MC980806.A09	/MMS/	09/26/1998	10/19/1998	107.307	31.999	17.163	28.7662	88.2650	40.0	1300.0
	1998	MC980806.A10	/MMS/	09/26/1998	10/19/1998	104.066	31.496	16.264	28.7662	88.2650	44.0	1300.0
	1998	MC980806.A11	/MMS/	09/26/1998	10/19/1998	96.440	30.682	15.295	28.7662	88.2650	48.0	1300.0
	1998	MC980806.A12	/MMS/	09/26/1998	10/19/1998	85.028	29.814	14.380	28.7662	88.2650	52.0	1300.0
	1998	MC980806.A13	/MMS/	09/26/1998	10/19/1998	56.786	19.561	9.832	28.7662	88.2650	56.0	1300.0
	1998	MC980806.A14	/MMS/	09/26/1998	10/19/1998	55.716	20.355	10.785	28.7662	88.2650	60.0	1300.0
	1998	MC980806.A15	/MMS/	09/26/1998	10/19/1998	74.502	29.185	14.927	28.7662	88.2650	64.0	1300.0
	1998	MC980806.A16	/MMS/	09/26/1998	10/19/1998	73.752	28.286	14.317	28.7662	88.2650	68.0	1300.0
	1998	MC980806.C01	/MMS/	09/26/1998	10/19/1998	33.071	11.024	6.442	28.7662	88.2650	500.0	1300.0
	1998	MC980806.C02	/MMS/	09/26/1998	10/19/1998	29.302	7.114	4.941	28.7662	88.2650	1310.0	1320.0
	1998	VK980807.A01	/MMS/	09/26/1998	10/19/1998	153.119	25.502	26.015	29.2120	87.8722	12.0	500.0
	1998	VK980807.A02	/MMS/	09/26/1998	10/19/1998	141.386	28.196	26.877	29.2120	87.8722	16.0	500.0
	1998	VK980807.A03	/MMS/	09/26/1998	10/19/1998	145.524	27.151	26.866	29.2120	87.8722	20.0	500.0
	1998	VK980807.A04	/MMS/	09/26/1998	10/19/1998	148.387	26.249	26.943	29.2120	87.8722	24.0	500.0
	1998	VK980807.A05	/MMS/	09/26/1998	10/19/1998	151.609	25.295	26.951	29.2120	87.8722	28.0	500.0
	1998	VK980807.A06	/MMS/	09/26/1998	10/19/1998	150.624	24.332	26.923	29.2120	87.8722	32.0	500.0
	1998	VK980807.A07	/MMS/	09/26/1998	10/19/1998	150.215	23.687	26.582	29.2120	87.8722	36.0	500.0
	1998	VK980807.A08	/MMS/	09/26/1998	10/19/1998	147.707	23.227	26.376	29.2120	87.8722	40.0	500.0
	1998	VK980807.A09	/MMS/	09/26/1998	10/19/1998	142.342	23.375	25.910	29.2120	87.8722	44.0	500.0
	1998	VK980807.A10	/MMS/	09/26/1998	10/19/1998	140.049	23.282	25.472	29.2120	87.8722	48.0	500.0

Table B-6. Speed statistics for energetic current events associated with tropical cyclones. (continued)

Event No.	Year	Filename	Directory	Event start date (m/d/y)	Event end date (m/d/y)	Maximum speed (cm·s^{-1})	Mean speed (cm·s^{-1})	Stand. dev. of speed (cm·s^{-1})	Latitude (°N)	Longitude (°W)	Depth (m)	Total water depth (m)
9	1998	VK980807.A11	/MMS/	09/26/1998	10/19/1998	137.241	23.163	24.674	29.2120	87.8722	52.0	500.0
	1998	VK980807.A12	/MMS/	09/26/1998	10/19/1998	135.663	22.377	23.825	29.2120	87.8722	56.0	500.0
	1998	VK980807.A13	/MMS/	09/26/1998	10/19/1998	138.226	21.304	24.272	29.2120	87.8722	60.0	500.0
	1998	VK980807.A14	/MMS/	09/26/1998	10/19/1998	127.512	17.320	22.083	29.2120	87.8722	64.0	500.0
	1998	VK980807.A15	/MMS/	09/26/1998	10/19/1998	125.929	17.380	22.164	29.2120	87.8722	68.0	500.0
	1998	VK980807.A16	/MMS/	09/26/1998	10/19/1998	132.106	19.839	24.006	29.2120	87.8722	72.0	500.0
	1998	VK980807.A17	/MMS/	09/26/1998	10/19/1998	132.480	19.816	23.753	29.2120	87.8722	76.0	500.0
	1998	VK980807.A18	/MMS/	09/26/1998	10/19/1998	132.184	19.744	23.909	29.2120	87.8722	80.0	500.0
	1998	VK980807.C01	/MMS/	09/26/1998	10/11/1998	128.395	18.973	23.098	29.2120	87.8722	200.0	500.0
	1998	VK980807.C02	/MMS/	09/26/1998	10/19/1998	97.002	14.642	13.386	29.2120	87.8722	300.0	500.0
	1998	VK980807.C03	/MMS/	09/26/1998	10/19/1998	65.101	12.163	10.068	29.2120	87.8722	490.0	500.0
	1998	VK980807.A19	/MMS/	09/26/1998	10/19/1998	161.808	34.563	17.270	29.0705	87.8568	12.0	1300.0
	1998	VK980807.A20	/MMS/	09/26/1998	10/19/1998	148.308	30.391	20.107	29.0705	87.8568	16.0	1300.0
	1998	VK980807.A21	/MMS/	09/26/1998	10/19/1998	136.940	28.796	19.464	29.0705	87.8568	20.0	1300.0
	1998	VK980807.A22	/MMS/	09/26/1998	10/19/1998	131.533	26.707	18.912	29.0705	87.8568	24.0	1300.0
	1998	VK980807.A23	/MMS/	09/26/1998	10/19/1998	120.877	24.965	18.167	29.0705	87.8568	28.0	1300.0
	1998	VK980807.A24	/MMS/	09/26/1998	10/19/1998	110.377	23.351	16.920	29.0705	87.8568	32.0	1300.0
	1998	VK980807.A25	/MMS/	09/26/1998	10/19/1998	96.116	21.589	15.725	29.0705	87.8568	36.0	1300.0
	1998	VK980807.A26	/MMS/	09/26/1998	10/19/1998	82.854	20.526	14.519	29.0705	87.8568	40.0	1300.0
	1998	VK980807.A27	/MMS/	09/26/1998	10/19/1998	70.830	20.233	13.393	29.0705	87.8568	44.0	1300.0
	1998	VK980807.A28	/MMS/	09/26/1998	10/19/1998	70.241	20.404	12.951	29.0705	87.8568	48.0	1300.0
	1998	VK980807.A29	/MMS/	09/26/1998	10/19/1998	68.101	20.592	13.523	29.0705	87.8568	52.0	1300.0
	1998	VK980807.A30	/MMS/	09/26/1998	10/19/1998	55.704	15.439	11.206	29.0705	87.8568	56.0	1300.0
	1998	VK980807.A31	/MMS/	09/26/1998	10/19/1998	61.059	15.615	11.394	29.0705	87.8568	60.0	1300.0
	1998	VK980807.A32	/MMS/	09/26/1998	10/19/1998	72.827	20.427	13.365	29.0705	87.8568	64.0	1300.0
	1998	VK980807.A33	/MMS/	09/26/1998	10/19/1998	76.287	20.315	12.933	29.0705	87.8568	68.0	1300.0
	1998	VK980807.A34	/MMS/	09/26/1998	10/19/1998	78.339	18.534	13.242	29.0705	87.8568	72.0	1300.0
	1998	VK980807.C04	/MMS/	09/26/1998	10/19/1998	54.281	9.272	8.457	29.0705	87.8568	500.0	1300.0
	1998	VK980808.C01	/MMS/	09/26/1998	10/19/1998	27.697	8.334	5.133	29.0705	87.8568	1290.0	1300.0
	1998	DD980812.A01	/MMS/	09/26/1998	10/19/1998	108.707	25.367	16.613	29.3712	87.3563	12.0	500.0
	1998	DD980812.A02	/MMS/	09/26/1998	10/19/1998	104.143	24.979	15.802	29.3712	87.3563	16.0	500.0
	1998	DD980812.A03	/MMS/	09/26/1998	10/19/1998	93.351	23.734	15.282	29.3712	87.3563	20.0	500.0
	1998	DD980812.A04	/MMS/	09/26/1998	10/19/1998	99.645	23.235	15.601	29.3712	87.3563	24.0	500.0
	1998	DD980812.A05	/MMS/	09/26/1998	10/19/1998	113.641	22.961	16.159	29.3712	87.3563	28.0	500.0

Table B-6. Speed statistics for energetic current events associated with tropical cyclones. (continued)

Event No.	Year	Filename	Directory	Event start date (m/d/y)	Event end date (m/d/y)	Maximum speed (cm·s^{-1})	Mean speed (cm·s^{-1})	Stand. dev. of speed (cm·s^{-1})	Latitude (°N)	Longitude (°W)	Depth (m)	Total water depth (m)
9	1998	DD980812.A06	/MMS/	09/26/1998	10/19/1998	118.084	22.752	16.644	29.3712	87.3563	32.0	500.0
	1998	DD980812.A07	/MMS/	09/26/1998	10/19/1998	114.661	22.679	17.018	29.3712	87.3563	36.0	500.0
	1998	DD980812.A08	/MMS/	09/26/1998	10/19/1998	111.668	22.444	17.378	29.3712	87.3563	40.0	500.0
	1998	DD980812.A09	/MMS/	09/26/1998	10/19/1998	113.492	21.605	17.804	29.3712	87.3563	44.0	500.0
	1998	DD980812.A10	/MMS/	09/26/1998	10/19/1998	113.789	21.163	17.947	29.3712	87.3563	48.0	500.0
	1998	DD980812.A11	/MMS/	09/26/1998	10/19/1998	113.373	20.718	18.081	29.3712	87.3563	52.0	500.0
	1998	DD980812.A12	/MMS/	09/26/1998	10/19/1998	112.730	19.993	18.217	29.3712	87.3563	56.0	500.0
	1998	DD980812.A13	/MMS/	09/26/1998	10/19/1998	117.850	19.448	19.007	29.3712	87.3563	60.0	500.0
	1998	DD980812.A14	/MMS/	09/26/1998	10/19/1998	117.526	19.823	19.170	29.3712	87.3563	64.0	500.0
	1998	DD980812.A15	/MMS/	09/26/1998	10/19/1998	119.822	20.318	19.325	29.3712	87.3563	68.0	500.0
	1998	DD980812.A16	/MMS/	09/26/1998	10/19/1998	121.443	20.176	19.755	29.3712	87.3563	72.0	500.0
	1998	DD980812.A17	/MMS/	09/26/1998	10/19/1998	119.861	19.440	19.525	29.3712	87.3563	76.0	500.0
	1998	DD980812.A18	/MMS/	09/26/1998	10/19/1998	115.981	18.036	18.471	29.3712	87.3563	80.0	500.0
	1998	DD980812.C01	/MMS/	09/26/1998	10/19/1998	110.084	16.284	15.676	29.3712	87.3563	200.0	500.0
	1998	DD980812.C02	/MMS/	09/26/1998	10/19/1998	85.670	16.904	12.807	29.3712	87.3563	300.0	500.0
	1998	DD980812.C03	/MMS/	09/26/1998	10/19/1998	72.003	13.158	9.946	29.3712	87.3563	490.0	500.0
	1998	DD980808.A01	/MMS/	09/26/1998	10/19/1998	202.837	30.467	22.425	29.0032	87.3532	12.0	1300.0
	1998	DD980808.A02	/MMS/	09/26/1998	10/19/1998	176.855	26.816	23.124	29.0032	87.3532	16.0	1300.0
	1998	DD980808.A03	/MMS/	09/26/1998	10/19/1998	161.485	25.733	22.276	29.0032	87.3532	20.0	1300.0
	1998	DD980808.A04	/MMS/	09/26/1998	10/19/1998	174.001	24.714	21.661	29.0032	87.3532	24.0	1300.0
	1998	DD980808.A05	/MMS/	09/26/1998	10/19/1998	156.170	23.673	21.236	29.0032	87.3532	28.0	1300.0
	1998	DD980808.A06	/MMS/	09/26/1998	10/19/1998	141.319	22.495	20.542	29.0032	87.3532	32.0	1300.0
	1998	DD980808.A07	/MMS/	09/26/1998	10/19/1998	125.455	21.551	19.604	29.0032	87.3532	36.0	1300.0
	1998	DD980808.A08	/MMS/	09/26/1998	10/19/1998	117.282	20.464	18.332	29.0032	87.3532	40.0	1300.0
	1998	DD980808.A09	/MMS/	09/26/1998	10/19/1998	102.837	19.469	16.283	29.0032	87.3532	44.0	1300.0
	1998	DD980808.A10	/MMS/	09/26/1998	10/19/1998	92.670	19.075	14.318	29.0032	87.3532	48.0	1300.0
	1998	DD980808.A11	/MMS/	09/26/1998	10/19/1998	77.131	18.482	12.880	29.0032	87.3532	52.0	1300.0
	1998	DD980808.A12	/MMS/	09/26/1998	10/19/1998	56.451	15.618	10.717	29.0032	87.3532	56.0	1300.0
	1998	DD980808.A13	/MMS/	09/26/1998	10/19/1998	50.472	14.963	9.949	29.0032	87.3532	60.0	1300.0
	1998	DD980808.A14	/MMS/	09/26/1998	10/19/1998	49.920	15.256	10.563	29.0032	87.3532	64.0	1300.0
	1998	DD980808.A15	/MMS/	09/26/1998	10/19/1998	53.422	14.454	10.762	29.0032	87.3532	68.0	1300.0
	1998	DD980808.A16	/MMS/	09/26/1998	10/19/1998	48.083	15.772	10.505	29.0032	87.3532	72.0	1300.0
	1998	DD980808.C01	/MMS/	09/26/1998	10/19/1998	34.813	14.569	7.347	29.0032	87.3532	500.0	1300.0
	1998	DD980808.C02	/MMS/	09/26/1998	10/19/1998	48.603	12.536	10.325	29.0032	87.3532	1290.0	1300.0

Table B-6. Speed statistics for energetic current events associated with tropical cyclones. (continued)

Event No.	Year	Filename	Directory	Event start date (m/d/y)	Event end date (m/d/y)	Maximum speed ($cm \cdot s^{-1}$)	Mean speed ($cm \cdot s^{-1}$)	Stand. dev. of speed ($cm \cdot s^{-1}$)	Latitude (°N)	Longitude (°W)	Depth (m)	Total water depth (m)
9	1998	DD980810.A01	/MMS/	09/26/1998	10/19/1998	156.826	22.485	21.475	29.3348	86.8520	12.0	500.0
	1998	DD980810.A02	/MMS/	09/26/1998	10/19/1998	159.905	23.694	20.093	29.3348	86.8520	16.0	500.0
	1998	DD980810.A03	/MMS/	09/26/1998	10/19/1998	159.066	22.629	19.236	29.3348	86.8520	20.0	500.0
	1998	DD980810.A04	/MMS/	09/26/1998	10/19/1998	139.394	21.541	17.525	29.3348	86.8520	24.0	500.0
	1998	DD980810.A05	/MMS/	09/26/1998	10/19/1998	130.437	20.912	16.683	29.3348	86.8520	28.0	500.0
	1998	DD980810.A06	/MMS/	09/26/1998	10/19/1998	121.074	20.437	15.759	29.3348	86.8520	32.0	500.0
	1998	DD980810.A07	/MMS/	09/26/1998	10/19/1998	110.401	20.288	14.632	29.3348	86.8520	36.0	500.0
	1998	DD980810.A08	/MMS/	09/26/1998	10/19/1998	100.749	20.445	13.076	29.3348	86.8520	40.0	500.0
	1998	DD980810.A09	/MMS/	09/26/1998	10/19/1998	74.166	20.424	10.963	29.3348	86.8520	44.0	500.0
	1998	DD980810.A10	/MMS/	09/26/1998	10/19/1998	62.613	20.137	9.366	29.3348	86.8520	48.0	500.0
	1998	DD980810.A11	/MMS/	09/26/1998	10/19/1998	48.073	19.076	8.665	29.3348	86.8520	52.0	500.0
	1998	DD980810.A12	/MMS/	09/26/1998	10/19/1998	45.069	18.028	7.981	29.3348	86.8520	56.0	500.0
	1998	DD980810.A13	/MMS/	09/26/1998	10/19/1998	45.838	17.578	8.072	29.3348	86.8520	60.0	500.0
	1998	DD980810.A14	/MMS/	09/26/1998	10/19/1998	42.218	16.300	7.839	29.3348	86.8520	64.0	500.0
	1998	DD980810.A15	/MMS/	09/26/1998	10/19/1998	44.031	16.270	7.758	29.3348	86.8520	68.0	500.0
	1998	DD980810.A16	/MMS/	09/26/1998	10/19/1998	39.041	16.045	7.624	29.3348	86.8520	72.0	500.0
	1998	DD980810.A17	/MMS/	09/26/1998	10/19/1998	38.037	15.422	7.465	29.3348	86.8520	76.0	500.0
	1998	DD980810.A18	/MMS/	09/26/1998	10/19/1998	38.485	13.783	7.321	29.3348	86.8520	80.0	500.0
	1998	DD980810.C01	/MMS/	09/26/1998	10/19/1998	49.059	14.801	7.298	29.3348	86.8520	200.0	500.0
	1998	DD980810.C02	/MMS/	09/26/1998	10/19/1998	52.828	9.694	7.629	29.3348	86.8520	300.0	500.0
	1998	DD980810.C03	/MMS/	09/26/1998	10/19/1998	39.598	11.980	9.044	29.3348	86.8520	490.0	500.0
	1998	EW980806.C01	/TAMU/	09/26/1998	10/19/1998	81.764	9.489	9.545	28.6190	89.9430	297.0	300.0

Notes by event number

1 1980: Hurricane ALLEN, 31 JUL-11 AUG:

These records give a good example of currents produced during a hurricane. The storm passed within 60 km south of the Brooks C mooring. The maximum speed at C at 200 m was 93.9 $cm \cdot s^{-1}$. Inertial motions are seen in all records at S and C. A detail of the time series of current stick vectors at Brooks moorings C and S during Hurricane Allen are plotted in Figure 6.1.2.-2. Data from Brooks C and S are plotted in Figure 6.3.2-2.

2 1983: Hurricane BARRY, 23-29 AUG

Hurricane Barry was a fast moving storm going east to west through the Gulf. It was a weak Tropical Depression when it passed over SAIC mooring A. Inertial oscillations occurred at 172 and 400 m about1-2 days after the closest approach. Data from SAIC A are plotted in Figure 6.3.3-2.

Table B-6. Speed statistics for energetic current events associated with tropical cyclones. (continued)

Notes by event number (continued)

3 1985: Hurricane ELENA, 28 AUG- 4 SEP

Hurricane Elena was a category 3 hurricane that occurred in the eastern Gulf. During August 29 through September 2, when it passed near SAIC moorings A and G, the storm was a category 1 hurricane. Some inertial motions are seen in the instrument records at 700 m and shallower. Peak velocity at 172 m is 82 $cm \cdot s^{-1}$. Data from SAIC A and G are plotted in Figure 6.3.3-2.

4 1987: Tropical Depression ONE, 9-17 AUG

This weak storm was moved over the central Gulf SAIC moorings EE, FF, and GG briefly on August 9. Weak inertial oscillations, with amplitudes of ~10 $cm \cdot s^{-1}$, occur at 725 m. Data from SAIC EE, FF, and GG are plotted in Figure 6.3.3-2.

5 1988: Hurricane FLORENCE, 7-11 SEP

Hurricane Florence was a category 1 storm when it passed 2° to the east of the central Gulf SAIC moorings EE, FF, and GG. No significant effect is seen in records deeper than 100 m. Inertial period oscillations were present at the 100 m records in EE, FF, and GG. Data from SAIC EE, FF, and GG are plotted in Figure 6.3.3-2.

6 1988: Hurricane GILBERT, 8-20 SEP

Hurricane Gilbert was a category 4 storm that passed through the southern Gulf. It was south of SAIC moorings EE, FF, and GG. Records from the 100 m instruments show inertial period oscillations for ~10 days after storm. Peak currents at GG approach 121 $cm \cdot s^{-1}$ at 100 m. Data from SAIC EE, FF, and GG are plotted in Figure 6.3.3-2. All MAMES data are plotted in Figure 6.3.9-2.

7 1992: Hurricane ANDREW, 16-28 AUG

Hurricane Andrew was a category 4 hurricane when it passed over the eastern Texas-Louisiana shelf and slope. The shelf circulation temporarily reversed in response to the storm passage. The storm had a small but noticeable effect on currents at LATEX mooring 49, which was off the shelf break off the south Texas coast. It passed just north of LATEX mooring 12. Large amplitude currents were seen at all depths at LATEX 12, with near-surface (14 m) maximum of 105 $cm \cdot s^{-1}$. Several days of inertial oscillations followed the storm's passage. The time series of current stick vectors at LATEX moorings 12 during Hurricane Andrew are plotted in Figure 6.1.2.-1. Data from LATEX 12 are plotted in Figure 6.3.4-2.

8 1997: Hurricane DANNY, 16-26 JUL

The genesis of Hurricane Danny was over the Texas-Louisiana slope. The hurricane then moved northeast over the Mississippi-Alabama shelf. There it affected currents at SAIC EIS instruments. The records show numerous examples of inertial oscillations and downward propagation of inertial energy. All SAIC EIS data are plotted in Figure 6.3.5-2. All Industry AT378 data are plotted in Figure 6.3.12-13.

9 1998: Hurricane EARL, 31 AUG-03 SEP, and Hurricane GEORGES, 15-29 SEP

Both hurricanes influenced currents in the central Gulf of Mexico and the DeSoto Canyon region. In particular, Hurricane Georges (category 2) produced strong surface currents in excess of 200 $cm \cdot s^{-1}$ and packets of inertial and sub-inertial oscillations between 500 m to 1300 m. Strong inertial oscillations and currents in excess of 100 $cm \cdot s^{-1}$ also accompanied Hurricane Earl. Data from SAIC EIS are plotted in 6.3.5-2. Details of Hurricane Georges are plotted in Figures 6.1.2-5, 6.1.5-1, 6.1.5-2, and 6.1.5-3. Due to the close proximity in time of the two events, their records are merged.

Table B-7. Speed statistics for energetic current events associated with extratropical (winter) cyclones. Given are the name of the file containing the event (keyed to the directory on the CD-ROM database), the start and stop dates used to characterize the event, maximum speed, mean speed, standard deviation of speed, mooring location, depth of the instrument, and total water depth. Comments on the event, keyed by the event number, are given in the notes below the table.

Event No.	Year	Filename	Directory	Event start date (m/d/y)	Event end date (m/d/y)	Maximum speed ($cm \cdot s^{-1}$)	Mean speed ($cm \cdot s^{-1}$)	Stand. dev. of speed ($cm \cdot s^{-1}$)	Latitude (°N)	Longitude (°W)	Depth (m)	Total water depth (m)
1	1978	DD771018.C01	/NODC_DEEP/	01/18/1978	01/30/1978	46.813	23.053	8.128	29.1900	87.6367	90.0	1047.0
	1978	DD771019.C01	/NODC_DEEP/	01/18/1978	01/30/1978	35.656	19.116	7.904	29.1900	87.6367	190.0	1047.0
	1978	DD771018.C02	/NODC_DEEP/	01/18/1978	01/30/1978	29.485	8.152	5.590	29.1900	87.6367	985.0	1047.0
2	1979	EL781026.C01	/NODC_DEEP/	01/12/1979	01/26/1979	34.752	16.178	8.107	27.6633	85.5217	157.0	1050.0
3	1979	EL781026.C03	/NODC_DEEP/	01/30/1979	02/05/1979	31.286	16.514	7.286	27.6633	85.5217	957.0	1050.0
4	1983	HH830127.C01	/NODC_DEEP/	02/05/1983	02/14/1983	66.851	41.727	11.144	25.7150	84.8850	172.0	1697.0
5	1983	HH830127.C01	/NODC_DEEP/	02/15/1983	02/19/1983	40.618	17.532	8.578	25.7150	84.8850	172.0	1697.0
6	1983	HH830127.C01	/NODC_DEEP/	02/20/1983	02/25/1983	37.211	19.662	6.895	25.7150	84.8850	172.0	1697.0
7	1983	HH830127.C01	/NODC_DEEP/	02/26/1983	03/15/1983	52.608	26.690	13.802	25.7150	84.8850	172.0	1697.0
8	1983	HH830127.C01	/NODC_DEEP/	03/16/1983	03/22/1983	43.137	28.213	7.874	25.7150	84.8850	172.0	1697.0
	1983	HH830127.C03	/NODC_DEEP/	03/16/1983	03/22/1983	23.722	6.652	4.116	25.7150	84.8850	1600.0	1697.0
9	1983	HH830127.C01	/NODC_DEEP/	03/23/1983	04/02/1983	50.367	23.092	12.665	25.7150	84.8850	172.0	1697.0
	1983	HH830127.C03	/NODC_DEEP/	03/23/1983	04/02/1983	22.219	5.849	4.415	25.7150	84.8850	1600.0	1697.0
10	1992	GC921023.C01	/TAMU/	11/04/1992	11/10/1992	27.594	14.833	4.922	27.9240	90.4950	19.0	505.0
	1992	GC921023.C02	/TAMU/	11/04/1992	11/10/1992	20.338	9.370	4.457	27.9240	90.4950	105.0	505.0
	1992	GC921022.C01	/TAMU/	11/04/1992	11/10/1992	4.804	1.869	0.704	27.9240	90.4950	495.0	505.0
	1992	EB921018.C01	/TAMU/	11/04/1992	11/10/1992	26.878	13.885	5.791	27.3690	95.8940	17.0	505.0
	1992	EB921018.C02	/TAMU/	11/04/1992	11/10/1992	25.492	11.437	5.749	27.3690	95.8940	105.0	505.0
	1992	EB921018.C03	/TAMU/	11/04/1992	11/10/1992	17.723	4.352	3.981	27.3690	95.8940	495.0	505.0
11	1992	GC921023.C01	/TAMU/	11/24/1992	12/01/1992	36.954	18.540	9.313	27.9240	90.4950	19.0	505.0
	1992	GC921023.C02	/TAMU/	11/24/1992	12/01/1992	26.116	12.964	5.758	27.9240	90.4950	105.0	505.0
	1992	GC921022.C01	/TAMU/	11/24/1992	12/01/1992	4.148	2.294	0.807	27.9240	90.4950	495.0	505.0
	1992	EB921018.C01	/TAMU/	11/24/1992	12/01/1992	46.966	31.230	8.700	27.3690	95.8940	17.0	505.0
	1992	EB921018.C02	/TAMU/	11/24/1992	12/01/1992	44.115	29.675	8.114	27.3690	95.8940	105.0	505.0
	1992	EB921018.C03	/TAMU/	11/24/1992	12/01/1992	11.357	3.509	2.623	27.3690	95.8940	495.0	505.0
12	1992	GC921023.C01	/TAMU/	12/09/1992	12/14/1992	22.809	10.462	5.418	27.9240	90.4950	19.0	505.0
	1992	GC921023.C02	/TAMU/	12/09/1992	12/14/1992	19.091	8.426	4.486	27.9240	90.4950	105.0	505.0
	1992	EB921018.C01	/TAMU/	12/09/1992	12/14/1992	71.853	40.107	13.960	27.3690	95.8940	17.0	505.0
	1992	EB921018.C02	/TAMU/	12/09/1992	12/14/1992	58.340	29.502	11.598	27.3690	95.8940	105.0	505.0
	1992	EB921018.C03	/TAMU/	12/09/1992	12/14/1992	13.036	3.286	3.011	27.3690	95.8940	495.0	505.0

Table B-7. Speed statistics for energetic current events associated with extratropical (winter) cyclones. (continued)

Event No.	**Year**	**Filename**	**Directory**	**Event start date (m/d/y)**	**Event end date (m/d/y)**	**Maximum speed ($cm \cdot s^{-1}$)**	**Mean speed ($cm \cdot s^{-1}$)**	**Stand. dev. of speed ($cm \cdot s^{-1}$)**	**Latitude (°N)**	**Longitude (°W)**	**Depth (m)**	**Total water depth (m)**
13	1993	GC930112.C01	/TAMU/	03/12/1993	04/07/1993	65.837	17.874	12.041	27.9290	90.4940	12.0	498.0
	1993	EB930119.C01	/TAMU/	03/12/1993	04/07/1993	21.390	5.374	3.777	27.3860	95.8990	491.0	501.0
14	1993	GC930112.C01	/TAMU/	04/08/1993	04/12/1993	45.718	18.007	10.174	27.9290	90.4940	12.0	498.0
15	1993	EB931212.C01	/TAMU/	12/20/1993	12/29/1993	34.372	17.351	7.618	27.3850	95.9020	12.0	500.0
16	1994	EB940330.C01	/TAMU/	04/22/1994	05/02/1994	48.966	21.576	10.482	27.3820	95.9000	10.0	498.0
	1994	EB940330.C02	/TAMU/	04/22/1994	05/02/1994	43.463	17.014	8.190	27.3820	95.9000	98.0	498.0
17	1994	EB940330.C01	/TAMU/	05/03/1994	05/12/1994	34.558	17.174	7.403	27.3820	95.9000	10.0	498.0
	1994	EB940330.C02	/TAMU/	05/03/1994	05/12/1994	21.359	9.680	4.806	27.3820	95.9000	98.0	498.0
	1994	GC940212.A01	/INDUSTRY/	05/03/1994	05/12/1994	35.536	20.146	5.675	27.7457	90.7310	31.0	894.6
	1994	GC940212.A02	/INDUSTRY/	05/03/1994	05/12/1994	35.536	20.416	5.543	27.7457	90.7310	39.0	894.6
	1994	GC940212.A03	/INDUSTRY/	05/03/1994	05/12/1994	38.221	20.038	5.868	27.7457	90.7310	47.0	894.6
	1994	GC940212.A04	/INDUSTRY/	05/03/1994	05/12/1994	37.122	20.054	6.157	27.7457	90.7310	55.0	894.6
	1994	GC940212.A05	/INDUSTRY/	05/03/1994	05/12/1994	35.851	20.913	6.245	27.7457	90.7310	63.0	894.6
	1994	GC940212.A06	/INDUSTRY/	05/03/1994	05/12/1994	37.849	21.193	6.037	27.7457	90.7310	71.0	894.6
	1994	GC940212.A07	/INDUSTRY/	05/03/1994	05/12/1994	38.422	21.435	6.210	27.7457	90.7310	79.0	894.6
	1994	GC940212.A08	/INDUSTRY/	05/03/1994	05/12/1994	40.253	21.112	6.942	27.7457	90.7310	87.0	894.6
	1994	GC940212.A09	/INDUSTRY/	05/03/1994	05/12/1994	36.603	20.111	6.759	27.7457	90.7310	95.0	894.6
	1994	GC940212.A10	/INDUSTRY/	05/03/1994	05/12/1994	38.021	18.783	6.817	27.7457	90.7310	103.0	894.6
	1994	GC940212.A11	/INDUSTRY/	05/03/1994	05/12/1994	32.827	17.339	6.935	27.7457	90.7310	111.0	894.6
	1994	GC940212.A12	/INDUSTRY/	05/03/1994	05/12/1994	30.509	15.462	6.166	27.7457	90.7310	119.0	894.6
	1994	GC940212.A13	/INDUSTRY/	05/03/1994	05/12/1994	29.852	14.923	5.543	27.7457	90.7310	127.0	894.6
	1994	GC940212.A14	/INDUSTRY/	05/03/1994	05/12/1994	31.966	14.266	6.017	27.7457	90.7310	135.0	894.6
	1994	GC940212.A15	/INDUSTRY/	05/03/1994	05/12/1994	26.632	12.102	5.099	27.7457	90.7310	143.0	894.6
	1994	GC940212.A16	/INDUSTRY/	05/03/1994	05/12/1994	32.512	13.370	5.911	27.7457	90.7310	151.0	894.6
	1994	GC940212.A17	/INDUSTRY/	05/03/1994	05/12/1994	31.567	12.230	5.918	27.7457	90.7310	159.0	894.6
	1994	GC940212.A18	/INDUSTRY/	05/03/1994	05/12/1994	23.970	10.503	4.859	27.7457	90.7310	167.0	894.6
	1994	GC940212.A19	/INDUSTRY/	05/03/1994	05/12/1994	24.250	10.730	5.393	27.7457	90.7310	175.0	894.6
	1994	GC940212.A20	/INDUSTRY/	05/03/1994	05/12/1994	25.031	10.942	5.391	27.7457	90.7310	183.0	894.6

Notes by event number

1 1978: January 18, January 20, and January 25

Small amplitude inertial oscillations of ~10 $cm \cdot s^{-1}$ occurred at NOAA M3 mooring in association with these three extratropical cyclones. Data from NOAA M3 are plotted in Figure 6.3.1-2.

Table B-7. Speed statistics for energetic current events associated with extratropical (winter) cyclones. (continued)

Notes by event number (continued)

2 1979: January 12

Small amplitude inertial oscillations occurred at the NOAA T1 mooring, with amplitudes of 10-15 $cm \cdot s^{-1}$ at 160 m. Data from NOAA T1 are plotted in Figure 6.3.1-2.

3 1979: January 30

Inertial oscillations occurred in the record for NOAA T1 at 950 m. These oscillations, however, may be associated with surface oscillations occurring two weeks prior to the passage of this extratropical cyclone. Data from NOAA T1 are plotted in Figure 6.3.1-2.

4 1983: February 5

The record for the upper(172 m) instrument at SAIC mooring A shows inertial period oscillations. Records for the middle (1100 m) and lower (1600 m) instruments show no effect. A large maximum speed of 67 $cm \cdot s^{-1}$ at 172 m is attributed to low-frequency motions that were independent of the extratropical cyclone. Data from SAIC A are plotted in Figure 6.3.3-2. The u- and v-velocity components at 172 m are shown in Figure A.7-1.

5 1983: February 15

The record for the upper (172 m) instrument at SAIC A shows inertial period oscillations. Records for the middle (1100 m) and lower (1600 m) instruments show no effect. Data from SAIC A are plotted in Figure 6.3.3-2. The u- and v-velocity components at 172 m are shown in Figure A.7-1.

6 1983: February 20

The record for the upper (172 m) instrument at SAIC A shows inertial period oscillations. Records for the middle (1100 m) and lower (1600 m) instruments show no effect. Data from SAIC A are plotted in Figure 6.3.3-2. The u- and v-velocity components at 172 m are shown in Figure A.7-1.

7 1983: February 26

The record for the upper (172 m) instrument at SAIC A shows inertial period oscillations. Records for the middle (1100 m) and lower (1600 m) instruments show no effect. Data from SAIC A are plotted in Figure 6.3.3-2. The u- and v-velocity components at 172 m are shown in Figure A.7-1.

8 1983: March 16

The record for the upper (172 m) instrument at SAIC A shows inertial period oscillations. The record for the middle (1100 m) instrument shows no effect. The record for the lower (1600 m) instrument shows an increase in the amplitude of the inertial period in the v-velocity component. Data from SAIC A are plotted in Figure 6.3.3-2. The u- and v-velocity components at 172 m are shown in Figure A.7-1.

9 1983: March 23

The record for the upper (172 m) instrument at SAIC A shows inertial period oscillations. The record for the middle (1100 m) instrument shows no effect. The record for the lower (1600 m) instrument shows an increase in the amplitude of the inertial period in the v-velocity component. Data from SAIC A are plotted in Figure 6.3.3-2. The u- and v-velocity components at 172 m are shown in Figure A.7-1.

10 1992: November 4

Strong inertial oscillations are seen in the records at LATEX 49, but are weaker at LATEX 12. Phasing of the oscillations indicates that effects from the extratropical cyclone occurred first at LATEX 49 then at LATEX 12. Data from LATEX 12 and 49 are plotted in Figure 6.3.4-2.

Table B-7. Speed statistics for energetic current events associated with extratropical (winter) cyclones. (continued)

Notes by event number (continued)

11 1992: November 24

Strong inertial oscillations are seen at LATEX 12, but are weaker at LATEX 49. Phasing of the oscillations indicates that effects from the extratropical cyclone occurred first at LATEX 49 then at LATEX 12. Data from LATEX 12 and 49 are plotted in Figure 6.3.4-2.

12 1992: December 9

Inertial oscillations are present in the records at LATEX 12 and 49. The phasing between the two moorings unclear is unclear. Data from LATEX 12 and 49 are plotted in Figure 6.3.4-2.

13 1993: March 12 (Storm of the Century)

Large current fluctuations and inertial oscillations occurred during passage of this extratropical cyclone at LATEX 12. A detail of this event is plotted in Figure 6.1.2-3. Only data from ~500 m depth were available from LATEX 49. Data from LATEX 12 and 49 are plotted in Figure 6.3.4-2.

14 1993: April 8

Strong (30 $cm \cdot s^{-1}$) inertial oscillations occurred at 14 m on LATEX 12. The oscillations persisted for 3-4 days after the storm. Data from LATEX 12 are plotted in Figure 6.3.4-2.

15 1993: December 20 and 22

Inertial oscillations were present in the record at 14 m on LATEX 12. Data from LATEX 12 are plotted in Figure 6.3.4-2.

16 1994: April 22

Inertial oscillations are seen in the record from LATEX 49. Comparison of the records at 14 and 102 m suggest there was a possible downward propagation of inertial energy . Data from LATEX 49 are plotted in Figure 6.3.4-2.

17 1994: May 3

Inertial oscillations occurred in records from LATEX 49 both before and after the extratropical cyclone. Inertial oscillations also are in the near-surface bins of the Industry GC200 record. Data from LATEX 49 are plotted in Figure 6.3.4-2. Industry GC200 data are in Figure 6.2.12-7.

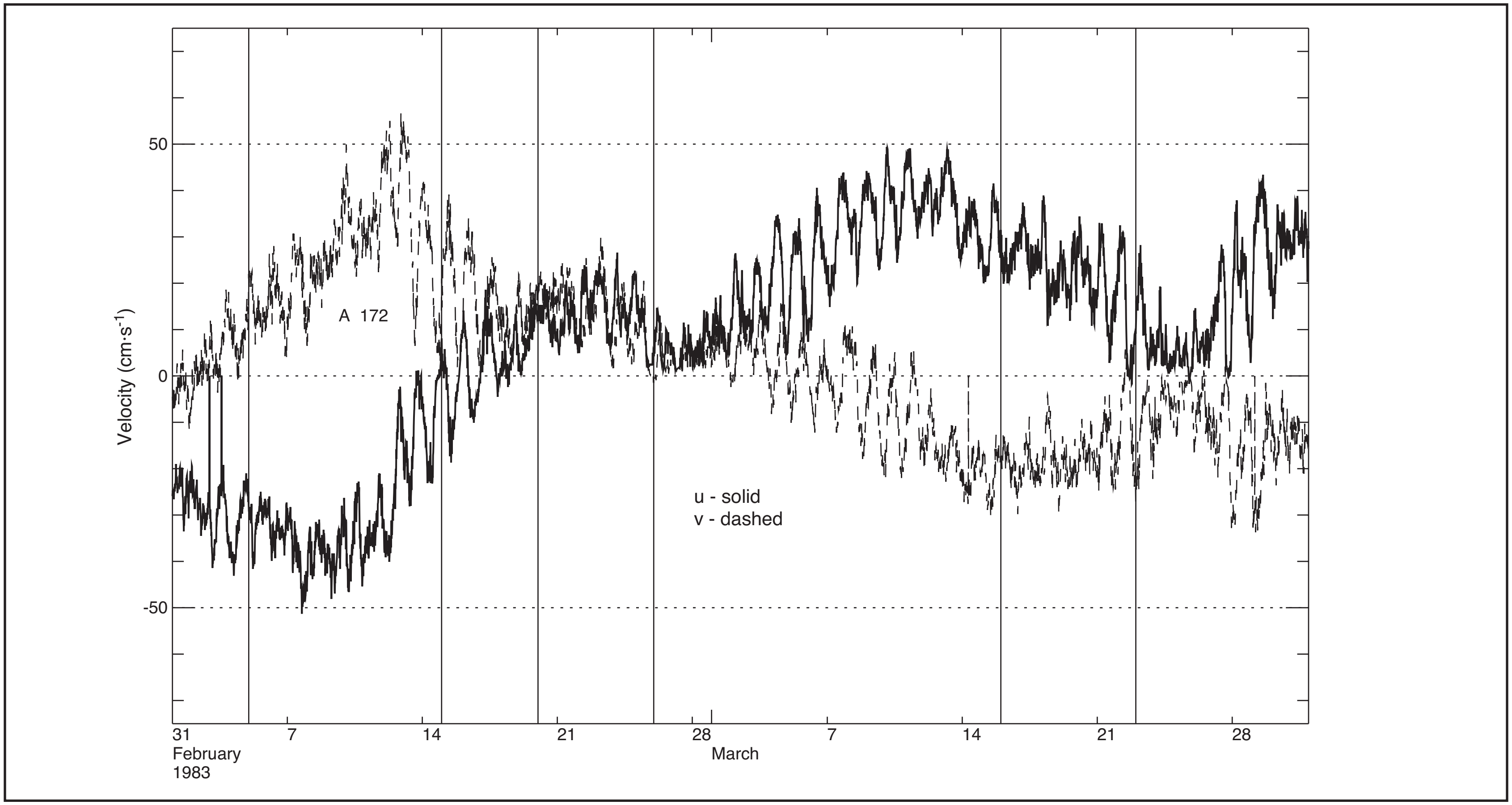

Figure B.7-1. Influence of extratropical cyclones on currents at 172 m in the eastern Gulf at SAIC 5-year mooring A, February and March 1983. Extratropical cyclones occurred on February 5, 15, 20, and 26, and March 16 and 23 (indicated by vertical lines). Velocity components are east-west (u, solid) and north-south (v, dashed). See also Table B-7, events 4 through 9.

Table B-8. Speed statistics for energetic deep barotropic motions, including bottom intensification. Given are the name of the file containing the event (keyed to the directory on the CD-ROM database), the start and stop dates used to characterize the event, maximum speed, mean speed, standard deviation of speed, mooring location, depth of the instrument, and total water depth. Comments on the event, keyed by the event number, are given in the notes below the table.

Event No.	**Year**	**Filename**	**Directory**	**Event start date (m/d/y)**	**Event end date (m/d/y)**	**Maximum speed ($cm \cdot s^{-1}$)**	**Mean speed ($cm \cdot s^{-1}$)**	**Stand. dev. of speed ($cm \cdot s^{-1}$)**	**Latitude (°N)**	**Longitude (°W)**	**Depth (m)**	**Total water depth (m)**
1	1985	MG850615.C05	/NODC_DEEP/	07/01/1985	08/31/1985	40.795	15.489	6.970	25.4917	94.1600	100.0	3500.0
	1985	MG850615.C06	/NODC_DEEP/	07/01/1985	08/31/1985	25.669	11.431	4.909	25.4917	94.1600	300.0	3500.0
	1985	MG850615.C07	/NODC_DEEP/	07/01/1985	08/31/1985	24.180	8.013	4.601	25.4917	94.1600	1000.0	3500.0
	1985	MG850615.C08	/NODC_DEEP/	07/01/1985	08/31/1985	21.291	7.797	5.089	25.4917	94.1600	1500.0	3500.0
	1985	MG850615.C09	/NODC_DEEP/	07/01/1985	08/31/1985	22.403	7.622	4.863	25.4917	94.1600	3000.0	3500.0
2	1985	MG850615.C01	/NODC_DEEP/	08/01/1985	08/31/1985	85.498	29.965	20.661	25.8717	94.8800	100.0	3000.0
	1985	MG850615.C02	/NODC_DEEP/	08/01/1985	08/31/1985	44.807	16.142	12.329	25.8717	94.8800	300.0	3000.0
	1985	MG850615.C03	/NODC_DEEP/	08/01/1985	08/31/1985	25.017	8.022	6.232	25.8717	94.8800	1000.0	3000.0
	1985	MG850615.C04	/NODC_DEEP/	08/01/1985	08/31/1985	27.352	12.286	6.994	25.8717	94.8800	1500.0	3000.0
3	1985	MG850615.C05	/NODC_DEEP/	09/01/1985	10/21/1985	59.928	13.190	13.525	25.4917	94.1600	100.0	3500.0
	1985	MG850615.C06	/NODC_DEEP/	09/01/1985	10/21/1985	25.016	6.998	4.867	25.4917	94.1600	300.0	3500.0
	1985	MG850615.C07	/NODC_DEEP/	09/01/1985	10/21/1985	18.954	5.944	2.740	25.4917	94.1600	1000.0	3500.0
	1985	MG850615.C08	/NODC_DEEP/	09/01/1985	10/21/1985	19.609	7.383	4.231	25.4917	94.1600	1500.0	3500.0
	1985	MG850615.C09	/NODC_DEEP/	09/01/1985	10/21/1985	18.769	7.833	4.385	25.4917	94.1600	3000.0	3500.0
4	1988	AB871109.C01	/NODC_DEEP/	08/01/1988	08/31/1988	89.884	55.221	12.370	25.6532	92.0333	100.0	3000.0
	1988	AB880409.C01	/NODC_DEEP/	08/01/1988	08/31/1988	37.809	21.953	5.614	25.6532	92.0333	300.0	3000.0
	1988	AB871109.C02	/NODC_DEEP/	08/01/1988	08/31/1988	19.238	8.756	4.522	25.6532	92.0333	725.0	3000.0
	1988	AB870406.C03	/NODC_DEEP/	08/01/1988	08/31/1988	24.554	13.002	6.747	25.6532	92.0333	1650.0	3000.0
	1988	AB880409.C02	/NODC_DEEP/	08/01/1988	08/31/1988	30.619	13.662	6.947	25.6532	92.0333	2500.0	3000.0
5	1998	DD980812.A01	/MMS/	09/01/1998	10/31/1998	179.442	25.386	17.369	29.3712	87.3563	12.0	500.0
	1998	DD980812.A02	/MMS/	09/01/1998	10/31/1998	150.841	24.997	16.638	29.3712	87.3563	16.0	500.0
	1998	DD980812.A03	/MMS/	09/01/1998	10/31/1998	127.838	23.788	15.665	29.3712	87.3563	20.0	500.0
	1998	DD980812.A04	/MMS/	09/01/1998	10/31/1998	106.385	22.781	14.896	29.3712	87.3563	24.0	500.0
	1998	DD980812.A05	/MMS/	09/01/1998	10/31/1998	113.641	21.719	14.364	29.3712	87.3563	28.0	500.0
	1998	DD980812.A06	/MMS/	09/01/1998	10/31/1998	118.084	21.165	13.789	29.3712	87.3563	32.0	500.0
	1998	DD980812.A07	/MMS/	09/01/1998	10/31/1998	114.661	20.783	13.449	29.3712	87.3563	36.0	500.0
	1998	DD980812.A08	/MMS/	09/01/1998	10/31/1998	111.668	20.335	13.498	29.3712	87.3563	40.0	500.0
	1998	DD980812.A09	/MMS/	09/01/1998	10/31/1998	113.492	19.821	13.886	29.3712	87.3563	44.0	500.0
	1998	DD980812.A10	/MMS/	09/01/1998	10/31/1998	113.789	19.909	14.191	29.3712	87.3563	48.0	500.0
	1998	DD980812.A11	/MMS/	09/01/1998	10/31/1998	113.373	19.960	14.481	29.3712	87.3563	52.0	500.0

Table B-8. Speed statistics for energetic deep barotropic motions, including bottom intensification. (continued)

Event No.	Year	Filename	Directory	Event start date (m/d/y)	Event end date (m/d/y)	Maximum speed (cm·s^{-1})	Mean speed (cm·s^{-1})	Stand. dev. of speed (cm·s^{-1})	Latitude (°N)	Longitude (°W)	Depth (m)	Total water depth (m)
5	1998	DD980812.A12	/MMS/	09/01/1998	10/31/1998	112.730	19.611	14.658	29.3712	87.3563	56.0	500.0
	1998	DD980812.A13	/MMS/	09/01/1998	10/31/1998	117.850	19.122	15.161	29.3712	87.3563	60.0	500.0
	1998	DD980812.A14	/MMS/	09/01/1998	10/31/1998	117.526	19.316	15.036	29.3712	87.3563	64.0	500.0
	1998	DD980812.A15	/MMS/	09/01/1998	10/31/1998	119.822	19.591	14.969	29.3712	87.3563	68.0	500.0
	1998	DD980812.A16	/MMS/	09/01/1998	10/31/1998	121.443	19.539	15.186	29.3712	87.3563	72.0	500.0
	1998	DD980812.A17	/MMS/	09/01/1998	10/31/1998	119.861	19.166	14.988	29.3712	87.3563	76.0	500.0
	1998	DD980812.A18	/MMS/	09/01/1998	10/31/1998	115.981	18.237	14.398	29.3712	87.3563	80.0	500.0
	1998	DD980812.C01	/MMS/	09/01/1998	10/31/1998	110.084	16.753	12.207	29.3712	87.3563	200.0	500.0
	1998	DD980812.C02	/MMS/	09/01/1998	10/31/1998	85.670	16.462	11.224	29.3712	87.3563	300.0	500.0
	1998	DD980812.C03	/MMS/	09/01/1998	10/31/1998	72.003	9.330	7.796	29.3712	87.3563	490.0	500.0
	1998	DD980808.A01	/MMS/	09/01/1998	10/31/1998	202.837	29.484	19.753	29.0032	87.3532	12.0	1300.0
	1998	DD980808.A02	/MMS/	09/01/1998	10/31/1998	177.568	26.924	20.995	29.0032	87.3532	16.0	1300.0
	1998	DD980808.A03	/MMS/	09/01/1998	10/31/1998	161.485	25.528	20.196	29.0032	87.3532	20.0	1300.0
	1998	DD980808.A04	/MMS/	09/01/1998	10/31/1998	174.001	24.609	19.158	29.0032	87.3532	24.0	1300.0
	1998	DD980808.A05	/MMS/	09/01/1998	10/31/1998	156.170	24.230	18.166	29.0032	87.3532	28.0	1300.0
	1998	DD980808.A06	/MMS/	09/01/1998	10/31/1998	141.319	24.061	17.720	29.0032	87.3532	32.0	1300.0
	1998	DD980808.A07	/MMS/	09/01/1998	10/31/1998	125.455	23.885	17.578	29.0032	87.3532	36.0	1300.0
	1998	DD980808.A08	/MMS/	09/01/1998	10/31/1998	117.282	23.516	17.225	29.0032	87.3532	40.0	1300.0
	1998	DD980808.A09	/MMS/	09/01/1998	10/31/1998	102.837	23.108	16.642	29.0032	87.3532	44.0	1300.0
	1998	DD980808.A10	/MMS/	09/01/1998	10/31/1998	92.670	22.323	15.409	29.0032	87.3532	48.0	1300.0
	1998	DD980808.A11	/MMS/	09/01/1998	10/31/1998	77.131	21.269	14.232	29.0032	87.3532	52.0	1300.0
	1998	DD980808.A12	/MMS/	09/01/1998	10/31/1998	60.004	17.270	11.242	29.0032	87.3532	56.0	1300.0
	1998	DD980808.A13	/MMS/	09/01/1998	10/31/1998	60.784	17.072	11.180	29.0032	87.3532	60.0	1300.0
	1998	DD980808.A14	/MMS/	09/01/1998	10/31/1998	66.430	18.429	13.209	29.0032	87.3532	64.0	1300.0
	1998	DD980808.A15	/MMS/	09/01/1998	10/31/1998	63.861	17.787	13.089	29.0032	87.3532	68.0	1300.0
	1998	DD980808.A16	/MMS/	09/01/1998	10/31/1998	59.146	18.693	12.340	29.0032	87.3532	72.0	1300.0
	1998	DD980808.C01	/MMS/	09/01/1998	10/31/1998	34.813	13.785	6.570	29.0032	87.3532	500.0	1300.0
	1998	DD980808.C02	/MMS/	09/01/1998	10/31/1998	48.603	8.392	7.837	29.0032	87.3532	1290.0	1300.0
6	1999	AT990829.A01	/MMS/	08/29/1999	10/25/1999	171.219	83.064	42.351	27.2933	89.7845	12.0	2001.0
	1999	AT990829.A02	/MMS/	08/29/1999	10/25/1999	171.224	88.143	38.901	27.2933	89.7845	16.0	2001.0
	1999	AT990829.A03	/MMS/	08/29/1999	10/25/1999	171.168	88.379	37.048	27.2933	89.7845	20.0	2001.0
	1999	AT990829.A04	/MMS/	08/29/1999	10/25/1999	166.227	87.429	36.339	27.2933	89.7845	24.0	2001.0
	1999	AT990829.A05	/MMS/	08/29/1999	10/25/1999	157.818	86.272	35.696	27.2933	89.7845	28.0	2001.0
	1999	AT990829.A06	/MMS/	08/29/1999	10/25/1999	154.805	85.104	35.059	27.2933	89.7845	32.0	2001.0

Table B-8. Speed statistics for energetic deep barotropic motions, including bottom intensification. (continued)

Event No.	Year	Filename	Directory	Event start date (m/d/y)	Event end date (m/d/y)	Maximum speed ($cm \cdot s^{-1}$)	Mean speed ($cm \cdot s^{-1}$)	Stand. dev. of speed ($cm \cdot s^{-1}$)	Latitude (°N)	Longitude (°W)	Depth (m)	Total water depth (m)
6	1999	AT990829.A07	/MMS/	08/29/1999	10/25/1999	147.711	83.988	34.454	27.2933	89.7845	36.0	2001.0
	1999	AT990829.A08	/MMS/	08/29/1999	10/25/1999	145.756	82.882	33.791	27.2933	89.7845	40.0	2001.0
	1999	AT990829.A09	/MMS/	08/29/1999	10/25/1999	145.566	81.722	33.000	27.2933	89.7845	44.0	2001.0
	1999	AT990829.A10	/MMS/	08/29/1999	10/25/1999	140.295	80.197	32.512	27.2933	89.7845	48.0	2001.0
	1999	AT990829.A11	/MMS/	08/29/1999	10/25/1999	138.110	78.540	31.745	27.2933	89.7845	52.0	2001.0
	1999	AT990829.A12	/MMS/	08/29/1999	10/25/1999	137.582	76.637	31.039	27.2933	89.7845	56.0	2001.0
	1999	AT990829.A13	/MMS/	08/29/1999	10/25/1999	133.277	74.624	30.039	27.2933	89.7845	60.0	2001.0
	1999	AT990829.A14	/MMS/	08/29/1999	10/25/1999	126.931	72.280	28.982	27.2933	89.7845	64.0	2001.0
	1999	AT990829.A15	/MMS/	08/29/1999	10/25/1999	114.214	49.286	25.863	27.2933	89.7845	68.0	2001.0
	1999	AT990829.A16	/MMS/	08/29/1999	10/25/1999	113.559	61.554	26.618	27.2933	89.7845	72.0	2001.0
	1999	AT990829.A17	/MMS/	08/29/1999	10/25/1999	120.070	68.505	27.596	27.2933	89.7845	76.0	2001.0
	1999	AT990829.A18	/MMS/	08/29/1999	10/25/1999	116.759	67.205	27.103	27.2933	89.7845	80.0	2001.0
	1999	AT990829.A19	/MMS/	08/29/1999	10/31/1999	99.538	56.490	21.180	27.2933	89.7845	106.0	2001.0
	1999	AT990829.A20	/MMS/	08/29/1999	10/31/1999	103.154	57.110	21.649	27.2933	89.7845	110.0	2001.0
	1999	AT990829.A21	/MMS/	08/29/1999	10/31/1999	103.837	56.072	21.168	27.2933	89.7845	114.0	2001.0
	1999	AT990829.A22	/MMS/	08/29/1999	10/31/1999	103.598	54.913	20.517	27.2933	89.7845	118.0	2001.0
	1999	AT990829.A23	/MMS/	08/29/1999	10/31/1999	99.214	53.756	19.818	27.2933	89.7845	122.0	2001.0
	1999	AT990829.A24	/MMS/	08/29/1999	10/31/1999	97.265	52.714	19.232	27.2933	89.7845	126.0	2001.0
	1999	AT990829.A25	/MMS/	08/29/1999	10/31/1999	96.813	51.642	18.811	27.2933	89.7845	130.0	2001.0
	1999	AT990829.A26	/MMS/	08/29/1999	10/31/1999	95.635	50.568	18.673	27.2933	89.7845	134.0	2001.0
	1999	AT990829.A27	/MMS/	08/29/1999	10/31/1999	94.996	49.631	18.490	27.2933	89.7845	138.0	2001.0
	1999	AT990829.A28	/MMS/	08/29/1999	10/31/1999	93.561	48.606	18.054	27.2933	89.7845	142.0	2001.0
	1999	AT990829.A29	/MMS/	08/29/1999	10/31/1999	92.749	47.717	17.925	27.2933	89.7845	146.0	2001.0
	1999	AT990829.A30	/MMS/	08/29/1999	10/31/1999	91.603	46.888	17.705	27.2933	89.7845	150.0	2001.0
	1999	AT990829.A39	/MMS/	08/29/1999	10/31/1999	97.079	46.638	18.131	27.2933	89.7845	150.0	2001.0
	1999	AT990829.A31	/MMS/	08/29/1999	10/31/1999	92.712	46.142	17.498	27.2933	89.7845	154.0	2001.0
	1999	AT990829.A40	/MMS/	08/29/1999	10/31/1999	95.535	44.961	17.573	27.2933	89.7845	154.0	2001.0
	1999	AT990829.A32	/MMS/	08/29/1999	10/31/1999	92.334	45.367	17.351	27.2933	89.7845	158.0	2001.0
	1999	AT990829.A41	/MMS/	08/29/1999	10/31/1999	89.214	43.755	15.819	27.2933	89.7845	158.0	2001.0
	1999	AT990829.A33	/MMS/	08/29/1999	10/31/1999	92.129	44.696	17.232	27.2933	89.7845	162.0	2001.0
	1999	AT990829.A42	/MMS/	08/29/1999	10/31/1999	90.997	44.081	16.827	27.2933	89.7845	162.0	2001.0
	1999	AT990829.A34	/MMS/	08/29/1999	10/31/1999	89.990	44.147	16.990	27.2933	89.7845	166.0	2001.0
	1999	AT990829.A43	/MMS/	08/29/1999	10/31/1999	87.003	43.610	16.837	27.2933	89.7845	166.0	2001.0
	1999	AT990829.A35	/MMS/	08/29/1999	10/31/1999	89.019	43.573	16.704	27.2933	89.7845	170.0	2001.0

Table B-8. Speed statistics for energetic deep barotropic motions, including bottom intensification. (continued)

Event No.	Year	Filename	Directory	Event start date (m/d/y)	Event end date (m/d/y)	Maximum speed (cm·s^{-1})	Mean speed (cm·s^{-1})	Stand. dev. of speed (cm·s^{-1})	Latitude (°N)	Longitude (°W)	Depth (m)	Total water depth (m)
6	1999	AT990829.A44	/MMS/	08/29/1999	10/31/1999	85.435	43.001	16.550	27.2933	89.7845	170.0	2001.0
	1999	AT990829.A36	/MMS/	08/29/1999	10/31/1999	88.728	42.996	16.516	27.2933	89.7845	174.0	2001.0
	1999	AT990829.A45	/MMS/	08/29/1999	10/31/1999	84.641	42.383	16.192	27.2933	89.7845	174.0	2001.0
	1999	AT990829.A37	/MMS/	08/29/1999	10/31/1999	87.077	42.492	16.033	27.2933	89.7845	178.0	2001.0
	1999	AT990829.A46	/MMS/	08/29/1999	10/31/1999	84.481	41.740	15.960	27.2933	89.7845	178.0	2001.0
	1999	AT990829.A38	/MMS/	08/29/1999	10/31/1999	96.058	41.693	15.450	27.2933	89.7845	182.0	2001.0
	1999	AT990829.A47	/MMS/	08/29/1999	10/31/1999	84.193	41.021	15.740	27.2933	89.7845	182.0	2001.0
	1999	AT990829.A48	/MMS/	08/29/1999	10/31/1999	85.535	40.352	15.571	27.2933	89.7845	186.0	2001.0
	1999	AT990829.A49	/MMS/	08/29/1999	10/31/1999	84.710	39.714	15.377	27.2933	89.7845	190.0	2001.0
	1999	AT990829.A50	/MMS/	08/29/1999	10/31/1999	83.707	39.108	15.220	27.2933	89.7845	194.0	2001.0
	1999	AT990829.A51	/MMS/	08/29/1999	10/31/1999	79.819	34.075	14.433	27.2933	89.7845	198.0	2001.0
	1999	AT990829.A52	/MMS/	08/29/1999	10/31/1999	70.778	27.193	11.108	27.2933	89.7845	202.0	2001.0
	1999	AT990829.A53	/MMS/	08/29/1999	10/31/1999	77.092	36.805	13.575	27.2933	89.7845	206.0	2001.0
	1999	AT990829.A54	/MMS/	08/29/1999	10/31/1999	75.477	37.105	14.654	27.2933	89.7845	210.0	2001.0
	1999	AT990829.A55	/MMS/	08/29/1999	10/31/1999	74.805	36.648	14.585	27.2933	89.7845	214.0	2001.0
	1999	AT990829.A56	/MMS/	08/29/1999	10/31/1999	75.402	36.202	14.422	27.2933	89.7845	218.0	2001.0
	1999	AT990829.A57	/MMS/	08/29/1999	10/31/1999	75.181	35.720	14.268	27.2933	89.7845	222.0	2001.0
	1999	AT990829.A58	/MMS/	08/29/1999	10/31/1999	73.324	35.145	14.140	27.2933	89.7845	226.0	2001.0
	1999	AT990829.A59	/MMS/	08/29/1999	10/31/1999	71.647	34.554	14.029	27.2933	89.7845	230.0	2001.0
	1999	AT990829.A60	/MMS/	08/29/1999	10/31/1999	67.959	33.150	13.418	27.2933	89.7845	234.0	2001.0
	1999	AT990829.A61	/MMS/	08/29/1999	10/31/1999	62.784	32.008	12.313	27.2933	89.7845	256.0	2001.0
	1999	AT990829.A62	/MMS/	08/29/1999	10/31/1999	62.966	31.734	12.238	27.2933	89.7845	260.0	2001.0
	1999	AT990829.A63	/MMS/	08/29/1999	10/31/1999	62.535	31.436	12.098	27.2933	89.7845	264.0	2001.0
	1999	AT990829.A64	/MMS/	08/29/1999	10/31/1999	61.366	31.115	11.932	27.2933	89.7845	268.0	2001.0
	1999	AT990829.A65	/MMS/	08/29/1999	10/31/1999	61.079	30.824	11.813	27.2933	89.7845	272.0	2001.0
	1999	AT990829.A66	/MMS/	08/29/1999	10/31/1999	60.691	30.475	11.701	27.2933	89.7845	276.0	2001.0
	1999	AT990829.A67	/MMS/	08/29/1999	10/31/1999	60.701	30.138	11.548	27.2933	89.7845	280.0	2001.0
	1999	AT990829.A68	/MMS/	08/29/1999	10/31/1999	60.076	29.818	11.460	27.2933	89.7845	284.0	2001.0
	1999	AT990829.A69	/MMS/	08/29/1999	10/31/1999	59.825	29.513	11.321	27.2933	89.7845	288.0	2001.0
	1999	AT990829.A70	/MMS/	08/29/1999	10/31/1999	58.963	29.264	11.162	27.2933	89.7845	292.0	2001.0
	1999	AT990829.A71	/MMS/	08/29/1999	10/31/1999	57.607	29.065	11.011	27.2933	89.7845	296.0	2001.0
	1999	AT990829.A72	/MMS/	08/29/1999	10/31/1999	57.191	28.816	10.885	27.2933	89.7845	300.0	2001.0
	1999	AT990829.A73	/MMS/	08/29/1999	10/31/1999	57.243	28.535	10.751	27.2933	89.7845	304.0	2001.0
	1999	AT990829.A74	/MMS/	08/29/1999	10/31/1999	56.230	28.293	10.626	27.2933	89.7845	308.0	2001.0

Table B-8. Speed statistics for energetic deep barotropic motions, including bottom intensification. (continued)

Event No.	Year	Filename	Directory	Event start date (m/d/y)	Event end date (m/d/y)	Maximum speed (cm·s^{-1})	Mean speed (cm·s^{-1})	Stand. dev. of speed (cm·s^{-1})	Latitude (°N)	Longitude (°W)	Depth (m)	Total water depth (m)
6	1999	AT990829.A75	/MMS/	08/29/1999	10/31/1999	55.473	28.147	10.589	27.2933	89.7845	312.0	2001.0
	1999	AT990829.A76	/MMS/	08/29/1999	10/31/1999	56.540	28.038	10.568	27.2933	89.7845	316.0	2001.0
	1999	AT990829.A77	/MMS/	08/29/1999	10/31/1999	55.336	27.906	10.470	27.2933	89.7845	320.0	2001.0
	1999	AT990829.A78	/MMS/	08/29/1999	10/31/1999	52.659	27.645	10.373	27.2933	89.7845	324.0	2001.0
	1999	AT990829.A79	/MMS/	08/29/1999	10/31/1999	52.277	27.431	10.349	27.2933	89.7845	328.0	2001.0
	1999	AT990829.A80	/MMS/	08/29/1999	10/31/1999	53.760	27.024	10.210	27.2933	89.7845	332.0	2001.0
	1999	AT990829.A83	/MMS/	08/29/1999	10/31/1999	61.304	30.565	11.315	27.2933	89.7845	332.0	2001.0
	1999	AT990829.A81	/MMS/	08/29/1999	10/31/1999	55.555	26.566	10.088	27.2933	89.7845	336.0	2001.0
	1999	AT990829.A82	/MMS/	08/29/1999	10/31/1999	57.369	26.432	10.381	27.2933	89.7845	340.0	2001.0
	1999	AT990829.A84	/MMS/	08/29/1999	10/31/1999	59.197	30.130	11.018	27.2933	89.7845	340.0	2001.0
	1999	AT990829.A85	/MMS/	08/29/1999	10/31/1999	56.640	29.629	10.795	27.2933	89.7845	348.0	2001.0
	1999	AT990829.A86	/MMS/	08/29/1999	10/31/1999	55.472	29.050	10.666	27.2933	89.7845	356.0	2001.0
	1999	AT990829.A87	/MMS/	08/29/1999	10/31/1999	55.095	28.600	10.472	27.2933	89.7845	364.0	2001.0
	1999	AT990829.A88	/MMS/	08/29/1999	10/31/1999	56.048	28.200	10.305	27.2933	89.7845	372.0	2001.0
	1999	AT990829.A89	/MMS/	08/29/1999	10/31/1999	54.089	27.753	10.143	27.2933	89.7845	380.0	2001.0
	1999	AT990829.A90	/MMS/	08/29/1999	10/31/1999	51.121	27.257	9.976	27.2933	89.7845	388.0	2001.0
	1999	AT990829.A91	/MMS/	08/29/1999	10/31/1999	49.742	26.876	9.810	27.2933	89.7845	396.0	2001.0
	1999	AT990829.A92	/MMS/	08/29/1999	10/31/1999	49.590	26.466	9.576	27.2933	89.7845	404.0	2001.0
	1999	AT990829.A93	/MMS/	08/29/1999	10/31/1999	49.262	26.018	9.416	27.2933	89.7845	412.0	2001.0
	1999	AT990829.A94	/MMS/	08/29/1999	10/31/1999	48.450	25.665	9.331	27.2933	89.7845	420.0	2001.0
	1999	AT990829.A95	/MMS/	08/29/1999	10/31/1999	48.664	25.142	9.260	27.2933	89.7845	428.0	2001.0
	1999	AT990829.A96	/MMS/	08/29/1999	10/31/1999	48.333	24.732	9.215	27.2933	89.7845	436.0	2001.0
	1999	AT990829.A97	/MMS/	08/29/1999	10/31/1999	46.795	24.293	9.012	27.2933	89.7845	444.0	2001.0
	1999	AT990829.A98	/MMS/	08/29/1999	10/31/1999	46.435	23.764	8.859	27.2933	89.7845	452.0	2001.0
	1999	AT990829.A99	/MMS/	08/29/1999	10/31/1999	44.163	23.282	8.669	27.2933	89.7845	460.0	2001.0
	1999	AT990829.Aa0	/MMS/	08/29/1999	10/31/1999	44.194	22.880	8.456	27.2933	89.7845	468.0	2001.0
	1999	AT990829.Aa1	/MMS/	08/29/1999	10/31/1999	42.003	22.249	8.353	27.2933	89.7845	476.0	2001.0
	1999	AT990829.Aa2	/MMS/	08/29/1999	10/31/1999	41.244	21.748	8.274	27.2933	89.7845	484.0	2001.0
	1999	AT990829.Aa3	/MMS/	08/29/1999	10/31/1999	41.877	21.374	8.070	27.2933	89.7845	492.0	2001.0
	1999	AT990829.Aa4	/MMS/	08/29/1999	10/31/1999	40.400	20.992	7.947	27.2933	89.7845	500.0	2001.0
	1999	AT990829.Aa5	/MMS/	08/29/1999	10/31/1999	40.554	20.634	7.819	27.2933	89.7845	508.0	2001.0
	1999	AT990829.Aa6	/MMS/	08/29/1999	10/31/1999	40.663	20.370	7.769	27.2933	89.7845	516.0	2001.0
	1999	AT990829.Aa7	/MMS/	08/29/1999	10/31/1999	38.420	19.897	7.725	27.2933	89.7845	524.0	2001.0
	1999	AT990829.Aa8	/MMS/	08/29/1999	10/31/1999	37.999	19.513	7.643	27.2933	89.7845	532.0	2001.0

Table B-8. Speed statistics for energetic deep barotropic motions, including bottom intensification. (continued)

Event No.	Year	Filename	Directory	Event start date (m/d/y)	Event end date (m/d/y)	Maximum speed ($cm{\cdot}s^{-1}$)	Mean speed ($cm{\cdot}s^{-1}$)	Stand. dev. of speed ($cm{\cdot}s^{-1}$)	Latitude (°N)	Longitude (°W)	Depth (m)	Total water depth (m)
6	1999	AT990829.Aa9	/MMS/	08/29/1999	10/31/1999	37.143	19.146	7.638	27.2933	89.7845	540.0	2001.0
	1999	AT990829.Ab0	/MMS/	08/29/1999	10/31/1999	37.488	18.891	7.510	27.2933	89.7845	548.0	2001.0
	1999	AT990829.Ab1	/MMS/	08/29/1999	10/31/1999	38.517	18.611	7.391	27.2933	89.7845	556.0	2001.0
	1999	AT990829.Ab2	/MMS/	08/29/1999	10/31/1999	38.336	18.353	7.280	27.2933	89.7845	564.0	2001.0
	1999	AT990829.Ab3	/MMS/	08/29/1999	10/31/1999	38.604	18.035	7.210	27.2933	89.7845	572.0	2001.0
	1999	AT990829.Ab4	/MMS/	08/29/1999	10/31/1999	36.912	17.815	7.233	27.2933	89.7845	580.0	2001.0
	1999	AT990829.Ab5	/MMS/	08/29/1999	10/31/1999	37.569	17.365	7.169	27.2933	89.7845	588.0	2001.0
	1999	AT990829.Ab6	/MMS/	08/29/1999	10/31/1999	35.798	11.931	6.097	27.2933	89.7845	658.0	2001.0
	1999	AT990829.Ab7	/MMS/	08/29/1999	10/31/1999	37.852	12.624	6.589	27.2933	89.7845	666.0	2001.0
	1999	AT990829.Ab8	/MMS/	08/29/1999	10/31/1999	38.585	12.713	6.687	27.2933	89.7845	674.0	2001.0
	1999	AT990829.Ab9	/MMS/	08/29/1999	10/31/1999	41.155	12.736	6.894	27.2933	89.7845	682.0	2001.0
	1999	AT990829.Ac0	/MMS/	08/29/1999	10/31/1999	43.901	12.657	6.980	27.2933	89.7845	690.0	2001.0
	1999	AT990829.Ac1	/MMS/	08/29/1999	10/31/1999	43.427	12.534	6.999	27.2933	89.7845	698.0	2001.0
	1999	AT990829.Ac2	/MMS/	08/29/1999	10/31/1999	42.844	12.353	7.161	27.2933	89.7845	706.0	2001.0
	1999	AT990829.Ac3	/MMS/	08/29/1999	10/31/1999	44.323	12.233	7.288	27.2933	89.7845	714.0	2001.0
	1999	AT990829.Ac4	/MMS/	08/29/1999	10/31/1999	44.804	12.162	7.357	27.2933	89.7845	722.0	2001.0
	1999	AT990829.Ac5	/MMS/	08/29/1999	10/31/1999	46.371	11.972	7.338	27.2933	89.7845	730.0	2001.0
	1999	AT990829.Ac6	/MMS/	08/29/1999	10/31/1999	44.976	11.896	7.358	27.2933	89.7845	738.0	2001.0
	1999	AT990829.Ac7	/MMS/	08/29/1999	10/31/1999	45.084	11.744	7.433	27.2933	89.7845	746.0	2001.0
	1999	AT990829.Ac8	/MMS/	08/29/1999	10/31/1999	49.036	11.633	7.514	27.2933	89.7845	754.0	2001.0
	1999	AT990829.Ac9	/MMS/	08/29/1999	10/31/1999	49.211	11.483	7.645	27.2933	89.7845	762.0	2001.0
	1999	AT990829.Ad0	/MMS/	08/29/1999	10/31/1999	50.525	11.223	7.668	27.2933	89.7845	770.0	2001.0
	1999	AT990829.Ad1	/MMS/	08/29/1999	10/31/1999	48.883	11.275	7.790	27.2933	89.7845	778.0	2001.0
	1999	AT990829.Ad2	/MMS/	08/29/1999	10/31/1999	48.685	11.242	7.744	27.2933	89.7845	786.0	2001.0
	1999	AT990829.Ad3	/MMS/	08/29/1999	10/31/1999	47.590	11.028	7.668	27.2933	89.7845	794.0	2001.0
	1999	AT990829.Ad4	/MMS/	08/29/1999	10/31/1999	47.566	10.971	7.610	27.2933	89.7845	802.0	2001.0
	1999	AT990829.Ad5	/MMS/	08/29/1999	10/31/1999	44.139	10.950	7.388	27.2933	89.7845	810.0	2001.0
	1999	AT990829.Ad6	/MMS/	08/29/1999	10/31/1999	42.503	10.909	7.306	27.2933	89.7845	818.0	2001.0
	1999	AT990829.Ad7	/MMS/	08/29/1999	10/31/1999	41.097	10.909	7.227	27.2933	89.7845	826.0	2001.0
	1999	AT990829.Ad8	/MMS/	08/29/1999	10/31/1999	40.359	10.840	7.263	27.2933	89.7845	834.0	2001.0
	1999	AT990829.Ad9	/MMS/	08/29/1999	10/31/1999	41.911	10.905	7.496	27.2933	89.7845	842.0	2001.0
	1999	AT990829.Ae0	/MMS/	08/29/1999	10/31/1999	42.230	10.703	7.621	27.2933	89.7845	850.0	2001.0
	1999	AT990829.Ae1	/MMS/	08/29/1999	10/31/1999	41.130	10.556	7.584	27.2933	89.7845	858.0	2001.0
	1999	AT990829.Ae2	/MMS/	08/29/1999	10/31/1999	44.967	10.519	7.647	27.2933	89.7845	866.0	2001.0

Table B-8. Speed statistics for energetic deep barotropic motions, including bottom intensification. (continued)

Event No.	Year	Filename	Directory	Event start date (m/d/y)	Event end date (m/d/y)	Maximum speed (cm·s^{-1})	Mean speed (cm·s^{-1})	Stand. dev. of speed (cm·s^{-1})	Latitude (°N)	Longitude (°W)	Depth (m)	Total water depth (m)
6	1999	AT990829.Ae3	/MMS/	08/29/1999	10/31/1999	43.494	10.435	7.743	27.2933	89.7845	874.0	2001.0
	1999	AT990829.Ae4	/MMS/	08/29/1999	10/31/1999	45.346	10.320	7.772	27.2933	89.7845	882.0	2001.0
	1999	AT990829.Ae5	/MMS/	08/29/1999	10/31/1999	46.032	10.378	7.895	27.2933	89.7845	890.0	2001.0
	1999	AT990829.Ae6	/MMS/	08/29/1999	10/31/1999	44.413	10.287	7.953	27.2933	89.7845	898.0	2001.0
	1999	AT990829.Ae7	/MMS/	08/29/1999	10/31/1999	46.538	10.290	8.023	27.2933	89.7845	906.0	2001.0
	1999	AT990829.Ae8	/MMS/	08/29/1999	10/31/1999	44.202	10.214	8.055	27.2933	89.7845	914.0	2001.0
	1999	AT990829.Ae9	/MMS/	08/29/1999	10/31/1999	43.533	10.093	8.142	27.2933	89.7845	922.0	2001.0
	1999	AT990829.Af0	/MMS/	08/29/1999	10/31/1999	44.985	10.039	8.204	27.2933	89.7845	930.0	2001.0
	1999	AT990829.Af1	/MMS/	08/29/1999	10/31/1999	46.622	10.025	8.245	27.2933	89.7845	938.0	2001.0
	1999	AT990829.Af2	/MMS/	08/29/1999	10/31/1999	43.910	9.993	8.219	27.2933	89.7845	946.0	2001.0
	1999	AT990829.Af3	/MMS/	08/29/1999	10/31/1999	44.709	9.947	8.230	27.2933	89.7845	954.0	2001.0
	1999	AT990829.Af4	/MMS/	08/29/1999	10/31/1999	45.902	9.952	8.164	27.2933	89.7845	962.0	2001.0
	1999	AT990829.Af5	/MMS/	08/29/1999	10/31/1999	45.082	10.147	8.260	27.2933	89.7845	970.0	2001.0
	1999	AT990829.Af6	/MMS/	08/29/1999	10/31/1999	44.949	10.168	8.216	27.2933	89.7845	978.0	2001.0
	1999	AT990829.Af7	/MMS/	08/29/1999	10/31/1999	46.029	10.205	8.203	27.2933	89.7845	986.0	2001.0
	1999	AT990829.Af8	/MMS/	08/29/1999	10/31/1999	42.745	10.137	8.208	27.2933	89.7845	994.0	2001.0
	1999	AT990829.Af9	/MMS/	08/29/1999	10/31/1999	43.445	10.084	8.188	27.2933	89.7845	1002.0	2001.0
	1999	AT990829.Ag0	/MMS/	08/29/1999	10/31/1999	40.933	10.148	8.147	27.2933	89.7845	1010.0	2001.0
	1999	AT990829.Ag1	/MMS/	08/29/1999	10/31/1999	41.260	10.227	8.091	27.2933	89.7845	1018.0	2001.0
	1999	AT990829.Ag2	/MMS/	08/29/1999	10/31/1999	39.498	10.044	8.112	27.2933	89.7845	1026.0	2001.0
	1999	AT990829.Ag3	/MMS/	08/29/1999	10/31/1999	43.563	10.034	8.211	27.2933	89.7845	1034.0	2001.0
	1999	AT990829.Ag4	/MMS/	08/29/1999	10/31/1999	40.679	10.006	8.289	27.2933	89.7845	1042.0	2001.0
	1999	AT990829.Ag5	/MMS/	08/29/1999	10/31/1999	43.060	10.012	8.227	27.2933	89.7845	1050.0	2001.0
	1999	AT990829.Ag6	/MMS/	08/29/1999	10/31/1999	44.087	10.091	8.322	27.2933	89.7845	1058.0	2001.0
	1999	AT990829.Ag7	/MMS/	08/29/1999	10/31/1999	43.985	10.260	8.407	27.2933	89.7845	1066.0	2001.0
	1999	AT990829.Ag8	/MMS/	08/29/1999	10/31/1999	43.618	10.417	8.332	27.2933	89.7845	1074.0	2001.0
	1999	AT990829.Ag9	/MMS/	08/29/1999	10/31/1999	43.586	10.666	8.357	27.2933	89.7845	1082.0	2001.0
	1999	AT990829.Ah0	/MMS/	08/29/1999	10/31/1999	45.787	10.658	8.488	27.2933	89.7845	1090.0	2001.0
	1999	AT990829.Ah1	/MMS/	08/29/1999	10/31/1999	43.214	10.936	8.470	27.2933	89.7845	1098.0	2001.0
	1999	AT990829.Ah2	/MMS/	08/29/1999	10/31/1999	43.674	11.163	8.531	27.2933	89.7845	1106.0	2001.0
	1999	AT990829.Ah3	/MMS/	08/29/1999	10/31/1999	46.573	11.150	8.739	27.2933	89.7845	1114.0	2001.0
	1999	AT990829.Ah4	/MMS/	08/29/1999	10/31/1999	48.703	11.413	8.733	27.2933	89.7845	1122.0	2001.0
	1999	AT990829.Ah5	/MMS/	08/29/1999	10/31/1999	46.373	11.574	8.617	27.2933	89.7845	1130.0	2001.0
	1999	AT990829.C01	/MMS/	08/29/1999	10/31/1999	51.572	10.693	8.520	27.2933	89.7845	800.0	2001.0

Table B-8. Speed statistics for energetic deep barotropic motions, including bottom intensification. (continued)

Event No.	Year	Filename	Directory	Event start date (m/d/y)	Event end date (m/d/y)	Maximum speed ($cm \cdot s^{-1}$)	Mean speed ($cm \cdot s^{-1}$)	Stand. dev. of speed ($cm \cdot s^{-1}$)	Latitude (°N)	Longitude (°W)	Depth (m)	Total water depth (m)
6	1999	AT990829.C02	/MMS/	08/29/1999	10/31/1999	40.315	9.243	7.302	27.2933	89.7845	1000.0	2001.0
	1999	AT990829.C03	/MMS/	08/29/1999	10/31/1999	49.663	11.985	10.485	27.2933	89.7845	1200.0	2001.0
	1999	AT990829.C04	/MMS/	08/29/1999	10/31/1999	53.401	14.943	11.353	27.2933	89.7845	1400.0	2001.0
	1999	AT990829.C05	/MMS/	08/29/1999	10/31/1999	52.290	15.978	11.306	27.2933	89.7845	1600.0	2001.0
	1999	AT990829.C06	/MMS/	08/29/1999	10/31/1999	54.617	16.857	11.657	27.2933	89.7845	1800.0	2001.0
	1999	AT990829.C07	/MMS/	08/29/1999	10/31/1999	50.959	16.675	10.591	27.2933	89.7845	1989.0	2001.0
	1999	GC990829.C01	/MMS/	08/29/1999	10/31/1999	95.005	27.635	21.393	27.2280	89.9710	1600.0	1998.0
	1999	GC990829.C02	/MMS/	08/29/1999	10/31/1999	85.574	25.175	19.469	27.2280	89.9710	1800.0	1998.0
	1999	GC990829.C03	/MMS/	08/29/1999	10/31/1999	90.082	22.697	16.182	27.2280	89.9710	1989.0	1998.0

Notes by event number

1 1985: Deep barotropic event, July - August

The records at SAIC R show a good example of a deep barotropic, bottom intensified event. It appears as a coherent, low-frequency wave seen throughout the water column. Data from SAIC R are plotted in Figure 6.3.3-5. A detail of this event is plotted in Figure 6.1.3-2. A detail of the currents during this event is shown in Figure A.8-1.

2 1985: Deep barotropic event, August

Strong southwestward currents are seen in the records for SAIC Q at 1000 and 1500 m. There is no surface expression of this event. Data from SAIC Q are plotted in Figure 6.3.3-5. A detail of this event is plotted in Figure 6.1.3-2. A detail of the currents during this event is shown in Figure A.8-2.

3 1985: Deep barotropic event, September - October

Another good example of a bottom intensified event with no surface expression is at SAIC R. Data from SAIC R are plotted in Figure 6.3.3-5. A detail of this event is plotted in Figure 6.1.3-2. A detail of the currents during this event is shown in Figure A.8-3.

4 1988: Deep barotropic event, August

A 25 $cm \cdot s^{-1}$ amplitude, low-frequency oscillation is seen in the lower waters at SAIC GG. The upper currents approach 75 $cm \cdot s^{-1}$. This event is coincident with the arrival of Eddy Murphy. Data from SAIC GG are plotted in Figure 6.3.3-8. A detail of this event is shown in Figure A.8-4.

5 1998: Bottom Intensification, September - October

The SAIC EIS moorings show a very good example of downward propagation of inertial energy and bottom-intensification. This event occurs just after Hurricane Georges. SAIC EIS data are plotted in Figure 6.3.5-2.

Table B-8. Speed statistics for energetic deep barotropic motions, including bottom intensification. (continued)

Notes by event number (continued)

6 1999: Bottom intensification, August-October

This event, seen in the SAIC EIS Extension data, coincides with the influence of Eddy Juggernaut. The currents are coherent in the lower 1000 m with a bottom depth of 2000 m. More information is given in Table A-3. SAIC EIS Extension data are plotted in Figures 6.3.6-2 and 6.3.6-3. A detail of this event is plotted in Figure 6.1.3-4.

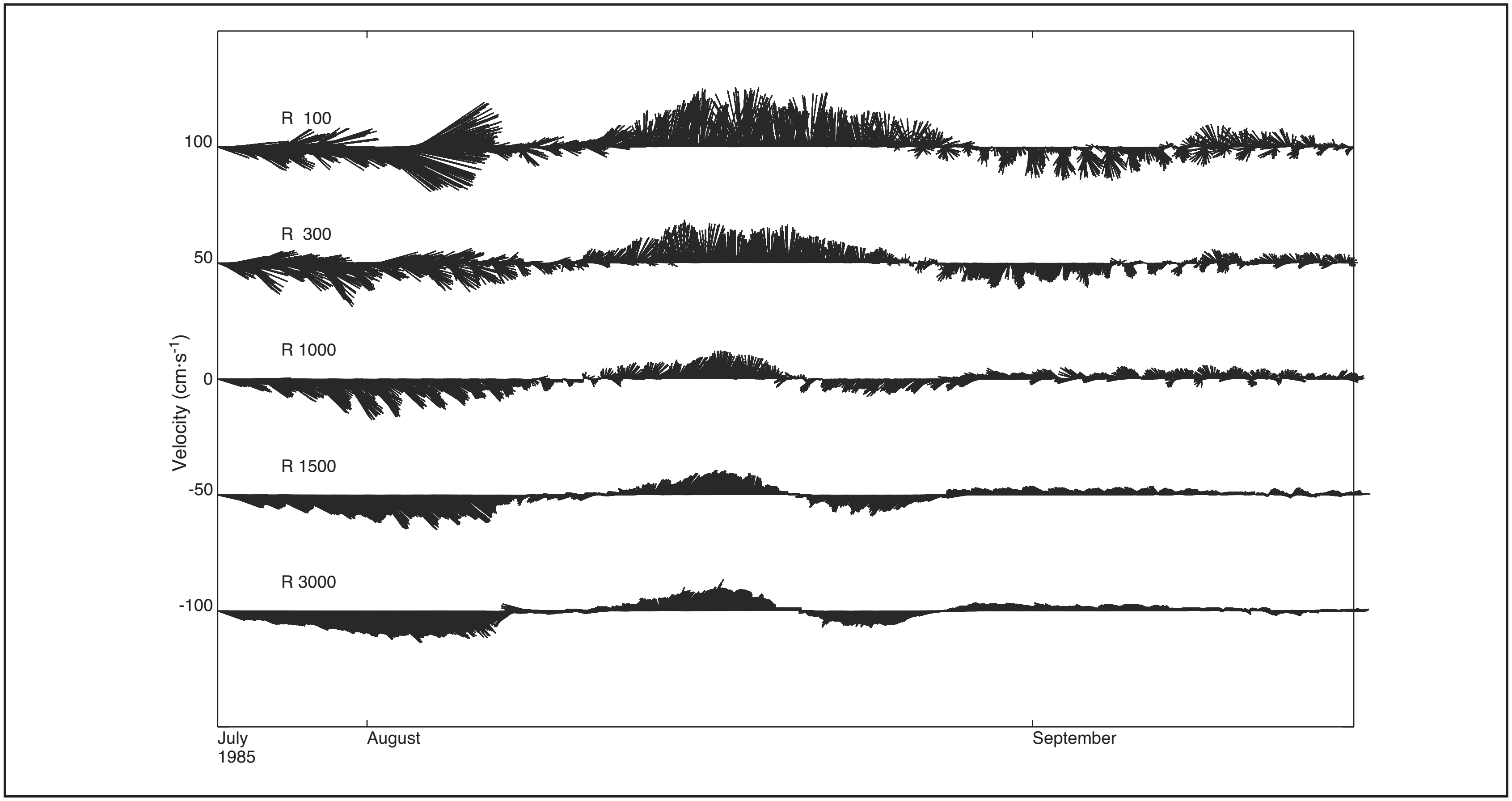

Figure B.8-1. A deep barotropic event with bottom intensification in the western Gulf at SAIC 5-year mooring R, July and August 1985. Note the low-frequency "wave" is throughout the water column. See also Table B-8, event 1.

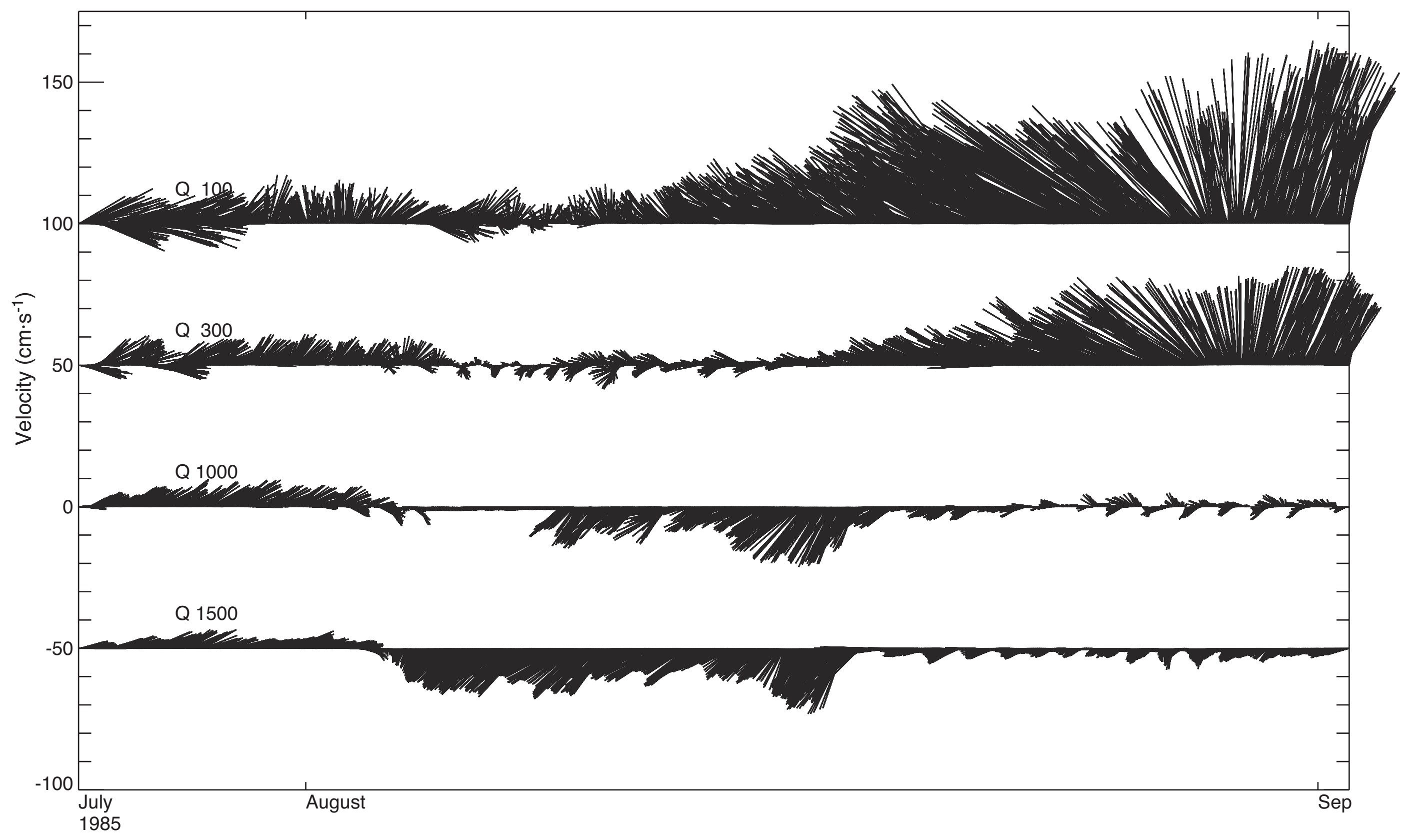

Figure B.8-2. A deep barotropic, bottom-intensified event in the western Gulf at SAIC 5-year mooring Q, August 1985. Note there is no surface expression of this event. See also Table B-8, event 2.

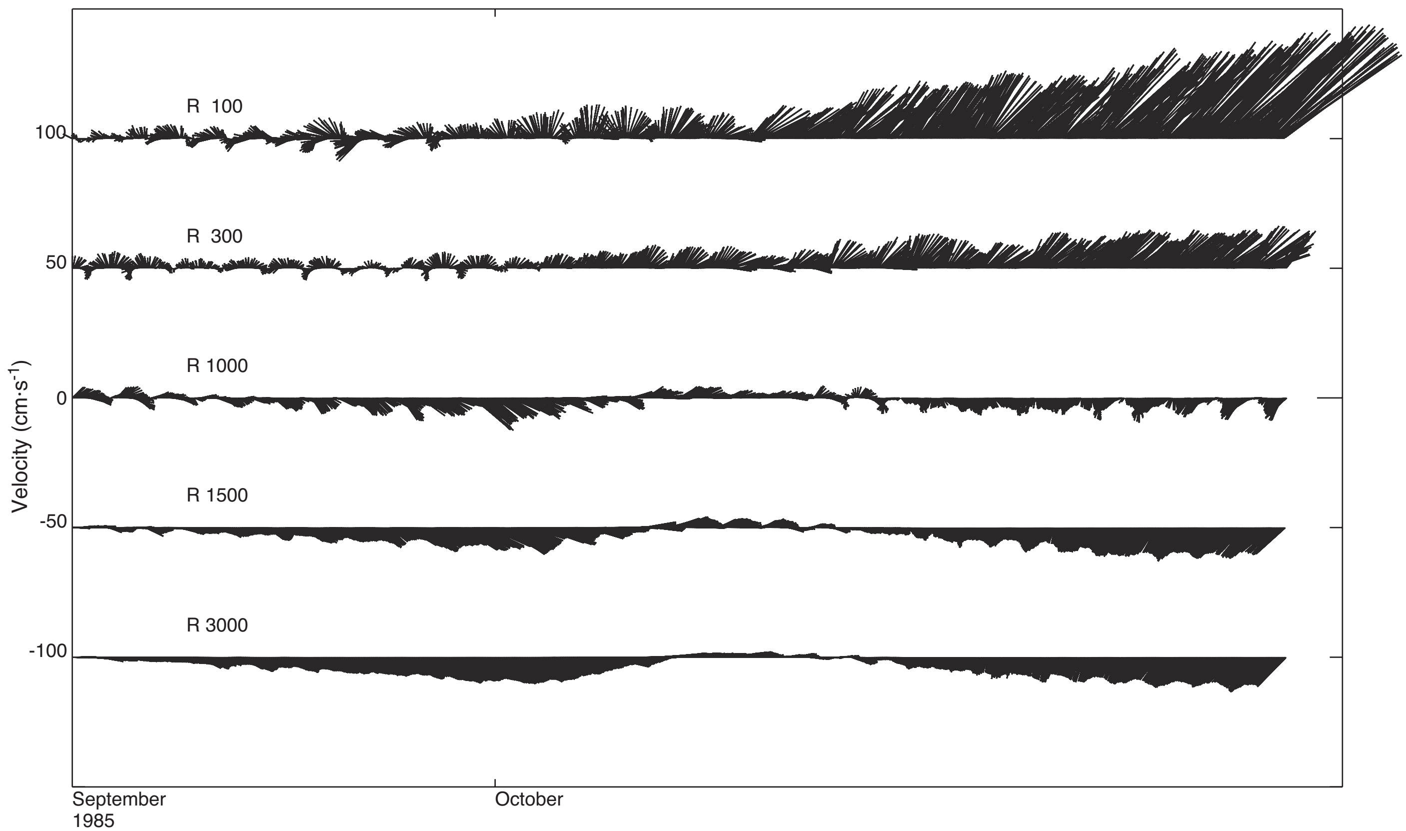

Figure B.8-3. A deep barotropic, bottom-intensified event in the western Gulf at SAIC 5-year mooring R, September and October 1985. Note there is no surface expression of the deep event. See also Table B-8, event 3.

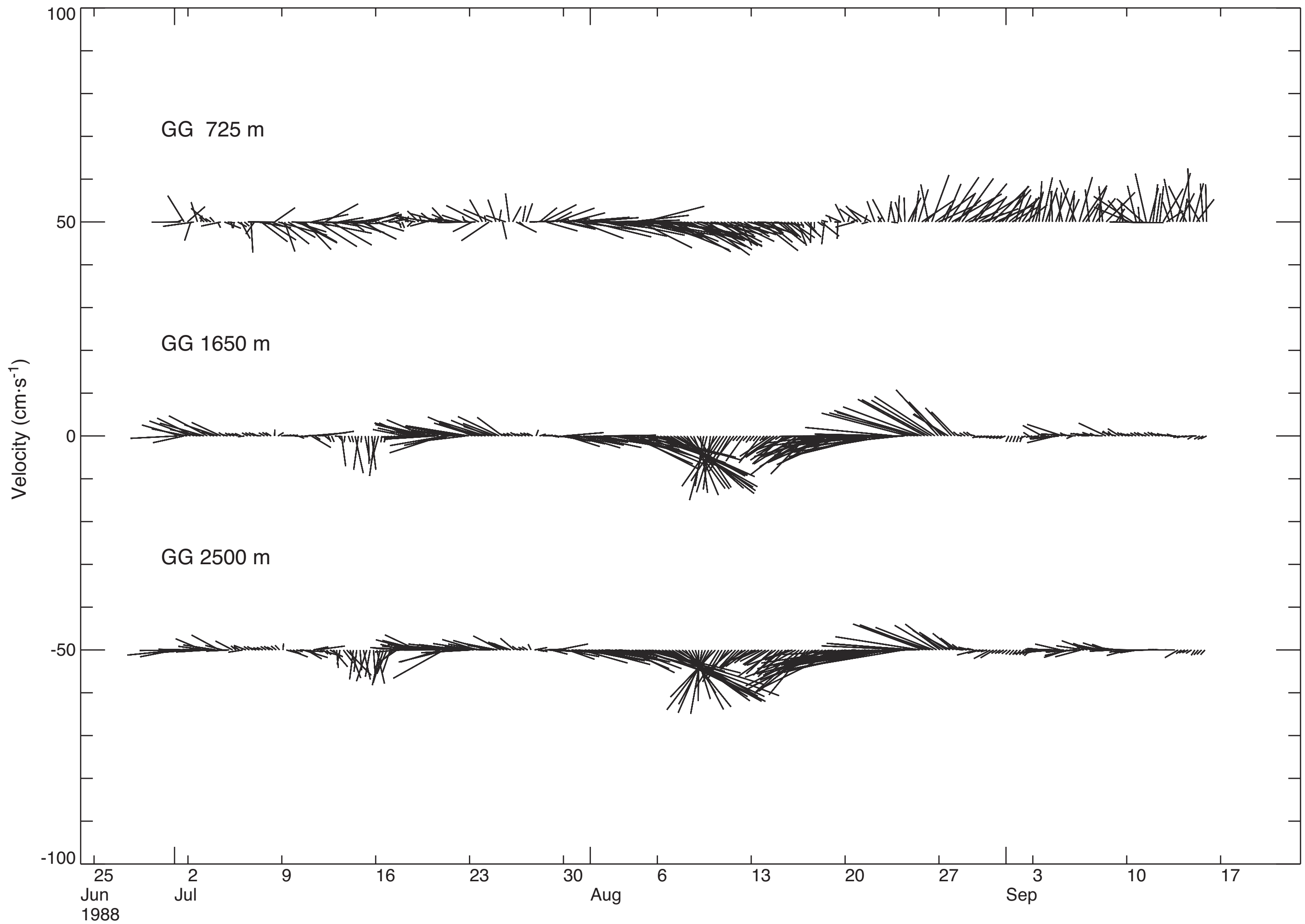

Figure B.8-4. A deep barotropic event in the central Gulf at SAIC 5-year mooring GG, August 1988. See also Table B-8, event 4.

Table B-9. Speed statistics for energetic current events associated with a deep anticyclonic eddy. Given are the name of the file containing the event (keyed to the directory on the CD-ROM database), the start and stop dates used to characterize the event, maximum speed, mean speed, standard deviation of speed, mooring location, depth of the instrument, and total water depth. Comments on the event, keyed by the event number, are given in the notes below the table.

Event No.	Year	Filename	Directory	Event start date (m/d/y)	Event end date (m/d/y)	Maxi-mum speed ($cm \cdot s^{-1}$)	Mean speed ($cm \cdot s^{-1}$)	Stand. dev. of speed ($cm \cdot s^{-1}$)	Latitude (°N)	Longi-tude (°W)	Depth (m)	Total water depth (m)
1	1985	MG850615.C07	/NODC_DEEP/	08/01/1985	08/10/1985	20.539	9.490	5.338	25.4917	94.1600	1000.0	3500.0
	1985	MG850612.C03	/NODC_DEEP/	08/01/1985	08/10/1985	9.714	4.988	1.875	25.4115	95.5300	1000.0	1508.0
	1985	AC850611.C02	/NODC_DEEP/	08/01/1985	08/10/1985	21.101	7.024	3.423	26.0117	95.1217	1000.0	2000.0
	1985	MG850615.C03	/NODC_DEEP/	08/01/1985	08/10/1985	20.255	5.931	5.119	25.8717	94.8800	1000.0	3000.0

Notes by event number

1 1985: Early August, Deep anticyclonic eddy

The effect of this deep anticyclonic eddy is best seen with the vector stick plots from 1000-m depth on SAIC moorings S (west-most mooring), P, Q, and R (east-most mooring). Currents are northward at S, northeastward at P and Q, and southward at R, exhibiting an anticyclonic circulation. The event is short lived, being only a few days in duration. There are inertial motions superimposed on the anticyclonic vectors. Data from SAIC S, P, Q, and R are plotted in Figure 6.3.3-5.

Table B-10. Speed statistics for energetic subsurface, mid-water column jets. Given are the name of the file containing the event (keyed to the directory on the CD-ROM database), the start and stop dates used to characterize the event, maximum speed, mean speed, standard deviation of speed, mooring location, depth of the instrument, and total water depth. Comments on the event, keyed by the event number, are given in the notes below the table.

Event No.	Year	Filename	Directory	Event start date (m/d/y)	Event end date (m/d/y)	Maximum speed ($cm \cdot s^{-1}$)	Mean speed ($cm \cdot s^{-1}$)	Stand. dev. of speed ($cm \cdot s^{-1}$)	Latitude (°N)	Longitude (°W)	Depth (m)	Total water depth (m)
1	1994	GC940212.A24	/INDUSTRY/	05/01/1994	05/31/1994	24.044	11.802	4.646	27.7457	90.7310	215.0	894.6
	1994	GC940212.A25	/INDUSTRY/	05/01/1994	05/31/1994	24.187	11.835	4.522	27.7457	90.7310	223.0	894.6
	1994	GC940212.A26	/INDUSTRY/	05/01/1994	05/31/1994	23.607	11.741	4.429	27.7457	90.7310	231.0	894.6
	1994	GC940212.A27	/INDUSTRY/	05/01/1994	05/31/1994	24.418	11.568	4.512	27.7457	90.7310	239.0	894.6
	1994	GC940212.A28	/INDUSTRY/	05/01/1994	05/31/1994	24.691	11.458	4.593	27.7457	90.7310	247.0	894.6
	1994	GC940212.A29	/INDUSTRY/	05/01/1994	05/31/1994	25.632	11.481	4.770	27.7457	90.7310	255.0	894.6
	1994	GC940212.A30	/INDUSTRY/	05/01/1994	05/31/1994	25.399	11.387	5.034	27.7457	90.7310	263.0	894.6
	1994	GC940212.A31	/INDUSTRY/	05/01/1994	05/31/1994	26.517	11.437	5.206	27.7457	90.7310	271.0	894.6
	1994	GC940212.A32	/INDUSTRY/	05/01/1994	05/31/1994	28.040	11.420	5.143	27.7457	90.7310	279.0	894.6
	1994	GC940212.A33	/INDUSTRY/	05/01/1994	05/31/1994	26.627	11.364	5.212	27.7457	90.7310	287.0	894.6
	1994	GC940212.A34	/INDUSTRY/	05/01/1994	05/31/1994	26.327	11.365	5.162	27.7457	90.7310	295.0	894.6
	1994	GC940212.A35	/INDUSTRY/	05/01/1994	05/31/1994	27.140	11.365	5.162	27.7457	90.7310	303.0	894.6
	1994	GC940212.A36	/INDUSTRY/	05/01/1994	05/31/1994	27.755	11.417	5.173	27.7457	90.7310	311.0	894.6
	1994	GC940212.A37	/INDUSTRY/	05/01/1994	05/31/1994	28.074	11.377	5.191	27.7457	90.7310	319.0	894.6
	1994	GC940212.A38	/INDUSTRY/	05/01/1994	05/31/1994	27.060	11.315	5.114	27.7457	90.7310	327.0	894.6
	1994	GC940212.A39	/INDUSTRY/	05/01/1994	05/31/1994	28.559	11.270	5.015	27.7457	90.7310	335.0	894.6
	1994	GC940212.A40	/INDUSTRY/	05/01/1994	05/31/1994	28.532	11.331	4.975	27.7457	90.7310	343.0	894.6
	1994	GC940212.A41	/INDUSTRY/	05/01/1994	05/31/1994	28.623	11.400	5.052	27.7457	90.7310	351.0	894.6
	1994	GC940212.A42	/INDUSTRY/	05/01/1994	05/31/1994	29.090	11.471	5.141	27.7457	90.7310	359.0	894.6
	1994	GC940212.A43	/INDUSTRY/	05/01/1994	05/31/1994	28.737	11.325	5.106	27.7457	90.7310	367.0	894.6
2	1997	MC970121.A01	/INDUSTRY/	04/04/1997	04/30/1997	76.585	35.233	13.768	28.3323	89.3669	20.0	837.6
	1997	MC970121.A02	/INDUSTRY/	04/04/1997	04/30/1997	68.033	33.432	12.747	28.3323	89.3669	36.0	837.6
	1997	MC970121.A03	/INDUSTRY/	04/04/1997	04/30/1997	59.452	31.374	11.932	28.3323	89.3669	52.0	837.6
	1997	MC970121.A04	/INDUSTRY/	04/04/1997	04/30/1997	58.977	29.302	11.608	28.3323	89.3669	68.0	837.6
	1997	MC970121.A05	/INDUSTRY/	04/04/1997	04/30/1997	55.471	27.562	11.632	28.3323	89.3669	84.0	837.6
	1997	MC970121.A06	/INDUSTRY/	04/04/1997	04/30/1997	50.000	24.914	11.494	28.3323	89.3669	100.0	837.6
	1997	MC970121.A07	/INDUSTRY/	04/04/1997	04/30/1997	46.717	21.539	10.430	28.3323	89.3669	116.0	837.6
	1997	MC970121.A08	/INDUSTRY/	04/04/1997	04/30/1997	39.217	19.072	8.541	28.3323	89.3669	132.0	837.6
	1997	MC970121.A09	/INDUSTRY/	04/04/1997	04/30/1997	35.892	17.528	6.935	28.3323	89.3669	148.0	837.6
	1997	MC970121.A10	/INDUSTRY/	04/04/1997	04/30/1997	34.015	16.591	6.605	28.3323	89.3669	164.0	837.6
	1997	MC970121.A11	/INDUSTRY/	04/04/1997	04/30/1997	30.806	15.749	6.272	28.3323	89.3669	180.0	837.6

Table B-10. Speed statistics for energetic subsurface, mid-water column jets. (continued)

Event No.	Year	Filename	Directory	Event start date (m/d/y)	Event end date (m/d/y)	Maximum speed ($cm \cdot s^{-1}$)	Mean speed ($cm \cdot s^{-1}$)	Stand. dev. of speed ($cm \cdot s^{-1}$)	Latitude (°N)	Longitude (°W)	Depth (m)	Total water depth (m)
2	1997	MC970121.A12	/INDUSTRY/	04/04/1997	04/30/1997	32.745	15.234	5.961	28.3323	89.3669	196.0	837.6
	1997	MC970121.A13	/INDUSTRY/	04/04/1997	04/30/1997	35.511	14.752	5.836	28.3323	89.3669	212.0	837.6
	1997	MC970121.A14	/INDUSTRY/	04/04/1997	04/30/1997	39.131	14.231	6.127	28.3323	89.3669	228.0	837.6
	1997	MC970121.A15	/INDUSTRY/	04/04/1997	04/30/1997	45.706	13.929	6.728	28.3323	89.3669	244.0	837.6
	1997	MC970121.A16	/INDUSTRY/	04/04/1997	04/30/1997	53.106	13.795	7.406	28.3323	89.3669	260.0	837.6
	1997	MC970121.A17	/INDUSTRY/	04/04/1997	04/30/1997	56.500	13.468	8.025	28.3323	89.3669	276.0	837.6
	1997	MC970121.A18	/INDUSTRY/	04/04/1997	04/30/1997	54.745	13.267	8.317	28.3323	89.3669	292.0	837.6
	1997	MC970121.A19	/INDUSTRY/	04/04/1997	04/30/1997	48.757	13.072	8.291	28.3323	89.3669	308.0	837.6
	1997	MC970121.A20	/INDUSTRY/	04/04/1997	04/30/1997	51.196	12.589	8.015	28.3323	89.3669	324.0	837.6
	1997	MC970121.A21	/INDUSTRY/	04/04/1997	04/30/1997	52.538	12.575	7.584	28.3323	89.3669	340.0	837.6
	1997	MC970121.A22	/INDUSTRY/	04/04/1997	04/30/1997	52.369	12.471	7.336	28.3323	89.3669	356.0	837.6
	1997	MC970121.A23	/INDUSTRY/	04/04/1997	04/30/1997	49.732	12.193	7.034	28.3323	89.3669	372.0	837.6
	1997	MC970121.A24	/INDUSTRY/	04/04/1997	04/30/1997	45.260	11.829	6.539	28.3323	89.3669	388.0	837.6
	1997	MC970121.A25	/INDUSTRY/	04/04/1997	04/30/1997	42.720	11.482	6.069	28.3323	89.3669	404.0	837.6
	1997	MC970121.A26	/INDUSTRY/	04/04/1997	04/30/1997	40.050	11.255	5.566	28.3323	89.3669	420.0	837.6
	1997	MC970121.A27	/INDUSTRY/	04/04/1997	04/30/1997	38.823	11.029	5.245	28.3323	89.3669	436.0	837.6
	1997	MC970121.A28	/INDUSTRY/	04/04/1997	04/30/1997	40.525	10.728	4.958	28.3323	89.3669	452.0	837.6
	1997	MC970121.A29	/INDUSTRY/	04/04/1997	04/30/1997	38.396	10.410	4.715	28.3323	89.3669	468.0	837.6
	1997	MC970121.A30	/INDUSTRY/	04/04/1997	04/30/1997	33.242	10.017	4.604	28.3323	89.3669	484.0	837.6
	1997	MC970121.A31	/INDUSTRY/	04/04/1997	04/30/1997	29.155	9.690	4.545	28.3323	89.3669	500.0	837.6
	1997	MC970121.A32	/INDUSTRY/	04/04/1997	04/30/1997	25.831	9.402	4.473	28.3323	89.3669	516.0	837.6
	1997	MC970121.A33	/INDUSTRY/	04/04/1997	04/30/1997	25.110	8.945	4.296	28.3323	89.3669	532.0	837.6
	1997	MC970121.A34	/INDUSTRY/	04/04/1997	04/30/1997	24.254	8.255	4.019	28.3323	89.3669	548.0	837.6
	1997	MC970121.A35	/INDUSTRY/	04/04/1997	04/30/1997	22.677	7.689	3.877	28.3323	89.3669	564.0	837.6
	1997	MC970121.A36	/INDUSTRY/	04/04/1997	04/30/1997	23.537	7.375	3.860	28.3323	89.3669	580.0	837.6
	1997	MC970121.A37	/INDUSTRY/	04/04/1997	04/30/1997	24.083	7.116	3.807	28.3323	89.3669	596.0	837.6
	1997	MC970121.A38	/INDUSTRY/	04/04/1997	04/30/1997	25.495	6.920	3.720	28.3323	89.3669	612.0	837.6
	1997	MC970121.A39	/INDUSTRY/	04/04/1997	04/30/1997	27.166	6.652	3.693	28.3323	89.3669	628.0	837.6
	1997	MC970121.A40	/INDUSTRY/	04/04/1997	04/30/1997	26.575	6.212	3.636	28.3323	89.3669	644.0	837.6
	1997	MC970121.A41	/INDUSTRY/	04/04/1997	04/30/1997	26.519	5.643	3.546	28.3323	89.3669	660.0	837.6
	1997	MC970121.A42	/INDUSTRY/	04/04/1997	04/30/1997	24.047	5.272	3.434	28.3323	89.3669	676.0	837.6
	1997	MC970121.A43	/INDUSTRY/	04/04/1997	04/30/1997	25.402	5.022	3.279	28.3323	89.3669	692.0	837.6
	1997	MC970121.A44	/INDUSTRY/	04/04/1997	04/30/1997	24.042	4.912	3.245	28.3323	89.3669	708.0	837.6
	1997	MC970121.A45	/INDUSTRY/	04/04/1997	04/30/1997	23.585	4.964	3.116	28.3323	89.3669	724.0	837.6

Table B-10. Speed statistics for energetic subsurface, mid-water column jets. (continued)

Event No.	Year	Filename	Directory	Event start date (m/d/y)	Event end date (m/d/y)	Maximum speed ($cm \cdot s^{-1}$)	Mean speed ($cm \cdot s^{-1}$)	Stand. dev. of speed ($cm \cdot s^{-1}$)	Latitude (°N)	Longitude (°W)	Depth (m)	Total water depth (m)
2	1997	MC970121.A46	/INDUSTRY/	04/04/1997	04/30/1997	22.611	5.031	2.982	28.3323	89.3669	740.0	837.6
	1997	MC970121.A47	/INDUSTRY/	04/04/1997	04/30/1997	23.243	5.088	2.894	28.3323	89.3669	756.0	837.6
	1997	MC970121.A48	/INDUSTRY/	04/04/1997	04/30/1997	24.352	5.108	2.961	28.3323	89.3669	772.0	837.6
	1997	MC970121.A49	/INDUSTRY/	04/04/1997	04/30/1997	25.812	5.160	3.064	28.3323	89.3669	788.0	837.6
	1997	MC970121.A50	/INDUSTRY/	04/04/1997	04/30/1997	19.164	6.301	3.327	28.3323	89.3669	804.0	837.6
3	1998	DD980812.A01	/MMS/	09/01/1998	10/31/1998	179.442	25.386	17.369	29.3712	87.3563	12.0	500.0
	1998	DD980812.A02	/MMS/	09/01/1998	10/31/1998	150.841	24.997	16.638	29.3712	87.3563	16.0	500.0
	1998	DD980812.A03	/MMS/	09/01/1998	10/31/1998	127.838	23.788	15.665	29.3712	87.3563	20.0	500.0
	1998	DD980812.A04	/MMS/	09/01/1998	10/31/1998	106.385	22.781	14.896	29.3712	87.3563	24.0	500.0
	1998	DD980812.A05	/MMS/	09/01/1998	10/31/1998	113.641	21.719	14.364	29.3712	87.3563	28.0	500.0
	1998	DD980812.A06	/MMS/	09/01/1998	10/31/1998	118.084	21.165	13.789	29.3712	87.3563	32.0	500.0
	1998	DD980812.A07	/MMS/	09/01/1998	10/31/1998	114.661	20.783	13.449	29.3712	87.3563	36.0	500.0
	1998	DD980812.A08	/MMS/	09/01/1998	10/31/1998	111.668	20.335	13.498	29.3712	87.3563	40.0	500.0
	1998	DD980812.A09	/MMS/	09/01/1998	10/31/1998	113.492	19.821	13.886	29.3712	87.3563	44.0	500.0
	1998	DD980812.A10	/MMS/	09/01/1998	10/31/1998	113.789	19.909	14.191	29.3712	87.3563	48.0	500.0
	1998	DD980812.A11	/MMS/	09/01/1998	10/31/1998	113.373	19.960	14.481	29.3712	87.3563	52.0	500.0
	1998	DD980812.A12	/MMS/	09/01/1998	10/31/1998	112.730	19.611	14.658	29.3712	87.3563	56.0	500.0
	1998	DD980812.A13	/MMS/	09/01/1998	10/31/1998	117.850	19.122	15.161	29.3712	87.3563	60.0	500.0
	1998	DD980812.A14	/MMS/	09/01/1998	10/31/1998	117.526	19.316	15.036	29.3712	87.3563	64.0	500.0
	1998	DD980812.A15	/MMS/	09/01/1998	10/31/1998	119.822	19.591	14.969	29.3712	87.3563	68.0	500.0
	1998	DD980812.A16	/MMS/	09/01/1998	10/31/1998	121.443	19.539	15.186	29.3712	87.3563	72.0	500.0
	1998	DD980812.A17	/MMS/	09/01/1998	10/31/1998	119.861	19.166	14.988	29.3712	87.3563	76.0	500.0
	1998	DD980812.A18	/MMS/	09/01/1998	10/31/1998	115.981	18.237	14.398	29.3712	87.3563	80.0	500.0
	1998	DD980812.C01	/MMS/	09/01/1998	10/31/1998	110.084	16.753	12.207	29.3712	87.3563	200.0	500.0
	1998	DD980812.C02	/MMS/	09/01/1998	10/31/1998	85.670	16.462	11.224	29.3712	87.3563	300.0	500.0
	1998	DD980812.C03	/MMS/	09/01/1998	10/31/1998	72.003	9.330	7.796	29.3712	87.3563	490.0	500.0
	1998	DD980808.A01	/MMS/	09/01/1998	10/31/1998	202.837	29.484	19.753	29.0032	87.3532	12.0	1300.0
	1998	DD980808.A02	/MMS/	09/01/1998	10/31/1998	177.568	26.924	20.995	29.0032	87.3532	16.0	1300.0
	1998	DD980808.A03	/MMS/	09/01/1998	10/31/1998	161.485	25.528	20.196	29.0032	87.3532	20.0	1300.0
	1998	DD980808.A04	/MMS/	09/01/1998	10/31/1998	174.001	24.609	19.158	29.0032	87.3532	24.0	1300.0
	1998	DD980808.A05	/MMS/	09/01/1998	10/31/1998	156.170	24.230	18.166	29.0032	87.3532	28.0	1300.0
	1998	DD980808.A06	/MMS/	09/01/1998	10/31/1998	141.319	24.061	17.720	29.0032	87.3532	32.0	1300.0
	1998	DD980808.A07	/MMS/	09/01/1998	10/31/1998	125.455	23.885	17.578	29.0032	87.3532	36.0	1300.0
	1998	DD980808.A08	/MMS/	09/01/1998	10/31/1998	117.282	23.516	17.225	29.0032	87.3532	40.0	1300.0

Table B-10. Speed statistics for energetic subsurface, mid-water column jets. (continued)

Event No.	Year	Filename	Directory	Event start date (m/d/y)	Event end date (m/d/y)	Maximum speed ($cm \cdot s^{-1}$)	Mean speed ($cm \cdot s^{-1}$)	Stand. dev. of speed ($cm \cdot s^{-1}$)	Latitude (°N)	Longitude (°W)	Depth (m)	Total water depth (m)
3	1998	DD980808.A09	/MMS/	09/01/1998	10/31/1998	102.837	23.108	16.642	29.0032	87.3532	44.0	1300.0
	1998	DD980808.A10	/MMS/	09/01/1998	10/31/1998	92.670	22.323	15.409	29.0032	87.3532	48.0	1300.0
	1998	DD980808.A11	/MMS/	09/01/1998	10/31/1998	77.131	21.269	14.232	29.0032	87.3532	52.0	1300.0
	1998	DD980808.A12	/MMS/	09/01/1998	10/31/1998	60.004	17.270	11.242	29.0032	87.3532	56.0	1300.0
	1998	DD980808.A13	/MMS/	09/01/1998	10/31/1998	60.784	17.072	11.180	29.0032	87.3532	60.0	1300.0
	1998	DD980808.A14	/MMS/	09/01/1998	10/31/1998	66.430	18.429	13.209	29.0032	87.3532	64.0	1300.0
	1998	DD980808.A15	/MMS/	09/01/1998	10/31/1998	63.861	17.787	13.089	29.0032	87.3532	68.0	1300.0
	1998	DD980808.A16	/MMS/	09/01/1998	10/31/1998	59.146	18.693	12.340	29.0032	87.3532	72.0	1300.0
	1998	DD980808.C01	/MMS/	09/01/1998	10/31/1998	34.813	13.785	6.570	29.0032	87.3532	500.0	1300.0
	1998	DD980808.C02	/MMS/	09/01/1998	10/31/1998	48.603	8.392	7.837	29.0032	87.3532	1290.0	1300.0

Notes by event number

1 1994: May

The records at Industry GC200 show an upward propagating wave packet with maximum speed of ~50 $cm \cdot s^{-1}$. This event lasts a few hours. The data are of high temporal (5 minute) and spatial (ADCP 8 m bins) resolution. Industry GC200 data are plotted in Figure 6.3.12-7. A detail of this event is shown in Figure 6.1.4-2.

2 1997: April

The records Industry MC628 show a downward propagating signal with maximum velocity of ~60 $cm \cdot s^{-1}$, centered at 300 m depth. The event lasts about 2 days. The peak jet speed equals the ambient surface speed. Data are of high temporal (10 minute) and spatial (ADCP 16 m bins) resolution. Industry MC628 data are plotted in Figure 6.3.12-13. A detail of this event is shown in Figure 6.1.4-1.

3 1998: September-October

The records at SAIC EIS mooring C3 show a very good example of downward inertial propagation of energy resulting from energetic atmospheric storms. Since lag between surface and subsurface expression of this energy could be several days, these types of events may be related to observations of mid-column jets. Data are from ADCP (upper 80 m in 4 m bins) and RCM8 (at 500 and 1300 m) instruments. SAIC EIS data are plotted in Figure 6.3.5-2. Details of this event are shown in Figures 6.1.5-1, 6.1.5-2, and 6.1.5-3.

The Department of the Interior Mission

As the Nation's principal conservation agency, the Department of the Interior has responsibility for most of our nationally owned public lands and natural resources. This includes fostering sound use of our land and water resources; protecting our fish, wildlife, and biological diversity; preserving the environmental and cultural values of our national parks and historical places; and providing for the enjoyment of life through outdoor recreation. The Department assesses our energy and mineral resources and works to ensure that their development is in the best interests of all our people by encouraging stewardship and citizen participation in their care. The Department also has a major responsibility for American Indian reservation communities and for people who live in island territories under U.S. administration.

The Minerals Management Service Mission

As a bureau of the Department of the Interior, the Minerals Management Service's (MMS) primary responsibilities are to manage the mineral resources located on the Nation's Outer Continental Shelf (OCS), collect revenue from the Federal OCS and onshore Federal and Indian lands, and distribute those revenues.

Moreover, in working to meet its responsibilities, the **Offshore Minerals Management Program** administers the OCS competitive leasing program and oversees the safe and environmentally sound exploration and production of our Nation's offshore natural gas, oil and other mineral resources. The MMS **Minerals Revenue Management** meets its responsibilities by ensuring the efficient, timely and accurate collection and disbursement of revenue from mineral leasing and production due to Indian tribes and allottees, States and the U.S. Treasury.

The MMS strives to fulfill its responsibilities through the general guiding principles of: (1) being responsive to the public's concerns and interests by maintaining a dialogue with all potentially affected parties and (2) carrying out its programs with an emphasis on working to enhance the quality of life for all Americans by lending MMS assistance and expertise to economic development and environmental protection.